

Methylomic and Transcriptomic Profiling of the Schizophrenia Brain

Submitted by

Joana Fortio Fernandes Pacheco Viana

to the University of Exeter

as a thesis for the degree of

Doctor of Philosophy in Medical Studies

In June 2016

This thesis is available for Library use on the understanding that it is copyright material and that no quotation from the thesis may be published without proper acknowledgement.

I certify that all material in this thesis which is not my own work has been identified and that no material has previously been submitted and approved for the award of a degree by this or any other University.

Signature:

Abstract

Schizophrenia is a severe psychiatric disorder that affects more than twenty-one million people worldwide, contributing significantly to the global burden of disease. A growing body of genetic, epigenetic and epidemiological evidence suggests that schizophrenia has its origins during neurodevelopment and that dysregulation of the immune system and infection may play a role in disease etiology. Twin and family studies have highlighted a considerable heritable component to schizophrenia; however the role of genetic variation in the etiology of the disorder is complex. In the majority of cases, susceptibility is attributed to the combined action of multiple common genetic risk variants of low penetrance.

Improved understanding about the biology of the genome has led to increased interest in the role of non-sequence-based variation in the etiology of neurodevelopmental phenotypes, including schizophrenia. The notion that epigenetic processes and gene expression dysregulation are involved in the onset of schizophrenia is supported by recent studies of disease-discordant monozygotic twins, clinical sample cohorts, and post-mortem brain tissue. To date, however, studies characterizing schizophrenia-associated methylomic and transcriptomic variation in the brain have been limited by small sample number or the assessment of a single brain region.

The main aim of this thesis was to undertake a comprehensive study of genomic variation across four brain regions in schizophrenia. The results provide further support for a neurodevelopmental origin to schizophrenia, as well as a role of the immune system on schizophrenia etiology. My analyses also suggest that epigenetic variation associated with polygenic burden for schizophrenia might play a role in the disease.

In summary, the work presented in this thesis represents the first analysis of epigenetic and gene expression variation associated with schizophrenia across multiple brain regions and highlights the utility of polygenic risk scores for identifying molecular pathways associated with etiological variation in complex disease.

Acknowledgements

A lot of people contributed to the success of this journey and I would like to thank every single person. I would like to start by thanking my first supervisor, Professor Jonathan Mill, for believing in my potential from the beginning, and for his continued enthusiasm, guidance and expertise. I would also like to thank my second supervisor, Dr Eduarda Santos, for being so supportive, present and kind all the way through.

I would like to thank Dr Ruth Pidsley, who started the 'schizophrenia brains' project and, perhaps without knowing, taught me what it means to be a good scientist. I am very thankful to everyone in the Complex Disease Epigenetics Group both in Exeter and London (there are too many of you to name), you are the best and most fun people I could ever wish to work with! In particular I would like to thank Therese and Eilís for their friendship, knowledge, help and support. Thank you to all the collaborators, students and staff in the University and in the different research groups who helped me in any way during my PhD.

I would also like to thank all the friends who were so important during these three years, all the friends who arrived and left Exeter in the meantime and marked my experience. Thank you to the salsa family for making my life so much more fun. Thank you to Lorena, for being the kindest friend. A big thank you to my 'vampires' Miriam, Afsoon, Magdalena and Trupti, my heart is full of love because of you. An immense thank you to George, for his love, incredible patience and endless support (and a special thank you to the Alfords & Co for their friendship and their delicious roast dinners). A huge thank you to Carolina, for being my unquestionable soulmate – there are no words.

Finally, I would like to thank my sister, brother, uncles, aunts and cousins (to summarise, all the Pachecos Vianas, extended version) for being the funniest and most fun family. The biggest thank you of all goes to my parents. Thank you for all the opportunities and for all the support. Most importantly, thank you for being the most amazing parents in the world.

I would like to dedicate this work, along with my past and future achievements, to my grandmother Isabelinha, who is the most intelligent, kind and wise woman I have ever known.

Table of Contents

Abstract	2
Acknowledgements	3
Table of Contents	4
Table of Figures	10
Table of Tables.....	19
Publications Arising from this Thesis.....	25
Declarations	27
List of Abbreviations	29
Chapter 1 - General Introduction	32
1.1. Schizophrenia	32
1.1.1. Clinical manifestation	32
1.1.2. Neuropathology of schizophrenia.....	33
1.1.3. Genetics of schizophrenia.....	36
1.1.3.1. Heritability and evidence from twin studies.....	36
1.1.3.2. Rare and <i>de novo</i> mutations.....	36
1.1.3.3. Schizophrenia as a polygenic disorder	36
1.1.4. Schizophrenia polygenic risk score.....	37
1.1.5. Neurodevelopmental origins of schizophrenia	38
1.1.6. Immunity and inflammation in schizophrenia	38
1.2. Gene expression and regulation	39
1.2.1. Introduction to epigenetics	41
1.2.2. Epigenetic mechanisms	43
1.2.2.1. DNA modifications	43
1.2.2.2. Histone modifications.....	46
1.2.2.3. Non-coding RNA.....	48
1.2.2.4. Interaction of different epigenetic mechanisms and gene expression regulation	48
1.2.2.5. Genetic mediation of the epigenome	50
1.3. Profiling the methylome.....	50
1.4. Epigenetic and gene expression studies in schizophrenia.....	52
1.4.1. Epigenetics of schizophrenia	52
1.4.1.1. Epigenetic studies of schizophrenia using post-mortem brain tissue	53

1.4.1.2. Epigenetic studies of schizophrenia using peripheral tissues	57
1.4.2. Transcriptomic variation in schizophrenia	60
1.4.3. Antipsychotic medication and the implications of epigenetic studies	62
1.5. Klinefelter syndrome	63
1.6. General aims of my thesis.....	64
Chapter 2 - Materials and Methods	67
2.1. Human sample cohorts	67
2.2. Nucleic acid extraction	67
2.2.1. Genomic DNA isolation using phenol-chloroform.....	68
2.2.2. Total RNA isolation from post-mortem human brain tissue.....	70
2.2.3. Total RNA clean-up.....	71
2.2.4. Determining the quality and quantity of isolated nucleic acids	74
2.3. DNA methylation profiling.....	78
2.3.1. Sodium bisulfite conversion	79
2.3.2. Infinium HumanMethylation450 BeadChip	80
2.3.2.1. Infinium HumanMethylation450 BeadChip data analysis.....	80
2.3.3. Bisulfite-PCR-pyrosequencing	82
2.3.3.1. Polymerase chain reaction	82
2.3.3.2. Agarose gel electrophoresis	85
2.3.3.3. Bisulfite-pyrosequencing.....	86
2.4. Genome-wide SNP profiling.....	89
2.5. Transcriptome profiling.....	89
2.5.1. Complementary DNA libraries preparation	90
2.5.2. cDNA libraries quantification and pooling	91
2.5.3. RNA sequencing.....	92
Chapter 3 - Methylomic profiling of schizophrenia in the brain	95
3.1. Introduction	95
3.2. Methods	97
3.2.1. Samples.....	97
3.2.1.1. Medical Research Council London Neurodegenerative Diseases Brain Bank.....	97
3.2.1.2. Douglas Bell-Canada Brain Bank	98
3.2.1.3. Medical Research Council Edinburgh Brain and Tissue Banks .	98
3.2.2. Samples and cohort quality control	104

3.2.3. Data pre-processing and normalisation	112
3.2.4. DNA methylation age calculation	117
3.2.5. Cell composition estimates	117
3.2.6. Identification of differentially methylated positions and regions	119
3.2.7. Additional probe annotation and enrichment analysis for regulatory regions and schizophrenia GWAS regions	121
3.2.8. Establishing multiple testing significance threshold for EWAS analysis	122
3.2.9. Cross-region multilevel model.....	122
3.2.10. Validation with bisulfite-PCR-pyrosequencing	123
3.3. Results	125
3.3.1. Overview of experimental strategy.....	125
3.3.2. No global DNA methylation changes or DNA methylation age acceleration in schizophrenia.....	127
3.3.3. Differently methylated positions associated with schizophrenia.....	130
3.3.4. Controlling for unknown confounding variables	156
3.3.5. Enrichment of overlap between schizophrenia-associated differently methylated positions and regulatory features and GWAS regions.....	161
3.3.6. Differentially methylated regions associated with schizophrenia ...	164
3.3.6.1. Differently methylated region in chromosome 17.....	169
3.3.7. Consistent methylomic markers of schizophrenia across brain regions	176
3.4. Discussion.....	186
3.4.1. Overview of results	186
3.4.2. Limitations.....	187
3.4.3. Implications, strengths and future directions	188
Chapter 4 - Methylomic profiling of schizophrenia polygenic risk burden in the brain	190
4.1. Introduction	190
4.2. Methods	192
4.2.1. Samples genotyping and quality control	192
4.2.2. Ethnicity prediction.....	194
4.2.3. Polygenic risk score calculation	196
4.2.4. DNA methylation data	196
4.2.5. Identification of differentially methylated positions and regions	198

4.2.6. Additional probe annotation and enrichment analysis for regulatory regions	199
4.2.7. Establishing multiple testing significance threshold for EWAS analysis	199
4.2.8. Cross-tissue mixed model.....	199
4.2.9. Methylation quantitative trait <i>loci</i>	200
4.3. Results	200
4.3.1. Overview of experimental strategy.....	200
4.3.2. Differently methylated positions associated with schizophrenia polygenic risk score	203
4.3.2.1. Enrichment of overlap between polygenic risk score-associated differently methylated positions and regulatory features.....	231
4.3.3. Differently methylated regions associated with schizophrenia polygenic risk score	233
4.3.4. Consistent methylomic markers of schizophrenia polygenic risk burden across brain regions	237
4.3.5. Comparison between methylomic analysis of schizophrenia PRS and diagnosed schizophrenia	247
4.3.6. Polygenic risk score-associated methylomic variation does not reflect direct genetic effects on DNA methylation	250
4.4. Discussion.....	256
4.4.1. Overview of results	256
4.4.2. Limitations.....	258
4.4.3. Implications, strengths and future directions.....	259
Chapter 5 - Systems-level analysis of DNA methylation in the schizophrenia brain	260
5.1. Chapter aims and structure	260
5.2. Background.....	260
5.2.1. Network analysis.....	260
5.2.2. Weighted gene co-methylation network analysis	264
5.2.3. Overview of experimental strategy.....	267
5.3. Data pre-processing and normalisation.....	269
5.4. Network construction and module detection	270
5.5. Similarities between separate networks for schizophrenia cases and non-psychiatric controls.....	272

5.5.1. Approaches to match networks for schizophrenia cases and non-psychiatric controls	275
5.5.1.1. Count the overlap of probes between each pair of modules from the controls and cases networks	275
5.5.1.2. Test for significant overlap of common probes between cases and controls modules	278
5.6. Networks including schizophrenia cases and non-psychiatric controls	279
5.6.1. Modules associated with several traits.....	279
5.6.2. Prefrontal cortex modules associated with schizophrenia.....	290
5.6.3. Gene ontology analysis on schizophrenia-associated modules.....	299
5.6.4. Exclusion of non-Caucasian samples	311
5.7. Fetal brain correlation network	318
5.8. Discussion.....	320
5.8.1. Overview of the results	320
5.8.2. Strengths, limitations and future directions	321
Chapter 6 - Transcriptomic profiling of schizophrenia prefrontal cortex.....	323
6.1. Introduction	323
6.2. Methods	324
6.2.1. Total RNA isolation from prefrontal cortex samples	324
6.2.2. Complementary DNA libraries preparation and RNA sequencing..	329
6.2.3. Data pre-processing.....	332
6.2.4. Inspection of raw data with <i>FastQC</i>	338
6.2.4.1. <i>Phred</i> quality scores	338
6.2.4.2. Per base sequence and GC content.....	340
6.2.4.3. Sequence duplication levels	343
6.2.5. Trimming of raw reads using <i>Trimmomatic</i>	344
6.2.6. Aligning reads to the human reference transcriptome and quantifying gene expression	349
6.2.7. Differential expression analysis.....	351
6.2.8. Gene and sample exclusion.....	351
6.2.8.1. Data normalisation.....	356
6.2.8.2. Differential expression analysis	358
6.3. Results.....	359
6.3.1. Overview of the experimental strategy	359

6.3.2. Differentially expressed genes between schizophrenia patients and non-psychiatric controls	361
6.3.3. Comparison with DNA methylation results.....	369
6.3.3.1. DNA methylation probes overlapping DE genes.....	369
6.3.3.2. Expressed genes overlapping differently methylated probes and regions.....	377
6.4. Discussion.....	383
6.4.1. Overview of the results	383
6.4.2. Limitations, strengths and future directions.....	384
Chapter 7 - Epigenomic and transcriptomic signatures of a Klinefelter syndrome (47,XXY) karyotype in the brain.....	386
Chapter 8 - General Discussion	400
8.1. Key findings from my research.....	400
8.1.1. Methylomic profiling of schizophrenia in the brain.....	400
8.1.2. Methylomic profiling of schizophrenia polygenic risk burden in the brain.....	401
8.1.3. Systems-level analysis of DNA methylation in the schizophrenia brain	401
8.1.4. Transcriptomic profiling of schizophrenia prefrontal cortex	402
8.1.5. Epigenomic and transcriptomic signatures of a Klinefelter syndrome (47,XXY) karyotype in the brain	402
8.2. Limitations	404
8.3. Integration of schizophrenia findings – strengths, implications and future directions.....	405
8.4. Conclusion	409
Appendix A – Supplementary Tables	416
Appendix B – Supplementary material of Chapter 7.....	491
Appendix C – Additional publications	508
Bibliography.....	555

Table of Figures

Figure 1.1. A simplified overview of the flow of information from DNA to protein in a eukaryote.....	40
Figure 1.2. Waddington's epigenetic landscape	41
Figure 1.3. DNA methylation involves the transfer of a methyl group to the 5 th position of the cytosine pyrimidine ring.....	43
Figure 1.4. Potential mechanisms of active demethylation of DNA regulated by ten-eleven-translocation (TET) family protein.....	45
Figure 1.5. Scheme of chromatin structure	47
Figure 1.6. Epigenomic information across tissues and marks profiled in the NIH Roadmap Epigenomics Consortium	49
Figure 1.7. Influence of neuropsychiatric drugs on the epigenome	63
Figure 1.8. Integration of Chapters 3 to 6 of this thesis	66
Figure 2.1. Overview of the genomic DNA extraction experimental procedure	69
Figure 2.2. Overview of the total RNA extraction experimental procedure	72
Figure 2.3. Overview of the RNA clean-up experimental procedure.....	73
Figure 2.4. A typical nucleic acid sample will have a very characteristic profile	74
Figure 2.5. Electropherogram detailing the regions that are indicative of RNA quality	75
Figure 2.6. A total RNA sample was degraded for varying times and the resulting samples were analyzed on the Agilent 2100 Bioanalyzer System using the Eukaryote Total RNA Nano assay	75
Figure 2.7. Electropherograms from samples ranging from intact (RNA Integrity Number (RIN) = 10), to degraded (RIN = 2)	76
Figure 2.8. Bioanalyzer electropherograms and gel electrophoresis images from a good quality (A) and a degraded sample (B)	76
Figure 2.9. Bioanalyzer electropherograms and gel electrophoresis images from a sample which was successfully rescued in the clean-up process	77
Figure 2.10. DNA sodium bisulfite treatment.....	78
Figure 2.11. Overview of the sodium bisulfite treatment experimental procedure	79
Figure 2.12. Example of an agarose gel used to inspect polymerase chain reaction (PCR) amplification products	86
Figure 2.13. The principles of pyrosequencing.....	88

Figure 2.14. Overview of the complementary DNA libraries preparation protocol	91
Figure 2.15. Example of a D1000 ScreenTape gel electrophoresis (A) and electropherogram (B) of a complementary DNA (cDNA) library	93
Figure 2.16. The data generation and analysis steps of a typical RNA sequencing experiment	94
Figure 3.1. Figure showing the anatomical location of the prefrontal cortex in the human brain	100
Figure 3.2. Figure showing the anatomical location of the basal ganglia (including the putamen) in the human brain	101
Figure 3.3. Figure showing the anatomical location of the hippocampus in the human brain	102
Figure 3.4. Figure showing the anatomical location of the cerebellum in the human brain	103
Figure 3.5. Hierarchical clustering of the thousand most variably-methylated probes across all samples	104
Figure 3.6. Multidimensional scaling of the thousand most variable probes across all samples	108
Figure 3.7. Example of multidimensional scaling plots for the thousand most variable probes across all the striatum MRC London Neurodegenerative Diseases Brain Bank samples	109
Figure 3.8. Example of multidimensional scaling plots of the X-chromosome (A) and Y-chromosome (B) probes across all the prefrontal cortex Douglas-Bell Canada Brain Bank samples	110
Figure 3.9. Example of bisulfite conversion plot	111
Figure 3.10. Example of a correlation plot for SNP probes for matched samples from two brain regions	112
Figure 3.11. Boxplots showing the β values distribution for each striatum samples from the Douglas-Bell Canada Brain Bank	115
Figure 3.12. Density plots showing the β values distribution for the striatum samples from the Douglas-Bell Canada Brain Bank	116
Figure 3.13. Neuronal proportion estimates calculated using the <i>CETS</i> package in R	118
Figure 3.14. Correlation between chronological age and neuronal proportion estimates	119
Figure 3.15. Example of a pyrogram of a successful pyrosequencing run assessing the DMR on the <i>RPH3AL</i> gene	124
Figure 3.16. Example of a pyrogram of a failed pyrosequencing run assessing the DMR on the <i>RPH3AL</i> gene	124
Figure 3.17. Overview of Chapter 3 experimental strategy	126

Figure 3.18. Correlation between chronological age and DNA methylation age	128
Figure 3.19. Correlation between chronological age and DNA methylation age separated by schizophrenia cases (red) and controls (black)	129
Figure 3.20. Quantile-quantile plot for the prefrontal cortex (PFC) case-control schizophrenia EWAS.....	132
Figure 3.21. Quantile-quantile plot for the striatum (STR) case-control schizophrenia EWAS.....	133
Figure 3.22. Quantile-quantile plot for the hippocampus (HC) case-control schizophrenia EWAS.....	133
Figure 3.23. Quantile-quantile plot for the cerebellum (CER) case-control schizophrenia EWAS.....	134
Figure 3.24. Manhattan plot for the prefrontal cortex (PFC) case-control schizophrenia EWAS.....	134
Figure 3.25. Manhattan plot for the striatum (STR) case-control schizophrenia EWAS.....	135
Figure 3.26. Manhattan plot for the hippocampus (HC) case-control schizophrenia EWAS.....	135
Figure 3.27. Manhattan plot for the cerebellum (CER) case-control schizophrenia EWAS.....	136
Figure 3.28. Heatmap showing the fifty top ranked schizophrenia-associated differently methylated positions in the prefrontal cortex (PFC)	145
Figure 3.29. Heatmap showing the fifty top ranked schizophrenia-associated differently methylated positions in the striatum (STR)	146
Figure 3.30. Heatmap showing the fifty top ranked schizophrenia-associated differently methylated positions in the hippocampus (HC).....	147
Figure 3.31. Heatmap showing the fifty top ranked schizophrenia-associated differently methylated positions in the cerebellum (CER)	148
Figure 3.32. Top ranked schizophrenia-associated differentially methylated positions (DMPs)	150
Figure 3.33. Correlation between DNA methylation differences for the fifty top ranked schizophrenia-associated probes identified in identified in the prefrontal cortex and the DNA methylation differences in the same probes in the remaining brain regions (y-axis)	151
Figure 3.34. Correlation between DNA methylation differences for the fifty top ranked schizophrenia-associated probes identified in identified in the striatum and the DNA methylation differences in the same probes in the remaining brain regions (y-axis).....	152

Figure 3.35. Correlation between DNA methylation differences for the fifty top ranked schizophrenia-associated probes identified in identified in the hippocampus and the DNA methylation differences in the same probes in the remaining brain regions (y-axis)	153
Figure 3.36. Correlation between DNA methylation differences for the fifty top ranked schizophrenia-associated probes identified in identified in the cerebellum and the DNA methylation differences in the same probes in the remaining brain regions (y-axis)	154
Figure 3.37. Schizophrenia-associated DNA methylation differences are robust to the addition of principal components (PC) capturing variation in DNA methylation data in the prefrontal cortex (PFC)	157
Figure 3.38. Schizophrenia-associated DNA methylation differences are robust to the addition of principal components (PC) capturing variation in DNA methylation data in the striatum (STR)	158
Figure 3.39. Schizophrenia-associated DNA methylation differences are robust to the addition of principal components (PC) capturing variation in DNA methylation data in the hippocampus (HC).....	159
Figure 3.40. Schizophrenia-associated DNA methylation differences are robust to the addition of principal components (PC) capturing variation in DNA methylation data in cerebellum (CER).....	160
Figure 3.41. Differentially methylated regions (DMRs) associated with schizophrenia	165
Figure 3.42. Validation of a schizophrenia-associated hypomethylated region within the <i>RPH3AL</i> gene in the prefrontal cortex (PFC)	171
Figure 3.43. Validation of a schizophrenia-associated hypomethylated region within the <i>RPH3AL</i> gene in the striatum (STR)	172
Figure 3.44. Manhattan plot showing the probes within 50 kilobases of the chr17:154410-154672 region in the prefrontal cortex.....	173
Figure 3.45. Manhattan plot showing the probes within 50 kilobases of the chr17:154410-154672 region in the striatum.....	173
Figure 3.46. Manhattan plot showing the probes within 50 kilobases of the chr17:154410-154672 region in the cerebellum	174
Figure 3.47. Probe cg15212418 shows dramatic DNA methylation (y-axis) changes associated with developmental age (x-axis) in fetal brain samples	174
Figure 3.48. Quantile-quantile plot for case-control schizophrenia EWAS	178
Figure 3.49. Manhattan plot for case-control schizophrenia EWAS	178
Figure 3.50. Heatmap showing the fifty top ranked schizophrenia-associated differentially methylated positions identified using a multi-region model incorporating prefrontal cortex (PFC), striatum (STR) and hippocampus (HC)	181

Figure 3.51. Heatmap showing differently methylated regions (DMRs) associated with schizophrenia identified using a multi-region model incorporating prefrontal cortex (PFC), striatum (STR) and hippocampus (HC)	185
Figure 4.1. Principal components (PC) 1 and 2 of genetic data for both the MRC London Neurodegenerative Diseases Brain Bank (LNDBB) and the Douglas-Bell Canada Brain Bank (DBCBB) cohorts	194
Figure 4.2. Principal component 2 of genetic data for both the MRC London Neurodegenerative Diseases Brain Bank (circle) and the Douglas-Bell Canada Brain Bank (triangle) vs respective polygenic risk scores (PRS)	195
Figure 4.3. Overview of Chapter 4 experimental strategy	202
Figure 4.4. Polygenic risk score in both schizophrenia cases and non-psychiatric controls included in the analyses of this chapter	203
Figure 4.5. Quantile-quantile plot for the prefrontal cortex (PFC) schizophrenia polygenic risk score EWAS	207
Figure 4.6. Quantile-quantile plot for the striatum (STR) schizophrenia polygenic risk score EWAS	207
Figure 4.7. Quantile-quantile plot for the hippocampus (HC) schizophrenia polygenic risk score EWAS	208
Figure 4.8. Quantile-quantile plot for the cerebellum (CER) schizophrenia polygenic risk score EWAS	208
Figure 4.9. Manhattan plot for the prefrontal cortex schizophrenia polygenic risk score EWAS	209
Figure 4.10. Manhattan plot for the striatum schizophrenia polygenic risk score EWAS	209
Figure 4.11. Manhattan plot for the hippocampus schizophrenia polygenic risk score EWAS	210
Figure 4.12. Manhattan plot for the cerebellum schizophrenia polygenic risk score EWAS	210
Figure 4.13. Top ranked schizophrenia polygenic risk score (PRS)-associated differentially methylated position (DMP) in the prefrontal cortex	212
Figure 4.14. Top ranked schizophrenia polygenic risk score (PRS)-associated differentially methylated positions (DMPs) in the striatum	212
Figure 4.15. Top ranked schizophrenia polygenic risk score (PRS)-associated differentially methylated positions (DMPs) in the cerebellum	213
Figure 4.16. Heatmap showing the fifty top ranked differentially methylated positions associated with schizophrenia polygenic risk score (PRS) in the prefrontal cortex (PFC)	222
Figure 4.17. Heatmap showing the fifty top ranked differentially methylated positions associated with schizophrenia polygenic risk score (PRS) in the striatum (STR)	223

Figure 4.18. Heatmap showing the fifty top ranked differently methylated positions associated with schizophrenia polygenic risk score (PRS) in the striatum (STR).....	224
Figure 4.19. Heatmap showing the fifty top ranked differently methylated positions associated with schizophrenia polygenic risk score (PRS) in the hippocampus (HC)	225
Figure 4.20. Correlation between DNA methylation differences for the fifty top ranked polygenic risk score (PRS)-associated probes identified in the prefrontal cortex and the DNA methylation differences in the same probes in the remaining brain regions (y-axis)	226
Figure 4.21. Correlation between DNA methylation differences for the fifty top ranked polygenic risk score (PRS)-associated probes identified in the striatum and the DNA methylation differences in the same probes in the remaining brain regions (y-axis).....	227
Figure 4.22. Correlation between DNA methylation differences for the fifty top ranked polygenic risk score (PRS)-associated probes identified in the hippocampus and the DNA methylation differences in the same probes in the remaining brain regions (y-axis)	228
Figure 4.23. Correlation between DNA methylation differences for the fifty top ranked polygenic risk score (PRS) associated probes identified in the cerebellum and the DNA methylation differences in the same probes in the remaining brain regions (y-axis)	229
Figure 4.24. Differentially methylated regions (DMRs) associated with schizophrenia polygenic risk score.....	236
Figure 4.25. Quantile-quantile plot for the schizophrenia polygenic risk score EWAS.....	239
Figure 4.26. Manhattan plot for the schizophrenia polygenic risk score EWAS	239
Figure 4.27. Examples of top ranked schizophrenia polygenic risk score-associated differentially methylated positions in the multilevel model including data from the prefrontal cortex (blue), striatum (green) and hippocampus (red).....	240
Figure 4.28. Heatmap showing the fifty top ranked differently methylated positions associated with schizophrenia polygenic risk score identified using a multi-region model incorporating prefrontal cortex (PFC), striatum (STR) and hippocampus (HC)	243
Figure 4.29. Heatmap showing differently methylated regions (DMRs) associated with schizophrenia polygenic risk score (PRS) identified using a multi-region model incorporating prefrontal cortex (PFC), striatum (STR) and hippocampus (HC)	246
Figure 4.30. Correlation between schizophrenia case-control EWAS and schizophrenia polygenic risk score EWAS for the prefrontal cortex	248
Figure 4.31. Correlation between schizophrenia case-control EWAS and schizophrenia polygenic risk score EWAS for the striatum.....	248

Figure 4.32. Correlation between schizophrenia case-control EWAS and schizophrenia polygenic risk score EWAS for the hippocampus	249
Figure 4.33. Correlation between schizophrenia case-control EWAS and schizophrenia polygenic risk score EWAS for the cerebellum.....	249
Figure 4.34. The relationship between lowest mQTL <i>P</i> -value and polygenic risk score (PRS) EWAS <i>P</i> -value for all DNA methylation probes associated (<i>P</i> < 1.00E-10) with genotype at a SNP incorporated in the schizophrenia PRS in prefrontal cortex (A), striatum (B) and cerebellum (C).....	255
Figure 5.1. Roadmap (A) and traffic patterns (B) of Boston, USA	262
Figure 5.2. Example of a correlation network	263
Figure 5.3. Overview of Weighted Gene Co-expression Network Analysis (WGCNA) methodology.....	265
Figure 5.4. Overview of Chapter 5 experimental strategy	268
Figure 5.5. Example of the analysis of network topology for various soft-thresholding power	271
Figure 5.6. Barplot showing the overlap between probes belonging to each module of the controls network and each module of the schizophrenia cases network in the prefrontal cortex	276
Figure 5.7. Barplot showing the overlap between 'hub probes' belonging to each module of the controls network and each module of the schizophrenia cases network in the prefrontal cortex	277
Figure 5.8. Heatmap showing the correlation coefficient between each prefrontal cortex module eigengene and different phenotypical traits	287
Figure 5.9. Heatmap showing the correlation coefficient between each striatum module eigengene and different phenotypical traits	288
Figure 5.10. Heatmap showing the correlation coefficient between each cerebellum module eigengene and different phenotypical traits.....	289
Figure 5.11. 'Brown' module of the prefrontal cortex (PFC) network (schizophrenia cases and non-psychiatric controls)	291
Figure 5.12. 'Black' module of the prefrontal cortex (PFC) network (schizophrenia cases and non-psychiatric controls)	292
Figure 5.13. Heatmap showing the correlation coefficient between each prefrontal cortex module eigengene and polygenic risk score and predicted ethnicity	315
Figure 5.14. Heatmap showing the correlation coefficient between each striatum module eigengene and polygenic risk score and predicted ethnicity.....	316
Figure 5.15. Heatmap showing the correlation coefficient between each cerebellum module eigengene and polygenic risk score and predicted ethnicity	317

Figure 6.1. Correlation between log ₂ of the observed and expected expression levels of the ERCC spike-in control transcripts.....	335
Figure 6.2. Example of plots produced by the <i>FastQ Screen</i> tool for the sample MS02 from the DBCBB	336
Figure 6.3. Example of plots produced by the <i>FastQ Screen</i> tool for the sample MS34 from the DBCBB	337
Figure 6.4. Example of a ‘per base sequence quality’ plot given by the <i>FastQC</i> software.....	339
Figure 6.5. Example of a ‘per sequence quality’ plot given by the <i>FastQC</i> software.....	340
Figure 6.6. Example of a ‘per base sequence content’ plot given by the <i>FastQC</i> software.....	341
Figure 6.7. Example of a ‘per base CG content’ plot given by the <i>FastQC</i> software.....	342
Figure 6.8. Example of a ‘per sequence GC content’ plot given by the <i>FastQC</i> software.....	343
Figure 6.9. Example of a ‘sequence duplication levels’ plot given by the <i>FastQC</i> software.....	344
Figure 6.10. Example of a ‘per base sequence quality’ plot given by the <i>FastQC</i> software before (A) and after (B) using <i>Trimmomatic</i>	346
Figure 6.11. Example of a ‘per base sequence content’ plot given by the <i>FastQC</i> software before (A) and after (B) using <i>Trimmomatic</i>	347
Figure 6.12. Example of a ‘per base CG content’ plot given by the <i>FastQC</i> software before (A) and after (B) using <i>Trimmomatic</i>	348
Figure 6.13. Principal component 1 (x-axis) versus principal component 2 (y-axis) of the raw gene counts.....	352
Figure 6.14. Example of multidimensional scaling plots for all samples included in the analyses of this chapter	353
Figure 6.15. Example of multidimensional scaling plots for all samples included in the analyses of this chapter	353
Figure 6.16. Log ₂ distribution of the raw gene counts (counts per million) estimated by <i>RSEM</i>	357
Figure 6.17. Log ₂ distribution of the raw gene counts (counts per million) estimated by <i>RSEM</i> (Li and Dewey, 2011) after excluding ERCC transcripts, genes on the sex chromosomes, incorrect assembly sequences, allelic variants and low expressed genes.....	357
Figure 6.18. Log ₂ distribution of the gene counts (counts per million) estimated by <i>RSEM</i> (Li and Dewey, 2011) after normalisation with <i>edgeR</i> (Robinson et al., 2010)	358
Figure 6.19. Overview of Chapter 6 experimental strategy	360

Figure 6.20. Quantile-quantile plot for the differential expression analysis.....	361
Figure 6.21. Volcano plot for the differential expression analysis.....	363
Figure 6.22. Log ₂ fold-change (FC) (y-axis) of the fifty top ranked differentially expressed genes in the prefrontal cortex	366
Figure 6.23. Counts per million (CPM) (y-axis) of the top ranked differentially expressed genes in the prefrontal cortex with less than 25 CPM	367
Figure 6.24. Counts per million (CPM) (y-axis) of the top ranked differentially expressed genes in the prefrontal cortex with more than 25 CPM	368
Figure 6.25. Methodological approach to investigate DNA methylation probes overlapping differentially expressed genes in schizophrenia.....	371
Figure. 6.26. Methodological approach to investigate expressed genes overlapping schizophrenia-associated differentially methylated regions (DMRs) (A) and top ranked differentially methylated positions (DMPs) in the PFC (B)	378
Chapter 7 - Figure 1. Reduced cerebellar mass in a 47,XXY patient comorbid for schizophrenia. Shown is the average cerebellar mass (in grams) across all samples compared with the cerebellar mass of the 47,XXY patient.....	388
Chapter 7 - Figure 2. Tissue-specific differences in global DNA methylation in a 47,XXY patient comorbid for schizophrenia	389
Appendix B - Figure S1. Multi-dimensional scaling plot of DNA methylation probes on the X-chromosome (A) and Y-chromosome (B)	494
Appendix B - Figure S2. Plot of <i>XIST</i> gene expression (A) and mean Y-chromosome gene expression (B)	495
Appendix B - Figure S3. Visualization of X-chromosome and Y-chromosome probe intensities for 47 prefrontal cortex samples run on the Illumina HumanOmniExpress BeadChip.....	496
Appendix B - Figure S4. Comparison of SNP probe intensities and allele frequencies between 47,XXY and a schizophrenia 46,XY patient.....	497
Appendix B - Figure S5. PCR-based sex-typing confirms the presence of the Y-chromosome in the 47,XXY patient	498
Appendix B - Figure S6. Comparison of cerebellum mass (g) between the 47,XXY patient, females and males	499
Appendix B - Figure S7. Comparison of global DNA methylation levels between the 47,XXY patient, females and males	500
Appendix B - Figure S8. Visualization of gene expression differences at the Eukaryotic Translation Initiation Factor 1AX (<i>EIF1AX</i>) gene	501

Table of Tables

Table 1.1. Changes in schizophrenia diagnostic criteria from DSM-IV to DSM-5	35
Table 1.2. Glossary of key epigenetic terms.....	42
Table 1.3. Summary of published DNA methylation studies on schizophrenia using post-mortem brain samples	55
Table 1.4. Summary of published DNA methylation studies on schizophrenia using peripheral tissues.....	58
Table 1.5. Summary of the most recently published transcriptomic studies on schizophrenia	61
Table 2.1. Nucleic acid extraction methods used in this thesis.....	67
Table 2.2. Polymerase chain reaction (PCR) reagents and quantities used in this thesis	84
Table 2.3. Standard polymerase chain reaction thermocycling conditions	84
Table 3.1. Tissue prediction for the cerebellum samples in this study using the DNA methylation age calculator	107
Table 3.2. Total number of probe included in the analyses after data normalisation and quality control	103
Table 3.3. Overview of samples included in the schizophrenia case versus control analysis.....	114
Table 3.4. Primers and assay conditions for the bisulfite-polymerase chain reaction pyrosequencing assay targeting the chr17:154410-154672 schizophrenia-associated differentially methylated region in the <i>RPH3AL</i> gene.....	123
Table 3.5. Top ranked schizophrenia-associated differentially methylated probes (DMPs) identified in the prefrontal cortex (PFC) meta-analysis.....	137
Table 3.6. Top ranked schizophrenia-associated differentially methylated probes (DMPs) identified in the striatum (STR) meta-analysis.....	139
Table 3.7. Top ranked schizophrenia-associated differentially methylated probes (DMPs) identified in the hippocampus (HC) linear regression analysis	141
Table 3.8. Top ranked schizophrenia-associated differentially methylated probes (DMPs) identified in the cerebellum (CER) meta-analysis.....	143
Table 3.9. Top ranked schizophrenia-associated differentially methylated positions (DMPs)	149
Table 3.11. Results of the Fisher's 2x2 exact tests for significant overlap between schizophrenia-associated differentially methylated positions (DMPs) in the prefrontal cortex and regulatory features.....	162
Table 3.12. Results of the Fisher's 2x2 exact tests for significant overlap between schizophrenia-associated differentially methylated positions (DMPs) in the striatum and regulatory features.....	162

Table 3.13. Results of the Fisher's 2x2 exact tests for significant overlap between schizophrenia-associated differently methylated positions (DMPs) in the hippocampus and regulatory features	162
Table 3.14. Results of the Fisher's 2x2 exact tests for significant overlap between schizophrenia-associated differently methylated positions (DMPs) in the cerebellum and regulatory features	163
Table 3.15. Results of the Fisher's 2x2 exact tests for significant overlap between schizophrenia-associated differently methylated positions (DMPs) in all the brain regions and GWAS regions	164
Table 3.16. Significant schizophrenia-associated differentially methylated regions (DMRs)	167
Table 3.17. Bisulfite-polymerase chain reaction-pyrosequencing validation across the DMR in the <i>RPH3AL</i> gene in both prefrontal cortex and striatum .	175
Table 3.18. Top ranked schizophrenia-associated differently methylated probes (DMPs) identified in the multiregion model incorporating the prefrontal cortex (PFC), striatum (STR) and hippocampus (HC) data	179
Table 3.19. Results for top ranked schizophrenia-associated probes identified in a previous study of cortical tissue.....	182
Table 3.20. Significant schizophrenia-associated differentially methylated regions (DMRs) identified in the multilevel model incorporating the prefrontal cortex, striatum and hippocampus data	183
Table 4.1. Table showing the brain region of origin of the DNA samples genotyped in the present chapter	192
Table 4.2. Overview of samples included in the schizophrenia polygenic risk score analysis.....	197
Table 4.3. Top ranked schizophrenia polygenic risk score (PRS)-associated differentially methylated positions (DMPs)	211
Table 4.4. Top ranked polygenic risk score-associated DMPs identified in the prefrontal cortex (PFC) meta-analysis	214
Table 4.5. Top ranked polygenic risk score-associated differentially methylated probes (DMPs) identified in the striatum (STR) meta-analysis	216
Table 4.6. Top ranked polygenic risk score-associated differentially methylated probes (DMPs) identified in the hippocampus (HC) linear regression	218
Table 4.7. Top ranked polygenic risk score-associated differentially methylated probes (DMPs) identified in the cerebellum (CER) meta-analysis.....	220
Table 4.8. Correlation between DNA methylation differences for the fifty top ranked polygenic risk score schizophrenia-associated probes identified in each brain region and the DNA methylation differences in the same probes in the remaining brain regions.....	230
Table 4.9. Results of the Fisher's 2x2 exact tests for significant overlap between polygenic risk score-associated differentially methylated positions (DMPs) in the prefrontal cortex and regulatory features.....	231

Table 4.10. Results of the Fisher's 2x2 exact tests for significant overlap between polygenic risk score-associated differently methylated positions (DMPs) in the striatum and regulatory features	232
Table 4.11. Results of the Fisher's 2x2 exact tests for significant overlap between polygenic risk score-associated differently methylated positions (DMPs) in the hippocampus and regulatory features	232
Table 4.12. Results of the Fisher's 2x2 exact tests for significant overlap between polygenic risk score-associated differently methylated positions (DMPs) in the cerebellum and regulatory features	232
Table 4.13. Differentially methylated regions (DMRs) significantly associated with polygenic score for schizophrenia.....	234
Table 4.14. Top ranked polygenic risk score-associated differently methylated probes (DMPs) identified in the multiregion model incorporating the prefrontal cortex (PFC), striatum (STR) and hippocampus (HC) data	241
Table 4.15. Significant polygenic risk score-associated differently methylated regions (DMRs) identified in the multilevel model incorporating the prefrontal cortex, striatum and hippocampus data.....	244
Table 4.16. Polygenic risk score (PRS)-associated DMPs located within schizophrenia-associated regions from the largest schizophrenia GWAS to date	251
Table 4.17. Results of the Fisher's 2x2 exact tests for significant overlap between polygenic risk score-associated differently methylated positions (DMPs) in all the brain regions and GWAS regions.....	254
Table 5.1. Glossary of weighted gene co-methylation analysis terminology ..	266
Table 5.2. Modules identified in the network using prefrontal cortex data from the non-psychiatric controls of the MRC London Neurodegenerative Diseases Brain Bank and Douglas-Bell Canada Brain Bank.....	273
Table 5.3. Modules identified in the network using prefrontal cortex data from the schizophrenia cases of the MRC London Neurodegenerative Diseases Brain Bank and Douglas-Bell Canada Brain Bank.....	274
Table 5.4. Modules identified in the network using prefrontal cortex data from both non-psychiatric cases and schizophrenia controls from the MRC London Neurodegenerative Diseases Brain Bank and Douglas-Bell Canada Brain Bank	281
Table 5.5. Modules identified in the network using striatum data from both non-psychiatric cases and schizophrenia controls from the MRC London Neurodegenerative Diseases Brain Bank and Douglas-Bell Canada Brain Bank	283
Table 5.6. Modules identified in the network using cerebellum data from both non-psychiatric cases and schizophrenia controls from the MRC London Neurodegenerative Diseases Brain Bank and Douglas-Bell Canada Brain Bank	285

Table 5.7. List of ‘hub probes’ (module membership > 0.80) from the prefrontal cortex modules ‘brown’, ‘black’, ‘tan’, ‘salmon’ and ‘darkgrey’	294
Table 5.8. Genes annotated to ‘hub probes’ of schizophrenia-associated modules that have an interaction with a hypothesised schizophrenia gene ...	297
Table 5.9. Association between modules identified in the prefrontal cortex and schizophrenia in the striatum (STR), hippocampus (HC) and cerebellum (CER)	298
Table 5.10. Pathway analysis in the prefrontal cortex ‘brown’ module using data from schizophrenia cases and controls	300
Table 5.11. Pathway analysis in the prefrontal cortex ‘black’ module using data from schizophrenia cases and controls	302
Table 5.12. Pathway analysis in the prefrontal cortex ‘tan’ module using data from schizophrenia cases and controls	304
Table 5.13. Pathway analysis in the prefrontal cortex ‘salmon’ module using data from schizophrenia cases and controls	306
Table 5.14. Pathway analysis in the prefrontal cortex ‘darkgrey’ module using data from schizophrenia cases and controls	309
Table 5.15. Modules identified in the network using prefrontal cortex data from Caucasian non-psychiatric cases and schizophrenia controls from the MRC London Neurodegenerative Diseases Brain Bank and Douglas-Bell Canada Brain Bank.....	312
Table 5.16. Modules identified in the network using striatum data from Caucasian non-psychiatric cases and schizophrenia controls from the MRC London Neurodegenerative Diseases Brain Bank and Douglas-Bell Canada Brain Bank.....	312
Table 5.17. Modules identified in the network using cerebellum data from Caucasian non-psychiatric cases and schizophrenia controls from the MRC London Neurodegenerative Diseases Brain Bank and Douglas-Bell Canada Brain Bank.....	314
Table 5.18. Association of the fetal brain modules with schizophrenia in the adult brain data.....	319
Table 6.1. Key RNA sequencing terms used in this Chapter.....	325
Table 6.2. RNA quantity and integrity information of the all the RNA samples extracted before and after the clean-up procedure.....	326
Table 6.3. Details of the complementary DNA (cDNA) libraries prepared	330
Table 6.4. Number of raw, trimmed and mapped reads for each sequenced library	333
Table 6.5. Criteria for sample exclusion or inclusion in the analyses performed in this chapter	354
Table 6.6. Demographic information on the final set of samples included in the analyses performed in this chapter.....	355

Table 6.7. Top ranked schizophrenia-associated differently expressed genes identified in the prefrontal cortex	362
Table 6.8. 450K array probes nominally associated with schizophrenia in the prefrontal cortex which are annotated to the differentially expressed genes using the Illumina gene annotation.....	372
Table 6.9. 450K array probes nominally associated with schizophrenia in the prefrontal cortex which the closest annotated transcription start site is one of the schizophrenia-associated differentially expressed genes.....	375
Table 6.10. 450K array probes nominally associated with schizophrenia in the prefrontal cortex that are annotated to the differentially expressed genes using the GREAT gene annotation	376
Table 6.11. Results of the schizophrenia differential expression analysis for the expressed genes annotated to the differentially methylated regions (DMRs) identified in Chapter 3	379
Table 6.12. Results of the schizophrenia differential expression analysis for the expressed genes annotated to the differentially methylated probes identified in the prefrontal cortex (Chapter 3)	380
Chapter 7 - Table 1. 47,XXY-associated differentially methylated regions in the prefrontal cortex	390
Chapter 7 - Table 2. 47,XXY-associated differentially methylated regions in the cerebellum.....	392
Chapter 7 - Table 3. 47,XXY-associated differentially expressed genes in the prefrontal cortex	393
Chapter 7 - Table 4. 47,XXY-associated differentially expressed genes in the cerebellum.....	395
Table 8.1. Key genes implicated in the studies presented in my thesis.....	408
Appendix A - Supplementary Table 1. Demographic data of all samples used in this thesis	415
Appendix A - Supplementary Table 2. Sentrix barcode ID information for all samples included in this thesis	418
Appendix A - Supplementary Table 3. Tissue prediction results for all samples included in Chapter 3 part 1	423
Appendix A - Supplementary Table 4. Tissue prediction results for all samples included in Chapter 3 part 2	431
Appendix A - Supplementary Table 5. Tissue prediction results for all samples included in Chapter 3 part 3	441
Appendix A - Supplementary Table 6. Methylation QTLs (mQTL) identified in the prefrontal cortex for SNPs included in the schizophrenia polygenic risk score (PRS)	451
Appendix A - Supplementary Table 7. Methylation QTLs (mQTL) identified in the striatum for SNPs included in the schizophrenia polygenic risk score (PRS).....	456

Appendix A - Supplementary Table 8. Methylation QTLs (mQTL) identified in the cerebellum for SNPs included in the schizophrenia polygenic risk score (PRS)	460
Appendix A - Supplementary Table 9. Overlap of probes assigned to each pair of schizophrenia cases and non-psychiatric controls modules	465
Appendix A - Supplementary Table 10. Percentage of probes in each of the non-psychiatric controls modules overlapping with each of the schizophrenia cases modules (1 to 27)	468
Appendix A - Supplementary Table 11. Percentage of probes in each of the non-psychiatric controls modules overlapping with each of the schizophrenia cases modules (28 to 54)	471
Appendix A - Supplementary Table 12. <i>P</i> -values of the hypergeometric test between pairs of non-psychiatric controls and schizophrenia (1 to 27) modules	474
Appendix A - Supplementary Table 13. <i>P</i> -values of the hypergeometric test between pairs of non-psychiatric controls and schizophrenia (28 to 54) modules	477
Appendix A - Supplementary Table 14. <i>P</i> -values of the Fisher's exact test between pairs of non-psychiatric controls and schizophrenia (1 to 27) modules	481
Appendix A - Supplementary Table 15. <i>P</i> -values of the Fisher's exact test between pairs of non-psychiatric controls and schizophrenia (28 to 54) modules	485
Appendix B - Table S1. Autosomal CNVs detected in the 47,XXY sample	502
Appendix B - Table S2. Rank of the 47,XXY patient against other samples for transcription of probes associated with <i>loci</i> believed to escape X-chromosome inactivation	503
Appendix B - Table S3. Rank of the 47,XXY patient against other samples for transcription of probes associated with <i>loci</i> residing in pseudoautosomal regions (<i>PAR</i>) 1 and 2.....	504
Appendix B - Table S4. Demographic and sample information for all samples included in this study	505

Publications Arising from this Thesis

Chapters 3 and 4 (accepted manuscript presented on **Appendix C**):

Viana J, Hannon E, Dempster E, Pidsley R, Macdonald R, Knox O, Spiers H, Troakes C, Al-Saraj S, Turecki G, Schalkwyk LC, Mill J. (In Press) Schizophrenia-associated methylomic variation: molecular signatures of disease and polygenic risk burden across multiple brain regions. *Human Molecular Genetics*.

The data generated in **Chapter 3** were also included for different analyses or as replication datasets on the following publications (articles presented on **Appendix C**):

Pidsley R, **Viana J**, Hannon E, Spiers H, Troakes C, Al-Sarraj S, Mechawar N, Turecki G, Schalkwyk L, Bray N, Mill J. (2014) Methylomic profiling of human brain tissue supports a neurodevelopmental origin for schizophrenia. *Genome Biology* 15(10):483.

Fisher HL*, Murphy TM*, Arseneault L, Caspi A, Moffitt TE, **Viana J**, Hannon E, Pidsley R, Burrage J, Dempster EL, Wong CC, Pariante CM, and Mill J. (2015) Methylomic Analysis of Monozygotic Twins Discordant for Childhood Psychotic Symptoms. *Epigenetics* 10(11):1014-23.

Hannon E, Spiers H, **Viana J**, Pidsley R, Burrage J, Murphy T, Troakes C, Turecki G, O'Donovan MC, Schalkwyk L, Bray N, Mill J. (2016) Methylation QTLs in the developing brain and their enrichment in schizophrenia risk *loci*. *Nature Neuroscience* 19:48–54.

Chapter 7:

Viana J*, Pidsley R*, Troakes C, Spiers H, Wong CCY, Al-Sarraj S, Craig I, Schalkwyk L, Mill J. (2014) Epigenomic and Transcriptomic Signatures of a Klinefelter's Syndrome (47,XXY) Karyotype in the Brain. *Epigenetics* 9(4):587-99.

During the course of my PhD I also co-authored other publications:

Hannon E, Dempster E, **Viana J**, Burrage J, Smith AR, Macdonald R, St Clair D, Mustard C, Breen G, Therman S, Kaprio J, Toulopoulou T, Hulshoff Pol HE, Bohlken MM, Kahn RS, Nenadic I, Hultman CM, Murray RM, Collier DA, Bass N, Gurling H, McQuillin A, Schalkwyk L, Mill J. (2016) An integrated genetic-epigenetic analysis of schizophrenia: evidence for co-localization of genetic associations and differential DNA methylation. *Genome Biology* 17(1):176.

Kumsta R*, Marzi S*, **Viana J**, Rutter M, Sonuga-Barke R and Mill J. (2016) Severe psychosocial deprivation in early childhood is associated with hypermethylation across a region of the CYP2E1 gene. *Translational Psychiatry* 6: e830.

Laing LV, **Viana J**, Dempster E, Trznadel M, Trunkfield L, Uren Webster TM, van Aerle R, Paull GC, Wilson R, Mill J and Santos EM. (2016) Bisphenol A causes reproductive toxicity and changes in epigenetic signalling pathways in mature zebrafish. *Epigenetics* 11(7):526-38.

*These authors contributed equally to the work.

Declarations

The samples used in **Chapter 3** were obtained from the Medical Research Council (MRC) London Neurodegenerative Diseases Brain Bank (LNDBB), at the Institute of Psychiatry, Psychology & Neuroscience, King's College London (courtesy of Dr Claire Troakes and Dr Safa Al-Sarraj), the Douglas-Bell Canada Brain Bank (DBCBB), Canada (courtesy of Dr Naguib Mechawar and Dr Gustavo Turecki), and the Edinburgh Brain and Tissue Banks (EBTB), at the University of Edinburgh (courtesy of Chris-Anne McKenzie). The samples used in **Chapter 4, 5** and **6** were obtained from the LNDBB and the DBCBB. The samples used in **Chapter 7** were obtained from the LNDBB.

All laboratory work was conducted by me at the University of Exeter Medical School laboratories with the exception of the following:

- DNA isolation and DNA methylation array and genotyping array processing of the prefrontal cortex and cerebellum samples from the LNDBB presented in **Chapters 3, 4, 5, 6** and **7**, which was carried out by Dr Ruth Pidsley as part of our initial study of DNA methylation changes in schizophrenia (Pidsley et al., 2014).
- Assistance for the PCR-pyrosequencing validation of DNA methylation changes in the chr17:154410-154672 region (**Chapter 3 section 3.3.6.1**) in the striatum samples was given by Ruby Macdonald, a placement student in our laboratory, with further assistance from Dr Emma Dempster.
- The complementary DNA libraries used in **Chapter 6** were prepared by me in collaboration with Audrey Farbos at the University of Exeter Sequencing Service.
- Illumina RNA sequencing of my libraries in **Chapter 6** was carried out by Audrey Farbos and Dr Karen Moore at the University of Exeter Sequencing Service.

The bioinformatics and statistical analyses were performed by me with exception of the following:

- The RNA sequencing data demultiplexing, contamination check and spike-in internal controls quality check (**Chapter 6**) were carried out by Dr Konrad Paszkiewicz at the University of Exeter Sequencing Service
- The polygenic risk scores calculation, ethnicity prediction and methylation quantitative trait *loci* analyses presented in **Chapter 4** were carried out with help from Dr Eilís Hannon.
- The multiple testing threshold used in **Chapters 3** and **4** was calculated by Dr Eilís Hannon.

Chapter 7 is presented in form of a peer-reviewed publication (Viana et al., 2014). First authorship of this publication is shared between me and Dr Ruth Pidsley and we both contributed equally to this work. **Appendix B** presents the supplementary material of **Chapter 7**.

List of Abbreviations

Abbreviation	Term
5caC	5-carboxylcytosine
5fC	5-formylcytosine
5hmC	5-hydroxymethylcytosine
5hmU	5-hydroxymethyluracil
ADHD	Attention-deficit/hyperactivity disorder
AID	Activation-induced deaminase
APS	Adenosine 5' phosphosulphate
ASD	Autism-spectrum disorder
BA	Brodman area
BER	Base-excision repair
bp	Base pairs
cAMP	Cyclic adenosine monophosphate
cDNA	complementary deoxyribonucleic acid
CER	Cerebellum
<i>CETS</i>	Cell epigenotype specific
chr	Chromosome
CpG	Cytosine-guanine dinucleotide
CPM	Counts per million
CTR	Controls
DBCBB	Douglas-Bell Canada Brain Bank
DE	differentially expressed
DHS(s)	DNase1 hypersensitivity site(s)
DMP(s)	differentially methylated probe(s)
DMR(s)	differentially methylated region(s)
DNA	Deoxyribonucleic acid
DNMT(s)	DNA methyltransferase(s)
DSM	Diagnostic and Statistical Manual of Mental Disorders
EBTB	Edinburgh Brain and Tissue Banks
EDTA	Ethylenediamine tetraacetic acid
eQTL	Expression quantitative trait <i>loci</i>
ERCC	External RNA Controls Consortium

EWAS	Epigenome-wide association studies
FC	Fold-change
FDR	False discovery rate
FGA(s)	First generation antipsychotic(s)
FPKM	Fragments per kilobase of transcript per million mapped reads
GLM	Generalised linear model
GO	Gene ontology
GREAT	Genomic regions enrichment of annotations tool
GWAS	Genome-wide association studies
HC	Hippocampus
HDCA(s)	Histone deacetylase(s)
HGNC	HUGO Gene Nomenclature Committee
HLA	Human leukocyte antigen
KS	Klinefelter syndrome
LD	Linkage disequilibrium
lncRNA	Long non-coding ribonucleic acid
LNDBB	MRC London Neurodegenerative Diseases Brain Bank
LREC	Local Research Ethics Committee
M	Methylated
MDS	Multidimensional scaling
ME	Module eigengene
MECP2	Methyl-CpG binding protein 2
MHC	Major histocompatibility complex
mirRNA	Micro ribonucleic acid
MM	Module membership
mQTL	Methylation quantitative trait <i>loci</i>
MRC	Medical Research Council
mRNA	Messenger ribonucleic acid
ncRNA	Non-coding ribonucleic acid
NGS	Next generation sequencing
NHI	National Institutes of Health
OECD	Organisation for Economic Co-operation and Development
OR	Odds ratio
PC	Principal component

PCR	Polymerase chain reaction
PFC	Prefrontal cortex
piRNA	Piwi-interacting ribonucleic acid
PPI	Protein-protein interactions
PPi	Pyrophosphate molecules
PRS	Polygenic risk score(s)
QC	Quality control
qPCR	Quantitative polymerase chain reaction
QQ	Quantile-quantile
RIN	Ribonucleic acid integrity number
RNA	Ribonucleic acid
RNA-seq	RNA sequencing
rRNA	Ribosomal ribonucleic acid
SAM	S-adenosylmethionine
SBS	Sequencing-by-synthesis
SCID I	Structured Clinical Interviews for DSM Disorders I
SGA(s)	Second generation antipsychotic(s)
siRNA	Small interfering ribonucleic acid
SMRT	Single-molecule real-time
snoRNA	Small nucleolar ribonucleic acid
SNP	Single nucleotide polymorphism
snRNA	Small nuclear ribonucleic acid
STR	Striatum
TDG	Thymine DNA glycosylase
TET	Ten-eleven translocation
TFBS(s)	Transcription factor binding site(s)
tRNA	Transporter ribonucleic acid
U	Unmethylated
WGCNA	Weighted-gene co-methylation analysis
XCI	X-chromosome inactivation

Chapter 1 - General Introduction

1.1. Schizophrenia

1.1.1. Clinical manifestation

Schizophrenia is a severe psychiatric disorder with neurodevelopmental origins that affects more than twenty-one million people worldwide, and contributes significantly to the global burden of disease (World Health Organization, 2013, World Health Organization, 2015). Schizophrenia onset occurs typically during adolescence or early adulthood, generally later in females than males (Hafner et al., 1994). Incidence rates are higher in males compared to females with a relative risk of approximately 1.4 (Aleman et al., 2003, McGrath et al., 2008).

The term schizophrenia was first used in 1908 by the Swiss psychiatrist Eugen Bleuler and over the last century the diagnostic criteria for schizophrenia has been the subject of considerable debate. The disorder is primarily defined by both 'positive' symptoms, such as hallucinations, delusions and interference with thought processes, and 'negative' symptoms, such as dysfunctional affective responses including apathy, lack of drive and social isolation, and altered cognition (Burmeister et al., 2008). Positive symptoms refer to symptoms present in affected individuals and absent in unaffected individuals, whereas negative symptoms are features absent in affected individuals and present in unaffected individuals. The wide range of symptoms means that multiple different clinical presentations are possible, with two schizophrenia patients potentially having few diagnosed symptoms in common.

This heterogeneity has led to multiple attempts to identify diagnostic subtypes within schizophrenia, not only to improve understanding of its aetiology and pathophysiology, but also improve therapy for these patients (Kendell, 1987). Despite these attempts to refine diagnosis, schizophrenia remains a broad clinical syndrome defined by reported subjective experiences (symptoms), loss of function (behavioural impairments) and variable patterns of course (Jablensky, 2010). Until 2013, according to the Diagnostic and Statistical Manual of Mental Disorders (DSM) IV, (American Psychiatric Association, 1994), schizophrenia was categorised into five different subtypes: paranoid, disorganised, catatonic, undifferentiated and residual type. In 2013, however,

these subtypes were eliminated from the updated DSM-5 (American Psychiatric Association, 2013) because they provided a poor description of the heterogeneity of schizophrenia, had low diagnostic stability, did not exhibit distinctive patterns of treatment response or longitudinal course, and were not heritable (Tandon et al., 2013). **Table 1.1** - taken from Tandon et al. (2013) - describes the updates in schizophrenia diagnostic criteria from DSM-IV (American Psychiatric Association, 1994) to DSM-5 (American Psychiatric Association, 2013). Despite these changes the core of diagnostic criteria in the latest DSM was maintained; schizophrenia remains within the schizophrenia disorders spectrum, which includes schizophreniform disorder, schizoaffective disorder and delusional disorder.

1.1.2. Neuropathology of schizophrenia

In this thesis my research focuses primarily on molecular alterations in the prefrontal cortex (PFC), striatum (STR), hippocampus (HC) and cerebellum (CER) in the context of schizophrenia. **Figures 3.1. to 3.4** in **Chapter 3** show the location of each of the regions in the human brain. Next I give an overview of the function of each brain region and their involvement in schizophrenia:

- The PFC is located in the anterior part of the frontal lobe (**Chapter 3 Figure 3.1**). It coordinates a broad range of functions including attention and the planning of motor and behavioural responses to internal and external stimuli, working with other brain regions to play a role in learning and memory and working memory (Tamminga and Buchsbaum, 2004). Decades of clinical, neuropathological, functional and brain connectivity research implicate it as one of the primary brain regions affected in schizophrenia (Shenton et al., 2001).
- The STR is composed by a group of contiguous subcortical structures located in the forebrain: the caudate, putamen and nucleus accumbens, and is part of the basal ganglia (**Chapter 3 Figure 3.2**). The basal ganglia are best known by their role in facilitating voluntary movement. The STR is one of the main components of the basal ganglia; it is connected and receives input from the cerebral cortex. It is therefore thought to be involved in several cortical functions, including cognition, motor and action planning, decision-making, motivation, reinforcement, and reward perception (Balleine et al., 2007). Although this structure has received much less attention than the PFC in the

context of schizophrenia, emerging evidence suggests that the STR might be involved in generating the cognitive symptoms observed in the disease. For an overview of the function of the STR and its possible involvement in schizophrenia see Simpson et al. (2010).

- The HC is located in the medial temporal lobe, under the cerebral cortex (**Chapter 3 Figure 3.3**). It is part of the limbic system and is involved in spatial navigation and the consolidation of information from short-term memory to long-term memory. The observation that schizophrenia patients can experience episodic memory loss (Ranganath et al., 2008) led to the suggestion that the HC could be involved in the disorder. Several neuroimaging, behavioural and molecular studies have implicated hippocampal dysfunction in schizophrenia (Heckers, 2001, Preston et al., 2005, Lodge and Grace, 2008, Tamminga et al., 2010).

- The CER is located in the hindbrain (**Chapter 3 Figure 3.4**). Its primary function is to coordinate motor activity; however mounting evidence suggests that the CER also plays a role in cognition (Rapoport et al., 2000). This concurs with evidence showing that cerebellar dysfunction is important in schizophrenia and neuropathological studies showing that patients with schizophrenia have cerebellar abnormalities, including a decrease in the density and size of Purkinje cells. For a detailed overview of the role of the CER in schizophrenia see the review by Andreasen and Pierson (2008).

Table 1.1. Changes in schizophrenia diagnostic criteria from DSM-IV to DSM-5. Table taken from Tandon et al. (2013).

DSM-IV criteria for schizophrenia	Proposed criteria for schizophrenia in DSM-5
<p>Criterion A. Characteristic symptoms Two (or more) of the following, each present for a significant portion of time during a 1-month period (or less if successfully treated)</p> <ol style="list-style-type: none"> (1) Delusions (2) Hallucinations (3) Disorganized speech (4) Grossly disorganized or catatonic behavior (5) Negative symptoms, i.e., affective flattening, alogia, or avolition <p>Note: Only one Criterion A symptom is required if delusions are bizarre or hallucinations consist of a voice keeping up a running commentary on the person's behavior or thoughts, or two or more voices conversing with each other</p>	<p>Criterion A. Characteristic symptoms: (Minor change) Two (or more) of the following, each present for a significant portion of time during a 1-month period (or less if successfully treated). At least one of these should include 1–3</p> <ol style="list-style-type: none"> 1. Delusions 2. Hallucinations 3. Disorganized speech 4. Grossly disorganized or catatonic behavior 5. Negative symptoms (i.e., diminished emotional expression or avolition) <p>Note: Deleted</p>
<p>Criterion B. Social/occupational dysfunction: For a significant portion of the time since the onset of the disturbance, one or more major areas of functioning, such as work, interpersonal relations, or self-care, are markedly below the level achieved prior to the onset (or when the onset is in childhood or adolescence, failure to achieve expected level of interpersonal, academic, or occupational achievement).</p>	<p>Criterion B. Social/occupational dysfunction (No change)</p>
<p>Criterion C. Duration: Continuous signs of the disturbance persist for at least 6 months. This 6-month period must include at least 1 month of symptoms (or less if successfully treated) that meet Criterion A (i.e., active-phase symptoms) and may include periods of prodromal or residual symptoms. During these prodromal or residual periods, the signs of the disturbance may be manifested by only negative symptoms or by two or more symptoms listed in Criterion A present in an attenuated form (e.g., odd beliefs, unusual perceptual experiences).</p>	<p>Criterion C. Duration of 6 months (No change)</p>
<p>Criterion D. Schizoaffective and major mood disorder exclusion Schizoaffective disorder and depressive or bipolar disorder with psychotic features have been ruled out because either (1) no major depressive or manic episodes have occurred concurrently with the active phase symptoms; or (2) if mood episodes have occurred during active-phase symptoms, their total duration has been brief relative to the duration of the active and residual periods.</p>	<p>Criterion D. Schizoaffective and mood disorder exclusion No change</p>
<p>Criterion E. Substance/general mood condition exclusion Substance/general medical condition exclusion: The disturbance is not attributed to the direct physiological effects of a substance (e.g., a drug of abuse, a medication) or another medical condition.</p>	<p>Criterion E. Substance/general mood condition exclusion No change</p>
<p>Criterion F. Relationship to Global Developmental Delay or Autism Spectrum Disorder: If there is a history of autism spectrum disorder, the additional diagnosis of schizophrenia is made only if prominent delusions or hallucinations are also present for at least 1 month (or less if successfully treated).</p>	<p>Criterion F. Relationship to Global Developmental Delay or Autism Spectrum Disorder — Minor Change If there is a history of autism spectrum disorder or other communication disorder of childhood onset, the additional diagnosis of schizophrenia is made only if prominent delusions or hallucinations are also present for at least 1 month (or less if successfully treated).</p>

1.1.3. Genetics of schizophrenia

1.1.3.1. Heritability and evidence from twin studies

Twin and family studies have highlighted a notable heritable component to schizophrenia, currently estimated at ~85% (Craddock et al., 2005). Concordance rates for diagnosed schizophrenia in monozygotic twins have been shown to be consistently higher (~50%) than in dizygotic twins (~17%), and adoption studies have provided further evidence that relatives of schizophrenia patients have an increased risk of developing the disorder (Riley and Kendler, 2006).

1.1.3.2. Rare and *de novo* mutations

Although schizophrenia genetic susceptibility is believed to be predominantly due to a polygenic burden of common genetic variants (see **section 1.1.3.3**), rare but highly penetrant inherited genomic alterations, such as copy number variants (Stefansson et al., 2014), *de novo* mutations (Xu et al., 2011, Purcell et al., 2014), and genetic translocations (St Clair et al., 1990), have been implicated in some cases of the disease. Furthermore, a recent study reported an increased retrotransposition of long interspersed nuclear element-1 (L1) copy number in brains of schizophrenia patients compared to controls, as well as in iPS-derived neurons of schizophrenia patients (Bundo et al., 2014).

1.1.3.3. Schizophrenia as a polygenic disorder

Initial genetic studies looking for genetic variants associated with schizophrenia took a candidate gene approach, selecting genes for study due to their presumed biological function. However, in these studies effect sizes are small and researchers have often been unable to replicate initial associations (Burmeister et al., 2008). Today, it is clear that schizophrenia susceptibility is predominantly attributed to the action of common genetic variants of low penetrance. The revolution precipitated by the onset of genome-wide association studies (GWAS) facilitated the identification of thousands of genes and genetic variants that contribute to complex diseases in humans. However, such studies need large sample sizes to increase the chance of detecting disease-associated variants, especially in heterogeneous disorders such as schizophrenia. In 2007 the Psychiatric Genomics Consortium (PGC) was created with the aim of 'uniting investigators around the world to conduct meta-

and mega-analyses of genome-wide genomic data for psychiatric disorders', including now 800 investigators from 38 countries (Psychiatric Genomics Consortium, 2016) and is an exemplar for collaboration in genetic studies across the biomedical sciences. The most recent schizophrenia GWAS carried out by the Schizophrenia Working Group of the PGC identified 128 common variants in 108 *loci* associated with schizophrenia (Schizophrenia Working Group of the Psychiatric Genomics, 2014). Despite these advances in understanding the genetic epidemiology of schizophrenia, little is known about the mechanisms by which schizophrenia risk variants mediate disease susceptibility in the brain (Fullard et al., 2016, Psych et al., 2015).

1.1.4. Schizophrenia polygenic risk score

In complex disorders such as schizophrenia, the variants reaching stringent genome-wide significance thresholds explain a limited amount of the observed heritability (International Schizophrenia, 2009, Schizophrenia Working Group of the Psychiatric Genomics, 2014), limiting their predictive power for clinical and aetiological applications. Polygenic risk scores (PRS) have recently generated interest as a way of using the information of nominally associated alleles with very small individual effects that collectively account for a substantial proportion of variation in disease risk (Dudbridge, 2013). This approach ideally involves combining multiple genetic markers into a single score for predicting disease risk.

A common method to calculate PRS is to count the number of risk alleles present in an individual's genome weighted by their effect size in the GWAS analysis in which they were identified. The most recent schizophrenia GWAS (Schizophrenia Working Group of the Psychiatric Genomics, 2014) calculated a schizophrenia PRS derived from all independent nominally significant associated alleles (association P -value < 0.05) that captures about 7% of total liability for the disorder in an European population. Although this is still not useful for clinical risk predication, it is possible that it may be predictive of chronicity, treatment resistance or useful in the stratification of patients (O'Donovan, 2015).

1.1.5. Neurodevelopmental origins of schizophrenia

The neurodevelopmental hypothesis of schizophrenia posits that the disease results from deficits arising during neurodevelopment. Mounting evidence from brain imaging, genetic, epigenetic and epidemiological studies support a neurodevelopmental origin of schizophrenia (for a comprehensive review on the neurodevelopmental model of schizophrenia see Rapoport et al. (2012) and Fatemi and Folsom (2009)). For example, several of the most robustly supported schizophrenia susceptibility genes identified in GWAS have known roles in early brain development and appear to impact on schizophrenia risk during this period (Kirov et al., 2009, Hill and Bray, 2012). Furthermore, several prenatal environmental insults including maternal stress (Khashan et al., 2008), hypoxia (Cannon et al., 2002), maternal infection (Brown and Derkits, 2010) and maternal malnutrition or famine (Susser et al., 1996) are well established associations with increased schizophrenia risk.

1.1.6. Immunity and inflammation in schizophrenia

Epidemiological studies have long suggested a role for dysregulation of the immune system and infection in schizophrenia (Sorensen et al., 2009, Benros et al., 2011, Nielsen et al., 2013). For example, an increased maternal level of the pro-inflammatory cytokine interleukin-8 during pregnancy is associated with an increased risk for schizophrenia in offspring (Brown et al., 2004) (for a review on maternal infection and schizophrenia risk see Brown and Derkits (2010)). This hypothesis is supported by schizophrenia transcriptomic studies which show enrichment of immune-related pathways in genes dysregulated in schizophrenia patients (Mistry et al., 2013, Roussos et al., 2012). Furthermore, genetic variants in the major histocompatibility complex (MHC) *locus* have been strongly associated with schizophrenia in recent GWAS studies (International Schizophrenia et al., 2009, Schizophrenia Working Group of the Psychiatric Genomics, 2014). The MHC *locus* spans several megabases on chromosome 6 and contains 18 highly polymorphic human leukocyte antigen (HLA) genes that encode proteins with antigen-presenting roles in the immune system (Benacerraf, 1981).

1.2. Gene expression and regulation

Understanding the molecular mechanisms that mediate gene regulation in a living organism is a central challenge of modern biology. The DNA sequence of an individual is identical across all somatic cells in the human body (except when rare somatic mutations occur), holding instructions for synthesising all the molecules that form the human body (Encode Project Consortium et al., 2007). However not all of this genetic information is required at all points during development or by all cells; it is estimated that only half of the ~19,000 protein coding genes within the mammalian genome are expressed in any cell type (Ezkurdia et al., 2014).

Figure 1.1 shows a simplified diagram of the gene expression process from DNA to protein. During transcription, a coding portion of the DNA (*i.e.* a protein coding gene) is used by a RNA polymerase as a template to generate a messenger RNA (mRNA) molecule. The mRNA molecules contain sequences called introns that are removed before the mature mRNA leaves the nucleus in a process called splicing. The remaining regions of the transcript, which include the protein-coding regions, are called exons, which are spliced together to produce the mature mRNA. After the mature mRNA leaves the nucleus it is used as a template to synthesise proteins in a process called translation.

The fine-scale temporal and spatial control of gene transcription (DNA to RNA) is regulated by the presence, absence and interplay of transcription factors and other co-factors as well as epigenetic marks. These marks include DNA modifications, histone modifications and the action of non-coding RNA (ncRNA) (Allis et al., 2015). In the next sections I describe some of the epigenetic modifications involved in transcriptional regulation, with particular focus on DNA methylation, and present supporting evidence for the dysregulation of gene expression and epigenetic mechanisms in schizophrenia.

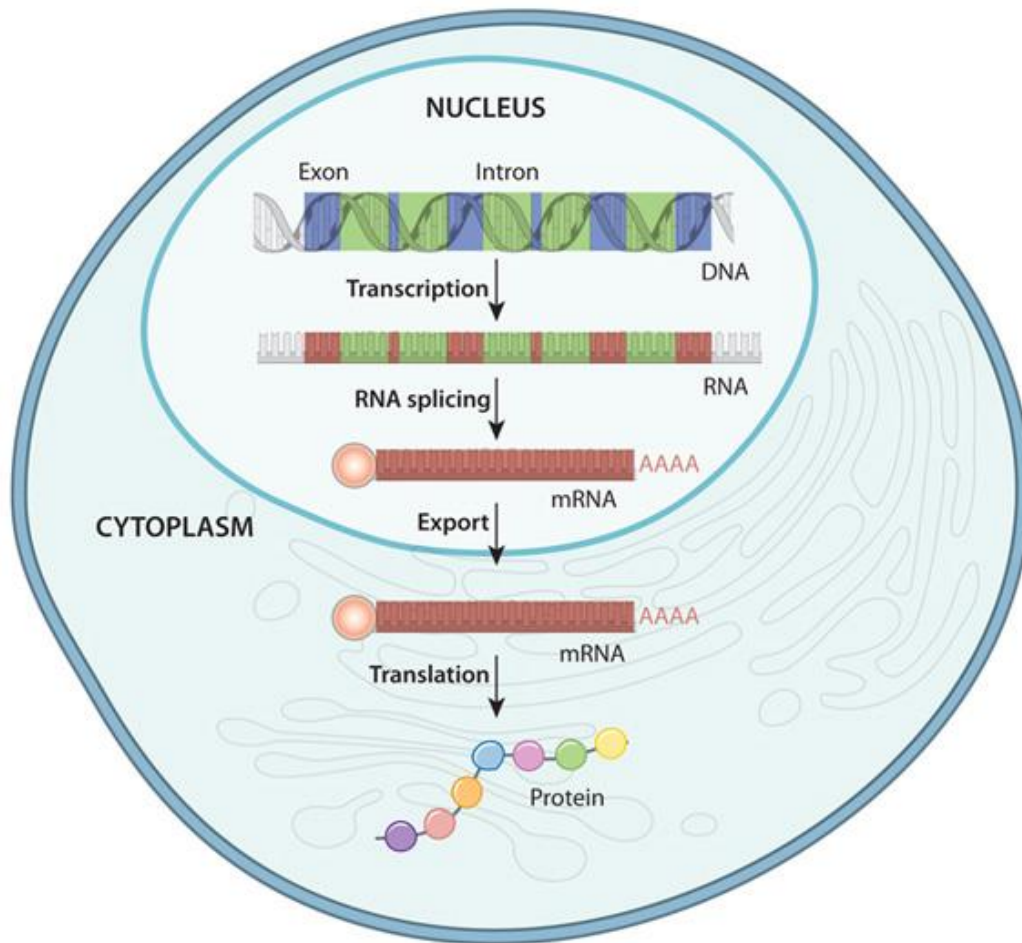


Figure 1.1. A simplified overview of the flow of information from DNA to protein in a eukaryote. Figure taken from Nature Education (2014).

1.2.1. Introduction to epigenetics

The term 'epigenetics' was introduced in 1942 by the embryologist Conrad Waddington to define the emerging branch of biology that '*...studies the causal interactions between genes and their products which bring the phenotype into being...*' (Waddington, 1942). Waddington illustrated his concept as an 'Epigenetic Landscape' (**Figure 1.2**), representing a metaphor for how gene regulation modulates cell fate during development. The figure shows a cell represented as a marble which is initially phenotypically plural, but becomes increasingly differentiated as it traverses down specific ridges and valleys within the landscape (Waddington, 1957). In modern usage epigenetics refers to the study of mitotically heritable, but reversible, changes in gene expression that occur independently of the genomic DNA sequence (Henikoff and Matzke, 1997). As such, epigenetic processes are critical for normal cellular development, tissue differentiation and the long-term regulation of gene function. For a glossary of key epigenetic terms used in this thesis see **Table 1.2**.

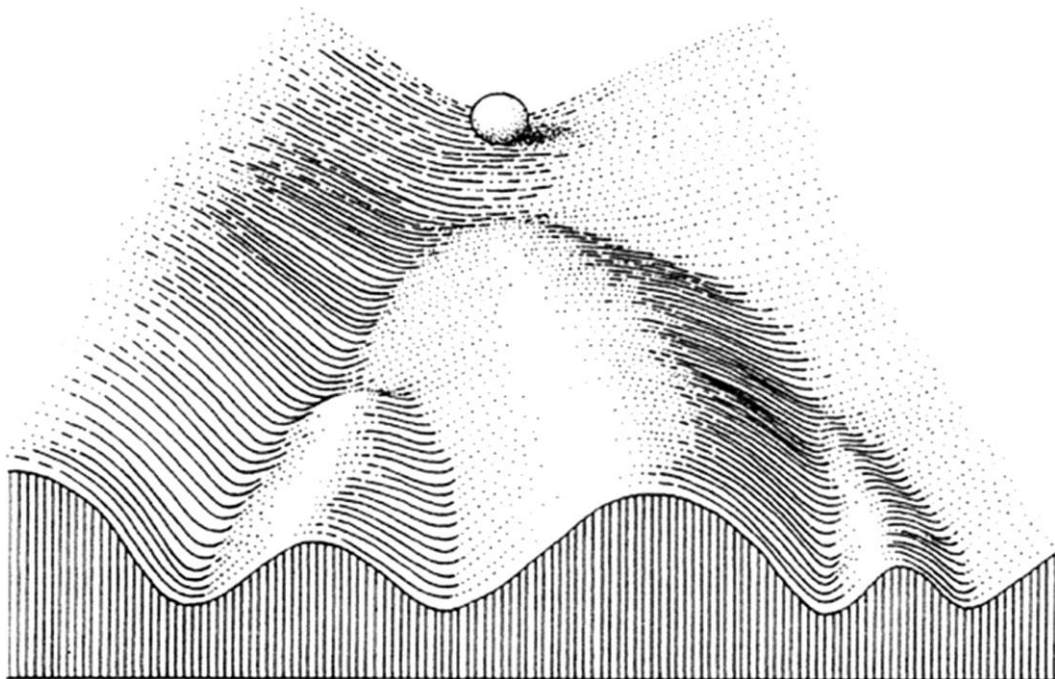


Figure 1.2. Waddington's epigenetic landscape. This figure represents the process of cellular differentiation during development; the marble represents a cell which has to follow a pathway through the different 'valleys' and 'peaks' of genetic regulation and the specific trajectory taken determines the cell fate. Figure taken from Waddington (1957).

Table 1.2. Glossary of key epigenetic terms.

Term	Key reference	Definition
Chromatin	(Berger, 2007)	A DNA-protein complex that constitutes the chromosomes. The structure of chromatin can be altered through covalent modifications made to the DNA or the proteins associated with it (histones). This facilitates movement between condensed (heterochromatic) and open (euchromatic) states.
CpG island	(Gardiner-Garden and Frommer, 1987)	Typically defined as 200 to 500 base pairs (bp) in length with a cytosine (C) and guanine (G) content of more than 50% and an observed/expected C-G dinucleotide (CpG) ratio of 0.6.
DNA hydroxymethylation	(Kriaucionis and Heintz, 2009, Tahiliani et al., 2009)	The oxidized product of active DNA demethylation produced by the action of ten-eleven translocation (TET) proteins. Known to be enriched in the central nervous system.
DNA methylation	(Jaenisch and Bird, 2003)	The addition of a methyl group to carbon 5 of the cytosine pyrimidine ring. DNA methylation in certain CpG-rich promoter regions acts to repress gene expression by disrupting the binding of transcription factors and recruitment of proteins associated with chromatin compaction.
Epigenetics	(Bird, 2007)	The study of mitotically heritable, but reversible, changes in gene expression that occur without a change in the genomic DNA sequence.
Epigenetic epidemiology	(Mill and Heijmans, 2013)	The integration of epigenetic analyses into population-based epidemiological research with the goal of identifying both the causes (that is, environmental, genetic or stochastic) and phenotypic consequences (that is, health and disease) of epigenomic variation.
Epigenetic inheritance	(Richards, 2006)	Epigenetic modifications are mitotically heritable and can therefore be maintained across cell division to contribute to cell line establishment. It is less clear (and controversial) whether epigenetic marks are inherited transgenerationally through meiosis in vertebrates.
Histone modifications	(Berger, 2007)	Post-translational, covalent additions made to N-terminal histone tails that modulate chromatin structure. Modifications include acetylation, methylation and phosphorylation.
Genomic imprinting	(Davies et al., 2005)	Monoallelic expression of genes in a parent-of-origin specific manner, regulated by allele-specific epigenetic marks established in the germline. This process is fundamental to normal mammalian development.
Non-coding RNA	(Encode Project Consortium et al., 2007, Kapranov et al., 2007)	RNA molecules that are not translated into protein that can have structural or regulatory consequences impacting directly upon gene transcription.
Nucleosome	(Luger et al., 1997)	DNA-histone complex consisting of 147 base pairs of DNA wrapped around eight histone proteins.
X-chromosome inactivation	(Avner and Heard, 2001)	A dosage compensation mechanism that, in humans, ensures that XY males and XX females have equivalent levels of gene expression from the X-chromosome.

1.2.2. Epigenetic mechanisms

Epigenetic mechanisms are integral to normal cellular differentiation and play a key role in the regulation of gene expression, X-chromosome inactivation (Avner and Heard, 2001), genomic imprinting (Morison et al., 2005) and the silencing of retroviral transposable elements (Walsh et al., 1998). Epigenetic mechanisms show distinct tissue-specific patterns and are highly dynamic during development (Rakyan et al., 2008). Once established during development, the epigenetic marks defining cellular phenotype are mitotically inherited, although evidence suggests epigenetic alterations can arise across the life span as a result of environmental influences or stochastic changes (Egger et al., 2004). There are several different forms of epigenetic processes including DNA or histone modifications and non-coding RNAs, which are each described in the following sections.

1.2.2.1. DNA modifications

DNA methylation is the most well characterised and stable epigenetic mechanism (Jirtle and Skinner, 2007) and plays a key role in the transcriptional regulation of the mammalian genome. In eukaryotes DNA methylation involves the transfer of a methyl group to the 5th position of the cytosine pyrimidine ring, usually (but not exclusively) at a CpG site (**Figure 1.3**). The reaction uses S-adenosylmethionine (SAM) as a methyl donor and is catalysed by a group of enzymes called DNA methyltransferases (DNMTs) (Klose and Bird, 2006). DNMT3a and DNMT3b are *de novo* methyltransferases which are responsible for establishing DNA methylation at unmethylated cytosines, whilst DNMT1 acts to maintain existing DNA methylation patterns (Lyko et al., 1999).

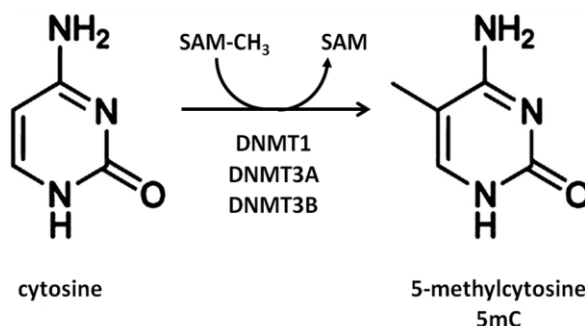


Figure 1.3. DNA methylation involves the transfer of a methyl group to the 5th position of the cytosine pyrimidine ring. Figure adapted from Ku et al. (2011).

Although it is widely accepted that DNA methylation can be both actively and passively removed from methylated cytosines (Tahiliani et al., 2009, Chen et al., 2003), the specific mechanisms driving active DNA demethylation have only recently been described. It has recently been shown that methyl groups can be removed by sequential oxidation of DNA methylation mediated by TET proteins via three intermediate modifications; 5-hydroxymethylcytosine (5hmC), 5-formylcytosine (5fC) and finally 5-carboxylcytosine (5caC) (He et al., 2011, Ito et al., 2011), which can then be removed by thymine DNA glycosylase (Zhang et al., 2012, Yu et al., 2012). **Figure 1.4** taken from Tan and Shi (2012) shows the proposed mechanisms of cytosine demethylation in the literature.

Although the 5hmC, 5fC and 5caC species were initially considered to be intermediate by-products of active 5mC demethylation, recent evidence suggests they may be epigenetic marks on their own (Booth et al., 2014, Booth et al., 2013, Booth et al., 2012, Bachman et al., 2015, Bachman et al., 2014). 5hmC in particular has gained recent attention given its potentially important role in the human brain and implication in neurological disorders (Cheng et al., 2015, Lunnon et al., 2016a). Furthermore, TET proteins have been implicated in meiosis, development, imprinting maintenance and stem-cell reprogramming (Yamaguchi et al., 2012, Gu et al., 2011, Ficz et al., 2011, Dawlaty et al., 2013), suggesting wide-ranging functional roles for other products of active DNA demethylation.

Since methylated cytosines are more liable to spontaneous deamination than unmethylated cytosines, CpG dinucleotides are less common in the genome than would be predicted by chance, and primarily occur in conserved clusters called 'CpG islands' (see **Table 1.2** for a definition) which are often located in gene promoters and are typically unmethylated (Bird, 1986). Epigenetic epidemiological research has primarily focused on DNA methylation at these CpG islands, although recent research highlights the functional importance of DNA methylation in other genomic regions (Jones, 2012). For example, exciting new research supports the hypothesis that intergenic DNA methylation might modulate alternative splicing (Maunakea et al., 2013). Furthermore, DNA methylation changes during brain development are overrepresented in regions flanking CpG islands (shores and shelves) and gene bodies (Spiers et al., 2015).

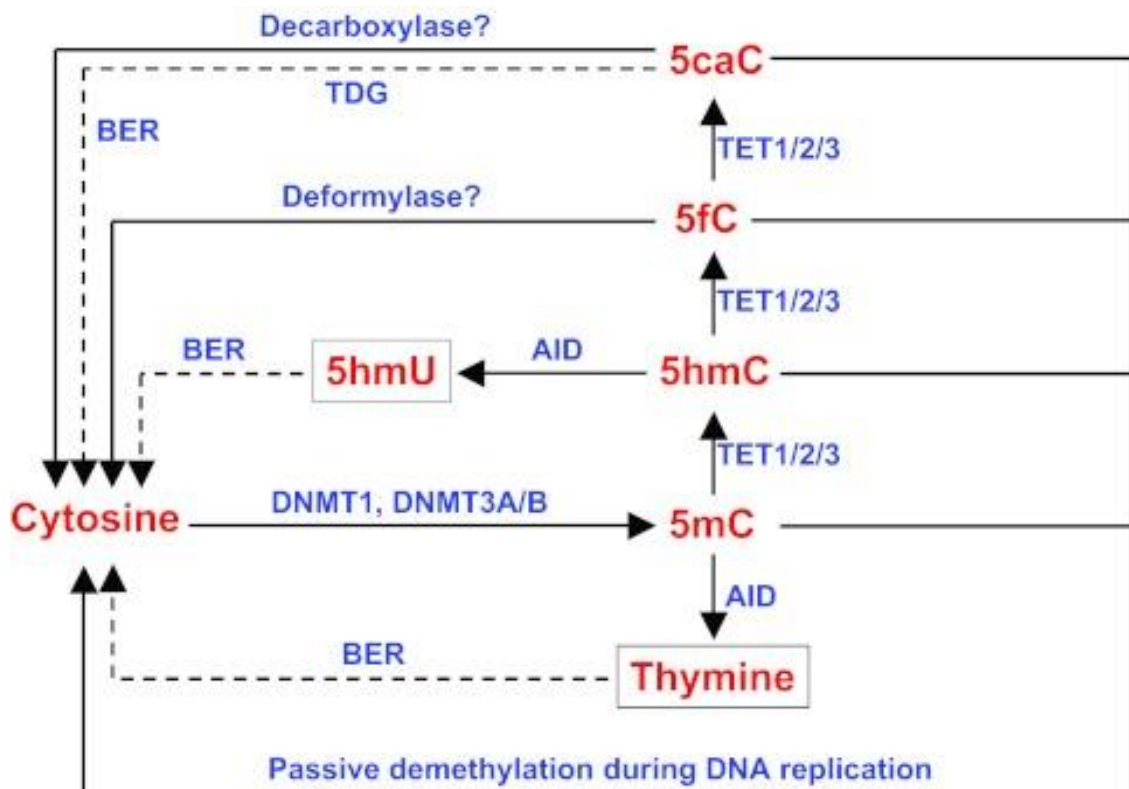


Figure 1.4. Potential mechanisms of active demethylation of DNA regulated by ten-eleven-translocation (TET) family protein. Figure taken and legend adapted from Tan and Shi (2012). TET proteins catalyse 5mC oxidation to 5hmC and further conversion into 5fC and 5caC. These may be recognized and excised by thymine DNA glycosylase (TDG) to generate cytosine and therefore complete demethylation. Alternatively, because 5hmC is more sensitive than 5mC to deamination (via activation-induced deaminase, AID), it can be converted to 5-hydroxymethyluracil (5hmU), which can in turn be converted to cytosine following base-excision repair (BER) pathway-mediated demethylation.

1.2.2.2. Histone modifications

Histone proteins package and order eukaryotic DNA into structural units called nucleosomes within the cell nucleus and are the primary protein component of chromatin (**Figure 1.5**). The nucleosome (see **Table 1.2** for a definition) is the building unit of chromatin and is comprised of DNA wrapped around histone proteins forming a 'spool'-like structure. Four types of histone protein – H2A, H2B, H3, H4 – combine to form the nucleosome's histone octamer core (Spencer and Davie, 1999). The N-terminal tails of the histone particles extend out from the nucleosome and are subject to post-synthesis modifications (Spencer and Davie, 1999).

A growing number of post-translational covalent histone modifications have been described (including acetylation, methylation, phosphorylation, SUMOylation, and ubiquitylation) (for a review on histone modifications see Kouzarides (2007)). Together these modifications form a complex, combinatorial 'histone code' which plays a role in gene expression regulation via alterations in chromatin structure (Berger, 2007). These alterations affect the access of the cell's transcriptional machinery to the DNA. In the condensed chromatin state (heterochromatin), in which the DNA and histone proteins are tightly packed, the access to DNA of transcription factors and other co-factors is blocked, repressing transcription. Conversely, an open chromatin state (euchromatin) allows the transcriptional machinery to access DNA and drive transcription (Grewal and Jia, 2007).

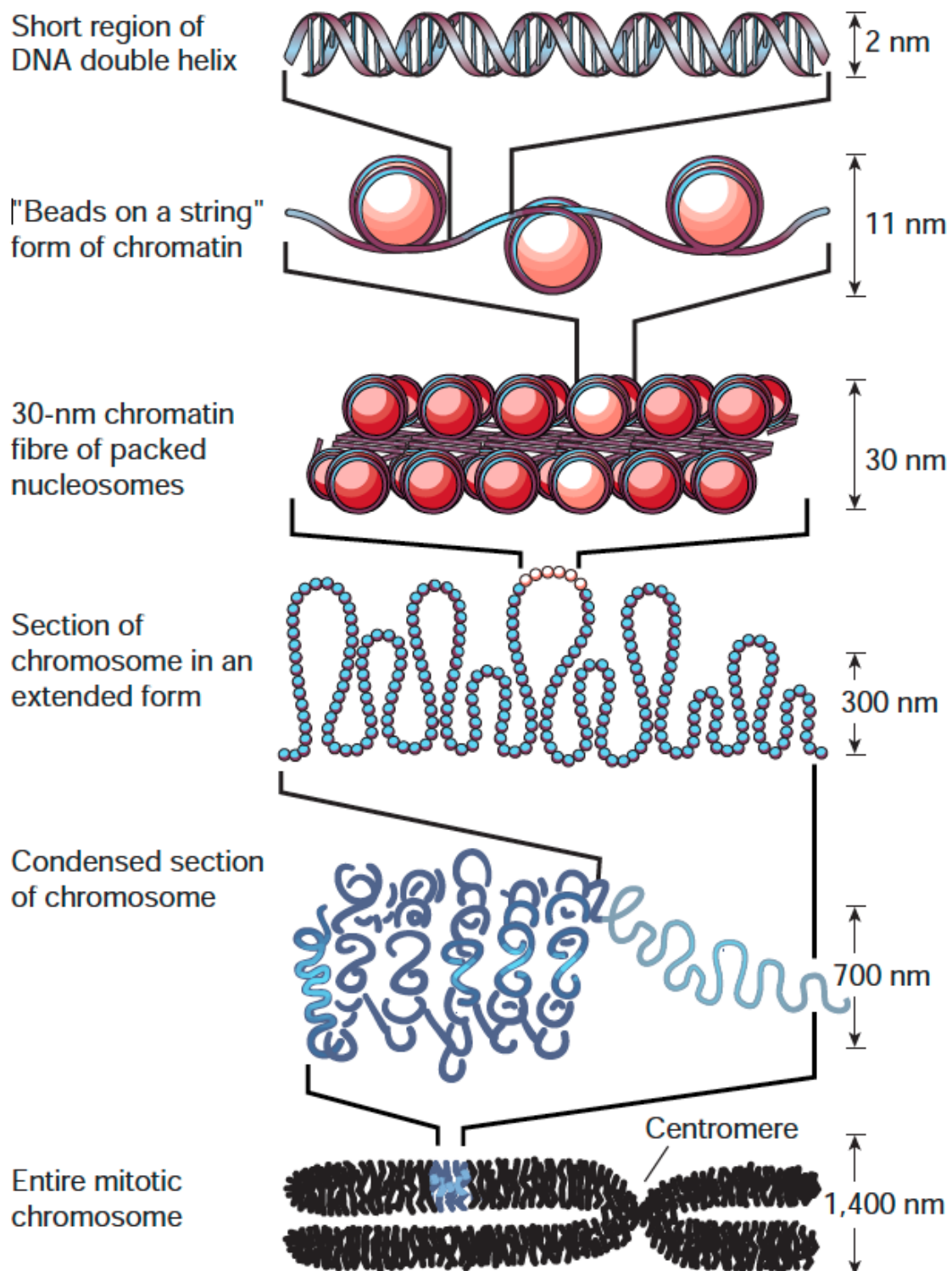


Figure 1.5. Scheme of chromatin structure. Figure adapted from Felsenfeld and Groudine (2003). The nucleosome is the most building unit of chromatin organisation. The “beads on a string” structure folds into a fibre 30nm in diameter, which then folds in to higher-order chromatin structures.

1.2.2.3. Non-coding RNA

Small non-coding RNAs (ncRNA) can take several forms, namely small interfering RNAs (siRNA), small temporal RNAs (stRNA), small nuclear RNAs (snRNAs), small nucleolar RNAs (snoRNAs), piwi-interacting RNAs (piRNA) and microRNAs (miRNAs) (Barry, 2014, Mattick and Makunin, 2006). Small ncRNAs are present in all life kingdoms and play diverse roles in regulating gene expression, epigenetic processes and defence against viruses (Finnegan and Matzke, 2003). Long noncoding RNAs (lncRNAs) appeared later in evolution and are present in invertebrates, vertebrates and plants and are particularly enriched in the cell nucleus. LncRNA forms are highly specific to each cell type and maintain certain features seen in coding RNAs, like promoter regions and intro-exon boundaries (Barry, 2014). The function of these long RNAs is still subject to debate, but they appear to play a role in chromatin regulation and shaping nuclear organization (Quinodoz et al., 2014) and have been implicated in neuronal differentiation and brain development and evolution (Lv et al., 2015, Ng and Stanton, 2013, Qureshi and Mehler, 2012).

1.2.2.4. Interaction of different epigenetic mechanisms and gene expression regulation

The epigenetic landscape of a given cell and the associated gene expression profile are established during development and maintained down the cell lineage through complex interactions that involve transcription factors, chromatin regulators, histone modifications, DNA modifications and ncRNA. Examples of interaction between DNA methylation and histone modifications include recruitment of histone deacetylases (HDACs) by DNMTs and methyl-CpG binding protein 2 (MECP2) (Nan et al., 1998, Saha and Pahan, 2006, Fuks et al., 2000, Fuks et al., 2001, Bachman et al., 2001). ncRNAs have also been found to interact with specific histone modifications (Dinger et al., 2008) and can function as modular scaffolds for histone modifying enzymes (Tsai et al., 2010).

However, the full extent of interactions between different epigenetic mechanisms to regulate gene expression in mammals remain largely poorly understood (Bernstein et al., 2010). One of the reasons is because the different epigenetic modifications discussed in **sections 1.2.2.1 to 1.2.2.3** are frequently studied in isolation, although recent international efforts have started annotating

combinatorial epigenomic signatures across the genome in a diverse range of cell types. The National Institutes of Health (NIH) Roadmap Epigenomics Consortium has set out to extensively examine these mechanisms in an integrative analysis of reference epigenomes and transcriptomes of over 100 human tissue types and provide a publicly accessible resource of epigenomic maps in stem cells and primary *ex vivo* tissues (Bernstein et al., 2010, Romanoski et al., 2015, Roadmap Epigenomics Consortium et al., 2015) (Figure 1.6).

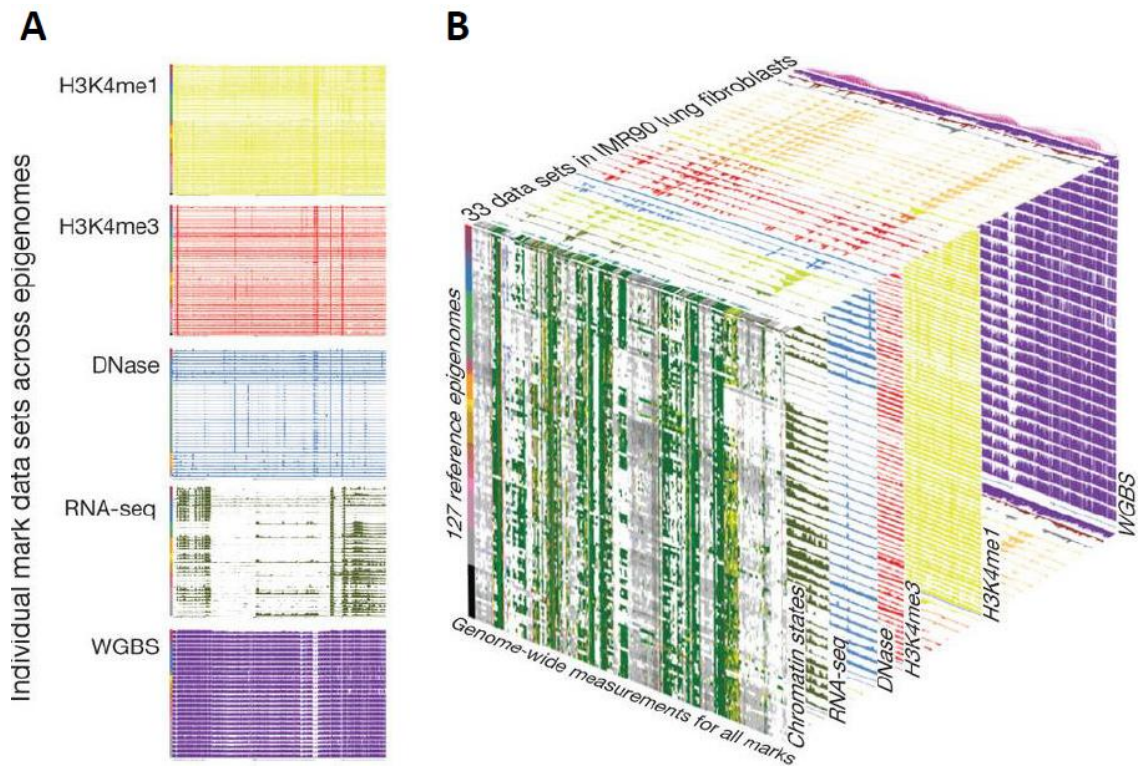


Figure 1.6. Epigenomic information across tissues and marks profiled in the NIH Roadmap Epigenomics Consortium. Adapted from Roadmap Epigenomics Consortium et al. (2015). A) Individual marks datasets across all epigenomes in which they are available; B) Relationship of figure panels highlights dataset dimensions.

1.2.2.5. Genetic mediation of the epigenome

Genetic variation has been shown to influence epigenetic modifications at specific sites across multiple tissues (Kasowski et al., 2013, Kilpinen et al., 2013, McVicker et al., 2013, Gutierrez-Arcelus et al., 2013) including the brain (Gibbs et al., 2010, Gamazon et al., 2013). This can occur in two ways; firstly, alterations in genome sequence may influence the establishment of epigenetic marks, for example a SNP located within the cytosine or guanine of a CpG site (a “CpG-SNP”) may potentially remove or introduce that CpG site; secondly, genetic polymorphisms may alter the epigenetic machinery directly. Genetic variants associated with changes in DNA methylation levels are denoted methylation quantitative trait *loci* (mQTLs). These frequently overlap genetic variants associated with gene expression changes, which are denoted expression quantitative trait *loci* (eQTLs). Therefore, it is possible that genetic mediation of the methylome provides a link between genetic variation and the establishment of complex phenotypes (Wagner et al., 2014, Gutierrez-Arcelus et al., 2013). Recent publications have studied the implication of eQTLs (Schizophrenia Working Group of the Psychiatric Genomics, 2014, Richards et al., 2012) and mQTLs (Hannon et al., 2016, Jaffe et al., 2016) in schizophrenia, providing support for the hypothesis that common variants associated with schizophrenia may function through influencing gene regulation to affect the disease phenotype.

1.3. Profiling the methylome

DNA modifications are erased by standard molecular biology approaches, including polymerase chain reaction (PCR). Therefore, the detection of DNA methylation requires exposure of the DNA to a methylation sensitive pre-treatment prior to DNA sequence analysis, of which the most commonly used is sodium bisulfite conversion (see **Chapter 2 section 2.3.1** for details). Whole genome bisulfite sequencing is considered the gold standard technique to profile DNA methylation, allowing the coverage of ~28 million CpG sites across the human genome. However, the high read depth needed to quantify the small DNA methylation changes that are commonly associated with complex disorders such as schizophrenia makes it, to this date, economically unfeasible for studies with large sample sizes (Ziller et al., 2015). The Illumina Infinium

HumanMethylation450 BeadChip (Illumina, San Diego, CA, USA; 450K array), and more recently the Illumina EPIC array, have become popular tools for screening over 450,000 CpG sites across the human genome (Dedeurwaerder et al., 2011). This approach represents the best compromise between coverage and cost, enabling DNA methylation quantification across the genome in a large number of samples. Furthermore, the widespread use of the 450K array has driven development of many novel bioinformatic methods and pipelines specific for this platform (Wilhelm-Benartzi et al., 2013), which has fostered its popularity and facilitated cross-study comparisons of findings and meta-analyses.

One limitation of standard bisulfite conversion-based approaches is that they do not distinguish between DNA methylation and other DNA modifications (Booth et al., 2012). Recent publications have described new methods of quantifying 5-methylcytosine, 5fC and 5hmC (Booth et al., 2012, Booth et al., 2014, Booth et al., 2013). Although these methods grant the comparison between levels of the three modifications in one same sample, they require three times the amount of screening in parallel. Single, non-modified and non-amplified molecule sequencing methods promise to overcome some of the problems faced by bisulfite conversion and amplification-based methods of epigenetic marks profiling. Single-molecule real-time (SMRT) sequencing allows the direct sequencing of different DNA modifications (Flusberg et al., 2010). This sequencing-by-synthesis method distinguishes between the several modified nucleotides by reading the different durations of fluorescently labelled nucleotides incorporation. Nanopore sequencing, on the other hand, involves translocating a single DNA molecule through a protein nanopore and sequencing it as the molecule passes through the pore, allowing the identification of different DNA modifications (Laszlo et al., 2013, Li et al., 2013, Ahmed et al., 2014). However, these single-cell sequencing techniques are novel and it is not clear how their use will be applicable to large cohorts of samples.

1.4. Epigenetic and gene expression studies in schizophrenia

Fully understanding the regulatory genomic changes associated with schizophrenia will enable researchers to develop molecular assays for improving clinical prognostic, disease subtyping and drug development. Schizophrenia is known to have a substantial genetic component, with several of the most robustly supported schizophrenia susceptibility genes playing important roles in early brain development (see **section 1.1.5**). Furthermore, epidemiological research suggests that prenatal environmental insults are also important (see **section 1.1.5**). These observations have led to a growing interest in the role of developmentally regulated epigenetic variation in the molecular etiology of schizophrenia (Dempster et al., 2013). The notion that epigenetic processes are involved in the onset of schizophrenia is supported by recent methylomic studies of disease-discordant monozygotic twins (Dempster et al., 2011), clinical sample cohorts (Aberg et al., 2014), and post-mortem brain tissue (Mill et al., 2008, Pidsley et al., 2014). In the following sections I describe and discuss epigenomic and transcriptomic research of schizophrenia developed to date.

1.4.1. Epigenetics of schizophrenia

It is being increasingly recognised that epigenetic dysregulation plays an important role in human health and disease (Egger et al., 2004). For example, aberrant promoter hypermethylation and associated with inappropriate gene silencing are well established mechanisms of cancer initiation and progression (Jones and Baylin, 2002). Furthermore, a growing number of studies provide evidence for epigenetic dysregulation in several complex psychiatric disorders (for a review see Labrie et al. (2012)). Although the last decade has witnessed tremendous advances in our understanding about the genetic basis of schizophrenia, a large amount of the variance in disease risk remains to be explained (see **section 1.1.3**). In this section I discuss the main evidence for epigenetic dysregulation in schizophrenia. This section is an updated version of a published review, which I co-authored (Dempster et al., 2013).

1.4.1.1. Epigenetic studies of schizophrenia using post-mortem brain tissue

As discussed above, different cell types in the human body express specific subsets of genes, regulated by cell-specific epigenetic factors including DNA methylation and histone modifications (Weber et al., 2005, Eckhardt et al., 2006, Doi et al., 2009). One of the major challenges in studying epigenetic changes in neuropsychiatric disorders is availability of samples of the primary target tissue (*i.e.*, the brain). Since it is not possible to perform *in vivo* epigenetic studies in the brain, only retrospective study designs using post-mortem brain samples are viable. These experiments are limited by access to high-quality, well-phenotyped samples. There are a number of potential confounders that could influence epigenetic analyses of such samples, including post-mortem interval, storage time, pH, and cellular heterogeneity (Pidsley and Mill, 2011). The small number of brain samples available for schizophrenia epigenetic research means that many investigations are limited in terms of their power to detect significant associations, especially given the small absolute changes that are likely to be uncovered and the heterogeneous cellular composition of the cerebral cortex. Ultimately, given the cell-specific differences identified in epigenetic gene regulation, it may be optimal to isolate specific cell types (*e.g.*, neurons, glia, and astrocytes) from brain tissue via processes such as laser capture microdissection.

Despite these limitations, in the last few years, researchers have made an effort to investigate epigenetic dysregulation in the schizophrenia brain. **Table 1.3** summarises DNA methylation studies on schizophrenia using post-mortem brain samples. These studies have primarily focused on only DNA methylation using small numbers of samples across very specific genomic regions (*i.e.*, promoter CpG islands associated with *a priori* candidate genes). A plethora of different methodological approaches have been used to interrogate epigenetic variation. The first studies were marked by little validation of disease-associated differences using alternative approaches or replication in additional samples. The most recent DNA methylation studies in schizophrenia have used the Illumina 450K array or its predecessor, the Illumina Infinium HumanMethylation27 BeadChip (Illumina, San Diego, CA, USA) (see **section**

1.3), with larger sample sizes and some effort to replicate (and validate) schizophrenia-associated differences.

Recently, we published a study that identified several differently methylated positions (DMP) and regions (DMR) in the PFC of individuals with schizophrenia. The top schizophrenia-associated DMPs were enriched for CpG sites that show dynamic DNA methylation changes during neurodevelopment (Pidsley et al., 2014, Spiers et al., 2015). Additionally, we identified modules of co-methylated CpG sites enriched for neuropsychiatric- and neurodevelopmental-linked genes. In another recent study we identified a significant enrichment of schizophrenia-associated GWAS variants in fetal brain mQTLs (Hannon et al., 2016). Similarly, Jaffe et al. (2016) identified an enrichment of DMPs associated with prenatal-postnatal transition in schizophrenia GWAS regions. Together this evidence supports the hypothesis that schizophrenia has an important, potentially epigenetic-mediated neurodevelopmental component (discussed above in **section 1.1.5**).

Table 1.3. Summary of published DNA methylation studies on schizophrenia using post-mortem brain samples. BA, Brodmann area; BD, bipolar disorder; DMP, differently methylated position; DMR, differently methylated region; FDR, false discovery rate; GEO, Gene Expression Omnibus database; LUMA, luminometric methylation assay; mQTL, methylation quantitative trait *loci*; MSP, methylation-specific PCR; MZ, monozygotic twins; PCR, polymerase chain reaction; mQTL, methylation quantitative trait *loci*.

Reference	Tissue Source	Sample Number	Method	Targeted / global / genome-wide	Key findings	Database accession number
Abdolmaleky et al. (2005)	Frontal cortex (BA 9 and 10)	5 schizophrenia patients, 5 controls	Methylation specific PCR (MSP) and bisulfite sequencing	Targeted	Schizophrenia-associated hypermethylation at <i>RELN</i> promoter.	-
Grayson et al. (2005)	Occipital cortex	10 schizophrenia patients, 10 controls	Direct sequencing of bisulfite-PCR amplicons	Targeted	Schizophrenia-associated hypermethylation of 4 CpG sites in the <i>RELN</i> promoter.	-
	Prefrontal cortex (BA 9 and 10)	5 schizophrenia patients, 5 controls		Targeted		
Iwamoto et al. (2005)	Post-mortem prefrontal cortex (BA10)	11 schizophrenia patients, 12 controls	Clonal sequencing of bisulfite-PCR amplicons	Targeted	Schizophrenia-associated hypermethylation and reduced expression of <i>SOX10</i> .	-
Abdolmaleky et al. (2006)	Frontal cortex (BA 46)	35 schizophrenia patients, 35 controls	MSP and bisulfite sequencing	Targeted	Schizophrenia-associated hypomethylation at <i>COMT</i> promoter in tissue samples from left side of brain.	-
	Frontal lobe (BA 9 and 10)	10 schizophrenia patients, 10 controls		Targeted		
Dempster et al. (2006)	Cerebellum	15 schizophrenia patients, 15 controls	Pyrosequencing of bisulfite-PCR amplicons	Targeted	No significant association with schizophrenia observed at <i>COMT</i> promoter.	-
Mill et al. (2008)	Frontal cortex	35 schizophrenia patients, 35 controls	Enrichment of unmethylated DNA and hybridization to CpG island microarrays	Genome-wide	Significant schizophrenia-associated differences in DNA methylation at multiple <i>loci</i> .	-
Tochigi et al. (2008)	Prefrontal cortex (BA 10)	15 schizophrenia patients, 15 controls	Pyrosequencing of bisulfite-PCR amplicons	Targeted	No association with schizophrenia observed at <i>RELN</i> .	-
Tolosa et al. (2010)	Both hemispheres of the superior temporal gyrus, parahippocampal gyrus and cingulate gyrus	293 schizophrenia patients, 340 controls	Clonal sequencing of bisulfite-PCR amplicons	Targeted	Schizophrenia-associated hypermethylation at <i>FOXP2</i> in the left parahippocampal gyrus.	-

Abdimaliky et al. (2011)	Frontal cortex (BA 46)	35 schizophrenia patients, 35 controls	MSP and bisulfite sequencing	Targeted	Schizophrenia-associated hypermethylation at <i>HTR2A</i> promoter.	-
Xiao et al. (2014)	Frontal cortex (BA 9) and cingulate gyrus (BA 24)	5 schizophrenia patients, 6 controls	MeDIP-seq	Genome-wide	Identification of 17 hyper- and 621 hypomethylated DMRs in BA9 and 620 hyper- and 29 hypomethylated DMRs in BA24 associated with schizophrenia, none at FDR level. Enrichment of introns and exons in the schizophrenia-associated DMRs in BA9 and intergenic regions in the schizophrenia-associated DMRs in BA24. Identification of 57 schizophrenia-associated genes overlapping with Mill et al. (2008). Overrepresentation of neuron development and axon guidance processes in the schizophrenia-associated DMRs.	-
Chen et al. (2014)	Cerebellum	39 schizophrenia patients, 43 controls (cerebellum)	Illumina 27K HumanMethylation microarray	Genome-wide	Four CpG sites showing correlated differential gene expression and methylation associated with schizophrenia, with an FDR threshold of 20%.	GEO: GSE38873
Numata et al. (2014)	Dorsolateral prefrontal cortex	106 schizophrenia patients, 110 controls	Illumina 27K HumanMethylation microarray	Genome-wide	Methylation status at 107 CpG sites significantly associated with schizophrenia. Several <i>cis</i> -mQTLs identified, including schizophrenia-associated risk SNPs.	-
Wockner et al. (2014)	Frontal cortex	24 schizophrenia patients, 24 controls	Illumina 450K HumanMethylation microarray and pyrosequencing	Genome-wide	Numerous schizophrenia-associated <i>loci</i> including <i>NOS1</i> , <i>AKT1</i> , <i>DTNBP1</i> , <i>DNMT1</i> , <i>PPP3CC</i> and <i>SOX10</i> .	GEO: GSE61107
Pidsley et al. (2014)	Prefrontal cortex and cerebellum	Discovery cohort: 21 schizophrenia patients, 23 controls Replication cohort: 18 schizophrenia patients, 15 controls	Illumina 450K HumanMethylation microarray and pyrosequencing	Genome-wide	Four schizophrenia-associated DMPs with a FDR threshold of 5% in the prefrontal cortex. One schizophrenia-associated DMR in the prefrontal cortex spanning the gene body of <i>NRN1</i> . Top schizophrenia-associated modules of co-methylated sites in the prefrontal cortex enriched for neuropsychiatric- and neurodevelopmental-linked genes schizophrenia. schizophrenia-associated DMPs in the prefrontal cortex were enriched for neurodevelopmental-associated DMPs.	GEO: GSE61431; GSE61380
Ruzicka et al. (2015)	Hippocampus	8 schizophrenia patients, 8 BD and 8 controls	Illumina 450K HumanMethylation microarray and pyrosequencing	Targeted	Analysis was restricted to 1,308 CpG sites in the vicinity of 27 genes of the <i>GAD67</i> regulatory network. Methylation status at 146 CpG sites significantly associated with schizophrenia and BD, with an FDR threshold of 5%. Identification of 54 DMRs associated with schizophrenia with a <i>P</i> -value < 0.01. Associations of 3 CpG sites at <i>MSX1</i> , <i>FOXP1</i> and <i>RUNX2</i> replicated by pyrosequencing.	-
Wockner et al. (2015)	Frontal cortex	24 schizophrenia patients, 24 controls + 2 publicly available cohorts from Pidsley et al., 2014	Illumina 450K HumanMethylation microarray	Genome-wide	Identification of several schizophrenia associated DMRs including <i>CERS3</i> , <i>DPPA5</i> , <i>REC8</i> , <i>PRDM9</i> , <i>L Y6G5C</i> and <i>DDX43</i> .	-
Jaffe et al. (2016)	Dorsolateral prefrontal cortex	108 schizophrenia patients and 136 controls	Illumina 450K HumanMethylation microarray	Genome-wide	Identification of 2,104 schizophrenia associated CpGs (Bonferroni-adjusted <i>P</i> < 0.05). Enrichment of DMPs associated with prenatal-postnatal transition in schizophrenia GWAS regions.	GEO: GSE74193
Hannon et al. (2016)	Prefrontal cortex (BA 9), striatum and cerebellum	166 human fetal brain samples	Illumina 450K HumanMethylation microarray	Genome-wide	Significant enrichment of schizophrenia-associated GWAS variants in fetal brain mQTLs.	GEO: GSE61431; GSE61380

1.4.1.2. Epigenetic studies of schizophrenia using peripheral tissues

Although understanding epigenetic dysregulation in the brain is crucial, investigating epigenetic changes in peripheral tissues of schizophrenia patients may be useful in the context of identifying disease biomarkers. Biomarkers are biological measures (e.g. molecular, physiological, anatomical measures) that can predict diagnosis, determine patient-specific aetiology and monitor the progress of disease. Clinical application of epigenetic biomarkers is close to be a reality in diseases where genetic regulation mechanisms undergo dramatic changes, such as cancer (Bock, 2009). Different areas of research such as transcriptomics, proteomics, immunology and epigenetics have aimed to identify molecular biomarkers for schizophrenia (Pickard, 2015).

Table 1.4 shows an overview of DNA methylation studies of schizophrenia using peripheral tissues. Aberg et al. (2014) identified several DMPs associated with disease using whole blood from a large number of schizophrenia patients and controls and a replication cohort, implicating genes relevant to neuronal differentiation, hypoxia and infection pathways. However this study did not account for cell composition heterogeneity. Recently, another study using whole blood from a large cohort identified several schizophrenia-associated DMPs with the Illumina 450K array, but failed to replicate any previously identified associations (Montano et al., 2016). Despite these advances, so far the different studies profiling DNA methylation changes in peripheral tissues of schizophrenia patients have failed to find consistent changes that could be used as biomarkers for the disease. As in post-mortem brain studies (**section 1.4.1.1**), we will need larger cohorts to achieve the replicative power needed to detect suitable biomarkers. Furthermore, these studies can be confounded with factors such as medication and smoking, which are sometimes difficult to account for. Before determining a clinical use of potential epigenetic biomarkers of schizophrenia, we first need to better understand which pathways are dysregulated in the disorder, as well which mechanisms are targeted by current antipsychotic medication (see **section 1.4.3**).

Table 1.4. Summary of published DNA methylation studies on schizophrenia using peripheral tissues. FDR, false discovery rate; FEP, first episode psychosis; GEO, Gene Expression Omnibus database; LUMA, luminometric methylation assay; MBD-seq, methyl-CpG binding domain protein-enriched genome sequencing; MSP, methylation-specific polymerase chain reaction; MZ, monozygotic twins; PCR, polymerase chain reaction.

Reference	Tissue Source	Sample Number	Method	Targeted / global / genome-wide	Key findings	Database accession number
Petronis et al. (2003)	Peripheral blood lymphocytes	1 MZ twin pair concordant for schizophrenia cases, 1 MZ twin pair discordant for schizophrenia cases	Clonal sequencing of bisulfite-PCR amplicons	Targeted	schizophrenia twin in pair discordant for schizophrenia had <i>DRD2</i> methylation levels "closer" to the affected concordant twin pair than to its unaffected co-twin	-
Zhang et al. (2007)	Peripheral blood leukocytes	48 same-sex sib pairs discordant for schizophrenia cases	MSP and direct bisulfite sequencing	Targeted	No significant association with schizophrenia at <i>DRD2</i>	-
McDonald et al. (2011)	Peripheral blood leukocytes	16 schizophrenia cases, 24 controls	MSP	Targeted	No association with schizophrenia observed at <i>NOTCH4</i>	-
Nohesara et al. (2011)	Saliva	20 schizophrenia cases, 20 unaffected family members, 25 controls.	MSP and bisulfite sequencing	Targeted	Schizophrenia-associated hypomethylation of <i>MB-COMT</i> promoter	-
Carrard et al. (2011)	Peripheral blood leukocytes	40 schizophrenia cases, 67 controls	High-resolution melting assay	Targeted	Schizophrenia-associated hypermethylation at <i>5HTR1A</i> promoter	-
Dempster et al. (2011)	Peripheral blood	22 MZ twin pairs discordant for schizophrenia cases	Illumina 27K HumanMethylation microarray	Genome-wide	Numerous loci with DNA methylation differences between discordant twins	-
Ghadirivasfi et al. (2011)	Saliva	63 schizophrenia cases, 76 controls. First-degree relatives: 15 schizophrenia cases,	MSP and bisulfite sequencing	Targeted	T102C polymorphic site of <i>HTR2A</i> significantly hypomethylated in patients and their first degree relatives compared to controls	-
Chen et al. (2012)	Peripheral blood cells	371 schizophrenia cases, 288 controls	MSP and bisulfite sequencing	Targeted	Significant hypermethylation at individual CpG sites in <i>MAOA</i> promoter in male but not female patients	-
Lott et al. (2013)	Whole blood	85 schizophrenia cases	Pyrosequencing of bisulfite-PCR amplicons	Targeted	Significant relationship between <i>COMT</i> promoter region methylation, physical activity and metabolic syndrome in 158Val/Met patients	-
Melas et al. (2012)	Peripheral blood leukocytes	177 schizophrenia cases, 171 controls	Luminometric methylation assay (LUMA)	Global	Significant global hypomethylation in schizophrenia associated with medication and age effects	-
			Pyrosequencing of bisulfite-PCR amplicons	Targeted	Schizophrenia-associated hypermethylation at <i>S-COMT</i>	-

Kinoshita et al. (2013)	Peripheral blood leukocytes	24 medication free-schizophrenia cases, 23 controls	Illumina 450K HumanMethylation microarray	Genome-wide	Methylation status at 10,747 CpG sites significantly associated with schizophrenia with an FDR threshold of 5%. 234 of these significantly different between discordant twins	-
		3 MZ twin pairs discordant for schizophrenia cases				
Ikegame et al. (2013)	Whole blood	100 schizophrenia cases, 100 controls	Pyrosequencing of bisulfite-PCR amplicons	Targeted	schizophrenia-associated hypermethylation at <i>BDNF</i> promoter 1	-
Nishioka et al. (2013)	Whole blood	18 FEschizophrenia cases, 15 controls	Illumina 27K HumanMethylation microarray	Genome-wide	Numerous schizophrenia-associated <i>loci</i>	-
Ota et al. (2014)	Whole blood	51 FEP, 51 controls	Clonal sequencing of bisulfite-PCR amplicons	Targeted	FEP-associated hypermethylation of four CpG sites at <i>GCH1</i> promoter	-
(Liu et al., 2014)	Whole blood	98 schizophrenia cases, 108 controls	Illumina 450K HumanMethylation microarray	Genome-wide	Numerous schizophrenia-associated <i>loci</i>	-
Aberg et al. (2014)	Whole blood	Discovery cohort: 760 schizophrenia cases, 738 controls	MBD-seq and pyrosequencing of bisulfite-PCR amplicons	Genome-wide	Methylation status at 139 sites significantly associated with schizophrenia with an FDR threshold of 1%. One site at <i>FAM63B</i> replicated in the pyrosequencing assay with a <i>P</i> -value lower than the multiple testing threshold. Several of the schizophrenia-associated sites were linked to hypoxia	-
		Replication cohort 1: 178 schizophrenia cases, 182 controls				
		Replication cohort 2: 561 schizophrenia cases, 582 controls				
Montano et al. (2016)	Whole blood	Discovery cohort: 689 schizophrenia cases and 645 controls Replication cohort: 247 schizophrenia cases and 250 controls	Illumina 450K HumanMethylation microarray	Genome-wide	923 schizophrenia-associated DMPs at an FDR threshold of 20%, 625 of which replicated. These included <i>RPS6KA1</i> , <i>MAD1L1</i> , <i>KLF13</i> , <i>SULT4A1</i> , <i>NPDC1</i> , <i>AUTS2</i> , <i>PIK3R1</i> and <i>PNPO</i>	-

1.4.2. Transcriptomic variation in schizophrenia

Early gene expression studies of schizophrenia primarily targeted GABAergic genes that are thought to be involved in the disease (Benes and Berretta, 2001), in particular *RELN* and *GAD67* (Guidotti et al., 2000). Several studies have reported decreased expression of these genes in post-mortem brain tissue of schizophrenia patients (Guidotti et al., 2000, Impagnatiello et al., 1998). In the last decade, several gene expression studies using microarrays have implicated immune and inflammatory, neurodevelopment and neurotransmission pathways in schizophrenia-associated transcriptomic abnormalities in the brain (Bowden et al., 2008, Narayan et al., 2008, Maycox et al., 2009, Torkamani et al., 2010, Schmitt et al., 2011). For a comprehensive review of gene expression analysis in schizophrenia using microarray technology see Kumarasinghe et al. (2012).

The advances in RNA sequencing (RNA-seq) techniques and analysis pipelines provide an opportunity to characterise the full extent of transcriptomic dysregulation in disease (Ozsolak and Milos, 2011). **Table 1.5** summarises the most recent transcriptomic studies in schizophrenia and their findings. It is notable that, despite general lack of replication of previous microarray findings, these novel studies largely implicate neurodevelopmental processes, inflammation and synaptic trafficking as the main pathways associated with schizophrenia.

Table 1.5. Summary of the most recently published transcriptomic studies on schizophrenia. mRNA, messenger RNA; qPCR, quantitative polymerase chain reaction; RT-PCR, real time polymerase chain reaction.

Reference	Tissue Source	Sample Number	Method	Key findings	Database accession number
Wu et al. (2012)	Superior temporal gyrus	Discovery cohort: 9 schizophrenia patients, 9 controls	mRNA sequencing (Illumina Genome Analyzer II) and qPCR	772 genes differently expressed between schizophrenia patients and controls. Three genes validated using qPCR. Gene ontology identified three schizophrenia -relevant functional clusters, namely neurotransmission, synaptic vesicle trafficking and neural development	ArrayExpress: E-MTAB-1030
		Validation cohort: 28 schizophrenia patients, 28 controls			
Xu et al. (2012)	Whole blood	3 schizophrenia patients, 3 controls	mRNA sequencing (Illumina Genome Analyzer II) and qPCR	198 genes differently expressed between schizophrenia patients and controls, 21 of these reached nominal significance and 19 were observed in the pooled sequencing. Differently expressed genes highly enriched in immune related pathways	-
		Pooled sequencing: 10 schizophrenia patients, 10 controls			
Hwang et al. (2013)	Hippocampus	Discovery cohort: 14 schizophrenia patients, 15 controls	mRNA sequencing (Illumina Genome Analyzer) and RT-PCR	144 genes differently expressed between schizophrenia patients and controls. Immune/inflammatory pathways were overrepresented in these genes. Several genes validated using RT-PCR	-
		Validation cohort: 33 schizophrenia patients, 34 controls			
Fillman et al. (2013)	Dorsolateral prefrontal cortex	Discovery cohort: 20 schizophrenia patients, 20 controls	mRNA sequencing (Life Technologies SOLiDv4) and qPCR	798 genes differently expressed between schizophrenia patients and controls. Pathway analysis identified inflammatory response as a key mechanism. Several genes validated using qPCR, including cytokines and immune modulators.	-
		Validation cohort: 37 schizophrenia patients, 37 controls			
Sainz et al. (2013)	Whole blood	36 schizophrenia patients and 40 controls	mRNA sequencing (Illumina Genome Analyzer Ix)	Identification of 200 genes differently expressed between schizophrenia patients and controls at an FDR threshold of 5%, including <i>GRIK3</i> , <i>LPL</i> , <i>S100B</i> , <i>SNCA</i> , <i>SYN2</i> , <i>TUBB2A</i> , <i>SELENBP1</i> and <i>CSMD1</i>	-
Gardiner et al. (2013)	Whole blood	114 schizophrenia or schizoaffective disorder patients and 80 controls	Gene expression array (Illumina HT-12_V3 beadchip) and qPCR	164 differently expressed between schizophrenia patients and controls. Results for 6 genes (<i>E/IF2C2</i> , <i>MEF2D</i> , <i>EVL</i> , <i>PI3</i> , <i>S100A12</i> and <i>DEFA4</i>) were validated using qPCR	-
Zhao et al. (2015)	Cingulate cortex (BA 24)	31 schizophrenia patients and 26 controls	mRNA sequencing (Illumina Genome Analyzer II and HiSeq 2000)	Identification of 105 genes differently expressed between schizophrenia patients and controls at an FDR threshold of 10%	-

1.4.3. Antipsychotic medication and the implications of epigenetic studies

Before the 1950s the treatment for schizophrenia consisted of electroconvulsive therapy. The first generation antipsychotics (FGAs) were discovered in the 1950s and the second generation antipsychotics (SGAs) were developed in the 1970s. The SGAs, contrary to FGAs, are less likely to cause extrapyramidal symptoms such as Parkinson-like movements (for a review on antipsychotic drugs see Miyamoto et al. (2005)). However, they introduced a new range of side-effects, such as weight gain and metabolic side effects (Hert et al., 2009). About 20% of the patients are resistant to current antipsychotic drugs and 40 to 70% of patients treated with clozapine (a commonly used antipsychotic drug) show an inadequate response (Bosia et al., 2015). Furthermore, most antipsychotic drugs act on reversing the symptoms rather than prevent the development of molecular dysfunction that underlies the disorder. They have poor effect on cognitive impairment and are not an efficient therapeutic of long term disability. Furthermore, even when effective, the molecular mechanism of action of several of these drugs remains elusive (Miyamoto et al., 2005) and understanding this would inform us about molecular pathways involved in schizophrenia itself.

Several studies have offered evidence that antipsychotic drugs might act through changes in epigenetic processes. The majority of the commonly used antipsychotics target serotonin and dopamine receptors and have been shown to induce changes in histone marks or DNA methylation, particularly in promoters of genes involved in GABAergic mechanisms (for a review of epigenetic effects of antipsychotic drugs see Bosia et al. (2015)). **Figure 1.7** summarises the epigenetic changes induced by a number of commonly-used antipsychotic medications (Boks et al., 2012). Assessing the effects of antipsychotic medication on epigenetic modifications in the brain is currently very difficult to achieve because most samples have poorly described medication information. Furthermore, even when this information is available is often impossible to distinguish between medication intake and disease status as all schizophrenia patients are usually prescribed some type of antipsychotic medication during their lifetime. The ideal study design would be to longitudinally assess DNA methylation changes in the brain during an

individuals' transition into disease, although such a study is clearly unfeasible at present. My current work is aiming to explore these mechanisms using animal models and will be the focus of my initial postdoctoral studies.

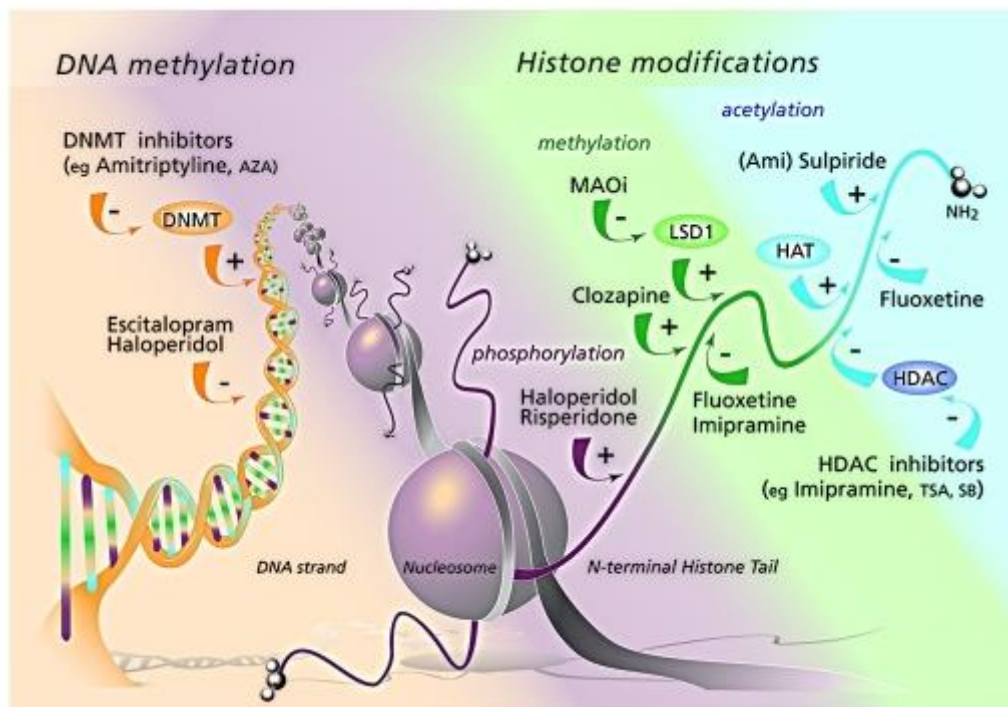


Figure 1.7. Influence of neuropsychiatric drugs on the epigenome. Image taken from Boks et al. (2012).

1.5. Klinefelter syndrome

As part of our first integrated “-omics” study of schizophrenia (Pidsley et al., 2014), we examined genome-wide patterns of DNA methylation, gene expression, and genetic variation in post-mortem CER and PFC brain tissue samples from schizophrenia patients and controls. During quality control steps on these data we identified an individual as having a Klinefelter syndrome (KS; 47,XXY karyotype). Klinefelter syndrome is the most common sex chromosome disorder, affecting approximately 1 in 400 to 800 men (van Rijn et al., 2006). Of note, comorbidity of schizophrenia-spectrum pathology have been reported in individuals with KS (van Rijn et al., 2006). For this reason, I decided to explore genomic variation in KS as part of my PhD; **Chapter 7** describes the first study to examine genome-wide patterns of DNA methylation and gene expression in two regions of the brain obtained post-mortem from a patient with a 47,XXY

karyotype. We identified widespread tissue-specific epigenomic and transcriptomic alterations, providing potential clues about the molecular consequences of KS. Further details on the clinical manifestation and evidence for epigenomic dysregulation in KS can be found in **Chapter 7**.

1.6. General aims of my thesis

Increased understanding about the functional complexity of the genome has led to growing recognition about the role of epigenetic variation in the aetiology of schizophrenia. Epigenetic processes act to dynamically control gene expression and are known to regulate key neurobiological and cognitive processes in the brain. Furthermore, mounting evidence suggests that genetic mediation of epigenetic processes and gene regulation may play a role in disease etiology. To date, our knowledge about dysregulation of transcriptomic and epigenomic mechanisms in the schizophrenia brain is limited and based on analyses of small numbers of samples obtained from a range of different cell and tissue types. The general aim of this thesis was to further our knowledge about the extent of methylomic and transcriptomic variation in the schizophrenia brain.

- In the first empirical chapter (**Chapter 3**) I aim to systematically investigate genome-wide methylomic variation associated with schizophrenia in four different brain regions; PFC, STR, HC and CER. The analyses were performed in a unique collection of two post-mortem brain cohorts using the Illumina 450K array. I identified multiple disease-associated DMPs and DMRs, many residing in the vicinity of genes previously implicated in schizophrenia.

- In the second empirical chapter (**Chapter 4**) I investigate DNA methylation variation associated with increased polygenic burden for schizophrenia. I identified multiple schizophrenia PRS-associated DMPs and DMRs in the PFC, STR, HC and CER, as well as associations across different brain regions. This study highlights the utility of PRS for identifying molecular pathways associated with etiological variation in complex disease.

- In the third empirical chapter (**Chapter 5**) I utilise a systems-level approach to explore the correlation structure of the schizophrenia methylome in each of the brain regions. This chapter describes my exploration of weighted gene network analysis and its application to DNA methylation data. I identified

several modules of co-methylated probes associated with schizophrenia in the PFC. Furthermore, I provide evidence that supports a neurodevelopmental origin of schizophrenia.

- In the fourth empirical chapter (**Chapter 6**) I profiled the transcriptome of the PFC of schizophrenia patients and controls using RNA-seq. In this chapter I describe the stringent quality control and analyses methods using to handle this dataset. I identified several differentially expressed genes associated with schizophrenia and provide evidence of schizophrenia-associated methylomic variation overlapping some of these genes.

- In the fifth empirical chapter (**Chapter 7**) I present the first study to examine genome-wide patterns of DNA methylation and gene expression in two regions of the post-mortem brain obtained from a patient with a 47,XXY karyotype. This chapter is presented in the format of a peer-reviewed publication (Viana et al., 2014).

Figure 1.8 describes the integration of the schizophrenia-relevant **Chapters 3 to 6**.

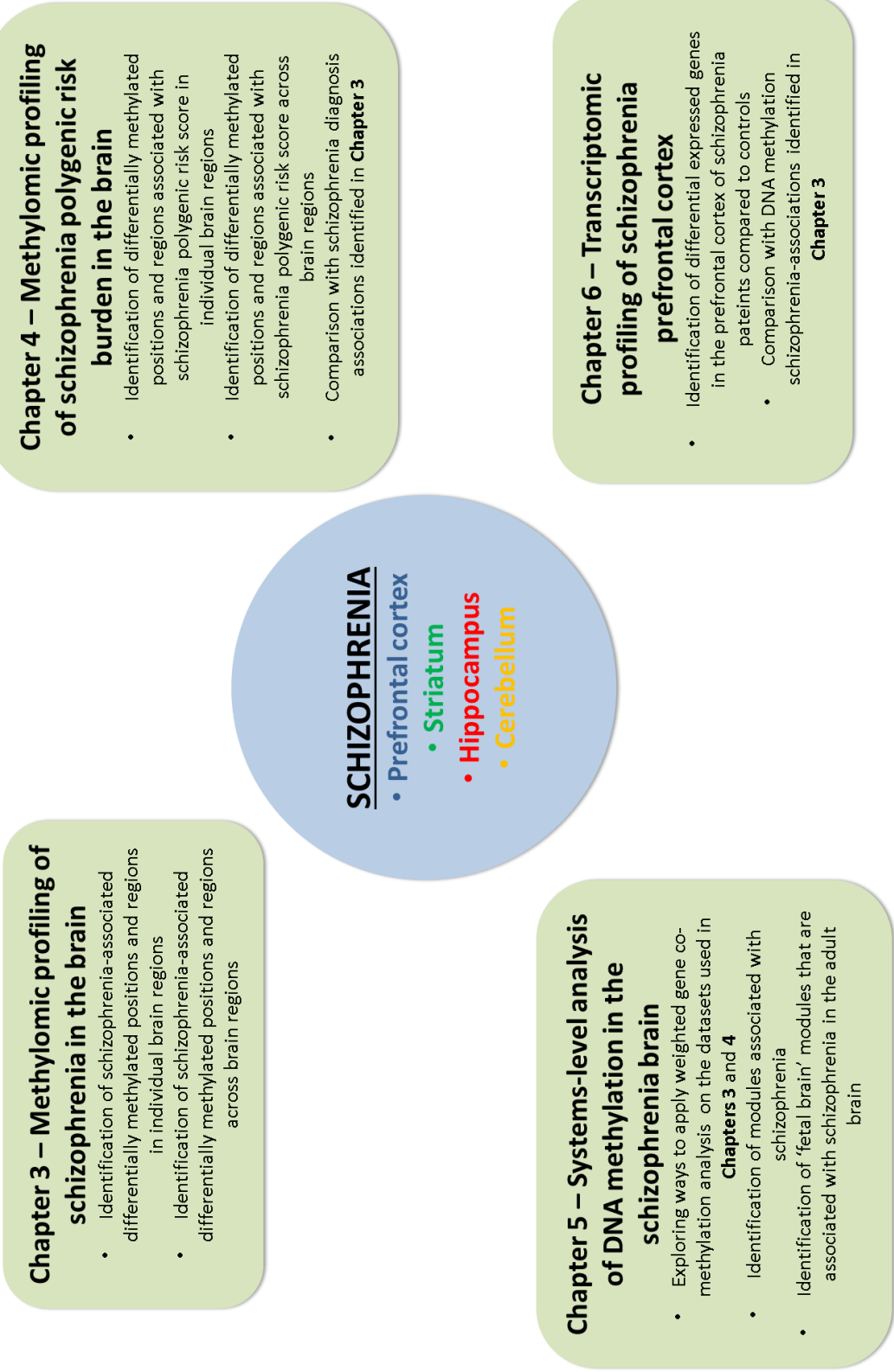


Figure 1.8. Integration of Chapters 3 to 6 of this thesis.

Chapter 2 - Materials and Methods

In this chapter I describe the general materials and methods used throughout my thesis in multiple chapters. Detailed descriptions of individual sample cohorts and methods specific to each analysis section are given in each of the empirical chapters

2.1. Human sample cohorts

I used tissue from the MRC London Neurodegenerative Diseases Brain Bank (LNDBB), Douglas-Bell Canada Brain Bank (DBCBB) and Edinburgh Brain and Tissue Banks (EBTB) to study genomic variation associated with schizophrenia. Each cohort comprises of multiple brain regions from schizophrenia patients and non-psychiatric controls. The use of these samples in the research presented in my thesis was approved by the University of Exeter Medical School Research Ethics Committee (reference number 13/02/009). Detailed information of each sample cohort is given in **Chapter 3 section 3.2.1**. Detailed information on the specific subset of samples used for individual analyses is given in each chapter.

2.2. Nucleic acid extraction

In this section I describe the methods used throughout my thesis to isolate nucleic acids (*i.e.* genomic DNA and total RNA) from tissue samples dissected from human brain tissue. All plastic-ware used during these procedures was sterile and RNase-free. Before starting experimental procedures, all the surfaces and materials were cleaned using ethanol and/or RNaseZap (Thermo Fisher Scientific, Waltham, MA, United States of America (USA)) to remove RNases present and avoid RNA degradation. **Table 2.1** describes the specific nucleic acid extraction methods used in each chapter.

Table 2.1. Nucleic acid extraction methods used in this thesis.

Chapters	Human brain regions	Nucleic acid	Extraction method	Protocol
3,4 & 5	Prefrontal cortex, striatum, hippocampus, cerebellum	DNA	Phenol-chloroform	section 2.2.1
6	Prefrontal cortex	RNA	miRNeasy Mini Kit (Qiagen, Venlo, Holland)	section 2.2.2
7	Prefrontal cortex, ceberellum	DNA	Phenol-chloroform	section 2.2.1

2.2.1. Genomic DNA isolation using phenol-chloroform

This section describes the isolation of genomic DNA from post-mortem human brain tissue. **Figure 2.1** shows an overview of the experimental procedure. ~50mg of frozen human brain tissue was excised from each sample using a sterile scalpel blade on a petri dish over dry ice and transferred to a sterile 1.5ml microcentrifuge tube. The tissue was homogenised in 500µl of lysis buffer (75mM NaCl, 10Mm TRIS-Cl pH=8, 0.1M EDTA pH=8, 0.5% SDS) using a DNase free, sterile plastic pestle. 1µl of DNase free RNase-A. 5µl of proteinase K (20mg/ml) (Thermo Fisher Scientific, Waltham, MA, USA) was added and the samples incubated in a water bath at 50°C overnight. After overnight incubation the samples were transferred to a water bath at 65°C for 20 minutes to deactivate the proteinase K, and then cooled to room temperature.

Phase-lock tubes were prepared in advance by adding a small amount of high vacuum grease (Dow Corning, Midland, Michigan (MI), USA) to a 2ml microcentrifuge tube and centrifuging for 5 minutes. The samples were transferred to these tubes and 500µl of phenol:chloroform:isoamyl alcohol (Thermo Fisher Scientific, Waltham, MA, USA) was added. The samples were mixed by inverting the tubes ~20 times and centrifuged at 13,000 rpm for 20 minutes. The upper layer of each sample was transferred to a new tube. 500µl of chloroform (Sigma-Aldrich Corporation, St. Louis, MO, USA) were added and the samples centrifuged at 13,000 rpm for 15 minutes. The upper layer was transferred to a new tube, another 500µl of chloroform added, and the samples centrifuged again at 13,000 rpm for 15 minutes. The upper layer was transferred with a pipette into new tubes. 1ml of cooled 100% ethanol (Sigma-Aldrich Corporation, St. Louis, MO, USA) was added and the samples slowly mixed by inverting to precipitate the DNA. The samples were centrifuged at 13,000 rpm for 15 minutes and the supernatant removed carefully and discarded. 500µl of 70% ethanol were added and the samples centrifuged at 13,000 rpm for 5 minutes. The supernatant was removed and the samples were left to air dry for 30 minutes or until dry. The DNA was resuspended in 100µl of 1M Tris-HCl (pH=7) buffer and left in a water bath at 37°C overnight to fully dissolve.

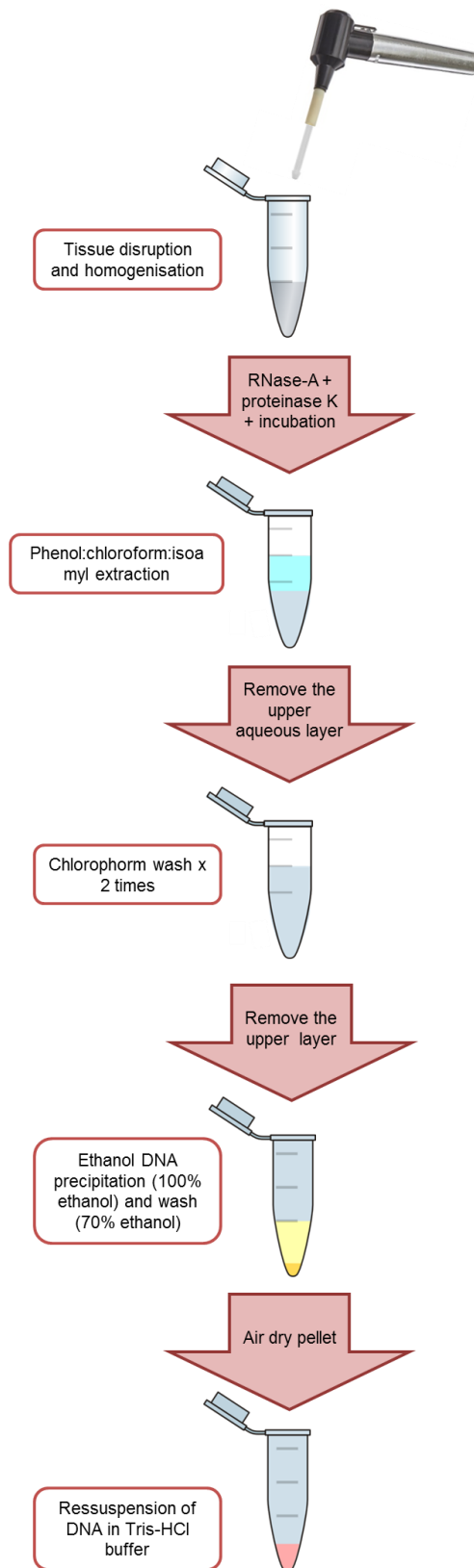


Figure 2.1. Overview of the genomic DNA extraction experimental procedure.

2.2.2. Total RNA isolation from post-mortem human brain tissue

This section describes the isolation of total RNA from post-mortem human brain tissue. Total RNA was extracted using the miRNeasy Mini Kit (Qiagen, Venlo, Holland). **Figure 2.2** shows an overview of the experimental procedure (taken from the miRNeasy Mini Kit Handbook (Qiagen, 2014)). All the reagents are provided with the kit unless otherwise stated. Before starting, the lysophilised RNase-Free DNase I (Qiagen, Venlo, Holland) was prepared by adding 550µl of RNase-free water, and 100% ethanol (Sigma-Aldrich Corporation, St. Louis, MO, USA) was added to the RPE and RWT buffers as indicated in the manufacturer instructions.

~30mg of frozen human brain tissue was excised from each sample using a sterile scalpel blade on a petri dish over dry ice and transferred into a sterile 1.5ml microcentrifuge tube. The tissue was homogenised in 350µl of QIAzol and using an RNase free, sterile plastic pestle. Another 350µl of QIAzol were added to each tube. The total 700µl of lysate were transferred into a QIAshredder column (Qiagen, Venlo, Holland) and centrifuged at 13,000rpm for 2 minutes. The samples were transferred to new microcentrifuge tubes and incubated at room temperature for 5 minutes. 140µl of chloroform (Sigma-Aldrich Corporation, St. Louis, MO, USA) was added and the samples mixed by shaking for 15 seconds. The samples were again incubated at room temperature for 2 minutes and then centrifuged at 13,000rpm at 4°C for 15 minutes.

The upper layer of each sample was transferred to a new microcentrifuge tube and 525µl of 100% ethanol added and mixed by pipetting. The samples were transferred to RNeasy Mini spin columns, centrifuged at 10,000rpm for 15 seconds and the flow-through discarded. 350µl of RWT buffer were added to each column, the samples were centrifuged at 10,000rpm for 15 seconds and the flow-through discarded. For each sample, 10µl of DNase I solution was added to 70µl of RDD buffer I (Qiagen, Venlo, Holland). 80µl of this solution was added to the centre of each column and the samples incubated at room temperature for 15 minutes. After incubation, 350µl of RWT buffer were added to each column, the samples were centrifuged at 10,000rpm for 15 seconds and the flow-through discarded. 500µl of RPE buffer were added to each column,

the samples were centrifuged at 10,000rpm for 15 seconds and the flow-through discarded. Another 500µl of RPE buffer were added to each column, the samples were centrifuged at 10,000rpm for 2 minutes and the flow-through discarded. The columns were placed in new collection tubes and centrifuged at 13,000rpm for 1 minute to dry. The columns were placed in the microcentrifuge tubes. 15µl of RNase-free water were added to the centre of each column and the samples centrifuged at 10,000rpm for 1 minute to elute the RNA. Another 15µl of RNase-free water were added to the centre of each column and the samples centrifuged at 10,000rpm for 1 minute to elute the remaining RNA.

2.2.3. Total RNA clean-up

From each of the total RNA samples isolated as described in **section 2.2.2**, 10µl were purified using the RNeasy MinElute Cleanup Kit (Qiagen, Venlo, Holland). **Figure 2.3** shows an overview of the experimental procedure (taken from the RNeasy MinElute Cleanup Kit Handbook (Qiagen, 2010)). All the reagents are provided with the kit unless otherwise stated. Before starting 100% ethanol (Sigma-Aldrich Corporation, St. Louis, MO, USA) was added to the RPE buffer as indicated in the manufacturer instructions. 80% ethanol was prepared using RNase-free water and 10µl of β-Mercaptoethanol (Sigma-Aldrich Corporation, St. Louis, MO, USA) was added per each 1ml of RLT buffer.

90µl of RNase-free water was added to 10µl of each RNA sample. 350µl of RLT buffer were added to each sample and mixed by pipetting, followed by 250µl of 100% ethanol (Sigma-Aldrich Corporation, St. Louis, MO, USA). The samples were transferred to an RNeasy MinElute spin columns, centrifuged at 10,000 rpm for 15 seconds and the flow-through discarded. The columns were placed into new tubes and 500µl of RPE buffer added to each. The samples were centrifuged at 10,000 rpm for 15 seconds and the flow-through discarded. 500µl of 80% ethanol were added, the columns centrifuged at 10,000rpm for 2 minutes and the flow-through discarded. The columns were placed in new tubes, the lids opened and centrifuged for at 13,000 rpm for 5 minutes. The tubes were rotated 180° from their previous position in the centrifuge and then spun again at 13,000rpm for 1 minute. The columns were then placed in new centrifuge tubes, 14µl of RNase-free water were added to the centre of the column and the samples centrifuged at 13,000rpm for 1 minute

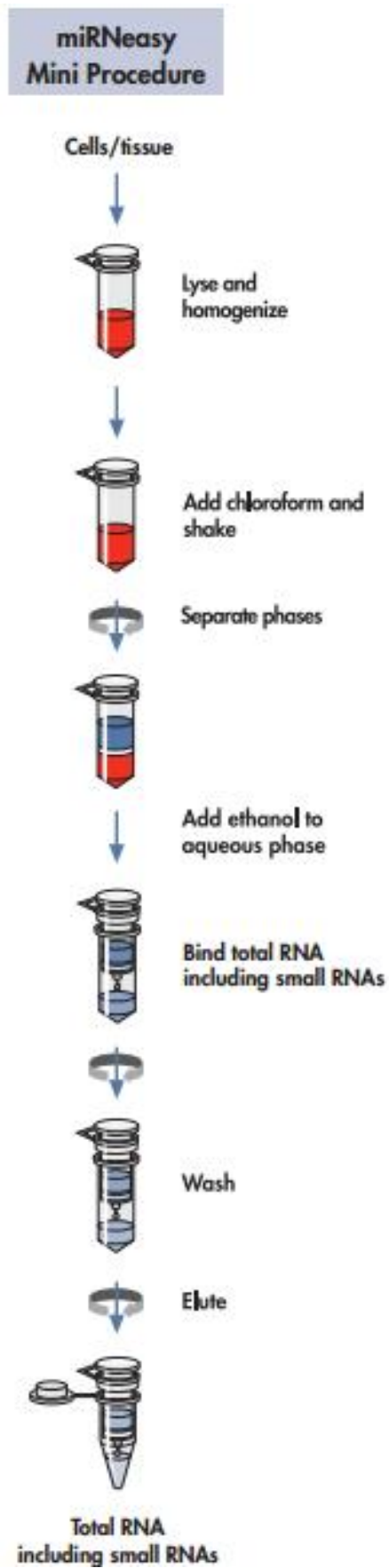


Figure 2.2. Overview of the total RNA extraction experimental procedure.
Figure taken from the miRNeasy Mini Kit Handbook (Qiagen, 2014).

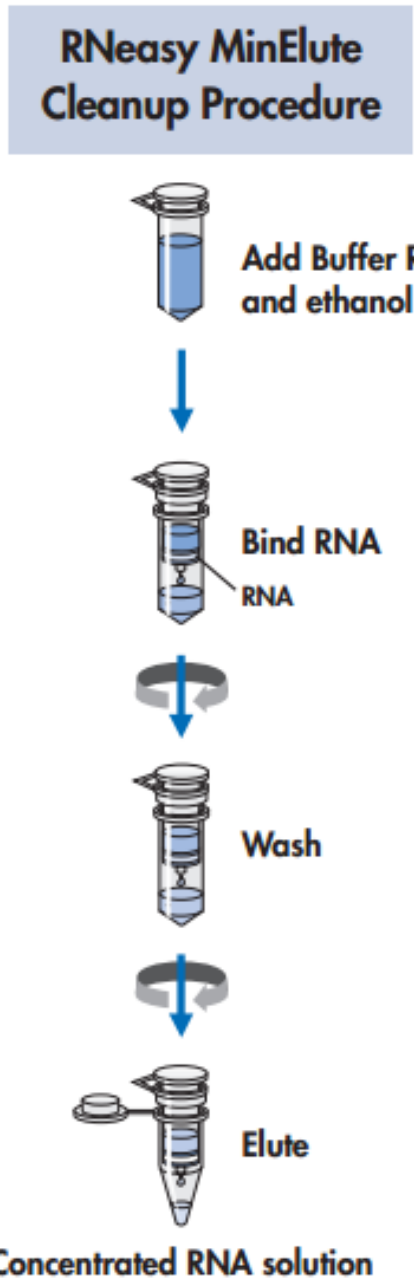


Figure 2.3. Overview of the RNA clean-up experimental procedure. Figure taken from the RNeasy MinElute Cleanup Kit Handbook (Qiagen, 2010).

2.2.4. Determining the quality and quantity of isolated nucleic acids

After extraction, DNA and RNA samples were quantified and checked for purity by spectrophotometry using a Nanodrop ND-8000 (Thermo Fisher Scientific, MA, USA). Nucleic acids absorb UV light at a wavelength of 260nm, whereas proteins absorb UV light at a wavelength of 280nm and other compounds such as ethylenediamine tetraacetic acid (EDTA), carbohydrates and phenol, at a wavelength of ~230nm. Therefore, the absorbency ratios of 260/280 and 260/230 indicate the presence of protein and other contaminants in the DNA and RNA samples. A 260/280 ratio of ~1.8 (for DNA) and ~2.0 (for RNA), and a 260/230 ratio between 1.8 and 2.2 is indicative of high purity sample. **Figure 2.4** shows an example of a typical nucleic acid nanodrop profile.

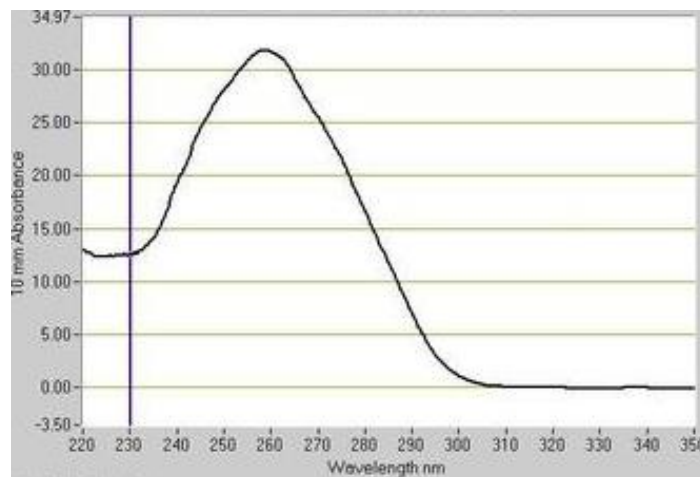


Figure 2.4. A typical nucleic acid sample will have a very characteristic profile.

The purity and integrity of RNA samples was further assessed using an Agilent 2100 Bioanalyzer Instrument (Agilent Technologies, Santa Clara, CA, USA) in conjunction with the Agilent RNA 6000 Nano Kit (Agilent Technologies, Santa Clara, CA, USA). The Bioanalyzer uses a fluorescent dye that binds to RNA on a gel electrophoresis chip. The Agilent Bioanalyzer software analyses the resulting electrophoresis gel and calculates an RNA integrity number (RIN), that can range between 1 (suggesting the RNA is highly degraded) and 10 (indicating the RNA has perfect integrity). **Figure 2.5** shows an electropherogram detailing the regions that are indicative of RNA quality (taken from Muelle et al. (2004)). **Figures 2.6** and **2.7** show the Bioanalyzer gel

electrophoresis images and electropherogram of RNA samples that were degraded for different periods of time, respectively (taken from Muelle et al. (2004)). Examples of good and poor quality RNA samples from the post-mortem brain tissues used in my work can be seen in example traces in **Figure 2.8**.

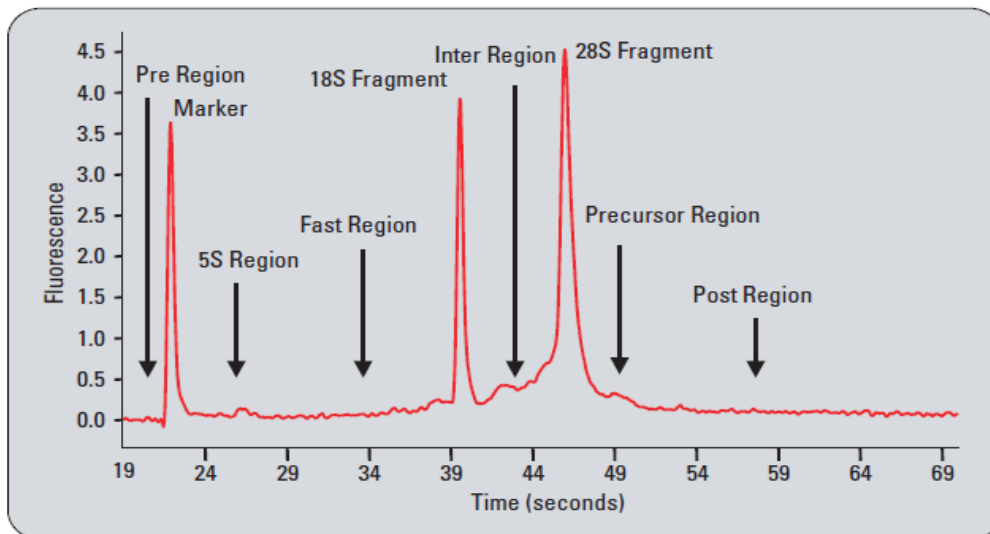


Figure 2.5. Electropherogram detailing the regions that are indicative of RNA quality. Figure and legend taken from the RNA Integrity Number (RIN) – Standardization of RNA Quality Control guide, Agilent Technologies (Muelle et al., 2004).

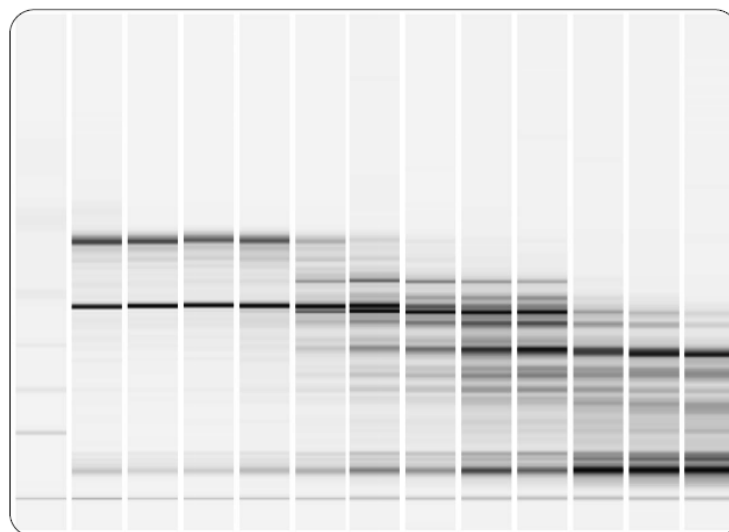


Figure 2.6. A total RNA sample was degraded for varying times and the resulting samples were analyzed on the Agilent 2100 Bioanalyzer System using the Eukaryote Total RNA Nano assay. A shift towards shorter fragment sizes (left to right) can be observed with progressing degradation. Figure taken and legend adapted from the RNA Integrity Number (RIN) – Standardization of RNA Quality Control guide, Agilent Technologies (Muelle et al., 2004).

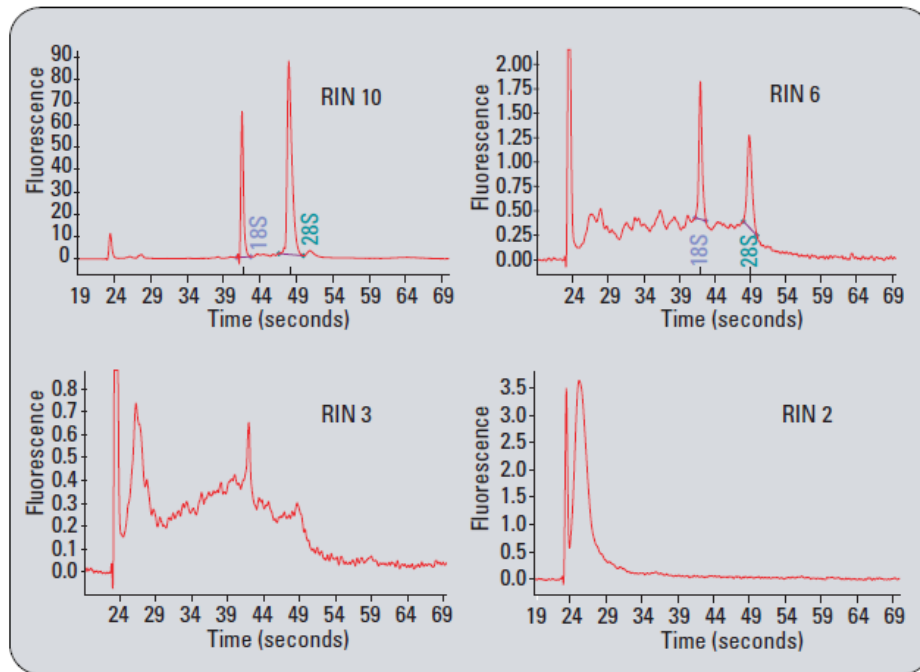


Figure 2.7. Electropherograms from samples ranging from intact (RNA Integrity Number (RIN) = 10), to degraded (RIN = 2). Figure taken and legend adapted from the RNA Integrity Number (RIN) – Standardization of RNA Quality Control guide, Agilent Technologies (Muelle et al., 2004).

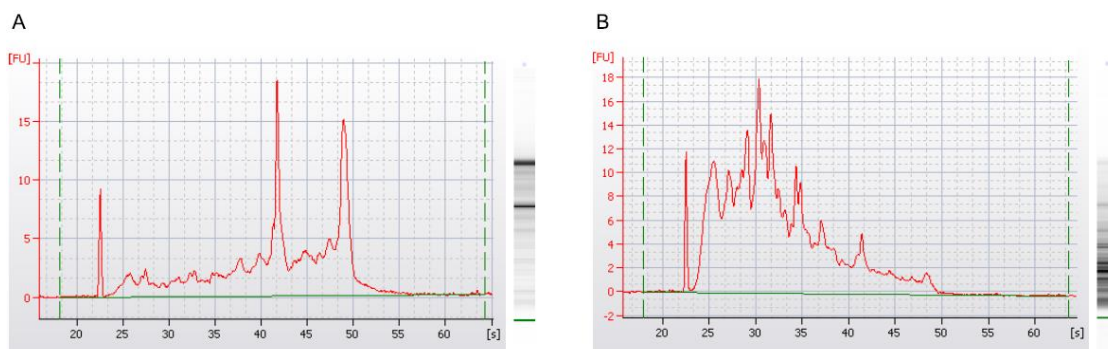


Figure 2.8. Bioanalyzer electropherograms and gel electrophoresis images from a good quality (A) and a degraded sample (B). Shown are the bioanalyzer results for the prefrontal cortex sample MS20 from the Douglas-Bell Canada Brain Bank with a RIN=8 (A; good quality) and the prefrontal cortex sample 50 from the MRC London Neurodegenerative Diseases Brain Bank with a RIN=2.6 (B; highly degraded).

RNA samples were run on the Bioanalyzer before and after clean-up (**Figure 2.9**) (see **Section 2.2.3**), in general confirming that the clean-up procedure improved the quality of the samples by removing heavily degraded RNA molecules. Final RIN numbers ranged between 1.9 and 8.3. The samples were characterized by relatively low RIN numbers, which is expected from post-mortem brain tissue that has variable post-mortem interval before dissection, and which has been stored for several decades and potentially subjected to several freeze-thaw cycles (Pidsley and Mill, 2011). The post-mortem human brain samples were prioritized for RNA sequencing based on RIN and concentration and the final cohort of samples used in the sequencing experiment had RIN numbers ranging between 4.2 and 8.3. The detailed quality and quantity information for each sample is further described in **Chapter 6 section 6.2.1**.

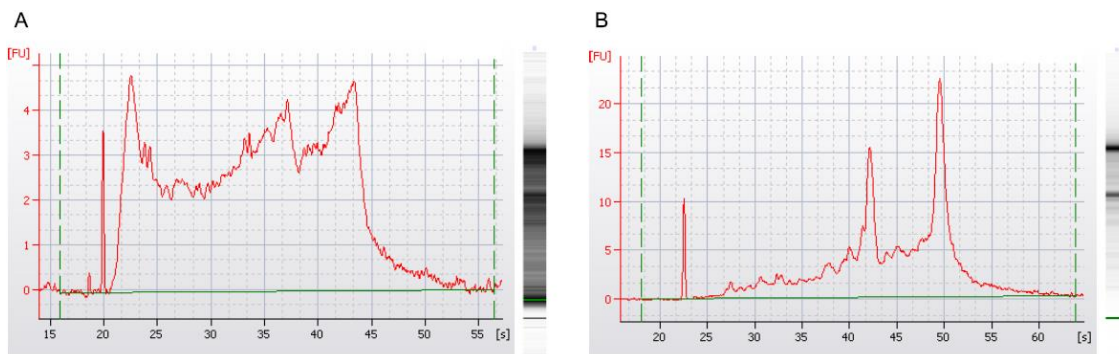


Figure 2.9. Bioanalyzer electropherograms and gel electrophoresis images from a sample which was successfully rescued in the clean-up process (see section 2.2.3). Shown are the bioanalyzer results for the prefrontal cortex sample 33 from the MRC London Neurodegenerative Diseases Brain Bank before (**A**; RIN= 2.4) and after (**B**; RIN =7.8) clean-up.

2.3. DNA methylation profiling

The mostly common used sequencing technologies are unable to distinguish between methylated and unmethylated cytosine residues due to their similar base-pairing characteristics. Sodium bisulfite (NaHSO_3) treatment of DNA molecules enables quantification of this modification through the deamination of non-methylated cytosines to uracil, which is then replaced by thymine during downstream procedures such as polymerase chain reaction (PCR). Methylated cytosines are protected from deamination, remaining as cytosines (Wang et al., 1980, Paul and Clark, 1996). **Figure 2.10** taken from the New England Biolabs (Ipswich, MA, USA) webpage (New England Biolabs, 2016) summarises the sodium bisulfite conversion process. A range of technologies can be subsequently used to quantify DNA methylation through comparison of expected and observed DNA sequences (Frommer et al., 1992). In this section I describe sodium bisulfite conversion followed by the different methods I utilised to profile DNA methylation across the research undertaken in this thesis.

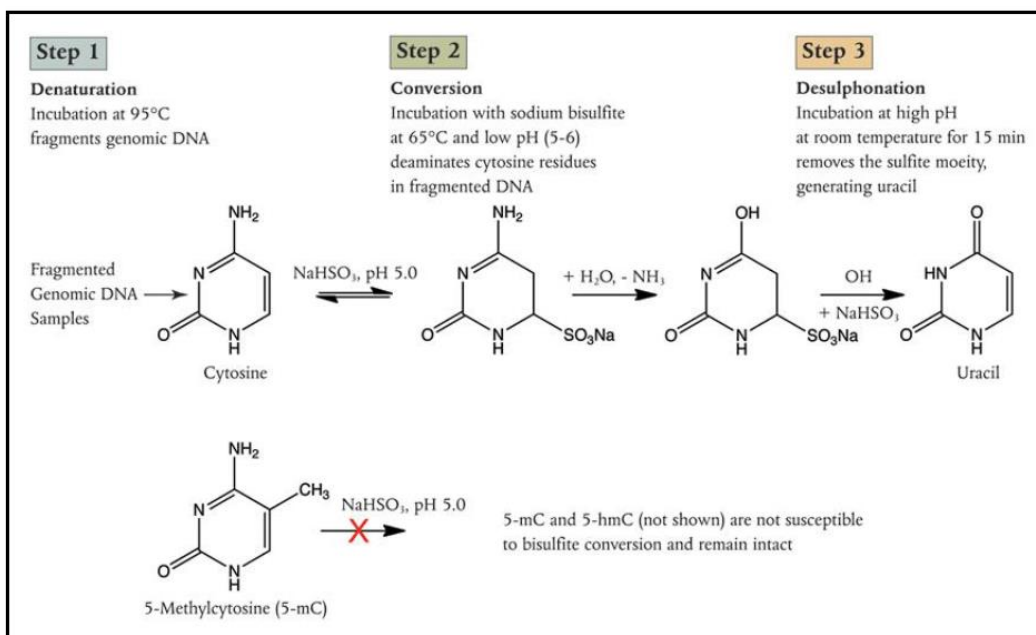


Figure 2.10. DNA sodium bisulfite treatment. Taken from New England Biolabs (Ipswich, MA, USA) webpage (New England Biolabs, 2016).

2.3.1. Sodium bisulfite conversion

Genomic human DNA was treated with sodium bisulfite using the EZ DNA Methylation-Gold Kit (Zymo Research, Irvine, CA, USA), according to manufacturer's instructions. **Figure 2.11** shows an overview of the experimental procedure (taken from Zymo Research webpage (2016)). Sodium bisulfite treated DNA was aliquotted and stored at -80°C until use in methylomic profiling.

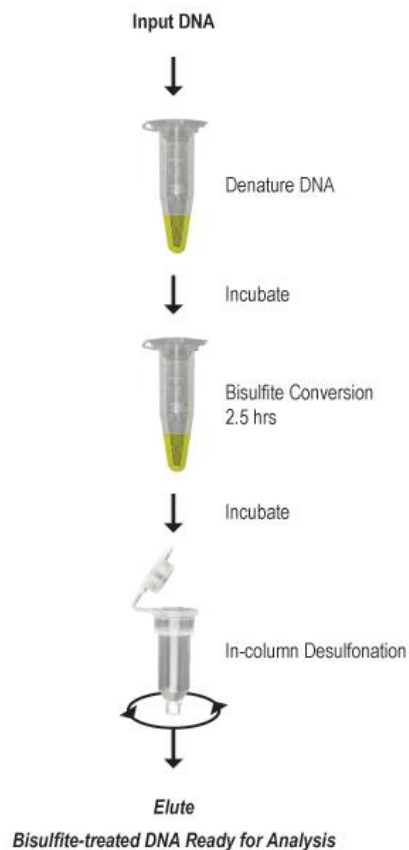


Figure 2.11. Overview of the sodium bisulfite treatment experimental procedure. Figure taken from Zymo Research webpage (2016).

2.3.2. Infinium HumanMethylation450 BeadChip

Following sodium bisulfite conversion, the human DNA samples used in this thesis were profiled using the Infinium HumanMethylation450 BeadChip (Illumina 450K array), scanned on an iScan Microarray Scanner (Illumina, San Diego, CA, USA) according to the manufacturer's instructions. The Illumina 450K array enables the quantification of DNA methylation levels at 485,577 CpG sites, covering 99% of RefSeq genes. The array also covers important regulatory regions such as CpG islands (96% covered), island shores and shelves, 5' and 3' UTRs, and promoters and gene bodies (Bibikova et al., 2011). The array uses two different types of chemistry, termed Infinium I and Infinium II probes. The first incorporates one of two probe types per CpG site with the same dye colour, one for the methylated (M) and the other for the unmethylated (U) state. The type I probe design is based on the assumption that the methylation status of CpG sites within 50bp are correlated with the query CpG (Illumina, 2015). This could be a source of bias when CpGs underlying the probe are not co-methylated with the query site.

The Infinium II probes use a single bead type with the DNA methylation state determined at the single base extension step after hybridization by two different dye colours (green for methylated sites and red for unmethylated sites). This design includes the addition of a degenerate R [A/G] base at underlying CpG sites, and therefore is less influenced by co-methylation patterns across nearby CpG sites.

2.3.2.1. Infinium HumanMethylation450 BeadChip data analysis

The DNA methylation level at each CpG site is determined by calculating the ratio of the intensity of the fluorescent signal for M (methylated) and U (unmethylated), which gives a β (DNA methylation) value for each site ranging from 0 (*i.e.* all cytosines at that site are unmethylated) to 1 (*i.e.* all cytosines at that site are methylated). The β value is calculated by the following equation:

$$\beta = \frac{\text{Intensity } M}{\text{Intensity } M + \text{Intensity } U + 100}$$

The Illumina 450K array has become one of the most popular methodologies to assess genome-wide DNA methylation in recent years. Considerable efforts

have been put into understanding the advantages and pitfalls of the technology. One of the disadvantages of using two types of probes is that they perform differently (Dedeurwaerder et al., 2011). For example, Infinium II probes are less accurate at detecting extreme levels of DNA methylation and present a larger variation across replicates than Infinium I probes. This realization led to the development of several normalisation methods and an ongoing debate about which analysis method is most suitable (Wang et al., 2015). Our research group has developed the *wateRmelon* package in R (Pidsley et al., 2013) which offers a range of normalisation function and tools that were used to pre-process and normalise the DNA methylation data presented in this thesis. Details on pre-processing and normalisation steps used in the DNA methylation datasets are described in **Chapter 3 sections 3.2.2 and 3.2.3.**

An additional issue is the presence of SNP variation within close proximity (10 base pairs (bp)) of the query CpG site. The DNA methylation data at these sites might be confounded by the polymorphism in the underlying genetic sequence (Chen et al., 2013, Price et al., 2013). Additionally, 6-8% of the probes in the array were found to cross-hybridise with other locations in the genome, not accurately estimating the DNA methylation levels at the annotated site (Chen et al., 2013, Price et al., 2013). Given these issues, two different research groups have developed additional annotation for the Illumina 450K array that allows the exclusion of cross-reactive and polymorphic probes from analysis. Details on the probe exclusion criteria and final number of probes included in the various analyses are present in **Chapter 3 section 3.2.3.**

A big confounder in epigenetic studies is the diverse (and variable) cell composition of different tissues or different samples (Jaffe and Irizarry, 2014). Even when working within the same brain region, different samples will have a different composition of neurons and other brain cells. Over recent years, researchers in the field have become increasingly more aware of the need to control for such differences. In 2013, our collaborators Guintivano and co-workers developed an algorithm to estimate neuronal composition from Illumina 450k human brain data (Guintivano et al., 2013). They identified cell epigenotype specific (*CETS*) markers based on DNA methylation differences between fluorescence-activated cell sorted (FACS) neuronal and non-neuronal nuclei. Using 10,000 *CETS* markers, they then developed and tested a method

to quantify the proportions of neurons and non-neurons as a proxy for cellular proportions. I used this approach to estimate neuronal to glia proportions in my datasets (and incorporated these estimates as covariates in subsequent analyses to control for cell composition differences across different samples with the exception of the cerebellum – see **Chapter 3 section 3.2.5**). The details on neuronal proportion estimates are presented in **Chapter 3 section 3.2.4**.

2.3.3. Bisulfite-PCR-pyrosequencing

In this thesis I used bisulfite-PCR-pyrosequencing to quantify DNA methylation across targeted regions and specific genomic regions identified using the 450K array (see **section 2.3.2**). The first step of this process is to treat the genomic DNA using sodium bisulfite (see **section 2.3.1**), followed by PCR to amplify specific target regions and pyrosequencing to quantify site-specific levels of DNA methylation.

2.3.3.1. Polymerase chain reaction

PCR is a method used to amplify a segment of DNA to generate thousands to millions copies of the same segment. These components are combined together and subject to cycles of heating and cooling in a thermocycler. During the first PCR step the mix is heated to a high temperature to activate the heat-sensitive polymerase taq. This is followed by three steps:

- 1) A denaturation step, where the mix is heated to 95°C to denature the double-stranded DNA;
- 2) An annealing step where the mix is cooled to a primer-specific temperature (usually between 50°C and 65°C) to allow the primers to anneal with high specificity to the correct annealing sequence in the DNA;
- 3) An elongation step at 72°C to allow the taq polymerase to synthesize the complementary strand of DNA using the deoxynucleotides (dNTPs).

These three steps are repeated for a number of cycles to allow the synthesis of an exponential number of DNA amplicons. The final number of amplicons will be 2^n , where n is the number of cycles. A final step at 72°C is added to allow a final extension.

Bisulfite-PCR uses bisulfite-converted genomic DNA as the reaction template (see **section 2.3.1**), which presents more of a challenge than using standard unconverted genomic DNA (Neumann, 2007) for a several reasons : i) extended sodium bisulfite incubations can lead to extensive damage to the DNA template; ii) bisulfite treatment leads to reduced sequence complexity (the DNA largely comprises three bases rather than four), leading to a higher redundancy of the target sequence; and iii) regions of interest often lie within CG-rich sequences, which become long stretches of thymines following bisulfite conversion, which can cause polymerase slippage. Together these consequences of sodium bisulfite treatment give a higher chance of mispriming and non-specific PCR amplification. This issue can be addressed with careful primer design, using the following criteria which are widely reported to be optimal for successful bisulfite-PCR:

1) Primers should not contain any CpG sites within their sequence to avoid discrimination between methylated or unmethylated DNA.

2) Primers should not be placed in a repetitive region.

3) Primers should contain non-CpG cytosines within their sequence to ensure exclusive amplification of bisulfite-converted DNA.

4) Primer length should be at least 20 bases long, to prevent non-specific amplification.

The cycling conditions, primer sequences and PCR reagents used in this thesis are presented in **Chapter 3 section 3.2.10**. The reagents used in the PCR reactions in this thesis, together with their description and quantities in a standard PCR reaction, are described in **Table 2.2**. **Table 2.3** describes the standard thermocycling conditions of a PCR reaction.

Table 2.2. Polymerase chain reaction (PCR) reagents and quantities used in this thesis.

Component	Function	PCR reagent (concentration)	Quantity (μ l)
Genomic DNA	Single-stranded sodium bisulfite converted genomic DNA provides the template for the PCR reaction	Sodium bisulfite converted DNA (see section 2.3.1) (10ng/ μ l)	2
DNA primers	Short, single-stranded oligonucleotides complementary to the target sequence	Forward and reverse primer mix (10 μ M)	2
DNA nucleotides	Nucleotide bases required for the synthesis of new DNA strands	dNTPs (2.5mM)	0.4
<i>Taq</i> DNA polymerase	Heat-resistant enzyme that extends primers to synthesize new DNA strands complementary to the target sequence using DNA nucleotides	Qiagen HotStar <i>Taq</i> Polymerase (5 units/ μ l) (Qiagen, Venlo, Holland)	0.15
PCR buffer	Buffer that maintains optimal pH for PCR reaction	10 x PCR buffer	2
Magnesium Chloride (MgCl ₂)	Required for <i>Taq</i> DNA polymerase function	MgCl ₂ (25mM)	0.4
Rnase/Dnase free water	Ensures consistent reaction volume	Water to a final volume of 20 μ l	13.05

Table 2.3. Standard polymerase chain reaction thermocycling conditions.

Step	Function	Temperature ($^{\circ}$ C)	Time
1. Initiation	DNA mix is heated to activate the <i>Taq</i> . Hot-start <i>Taq</i> reduces mispriming and primer-dimer formation	95	15 minutes
2. Denaturation	High temperatures denature the double stranded DNA into single stranded DNA	95	20 seconds
3. Annealing	Lower temperatures allow the primers to anneal. Annealing temperature is selected carefully - too high and the primers are unable to anneal, too low and non-specific amplification occurs.	50 - 65	30 seconds
4. Extension	<i>Taq</i> DNA polymerase uses dNTPs to build the complementary DNA strand	72	1 minute
5. Final extension	Remaining single stranded DNA is fully extended	72	3 minutes
6. Finish	Products are kept at low temperatures	4	∞

2.3.3.2. Agarose gel electrophoresis

Agarose gel electrophoresis is a commonly used technique for the separation of DNA molecules based on their size. It is most commonly used to assess the quality and quantity of DNA and determining the success of molecular biology techniques such as PCR amplification. An agarose gel is a three-dimensional matrix containing pores through which molecules can pass. The gel is obtained by melting agarose powder at a concentration that can typically range from 0.8 to 1.0%, in tris-borate EDTA (TBE) buffer. The concentration of agarose influences the size of the pores in the matrix; therefore the concentration of agarose selected is dependent on the size of molecule to be separated. After addition of a DNA sample to the gel matrix, an electrical charge is applied across it, causing the negatively charged DNA to migrate towards the positive terminal, at a speed determined by the DNA fragment size. Smaller molecules are able to move through the matrix faster, and move further through the gel. The separated DNA is then viewed using a stain, most commonly ethidium bromide, which intercalates into the DNA structure allowing it to be visualised under UV light. The UV light is absorbed by the ethidium bromide and re-emitted as visible light, allowing the fragments the DNA to be observed. In this thesis, agarose gel electrophoresis was used for the inspection of PCR products (see **section 2.3.3.1**) using a 1.5% gel. **Figure 2.12** shows an example of an agarose gel used to inspect PCR amplification products.



Figure 2.12. Example of an agarose gel used to inspect polymerase chain reaction (PCR) amplification products. All samples amplified successfully during PCR except for sample 3. L, 1,000bp ladder, W, water (negative control).

2.3.3.3. Bisulfite-pyrosequencing

Pyrosequencing is a highly-sensitive ‘sequencing-by-synthesis’ technique often used to quantify DNA methylation at individual CpG sites in short DNA fragments (<200bp). The method works by monitoring the real-time incorporation of nucleotides via detection of the light signal resulting from the release of pyrophosphate molecules (PPi) during DNA elongation (Tost and Gut, 2007). DNA methylation analysis by pyrosequencing uses single-stranded, biotin-labelled bisulfite-PCR amplicons as a template (see **section 2.3.3.1**).

Figure 2.13 adapted from the Qiagen website (Qiagen, 2016) illustrates the principles of pyrosequencing. In summary:

1) A sequencing primer is hybridised to the template and incubated with DNA polymerase, ATP sulfurylase, luciferase, and apyrases, substrates, adenosine 5′ phosphosulphate (APS) and luciferin.

2) dNTPs are then dispensed sequentially, and release PPi molecules when incorporated into the DNA elongation strand, in a quantity equimolar to the amount of incorporated nucleotide.

3) In the presence of APS, ATP-sulfurylase converts PPi to ATP which provides energy for luciferase to generate visible light in amounts that are proportional to the amount of ATP. The luminescence is detected by a charge

couple device chip and visualised as a peak in the raw data output with a height proportional to the number of nucleotides incorporated.

4) Unincorporated dNTPs and ATPs are continuously degraded by a nucleotide-degrading enzyme, apyrase.

In the work carried out in this thesis, bisulfite-pyrosequencing primers (specific to bisulfite-converted DNA) were designed using the PyroMarkQ24 Assay Design Software version 2.0 (Qiagen, Venlo, Holland). A biotin label was incorporated into the primer to allow capture of single-strands of DNA. For each sample, PCR was performed in duplicated as described in **section 2.3.3.1**. Subsequently, 10µl of each PCR duplicate were mixed to make a total of 20µl PCR product for each sample. The PCR products were incubated for 10 minutes with Streptavidin Sepharose beads (Qiagen, Venlo, Holland) to immobilise and capture the biotin-labelled DNA strands. This was followed by washes in 70% ethanol (Sigma-Aldrich Corporation, St. Louis, MO, USA), denaturation solution (0.2M NaOH), and Pyromark wash buffer (Qiagen, Venlo, Holland). Denatured PCR products were then sequenced using 0.3µM sequencing primer and Qiagen Pyromark enzyme and substrate in a PyroMark Q24 Instrument (Qiagen, Venlo, Holland). Details about the assays, primers and conditions used for pyrosequencing are presented in **Chapters 3 section 3.2.10** and **Chapter 7 Materials and Methods**. For an example of a pyrogram trace see **Figure 3.15** in **Chapter 3 section 3.2.10**.

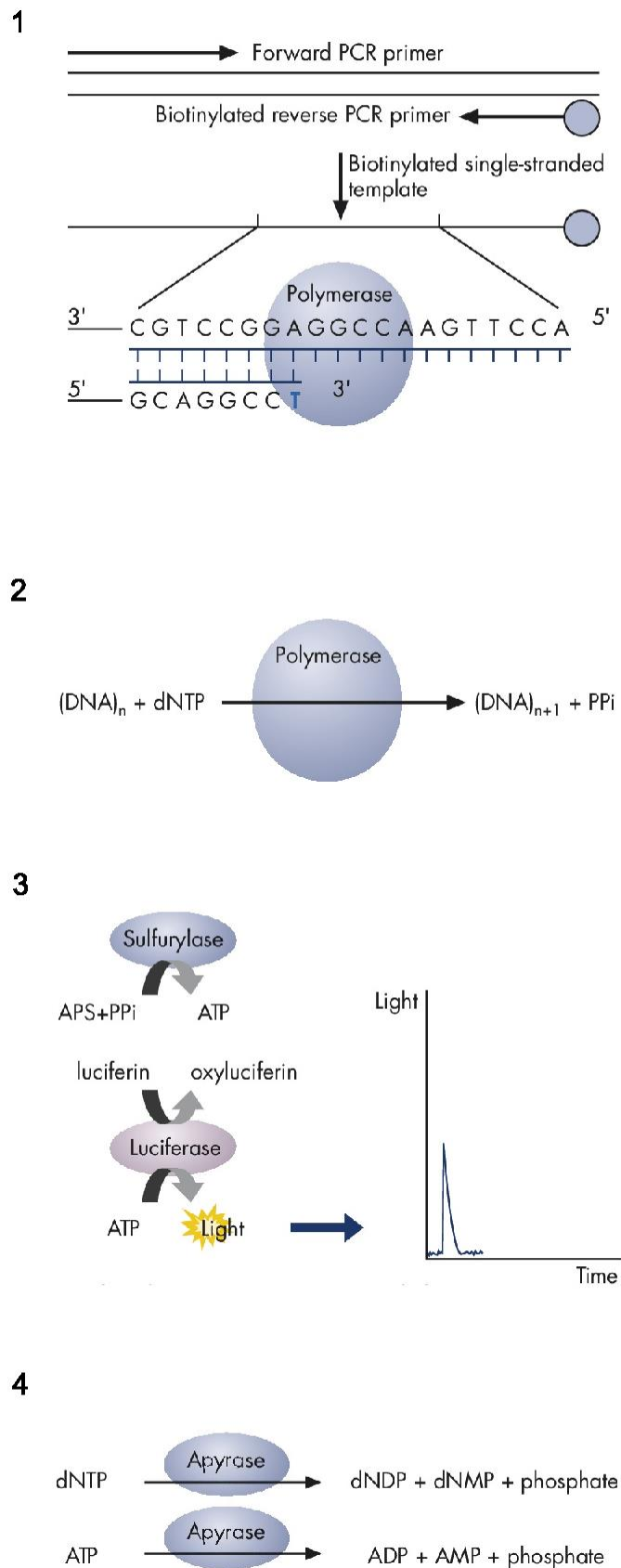


Figure 2.13. The principles of pyrosequencing. Figure adapted from the Qiagen website (Qiagen, 2016).

2.4. Genome-wide SNP profiling

In this section I describe the method used to profile common genetic common variation and calculate schizophrenia polygenic risk score in the samples used in **Chapters 3 to 6**. The samples were genotyped using the Infinium HTS HumanOmniExpress-24 BeadChip Kit v1-0 and processed on an iScan Microarray Scanner (Illumina, San Diego, CA, USA), according to manufacturer's instructions. The array was designed to analyse up to 750,000 SNPs and copy number variant (CNV) markers across the genome. Similarly to the 450K array described above, the Illumina OmniExpress SNP array uses two different types of Infinium probes. In the type I probe, the 3' end of the primer overlaps with the SNP site and the intensity signal is only generated if there is a perfect match and extension occurs. In the type II probe, the 3' end of the primer is positioned directly adjacent to the SNP site, or in the case of a non-polymorphic probe, directly adjacent to the non-polymorphic site (Illumina, 2013). Allele-specific single base extension of the primer incorporates a biotin nucleotide (in case of a C or G) or a dinitrophenyl labelled nucleotide (in case of an A or T). The overall signal-to-noise ratio is improved by signal amplification of the incorporated label. The details of SNP array data quality control and analysis are described in **Chapter 4 section 4.2.1**.

2.5. Transcriptome profiling

In this section I describe the methods used to profile the transcriptome of the samples used in **Chapter 6** using highly-parallel RNA sequencing (RNA-seq). The first step of RNA-seq is to create libraries of double stranded DNA (cDNA) complementary to messenger RNA (mRNA) molecules. Before library preparation it is necessary to remove all ribosomal RNA (rRNA) present in the sample that could confound the quantification of mRNA molecules. The method used for this step depends primarily on the quality of the sample. I used rRNA depletion given the low quality of RNA retrieved from a number of the post-mortem brain samples (see **Chapter 6 section 6.2.1**). RNA depletion enables subsequent sequencing of all non-rRNA molecules including mRNA molecules that are not intact, being ideal for partially-degraded RNA samples. I will first describe the method used for complementary DNA (cDNA) library preparation followed by RNA sequencing (RNA-seq).

2.5.1. Complementary DNA libraries preparation

To prepare cDNA libraries from total RNA from post-mortem brain tissue, I used the TruSeq Stranded Total RNA with Ribo-Zero Gold Library Preparation LT kit (Illumina, San Diego, CA, USA). The protocol was carried following manufacturer's instructions. The human cDNA libraries were prepared by myself in conjunction with Audrey Farbos, a research technician from the Exeter Sequencing Service.

The protocol consists in the following six steps (**Figure 2.14**):

- 1) **Deplete and fragment RNA** – this step aims to remove rRNA using biotinylated, target-specific oligos combined with Ribo-Zero rRNA removal beads. The specific kit used in my analyses (Gold) depletes samples of both cytoplasmic and mitochondrial rRNA. After the rRNA is depleted, the remaining RNA is purified, fragmented, and primed for cDNA synthesis.
- 2) **First strand cDNA synthesis** – in this step the cleaved RNA fragments are copied into first strand cDNA using reverse transcriptase and random primers.
- 3) **Second strand cDNA synthesis** - this process removes the RNA template and synthesizes a replacement strand, incorporating dUTP in place of dTTP to generate double stranded cDNA. At the end of this step we have blunt ended DNA.
- 4) **Adenylate 3' ends** - A single 'A' nucleotide is added to the 3' ends of the blunt cDNA fragments to prevent them from ligating to each other during the ligation of the adapter. A corresponding single 'T' nucleotide on the 3' end of the adapter provides a complementary overhang for ligating the adapter to the fragment. This strategy ensures a low rate of chimera (concatenated template) formation.
- 5) **Ligate adapters** - this process ligates multiple indexing adapters to the ends of the cDNA. The adapters are known barcode DNA sequences that allow the labelling and posterior identification of individual samples.
- 6) **PCR amplification** - the labelled cDNA fragments are then purified and enriched with PCR to create the final cDNA library.

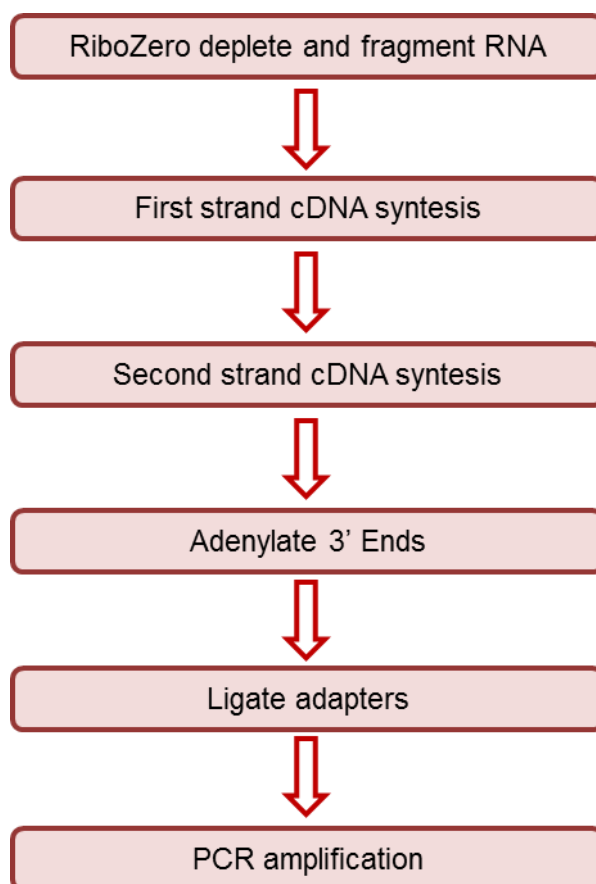


Figure 2.14. Overview of the complementary DNA libraries preparation protocol.

2.5.2. cDNA libraries quantification and pooling

After preparation, the cDNA libraries were quantified using D1000 ScreenTapes (Agilent Technologies, Santa Clara, CA, USA) processed on a 2200 TapeStation Instrument (Agilent Technologies, Santa Clara, CA, USA), according to manufacturer's instructions. The TapeStation uses an electrophoresis-based approach to analyse DNA or RNA, giving an accurate measure of quality and fragment size. The tape used allows the analysis of DNA fragments ranging from 35 to 1000bp. The cDNA libraries prepared should have an average fragment size of 260-300bp. **Figure 2.15** shows an example of the tape gel electrophoresis and electropherogram of a cDNA library. To quantify cDNA molarity and fragment size I isolated the region from 150 to 900bp (red in **Figure 2.15 B**) in the TapeStation Instrument software. I also isolated the region from 50 to 150bp (green in **Figure 2.15 B**) to make sure there was no contamination of small fragment DNA. Specific details on the

quantification of the resulting cDNA libraries are presented in **Chapter 6 section 6.2.2**.

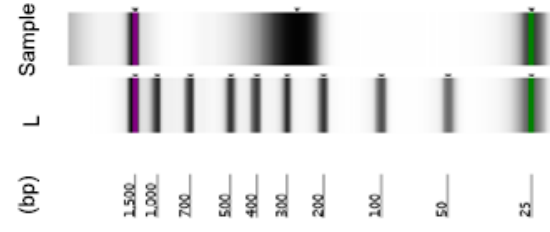
2.5.3. RNA sequencing

The sequencing of the libraries was performed using the Illumina HiSeq 2500 Ultra-High-Throughput Sequencing System (Illumina, San Diego, CA, USA), which performs next generation sequencing (NGS). NGS allows the massive parallel sequencing of millions of DNA molecules at the same time and developed from Sanger sequencing, a gold-standard method developed by Frederick Sanger in the 1970s (Sanger et al., 1977).

Following the library preparation steps described above (**section 2.5.1**), the libraries were loaded into a flow cell for cluster generation by bridge amplification. In the flow cell, the cDNA fragments are captured on a lawn of surface-bound oligos complementary to the library adapters. Each fragment is then amplified into distinct clonal fragments and ready for sequencing. Each cluster of clonal molecules will act as an individual sequencing reaction.

Illumina NGS chemistry is a sequencing-by-synthesis method (SBS). Briefly, a fluorescently labelled reversible terminator is imaged as each dNTP is added, and then cleaved to allow incorporation of the next base. Since all 4 reversible terminator-bound dNTPs are present during each sequencing cycle, natural competition minimizes incorporation bias. We performed paired-end sequencing, which involves sequencing both the forward and reverse template strands of each cDNA fragment. This increases the accuracy when aligning the data to a reference genome, especially in repetitive areas of the genome. **Figure 2.16**, taken from Martin and Wang (2011) show the workflow of a typical RNA-sequencing experiment. Details on RNA-sequencing and data analysis can be found in **Chapter 6 sections 6.1 and 6.2**.

A



B

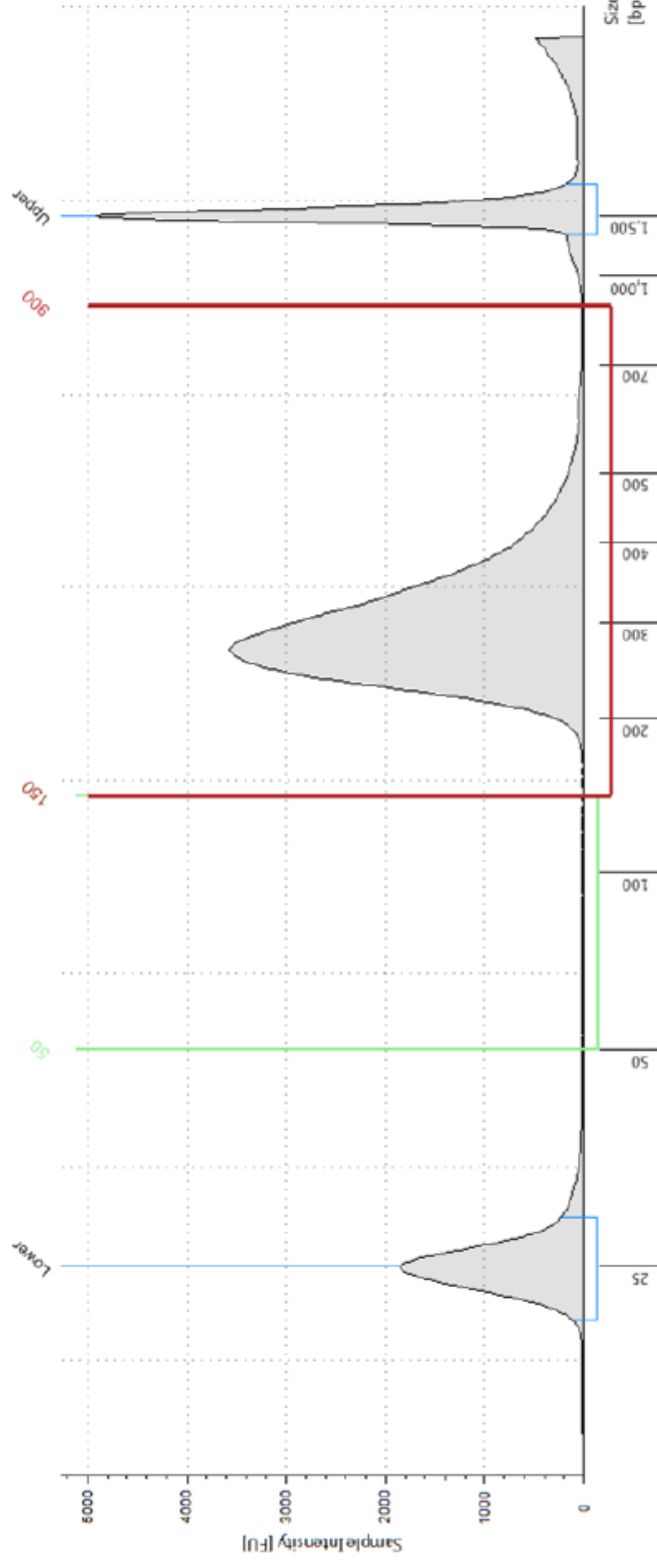


Figure 2.15. Example of a D1000 ScreenTape gel electrophoresis (A) and electropherogram (B) of a complementary DNA (cDNA) library. Shown is the cDNA library quantification of the sample 9 from the MRC London Neurodegenerative Diseases Brain Bank. The electropherogram (B) shows the lower and upper marker, the region (red) between 150 and 900bp used for quantification, and the region (green) between 50 and 150bp used to guarantee there was no small fragment cDNA contamination. L, ladder, bp, base pairs.

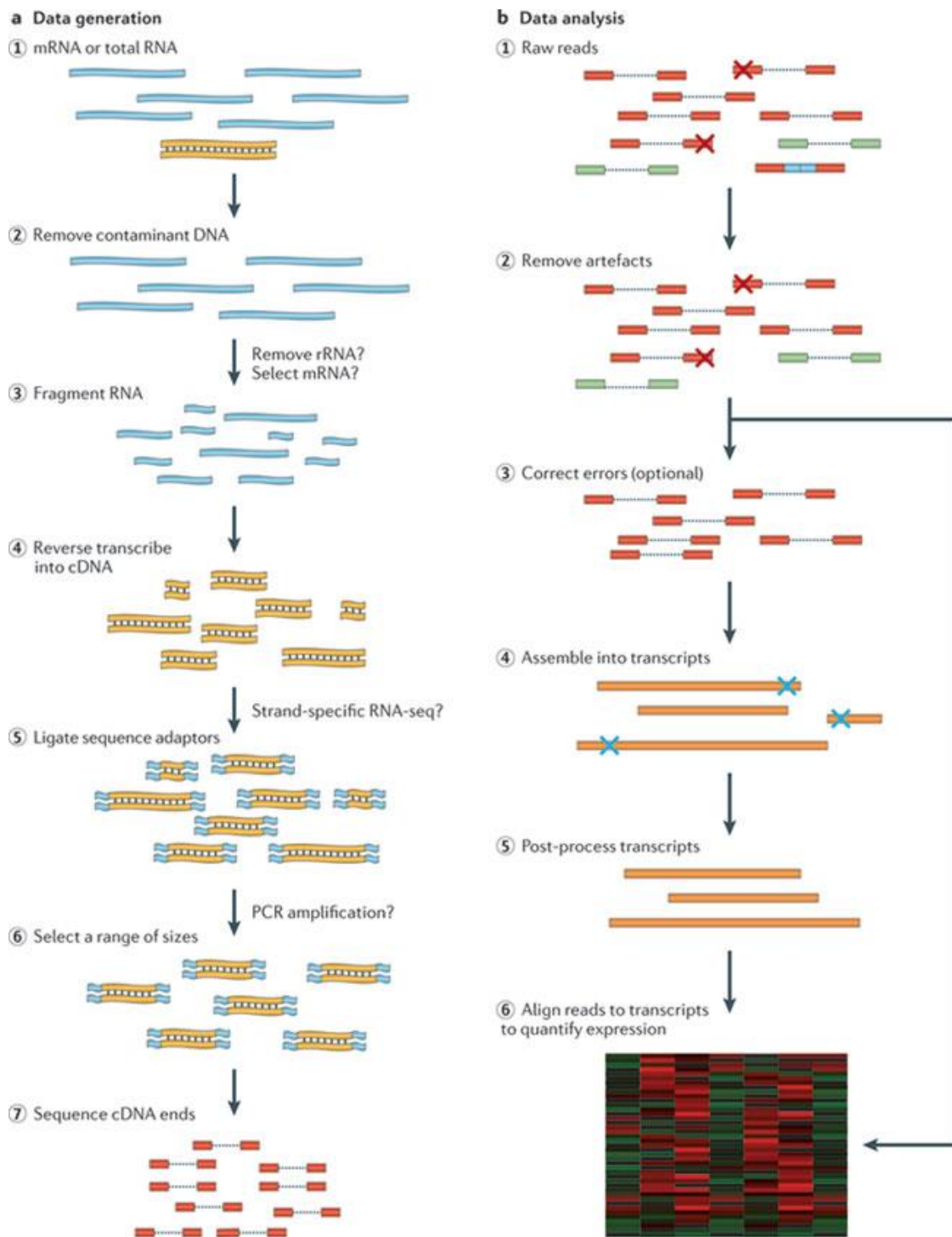


Figure 2.16. The data generation and analysis steps of a typical RNA sequencing experiment. Figure and legend taken from Martin and Wang (2011).

Chapter 3 - Methylomic profiling of schizophrenia in the brain

3.1. Introduction

Schizophrenia is a severe neurodevelopmental disorder, characterized by episodic psychosis, hallucinations, delusion and altered cognitive function (Burmeister et al., 2008). The disorder affects more than twenty-one million people worldwide contributing significantly to the global burden of disease (World Health Organization, 2013, World Health Organization, 2015). Twin and family studies have highlighted a notable heritable component to schizophrenia (Craddock et al., 2005), however the role of genetic variation in the etiology of the disorder is complex. Rare, highly penetrant mutations have been implicated in some cases of schizophrenia; these include copy number variants (Stefansson et al., 2014), *de novo* coding mutations (Xu et al., 2011, Purcell et al., 2014), or genomic translocations (St Clair et al., 1990). In most cases of schizophrenia, however, susceptibility is attributed to the combined action of multiple common genetic variants of low penetrance (Schizophrenia Working Group of the Psychiatric Genomics, 2014).

A growing body of evidence suggest that schizophrenia has its origins during neurodevelopment. Several of the most robustly supported schizophrenia susceptibility genes have known roles in early brain development and appear to impact on schizophrenia risk during this period (Kirov et al., 2009, Hill and Bray, 2012). Furthermore, epidemiological studies have shown that prenatal environmental insults are also important, with established associations between hypoxia (Cannon et al., 2002), maternal infection (Brown and Derkits, 2010), maternal stress (Khashan et al., 2008), and maternal malnutrition or famine (Susser et al., 1996) and risk for developing schizophrenia. These observations have led to a growing interest in the role of developmentally regulated epigenetic variation in the molecular etiology of schizophrenia (Dempster et al., 2013). Despite the advances in understanding the genetic and environmental epidemiology of schizophrenia, little is known about the mechanisms by which schizophrenia risk factors interplay and mediate disease susceptibility in the brain.

Improved understanding of the biology of the genome has led to increased interest in the role of non-DNA sequence-based variation in the etiology of neurodevelopmental phenotypes, including schizophrenia. Epigenetic processes have been hypothesised to mediate associations between genetic risk burden, environmental risk exposure and phenotype. Furthermore, a growing number of studies provide evidence for the dysregulation of epigenetic mechanisms in complex psychiatric disorders (Labrie et al., 2012, Pidsley and Mill, 2011, Dempster et al., 2013, Fullard et al., 2016). The notion that epigenetic processes are involved in the onset of schizophrenia is supported by recent methylomic studies of disease-discordant monozygotic twins (Dempster et al., 2011), clinical sample cohorts (Aberg et al., 2014), and post-mortem brain tissue (Mill et al., 2008, Jaffe et al., 2016, Pidsley et al., 2014). To date, such studies have primarily focused on DNA methylation at CpG dinucleotides, as this is the best characterised and most stable epigenetic modification. To date, studies characterizing schizophrenia-associated methylomic variation have been limited by small sample number or the assessment of a single brain region (Chen et al., 2014, Numata et al., 2014, Wockner et al., 2014, Pidsley et al., 2014, Jaffe et al., 2016, Ruzicka et al., 2015).

A previous study by our group investigated schizophrenia-associated methylomic variation in the adult brain and its relationship to changes in DNA methylation during human fetal brain development (Pidsley et al., 2014). The data presented in that initial study strongly support the hypothesis that schizophrenia has an important early neurodevelopmental component, and suggest that epigenetic mechanisms may mediate the relationship between neurodevelopmental disturbances and risk of disease. In this chapter I describe a follow-on study using additional post-mortem brain samples dissected from multiple regions of the brain.

3.2. Methods

3.2.1. Samples

I obtained tissue from three human post-mortem brain banks to study methylomic variation associated with schizophrenia. Each cohort comprises of multiple brain regions from schizophrenia patients and non-psychiatric controls. The use of these samples in the research presented here was approved by the University of Exeter Medical School Research Ethics Committee (reference number 13/02/009).

3.2.1.1. Medical Research Council London Neurodegenerative Diseases Brain Bank

The MRC London Neurodegenerative Diseases Brain Bank (LNDBB) (MRC London Neurodegenerative Disease Brain Bank website, 2016) was established in 1989 in the Department of Neuropathology, Institute of Psychiatry, King's College London and is part of the United Kingdom (UK) Brain Banks Network funded by the Medical Research Council (MRC). It primarily focuses on neurodegenerative diseases including Alzheimer's disease, Frontotemporal dementias and Motor Neurone Disease but it also holds a number of other disease collections including various movement disorders, HIV, autism and schizophrenia. I obtained post-mortem prefrontal cortex (PFC; Brodmann Area (BA) 9), cerebellum (CER), striatum (STR; putamen) and hippocampus (HC) samples from a total of 23 schizophrenia patients and 29 non-psychiatric controls who donated their brains to the LNDBB. Subjects were approached in life for written consent for brain banking, and all tissue donations were collected and stored following legal and ethical guidelines (National Health Service reference number 08/MRE09/38; the Human Tissue Authority license number for the LNDBB brain bank is 12293). Samples were dissected by a trained neuropathologist, snap-frozen and stored at -80°C. Schizophrenia patients were diagnosed by trained psychiatrists according to Diagnostic and Statistical Manual of Mental Disorders (DSM) criteria (for the latest edition see American Psychiatric Association (2013)). In the beginning of this project I visited the LNDBB and personally collected relevant information from the medical records of these samples.

3.2.1.2. Douglas Bell-Canada Brain Bank

The Douglas-Bell Canada Brain Bank (DBCBB) (Douglas-Bell Canada Brain Bank website, 2016) was established in 1980 and is based at the Douglas Mental Health University Institute (a McGill University affiliate), Montreal, Québec, Canada. The bank collects brains from people who suffered from different neurodegenerative diseases such as Parkinson's disease, Alzheimer's disease, and other dementias, as well as diverse mental disorders, including schizophrenia, major depression, bipolar disorder, and substance use disorders. I obtained post-mortem PFC (BA9), CER and STR (putamen) samples from a total of 18 schizophrenia patients and 18 non-psychiatric controls who donated their brains to the DBCBB. Samples were collected post-mortem following consent obtained with next of kin, according to tissue banking practices regulated by the Quebec Health Research Fund, and based on the Organisation for Economic Co-operation and Development (OECD) Guidelines on Human Biobanks and Genetic Research Databases. Samples were dissected by neuropathology technicians, snap-frozen and stored at -80°C. Psychiatric diagnoses were based on best-estimate diagnostic procedures, following Structured Clinical Interviews for DSM Disorders I (SCID I) (for the latest edition see American Psychiatric Association (2013)) conducted with informants.

3.2.1.3. Medical Research Council Edinburgh Brain and Tissue Banks

The Edinburgh Brain and Tissue Banks (EBTB) (Edinburgh Brain and Tissue Banks website, 2016) were established in 1990 at the University of Edinburgh, UK. The banks are part of the UK Brain Banks Network funded by the MRC and include Creutzfeldt-Jakob disease, human immunodeficiency virus, stroke, motor neurone disease, dementia and sudden death banks. I obtained post-mortem PFC (BA9), CER, basal ganglia (STR)¹ and HC samples from a total of 8 schizophrenia patients and 9 non-psychiatric controls who donated their brains to the EBTB. All individuals died suddenly and unexpectedly and the next-of-kin of all individuals authorised the use of the tissue for research

¹ As the EBTB could not clarify which part of the basal ganglia the samples were collected from I will refer to these samples as STR for simplicity.

purposes by completing and signed an Authorisation Form, confirming their wish of donating the brains (consistent with the requirements of the Human Tissue (Scotland) Act 2006). All samples were collected and stored in accordance with good clinical practice requirements, legal and ethical guidelines. The medical records of all schizophrenia cases were assessed by two Consultant Psychiatrists and diagnosis made according to DSM criteria (for the latest edition see American Psychiatric Association (2013)). The samples stored in the Edinburgh Banks are fully authorised for research by families and ethically approved for research use in accordance with the terms of current UK Human Tissue legislation. The Brain Bank has local Research Ethics Committee approval (LREC 2003/8/37) and works within the legal framework of the Human Tissue (Scotland) Act 2006.

Figures 3.1 to 3.4 show the anatomical location of the PFC (**A**), basal ganglia (including the STR; putamen) (**B**), HC (**C**) and CER (**D**) in the human brain, respectively. An overview of the functions of each of these brain regions and their relevance to schizophrenia is given in **Chapter 1 Section 1.1.2**. Demographic data of all samples is presented in **Appendix A - Supplementary Table 1**. DNA was isolated from tissue samples as described in the **Chapter 2 section 2.2**. Briefly, genomic DNA was isolated using a standard phenol-chloroform extraction protocol and tested for degradation and purity using spectrophotometry. 500 ng DNA from each sample was treated with sodium bisulfite using the EZ-96 Gold DNA methylation kit (Zymo Research, Irvine, CA, USA). DNA methylation was quantified using the Illumina Infinium HumanMethylation450 BeadChip (Illumina, San Diego, CA, USA) run on an Illumina HiScan System (Illumina, San Diego, CA, USA) using the manufacturers' standard protocol. **Appendix A - Supplementary Table 2** includes sentrix barcode ID information for all samples.

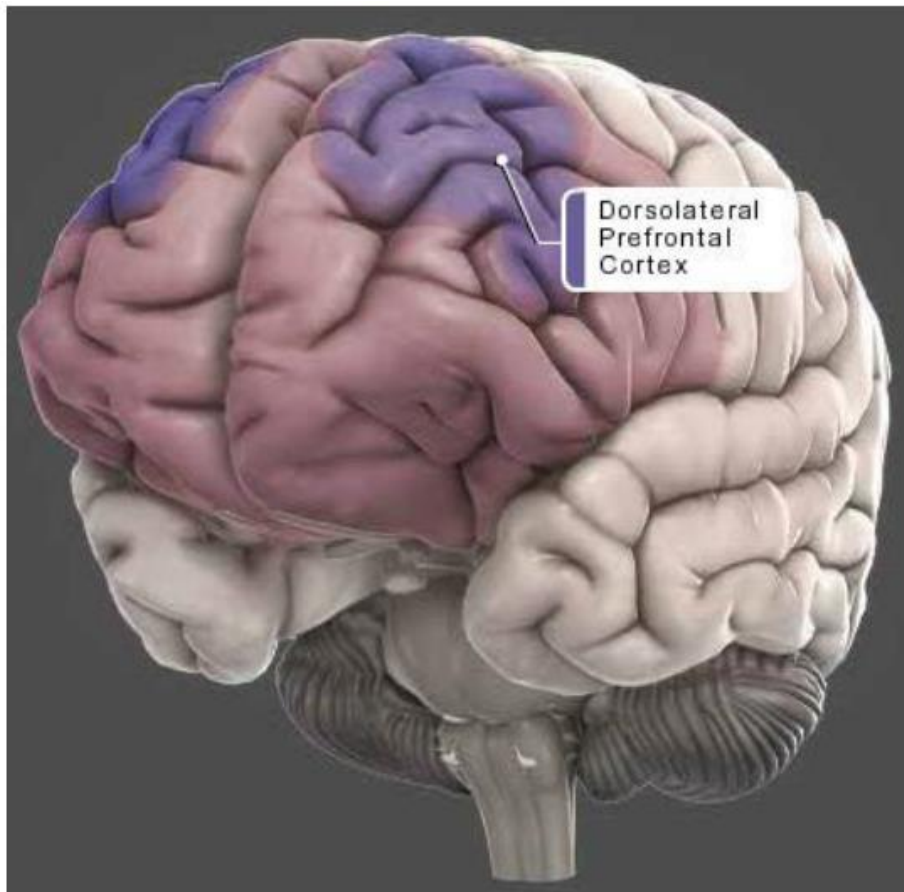


Figure 3.1. Figure showing the anatomical location of the prefrontal cortex in the human brain. Adapted from Genes to Cognition Online (Cold Spring Harbor Laboratory, 2009).

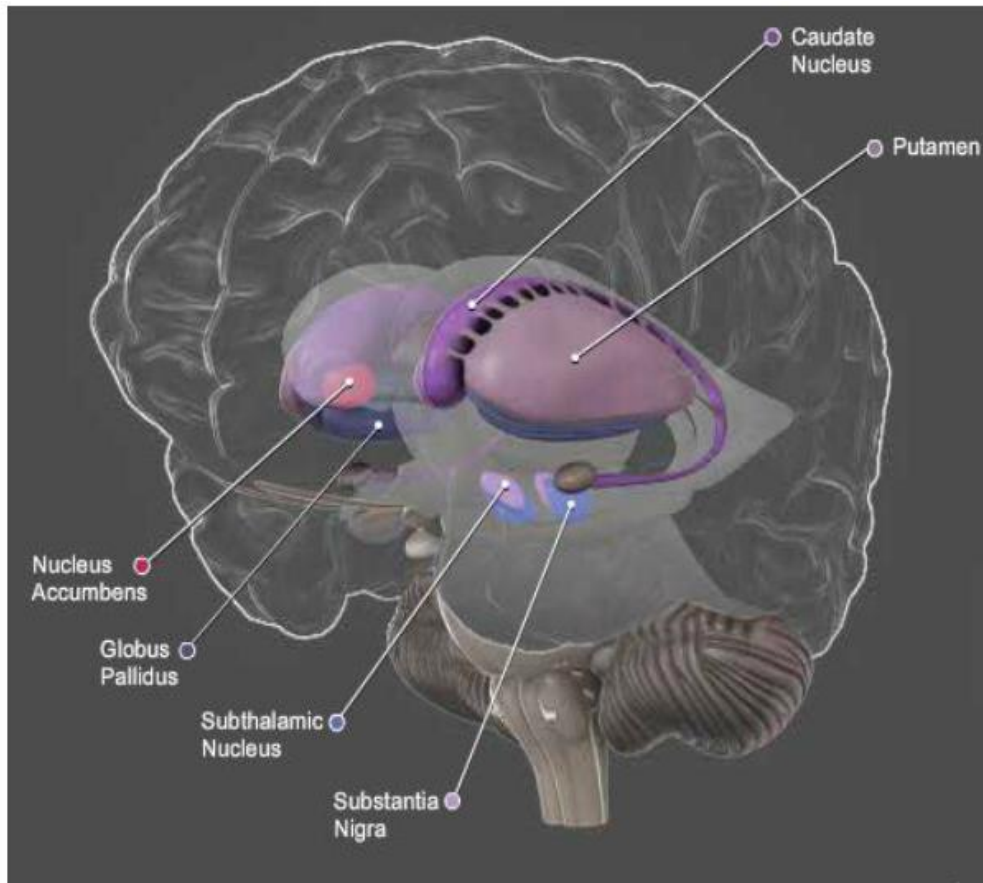


Figure 3.2. Figure showing the anatomical location of the basal ganglia (including the putamen) in the human brain. Adapted from Genes to Cognition Online (Cold Spring Harbor Laboratory, 2009).

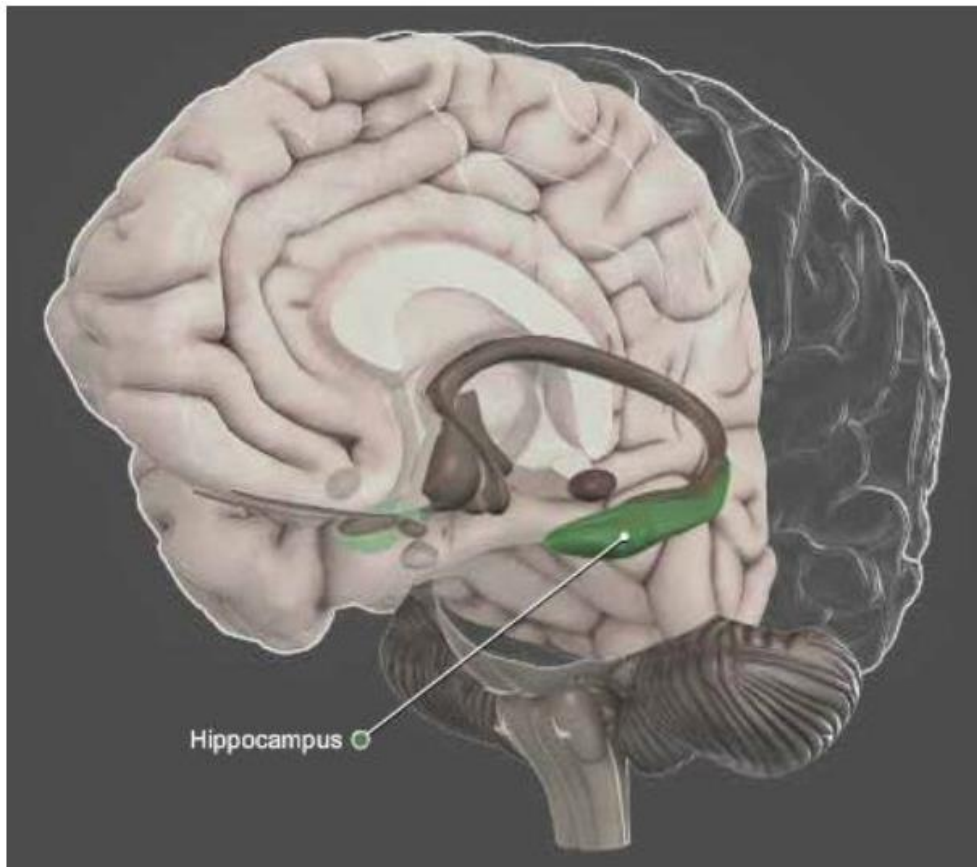


Figure 3.3. Figure showing the anatomical location of the hippocampus in the human brain. Adapted from Genes to Cognition Online (Cold Spring Harbor Laboratory, 2009).

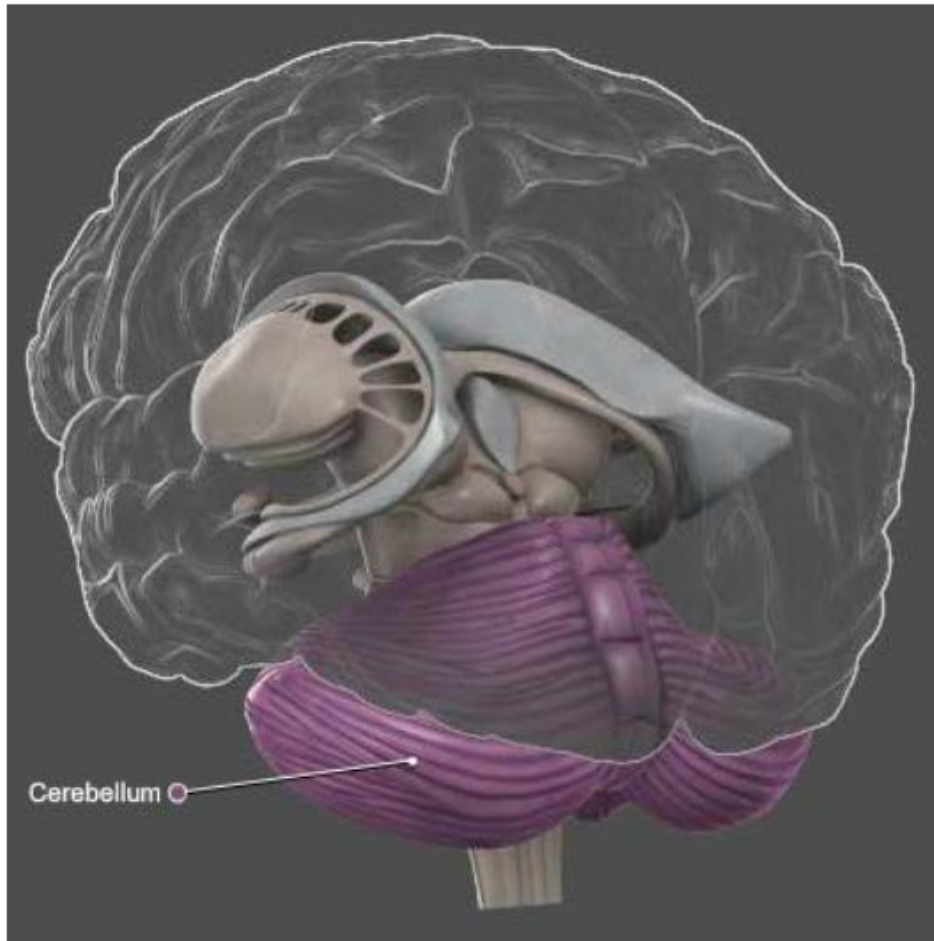


Figure 3.4. Figure showing the anatomical location of the cerebellum in the human brain. Adapted from Genes to Cognition Online (Cold Spring Harbor Laboratory, 2009).

3.2.2. Samples and cohort quality control

Quality control (QC) and normalisation steps were performed on the raw Illumina 450K array data generated from the three cohorts separately. Signal intensities for each probe were extracted using Illumina *GenomeStudio* software (Illumina, San Diego, CA, USA) and imported into R (R Core Team, 2015) using the *methyumi* and *minfi* packages (Aryee et al., 2014, Davis S, 2015). The standard deviation across all samples from all cohorts and brain regions was calculated for each probe. The thousand probes with highest standard deviation across all samples were plotted to visualise differences across brain regions and sample cohorts (**Figure 3.5**).

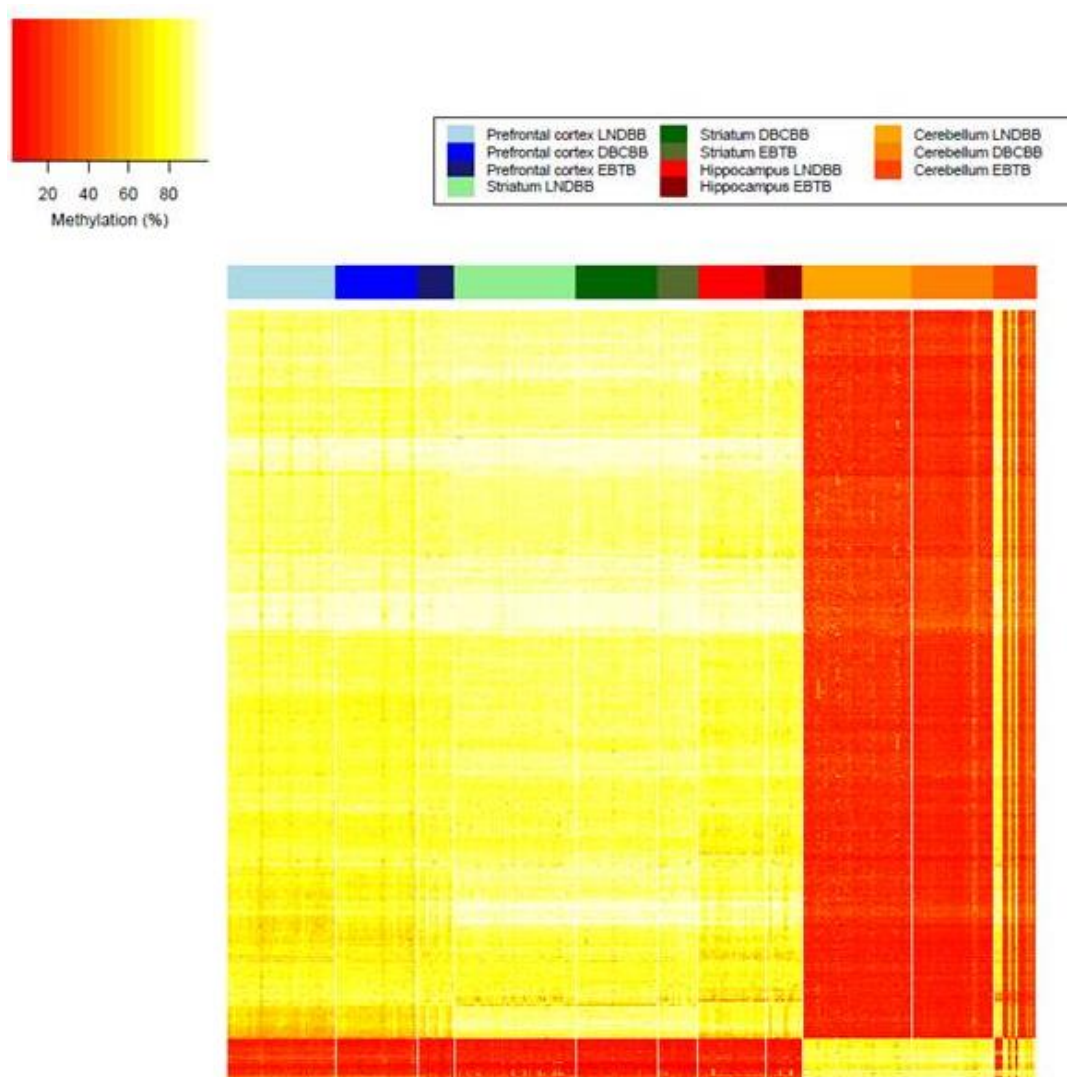


Figure 3.5. Hierarchical clustering of the thousand most variably-methylated probes across all samples. LNDBB, MRC London Neurodegenerative Diseases Brain Bank; DBCBB, Douglas-Bell Canada Brain Bank; EBTB, Edinburgh Brain and Tissue Banks.

As expected, all brain regions show distinct DNA methylation profiles that are consistent across cohorts, with the CER being a clear outlier, concurring with data from previous studies (Davies et al., 2012, Hannon et al., 2016, Ladd-Acosta et al., 2007). Of note, ES12, ES13, ES14, ES15, ES16 and ES18 CER samples from the EBTB cohort appear considerably different from the CER samples from the other two cohorts, suggesting these samples might actually represent a different region of the brain. To further investigate this I used an algorithm within the online DNA methylation age calculator to predict the tissue of origin of each sample (Horvath, 2016) (see **section 3.2.4** for specific details). The tissue prediction feature of this tool can be helpful in identifying mislabelled samples, however this feature has not been published and the author suggests caution in interpreting the predictions (see the online tool tutorial by Horvath (2013b)). **Appendix A - Supplementary Tables 3 to 5** show the tissue prediction results for all samples in this study and **Table 3.1** shows the tissue prediction only for the CER samples. Whereas the majority CER samples are predicted as cerebellum (“Brain CRBLM”) and have a high cerebellum prediction value (0.48 ± 0.06), the EBTB samples highlighted in grey are not predicted as cerebellum and show a considerably lower cerebellum prediction value (0.03 ± 0.01). This is consistent with the multidimensional scaling (MDS) plot of the thousand most variable probes across all samples (**Figure 3.6**), showing the samples from the same brain regions clustering together with exception of the same EBTB CER samples. Furthermore, these samples present a higher prediction value for pons (< 0.10) than the remaining samples, suggesting that they might have been dissected from pons, a structure lying between the midbrain and the medulla oblongata and in front of the CER (**Appendix A - Supplementary Table 3**). In light of these observations I decided to exclude the entire EBTB cohort from any further analysis.

Table 3.1. Tissue prediction for the cerebellum samples in this study using the DNA methylation age calculator (Horvath, 2016). Brain CRBLM, cerebellum; LNDBB , MRC London Neurodegenerative Diseases Brain Bank; DBCBB, Douglas-Bell Canada Brain Bank; EBTB, Edinburgh Brain and Tissue Banks. Highlighted in grey are the samples that are not predicted correctly as cerebellum samples.

Sample ID	Brain Bank	Group	450K Barcode	Predicted tissue	Probability from Brain cerebellum
MS01	DBCBB	schizophrenia	9647450027_R06C01	Brain CRBLM	0.52
MS03	DBCBB	schizophrenia	9647455007_R02C02	Brain CRBLM	0.44
MS04	DBCBB	schizophrenia	9647450013_R02C02	Brain CRBLM	0.53
MS05	DBCBB	control	9647450019_R04C02	Brain CRBLM	0.47
MS06	DBCBB	schizophrenia	9647450013_R05C02	Brain CRBLM	0.48
MS07	DBCBB	schizophrenia	9647450019_R05C02	Brain CRBLM	0.48
MS08	DBCBB	control	9647450027_R02C01	Brain CRBLM	0.48
MS09	DBCBB	control	9647450013_R04C02	Brain CRBLM	0.49
MS10	DBCBB	control	9647450019_R06C01	Brain CRBLM	0.52
MS11	DBCBB	schizophrenia	9647450013_R01C01	Brain CRBLM	0.46
MS12	DBCBB	schizophrenia	9647450019_R05C01	Brain CRBLM	0.47
MS13	DBCBB	control	9647455007_R01C01	Brain CRBLM	0.47
MS14	DBCBB	control	9647450013_R06C02	Brain CRBLM	0.48
MS15	DBCBB	control	9647450013_R06C01	Brain CRBLM	0.47
MS16	DBCBB	control	9647450027_R03C01	Brain CRBLM	0.52
MS17	DBCBB	control	9647450013_R04C01	Brain CRBLM	0.43
MS18	DBCBB	schizophrenia	9647450019_R01C01	Brain CRBLM	0.48
MS19	DBCBB	control	9553932139_R04C02	Brain CRBLM	0.55
MS20	DBCBB	schizophrenia	9647455007_R03C02	Brain CRBLM	0.48
MS21	DBCBB	schizophrenia	9647450019_R01C02	Brain CRBLM	0.51
MS22	DBCBB	control	9553932139_R05C02	Brain CRBLM	0.54
MS23	DBCBB	schizophrenia	9647450019_R04C01	Brain CRBLM	0.45
MS25	DBCBB	schizophrenia	9647450027_R02C02	Brain CRBLM	0.45
MS26	DBCBB	control	9647455007_R04C01	Brain CRBLM	0.52
MS27	DBCBB	schizophrenia	9647450027_R01C02	Brain CRBLM	0.47
MS28	DBCBB	schizophrenia	9647450013_R02C01	Brain CRBLM	0.47
MS30	DBCBB	schizophrenia	9647450013_R01C02	Brain CRBLM	0.51
MS31	DBCBB	control	9647455007_R06C02	Brain CRBLM	0.48
MS32	DBCBB	schizophrenia	9647450027_R06C02	Brain CRBLM	0.47
MS33	DBCBB	control	9553932139_R06C02	Brain CRBLM	0.58
MS34	DBCBB	control	9647450027_R04C02	Brain CRBLM	0.45
MS35	DBCBB	control	9647450027_R04C01	Brain CRBLM	0.49
MS36	DBCBB	control	9647450013_R03C01	Brain CRBLM	0.48
ES01	EBTB	schizophrenia	9553932139_R03C02	Brain CRBLM	0.47
ES02	EBTB	control	9647455007_R03C01	Brain CRBLM	0.47
ES03	EBTB	control	9647455007_R05C02	Brain CRBLM	0.48
ES04	EBTB	control	9647450027_R05C02	Brain CRBLM	0.54
ES05	EBTB	schizophrenia	9647450019_R06C02	Brain CRBLM	0.5
ES06	EBTB	schizophrenia	9647455007_R04C02	Brain CRBLM	0.46
ES07	EBTB	schizophrenia	9647455007_R05C01	Brain CRBLM	0.17
ES09	EBTB	schizophrenia	9647455007_R06C01	Brain CRBLM	0.2
ES10	EBTB	control	9647450019_R03C02	Brain CRBLM	0.48
ES11	EBTB	schizophrenia	9647455007_R02C01	Brain CRBLM	0.5
ES12	EBTB	schizophrenia	9647450013_R05C01	GlialCell	0.02
ES13	EBTB	control	9647450027_R01C01	GlialCell	0.04
ES14	EBTB	control	9647450013_R03C02	GlialCell	0.02
ES15	EBTB	control	9647450019_R02C02	GlialCell	0.02

ES16	EFTB	control	9647450019_R02C01	GlialCell	0.03
ES17	EFTB	control	9647450027_R05C01	Brain CRBLM	0.33
ES18	EFTB	schizophrenia	9647455007_R01C02	GlialCell	0.04
1	LNDBB	schizophrenia	6042316042_R03C01	Brain CRBLM	0.51
2	LNDBB	schizophrenia	6042316047_R02C01	Brain CRBLM	0.46
3	LNDBB	schizophrenia	6042316024_R06C02	Brain CRBLM	0.46
4	LNDBB	schizophrenia	6042316042_R05C01	Brain CRBLM	0.49
5	LNDBB	schizophrenia	6042316024_R03C01	Brain CRBLM	0.5
6	LNDBB	schizophrenia	6042316031_R03C02	Brain CRBLM	0.49
7	LNDBB	schizophrenia	6042316024_R04C01	Brain CRBLM	0.47
8	LNDBB	schizophrenia	6042316024_R04C02	Brain CRBLM	0.48
9	LNDBB	schizophrenia	6042316031_R05C02	Brain CRBLM	0.46
10	LNDBB	schizophrenia	6042316024_R02C02	Brain CRBLM	0.51
11	LNDBB	schizophrenia	6042316024_R02C01	Brain CRBLM	0.51
12	LNDBB	schizophrenia	6042316024_R01C01	Brain CRBLM	0.47
13	LNDBB	schizophrenia	6042316042_R05C02	Brain CRBLM	0.48
14	LNDBB	schizophrenia	6042316031_R01C01	Brain CRBLM	0.5
15	LNDBB	schizophrenia	6042316047_R03C02	Brain CRBLM	0.45
16	LNDBB	schizophrenia	6042316031_R06C01	Brain CRBLM	0.53
17	LNDBB	schizophrenia	6042316024_R05C02	Brain CRBLM	0.46
18	LNDBB	schizophrenia	6042316042_R04C02	Brain CRBLM	0.51
19	LNDBB	schizophrenia	6042316031_R02C01	Brain CRBLM	0.49
20	LNDBB	schizophrenia	6042316031_R04C02	Brain CRBLM	0.49
23	LNDBB	schizophrenia	6042316031_R02C02	Brain CRBLM	0.48
25	LNDBB	control	6042316042_R01C02	Brain CRBLM	0.45
26	LNDBB	control	6042316031_R03C01	Brain CRBLM	0.46
28	LNDBB	control	6042316047_R06C01	Brain CRBLM	0.48
30	LNDBB	control	6042316024_R06C01	Brain CRBLM	0.5
31	LNDBB	control	6042316042_R06C02	Brain CRBLM	0.49
32	LNDBB	control	6042316047_R05C01	Brain CRBLM	0.55
33	LNDBB	control	6042316042_R02C02	Brain CRBLM	0.48
34	LNDBB	control	6042316031_R06C02	Brain CRBLM	0.52
35	LNDBB	control	6042316047_R05C02	Brain CRBLM	0.52
37	LNDBB	control	6042316024_R05C01	Brain CRBLM	0.5
38	LNDBB	control	6042316047_R04C02	Brain CRBLM	0.51
39	LNDBB	control	6042316031_R01C02	Brain CRBLM	0.43
40	LNDBB	control	6042316047_R04C01	Brain CRBLM	0.48
41	LNDBB	control	6042316042_R04C01	Brain CRBLM	0.44
42	LNDBB	control	6042316031_R05C01	Brain CRBLM	0.42
44	LNDBB	control	6042316031_R04C01	Brain CRBLM	0.47
45	LNDBB	control	6042316042_R03C02	Brain CRBLM	0.47
46	LNDBB	control	6042316042_R01C01	Brain CRBLM	0.52
47	LNDBB	control	6042316042_R02C01	Brain CRBLM	0.5
49	LNDBB	control	6042316024_R01C02	Brain CRBLM	0.46
51	LNDBB	control	6042316042_R06C01	Brain CRBLM	0.51
52	LNDBB	control	6042316047_R01C01	Brain CRBLM	0.54
53	LNDBB	control	6042316047_R02C02	Brain CRBLM	0.49

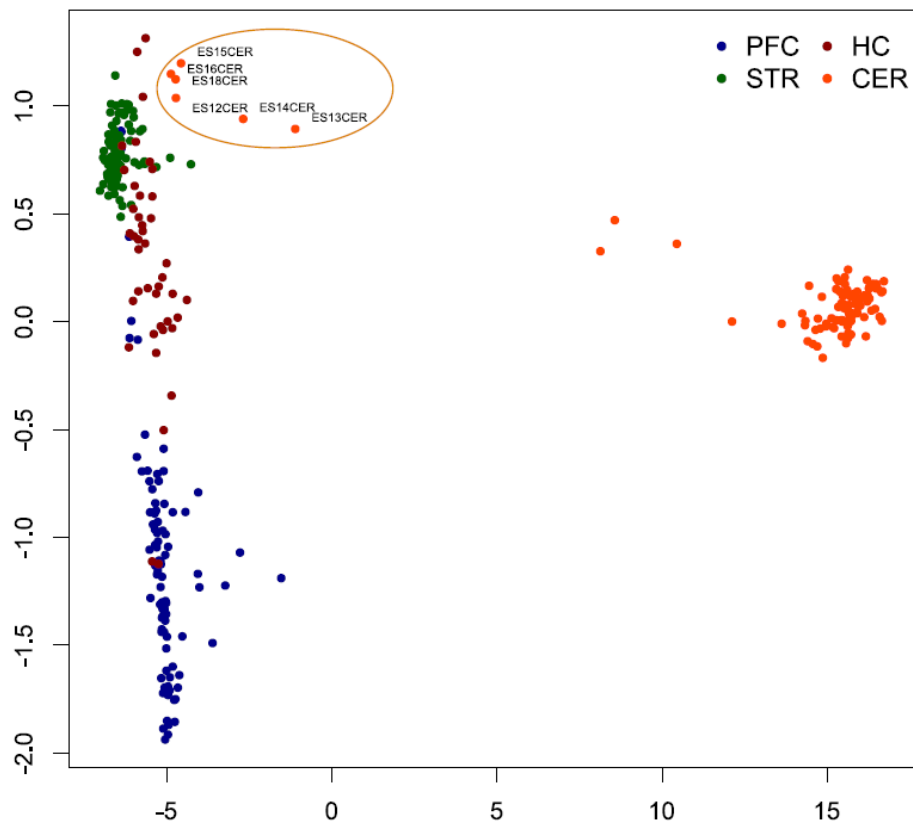


Figure 3.6. Multidimensional scaling of the thousand most variable probes across all samples. Six cerebellum samples from the Edinburgh Brain and Tissue Banks (circled) do not cluster with the remaining cerebellum samples. PFC, prefrontal cortex (blue); CER, cerebellum (orange); STR, striatum (green) and HC, hippocampus (dark red).

MDS plots of probes located on each of the autosomal chromosomes and for the thousand most variable probes across all samples were used to check for DNA extraction, bisulfite treatment and microarray batch effects. **Figure 3.7** shows an example of MDS plots coloured by microarray chip (**A**) and DNA extraction batch (**B**); the samples cluster by sex but not by colours, indicating that no obvious batch effects were identified. MDS plots of probes on each sex chromosome were used to check that the predicted sex corresponded with the reported sex for each individual. One individual from each cohort was identified as having a 47,XXY karyotype (presence of 2 X-chromosomes and 1 Y-chromosome consistently across all brain regions) and excluded from my schizophrenia analysis (a detailed analysis of genomic variation in one of these 47,XXY (Klinefelter Syndrome) samples is presented in **Chapter 7**). **Figure 3.8** shows examples of such MDS plots for probes on the X (**A**) and Y (**B**)

chromosomes of the 47,XXY sample from the DBCBB cohort. Another CER sample showed different predicted and reported sex and was excluded from analysis. The DNA Methylation age calculator (Horvath, 2016) also predicts sex from DNA methylation data (see **section 3.2.4** for specific details on this tool). All the samples that survived QC had matching reported sex with the sex predicted by the age calculator (**Appendix A - Supplementary Table 3**).

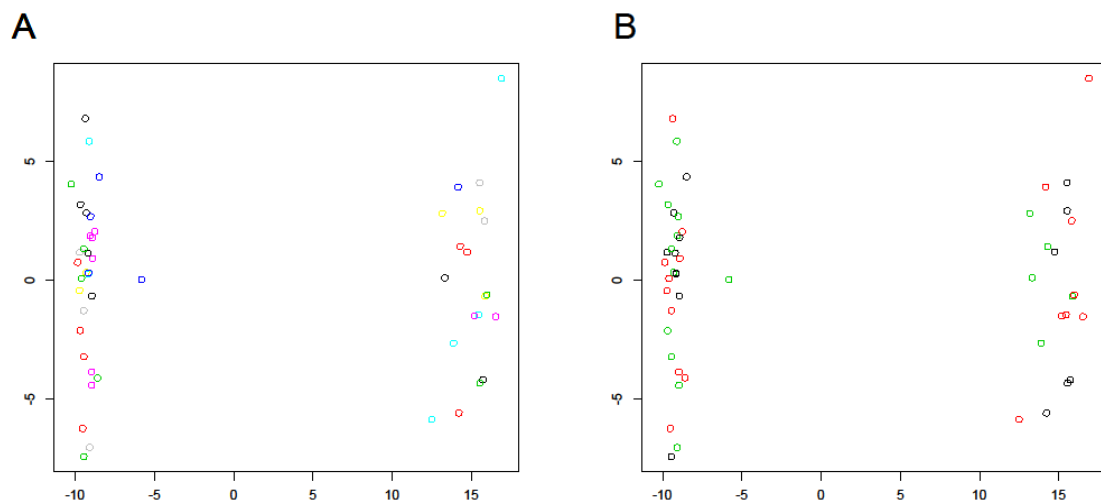


Figure 3.7. Example of multidimensional scaling plots for the thousand most variable probes across all the striatum MRC London Neurodegenerative Diseases Brain Bank samples. The samples are coloured by chip array (A) and DNA extraction batch (B) and in both cases show no batch effects. The clustering is probably due to sex differences.

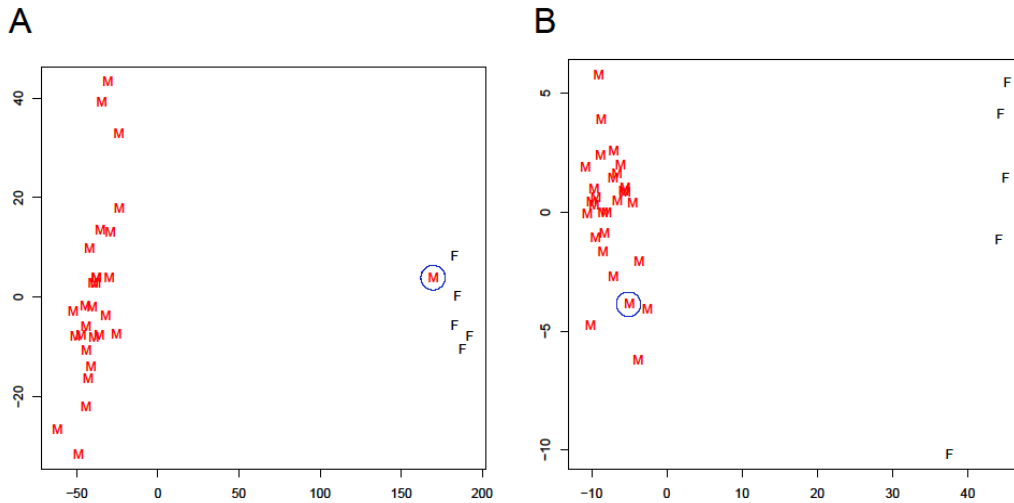


Figure 3.8. Example of multidimensional scaling plots of the X-chromosome (A) and Y-chromosome (B) probes across all the prefrontal cortex Douglas-Bell Canada Brain Bank samples. The sample circled in blue clusters with females for the X-chromosome probes (A) and with males for the Y-chromosome probes (B).

The ten sodium bisulfite conversion control probes on the array were used to calculate the efficiency of the conversion reaction and samples showing a score less than 90% were excluded from analysis (PFC: 2; STR: 1; CER: 0; HC: 0). **Figure 3.9** shows an example of the conversion plot for the LNDBB and DBCBB PFC samples. Correlation data from the 65 SNP probes on the array between brain region pairs confirmed that matched tissues were sourced from the same individual. **Figure 3.10** shows an example of a correlation plot between DBCBB CER and PFC samples. **Appendix A - Supplementary Table 2** provides detailed information on exclusion criteria for each sample profiled in the course of this study.

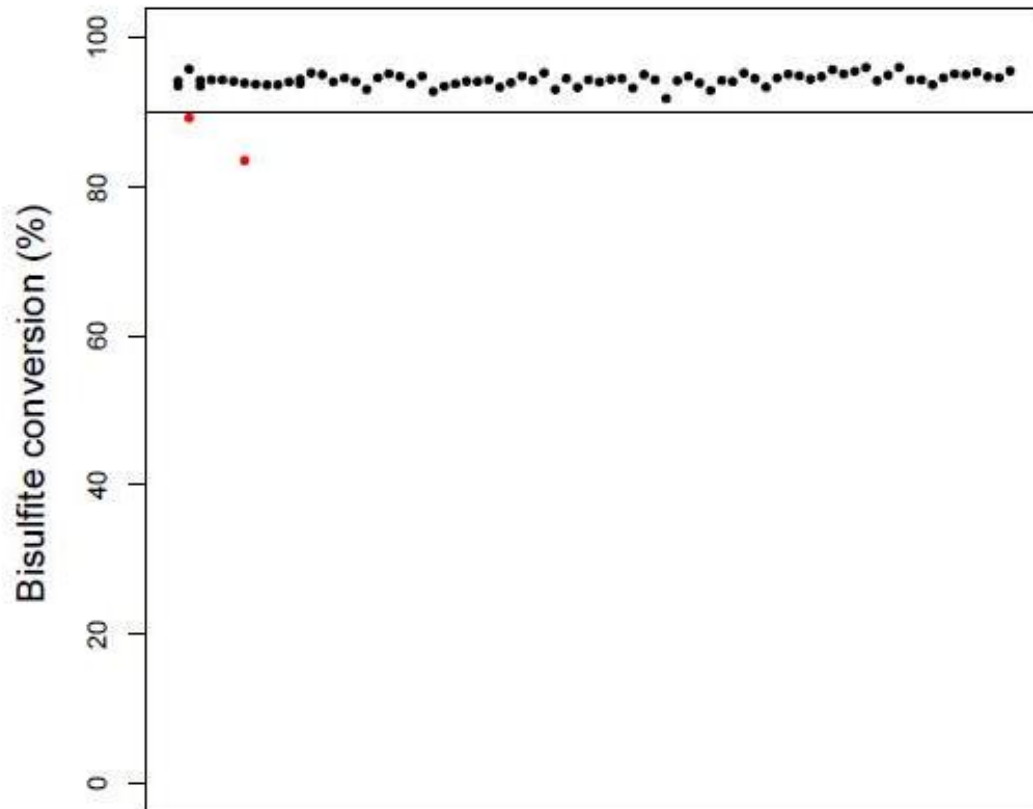


Figure 3.9. Example of bisulfite conversion plot. Shown are the bisulfite conversion values (y-axis) for the MRC London Neurodegenerative Diseases Brain Bank and Douglas-Bell Canada Brain Bank prefrontal cortex samples. The samples in red are below the 90% bisulfite conversion threshold (horizontal line) and were excluded from further analysis.

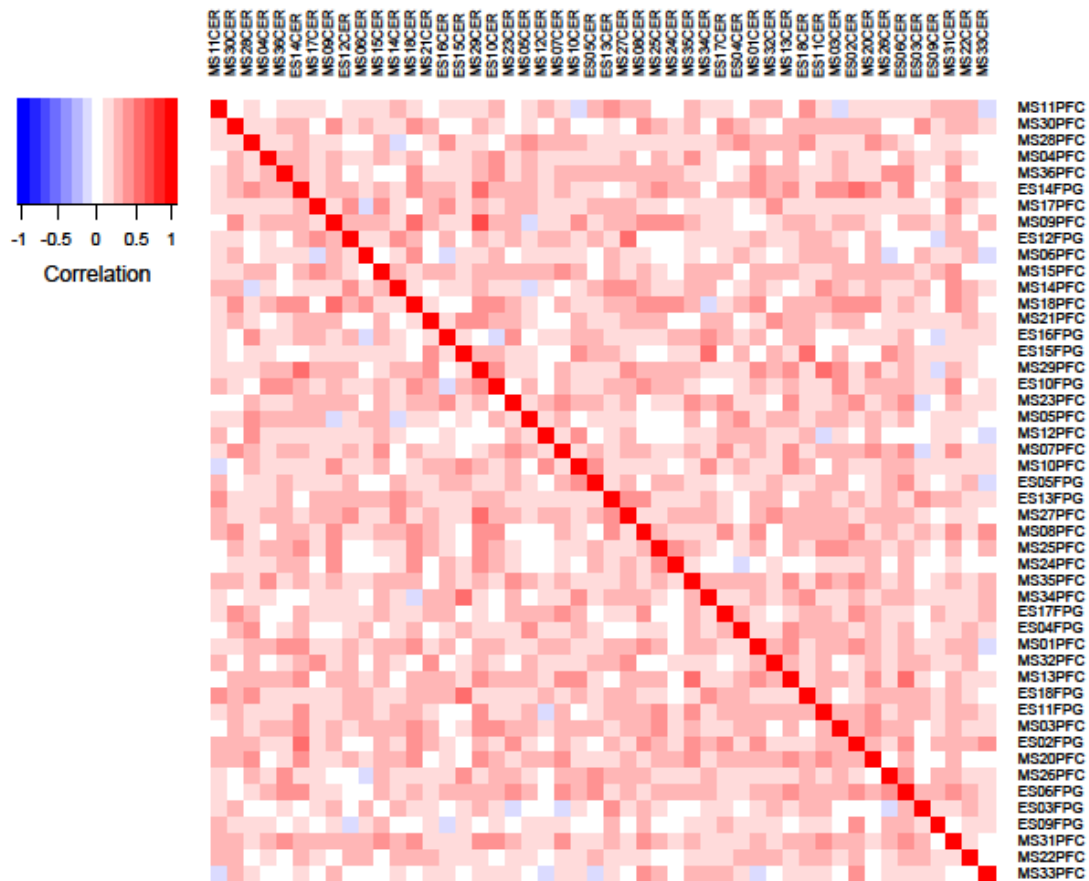


Figure 3.10. Example of a correlation plot for SNP probes for matched samples from two brain regions. The figure shows correlation of the 65 SNP probes on the 450K array between prefrontal cortex (PFC; vertical) and cerebellum (CER; horizontal) samples from the Douglas-Bell Canada Brain Bank. High positive correlation (red) indicates that matched tissues were sourced from the same individual, with lower correlations for all other comparisons.

3.2.3. Data pre-processing and normalisation

The 65 SNP probes, probes on sex chromosomes, cross-hybridizing probes (Price et al., 2013, Chen et al., 2013) and probes containing a SNP with minor allele frequency >5% within 10 base pairs (bp) of the single base extension were excluded from analysis (**Chapter 2 section 2.3.2.1**). The *pfilter* function of the *wateRmelon* package (Pidsley et al., 2013) was used to filter data by beadcount and detection *P*-value. Samples with >1% probes with a detection *P*-value >0.01 were removed (PFC: 1; STR: 1; CER: 1; HC: 2) and probes with a

detection P -value > 0.05 in at least 1% of samples and/or a beadcount <3 in 5% of samples were also removed. Reasons for exclusion for each sample are presented in **Appendix A - Supplementary Table 2**. The *dasen* function in *wateRmelon* was used to normalise the data as previously described (Pidsley et al., 2013). **Table 3.2** summarises the number of probes that survived QC in each cohort and brain region and were included in the differently methylated probe analyses and **Table 3.3** and **Appendix A - Supplementary Tables 1** and **3** summarise the demographic and sentrix barcode ID for the samples included in the analyses, respectively. DNA methylation (β) values were calculated from unmethylated (U) and methylated (M) signal $[M/(U + M + 100)]$ and ranged from 0 to 1 (corresponding to 0 to 100% DNA methylation). **Figure 3.11** shows the example of β values distribution before (**A**; raw data) and after normalisation (**B**) of the DBCBB STR samples. As is evident from the figure, one sample (MS07STR) failed and was excluded during QC. **Figure 3.12** shows the density of β values distribution for all probes, type I probes and type II probes before (**A**) and after (**B**) normalisation. A sensitivity test was performed using the *G*Power* software (Faul et al., 2007) and revealed the ability to detected a DNA methylation difference of 9.12% at a P -value < 0.05 and 49.49% at the multiple testing threshold used in this study (see **Section 3.2.8**) (sample size of 88 individuals, 80% statistical power).

Table 3.2. Total number of probe included in the analyses after data normalisation and quality control. DBCBB, Douglas-Bell Canada Brain Bank; LNDBB, MRC London Neurodegenerative Diseases Brain Bank.

	Prefrontal cortex	Striatum	Hippocampus	Cerebellum
LNDBB	415,426	419,489	417,213	410,756
DBCBB	417,033	417,470	-	417,039
Meta-analysis	413,201	417,046	-	409,311

Table 3.3. Overview of samples included in the schizophrenia case versus control analysis. LNDBB, MRC London Neurodegenerative Diseases Brain Bank; DBCBB, Douglas-Bell Canada Brain Bank.

	N	Sex (male:female)	Age at death	Brain weight (g)	pH
LNDBB	schizophrenia	11:9	62.05 ± 15.87	1232.94 ± 129.22	6.64 ± 0.28
	controls	17:6	62.04 ± 18.74	1368.48 ± 185.22	6.49 ± 0.33
	total	28:15	62.05 ± 17.26	1310.88 ± 175.52	6.56 ± 0.31
	<i>P</i>	-	1.00	0.01	0.13
LNDBB	schizophrenia	11:10	61.76 ± 16.61	1227.44 ± 123.68	6.60 ± 0.30
	controls	20:8	63.43 ± 18.16	1360.52 ± 184.59	6.46 ± 0.33
	total	31:18	62.71 ± 17.36	1302.10 ± 172.37	6.53 ± 0.32
	<i>P</i>	-	0.74	0.01	0.17
LNDBB	schizophrenia	10:4	60.71 ± 15.93	1271.25 ± 139.22	6.63 ± 0.28
	controls	11:2	61.92 ± 17.80	1415.27 ± 173.82	6.48 ± 0.41
	total	21:6	61.30 ± 16.54	1340.13 ± 169.81	6.56 ± 0.34
	<i>P</i>	-	0.85	0.04	0.31
LNDBB	schizophrenia	11:10	61.76 ± 16.61	1227.44 ± 123.68	6.60 ± 0.30
	controls	17:6	61.39 ± 19.25	1361.30 ± 185.03	6.46 ± 0.33
	total	28:16	61.57 ± 17.83	1232.41 ± 172.79	6.60 ± 0.32
	<i>P</i>	-	0.95	0.01	0.15
LNDBB	schizophrenia	15:3	45.50 ± 16.61	1431.78 ± 188.16	6.23 ± 0.22
	controls	13:2	42.27 ± 14.80	1462.96 ± 175.17	6.12 ± 0.32
	total	28:5	44.03 ± 15.65	1447.37 ± 179.32	6.18 ± 0.27
	<i>P</i>	-	0.56	0.64	0.27
LNDBB	schizophrenia	13:3	46.25 ± 17.10	1410.90 ± 193.35	6.21 ± 0.22
	controls	14:3	45.65 ± 16.82	1438.02 ± 180.91	6.09 ± 0.31
	total	27:6	45.94 ± 16.69	1426.27 ± 183.61	6.15 ± 0.27
	<i>P</i>	-	0.92	0.70	0.23
LNDBB	schizophrenia	14:2	44.56 ± 15.84	1404.62 ± 161.90	6.25 ± 0.22
	controls	14:3	45.65 ± 16.82	1438.02 ± 180.91	6.09 ± 0.31
	total	28:5	45.12 ± 16.10	1422.94 ± 170.58	6.17 ± 0.28
	<i>P</i>	-	0.85	0.59	0.10
DBCBB	schizophrenia	13:3	46.25 ± 17.10	1410.90 ± 193.35	6.21 ± 0.22
	controls	14:3	45.65 ± 16.82	1438.02 ± 180.91	6.09 ± 0.31
	total	27:6	45.94 ± 16.69	1426.27 ± 183.61	6.15 ± 0.27
	<i>P</i>	-	0.92	0.70	0.23
DBCBB	schizophrenia	14:2	44.56 ± 15.84	1404.62 ± 161.90	6.25 ± 0.22
	controls	14:3	45.65 ± 16.82	1438.02 ± 180.91	6.09 ± 0.31
	total	28:5	45.12 ± 16.10	1422.94 ± 170.58	6.17 ± 0.28
	<i>P</i>	-	0.85	0.59	0.10

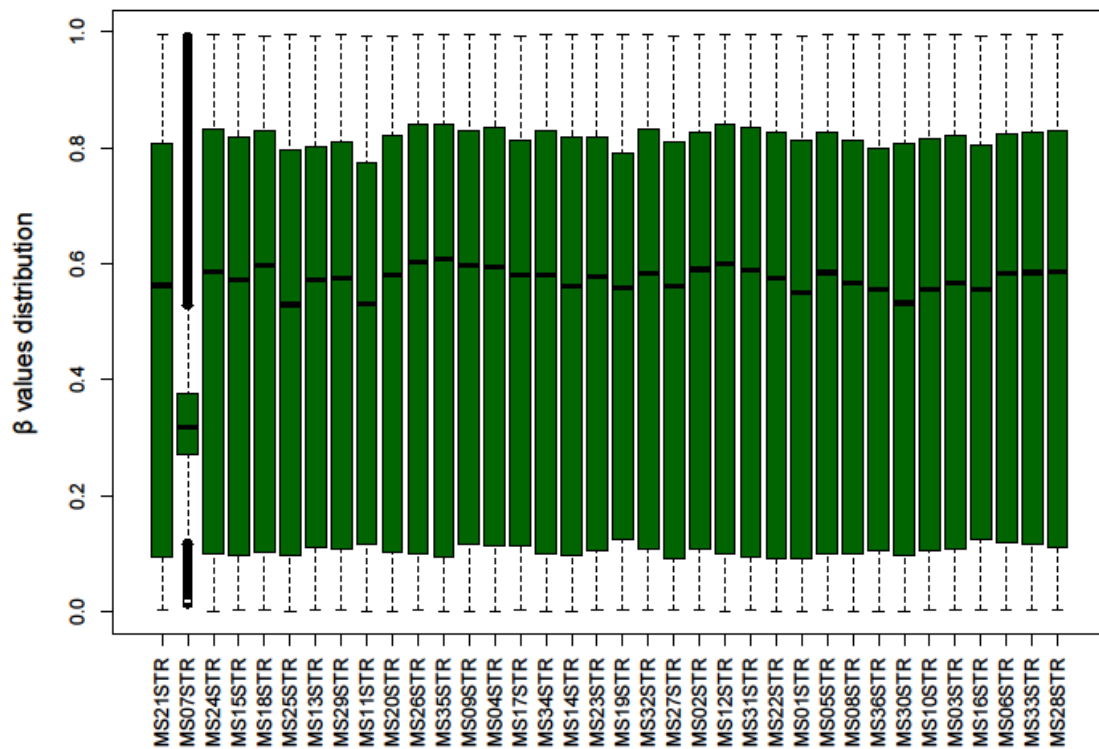
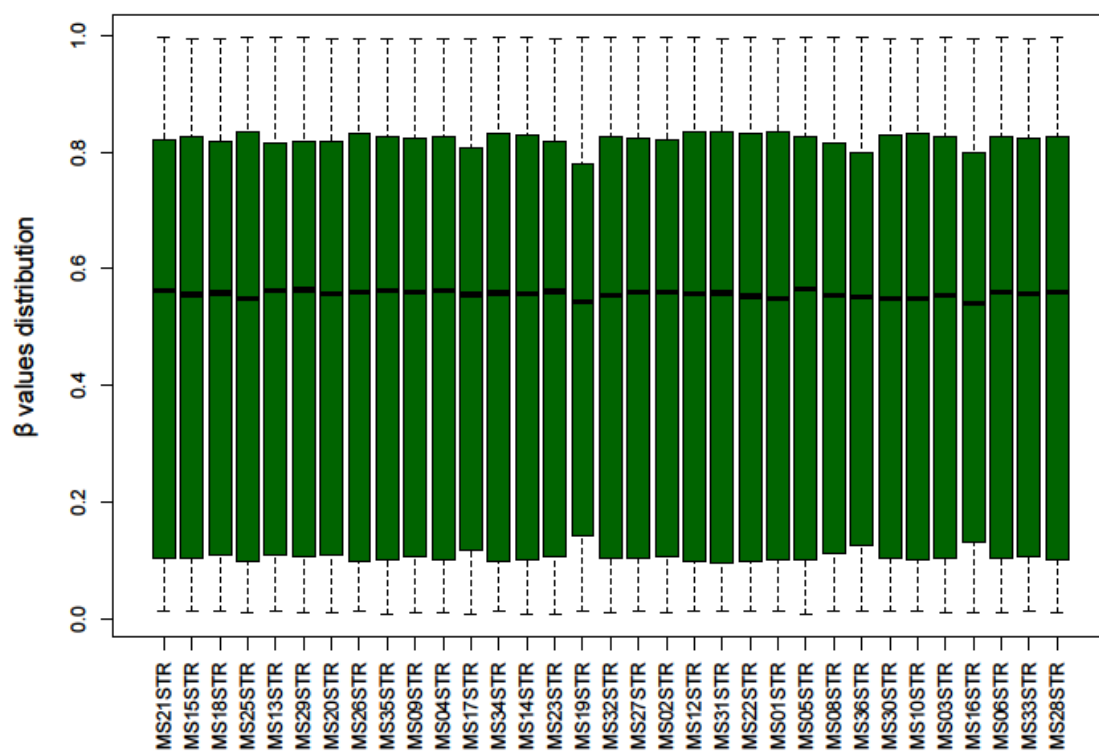
A**B**

Figure 3.11. Boxplots showing the β values distribution for each striatum samples from the Douglas-Bell Canada Brain Bank. Shown are the β values distribution before (A) and after (B) quality control and normalisation steps.

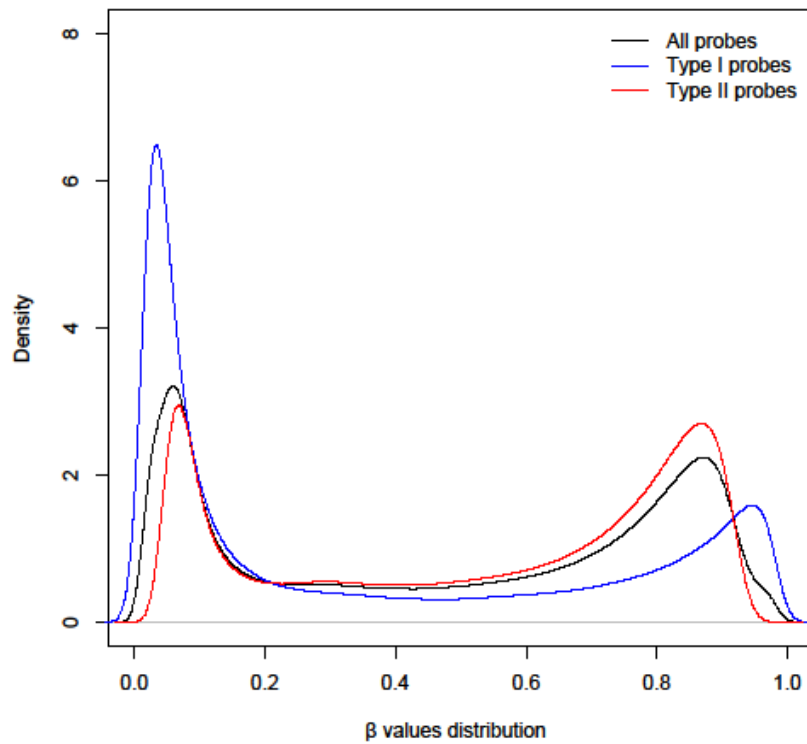
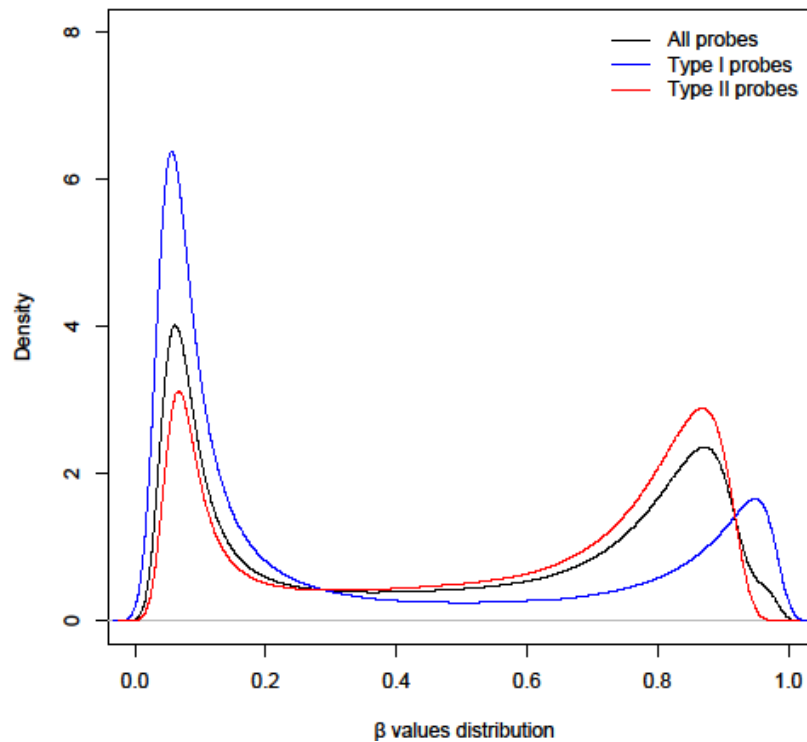
A**B**

Figure 3.12. Density plots showing the β values distribution for the striatum samples from the Douglas-Bell Canada Brain Bank. Shown are the β values distribution before (A) and after (B) quality control and normalisation steps for all probes (black), type I probes (blue) and type II probes (red).

3.2.4. DNA methylation age calculation

The DNA methylation age online calculator (Horvath, 2013a, Horvath, 2015, Horvath, 2016) was used to estimate DNA methylation age for each sample. The DNA methylation age calculator was developed using 8,000 samples from a broad range of healthy tissues, cancer tissues and cell lines. The calculator allows the estimation of DNA methylation age from a complete 450K dataset, using weighted average data from 353 'clock CpGs', which is then transformed to DNA methylation age using a calibration function. DNA methylation age for each sample in this study is presented in **Appendix A - Supplementary Table 1**. I calculated the correlation coefficients between the chronological age and DNA methylation age for each brain region from each sample. To test whether there is DNA methylation age acceleration in schizophrenia, I performed a regression model with DNA methylation age values as the dependent variable, chronological age and diagnosis as fixed effects and an interaction term between chronological age and diagnosis.

3.2.5. Cell composition estimates

The epigenetic profile of a cell contributes to its unique gene expression pattern and DNA methylation is known to be a mark of cell and tissue type (Roadmap Epigenomics Consortium et al., 2015, Rivera and Ren, 2013). This has obvious implications in EWAS that use bulk tissue samples with a heterogeneous population of cells and in recent years different approaches have emerged that allow us to estimate cell type composition in different human tissues (Houseman et al., 2015, Guintivano et al., 2013).

I estimated neuronal composition for each sample using the *Cell EpigenoType Specific (CETS)* package in R (Guintivano et al., 2013). Neuronal composition estimates for each sample are presented in **Appendix A - Supplementary Table 1** and **Figure 3.13**. The CER neuronal estimates derived from *CETS* correlated significantly with age ($\rho = 0.48$, $P = 1.26E-05$) in contrast to PFC ($\rho = 0.06$, $P = 0.58$), STR ($\rho = -0.24$, $P = 0.032$) and HC ($\rho = 0.09$, $P = 0.65$) estimates (**Figure 3.14**). This concurs with data reported by Guintivano et al. (2013) and is likely explained by age-related variation in the proportion of NeuN expressing and non-expressing neurons (e.g. Purkinje neurons) in the CER. Purkinje neuron (NeuN⁻) levels relative to granule neurons (NeuN⁺) have been observed

to decrease with age in mice (Sturrock, 1990, Sturrock, 1989b, Sturrock, 1989a). These observations make CETS unsuitable for estimating cell composition in this brain region (Guintivano et al., 2013). For this reason, subsequent analyses on CER did not include neuronal proportion estimates as an independent variable.

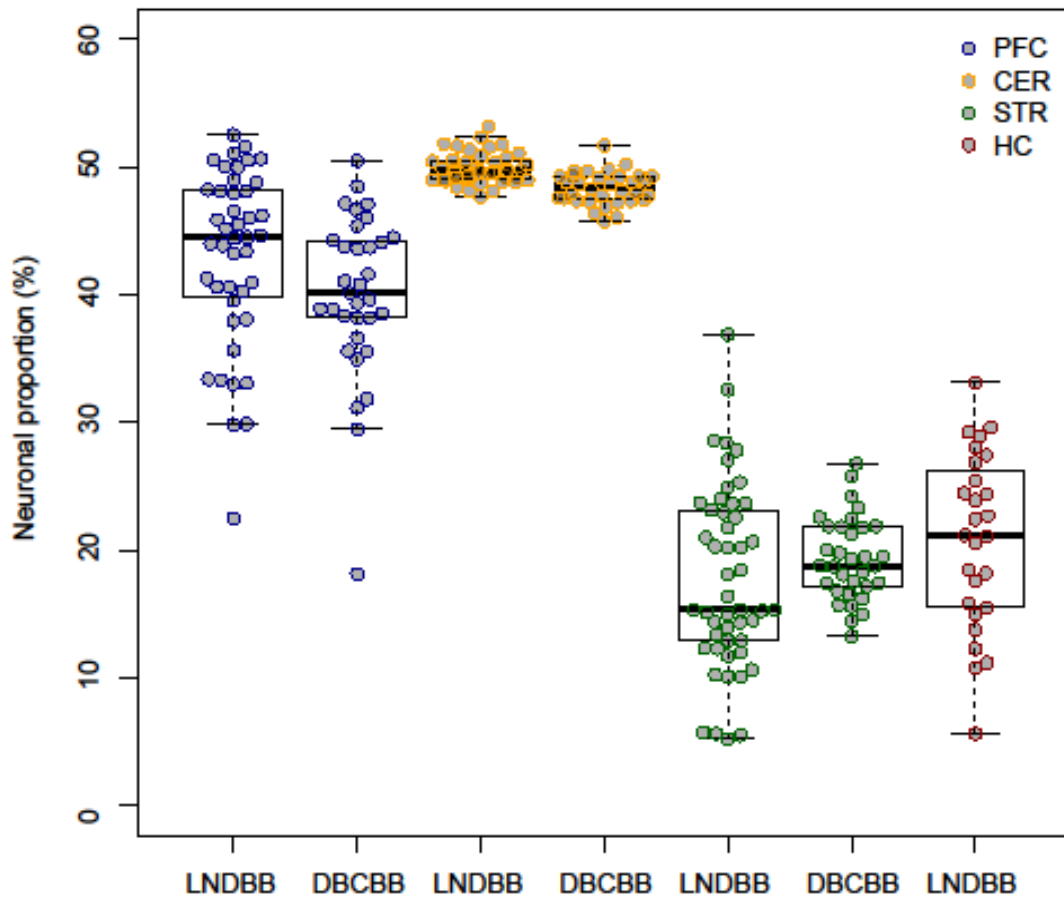


Figure 3.13. Neuronal proportion estimates calculated using the *CETS* package in R (Guintivano et al., 2013). Shown are neuronal proportion estimates (y-axis) for prefrontal cortex (PFC; blue), cerebellum (CER; yellow), striatum (STR; green) and hippocampus (HC; red) samples from both the MRC London Neurodegenerative Diseases Brain Bank (LNDBB) and Douglas-Bell Canada Brain Bank (DBCBB).

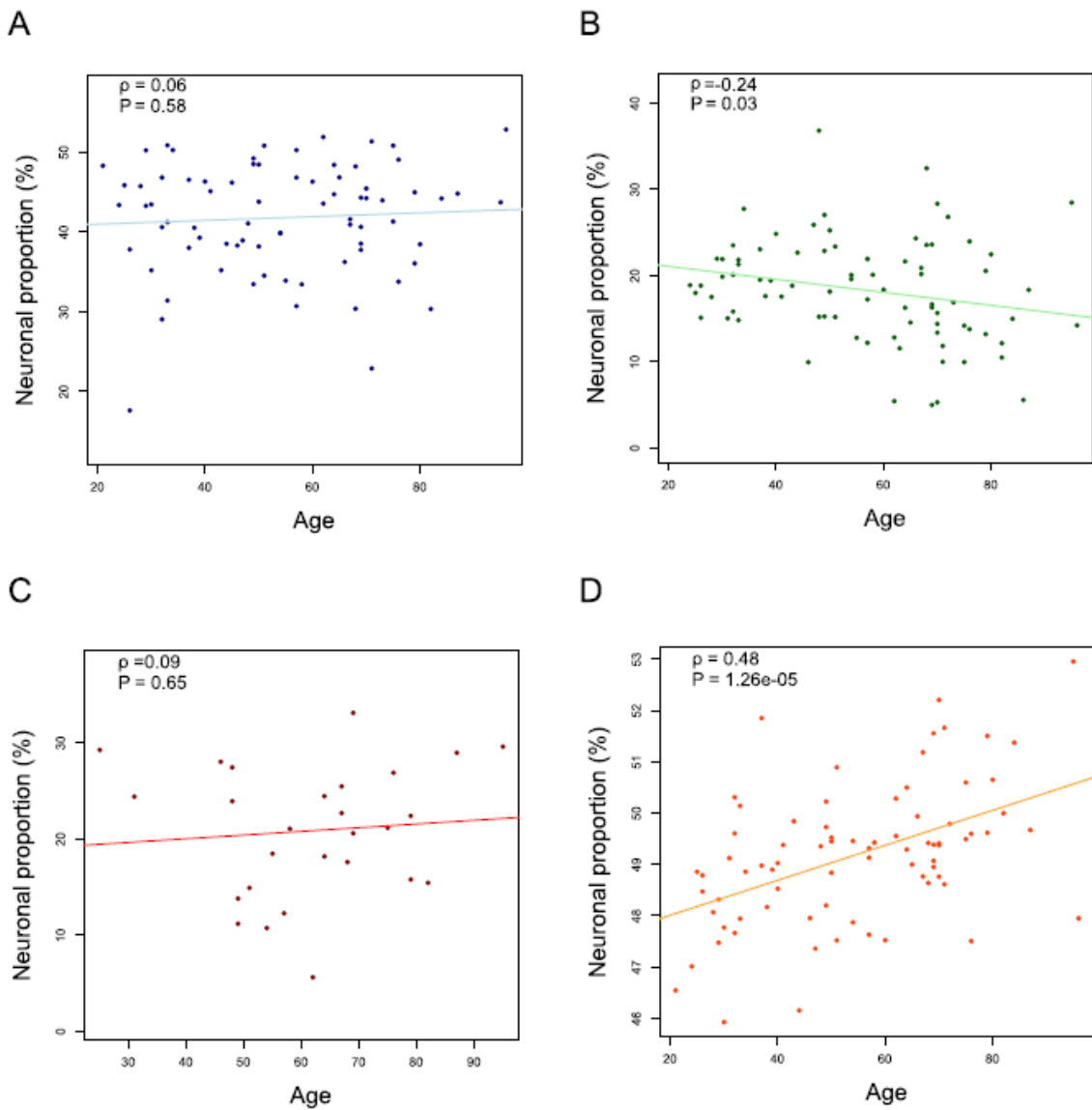


Figure 3.14. Correlation between chronological age and neuronal proportion estimates. Shown is the correlation between chronological age (x-axis) and neuronal proportion estimates (y-axis) in the prefrontal cortex (A), striatum (B), hippocampus (C) and cerebellum (D). Neuronal proportion estimates were calculated using the *CETS* package (Guintivano et al., 2013).

3.2.6. Identification of differentially methylated positions and regions

To identify schizophrenia-associated DNA methylation differences at the individual probe level in each brain region I performed a linear regression using the pre-processed and normalised DNA methylation (β) values of each cohort as the dependent variable and disease status, chronological age, sex and neuronal proportion estimates as independent variables. Neuronal proportion

estimates were not included as a variable for CER samples as described above (**section 3.2.2**). Given the nature of these samples, medication, smoking status and other important phenotypical information was not available and therefore I could not include these as independent variables.

The adjusted DNA methylation values for each probe and sample were calculated as follows:

- a) repeating the linear regression model for each brain region and cohort without including diagnosis as an independent variable;
- b) calculating the sum of the regression residuals and intercept for each probe and sample.

The resulting *P*-values of the linear regression in the HC LNDBB data were used to identify differentially methylated CpG sites in this brain region. For tissues collected from both brain banks (PFC, STR and CER), a fixed effect meta-analysis on the adjusted mean DNA methylation values computed with inverse variance weights was performed in each probe using the *metacont* function from the *meta* package in R (Schwarzer, 2015). Only the probes that survived QC and were common to both cohorts in each brain region were used in the meta-analysis (**Table 3.2**).

To identify differentially methylated regions (DMRs), I identified spatially correlated *P*-values in our data using the Python module *comb-p* (Pedersen et al., 2012) to group spatially correlated DMPs (seed *P*-value < 1.00E-3, minimum of two probes) at a maximum distance of 300bp in each brain region. DMR *P*-values were corrected for multiple testing using Šidák correction (Šidák, 1967), which corrects the combined *P* for n_a/n_r tests, where n_a is the total number of probes tested in the initial EWAS and n_r the number of probes in the given region.

Permutation tests were performed for multiple purposes. The sample was randomly split into cases and controls 2,000 times (matching the numbers in each group in the real analysis), and for each permutation an EWAS was performed using a linear regression model for each cohort and brain region which were combined using a meta-analysis of both cohorts for PFC, STR and CER, as described above. The 2.5th and 97.5th percentiles of the *P*-values for

each permutation were calculated and used to compute the 95% confidence intervals presented in the quantile-quantile (QQ) plots for each analysis (Figures 3.20 to 3.23, section 3.3.3).

3.2.7. Additional probe annotation and enrichment analysis for regulatory regions and schizophrenia GWAS regions

I annotated the probes on the 450K array using the Genomic Regions Enrichment of Annotations Tool (GREAT) (McLean et al., 2010). GREAT associates genomic regions with genes by defining a *cis*-regulatory region for each gene in the genome. In the context of this study, annotating 450K probes of interest with GREAT (*i.e.* DMPs and DMRs) can provide information on whether these probes lie within putative regulatory regions mapped to genes of interest.

Probes were also annotated to transcription factor binding sites (TFBSs) and DNase1 hypersensitivity sites (DHSs) using published 450K array probe annotation (Slieker et al., 2013) based on data made publically available as part of the ENCODE project (ENCODE Project Consortium, 2012, Maurano et al., 2012). The overlap between these regulatory features and different thresholds of DMPs (50 top ranked, DMPs $P < 1.00E-03$ and DMPs $P < 0.05$) was tested for enrichment using a two sided Fisher's 2x2 exact test (Fisher, 1922).

A recent large-scale GWAS of schizophrenia identified 128 independent associations spanning 108 genomic regions in a meta-analysis of over 80,000 samples (Schizophrenia Working Group of the Psychiatric Genomics, 2014). 5006, 5058, 5066 and 4951 Illumina 450K array probes included in our PFC, STR, HC and CER analyses, respectively, were located within these broad genomic regions. The overlap between different thresholds of DMPs (50 top ranked, DMPs $P < 1.00E-03$ and DMPs $P < 0.05$) and GWAS regions was tested for enrichment using a two sided Fisher's 2x2 exact test (Fisher, 1922).

3.2.8. Establishing multiple testing significance threshold for EWAS analysis

To establish a stringent multiple-testing significance threshold to identify schizophrenia-associated DMPs, the data from a large schizophrenia Illumina 450K dataset ($n = 675$ individuals) from another ongoing study in our lab (Hannon E et al., under review) was randomly split into cases and controls 5,000 times, and for each permutation an EWAS was performed using a linear regression model controlling for age, sex, smoking and cell composition and the probe-level P -values were recorded. The minimum (or most significant) P -value was identified for each permutation and the 5th quantile across the permutations was used to estimate the nominal P -value for 5% family-wise error ($P = 1.66E-07$).

3.2.9. Cross-region multilevel model

As reported in previous studies (Davies et al., 2012, Hannon et al., 2016, Ladd-Acosta et al., 2007), my data show that at a global level the CER is very distinct to the other three brain regions included in this study (**Figures 3.5 and 3.6**); for this reason I excluded the CER from the multi-region model and focused on identifying consistent signals across the PFC, STR and HC. To identify homogeneous DNA methylation effects across PFC, STR and HC data a null model of no heterogeneity was fitted using disease, sex, age and cohort as fixed effects. As the brain regions were dissected from the same set of individuals, each individual's DNA methylation values are potentially non-independent across brain regions. In addition, DNA methylation values within a brain region are also expected to be correlated across individuals, therefore both of these covariates were included as random effects. The *comb-p* tool (Pedersen et al., 2012) was then used to identify significant DMRs across the three brain regions, using the P -values of the cross-region model as described in **section 3.2.6**.

3.2.10. Validation with bisulfite-PCR-pyrosequencing

Independent technical verification was performed using bisulfite-PCR-pyrosequencing on region chr17:154420-154443 within the *RPH3AL* gene that was consistently associated with schizophrenia (see **section 3.3.3.1**). The validation was performed in the PFC and STR samples used for 450K array analysis. Pyrosequencing assays were designed using the PyroMark Assay design software (Qiagen, Hilden, Germany). PCR amplification was performed on sodium bisulfite treated DNA (see **section 3.2.2**) in duplicate. Fully methylated control samples and negative controls were included in all experiments. Primers and assay conditions are presented in **Table 3.4**. The assay covers five CpG sites, although the final two CpGs were excluded from analysis due to variable quality at the end of the sequencing assay. DNA methylation was quantified across amplicons using the Pyromark Q24 system (Qiagen) following the manufacturer's standard instructions. DNA methylation values were retrieved using the Pyromark Q24 CpG 2.0.6 software (Qiagen, Hilden, Germany). **Figures 3.15** and **3.16** show examples of a successful and failed pyrosequencing run, respectively. **Appendix A - Supplementary Table 2** presents information on excluded samples from pyrosequencing analyses. For a full description of bisulfite-PCR-pyrosequencing methodology please see **Chapter 2 section 2.3.3**.

Table 3.4. Primers and assay conditions for the bisulfite-polymerase chain reaction pyrosequencing assay targeting the chr17:154410-154672 schizophrenia-associated differentially methylated region in the *RPH3AL* gene.

CpG	450K probe	Genomic coordinates (hg19)	Annealing PCR Temperature (°C)	PCR primer reverse	PCR primer forward	Sequencing primer
1	-	chr17:154444	60	5'-ACAAAAAT	5'-Biotin-ATAATA	5'-
2	-	chr17:154429		CCAACCAA	TAATTAGAGGG	CCAAACTCATT
3	cg11940040	chr17:154420		ACTCATTA-3'	GAAGGAAGTT-3'	AATTCTCCTA-3'

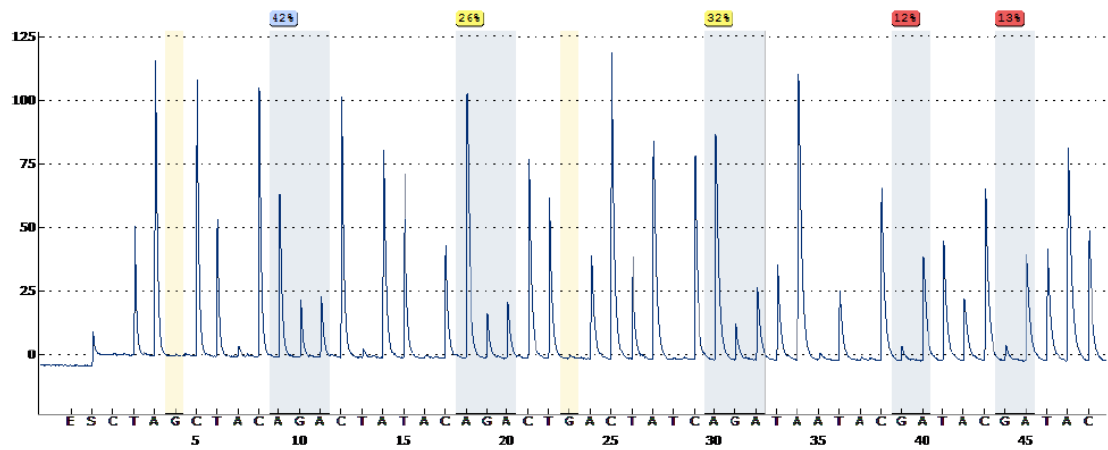


Figure 3.15. Example of a pyrogram of a successful pyrosequencing run assessing the DMR on the *RPH3AL* gene. Shown is the pyrogram for a striatum sample from the MRC London Neurodegenerative Diseases Brain Bank (ID = 16STR). The assay covers five CpG, although the final two CpGs were excluded from analysis due to variable quality at the end of the sequencing assay.

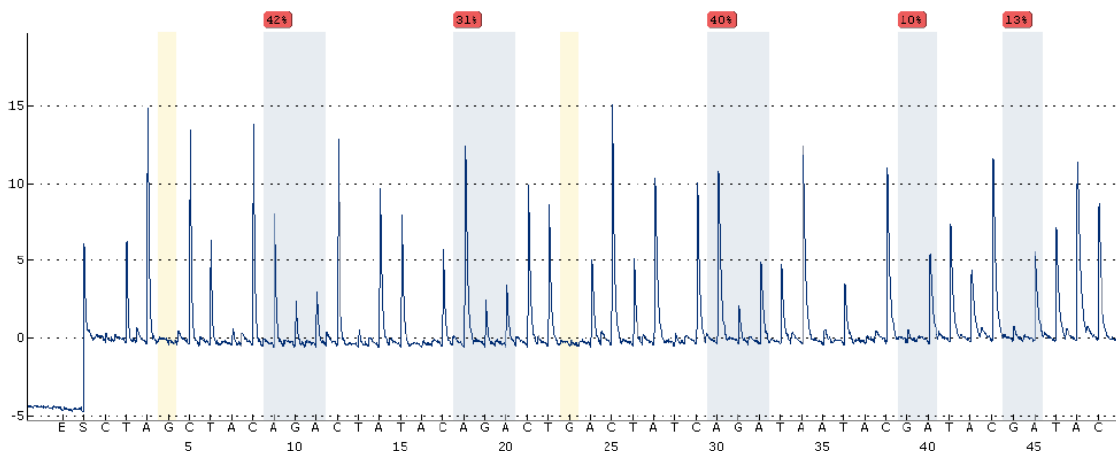


Figure 3.16. Example of a pyrogram of a failed pyrosequencing run assessing the DMR on the *RPH3AL* gene. Shown is the pyrogram for a prefrontal cortex sample from the MRC London Neurodegenerative Diseases Brain Bank (ID = 16PFC). This sample was excluded from analysis (see **Appendix A - Supplementary Table 2**)

3.3. Results

3.3.1. Overview of experimental strategy

In total, I quantified genome-wide patterns of DNA methylation in 341 samples derived from four brain regions dissected from 105 individuals (49 schizophrenia and 56 non-psychiatric controls) obtained from 3 independent brain banks, using the Illumina Infinium HumanMethylation450 BeadChip (450K array) (Illumina Inc., San Diego, CA, USA) (see **section 3.2.1**). Based on my initial QC, I excluded the entire EBTB cohort due to uncertainty of brain region for some of the CER samples (see **section 3.2.2**). Additionally I excluded 2 individuals that were identified with a 47,XXY karyotype (see **Chapter 7**), 3 samples that failed bisulfite conversion, 1 sample with the wrong reported sex and 5 samples that failed based on the detection *P*-value (**Appendix A - Supplementary Table 2**). Overall, this represents very stringent filtering of the data used in my subsequent analyses.

In total, data from 76 PFC (38 schizophrenia and 38 controls), 82 STR (37 schizophrenia and 45 controls), 33 HC (16 schizophrenia and 17 controls) and 77 CER (37 schizophrenia and 40 controls) samples from both the LNDBB and DBCBB passed stringent QC metrics and were used for analysis (demographics for these samples are presented in **Table 3.3**). A linear regression was performed in each brain region from each cohort separately and for tissues collected from both brain banks (PFC, STR and CER) a fixed-effect meta-analysis approach was used to combine analyses results from both cohorts. The initial analyses focused on identifying DMPs and DMRs associated with disease status. Analyses were initially performed independently for each brain region, subsequently employed a multi-level model to identify consistent DNA methylation associations with schizophrenia present across the PFC, STR, and HC. An overview of the analysis approach in this chapter is given in **Figure 3.7** and a representation on how this analysis integrates with the remaining chapters is given in **Chapter 1 Figure 1.8**.

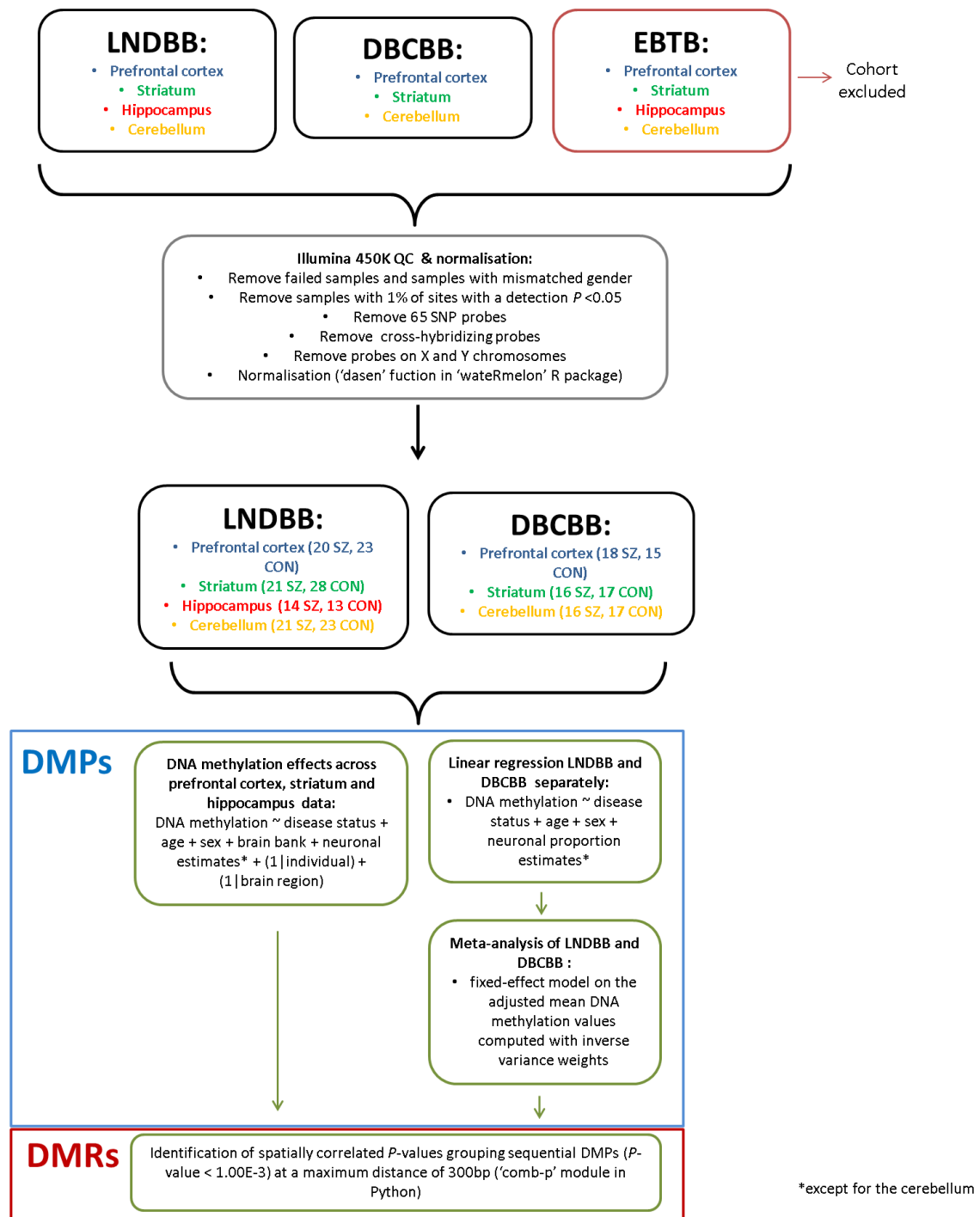


Figure 3.17. Overview of Chapter 3 experimental strategy.

3.3.2. No global DNA methylation changes or DNA methylation age acceleration in schizophrenia

As expected, no global differences in DNA methylation - estimated by averaging across all probes on the array included in our analysis - were identified between schizophrenia patients and controls in any of the four brain regions (PFC: schizophrenia (SZ) = 48.43%, controls (CTR) = 48.57%, $P = 0.51$; STR: SZ = 49.20%, CTR = 49.16%, $P = 0.12$; HC: SZ = 48.44%, CTR = 48.38%, $P = 0.05$; CER: SZ = 47.25%, CTR = 47.27%, $P = 0.89$). Furthermore, the estimated DNA methylation age for each sample calculated using an epigenetic clock based on DNA methylation values (Horvath, 2013a, Horvath, 2015) was strongly correlated with actual chronological age in each brain region (**Figure 3.18**), with no evidence for accelerated “DNA methylation aging” in affected individuals (**Figure 3.19**). Taken together, these data indicate that schizophrenia is not associated with any systemic methylomic differences in the brain regions tested in this study, as would be expected from a common, complex disorder.

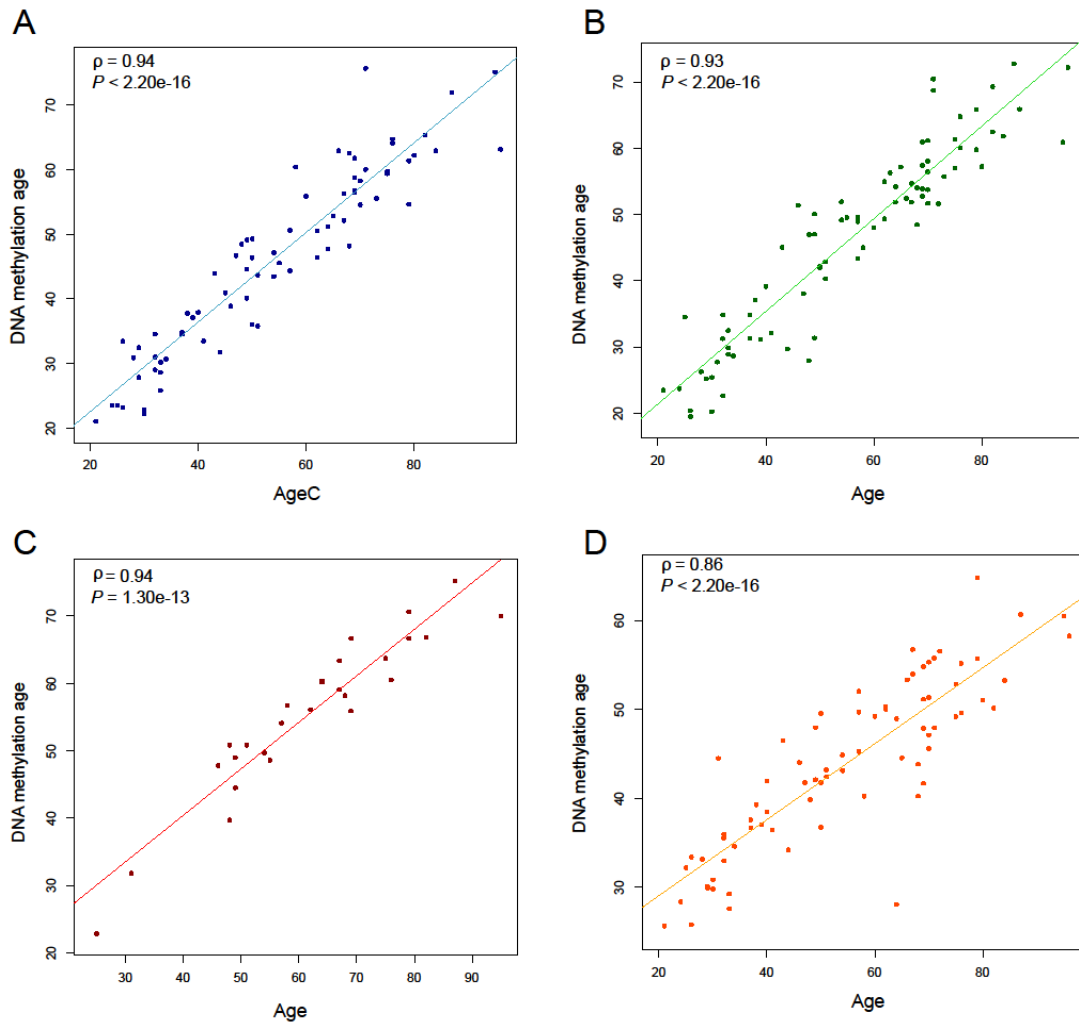


Figure 3.18. Correlation between chronological age and DNA methylation age. Shown is the correlation between chronological age (x-axis) and DNA methylation age (y-axis) for samples from both cohorts for A) prefrontal cortex, B) striatum, C) hippocampus, and D) cerebellum. DNA methylation age was calculated using the DNA methylation age online calculator (Horvath, 2016, Horvath, 2013a). ρ , Pearson's correlation coefficient.

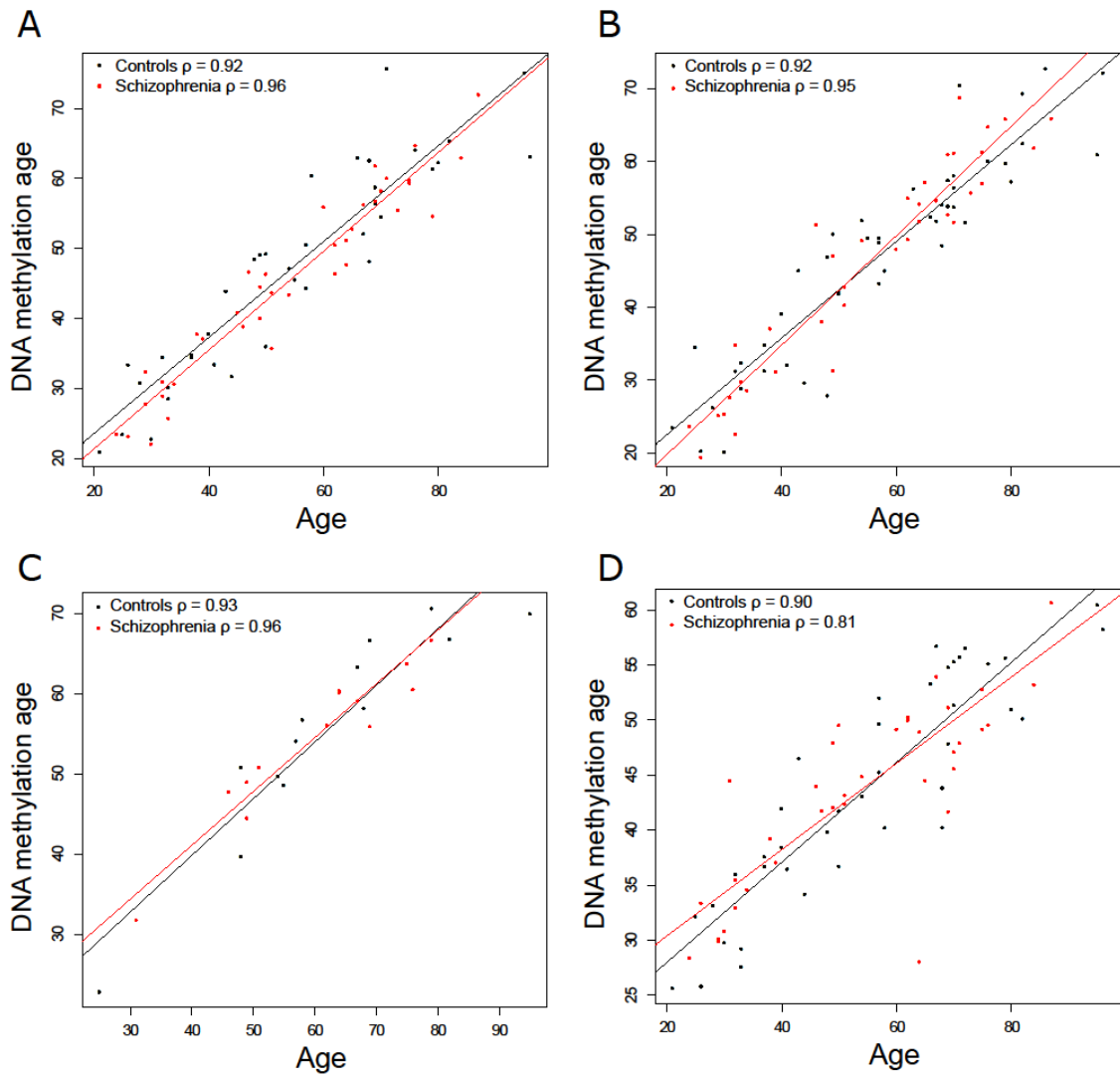


Figure 3.19. Correlation between chronological age and DNA methylation age separated by schizophrenia cases (red) and controls (black). Shown is the correlation between chronological age (x-axis) and DNA methylation age (y-axis) for samples from both cohorts for A) prefrontal cortex, B) striatum, C) hippocampus, and D) cerebellum. ρ , Pearson's correlation coefficient.

3.3.3. Differently methylated positions associated with schizophrenia

My first analyses focused on identifying DNA methylation differences between schizophrenia cases and non-psychiatric controls. There was widespread evidence for schizophrenia-associated variation at specific *loci* across the genome in each brain region. QQ plots for the analyses in each tissue are shown in **Figures 3.20 to 3.23**, highlighting little evidence of systematic *P*-value inflation (PFC $\lambda = 1.18$, STR $\lambda = 1.02$, HC $\lambda = 1.13$, CER $\lambda = 1.23$) in any of the four brain regions. Manhattan plots for the analyses in each brain region are shown in **Figures 3.24 to 3.27**. The fifty top ranked schizophrenia-associated DMPs in each brain region are listed in **Tables 3.5 to 3.8** and **Figures 3.28 to 3.31**, with those passing a highly stringent family-wise significance threshold ($P < 1.66E-07$, see **section 3.1.3**), shown in **Table 3.9** and **Figure 3.32**.

Although the specific list of top ranked DMPs identified in each tissue is distinct, many DMPs are characterised by consistent effects across brain regions (**Figures 3.28 to 3.31**), and for DMPs identified in each of the four individual brain regions, schizophrenia-associated DNA methylation differences are significantly positively correlated with those at the same probes in the other three brain regions (**Figures 3.33 to 3.36** and **Table 3.10**).

Of note, genes annotated to several of these top ranked probes have been previously implicated in the etiology and pathophysiology of schizophrenia. For example:

- The top ranked DMP - cg08743050, which is significantly hypomethylated in PFC ($P = 1.84E-08$) - is located in the gene body of the neural cell adhesion molecule 1 (*NCAM1*) gene, which encodes a cell adhesion protein with a well-established role in neurodevelopment and synaptic plasticity (Ronn et al., 1998, Sunshine et al., 1987).
- cg08103144 is significantly hypomethylated in STR ($P = 3.64E-08$) and located within the synaptopodin gene (*SYNPO*), a gene encoding an actin-associated protein that plays a role in actin-based cell shape and motility that has been shown to be differentially expressed in schizophrenia brains (Focking et al., 2015).

- cg22221320 is significantly hypermethylated in STR ($P = 7.88E-08$) and located in the guanylate binding protein 4 (*GBP4*), a gene that has been found to be differentially expressed in schizophrenia patients (Sanders et al., 2013).

- Also of interest is cg15607358, which is hypermethylated in STR ($P = 1.03E-05$) and annotated to the solute carrier family 6-neurotransmitter transporter GABA-member 13 (*SLC6A13*) gene, also known as GABA transporter 2 (*GAT2*), which is a transporter of the key inhibitory neurotransmitter GABA. The GABAergic system has been extensively implicated in neurodevelopment and schizophrenia pathology (Schmidt and Mirnics, 2015).

Other DMPs were also of potential interest in the context of schizophrenia such as:

- cg20044211 is significantly hypermethylated in PFC ($P = 7.54E-06$) and annotated to the gene body of the *NOTCH4* gene, which is a member of the NOTCH pathway with an important role in neurodevelopment (Lasky and Wu, 2005).

- cg19028706 is significantly hypomethylated in PFC ($P = 6.71E-06$) and annotated to the gene body of trafficking protein kinesin binding 1 (*TRAK1*). This gene encodes a protein that complexes with the protein encoded by the disrupted in schizophrenia 1 (*DISC1*) gene. A balanced translocation involving *DISC1* that segregates with several major psychiatric disorders including schizophrenia has been intensively studied in a Scottish pedigree (St Clair et al., 1990), although the involvement of this *locus* in the etiology of the disorder remains controversial and common genetic variation in this region was not identified in recent GWAS analyses (Schizophrenia Working Group of the Psychiatric Genomics, 2014). The complex involving *TRAK1* and *DISC1* plays a role in mitochondrial transport in neuronal axons (Ogawa et al., 2014, Norkett et al., 2016)

- cg10071493 is hypermethylated in PFC ($P = 2.13E-06$) and is annotated to the calcium channel voltage-dependent T type alpha 1H subunit (*CACNA1H*) gene in the GREAT annotation database (McLean et al., 2010) (the probes is located 23726bp upstream the transcription start site of the gene) (see **section 3.2.7** for details on the GREAT annotation). This gene encodes a protein in the

voltage-dependent calcium channel complex, previously implicated in epilepsy (Eckle et al., 2014).

- cg10383028 probe is hypomethylated in HC ($P = 5.30E-06$) and annotated to the transcription start site of the calcium voltage-gated channel subunit alpha1 G (*CACNA1G*) gene.

Notably, variation in other voltage-gated calcium channel genes has been implicated in schizophrenia, including common genetic variants in *CACNA1C*, *CACNB2* and *CACNA1I* in the latest schizophrenia GWAS (Schizophrenia Working Group of the Psychiatric Genomics, 2014).

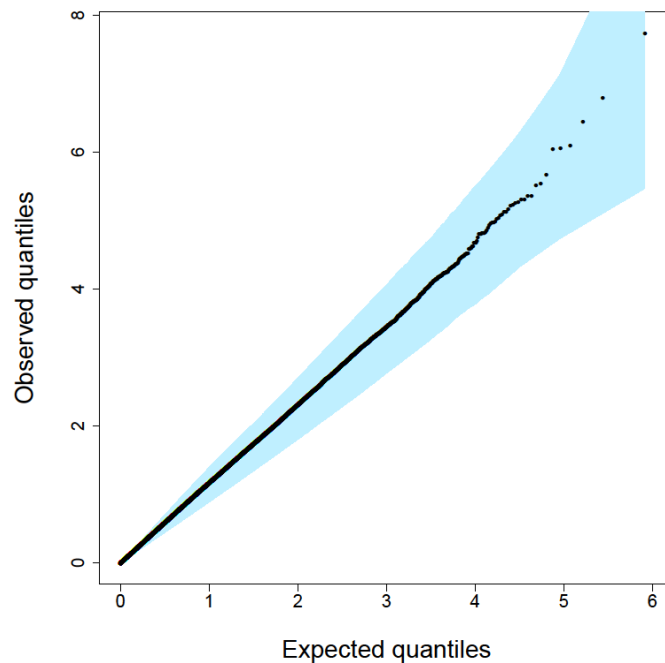


Figure 3.20. Quantile-quantile plot for the prefrontal cortex (PFC) case-control schizophrenia EWAS. Shown are the expected (x-axis) and observed (y-axis) quantiles observed in the meta-analysis of the PFC of both the MRC London Neurodegenerative Diseases Brain Bank and Douglas-Bell Canada Brain Bank. Blue shading indicates 95% confidence intervals. $\lambda = 1.18$.

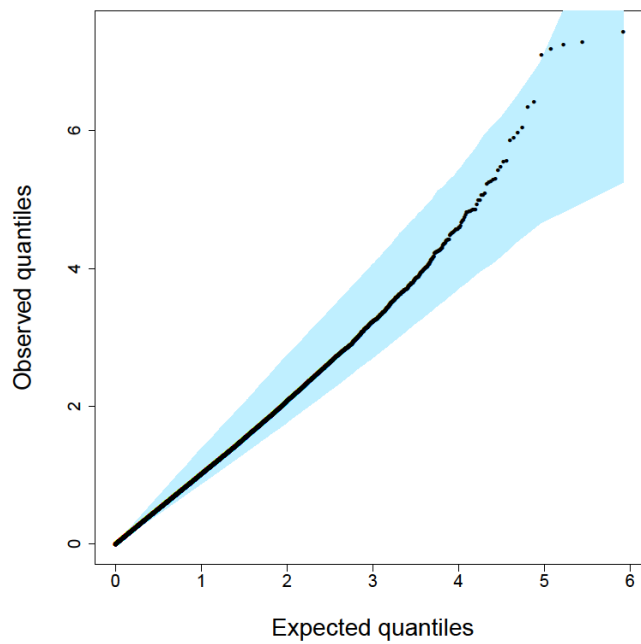


Figure 3.21. Quantile-quantile plot for the striatum (STR) case-control schizophrenia EWAS. Shown are the expected (x-axis) and observed (y-axis) quantiles observed in the meta-analysis of the STR of both the MRC London Neurodegenerative Diseases Brain Bank and Douglas-Bell Canada Brain Bank. Blue shading indicates 95% confidence intervals. $\lambda = 1.02$.

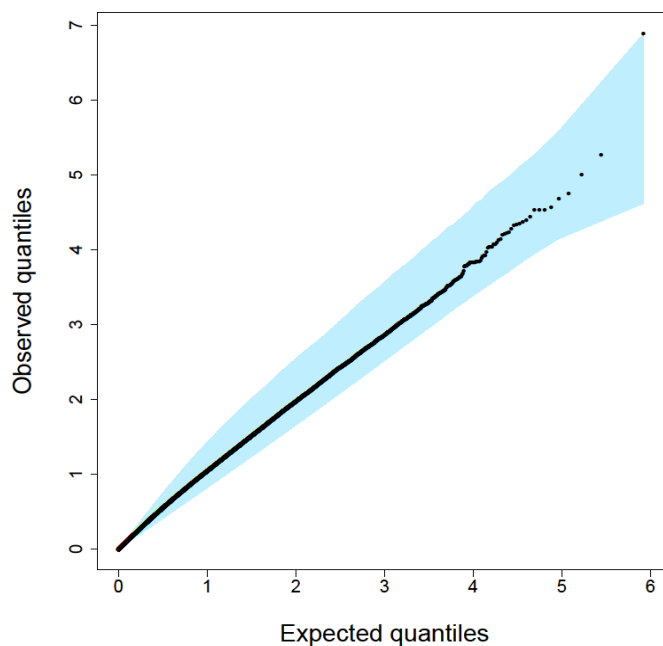


Figure 3.22. Quantile-quantile plot for the hippocampus (HC) case-control schizophrenia EWAS. Shown are the expected (x-axis) and observed (y-axis) quantiles observed in the linear regression analysis of the HC data from the MRC London Neurodegenerative Diseases Brain Bank. Blue shading indicated 95% confidence intervals. $\lambda = 1.13$.

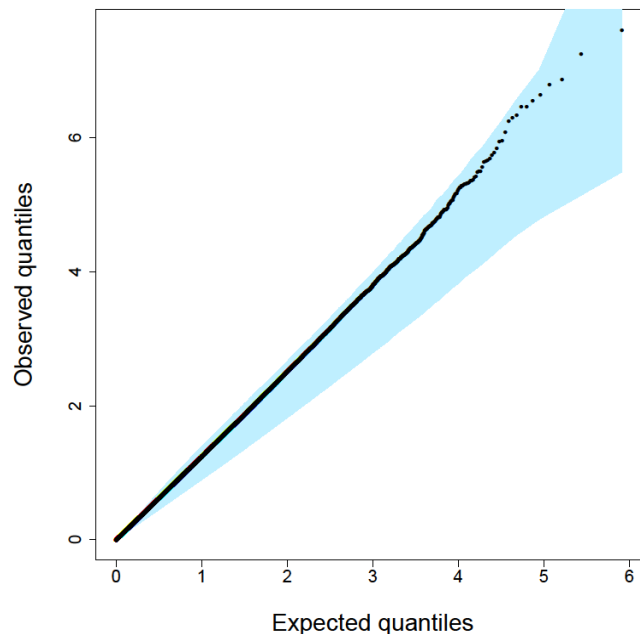


Figure 3.23. Quantile-quantile plot for the cerebellum (CER) case-control schizophrenia EWAS. Shown are the expected (x-axis) and observed (y-axis) quantiles observed in the meta-analysis of the CER of both the MRC London Neurodegenerative Diseases Brain Bank and Douglas-Bell Canada Brain Bank. Blue shading indicates 95% confidence intervals. $\lambda = 1.23$.

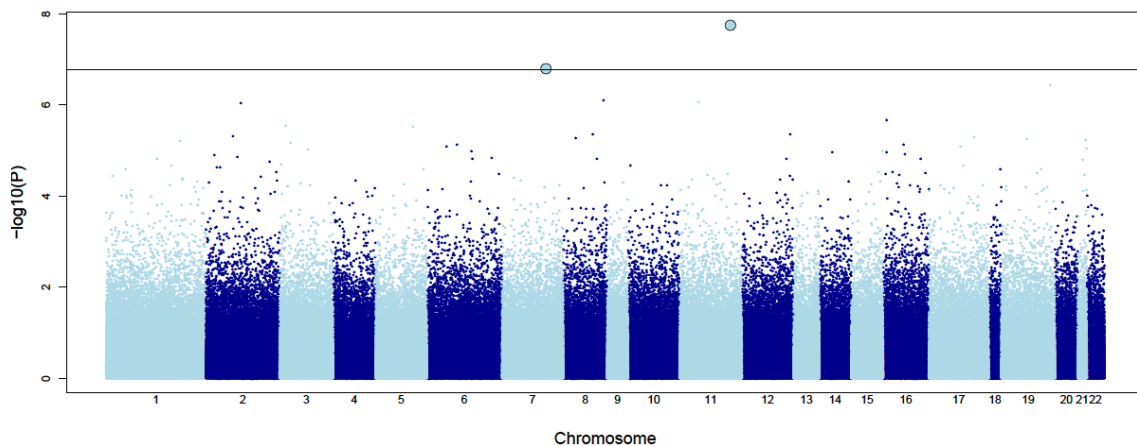


Figure 3.24. Manhattan plot for the prefrontal cortex (PFC) case-control schizophrenia EWAS. Shown are the $-\log_{10}(P\text{-values})$ (y-axis) of the meta-analysis of the PFC of both the MRC London Neurodegenerative Diseases Brain Bank and Douglas-Bell Canada Brain Bank by chromosomal position (x-axis). The horizontal line indicates a stringent multiple-testing significance threshold ($P = 1.66E-07$) (see **section 3.2.8**).

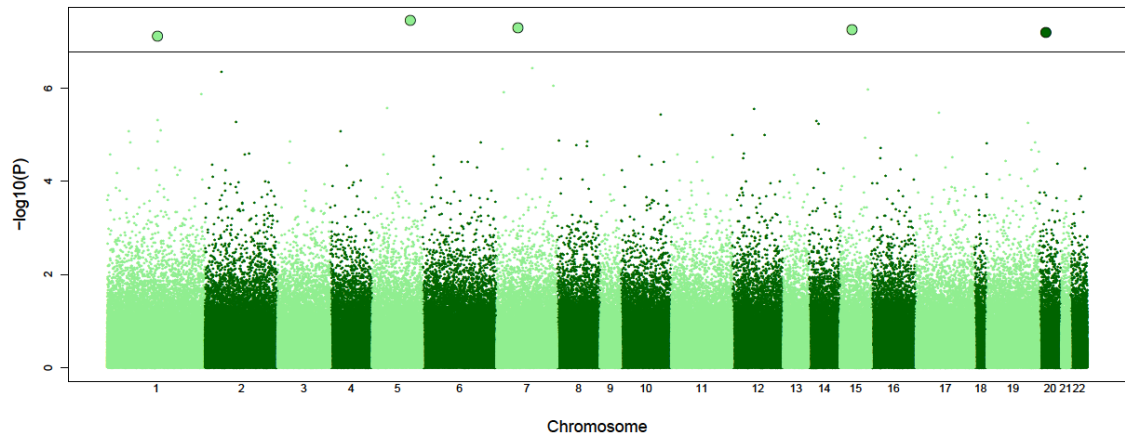


Figure 3.25. Manhattan plot for the striatum (STR) case-control schizophrenia EWAS. Shown are the $-\log_{10}(P\text{-values})$ (y-axis) of the meta-analysis of the STR of both the MRC London Neurodegenerative Diseases Brain Bank and Douglas-Bell Canada Brain Bank by chromosomal position (x-axis). The horizontal line indicates a stringent multiple-testing significance threshold ($P = 1.66\text{E-}07$) (see **section 3.2.8**).

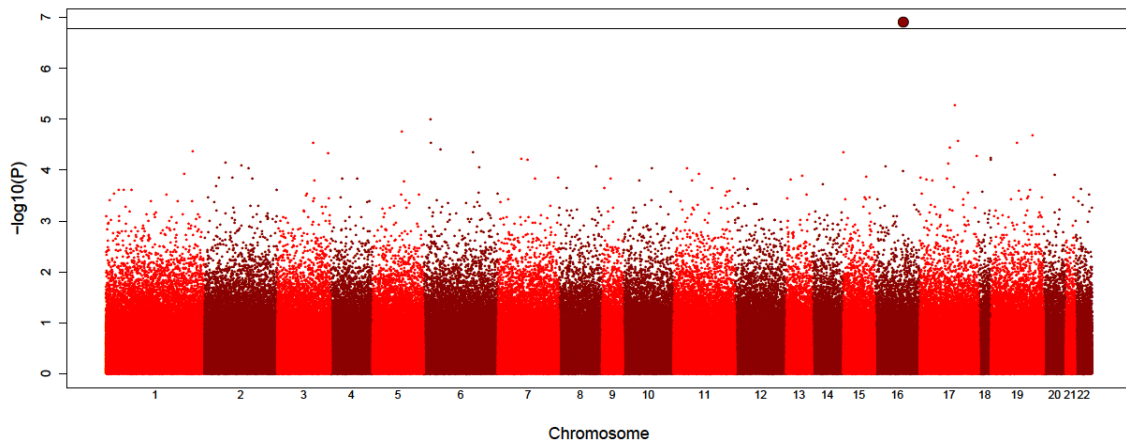


Figure 3.26. Manhattan plot for the hippocampus (HC) case-control schizophrenia EWAS. Shown are the $\log_{10}(P\text{-values})$ (y-axis) of the linear regression analysis of the HC data from the MRC London Neurodegenerative Diseases Brain Bank by chromosomal position (x-axis). The horizontal line indicates a stringent multiple-testing significance threshold ($P = 1.66\text{E-}07$) (see **section 3.2.8**).

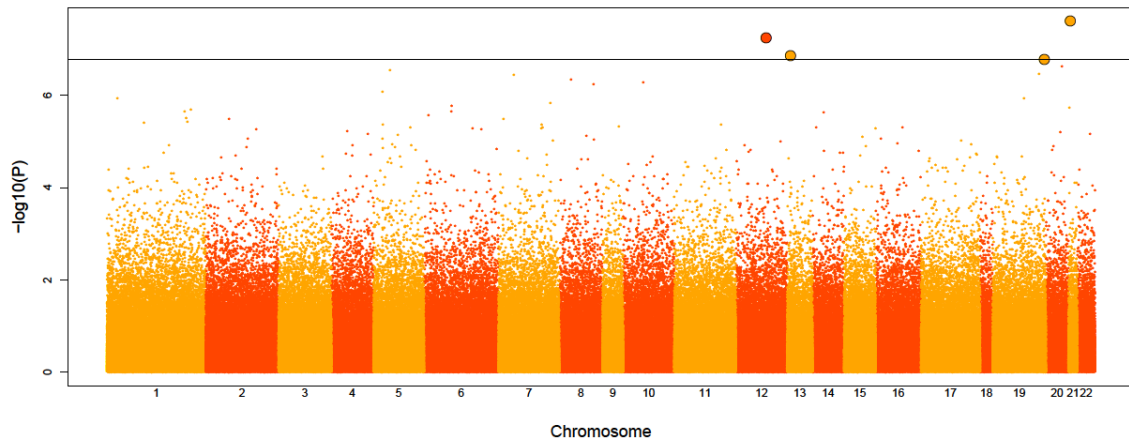


Figure 3.27. Manhattan plot for the cerebellum (CER) case-control schizophrenia EWAS. Shown are the $-\log_{10}(P\text{-values})$ (y-axis) of the meta-analysis of the CER of both the MRC London Neurodegenerative Diseases Brain Bank and Douglas-Bell Canada Brain Bank by chromosomal position (x-axis). The horizontal line indicates a stringent multiple-testing significance threshold ($P = 1.66E-07$) (see **section 3.2.8**).

Table 3.5. Top ranked schizophrenia-associated differently methylated probes (DMPs) identified in the prefrontal cortex (PFC) meta-analysis. Listed for each PFC DMP (grey) are corresponding results from the striatum (STR; $P < 0.05$ in green), hippocampus (HC; $P < 0.05$ in red) and cerebellum (CER; $P < 0.05$ in orange) meta-analyses (PFC, STR and CER) or linear regression (HC). Illumina and Genomic Regions Enrichment of Annotation Tool (GREAT) annotation (McLean et al., 2010) is listed for each DMP.

Probe ID	Genomic position (hg19)	Illumina gene annotation	Gene region	GREAT annotation (McLean et al., 2010)	Methylation difference PFC (%)	P PFC	Methylation difference STR (%)	P STR	Methylation difference HC (%)	P HC	Methylation difference CER (%)	P CER
cg08743050	chr11:113113936	NCAM1	Body	TTC12; NCAM1	-3.80	1.84E-08	-0.59	0.56	-2.53	0.18	-0.48	0.29
cg05686445	chr7:127636396	C7orf54; SND1	TSS1500; Body	LRRC4; SND1	-3.65	1.63E-07	-0.67	0.51	3.17	0.26	-0.75	0.50
cg26778001	chr19:55142181	LILRB1	5'UTR	LILRB1	2.48	3.64E-07	1.83	0.01	1.09	0.34	3.75	4.02E-04
cg26173173	chr8:144642813	GSDMD	Body	GSDMD; C6orf73	3.11	8.06E-07	1.39	0.08	1.73	0.30	1.21	0.18
cg03325693	chr1:34196316	ABTB2	Body	NAT10; ABTB2	-2.36	8.73E-07	-1.28	0.05	0.28	0.88	-0.08	0.88
cg16782339	chr2:109847146	SH3RF3	Body	SH3RF3; SEPT10	1.83	9.12E-07	0.11	0.78	-1.86	0.05	0.19	0.79
cg10071493	chr16:1179514	-	-	C1QTNF8; CACNA1H	3.69	2.13E-06	-0.42	0.54	0.64	0.72	0.03	0.97
cg18812956	chr3:19987665	RAB5A	TSS1500	RAB5A	4.68	2.90E-06	1.70	0.22	1.49	0.58	1.83	0.28
cg23303408	chr5:145718597	POU4F3	5'UTR; 1stExon	POU4F3	-1.93	3.04E-06	-0.56	0.18	0.15	0.88	-0.09	0.79
cg24281764	chr12:1323330505	MMP17	Body	ULK1; MMP17	0.71	4.38E-06	-8.18E-02	0.67	-0.10	0.76	-0.09	0.51
cg10654165	chr8:105479705	DPYS	TSS1500	DPYS	2.24	4.39E-06	-1.61	0.02	-0.29	0.82	0.24	0.82
cg16204289	chr2:75796759	FAM176A	5'UTR; 1stExon	MIRPL19; FAM176A	1.51	4.86E-06	-3.14E-02	0.95	0.19	0.75	0.44	0.37
cg17901382	chr17:73514798	TSEN54	Body	CASKIN2; TSEN54	2.69	4.98E-06	9.09E-04	1.00	0.38	0.76	-1.99	0.25
cg10932125	chr8:28929689	KIF13B	Body	HMBOX1; KIF13B	2.37	5.38E-06	-0.63	0.31	0.87	0.36	0.97	0.13
cg20098710	chr19:19640075	YJEFN3	Body	YJEFN3	-2.88	5.61E-06	-0.75	0.46	0.57	0.77	-0.52	0.51
cg20383948	chr21:46898137	COL18A1	Body	COL18A1; SLC19A1	-3.70	5.89E-06	0.60	0.55	-3.29	0.09	1.21	0.02
cg16350225	chr1:167666363	RCSL1	Body	CREG1; MPZL1	4.28	6.08E-06	-0.47	0.64	2.08	0.28	2.91	0.01
cg19028706	chr3:42158765	TRAK1	Body	TRAK1; CCK	-3.49	6.71E-06	-0.18	0.89	2.15	0.32	-0.35	0.61
cg07405426	chr16:30825646	-	-	ZNF629; BCL7C	0.70	7.44E-06	-0.45	0.06	0.32	0.41	-0.47	0.02
cg20044211	chr6:32185995	NOTCH4	Body	GPSM3; NOTCH4	2.69	7.54E-06	1.30	0.04	2.69	0.17	1.68	0.03
cg10072351	chr17:45000308	GOSR2	TSS200	GOSR2	-0.61	8.09E-06	0.06	0.76	0.30	0.76	-0.56	0.06
cg26088561	chr6:30619080	C6orf136	Body	C6orf136; DHX16	-2.62	8.26E-06	0.84	0.20	2.61	0.02	-0.44	0.65
cg04314225	chr21:47844134	PCNT	Body	DIP2A; PCNT	2.09	9.18E-06	0.34	0.64	-1.09	0.26	1.03	0.23

cg06099244	chr3:112739834	C3orf17	TSS1500	C3orf17	9.47E-06	-0.16	0.78	1.10	0.43	0.25	0.74
cg06777813	chr15:101085111	LASS3	TSS200	CERS3	1.02E-05	2.07	0.06	1.15	0.52	3.22	1.91E-03
cg02272814	chr6:46655782	TDRD6	1stExon; 5'UTR	TDRD6	1.06E-05	0.27	0.66	2.78	0.04	1.19	0.09
cg27059530	chr14:67707359	MPP5	TSS1500	MPP5	1.08E-05	-0.55	0.04	-1.02	0.08	0.14	0.52
cg07243041	chr16:1135931	-	-	C1QTNF8; SSTR5	1.11E-05	0.55	0.16	1.14	0.25	0.64	0.42
cg14125292	chr16:34407918	-	-	BC068290	1.17E-05	0.74	0.25	2.60	0.07	-0.33	0.73
cg18705408	chr2:20212524	MAATN3	TSS200	MAATN3	1.26E-05	-0.25	0.19	0.01	0.97	-0.14	0.43
cg09741917	chr2:98702260	VWA3B	TSS1500	CNGA3; TMEM131	1.40E-05	0.36	0.42	0.35	0.66	0.43	0.53
cg25529303	chr6:151186601	MTHFD1L	TSS200	MTHFD1L	1.46E-05	-0.70	0.34	1.10	0.53	-1.15	0.06
cg08633665	chr8:128972829	MIR1205; PVT1	TSS200; Body	MYC	1.52E-05	-0.14	0.84	0.86	0.54	1.75	0.01
cg16679302	chr16:85622276	-	-	KIAA0182; KIAA0513	1.52E-05	0.53	0.61	1.87	0.30	-1.55	0.37
cg25049698	chr6:50692605	TFAP2D	Body	TFAP2B; TFAP2D	1.54E-05	0.20	0.72	1.38	0.23	0.27	0.59
cg02213139	chr1:85527754	WDR63	TSS1500	MCOLN3; SYDE2	1.54E-05	0.39	0.30	-0.74	0.44	-0.08	0.86
cg27645498	chr12:125145553	-	-	NCOR2; SCARB1	1.54E-05	-0.35	0.73	-2.16	0.26	-0.96	0.18
cg02370100	chr21:43655256	ABCG1	Body	ABCG1; TFF3	1.56E-05	-0.75	0.25	-0.75	0.55	0.04	0.93
cg24044052	chr2:231191662	SP140L	TSS1500	SP140L	1.75E-05	0.34	0.63	1.30	0.39	0.44	0.44
ch.3.183336F	chr3:9516816	SETD5	Body	LHFPL4; THUMPD3	2.00E-05	0.15	0.69	0.63	0.45	0.27	0.58
cg26963844	chr17:47929214	-	-	TAC4	2.09E-05	-0.29	0.53	-1.47	0.07	-0.05	0.86
cg26548293	chr1:153606178	C1orf77; S100A13	TSS1500; 5'UTR	CHTOP	2.11E-05	1.53	0.19	-0.37	0.90	2.81	0.02
cg15081722	chr10:1517340	ADARB2	Body	ID1; ADARB2	2.12E-05	1.73	0.14	-0.43	0.85	2.52	0.11
cg06477164	chr2:37375682	EIF2AK2	TSS1500; 5'UTR	EIF2AK2; CCDC75	2.34E-05	0.09	0.84	-0.03	0.98	1.04	0.11
cg22488717	chr2:26785946	C2orf70	Body	OTOF	2.39E-05	-0.57	0.30	-1.40	0.31	0.05	0.95
cg02565255	chr5:177503040	-	-	PROP1; N4BP3	2.54E-05	0.19	0.57	-0.58	0.34	-0.06	0.84
cg11321921	chr18:77235850	NFATC1	Body	CTDP1; NFATC1	2.54E-05	0.37	0.36	0.22	0.78	0.07	0.88
cg09789590	chr19:46800479	HIF3A	Body; TSS1500	HIF3A	2.60E-05	-0.52	0.41	-1.38	0.17	0.74	0.01
cg03944444	chr1:16785803	NECAP2	3'UTR	NECAP2; NBPF1	2.62E-05	1.19	0.13	-0.93	0.58	0.60	0.35
cg26819783	chr2:240653447	-	-	HDAC4; NDUFA10	3.01E-05	-0.51	0.24	1.23	0.06	0.74	0.08

Table 3.6. Top ranked schizophrenia-associated differentially methylated probes (DMPs) identified in the striatum (STR) meta-analysis. Listed for each STR DMP (grey) are corresponding results from the prefrontal cortex (PFC; $P < 0.05$ in blue), hippocampus (HC; $P < 0.05$ in red) and cerebellum (CER; $P < 0.05$ in orange) meta-analyses (PFC, STR and CER) or linear regression (HC). Illumina and Genomic Regions Enrichment of Annotation Tool (GREAT) annotation (McLean et al., 2010) is listed for each DMP.

Probe ID	Genomic position (hg19)	Illumina gene annotation	Gene region	GREAT annotation (McLean et al., 2010)	Methylation difference (%) STR	P STR	Methylation difference (%) PFC	P PFC	Methylation difference (%) HC	P HC	Methylation difference (%) CER	P CER
cg08103144	chr5:150028986	SYNPO	Body	MYOZ3; SYNPO	-3.17	3.64E-08	0.68	0.21	0.24	0.84	0.83	0.29
cg03847432	chr7:43391524	HECW1	Body	STK17A; HECW1	2.71	5.23E-08	0.74	0.31	3.30	0.01	1.32	0.18
cg22182016	chr15:57998894	GRINL1A; GCOM1	TSS200; Body	POLR2M	-0.51	5.67E-08	-0.05	0.55	0.17	0.34	-0.13	0.10
cg25361651	chr20:29847402	DEFB115	Body	DEFB115; DEFB116	4.43	6.52E-08	1.03	0.32	-1.80	0.46	-	-
cg22221320	chr1:89664340	GBP4	Body	GBP4	6.93	7.89E-08	3.75	0.02	-0.05	0.99	2.68	0.12
cg02049663	chr7:99686396	COPS6	TSS200	COPS6	-0.64	3.76E-07	-0.27	0.03	0.13	0.74	-0.24	0.10
cg23245620	chr2:45172972	SIX3	3'UTR	SIX3; SIX2	3.49	4.47E-07	-0.78	0.44	2.48	0.14	-1.09	0.15
cg07514654	chr7:157258062	-	-	DNAJB6	-4.07	8.90E-07	-2.63	0.04	-0.33	0.89	-1.81	0.13
cg01663682	chr15:93447777	CHD2	Body	CHD2; RGMA	-1.26	1.06E-06	-0.10	0.64	-1.54	0.05	-0.49	0.04
cg27203372	chr7:26383310	IQCE	Body	TTYH3; IQCE	1.48	1.26E-06	0.26	0.57	1.09	0.19	0.08	0.84
cg02454364	chr1:236156917	NID1	Body	LYST; NID1	-2.86	1.36E-06	0.07	0.58	-0.16	0.64	-0.46	0.08
cg24741713	chr5:59064389	PDE4D	Body	PDE4D	-1.30	2.76E-06	0.18	0.60	-1.64	0.02	-0.26	0.44
cg03226218	chr12:57082170	PTGES3	TSS200	PTGES3	-0.59	2.80E-06	0.03	0.81	-0.36	0.37	-0.03	0.88
cg02443072	chr17:37183683	-	-	PLXDC1; LASP1	-1.62	3.32E-06	-1.32	0.01	-1.08	0.10	-0.41	0.34
cg03804621	chr10:124638756	FAM24B; LOC399815	5'UTR; TSS1500	FAM24B	5.44	3.71E-06	4.36	0.002	1.46	0.52	6.02	6.58E-05
cg21365602	chr1:89664407	GBP4	Body	GBP4	6.23	4.99E-06	4.46	8.42E-04	0.54	0.86	4.49	5.97E-04
cg16685608	chr14:52211579	-	-	GNG2; FRMD6	3.48	5.06E-06	2.20	0.02	-0.94	0.50	1.24	0.30
cg18122392	chr2:99013409	CNGA3	Body	INPP4A; CNGA3	-1.99	5.37E-06	0.67	0.18	-0.54	0.40	0.04	0.94
cg12253200	chr19:49123013	RPL18; SPHK2	TSS1500; 5'UTR	RPL18; SPHK2	-1.00	5.55E-06	-0.29	0.19	-0.99	0.04	-0.35	0.17
cg18116486	chr14:58667316	ACTR10	Body	ACTR10	-0.84	5.95E-06	-0.21	0.33	-0.54	0.22	0.15	0.53
cg05612904	chr1:101491636	DPH5	TSS1500	DPH5	-0.64	8.13E-06	-0.04	0.78	-1.14	0.10	-0.04	0.78
cg05461666	chr1:20573259	-	-	PLA2G2C; VWA5B1	1.36	8.45E-06	0.63	0.03	2.03	0.40	0.30	0.32

cg06768993	chr4:8443412	ACOX3	TSS1500	ACOX3; METTL19	3.28	8.57E-06	2.03	0.03	1.27	0.46	3.37	9.12E-04
cg24688803	chr12:105478590	ALDH1L2	TSS1500	ALDH1L2	2.66	1.03E-05	1.62	0.05	0.46	0.78	-0.85	0.46
cg15607358	chr12:372049	SLC6A13	TSS200	SLC6A13	4.49	1.03E-05	-0.91	0.41	0.26	0.87	-0.73	0.53
cg15559640	chr15:89010445	MRPS11; MRPL46	TSS1500; 1stExon	MRPS11; MRPL46	-0.98	1.18E-05	-0.26	0.22	-0.61	0.17	-0.22	0.31
cg18803856	chr8:1495169	DLGAP2	5'UTR	CLN8; DLGAP2	1.73	1.37E-05	0.83	0.09	-0.80	0.44	0.36	0.35
cg25924911	chr3:45838094	SLC6A20	TSS200	SLC6A20	0.69	1.38E-05	-0.11	0.34	-0.04	0.88	0.05	0.78
cg22513099	chr8:117788299	-	-	UTP23; RAD21	3.93	1.39E-05	-0.19	0.85	3.70	0.13	3.12	4.93E-03
cg13938909	chr1:89873226	LOC400759	TSS200	LRRCC8B; GBP6	4.35	1.44E-05	2.08	0.02	3.25	0.22	-	-
cg26823162	chr19:55792075	HSPBP1	TSS1500	BRSKI; HSPBP1	1.44	1.47E-05	0.74	0.05	0.52	0.54	0.77	0.14
cg11225745	chr1:22927925	EPHA8	Body	C1QA; EPHA8	1.73	1.49E-05	-0.14	0.73	0.55	0.50	-0.79	0.03
cg11584284	chr6:130690629	-	-	TMEM200A; L3MBTL3	1.98	1.49E-05	-0.36	0.51	0.26	0.83	0.35	0.71
cg07500432	chr18:77918588	PAR6G; LOC100730522	Body	ADNP2; PAR6G	4.64	1.54E-05	6.69	6.25E-05	5.11	1.00E-03	3.14	0.04
cg04682911	chr8:59971099	TOX	Body	NSMAF; TOX	-1.35	1.66E-05	-0.01	0.97	0.83	0.33	0.70	0.19
cg10207277	chr8:14449243	CSMD3	TSS200	CSMD3	-0.83	1.80E-05	0.01	0.98	0.32	0.46	-0.08	0.73
cg04278794	chr16:3406339	OR2C1	1stExon	OR2C1	3.11	1.97E-05	0.48	0.62	1.44	0.33	1.78	0.06
cg11794120	chr7:2087905	MAD1L1	Body	MAD1L1; ELFN1	-1.43	2.03E-05	-0.97	0.04	-0.93	0.42	1.25	4.09E-03
cg00996764	chr19:51382591	KLK2	3'UTR	KLK2; KLK4	1.82	2.16E-05	-0.32	0.45	-0.39	0.66	0.80	0.19
cg07777224	chr19:58919807	ZNF584	TSS1500	ZNF584	-1.41	2.37E-05	-0.05	0.82	1.09	0.35	-0.23	0.46
cg21008684	chr2:157198370	-	-	GPD2; NR4A2	-0.76	2.54E-05	-0.13	0.55	-0.38	0.19	-0.05	0.82
cg01837362	chr12:34492938	-	-	ALG10	5.26	2.56E-05	4.78	5.15E-04	5.90	0.03	6.01	8.20E-05
cg09063683	chr5:37890150	-	-	EGFLAM; GDNF	-3.24	2.70E-05	-0.99	0.19	-5.56	8.44E-04	-1.52	0.05
cg10042645	chr11:2308589	-	-	ASCL2; C11orf21	2.16	2.70E-05	0.25	0.66	2.81	0.01	0.54	0.36
cg18743464	chr2:131089942	-	-	TUBA3E; CCDC115	2.73	2.71E-05	1.34	0.05	0.53	0.68	1.53	0.18
cg13897348	chr1:1549699	MIB2	TSS1500	MIB2	4.57	2.73E-05	-0.45	0.69	-0.01	1.00	-1.56	0.11
cg15212418	chr17:155045	RPH3AL	Body	DOC2B; RPH3AL	-9.74	2.86E-05	-7.39	1.24E-03	-9.06	0.07	-9.30	2.12E-03
cg13647960	chr10:68582091	CTNNA3	Body	LRRTM3	2.93	2.92E-05	-	-	-0.89	0.58	-	-
cg21196747	chr6:27521385	-	-	ZNF184; HIST1H2BL	-2.93	2.99E-05	-2.25	0.01	-0.79	0.71	-3.11	2.18E-04
cg18444231	chr17:55058723	SCPEP1	Body	AKAP1; SCPEP1	3.76	3.02E-05	1.84	0.05	6.77	0.003	-0.03	0.98

Table 3.7. Top ranked schizophrenia-associated differentially methylated probes (DMPs) identified in the hippocampus (HC) linear regression analysis. Listed for each HC DMP (grey) are corresponding results from the prefrontal cortex (PFC; $P < 0.05$ in blue), striatum (STR; $P < 0.05$ in green) and cerebellum (CER; $P < 0.05$ in orange) meta-analyses. Illumina and Genomic Regions Enrichment of Annotation Tool (GREAT) annotation (McLean et al., 2010) is listed for each DMP.

Probe ID	Genomic position (hg19)	Illumina gene annotation	Gene region	GREAT annotation (McLean et al., 2010)	Methylation difference (%) HC	P HC	Methylation difference PFC (%)	P PFC	Methylation difference STR (%)	P STR	Methylation difference CER (%)	P CER
cg07751266	chr16:67515323	ATP6V0D1	TSS1500	ATP6V0D1	-1.35	1.27E-07	-0.13	0.41	-0.27	0.30	-0.26	0.21
cg10383028	chr17:48638097	CACNA1G	TSS1500	CACNA1G	-0.59	5.30E-06	-0.09	0.29	0.02	0.84	0.17	0.12
cg20871346	chr6:17021625	-	-	RBM24; ATXN1	-6.14	9.89E-06	0.46	0.41	-0.47	0.53	-0.09	0.91
cg01422136	chr5:132362224	ZCCHC10	1stExon	ZCCHC10	-1.56	1.75E-05	-0.03	0.89	0.05	0.82	0.13	0.56
cg23082877	chr19:49243427	RASIP1	Body	RASIP1	-4.37	2.03E-05	0.01	0.98	-0.55	0.51	-1.42	0.08
cg16250023	chr17:58470033	USP32	TSS1500	USP32	-0.92	2.71E-05	0.02	0.90	-0.22	0.11	-0.09	0.59
cg25119073	chr19:23870151	ZNF675	TSS200	ZNF675	-2.56	2.87E-05	-0.12	0.78	-0.43	0.30	0.11	0.84
cg23860886	chr6:18155593	KDM1B; TPMT	TSS200; TSS1500	TPMT; KDM1B	-1.05	2.89E-05	-0.06	0.68	0.14	0.53	-0.02	0.90
cg23201032	chr3:134369828	KY	5'UTR; 1stExon	KY	-0.91	2.91E-05	0.27	0.18	-0.13	0.38	0.10	0.52
cg05092310	chr17:43226346	HEXIM1	1stExon; 5'UTR	HEXIM2; HEXIM1	-1.01	3.56E-05	-0.17	0.32	-0.18	0.46	0.32	0.15
cg19115272	chr6:30139538	TRIM15	Body	TRIM10; TRIM26	-1.06	3.95E-05	-0.02	0.91	-0.05	0.67	0.02	0.90
cg07158797	chr1:215740701	KCTD3	TSS200	KCTD3	1.37	4.22E-05	-0.05	0.66	-0.22	0.18	-0.09	0.56
cg05167468	chr15:21905516	-	-	OR4M2	2.37	4.39E-05	0.11	0.72	-0.14	0.72	0.25	0.58
cg08266474	chr6:84904847	KIAA1009	Body	KIAA1009; MIRAP2	5.21	4.52E-05	0.29	0.59	0.72	0.25	1.38	0.02
cg21106136	chr3:194405973	FAM43A	TSS1500	LSG1; XYLT1	7.73	4.65E-05	-0.04	0.96	1.52	0.15	-	-
cg12167135	chr17:80573887	WDR45L	Body	WDR45L; FOXK2	-3.96	5.23E-05	0.03	0.98	-0.27	0.75	0.79	0.33
cg13590055	chr18:77917647	LOC100130522; PARD6G	Body; 3'UTR	ADNP2; PARD6G	12.85	5.80E-05	8.89	1.33E-04	7.99	6.91E-05	4.18	0.01
cg20195319	chr7:47568297	TNS3	5'UTR	TNS3	1.88	5.99E-05	0.00	1.00	0.49	0.07	0.03	0.95
cg01310473	chr7:76829168	CCDC146; FGL2	Body; TSS200	FGL2	3.58	6.15E-05	-0.44	0.55	1.37	0.03	-1.95	0.07
cg19815565	chr18:77917615	LOC100130522; PARD6G	Body; 3'UTR	ADNP2; PARD6G	12.76	6.24E-05	8.06	6.77E-04	8.57	2.23E-04	4.03	0.06
cg01657493	chr2:64681082	HSPC159	TSS1500	LGALS1	-2.05	7.10E-05	0.35	0.19	-0.41	0.28	-0.03	0.92
cg18938150	chr17:42144162	LSM12	5'UTR	G6PC3	-1.12	7.37E-05	0.05	0.77	0.11	0.49	-0.19	0.40
cg03075791	chr2:120774652	EPB41L5	5'UTR	EPB41L5; TMEIM185B	2.96	7.94E-05	0.39	0.60	0.11	0.83	0.68	0.25
cg02851167	chr8:143378153	TSNARE1	Body	FLJ43860;	3.52	8.30E-05	-0.32	0.61	0.43	0.45	0.60	0.42

cg09851072	chr16:4749498	ANKS3	TSMARE1 NUDT16L1; ZNF500	Body	-2.02	8.42E-05	-0.26	0.46	0.28	0.54	-0.37	0.46
cg08681110	chr6:114178501	MARCKS	MARCKS	TSS200	-2.11	8.98E-05	0.18	0.51	-0.18	0.54	0.74	9.61E-04
cg07152487	chr11:14665355	PDE3B; PSMA1	PDE3B	1stExon; TSS200; 5'UTR	0.99	9.08E-05	-0.09	0.48	-0.03	0.89	0.17	0.34
cg24023498	chr2:157199345	-	GPD2; NR4A2	-	-2.26	9.08E-05	-0.69	0.07	-0.23	0.71	0.28	0.40
cg05134775	chr10:98273510	TLL2	TLL2	1stExon; 5'UTR	0.81	9.25E-05	0.07	0.61	-0.15	0.22	-0.11	0.36
cg04044983	chr16:67280079	FHOD1	SLC9A5; FHOD1	Body	-1.51	1.06E-04	-0.24	0.41	-0.01	0.97	-0.25	0.46
cg18489266	chr11:59323918	-	OR4D9; OSBP	-	4.56	1.17E-04	-1.19	0.02	-0.48	0.51	0.29	0.62
cg12591668	chr1:192520335	-	RGS1; RGS21	-	4.52	1.18E-04	0.53	0.49	1.02	0.11	-0.35	0.63
cg03532879	chr20:37209395	ADIG	ADIG	TSS1500	6.73	1.23E-04	-0.22	0.70	1.41	0.14	-0.48	0.47
cg24122364	chr13:99574736	DOCK9	SLC15A1; DOCK9	Body	-10.93	1.27E-04	-1.08	0.40	-1.37	0.40	-0.11	0.93
cg15193475	chr15:80998711	FAM108C1	KIAA1199; FAM108C1	Body	3.65	1.37E-04	1.06	0.11	1.26	0.07	1.33	0.02
cg01896926	chr17:685509	GLOD4; RNMTL1	RNMTL1; GLOD4	5'UTR; 1stExon; TSS200	-0.49	1.41E-04	0.03	0.84	-0.07	0.44	0.24	0.08
cg21328651	chr7:158742190	-	ESYT2; VIPR2	-	2.35	1.42E-04	1.37	0.02	0.50	0.13	-0.20	0.66
cg09414612	chr2:85838835	C2orf68	USP39	Body	-0.81	1.42E-04	0.13	0.49	-0.05	0.57	0.23	0.03
cg22573675	chr2:38762739	-	ATL2; HNRPLL	-	-3.36	1.42E-04	-0.10	0.81	0.38	0.39	1.07	0.35
cg22761176	chr2:173539542	-	RAPGEF4; PDK1	-	-6.09	1.44E-04	-1.14	0.29	0.41	0.67	0.37	0.75
cg00645229	chr4:15429531	C1QTNF7	C1QTNF7	TSS200; Body; 5'UTR	-3.53	1.46E-04	0.66	0.36	0.60	0.35	1.32	3.08E-03
cg12271317	chr4:108972693	LEF1	HADH; LEF1	3'UTR; Body	-3.33	1.47E-04	0.41	0.26	0.14	0.76	-0.22	0.77
cg23213170	chr9:108320507	FKTN	FKTN	5'UTR	-1.37	1.47E-04	0.05	0.75	-0.20	0.26	-0.30	0.14
cg25512683	chr17:41003399	AOC3	AOC3	1stExon	3.59	1.47E-04	-0.58	0.38	-0.48	0.44	0.64	0.34
cg24799451	chr11:134093757	NCAPD3; VPS26B	VPS26B; NCAPD3	1stExon; TSS1500	-1.07	1.48E-04	-0.18	0.28	-0.22	0.34	0.03	0.87
cg09442740	chr7:100482960	SRR7	UFSP1; SRR7	Body	1.60	1.48E-04	0.34	0.15	0.25	0.77	-0.51	0.21
cg12859716	chr17:6552190	MED31	KIAA0753; MED31	Body	4.41	1.53E-04	0.58	0.24	0.25	0.63	0.36	0.54
cg08634721	chr13:30169482	SLC7A1	SLC7A1	5'UTR	-1.77	1.54E-04	-	-	-0.11	0.64	-0.13	0.64
cg25201910	chr3:138327818	FAIM	FAIM	5'UTR; TSS200	-2.77	1.59E-04	-0.39	0.40	-0.05	0.90	-0.44	0.37
cg12799790	chr10:54071134	-	DKK1	-	6.39	1.61E-04	-	-	1.86	0.03	1.22	0.35

Table 3.8. Top ranked schizophrenia-associated differentially methylated probes (DMPs) identified in the cerebellum (CER) meta-analysis. Listed for each CER DMP (grey) are corresponding results from the prefrontal cortex (PFC; $P < 0.05$ in blue), striatum (STR; $P < 0.05$ in green) and hippocampus (HC; $P < 0.05$ in red) meta-analyses (PFC, STR and CER) or linear regression (HC). Illumina and Genomic Regions Enrichment of Annotation Tool (GREAT) annotation (McLean et al., 2010) is listed for each DMP.

Probe ID	Genomic position (hg19)	Illumina gene annotation	Gene region	GREAT annotation (McLean et al., 2010)	Methylation difference (%) CER	P CER	Methylation difference PFC (%)	PPFC	Methylation difference STR (%)	P STR	Methylation difference HC (%)	PHC
cg14609448	chr21:34896882	GART	Body; 3'UTR	DNAJC28; GART	2.29	2.48E-08	0.15	0.81	-0.02	0.95	-0.57	0.70
cg01757160	chr12:96588951	ELK3	5'UTR	ELK3	0.56	5.74E-08	0.15	0.31	0.03	0.88	-0.30	0.44
cg09757430	chr13:28397122	-	-	PDX1; GSX1	-3.13	1.37E-07	1.21	0.23	-0.31	0.77	-2.05	0.38
cg20751795	chr19:58281019	ZNF586	TSS200	ZNF586	0.57	1.64E-07	0.18	0.10	-0.02	0.89	-0.44	0.03
cg01692482	chr20:52198378	ZNF217	1stExon	ZNF217; TSHZ2	2.51	2.30E-07	0.12	0.87	-1.05	0.09	-0.69	0.47
cg02688226	chr5:68665548	RAD17; TAF9	TSS200; 1stExon; 5'UTR; TSS1500	RAD17; TAF9	-0.51	2.84E-07	-0.17	0.10	-4.30E-03	0.97	-0.20	0.38
cg02966813	chr19:52495464	ZNF615	3'UTR	ZNF350; ZNF615	3.42	3.47E-07	0.72	0.41	0.02	0.98	1.17	0.51
cg23055921	chr7:26112215	-	-	NPVF; NFE2L3	4.18	3.49E-07	1.58	0.06	0.71	0.40	2.36	0.22
cg22230538	chr8:28258841	-	-	FZD3; ZNF395	0.45	4.59E-07	0.18	0.06	0.13	0.25	-0.24	0.42
cg10432626	chr10:72033567	-	-	PPA1; NPPFR1	2.09	5.09E-07	0.53	0.26	0.15	0.77	1.80	0.19
cg18618431	chr8:134531916	ST3GAL1	5'UTR	NDRG1; ST3GAL1	2.36	5.65E-07	-0.90	0.10	-0.29	0.51	1.34	0.20
cg10589310	chr5:23507030	PRDM9	TSS1500	PRDM9	5.08	8.37E-07	1.88	0.02	2.12	0.01	3.53	0.03
cg12830694	chr19:38747796	PPP1R14A	TSS1500	PPP1R14A	1.68	1.13E-06	0.44	0.20	0.42	0.20	-0.36	0.53
cg22530668	chr1:5919081	-	-	NPHP4	2.00	1.13E-06	0.59	0.18	0.40	0.45	-0.29	0.76
cg13043509	chr7:150434452	GIMAP5	1stExon; 5'UTR	GIMAP1-GIMAP5; TIME176B	4.36	1.44E-06	1.94	0.05	0.79	0.36	-0.15	0.91
cg10303653	chr6:32049516	TNXB	Body	TNXB; CYP21A2	-5.91	1.66E-06	0.49	0.55	-0.15	0.84	-1.78	0.06
cg20220242	chr21:30392188	RWDD2B	TSS1500	USP16; RWDD2B	5.92	1.82E-06	3.15	0.02	3.28	4.13E-03	1.22	0.63
cg22401939	chr1:206731166	RASSF5	Body	RASSF5; EIF2D	-3.73	2.06E-06	-0.18	0.81	0.78	0.38	0.60	0.74
cg22135102	chr6:32036897	TNXB	Body	CYP21A2; TNXB	-2.99	2.20E-06	0.16	0.76	0.11	0.83	-0.21	0.86
cg00208830	chr1:183154778	LAMC2	TSS1500	LAMC2	-3.54	2.24E-06	-0.70	0.19	-0.16	0.78	-1.65	0.16
cg13259118	chr14:62161958	HIF1A	TSS200	HIF1A	-0.77	2.31E-06	-0.33	0.03	-0.16	0.32	-0.60	0.16
cg02397497	chr6:10412073	TFAP2A	Body; 5'UTR; 1stExon	OFCC1; TFAP2A	1.23	2.73E-06	-0.52	0.45	-0.16	0.72	0.66	0.51
cg08917060	chr1:197872294	C1orf53	Body	DENND1B; LHX9	-1.09	3.15E-06	-0.19	0.47	0.01	0.98	0.35	0.71
cg26125384	chr2:70314274	PCBP1	TSS1500	PCBP1	-2.02	3.19E-06	-0.35	0.30	-0.64	0.22	1.35	0.26

cg00846140	chr7:1892569	MAD1L1	Body	ELFN1; MAD1L1	2.29	3.25E-06	0.55	0.25	0.26	0.67	1.52	0.06
cg05695876	chr1:201665422	NAV1	Body	IPO9; NAV1	-2.89	3.75E-06	-1.17	0.32	-0.67	0.52	-1.13	0.61
cg01664124	chr1:42928162	-	-	PIH; PPCS	2.77	3.86E-06	0.46	0.41	2.00	1.03E-03	2.11	0.05
cg24919344	chr5:24208918	-	-	CDH10; PRDM9	-3.85	4.27E-06	-2.44	0.01	1.44	0.05	-1.52	0.40
cg19467738	chr11:94823267	ENDOD1	1stExon	ENDOD1	0.66	4.34E-06	0.06	0.68	0.14	0.21	0.06	0.86
ch.7.124218544F	chr7:124431308	-	-	GPR37; POT1	-3.11	4.35E-06	-0.09	0.90	-0.34	0.60	-1.20	0.27
cg14629665	chr9:136819477	VAI2	Body	SARDH; VAI2	-3.17	4.66E-06	-0.59	0.47	0.26	0.81	1.52	0.48
cg23461926	chr5:147691991	SPINK7	5'UTR; 1stExon	SPINK7	3.48	4.83E-06	0.30	0.60	0.35	0.60	2.86	0.05
cg03919836	chr16:58426331	GINS3	5'UTR; 1stExon	GINS3	0.88	4.83E-06	-0.13	0.44	-0.42	0.04	-0.49	0.31
cg18710945	chr14:24887496	NYNRIN	3'UTR	CBLN3; NYNRIN	2.17	4.89E-06	0.56	0.25	-0.27	0.59	1.30	0.28
cg13169491	chr7:128368940	FAM71F1	Body	CALU; METTL2B	-2.64	4.96E-06	-0.76	0.04	-0.13	0.65	-2.67	0.02
cg20975713	chr15:102284772	TARSL2	TSS200	TARSL2	-0.99	5.13E-06	0.07	0.70	0.14	0.60	-0.02	0.97
cg18100830	chr7:123903317	-	-	TMEM229A; GPR37	-5.07	5.27E-06	-0.37	0.48	0.66	0.39	-0.69	0.47
cg25830605	chr6:79758654	PHIP	Body	PHIP; IRAK1BP1	2.32	5.29E-06	-0.76	0.46	-0.16	0.78	0.41	0.85
cg19267163	chr6:125004984	NKAIN2	Body	RNF217; NKAIN2	-5.12	5.46E-06	-1.39	0.12	0.23	0.79	2.61	0.13
cg17753475	chr2:180477963	ZNF385B	Body	SESTD1; ZNF385B	3.05	5.54E-06	0.63	0.15	-0.63	0.49	1.27	0.40
cg04609245	chr4:41646293	LIMCH1	Body	PHOX2B; LIMCH1	-2.99	5.91E-06	-2.55	1.95E-03	-0.91	0.26	2.09	0.10
cg01758993	chr20:44993436	SLC35C2	TSS1500	SLC35C2	-3.27	6.19E-06	-0.90	0.03	0.13	0.82	1.54	0.29
cg07393322	chr22:43117318	A4GALT	TSS1500	A4GALT	-2.25	6.79E-06	-0.67	0.22	0.17	0.81	-0.93	0.47
cg05388307	chr4:166248715	SC4MOL	TSS200	MSMO1	0.51	6.89E-06	-0.09	0.45	0.05	0.72	-0.56	0.03
cg00954536	chr5:110427846	WDR36	TSS200	WDR36	-1.28	7.02E-06	-0.23	0.39	-0.07	0.88	-0.72	0.37
cg21349849	chr8:99916884	-	-	STK3; OSR2	2.96	7.41E-06	0.65	0.17	-0.62	0.20	1.61	0.09
cg04484842	chr15:72410733	MYO9A; SENP8	TSS1500; 1stExon; 5'UTR	MYO9A; SENP8	0.56	7.87E-06	0.08	0.57	-0.05	0.76	-2.33E-03	0.99
cg04362002	chr5:23506738	PRDM9	TSS1500	PRDM9	4.16	8.53E-06	1.42	0.10	1.56	0.06	2.22	0.19
cg27316811	chr16:1576146	IFT140	Body	TMEM204; TELO2	1.39	8.60E-06	0.56	0.04	0.54	0.12	-1.10	0.12
cg08722395	chr2:144692640	-	-	GTDC1; ARHGAP15	2.71	8.85E-06	-0.87	0.27	1.36	0.04	-0.20	0.86

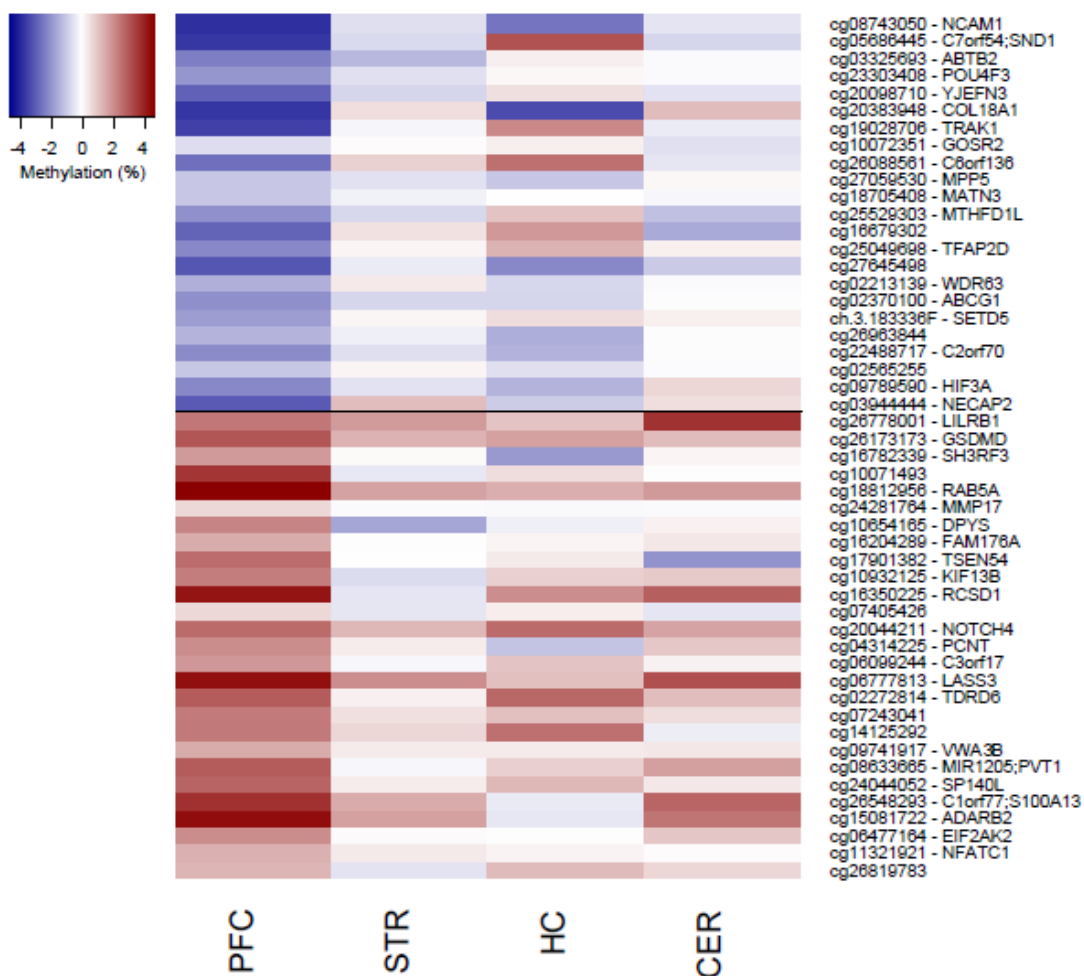


Figure 3.28. Heatmap showing the fifty top ranked schizophrenia-associated differentially methylated positions in the prefrontal cortex (PFC). Shown for each probe is the mean DNA methylation difference between cases and controls, with the corresponding difference at the same probe for the three other brain regions (striatum (STR), hippocampus (HC) and cerebellum (CER)) dissected from the same individuals. Probes are ordered by *P*-value for hypomethylated (blue, top) and hypermethylated (red, bottom) *loci* within the PFC.

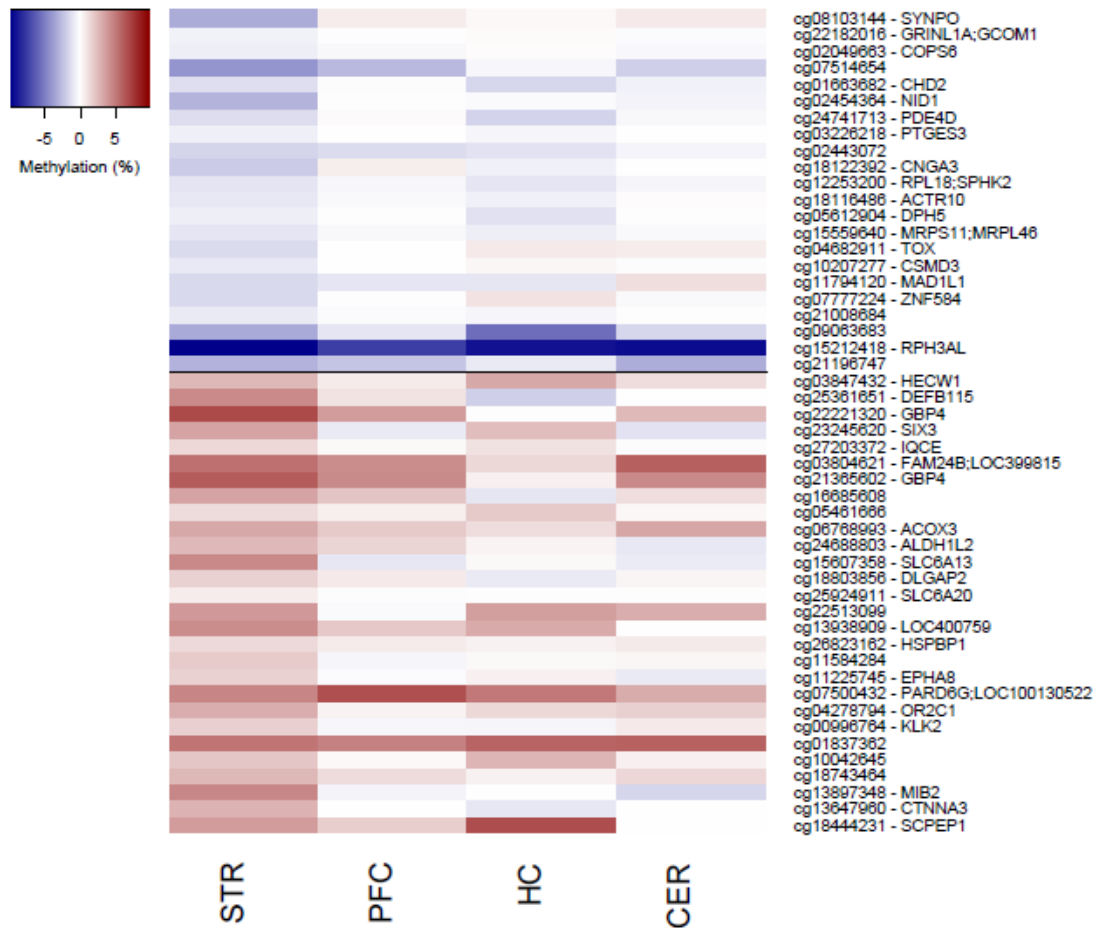


Figure 3.29. Heatmap showing the fifty top ranked schizophrenia-associated differentially methylated positions in the striatum (STR). Shown for each probe is the mean DNA methylation difference between cases and controls, with the corresponding difference at the same probe for the three other brain regions (prefrontal cortex (PFC), hippocampus (HC) and cerebellum (CER)) dissected from the same individuals. Probes are ordered by *P*-value for hypomethylated (blue, top) and hypermethylated (red, bottom) *loci* within the STR.

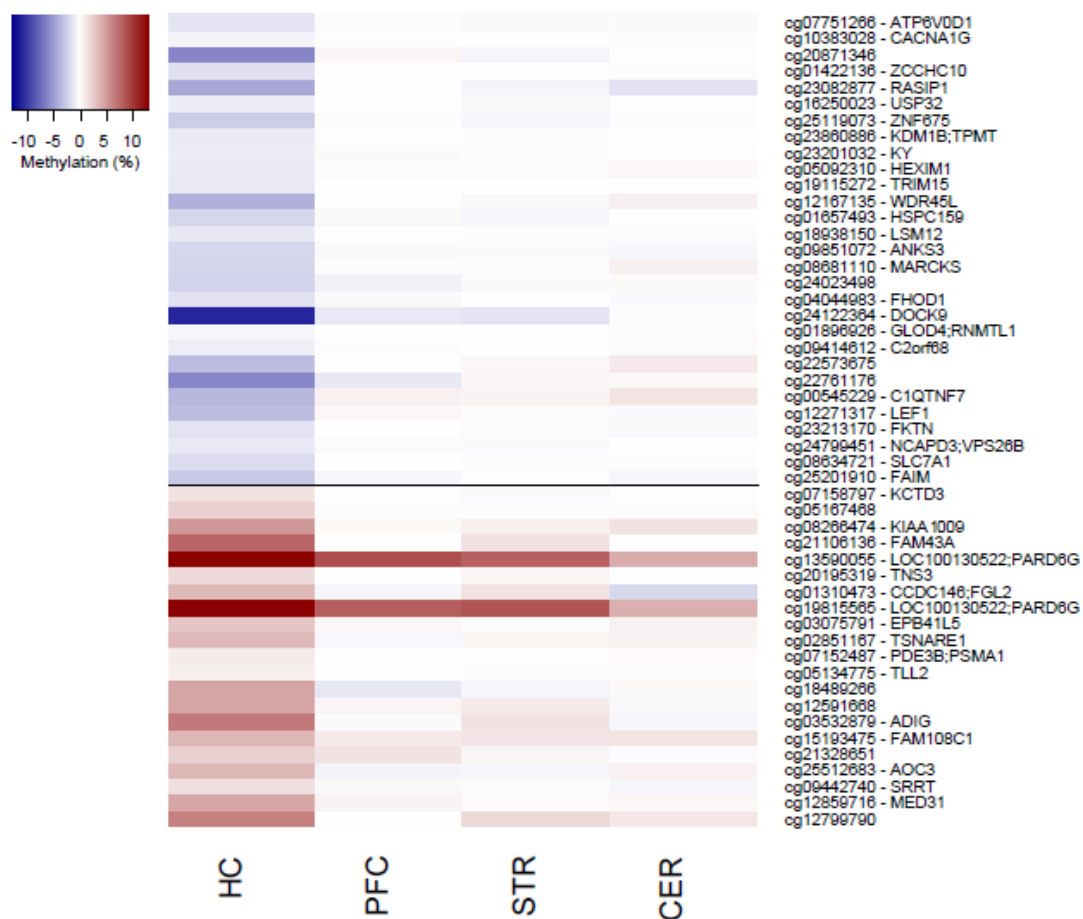


Figure 3.30. Heatmap showing the fifty top ranked schizophrenia-associated differentially methylated positions in the hippocampus (HC). Shown for each probe is the mean DNA methylation difference between cases and controls, with the corresponding difference at the same probe for the three other brain regions (prefrontal cortex (PFC), striatum (STR) and cerebellum (CER)) dissected from the same individuals. Probes are ordered by *P*-value for hypomethylated (blue, top) and hypermethylated (red, bottom) *loci* within the HC.

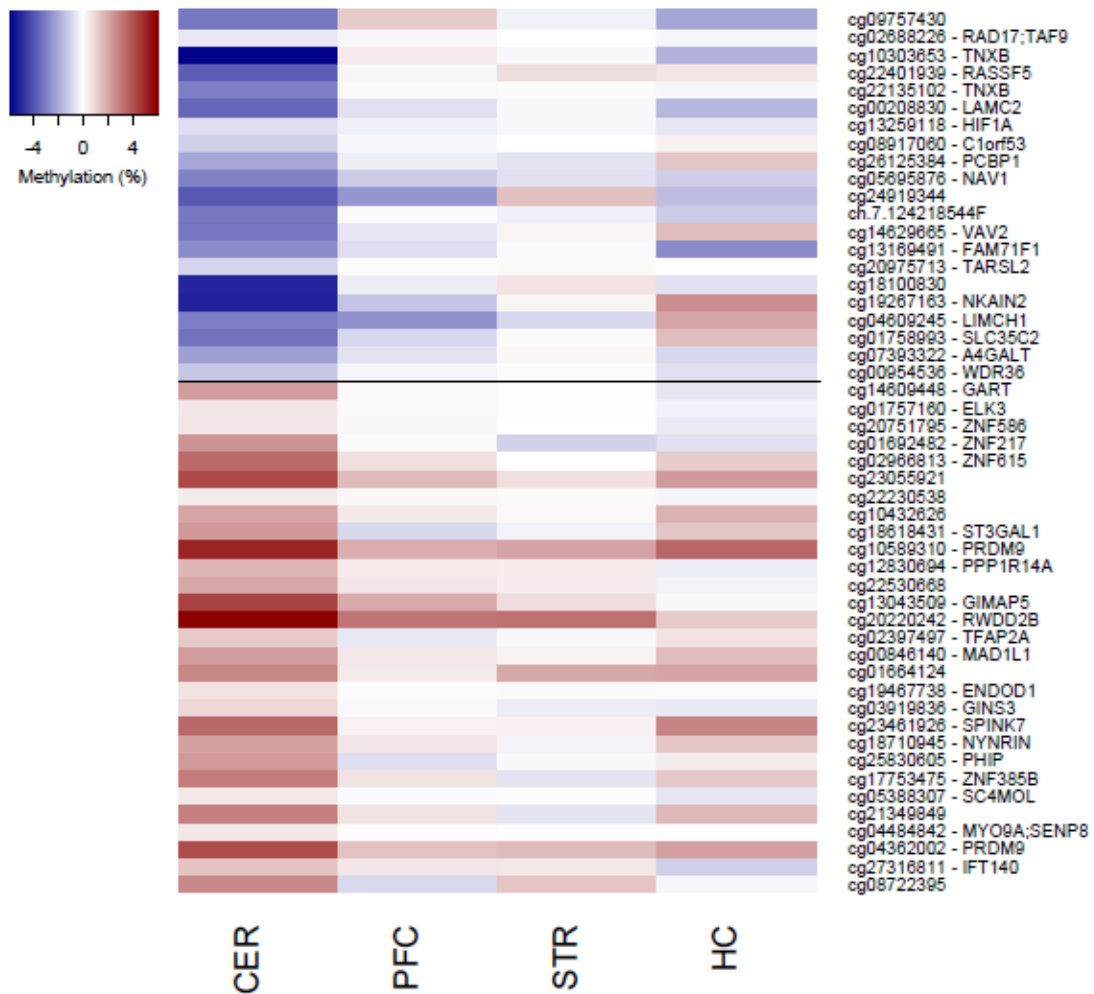


Figure 3.31. Heatmap showing the fifty top ranked schizophrenia-associated differentially methylated positions in the cerebellum (CER). Shown for each probe is the mean DNA methylation difference between cases and controls, with the corresponding difference at the same probe for the three other brain regions (prefrontal cortex (PFC), striatum (STR) and hippocampus (HC)) dissected from the same individuals. Probes are ordered by *P*-value for hypomethylated (blue, top) and hypermethylated (red, bottom) *loci* within the CER.

Table 3.9. Top ranked schizophrenia-associated differentially methylated positions (DMPs). Shown are DMPs associated with schizophrenia at a highly stringent significance threshold ($P < 1.66E-07$) (see Materials and Methods). Top ranked schizophrenia-associated DMPs for each of the four brain regions profiled are presented in **Tables 3.5 to 3.8**. Illumina and Genomic Regions Enrichment of Annotation Tool (GREAT) (McLean et al., 2010) annotations are listed for each DMP.

Probe ID	Genomic position (hg19)	Illumina gene annotation	Genic region	GREAT annotation (McLean et al., 2010)	Brain region	DNA methylation difference (%)	P
cg08743050	chr11:113113936	<i>NCAM1</i>	Body	<i>TTC12</i> ; <i>NCAM1</i>	Prefrontal cortex	-3.80	1.84E-08
cg14609448	chr21:34896882	<i>GART</i>	Body; 3'UTR	<i>DNAJC28</i> ; <i>GART</i>	Cerebellum	2.29	2.48E-08
cg08103144	chr5:150028986	<i>SYNPO</i>	Body	<i>MYOZ3</i> ; <i>SYNPO</i>	Striatum	-3.17	3.64E-08
cg03847432	chr7:43391524	<i>HECW1</i>	Body	<i>STK17A</i> ; <i>HECW1</i>	Striatum	2.71	5.23E-08
cg22182016	chr15:57998894	<i>GRINL1A</i> ; <i>GCOM1</i>	TSS200; Body	<i>POLR2M</i>	Striatum	-0.51	5.67E-08
cg01757160	chr12:96588951	<i>ELK3</i>	5'UTR	<i>ELK3</i>	Cerebellum	0.57	5.74E-08
cg25361651	chr20:29847402	<i>DEFB115</i>	Body	<i>DEFB115</i> ; <i>DEFB116</i>	Striatum	4.43	6.52E-08
cg22221320	chr1:89664340	<i>GBP4</i>	Body	<i>GBP4</i>	Striatum	6.93	7.88E-08
cg07751266	chr16:67515323	<i>ATP6V0D1</i>	TSS1500	<i>ATP6V0D1</i>	Hippocampus	-1.35	1.27E-07
cg09757430	chr13:28397122	-	-	<i>PDX1</i> ; <i>GSX1</i>	Cerebellum	-3.13	1.37E-07
cg05686445	chr7:127636396	<i>C7orf54</i> ; <i>SND1</i>	TSS1500; Body	<i>LRRC4</i> ; <i>SND1</i>	Prefrontal cortex	-3.65	1.63E-07
cg20751795	chr19:58281019	<i>ZNF586</i>	TSS200	<i>ZNF586</i>	Cerebellum	0.57	1.64E-07

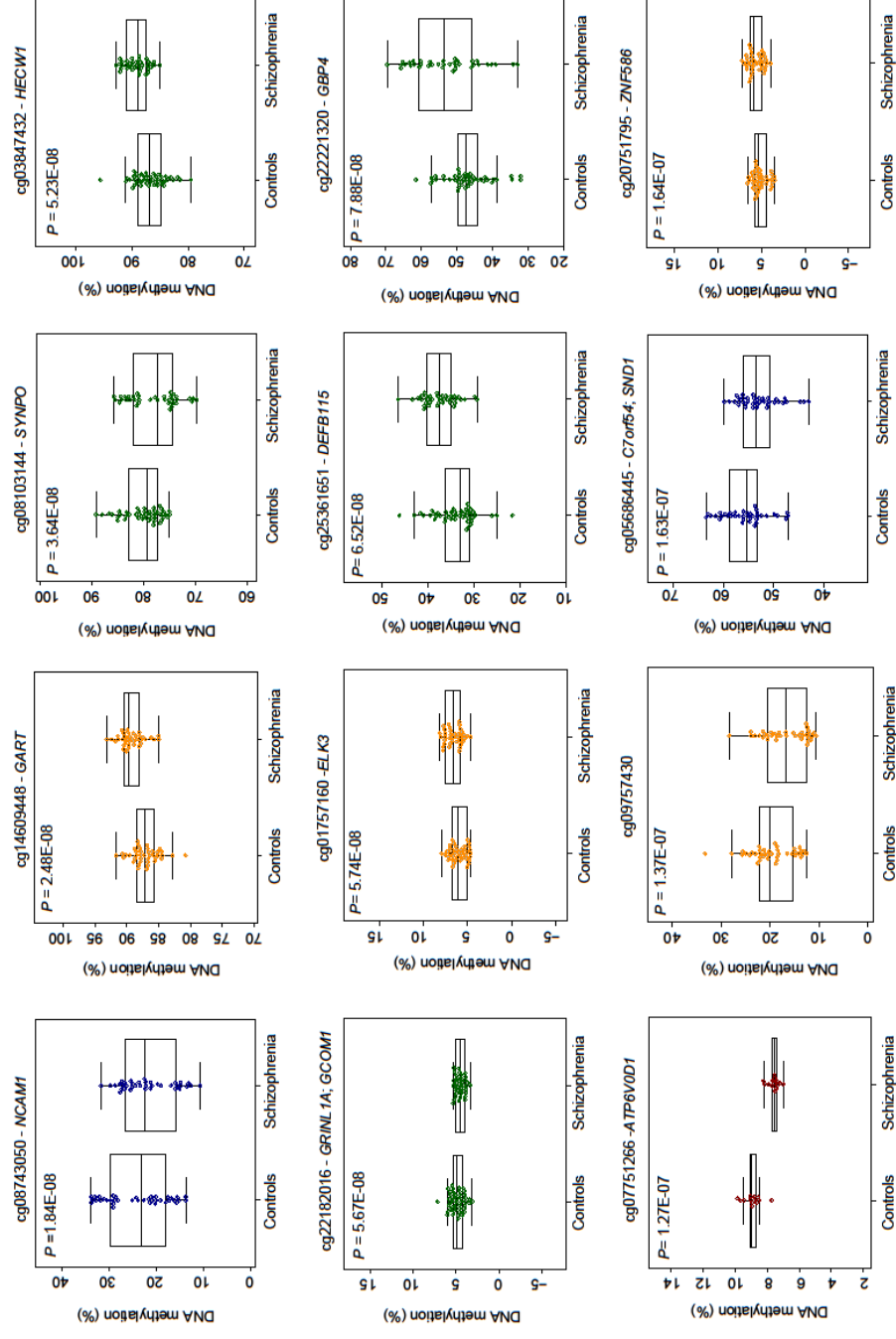


Figure 3.32. Top ranked schizophrenia-associated differentially methylated positions (DMPs). Shown are adjusted DNA methylation values (y-axis) for 12 DMPs associated with schizophrenia at a highly stringent significance threshold ($P < 1.66E-07$) (see section 3.2.8). Additional information on these DMPs is given in Table 3.9. Colour depicts brain region in which the schizophrenia-association was identified: prefrontal cortex = blue, striatum = green, hippocampus = red, and cerebellum = yellow.

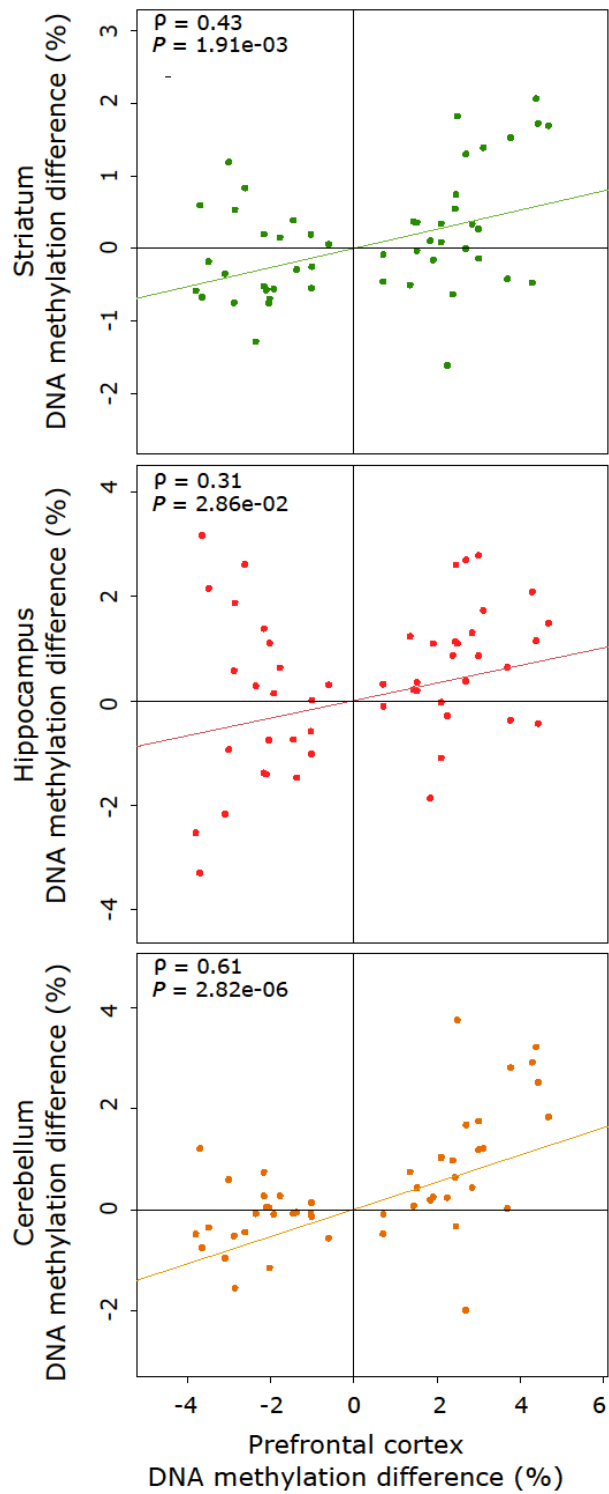


Figure 3.33. Correlation between DNA methylation differences for the fifty top ranked schizophrenia-associated probes identified in identified in the prefrontal cortex and the DNA methylation differences in the same probes in the remaining brain regions (y-axis). Striatum = green; hippocampus = red; cerebellum = orange. ρ , Pearson's correlation coefficient.

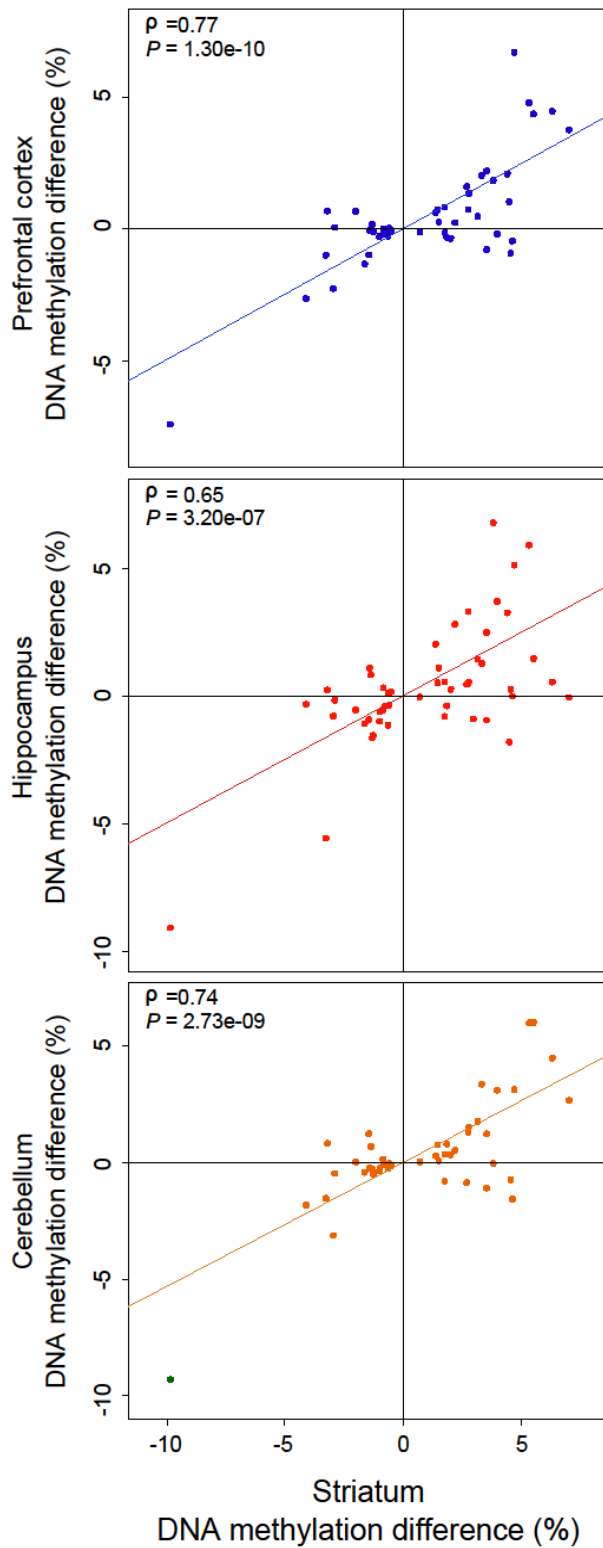


Figure 3.34. Correlation between DNA methylation differences for the fifty top ranked schizophrenia-associated probes identified in identified in the striatum and the DNA methylation differences in the same probes in the remaining brain regions (y-axis). Prefrontal cortex = blue; hippocampus = red; cerebellum = orange. ρ , Pearson's correlation coefficient.

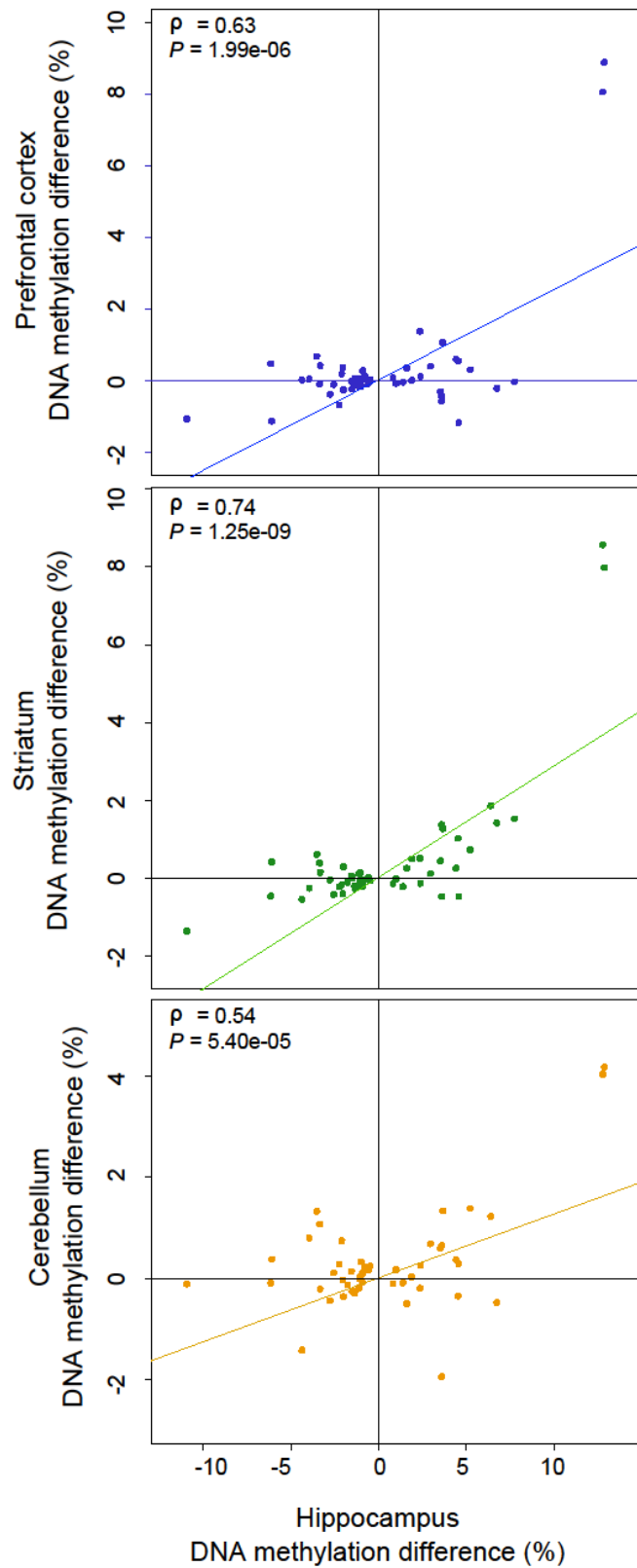


Figure 3.35. Correlation between DNA methylation differences for the fifty top ranked schizophrenia-associated probes identified in identified in the hippocampus and the DNA methylation differences in the same probes in the remaining brain regions (y-axis). Prefrontal cortex = blue; striatum = green; cerebellum = orange. ρ , Pearson's correlation coefficient.

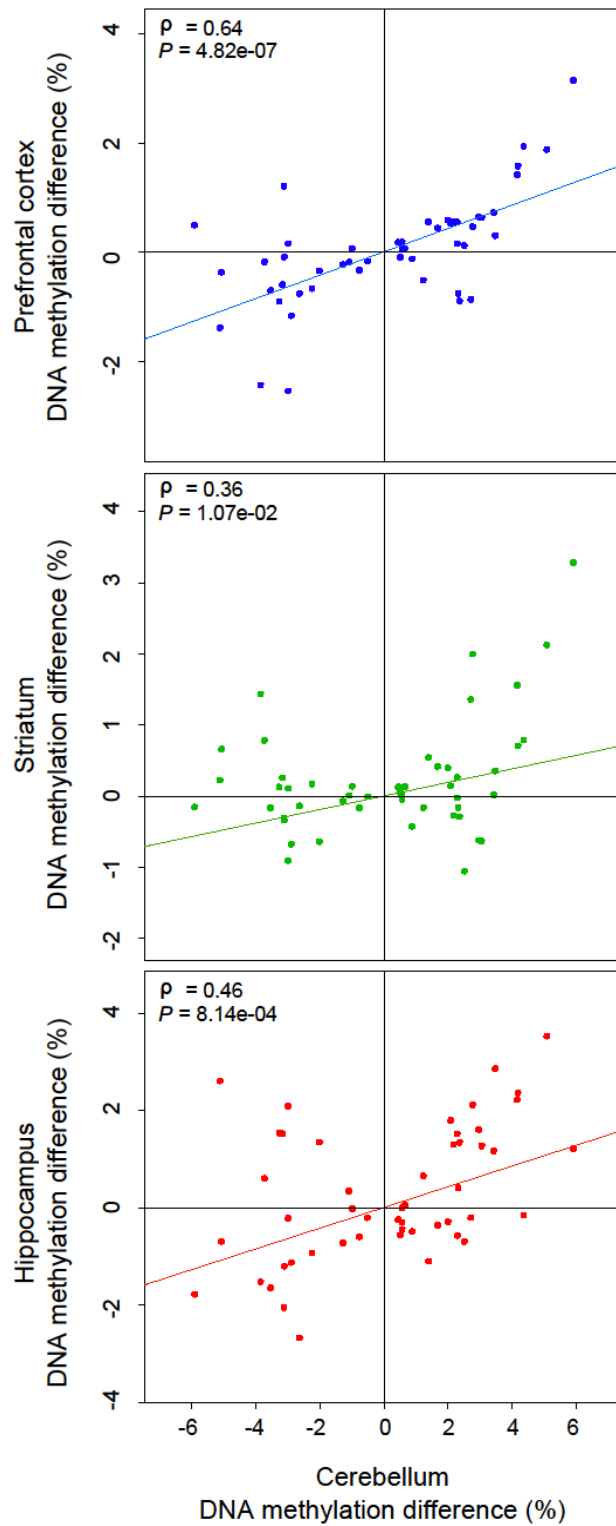


Figure 3.36. Correlation between DNA methylation differences for the fifty top ranked schizophrenia-associated probes identified in identified in the cerebellum and the DNA methylation differences in the same probes in the remaining brain regions (y-axis). Prefrontal cortex = blue; striatum = green; hippocampus = red. ρ , Pearson's correlation coefficient.

Table 3.10. Correlation between DNA methylation differences for the fifty top ranked schizophrenia-associated probes identified in each brain region and the DNA methylation differences in the same probes in the remaining brain regions. Presented are the Pearson's correlation coefficient (ρ) and the associated P -values.

	Prefrontal cortex		Striatum		Hippocampus		Cerebellum			
	ρ	P	ρ	P	ρ	P	ρ	P		
50 top ranked probes	Prefrontal cortex		-	-	0.43	1.90E-03	0.31	0.03	0.61	2.82E-06
	Striatum		0.77	1.30E-10	-	-	0.65	3.19E-07	0.74	2.73E-09
	Hippocampus		0.63	2.00E-06	0.74	1.25E-09	-	-	0.54	5.40E-05
	Cerebellum		0.64	4.80E-07	0.36	0.01	0.46	8.14E-04	-	-

3.3.4. Controlling for unknown confounding variables

As mentioned previously (**section 3.2.6**), detailed data regarding medication, smoking status and other important phenotypical information was not available for the post-mortem samples used in this thesis and therefore I could not include these as independent variables in my analysis model. Because it is likely that these or other unmeasured factors beyond the variables included in my analysis model (*i.e.* age, sex, and neuronal proportion estimates) confound the analyses results, however, I investigated the impact of additional surrogate variables capturing variation in DNA methylation on the association statistics for schizophrenia-associated DMPs.

To do this I repeated the EWAS linear regression iteratively including up to 10 principal components (PCs) derived from the DNA methylation data as independent variables. I compared these to the DNA methylation differences from the initial analysis model. In all tissues, I observed a strong positive correlation for schizophrenia-associated DNA methylation differences between analyses (**Figures 3.37 to 3.40**). This sensitivity analysis implies that although additional confounders potentially exist in the dataset, the identified schizophrenia-associated DMPs are relatively robust to the major PCs associated with methylomic variance.

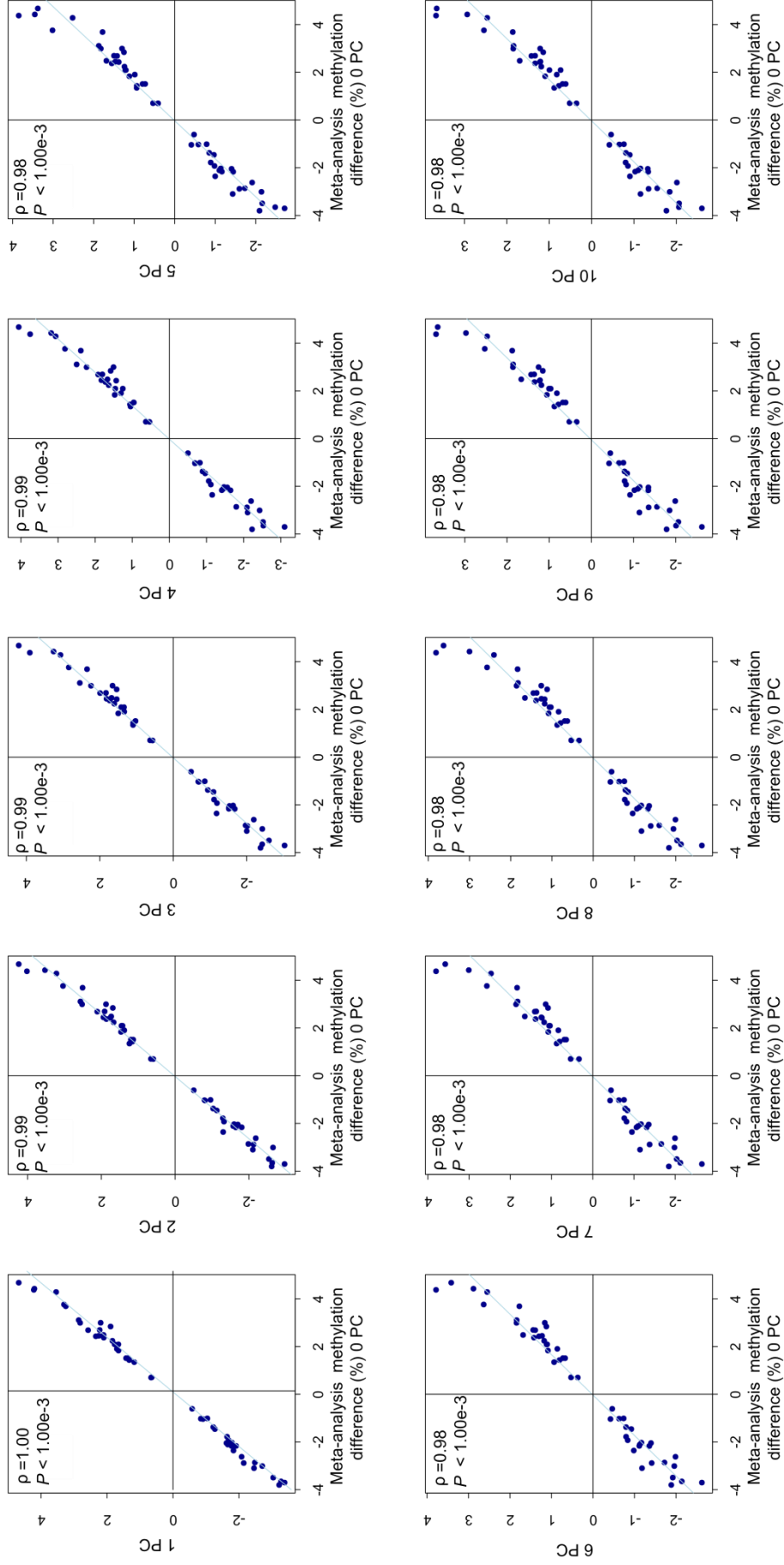


Figure 3.37. Schizophrenia-associated DNA methylation differences are robust to the addition of principal components (PC) capturing variation in DNA methylation data in the prefrontal cortex (PFC). Shown is the correlation (ρ , Pearson's correlation coefficient) of DNA methylation differences for the fifty top ranked PFC schizophrenia-associated DMPs (x-axis) with differences at the same positions in an EWAS iteratively adding 1 to 10 PCs as independent co-variables (y-axis).

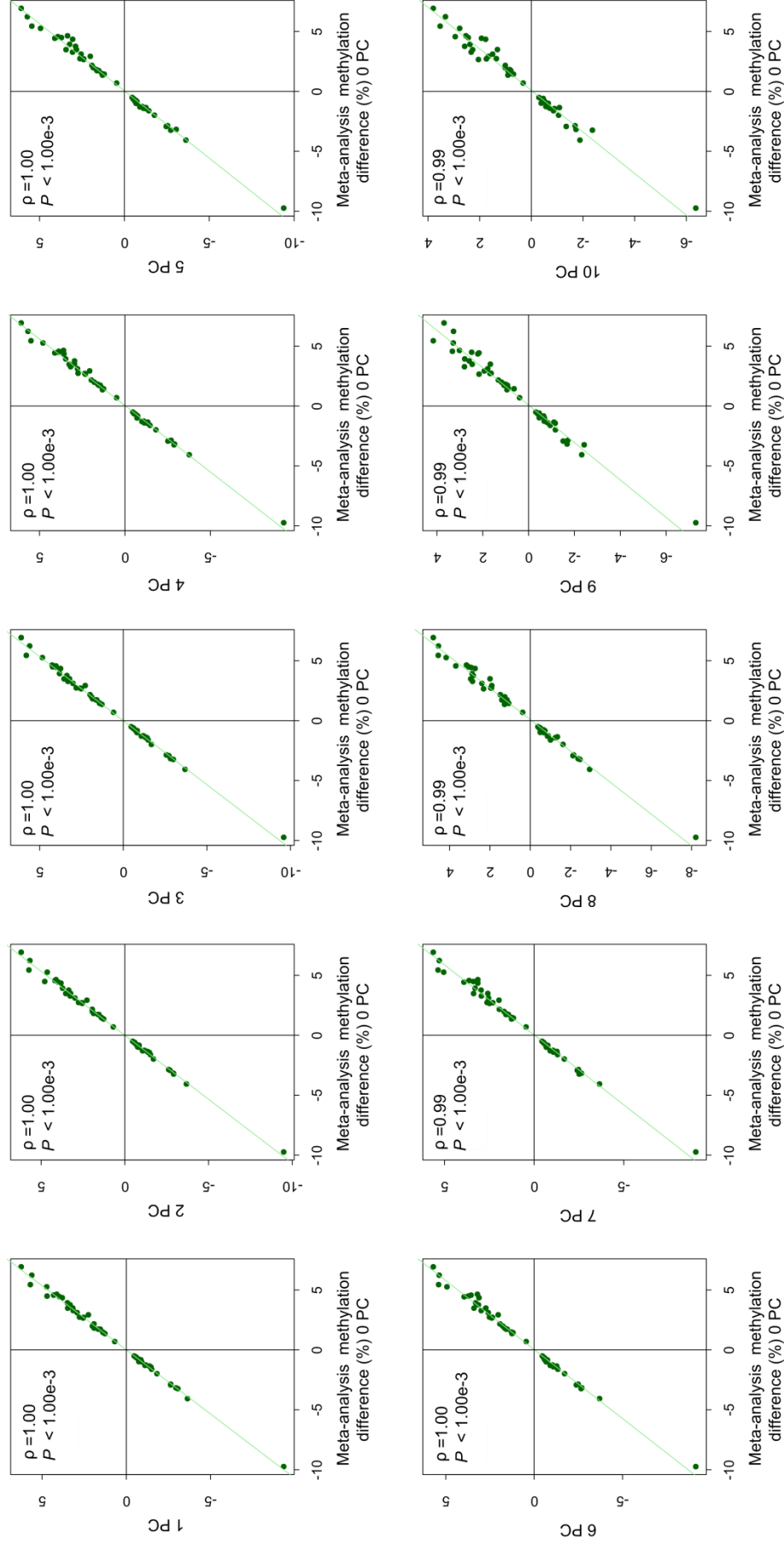


Figure 3.38. Schizophrenia-associated DNA methylation differences are robust to the addition of principal components (PC) capturing variation in DNA methylation data in the striatum (STR). Shown is the correlation (ρ , Pearson's correlation coefficient) of DNA methylation differences for the fifty top ranked STR schizophrenia-associated DMPs (x-axis) with differences at the same positions in an EWAS iteratively adding 1 to 10 PCs as independent co-variables (y-axis).

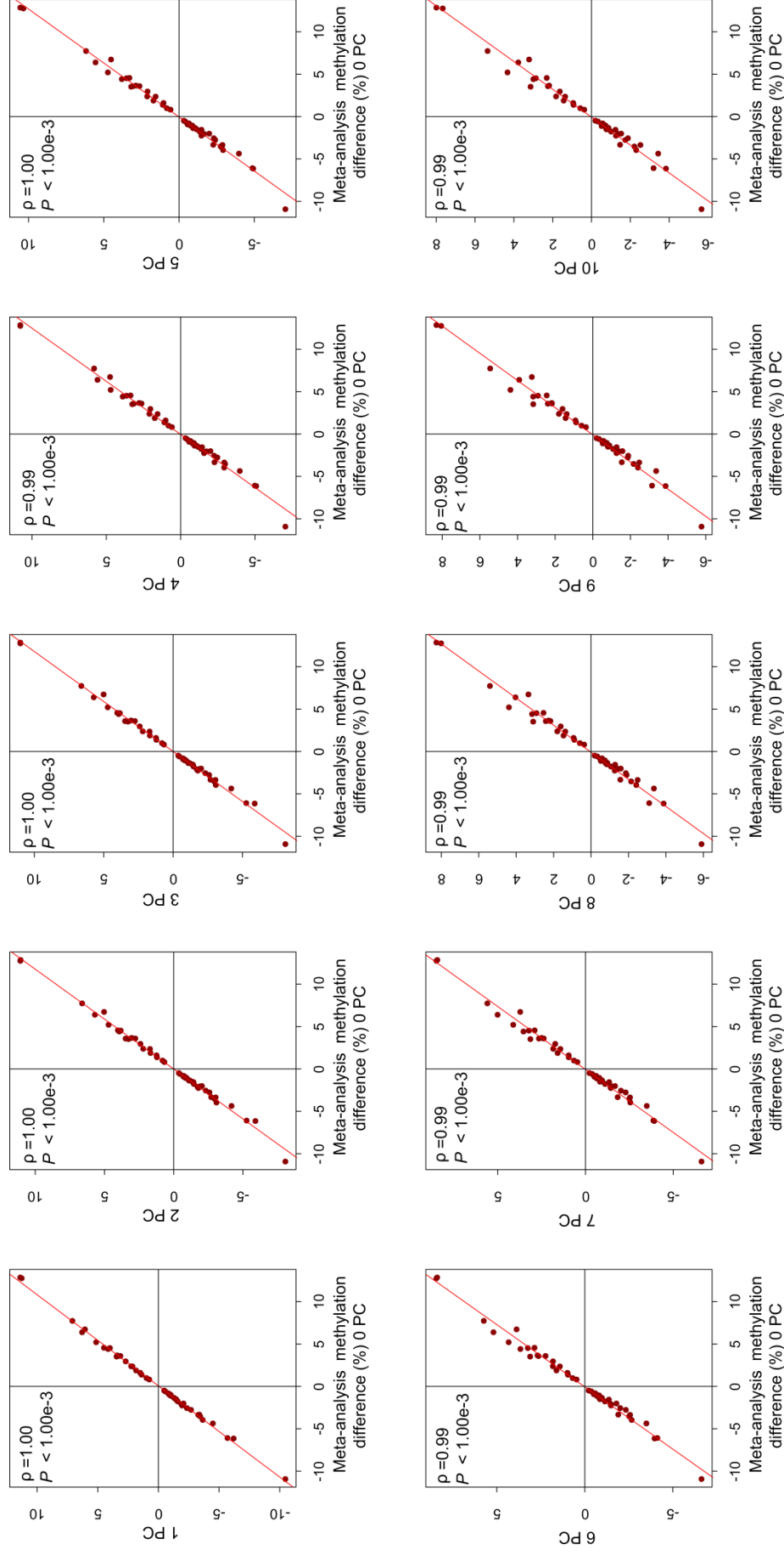


Figure 3.39. Schizophrenia-associated DNA methylation differences are robust to the addition of principal components (PC) capturing variation in DNA methylation data in the hippocampus (HC). Shown is the correlation (ρ , Pearson's correlation coefficient) of DNA methylation differences for the fifty top ranked HC schizophrenia-associated DMPs (x-axis) with differences at the same positions in an EWAS iteratively adding 1 to 10 PCs as independent co-variables (y-axis).

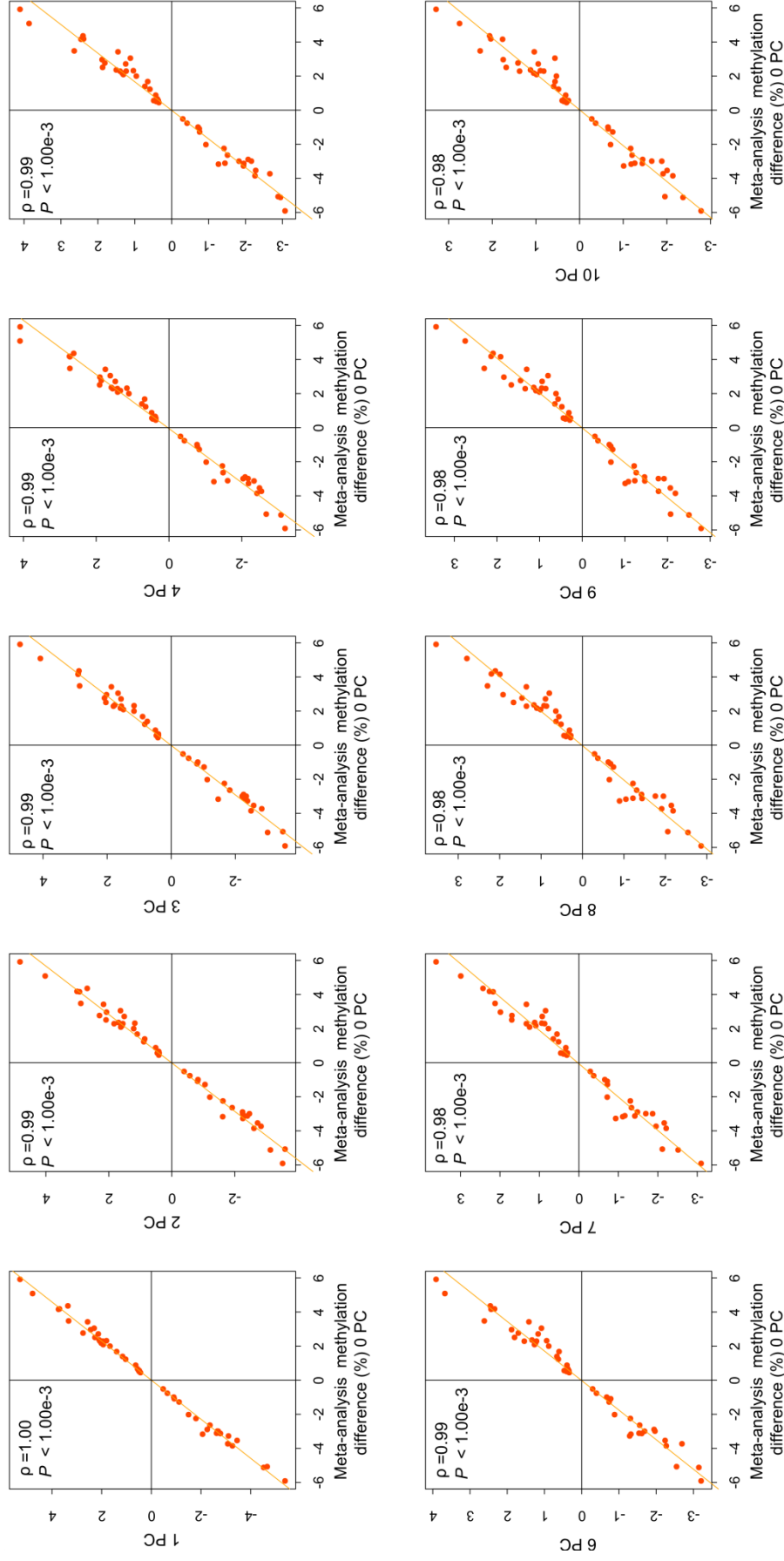


Figure 3.40. Schizophrenia-associated DNA methylation differences are robust to the addition of principal components (PC) capturing variation in DNA methylation data in cerebellum (CER). Shown is the correlation (ρ , Pearson's correlation coefficient) of DNA methylation differences for the fifty top ranked CER schizophrenia-associated DMPs (x-axis) with differences at the same positions in an EWAS iteratively adding 1 to 10 PCs as independent co-variables (y-axis).

3.3.5. Enrichment of overlap between schizophrenia-associated differently methylated positions and regulatory features and GWAS regions

The 450K array probes were annotated to TFBSs and DHSs using published data (Sliker et al., 2013, ENCODE Project Consortium, 2012, Maurano et al., 2012) and the overlap between schizophrenia-associated DMPs identified in the different brain regions and these regulatory features tested for enrichment using a two sided Fisher's 2x2 exact test (Fisher, 1922). **Tables 3.11** to **3.14** present the results of these tests for all brain regions.

The fifty top ranked probes from each brain region show no significant overlap with either of the regulatory features at the Bonferroni corrected threshold for the twenty-four tests ($P = 2.08E-03$). PFC schizophrenia-associated DMPs (**Table 3.11**) show a significant under-enrichment for TFBS at the significance threshold of $P < 1.00E-03$ (odds ratio (OR) = 0.78 and $P = 4.61E-05$) and $P < 0.05$ (OR = 0.86 and $P = 1.03E-39$), and a significant under-enrichment for DHS at the significance threshold of $P < 1.00E-03$ (OR = 0.88 and $P = 2.03E-26$). In the STR (**Table 3.12**), DMPs associated with schizophrenia with a $P < 0.05$ show an enrichment for both DHS (OR = 1.06 and $P = 6.14E-05$) and TFBS (OR = 1.11 and $P = 4.38E-13$). In the HC (**Table 3.13**), DMPs associated with schizophrenia with a $P < 0.05$ show an enrichment for TFBS (OR = 1.10 and $P = 3.47E-11$).). In the CER (**Table 3.14**), DMPs associated with schizophrenia with a $P < 0.05$ show an enrichment for TFBS (OR = 1.04 and $P = 6.10E-04$)

Table 3.11. Results of the Fisher’s 2x2 exact tests for significant overlap between schizophrenia-associated differently methylated positions (DMPs) in the prefrontal cortex and regulatory features. Shown are the results for overlap enrichment with the 50 top ranked probes, DMPs with an association *P*-value < 1.00E-03 and DMPs with an association *P*-value < 0.05. DHS, DNA hypersensitivity sites; TFBS, transcription factor binding sites.

	DHS		TFBS	
	Odds ratio	<i>P</i>	Odds ratio	<i>P</i>
Top ranked 50	1.03	1	1.27	0.40
<i>P</i> < 1.00E-03	0.83	3.03E-03	0.78	4.61E-05
<i>P</i> < 0.05	0.88	2.03E-26	0.86	1.03E-39

Table 3.12. Results of the Fisher’s 2x2 exact tests for significant overlap between schizophrenia-associated differently methylated positions (DMPs) in the striatum and regulatory features. Shown are the results for overlap enrichment with the 50 top ranked probes, DMPs with an association *P*-value < 1.00E-03 and DMPs with an association *P*-value < 0.05. DHS, DNA hypersensitivity sites; TFBS, transcription factor binding sites.

	DHS		TFBS	
	Odds ratio	<i>P</i>	Odds ratio	<i>P</i>
Top ranked 50	1.13	0.78	0.73	0.32
<i>P</i> < 1.00E-03	1.11	0.21	1.05	0.58
<i>P</i> < 0.05	1.06	6.14E-05	1.11	4.38E-13

Table 3.13. Results of the Fisher’s 2x2 exact tests for significant overlap between schizophrenia-associated differently methylated positions (DMPs) in the hippocampus and regulatory features. Shown are the results for overlap enrichment with the 50 top ranked probes, DMPs with an association *P*-value < 1.00E-03 and DMPs with an association *P*-value < 0.05. DHS, DNA hypersensitivity sites; TFBS, transcription factor binding sites.

	DHS		TFBS	
	Odds ratio	<i>P</i>	Odds ratio	<i>P</i>
Top ranked 50	2.00	0.02	1.94	0.02
<i>P</i> < 1.00E-03	1.09	0.48	1.01	0.91
<i>P</i> < 0.05	1.02	9.23E-02	1.10	3.47E-11

Table 3.14. Results of the Fisher's 2x2 exact tests for significant overlap between schizophrenia-associated differently methylated positions (DMPs) in the cerebellum and regulatory features. Shown are the results for overlap enrichment with the 50 top ranked probes, DMPs with an association P -value $< 1.00E-03$ and DMPs with an association P -value < 0.05 . DHS, DNA hypersensitivity sites; TFBS, transcription factor binding sites.

	DHS		TFBS	
	Odds ratio	P	Odds ratio	P
Top ranked 50	1.03	1.00	0.99	1.00
$P < 1.00E-03$	1.06	0.26	1.08	0.11
$P < 0.05$	1.03	7.53E-03	1.04	6.10E-04

I tested the same sets of DMPs (top ranked fifty, $P < 1.00E-03$ and $P < 0.05$) for significant overlap with probes within genomic regions associated with schizophrenia in the latest schizophrenia GWAS (Schizophrenia Working Group of the Psychiatric Genomics, 2014). A total of 5006, 5058, 5066 and 4951 Illumina 450K array probes included in our PFC, STR, HC and CER analyses, respectively, were located within these broad genomic regions. None of the different sets of schizophrenia-associated DMPs from any of the brain regions show a significant overlap with GWAS regions (at Bonferroni corrected threshold for the twelve tests $P = 4.17E-03$) (**Table 3.15**).

Table 3.15. Results of the Fisher's 2x2 exact tests for significant overlap between schizophrenia-associated differentially methylated positions (DMPs) in all the brain regions and GWAS regions. Shown are the results for the overlap between the 50 top ranked probes, DMPs with an association P -value $< 1.00E-03$ and DMPs with an association P -value < 0.05 . OR = odds ratio and probes within genomic regions associated with schizophrenia (Schizophrenia Working Group of the Psychiatric Genomics, 2014).

	PFC OR	PFC P	STR OR	STR P	HC OR	HC P	CER OR	CER P
Top ranked 50	1.66	0.46	1.66	0.46	0.00	1.00	0.00	1.00
$P < 1.00E-03$	0.62	0.20	0.52	0.27	0.56	0.59	0.97	1.00
$P < 0.05$	0.94	0.28	1.08	0.24	1.01	0.92	0.98	0.73

3.3.6. Differentially methylated regions associated with schizophrenia

I next used *comb-p* (Pedersen et al., 2012) (**section 3.2.6**) to identify spatially correlated regions of differential DNA methylation significantly associated with schizophrenia (\check{S} idák-corrected $P < 0.05$, number of consecutive probes ≥ 2) in each of the 4 brain regions (**Figure 3.41** and **Table 3.16**). One region (*PRSS30P*; *TMPRSS8*) was identified in both PFC and CER and seven regions showed a nominally significant association with schizophrenia (median P -value across all probes) in at least one other brain region (*GBP4*, *PRDM9*, *FAM24B/LOC399815*, *CAT*, *TFDP1/TMCO3*, *PRSS30P/TMPRSS8*, *DOC2B/RPH3AL*). Although the remaining 18 regions were associated with disease in only one brain region, many of these DMRs are characterised by consistent schizophrenia-associated differences in DNA methylation across multiple brain regions (**Figure 3.41**).

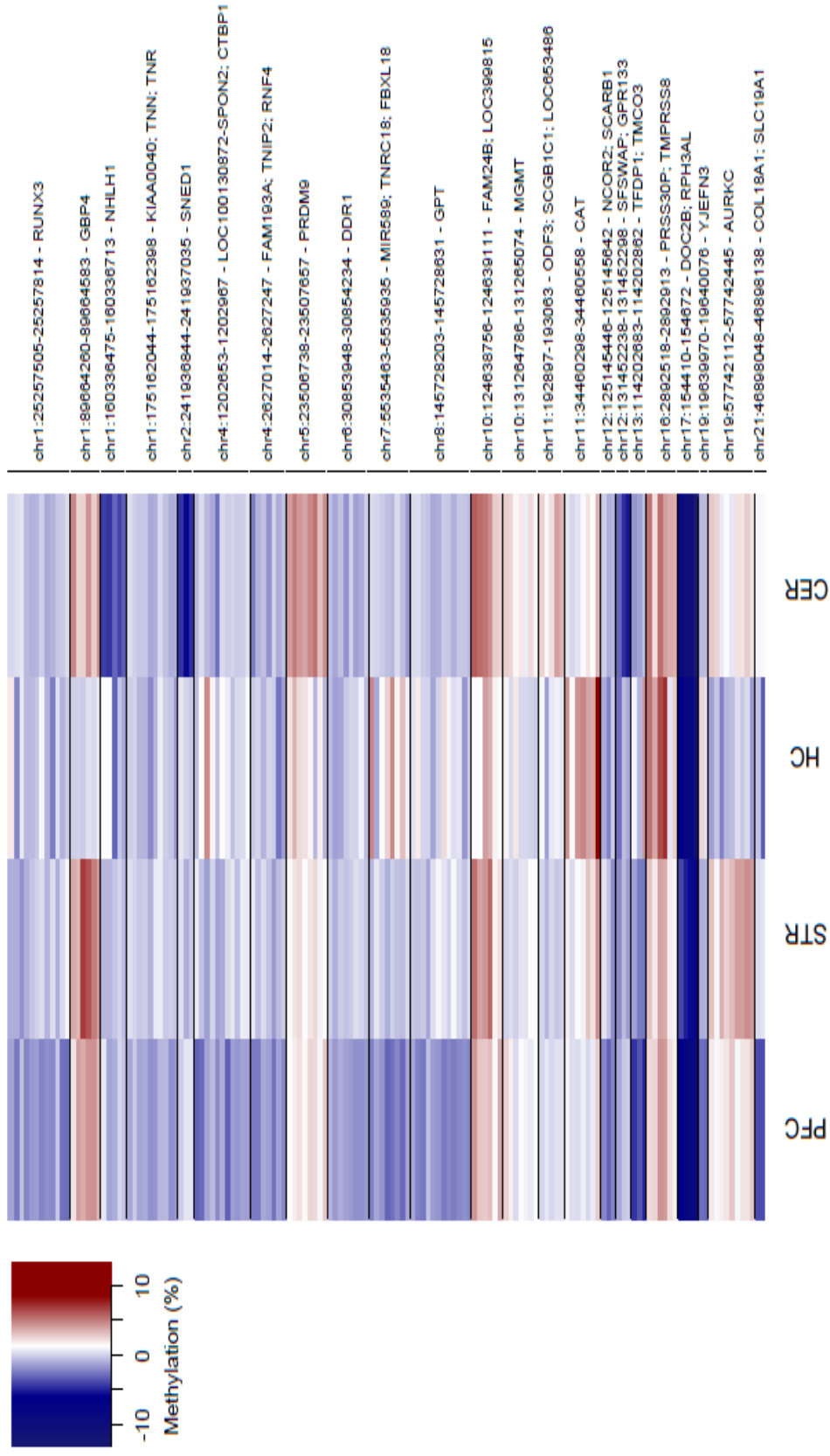


Figure 3.41. Differentially methylated regions (DMRs) associated with schizophrenia. Shown in chromosomal order are DMRs associated with schizophrenia identified in any of the four brain regions. DNA methylation differences for individual probes within each DMR are also shown for the other three brain regions (blue = hypomethylation, red = hypermethylation).

Of note, DMRs were identified in the vicinity of several genes previously implicated in the etiology of schizophrenia including *PRDM9*; this gene encodes a protein with histone H3K4 trimethyltransferase activity during meiosis (Berg et al., 2010) and has been previously hypothesised to play a role in schizophrenia (Crow, 2011). Two different sets of probes in the transcription start site of *PRDM9* (chr5:23506738-23507031; chr5:23507450-23507657) show significant hypermethylation in the CER. The probe in between these two regions (cg25336267) was excluded during QC thus it is possible that the entire region chr5:23506738-23507657 within the *PRDM9* gene is significantly associated with schizophrenia in the CER. The chr19:19639970-19640076 DMR within the YjeF N-terminal domain containing 3 (*YJEFN3*) gene identified in the PFC overlaps with the chr19:19374022-19658022 region identified in the latest schizophrenia GWAS (most significant association: rs2905426 – $P = 3.63E-10$) (Schizophrenia Working Group of the Psychiatric Genomics, 2014). Additionally, a region in chr6:30853948-30854234 is significantly associated with schizophrenia in PFC and located within the discoidin domain receptor tyrosine kinase 1 (*DDR1*) gene. This gene has been shown to be upregulated during oligodendrocytes differentiation and remyelination (Roig et al., 2010, Letzen et al., 2010).

Table 3.16. Significant schizophrenia-associated differentially methylated regions (DMRs). Shown in chromosomal order is the location of significant (Šidák-corrected $P < 0.05$). DMRs identified in each of the four brain regions, with the median P -value for DMR probes given for the other three brain regions (bold denotes median $P < 0.05$ and grey boxes denote regions that were not identified in that brain region). The 'Gene' column lists the combined Illumina and Genomic Regions Enrichment of Annotation Tool (GREAT) annotation (McLean et al., 2010).

Region	Gene	Probes	N probes	Prefrontal cortex		Striatum		Hippocampus		Cerebellum	
				Median P	Šidák P	Median P	Šidák P	Median P	Šidák P	Median P	Šidák P
chr1:25257505-25257814	RUNX3	cg07996594; cg04221877; cg15014975; cg24019564; cg10993442; cg24842859; cg20695936; cg13106389; cg18087266; cg25882256; cg04250451; cg10013501	12	1.22E-02	1.02E-02	0.36		0.66		0.29	
chr1:89664260-89664583	GBP4	cg23978657; cg02482460; cg22221320; cg21365602; cg20410995; cg14563196	6	8.36E-03		5.36E-04	3.16E-12	0.93		7.06E-02	
chr1:160336475-160336713	NHLH1	cg18023842; cg08247612; cg13992678; cg00006397; cg00881010	5	0.24		0.62		0.42		8.00E-04	1.64E-05
chr1:175162044-175162398	KIAA0040; TMN; TNR	cg11908570; cg22626041; cg26563563; cg17839543; cg18880390; cg00099768; cg13857382; cg11973900; cg08873628; cg00321850	10	2.34E-02	7.62E-04	0.47		0.25		0.25	
chr2:241936844-241937035	SNED1	cg16937168; cg03785076; cg21304158	3	0.45		0.74		0.89		5.16E-05	6.68E-05
chr4:1202653-1202967	LOC100130872-SPON2; CTBP1	cg14527262; cg04228083; cg17227257; cg16721321; cg26130533; cg14505741; cg11104416; cg18085660; cg11888738; cg01638225; cg21082272	11	3.61E-02	1.32E-02	0.41		0.66		0.72	
chr4:2627014-2627247	FAM193A; TNIP2; RNF4	cg25790133; cg05083414; cg05949640; cg22980079; cg14549256; cg20163033; cg00097088	7	7.22E-03	2.99E-02	0.56		0.94		0.44	
chr5:23506738-23507031	PRDM9	cg04362002; cg10589310	2	5.91E-02		3.76E-02		0.11		4.69E-06	3.65E-05
chr5:23507450-23507657		cg22054885; cg19837938; cg02444433; cg25472530; cg22079902; cg01667892	6	0.10		0.11		0.45		5.33E-04	5.49E-08
chr6:30853948-30854234	DDR1	cg116215084; cg25251478; cg26321999; cg00934322; cg07187855; cg24566261; cg09965419; cg17091577	8	2.28E-02	7.87E-03	0.75		0.73		0.21	

chr7:5535463-5535935	MIR569; TNRC18; FBXL18	cg01942816; cg22108567; cg25343388; cg09286367; cg17419731; cg01024247; cg00966405; cg04155485	8	5.48E-03	3.44E-03	0.55	0.36		0.54
chr8:145728203-145728631	GPT	cg16587265; cg14476479; cg23793500; cg00280345; cg16582889; cg07658280; cg26572973; cg05241828; cg09957864; cg25600446; cg06110286; cg19352605	12	1.80E-03	5.53E-09	0.49	0.74		0.51
chr10:124638756-124639111	FAM24B; LOC399815	cg03804621; cg16299003; cg11218091; cg14708218; cg18195080; cg15252215	6	1.05E-02		4.88E-03	0.47		5.15E-03
chr10:131264786-131265074	MGMT	cg36950715; cg02330106; cg12575438; cg02022136; cg23998405; cg01341123; cg25946389	7	0.13		0.54	0.83		1.01E-02
chr11:192897-193063	ODF3; SCGB1C1; LOC653486	cg18793661; cg22280333; cg03960562; cg02378673; cg20297976	5	0.26		0.62	0.25		4.55E-04
chr11:34460298-34460558	CA17	cg20731136; cg06027906; cg07768201; cg03720043; cg02109652; cg06908474; cg01847719	7	0.36		3.61E-02	1.00E-02	9.44E-04	0.21
chr12:125145446-125145642	NCOR2; SCARB1	cg12077664; cg27645498; cg19888509	3	2.00E-03	2.20E-02	0.56	0.59		0.18
chr12:131452238-131452298	SFSWAP; GPR133	cg24336338; cg03776878; cg23617848	3	0.80		0.23	0.59		1.20E-04
chr13:114202683-114202862	TFDP1; TMCO3	cg16567723; cg24121069; cg11312353	3	6.38E-04	1.94E-02	0.12	0.74		9.18E-03
chr16:2892518-2892913	PRSS30P; TMPRSS8	cg07645761; cg00491180; cg01006802; cg27137258; cg10448227; cg10186456	6	7.18E-03	5.65E-03	3.91E-02	0.12		4.27E-03
chr17:154410-154672	DOC2B; RPH3AL	cg08770870; cg11940040; cg10440639; cg23246911	4	8.27E-04	1.02E-04	7.14E-03	1.78E-02		3.86E-03
chr19:19639970-19640076	YJEFN3	cg11244672; cg20098710	2	3.00E-04	4.49E-02	0.43	0.50		0.54
chr19:57742112-57742445	AURKC	cg25802888; cg19568003; cg18644286; cg26332114; cg19603903; cg23371413; cg06643849; cg25432232; cg22711741	9	0.23		1.34E-02	0.86	2.64E-03	0.27
chr21:46898048-46898138	COL18A1; SLC19A1	cg03208198; cg20383948	2	1.30E-04	2.31E-02	0.68	0.49		0.14

3.3.6.1. Differently methylated region in chromosome 17

A DMR spanning four probes within an intron of the *RPH3AL* gene on chromosome 17, which encodes a protein that plays a direct regulatory role in calcium-ion-dependent exocytosis, is consistently hypomethylated in schizophrenia patients across all four brain regions (PFC: median DNA methylation difference = -8.03%, median $P = 8.27E-04$; STR: median DNA methylation difference = -5.32%, median $P = 7.14E-03$; HC: median DNA methylation difference = -7.84%, median $P = 1.78E-02$; CER: median DNA methylation difference = -10.24, median $P = 3.86E-03$) (**Figures 3.42 A and B, Figures 3.43 A and B and Figures 3.44 to 3.46**). A consecutive probe (cg15212418 - chr17:155046) also showed significant hypomethylation in PFC, STR and CER (PFC: DNA methylation difference = -7.39%, $P = 1.24E-3$; STR: DNA methylation difference = -9.74%, $P = 2.86E-05$; CER: DNA methylation difference = -9.30%, $P = 2.12E-3$). This probe was not contained in the DMR, probably due to the window size used in *comb-p* (300bp), but it is clearly part of a coordinated sequence of differently methylated CpGs (**Figures 3.44 to 3.46**). Interestingly, this probe shows a dramatic Bonferroni-significant increase in DNA methylation associated with brain development in a study by our group using fetal brain samples (regression coefficient= 0.29, $P = 2.56E-10$ in Spiers et al. (2015)) (**Figure 3.47**). This is particularly interesting since schizophrenia has been suggested to have neurodevelopmental origins (Owen et al., 2011, Weinberger, 1995). The probes within this DMR are also annotated to the double C2-like domains beta (*DOC2B*) gene in the GREAT annotation database (McLean et al., 2010). The DMR is located upstream the transcription start site of this gene (**Figures 3.44 to 3.46**), which encodes a protein that regulates calcium-dependent neurotransmitter release in synapses (Groffen et al., 2010). Synapses are the junctions between two neurons that allow the electrical or chemical signal to pass from one neuron to the other. Synaptic dysfunction has long been implicated in schizophrenia etiology (for a review see Pocklington et al. (2014)).

To validate the differences identified across this DMR using the Illumina 450K array we employed bisulfite-PCR-pyrosequencing to quantify DNA methylation across an amplicon spanning three CpG sites (cg11940040 and two adjacent CpG sites not on the 450K array) in the PFC (n = 35 schizophrenia and 36 controls) and STR (n = 36 schizophrenia and 41 controls) samples (**Appendix A - Supplementary Table 2** presents samples excluded in the pyrosequencing). All three sites were significantly hypomethylated in schizophrenic patients compared to controls in both brain regions (**Table 3.17** and **Figures 3.42 C** and **3.43 C**), with DNA methylation differences reflecting those identified using the 450K array (PFC: average DNA methylation difference = -8.68%, $P = 1.72E-03$; STR: average DNA methylation difference = -5.33%, $P = 1.41E-02$).

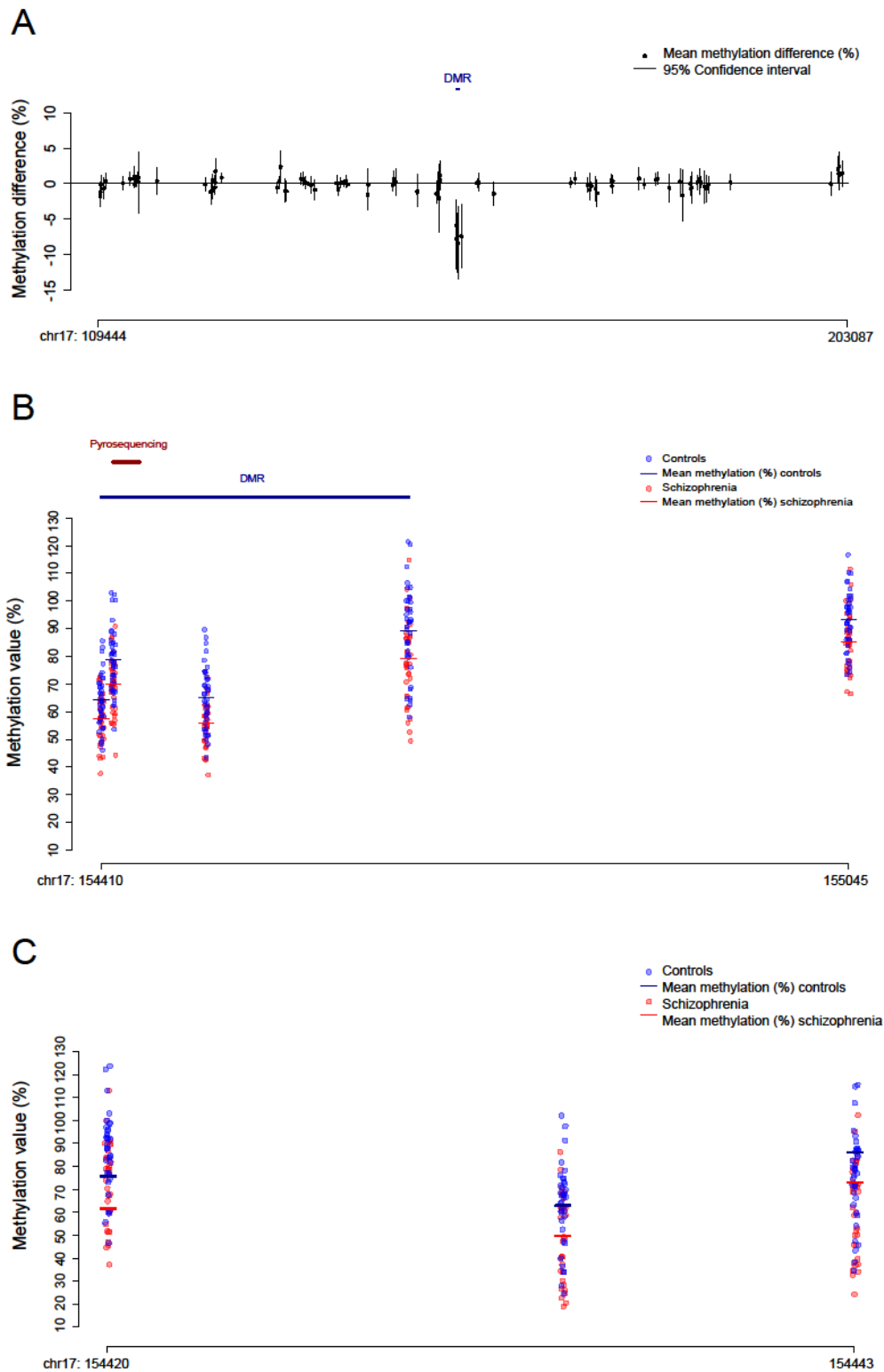


Figure 3.42. Validation of a schizophrenia-associated hypomethylated region within the *RPH3AL* gene in the prefrontal cortex (PFC). The chr17:154410-154672 schizophrenia-associated region identified using the Illumina 450K array (**A** and **B**) in the PFC samples. We used bisulfite-PCR-pyrosequencing to validate schizophrenia-associated hypomethylation at cg11940040 and two adjacent CpG sites not present in the array (**C**).

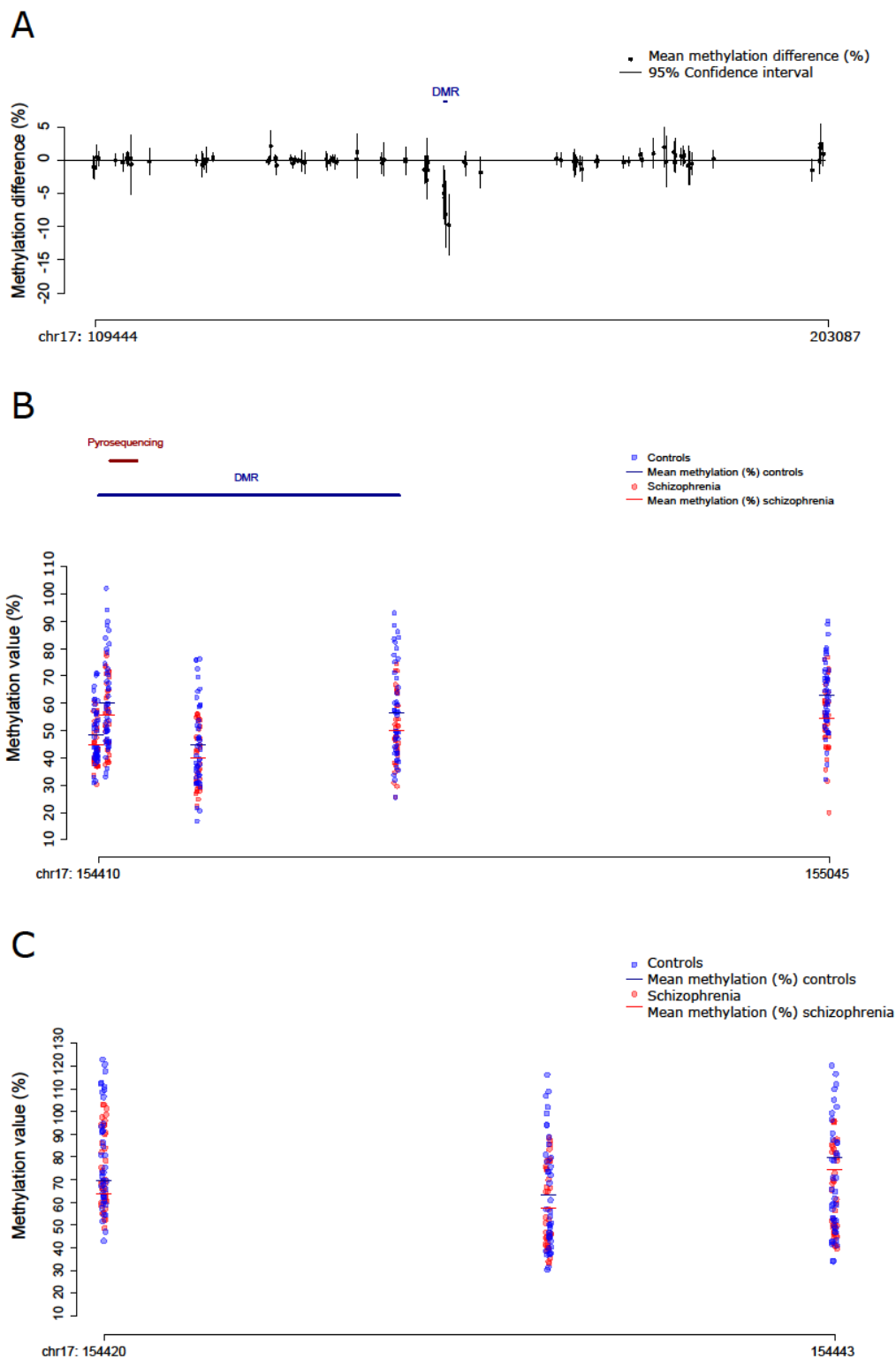


Figure 3.43. Validation of a schizophrenia-associated hypomethylated region within the *RPH3AL* gene in the striatum (STR). The chr17:154410-154672 schizophrenia-associated region identified using the Illumina 450K array (**A** and **B**) in the PFC samples. We used bisulfite-PCR-pyrosequencing to validate schizophrenia-associated hypomethylation at cg11940040 and two adjacent CpG sites not present in the array (**C**).

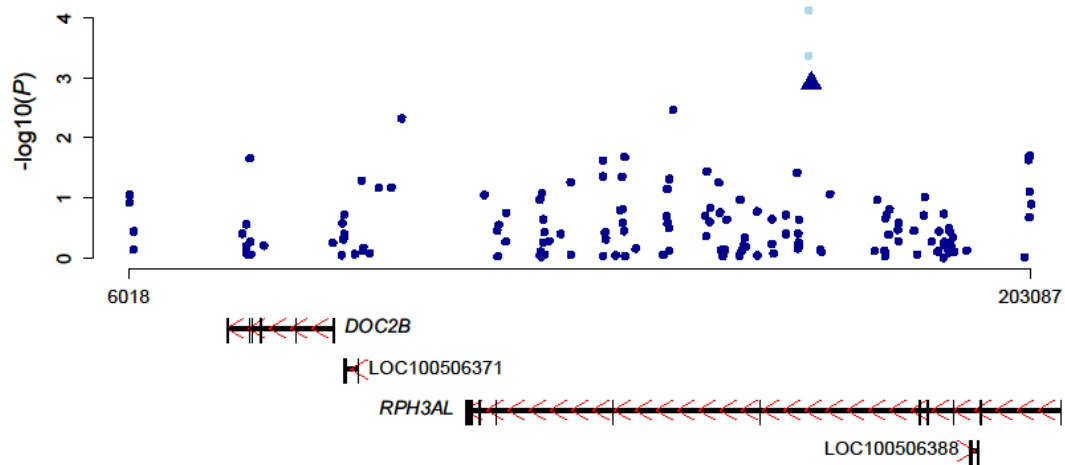


Figure 3.44. Manhattan plot showing the probes within 50 kilobases of the chr17:154410-154672 region in the prefrontal cortex. Shown are the $-\log_{10}(P)$ -values (y-axis) of the meta-analysis of the prefrontal cortex by chromosomal position (x-axis). The points in lighter blue show the probes identified in the differently methylated region and the triangle shape shows the cg11940040 probe.

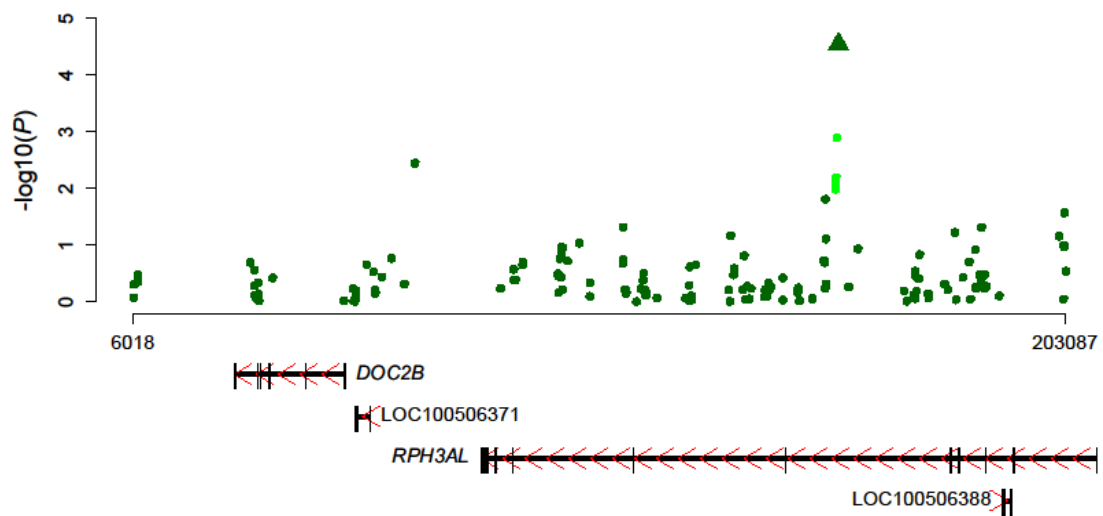


Figure 3.45. Manhattan plot showing the probes within 50 kilobases of the chr17:154410-154672 region in the striatum. Shown are the $-\log_{10}(P)$ -values (y-axis) of the meta-analysis of the striatum by chromosomal position (x-axis). The points in lighter green show the probes identified in the differently methylated region and the triangle shape shows the cg11940040 probe.

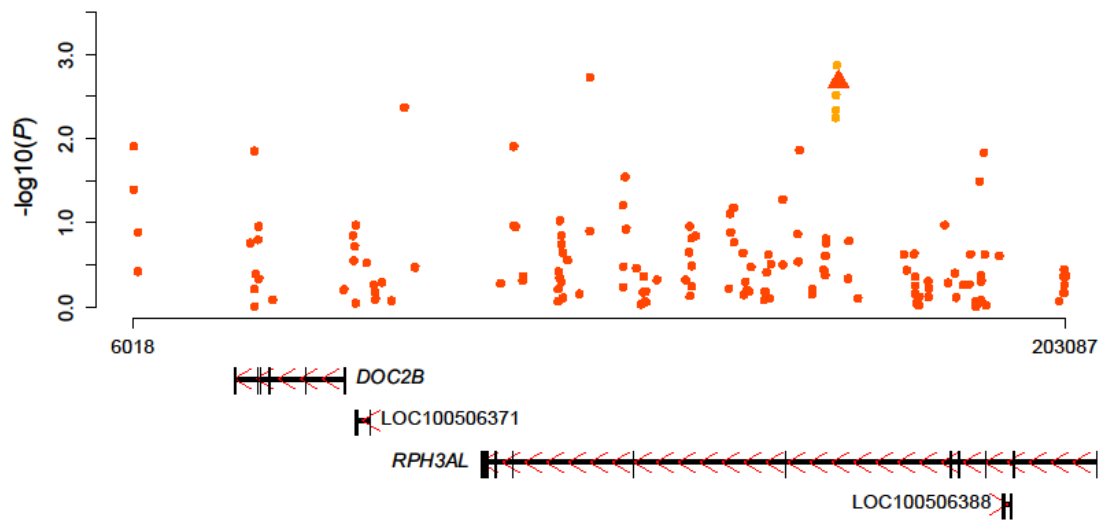


Figure 3.46. Manhattan plot showing the probes within 50 kilobases of the chr17:154410-154672 region in the cerebellum. Shown are the $-\log_{10}(P)$ -values (y-axis) of the meta-analysis of the cerebellum by chromosomal position (x-axis). The points in lighter orange show the probes identified in the differently methylated region and the triangle shape shows the cg11940040 probe.

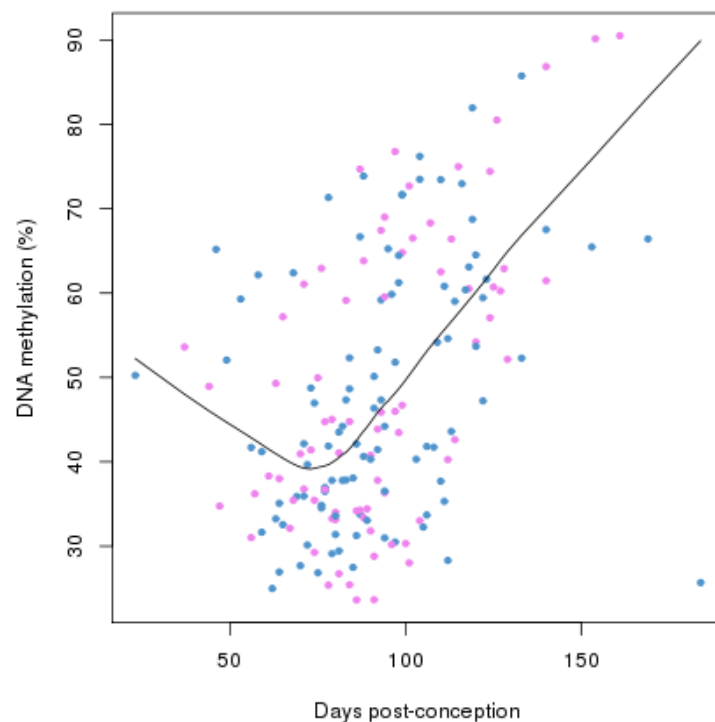


Figure 3.47. Probe cg15212418 shows dramatic DNA methylation (y-axis) changes associated with developmental age (x-axis) in fetal brain samples (Spiers et al., 2015). This probe shows significant DNA hypomethylation in schizophrenia brains and is adjacent to the schizophrenia-associated DMR in the *RPH3AL* gene (chr17:154410-154672).

Table 3.17. Bisulfite-polymerase chain reaction-pyrosequencing validation across the DMR in the *RPH3AL* gene in both prefrontal cortex and striatum.

CpG	450K probe	Genomic coordinates (hg19)	Prefrontal cortex			Striatum				
			450K		Pyrosequencing		450K		Pyrosequencing	
			Methylation difference (%)	P	Methylation difference (%)	P	Methylation difference (%)	P	Methylation difference (%)	P
1	-	chr17:154444	-	-	-8.86	1.61E-03	-	-	-5.09	1.82E-02
2	-	chr17:154429	-	-	-8.16	1.83E-03	-	-	-5.10	1.50E-02
3	cg11940040	chr17:154420	-7.76	4.36E-04	-9.03	1.97E-03	-5.04	7.89E-03	-5.84	1.24E-02
Average	-	-	-	-	-8.68	1.72E-03	-	-	-5.33	1.41E-02

3.3.7. Consistent methylomic markers of schizophrenia across brain regions

I next employed a multi-level model to further explore consistent schizophrenia-associated differences across multiple brain regions (see **section 3.2.9**). As reported in previous analyses of epigenetic variation in the human brain (Davies et al., 2012, Hannon et al., 2016, Ladd-Acosta et al., 2007), my data indicate that the CER is very distinct at a global level to the other three brain regions included in this study (**Figures 3.5** and **3.6**); for this reason I excluded the CER from the cross-region model and focused on identifying consistent signals across the PFC, STR and HC. **Figures 3.48** and **3.49** present the QQ and Manhattan plot for this analysis, respectively. Of note, there is some inflation in the distribution of *P*-values in the multi-region case-control analysis ($\lambda = 1.43$); although the multilevel model used is designed to control for the non-independence of brain regions from the same individual, it is possible that combining datasets has resulted in some residual inflation. Compared to other published EWAS analyses, however, this inflation is relatively modest and I did not identify an excessively large number of DMPs passing our stringent family-wise significance threshold. **Table 3.18** and **Figure 3.50** lists the fifty top ranked cross-region DMPs.

Although no DMP reached the highly stringent multiple testing significance threshold ($P < 1.66E-07$, see **section 3.2.8**), some cross-region DMPs are of interest. For example, the cg07500432 shows consistent schizophrenia-associated hypermethylation in all three brain regions. This probe is within an intron of the par-6 family cell polarity regulator gamma (*PARD6G*) gene, which encodes a protein involved in asymmetrical cell division and cell polarization processes. Of more interest is the fact that this probe is also annotated to the activity-dependent neuroprotective protein homeobox 2 (*ADNP2*) gene in the GREAT annotation (McLean et al., 2010) (the probe is located 51,674kb upstream the *ADNP2* gene). This gene is highly expressed in the brain compared to other tissues and has been suggested to play a role in neurodevelopment (Kushnir et al., 2008) and has been previously implicated in schizophrenia (Merenlender-Wagner et al., 2015). The DMP analysis also provides further support for several *loci* identified in our previous study of schizophrenia prefrontal cortex 17 including *GSDMD* (cg26173173: $P = 4.28E-$

05), *RASA3* (cg24803255: $P = 1.51E-04$), *PPFIA1* (cg08171022: $P = 1.19E-02$) and *MYT1L* (cg00236305: $P = 4.62E-04$) (**Table 3.19**), suggesting that DNA methylation differences at these *loci* consistent effects across the three regions.

Significant schizophrenia-associated cross-region DMRs are presented in **Table 3.20** and **Figure 3.51**. Of note, the top ranked cross-region DMRs include a highly-significant signal spanning 11 CpG sites (Šidák-corrected $P = 8.90E-11$) annotated to *WNT5A*, an important neurodevelopmental *locus* (Horigane et al., 2016), in addition to regions annotated several *loci* discussed above such as *GBP4* (Šidák-corrected $P = 0.01$), *PRDM9* (Šidák-corrected $P = 0.04$) and *RPH3AL* (Šidák-corrected $P = 1.23E-05$).

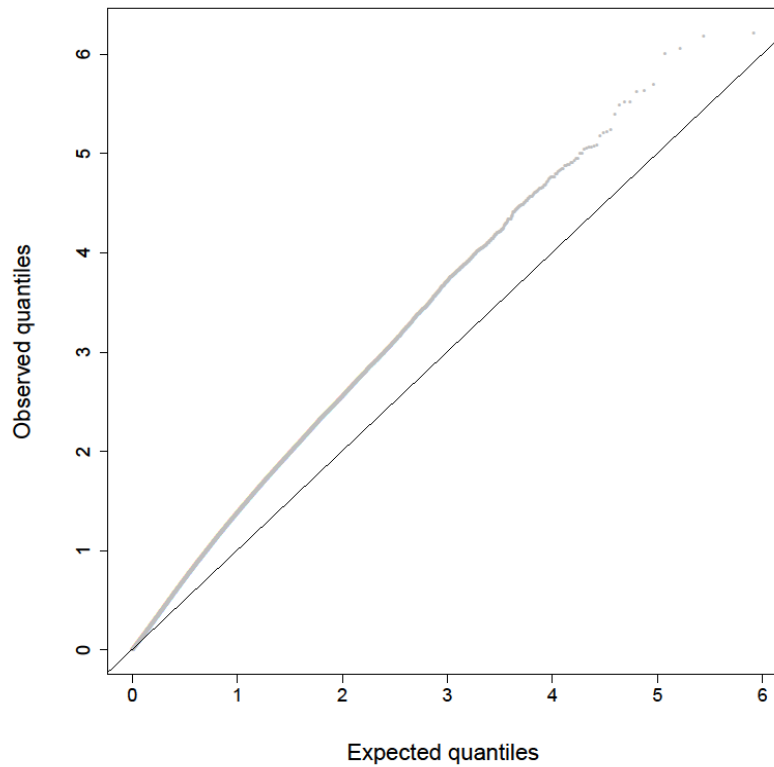


Figure 3.48. Quantile-quantile plot for case-control schizophrenia EWAS. Shown are the expected (x-axis) and observed (y-axis) quantiles observed in the multi-level model including data from the PFC, STR and HC.

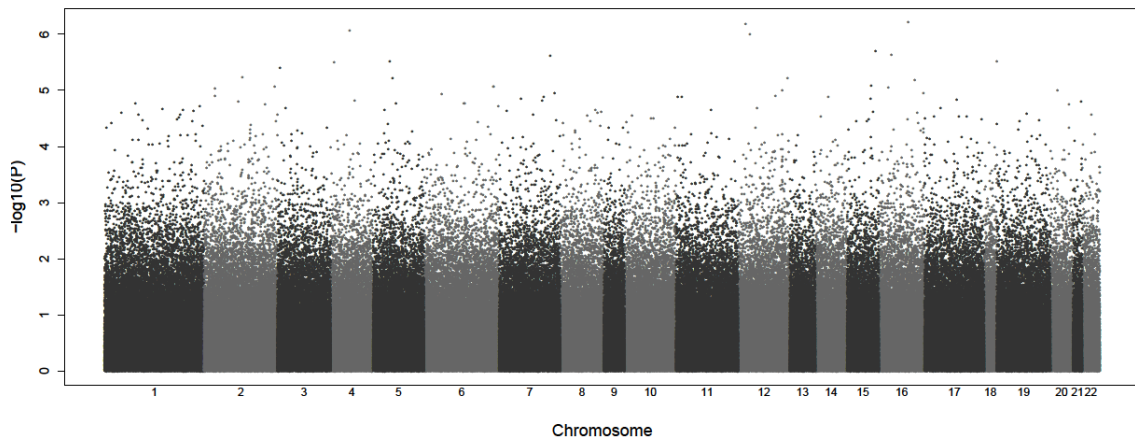


Figure 3.49. Manhattan plot for case-control schizophrenia EWAS. Shown are the $\log_{10}(P\text{-values})$ (y-axis) of the multi-level model including data from the PFC, STR and HC by chromosomal position (x-axis).

Table 3.18. Top ranked schizophrenia-associated differentially methylated probes (DMPs) identified in the multiregion model incorporating the prefrontal cortex (PFC), striatum (STR) and hippocampus (HC) data. Listed for each DMP are results from the multilevel model (grey) and corresponding results from the prefrontal cortex (PFC; $P < 0.05$ in blue), striatum (STR; $P < 0.05$ in green) and hippocampus (HC; $P < 0.05$ in red) meta-analyses (PFC and STR) or linear regression (HC). Also shown is the association with schizophrenia polygenic burden (multiregion model, $P < 0.05$ in purple). Illumina and Genomic Regions Enrichment of Annotation Tool (GREAT) annotation (McLean et al., 2010) is listed for each DMP.

Probe ID	Genomic position (hg19)	Illumina gene annotation	Gene region	GREAT annotation (McLean et al., 2010)	Methylation difference (%) multilevel model	Methylation difference (%) PFC	Methylation difference (%) STR	Methylation difference (%) HC	P HC	Polygenic risk score methylation difference (%) multiregion model	Polygenic risk score P multiregion model
cg05966228	chr16:67666442	CTCF	Body	ACD; CTCF	-3.07	-1.73	-1.99	-3.97	0.02	-0.27	6.70E-03
cg19091779	chr12:13200089	KIAA1467	Body	KIAA1467; GSG1	1.90	1.51	1.49	2.51	0.01	0.15	0.01
cg08575268	chr4:57411000	-	-	ARL9; HOPX	-1.53	-0.69	-1.62	-0.97	0.16	-0.17	4.86E-04
cg01837362	chr12:34492938	-	-	ALG10	6.12	4.78	5.26	5.90	0.03	0.31	0.12
cg01663682	chr15:93447777	CHD2	Body	CHD2; RGM A	-0.96	-0.10	-1.26	-1.54	0.05	-9.72E-02	4.40E-03
cg16669395	chr16:10208417	GRIN2A	Body	GRIN2A	-3.58	-2.79	-2.75	-2.22	0.27	-0.19	0.12
cg23749029	chr7:148923218	ZNF282	3'UTR	ZNF282; ZNF282	-1.79	-1.34	-1.01	-2.81	0.02	-0.13	0.03
cg07500432	chr18:77918588	PAR6G; LOC100130522	Body	ADNP2; PAR6G	6.09	6.69	4.64	5.11	1.32E-03	0.64	2.01E-03
cg00067720	chr5:67521141	PIK3R1	TSS1500	SLC30A5; PIK3R1	-3.30	-1.24	-2.42	-1.99	0.25	-0.35	2.02E-03
cg21299345	chr4:1597692	-	-	FAM53A; CRIPAK	1.39	1.13	0.87	1.76	0.05	0.10	0.05
cg13441156	chr3:10335288	GHRL	TSS1500	GHRL	2.98	2.75	2.24	2.47	0.13	0.19	0.08
cg26228577	chr2:121624862	GLI2	Body	GLI2; TFCEP2L1	-2.58	-0.82	-2.33	-2.00	0.10	-0.15	0.12
cg01302436	chr12:132865713	GALNT9	Body	GALNT9; NOC4L	-4.38	-2.32	-0.48	-5.61	0.03	-0.47	1.65E-03
cg07228402	chr5:77917917	LHFP2	5'UTR	LHFP2; SCAMP1	3.35	2.94	3.22	2.77	0.23	0.14	0.27
cg18806980	chr16:84438123	ATP2C2	Body	ATP2C2; KIAA1609	2.03	1.36	1.94	2.96	0.01	0.17	0.02
cg16040341	chr15:83544284	HOMER2	Body	WHAMM; HOMER2	-2.04	-1.15	-1.64	-1.51	0.15	-0.22	1.56E-03
cg16757441	chr2:241419011	ANKMY1	3'UTR	GPC1; ANKMY1	1.96	1.42	1.32	1.55	0.09	0.18	0.01
cg04230050	chr6:166144874	-	-	PDE10A; T	1.69	1.27	1.91	0.93	0.27	0.06	0.38
cg19353294	chr6:164200967	-	-	QKI	1.97	0.95	1.59	4.22	8.92E-03	0.08	0.28
cg23754665	chr16:3313947	-	-	ZNF263; MEFV	1.68	0.92	1.80	2.25	2.47E-03	0.06	0.32
cg24538947	chr2:26785301	C2orf70	TSS200	OTOF	-2.33	-0.72	-2.28	-2.69	0.05	-0.32	7.76E-05

cg11484348	chr20:29896479	DEFB116	TSS200	DEFB116	9.97E-06	2.71	1.13E-03	3.37	2.06E-04	5.41	0.02	0.25	0.06
cg00254608	chr12:124813321	NCOR2	Body	NCOR2; ZNF664	1.00E-05	-1.75	0.05	-3.02	3.92E-03	-1.19	0.45	-0.25	0.06
cg00183888	chr7:155276880	-	-	RBM33; EN2	1.11E-05	-1.42	0.06	-1.40	0.05	-1.94	0.19	-0.28	2.86E-03
cg10091053	chr16:89603535	SPG7	Body; 3'UTR	RPL13; SPG7	1.13E-05	-1.91	8.02E-03	-1.56	0.03	-3.88	0.07	-0.27	0.01
cg19988490	chr6:30167065	TRIM26	5'UTR	TRIM10; TRIM26	1.16E-05	1.19	0.04	1.72	2.16E-03	1.83	0.10	0.08	0.23
cg14835517	chr12:113917417	-	-	LHX5; RBM19	1.24E-05	-1.33	0.01	-1.23	7.42E-03	-1.28	0.09	-0.14	7.37E-03
cg22488717	chr2:26785946	C2orf70	Body	OTOF	1.25E-05	-2.11	2.39E-05	-0.57	0.30	-1.40	0.31	-0.11	0.11
cg03608093	chr11:691457	DEAF1	Body	TMEIM80	1.29E-05	-1.60	9.76E-03	-1.28	0.04	-1.90	0.07	-6.42E-02	0.40
cg19567740	chr7:128527122	KCP	Body	KCP; ATP6V1F	1.31E-05	1.38	0.03	1.64	3.16E-03	2.78	9.08E-03	0.03	0.64
cg27059530	chr14:67707359	MPP5	TSS1500	MPP5	1.31E-05	-1.02	1.08E-05	-0.55	0.04	-1.02	0.08	-5.21E-02	0.06
cg24439505	chr11:2172098	INS-IGF2	Body; TSS1500	IGF2; INS-IGF2	1.33E-05	-2.39	2.14E-04	-1.13	0.13	-5.51	4.85E-03	-0.15	0.14
cg09941712	chr15:81068966	-	-	KIAA1199	1.41E-05	-1.03	0.03	-1.21	5.53E-04	-1.17	0.11	-7.84E-02	0.10
cg20413415	chr7:43351469	HECW1	Body	STK17A; HECW1	1.42E-05	1.12	7.51E-04	1.02	0.01	1.43	0.10	0.05	0.21
cg03496533	chr17:46035183	PRR15L	TSS200	CDK5RAP3; PNPO	1.47E-05	1.68	0.01	1.67	0.08	2.33	0.15	0.07	0.49
cg24652994	chr7:122011261	CADPS2	Body	FEZF1; RNF133	1.50E-05	1.01	8.53E-03	0.61	0.09	1.95	0.11	0.06	0.22
cg23092072	chr4:87927706	AFF1	Body; TSS1500	AFF1; HSD17B13	1.51E-05	-0.56	0.03	-2.30	8.19E-03	-0.98	0.18	-0.16	0.08
cg11029358	chr21:46875433	COL18A1	5'UTR; 1stExon; Body	COL18A1	1.60E-05	-1.65	0.03	-2.19	9.00E-04	-2.44	0.06	-7.41E-02	0.44
cg08775629	chr2:107457756	ST6GAL2	Body	RGPD3; ST6GAL2	1.61E-05	-1.45	0.06	-1.64	0.02	-2.78	0.09	-2.59E-01	3.99E-03
cg00369811	chr6:37673597	-	-	ZFAND3; MDGA1	1.72E-05	-0.69	0.04	-1.67	3.94E-05	-0.53	0.58	-3.72E-02	0.42
cg11348994	chr5:95769993	PCSK1	TSS1500	PCSK1	1.73E-05	-1.34	0.01	-2.22	0.01	-0.73	0.40	-0.34	2.22E-04
cg14843030	chr1:32716051	LCK	TSS1500	LCK; EIF3I	1.73E-05	1.09	0.04	1.62	4.97E-04	2.66	0.02	0.14	0.03
cg14418226	chr6:40996092	UNC5CL	3'UTR	LRFN2; UNC5CL	1.74E-05	-1.06	0.08	-1.44	3.97E-03	-1.78	0.17	-1.72E-01	0.02
cg18864882	chr20:60371478	CDH4	Body	TAF4; CDH4	1.77E-05	2.18	0.02	2.68	4.38E-04	2.20	0.15	0.16	0.14
cg25476129	chr2:220341206	SPEG	Body	GMPPA; SPEG	1.80E-05	-0.22	0.72	-2.82	1.02E-04	-2.80	0.01	-0.26	1.19E-03
cg04245131	chr1:235133338	-	-	IRF2BP2; TOMM20	1.90E-05	-1.68	9.98E-03	-1.24	0.08	-1.54	0.14	-0.27	2.47E-03
cg00632364	chr6:170401305	-	-	DLL1; C6orf70	1.95E-05	-1.46	0.14	-2.80	3.95E-03	-1.36	0.59	-0.28	0.02
cg21637761	chr17:20107320	CYTSB	Body	SPECC1; LGALS9B	2.04E-05	-2.17	7.54E-03	-1.82	0.01	-3.23	0.03	-0.27	6.98E-03
cg27597505	chr12:54148217	-	-	HOXC13; CALCOCO1	2.07E-05	-2.44	1.30E-03	-1.42	0.04	-0.95	0.43	-0.14	0.10
cg19459454	chr3:32509030	-	-	CMTM6; CMTM7	2.10E-05	-3.44	6.15E-05	-1.20	0.13	-2.65	0.20	-0.25	0.03

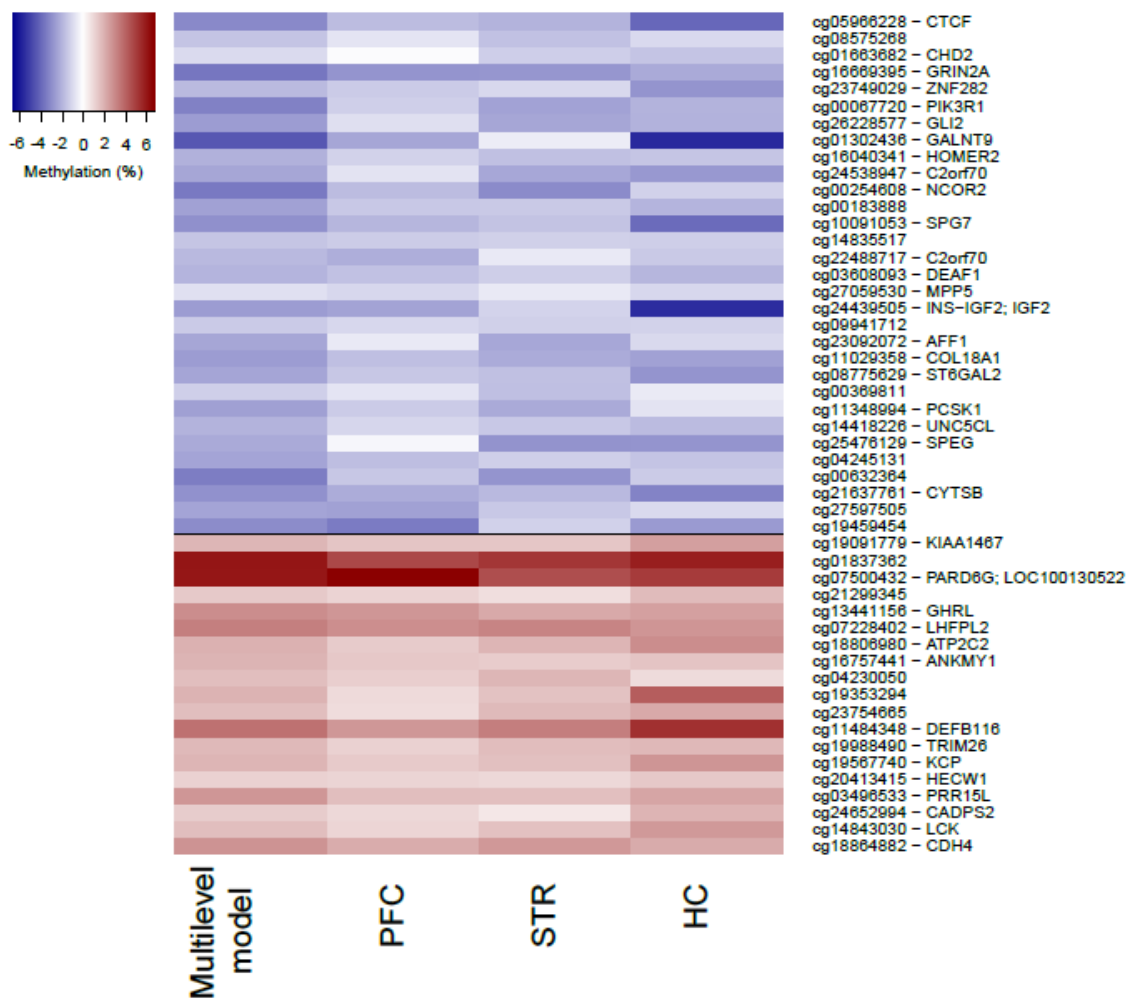


Figure 3.50. Heatmap showing the fifty top ranked schizophrenia-associated differentially methylated positions identified using a multi-region model incorporating prefrontal cortex (PFC), striatum (STR) and hippocampus (HC). Shown for each probe is the DNA methylation difference between cases and controls, with the corresponding difference at the same probe for the three individual brain regions. Probes are ordered by *P*-value for hypomethylated (blue, top) and hypermethylated (red, bottom) *loci* from the multi-region model.

Table 3.19. Results for top ranked schizophrenia-associated probes identified in a previous study of cortical tissue (Pidsley et al., 2014). Shown are data for each brain region for probes previously associated with schizophrenia (FDR < 0.10) in the cortex by Pidsley et al (2014) (Pidsley et al., 2014).

Probe	Gene	Pidsley et al. Methylation difference (%)	Pidsley et al. P	PFC methylation difference (%)	PFC P	STR methylation difference (%)	STR P	HC methylation difference (%)	HC P	CER methylation difference (%)	CER P	Multilevel model methylation difference (%)	Multilevel model P
cg26173173	GSDMD	4	1.16E-07	3.11	8.06E-07	1.39	7.59E-02	1.73	2.99E-01	1.21	1.81E-01	2.47	4.28E-05
cg24803255	RASA3	-9	1.25E-07	-3.23	8.98E-05	-0.99	5.26E-02	0.58	7.98E-01	-1.35	3.03E-01	-2.61	1.51E-04
cg00903099	HTR5A	-2	2.40E-07	-1.25	2.42E-04	-0.09	8.79E-01	-0.07	9.62E-01	0.06	8.75E-01	-0.67	1.36E-01
cg08171022	PPFIA1	-5	2.85E-07	-2.49	6.26E-04	0.14	8.76E-01	-1.03	5.84E-01	-1.01	1.38E-01	-1.82	1.19E-02
cg02857643	CACNA1G	-5	1.63E-06	-0.04	9.44E-01	-0.65	6.40E-02	0.06	8.60E-01	0.25	3.17E-01	-0.82	2.09E-02
cg00236305	MYT1L	-6	1.75E-06	-2.4	3.68E-04	0.04	9.13E-01	-0.82	4.53E-01	-2.66	1.12E-01	-1.56	4.62E-04
cg14966346	KLC1	-5	2.51E-06	-1.63	1.46E-02	0.06	8.93E-01	-0.8	4.92E-01	-0.38	7.05E-01	-1.22	3.53E-03
cg13079528	SDK1	-8	2.75E-06	-2.24	1.44E-02	0.08	9.18E-01	-2.02	2.35E-01	0.32	1.74E-01	-1.28	3.52E-02
cg14429765	MCPH1	3	2.79E-06	-	-	-	-	-	-	-	-	-	-
cg08602214	RHOBTB2	-7	2.87E-06	-1.93	2.41E-03	-0.28	6.41E-01	-1.82	1.61E-01	-0.27	4.95E-01	-1.08	3.45E-02
cg19735533	-	-6	2.94E-06	-1.45	6.34E-02	0.51	1.54E-01	-0.5	6.58E-01	0.13	8.21E-01	-0.44	3.52E-01
cg09507608	-	-6	2.95E-06	-2.64	1.85E-03	-0.71	4.26E-01	-1.39	5.89E-01	-0.54	4.82E-01	-1.52	3.78E-02
cg23844013	C8A	3	3.20E-06	1.82	1.04E-04	-0.28	5.79E-01	-0.41	7.84E-01	0.7	3.39E-01	0.44	3.28E-01
cg26578910	PRKD2	-4	3.47E-06	-2.01	7.61E-05	-0.35	7.04E-01	-0.03	9.81E-01	0.4	2.91E-01	-0.02	9.81E-01
cg21847368	MCF2L	-3	3.70E-06	-1.29	8.90E-03	0.6	2.71E-01	1.71	1.05E-01	1.42	8.20E-02	-0.55	1.72E-01
cg03607729	LCMT1	-4	4.19E-06	-0.44	3.49E-01	-0.25	5.66E-01	-0.77	4.06E-01	0.57	1.97E-01	-0.9	2.53E-02
cg10248981	LHPP	-7	4.32E-06	-2.85	7.43E-04	0.43	7.63E-01	-4.24	1.43E-01	-0.36	8.47E-01	-2.12	4.93E-02
cg03445663	HDLBP	-8	4.59E-06	-2.5	1.67E-03	0.13	5.28E-01	-0.76	6.24E-01	-0.93	2.54E-01	-1.92	1.30E-03
cg15079231	VIPR1	-4	4.93E-06	-2.08	5.59E-04	0.18	7.74E-01	-0.29	8.43E-01	0.32	6.27E-01	-0.91	6.35E-02
cg21341878	ZFYVE28	-5	5.14E-06	-1.63	1.47E-02	0.18	6.06E-01	-0.59	5.55E-01	-1.24	4.28E-01	-1.1	9.27E-03
cg04922803	GLT8D2	6	5.19E-06	2.75	1.11E-02	-0.36	8.09E-01	1.7	4.73E-01	1.01	5.24E-01	0.24	8.46E-01
cg18857062	CRIP3	-4	5.29E-06	-2.63	9.65E-05	1.25	1.97E-01	-0.9	6.35E-01	-0.7	1.51E-01	-1.23	1.04E-01

Table 3.20. Significant schizophrenia-associated differently methylated regions (DMRs) identified in the multilevel model incorporating the prefrontal cortex, striatum and hippocampus data. Shown in chromosomal order is the location of significant (Šidák-corrected $P < 0.05$) DMRs identified in the multilevel model. The column “Gene” represents the combined Illumina and Genomic Regions Enrichment of Annotation Tool (GREAT) annotation (McLean et al., 2010).

Region	Gene	Probes	N probes	Median P	Šidák P
chr1:89664260-89664546	GBP4	cg23978657; cg02482460; cg22221320; cg21365602; cg20410995	5	3.67E-03	0.01
chr3:32509018-32509332	CMTM6; CMTM7	cg00718400; cg19459454; cg13050802; cg05625284; cg16621749; cg05651657	6	4.36E-03	3.32E-03
chr3:49170496-49170850	LAMB2	cg01919208; cg02954987; cg08234664; cg05654765; cg14099457; cg11566975	6	9.57E-03	8.60E-03
chr3:55517496-55518442	WNT5A; LRMT1	cg20746482; cg08852968; cg27364162; cg18562578; cg18010752; cg17679453; cg04941246; cg24216596; cg08666668; cg02867696; cg23456221	11	1.06E-03	8.90E-11
chr5:23507450-23507657	PRDM9	cg22054885; cg19837938; cg02444433; cg25472530; cg22079902; cg01667892	6	7.27E-03	0.04
chr6:30043049-30043419	RNF39	cg23500724; cg10865856; cg24016627; cg23939808; cg12967914; cg00853042; cg23027574; cg05853632; cg22105332; cg19006429; cg27532187; cg01631162	12	1.36E-02	5.82E-04
chr6:31648650-31649094	LY6G5C	cg08226747; cg18581937; cg19387310; cg25188387; cg07845406; cg17990278; cg03588325; cg23642766; cg06667222; cg14102811; cg14463529; cg07151644; cg09295695	13	2.37E-02	3.38E-03
chr6:33739406-33739654	LEMD2; IP6K3	cg07979401; cg18005901; cg16010596; cg13859433	4	1.43E-03	0.04
chr6:40995889-40996214	UNC5CL; LRFN2	cg21774121; cg24419528; cg00592058; cg14418226; cg21128951	5	2.03E-03	2.87E-05

chr10:63809073-63809171	ARID5B; RTKN2	cg14789659; cg00928816; cg20746552; cg16389209; cg07520810; cg16401465	6	3.78E-03	4.51E-03
chr10:124638756-124639013	FAM24B; LOC399815	cg03804621; cg16299003; cg11218091; cg14708218; cg18195080	5	1.39E-03	4.44E-04
chr10:134994186-134994456	KNDC1; UTF1	cg13609319; cg18398637; cg06517181; cg08815970; cg09274040	5	2.72E-04	4.10E-03
chr11:6341717-6341909	PRKCDBP	cg16459349; cg20938665; cg02273041; cg27132391; cg15202102; cg26678920; cg05628549; cg10064871	8	1.12E-02	0.03
chr12:124864528-124864682	NCOR2; ZNF664	cg04930596; cg07241090; cg17387577; cg17825194	4	1.79E-04	2.64E-04
chr14:36983129-36983695	SFTA3; MBIP; NKX2-1	cg23542968; cg10385303; cg16478719; cg22945387; cg27294268; cg05372242; cg04330513	5	1.04E-02	6.79E-04
chr16:67184918-67185195	B3GNT9	cg08659394; cg05527491; cg06212637; cg20984188; cg02771381; cg02724047	6	5.84E-03	9.98E-03
chr16:89603535-89603818	SPG7; RPL13	cg10091053; cg02207944; cg03740221; cg00855299	4	4.37E-03	5.41E-03
chr17:154410-154672	RPH3AL; DOC2B	cg08770870; cg11940040; cg10440639; cg23246911	4	1.77E-04	1.23E-05
chr17:76220608-76220956	BIRC5; EPR1; TMEIM235	cg11912239; cg10140240; cg00017271; cg19272238; cg07366188; cg10070788	6	6.10E-03	1.42E-03
chr19:57149436-57149631	ZNF835; ZNF71	cg07962143; cg15091407; cg02940165; cg14627089	4	3.06E-03	0.03
chr20:37230326-37230613	C20orf95; ARHGAP40	cg01025836; cg00557360; cg04608177; cg03356734; cg06301550; cg08438366	6	5.14E-03	0.03
chr21:46875142-46875434	COL18A1	cg02124724; cg16121744; cg14903689; cg07279557; cg11029358	5	8.81E-03	5.86E-03

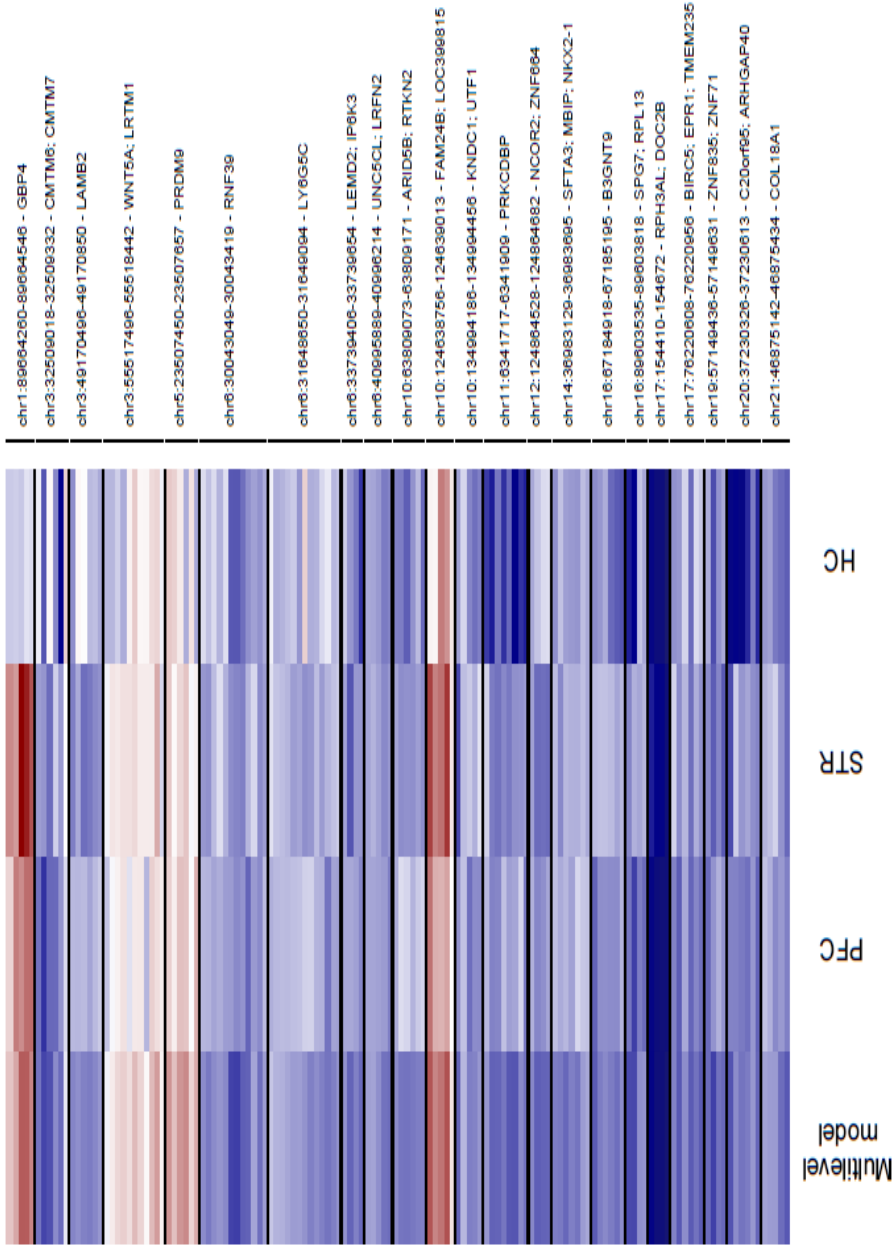


Figure 3.51. Heatmap showing differently methylated regions (DMRs) associated with schizophrenia identified using a multi-region model incorporating prefrontal cortex (PFC), striatum (STR) and hippocampus (HC). Shown in chromosomal order are schizophrenia-associated DNA methylation differences in each of the significant DMRs, with disease-associated differences in the corresponding probes shown for the three individual brain regions (blue = hypomethylation, red = hypermethylation).

3.4. Discussion

3.4.1. Overview of results

In this study I quantified genome-wide patterns of DNA methylation in post-mortem brain samples isolated from PFC, STR, HC and CER obtained from three independent cohorts of schizophrenia patients and controls. One of the cohorts was removed from analyses during stringent QC steps due to the detection of the incorrect tissue type for one brain region, and the two remaining cohorts were used in all subsequent analyses. I identified numerous DMPs and DMRs associated with disease in each individual brain region. Although the specific list of top ranked DMPs identified in each brain region is distinct, many of these were characterised by consistent effects across brain regions. The multilevel model across PFC, STR and HC data identified differential methylation in DMPs and DMRs across all three brain regions.

Genes annotated to several of the schizophrenia-associated DMPs and DMRs identified have been previously implicated in the pathophysiology of schizophrenia or have relevant roles in brain function; such as *NCAM1* (which encodes a neural cell adhesion molecule with a well-established role in neurodevelopment and synaptic plasticity) (Sunshine et al., 1987, Ronn et al., 1998), *SYNPO* (which encodes a actin-associated protein that is associated with postsynaptic densities and dendritic spines and differentially expressed in schizophrenia brain) (Focking et al., 2015), *GBP4* (which encodes a gene that has been found to be differentially expressed in schizophrenia patients) (Sanders et al., 2013) and *PRDM9* (which encodes a protein with histone H3K4 trimethyltransferase activity during meiosis that has been previously hypothesized to play a role in schizophrenia) (Berg et al., 2010, Crow, 2011), among others.

There is no evidence for enrichment of probes within TFBS and DHS regions in the fifty top ranked DMPs for each brain region. At more relaxed thresholds of significance, however, the PFC DMPs show a significant under-enrichment for TFBS and DHS, the STR and CER DMPs show a significant enrichment for both DHS and TFBS and the HC DMPs have a significant enrichment for TFBS.

3.4.2. Limitations

Despite this being, to my knowledge, the first study to quantify DNA methylation across four different brain regions from schizophrenia patients and controls, using samples from independent brain banks, this study has a number of important limitations.

First, the number of samples assessed in this study is relatively low, especially for analyses involving the HC, which was only available from one of the two cohorts used in the analyses. The small number of samples limits the power to detect significant associations with schizophrenia (Dempster et al., 2013). Future efforts by the community should focus on extending participation in brain-banking efforts to maximise the number of samples available for molecular epidemiology. Second, these data arise from measuring DNA methylation at a single, post-mortem time point. Given the dynamic nature of epigenetic processes, it would be important to measure DNA methylation in the living brain at different time points, which is currently impossible.

Third, because epigenetic processes play an important role in defining cell type-specific patterns of gene expression (Roadmap Epigenomics Consortium et al., 2015, Talens et al., 2010, Varley et al., 2013), the use of bulk tissue from each brain region is a potential confounder in DNA methylation studies (Guintivano et al., 2013, Heijmans and Mill, 2012). Despite my efforts to control for the effect of cell type diversity in DNA methylation quantification in the analyses using *in silico* approaches to estimate neuronal proportions, this approach is not suitable to estimate the neuronal proportion in the CER and cannot inform about disease relevant DNA methylation changes specific to individual brain cell types.

Forth, there is increasing awareness of the importance of 5-hydroxymethyl cytosine (5-hmC) in the human brain (Branco et al., 2012, Kriaucionis and Heintz, 2009), although this modification cannot be distinguished from DNA methylation using standard bisulfite-based approaches (Lunnon et al., 2016b, Booth et al., 2012). It is therefore plausible that many of the differences identified in this study are confounded by modifications other than DNA methylation. To date and to my knowledge, no study has evaluated the role of 5-hmC in schizophrenia or any other psychiatric disorder, although novel

profiling methods should make this feasible in the near future (Lunnon et al., 2016b). Future work by our group and others is focussing on using novel single-cell approaches to examine cellular heterogeneity in complex tissues such as the brain and facilitate the identification of pathological changes in specific cells (and cell types).

Finally, although I controlled for age, sex and neuronal composition estimates (where possible) in the analyses, it is plausible that other factors may be confounding the case-control analyses of schizophrenia. For example, epidemiological data highlights a much higher rate of smoking in schizophrenia patients compared to unaffected controls (Dalack et al., 1998, de Leon and Diaz, 2005). Although smoking has been shown to have striking effects on DNA methylation in blood (Elliott et al., 2014), none of the robust smoking-associated DMPs identified in blood are amongst the schizophrenia DMPs identified in any of the four brain regions assessed in this chapter. Furthermore, I investigated the impact of including additional PC as independent variables capturing variation in DNA methylation on the association statistics for schizophrenia-associated DMPs, finding that the identified schizophrenia-associated DMPs are relatively robust to the major PCs associated with methylomic variance.

3.4.3. Implications, strengths and future directions

Despite the relatively small sample size, I was able to identify a number of DMPs and DMRs passing the stringent significance threshold in both the analyses of diagnosed schizophrenia. Furthermore, although the magnitude of DNA methylation change at the differentially methylated *loci* was relatively small (*i.e.* involving a relative small proportion of cells in a given brain region), we were able to technically validate the Illumina 450K array data using bisulfite-pyrosequencing. Definitively distinguishing cause from effect in epigenetic epidemiology is difficult, especially for disorders like schizophrenia that manifest in inaccessible tissues such as the brain and are therefore particularly refractory to longitudinal study (Heijmans and Mill, 2012). However, the observation of consistent changes across multiple brain regions in two independent cohorts for many DMPs and DMRs suggests that the identified *loci* are potentially directly relevant to the schizophrenia pathogenesis.

Finally, although this study presents novel evidence for associations between schizophrenia diagnosis and variable DNA methylation across different brain regions, replication using larger sample sizes is required to further support these results. Future studies should focus on understanding the transcriptional consequences of the observed associations, and testing whether these associations are causal or a consequence of disease and/or medication.

In summary, these data provide evidence for extensive differences in DNA methylation across multiple brain regions in schizophrenia. To my knowledge, this study represents the first analysis of epigenetic variation associated with schizophrenia across multiple brain regions.

Chapter 4 - Methylomic profiling of schizophrenia polygenic risk burden in the brain

4.1. Introduction

Twin and family studies have highlighted a notable heritable component to schizophrenia (Craddock et al., 2005), however the role of genetic variation in the etiology of the disorder is complex. Rare, highly penetrant inherited and *de novo* mutations have been implicated in some cases of schizophrenia (Xu et al., 2011, St Clair et al., 1990, Stefansson et al., 2014, Purcell et al., 2014), although susceptibility is predominantly attributed to the action of common genetic variants of low penetrance. Recently, a large-scale genome-wide association study (GWAS) identified 108 independent genomic *loci* exhibiting genome-wide significant association with schizophrenia (Schizophrenia Working Group of the Psychiatric Genomics, 2014).

Genetic variation has been shown to influence DNA methylation in the human brain (Gibbs et al., 2010, Gamazon et al., 2013). Genetic variants associated with variation in DNA methylation levels are denoted methylation quantitative trait *loci* (mQTLs) and evidence suggest that genetic mediation of the methylome provides a link between genetic variation and the establishment of complex phenotypes (Wagner et al., 2014, Gutierrez-Arcelus et al., 2013). Recent publications from our group and others have studied the implication of mQTLs (Hannon et al., 2016, Jaffe et al., 2016) in schizophrenia, providing support for the hypothesis that common variants associated with schizophrenia may function through directly influencing the methylome to affect the disease phenotype.

Polygenic risk scores (PRS) are defined as the sum of trait-associated alleles across many genetic *loci*, weighted by effect sizes estimated by GWAS analyses. There has been recent interest in using PRS as disease biomarkers, although their utility for exploring the molecular genomic mechanisms involved in disease pathogenesis is largely unexplored. For example, PRS-associated epigenetic variation is potentially less affected by factors associated with the disease itself (e.g. medication exposure, stress, and smoking), which can confound case-control analyses.

The most recent schizophrenia GWAS (Schizophrenia Working Group of the Psychiatric Genomics, 2014) calculated that a schizophrenia PRS derived from all independent nominally significant associated alleles (association P -value < 0.05) captures about 7% of total liability for the disorder in an European population. Although this is not currently useful for clinical risk predication, it could be predictive of chronicity, treatment resistance or useful in the stratification of patients (O'Donovan, 2015). So far schizophrenia PRS have been used to investigate several schizophrenia-linked traits such as creativity (Power et al., 2015), cognitive decline (Liebers et al., 2016) and antipsychotic drug response (Frank et al., 2015). A recent study suggests that schizophrenia PRS correlates with negative symptoms and anxiety disorder but not with psychotic experiences or depression in adolescents from a population-based birth cohort (Jones et al., 2016).

Despite the recent advances in understanding the genetic epidemiology of schizophrenia, little is known about the mechanisms by which schizophrenia risk variants mediate disease susceptibility in the brain (Fullard et al., 2016, Psych et al., 2015). In this chapter I investigate whether schizophrenia PRS impacts on DNA methylation, and whether this impact is independent from direct genetic effects on DNA methylation (*i.e.* mQTLs). I identified several differently methylated positions (DMP) and regions (DMR) in all four brain regions investigated and across brain regions. I show that these associations, showing that PRS-associated *loci* are independent from disease-associated methylomic variation and are not the consequence of *cis*-acting brain mQTLs. These data highlight the utility of PRS for identifying molecular pathways associated with etiological variation in complex disease.

4.2. Methods

4.2.1. Samples genotyping and quality control

The 88 individuals (n = 41 schizophrenia patients and n = 47 non-psychiatric controls) from the LNDBB and DBCBB used in the final DNA methylation dataset (see **Chapter 3**) were selected for genotyping. Detailed information about the sample cohorts is given in **Chapter 3 Section 3.2.1** and **Supplementary Table 1** and detailed DNA extraction information is described in **Chapter 2 section 2.2**. Genomic DNA (~200 ng) from each individual was used for genotyping on the Illumina Infinium HTS HumanOmniExpress-24 BeadChip v1-0 using an iScan Microarray Scanner (Illumina, San Diego, CA, USA), and I processed each sample according to manufacturer' standard instructions. The brain region of origin of each genotyped sample is given in **Table 4.1**. Illumina *GenomeStudio* software was used for genotype calling and the data were exported as *.ped* and *.map* files. *PLINK* (Purcell et al., 2007) was used to remove samples with > 5% missing data and SNPs with > 1% missing values, Hardy-Weinberg equilibrium $P < 1.00E-03$ or minor allele frequency of < 5%.

Table 4.1. Table showing the brain region of origin of the DNA samples genotyped in the present chapter. Detailed information of all samples of all samples is presented in **Appendix A - Supplementary Table 1**.

Individual	Brain Bank	Group	Brain region used for genotyping	Genotyping array barcode
1	LNDBB	schizophrenia	prefrontal cortex	7942519024_R03C01
2	LNDBB	schizophrenia	prefrontal cortex	7942519024_R02C02
3	LNDBB	schizophrenia	prefrontal cortex	7942519009_R02C01
4	LNDBB	schizophrenia	prefrontal cortex	7942519009_R05C02
5	LNDBB	schizophrenia	prefrontal cortex	7930649111_R01C01
6	LNDBB	schizophrenia	prefrontal cortex	7942519009_R03C01
7	LNDBB	schizophrenia	prefrontal cortex	7930649111_R04C02
8	LNDBB	schizophrenia	prefrontal cortex	7942519009_R04C02
9	LNDBB	schizophrenia	prefrontal cortex	7942519009_R01C01
10	LNDBB	schizophrenia	prefrontal cortex	7942519009_R04C01
11	LNDBB	schizophrenia	prefrontal cortex	7930649095_R06C01
12	LNDBB	schizophrenia	striatum	9933568129_R04C02
13	LNDBB	schizophrenia	prefrontal cortex	7930649111_R03C02
14	LNDBB	schizophrenia	prefrontal cortex	7930649111_R03C01
15	LNDBB	schizophrenia	prefrontal cortex	7930649095_R03C02
16	LNDBB	schizophrenia	prefrontal cortex	7942519009_R06C02
17	LNDBB	schizophrenia	prefrontal cortex	7942519024_R06C02
18	LNDBB	schizophrenia	prefrontal cortex	7942519024_R04C02
19	LNDBB	schizophrenia	prefrontal cortex	7942519024_R05C01
20	LNDBB	schizophrenia	prefrontal cortex	7930649095_R05C02
21	LNDBB	schizophrenia	prefrontal cortex	7930649095_R01C01
23	LNDBB	schizophrenia	prefrontal cortex	7942519009_R01C02
24	LNDBB	schizophrenia	prefrontal cortex	7942519024_R01C01
25	LNDBB	control	prefrontal cortex	7930649095_R05C01

26	LNDBB	control	prefrontal cortex	7930649095_R03C01
27	LNDBB	control	striatum	9933568081_R07C01
28	LNDBB	control	prefrontal cortex	7930649095_R04C02
30	LNDBB	control	prefrontal cortex	7942519009_R02C02
31	LNDBB	control	prefrontal cortex	7942519009_R06C01
32	LNDBB	control	prefrontal cortex	7930649111_R05C02
33	LNDBB	control	prefrontal cortex	7930649095_R02C01
34	LNDBB	control	striatum	9933568081_R04C01
35	LNDBB	control	prefrontal cortex	7942519024_R01C02
36	LNDBB	control	striatum	9933568129_R06C02
37	LNDBB	control	prefrontal cortex	7930649111_R02C01
38	LNDBB	control	prefrontal cortex	7942519024_R06C01
39	LNDBB	control	striatum	9933568129_R11C02
40	LNDBB	control	prefrontal cortex	7930649095_R02C02
41	LNDBB	control	prefrontal cortex	7942519024_R05C02
42	LNDBB	control	prefrontal cortex	7930649095_R04C01
43	LNDBB	control	striatum	9933568081_R08C01
44	LNDBB	control	prefrontal cortex	7930649111_R06C02
45	LNDBB	control	prefrontal cortex	7930649111_R01C02
46	LNDBB	control	prefrontal cortex	7930649111_R05C01
47	LNDBB	control	prefrontal cortex	7942519009_R03C02
49	LNDBB	control	prefrontal cortex	7930649095_R01C02
50	LNDBB	control	striatum	9933568081_R11C01
51	LNDBB	control	prefrontal cortex	7930649111_R04C01
52	LNDBB	control	prefrontal cortex	7942519024_R02C01
53	LNDBB	control	prefrontal cortex	7942519024_R04C01
54	LNDBB	control	prefrontal cortex	7930649111_R02C02
MS01	DBCBB	schizophrenia	cerebellum	9933568081_R02C01
MS02	DBCBB	schizophrenia	prefrontal cortex	9933568129_R11C01
MS03	DBCBB	schizophrenia	cerebellum	9933568157_R06C02
MS04	DBCBB	schizophrenia	cerebellum	9933568129_R03C01
MS05	DBCBB	control	cerebellum	9933568129_R09C01
MS06	DBCBB	schizophrenia	striatum	9933568129_R08C01
MS07	DBCBB	schizophrenia	cerebellum	9933568129_R12C02
MS08	DBCBB	control	cerebellum	9933568129_R07C01
MS09	DBCBB	control	striatum	9933568129_R08C02
MS10	DBCBB	control	striatum	9933568129_R09C02
MS11	DBCBB	schizophrenia	prefrontal cortex	9933568129_R03C02
MS12	DBCBB	schizophrenia	striatum	9933568129_R06C01
MS13	DBCBB	control	cerebellum	9933568129_R04C01
MS14	DBCBB	control	striatum	9933568129_R10C01
MS15	DBCBB	control	striatum	9933568081_R05C01
MS16	DBCBB	control	striatum	9933568129_R02C02
MS17	DBCBB	control	striatum	9933568129_R02C01
MS18	DBCBB	schizophrenia	striatum	9933568157_R12C02
MS19	DBCBB	control	cerebellum	9933568081_R06C01
MS20	DBCBB	schizophrenia	striatum	9933568129_R01C01
MS21	DBCBB	schizophrenia	striatum	9933568081_R10C01
MS22	DBCBB	control	striatum	9933568129_R07C02
MS23	DBCBB	schizophrenia	striatum	9933568129_R10C02
MS24	DBCBB	control	striatum	9933568081_R09C01
MS25	DBCBB	schizophrenia	striatum	9933568157_R05C02
MS26	DBCBB	control	striatum	9933568157_R08C02
MS27	DBCBB	schizophrenia	striatum	9933568157_R07C02
MS28	DBCBB	schizophrenia	striatum	9933568081_R03C01
MS29	DBCBB	schizophrenia	cerebellum	9933568157_R09C02
MS30	DBCBB	schizophrenia	striatum	9933568157_R10C02
MS31	DBCBB	control	striatum	9933568129_R01C02
MS32	DBCBB	schizophrenia	striatum	9933568129_R05C01
MS33	DBCBB	control	striatum	9933568081_R01C01
MS34	DBCBB	control	prefrontal cortex	9933568157_R11C02
MS35	DBCBB	control	striatum	9933568129_R12C01
MS36	DBCBB	control	cerebellum	9933568129_R05C02

4.2.2. Ethnicity prediction

Sample ethnicity was determined by merging the genotypes with data from HapMap Phase 3 (Wellcome Trust Sanger Institute, 2016) and linkage disequilibrium (LD) pruning the overlapping SNPs such that no pair of SNPs within 1500 bp had $r^2 > 0.20$. *GCTA* software (Yang et al., 2011) was then used to calculate principal components (PC) of the genetic data, which were visually inspected to predict ethnicity for each sample (**Figure 4.1**) by comparison with the known ethnicities of the HapMap sample. The schizophrenia GWAS used to calculate schizophrenia PRS in this chapter was carried out mainly in patients of European ancestry. Therefore I decided to exclude samples predicted as ancestry outliers (non-Caucasians; PC 2 < 0.03; n = 10) from further analyses of PRS, to avoid population stratification. In general these samples show higher schizophrenia PRS than Caucasian samples regardless of disease status (**Figure 4.2**) (see **section 4.2.3** for PRS calculation), hence their inclusion could confound results. Sentrrix barcodes and sample exclusion criteria are presented in **Appendix A - Supplementary Table 2**.

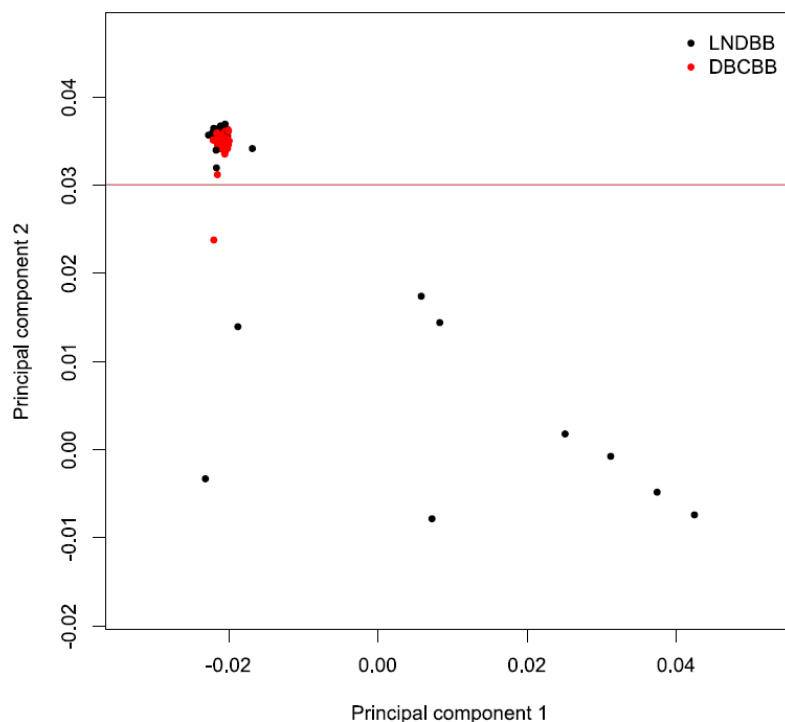


Figure 4.1. Principal components (PC) 1 and 2 of genetic data for both the MRC London Neurodegenerative Diseases Brain Bank (LNDBB) and the Douglas-Bell Canada Brain Bank (DBCBB) cohorts. The samples with a PC 2 < 0.03 (red line) were determined as ancestry outliers and removed from all the polygenic risk score analyses.

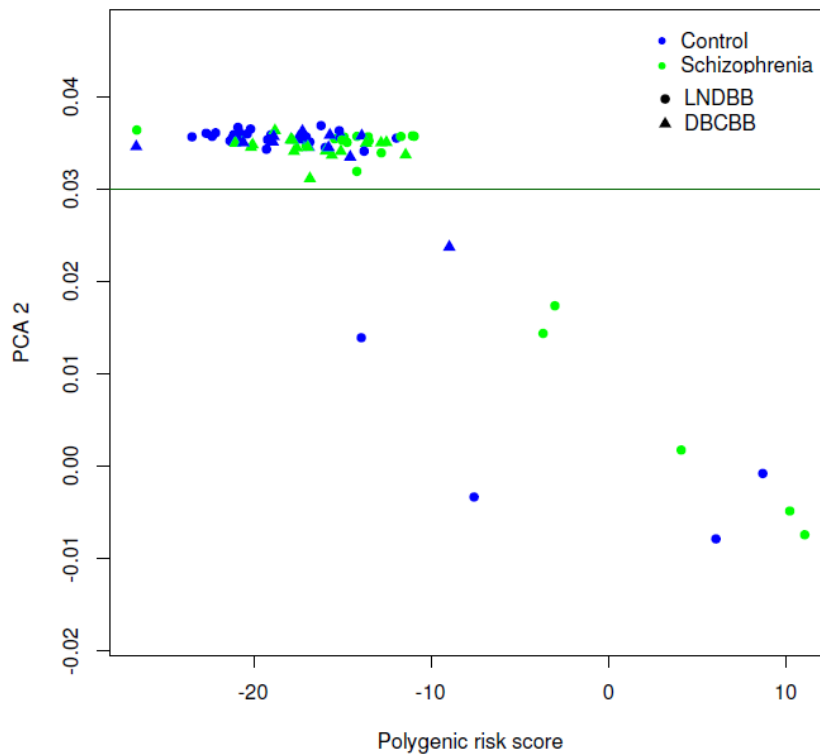


Figure 4.2. Principal component 2 of genetic data for both the MRC London Neurodegenerative Diseases Brain Bank (circle) and the Douglas-Bell Canada Brain Bank (triangle) vs respective polygenic risk scores (PRS). The samples with a principal component 2 < 0.03 (green line) were determined as ancestry outliers and removed from all the polygenic risk score analyses. In general, non-Caucasian samples show higher PRS than Caucasian samples regardless of whether they are schizophrenia cases (green) or controls (blue).

4.2.3. Polygenic risk score calculation

To impute variation at SNPs not present on the array used in this study (see **Section 4.2.1**), genotypes were recoded into *.vcf* files using *PLINK1.9* (Chang et al., 2015) and *VCFtools* (Danecek et al., 2011) before uploading to the Michigan Imputation Server (Cloudgene, 2016), which uses SHAPEIT (Delaneau et al., 2012) to phase haplotypes, and Minimac3 (Howie et al., 2012) with the most recent 1000 Genomes reference panel (phase 3, version 5) (EMBL-EBI, 2016).

PRS were calculated in *PLINK* (Purcell et al., 2007) using the imputation dosages and the score file downloaded from the Psychiatric Genomics Consortium (PGC) website (Psychiatric Genomics Consortium, 2015) where schizophrenia GWAS results have been clumped, retaining the best association (identified by *P*-value) in each LD block. Data from all the schizophrenia-associated genetic variants at a *P*-value < 0.05 (a total of 99,940 genetic variants) were included because this was the association threshold at which SNPs explained the most variance (Psychiatric Genomics Consortium, 2015). PRS for each sample are presented in **Appendix A - Supplementary Table 1**.

4.2.4. DNA methylation data

The DNA methylation data from the PFC (33 schizophrenia and 34 controls), STR (32 schizophrenia and 39 controls), HC (11 schizophrenia and 12 controls) and CER (33 schizophrenia and 35 controls) samples used in this chapter were pre-processed and normalised as described in **Chapter 3 section 3.2.3** and the probes included in all the analyses are the same (**Table 3.2**). Detailed demographic data of all samples are presented in **Appendix A - Supplementary Table 1**. **Table 4.2** presents summary demographic information on the samples included in this chapter and **Appendix A - Supplementary Table 2** presents reasons for exclusion for both DNA methylation and genotyping data and barcode array information. Neuronal proportion estimates for each sample were calculated using the *CETS* package in R (Guintivano et al., 2013) for each brain region, as described in **Chapter 3, section 3.2.5** and are presented in **Appendix A - Supplementary Table 1**.

Table 4.2. Overview of samples included in the schizophrenia polygenic risk score analysis. LNDDB, MRC London Neurodegenerative Diseases Brain Bank; DBCBB, Douglas-Bell Canada Brain Bank.

	N	Sex (male:female)	Age at death	Brain weight (g)	pH	Polygenic risk score
LNDDB	schizophrenia		65.68 ± 14.61	1222.46 ± 140.74	6.64 ± 0.29	-15.50 ± 0.29
	controls	9:7	62.70 ± 19.76	1389.50 ± 186.12	6.46 ± 0.34	-18.83 ± 0.34
	total	23:13	64.03 ± 17.49	1323.70 ± 186.72	6.54 ± 0.33	-17.31 ± 0.33
	<i>P</i>	-	0.61	0.01	0.10	0.01
LNDDB	schizophrenia		65.94 ± 14.19	1220.36 ± 135.45	6.61 ± 0.3	-15.34 ± 3.81
	controls	9:8	65.22 ± 19	1385.26 ± 190.23	6.44 ± 0.34	-18.75 ± 3.20
	total	16:7	65.53 ± 16.92	1315.30 ± 186.17	6.52 ± 0.33	-17.30 ± 3.83
	<i>P</i>	25:15	0.89	0.01	0.12	0.01
LNDDB	schizophrenia		65.91 ± 13.17	1255.11 ± 158.25	6.63 ± 0.29	-14.79 ± 2.79
	controls	8:3	62.58 ± 18.43	1422.10 ± 181.66	6.43 ± 0.39	-20.55 ± 2.28
	total	10:2	64.17 ± 15.86	1343 ± 187	6.53 ± 0.35	-17.79 ± 3.84
	<i>P</i>	18:5	0.62	0.05	0.21	3.08E-05
LNDDB	schizophrenia		65.94 ± 14.19	1220.36 ± 135.45	6.61 ± 0.3	-15.34 ± 3.81
	controls	9:8	63.11 ± 20.22	1386.21 ± 190.62	6.44 ± 0.33	-18.69 ± 3.14
	total	13:6	64.44 ± 17.44	1315.85 ± 186.61	6.52 ± 0.33	-17.07 ± 3.83
	<i>P</i>	22:14	0.63	0.01	0.11	0.01
LNDDB	schizophrenia		46.24 ± 16.81	1404.62 ± 161.9	6.25 ± 0.21	-16.64 ± 2.87
	controls	14:3	46.75 ± 16.72	1430.09 ± 183.76	6.06 ± 0.29	-18.41 ± 3.11
	total	12:2	46.48 ± 16.51	1418.20 ± 171.41	6.16 ± 0.27	-17.52 ± 3.08
	<i>P</i>	26:5	0.93	0.69	0.05	0.11
LNDDB	schizophrenia		47.13 ± 17.32	1377.48 ± 157.92	6.23 ± 0.21	-16.90 ± 2.78
	controls	12:3	46.75 ± 16.72	1430.09 ± 183.76	6.06 ± 0.29	-18.41 ± 3.11
	total	13:3	46.94 ± 16.73	1407.54 ± 172.11	6.14 ± 0.27	-17.68 ± 3.01
	<i>P</i>	25:6	0.95	0.42	0.08	0.16
LNDDB	schizophrenia		44.56 ± 15.84	1404.62 ± 161.9	6.25 ± 0.22	-16.84 ± 2.86
	controls	14:2	46.75 ± 16.72	1430.09 ± 183.76	6.06 ± 0.29	-18.41 ± 3.11
	total	13:3	45.66 ± 16.06	1418.20 ± 171.41	6.16 ± 0.27	-17.65 ± 3.05
	<i>P</i>	27:5	0.71	0.69	0.04	0.15
DBCBB	schizophrenia		46.24 ± 16.81	1404.62 ± 161.9	6.25 ± 0.21	-16.64 ± 2.87
	controls	14:3	46.75 ± 16.72	1430.09 ± 183.76	6.06 ± 0.29	-18.41 ± 3.11
	total	12:2	46.48 ± 16.51	1418.20 ± 171.41	6.16 ± 0.27	-17.52 ± 3.08
	<i>P</i>	26:5	0.93	0.69	0.05	0.11
DBCBB	schizophrenia		47.13 ± 17.32	1377.48 ± 157.92	6.23 ± 0.21	-16.90 ± 2.78
	controls	12:3	46.75 ± 16.72	1430.09 ± 183.76	6.06 ± 0.29	-18.41 ± 3.11
	total	13:3	46.94 ± 16.73	1407.54 ± 172.11	6.14 ± 0.27	-17.68 ± 3.01
	<i>P</i>	25:6	0.95	0.42	0.08	0.16
DBCBB	schizophrenia		44.56 ± 15.84	1404.62 ± 161.9	6.25 ± 0.22	-16.84 ± 2.86
	controls	14:2	46.75 ± 16.72	1430.09 ± 183.76	6.06 ± 0.29	-18.41 ± 3.11
	total	13:3	45.66 ± 16.06	1418.20 ± 171.41	6.16 ± 0.27	-17.65 ± 3.05
	<i>P</i>	27:5	0.71	0.69	0.04	0.15

4.2.5. Identification of differentially methylated positions and regions

To identify PRS-associated DNA methylation differences at the single probe level in each brain region I performed a linear regression of the pre-processed and normalised DNA methylation (β) values in each cohort using the imputed PRS, age, sex and neuronal proportion estimates as independent variables. Neuronal proportion estimates were not included as independent variables in the CER analysis for reasons described in **Chapter 3 section 3.2.5**. Given the nature of the samples used in this study, information about medication, smoking status and other phenotypic information was not available and could not be included as covariates in analyses. The adjusted DNA methylation values for each probe and sample were calculated as described in **Chapter 3 section 3.2.6**.

The resulting P -values of the linear regression in the HC LNDBB data were used to identify differentially methylated positions (DMPs) in this brain region. For tissues collected from both brain banks (*i.e.* PFC, STR and CER), a fixed-effect meta-analysis based on the linear regression estimates and their standard errors was computed with inverse variance weights using the *metagen* function from the *meta* package in R (Schwarzer, 2015). Only probes that passed the stringent QC metrics and were common to both cohorts in each brain region were used in the meta-analysis (**Table 3.2** in **Chapter 3**).

To identify differentially methylated regions (DMRs), I identified spatially correlated P -values in the data using the Python module *comb-p* (Pedersen et al., 2012) to group spatially correlated DMPs (seed P -value $< 1.00E-3$, minimum of two probes) at a maximum distance of 300bp in each brain region. DMR P -values were corrected for multiple testing using Šidák correction (Šidák, 1967), which corrects the combined P for n_a/n_r tests, where n_a is the total number of probes tested in the initial EWAS and n_r the number of probes in the given region.

4.2.6. Additional probe annotation and enrichment analysis for regulatory regions

I annotated the probes on the Illumina 450K array using the GREAT annotation tool (McLean et al., 2010). Probes were also annotated to transcription factor binding sites (TFBSs) and DNase1 hypersensitivity sites (DHSs) (Sliker et al., 2013, ENCODE Project Consortium, 2012, Maurano et al., 2012). Details on these annotations are provided in **Chapter 3 section 3.2.7**. The overlap between these regulatory features and different thresholds of DMPs (50 top ranked, DMPs $P < 1.00E-03$ and DMPs $P < 0.05$) were tested for enrichment using a two sided Fisher's 2x2 exact test (Fisher, 1922).

The overlap between the 450K probes within genomic regions identified in the latest GWAS (Schizophrenia Working Group of the Psychiatric Genomics, 2014) (see **Chapter 3 section 3.2.7**) and the same thresholds of DMPs for each brain region was also tested for enrichment using a two sided Fisher's 2x2 exact test (Fisher, 1922).

4.2.7. Establishing multiple testing significance threshold for EWAS analysis

To establish a stringent multiple-testing significance threshold to identify schizophrenia-associated DMPs, the data from another large schizophrenia Illumina 450K dataset ($n = 675$ individuals) from an ongoing study in our lab (Hannon E et al., under review) were randomly split into cases and controls 5,000 times, and for each permutation an EWAS was performed using a linear regression model controlling for age, sex, smoking and cell composition and the probe-level P -values were recorded. The minimum (or most significant) P -value was identified for each permutation and the 5th quantile across the permutations was used to estimate the nominal P -value for 5% family-wise error ($P = 1.66E-07$).

4.2.8. Cross-tissue mixed model

To identify homogeneous DNA methylation effects across PFC, STR and HC data a null model of no heterogeneity was fitted using disease, sex, age and cohort as fixed effects. I excluded the CER from the multi-region model for reasons described on **Chapter 3 section 3.2.9**. As the brain regions were

dissected from the same set of individuals, each individual's DNA methylation values are potentially non-independent across brain regions. In addition, DNA methylation values within a brain region are also expected to be correlated across individuals, therefore both of these covariates were included as random effects. The *comb-p* algorithm (Pedersen et al., 2012) was then used to identify significant DMRs across the three brain regions, using the *P*-values of the cross-region model as described in **section 4.2.5**.

4.2.9. Methylation quantitative trait *loci*

To test whether the PRS associations identified reflect a direct *cis*-genetic effect on DNA methylation, we next characterized brain mQTLs associated with the 99,904 variants included in the PRS calculation, using a genome-wide mQTL significance threshold of $P = 3.69E-13$, as described in a recent paper from our group (Hannon et al., 2016). In summary, an additive linear model was fitted to test if the number of alleles (coded 0, 1 and 2) predicted DNA methylation at each site, including covariates for age, sex, brain bank and the first two principal components from the genotype data to control for ethnicity differences. Given the low number of samples from the HC, mQTL analyses were not performed for this brain region.

4.3. Results

4.3.1. Overview of experimental strategy

In **Chapter 3**, I identify schizophrenia-associated DNA methylation differences in the PFC, STR, HC and CER samples from the LNDBB and DBCBB cohorts using the Illumina Infinium HumanMethylation450 BeadChip (Illumina Inc., San Diego, CA, USA) (see **Chapter 3**). In the present chapter I aimed to identify DNA methylation differences associated with schizophrenia polygenic risk burden and compare these to schizophrenia-associated differences and direct *cis*-genetic effects on DNA methylation.

I genotyped the schizophrenia patients and non-psychiatric controls using the Illumina Infinium HTS HumanOmniExpress-24 BeadChip v1-0 (Illumina Inc., San Diego, CA, USA). One sample was excluded based on stringent QC of the genotyping data. To avoid population stratification effects, ethnicity was

determined using data from HapMap Phase 3 (see **section 4.2.2**) and non-Caucasian ancestry outliers ($n = 10$) were excluded from subsequent analyses. In total, the genotyping and DNA methylation data from 67 PFC (33 schizophrenia and 34 controls), 71 STR (32 schizophrenia and 39 controls), 23 HC (11 schizophrenia and 12 controls) and 68 CER (33 schizophrenia and 35 controls) samples from both the LNDBB and DBCBB passed stringent QC metrics and were used for analysis (demographic summaries for these samples are presented in **Table 4.2**). SNP data were imputed using the latest data release from the 1,000 Genomes project, and a PRS for each sample was generated using data from the recent schizophrenia GWAS (Schizophrenia Working Group of the Psychiatric Genomics, 2014).

A linear regression was performed in each brain region from each cohort separately and for tissues collected from both brain banks (PFC, STR and CER) a fixed-effect meta-analysis approach was used to combine analyses results from both cohorts. The initial analyses focused on identifying DMPs and DMRs associated with schizophrenia PRS. Analyses were first performed independently for each brain region, and I subsequently employed a multi-level model to identify consistent DNA methylation associations with PRS present across the PFC, STR, and HC. An overview of the analysis approach in this chapter is given in **Figure 3.3** and a representation on how this analysis integrates with the remaining chapters is given in **Chapter 1 Figure 1.8**.

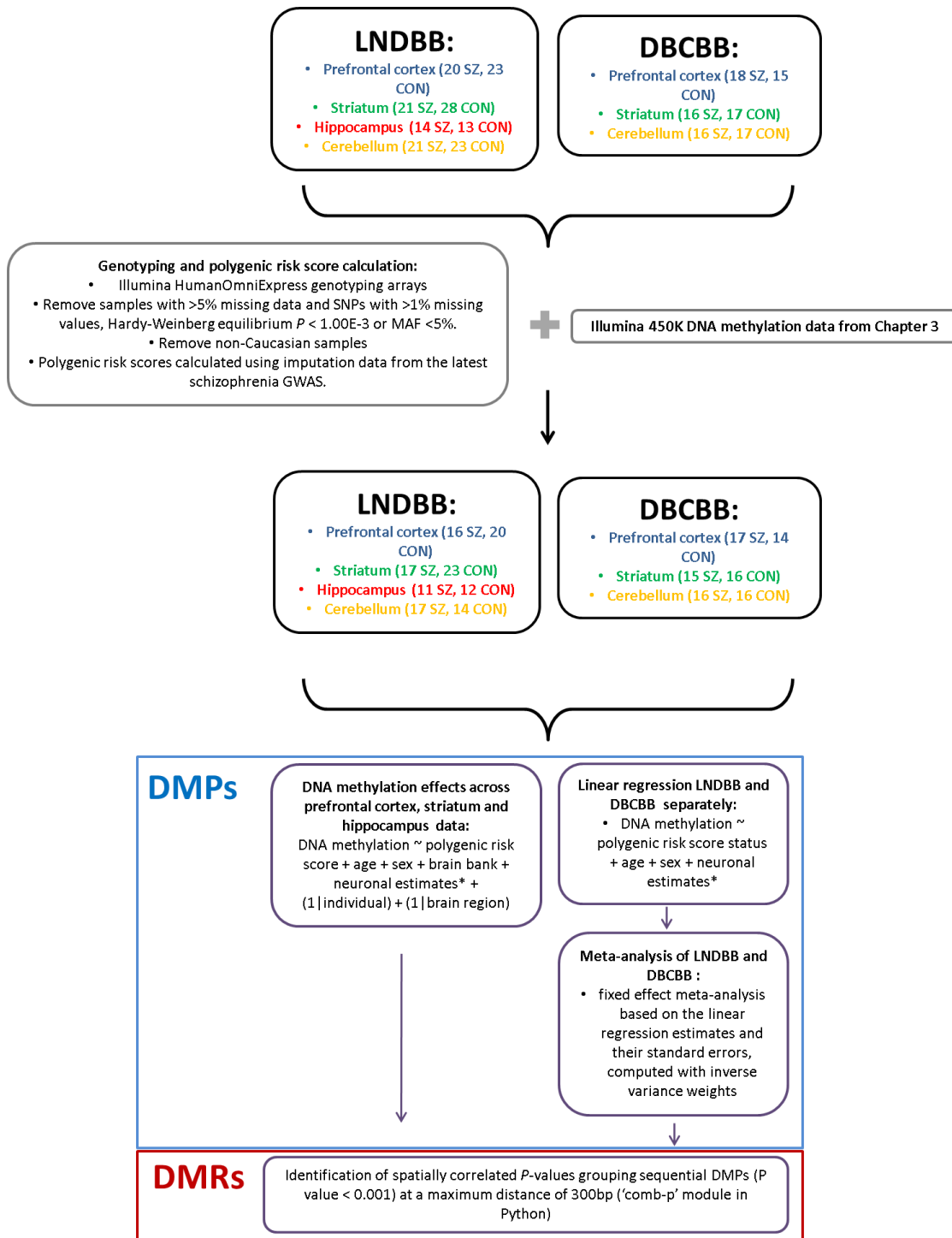


Figure 4.3. Overview of Chapter 4 experimental strategy.

4.3.2. Differently methylated positions associated with schizophrenia polygenic risk score

In this chapter, I wanted to explore whether an increased burden of polygenic variants associated with schizophrenia was itself associated with variation in DNA methylation in the brain. Despite the relatively small sample size, it was striking that schizophrenia patients ($n = 34$) were characterized by a significantly higher PRS than controls ($n = 40$) ($P = 4.43E-03$) (**Figure 4.4**), highlighting the robust nature of the schizophrenia PRS and the power of this approach for classifying genetic risk.

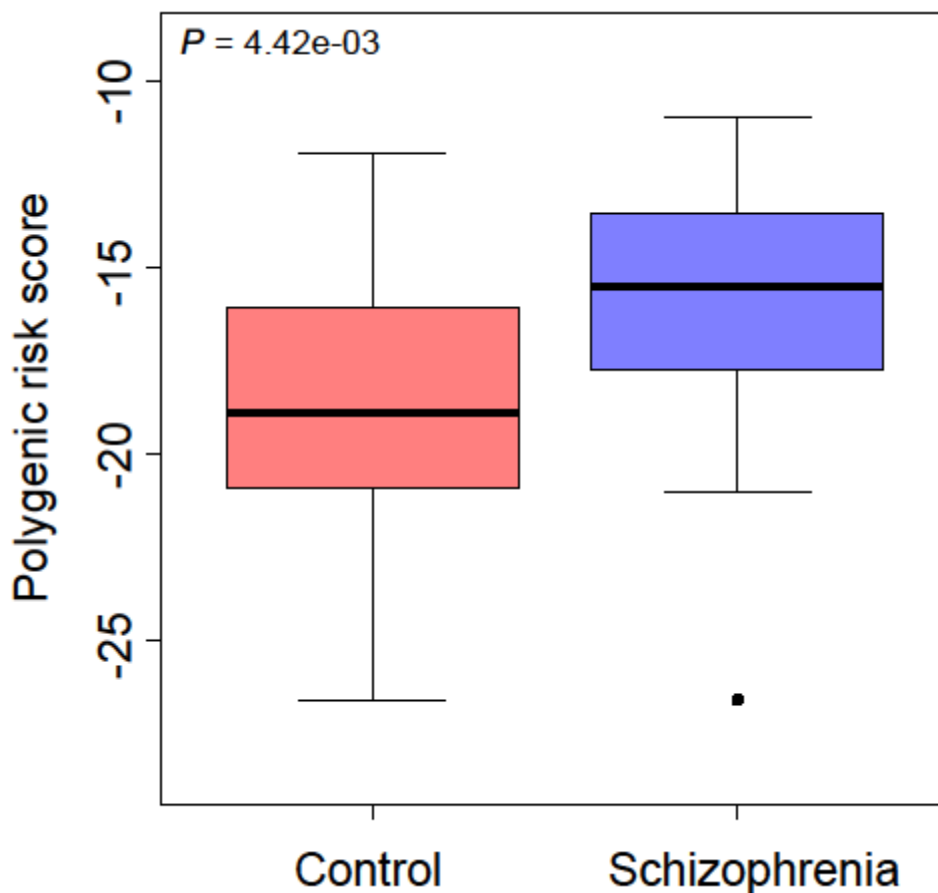


Figure 4.4. Polygenic risk score in both schizophrenia cases and non-psychiatric controls included in the analyses of this chapter.

I employed a linear model controlling for age, sex, and neuronal estimates (except in the CER, as described in **section 4.2.5**), followed by a fixed-effect meta-analysis to identify DNA methylation variation associated with the schizophrenia PRS. Quantile-quantile (QQ) plots for the analyses in each tissue are shown in **Figures 4.5 to 4.8**, highlighting little evidence of systematic P -

value inflation (PFC $\lambda = 0.96$, STR $\lambda = 1.10$, HC $\lambda = 1.17$, CER $\lambda = 1.26$) in any of the four brain regions. Manhattan plots for the analyses in each brain region are shown in **Figures 4.9 to 4.12**.

The PRS-associated DMPs passing the stringent family-wise significance threshold ($P < 1.66E-07$, see **section 4.2.7**), are listed in **Table 4.3** and presented in **Figures 4.13 to 4.15**. The fifty top ranked PRS-associated DMPs in each brain region presented in **Tables 4.4 to 4.7** and **Figures 4.16 to 4.19**. Although the specific top ranked PRS-associated *loci* in each brain region are distinct, effect sizes at PRS-associated DMPs are significantly correlated across brain regions (**Figures 4.20 to 4.23** and **Table 4.8**), with the exception of the HC where the low number of samples ($n = 23$) means my analysis is probably underpowered to detect robust effects.

Several PRS-associated DMPs are of relevance in the context of schizophrenia and associated neurobiological functions. These include:

- cg12595281, which is characterised by a significant increase of DNA methylation with increased PRS in the STR ($P = 6.85E-08$) (**Table 4.5** and **Figure 4.14**) and is annotated to the transcription start site of the *repulsive guidance molecule family member a (RGMA)* gene. This gene encodes an axon guidance protein thought to be important in interneuron migration and differentiation during neurogenesis (O'Leary et al., 2013, Matsunaga et al., 2004).

- cg19852211, which is characterised by increased DNA methylation with increased PRS in the PFC ($P = 3.25E-05$) (**Table 4.4**) and is annotated to the cluster of *protocadherin alpha* genes 1 to 4 (*PCDHA1*, *PCDHA2*, *PCDHA3* and *PCDHA4*). These genes are organised in a cluster and encode integral plasma membrane, cell adhesion proteins localised at synaptic junctions in neurons (Hamada and Yagi, 2001, Kohmura et al., 1998).

- cg04293307, which is characterised by increased DNA methylation with increased PRS in the PFC ($P = 6.07E-06$) (**Table 4.4**) and is annotated to the gene body of *AXIN2*, a gene that encodes a protein known component of the Wnt signalling pathway (Kikuchi, 1999). This pathway plays a crucial role in controlling self-renewal and differentiation during neurodevelopment (Kalani et al., 2008, Nusse, 2008).

- cg15022015, which is characterised by increased DNA methylation with increased PRS in the STR ($P = 3.82E-06$) (**Table 4.5**) and is annotated to the gene body of the *regulatory associated protein of MTOR, complex 1 (RPTOR)* gene. Ablation of the protein encoded by this gene in oligodendrocytes has revealed a potential role of this protein in the central nervous system myelination during mouse development (Bercury et al., 2014).

- cg07984684, which is characterised by increased DNA methylation with increased PRS in the CER ($P = 3.12E-07$) (**Table 4.7**) and is annotated to the transcription start site of the *charged multivesicular body protein 1A (CHMP1A)* gene. Mochida *et al.* linked loss-of function mutations in this gene reduced cerebellar and cerebral cortical size (Mochida et al., 2012). In the same study, knockout of the *CHMP1A* orthologue in zebrafish (*chmp1a*) resulted in reduced cerebellum and forebrain volume in these animals.

Other DMPs associated with PRS are annotated to genes that have been implicated in other neurological and neurodevelopmental disorders related to schizophrenia including autism-spectrum disorder (ASD), attention-deficit/hyperactivity disorder (ADHD) and language deficits:

- cg01682070 shows increased DNA methylation with increased PRS in the CER ($P = 4.20E-08$) (**Table 4.7** and **Figure 4.15**). This probe is within the gene body of the *thousand-and-one-amino acid 2 kinase (TAOK2)* gene, which encodes a protein that is thought to play an essential role in dendrite morphogenesis (de Anda et al., 2012). Microdeletions and duplications in chromosome 16 affecting this gene have been implicated in ASD (Weiss et al., 2008), another neurodevelopmental disease.

- cg0486234 shows increase DNA methylation associated with increased PRS in the PFC ($P = 8.04E-06$) (**Table 4.4**). The probe is annotated to the *RNA binding protein, fox-1 homolog (C. elegans) 1 gene (RBFox1)*. This gene encodes a protein thought to regulate a network of genes involved in synaptic function and calcium signalling (Lee et al., 2016). Chromosomal translocations and copy number variations in this gene have been associated with ASD (Martin et al., 2007, Sebat et al., 2007).

- cg19376461 shows increased DNA methylation associated with increased PRS in the STR ($P = 2.11E-06$) (**Table 4.5**). This probe is annotated

to the gene body of the *inner mitochondrial membrane peptidase subunit 2* (*IMMP2L*) gene. This gene encodes a protein involved in processing the signal peptide sequences used to direct mitochondrial proteins to the mitochondria. Deletions in this gene have been implicated in several neuropsychiatric disorders ADHD (Elia et al., 2010), ASD (Maestrini et al., 2010) and Tourette syndrome (Patel et al., 2011).

- cg01331540 shows increased DNA methylation associated with increased PRS in the STR ($P = 5.39E-06$) (**Table 4.5**). The probe is annotated to the gene body of the *forkhead box P* (*FOXP1*) gene. Deletions, mutations and chromosomal aberrations affecting this gene have been associated with several neurodevelopmental conditions, such as ASD, speech and language deficits and motor development delay (Talkowski et al., 2012, Hamdan et al., 2010, O'Roak et al., 2011). This gene also seems to be important in striatal development in mice (Bacon et al., 2015).

Epidemiological studies have long suggested a role of the immune system dysregulation in schizophrenia (Benros et al., 2011, Nielsen et al., 2013) and infection (Sorensen et al., 2009), a hypothesis that was supported by schizophrenia transcriptomic (Mistry et al., 2013, Roussos et al., 2012) and GWAS analyses (International Schizophrenia et al., 2009, Schizophrenia Working Group of the Psychiatric Genomics, 2014). Interestingly, two of the PRS-associated DMPs in the PFC are annotated to genes that play an important role in the immune system. First, cg14595786 ($P = 2.45E-07$) (**Table 4.4**) is annotated to the transcription start site of the *sialic acid binding Ig like lectin 9* (*SIGLEC9*) gene. The siglecs are a family of lectins thought to promote cell–cell interactions and regulate cell function in the innate and adaptive immune systems (Crocker et al., 2007). The SIGLEC9 membrane protein is expressed in monocytes, neutrophils and natural killer cells (Zhang et al., 2000, Angata and Varki, 2000). Second, cg01948217 ($P = 7.02E-07$) (**Table 4.4**) is annotated to the transcription start site of the *bactericidal/permeability-increasing protein* (*BPI*) gene, which encodes a neutrophil-expressed protein that plays a role in inflammatory response to Gram-negative bacteria (Marra et al., 1992).

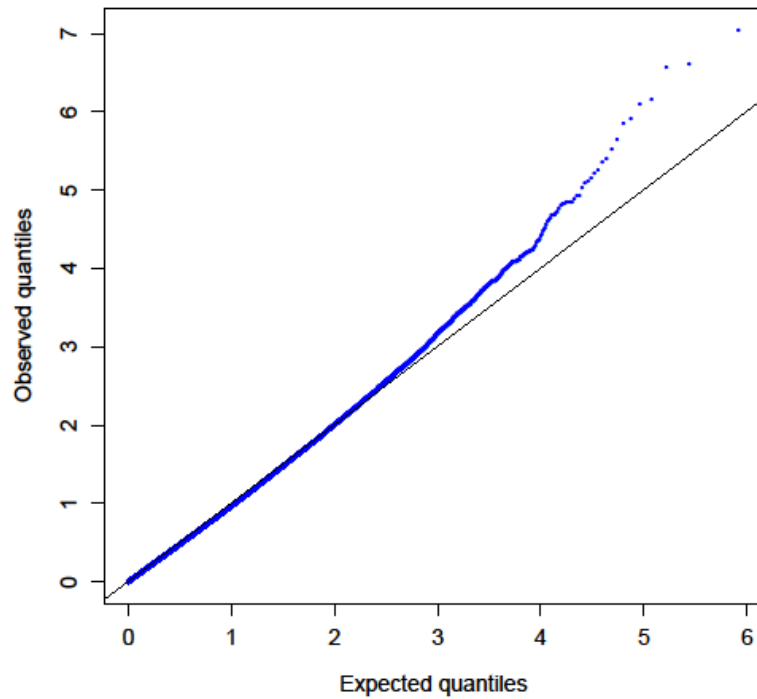


Figure 4.5. Quantile-quantile plot for the prefrontal cortex (PFC) schizophrenia polygenic risk score EWAS. Shown are the expected (x-axis) and observed (y-axis) quantiles observed in the meta-analysis of the (PFC) of both cohorts. $\lambda = 0.96$.

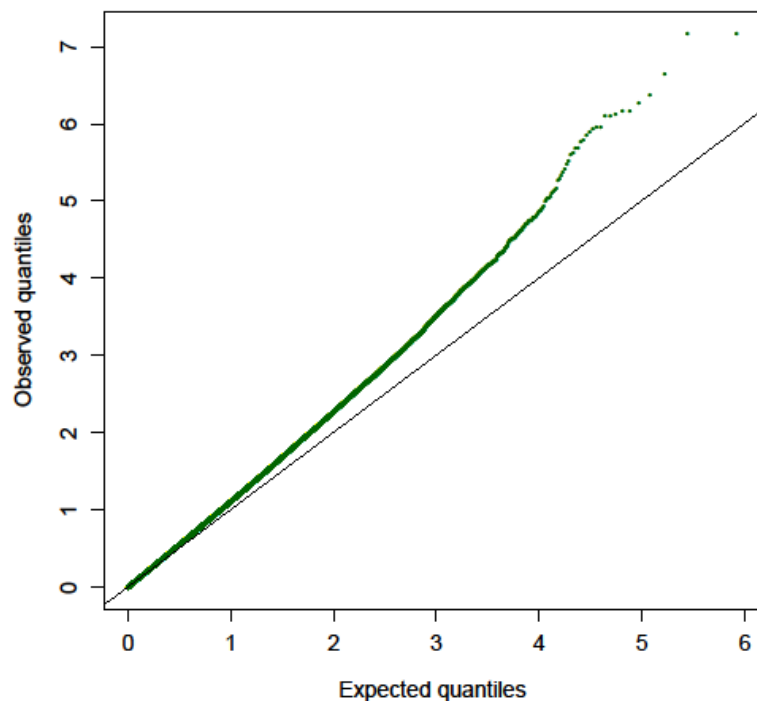


Figure 4.6. Quantile-quantile plot for the striatum (STR) schizophrenia polygenic risk score EWAS. Shown are the expected (x-axis) and observed (y-axis) quantiles observed in the meta-analysis of the STR of both cohorts. $\lambda = 1.10$.

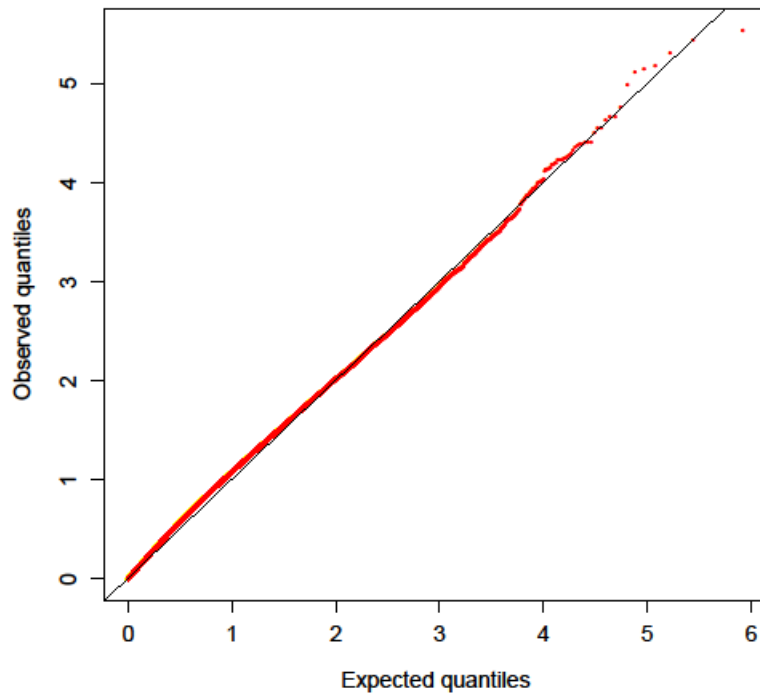


Figure 4.7. Quantile-quantile plot for the hippocampus (HC) schizophrenia polygenic risk score EWAS. Shown are the expected (x-axis) and observed (y-axis) quantiles observed in the meta-analysis of the HC of the MRC London Neurodegenerative Diseases Brain Bank samples. $\lambda = 1.17$.

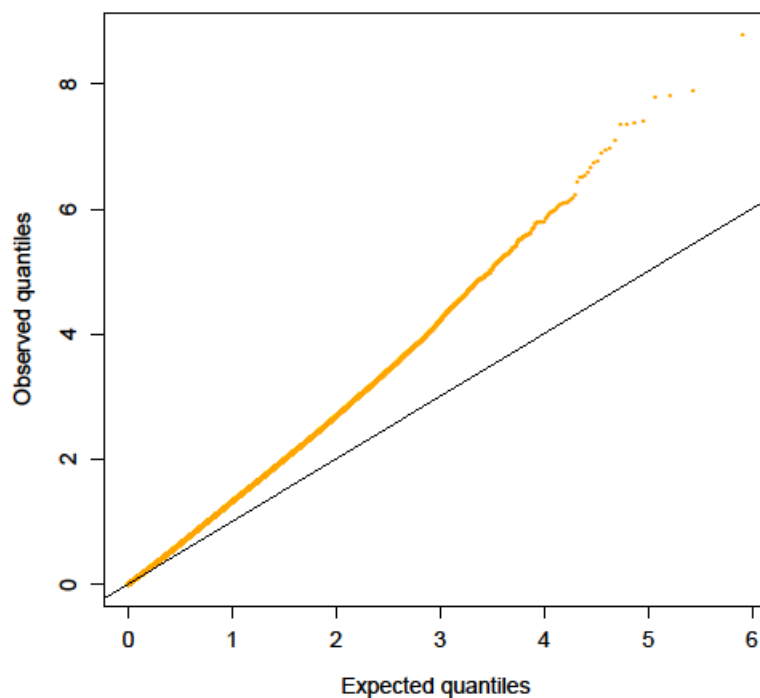


Figure 4.8. Quantile-quantile plot for the cerebellum (CER) schizophrenia polygenic risk score EWAS. Shown are the expected (x-axis) and observed (y-axis) quantiles observed in the meta-analysis of the CER of both cohorts. $\lambda = 1.26$.

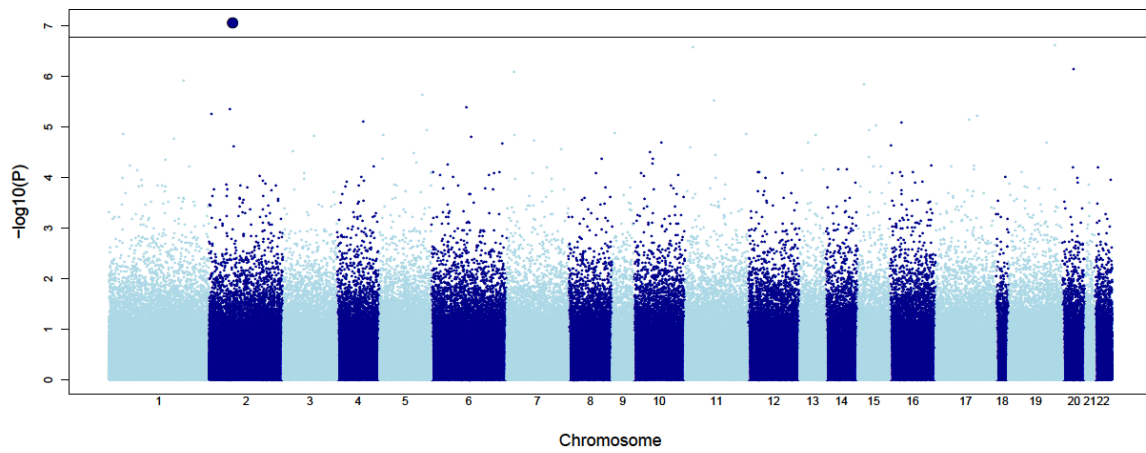


Figure 4.9. Manhattan plot for the prefrontal cortex schizophrenia polygenic risk score EWAS. Shown are the $-\log_{10}(P\text{-values})$ (y-axis) of the meta-analysis of the prefrontal cortex of both cohorts by chromosomal position (x-axis). The horizontal line indicates a stringent multiple-testing significance threshold ($P = 1.66\text{E-}07$) (see **section 4.2.7**).

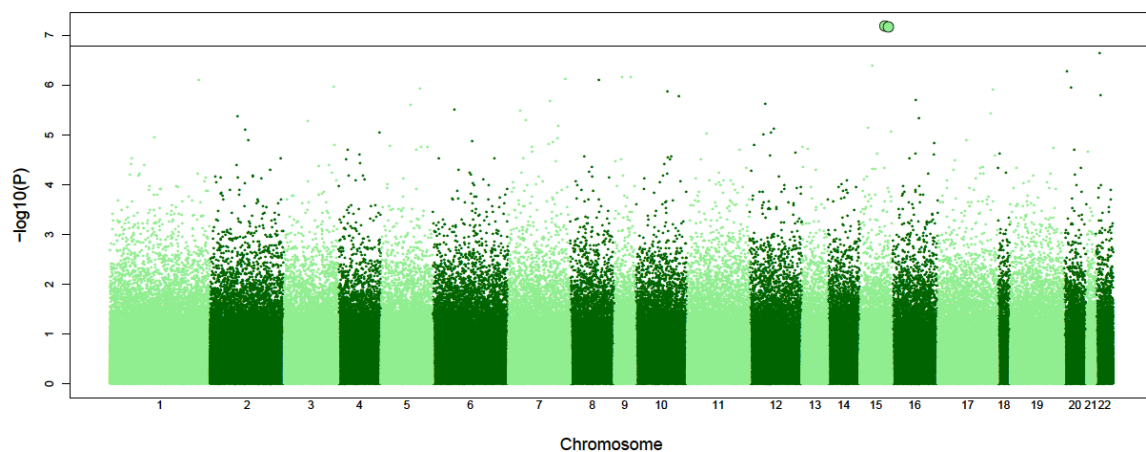


Figure 4.10. Manhattan plot for the striatum schizophrenia polygenic risk score EWAS. Shown are the $-\log_{10}(P\text{-values})$ (y-axis) of the meta-analysis of the striatum of both cohorts by chromosomal position (x-axis). The horizontal line indicates a stringent multiple-testing significance threshold ($P = 1.66\text{E-}07$) (see **section 4.2.7**).

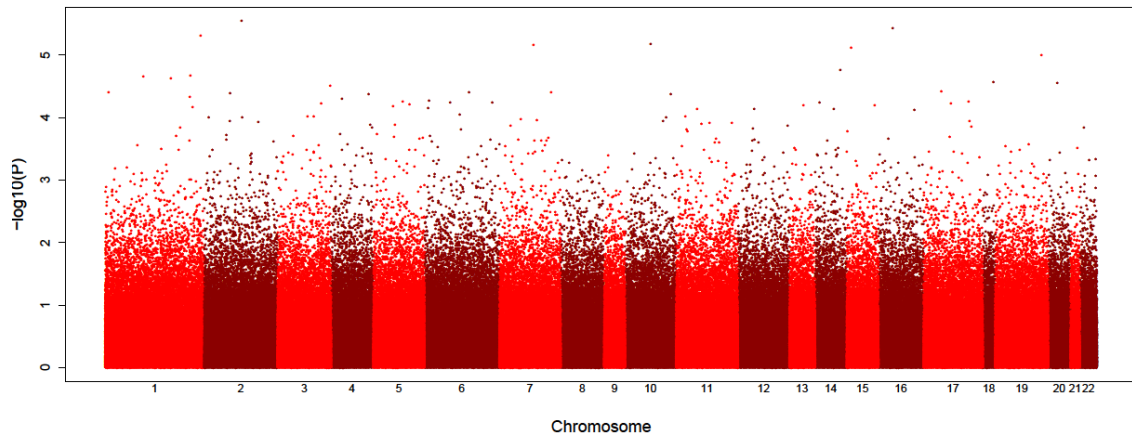


Figure 4.11. Manhattan plot for the hippocampus schizophrenia polygenic risk score EWAS. Shown are the $-\log_{10}(P\text{-values})$ (y-axis) of the linear regression analysis of the hippocampus data from the MRC London Neurodegenerative Diseases Brain Bank by chromosomal position (x-axis). The horizontal line indicates a stringent multiple-testing significance threshold ($P = 1.66\text{E-}07$) (see **section 4.2.7**).

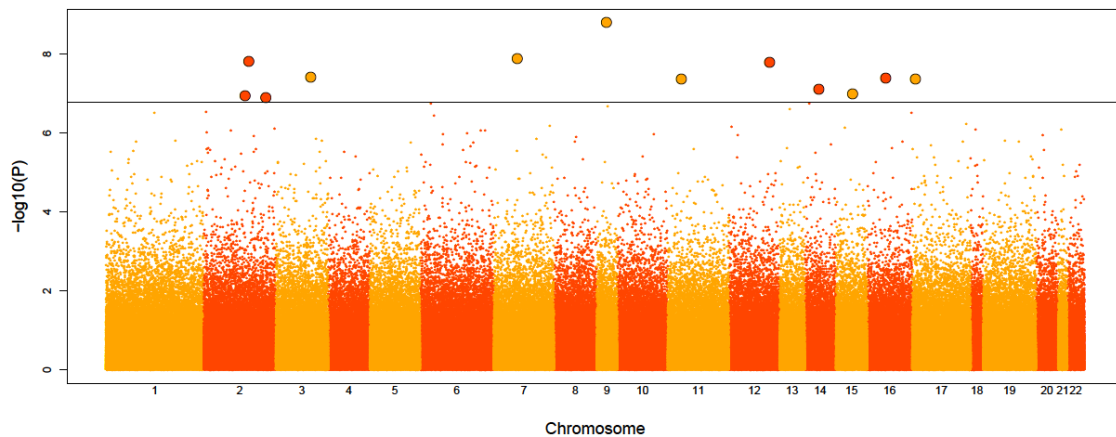


Figure 4.12. Manhattan plot for the cerebellum schizophrenia polygenic risk score EWAS. Shown are the $-\log_{10}(P\text{-values})$ (y-axis) of the meta-analysis of the cerebellum of both cohorts by chromosomal position (x-axis). The horizontal line indicates a stringent multiple-testing significance threshold ($P = 1.66\text{E-}07$) (see **section 4.2.7**).

Table 4.3. Top ranked schizophrenia polygenic risk score (PRS)-associated differentially methylated positions (DMPs). Shown are DMPs associated with schizophrenia at a highly stringent significance threshold ($P < 1.66E-07$) (see section 4.2.7). Top ranked PRS-associated DMPs for each of the four brain regions profiled are presented in Tables 4.4 to 4.7. Illumina and Genomic Regions Enrichment of Annotation Tool (GREAT) (McLean et al., 2010) annotations are listed for each DMP.

Probe ID	Genomic position (hg19)	Illumina gene annotation	GREAT				DNA methylation difference (%)	P
			McLean et al., 2010	Gene region	Brain region			
cg20640266	chr9:116811789	ZNF618	AMBP; ZNF618	Body	Cerebellum	0.598	1.62E-09	
cg27150552	chr7:48026856	SUNC1	HUS1; SUN3	3'UTR	Cerebellum	0.340	1.30E-08	
cg05209768	chr2:164573665	FIGN	KCNH7; FIGN	Body	Cerebellum	0.697	1.55E-08	
cg07793808	chr12:122019006	KDM2B	KDM2B	TSS200; TSS1500	Cerebellum	-0.186	1.66E-08	
cg10218777	chr3:133180261	BFSP2	CDV3; BFSP2	Body	Cerebellum	0.670	3.86E-08	
cg01682070	chr16:29996774	TAOK2	HIRIP3; TAOK2	Body	Cerebellum	0.317	4.20E-08	
cg11786558	chr17:2266589	SGSM2	SGSM2; MNT	Body	Cerebellum	0.692	4.35E-08	
cg26053083	chr11:14995770	-	CALCA	-	Cerebellum	-0.149	4.41E-08	
cg26893445	chr15:85924187	AKAP13	AKAP13	5'UTR	Striatum	0.146	6.73E-08	
cg12595281	chr15:93633172	RGMA	RGMA	TSS1500	Striatum	0.683	6.85E-08	
cg01022840	chr14:71250264	MAP3K9	MAP3K9; TTC9	Body	Cerebellum	0.633	7.86E-08	
cg18847009	chr2:70175826	-	ASPRV1; MXD1	-	Prefrontal cortex	-0.511	8.98E-08	
cg08478539	chr15:68640339	ITGA11	FEM1B; ITGA11	Body	Cerebellum	0.693	1.06E-07	
cg23788334	chr2:137181176	-	THSD7B; CXCR4	-	Cerebellum	-0.131	1.15E-07	
cg16904520	chr2:230590962	-	DNER; TRIP12	-	Cerebellum	0.255	1.25E-07	

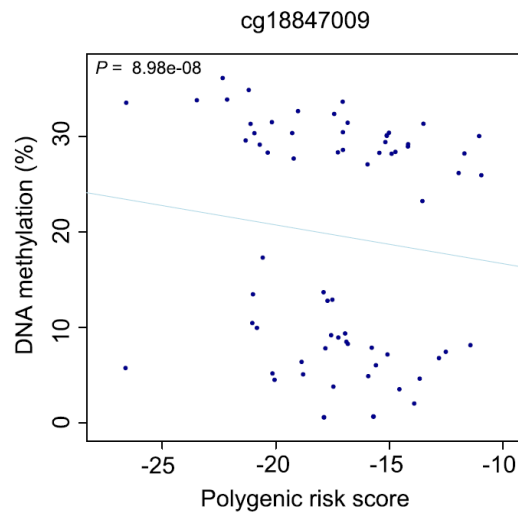


Figure 4.13. Top ranked schizophrenia polygenic risk score (PRS)-associated differentially methylated position (DMP) in the prefrontal cortex. Shown are adjusted DNA methylation values (y-axis) for the DMP associated with PRS (x-axis) in the prefrontal cortex at a highly stringent significance threshold ($P < 1.66E-07$) (see **section 4.2.7**). Additional information on these DMPs is given in **Table 4.3**.

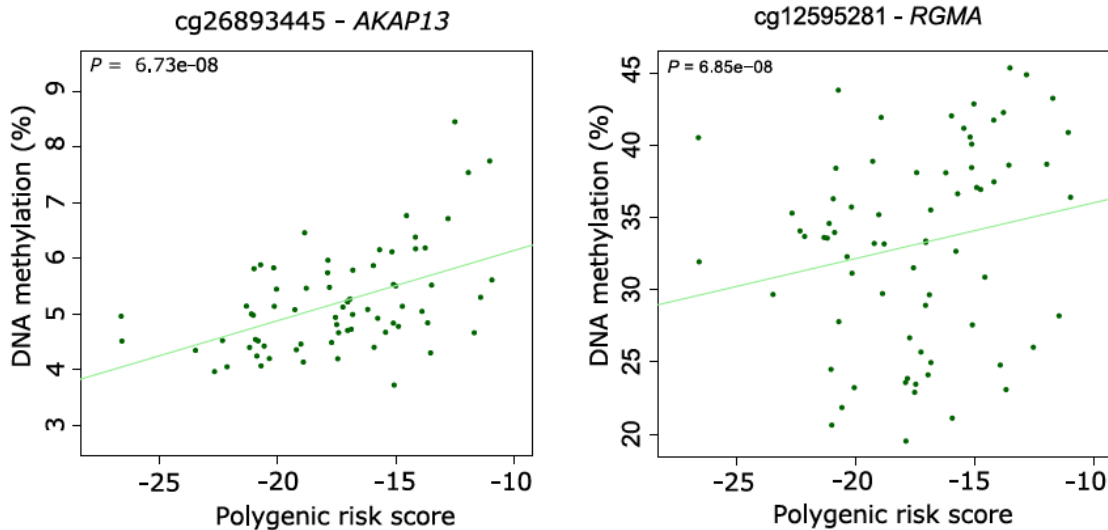


Figure 4.14. Top ranked schizophrenia polygenic risk score (PRS)-associated differentially methylated positions (DMPs) in the striatum. Shown are adjusted DNA methylation values (y-axis) for the DMPs associated with PRS (x-axis) in the striatum at a highly stringent significance threshold ($P < 1.66E-07$) (see **section 4.2.7**). Additional information on these DMPs is given in **Table 4.3**.

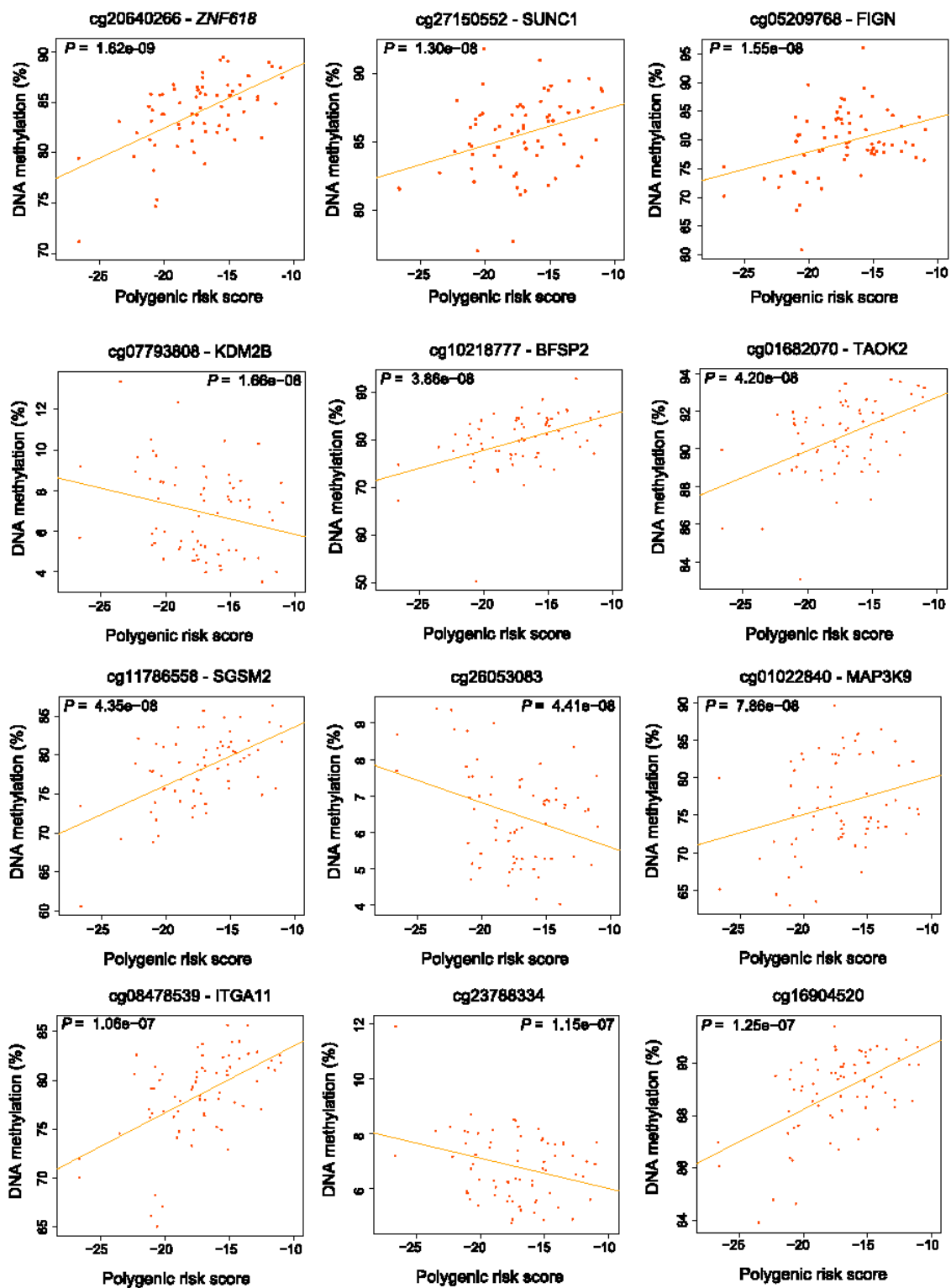


Figure 4.15. Top ranked schizophrenia polygenic risk score (PRS)-associated differentially methylated positions (DMPs) in the cerebellum. Shown are adjusted DNA methylation values (y-axis) for the DMPs associated with PRS (x-axis) in the cerebellum at a highly stringent significance threshold ($P < 1.66E-07$) (see **section 4.2.7**). Additional information on these DMPs is given in **Table 4.3**.

Table 4.4. Top ranked polygenic risk score-associated DMPs identified in the prefrontal cortex (PFC) meta-analysis. Listed for each PFC DMP (grey) are corresponding results from the striatum (STR; $P < 0.05$ in green), hippocampus (HC; $P < 0.05$ in red) and cerebellum (CER; $P < 0.05$ in orange) meta-analyses (PFC, STR and CER) or linear regression (HC). Also shown is the association with schizophrenia diagnosis in PFC ($P < 0.05$ in blue). The methylation difference is measured per PRS unit. Illumina and Genomic Regions Enrichment of Annotation Tool (GREAT) annotation (McLean et al., 2010) is listed for each DMP.

Probe ID	Genomic position (hg19)	Illumina gene annotation	Gene region	GREAT annotation (McLean et al., 2010)	Methylation difference PFC (%)	P PFC	Methylation difference STR (%)	P STR	Methylation difference HC (%)	P HC	Methylation difference CER (%)	P CER	Disease PFC methylation difference (%)	Disease PFC P
cg18847009	chr2:70175826	-	-	ASPRV1; MXD1	-0.51	8.98E-08	-0.32	0.02	-0.79	1.07E-03	-0.20	0.22	-1.12	0.11
cg14595786	chr19:51626986	SIGLEC9	TSS1500	SIGLEC9	0.54	2.45E-07	0.12	0.44	0.63	0.04	0.17	0.20	2.72	1.98E-03
cg05090695	chr11:2907670	CDKN1C	TSS1500	CDKN1C	-0.53	2.65E-07	0.16	0.21	-0.30	0.06	-0.05	0.12	-0.56	0.43
cg01948217	chr20:36932385	BPI	TSS200	BPI	0.66	7.02E-07	0.24	0.20	0.00	0.99	-0.14	0.34	-0.03	0.97
cg01986619	chr7:2613963	IQCE	Body	TTYH3; IQCE	0.48	8.15E-07	-0.11	0.41	0.37	0.04	-0.13	0.30	1.04	0.13
cg20678082	chr11:168356591	-	-	TBX19; XCL2	-0.66	1.23E-06	-0.08	0.65	-0.32	0.27	-0.21	0.34	-0.91	0.34
cg17460228	chr15:41052250	-	-	FAM82A2; GCHFR	0.38	1.42E-06	0.28	0.11	0.60	0.02	-0.05	0.68	0.93	0.11
cg04221388	chr5:167689716	ODZ2	Body	WWC1; ODZ2	0.23	2.28E-06	0.02	0.70	-0.13	0.33	-0.05	0.58	0.58	0.16
		SNORD27; SLC3A2;												
cg26283550	chr11:62623419	SNORD28; SNORD25; SNORD26; SNHG1	TSS1500; TSS200	SLC3A2	-0.08	2.96E-06	0.00	0.97	0.03	0.48	-0.02	0.50	-0.07	0.59
		ZBTB22; TAPBP	Body;											
cg03000593	chr6:33283162	TAPBP	TSS1500	TAPBP	-0.58	4.06E-06	0.02	0.84	0.19	0.37	-0.04	0.80	-0.28	0.72
cg17926234	chr2:61404587	AHSA2	1stExon; 5'UTR	AHSA2	0.10	4.41E-06	-0.02	0.83	0.00	0.96	0.00	0.96	0.10	0.57
cg23822732	chr2:2692854	-	-	TRAPPC12; MYT1L	0.23	5.53E-06	-0.09	0.12	0.16	0.14	-0.04	0.56	0.82	0.03
cg04293307	chr17:63553581	AXIN2	Body	AXIN2; RGS9	0.54	6.07E-06	0.02	0.91	0.44	0.15	0.41	0.03	0.49	0.63
cg25489169	chr17:46689639	HOXB7	TSS1500	HOXB7	-0.17	7.07E-06	0.11	0.10	-0.04	0.73	-0.06	0.26	-0.48	0.06
cg12463346	chr4:102268854	PPP3CA	TSS1500	PPP3CA	0.08	7.72E-06	0.02	0.43	0.09	0.21	0.03	0.22	0.11	0.31
cg04862340	chr16:6534204	A2BP1	5'UTR	RBFOX1	0.86	8.04E-06	-	-	-	-	-	-	1.23	0.32
cg27454589	chr15:71509548	THSD4	Body	NR2E3; THSD4	0.28	9.12E-06	0.06	0.63	0.06	0.80	-0.03	0.77	0.58	0.26
cg02489245	chr15:53495286	-	-	UNC13C; ONECUT1	0.29	1.15E-05	0.08	0.35	0.11	0.41	0.02	0.88	1.03	0.02
cg05987933	chr5:176513799	FGFR4	TSS200	FGFR4	-0.17	1.15E-05	-0.13	0.22	-0.33	0.08	-0.13	0.11	-0.25	0.35
cg13548543	chr9:34460044	DNAI1; C9orf25	Body; TSS1500	DNAI1; ENHO	0.40	1.30E-05	0.06	0.70	0.32	0.32	-0.10	0.42	0.25	0.72

cg08506743	chr11:131779750	NTM	TSS1500; Body	NTM	-0.32	1.39E-05	0.07	0.40	-0.01	0.96	0.20	0.09	-0.72	0.15
cg16037569	chr1:9710867	PIK3CD	TSS1500	PIK3CD	0.48	1.40E-05	0.29	0.14	0.14	0.77	0.05	0.76	0.42	0.58
cg26994839	chr5:15111271	LPCAT1	Body	SLC6A3; LPCAT1	0.26	1.45E-05	-0.08	0.35	0.13	0.29	0.20	0.04	1.35	1.18E-03
cg24202468	chr13:99195339	STK24	Body	RNF119B; STK24	0.57	1.45E-05	0.21	0.20	0.54	0.02	0.07	0.64	0.91	0.26
cg09055236	chr7:2673197	TTYH3	Body	AMZ1; TTYH3	0.27	1.46E-05	-0.05	0.58	0.24	0.14	-0.06	0.24	0.86	0.04
cg22930808	chr3:122281881	PARP9; DTX3L	5UTR; TSS1500	DTX3L	0.56	1.47E-05	0.39	9.87E-04	0.04	0.82	0.18	0.06	0.71	0.37
cg17552088	chr6:38087605	ZFAND3	Body	ZFAND3; BTBD9	0.68	1.59E-05	0.43	0.01	-0.10	0.83	0.30	0.11	-0.06	0.95
cg10119001	chr1:153114766	SPRR2C	TSS1500	SPRR2F; SPRR2G	0.44	1.73E-05	0.08	0.64	0.58	0.14	0.32	0.03	1.10	0.11
cg23630131	chr7:65973040	-	-	KCTD7; TPST1	0.64	1.89E-05	0.14	0.54	0.09	0.71	0.13	0.61	1.36	0.19
cg15928016	chr10:94064371	MAR05	Body	MARCH5; IDE	0.58	2.01E-05	-0.07	0.58	0.45	0.22	0.40	3.78E-04	1.48	0.08
cg00735454	chr13:44595496	LOC121838	TSS1500	ENOX1; SERP2	0.83	2.06E-05	0.40	0.01	0.26	0.31	0.22	0.15	0.83	0.47
cg23696248	chr19:45260501	BCL3	Body	CBLC; BCL3	-0.27	2.08E-05	0.14	0.19	-0.32	0.18	-0.28	0.04	-0.35	0.39
cg19851574	chr6:167178233	RPS6K42	Body	BRP44L; RPS6K42	0.23	2.10E-05	0.03	0.52	-0.20	0.17	0.12	0.26	-0.15	0.66
cg06951750	chr16:614645	C16orf11	Body	PIGQ; SOLH	0.61	2.31E-05	0.24	0.09	0.43	0.03	0.12	0.20	1.97	0.01
cg07410044	chr2:71222186	TEX261	TSS200	TEX261	0.14	2.42E-05	0.00	0.98	0.06	0.47	0.05	0.30	0.56	0.01
cg21136371	chr1:11991065	-	-	MRPL23; IGF2	-0.35	2.49E-05	-0.24	0.02	-0.05	0.83	-0.05	0.75	-0.82	0.17
cg06105987	chr7:151483394	PRKAG2	Body	RHEB; PRKAG2	-0.05	2.77E-05	0.01	0.54	-0.03	0.29	0.00	0.95	-0.05	0.59
cg24368167	chr3:38179936	ACAA1; MYD88	TSS1500; TSS200	ACAA1; MYD88	-0.27	2.97E-05	-0.06	0.32	-0.22	0.02	-0.12	0.06	-0.32	0.42
cg15353031	chr10:50887632	C10orf53	TSS200	CHAT; OGDHL	-0.14	3.12E-05	-0.07	0.12	0.05	0.52	0.07	0.02	-0.11	0.61
cg19852211	chr5:140187240	PCDHA2; PCDHA1; PCDHA4; PCDHA3	Body; 1stExon	PCDHAC2; ZMAT2	0.33	3.25E-05	-0.14	0.04	0.12	0.29	0.04	0.64	0.54	0.24
cg10998122	chr11:64008466	FKBP2	TSS1500; 1stExon; 5UTR; TSS200	FKBP2	0.11	3.65E-05	0.05	0.60	0.04	0.63	0.02	0.61	-0.09	0.63
cg01868896	chr15:52581521	MYO5C	Body	GNB5; MYO5C	0.43	3.89E-05	-0.02	0.90	0.24	0.53	0.22	0.16	1.75	9.40E-03
cg08616269	chr10:70480892	CCAR1	TSS200	CCAR1	0.19	4.18E-05	-0.04	0.43	-0.02	0.76	0.05	0.34	0.46	0.14
cg19526685	chr8:126963507	-	-	TRIB1; FAM84B	0.47	4.30E-05	-0.01	0.94	-0.11	0.63	-0.23	0.05	-0.01	0.99
cg11832804	chr5:1279449	TERT	Body	TERT; SLC6A18	0.15	4.35E-05	0.05	0.20	-0.03	0.51	0.03	0.41	0.37	0.06
cg25730577	chr1:110453002	CSF1	TSS1500	CSF1	-0.25	4.51E-05	-0.08	0.37	-0.35	2.09E-03	-0.08	0.22	-0.55	0.15
cg04245568	chr16:88453579	-	-	ZNF469; BAMP	0.11	5.88E-05	-0.01	0.68	-0.08	0.15	0.04	0.15	0.80	0.35
cg04410989	chr20:35578437	SAMHD1	N_Shore	DSN1; SAMHD1	0.29	6.34E-05	0.20	0.07	0.15	0.45	0.10	0.20	-0.45	0.36
cg00379630	chr6:159736614	-	-	FNDC1; SOD2	0.50	7.87E-05	-0.14	0.14	-0.04	0.83	0.01	0.95	-1.04	0.14
cg04021074	chr10:14816947	FAM107B	TSS200	FRMD4A; CDNF	0.30	8.08E-05	0.18	0.02	0.13	0.52	0.09	0.48	-0.08	0.46

Table 4.5. Top ranked polygenic risk score-associated differentially methylated probes (DMPs) identified in the striatum (STR) meta-analysis. Listed for each STR DMP (grey) are corresponding results from the prefrontal cortex (PFC; $P < 0.05$ in blue), hippocampus (HC; $P < 0.05$ in red) and cerebellum (CER; $P < 0.05$ in orange) meta-analyses (PFC, STR and CER) or linear regression (HC). Also shown is the association with schizophrenia diagnosis in STR ($P < 0.05$ in green). The methylation difference is measured per PRS unit. Illumina and Genomic Regions Enrichment of Annotation Tool (GREAT) annotation (McLean et al., 2010) is listed for each DMP.

Probe ID	Genomic position (hg19)	Illumina gene annotation	Gene region	GREAT annotation (McLean et al., 2010)	Methylation difference (%) STR	P STR	Methylation difference PFC (%)	PPFC	Methylation difference HC (%)	P HC	Methylation difference CER (%)	P CER	Disease STR P	Disease STR methylation difference (%)
cg26893445	chr15:85924187	AKAP13	5'UTR	AKAP13	0.15	6.73E-08	-0.01	0.71	0.13	0.13	-0.03	0.17	0.81	0.05
cg12595281	chr15:93633172	RGMA	TSS1500	RGMA	0.68	6.86E-08	0.16	0.33	0.28	0.36	0.26	0.19	0.97	-0.04
cg13567870	chr22:24995852	C22orf36; GGT1	Body; 5'UTR	GGT1; PIWIL3	0.24	2.29E-07	0.13	0.31	0.37	0.27	0.03	0.61	0.11	0.54
cg25188724	chr15:58674907	-	-	LIPC; AQP9	0.50	4.16E-07	-0.01	0.89	0.19	0.43	0.07	0.46	0.14	0.95
cg18651578	chr20:5844315	C20orf196	3'UTR	GPCPD1; CHGB	0.46	5.30E-07	0.05	0.77	0.05	0.88	0.09	0.54	0.72	0.28
cg13954067	chr9:136679658	VAV2	Body	SARDH; VAV2	-0.65	6.87E-07	-0.29	0.05	0.20	0.46	-0.27	0.14	1.17E-03	-2.78
cg25327452	chr9:100000464	KIAA1529	TSS1500	C9orf174; ZNF322	-0.19	7.01E-07	0.03	0.33	-0.03	0.66	-0.02	0.62	6.06E-03	-0.73
cg25789405	chr7:156263914	-	-	SHH; C7orf13	-0.16	7.65E-07	-0.02	0.76	0.07	0.39	-1.69E-03	0.97	0.76	-0.09
cg06854438	chr1:220263111	BPNT1	1stExon; 5'UTR	IARS2; BPNT1	-0.15	7.82E-07	0.05	0.50	-0.05	0.76	-0.03	0.49	0.28	-0.26
cg26064870	chr8:102944342	NCALD	5'UTR	NCALD; GRHL2	0.36	7.84E-07	0.05	0.47	0.03	0.83	2.45E-03	0.98	0.02	1.06
cg03293330	chr3:187385312	-	-	SST; RTP4	0.63	1.09E-06	-	-	-0.05	0.85	0.28	0.11	0.04	1.76
cg14372324	chr20:30347798	TPX2	Body	MYLK2; TPX2	1.32	1.11E-06	0.60	0.08	1.66	0.07	1.00	1.31E-03	0.03	3.54
cg15674825	chr5:150052349	MYOZ3	Body	MYOZ3; RBM22	0.42	1.16E-06	-0.01	0.88	-0.36	0.20	-0.10	0.62	0.83	0.15
cg05415496	chr17:79519191	C17orf70	1stExon; 5'UTR	C17orf70	-0.07	1.25E-06	-0.01	0.65	0.03	0.08	-3.09E-04	0.98	0.01	-0.22
cg24646359	chr10:102288877	NDUFB8	Body	NDUFB8	-0.18	1.38E-06	0.01	0.77	0.04	0.82	3.40E-03	0.92	0.02	-0.60
cg23664774	chr22:29446636	ZNRF3	Body	KREMEN1; ZNRF3	0.47	1.62E-06	0.02	0.86	0.10	0.71	0.05	0.83	0.89	0.10
cg07986469	chr10:129795003	PTPRE	5'UTR	PTPRE; MKI67	0.57	1.71E-06	0.20	0.06	0.09	0.68	-0.01	0.85	0.39	0.68
cg09493966	chr16:51165636	-	-	SALL1; CYLD	0.50	2.04E-06	0.01	0.95	-0.35	0.03	-0.18	0.21	0.38	0.60
cg19376461	chr7:110358708	IMMP2L	Body	LRRN3	0.43	2.11E-06	-0.17	0.18	0.32	0.07	-0.14	0.54	0.40	0.51
cg06452647	chr12:49961750	MCRS1	5'UTR	MCRS1	-0.11	2.40E-06	0.03	0.42	-0.01	0.92	-0.10	2.93E-03	0.07	-0.32
cg11427534	chr5:132155233	-	-	SEPT8; SHROOM1	0.47	2.48E-06	0.04	0.78	0.02	0.93	-0.39	0.08	0.86	-0.19
cg01020037	chr6:31047822	-	-	C6orf15; MUC22	-0.26	3.09E-06	0.09	0.27	-0.36	0.03	-0.07	0.43	0.10	-0.72

cg22244135	chr7:7226343	C1GALT1	5'UTR	C1GALT1; COL28A1	0.22	3.33E-06	-0.06	0.27	0.17	0.07	0.13	0.09	6.54E-03	0.93
cg15022015	chr17:78869527	RPTOR	Body	CHIMP6; RPTOR	0.28	3.82E-06	0.10	0.17	0.13	0.12	0.07	0.42	0.20	0.58
cg17689581	chr2:82508075	-	-	NONE	0.36	4.35E-06	-0.05	0.69	-0.20	0.34	0.23	3.72E-03	0.28	0.56
cg26570279	chr16:58324876	KLKBL4	Body	PRSS54; CCDC113	0.22	4.60E-06	-0.06	0.36	0.08	0.16	0.05	0.58	0.60	0.18
cg12988813	chr7:27946471	JAZF1	Body	TAX1BP1; JAZF1	0.53	5.20E-06	0.21	0.20	0.16	0.49	0.16	0.05	0.13	1.18
cg01331540	chr3:71027020	FOXP1	Body	FOXP1	0.30	5.39E-06	0.09	0.48	-0.01	0.97	0.34	0.02	0.14	0.74
cg17095753	chr7:140623924	BRAF	Body	BRAF	-0.19	6.72E-06	0.01	0.78	-0.13	0.13	-0.02	0.66	0.25	-0.34
cg22129639	chr15:43785364	TP53BP1	TSS200; 5'UTR	TP53BP1	-0.43	7.13E-06	-0.04	0.44	-0.37	0.19	-0.04	0.61	0.25	-0.81
cg20548182	chr12:59426481	-	-	SLC16A7; LRIG3	0.26	7.68E-06	-0.04	0.65	-0.07	0.54	0.15	0.11	0.63	0.21
cg03292206	chr2:111424914	BUB1	Body	RGPD6; BUB1	0.52	7.79E-06	0.14	0.45	-0.07	0.81	0.03	0.81	0.06	1.44
cg26509022	chr15:101419296	ALDH1A3	TSS1500	ALDH1A3	0.61	8.77E-06	-0.02	0.90	-0.06	0.83	0.53	0.15	0.12	1.55
cg22708290	chr12:56368226	RAB5B	5'UTR	RAB5B	-0.52	8.99E-06	-0.01	0.94	-0.02	0.92	-0.21	0.18	0.61	-0.41
cg02549170	chr4:186436021	PDLIM3	Body	CCDC110; PDLIM3	0.19	9.08E-06	-0.01	0.91	-0.03	0.74	0.01	0.89	0.11	0.51
cg12449325	chr11:34814081	-	-	PDHX; EHF	0.40	9.42E-06	-0.05	0.44	0.03	0.90	0.06	0.43	0.33	0.56
cg08135379	chr12:47474763	AMIGO2	TSS1500	AMIGO2	0.42	1.00E-05	0.04	0.80	0.02	0.91	0.13	0.43	0.45	0.51
cg26008841	chr1:55450605	TMEM61	Body	BSND; TMEM61	0.33	1.14E-05	0.07	0.35	0.11	0.52	0.10	0.39	0.19	0.68
cg08600218	chr7:139412996	HIPK2	Body	HIPK2; CLEC2L	0.44	1.20E-05	0.01	0.95	0.30	0.12	0.06	0.48	0.60	0.37
cg21940313	chr17:41620911	ETV4	Body	ETV4; DHX8	0.44	1.27E-05	0.14	0.18	-0.05	0.84	0.46	3.82E-03	0.18	0.89
cg26075039	chr2:121684535	GLI2	Body	GLI2; TFCP2L1	1.23	1.32E-05	0.89	0.02	-0.75	0.19	0.42	0.18	0.60	0.91
cg17066531	chr6:36922415	PI16	5'UTR; 1stExon	PI16	0.46	1.34E-05	-0.03	0.78	-0.16	0.52	0.20	0.43	0.26	0.78
cg27263448	chr7:127637871	C7orf54; SND1	Body	LRRC4; SND1	0.15	1.42E-05	0.02	0.78	0.05	0.66	-0.04	0.85	0.32	0.28
cg05544885	chr16:88807707	FAM38A	Body	CTU2; PIEZO1	0.33	1.46E-05	0.14	0.08	-0.03	0.86	0.15	0.05	0.19	0.71
cg01379237	chr3:189983744	-	-	LEPREL1; CLDN1	0.57	1.63E-05	0.16	0.42	0.13	0.60	0.03	0.87	0.48	-0.16
cg05494483	chr5:17001489	-	-	BASP1; MYO10	-0.32	1.67E-05	0.25	0.03	0.07	0.60	0.11	0.24	6.99E-03	1.48
cg02141675	chr5:153569408	GALNT10	TSS1500	GALNT10	-0.19	1.74E-05	-0.01	0.83	-0.14	0.20	0.04	0.59	0.07	1.71
cg10939579	chr13:20768309	GJB2	TSS1500	GJB2	-0.68	1.76E-05	-0.09	0.65	0.34	0.40	-	-	0.32	-0.53
cg11593949	chr7:45927735	IGFBP1	TSS1500	IGFBP1	0.38	1.79E-05	0.20	0.17	0.40	0.12	-0.04	0.84	0.04	-0.65
cg08820821	chr19:49588236	SNRNP70	TSS1500	SNRNP70	-0.23	1.80E-05	0.03	0.62	0.02	0.77	0.00	0.97	0.53	0.79

Table 4.6. Top ranked polygenic risk score-associated differentially methylated probes (DMPs) identified in the hippocampus (HC) linear regression. Listed for each HC DMP (grey) are corresponding results from the prefrontal cortex (PFC; $P < 0.05$ in blue), striatum (STR; $P < 0.05$ in green) and cerebellum (CER; $P < 0.05$ in orange) meta-analyses. Also shown is the association with schizophrenia diagnosis in HC ($P < 0.05$ in red). The methylation difference is measured per PRS unit. Illumina and Genomic Regions Enrichment of Annotation Tool (GREAT) annotation (McLean et al., 2010) is listed for each DMP.

Probe ID	Genomic position (hg19)	Illumina gene annotation	Gene region	GREAT annotation (McLean et al., 2010)	Methylation difference (% HC)	P HC	Methylation difference PFC (%)	PPFC	Methylation difference STR (%)	P STR	Methylation difference CER (%)	P CER	Disease HC methylation difference (%)	Disease HC P
cg03075791	chr2:120774662	EPB41L5	5'UTR	EPB41L5; TMEM185B	0.48	2.85E-06	0.16	0.27	-0.01	0.90	0.15	0.07	2.96	7.94E-05
cg01305596	chr16:162282299	ABCC1	Body	ABCC6; ABCC1	0.12	3.67E-06	0.01	0.71	0.03	0.11	2.30E-03	0.91	0.57	6.14E-03
cg16365352	chr1:236954819	-	-	MTR	0.63	4.88E-06	-0.01	0.87	0.02	0.81	0.11	0.26	3.21	2.04E-03
cg04074321	chr10:88296423	-	-	OPN4; WAPAL	-0.92	6.59E-06	0.04	0.74	0.17	0.19	0.05	0.79	-5.04	1.45E-03
cg00555456	chr7:96745696	ACN9	TSS1500	ACN9	-0.85	6.96E-06	-0.11	0.57	0.11	0.33	0.05	0.72	-4.49	1.77E-03
cg05239158	chr15:35842016	-	-	ZNF770	-0.97	7.69E-06	-0.08	0.62	0.23	0.14	0.21	0.33	-5.20	8.73E-04
cg02315597	chr19:52598999	ZNF841	5'UTR; 1stExon	ZNF841	-0.20	1.02E-05	0.02	0.54	-0.04	0.28	-0.03	0.52	-0.80	0.02
cg23811289	chr14:101440409	SNORD114-17	TSS1500	DIO3; RTL1	0.53	1.73E-05	-0.14	0.41	0.11	0.36	0.23	0.21	2.72	4.38E-03
cg22502856	chr1:209825678	LAMB3	TSS1500; 5'UTR; TSS200	LAMB3	0.37	2.14E-05	0.05	0.29	-0.06	0.31	6.86E-04	0.99	2.06	1.40E-03
cg04487827	chr1:44434389	DPH2	TSS1500	DPH2	-0.60	2.18E-05	-0.23	2.26E-03	0.09	0.41	0.07	0.45	-3.64	1.98E-03
cg27105205	chr1:154934396	PYGO2	TSS200	PYGO2	0.11	2.33E-05	-0.01	0.61	-0.01	0.41	1.92E-04	0.99	0.53	0.02
cg01200150	chr18:76322683	-	-	SALL3	-1.37	2.76E-05	-0.11	0.46	0.13	0.49	0.31	0.05	-6.31	0.01
cg19832184	chr20:33578069	MYH7B; MIR499	Body; TSS200	MYH7B; TRPC4AP	0.53	2.82E-05	0.06	0.52	0.01	0.92	0.09	0.38	2.75	3.02E-03
cg08370082	chr3:196616876	SENP5	Body	SENP5; NCBP2	1.16	3.14E-05	0.18	0.40	-0.15	0.46	-	-	4.83	0.02
cg25246281	chr17:27188748	MIR451; MIR144	TSS1500; TSS200	ERAL1; FLOT2	0.76	3.84E-05	0.06	0.58	0.02	0.80	-0.09	0.50	4.17	1.40E-03
cg14833040	chr6:47197781	-	-	GPR110; TNFRSF21	0.24	3.93E-05	0.05	0.32	0.10	0.04	0.04	0.50	1.03	0.02
cg26045524	chr7:150035522	RARRES2	3'UTR	ACTR3C; RARRES2	0.55	3.95E-05	0.04	0.72	0.31	0.02	0.20	0.23	2.48	0.02
cg11956108	chr1:1895061	KIAA1751	Body	GABRD; TIME52	0.31	3.96E-05	0.07	0.45	-0.11	0.21	0.03	0.73	1.65	6.54E-03
cg14183864	chr2:74699903	MIRPL53	5'UTR; 1stExon	MRPL53	-0.15	4.03E-05	0.01	0.70	-0.01	0.77	0.03	0.41	-0.77	5.82E-03
cg18961589	chr10:133598669	-	-	PPP2R2D	-0.38	4.21E-05	-0.02	0.82	0.07	0.39	0.09	0.24	-2.34	7.37E-04
cg20810675	chr4:171604188	-	-	AADAT	0.94	4.29E-05	0.12	0.53	-0.03	0.87	-0.04	0.82	4.91	5.79E-03

cg09936645	chr1:207627581	CR2	TSS200	CR2	-0.06	4.75E-05	0.03	0.05	0.02	0.37	-3.50E-03	0.82	-0.22	0.05
cg14069049	chr4:11430698	HS3ST1	TSS200	HS3ST1	-0.19	5.01E-05	0.09	0.02	2.38E-03	0.93	-0.01	0.64	-1.12	1.45E-03
cg18290739	chr6:10389490	-	-	OFCC1; TFAP2A	0.95	5.28E-05	-0.10	0.58	0.03	0.85	0.14	0.38	3.57	0.05
cg01422136	chr5:132362224	ZCCHC10	1stExon	ZCCHC10	-0.23	5.50E-05	0.02	0.57	-0.07	0.02	-0.01	0.78	-1.56	1.75E-05
cg19159842	chr17:73727435	ITGB4	Body	ITGB4; GALK1	0.58	5.65E-05	0.08	0.55	0.02	0.83	-1.05E-03	0.99	1.97	0.12
cg15043711	chr6:31797954	HSPA1B	3'UTR; 1stExon	HSPA1B; NEU1	-0.39	5.68E-05	-0.04	0.71	-0.16	0.02	-0.18	0.04	-2.20	3.39E-03
cg07057342	chr14:31915923	C14orf126	3'UTR	HEATR5A; C14orf126	0.83	5.75E-05	-0.05	0.75	-0.17	0.29	0.36	5.90E-03	3.90	7.32E-03
cg18959411	chr6:160182805	ACAT2	TSS200	ACAT2	-0.13	5.76E-05	-0.04	0.44	-0.04	0.23	-0.04	0.16	-0.92	8.64E-04
cg02441618	chr17:40936570	WNK4	Body	WNK4; CCDC56	-0.89	5.91E-05	0.11	0.32	-0.03	0.84	-0.14	0.44	-3.69	0.06
cg14228238	chr3:168864123	MECOM	TSS200; Body; 5'UTR	MECOM	-0.60	5.94E-05	0.16	0.16	0.15	0.13	0.01	0.81	-2.56	0.02
cg01204911	chr5:142187317	ARHGAP26	Body	ARHGAP26; NR3C1	-0.69	6.27E-05	0.05	0.64	-0.09	0.39	0.01	0.79	-2.60	0.03
cg23433530	chr15:93014435	C15orf32	TSS1500	ST8SIA2; FAM174B	0.69	6.37E-05	0.04	0.64	0.10	0.23	0.12	0.19	3.87	1.03E-03
cg06135282	chr13:86370102	SLITRK6	Body	SLITRK6	0.43	6.45E-05	0.08	0.45	-0.06	0.38	0.10	0.16	2.23	2.99E-03
cg21985690	chr5:79330669	THBS4	TSS1500	THBS4	1.45	6.52E-05	0.04	0.79	0.08	0.57	0.10	0.56	7.31	3.37E-03
cg07158797	chr1:215740701	KCTD3	TSS200	KCTD3	0.20	6.92E-05	2.35E-03	0.92	0.00	0.97	-0.02	0.51	1.37	4.22E-05
cg15815726	chr6:7129714	RREB1	5'UTR	RREB1; SSR1	0.95	6.98E-05	0.29	0.13	0.25	0.27	-0.04	0.84	5.35	3.06E-03
cg12100385	chr14:88602662	-	-	GPR65; KCNK10	0.35	7.29E-05	-0.01	0.88	-0.06	0.41	0.08	0.11	0.93	0.18
cg03196189	chr12:51488916	TFCP2	3'UTR	C-SRNP2; TFCP2	0.35	7.36E-05	-0.01	0.94	0.07	0.22	-0.04	0.74	2.01	1.95E-03
cg10374499	chr11:44601397	CD82	5'UTR	TSPAN18; CD82	0.84	7.39E-05	0.18	0.13	0.24	0.14	0.01	0.92	2.65	0.13
cg05529754	chr16:85045486	ZDHHC7	TSS1500	ZDHHC7	-0.25	7.44E-05	-0.01	0.82	-0.06	0.22	0.03	0.39	-1.27	4.49E-03
cg18187593	chr6:33290972	DAXX	TSS200	DAXX	-0.18	9.01E-05	0.00	0.91	-0.01	0.79	0.02	0.50	-0.81	0.01
cg12930930	chr11:5372503	OR51B6	TSS1500	OR51B6	0.86	9.49E-05	0.25	0.22	0.33	0.01	0.22	0.20	4.25	6.28E-03
cg00060320	chr3:134369974	KY	TSS200	KY	-0.10	9.58E-05	0.03	0.32	-0.05	0.09	-0.01	0.69	-0.67	3.99E-04
cg02863947	chr3:119499190	NR1I2	TSS200	NR1I2	0.32	9.78E-05	-0.01	0.90	0.04	0.50	0.05	0.53	2.01	2.90E-04
cg21759953	chr2:121748257	GLI2	3'UTR	GLI2; TFCEP2L1	0.30	9.83E-05	-0.03	0.68	0.03	0.56	-0.03	0.63	1.56	3.39E-03
cg01962750	chr2:8298983	-	-	ID2	-0.61	9.90E-05	0.08	0.52	-0.03	0.75	-0.12	0.37	-2.72	0.02
cg04944537	chr10:125428817	GPR26	Body	GPR26; CPXM2	0.49	1.01E-04	0.06	0.62	0.08	0.29	-4.56E-03	0.95	2.61	2.22E-03
cg16216907	chr7:42267430	GLI3	5'UTR	INHBA; GLI3	-1.13	1.08E-04	0.13	0.44	0.03	0.89	-0.06	0.64	-4.99	0.01
cg09442740	chr7:100482960	SRRT	Body	UFSP1; SRRT	0.23	1.09E-04	0.03	0.56	-0.06	0.69	0.03	0.72	1.60	1.48E-04

Table 4.7. Top ranked polygenic risk score-associated differentially methylated probes (DMPs) identified in the cerebellum (CER) meta-analysis. Listed for each CER DMP (grey) are corresponding results from the prefrontal cortex (PFC; $P < 0.05$ in blue), striatum (STR; $P < 0.05$ in green) and hippocampus (HC; $P < 0.05$ in red) meta-analyses (PFC, STR and CER) or linear regression (HC). Also shown is the association with schizophrenia diagnosis in CER ($P < 0.05$ in orange). The methylation difference is measured per PRS unit. Illumina and Genomic Regions Enrichment of Annotation Tool (GREAT) annotation (McLean et al., 2010) is listed for each DMP.

Probe ID	Genomic position (hg19)	Illumina gene annotation	Gene region	GREAT annotation (McLean et al., 2010)	Methylation difference (% CER)	P CER	Methylation difference PFC (%)	P PFC	Methylation difference STR (%)	P STR	Methylation difference HC (%)	P HC	Disease methylation difference (%)	Disease CER P
cg20640286	chr9:116811789	ZNF618	Body	AMBIP; ZNF618	0.60	1.62E-09	-0.02	0.93	0.12	0.10	0.02	0.88	1.20	0.11
cg27150552	chr7:48026856	SUNC1	3'UTR	HUS1; SUNC3	0.34	1.30E-08	-0.13	0.30	-0.02	0.89	0.47	0.06	0.84	0.18
cg05209768	chr2:164573665	FIGN	Body	KCNH7; FIGN	0.70	1.55E-08	-0.04	0.82	0.01	0.96	0.47	0.16	2.00	0.04
cg07793808	chr12:122019006	KDM2B	TSS200; TSS1500	KDM2B	-0.19	1.66E-08	0.05	0.62	-0.02	0.91	-0.39	0.23	-0.23	0.36
cg10218777	chr3:133180261	BFSP2	Body	CDV3; BFSP2	0.67	3.86E-08	0.06	0.69	0.05	0.79	0.45	0.20	2.91	6.54E-03
cg01682070	chr16:29996774	TAOK2	Body	HIRIP3; TAOK2	0.32	4.20E-08	0.03	0.64	0.04	0.50	0.02	0.83	0.87	0.04
cg11786558	chr17:2266589	SGSM2	Body	SGSM2; MNT	0.69	4.35E-08	0.04	0.80	0.02	0.87	-0.10	0.69	1.28	0.14
cg26053083	chr11:14995770	-	-	CALCA	-0.15	4.41E-08	-0.02	0.70	-0.06	0.10	-0.08	0.19	-0.29	0.14
cg01022840	chr14:71250264	MAP3K9	Body	MAP3K9; TTC9	0.63	7.86E-08	-0.01	0.91	0.13	0.20	0.34	0.25	1.94	0.03
cg08478539	chr15:68640339	ITGA11	Body	FEM1B; ITGA11	0.69	1.06E-07	1.24E-03	0.99	0.11	0.41	0.02	0.94	1.41	0.14
cg23788334	chr2:137181176	-	-	THSD7B; CXCR4	-0.13	1.15E-07	-0.04	0.37	0.01	0.75	-0.05	0.53	-0.15	0.38
cg16904520	chr2:230590962	-	-	DNER; TRIP12	0.26	1.25E-07	-0.04	0.79	0.10	0.60	0.08	0.78	1.27	9.37E-04
cg09987651	chr6:27463667	-	-	ZNF184; HIST1H2BL	-0.50	1.76E-07	0.01	0.96	-0.08	0.42	-0.31	0.06	-0.86	0.24
cg03314644	chr14:31890001	-	-	HEATR5A	-0.34	1.82E-07	-0.01	0.93	-0.04	0.74	-0.36	0.14	-0.48	0.29
cg03812240	chr9:125107355	-	-	RBM18; PTGS1	0.28	2.13E-07	-4.47E-03	0.95	0.04	0.59	0.03	0.92	0.23	0.60
cg13846270	chr13:51417929	DLEU7	TSS200	RNASEH2B; ST13P4	-0.84	2.55E-07	-0.11	0.50	-0.13	0.38	-0.44	0.14	-3.95	2.06E-04
cg14595617	chr2:3105137	-	-	MYT1L; TRAPPC12	0.48	2.96E-07	0.02	0.71	0.14	0.01	-0.04	0.75	0.13	0.84
cg07984684	chr16:89724635	C16orf55; CHMP1A	Body; TSS1500	CHMP1A	-0.19	3.12E-07	0.04	0.52	0.01	0.89	-0.06	0.57	-0.44	0.11
cg17788761	chr1:78340579	FAM73A	Body	NEXN; FAM73A	0.62	3.15E-07	-0.04	0.85	0.07	0.55	0.58	0.02	2.34	8.32E-03
cg06343355	chr6:29521023	-	-	MAS1L; UBD	-0.56	3.72E-07	0.13	0.25	-0.09	0.37	2.23E-03	0.99	-0.99	0.30
cg08853103	chr17:79514978	C17orf70	Body	C17orf70; FSCN2	0.40	5.87E-07	-0.02	0.83	0.01	0.93	0.17	0.22	1.51	0.02
cg01580578	chr7:156889041	-	-	MXN1; UBE3C	-0.72	6.52E-07	-0.28	0.06	-0.19	0.16	-0.53	0.07	-1.68	0.10

cg02583247	chr12:4555311	FGF6	TSS1500 5'UTR;	FGF6	6.96E-07	0.37	9.40E-07	0.35	5.17E-04	0.99	0.32	0.01	0.64	0.22
cg12374123	chr15:45406327	DUOX2; DUOX2	TSS200; 1stExon	DUOX2; DUOX2	7.45E-07	-0.59	7.45E-07	0.17	0.08	0.48	-0.27	0.15	-2.12	0.01
cg19321126	chr2:242211919	HDLBP	5'UTR	HDLBP	7.81E-07	0.09	7.81E-07	0.02	-4.24E-03	0.87	0.09	0.14	0.41	3.40E-03
cg20755721	chr21:38070524	SIM2	TSS1500	SIM2	8.17E-07	-0.49	8.17E-07	0.74	0.04	0.70	-0.32	0.14	-1.19	0.09
cg05919625	chr18:32870178	ZNF271; ZNF3970S	TSS200; 5'UTR; 1stExon	ZNF271; ZSCAN30	8.17E-07	-0.10	8.17E-07	0.37	-3.25E-03	0.87	-0.05	0.16	-0.18	0.21
cg19575244	chr6:157094085	-	-	ARID1B	8.49E-07	0.46	8.49E-07	0.81	0.14	0.30	0.37	0.16	1.31	0.09
cg15034300	chr2:85134468	-	-	KCMF1; TMSB10	8.61E-07	-0.80	8.61E-07	0.44	0.16	0.09	-0.38	0.16	0.34	0.79
cg11468000	chr6:139694674	CITED2	Body	CITED2	8.83E-07	-0.15	8.83E-07	0.90	-0.06	0.12	-0.12	0.13	0.15	0.51
cg15506890	chr2:3487001	-	-	ADI1; TRAPPC12	9.40E-07	1.27	9.40E-07	4.62 E-03	0.62	8.69 E-04	-0.04	0.91	1.89	0.33
cg05447008	chr6:73331114	KCNQ5	TSS1500	KCNQ5	1.01E-06	-0.09	1.01E-06	0.54	-8.27E-04	0.98	0.03	0.53	-0.22	0.09
cg14308867	chr6:31603476	BAT2	Body	PRRC2A; BAG6	1.05E-06	0.30	1.05E-06	0.99	-0.01	0.89	-0.06	0.65	0.65	0.12
cg26656452	chr10:115313165	HABP2	Body	HABP2	1.08E-06	0.41	1.08E-06	0.48	0.03	0.55	-0.03	0.78	1.14	0.04
cg13159946	chr20:30073521	NCRNA000 28	TSS200	HM13; REM1	1.11E-06	-0.75	1.11E-06	0.17	-0.44	0.02	-0.89	0.03	-0.35	0.78
cg14597361	chr12:22778766	ETNK1	Body	ETNK1	1.14E-06	-0.16	1.14E-06	0.75	-0.07	0.07	0.02	0.76	-0.29	0.22
cg08041245	chr2:179516579	TTN; MIR548N	Body	TTN; PLEKHA3	1.20E-06	0.56	1.20E-06	0.31	-0.02	0.82	0.28	0.02	2.22	0.01
cg24523948	chr8:72916620	-	-	MSC; TRPA1	1.27E-06	-0.66	1.27E-06	0.53	0.02	0.89	0.33	0.26	-2.60	6.54E-03
cg10569616	chr7:124536676	POT1	Body; 5'UTR	GPR37; POT1	1.37E-06	0.45	1.37E-06	0.26	0.07	0.51	0.22	0.37	1.07	0.11
cg11630392	chr3:150920964	GPR171; MED12L	1stExon; Body; 5'UTR	GPR171	1.44E-06	0.63	1.44E-06	0.72	0.04	0.82	-	-	2.23	0.02
cg15094071	chr3:183525728	YEATS2	Body	MAP6D1; YEATS2	1.58E-06	0.29	1.58E-06	0.50	-0.02	0.80	-0.25	0.20	0.63	0.13
cg20981127	chr19:17357587	NR2F6	TSS1500	NR2F6	1.59E-06	-0.60	1.59E-06	0.87	-0.05	0.45	-0.32	0.15	-0.84	0.40
cg05266784	chr1:160312524	COPA;	Body;	NCSTN; COPA	1.60E-06	-0.19	1.60E-06	0.58	-0.02	0.74	-0.16	0.30	-0.23	0.42
cg02783970	chr17:78121126	EIF4A3	TSS1500	EIF4A3	1.63E-06	-0.07	1.63E-06	0.13	-0.02	0.39	-0.11	0.12	-0.14	0.28
cg17152101	chr1:32509371	KHDRBS1	3'UTR	TMEM39B; KHDRBS1	1.63E-06	0.47	1.63E-06	0.85	0.13	0.22	0.05	0.84	0.91	0.30
cg18559785	chr19:42915372	LIPE	Body	GNFN; LIPE	1.65E-06	0.37	1.65E-06	0.06	-0.04	0.71	0.07	0.69	1.07	0.09
cg11629408	chr8:67415435	C8orf46	Body	ADHFE1; MYBL1	1.65E-06	0.28	1.65E-06	0.90	0.27	1.14 E-03	0.18	0.29	0.18	0.65
cg17561452	chr16:84224707	ADAD2	TSS200	TAF1C; ADAD2	1.66E-06	0.48	1.66E-06	0.89	0.02	0.89	-0.08	0.69	1.92	0.01
cg02400308	chr5:160048139	ATP10B	Body	PTTG1; ATP10B	1.71E-06	0.24	1.71E-06	0.22	0.10	0.11	-0.15	0.41	0.31	0.42
cg06845571	chr6:108279703	SEC63	TSS1500	SEC63	1.72E-06	-0.18	1.72E-06	0.84	-0.05	0.44	-0.22	0.12	-0.28	0.26

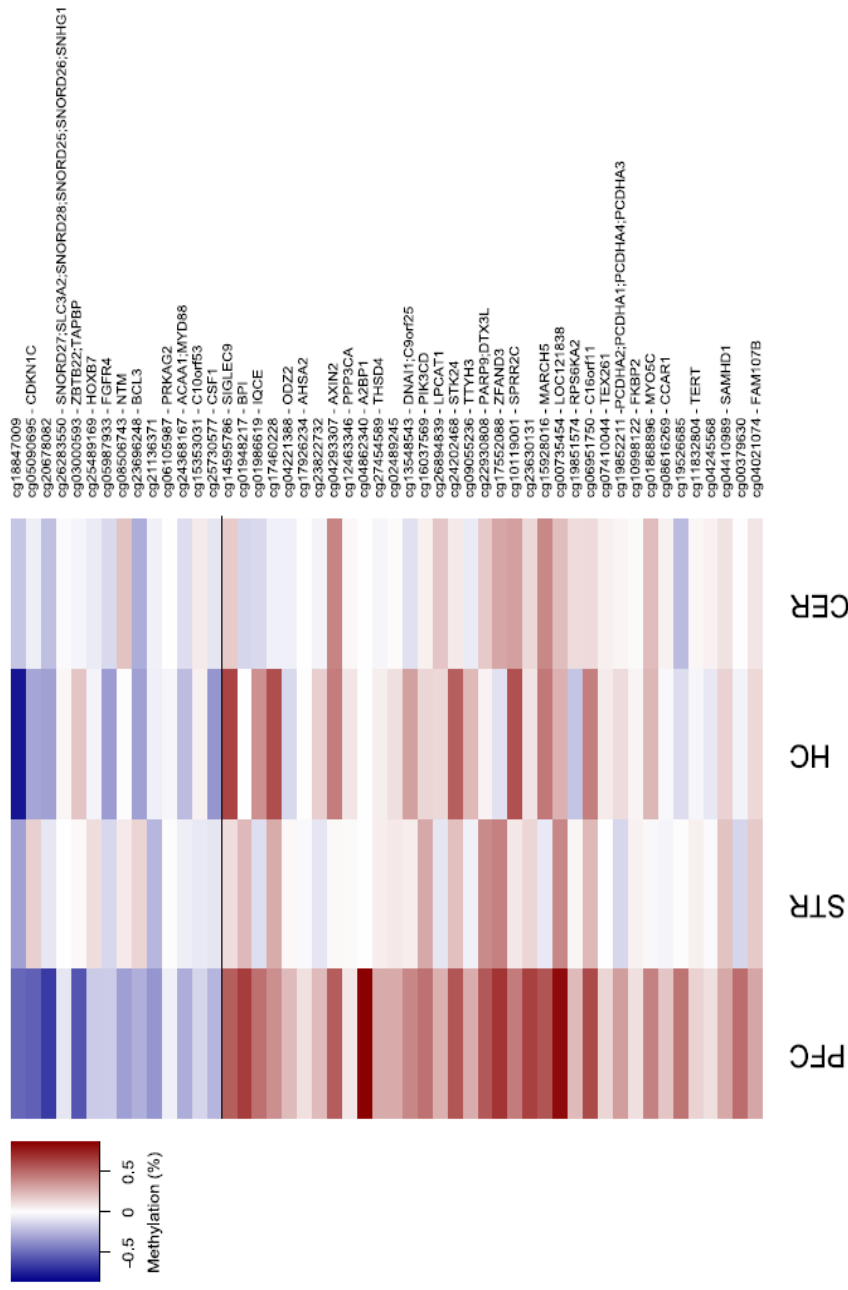


Figure 4.16. Heatmap showing the fifty top ranked differently methylated positions associated with schizophrenia polygenic risk score (PRS) in the prefrontal cortex (PFC). Shown for each probe is the DNA methylation effect size associated with PRS, with the corresponding effect at the same probe for the three other brain regions (striatum (STR), hippocampus (HC) and cerebellum (CER)) dissected from the same individuals. Probes are ordered by *P*-value for PRS-associated hypomethylation (blue, top) and hypermethylation (red, bottom) *loci* within the PFC.

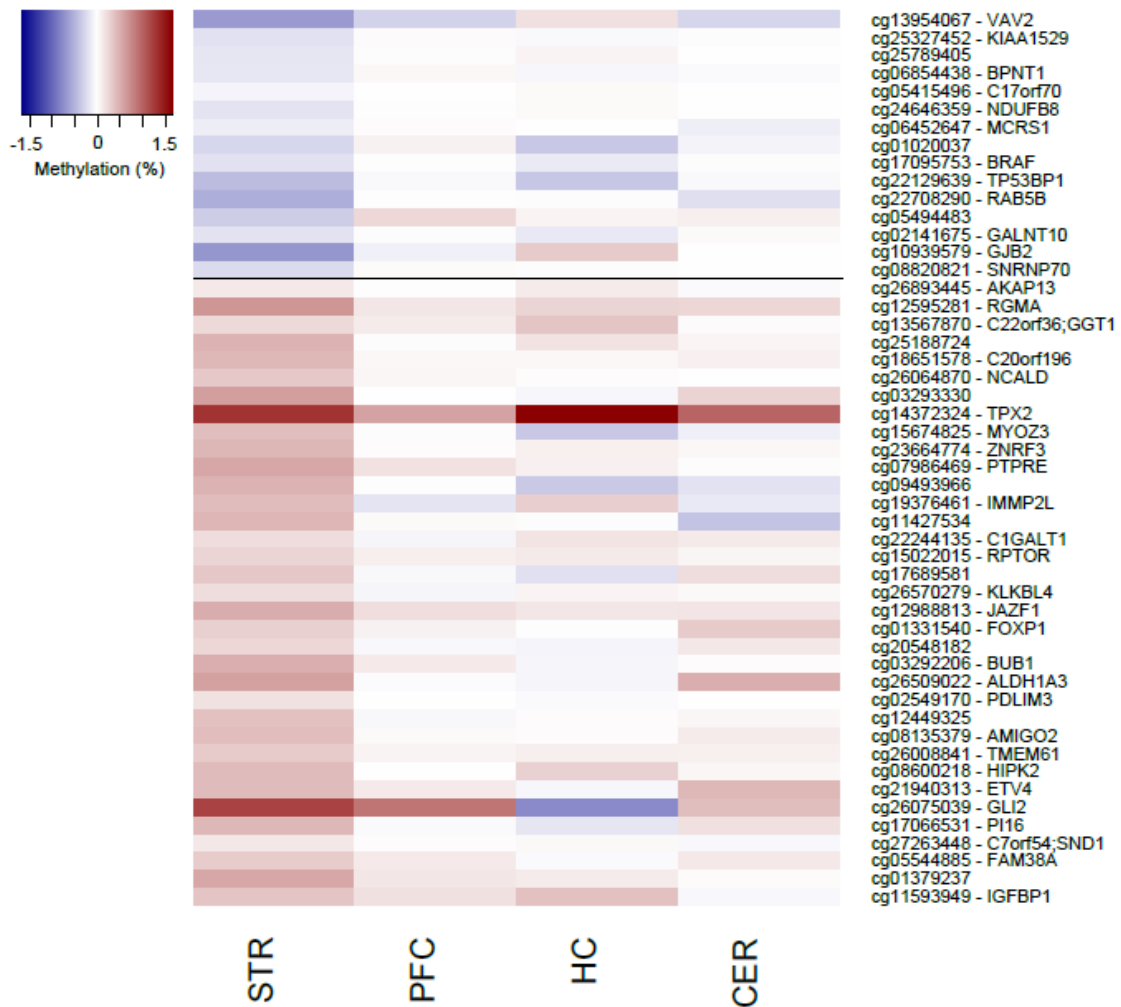


Figure 4.17. Heatmap showing the fifty top ranked differently methylated positions associated with schizophrenia polygenic risk score (PRS) in the striatum (STR). Shown for each probe is the DNA methylation effect size associated with PRS, with the corresponding effect at the same probe for the three other brain regions (prefrontal cortex (PFC), hippocampus (HC) and cerebellum (CER)) dissected from the same individuals. Probes are ordered by *P*-value for PRS-associated hypomethylation (blue, top) and hypermethylation (red, bottom) *loci* within the STR.

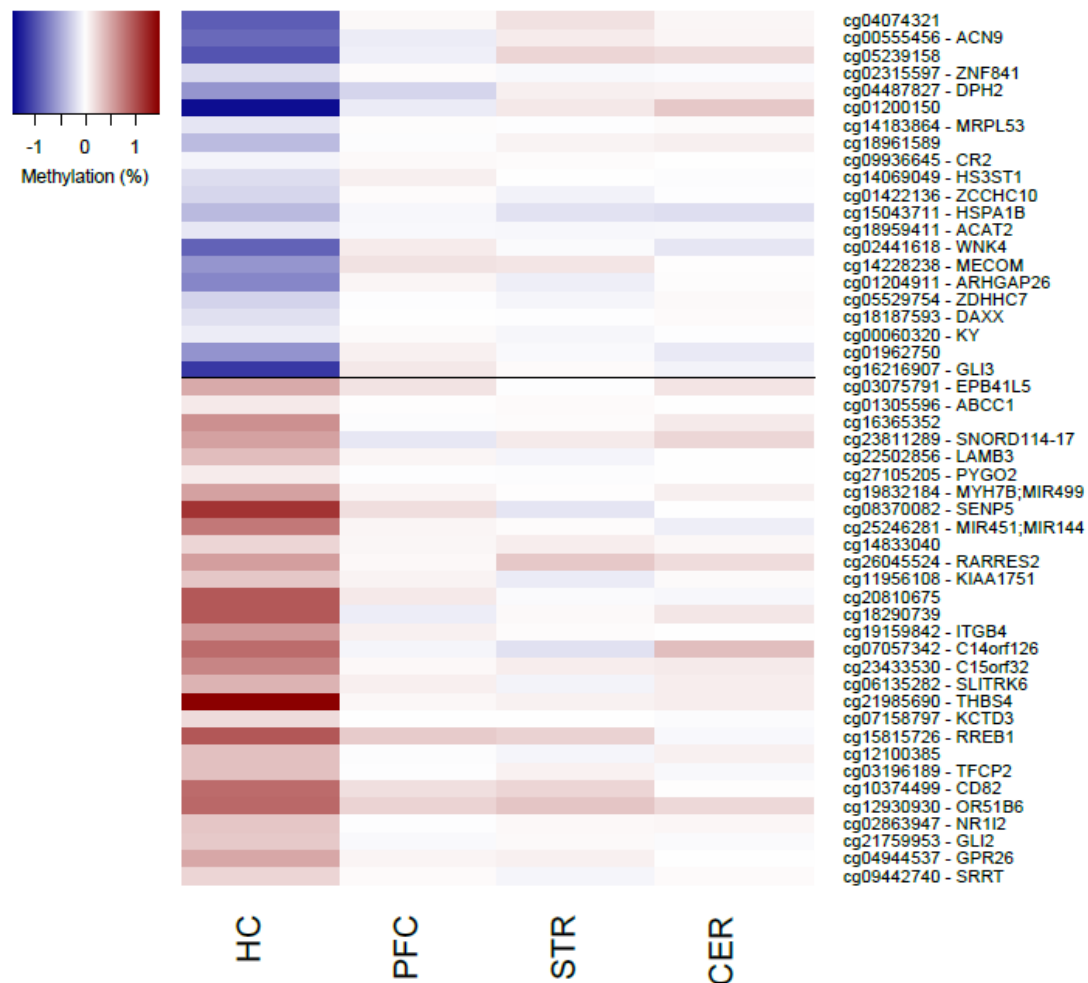


Figure 4.18. Heatmap showing the fifty top ranked differentially methylated positions associated with schizophrenia polygenic risk score (PRS) in the striatum (STR). Shown for each probe is the DNA methylation effect size associated with PRS, with the corresponding effect at the same probe for the three other brain regions (prefrontal cortex (PFC), hippocampus (HC) and cerebellum (HC)) dissected from the same individuals. Probes are ordered by *P*-value for PRS-associated hypomethylation (blue, top) and hypermethylation (red, bottom) *loci* within the STR.

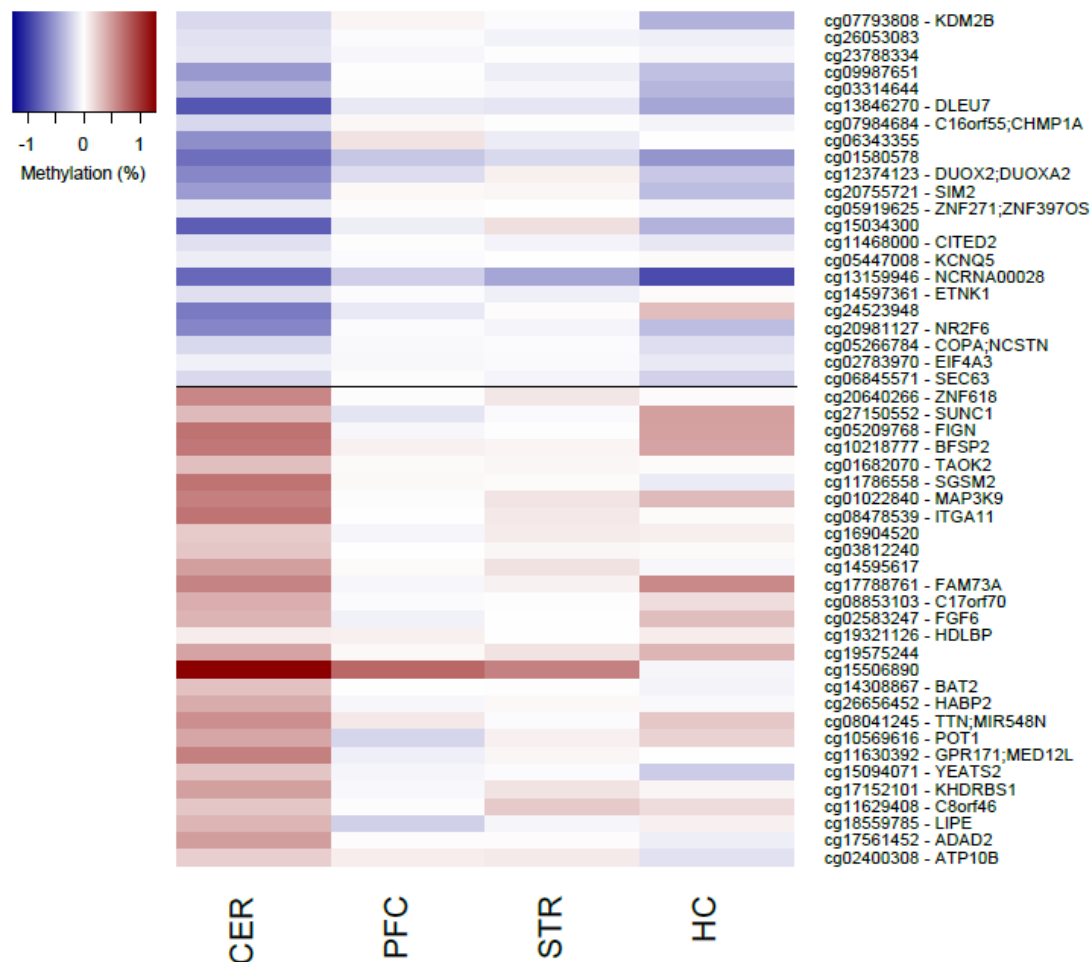


Figure 4.19. Heatmap showing the fifty top ranked differently methylated positions associated with schizophrenia polygenic risk score (PRS) in the hippocampus (HC). Shown for each probe is the DNA methylation effect size associated with PRS, with the corresponding effect at the same probe for the three other brain regions (prefrontal cortex (PFC), striatum (STR) and cerebellum (CER)) dissected from the same individuals. Probes are ordered by *P*-value for PRS-associated hypomethylation (blue, top) and hypermethylation *loci* within the HC.

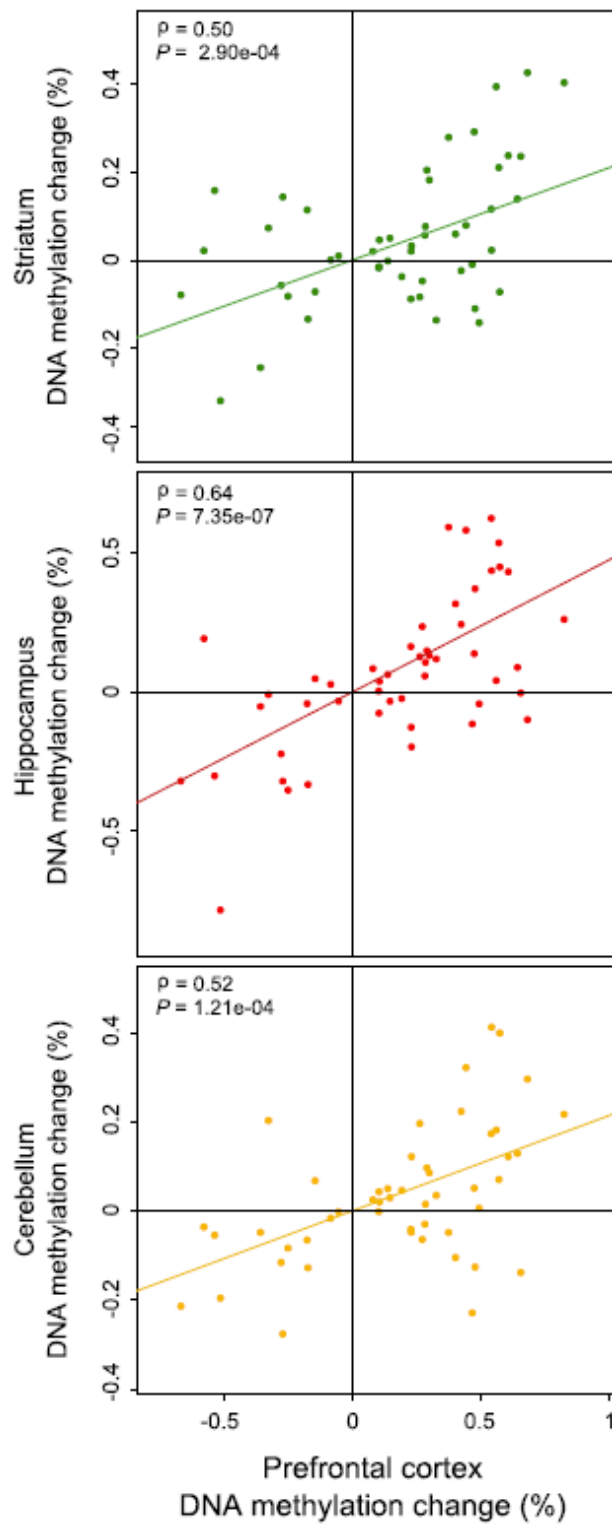


Figure 4.20. Correlation between DNA methylation differences for the fifty top ranked polygenic risk score (PRS)-associated probes identified in the prefrontal cortex and the DNA methylation differences in the same probes in the remaining brain regions (y-axis). Striatum = green; hippocampus = red; cerebellum = orange. ρ = Pearson's correlation coefficient. The DNA methylation difference is measured per PRS unit.

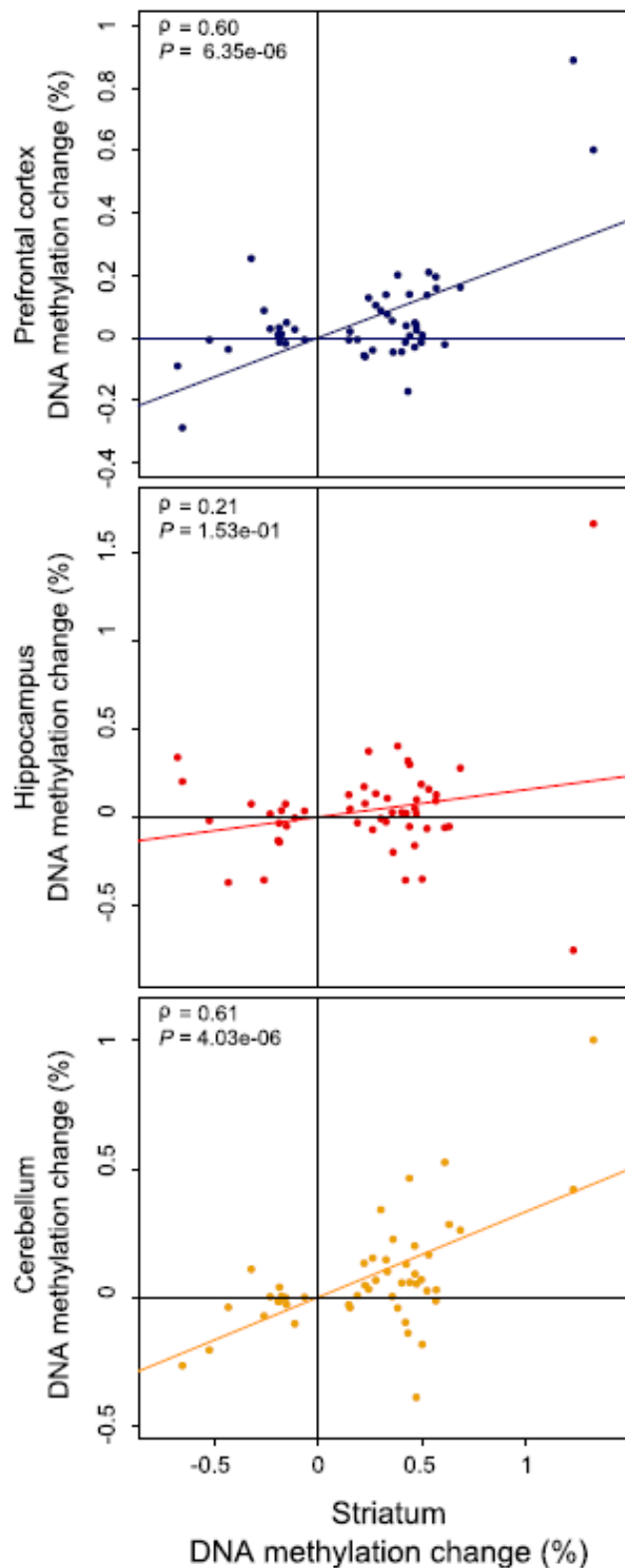


Figure 4.21. Correlation between DNA methylation differences for the fifty top ranked polygenic risk score (PRS)-associated probes identified in the striatum and the DNA methylation differences in the same probes in the remaining brain regions (y-axis). Prefrontal cortex = blue; hippocampus = red; cerebellum = orange. ρ = Pearson's correlation coefficient. The DNA methylation difference is measured per PRS unit.

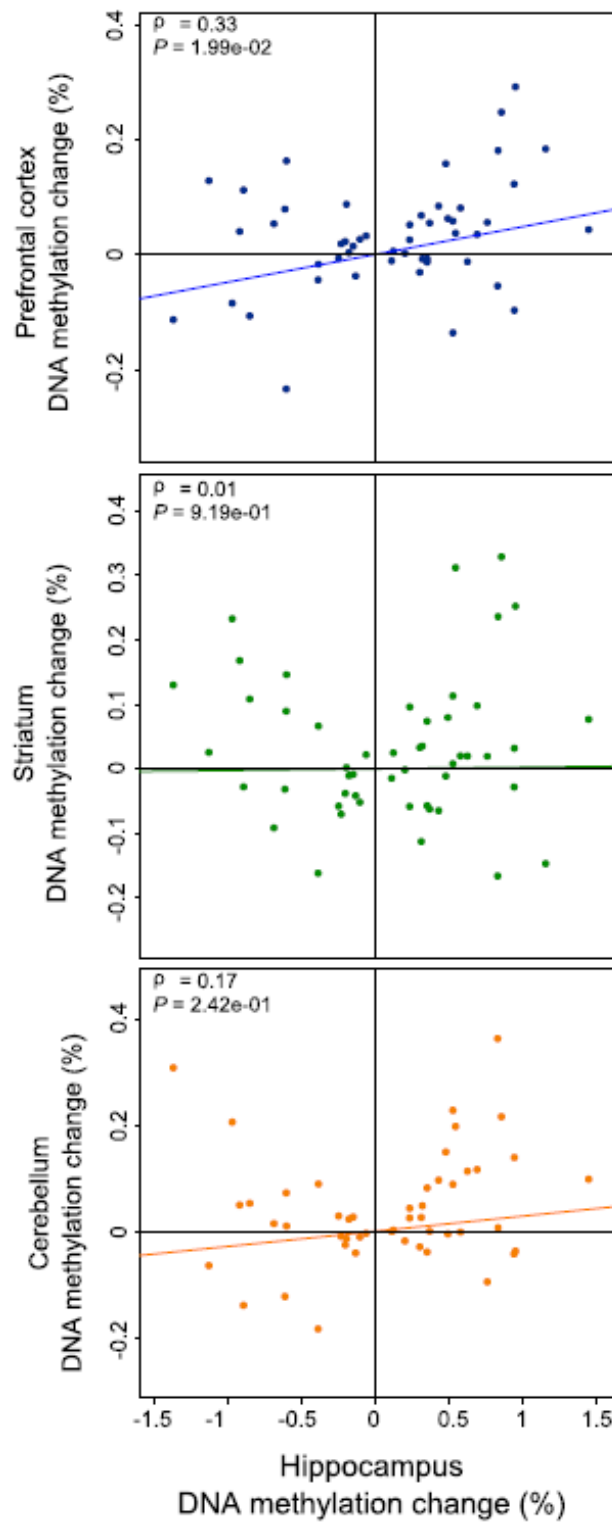


Figure 4.22. Correlation between DNA methylation differences for the fifty top ranked polygenic risk score (PRS)-associated probes identified in the hippocampus and the DNA methylation differences in the same probes in the remaining brain regions (y-axis). Prefrontal cortex = blue; striatum = green; cerebellum = orange. ρ = Pearson's correlation coefficient. The DNA methylation difference is measured per PRS unit.

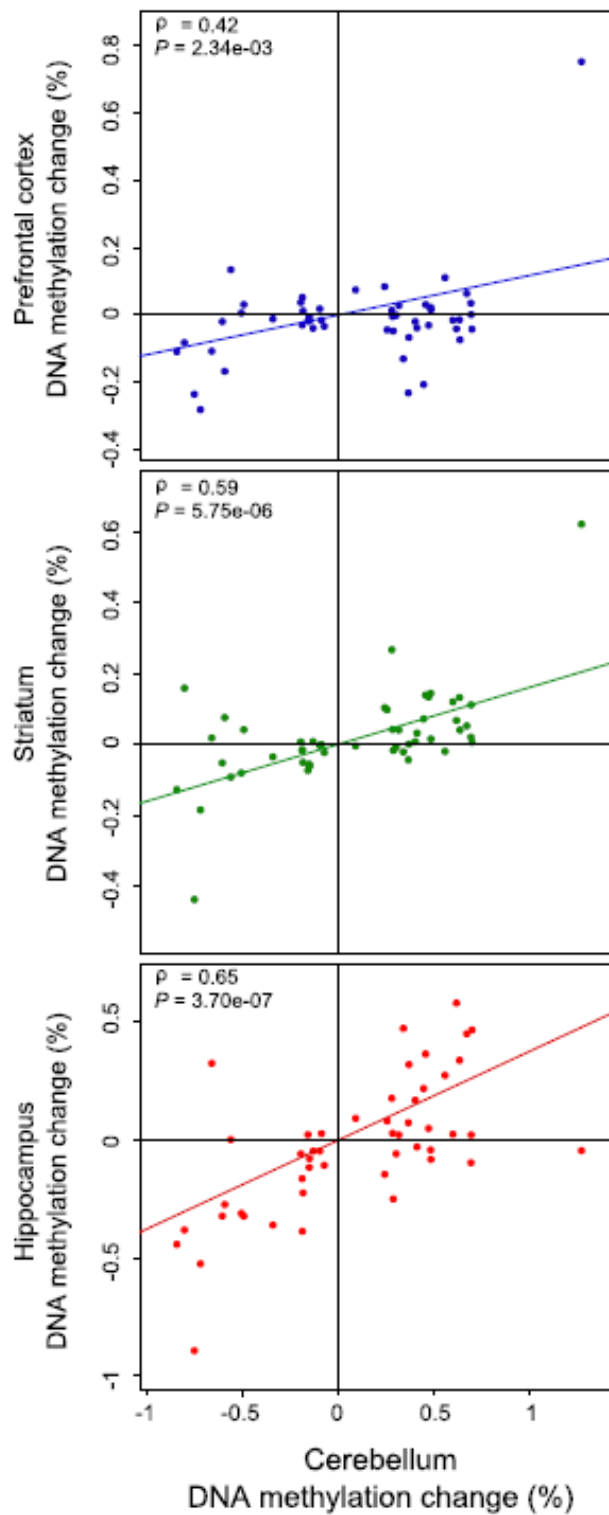


Figure 4.23. Correlation between DNA methylation differences for the fifty top ranked polygenic risk score (PRS) associated probes identified in the cerebellum and the DNA methylation differences in the same probes in the remaining brain regions (y-axis). Prefrontal cortex = blue; striatum = green; hippocampus = red. ρ = Pearson's correlation coefficient. The DNA methylation difference is measured per PRS unit.

Table 4.8. Correlation between DNA methylation differences for the fifty top ranked polygenic risk score schizophrenia-associated probes identified in each brain region and the DNA methylation differences in the same probes in the remaining brain regions. Presented are the Pearson's correlation coefficient (ρ) and the associated P -values.

50 top ranked probes	Prefrontal cortex		Striatum		Hippocampus		Cerebellum	
	ρ	P	ρ	P	ρ	P	ρ	P
	Prefrontal cortex	-	-	0.50	2.90E-04	0.64	7.35E-07	0.52
Striatum	0.60	6.40E-06	-	-	0.21	0.15	0.61	4.03E-06
Hippocampus	0.33	0.02	0.01	0.92	-	-	0.17	0.24
Cerebellum	0.42	0.00	0.59	5.75E-06	0.65	3.70E-07	-	-

4.3.2.1. Enrichment of overlap between polygenic risk score-associated differently methylated positions and regulatory features

The Illumina 450K array probes were annotated to TFBSs and DHSs using published data (Slieker et al., 2013, ENCODE Project Consortium, 2012, Maurano et al., 2012) and the overlap between PRS-associated DMPs identified in the different brain regions and these regulatory features tested for enrichment using a two sided Fisher's 2x2 exact test (Fisher, 1922). **Tables 4.9** to **4.12** present the results of these tests for all brain regions.

The fifty top ranked and DMPs with a P -value $< 1.00E-03$ show no significant enrichment for probes overlapping DHS or TFBS in any of the brain regions at the Bonferroni corrected threshold for the twenty-four tests ($P = 2.08E-03$). DMPs with a P -value < 0.05 show a significant under-enrichment for probes overlapping TFBS in the PFC (**Table 4.9**), STR (**Table 4.10**) and CER (**Table 4.12**), but not the HC (**Table 4.11**). The same set of probes show a significant under-enrichment for probes overlapping DHS in the PFC (**Table 4.9**) but not the other brain regions.

Table 4.9. Results of the Fisher's 2x2 exact tests for significant overlap between polygenic risk score-associated differently methylated positions (DMPs) in the prefrontal cortex and regulatory features. Shown are the results for overlap enrichment with the 50 top ranked probes, DMPs with an association P -value $< 1.00E-03$ and DMPs with an association P -value < 0.05 . DHS, DNA hypersensitivity sites; TFBS, transcription factor binding sites.

	DHS		TFBS	
	Odds ratio	P	Odds ratio	P
Top ranked 50	1.31	0.40	1.00	1.00
$P < 1.00E-03$	0.84	0.04	0.90	0.22
$P < 0.05$	0.92	8.11E-09	0.92	3.13E-08

Table 4.10. Results of the Fisher’s 2x2 exact tests for significant overlap between polygenic risk score-associated differently methylated positions (DMPs) in the striatum and regulatory features. Shown are the results for overlap enrichment with the 50 top ranked probes, DMPs with an association *P*-value < 1.00E-03 and DMPs with an association *P*-value < 0.05. DHS, DNA hypersensitivity sites; TFBS, transcription factor binding sites.

	DHS		TFBS	
	Odds ratio	<i>P</i>	Odds ratio	<i>P</i>
Top ranked 50	1.13	0.78	0.67	0.20
<i>P</i> < 1.00E-03	1.06	0.31	0.89	0.04
<i>P</i> < 0.05	0.99	0.43	0.88	1.26E-22

Table 4.11. Results of the Fisher’s 2x2 exact tests for significant overlap between polygenic risk score-associated differently methylated positions (DMPs) in the hippocampus and regulatory features. Shown are the results for overlap enrichment with the 50 top ranked probes, DMPs with an association *P*-value < 1.00E-03 and DMPs with an association *P*-value < 0.05. DHS, DNA hypersensitivity sites; TFBS, transcription factor binding sites.

	DHS		TFBS	
	Odds ratio	<i>P</i>	Odds ratio	<i>P</i>
Top ranked 50	1.04	0.89	1.18	0.57
<i>P</i> < 1.00E-03	0.94	0.57	1.00	1.00
<i>P</i> < 0.05	1.00	0.97	1.04	5.29E-03

Table 4.12. Results of the Fisher’s 2x2 exact tests for significant overlap between polygenic risk score-associated differently methylated positions (DMPs) in the cerebellum and regulatory features. Shown are the results for overlap enrichment with the 50 top ranked probes, DMPs with an association *P*-value < 1.00E-03 and DMPs with an association *P*-value < 0.05. DHS, DNA hypersensitivity sites; TFBS, transcription factor binding sites.

	DHS		TFBS	
	Odds ratio	<i>P</i>	Odds ratio	<i>P</i>
Top ranked 50	0.74	0.32	0.56	0.05
<i>P</i> < 1.00E-03	0.94	0.37	0.89	0.11
<i>P</i> < 0.05	0.97	9.68E-03	0.91	7.87E-13

4.3.3. Differently methylated regions associated with schizophrenia polygenic risk score

I used *comb-p* (Pedersen et al., 2012) to identify spatially correlated regions of differential DNA methylation associated with schizophrenia PRS (Šidák-corrected $P < 0.05$, number of consecutive probes ≥ 2). PRS-associated DMRs in each of the four brain regions are listed in **Table 4.13** and **Figure 4.24**. Although all PRS-associated DMRs were identified in just one brain region (**Table 4.13**), the majority are characterised by consistent effects across all brain regions (**Figure 4.24**). Interestingly, most DMRs show decreased DNA methylation with PRS (blue).

Two DMRs identified in the PFC spanning *RNF39* and *HLA-DPB2* reside within the major histocompatibility complex (MHC) on chromosome 6. The MHC *locus* spans several megabases on chromosome 16 and contains 18 highly polymorphic human leukocyte antigen (HLA) genes that encode proteins with antigen-presenting roles in the immune system (Benacerraf, 1981). Of note, genetic variants in the MHC *locus* have been strongly linked to schizophrenia GWAS studies (International Schizophrenia et al., 2009, Schizophrenia Working Group of the Psychiatric Genomics, 2014), highlighting the potential importance of the immune system in schizophrenia etiology already mentioned (**section 4.3.2**)

Table 4.13. Differentially methylated regions (DMRs) significantly associated with polygenic score for schizophrenia. Shown in chromosomal order is the location of significant (Šidák-corrected $P < 0.05$) DMRs identified in each of the four brain regions, with the median P -value for DMR probes given for the other three brain (bold denotes median $P < 0.05$ and grey boxes denote regions that were not identified in that brain region). The 'gene' column lists the combined Illumina and Genomic Regions Enrichment of Annotation Tool (GREAT) annotation (McLean et al., 2010).

Region	Gene	Probes	N probes	Prefrontal cortex		Cerebellum		Striatum		Hippocampus	
				Median P	Šidák P	Median P	Šidák P	Median P	Šidák P	Median P	Šidák P
chr1:84326547-84326857	TTL7	cg08882038; cg07807165; cg02531516; cg18116902; cg26347197; cg24955204; cg02483449	7	0.40		0.05	0.03	0.88		0.11	
chr1:168356537-168356674	TBX19; XCL2	cg22695117; cg20678082; cg10555800; cg06122518	4	0.02	0.02	0.13		0.39		0.14	
chr2:3486706-3487165	ADI1; TRAPPC12	cg14053828; cg15541040; cg15506890; cg08493051	4	0.03		2.82E-03	3.63E-04	0.03		0.84	
chr2:97405651-97405880	LMAN2L	cg13915892; cg04771938; cg17340948; cg17526658; cg12930819; cg04918358; cg15007626	7	0.66		5.73E-03	9.07E-03	0.59		0.57	
chr4:74847646-74848017	PF4	cg15158783; cg21043213; cg16072462; cg15398841; cg02530824; cg06834998; cg05509609; cg13126871	8	3.39E-03	2.10E-05	0.16		0.03		0.02	
chr5:102898463-102898730	NUDT12	cg02976617; cg13665998; cg09166085; cg07655627	4	2.27E-03	0.01	0.08		3.91E-03		0.31	
chr5:493262-493614	SLC9A3; EXOC3	cg19107578; cg25518170; cg20402284; cg25346936	4	0.76		1.17E-03	3.87E-04	0.67		0.72	
chr5:497397-497640		cg22985016; cg16555556; cg14533753; cg00190355	4	0.49		5.41E-03	0.05	0.17		0.82	
chr6:30042919-30043419	RNF39	cg12704854; cg11562284; cg02552311; cg03219282; cg24766429; cg23500724; cg10865856; cg24016627; cg23939808; cg12967914; cg00853042; cg23027574; cg05853632; cg22105332; cg19006429; cg27532187; cg01631162	17	0.06	2.99E-04	0.40		0.41		0.23	

chr6:33084549-33084841	HLA-DPB2; COL11A2	cg03943025; cg08693832; cg27264993; cg21870640; cg08088295; cg17833071; cg23075555; cg13524302; cg02662362; cg24465429; cg24266485	11	0.03	0.04	0.11	0.19	0.23
chr11:2907670-2907755	CDKN1C	cg05090695; cg11744767; cg05559445; cg23225147	4	1.08E-03	1.93E-04	0.08	0.40	0.06
chr12:75784617-75785098	GLIPR1L2	cg14292619; cg00108944; cg23588049; cg12351126; cg02415057; cg07311024; cg02071292	7	0.66		1.27E-03	2.49E-07	0.19
chr13:51417846-51418222	DLEU7; RNASEH2B; ST13P4	cg20170533; cg08274637; cg13846270; cg27051129; cg10359157; cg20400592; cg05965387; cg17288288; cg03389701	9	0.50		8.88E-03	5.83E-04	0.28
chr13:113540400-113540632	ATP11A; MCF2L	cg17842918; cg11462099; cg26666292; cg11520003	4	0.53		0.17	2.57E-03	0.70
chr16:66400320-66400600	CDH5	cg08872742; cg02078525; cg00401972; cg00044665; cg16471830; cg22319147	6	0.68		0.56	6.43E-03	0.74
chr19:2650727-2650864	GNG7; GADD45B	cg03070741; cg01250212; cg27324541; cg10350536	4	0.43		0.65	3.07E-03	0.72
chr19:11784514-11784956	ZNF833	cg04598224; cg05950877; cg26772540; cg25394203; cg21771200; cg15209566; cg02274869	7	0.44		4.66E-03	1.81E-04	0.66
chr19:17357315-17357642	NR2F6	cg06108395; cg20981127; cg16749578; cg24057642	4	0.44		4.68E-04	2.12E-07	0.13
chr19:47287964-47288264	SLC1A5; STRN4	cg02711608; cg25607249; cg21766592; cg12165685; cg11645155; cg01406381	6	0.33		0.51	1.52E-03	7.62E-05
chr20:30073399-30073577	NCRNA0028; HMT1; REM1	cg15537254; cg13159946; cg02991085; cg25502144; cg21846177	5	0.17		5.15E-04	2.06E-04	0.29
chr20:32308081-32308344	PXMP4	cg27194921; cg25092328; cg20589882; cg06231372; cg12297619; cg24270031	6	0.02		0.03	0.02	0.25
chr22:38071534-38071678	LGALS1	cg21064451; cg21737444; cg01264106; cg08885221; cg27619353; cg19853760	6	0.65		1.22E-03	2.30E-07	0.43

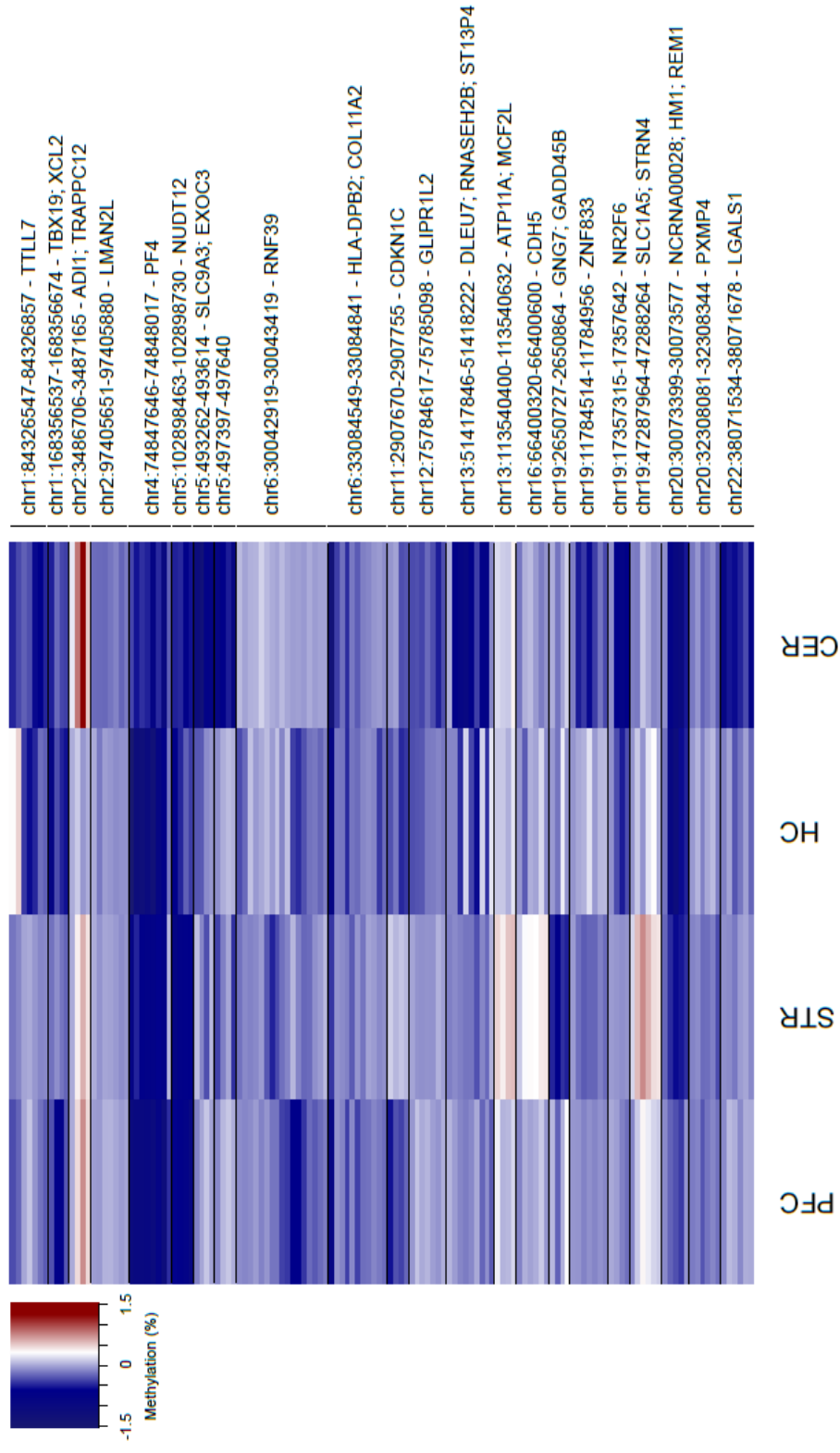


Figure 4.24. Differentially methylated regions (DMRs) associated with schizophrenia polygenic risk score. Shown in chromosomal order are DMRs associated with schizophrenia identified in any of the four brain regions. DNA methylation differences for individual probes within each DMR are also shown for the other three brain regions (blue = hypomethylation, red = hypermethylation).

4.3.4. Consistent methylomic markers of schizophrenia polygenic risk burden across brain regions

I next employed a multi-level model including data from the PFC, STR and HC (see **section 4.2.8**) to identify consistent PRS-associated DMPs across these brain regions. The QQ and Manhattan plots for this analysis are presented in **Figures 4.25** and **4.26**. There is some inflation in the distribution of P -values in the multi-region case-control analysis ($\lambda = 1.33$), although less than the inflation observed in the disease-controls multilevel analysis presented on **Chapter 3 (section 3.3.7)**.

Of interest, several DMPs were relevant in the context of schizophrenia:

- The top ranked PRS-associated DMP (cg04910228), at which PRS is negatively correlated with DNA methylation (estimate = -0.38%, $P = 6.50E-07$), is located within the *TSNAX-DISC1* locus on chromosome 1 (**Figure 4.27 A**). A balanced translocation involving this gene that segregates with several major psychiatric disorders including schizophrenia has been intensively studied in a Scottish pedigree (St Clair et al., 1990), although the involvement of this locus in the etiology of the disorder remains controversial and common genetic variation in this region was not identified in recent GWAS analyses (Sullivan, 2013, Porteous et al., 2014). These data suggest that an increased polygenic burden for schizophrenia may impact upon regulatory variation of the *DISC1* locus in the brain;

- cg08619378 is annotated to the gene body of the *adenylate cyclase 1* (*ADCY1*) gene and shows decreased DNA methylation with increased PRS across brain regions ($P = 1.73E-05$) (**Figure 4. 27 B**). The protein encoded by this gene is primarily expressed in the brain and its role is to couple Ca(2+) to cyclic AMP (cAMP), which is involved in synaptic functions such as long-term potentiation, long-term depression, and depotentiation, processes important for memory formation (Wang and Zhang, 2012, Wang et al., 2004)

- A probe annotated the 5'UTR of the *microtubule associated protein tau* (*MAPT*) gene decreases DNA methylation with PRS (cg26019600, $P = 2.99E-05$) (**Figure 4.27 C**). This gene encodes several different isoforms of the tau protein, which have a crucial role in keeping the function of microtubules and axonal transport. Several mutations in this gene have been strongly linked to

multiple neurodegenerative disorders including Alzheimer's disease, Parkinson's disease, frontotemporal dementia, amongst others (for a review see Zhang et al. (2015)).

Next I identified PRS-associated DMRs consistent across PFC, STR and HC using *comb-p* (Pedersen et al., 2012) in the *P*-values from the cross-region multilevel model. Top ranked cross-region DMPs associated with schizophrenia PRS are presented in **Table 4.14** and **Figure 4.28** and DMRs are presented in **Table 4.15** and **Figure 4.29**.

Of interest:

- A PRS-associated DMR of 6 probes spanning *WNT5A* is within the schizophrenia-associated DMR spanning 11 probes in the same gene described in **Chapter 3 section 3.3.7**. This is an important cross-brain region association with both schizophrenia polygenic risk burden and schizophrenia diagnosis given the previously discussed neurodevelopmental relevance of this *locus* (**Chapter 3 section 3.3.6.1**).

- In addition to the 17 probe-wide DMR spanning *RNF39* that was identified again (see above **section 4.3.3**), another PRS-associated DMR within the MHC region in chromosome 6 was identified in the cross-brain region model (*HLA-J*), reinforcing the association of DNA methylation variation at *loci* within this region with schizophrenia polygenic risk burden.

- Another DMR is annotated to the *lymphocyte-specific protein 1 (LSP1)* gene which encodes an intracellular F-actin binding protein expressed in immune cells such as lymphocytes, neutrophils and macrophages (Pulford et al., 1999).

- A DMR in chromosome 16 is annotated to the *interferon regulatory factor 8 (IRF8)* gene, which encodes a protein that plays an important role in immune cells differentiation and cell fate (Yanez and Goodridge, 2016).

- A DMR spanning 7 probes in the *glial cell derived neurotrophic factor (GDNF)* gene shows significant association with schizophrenia PRS. This gene encodes a neurotrophic factor that promotes the differentiation and survival to different types of neurons and has been implicated in Parkinson's disease (Ibanez, 2008). GDNF has been shown to be important for the survival of

catecholaminergic neuron survival (these include dopaminergic, epinephrine and norepinephrine neurons) both *in vivo* (Pascual et al., 2008) and *in vitro* (Lin et al., 1993), although this has recently been disputed (Kopra et al., 2015).

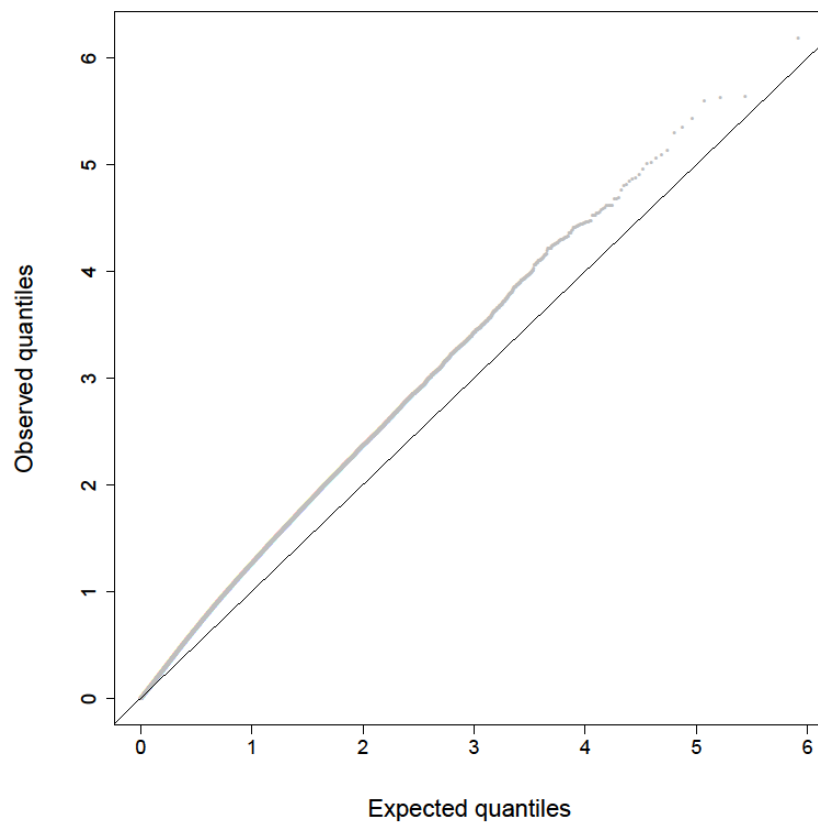


Figure 4.25. Quantile-quantile plot for the schizophrenia polygenic risk score EWAS. Shown are the expected (x-axis) and observed (y-axis) quantiles observed in the multi-level model including data from the PFC, STR and HC.

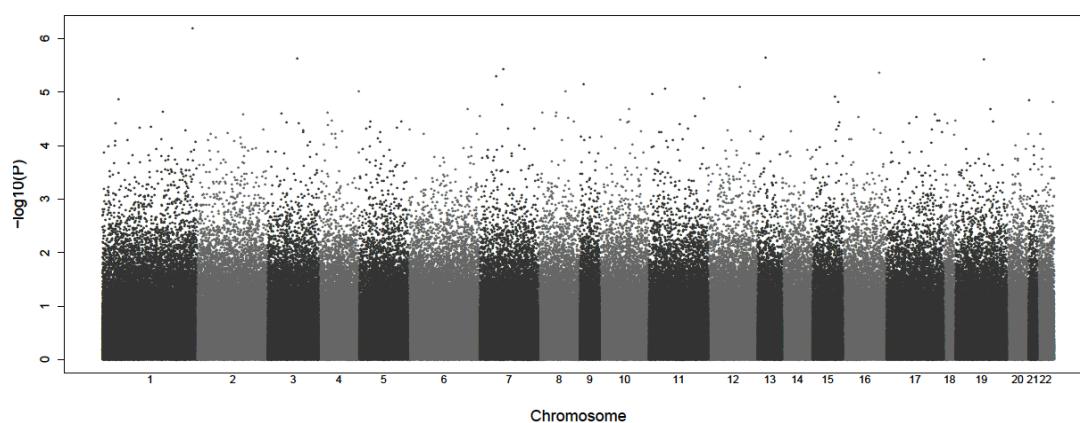


Figure 4.26. Manhattan plot for the schizophrenia polygenic risk score EWAS. Shown are the $-\log_{10}(P\text{-values})$ (y-axis) of the multi-level model including data from the PFC, STR and HC by chromosomal position (x-axis).

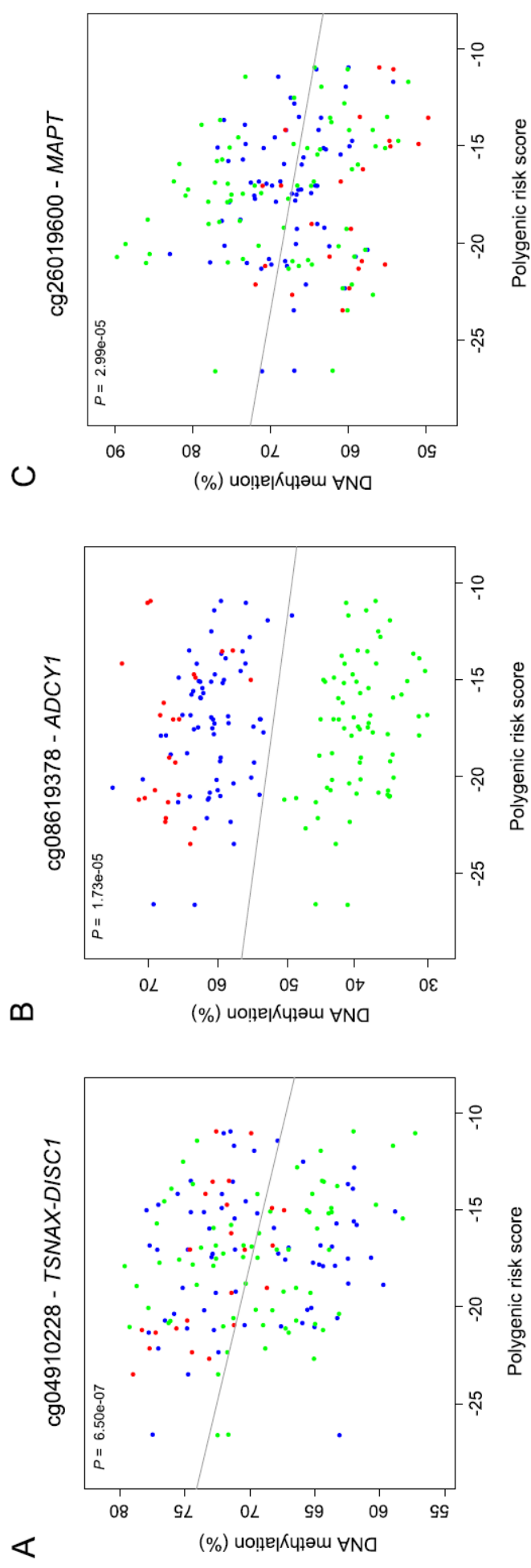


Figure 4.27. Examples of top ranked schizophrenia polygenic risk score-associated differentially methylated positions in the multilevel model including data from the prefrontal cortex (blue), striatum (green) and hippocampus (red).

Table 4.14. Top ranked polygenic risk score-associated differentially methylated probes (DMPs) identified in the multiregion model incorporating the prefrontal cortex (PFC), striatum (STR) and hippocampus (HC) data. Listed for each DMP are corresponding results from the multilevel model (grey) and corresponding results from the prefrontal cortex (PFC; $P < 0.05$ in blue), striatum (STR; $P < 0.05$ in green) and hippocampus (HC; $P < 0.05$ in red) meta-analyses (PFC and STR) or linear regression (HC). Also shown is the association with schizophrenia diagnosis (multi-region model, $P < 0.05$ in purple). The DNA methylation difference is measured per PRS unit. Illumina and Genomic Regions Enrichment of Annotation Tool (GREAT) annotation (McLean et al., 2010) is listed for each DMP.

Probe ID	Genomic position (hg19)	Illumina gene annotation	Gene region	GREAT annotation (McLean et al., 2010)	Methylation difference (%) multilevel model	P multilevel model	Methylation difference PFC (%)	P PFC	Methylation difference STR (%)	P STR	Methylation difference HC (%)	P HC	Disease methylation difference (%)	Disease P
cg04910228	chr1:231739450	TSNAX-DISC1	Body	DISC1; TSNAX	-0.38	6.50E-07	-0.23	0.03	-0.43	8.49E-05	-0.54	4.56E-03	-0.97	0.09
cg00736454	chr13:44595496	LOC121838	TSS1500	ENOX1; SERP2	0.58	2.28E-06	0.83	2.06E-05	0.40	0.01	0.26	0.31	0.53	0.52
cg22930808	chr3:122281881	PARP9; DTX3L	5'UTR; TSS1500	DTX3L	0.41	2.33E-06	0.56	1.47E-05	0.39	9.87E-04	0.04	0.82	0.92	0.12
cg21062760	chr19:36205574	ZBTB32	Body	MLL4	-0.36	2.50E-06	-0.32	5.87E-03	-0.25	0.01	-0.59	0.05	-1.57	3.78E-03
cg01495332	chr7:50798564	GRB10	5'UTR; Body	DDC; GRB10	-0.52	3.67E-06	-0.28	0.10	-0.59	5.72E-04	-0.61	0.03	-1.93	0.02
cg09735146	chr16:85845936	-	-	IRF8; COX411	-0.49	4.39E-06	-0.40	9.68E-03	-0.27	0.06	-0.82	0.01	-1.99	6.11E-03
cg12988813	chr7:27946471	JAZF1	Body	TAX1BP1; JAZF1	0.42	4.98E-06	0.21	0.20	0.53	5.20E-06	0.16	0.49	1.09	0.08
cg14054620	chr9:38622748	C9orf122	Body	IGFBPL1; CNTNAP3	0.64	7.24E-06	0.14	0.40	0.70	3.82E-04	0.80	0.04	2.04	0.04
cg23539745	chr12:106142108	-	-	APPL2; NUAK1	0.63	8.04E-06	0.28	0.04	0.29	0.02	0.21	0.09	-0.95	0.30
cg07535191	chr11:27250166	-	-	BBOX1; LGR4	0.51	8.67E-06	0.26	0.12	0.48	1.34E-03	1.10	4.26E-03	1.96	7.97E-03
cg26064870	chr8:102944342	NCALD	5'UTR	NCALD; GRHL2	0.22	9.56E-06	0.05	0.47	0.36	7.84E-07	0.03	0.83	0.98	2.36E-03
cg09357276	chr4:188917856	ZFP42	5'UTR	ZFP42	-0.49	9.74E-06	-0.30	0.02	-0.44	2.70E-03	-0.75	0.07	-2.24	2.76E-03
cg26937267	chr11:1315171	TOLLIP	Body	TOLLIP; MUC5B	-0.42	1.09E-05	-0.26	0.04	-0.38	1.13E-03	-0.41	0.20	-1.44	0.03
cg24640510	chr15:80988694	FAM108C1	Body	KIAA1199; FAM108C1	0.27	1.24E-05	0.12	0.10	0.28	5.52E-03	0.42	0.01	0.48	0.25
cg26840462	chr11:125220543	PKNOX2	5'UTR	FEZ1; PKNOX2	-0.25	1.31E-05	-0.25	9.52E-03	-0.11	8.15E-03	-0.07	0.52	-0.56	0.16
cg11717194	chr1:11990078	-	-	PLOD1; KIAA2013	-0.34	1.37E-05	-0.34	2.07E-04	-0.30	0.01	-0.25	0.02	-1.57	2.28E-03
cg00324562	chr21:27106440	ATP5J; GABPA	5'UTR; Body; TSS1500	GABPA	-0.11	1.43E-05	-0.07	0.08	-0.09	0.01	-0.11	0.05	-0.47	2.50E-03

cg21245653	chr22:50426164	-	-	PIM3; MLC1	0.67	1.53E-05	0.66	1.09E-04	0.23	0.07	0.05	0.60	-0.90	0.37
cg12382398	chr15:90358537	ANPEP	TSS1500	ANPEP	-0.30	1.55E-05	-0.09	0.31	-0.36	3.55E-04	-0.57	0.03	-0.83	0.09
cg08619378	chr7:45616358	ADCY1	Body	IGFBP1; ADCY1	-0.47	1.73E-05	-0.51	3.05E-03	-0.48	1.73E-04	-0.19	0.50	-1.30	0.07
cg27247731	chr10:100994441	HPSE2	Body	HPSE2	-0.20	2.04E-05	-0.07	0.28	-0.22	4.81E-03	-0.46	3.18E-03	-0.59	0.07
cg13379208	chr6:142564220	-	-	GPR126; VTA1	0.40	2.06E-05	0.34	4.64E-03	0.35	2.10E-03	0.46	0.03	1.90	4.03E-03
cg18851960	chr19:43979739	PHLDB3	Body	LYPD3; ETHE1	-0.38	2.07E-05	-0.35	5.42E-03	-0.31	6.27E-03	-0.29	0.34	-1.20	0.05
cg00224508	chr1:151031323	CDC42SE1; MLLT11	5'UTR; TSS1500	MLLT11; CDC42SE1	-0.14	2.37E-05	-0.07	0.15	-0.20	5.04E-04	-0.14	0.04	-0.86	7.84E-05
cg24149904	chr8:6691719	XKR5	Body	XKR5; AGPAT5	-0.36	2.38E-05	-0.22	0.10	-0.33	0.01	-0.58	0.03	-1.39	0.02
cg24388251	chr8:55618220	-	-	XKR4; RP1	0.40	2.41E-05	0.39	9.41E-04	0.16	0.16	0.39	0.11	1.84	2.41E-03
cg01275038	chr4:7287492	SORCS2	Body	SORCS2; PSAPL1	0.52	2.42E-05	0.33	0.03	0.48	5.68E-03	1.06	1.87E-04	2.93	4.02E-04
cg07304068	chr3:47823820	SMARCC1	TSS1500	SMARCC1	-0.09	2.53E-05	-0.03	0.18	-0.11	9.63E-04	-0.13	0.07	-0.44	2.89E-03
cg26574247	chr17:77712786	ENPP7	3'UTR	CBX2; ENPP7	0.39	2.59E-05	0.42	5.88E-03	0.24	0.03	0.37	0.17	1.31	0.03
cg16429927	chr2:172430723	-	-	DYNC112; CYBRD1	-0.31	2.61E-05	-0.18	0.13	-0.37	2.20E-04	-0.45	0.02	-1.46	2.95E-03
cg22133973	chr6:170789640	-	-	PSMB1; FAM120B	-0.39	2.79E-05	-0.22	0.07	-0.39	2.20E-03	-0.72	0.03	-1.42	0.05
cg20645973	chr11:102402091	MMP7	TSS1500	MMP7	0.31	2.80E-05	0.26	0.03	0.18	0.06	0.30	0.15	1.24	7.97E-03
cg26205771	chr8:53851156	NPBWR1	TSS1500	NPBWR1	-0.36	2.81E-05	-0.22	0.04	-0.27	0.02	-0.25	0.10	-1.50	0.02
cg26019600	chr17:43978704	MAPT	5'UTR	STH; MAPT	-0.57	2.99E-05	-0.41	0.02	-0.42	0.03	-0.80	0.04	-2.81	1.59E-03
cg27662639	chr16:22312063	POLR3E	5'UTR	POLR3E; CDR2	-0.34	2.99E-05	-0.24	0.08	-0.38	5.83E-04	-0.42	0.04	-1.56	5.79E-03
cg25448355	chr8:121224799	COL14A1	Body	COL14A1; MRPPL13	0.33	2.99E-05	0.10	0.41	0.30	4.86E-03	0.36	0.09	0.16	0.77
cg26960370	chr10:73576410	PSAP	3'UTR	C10orf54; PSAP	-0.23	3.34E-05	-0.21	0.03	-0.15	0.04	-0.19	0.19	-1.01	7.03E-03
cg19746982	chr18:775252568	-	-	KCNG2; CTDP1	0.32	3.37E-05	0.28	0.02	0.30	2.77E-03	0.14	0.44	0.73	0.15
cg02289038	chr4:24915774	CCDC149	TSS1500; 5'UTR	LG2; SOD3	0.21	3.40E-05	0.06	0.40	0.19	2.02E-03	0.47	5.61E-03	0.90	0.01
cg18268547	chr17:79615552	TSPAN10	3'UTR	TSPAN10; PDE6G	-0.45	3.42E-05	-0.52	6.02E-03	-0.53	2.18E-04	-0.19	0.61	-1.45	0.04
cg15022015	chr17:78869527	RPTOR	Body	CHMP6; RPTOR	0.18	3.44E-05	0.10	0.17	0.28	3.82E-06	0.13	0.12	0.46	0.10
cg02683714	chr8:142500299	FLJ43860	Body	FLJ43860; PTP4A3	0.76	3.49E-05	0.32	0.11	0.34	9.76E-04	0.17	0.24	-0.87	0.46
cg21886364	chr5:39398185	DAB2	5'UTR	C9; DAB2	0.88	3.52E-05	0.68	6.07E-03	0.81	3.11E-04	0.55	0.18	0.39	0.78
cg23504719	chr10:99735010	CRTAC1	Body	CRTAC1; GOLGA7B	-0.65	3.56E-05	-0.49	0.02	-0.71	2.16E-04	-0.87	0.01	-2.71	0.01
cg13652372	chr19:46177461	MIR642; GIPR	TSS1500; Body	GIPR; SNRPD2	0.18	3.60E-05	0.04	0.61	0.22	1.16E-04	0.22	0.09	0.72	8.89E-03
cg27328876	chr5:172098275	NEURL1B	Body	NEURL1B; DUSP1	0.14	3.61E-05	0.04	0.44	0.08	0.06	0.30	8.96E-03	0.66	7.08E-03
cg27292417	chr3:53850724	CHDH	3'UTR	CHDH; CACNA1D	0.64	3.70E-05	0.32	0.06	0.57	0.01	1.41	2.44E-03	1.55	0.13
cg09504568	chr15:93127028	-	-	FAM174B; ST8SIA2	0.72	3.70E-05	0.52	3.67E-03	0.30	0.05	0.03	0.75	-1.04	0.36
cg20276630	chr10:97055439	-	-	PDLIM1	-0.28	3.75E-05	-0.23	0.01	-0.21	0.08	-0.31	0.08	-1.05	0.02
cg17865653	chr18:22005767	IMPACT	TSS1500	IMPACT	0.21	3.79E-05	0.18	0.03	0.14	0.02	0.32	0.11	0.91	8.87E-03

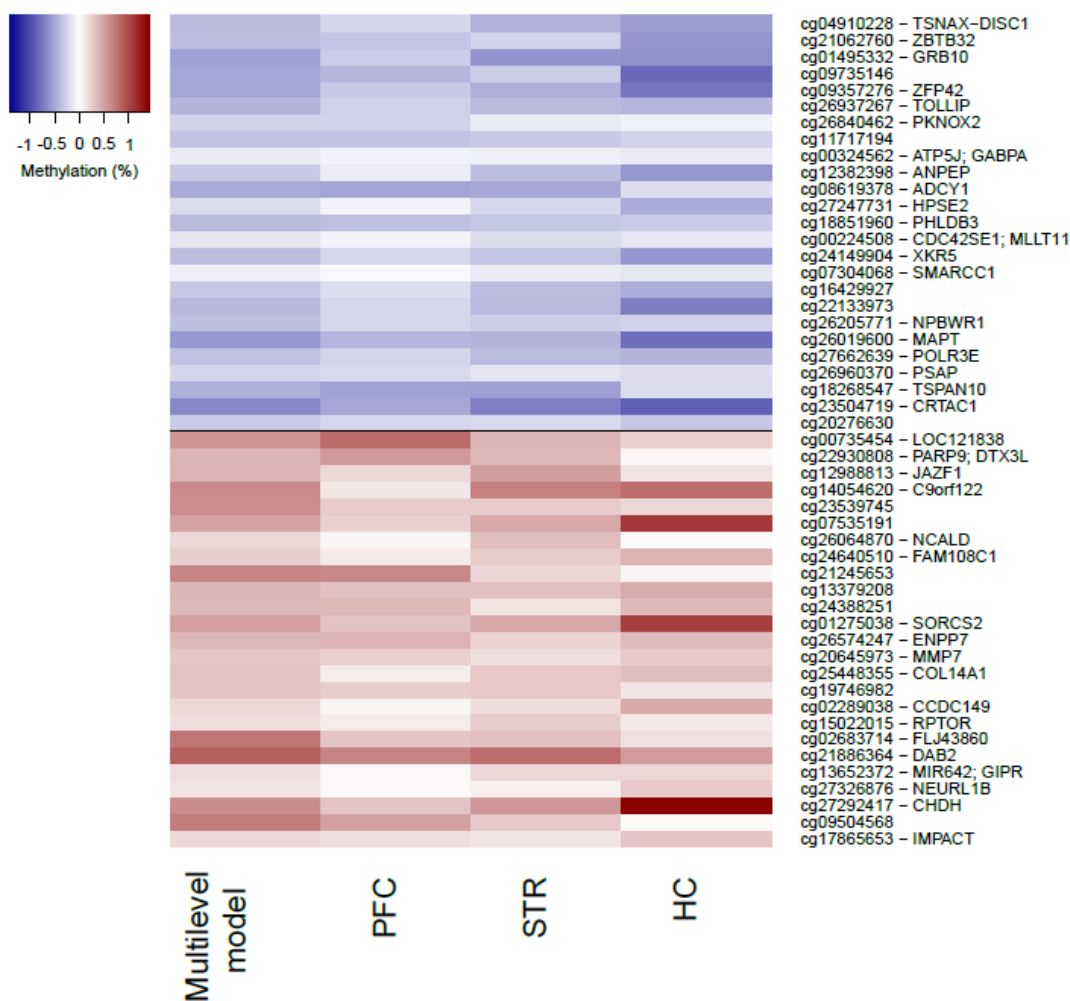


Figure 4.28. Heatmap showing the fifty top ranked differentially methylated positions associated with schizophrenia polygenic risk score identified using a multi-region model incorporating prefrontal cortex (PFC), striatum (STR) and hippocampus (HC). Shown for each probe is the DNA methylation effect size, with the corresponding difference at the same probe for the three individual brain regions. Probes are ordered by *P*-value for PRS-associated hypomethylation (blue, top) and hypermethylation (red, bottom) *loci* from the multi-region model.

Table 4.15. Significant polygenic risk score-associated differently methylated regions (DMRs) identified in the multilevel model incorporating the prefrontal cortex, striatum and hippocampus data. Shown in chromosomal order is the location of significant (Šidák-corrected $P < 0.05$) DMRs identified in the multilevel model. The column “Gene” represents the combined Illumina and Genomic Regions Enrichment of Annotation Tool (GREAT) annotation (McLean et al., 2010).

Region	Gene	Probes	N probes	Median P	Šidák P
chr1:156358116-156358613	<i>RHBG</i> ; <i>C1orf61</i>	cg24361162; cg098989644; cg12062819; cg23842796; cg20433275; cg15575683	6	2.34E-03	1.05E-04
chr3:55517806-55518143	<i>WNT5A</i> ; <i>LRTM1</i>	cg27364162; cg18562578; cg18010752; cg17679453; cg04941246; cg24216596	6	4.56E-03	0.02
chr4:74847646-74847830	<i>PF4</i>	cg15158783; cg21043213; cg16072462; cg15398841; cg02530824; cg06834998; cg05509609	7	7.45E-03	9.05E-03
chr5:37834672-37835169	<i>GDNF</i> ; <i>NUP155</i>	cg07423205; cg21590264; cg26473844; cg18725867; cg08204023; cg18182111; cg20683765	7	1.90E-03	1.73E-06
chr5:92908771-92909070	<i>FLJ42709</i> ; <i>NR2F1</i>	cg02020829; cg22217860; cg06668065	3	2.71E-04	0.03
chr5:102898223-102898730	<i>NUDT12</i>	cg07666882; cg02976617; cg13665998; cg09166085; cg07655627	5	1.21E-03	1.15E-04
chr6:28583971-28584289	<i>SCAND3</i> ; <i>TRIM27</i>	cg01400884; cg02246609; cg01309870; cg04626491; cg09470274; cg20450471; cg09897374; cg00919411; cg15967709; cg03682719; cg20839206; cg22121557; cg03858673; cg24114014; cg04645150; cg11111740	16	0.02	5.28E-03
chr6:29974715-29975081	<i>HLA-J</i> ; <i>NCRNA00171</i>	cg04566848; cg24725574; cg01814945; cg23313031; cg19448822; cg13207333; cg11867546; cg23483840; cg08163199; cg25318809; cg14781281; cg08325845; cg15726260; cg12976581; cg144432143; cg21330423; cg09659004; cg15364169	18	0.03	0.02
chr6:30042919-30043419	<i>RNF39</i>	cg12704854; cg11562284; cg02552311; cg03219282; cg24766429; cg23500724; cg10865856; cg24016627; cg23939808; cg12967914; cg00853042; cg23027574; cg05853632; cg22105332; cg19006429; cg27532187; cg01631162	17	0.02	7.36E-04

chr6:30853948-30854234	<i>DDR1</i>	cg16215084; cg25251478; cg26321999; cg00934322; cg07187855; cg24566261; cg09965419; cg17091577	8	9.06E-03	0.02
chr6:42927993-42928346	<i>GMMT</i>	cg25671484; cg16682276; cg23093754; cg24153763; cg27588902; cg09436375; cg17345569; cg07941301; cg04013093; cg11409096; cg23696834	11	0.02	0.03
chr7:29519388-29519657	<i>CHN2; PRR15</i>	cg02844647; cg04635849; cg03100044; cg21251563; cg16920620; cg00615485	6	7.75E-03	0.03
chr7:95025736-95025956	<i>PON3; PON1; PON2</i>	cg07121856; cg23230584; cg08520743; cg08828819; cg04685170; cg15927196; cg15500865; cg25572105	8	0.02	0.01
chr7:156870822-156871089	<i>MNX1; UBE3C</i>	cg24880736; cg02456451; cg00173659	3	8.86E-04	0.03
chr8:37824306-37824766	<i>ADRB3</i>	cg02174634; cg23460057; cg10357888; cg01386493; cg19806221	5	5.97E-04	2.50E-04
chr10:99734912-99735203	<i>CRTAC1; GOLGA7B</i>	cg27110886; cg23504719; cg23245905; cg08930881	4	1.26E-03	0.01
chr11:1891872-1892393	<i>LSP1; TNNT3</i>	cg27261733; cg08276062; cg24552015; cg09989681; cg20331155; cg21529477; cg22043296; cg26897904; cg26868156; cg15079934; cg087566594	11	5.69E-03	8.89E-05
chr12:54070294-54070592	<i>ATP5G2</i>	cg17561241; cg02541613; cg22546318; cg02056144; cg22997177; cg27479634; cg19842134	7	1.72E-03	3.57E-04
chr16:85845626-85845937	<i>IRF8; COX4I1</i>	cg03889236; cg05312293; cg06521653; cg09735146	4	3.19E-03	8.76E-03
chr20:32308081-32308481	<i>PXMP4</i>	cg27194921; cg25092328; cg20588982; cg06231372; cg12297619; cg24270031; cg04730850	7	8.06E-03	6.46E-03
chr20:37230326-37230613	<i>C20orf95; ARHGAP40</i>	cg01025836; cg00557360; cg04608177; cg03356734; cg06301550; cg08438366	6	9.35E-04	3.18E-06

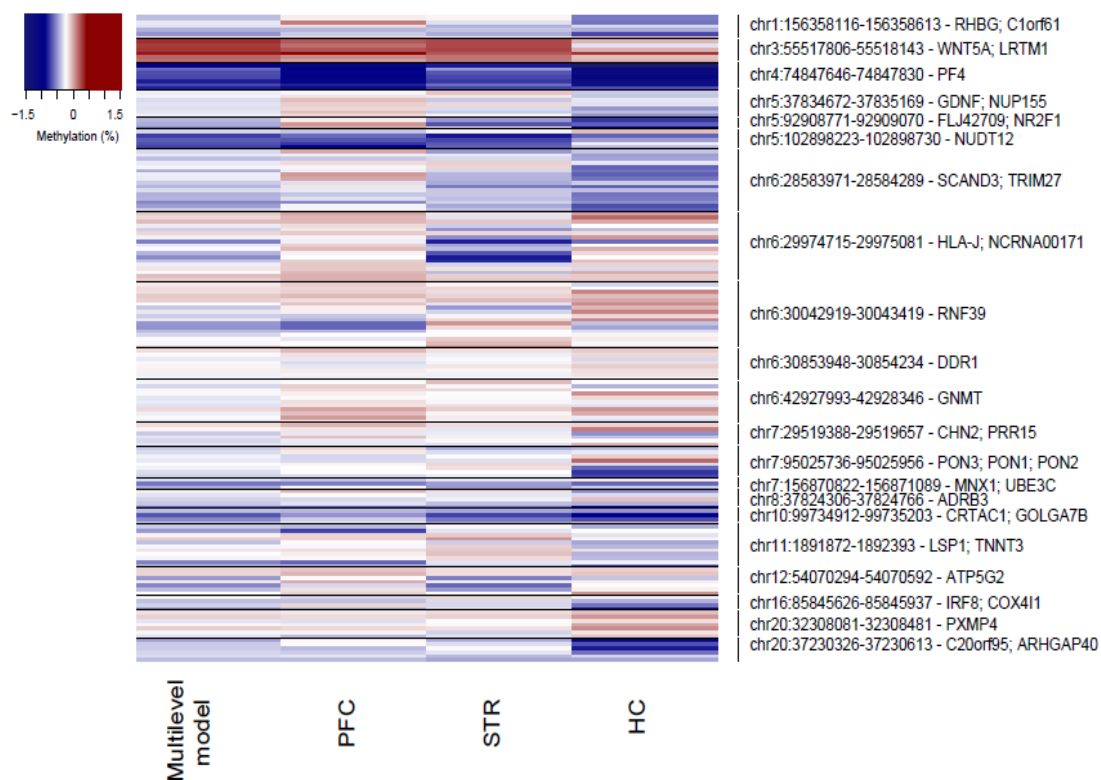


Figure 4.29. Heatmap showing differentially methylated regions (DMRs) associated with schizophrenia polygenic risk score (PRS) identified using a multi-region model incorporating prefrontal cortex (PFC), striatum (STR) and hippocampus (HC). Shown in chromosomal order are PRS DNA methylation differences in each of the significant DMRs, with disease-associated differences in the corresponding probes shown for the three individual brain regions (blue = hypomethylation, red = hypermethylation).

4.3.5. Comparison between methylomic analysis of schizophrenia PRS and diagnosed schizophrenia

In this section I compare the PRS EWAS results presented in this chapter with the schizophrenia EWAS results presented in **Chapter 3**. Of note, in this section I refer to both the ‘DNA methylation difference’ from the schizophrenia EWAS and the ‘DNA methylation change per PRS unit’ from the PRS EWAS as ‘effect size’ for simplicity. Although there is no direct overlap between the top ranked schizophrenia-associated DMPs (**Chapter 3 section 3.3.3 Tables 3.5 to 3.8**) and PRS-associated DMPs (**Tables 4.4 to 4.7**), as expected the effect sizes at the top ranked PRS-associated probes are significantly correlated with those at the same sites in the schizophrenia EWAS, and vice versa, across all brain regions (**Figures 4.30 to 4.33**).

Next, I investigated whether including PRS as an independent co-variate in the schizophrenia EWAS had any effects on the schizophrenia EWAS associations. Because the PRS analyses only included Caucasian samples, I repeated the schizophrenia EWAS (as described in **Chapter 3 section 3.2.6**) using only the samples included in the PRS analysis ($n = 88$), with and without the inclusion of PRS as a covariate and compared the results. For the top ranked schizophrenia-associated DMPs, there was a high correlation of effect size and P -value detected in the schizophrenia EWAS with those identified in the PRS EWAS across all four brain regions (Effect size: $\rho > 0.99$ in all brain regions; P -value: $\rho > 0.99$ in the PFC and CER, $\rho = 0.84$ in the STR and $\rho = 0.56$ in the HC), indicating that polygenic risk burden is not impacting greatly on schizophrenia-associated differences.

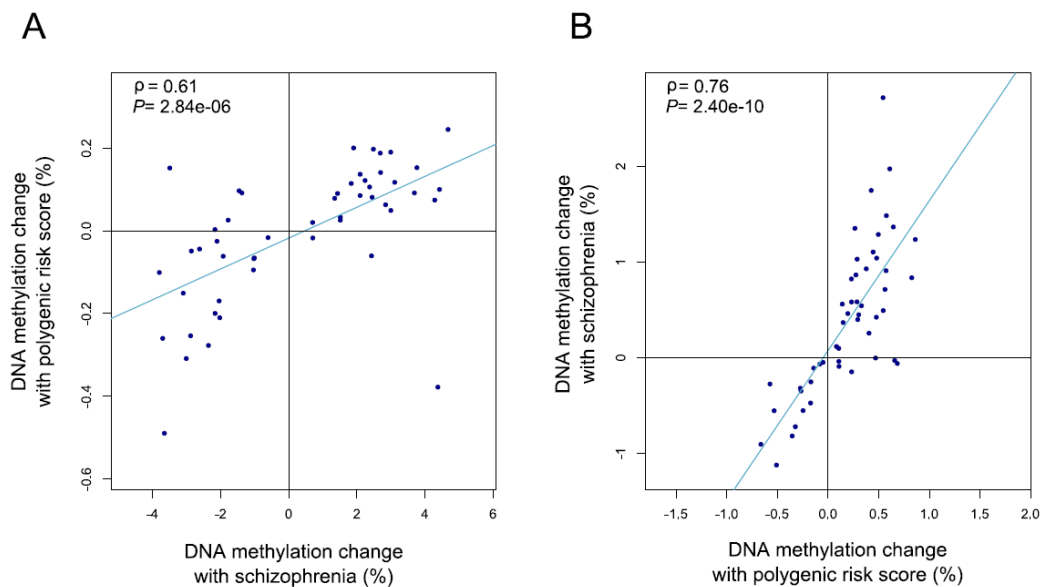


Figure 4.30. Correlation between schizophrenia case-control EWAS and schizophrenia polygenic risk score EWAS for the prefrontal cortex. A) Correlation between and effect sizes in the PRS EWAS (y-axis) for the DMPs identified in the case-control EWAS. B) Correlation between effect sizes in the PRS EWAS (x-axis) and DNA methylation differences in the case-control EWAS (y-axis) in the PRS EWAS.

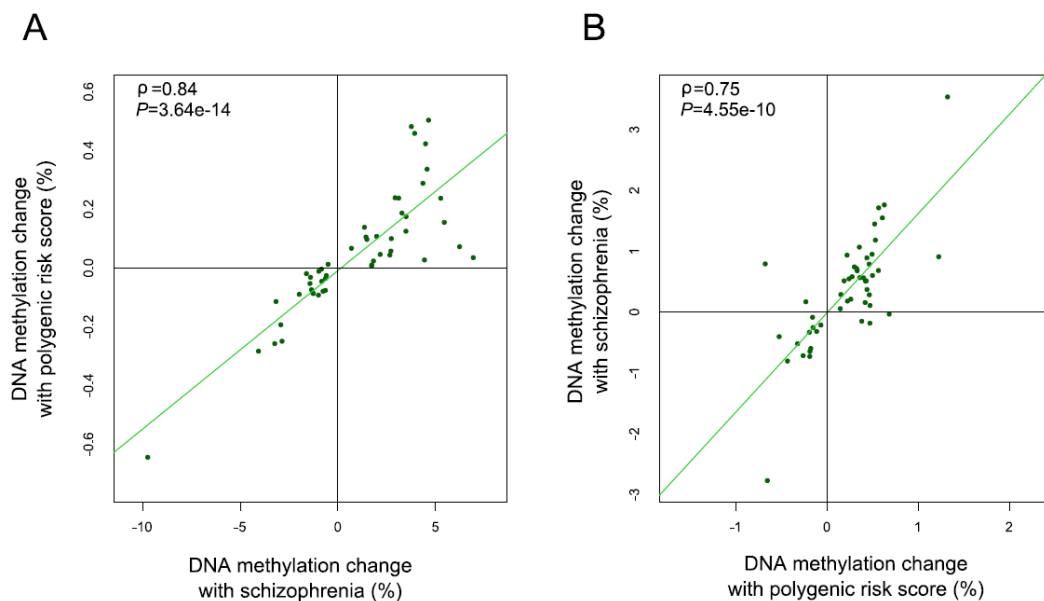


Figure 4.31. Correlation between schizophrenia case-control EWAS and schizophrenia polygenic risk score EWAS for the striatum. A) Correlation between and effect sizes in the PRS EWAS (y-axis) for the DMPs identified in the case-control EWAS. B) Correlation between effect sizes in the PRS EWAS (x-axis) and DNA methylation differences in the case-control EWAS (y-axis) in the PRS EWAS.

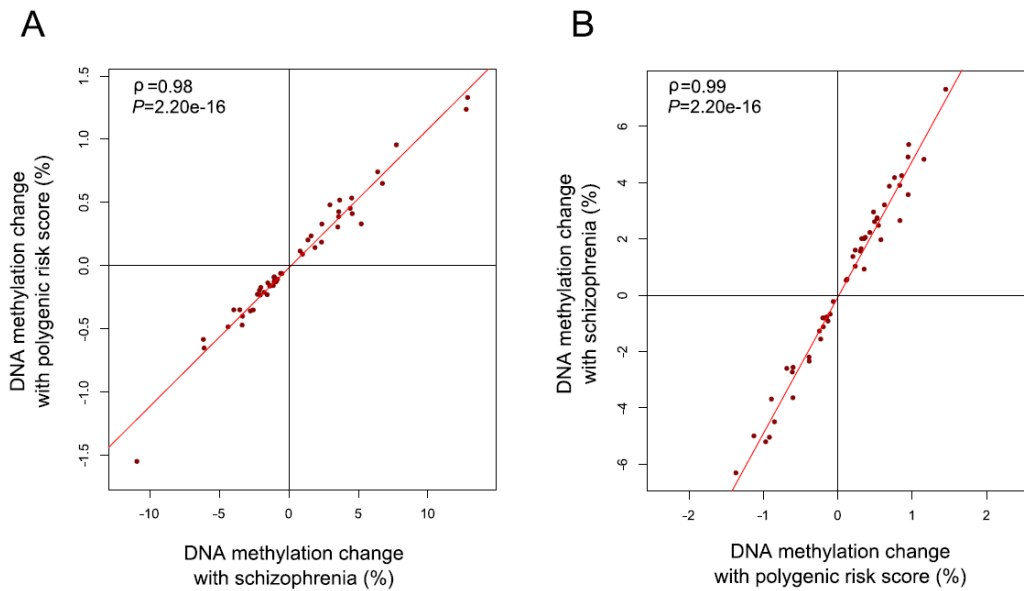


Figure 4.32. Correlation between schizophrenia case-control EWAS and schizophrenia polygenic risk score EWAS for the hippocampus. A) Correlation between and effect sizes in the PRS EWAS (y-axis) for the DMPs identified in the case-control EWAS. B) Correlation between effect sizes in the PRS EWAS (x-axis) and DNA methylation differences in the case-control EWAS (y-axis) in the PRS EWAS.

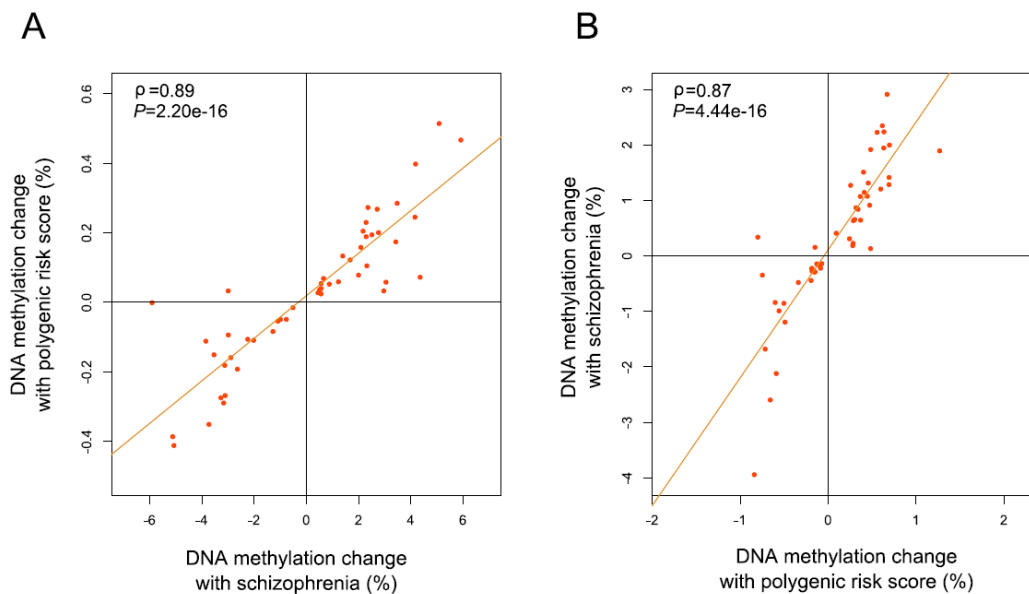


Figure 4.33. Correlation between schizophrenia case-control EWAS and schizophrenia polygenic risk score EWAS for the cerebellum. A) Correlation between and effect sizes in the PRS EWAS (y-axis) for the DMPs identified in the case-control EWAS. B) Correlation between effect sizes in the PRS EWAS (x-axis) and DNA methylation differences in the case-control EWAS (y-axis) in the PRS EWAS.

4.3.6. Polygenic risk score-associated methylomic variation does not reflect direct genetic effects on DNA methylation

A total of 5,006, 5,058, 5,066 and 4,951 Illumina 450K array probes included in the PFC, STR, HC and CER analyses, respectively, were located within genomic regions associated with schizophrenia in the latest schizophrenia GWAS (Schizophrenia Working Group of the Psychiatric Genomics, 2014). Interestingly, one of the top ranked PRS-associated DMPs was located within a GWAS-nominated genomic region - cg01682070 (annotated to *TAOK2*), at which DNA methylation was positively correlated with PRS in the CER ($P = 4.30E-08$) (this *locus* was discussed in **section 4.3.2**). Additionally, a number of nominally-significant PRS-associated DMPs ($P < 1.00E-03$) co-localize to GWAS regions (**Table 4.16**). However, despite this, none of the different sets of PRS-associated DMPs from any of the brain regions show a significant overlap with GWAS regions (**Table 3.17**) (Bonferroni corrected $P = 4.17E-03$).

To assess whether PRS associations were direct effects of genetic variation, mQTLs associated with the 99,904 variants used to derive the PRS were calculated, using linkage disequilibrium (LD)-pruned independent SNPs and a genome-wide mQTL significance threshold of $P = 3.69E-13$ (Hannon et al., 2016). Given the low number of samples from the HC, mQTL analyses were not performed for this brain region. In total we identified 255 associations between genetic variants and DNA methylation sites in the PFC, representing 198 unique SNPs (**Appendix A - Supplementary Table 6**), with 247 mQTL pairs (representing 201 independent SNPs) identified in the STR (**Appendix A - Supplementary Table 7**) and 282 mQTL pairs (representing 219 independent SNPs) identified in the CER (**Appendix A - Supplementary Table 8**). None of the top ranked PRS-associated DMPs in any of the three brain regions, in addition to those identified in the multi-region model, were significantly associated with any of the genetic variants included in the PRS calculation. Because it is possible that weaker-effect mQTLs may still underlie some of the PRS-associated epigenetic variation, I subsequently relaxed our mQTL significance threshold to $P < 1.00E-10$, again finding no overlap with PRS-associated DMPs (**Figure 4.34**). These data indicate that PRS-associated epigenetic variation does not directly result from genetic influences on DNA methylation in any of the brain regions tested.

Table 4.16. Polygenic risk score (PRS)-associated DMPs located within schizophrenia-associated regions from the largest schizophrenia GWAS to date (Schizophrenia Working Group of the Psychiatric Genomics, 2014). Listed are all probes significant at $P < 1.00E-03$ within the 108 genomic regions associated with schizophrenia in the GWAS analysis.

Probe	Brain region	Methylation difference (%)	P	P Rank	Illumina gene annotation	GWAS region	Best SNP	Min P
cg01682070	Cerebellum	0.32	4.20E-08	6	TAOK2	chr16:29924377-30144877	rs12691307	4.548E-11
cg17297362	Cerebellum	0.54	9.34E-06	134	KCNJ13; GIGYF2	chr2:233559301-233753501	rs6704768	2.315E-12
cg13060642	Cerebellum	0.29	2.58E-05	250	STAB1	chr3:52541105-52903405	rs2535627	4.264E-11
cg10581241	Cerebellum	-0.25	2.90E-05	268	MDK	chr11:46342943-46751213	chr11_46350213_D	1.259E-11
cg08365687	Cerebellum	0.30	3.24E-05	287	NT5DC2; LOC440957	chr3:52541105-52903405	rs2535627	4.264E-11
cg19852211	Prefrontal cortex	0.33	3.25E-05	40	PCDHA1; PCDHA2; PCDHA3; PCDHA4	chr5:140023664-140222664	chr5_140143664_I	4.849E-08
cg01816191	Cerebellum	0.45	4.77E-05	361	FXR1	chr3:180588843-181205585	chr3_180594593_I	1.301E-11
cg05682745	Prefrontal cortex	0.62	6.30E-05	58	SRPK2	chr7:104598064-105063064	rs6466055	1.127E-09
cg10301212	Cerebellum	0.21	7.17E-05	445	TAF5	chr10:104423800-105165583	rs11191419	6.198E-19
cg12841920	Cerebellum	0.41	7.81E-05	464	TRANK1	chr3:36843183-36945783	rs75968099	1.053E-13
cg170371491	Multilevel model	0.16	7.84E-05	108	-	chr11:57386294-57682294	rs9420	2.243E-09
cg20416874	Multilevel model	-0.32	8.36E-05	114	RERE	chr1:8411184-8638984	chr1_8424984_D	1.166E-09
cg08036435	Cerebellum	0.52	8.63E-05	496	TMTC1	chr12:29905265-29940365	rs679087	3.906E-08
cg24403305	Striatum	0.21	1.16E-04	199	MAD1L1	chr7:1896096-2190096	chr7_2025096_I	8.2E-15
cg25151353	Cerebellum	0.05	1.47E-04	696	DGKZ	chr11:46342943-46751213	chr11_46350213_D	1.259E-11
cg09524078	Cerebellum	-0.11	1.50E-04	704	NEK4	chr3:52541105-52903405	rs2535627	4.264E-11
cg01959848	Prefrontal cortex	0.16	1.61E-04	134	TMX2; MED19	chr11:57386294-57682294	rs9420	2.243E-09
cg13997124	Prefrontal cortex	-0.18	1.66E-04	137	ZNF323	chr6:28303247-28712247	rs115329265	3.48E-31
cg01758942	Cerebellum	0.29	1.85E-04	809	STAB1	chr3:52541105-52903405	rs2535627	4.264E-11
cg17432688	Prefrontal cortex	0.13	2.08E-04	163	-	chr12:123448113-	rs2851447	1.859E-14

cg08426047	Striatum	-0.20	2.22E-04	329	ZSCAN2	chr15:84661161-85153461	rs950169	1.618E-11
cg06094113	Cerebellum	-0.30	2.23E-04	910	BTBD18	chr11:57386294-57682294	rs9420	2.243E-09
cg03513874	Prefrontal cortex	0.23	2.35E-04	177	-	chr2:198148577-198835577	rs6434928	2.064E-11
cg09174610	Striatum	-0.09	2.35E-04	345	-	chr12:123448113-123909113	rs2851447	1.859E-14
cg01964765	Striatum	-0.19	2.63E-04	374	SETD8	chr12:123448113-123909113	rs2851447	1.859E-14
cg11915388	Cerebellum	-0.54	2.79E-04	1041	FAM109B	chr22:42315744-42689414	rs6002655	1.709E-09
cg08210507	Hippocampus	-1.08	2.83E-04	105	MAD1L1	chr7:1896096-2190096	chr7_2025096_I	8.2E-15
cg19784816	Cerebellum	0.49	2.84E-04	1054	ITIH1	chr3:52541105-52903405	rs2535627	4.264E-11
cg17037149	Striatum	0.16	3.11E-04	422	-	chr11:57386294-57682294	rs9420	2.243E-09
cg09075743	Striatum	0.33	3.29E-04	441	MAD1L1	chr7:1896096-2190096	chr7_2025096_I	8.2E-15
cg11558328	Multilevel model	-0.16	3.98E-04	433	ARHGAP1; ZNF408	chr11:46342943-46751213	chr11_46350213_D	1.259E-11
cg06789500	Hippocampus	-1.26	3.99E-04	151	MAD1L1	chr7:1896096-2190096	chr7_2025096_I	8.2E-15
cg25563625	Striatum	0.24	4.01E-04	509	PITPNM2	chr12:123448113-123909113	rs2851447	1.859E-14
cg23258881	Multilevel model	0.10	4.28E-04	467	PLEKHO1	chr1:14998890-150242490	rs140505938	4.487E-10
cg09482816	Cerebellum	0.05	4.64E-04	1462	LRP1	chr12:57428314-57682971	rs12826178	2.015E-12
cg10571824	Cerebellum	0.06	4.67E-04	1472	MAD1L1	chr7:1896096-2190096	chr7_2025096_I	8.2E-15
cg24333192	Cerebellum	-0.12	4.71E-04	1476	-	chr6:28303247-28712247	rs115329265	3.48E-31
cg06271067	Cerebellum	0.44	4.76E-04	1492	CUL3	chr2:225334096-225467796	rs11685299	1.115E-08
cg084260471	Multilevel model	-0.17	4.97E-04	547	ZSCAN2	chr15:84661161-85153461	rs950169	1.618E-11
cg00026230	Striatum	-0.10	5.24E-04	602	ALDOA	chr16:29924377-30144877	rs12691307	4.548E-11
cg27177954	Prefrontal cortex	-0.05	5.35E-04	341	L3MBTL2	chr22:41408556-41675156	rs9607782	2.069E-11
cg18296956	Hippocampus	-0.39	5.51E-04	206	VTRNA1-1	chr5:140023664-140222664	chr5_140143664_I	4.849E-08
cg01449141	Hippocampus	-0.20	5.57E-04	208	SCAND3	chr6:28303247-28712247	rs115329265	3.48E-31
cg02164492	Cerebellum	-0.17	5.65E-04	1682	-	chr11:46342943-46751213	chr11_46350213_D	1.259E-11

cg082105071	Multilevel model	-0.47	5.73E-04	638	MAD1L1	chr7:1896096-2190096	chr7_2025096_I	8.2E-15
cg04502927	Striatum	-0.14	6.16E-04	695	ZSWIM6	chr5:60499143-60843543	rs4391122	1.099E-14
cg02227292	Striatum	-0.73	6.21E-04	699	-	chr6:28303247-28712247	rs115329265	3.48E-31
cg05777052	Multilevel model	0.31	6.31E-04	686	-	chr15:40566759-40602237	rs56205728	4.178E-09
cg12555369	Hippocampus	0.86	6.55E-04	239	USMG5	chr10:104423800-105165583	rs11191419	6.198E-19
cg01364621	Multilevel model	0.19	7.05E-04	762	-	chr1:2372401-2402501	rs4648845	8.701E-10
cg00969047	Cerebellum	0.07	7.10E-04	1982	NXPH4	chr12:57428314-57682971	rs12826178	2.015E-12
cg02927836	Cerebellum	-0.22	7.46E-04	2024	CNNM2	chr10:104423800-105165583	rs11191419	6.198E-19
cg271779541	Multilevel model	-0.05	7.58E-04	801	L3MBTL2	chr22:41408556-41675156	rs9607782	2.069E-11
cg14915854	Cerebellum	-0.40	7.67E-04	2062	ZNF408; ARHGAP1	chr11:46342943-46751213	chr11_46350213_D	1.259E-11
cg16179182	Hippocampus	-0.96	7.76E-04	285	VTRNA1-1	chr5:140023664-140222664	chr5_140143664_I	4.849E-08
cg00749118	Striatum	0.37	7.98E-04	841	MAD1L1	chr7:1896096-2190096	chr7_2025096_I	8.2E-15
cg19925755	Cerebellum	0.32	8.02E-04	2128	NT5C2	chr10:104423800-105165583	rs11191419	6.198E-19
cg07251194	Prefrontal cortex	-0.26	8.14E-04	467	TSNAXIP1	chr16:67709340-68311340	rs8044995	1.513E-08
cg00055811	Cerebellum	0.53	8.18E-04	2157	RERE	chr1:8411184-8638984	chr1_8424984_D	1.166E-09
cg12846190	Cerebellum	-0.52	8.25E-04	2172	C10orf26	chr10:104423800-105165583	rs11191419	6.198E-19
cg16085276	Multilevel model	-0.06	8.40E-04	884	NDUFA6	chr22:42315744-42689414	rs6002655	1.709E-09
cg03315484	Cerebellum	-0.12	8.45E-04	2215	KDM3B	chr5:137598121-137948092	rs3849046	4.666E-09
cg24808162	Multilevel model	-0.28	8.76E-04	922	PTRF	chr1:44029384-44128084	rs11210892	3.394E-10
cg25974723	Striatum	-0.11	9.26E-04	949	PRR12	chr19:50067499-50135399	rs56873913	4.686E-08
cg06015834	Hippocampus	-0.65	9.33E-04	355	DOC2A	chr16:29924377-30144877	rs12691307	4.548E-11
cg03293350	Cerebellum	0.41	9.61E-04	2442	TCF4	chr18:52747686-53200117	rs9636107	3.337E-12
cg15518294	Cerebellum	0.48	9.92E-04	2485	NGEF	chr2:233559301-233753501	rs6704768	2.315E-12
cg072511941	Multilevel model	-0.18	9.99E-04	1051	TSNAXIP1	chr16:67709340-68311340	rs8044995	1.513E-08

Table 4.17. Results of the Fisher’s 2x2 exact tests for significant overlap between polygenic risk score-associated differently methylated positions (DMPs) in all the brain regions and GWAS regions Shown are the results for the overlap between the 50 top ranked probes, DMPs with an association *P*-value < 1.00E-03 and DMPs with an association *P*-value < 0.05. OR = odds ratio and probes within genomic regions associated with schizophrenia (Schizophrenia Working Group of the Psychiatric Genomics, 2014).

	PFC OR	PFC <i>P</i>	STR OR	STR <i>P</i>	HC OR	HC <i>P</i>	CER OR	CER <i>P</i>
Top ranked 50	1.66	0.46	0.00	1.00	0.00	1.00	1.67	0.46
P < 1.00E-03	1.09	0.83	1.17	0.53	1.52	0.24	0.85	0.53
P <0.05	0.97	0.71	1.02	0.71	0.94	0.29	0.98	0.76

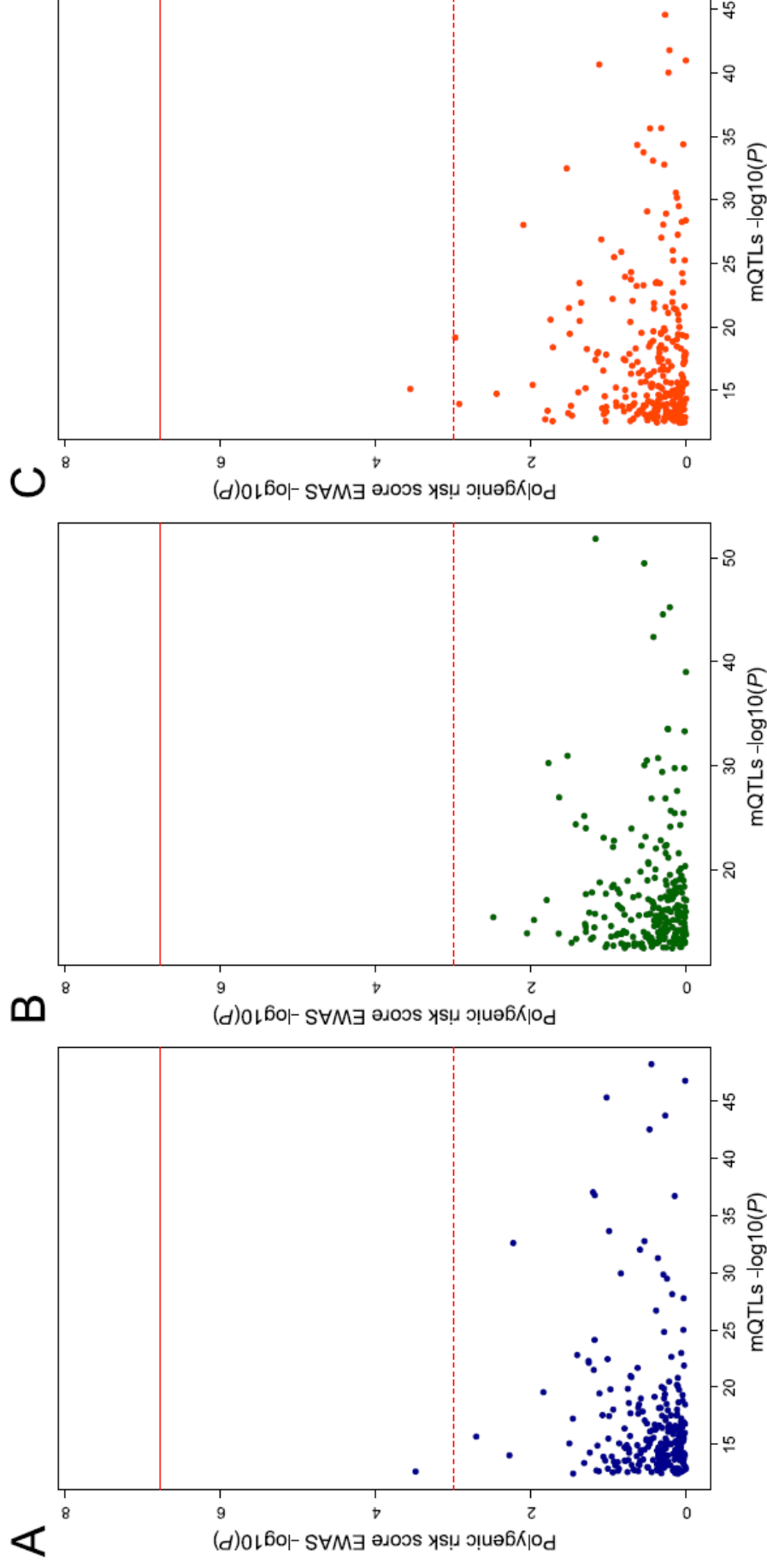


Figure 4.34. The relationship between lowest mQTL P -value and polygenic risk score (PRS) EWAS P -value for all DNA methylation probes associated ($P < 1.00E-10$) with genotype at a SNP incorporated in the schizophrenia PRS in prefrontal cortex (A), striatum (B) and cerebellum (C). The solid red line indicates a stringent PRS EWAS threshold of $P < 1.66E-07$. The dashed red line indicates a lenient PRS EWAS threshold of $P < 1.00E-03$.

4.4. Discussion

4.4.1. Overview of results

In this chapter I examined the association between DNA methylation and schizophrenia polygenic risk score in post-mortem brain samples isolated from PFC, STR, HC and CER. I identified numerous DMPs and DMRs associated polygenic risk burden in individual brain regions as well as across brain regions. Many of the PRS-associated *loci* have been previously implicated in the etiology of schizophrenia, most notably several regions in the MHC region, which has been implicated in schizophrenia in genetic studies (International Schizophrenia et al., 2009, Schizophrenia Working Group of the Psychiatric Genomics, 2014) and *GADD45B* which plays a role in neurogenesis and previously found to be differentially methylated in psychosis (Gavin et al., 2012). Strikingly, the top ranked probe associated with PRS in the multi-region model (*i.e.* across PFC, STR and HC) is located in the gene body of *DISC1*, a gene previously strongly linked to schizophrenia in a Scottish pedigree with a balanced translocation spanning the *locus* (St Clair et al., 1990). The data suggest that an increased PRS for schizophrenia may impact upon regulatory variation of the *DISC1 locus* in the brain, implicating a potentially common functional pathway between polygenic and highly penetrant single *locus* etiologies that warrants further investigation.

Other PRS-associated *loci*, such as *SIGLEC9* and *BPI*, encode proteins that play crucial roles in the immune system (Crocker et al., 2007, Zhang et al., 2000, Angata and Varki, 2000). This is an important observation given the hypothesised involvement of the immune system and inflammation response in schizophrenia (see **Chapter 1 section 1.1.6**). Furthermore, several PRS-associated *loci* are of relevance in the context of neuronal function and neurodevelopment, such as *RGMA* (which encodes an axon guidance protein thought to be important in interneuron migration and differentiation during neurogenesis (O'Leary et al., 2013, Matsunaga et al., 2004)), the cluster of genes *PCDHA 1 to 4* (which encode integral plasma membrane, cell adhesion proteins localised at synaptic junctions in neurons (Hamada and Yagi, 2001,

Kohmura et al., 1998)), *AXIN2* (which encodes a known component of the Wnt signalling pathway (Kikuchi, 1999), a pathway that plays a crucial role in controlling self-renewal and differentiation during neurodevelopment (Kalani et al., 2008, Nusse, 2008)) and *GDNF* (which encodes a neurotrophic factor that promotes the differentiation and survival to different types of neurons and has been implicated in Parkinson's disease (Ibanez, 2008)). Finally, some of the PRS-associated *loci* have been previously implicated in other neurodevelopmental disorders, in particular ASD, including *TAOK2*, *RBFOX1*, *IMMP2L* and *FOXP1*.

Many of the DMPs and DMRs associated with increased genetic burden for schizophrenia are independent of the changes observed associated with a diagnosis of schizophrenia itself, identified in the case-control analyses presented in **Chapter 3**. However, although there was no direct overlap between the top ranked schizophrenia-associated and PRS-associated DMPs, as expected, the effect sizes at the top ranked PRS-associated probes were significantly correlated with those at the same sites in the case-control analysis, indicating that schizophrenia PRS is not completely independent from disease diagnosis. Furthermore, there was no evidence for direct genetic effects on DNA methylation for variants included in the PRS (*i.e.* via mQTLs and enrichment of DMPs in GWAS regions), indicating that the PRS-associated epigenetic variation observed does not directly result from *cis*-genetic influences on DNA methylation.

4.4.2. Limitations

The study presented in this chapter has a number of important limitations. First, the limitations discussed in **Chapter 3 (section 3.4.2)** are also relevant in the context of this chapter. In summary, the number of samples assessed in this study is relatively low, which limits the power to detect significant associations (Dempster et al., 2013); the use of bulk tissue from each brain region is a potential confounder in DNA methylation studies (Guintivano et al., 2013, Heijmans and Mill, 2012); it is possible that many of the differences identified in this study are confounded by modifications other than DNA methylation and it is also possible that factors not accounted as covariates in the analyses (*i.e.* smoking, medication) may be confounding the PRS EWAS results.

In addition to these, there are other limitations that should be considered. First, PRS were calculated using the data from the latest and largest schizophrenia GWAS to date, incorporating all independent nominally significant associated alleles ($P < 0.05$). The authors predicted that the PRS explained only about 7% of total liability for the disorder (Schizophrenia Working Group of the Psychiatric Genomics, 2014). Although this is the schizophrenia GWAS capturing the most genetic variance to date, a large proportion of the variance remains unexplained. However it is worth noting that the PRS score was found to be significantly higher in schizophrenia cases compared to controls in the relatively small number of samples, highlighting the robust nature of the schizophrenia PRS. Second, the GWAS was carried out mainly in patients of European ancestry to avoid population stratification, therefore for the same reason I only used Caucasian samples on the analysis presented here. To date no high-powered schizophrenia GWAS has been performed in non-Caucasian samples, in particular from African ancestry, which have fundamentally different LD structures from Caucasian populations (International HapMap, 2005). Finally, schizophrenia PRS is not completely independent from diagnosis and the underlying correlation might confound the results, although the overlap of between schizophrenia-associated DNA methylation changes and PRS-associated changes was minimal suggesting that PRS is having independent effects on DNA methylation.

4.4.3. Implications, strengths and future directions

To my knowledge, this is the first study investigating DNA methylation changes associated with schizophrenia polygenic risk burden, or any other complex disease phenotype. It highlights the utility of PRS for identifying molecular pathways associated with etiological variation, which complement the associations identified with schizophrenia diagnosis. Although schizophrenia PRS is not useful for clinical risk predication, it is possible that it may be predictive of chronicity, treatment resistance or in the stratification of patients (O'Donovan, 2015). Furthermore, the identification of PRS-associated variation in DNA methylation is potentially less confounded by medication intake and other disease-associated exposures that can influence case-control analyses. Future studies should focus on understanding by which mechanisms an increased schizophrenia polygenic burden influences epigenetic regulation if not by a direct, *cis*-genetic influence on DNA methylation as my data suggest. Finally, although the resulting combined data from **Chapter 3** and the present chapter present novel evidence for associations between schizophrenia diagnosis, schizophrenia polygenic burden and variable DNA methylation across different brain regions, further replication using larger sample sizes is required to further validate these results. Future studies should also focus on understanding the transcriptional consequences of the observed associations.

Chapter 5 - Systems-level analysis of DNA methylation in the schizophrenia brain

5.1. Chapter aims and structure

In this chapter I was interested in studying the co-methylation structure of the DNA methylation across the genome in each of the four brain regions assessed, and exploring differences in that structure between schizophrenia patients and non-psychiatric controls. This chapter describes my exploration of network analysis methodology and its application to my DNA methylation data; it is structured in comprehensive sections that explain the rationale and the results of each approach in a stepwise manner.

5.2. Background

One of the main aims of my thesis was to identify variable DNA methylation associated with schizophrenia using tissue from four different brain regions (prefrontal cortex (PFC), striatum (STR), hippocampus (HC) and cerebellum (CER)). In **Chapters 3** and **4** I investigated DNA methylation changes associated with schizophrenia and schizophrenia polygenic risk burden at individual CpG sites and extended these analyses to explore regions of consecutive differentially methylated CpG sites across the genome. In the present chapter I aim to take a systems-level approach by exploring networks of highly correlated CpG sites. My aim was to explore the co-methylation structure of DNA methylation in each of the brain regions, independently of genomic position, and investigate which modules of co-methylated *loci* are altered in schizophrenia (for a definition of module see **Table 5.1**).

5.2.1. Network analysis

Biological systems, such as the genome, a cell or an organism, are made up of individual parts (*e.g.* molecules or organs) which interact dynamically to make the system function. Although it is important to investigate changes in individual components of a biological system, it is crucial to understand how the different parts of the system interact; in other words, to understand both the underlying structure and dynamics of the system. Because a system is not just a list of its components, its properties cannot be fully understood by studying these

components separately. Furthermore, a small change in an individual component of a regulatory system will potentially have major effects on the entire system. This is analogous to a transport network system – although it is important to draw and study the static roadmaps, it is crucial to understand traffic patterns, why they emerge and how to control them (Kitano, 2002). **Figure 5.1** shows the example of the roadmaps in Boston, USA (**A**) and an analysis of traffic patterns in the same city (**B**) (taken from Wang (2012)). Just by analysing the roadmaps is not possible to conclude which areas of Boston are more affluent and might be more affected by a traffic disruption.

Network analysis provides a way of representing the complex interactions between the interconnected components of a given system (Zhang and Horvath, 2005). It has been widely used in a broad range of disciplines, from social and economic studies (Jackson, 2010) to molecular biology (Barabasi and Oltvai, 2004). Examples of the latter are gene co-expression networks (Parikshak et al., 2013, Zhang and Horvath, 2005, Voineagu et al., 2011), protein-protein interaction networks (Schwikowski et al., 2000), and cell-cell interaction networks (Hartwell et al., 1999). The rapid progress in genomic, transcriptomic and epigenomic profiling techniques enables us to collect a large amount of data and gives us a unique opportunity to understand the dynamics and structure of entire biological systems. Additionally, the individual interrogation of thousands or millions of genomic positions or genes across the genome generates a multiple comparison problem that such data reduction techniques can mitigate.

Figure 5.2 shows an example of a correlation network where the main components of the network are described as ‘nodes’ and the interactions between them as ‘edges’. On a gene co-expression network, for example, the genes would be the nodes and the pair-wise correlation of their expression profiles determines which edges are included. In a network of co-methylated CpG sites, the nodes would be the individual CpG sites and the edges would be defined from the pair-wise correlation of their DNA methylation profiles

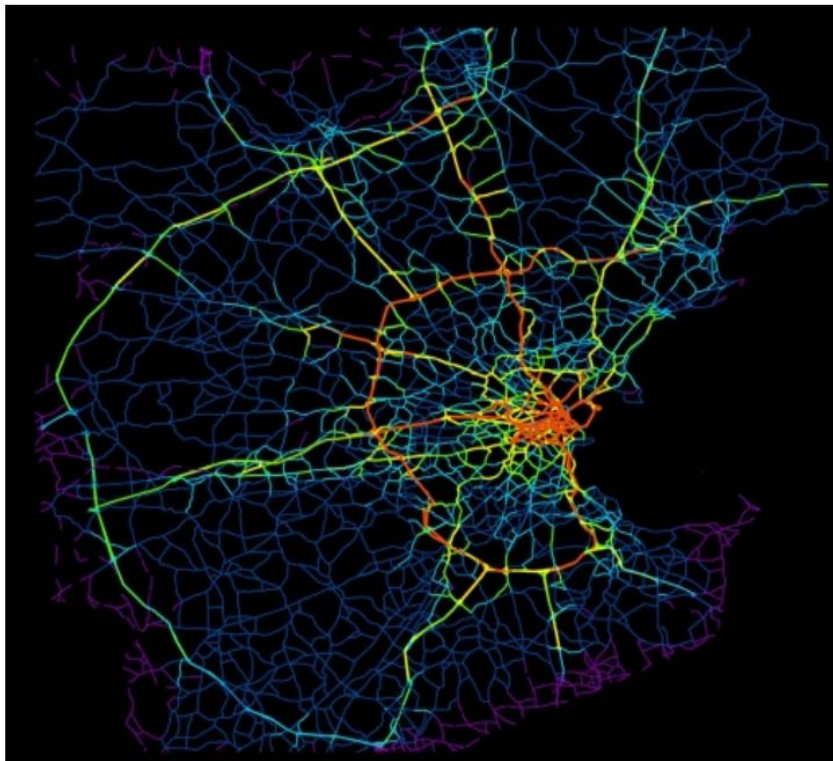
A**B**

Figure 5.1. Roadmap (A) and traffic patterns (B) of Boston, USA. Figure B was taken from the MIT News website (Wang, 2012).

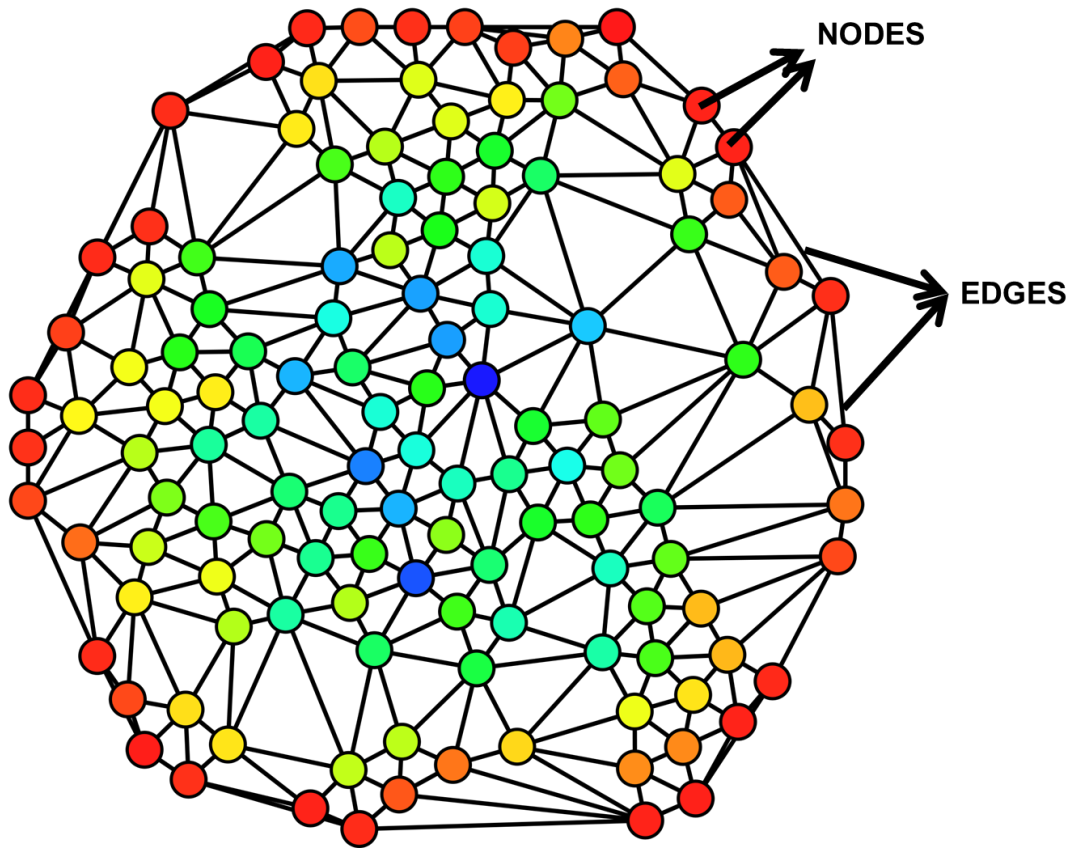


Figure 5.2. Example of a correlation network.

5.2.2. Weighted gene co-methylation network analysis

In this chapter I applied the weighted gene co-methylation network analysis (WGCNA) approach (Zhang and Horvath, 2005) to the DNA methylation data, using the *WGCNA* package (Langfelder and Horvath, 2008) in R (R Core Team, 2015). The package was developed to construct networks from gene expression data, but it can be used with any matrix of correlation coefficients.

Figure 5.3 taken from Langfelder and Horvath (2008) describes the general WGCNA methodology applied to gene expression data. Briefly, the first step is to construct a network of genes that are co-regulated (*i.e.* vary together) in the dataset. This network represents one system that is broken up into several modules of co-regulated genes, which will represent the main subcomponents of the network. In gene co-expression networks, for example, the defined modules represent functionally distinct groups of co-expressed genes with similar functions (Carlson et al., 2006). These modules are interesting entities and can then be explored in several ways; for example, the modules can be correlated with traits of interest (*e.g.* diagnosis, sex, age), pathway or gene ontology analysis can be used to identify biological functions associated with each module, or the central genes of each module can be identified and further investigated.

I applied this methodology to the DNA methylation datasets generated for each brain region separately (described in **Chapter 3 section 3.2**). **Table 5.1** has been adapted from Langfelder and Horvath (2008) to be applicable to DNA methylation data and summarises some of the terminology used in throughout this chapter.

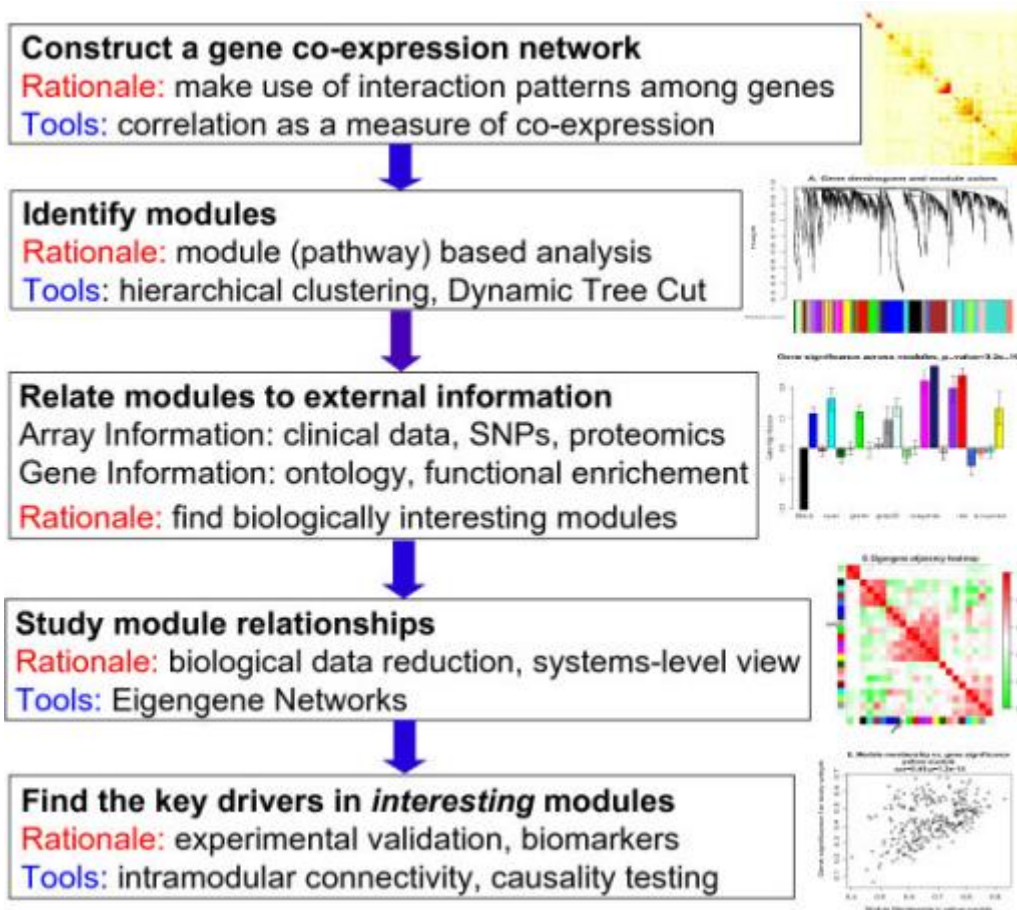


Figure 5.3. Overview of Weighted Gene Co-expression Network Analysis (WGCNA) methodology. This flowchart presents a brief overview of the main steps of WGCNA. Figure and legend taken from Langfelder and Horvath (2008).

Table 5.1. Glossary of weighted gene co-methylation analysis terminology (adapted from Langfelder and Horvath (2008)).

Term	Definition
Co-methylation network	Co-methylation networks are defined as undirected, weighted networks of DNA methylation sites (<i>i.e.</i> Illumina 450K array probes). The nodes of the network correspond to DNA methylation probes, and the edges between probes represent the pair-wise correlations between these probes. During the network construction, the absolute value of the correlation coefficients are raised to a power (soft-thresholding), to emphasize high or strong correlations at the expense of low or weak correlations, to allow modules of highly correlated probes to be identified.
Module	Modules are clusters within the global network of highly interconnected probes. In a signed network, modules correspond to positively correlated probes, whereas in an unsigned network, modules correspond to clusters of probes which may be positively or negatively correlated.
Module eigengene (ME)	The module eigengene (ME) is defined as the first principal component calculated from the DNA methylation values of all members (of that modules). It can be considered representative of the overall DNA methylation profile in a given module.
Module membership (MM)	For each probe, module membership (MM) is defined as the correlation between its DNA methylation values and the ME of a given module. The MM measure can be defined for all probes irrespective of which module they were allocated to.
Hub probe	The term is used to describe 'highly connected' probes within a particular module. In this project I consider 'hub probes' as those belonging to a given module with a high module membership to that module ($MM > 0.80$).

5.2.3. Overview of experimental strategy

I applied WGCNA to DNA methylation data from 76 PFC (38 schizophrenia and 38 controls), 82 STR (37 schizophrenia and 45 controls), 33 HC (16 schizophrenia and 17 controls) and 77 CER (37 schizophrenia and 40 controls) samples to i) identify discrete modules of co-methylated CpG sites and ii) test the association of their first principal component (ME, see **Table 5.1**) with schizophrenia and other traits. For details on the samples and demographic information relating to the samples used in this analysis, please see **Chapter 3 section 3.2**.

The initial approach focused on creating networks of Illumina 450K array probes for schizophrenia patients and non-psychiatric controls separately within each brain region and identifying both overlapping and unique modules of co-methylated probes between cases and controls networks. This approach is based on my observation that within a given brain region schizophrenia cases and controls are not characterised by systemic methylomic differences (see **Chapter 3 section 3.3.2**). Therefore I expected to see broadly similar structures between both cases and controls networks within the same brain region with a few dissimilarities related to disease. After using this approach (see below) I concluded it was not the optimal method to use. I subsequently created networks for all samples from each brain region (*i.e.* including both schizophrenia cases and controls) and tested for a significant association of each module with schizophrenia status, schizophrenia polygenic risk score (PRS) and other traits of interest. I performed gene ontology (GO) enrichment analysis on the genes belonging to the schizophrenia-associated modules.

Finally, I imposed the structure of modules of co-methylated probes identified in a fetal brain dataset generated by our lab (Spiers et al., 2015) to my adult brain data (schizophrenia cases + controls) and tested these for association with schizophrenia. This approach was used to explore the hypothesis that schizophrenia has neurodevelopmental origins, and may result from genomic dysregulation during periods of brain development (see **Chapter 1 section 1.1.5**). In the following sections I will describe each of these steps and corresponding results. An overview of the analysis approach in this chapter is

presented in **Figure 5.4** and a representation on how this analysis integrates with the other chapters in this thesis is given in **Chapter 1 Figure 1.8**.

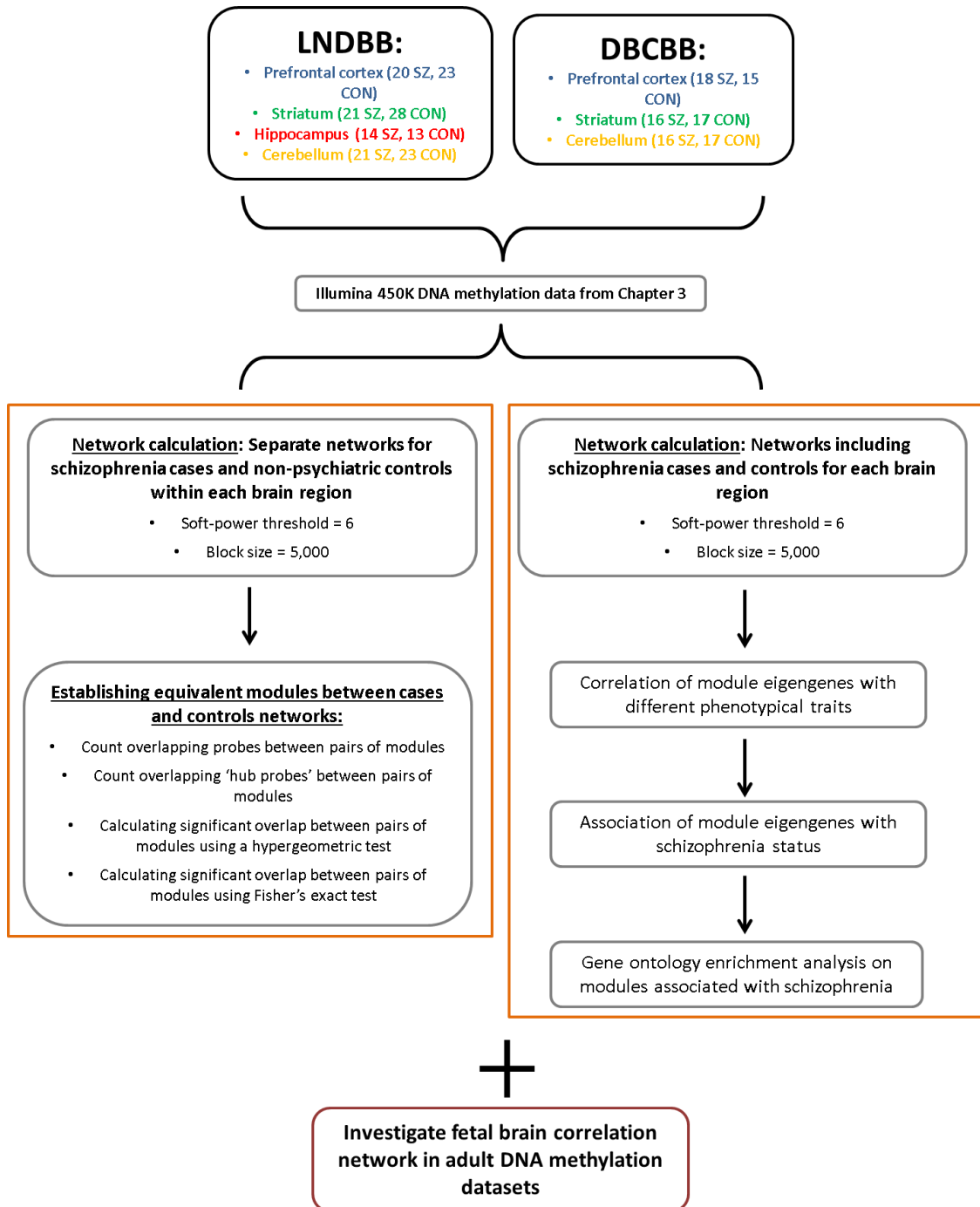


Figure 5.4. Overview of Chapter 5 experimental strategy.

5.3. Data pre-processing and normalisation

I performed WGCNA on Illumina 450K array data generated on samples from the PFC, STR, HC and CER from the MRC London Neurodegenerative Diseases Brain Bank (LNDBB) and the Douglas-Bell Canada Brain Bank (DBCBB) cohorts that were used for analyses in **Chapter 3**. Laboratory and data quality control (QC) procedures are described in **Chapter 2 sections 2.2 to 2.4** and **Chapter 3 section 3.2.3**. Detailed demographic information on all samples is presented in **Appendix A - Supplementary Table 1** and sample exclusion criteria are described in **Appendix A - Supplementary Table 2**. **Table 3.3** gives an overview of available demographic data available for the samples included in the analyses in this chapter.

Briefly, data were pre-processed and normalised using the *pfilter* and *dasen* functions of the *wateRmelon* package (Pidsley et al., 2013) in R (R Core Team, 2015) as described in **Chapter 3 section 3.2.3**. For tissues collected from both brain banks (PFC, STR and CER) array data obtained from both cohorts were pre-processed and normalised together. In total, 413,563, 417,447, 409,762 and 417,213 probes survived QC, respectively and were included in the network analyses of PFC, STR, HC and CER presented here. Adjusted DNA methylation values were calculated for each probe by fitting a linear regression model separately for each brain region including sex, age, brain bank and neuronal proportion estimates (except in the CER - for reasons described in **Chapter 3 section 3.2.5**) as independent variables, as described in **Chapter 3 section 3.2.6**.

5.4. Network construction and module detection

The *WGCNA* package (Langfelder and Horvath, 2008), implemented in R (R Core Team, 2015), was used to generate networks of co-methylated probes. The functions described here are part of this package unless otherwise stated. *WGCNA* uses a soft-thresholding approach for the construction of biological networks since this preserves the continuous nature of the underlying correlation information (Zhang and Horvath, 2005). Networks were created for 1) schizophrenia cases only, 2) non-psychiatric controls only and 3) both cases and controls together for each brain region, totalling 12 networks. The rationale for this approach is presented in **section 5.2.3** and throughout the next sections of this chapter.

I used the *pickSoftThreshold* function, which assesses scale free topology for multiple soft-thresholding powers, to inform my decision about which soft-thresholding power would be the most appropriate for the network construction. Of note, a network is said to follow a scale free topology if it follows a power law distribution. I based the calculation on a maximum block size of 5,000, which is the maximum number of probes that the function included in each block for calculation so that it can be handled by available computing infrastructure. This number was kept consistent for all networks. The proposed methodology of the *WGCNA* package, based on work from Zhang and Horvath (2005), is to choose the optimum soft-thresholding power to satisfy the criterion of scale-free topology. To do this I inspected plots showing the scale free topology, fitting index R^2 versus the different soft-thresholding powers. **Figure 5.5** shows an example of such plot for the DBCBB cerebellum (cases + controls) network. Both Zhang and Horvath (2005) and Langfelder and Horvath (2008) suggest that it is optimal to choose the lowest soft-thresholding power (x-axis) for which the curve flattens out upon reaching a high R^2 value (>0.80) (y-axis). To be consistent across all networks I chose the power 6, which was the lowest power that satisfied the R^2 criterion in all the datasets. This also the default value used by the authors of the package (Langfelder and Horvath, 2008).

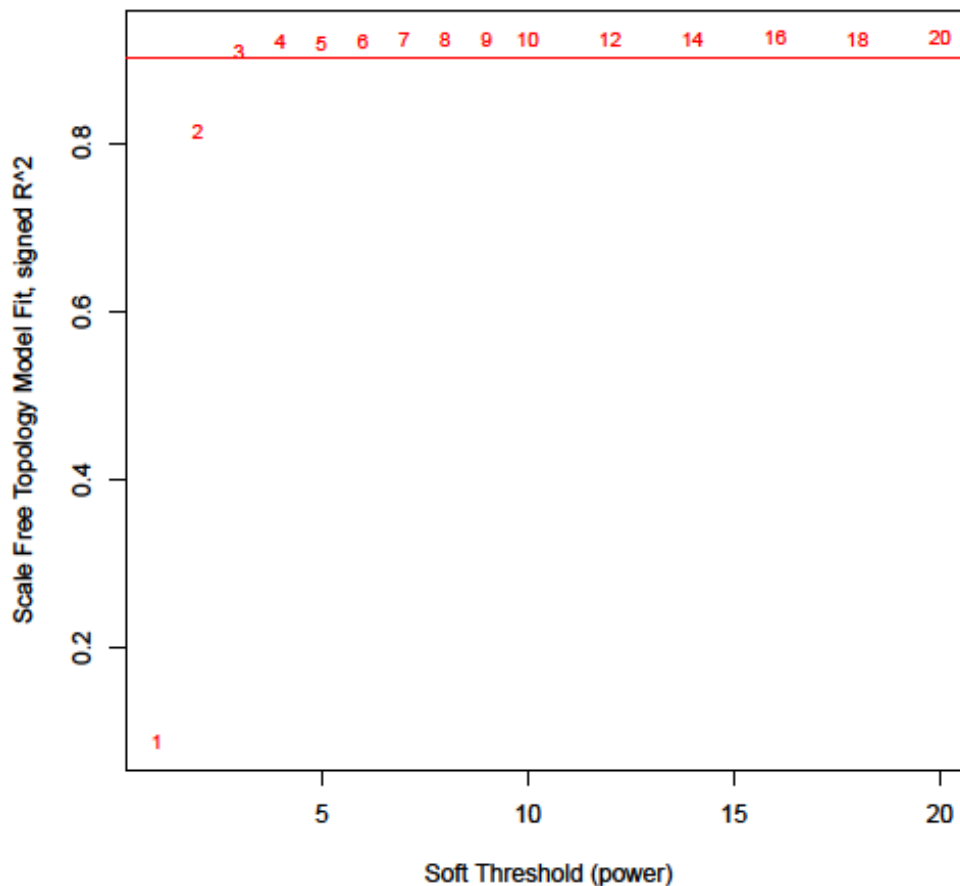


Figure 5.5. Example of the analysis of network topology for increasing soft-thresholding powers. Shown is the scale free topology fitting index R^2 (y-axis) versus soft-thresholding power (x-axis) for the cerebellum Douglas-Bell Canada Brain Bank (cases + controls) network.

Unsigned networks were created using the *blockwiseModules* function with a soft-threshold parameter of 6 with a block size of 5,000. An unsigned network will consider the absolute correlation between two probes irrespective of whether they are positively or negatively correlated (see term ‘Module’ on **Table 5.1**). Each module was labelled with a unique arbitrary colour name. For each module within each network, the first principal component from the matrix of DNA methylation values of was calculated using the *moduleEigengenes* function to give a module eigengene (ME) for each module (see term ‘Module eigengene’ on **Table 5.1**). A module membership (MM) measure for each module was calculated for each probe by calculating Pearson’s correlation coefficient between the DNA methylation values and the ME (see term ‘Module membership’ on **Table 5.1**).

5.5. Similarities between separate networks for schizophrenia cases and non-psychiatric controls

My first approach was to generate DNA methylation networks for schizophrenia cases and controls separately for each brain region (see **section 5.4**). This approach is based on my observation that within each brain region schizophrenia cases and controls are not characterised by systemic methylomic differences (see **Chapter 3 section 3.3.2**). Therefore I expected to see considerable similarity between modules of co-methylated probes in both case and control networks within the same brain region with small differences in modules associated with disease. To test this hypothesis, I started by exploring the PFC networks generated separately for schizophrenia cases and controls. **Tables 5.2** and **5.3** present the number, colour and size of modules in the controls and schizophrenia cases network, respectively. Every network has a 'grey', module that is comprised of all probes that were not assigned to any specific module. The 'grey' modules of all networks were disregarded in all following analyses.

Table 5.2. Modules identified in the network using prefrontal cortex data from the non-psychiatric controls of the MRC London Neurodegenerative Diseases Brain Bank and Douglas-Bell Canada Brain Bank.

Module	Module colour	N Probes
0	grey	144546
1	turquoise	57824
2	Blue	10014
3	brown	9801
4	yellow	9072
5	green	8542
6	Red	8126
7	black	8064
8	Pink	7369
9	magenta	7036
10	purple	6836
11	greenyellow	6642
12	Tan	6533
13	salmon	6514
14	cyan	6386
15	midnightblue	6283
16	lightcyan	5997
17	grey60	5945
18	lightgreen	5744
19	lightyellow	5386
20	royalblue	4969
21	darkred	4461
22	darkgreen	3968
23	darkturquoise	3960
24	darkgrey	3902
25	orange	3585
26	darkorange	3451
27	white	3431
28	skyblue	3361
29	saddlebrown	3230
30	steelblue	2950
31	paleturquoise	2926
32	violet	2839
33	darkolivegreen	2779
34	darkmagenta	2708
35	sienna3	2428
36	yellowgreen	2388
37	skyblue3	2192
38	plum1	2099
39	orangered4	1966
40	mediumpurple3	1732
41	lightsteelblue1	1646
42	lightcyan1	1503
43	ivory	1411
44	floralwhite	1341
45	darkorange2	1021
46	brown4	906
47	bisque4	787
48	darkslateblue	724
49	plum2	592
50	thistle2	544
51	thistle1	524
52	salmon4	483
53	palevioletred3	472
54	navajowhite2	469
55	maroon	440
56	lightpink4	379
57	lavenderblush3	336
58	honeydew1	334
59	darkseagreen4	291
60	coral1	170
61	antiquewhite4	160
62	coral2	160
63	mediumorchid	159
64	skyblue2	144
65	yellow4	125
66	skyblue1	124
67	plum	117
68	orangered3	108
69	mediumpurple2	108

Table 5.3. Modules identified in the network using prefrontal cortex data from the schizophrenia cases of the MRC London Neurodegenerative Diseases Brain Bank and Douglas-Bell Canada Brain Bank.

Module	Module colour	N Probes
0	grey	126049
1	turquoise	113624
2	blue	29578
3	brown	25900
4	yellow	10804
5	green	10670
6	red	8832
7	black	6859
8	pink	6621
9	magenta	6435
10	purple	4840
11	greenyellow	4181
12	tan	4097
13	salmon	4059
14	cyan	3736
15	midnightblue	3458
16	lightcyan	3178
17	grey60	3094
18	lightgreen	2824
19	lightyellow	2664
20	royalblue	2353
21	darkred	1951
22	darkgreen	1850
23	darkturquoise	1597
24	darkgrey	1582
25	orange	1577
26	darkorange	1487
27	white	1445
28	skyblue	1358
29	saddlebrown	1337
30	steelblue	1247
31	paleturquoise	1088
32	violet	1053
33	darkolivegreen	1019
34	darkmagenta	997
35	sienna3	890
36	yellowgreen	878
37	skyblue3	805
38	plum1	800
39	orangered4	755
40	mediumpurple3	747
41	lightsteelblue1	684
42	lightcyan1	682
43	ivory	614
44	floralwhite	594
45	darkorange2	467
46	brown4	426
47	bisque4	325
48	darkslateblue	320
49	plum2	243
50	thistle2	232
51	thistle1	189
52	salmon4	168
53	palevioletred3	159
54	navajowhite2	141

5.5.1. Approaches to match networks for schizophrenia cases and non-psychiatric controls

I attempted to match each module derived from the control network with at least one corresponding module from the case network using the following approaches: i) counting the overlap of probes between each control and case modules and ii) testing for significant overlap of common probes between each pair of modules. The next sections present the results of each of those methodologies.

5.5.1.1. Count the overlap of probes between each pair of modules from the controls and cases networks

The first approach to match the cases and control networks to find overlapping and unique modules within each brain region involved counting the overlapping probes between each pair of modules from the cases and controls networks. **Appendix A - Supplementary Table 9** presents the overlap of probes assigned to each pair of cases and controls modules. **Figure 5.6** shows a graphical representation of these overlaps, with each bar representing one module from the controls network and the colours representing the schizophrenia modules. The area of a given colour within each bar is proportional to the overlap of probes between the control module (bar) and that respective schizophrenia module (colour).

Appendix A - Supplementary Tables 10 and 11 (schizophrenia modules 1-27 and 28-54, respectively) show the percentage overlap of each control module with each schizophrenia module (expressed as a percentage of the size of the respective control module). It is clear from these tables and figure that each of the control modules, in particular for the larger modules, have some degree of overlap with all the schizophrenia modules, and vice-versa. Using this method it was not possible to establish a clear matching between the modules in the cases and the controls networks. Similarly, I counted the overlap of 'hub probes' between each pair of modules, defining 'hub probes' as probes assigned to a module and that have a MM > 0.80 (see **Table 5.1**). **Figure 5.7** shows a graphical representation of that overlap. Again, it was not possible to conclusively establish which module of the controls network corresponded to which module of the schizophrenia network.

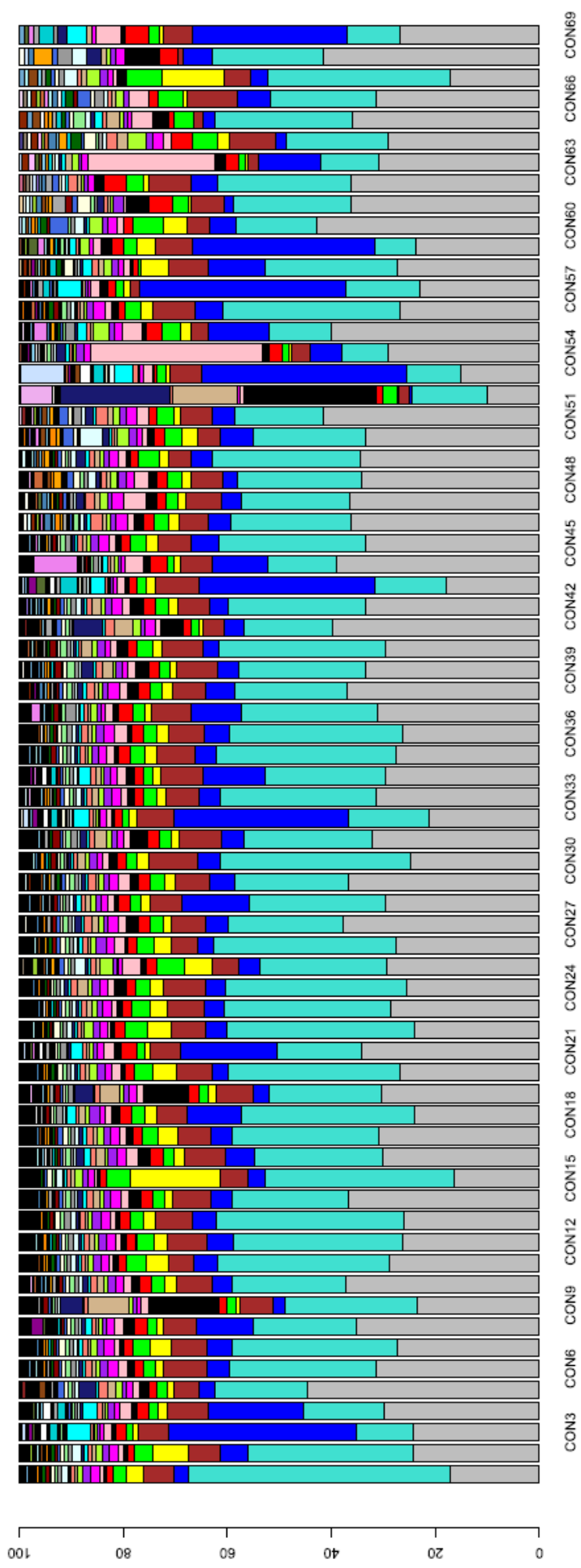


Figure 5.6. Barplot showing the overlap between probes belonging to each module of the controls network and each module of the schizophrenia cases network in the prefrontal cortex. Each bar (x-axis) represents one control (CON) module whereas the colours represent the schizophrenia modules. The extent of the colours within each bar represents the percentage (y-axis) of probes in each control module (bar) overlapping with the schizophrenia modules represented by the respective colours.

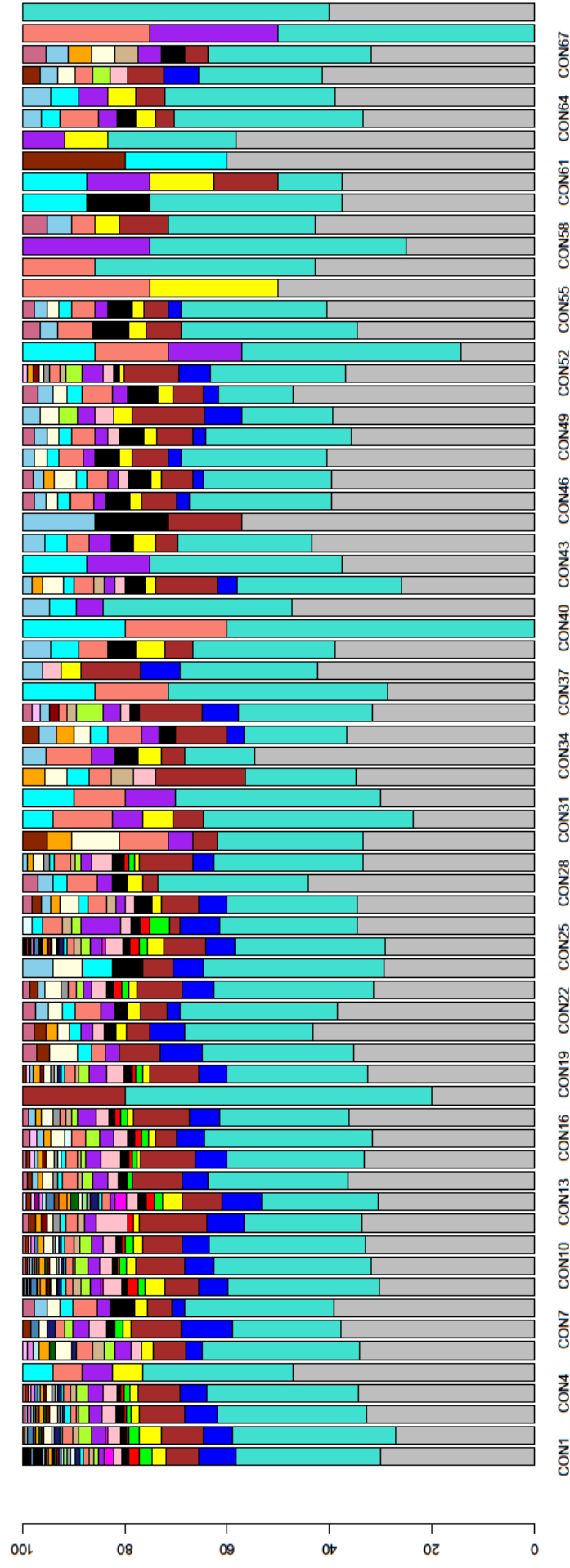


Figure 5.7. Barplot showing the overlap between ‘hub probes’ belonging to each module of the controls network and each module of the schizophrenia cases network in the prefrontal cortex. Each bar (x-axis) represents one control (CON) module whereas the colours represent the schizophrenia modules. The extent of the colours within each bar represents the percentage (y-axis) of ‘hub probes’ in each control module (bar) overlapping with the schizophrenia modules represented by the respective colours.

5.5.1.2. Test for significant overlap of common probes between cases and controls modules

I next applied a hypergeometric test using the *phyper* function in R (R Core Team, 2015), which determines the probability of the overlap between two lists of genes to be a chance event (Fury et al., 2006). **Appendix A - Supplementary Tables 12 and 13** (schizophrenia modules 1-27 and 28-54, respectively) present the *P*-values of the hypergeometric test between all pairs of schizophrenia and control modules. Again, all control modules show significant overlap with at least one schizophrenia module, making it unfeasible to definitively establish a correspondent schizophrenia module for each control module.

Finally, I used the *matchLabels* function from the *WGCNA* package (Langfelder and Horvath, 2008). This function calculates the significant overlap between modules of two networks using a Fisher's exact test (Fisher, 1922) and relabels the 'reference network' modules (here the schizophrenia network) based on a 'source network' (here controls network). **Appendix A - Supplementary Tables 14 and 15** (schizophrenia modules 1-27 and 28-54, respectively) present the *P*-values of the Fisher's exact test from the *matchLabels* function. The function redistributed the 54 modules of the schizophrenia network into 88 new modules, a considerably higher number, which indicates that the two networks could not be matched effectively. The Fisher's exact test *P*-values support this conclusion, with most modules overlapping significantly with more than one module of the other network. This is not surprising given that the hypergeometric test and the Fisher's exact test use similar approaches.

As mentioned above, I used these approaches on the PFC schizophrenia cases and controls networks, which proved unsuccessful. This could be due to the small sample size in both schizophrenia patients and controls groups of samples or the high number of probes used to create the networks (see **section 5.4** for further discussion on this topic). As the attempt to establish an overlap between modules was unsuccessful in the PFC, I proceeded to explore the networks of cases and controls together in each brain region (see following sections).

5.6. Networks including schizophrenia cases and non-psychiatric controls

After an initial exploration of the PFC networks derived from schizophrenia patients and controls separately (**section 5.5**) I concluded that identifying overlapping and dissimilar modules between the two was not the optimal approach to use. Therefore I next created networks of co-methylated probes including schizophrenia cases and non-psychiatric controls for each brain region. 34 modules were identified in the PFC network, 29 in the STR, 97 in the HC and 32 in the CER. The high number of modules identified in the HC data compared to the other brain tissues results from the small number of samples available for this tissue, and suggests that it might be inappropriate to perform network analysis on these data due to the amount of noise. Therefore the HC network was not considered for further analysis. **Tables 5.4** to **5.6** present the number of probes and arbitrary colour label for each module for the PFC, STR and CER networks.

5.6.1. Modules associated with several traits

To identify modules associated with specific traits, a Pearson's correlation coefficient was calculated for each module between the ME and disease status, brain bank, sex, age, neuronal proportion estimates (except for the CER), PRS and ethnicity (for details on these two traits please see **Chapter 4**). **Tables 5.4** to **5.6** show the correlation coefficients (ρ) and P -values for these correlations. Since I included DNA methylation values with age, sex, brain bank and neuronal estimates (except in the CER) regressed out, these would not be expected to correlate with any of the modules in the networks. In cases where such co-variables have not been regressed out is common to see modules of co-methylated probes strongly associated with them (Pidsley et al., 2014, Spiers et al., 2015). **Figures 5.8** to **5.10** show the heatmaps of the correlation coefficients between the ME and disease status, PRS and ethnicity.

Interestingly, in the three networks there are modules which are significantly correlated ($P < 0.05$) with schizophrenia PRS (PFC: 'pink', 'darkorange', 'white', 'violet' and 'darkmagenta', STR: 'lightcyan' and 'orange', CER: 'green', 'darkgreen', 'darkturquoise', 'darkgrey' and 'saddlebrown'). The majority of these modules however also correlate significantly with ethnicity. To investigate whether these correlations resulted from variation in schizophrenia polygenic risk burden or the presence of (ethnic) outliers I later repeated the construction of the networks including only Caucasian samples (these results are presented in **section 5.6.4**).

As schizophrenia diagnosis is a dichotomous trait, I performed an independent t-test between the ME and disease status for each module to identify modules associated with schizophrenia within each network. The t-test P -values are presented in **Tables 5.8 to 5.10**. Five PFC modules were nominally associated with schizophrenia (**Table 5.4 and Figure 5.8**) (P -values – 'brown': 0.05, 'black': 0.05, 'tan': 0.04, 'salmon': 0.04 and 'darkgrey': 0.04), although none of these survived Bonferroni correction for the 95 modules tested; $P = 5.26E-04$. The STR and CER networks, in contrast, had no modules even nominally associated with schizophrenia. The five schizophrenia-associated modules in the PFC network are described in more detail in the next section (**section 5.6.2**)

Table 5.4. Modules identified in the network using prefrontal cortex data from both non-psychiatric cases and schizophrenia controls from the MRC London Neurodegenerative Diseases Brain Bank and Douglas-Bell Canada Brain Bank. Shown are the coefficients (ρ) and P -values of Pearson's correlations and/or t-tests between each module eigengene and different phenotypical traits. Significant correlations/t-tests ($P < 0.05$) are shown in bold.

Module no.	Module colour	N Probes	Disease status ρ	t-test P	Brain bank P	Sex ρ	Age ρ	Neuronal proportion estimates P	Polygenic risk score ρ	correlation P	Ethnicity ρ	correlation P
0	grey	273015	-	-	-	-	-	-	-	-	-	-
1	turquoise	60418	-0.12	0.29	-1.60E-16	2.80E-16	1.87E-16	-4.34E-17	-1.56E-03	0.99	0.08	0.49
2	blue	34302	0.16	0.17	8.17E-16	-1.04E-16	-2.79E-16	-1.51E-16	-8.43E-02	0.47	-0.19	0.11
3	brown	12077	-0.23	0.05	-1.67E-16	3.59E-16	1.03E-16	3.34E-17	4.44E-04	1.00	0.08	0.47
4	yellow	8298	-0.05	0.66	-1.60E-16	2.34E-17	-1.50E-16	2.63E-16	-4.40E-03	0.97	-9.32E-03	0.94
5	green	6442	0.21	0.07	-2.17E-17	1.96E-16	1.09E-16	3.75E-17	-3.27E-02	0.78	-9.36E-02	0.42
6	red	3120	-0.20	0.08	-3.47E-18	-9.11E-17	1.73E-16	-1.21E-16	-4.64E-02	0.69	0.07	0.56
7	black	2801	-0.23	0.05	9.80E-17	-2.17E-16	-2.66E-16	1.54E-16	-4.71E-02	0.69	-1.97E-02	0.87
8	pink	1605	-0.02	0.84	-2.17E-17	-1.43E-17	1.76E-16	2.36E-17	-0.39	4.41E-04	-0.55	3.19E-07
9	magenta	1585	0.21	0.06	-2.35E-16	8.67E-17	-5.09E-16	1.89E-16	0.03	0.77	-3.53E-02	0.76
10	purple	1327	-0.20	0.09	-6.59E-17	1.09E-16	1.49E-16	1.78E-16	0.03	0.79	0.07	0.54
11	greenyellow	1308	-0.02	0.84	-9.19E-17	1.15E-16	-6.07E-17	2.36E-16	-5.35E-02	0.65	-4.06E-02	0.73
12	tan	1247	0.24	0.04	-3.38E-17	-1.80E-17	-2.62E-17	-3.61E-17	-2.03E-02	0.86	-9.57E-02	0.41
13	salmon	957	0.23	0.04	1.91E-17	8.28E-17	1.78E-17	1.04E-17	5.70E-03	0.96	-6.73E-02	0.56
14	cyan	707	-0.13	0.28	1.58E-16	0	0	-2.95E-17	7.46E-03	0.95	0.02	0.83
15	midnightblue	529	-0.18	0.11	4.92E-17	9.24E-17	-2.15E-16	3.17E-17	-4.29E-02	0.71	0.04	0.71

16	lightcyan	422	-0.12	0.30	-9.37E-17	-1.30E-16	-1.91E-16	5.03E-17	2.02E-03	0.99	0.01	0.91
17	grey60	358	-0.16	0.18	7.81E-17	8.50E-17	-1.16E-16	2.21E-17	-6.89E-02	0.55	0.04	0.73
18	lightgreen	305	0.10	0.40	9.97E-18	1.34E-17	-1.69E-17	3.69E-18	-4.07E-02	0.73	-2.06E-02	0.86
19	lightyellow	257	0.09	0.43	7.81E-17	-8.67E-18	3.23E-16	-1.45E-16	0.09	0.44	0.01	0.91
20	royalblue	255	-0.15	0.21	1.06E-16	-2.34E-17	5.14E-16	6.59E-17	0.01	0.91	0.01	0.91
21	darkred	239	-0.07	0.56	2.53E-16	2.04E-16	3.22E-16	7.29E-17	-6.22E-02	0.59	0.09	0.46
22	darkgreen	239	-0.10	0.39	-1.47E-16	-7.74E-17	3.46E-16	4.58E-17	-7.74E-02	0.51	0.06	0.58
23	darkturquoise	204	0.13	0.26	4.89E-16	2.57E-16	-1.21E-16	2.31E-16	-1.10E-01	0.34	-3.54E-02	0.76
24	darkgrey	186	0.24	0.04	1.19E-16	-4.99E-17	-3.36E-16	1.19E-16	-3.57E-02	0.76	6.78E-04	1.00
25	orange	171	-0.12	0.32	-2.18E-17	-1.01E-16	-6.91E-17	9.16E-17	-5.95E-02	0.61	-8.09E-02	0.49
26	darkorange	165	0.07	0.54	-8.93E-17	2.60E-17	-1.73E-18	-1.20E-16	-0.46	2.83E-05	-0.52	1.54E-06
27	white	156	0.01	0.92	6.16E-17	9.11E-17	-4.69E-16	7.76E-17	0.36	1.29E-03	0.31	5.69E-03
28	skyblue	142	0.01	0.96	-1.78E-17	-1.58E-16	-2.99E-16	2.08E-16	-5.62E-02	0.63	-9.70E-02	0.40
29	saddlebrown	135	0.08	0.51	-1.10E-16	-2.01E-16	1.25E-16	-1.97E-16	0.05	0.69	-3.16E-03	0.98
30	steelblue	127	-0.10	0.37	-8.67E-19	-1.45E-16	-1.67E-16	-2.06E-16	-0.12	0.32	-5.29E-02	0.65
31	paleturquoise	125	0.15	0.19	9.97E-17	8.24E-18	9.54E-18	1.91E-16	-1.66E-02	0.89	8.81E-03	0.94
32	violet	120	-0.09	0.46	4.90E-17	-3.90E-17	3.38E-16	-1.98E-16	-0.29	0.01	-0.41	2.20E-04
33	darkolivegreen	112	0.22	0.06	-6.77E-17	-2.63E-16	8.67E-19	-1.01E-16	-1.86E-02	0.87	0.01	0.92
34	darkmagenta	107	0.08	0.49	1.65E-17	1.68E-16	1.58E-16	-2.49E-18	0.25	0.03	0.39	4.89E-04

Table 5.5. Modules identified in the network using striatum data from both non-psychiatric cases and schizophrenia controls from the MRC London Neurodegenerative Diseases Brain Bank and Douglas-Bell Canada Brain Bank. Shown are the coefficients (ρ) and P -values of Pearson's correlations and/or t -tests between each module eigengene and different phenotypical traits. Significant correlations/ t -tests ($P < 0.05$) are shown in bold.

Module no.	Module colour	N Probes	Disease status ρ	t -test P	Brain bank P	Sex ρ	Age ρ	Neuronal proportion estimates ρ	Polygenic risk score ρ	correlation P	Ethnicity ρ	correlation P
0	grey	194146	-	-	-	-	-	-	-	-	-	-
1	turquoise	68690	0.28	0.26	-1.73E-16	-8.59E-17	-4.38E-16	6.47E-10	0.02	0.85	0.06	0.57
2	blue	40022	0.41	0.39	-1.73E-16	-2.99E-16	1.97E-16	-5.55E-10	-3.29E-02	0.77	-7.98E-02	0.48
3	brown	27615	0.80	0.81	-2.08E-16	2.02E-16	-3.16E-16	7.34E-10	-7.50E-02	0.50	0.02	0.88
4	yellow	18714	0.47	0.48	5.55E-17	-3.42E-16	-3.21E-16	-5.28E-11	-2.01E-02	0.86	-0.11	0.32
5	green	14304	0.66	0.66	-9.37E-17	-5.77E-17	-1.40E-16	-2.93E-10	0.03	0.81	0.05	0.68
6	red	13299	0.23	0.20	6.59E-17	1.57E-16	-6.01E-17	9.19E-11	0.04	0.73	0.02	0.84
7	black	8497	0.90	0.90	-2.69E-17	-4.49E-17	-4.53E-17	-4.12E-10	0.02	0.83	-3.52E-02	0.75
8	pink	6099	0.27	0.23	3.56E-17	1.42E-16	6.98E-17	3.55E-10	-0.06	0.59	0.06	0.58
9	magenta	5689	0.38	0.39	-1.08E-16	1.13E-16	0.00E+00	-2.31E-10	0.04	0.74	0.01	0.93
10	purple	4003	0.14	0.12	1.34E-16	2.76E-16	2.47E-17	6.58E-10	0.01	0.92	0.06	0.59
11	greenyellow	3338	0.48	0.45	1.15E-17	-2.26E-16	-2.38E-16	-6.52E-10	-4.80E-02	0.67	-8.16E-02	0.47
12	tan	2319	0.46	0.50	6.94E-18	-1.35E-16	1.41E-16	-2.03E-10	-0.11	0.34	-0.18	0.10
13	salmon	2295	0.83	0.83	-1.04E-17	-6.59E-17	1.01E-16	-4.63E-10	-8.72E-02	0.44	-0.22	0.04
14	cyan	2059	0.41	0.39	-1.26E-16	-1.4E-17	-1.1E-16	-4.09E-10	0.06	0.56	-9.25E-02	0.41
15	midnightblue	954	0.81	0.80	-3.16E-17	-2.59E-16	-3.13E-16	-5.13E-10	-3.08E-02	0.78	-0.12	0.30
16	lightcyan	718	0.34	0.34	-3.82E-17	-3.24E-16	-1.09E-16	-1.15E-09	0.22	0.04	0.08	0.45
17	grey60	706	0.17	0.15	3.77E-17	4.99E-18	-1.06E-17	-5.02E-10	0.11	0.33	0.03	0.79

18	lightgreen	705	1.00	1.00	1.00	-1.95E-16	-1.73E-16	1.56E-16	-5.23E-10	0.03	0.78	-4.43E-03	0.97
19	lightyellow	693	0.33	0.33	0.32	-1.03E-16	-1.75E-16	4.42E-17	4.14E-10	-0.15	0.17	-5.32E-02	0.63
20	royalblue	686	0.77	0.77	0.79	6.85E-17	1.30E-15	-7.37E-18	7.22E-10	0.02	0.84	6.40E-03	0.95
21	darkred	369	0.44	0.44	0.49	2.81E-16	-5.50E-17	-1.07E-16	1.29E-09	0.10	0.35	0.11	0.31
22	darkgreen	346	0.48	0.48	0.52	-2.22E-16	3.47E-16	4.16E-17	-2.68E-10	0.03	0.80	0.03	0.79
23	darkturquoise	296	0.95	0.95	0.95	-1.10E-16	4.33E-16	-1.12E-16	4.77E-10	0.05	0.64	0.18	0.11
24	darkgrey	168	0.79	0.79	0.79	1.91E-16	5.21E-16	-9.54E-18	4.77E-10	-6.66E-02	0.55	-0.12	0.27
25	orange	168	0.37	0.37	0.33	-2.47E-16	-2.22E-16	4.99E-17	-1.08E-10	-0.39	3.06E-04	-0.44	4.10E-05
26	darkorange	166	0.73	0.73	0.73	3.73E-17	2.83E-16	-1.45E-16	3.16E-10	0.03	0.80	0.05	0.67
27	white	137	0.63	0.63	0.64	-2.57E-16	4.63E-16	1.14E-16	7.46E-10	-9.87E-02	0.38	-3.82E-03	0.97
28	skyblue	125	0.30	0.30	0.35	-1.54E-16	-3.00E-16	1.47E-16	-4.78E-10	-0.11	0.33	-3.36E-03	0.98
29	saddlebrown	121	0.79	0.79	0.79	-2.22E-16	5.34E-16	2.55E-16	8.86E-10	-8.93E-02	0.42	-7.99E-02	0.48

Table 5.6. Modules identified in the network using cerebellum data from both non-psychiatric cases and schizophrenia controls from the MRC London Neurodegenerative Diseases Brain Bank and Douglas-Bell Canada Brain Bank. Shown are the coefficients (ρ) and P -values of Pearson's correlations and/or t -tests between each module eigengene and different phenotypical traits. Significant correlations/ t -tests ($P < 0.05$) are shown in bold.

Module	Module colour	N Probes	Disease status ρ	t-test P	Brain bank ρ	Sex ρ	Age ρ	Polygenic risk score ρ	correlation P	Ethnicity ρ	correlation P
0	grey	159974	-	-	-	-	-	-	-	-	-
1	turquoise	64761	-0.03	0.79	4.97E-16	-2.08E-16	8.67E-18	0.03	0.80	0.11	0.34
2	blue	22683	-0.03	0.81	-8.89E-17	1.25E-16	-2.36E-16	-1.11E-02	0.92	0.06	0.63
3	brown	21473	0.20	0.83	-1.62E-16	4.43E-16	-3.10E-16	0.09	0.43	0.09	0.43
4	yellow	19912	-0.08	0.07	3.64E-17	-3.13E-16	-2.12E-16	7.78E-03	0.95	-4.70E-02	0.68
5	green	18463	-0.16	0.52	-3.19E-16	-6.83E-17	-9.06E-17	-0.23	0.04	-0.42	1.70E-04
6	red	16814	-0.07	0.16	9.80E-17	3.90E-18	-1.60E-16	-0.10	0.37	-4.45E-02	0.70
7	black	10211	0.09	0.55	2.80E-16	-4.34E-16	-2.31E-16	-0.21	0.06	-0.29	9.60E-03
8	pink	8681	-0.09	0.44	3.43E-17	1.92E-16	-2.83E-16	-0.11	0.36	-0.20	0.08
9	magenta	7959	-0.05	0.43	-3.64E-17	3.88E-16	5.55E-17	-0.16	0.16	-0.26	0.02
10	purple	6521	-0.07	0.68	4.82E-16	-7.15E-16	-5.48E-16	0.16	0.17	0.02	0.87
11	greenyellow	6420	0.18	0.55	4.77E-17	-5.38E-17	-2.08E-17	0.05	0.68	0.09	0.42
12	tan	6054	-0.08	0.11	-9.19E-17	-1.88E-16	-9.54E-17	0.05	0.70	-3.81E-02	0.74
13	salmon	3895	0.14	0.47	1.91E-17	-3.04E-17	-2.60E-17	-2.80E-02	0.81	-3.88E-02	0.74
14	cyan	3893	-0.22	0.20	-1.22E-16	-8.28E-17	-1.47E-16	-1.62E-02	0.89	0.05	0.67
15	midnightblue	3459	0.13	0.05	-7.63E-17	1.83E-16	8.50E-17	0.08	0.50	0.06	0.61
16	lightcyan	3437	-0.04	0.23	-8.80E-17	-2.62E-16	1.28E-16	0.02	0.85	-4.75E-03	0.97
17	grey60	3400	-0.13	0.74	6.64E-17	-1.99E-16	1.36E-17	-8.14E-02	0.48	0.10	0.41
18	lightgreen	3194	0.15	0.26	1.15E-16	-1.65E-16	2.80E-16	-4.51E-03	0.97	0.03	0.79

19	lightyellow	2964	0.15	0.18	6.94E-17	7.46E-17	1.03E-16	0.15	0.18	0.06	0.62
20	royalblue	2544	-0.04	0.18	5.20E-18	-4.29E-17	1.04E-17	-4.54E-02	0.69	0.04	0.70
21	darkred	2461	0.14	0.73	-4.25E-17	6.42E-17	2.75E-17	0.16	0.16	0.01	0.90
22	darkgreen	2259	0.13	0.21	2.09E-16	5.83E-17	1.58E-16	-0.25	0.03	-0.19	0.11
23	darkturquoise	2055	0.00	0.24	1.68E-16	-1.20E-16	-2.78E-17	-0.36	1.42E-03	-0.43	1.15E-04
24	darkgrey	1563	-0.09	0.98	-3.60E-17	1.14E-16	4.73E-17	0.24	0.04	0.10	0.37
25	orange	1551	0.19	0.43	-6.42E-17	4.94E-17	1.43E-16	-0.10	0.39	0.02	0.84
26	darkorange	1505	-0.02	0.09	1.24E-16	-3.67E-16	-1.64E-16	0.11	0.33	0.05	0.68
27	white	420	-0.15	0.89	1.08E-16	8.07E-17	-1.04E-16	0.02	0.86	-0.13	0.24
28	skyblue	390	-0.02	0.19	1.42E-16	-1.56E-17	-2.69E-17	-1.43E-02	0.90	-4.22E-02	0.72
29	saddlebrown	343	-0.10	0.88	9.84E-17	-9.30E-17	-5.29E-17	-0.29	9.67E-03	-0.44	6.27E-05
30	steelblue	223	-0.14	0.37	6.59E-17	-2.65E-16	-1.01E-16	-7.27E-03	0.95	-8.66E-03	0.94
31	paleturquoise	148	0.10	0.22	3.51E-17	-6.29E-18	7.81E-18	-6.43E-03	0.96	-5.32E-02	0.65
32	violet	132	-0.03	0.37	-1.27E-16	1.87E-16	3.60E-17	0.29	0.01	0.14	0.23

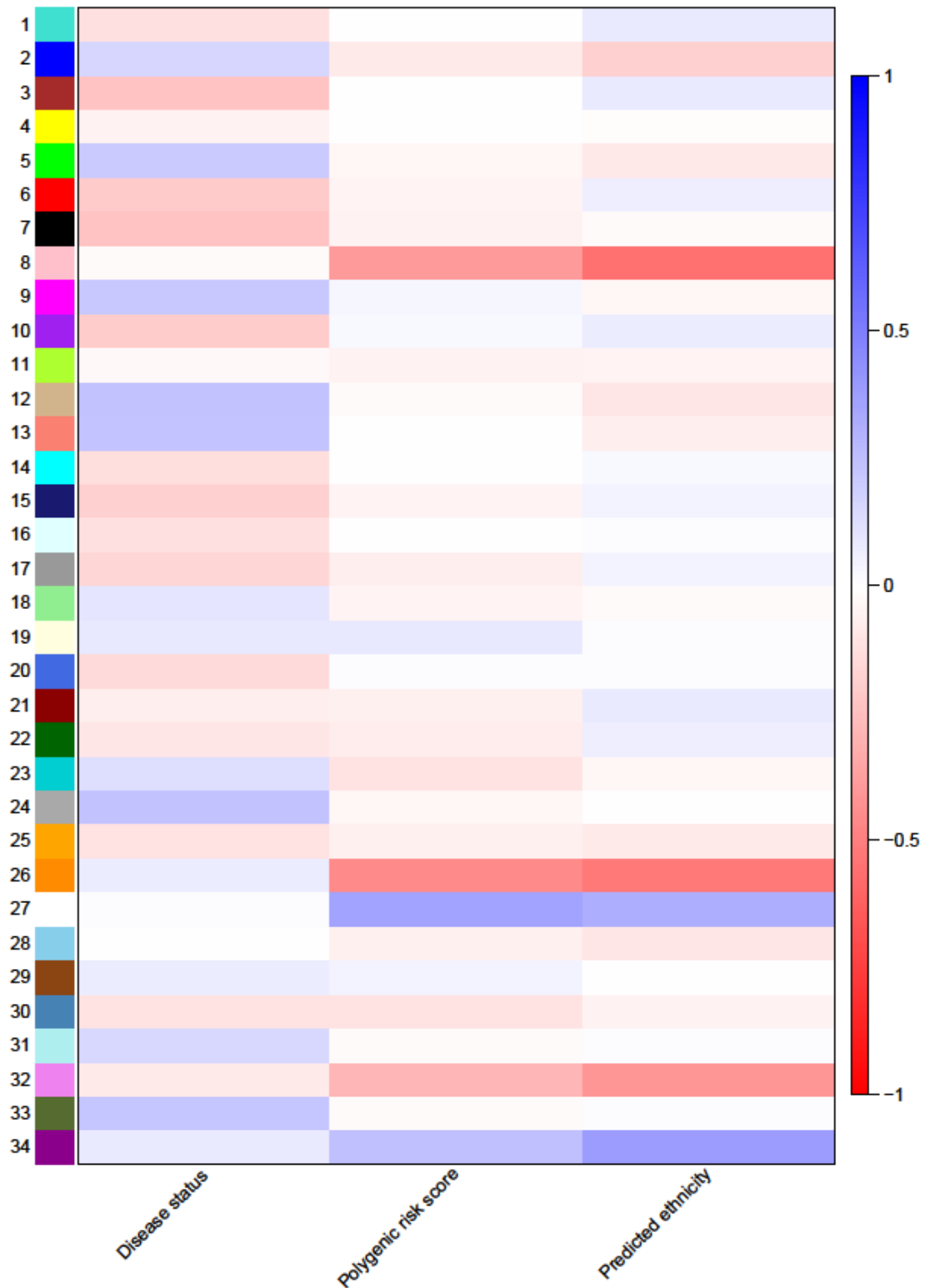


Figure 5.8. Heatmap showing the correlation coefficient between each prefrontal cortex module eigengene and different phenotypical traits. Shown are the modules identified in the network using prefrontal cortex data from both non-psychiatric cases and schizophrenia controls from the MRC London Neurodegenerative Diseases Brain Bank and Douglas-Bell Canada Brain Bank.

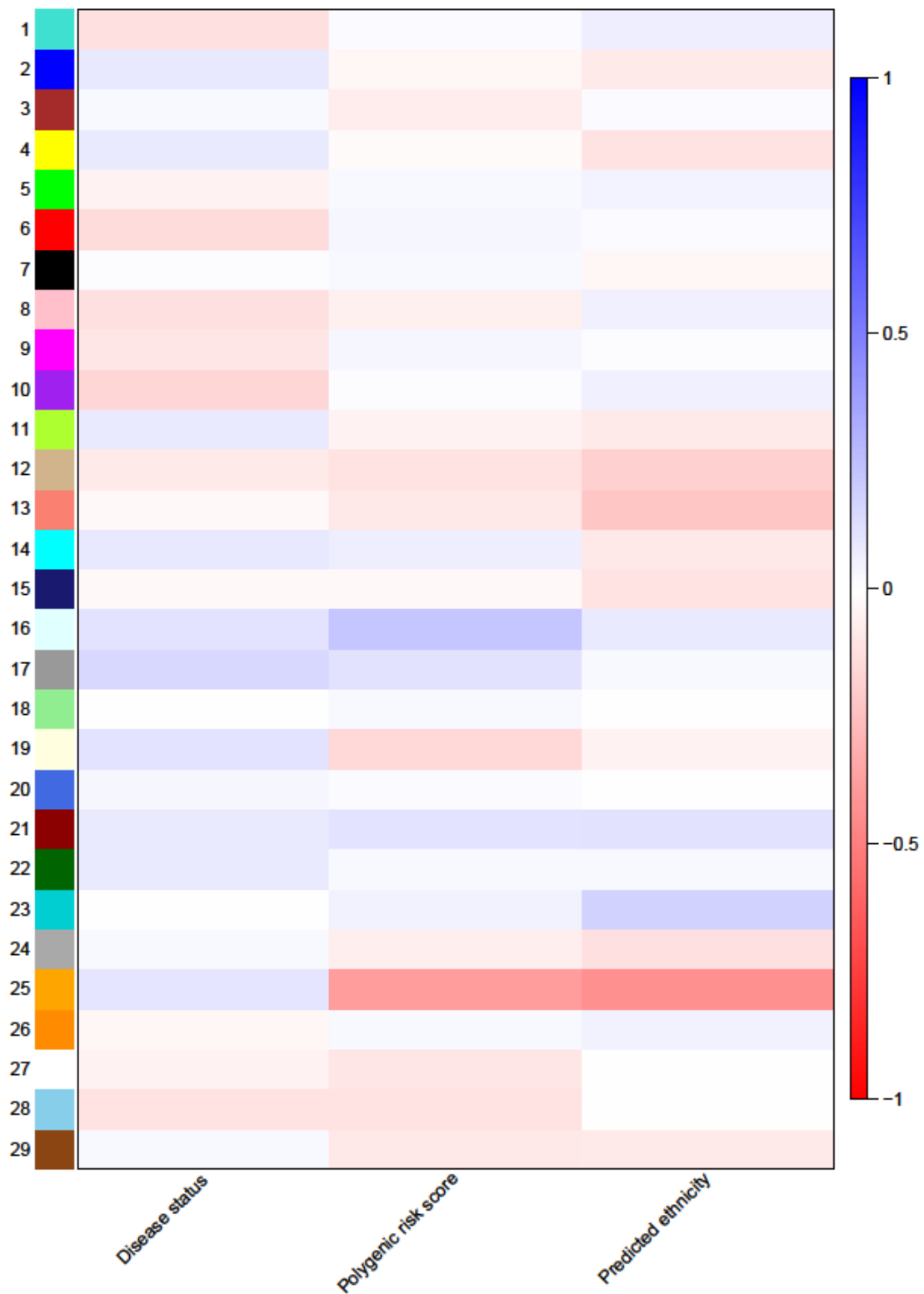


Figure 5.9. Heatmap showing the correlation coefficient between each striatum module eigengene and different phenotypical traits. Shown are the modules identified in the network using striatum data from both non-psychiatric cases and schizophrenia controls from the MRC London Neurodegenerative Diseases Brain Bank and Douglas-Bell Canada Brain Bank.

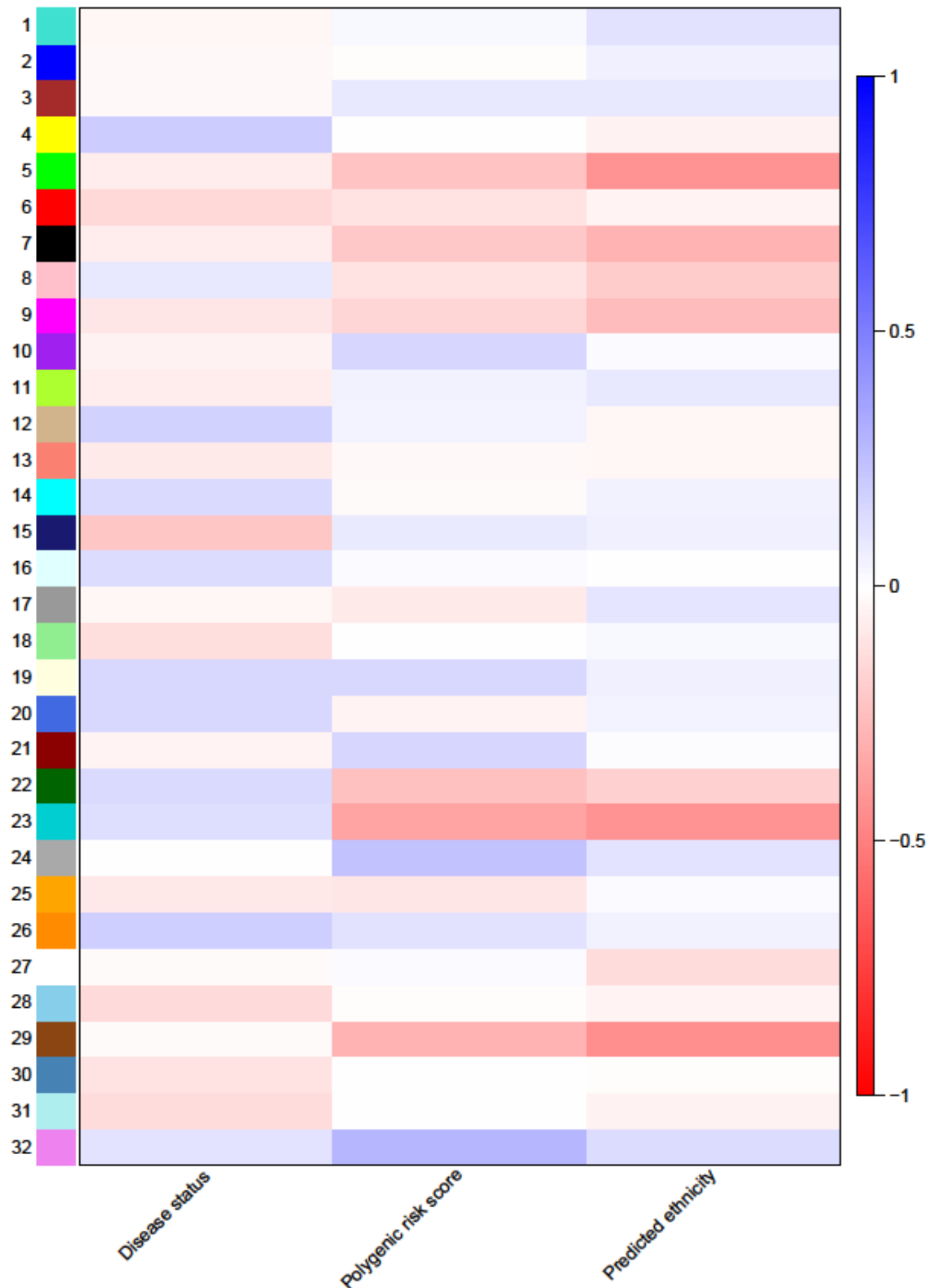


Figure 5.10. Heatmap showing the correlation coefficient between each cerebellum module eigengene and different phenotypical traits. Shown are the modules identified in the network using cerebellum data from both non-psychiatric cases and schizophrenia controls from the MRC London Neurodegenerative Diseases Brain Bank and Douglas-Bell Canada Brain Bank.

5.6.2. Prefrontal cortex modules associated with schizophrenia

Figures 5.11 and **5.12** were created using Cytoscape v3.2.1 (Lopes et al., 2010) and show the stronger correlations ($\rho > 0.80$) between the ‘hub probes’ (MM > 0.80) in the ‘brown’ and ‘black’ PFC module. Shown are the genes annotated to the respective ‘hub probes’, unless the probe is not annotated to a gene, in which case the probe name is shown. The remaining three modules do not have enough ‘hub probes’ to create a meaningful graphic representation.

Table 5.7 presents the ‘hub probes’ (MM > 0.80) and their annotated genes for all five modules associated with schizophrenia in the PFC. Of relevance, three of these genes are particularly interesting in the context of schizophrenia:

- The *lysine demethylase 3B (KDM3B)* gene (cg03315484, ‘black’ module) is one of the genes implicated in the largest schizophrenia GWAS to date (Schizophrenia Working Group of the Psychiatric Genomics, 2014))
- The *ankyrin 3 (ANK3)* gene (cg22150335, ‘brown’ module) encodes a protein found on the axons and nodes of Ranvier of neurons in the central and peripheral nervous systems and has been previously implicated in schizophrenia and bipolar disorder (Ferreira et al., 2008, Wirgenes et al., 2014).
- The *MTOR, complex 1 (RPTOR)* gene is annotated to a probe significantly associated with PRS (cg15022015, associated with PRS in the STR: $P = 3.82E-06$ and multi-region model: $P = 3.44E-05$. See **Chapter 4 section 4.3.4** for details). Of note, this is a distinct probe from o the ‘brown’ module ‘hub probe’ (cg10281768) annotated to the same gene.

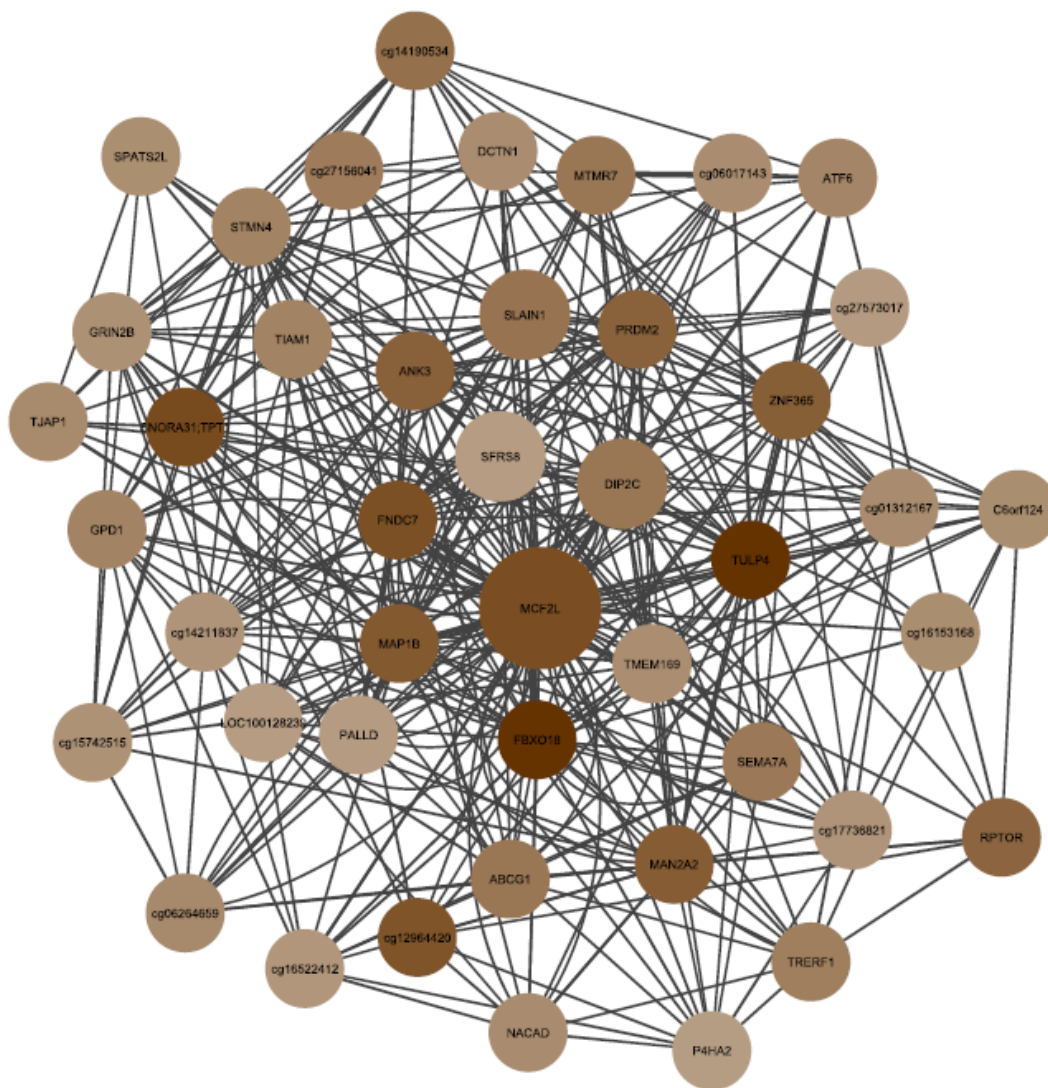


Figure 5.11. 'Brown' module of the prefrontal cortex (PFC) network (schizophrenia cases and non-psychiatric controls). The figure shows the strongest correlations ($\rho > 0.80$) between the 'hub probes' ($MM > 0.80$) in the 'brown' PFC module. Shown are the genes annotated to the respective 'hub probes'. If the probe is not annotated to a gene the probe name is presented. The size of the circles indicates the degree of the node, or in other words the number of strong correlations ($\rho > 0.80$) between the probes annotated to that gene and other probes (larger meaning higher number of connections). The colour of the circle represents module membership (darker colour means higher module membership).

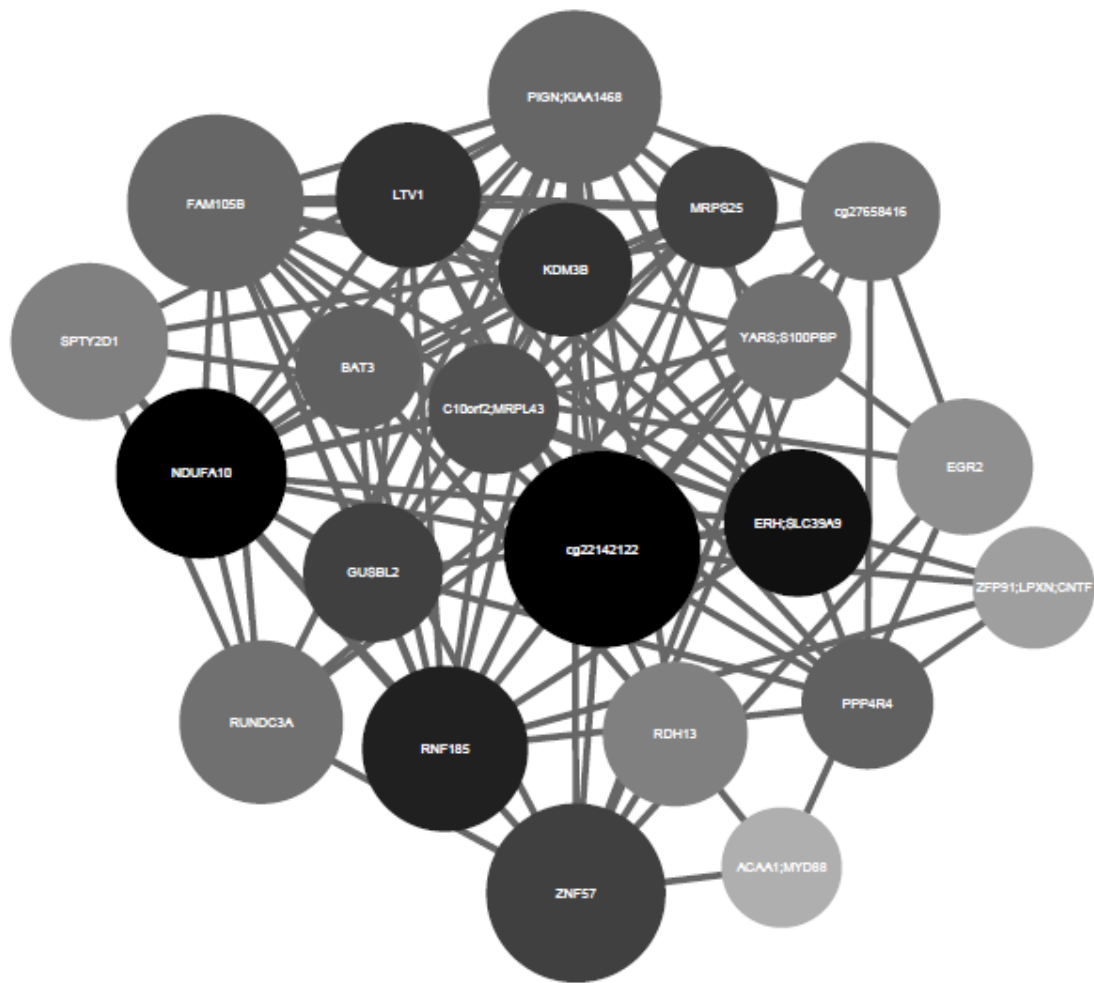


Figure 5.12. 'Black' module of the prefrontal cortex (PFC) network (schizophrenia cases and non-psychiatric controls). The figure shows the stronger correlations ($\rho > 0.80$) between the 'hub probes' ($MM > 0.80$) in the 'black' PFC module. Shown are the genes annotated to the respective 'hub probes'. If the probe is not annotated to a gene the probe name is presented. The size of the circles indicates the degree of the node, or in other words the number of strong correlations ($\rho > 0.80$) between the probes annotated to that gene and other probes (larger meaning higher number of connections). The colour of the circle represents module membership (darker colour means higher module membership).

Table 5.7. List of 'hub probes' (module membership > 0.80) from the prefrontal cortex modules 'brown', 'black', 'tan', 'salmon' and 'darkgrey'

Probe ID	Genomic position (hg19)	Module membership	Module no.	Module colour	Illumina gene annotation	Gene region
cg01411652	chr1:14113172	0.81	3	brown	<i>PRDM2</i>	Body; 3'UTR
cg11413570	chr1:109260678	0.80	3	brown	<i>FNDC7</i>	Body
cg03391019	chr1:161927947	0.81	3	brown	<i>ATF6</i>	Body
cg06492521	chr10:532357	0.81	3	brown	<i>DIP2C</i>	Body
cg18503829	chr10:729956	0.83	3	brown	<i>DIP2C</i>	Body
cg10610648	chr10:5969457	0.80	3	brown	<i>FBXO18</i>	Body
cg22150335	chr10:62148959	0.83	3	brown	<i>ANK3</i>	Body
cg02712553	chr10:64136038	0.81	3	brown	<i>ZNF365</i>	Body
cg06017143	chr11:82403271	0.80	3	brown	-	-
cg00704554	chr11:133902198	0.83	3	brown	<i>LOC100128239</i>	Body
cg17174980	chr12:14109514	0.80	3	brown	<i>GRIN2B</i>	5'UTR
cg23251170	chr12:50496350	0.81	3	brown	<i>GPD1</i>	TSS1500
cg09814354	chr12:132278430	0.82	3	brown	<i>SFRS8</i>	Body
cg01614703	chr12:132278510	0.81	3	brown	<i>SFRS8</i>	Body
cg16522412	chr13:33926811	0.81	3	brown	-	-
cg11218434	chr13:45911764	0.80	3	brown	<i>SNORA31; TPT1</i>	TSS200; Body
cg12964420	chr13:50975679	0.81	3	brown	-	-
cg25253705	chr13:78314465	0.82	3	brown	<i>SLAIN1</i>	Body; TSS1500
cg08504583	chr13:78315584	0.81	3	brown	<i>SLAIN1</i>	Body; 5'UTR
cg02676602	chr13:113698408	0.81	3	brown	<i>MCF2L</i>	Body
cg02810375	chr13:113698416	0.82	3	brown	<i>MCF2L</i>	Body
cg07443074	chr13:113698946	0.80	3	brown	<i>MCF2L</i>	Body
cg22495636	chr13:113698951	0.83	3	brown	<i>MCF2L</i>	Body
cg12314335	chr13:113699016	0.86	3	brown	<i>MCF2L</i>	Body
cg14190534	chr14:90848416	0.86	3	brown	-	-
cg18335991	chr15:74724562	0.84	3	brown	<i>SEMA7A</i>	Body; 5'UTR
cg17017272	chr15:91447374	0.84	3	brown	<i>MAN2A2</i>	TSS200
cg27573017	chr17:48258708	0.82	3	brown	-	-
cg10281768	chr17:78720226	0.81	3	brown	<i>RPTOR</i>	Body
cg14211837	chr18:53695649	0.84	3	brown	-	-
cg01312167	chr2:54292798	0.84	3	brown	-	-
cg17736821	chr2:64844761	0.82	3	brown	-	-
cg06264659	chr2:64998062	0.80	3	brown	-	-
cg06909228	chr2:74602278	0.81	3	brown	<i>DCTN1</i>	Body; TSS1500
cg02882004	chr2:201334663	0.81	3	brown	<i>SPATS2L</i>	Body
cg20968678	chr2:216948982	0.80	3	brown	<i>TMEM169</i>	5'UTR

cg26648185	chr21:32927013	0.83	3	brown	<i>TIAM1</i>	5'UTR
cg27243685	chr21:43642366	0.81	3	brown	<i>ABCG1</i>	Body; 5'UTR
cg06044751	chr4:169789830	0.80	3	brown	<i>PALLD</i>	5'UTR; Body
cg16153168	chr5:68114337	0.82	3	brown	-	-
cg02073775	chr5:71478626	0.81	3	brown	<i>MAP1B</i>	Body
cg22485921	chr5:131557716	0.81	3	brown	<i>P4HA2</i>	5'UTR
cg11548059	chr6:42225756	0.83	3	brown	<i>TRERF1</i>	Body
cg11910652	chr6:43457274	0.80	3	brown	<i>TJAP1</i>	5'UTR; Body; TSS200
cg10296548	chr6:158797675	0.81	3	brown	<i>TULP4</i>	Body
cg00035268	chr6:168225394	0.81	3	brown	<i>C6orf124</i>	Body
cg00733493	chr7:45126655	0.80	3	brown	<i>NACAD</i>	Body
cg27156041	chr7:98199360	0.81	3	brown	-	-
cg15742515	chr8:1402185	0.82	3	brown	-	-
cg03080147	chr8:17270347	0.82	3	brown	<i>MTMR7</i>	Body
cg02130905	chr8:27116213	0.80	3	brown	<i>STMN4</i>	TSS1500
cg02504327	chr1:33283743	0.81	7	black	<i>YARS;</i> <i>S100PBP</i>	TSS200; 5'UTR
cg24868421	chr10:64577216	0.81	7	black	<i>EGR2</i>	5'UTR; TSS1500
cg10309340	chr10:102747329	0.80	7	black	<i>C10orf2;</i> <i>MRPL43</i>	1stExon; 5'UTR; TSS200
cg04375578	chr11:18655531	0.82	7	black	<i>SPTY2D1</i>	Body
cg04570322	chr11:58345695	0.81	7	black	<i>ZFP91; LPXN;</i> <i>ZFP91-CNTF</i>	TSS1500; TSS200
cg04509559	chr14:69864994	0.81	7	black	<i>ERH;</i> <i>SLC39A9</i>	1stExon; 5'UTR; TSS1500
cg00748938	chr14:94641781	0.84	7	black	<i>PPP4R4</i>	Body
cg18495307	chr17:42385942	0.83	7	black	<i>RUNDC3A</i>	1stExon; 5'UTR
cg18661731	chr18:59854239	0.80	7	black	<i>PIGN;</i> <i>KIAA1468</i>	5'UTR; 1stExon; TSS1500
cg10661629	chr19:2900748	0.82	7	black	<i>ZNF57</i>	TSS200
cg02279127	chr19:55574702	0.81	7	black	<i>RDH13</i>	TSS200; 5'UTR
cg23348161	chr2:240964931	0.86	7	black	<i>NDUFA10</i>	TSS200
cg11672225	chr22:31556238	0.85	7	black	<i>RNF185</i>	1stExon; Body; 5'UTR
cg00001245	chr3:15106710	0.80	7	black	<i>MRPS25</i>	1stExon; 5'UTR
cg00884680	chr3:38178684	0.84	7	black	<i>ACAA1;</i> <i>MYD88</i>	1stExon; Body; 5'UTR; TSS1500
cg26395828	chr5:14665166	0.85	7	black	<i>FAM105B</i>	Body

cg03315484	chr5:137688433	0.88	7	black	<i>KDM3B</i>	1stExon; 5'UTR
cg27658416	chr6:28603033	0.85	7	black	-	-
cg22142122	chr6:28979338	0.82	7	black	-	-
cg17615061	chr6:31620208	0.82	7	black	<i>BAT3</i>	1stExon; TSS200; 5'UTR
cg10189605	chr6:58287430	0.86	7	black	<i>GUSBL2</i>	Body
cg23493127	chr6:144164392	0.82	7	black	<i>LTV1</i>	TSS200
cg25214914	chr1:155910523	0.83	12	tan	<i>RXFP4</i>	TSS1500
cg04130507	chr1:182030753	0.80	12	tan	<i>ZNF648</i>	5'UTR; 1stExon
cg27454102	chr10:32428473	0.84	12	tan	-	-
cg09519218	chr10:126390317	0.81	12	tan	<i>FAM53B</i>	Body
cg27274382	chr11:76376064	0.80	12	tan	<i>LRRC32</i>	Body
cg02054358	chr17:70335431	0.81	12	tan	-	-
cg23787321	chr2:43385844	0.80	12	tan	-	-
cg05082708	chr4:4765299	0.81	12	tan	-	-
cg04859102	chr6:31527893	0.81	12	tan	-	-
cg11869828	chr11:116700447	0.80	13	salmon	<i>APOC3</i>	TSS200
cg12332902	chr2:98330020	0.84	13	salmon	<i>ZAP70</i>	TSS200
cg12003230	chr21:44899139	0.83	13	salmon	<i>C21orf84</i>	TSS1500
cg16562486	chr1:2925740	0.89	24	darkgrey	-	-
cg27518860	chr1:35250839	0.91	24	darkgrey	<i>GJB3</i>	Body
cg10702366	chr1:60070383	0.96	24	darkgrey	<i>FGGY</i>	Body
cg13444583	chr10:132600162	0.88	24	darkgrey	-	-
cg09538401	chr11:111171330	0.88	24	darkgrey	<i>C11orf93</i> ; <i>C11orf92</i>	5'UTR; TSS1500
cg15774028	chr17:78183443	0.94	24	darkgrey	<i>SGSH</i>	3'UTR
cg00141153	chr17:78183500	0.89	24	darkgrey	<i>SGSH</i>	3'UTR
cg15458322	chr19:10070965	0.89	24	darkgrey	<i>COL5A3</i>	3'UTR
cg16889990	chr19:57631478	0.84	24	darkgrey	<i>USP29</i>	TSS200
cg05761971	chr2:38177677	0.93	24	darkgrey	<i>FAM82A1</i>	5'UTR; 1stExon; Body
cg18033443	chr3:14584240	0.83	24	darkgrey	<i>GRIP2</i>	TSS1500
cg25785495	chr3:134910848	0.82	24	darkgrey	<i>EPHB1</i>	Body
cg00699947	chr4:4592560	0.85	24	darkgrey	-	-
cg02645905	chr9:140612442	0.81	24	darkgrey	<i>EHMT1</i>	Body

Recently, a study reported over 500 novel interactions with genes previously implicated in schizophrenia using a new protein-protein interactions (PPI) approach (Ganapathiraju et al., 2016). PPI maps can aid understanding complex regulatory networks underlying disease etiology by identifying groups of genes that interact with liability genes for a particular disease. The authors of this study identified 365 new interactions with genes from the latest schizophrenia GWAS (Schizophrenia Working Group of the Psychiatric Genomics, 2014) and 147 new interactions with genes that were implicated in schizophrenia prior to the GWAS era (*i.e.* as candidate genes).

I next investigated whether the genes annotated to the 'hub probes' of the schizophrenia-associated modules are present in the interactions identified by Ganapathiraju et al. (2016). To do this I used the list of interacting genes in the Supplementary File 2 from their paper (Ganapathiraju et al., 2016) and the online tool the authors made available to investigate the PPI identified in all of their studies (Ganapathiraju, 2012-2016). **Table 5.8** shows the genes annotated to 'hub probes' of schizophrenia-associated modules that have an interaction with at least one schizophrenia-linked gene in Ganapathiraju et al. (2016).

Interestingly, two genes of the 'brown' module interact with *disrupted in schizophrenia 1 (DISC1)* gene. A balanced translocation involving this gene that segregates with several major psychiatric disorders including schizophrenia has been intensively studied in a Scottish pedigree (St Clair et al., 1990). Furthermore, I identified PRS-associated differential DNA methylation at a probe annotated to this gene in a cross-region model including data from PFC, STR and HC (see **Chapter 4 section 4.3.4**). Furthermore, 7 genes from the 'brown', 'black', 'salmon' and 'darkgrey' modules have interactions with genes associated with schizophrenia in the latest GWAS (Schizophrenia Working Group of the Psychiatric Genomics, 2014).

Table 5.8. Genes annotated to 'hub probes' of schizophrenia-associated modules that have an interaction with a hypothesised schizophrenia gene (Ganapathiraju et al., 2016). Shown is the gene annotated to the 'hub probe' and respective module, the interacting gene and the study where the association with schizophrenia was published.

Probe(s) ID(s)	Module no.	Module colour	Gene in module	Interaction	Association with schizophrenia
cg02712553	3	brown	ZNF365	DISC1	St Clair et al. (1990)
cg06909228	3	brown	DCTN1		
cg18335991	3	brown	SEMA7A	CHRNA5	
cg17017272	3	brown	MAN2A2	FES	
cg10296548	3	brown	TULP4	MAD1L1	Schizophrenia Working Group of the
cg24868421	7	black	EGR2	NAB2	Psychiatric Genomics (2014)
cg23348161	7	black	NDUFA10	CUL3	
cg12332902	13	salmon	ZAP70		
cg15774028;	24	darkgrey	SGSH	DRD2	
cg00141153					

To test if the same modules were associated with schizophrenia in the other brain tissues I imposed the PFC network structure on the data from the other brain regions. To do this I calculated the ME of the PFC modules using the STR, HC and CER data and performed an independent t-test between the MEs of schizophrenia cases and controls as described above. None of the five modules were associated with schizophrenia in the other brain regions (**Table 5.9**) suggesting the effects were specific to the PFC.

Table 5.9. Association between modules identified in the prefrontal cortex and schizophrenia in the striatum (STR), hippocampus (HC) and cerebellum (CER). Shown are the *P*-values for the t-tests between disease status and eigengenes for each prefrontal cortex module. None are significantly associated with schizophrenia in any of the three other brain regions. Highlighted in grey are the modules that were nominally associated with schizophrenia in the PFC network.

PFC module No.	PFC module colour	<i>P</i> PFC	<i>P</i> STR	<i>P</i> HC	<i>P</i> CER
3	brown	0.05	0.30	0.64	0.54
7	black	0.05	0.31	0.11	0.24
12	tan	0.04	0.32	0.93	0.40
13	salmon	0.04	0.37	0.40	0.58
24	darkgrey	0.04	0.86	0.13	0.11

5.6.3. Gene ontology analysis on schizophrenia-associated modules

I next performed an enrichment analysis on GO terms associated with genes belonging to each PFC schizophrenia-associated module to test for a significant enrichment of particular GO terms (Ashburner et al., 2000). I used an approach developed by our group, as described in Lunnon et al. (2016b). In summary, all probes within each module were annotated to genes using the standard Illumina annotation file (GRCh37/hg19). A logistic regression model was used to test if genes in each module predicted pathway membership, while controlling for the number of probes in each network annotated to each gene. Pathways were downloaded from the GO website (Gene Ontology Consortium, 2015) and mapped to genes including all parent ontology terms. All genes with at least one 450k probe annotated and mapped to at least one GO pathway were considered. Pathways were filtered to those containing between 10 and 2000 genes. After applying this method to all pathways, the list of significant pathways ($P < 0.05$) was refined by grouping related pathways to control for the effect of overlapping genes. This was achieved by taking the most significant pathway, and retesting all remaining significant pathways while controlling additionally for this best term. If the test genes no longer predicted the pathway, the term was said to be explained by the more significant pathway, and hence these pathways were grouped together. This algorithm was repeated, taking the next most significant term, until all pathways were considered as the most significant or found to be explained by a more significant term.

Tables 5.10 to 5.14 present pathways with a P -value $< 1.00E-03$ ranked by significance for the 5 PFC modules. Notably, the eleven most significantly enriched pathways on the largest ('brown') module are neuronal function- and neurodevelopment-relevant pathways, such as GO:0007399 - nervous system development, GO:0097458 – neuron part and GO:0010975 - regulation of neuron projection development.

Table 5.10. Pathway analysis in the prefrontal cortex ‘brown’ module using data from schizophrenia cases and controls. Analysis testing for a significant enrichment of genes belonging to the prefrontal cortex ‘brown’ module overlapping gene ontology (GO) terms.

GO term	ID	Total genes in pathway	Module genes in pathway	P
GO:0097458	neuron part	830	365	2.07E-15
GO:0007399	nervous system development	1804	721	2.31E-15
GO:0030054	cell junction	778	332	3.47E-13
GO:0045202	Synapse	514	240	1.00E-12
GO:0042995	cell projection	1334	522	1.25E-12
GO:0010975	regulation of neuron projection development	248	126	3.87E-11
GO:0006928	cellular component movement	1199	460	1.54E-10
GO:0050793	regulation of developmental process	1612	594	1.76E-10
GO:0019226	transmission of nerve impulse	629	264	4.57E-10
GO:0030424	Axon	278	142	6.04E-10
GO:0051960	regulation of nervous system development	517	228	7.45E-10
GO:0008092	cytoskeletal protein binding	696	284	1.53E-09
GO:0035556	intracellular signal transduction	1423	522	1.69E-09
GO:0000904	cell morphogenesis involved in differentiation	586	261	5.84E-09
GO:0051056	regulation of small GTPase mediated signal transduction	380	175	1.01E-08
GO:0016301	kinase activity	766	297	1.72E-08
GO:0007268	synaptic transmission	608	249	2.10E-08
GO:0048167	regulation of synaptic plasticity	104	61	2.12E-08
GO:0019220	regulation of phosphate metabolic process	1502	548	2.24E-08
GO:0051270	regulation of cellular component movement	538	218	2.76E-08
GO:0007155	cell adhesion	798	324	9.83E-08
GO:0007169	transmembrane receptor protein tyrosine kinase signaling pathway	554	228	1.55E-07
GO:1902531	regulation of intracellular signal transduction	1240	450	1.65E-07
GO:0035023	regulation of Rho protein signal transduction	135	66	3.51E-07
GO:0006897	Endocytosis	362	146	3.52E-07
GO:0030695	GTPase regulator activity	273	125	4.13E-07
GO:0043547	positive regulation of GTPase activity	161	80	9.81E-07
GO:0031252	cell leading edge	289	131	1.01E-06
GO:0051128	regulation of cellular component organization	1411	503	1.06E-06
GO:0010648	negative regulation of cell communication	839	318	1.17E-06
GO:0030426	growth cone	110	58	1.17E-06
GO:0009605	response to external stimulus	1154	413	1.21E-06
GO:0031226	intrinsic component of plasma membrane	1249	434	2.18E-06
GO:0034330	cell junction organization	178	82	2.94E-06
GO:0005085	guanyl-nucleotide exchange factor activity	175	87	2.97E-06
GO:0070848	response to growth factor	549	219	3.16E-06
GO:0071526	semaphorin-plexin signaling pathway	16	13	4.84E-06
GO:0009611	response to wounding	998	342	5.62E-06
GO:0030111	regulation of Wnt signaling pathway	195	90	6.54E-06
GO:0045121	membrane raft	203	89	6.74E-06
GO:0048471	perinuclear region of cytoplasm	506	191	7.80E-06
GO:0018212	peptidyl-tyrosine modification	122	60	1.04E-05
GO:0005231	excitatory extracellular ligand-gated ion channel activity	48	26	1.34E-05
GO:0007612	Learning	99	51	1.42E-05
GO:0008289	lipid binding	535	195	1.66E-05
GO:0015020	glucuronosyltransferase activity	27	17	1.84E-05
GO:0016772	transferase activity	901	322	1.94E-05

GO:0043551	regulation of phosphatidylinositol 3-kinase activity	30	19	2.23E-05
GO:0005794	Golgi apparatus	1183	399	2.31E-05
GO:0070307	lens fiber cell development	12	10	2.59E-05
GO:0044089	positive regulation of cellular component biogenesis	24	18	3.78E-05
GO:0030168	platelet activation	210	85	4.87E-05
GO:0032940	secretion by cell	404	153	4.89E-05
GO:0006029	proteoglycan metabolic process	84	41	5.93E-05
GO:0019899	enzyme binding	1183	416	6.65E-05
GO:0015081	sodium ion transmembrane transporter activity	125	53	6.75E-05
GO:0031338	regulation of vesicle fusion	14	10	7.20E-05
GO:0005328	neurotransmitter:sodium symporter activity	21	14	8.80E-05
GO:0045913	positive regulation of carbohydrate metabolic process	47	25	9.13E-05
GO:0030198	extracellular matrix organization	310	129	9.24E-05
GO:0035591	signaling adaptor activity	61	31	9.68E-05
GO:0048745	smooth muscle tissue development	19	13	1.03E-04
GO:0031012	extracellular matrix	422	162	1.25E-04
GO:0019902	phosphatase binding	131	59	1.26E-04
GO:0045161	neuronal ion channel clustering	12	10	1.41E-04
GO:0061097	regulation of protein tyrosine kinase activity	50	26	1.45E-04
GO:0006811	ion transport	983	329	1.49E-04
GO:0048306	calcium-dependent protein binding	47	24	1.50E-04
GO:0000979	RNA polymerase II core promoter sequence-specific DNA binding	29	18	1.67E-04
GO:0001568	blood vessel development	425	162	1.87E-04
GO:0005057	receptor signaling protein activity	131	56	1.89E-04
GO:0048013	ephrin receptor signaling pathway	28	17	2.27E-04
GO:0019897	extrinsic component of plasma membrane	87	41	2.53E-04
GO:0005509	calcium ion binding	661	249	2.80E-04
GO:0009986	cell surface	500	171	3.23E-04
GO:0016358	dendrite development	64	35	3.80E-04
GO:0030010	establishment of cell polarity	63	35	4.04E-04
GO:0007158	neuron cell-cell adhesion	10	8	4.10E-04
GO:0032863	activation of Rac GTPase activity	10	8	4.31E-04
GO:0043235	receptor complex	256	109	4.36E-04
GO:0005544	calcium-dependent phospholipid binding	28	15	4.68E-04
GO:0045833	negative regulation of lipid metabolic process	61	29	4.92E-04
GO:0045620	negative regulation of lymphocyte differentiation	30	16	5.02E-04
GO:0090004	positive regulation of establishment of protein localization to plasma membrane	21	13	5.65E-04
GO:0018210	peptidyl-threonine modification	42	22	5.81E-04
GO:0072006	nephron development	86	41	5.90E-04
GO:0001106	RNA polymerase II transcription corepressor activity	18	12	6.64E-04
GO:0010893	positive regulation of steroid biosynthetic process	12	9	6.86E-04
GO:0030276	clathrin binding	23	13	6.91E-04
GO:0050853	B cell receptor signaling pathway	30	16	7.20E-04
GO:0072661	protein targeting to plasma membrane	18	13	8.75E-04
GO:0005942	phosphatidylinositol 3-kinase complex	14	9	8.78E-04
GO:0060191	regulation of lipase activity	117	52	9.98E-04

Table 5.11. Pathway analysis in the prefrontal cortex ‘black’ module using data from schizophrenia cases and controls. Analysis testing for a significant enrichment of genes belonging to the prefrontal cortex 7.black module overlapping gene ontology (GO) terms.

GO term	ID	Total genes in pathway	Module genes in pathway	<i>P</i>
GO:0032434	regulation of proteasomal ubiquitin-dependent protein catabolic process	67	23	1.02E-07
GO:0034593	phosphatidylinositol bisphosphate phosphatase activity	13	8	1.27E-07
GO:0044265	cellular macromolecule catabolic process	669	123	2.15E-07
GO:0007049	cell cycle	1210	208	4.35E-06
GO:0042809	vitamin D receptor binding	14	7	4.93E-06
GO:0009894	regulation of catabolic process	670	138	7.07E-06
GO:0003723	RNA binding	869	148	7.49E-06
GO:0044772	mitotic cell cycle phase transition	275	58	2.06E-05
GO:0005654	nucleoplasm	1398	234	2.40E-05
GO:0009263	deoxyribonucleotide biosynthetic process	12	6	2.96E-05
GO:0031625	ubiquitin protein ligase binding	158	38	4.14E-05
GO:0044389	small conjugating protein ligase binding	158	38	4.14E-05
GO:0005811	lipid particle	50	15	4.54E-05
GO:0006661	phosphatidylinositol biosynthetic process	87	23	4.66E-05
GO:0016126	sterol biosynthetic process	36	12	5.17E-05
GO:0016780	phosphotransferase activity	15	7	5.72E-05
GO:0015630	microtubule cytoskeleton	898	158	5.72E-05
GO:0034708	methyltransferase complex	75	20	6.05E-05
GO:0051641	cellular localization	1713	276	6.99E-05
GO:0043981	histone H4-K5 acetylation	13	6	7.28E-05
GO:0043982	histone H4-K8 acetylation	13	6	7.28E-05
GO:0045717	negative regulation of fatty acid biosynthetic process	10	5	7.62E-05
GO:0009132	nucleoside diphosphate metabolic process	25	9	8.49E-05
GO:0000050	urea cycle	10	5	8.99E-05
GO:0032042	mitochondrial DNA metabolic process	13	6	1.03E-04
GO:0016241	regulation of macroautophagy	23	9	1.05E-04
GO:0031312	extrinsic component of organelle membrane	10	5	1.06E-04
GO:2001251	negative regulation of chromosome organization	40	13	1.16E-04
GO:0001953	negative regulation of cell-matrix adhesion	20	8	1.23E-04
GO:0043249	erythrocyte maturation	10	5	1.29E-04
GO:0048505	regulation of timing of cell differentiation	11	6	1.42E-04
GO:0061028	establishment of endothelial barrier	13	6	1.76E-04
GO:0050768	negative regulation of neurogenesis	96	27	1.83E-04
GO:0090344	negative regulation of cell aging	13	6	1.88E-04
GO:1902337	regulation of apoptotic process involved in morphogenesis	10	5	2.02E-04

GO:0010884	positive regulation of lipid storage	18	7	2.05E-04
GO:0010762	regulation of fibroblast migration	16	7	2.09E-04
GO:1902494	catalytic complex	726	123	2.19E-04
GO:0048008	platelet-derived growth factor receptor signaling pathway	32	11	2.71E-04
GO:0045879	negative regulation of smoothed signaling pathway	24	9	2.86E-04
GO:0043555	regulation of translation in response to stress	11	5	3.18E-04
GO:2000058	regulation of protein ubiquitination involved in ubiquitin-dependent protein catabolic process	17	7	3.62E-04
GO:0006464	cellular protein modification process	1892	296	4.05E-04
GO:0036211	protein modification process	1892	296	4.05E-04
GO:0019012	Virion	15	6	4.24E-04
GO:0019028	viral capsid	15	6	4.24E-04
GO:0044423	virion part	15	6	4.24E-04
GO:0008409	5'-3' exonuclease activity	11	5	4.32E-04
GO:0006260	DNA replication	207	41	4.46E-04
GO:0006974	cellular response to DNA damage stimulus	626	106	4.46E-04
GO:0010833	telomere maintenance via telomere lengthening	36	11	4.68E-04
GO:0034061	DNA polymerase activity	32	10	4.77E-04
GO:0005524	ATP binding	1430	231	4.93E-04
GO:0090317	negative regulation of intracellular protein transport	65	17	5.20E-04
GO:0030522	intracellular receptor signaling pathway	167	35	5.30E-04
GO:0043009	chordate embryonic development	589	112	5.45E-04
GO:0005730	Nucleolus	636	105	6.42E-04
GO:0016197	endosomal transport	142	30	6.56E-04
GO:0001501	skeletal system development	412	83	6.89E-04
GO:0005669	transcription factor TFIID complex	20	7	7.25E-04
GO:0048488	synaptic vesicle endocytosis	18	7	7.60E-04
GO:0032269	negative regulation of cellular protein metabolic process	472	88	7.86E-04
GO:0060079	regulation of excitatory postsynaptic membrane potential	41	14	8.31E-04
GO:0031648	protein destabilization	20	7	8.58E-04
GO:2000178	negative regulation of neural precursor cell proliferation	17	7	8.79E-04
GO:0033057	multicellular organismal reproductive behavior	20	7	9.05E-04
GO:0031941	filamentous actin	19	7	9.57E-04

Table 5.12. Pathway analysis in the prefrontal cortex ‘tan’ module using data from schizophrenia cases and controls. Analysis testing for a significant enrichment of genes belonging to the prefrontal cortex 12.tan module overlapping gene ontology (GO) terms.

GO term	ID	Total genes in pathway	Module genes in pathway	P
GO:1901379	regulation of potassium ion transmembrane transport	20	7	1.51E-10
GO:0043268	positive regulation of potassium ion transport	16	6	7.03E-10
GO:0017166	vinculin binding	10	4	4.85E-09
GO:0034767	positive regulation of ion transmembrane transport	22	6	2.48E-07
GO:0043034	costamere	17	5	4.39E-07
GO:0032012	regulation of ARF protein signal transduction	42	9	6.08E-07
GO:0044304	main axon	50	10	6.43E-07
GO:0035591	signaling adaptor activity	61	10	1.56E-06
GO:1902531	regulation of intracellular signal transduction	1240	91	1.59E-06
GO:0032794	GTPase activating protein binding	14	4	1.99E-06
GO:0072677	eosinophil migration	10	3	2.11E-06
GO:0044295	axonal growth cone	12	4	2.53E-06
GO:0019226	transmission of nerve impulse	629	55	3.18E-06
GO:0042993	positive regulation of transcription factor import into nucleus	34	6	3.85E-06
GO:0042753	positive regulation of circadian rhythm	10	3	4.41E-06
GO:0033268	node of Ranvier	14	4	6.18E-06
GO:1901016	regulation of potassium ion transmembrane transporter activity	15	4	6.29E-06
GO:0030054	cell junction	778	65	6.34E-06
GO:0043270	positive regulation of ion transport	139	16	8.18E-06
GO:0070098	chemokine-mediated signaling pathway	27	5	8.67E-06
GO:0006897	endocytosis	362	32	9.74E-06
GO:0046689	response to mercury ion	11	3	1.08E-05
GO:0005085	guanyl-nucleotide exchange factor activity	175	22	1.13E-05
GO:0048584	positive regulation of response to stimulus	1344	88	1.20E-05
GO:0004673	protein histidine kinase activity	10	3	1.31E-05
GO:0036041	long-chain fatty acid binding	11	3	1.48E-05
GO:0005083	small GTPase regulator activity	166	20	2.71E-05
GO:0015695	organic cation transport	19	4	4.54E-05
GO:0030506	ankyrin binding	20	5	6.65E-05
GO:0017124	SH3 domain binding	115	14	6.95E-05
GO:0009312	oligosaccharide biosynthetic process	13	3	7.23E-05
GO:0016023	cytoplasmic membrane-bounded vesicle	927	62	8.53E-05
GO:0005249	voltage-gated potassium channel activity	83	11	8.68E-05
GO:0008092	cytoskeletal protein binding	696	55	9.75E-05
GO:0051707	response to other organism	558	35	9.87E-05
GO:0009415	response to water	11	3	1.06E-04

GO:0005925	focal adhesion	126	15	1.47E-04
GO:0097481	neuronal postsynaptic density	11	3	1.69E-04
GO:0050954	sensory perception of mechanical stimulus	135	16	2.01E-04
GO:0019894	kinesin binding	25	5	2.09E-04
GO:0048525	negative regulation of viral process	47	6	2.12E-04
GO:0030676	Rac guanyl-nucleotide exchange factor activity	11	3	2.73E-04
GO:0003013	circulatory system process	272	23	2.75E-04
GO:0001945	lymph vessel development	20	4	3.22E-04
GO:0005680	anaphase-promoting complex	23	4	3.32E-04
GO:0050775	positive regulation of dendrite morphogenesis	13	3	3.83E-04
GO:0090344	negative regulation of cell aging	13	3	3.91E-04
GO:0006972	hyperosmotic response	24	4	4.00E-04
GO:0016235	aggresome	22	4	4.16E-04
GO:0010453	regulation of cell fate commitment	28	5	4.19E-04
GO:1902603	carnitine transmembrane transport	12	3	4.26E-04
GO:0005887	integral component of plasma membrane	1202	76	4.32E-04
GO:0072283	metanephric renal vesicle morphogenesis	11	3	4.53E-04
GO:0001775	cell activation	582	40	4.61E-04
GO:0031998	regulation of fatty acid beta-oxidation	13	3	4.75E-04
GO:0042088	T-helper 1 type immune response	17	3	5.68E-04
GO:0050848	regulation of calcium-mediated signaling	35	5	6.11E-04
GO:0051225	spindle assembly	42	6	6.48E-04
GO:0051270	regulation of cellular component movement	538	41	6.85E-04
GO:0008015	blood circulation	270	22	7.45E-04
GO:0010939	regulation of necrotic cell death	16	3	7.73E-04
GO:0043368	positive T cell selection	20	4	8.18E-04
GO:0004672	protein kinase activity	579	44	8.61E-04
GO:0045408	regulation of interleukin-6 biosynthetic process	18	3	9.71E-04

Table 5.13. Pathway analysis in the prefrontal cortex ‘salmon’ module using data from schizophrenia cases and controls. Analysis testing for a significant enrichment of genes belonging to the prefrontal cortex 13.salmon module overlapping gene ontology (GO) terms.

GO term	ID	Total genes in pathway	Module genes in pathway	P
GO:0043535	regulation of blood vessel endothelial cell migration	43	10	2.81E-12
GO:0007155	cell adhesion	798	73	1.03E-11
GO:0051270	regulation of cellular component movement	538	50	2.50E-11
GO:0043537	negative regulation of blood vessel endothelial cell migration	20	6	4.70E-11
GO:0090049	regulation of cell migration involved in sprouting angiogenesis	15	5	1.27E-10
GO:0007156	homophilic cell adhesion	135	25	3.57E-10
GO:0003951	NAD+ kinase activity	16	5	1.46E-09
GO:0015271	outward rectifier potassium channel activity	10	4	1.33E-08
GO:0040013	negative regulation of locomotion	169	20	1.64E-08
GO:0071435	potassium ion export	10	4	2.85E-08
GO:0001570	vasculogenesis	69	11	5.94E-08
GO:0048747	muscle fiber development	34	7	7.30E-08
GO:0019048	modulation by virus of host morphology or physiology	25	6	7.63E-08
GO:0001944	vasculature development	452	39	9.75E-08
GO:0001945	lymph vessel development	20	5	1.40E-07
GO:0050951	sensory perception of temperature stimulus	14	4	2.33E-07
GO:0002042	cell migration involved in sprouting angiogenesis	15	4	3.46E-07
GO:0031362	anchored component of external side of plasma membrane	16	4	3.64E-07
GO:0060840	artery development	55	9	6.39E-07
GO:0010631	epithelial cell migration	60	9	6.90E-07
GO:0090132	epithelium migration	60	9	6.90E-07
GO:0060841	venous blood vessel development	15	4	8.76E-07
GO:0043551	regulation of phosphatidylinositol 3-kinase activity	30	6	9.91E-07
GO:0031664	regulation of lipopolysaccharide-mediated signaling pathway	16	4	1.02E-06
GO:1901888	regulation of cell junction assembly	40	7	1.12E-06
GO:0043547	positive regulation of GTPase activity	161	19	1.53E-06
GO:0045909	positive regulation of vasodilation	25	5	2.19E-06
GO:0005509	calcium ion binding	661	52	2.42E-06
GO:0045834	positive regulation of lipid metabolic process	98	12	2.54E-06
GO:0006012	galactose metabolic process	11	3	2.68E-06
GO:0046503	glycerolipid catabolic process	28	5	2.98E-06
GO:0034763	negative regulation of transmembrane transport	16	4	3.54E-06
GO:0042887	amide transmembrane transporter activity	15	4	3.77E-06

GO:0004089	carbonate dehydratase activity	12	3	4.35E-06
GO:0002281	macrophage activation involved in immune response	11	3	5.89E-06
GO:0002832	negative regulation of response to biotic stimulus	19	4	6.68E-06
GO:0071467	cellular response to pH	12	3	8.27E-06
GO:0009611	response to wounding	998	60	9.62E-06
GO:0038084	vascular endothelial growth factor signaling pathway	11	3	1.04E-05
GO:0009628	response to abiotic stimulus	902	55	1.26E-05
GO:0032101	regulation of response to external stimulus	463	31	1.51E-05
GO:0072044	collecting duct development	11	3	1.70E-05
GO:0009415	response to water	11	3	1.70E-05
GO:0046885	regulation of hormone biosynthetic process	18	4	2.20E-05
GO:0032720	negative regulation of tumor necrosis factor production	29	5	2.57E-05
GO:0030214	hyaluronan catabolic process	13	3	2.67E-05
GO:0001701	in utero embryonic development	360	29	3.39E-05
GO:0043271	negative regulation of ion transport	62	8	3.51E-05
GO:0006066	alcohol metabolic process	310	23	3.81E-05
GO:0060039	pericardium development	17	4	4.01E-05
GO:0005901	Caveola	63	9	4.36E-05
GO:0017158	regulation of calcium ion-dependent exocytosis	27	5	5.09E-05
GO:0032332	positive regulation of chondrocyte differentiation	18	4	5.43E-05
GO:0016575	histone deacetylation	25	5	6.58E-05
GO:0060976	coronary vasculature development	12	3	7.66E-05
GO:0043406	positive regulation of MAP kinase activity	185	16	9.17E-05
GO:0034358	plasma lipoprotein particle	38	5	1.16E-04
GO:0032317	regulation of Rap GTPase activity	14	3	1.23E-04
GO:0042219	cellular modified amino acid catabolic process	15	3	1.24E-04
GO:0003158	endothelium development	59	8	1.26E-04
GO:0043500	muscle adaptation	27	5	1.29E-04
GO:0070412	R-SMAD binding	21	4	1.43E-04
GO:0019838	growth factor binding	110	12	1.46E-04
GO:0018108	peptidyl-tyrosine phosphorylation	120	13	1.56E-04
GO:0002920	regulation of humoral immune response	42	5	1.65E-04
GO:0045920	negative regulation of exocytosis	13	3	1.69E-04
GO:0050900	leukocyte migration	216	16	1.87E-04
GO:0032153	cell division site	44	6	1.88E-04
GO:0032155	cell division site part	44	6	1.88E-04
GO:0070887	cellular response to chemical stimulus	1868	96	1.99E-04
GO:0061061	muscle structure development	417	32	2.19E-04
GO:0035810	positive regulation of urine volume	15	3	2.20E-04
GO:0061298	retina vasculature development in camera-type eye	14	3	2.21E-04
GO:0014910	regulation of smooth muscle cell migration	33	5	2.24E-04
GO:0048008	platelet-derived growth factor receptor signaling pathway	32	5	2.46E-04

GO:0010243	response to organonitrogen compound	671	44	2.50E-04
GO:0097061	dendritic spine organization	13	3	2.54E-04
GO:0048569	post-embryonic organ development	15	3	2.55E-04
GO:0042588	zymogen granule	13	3	2.57E-04
GO:0018146	keratan sulfate biosynthetic process	29	4	2.92E-04
GO:0048841	regulation of axon extension involved in axon guidance	13	3	3.03E-04
GO:0001941	postsynaptic membrane organization	13	3	3.23E-04
GO:0006656	phosphatidylcholine biosynthetic process	25	4	3.41E-04
GO:0051904	pigment granule transport	17	3	3.49E-04
GO:0051905	establishment of pigment granule localization	17	3	3.49E-04
GO:0071813	lipoprotein particle binding	26	4	3.60E-04
GO:0071814	protein-lipid complex binding	26	4	3.60E-04
GO:0048638	regulation of developmental growth	127	13	3.89E-04
GO:0034405	response to fluid shear stress	25	4	3.95E-04
GO:0071695	anatomical structure maturation	46	6	3.98E-04
GO:0030510	regulation of BMP signaling pathway	63	8	5.13E-04
GO:0042886	amide transport	73	8	5.62E-04
GO:0030029	actin filament-based process	381	30	5.63E-04
GO:0001754	eye photoreceptor cell differentiation	40	5	6.14E-04
GO:0035850	epithelial cell differentiation involved in kidney development	23	4	6.59E-04
GO:0043198	dendritic shaft	32	5	7.44E-04
GO:0001848	complement binding	10	2	7.76E-04
GO:0035428	hexose transmembrane transport	10	2	8.04E-04
GO:0042056	chemoattractant activity	20	3	8.56E-04
GO:0043548	phosphatidylinositol 3-kinase binding	23	4	8.77E-04
GO:0005372	water transmembrane transporter activity	11	2	9.71E-04

Table 5.14. Pathway analysis in the prefrontal cortex 'darkgrey' module using data from schizophrenia cases and controls. Analysis testing for a significant enrichment of genes belonging to the prefrontal cortex 24.darkgrey module overlapping gene ontology (GO) terms.

GO term	ID	Total genes in pathway	Module genes in pathway	P
GO:0032806	carboxy-terminal domain protein kinase complex	10	2	9.73E-12
GO:0004115	3'5'-cyclic-AMP phosphodiesterase activity	10	2	4.28E-11
GO:0019098	reproductive behavior	30	3	1.74E-08
GO:0005527	macrolide binding	15	2	8.80E-08
GO:0005528	FK506 binding	15	2	8.80E-08
GO:0006029	proteoglycan metabolic process	84	5	3.00E-07
GO:0033363	secretory granule organization	18	2	7.64E-07
GO:0045822	negative regulation of heart contraction	18	2	9.01E-07
GO:0050885	neuromuscular process controlling balance	58	4	1.56E-06
GO:0031290	retinal ganglion cell axon guidance	18	2	1.66E-06
GO:0060384	Innervation	18	2	1.82E-06
GO:0005201	extracellular matrix structural constituent	62	4	1.93E-06
GO:0072676	lymphocyte migration	20	2	3.42E-06
GO:0034110	regulation of homotypic cell-cell adhesion	19	2	3.52E-06
GO:0009100	glycoprotein metabolic process	340	10	1.24E-05
GO:0050877	neurological system process	1168	24	1.29E-05
GO:0031683	G-protein beta/gamma-subunit complex binding	21	2	1.61E-05
GO:0008146	sulfotransferase activity	50	3	2.39E-05
GO:0010880	regulation of release of sequestered calcium ion into cytosol by sarcoplasmic reticulum	23	2	3.19E-05
GO:0060119	inner ear receptor cell development	25	2	4.91E-05
GO:0016266	O-glycan processing	52	3	7.66E-05
GO:0060326	cell chemotaxis	137	5	8.51E-05
GO:0004435	phosphatidylinositol phospholipase C activity	28	2	1.03E-04
GO:0044705	multi-organism reproductive behavior	28	2	1.26E-04
GO:0031589	cell-substrate adhesion	131	5	1.81E-04
GO:0034704	calcium channel complex	54	3	1.87E-04
GO:0046942	carboxylic acid transport	190	6	2.36E-04
GO:0061515	myeloid cell development	29	2	3.35E-04
GO:0015250	water channel activity	10	1	4.40E-04

GO:0005001	transmembrane receptor protein tyrosine phosphatase activity	20	2	4.89E-04
GO:0019198	transmembrane receptor protein phosphatase activity	20	2	4.89E-04
GO:0021955	central nervous system neuron axonogenesis	29	2	4.93E-04
GO:0007040	lysosome organization	34	2	5.04E-04
GO:0019855	calcium channel inhibitor activity	10	1	5.31E-04
GO:0032515	negative regulation of phosphoprotein phosphatase activity	10	1	5.56E-04
GO:0045717	negative regulation of fatty acid biosynthetic process	10	1	5.88E-04
GO:0051775	response to redox state	10	1	5.99E-04
GO:0015651	quaternary ammonium group transmembrane transporter activity	10	1	6.02E-04
GO:0071295	cellular response to vitamin	10	1	6.75E-04
GO:0004887	thyroid hormone receptor activity	10	1	6.78E-04
GO:0090280	positive regulation of calcium ion import	10	1	6.97E-04
GO:0097435	fibril organization	10	1	7.13E-04
GO:0071498	cellular response to fluid shear stress	10	1	7.36E-04
GO:0090140	regulation of mitochondrial fission	10	1	7.36E-04
GO:0031045	dense core granule	10	1	8.01E-04
GO:0048711	positive regulation of astrocyte differentiation	10	1	8.38E-04
GO:0090184	positive regulation of kidney development	10	1	8.53E-04
GO:0042581	specific granule	11	1	9.85E-04

5.6.4. Exclusion of non-Caucasian samples

The PFC, STR and CER networks all contain modules that are significantly correlated with PRS (see **section 5.6.1**). Most of these modules, however, are also correlated with ethnicity (identified from genotype data). To investigate whether the associations with PRS were a result of the inclusion of non-Caucasian samples in the networks I repeated the generation of the networks excluding these samples (for details on sample ethnicity derived from genetic data see **Chapter 4 section 4.2.2**).

Tables 5.15 to 5.17 present the number of modules for each brain region network, probes in each module and results of Pearson's correlation between each module's ME and PRS and ethnicity. **Figures 5.13 to 5.15** show the heatmaps for these correlations. The PFC and STR networks have no modules associated with PRS after the exclusion of non-Caucasian samples, indicating that the initial observations were potentially driven by ancestry outliers. In contrast, the CER network contained three modules associated with PRS. Given the differences already observed in the CER DNA methylation data compared to the other brain regions present in this study (see **Chapter 3 sections 3.2.2 and 3.2.5**), these associations need a more careful exploration.

Table 5.15. Modules identified in the network using prefrontal cortex data from Caucasian non-psychiatric cases and schizophrenia controls from the MRC London Neurodegenerative Diseases Brain Bank and Douglas-Bell Canada Brain Bank. Shown are the coefficients (ρ) and P -values of Pearson's correlations between each module eigengene and polygenic risk score and ethnicity.

Module	Module colour	N Probes	Polygenic risk score		Ethnicity	
			ρ	correlation P	P	correlation P
0	grey	254126	-	-	-	-
1	turquoise	78101	-8.04E-02	0.52	0.02	0.84
2	blue	19802	0.08	0.52	-1.06E-02	0.93
3	brown	10058	-0.13	0.28	-9.10E-02	0.46
4	yellow	8356	-1.76E-02	0.89	-1.12E-01	0.37
5	green	7933	0.03	0.80	0.10	0.44
6	red	7657	-0.16	0.19	-6.80E-02	0.58
7	black	5394	-0.01	0.91	-7.32E-02	0.56
8	pink	3279	-0.11	0.39	-1.79E-02	0.89
9	magenta	2950	-0.12	0.35	-0.10	0.42
10	purple	2015	0.12	0.35	-0.14	0.26
11	greenyellow	2012	0.15	0.23	-5.70E-02	0.65
12	tan	1677	0.15	0.23	0.09	0.47
13	salmon	898	-8.99E-02	0.47	0.12	0.33
14	cyan	848	1.55E-03	0.99	-1.12E-02	0.93
15	midnightblue	792	-7.64E-03	0.95	0.24	0.05
16	lightcyan	777	0.07	0.60	-1.57E-01	0.21
17	grey60	754	-0.12	0.34	0.05	0.72
18	lightgreen	587	0.19	0.13	-5.71E-02	0.65
19	lightyellow	513	-0.12	0.35	0.05	0.66
20	royalblue	459	-0.12	0.35	-8.21E-02	0.51
21	darkred	440	0.04	0.77	0.07	0.58
22	darkgreen	429	-5.14E-03	0.97	0.03	0.81
23	darkturquoise	420	0.06	0.62	0.08	0.55
24	darkgrey	419	0.11	0.37	0.04	0.75
25	orange	324	0.02	0.86	0.02	0.89
26	darkorange	317	-0.15	0.24	0.09	0.47
27	white	264	-0.19	0.12	0.08	0.52
28	skyblue	241	-1.38E-02	0.91	0.03	0.83
29	saddlebrown	232	-8.90E-02	0.47	-8.39E-02	0.50
30	steelblue	204	-8.76E-02	0.48	0.17	0.18
31	paleturquoise	203	-9.60E-02	0.44	0.04	0.73
32	violet	197	-0.14	0.25	0.21	0.09
33	darkolivegreen	186	0.14	0.26	0.09	0.48
34	darkmagenta	176	0.03	0.80	-1.55E-01	0.21
35	sienna3	151	-1.31E-02	0.92	-1.92E-01	0.12
36	yellowgreen	137	6.81E-03	0.96	-2.08E-02	0.87
37	skyblue3	134	0.02	0.88	0.14	0.26
38	plum1	101	0.12	0.32	-4.64E-02	0.71

Table 5.16. Modules identified in the network using striatum data from Caucasian non-psychiatric cases and schizophrenia controls from the MRC London Neurodegenerative Diseases Brain Bank and Douglas-Bell Canada Brain Bank. Shown are the coefficients (ρ) and P -values of Pearson's correlations between each module eigengene and polygenic risk score and ethnicity.

Module	Module colour	N Probes	Polygenic risk score		Ethnicity	
			ρ	correlation P	ρ	correlation P
0	grey	191031	-	-	-	-
1	turquoise	68834	1.84E-03	0.28	-8.56E-02	0.79
2	blue	23456	-1.19E-02	0.99	-1.64E-02	0.48
3	brown	22049	0.09	0.92	0.02	0.89
4	yellow	17218	0.04	0.45	0.04	0.86
5	green	14078	0.13	0.77	8.34E-03	0.73
6	red	13654	-0.02	0.27	0.10	0.94
7	black	11055	0.12	0.85	0.09	0.43
8	pink	8284	0.07	0.33	0.11	0.48
9	magenta	6852	0.09	0.58	0.04	0.38
10	purple	6032	-3.82E-02	0.46	-0.11	0.72
11	greenyellow	5786	-0.12	0.75	-1.24E-02	0.34
12	tan	5232	-0.15	0.33	0.07	0.92
13	salmon	5164	-6.90E-02	0.20	-5.22E-02	0.57
14	cyan	4920	-7.30E-02	0.57	-3.06E-02	0.67
15	midnightblue	3992	0.17	0.55	-7.27E-02	0.80
16	lightcyan	2890	0.18	0.16	-3.50E-03	0.55
17	grey60	1742	0.05	0.14	-2.09E-02	0.98
18	lightgreen	888	-6.60E-04	0.67	-4.22E-02	0.86
19	lightyellow	742	-0.04	1.00	-0.13	0.73
20	royalblue	474	0.11	0.73	0.02	0.30
21	darkred	423	-0.18	0.35	0.16	0.85
22	darkgreen	379	-0.17	0.14	-1.43E-02	0.19
23	darkturquoise	360	-1.34E-02	0.17	-8.34E-02	0.91
24	darkgrey	281	-0.12	0.91	0.07	0.49
25	orange	274	0.17	0.33	-0.11	0.56
26	darkorange	237	-0.22	0.17	-8.43E-02	0.35
27	white	189	-0.18	0.07	-2.81E-02	0.48
28	skyblue	176	-0.14	0.12	-7.01E-02	0.82
29	saddlebrown	143	0.11	0.24	0.55	0.56
30	steelblue	141	-0.15	0.37	0.08	0.00
31	paleturquoise	136	-0.17	0.21	0.05	0.51
32	violet	112	-0.17	0.15	-9.96E-02	0.68
33	darkolivegreen	112	-5.18E-02	0.16	0.14	0.41
34	darkmagenta	111	-5.18E-02	0.67	0.14	0.26

Table 5.17. Modules identified in the network using cerebellum data from Caucasian non-psychiatric cases and schizophrenia controls from the MRC London Neurodegenerative Diseases Brain Bank and Douglas-Bell Canada Brain Bank. Shown are the coefficients (ρ) and P -values of Pearson's correlations between each module eigengene and polygenic risk score and ethnicity. Significant correlations ($P < 0.05$) are shown in bold.

Module	Module colour	N Probes	Polygenic risk score		Ethnicity	
			ρ	correlation P	P	correlation P
0	grey	153386	-	-	-	-
1	turquoise	62966	0.02	0.84	-0.14	0.24
2	blue	29356	-3.65E-03	0.98	-2.48E-02	0.84
3	brown	26545	-0.18	0.14	-4.06E-02	0.74
4	yellow	23161	5.20E-03	0.97	0.14	0.25
5	green	18048	-0.25	0.04	-0.15	0.23
6	red	11976	0.04	0.76	0.26	0.03
7	black	10625	-5.92E-02	0.63	0.43	2.93E-04
8	pink	9220	-0.23	0.06	-5.80E-02	0.64
9	magenta	6576	7.79E-03	0.95	0.19	0.12
10	purple	6520	0.05	0.67	0.02	0.87
11	greenyellow	5775	-0.17	0.16	-0.17	0.15
12	tan	5277	0.13	0.27	0.14	0.24
13	salmon	4998	0.63	7.32E-09	-0.11	0.39
14	cyan	4588	0.02	0.88	0.29	0.02
15	midnightblue	4030	0.06	0.60	-0.15	0.22
16	lightcyan	3849	9.12E-03	0.94	0.10	0.40
17	grey60	3512	0.47	5.79E-05	-5.68E-02	0.65
18	lightgreen	3273	-8.67E-02	0.48	-3.26E-02	0.79
19	lightyellow	3183	-2.10E-02	0.86	0.16	0.19
20	royalblue	3061	0.57	4.98E-07	0.21	0.08
21	darkred	2062	-7.33E-02	0.55	-6.38E-02	0.61
22	darkgreen	1830	-0.10	0.40	-9.21E-04	0.99
23	darkturquoise	1793	0.24	0.05	0.11	0.37
24	darkgrey	1571	0.04	0.74	0.21	0.08
25	orange	972	-4.90E-02	0.69	-0.20	0.11
26	darkorange	481	-0.18	0.13	0.01	0.91
27	white	346	-0.11	0.39	0.12	0.32
28	skyblue	324	2.65E-03	0.98	-8.98E-02	0.47
29	saddlebrown	174	-0.29	0.02	-0.17	0.16
30	steelblue	173	8.55E-04	0.99	0.02	0.89
31	paleturquoise	111	-8.11E-02	0.51	0.14	0.27

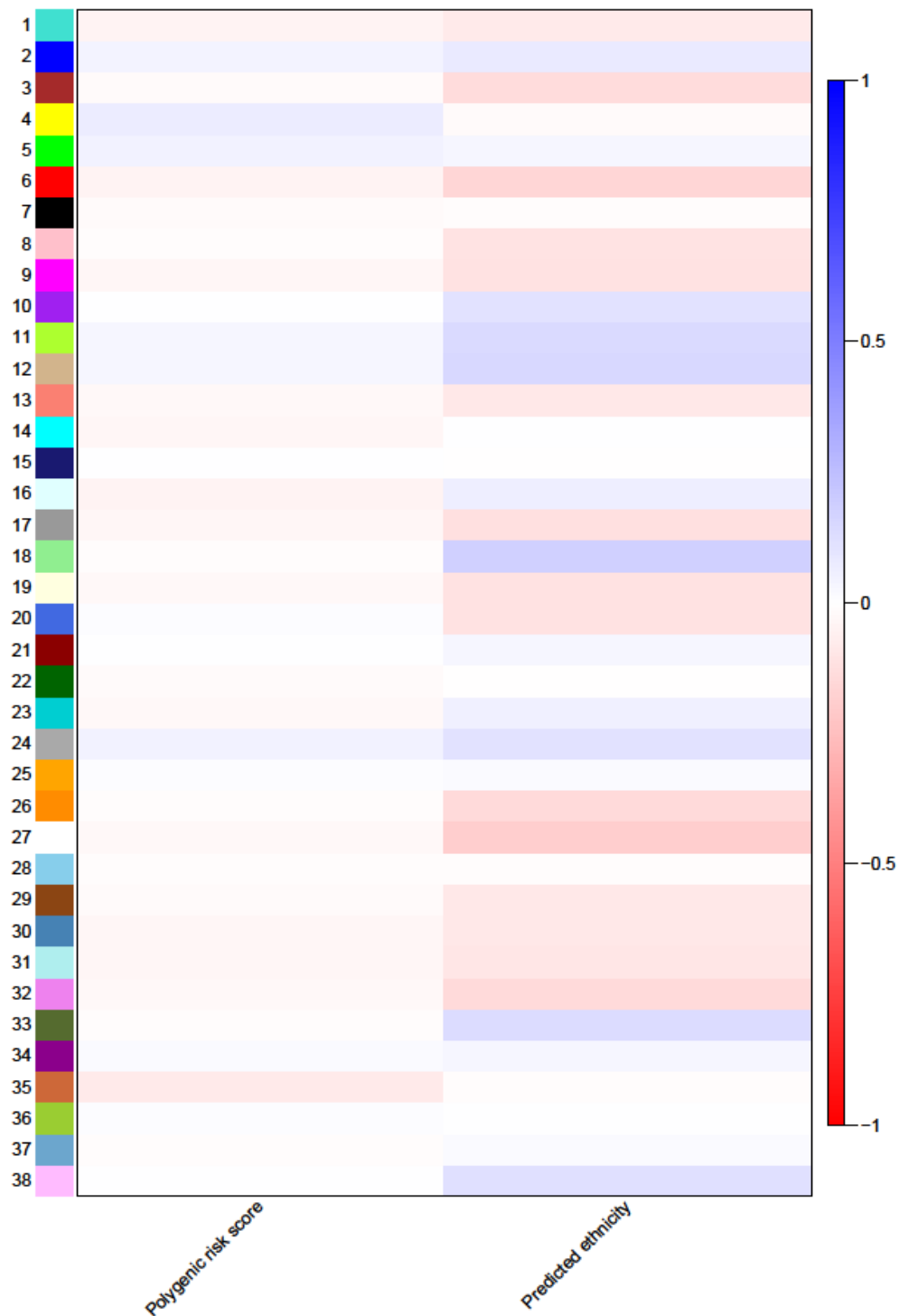


Figure 5.13. Heatmap showing the correlation coefficient between each prefrontal cortex module eigengene and polygenic risk score and ethnicity. Shown are the modules identified in the network using prefrontal cortex data from the Caucasians non-psychiatric cases and schizophrenia controls from the MRC London Neurodegenerative Diseases Brain Bank and Douglas-Bell Canada Brain Bank.

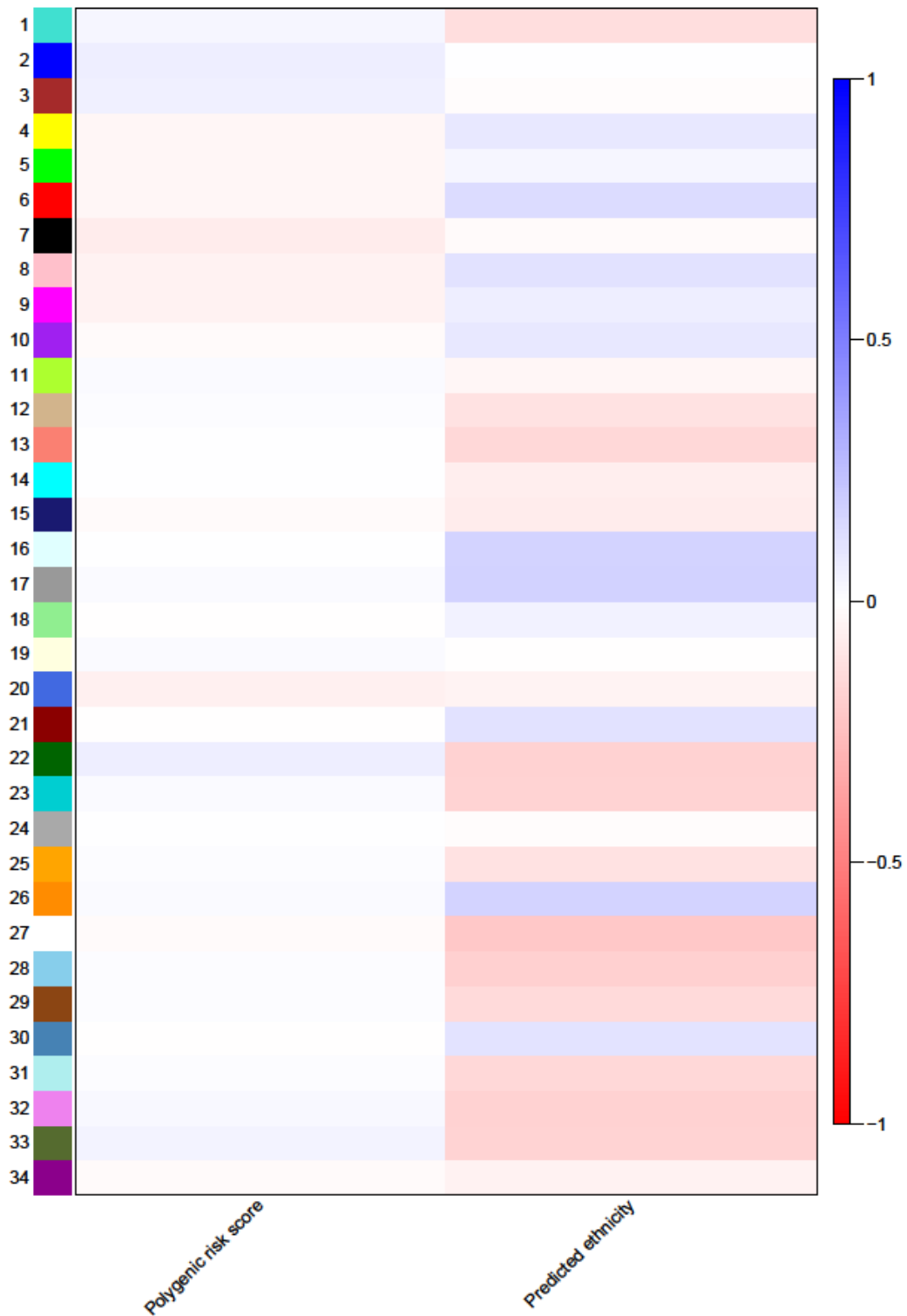


Figure 5.14. Heatmap showing the correlation coefficient between each striatum module eigengene and polygenic risk score and ethnicity. Shown are the modules identified in the network using striatum data from the Caucasians non-psychiatric cases and schizophrenia controls from the MRC London Neurodegenerative Diseases Brain Bank and Douglas-Bell Canada Brain Bank.

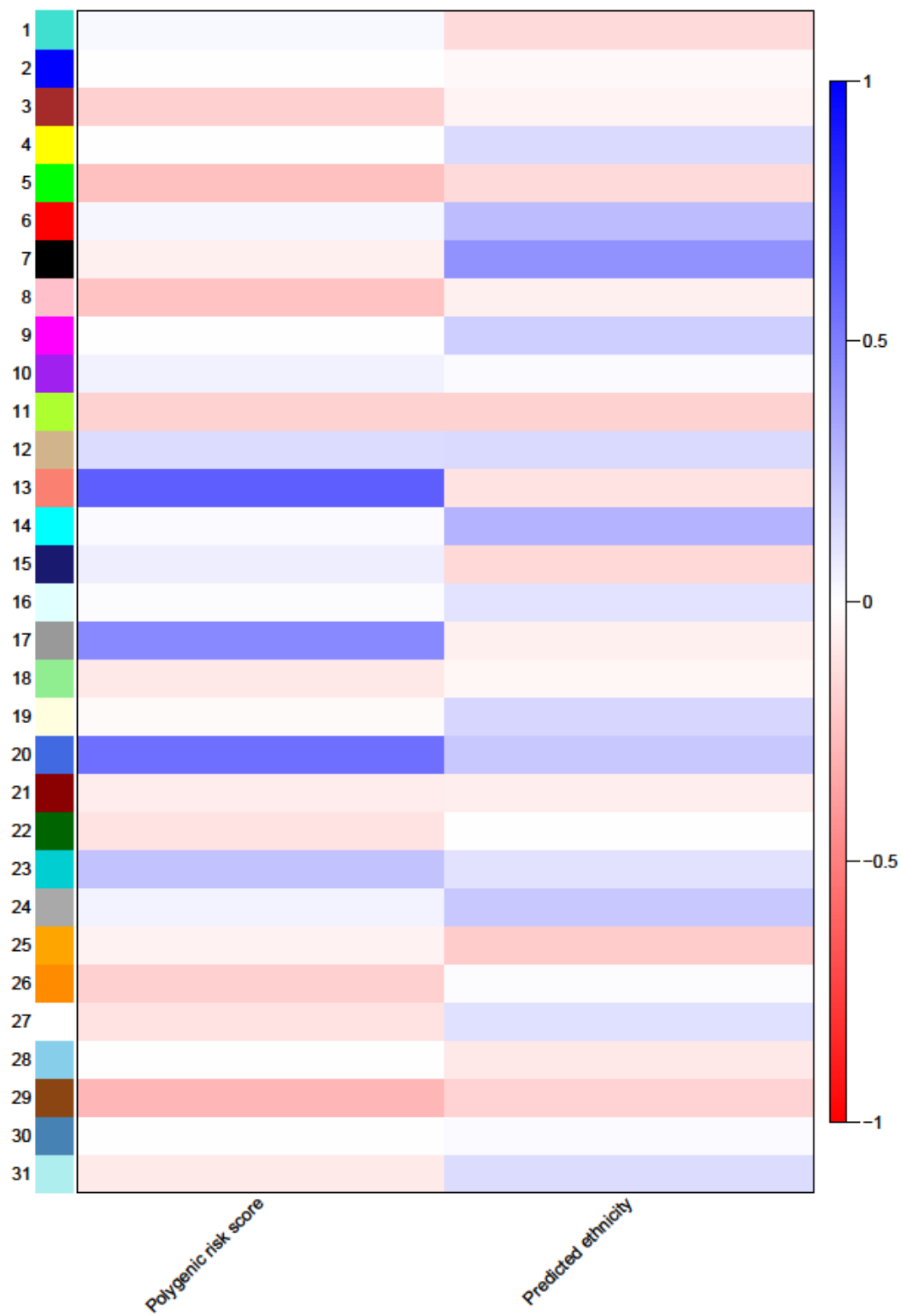


Figure 5.15. Heatmap showing the correlation coefficient between each cerebellum module eigengene and polygenic risk score and ethnicity. Shown are the modules identified in the network using cerebellum data from the Caucasians non-psychiatric cases and schizophrenia controls from the MRC London Neurodegenerative Diseases Brain Bank and Douglas-Bell Canada Brain Bank.

5.7. Fetal brain correlation network

Given previous evidence for a neurodevelopmental basis to schizophrenia (Spiers et al., 2015) I next investigated whether co-methylated modules identified in human fetal brain were also associated with schizophrenia. Previously our group generated an Illumina 450K array dataset from fetal brain samples ($n = 179$), ranging from 23 to 184 days post-conception (Spiers et al., 2015) and showed that there were several co-methylated modules strongly associated with brain development. For each brain region network I imposed the module structure of the fetal brain network by calculating the MEs of the modules identified in the fetal brain dataset for each of the adult brain samples and testing for association between the ME and schizophrenia within each adult brain region using an independent sample t-test as described above (**section 5.6.2**).

Table 5.18 presents the P -values of these tests for all the fetal brain modules. Although none of the modules was significantly associated with schizophrenia at a Bonferroni corrected threshold (corrected for the 92 tests; $P = 5.43E-04$), seven PFC, 1 HC and 1 CER modules were nominally associated with schizophrenia. Strikingly, five of the PFC schizophrenia-associated modules (P -values: 'brown': 0.04, 'darkgreen': 0.02, 'grey60': 0.02, 'red': 0.02 and 'yellow': 0.02) were also significantly correlated with fetal age in Spiers et al. (2015). The largest of these modules (fetal 'brown' module) was highly enrichment for probes annotated to genes in pathways relevant to neurodevelopment (Spiers et al., 2015). These observations have particular relevance since schizophrenia has been suggested to have neurodevelopmental origins (Owen et al., 2011, Weinberger, 1995), as discussed in **Chapter 1 section 1.1.5**.

Table 5.18. Association of the fetal brain modules with schizophrenia in the adult brain data. Shown are the t-test *P*-values for schizophrenia cases and controls in the adult prefrontal cortex, striatum, hippocampus and cerebellum datasets using the fetal brain module structure and the correlation coefficients (with respective *P*-values) with fetal age from Spiers et al. (2015).

	<i>P</i> Prefrontal cortex	<i>P</i> Striatum	<i>P</i> Hippocampus	<i>P</i> Cerebellum	<i>P</i> correlation with fetal age (Spiers et al., 2015)
black	0.52	0.42	0.43	0.97	0.01 (8.75E-01)
blue	0.20	0.26	0.14	0.62	-0.14 (6.44E-02)
brown	0.04	0.99	0.37	0.57	0.54 (5.63E-15)
cyan	0.44	0.66	0.40	0.42	-0.22 (3.42E-03)
darkgreen	0.02	0.64	0.42	0.24	-0.45 (1.61E-10)
darkred	0.15	0.71	0.57	0.93	0.31 (2.30E-05)
green	0.12	0.40	0.21	0.58	-0.12 (9.72E-02)
greenyellow	0.16	0.37	0.19	0.61	-0.32 (9.86E-06)
grey60	0.02	1.00	0.39	0.28	-0.52 (1.59E-13)
lightcyan	8.28E-03	0.62	0.04	0.23	-0.01 (9.40E-01)
lightgreen	0.05	0.81	0.36	0.91	-0.05 (5.23E-01)
lightyellow	0.12	0.58	0.22	0.73	-0.22 (3.31E-03)
magenta	0.18	0.47	0.11	0.14	-0.21 (5.64E-03)
midnightblue	0.04	0.88	0.72	0.22	0.12 (9.63E-02)
pink	0.10	0.91	0.27	0.49	0.47 (3.84E-11)
purple	0.67	0.33	0.64	0.03	0.06 (3.99E-01)
red	0.02	0.85	0.36	0.38	-0.23 (1.68E-03)
royalblue	0.30	0.28	0.18	0.10	0.05 (4.91E-01)
salmon	0.08	0.75	0.25	0.57	0.22 (2.56E-03)
tan	0.09	0.99	0.27	0.72	0.33 (4.81E-06)
turquoise	0.09	0.46	0.20	0.47	0.19 (9.87E-03)
yellow	0.02	0.90	0.36	0.46	-0.59 (3.94E-18)

5.8. Discussion

5.8.1. Overview of the results

In this chapter I used WGCNA to study the co-methylation structure of DNA methylation in each of the four brain regions, exploring differences in network structures between schizophrenia patients and controls. The initial approach focused on creating separate networks for schizophrenia patients and non-psychiatric controls within each brain region and identifying overlapping and unique modules of co-methylated probes between cases and controls networks. I attempted to match each module of the control network with at least one corresponding module from the schizophrenia network and concluded that this was not possible and therefore this was not the optimal method to use.

I subsequently created networks for each brain region using the entire set of samples (*i.e.* including both schizophrenia cases and controls) and tested for a significant association of these with schizophrenia status, schizophrenia PRS and other traits of interest. Several modules in each brain region are correlated with PRS, although these are also associated with ethnicity, except in the cerebellum. I repeated the networks including only Caucasian samples and retested for correlation with PRS. None of the new modules are correlated with PRS in the PFC and STR after excluding non-Caucasian samples. In the CER, three modules are correlated with PRS after excluding the non-Caucasian samples, although, given the differences already observed in the CER DNA methylation data compared to the other brain regions present in this study (see **Chapter 3 sections 3.2.2 and 3.2.5**), these associations need to be explored further.

Five modules are nominally associated with schizophrenia in the PFC network and none in the STR and CER networks. Three of the genes annotated to the 'hub probes' of the PFC schizophrenia-associated modules are particularly interesting in the context of schizophrenia: *KDM3B* ('black' module) (Schizophrenia Working Group of the Psychiatric Genomics, 2014), *ANK3* ('brown' module) (Ferreira et al., 2008, Wirgenes et al., 2014) and *RPTOR* ('brown' module, associated with PRS in **Chapter 4 section 4.3.4**). Furthermore, two genes of the 'brown' module showed interactions with the *DISC1* gene in a recent study reporting novel interaction networks with

schizophrenia-linked genes (Ganapathiraju et al., 2016). Seven other genes belonging to the PFC schizophrenia-associated modules also had interactions with genes associated with schizophrenia in the latest GWAS (Schizophrenia Working Group of the Psychiatric Genomics, 2014). GO enrichment analysis revealed that the eleven most significantly enriched pathways on the largest (PFC 'brown') schizophrenia-associated module are neuronal function- and neurodevelopment-relevant pathways.

Finally, I imposed the structure of modules of co-methylated probes identified in a fetal brain dataset (Spiers et al., 2015) to my adult brain data and tested these for association with schizophrenia. Strikingly, five schizophrenia-associated 'fetal network' modules in the PFC were also significantly correlated with fetal age in Spiers et al. (2015) and the largest of these modules (fetal 'brown' module) was highly enriched for probes annotated to genes in pathways relevant to neurodevelopment (Spiers et al., 2015). These observations have particular relevance since schizophrenia has been suggested to have neurodevelopmental origins (Owen et al., 2011, Weinberger, 1995).

5.8.2. Strengths, limitations and future directions

This chapter represents a first step in exploring the network structure of the DNA methylation data generated in this thesis and how this structure is affected in different brain regions of schizophrenia patients. I identified modules of co-methylated sites nominally associated with schizophrenia in the PFC and genes central to those modules that have been previously linked to schizophrenia or have shown to interact with schizophrenia linked-genes. Five modules of co-methylated probes that were correlated with fetal age in Spiers et al. (2015) are also found to be associated with schizophrenia in the PFC. Furthermore, both the largest schizophrenia-associated module identified in the PFC dataset and the largest fetal module associated with schizophrenia in the PFC are enriched for probes in pathways relevant to neurodevelopment. These observations support a neurodevelopmental origin of schizophrenia.

In future studies, it would be important to explore the networks of both schizophrenia patients and non-psychiatric controls separately. This would potentially allow studying modules of co-methylated probes that are unique or missing from the schizophrenia network, as well as exploring modules that are

disrupted between the two networks. It was not possible to use this approach in this chapter (see **section 5.5**), which could be due to the small sample size for schizophrenia patients and controls from each brain region. Another likely reason is the number of probes used to create the networks. Networks of co-expression genes are usually constructed using thousands to dozens of thousands of genes (Parikshak et al., 2013, Zhang and Horvath, 2005, Voineagu et al., 2011). The inclusion of ~480,000 probes will potentially increase the noise in the network. In the future, ways of reducing the amount of probes in the network should be explored. For example:

- Exclude non-variable probes across all samples;
- Combine adjacent probes into regions of correlated probes and create a common metric to represent these probes;
- Combine probes annotated to a single gene or gene feature and create a common metric to represent these probes.

All these suggestions have potential limitations and should be explored carefully. The use of systems-level approaches to explore the epigenome has not been widely applied, and new analytical approaches are required. After refining the WGCNA approach for use in DNA methylation data, it will be important to study more carefully which co-methylated modules are associated with schizophrenia and schizophrenia polygenic burden in the different brain regions.

In summary, this chapter presents a first step in exploring network analysis in DNA methylation data. I identified several modules of co-methylated probes associated with schizophrenia in the PFC and report additional evidence that supports a neurodevelopmental origin of schizophrenia. However, this methodology needs to be further refined to be suitable to use in large DNA methylation datasets.

Chapter 6 - Transcriptomic profiling of schizophrenia prefrontal cortex

6.1. Introduction

The 'transcriptome' refers to the complete population of transcripts expressed in a cell and their quantity, at a given developmental stage or physiological condition (*e.g.* disorder). Cataloguing and quantifying the transcriptome is a crucial step in interpreting the functional elements of the genome and for understanding the role of gene regulation in development and disease.

To date only a few studies have attempted to profile transcriptomic differences in schizophrenia brain compared to healthy individuals. A comprehensive overview of recent gene expression studies in schizophrenia is given in **Chapter 1 section 1.1.3**. Initial studies focused on characterising gene expression levels of individual candidate genes linked to schizophrenia based on their function utilising quantitative polymerase chain reaction (qPCR). Recently, several studies have taken a transcriptome-wide, hypothesis free approach. Although this represents a significant advance in the field of schizophrenia genomics research, such studies have primarily focussed on peripheral tissues (which may have limited utility for understanding gene expression differences in the brain) or used small sample sizes of post-mortem brain tissue.

The RNA sequencing (RNA-seq) method was developed in 2008 (Nagalakshmi et al., 2008) and has since then revolutionised the study of transcriptomic variation. Previously, the most popular choice for transcriptomic profiling was microarray based methods. RNA-seq represents an improvement compared to gene expression arrays since it allows for the full coverage of the transcriptome and the identification of new transcripts and isoforms (Wilhelm and Landry, 2009, Haas and Zody, 2010, Wang et al., 2009). There are also less problems with cross-hybridization artifacts and the poor quantification of low and highly expressed genes. The wide uptake of RNA-seq has meant that several pre-processing, aligning and analysis pipelines have been developed (Conesa et al., 2016), including analysis pipelines appropriate for case-control studies (Robinson et al., 2010).

In this Chapter I undertook a case-control RNA-seq gene expression study using post-mortem brain samples from schizophrenia patients and controls. I identified several disease-relevant genes showing expression changes in schizophrenia, with several of these annotated to CpG sites showing schizophrenia-associated DNA methylation variation in **Chapter 3**.

6.2. Methods

6.2.1. Total RNA isolation from prefrontal cortex samples

In this chapter I profiled transcriptomic variation in the prefrontal cortex (PFC) using RNA isolated from schizophrenia patients and non-psychiatric controls from the Medical Research Council (MRC) London Neurodegenerative Diseases Brain Bank (LNDBB) and Douglas-Bell Canada Brain Bank (DBCBB). Details on these sample cohorts are given in **Chapter 3 section 3.2.1**. Total RNA was isolated from the PFC of 39 schizophrenia patients and 45 controls. **Appendix A - Supplementary Table 1** presents demographic information on all the samples included in this Chapter. Total RNA was isolated using the miRNeasy Mini Kit (Qiagen, Venlo, Holland) followed by a clean-up to remove fragmented RNA using the RNeasy MinElute Cleanup Kit (Qiagen, Venlo, Holland). The purity and integrity of RNA samples was assessed before and after clean-up using a Nanodrop ND-8000 (Thermo Fisher Scientific, MA, USA) and the Agilent RNA 6000 Nano Kit ran on an Agilent 2100 Bioanalyzer Instrument (Agilent Technologies, Santa Clara, CA, USA). Details on total RNA isolation, cleaning and quality check are described in **Chapter 2 section 2.2**. **Table 6.2** gives an overview of the RNA concentration and RNA integrity number (RIN) results from the Bioanalyzer Instrument and 260/280 and 260/230 ratios from the Nanodrop for all samples extracted, before and after the clean-up. Details on these measures can be found in **Chapter 2 section 2.2.2**.

Table 6.1. Key RNA sequencing terms used in this Chapter.

Term	Definition
Library	For each sample, a library is a collection of complementary DNA fragments, which are flanked by specific constant sequences (known as adapters) that are necessary for sequencing
Reads	Short sequences of DNA representing the output from the sequencing of the library
Alignment or mapping	The process of finding the position of a sequencing read on the reference genome or transcriptome
Counts	The number of paired reads that align to a particular feature (<i>i.e.</i> gene or transcript)
Counts per million (CPM)	Counts normalised by the number of fragments sequenced (size of the library sequenced) multiplied by one million: $CPM_i = \frac{X_i}{N} = \frac{X_i}{N} \cdot 10^6$ where X is the number of counts of gene/transcript and N is the library size
Fragments per kilobase of transcript per million mapped reads (FPKM)	Counts normalised by the number of fragments sequenced (size of the library sequenced) and the length of each fragment: $FPKM_i = \frac{X_i}{\left(\frac{\tilde{l}_i}{10^3}\right) \left(\frac{N}{10^6}\right)} = \frac{X_i}{\tilde{l}_i N} \cdot 10^9$ where X is the number of the counts of gene/transcript, N is the library size and \tilde{l} is the length in base pairs of the gene/transcript

Table 6.2. RNA quantity and integrity information of the all the RNA samples extracted before and after the clean-up procedure.

Highlighted in grey are the samples chosen for sequencing based on their quality metrics. RIN, RNA integrity number.

Sample	Brain bank	Group	Age	Gender	Before clean-up				After clean-up				Sample sequenced	
					Concentration (ng/ml)	Quantity (ng)	RIN	260/280 ratio	260/230 ratio	Concentration (ng/ml)	RIN	260/280 ratio		260/230 ratio
1	LNDDB	schizophrenia	67	M	279.82	6995.51	6.60	2.09	2.11	362.54	6.70	2.09	1.71	yes
2	LNDDB	schizophrenia	79	M	435.94	10898.42	3.30	2.09	2.16	186.75	6.00	2.04	1.96	yes
3	LNDDB	schizophrenia	69	F	84.35	2108.74	2.40	2.11	1.70	151.73	3.60	2.05	1.62	no
4	LNDDB	schizophrenia	76	F	-	-	-	2.10	1.67	-	-	2.07	0.73	no
5	LNDDB	schizophrenia	84	F	339.75	8493.71	4.90	2.03	1.74	199.03	5.50	2.02	1.16	no
6	LNDDB	schizophrenia	87	M	199.66	4991.55	3.10	2.11	0.49	389.04	3.00	2.12	2.05	no
7	LNDDB	schizophrenia	32	F	-	-	-	2.08	2.06	-	-	2.09	1.94	no
8	LNDDB	schizophrenia	70	F	161.08	4027.03	5.10	2.02	1.81	226.78	5.50	2.27	1.77	yes
9	LNDDB	schizophrenia	49	F	458.45	11461.26	4.70	2.10	1.25	167.72	6.40	2.05	2.03	yes
10	LNDDB	schizophrenia	46	M	184.85	4621.21	3.20	2.14	2.09	187.19	4.20	2.17	0.63	no
11	LNDDB	schizophrenia	62	M	129.06	3226.38	2.70	2.04	1.75	96.37	5.00	2.08	1.48	yes
12	LNDDB	schizophrenia	31	M	81.05	2026.33	4.10	1.90	0.54	101.43	2.70	1.92	1.78	no
13	LNDDB	schizophrenia	51	M	407.34	10183.62	3.30	2.11	0.85	213.28	6.20	1.98	0.77	yes
14	LNDDB	schizophrenia	62	M	65.81	1645.29	7.20	2.05	1.51	160.72	6.50	2.12	0.77	yes
15	LNDDB	schizophrenia	34	F	106.90	2672.50	4.40	2.10	1.20	126.88	5.00	2.07	1.66	yes
16	LNDDB	schizophrenia	75	F	81.99	2049.73	5.30	2.15	2.13	264.83	6.60	2.14	2.09	yes
18	LNDDB	schizophrenia	64	M	201.42	5035.39	6.00	2.12	1.32	142.72	6.20	1.89	1.17	yes
19	LNDDB	schizophrenia	49	M	657.05	16426.34	3.70	2.06	0.91	183.65	6.60	2.07	1.59	yes
20	LNDDB	schizophrenia	71	F	106.04	2651.08	6.10	2.07	1.94	173.48	6.00	2.08	1.48	yes
22	LNDDB	schizophrenia	75	F	287.14	7178.47	7.70	2.08	1.38	347.42	8.00	2.10	1.73	yes
23	LNDDB	schizophrenia	64	M	506.43	12660.78	3.40	2.07	2.07	346.82	4.00	1.96	1.75	no
24	LNDDB	schizophrenia	45	M	219.33	5483.34	7.00	2.09	1.81	443.16	8.00	2.09	2.10	yes
25	LNDDB	control	25	M	231.00	5774.90	8.00	1.97	0.56	241.93	8.30	2.04	1.04	yes
26	LNDDB	control	49	M	305.20	7630.04	5.40	2.09	0.64	168.67	6.70	2.08	1.57	yes
27	LNDDB	control	82	F	97.90	2447.49	6.20	2.14	2.04	139.99	6.20	2.11	1.96	yes
28	LNDDB	control	82	F	109.62	2740.62	2.50	2.09	1.79	71.02	2.70	2.05	1.52	no
29	LNDDB	control	63	F	205.24	5130.88	6.70	2.07	1.67	345.23	6.80	2.09	0.89	yes
30	LNDDB	control	68	F	73.22	1830.62	2.60	2.08	1.50	55.39	3.00	2.09	0.52	no
31	LNDDB	control	33	F	151.79	3794.76	3.90	2.16	1.23	102.99	5.30	2.13	0.51	yes

32	LNDBB	control	50	M	127.57	3189.32	6.90	2.12	1.24	133.12	6.80	1.99	1.24	yes
33	LNDBB	control	57	M	274.74	6868.62	2.40	2.08	2.07	222.02	7.80	2.09	1.57	yes
34	LNDBB	control	58	M	186.13	4653.22	3.20	2.06	2.07	458.38	4.20	2.12	2.10	yes
35	LNDBB	control	68	F	128.18	3204.51	2.20	2.07	1.79	96.13	3.20	2.09	1.55	no
36	LNDBB	control	86	M	0.98	24.53	-	2.10	0.57	197.80	2.10	2.05	1.69	no
37	LNDBB	control	71	M	175.07	4376.69	3.20	2.10	1.97	125.06	3.50	2.09	1.13	no
38	LNDBB	control	95	M	221.55	5538.87	2.40	2.12	2.11	246.44	2.30	2.08	1.78	no
39	LNDBB	control	40	M	133.25	3331.25	3.50	2.11	1.47	114.92	3.50	2.06	1.50	no
40	LNDBB	control	54	M	324.34	8108.57	2.90	2.13	1.87	141.49	6.00	2.12	0.99	yes
41	LNDBB	control	76	F	37.78	944.61	2.50	2.10	1.59	46.87	2.70	2.07	0.92	no
42	LNDBB	control	67	M	355.47	8886.83	3.30	2.09	1.79	158.37	4.40	2.17	0.20	no
43	LNDBB	control	70	M	129.06	3226.38	2.70	2.06	1.85	163.41	4.20	2.05	1.92	yes
44	LNDBB	control	96	F	164.19	4104.81	3.50	2.15	0.44	176.35	5.60	2.11	0.90	yes
45	LNDBB	control	37	M	100.70	2517.43	4.40	2.06	1.83	173.86	4.80	2.07	1.58	yes
46	LNDBB	control	40	M	28.67	716.77	2.80	2.09	1.62	50.54	6.30	2.03	0.56	yes
47	LNDBB	control	70	M	709.03	17725.66	4.60	2.08	2.12	374.51	5.90	2.05	1.10	yes
49	LNDBB	control	69	M	105.01	2625.14	3.00	1.98	1.61	158.66	4.30	2.07	2.11	yes
50	LNDBB	control	48	M	369.28	9231.96	2.60	2.13	1.62	525.49	2.60	2.12	1.37	no
51	LNDBB	control	48	M	300.40	7509.99	4.00	2.06	1.93	202.11	6.50	2.09	2.07	yes
52	LNDBB	control	80	M	201.42	5035.39	6.00	2.16	2.13	227.87	3.20	1.97	1.50	no
53	LNDBB	control	79	M	326.80	8170.07	3.20	2.08	1.32	181.12	3.50	2.10	0.25	no
54	LNDBB	control	55	M	81.52	2037.89	2.30	2.05	1.68	108.24	2.60	1.84	1.02	no
MS01PFC	DBCBB	schizophrenia	70	M	98.06	2451.46	7.50	2.14	1.03	119.50	8.20	2.10	0.34	yes
MS02PFC	DBCBB	schizophrenia	73	F	233.93	5848.22	5.20	2.09	2.01	96.23	6.50	2.05	1.37	yes
MS03PFC	DBCBB	schizophrenia	30	M	100.52	2513.08	7.20	2.10	1.98	37.06	7.00	1.82	1.12	yes
MS04PFC	DBCBB	schizophrenia	60	F	259.40	6485.05	6.80	2.04	1.56	169.81	7.50	2.06	1.66	yes
MS05PFC	DBCBB	control	57	F	106.63	2665.82	2.40	2.08	1.54	69.92	5.90	1.94	0.88	yes
MS06PFC	DBCBB	schizophrenia	51	F	62.08	1551.92	4.00	2.09	0.98	131.86	7.90	2.06	1.88	yes
MS07PFC	DBCBB	schizophrenia	50	M	94.13	2353.30	2.50	2.11	1.66	36.53	5.50	1.82	1.03	no
MS08PFC	DBCBB	control	57	M	209.42	5235.39	6.60	2.12	0.49	114.08	7.30	2.07	1.52	yes
MS09PFC	DBCBB	control	50	F	105.67	2641.87	5.00	2.06	0.87	79.68	5.70	2.14	0.82	yes
MS10PFC	DBCBB	control	43	M	213.27	5331.72	3.40	2.13	0.67	110.39	3.40	2.01	1.65	no
MS11PFC	DBCBB	schizophrenia	29	M	125.94	3148.48	4.30	2.08	2.01	79.27	7.50	2.05	1.50	yes
MS12PFC	DBCBB	schizophrenia	24	M	135.78	3394.41	3.50	2.05	1.04	12.89	3.80	2.44	1.63	no
MS13PFC	DBCBB	control	44	M	124.19	3104.70	2.50	2.08	2.07	145.08	2.60	2.03	1.04	no
MS14PFC	DBCBB	control	28	M	1.99	49.70	-	2.44	0.91	1.42	-	1.64	0.17	no
MS15PFC	DBCBB	control	26	M	141.23	3530.67	2.10	2.11	0.68	33.12	4.70	2.30	0.07	no

MS17PFC	DBCBB	control	30	M	141.86	3546.52	5.50	2.04	0.65	64.46	6.80	2.07	1.03	yes
MS18PFC	DBCBB	control	72	F	121.21	3030.25	2.40	2.12	0.77	57.96	3.50	2.07	0.94	no
MS20PFC	DBCBB	schizophrenia	38	M	204.26	5106.58	8.00	2.08	1.96	104.47	7.80	2.00	1.66	yes
MS21PFC	DBCBB	schizophrenia	39	M	304.58	7614.49	6.10	2.09	2.10	125.30	6.50	2.11	1.21	yes
MS22PFC	DBCBB	control	37	M	30.61	765.31	2.40	2.03	0.56	37.03	4.70	1.64	0.40	no
MS23PFC	DBCBB	schizophrenia	47	M	128.09	3202.22	2.40	2.09	1.44	76.37	5.10	1.81	0.62	no
MS25PFC	DBCBB	schizophrenia	65	M	237.37	5934.13	2.30	2.09	2.07	124.11	2.30	2.14	1.81	no
MS26PFC	DBCBB	control	41	M	22.79	569.68	1.50	1.97	1.65	33.04	5.30	2.26	0.57	no
MS27PFC	DBCBB	schizophrenia	26	M	40.35	1008.68	3.20	2.03	1.99	29.50	6.30	2.17	0.20	no
MS28PFC	DBCBB	schizophrenia	29	M	163.35	4083.85	4.90	2.10	1.63	22.32	1.90	1.53	0.80	no
MS29PFC	DBCBB	schizophrenia	33	M	85.92	2148.12	4.70	2.09	1.38	5.36	-	1.73	1.21	no
MS30PFC	DBCBB	schizophrenia	32	M	320.56	8014.09	4.90	2.12	0.70	153.79	6.80	2.08	1.81	yes
MS31PFC	DBCBB	control	33	M	76.15	1903.68	4.60	2.10	2.05	-	-	-	-	no
MS32PFC	DBCBB	schizophrenia	54	M	181.20	4530.01	2.70	2.12	1.22	11.35	-	1.54	1.29	no
MS33PFC	DBCBB	control	66	M	121.38	3034.48	5.00	2.10	0.94	73.64	7.30	1.97	1.16	yes
MS34PFC	DBCBB	control	21	M	248.46	6211.49	6.70	2.10	2.09	27.97	6.50	1.85	1.20	yes
MS35PFC	DBCBB	control	32	M	158.07	3951.65	5.60	2.11	1.76	77.61	5.80	1.89	1.25	yes
MS36PFC	DBCBB	control	69	M	130.59	3264.84	2.50	2.13	1.90	94.92	3.50	1.86	0.37	no

6.2.2. Complementary DNA libraries preparation and RNA sequencing

Based on these quality measures I selected the 23 optimal schizophrenia samples and the 23 optimal non-psychiatric control samples for inclusion in the subsequent RNA-seq experiment. **Table 6.2** provides details about the samples selected for sequencing (highlighted in grey).

Complementary DNA (cDNA) libraries were generated from 500ng of the selected RNA samples using the TruSeq Stranded Total RNA with Ribo-Zero Gold Library Preparation LT kit (Illumina, San Diego, CA, USA). Details on cDNA library preparation are presented in **Chapter 2 section 2.5.1**. External RNA Controls Consortium (ERCC) spike-in control mixes (Ambion, Thermo Fisher Scientific, Waltham, MA, USA) were added to each RNA sample during the preparation of the libraries, according to the manufacturer's instructions. The fragment size range, molarity and the quality of the libraries was assessed using D1000 ScreenTapes (Agilent Technologies, Santa Clara, CA, USA) processed on a 2200 TapeStation Instrument (Agilent Technologies, Santa Clara, CA, USA) as described in **Chapter 2 section 2.5.2**. For an example of the quantification of the resulting cDNA libraries see **Figure 2.15** in **Chapter 2**.

The samples were multiplexed, with 8 samples run per sequencing lane, with each pool containing an equal amount of each individual library to make a final concentration of 10mM. To accomplish this, individual "barcode" sequences were added to each sample so they could be de-multiplexed and distinguished during data analysis. **Table 6.3** presents details on each sample library, including the Illumina TruSeq adapter barcode used for each sample and whether spike-in mix 1 or 2 was added. After I had prepared the libraries, the sequencing of the libraries was performed by the University of Exeter Sequencing Service on an Illumina HiSeq 2500 Sequencing System to generate paired-end reads, according to manufacturer's instructions (see **Chapter 2 section 2.5.3** for more details on pair-ended sequencing). Samples were randomised for sex and diagnosis throughout the total RNA isolation, cDNA preparation and sequencing lane allocation processes.

Table 6.3. Details of the complementary DNA (cDNA) libraries prepared. The samples are ordered by sample name within each sequencing lane.

Sample	Brain Bank	Group	Sequencing lane	TruSeq Illumina adaptor name	Adaptor barcode Sequence	ERCC Spike-in mix	Average cDNA fragment size	Molarity (nM)
15	LNDDB	schizophrenia	1	Illumina TruSeq index 22	CGTACG	2	303	147
18	LNDDB	schizophrenia	1	Illumina TruSeq index 9	GATCAG	2	308	143
22	LNDDB	schizophrenia	1	Illumina TruSeq index 25	ACTGAT	1	304	163
44	LNDDB	control	1	Illumina TruSeq index 21	GTTTCG	2	317	163
MS04	DBCBB	schizophrenia	1	Illumina TruSeq index 20	GTGGCC	2	310	166
MS09	DBCBB	control	1	Illumina TruSeq index 27	ATTCCT	1	301	130
MS34	DBCBB	control	1	Illumina TruSeq index 8	ACTTGA	1	338	64.6
MS35	DBCBB	control	1	Illumina TruSeq index 23	GAGTGG	2	292	136
1	LNDDB	schizophrenia	2	Illumina TruSeq index 20	GTGGCC	1	311	133
8	LNDDB	schizophrenia	2	Illumina TruSeq index 21	GTTTCG	1	302	155
13	LNDDB	schizophrenia	2	Illumina TruSeq index 23	GAGTGG	1	320	121
19	LNDDB	schizophrenia	2	Illumina TruSeq index 27	ATTCCT	2	310	149
27	LNDDB	control	2	Illumina TruSeq index 25	ACTGAT	2	304	150
34	LNDDB	control	2	Illumina TruSeq index 22	CGTACG	2	296	166
MS05	DBCBB	control	2	Illumina TruSeq index 19	GTGAAA	1	298	134
MS17	DBCBB	control	2	Illumina TruSeq index 18	GTCCGC	1	348	41.6
25	LNDDB	control	3	Illumina TruSeq index 15	ATGTCA	2	357	38.2
26	LNDDB	control	3	Illumina TruSeq index 9	GATCAG	2	342	55.3
29	LNDDB	control	3	Illumina TruSeq index 13	AGTCAA	1	350	43
32	LNDDB	control	3	Illumina TruSeq index 12	CTTGTA	2	289	155
49	LNDDB	control	3	Illumina TruSeq index 14	AGTTCC	1	295	102
MS01	DBCBB	schizophrenia	3	Illumina TruSeq index 11	GGCTAC	2	282	111
MS21	DBCBB	schizophrenia	3	Illumina TruSeq index 16	CCGTCC	1	332	57.1
MS30	DBCBB	schizophrenia	3	Illumina TruSeq index 10	TAGCTT	1	322	115
9	LNDDB	schizophrenia	6	Illumina TruSeq index 1	ATCACG	2	318	115
11	LNDDB	schizophrenia	6	Illumina TruSeq index 2	CGATGT	1	307	87.5

31	LNDBB	control	6	Illumina TruSeq index 7	CAGATC	2	303	89.8
43	LNDBB	control	6	Illumina TruSeq index 6	GCCAAT	2	311	154
51	LNDBB	control	6	Illumina TruSeq index 3	TTAGGC	2	302	110
MS02	DBCBB	schizophrenia	6	Illumina TruSeq index 5	ACAGTG	1	308	106
MS06	DBCBB	schizophrenia	6	Illumina TruSeq index 4	TGACCA	1	319	151
2	LNDBB	schizophrenia	7	Illumina TruSeq index 15	ATGTCA	2	324	165
16	LNDBB	schizophrenia	7	Illumina TruSeq index 14	AGTTCC	2	316	165
20	LNDBB	schizophrenia	7	Illumina TruSeq index 8	ACTTGA	1	322	156
40	LNDBB	control	7	Illumina TruSeq index 10	TAGCTT	1	310	161
45	LNDBB	control	7	Illumina TruSeq index 16	CCGTCC	1	308	151
46	LNDBB	control	7	Illumina TruSeq index 12	CTTGTA	1	304	125
47	LNDBB	control	7	Illumina TruSeq index 11	GGCTAC	2	308	146
MS11	DBCBB	schizophrenia	7	Illumina TruSeq index 13	AGTCAA	1	313	146
14	LNDBB	schizophrenia	8	Illumina TruSeq index 2	CGATGT	1	315	159
24	LNDBB	schizophrenia	8	Illumina TruSeq index 6	GCCAAT	2	309	162
33	LNDBB	control	8	Illumina TruSeq index 3	TTAGGC	2	314	161
MS03	DBCBB	schizophrenia	8	Illumina TruSeq index 5	ACAGTG	2	295	147
MS08	DBCBB	control	8	Illumina TruSeq index 1	ATCAGG	1	301	155
MS20	DBCBB	schizophrenia	8	Illumina TruSeq index 7	CAGATC	2	304	170
MS33	DBCBB	control	8	Illumina TruSeq index 8	ACTTGA	1	301	132

6.2.3. Data pre-processing

Raw data were de-multiplexed using the index barcode information provided in **Table 6.3** and the raw data for each sample were stored as *.fastq* files. The numbers of raw reads from Read 1 (R1), Read 2 (R2) and Paired Reads (R1+R2) for each sample is presented in **Table 6.4**. Each Illumina HiSeq 2500 lane provides ~200 million paired-end reads (Exeter Sequencing Service, 2015). I multiplexed 8 samples per lane; therefore I expected to obtain ~25 million paired-end reads per sample. As **Table 6.4** shows, all samples show considerably good sequencing coverage and therefore none of the samples was excluded based on low read coverage.

As part of the initial quality control (QC) steps performed by the Exeter Sequencing Service, Dr Konrad Paszkiewicz assessed the dynamic range for each of the samples using the ERCC spike-in controls (Jiang et al., 2011). The ERCC controls (Ambion, Thermo Fisher Scientific, Waltham, MA, USA) are a set of 92 unlabelled, poly-adenylated transcripts designed to be added to an RNA analysis experiment after sample isolation. The data generated for these transcripts during sequencing can then be compared with expected fold-changes provided by the manufacturer (Thermo Fisher Scientific, 2012). In this experiment sample 15 from the LBDBB failed to show a good correlation between observed and expected expression levels of the ERCC transcripts. **Figure 6.1** shows the examples of sample MS06 from the DBCBB (**A**) and sample 15 from the LBDBB (**B**). On a successful sample (**A**), the expected expression levels ($\log_2(\text{FPKM})$; y-axis) should appear proportional to the observed expression (x-axis) levels throughout most of the range. For details on the FPKM measure see **Table 6.1**.

Table 6.4. Number of raw, trimmed and mapped reads for each sequenced library.

Sample	Raw reads R1	Raw reads R2	Raw paired reads	Trimmed reads R1	Trimmed reads R2	Trimmed paired reads	% Trimmed paired reads	Mapped paired reads	Unique mapped reads	% Unique mapped reads
1	22,022,362	22,022,362	44,044,724	19,737,657	19,737,657	39,475,314	89.63	82,694,670	33,045,883	75.03
2	36,507,236	36,507,236	73,014,472	32,743,321	32,743,321	65,486,642	89.69	137,782,088	54,350,203	74.44
8	24,379,434	24,379,434	48,758,868	21,848,457	21,848,457	43,696,914	89.62	94,970,386	36,044,222	73.92
9	35,228,080	35,228,080	70,456,160	31,699,701	31,699,701	63,399,402	89.98	142,326,800	51,554,779	73.17
11	15,507,652	15,507,652	31,015,304	13,708,674	13,708,674	27,417,348	88.40	62,279,464	22,266,347	71.79
13	23,953,451	23,953,451	47,906,902	21,216,683	21,216,683	42,433,366	88.57	90,774,484	35,177,727	73.43
14	24,798,825	24,798,825	49,597,650	22,383,851	22,383,851	44,767,702	90.26	95,661,926	37,181,159	74.97
15	19,097,235	19,097,235	38,194,470	16,059,545	16,059,545	32,119,090	84.09	66,844,292	27,105,803	70.97
16	35,742,983	35,742,983	71,485,966	32,041,115	32,041,115	64,082,230	89.64	140,566,028	52,654,471	73.66
18	27,913,509	27,913,509	55,827,018	25,179,757	25,179,757	50,359,514	90.21	83,489,526	44,137,940	79.06
19	37,349,087	37,349,087	74,698,174	33,177,004	33,177,004	66,354,008	88.83	148,940,126	54,474,639	72.93
20	21,387,308	21,387,308	42,774,616	15,163,656	15,163,844	30,327,500	70.90	68,444,996	24,762,860	57.89
22	19,700,598	19,700,598	39,401,196	16,815,428	16,815,428	33,630,856	85.35	68,491,022	28,254,456	71.71
24	13,410,955	13,410,955	26,821,910	11,676,892	11,676,892	23,353,784	87.07	50,036,030	19,240,093	71.73
25	29,397,221	29,397,221	58,794,442	26,194,076	26,194,076	52,388,152	89.10	117,695,800	42,847,880	72.88
26	25,157,490	25,157,490	50,314,980	23,110,516	23,110,516	46,221,032	91.86	106,063,442	37,206,511	73.95
27	25,476,024	25,476,024	50,952,048	23,257,529	23,257,529	46,515,058	91.29	105,895,278	37,221,490	73.05
29	21,208,006	21,208,006	42,416,012	17,916,108	17,916,108	35,832,216	84.48	76,759,346	29,802,156	70.26
31	20,076,041	20,076,041	40,152,082	18,305,203	18,305,203	36,610,406	91.18	82,685,816	29,557,574	73.61
32	23,056,617	23,056,617	46,113,234	21,306,636	21,306,636	42,613,272	92.41	99,414,198	34,088,653	73.92
33	15,198,805	15,198,805	30,397,610	13,138,163	13,138,163	26,276,326	86.44	54,204,792	22,062,152	72.58
34	21,895,739	21,895,739	43,791,478	18,654,893	18,654,893	37,309,786	85.20	76,229,954	31,294,444	71.46
40	22,810,546	22,810,546	45,621,092	20,657,514	20,657,514	41,315,028	90.56	94,217,408	33,551,666	73.54
43	34,379,919	34,379,919	68,759,838	30,401,870	30,401,870	60,803,740	88.43	134,630,726	50,514,554	73.47
44	27,077,129	27,077,129	54,154,258	23,552,979	23,552,979	47,105,958	86.98	71,054,894	42,347,065	78.20
45	21,764,436	21,764,436	43,528,872	19,424,642	19,424,642	38,849,284	89.25	85,845,448	32,148,458	73.86
46	35,203,960	35,203,960	70,407,920	32,247,555	32,247,555	64,495,110	91.60	152,164,264	51,681,388	73.40

47	24,044,003	24,044,003	48,088,006	21,502,237	43,004,474	89.43	90,512,832	35,814,681	74.48
49	28,112,673	28,112,673	56,225,346	24,992,133	49,984,266	88.90	121,158,652	39,452,744	70.17
51	52,462,890	52,462,890	104,925,780	46,275,141	92,550,282	88.21	194,329,070	77,698,097	74.05
MS01	21,965,168	21,965,168	43,930,336	19,723,836	39,447,672	89.80	90,352,870	31,671,098	72.09
MS02	30,511,201	30,511,201	61,022,402	27,395,656	54,791,312	89.79	123,237,214	44,307,305	72.61
MS03	29,134,445	29,134,445	58,268,890	25,785,581	51,571,162	88.51	101,280,234	43,280,614	74.28
MS04	23,780,243	23,780,243	47,560,486	20,979,530	41,959,060	88.22	58,984,380	37,961,489	79.82
MS05	25,669,043	25,669,043	51,338,086	23,242,975	46,485,950	90.55	106,820,460	37,695,377	73.43
MS06	31,862,762	31,862,762	63,725,524	28,710,353	57,420,706	90.11	132,721,426	45,754,111	71.80
MS08	23,865,250	23,865,250	47,730,500	21,956,388	43,912,776	92.00	97,274,086	35,970,134	75.36
MS09	23,326,142	23,326,142	46,652,284	19,362,352	38,724,704	83.01	64,464,116	34,122,372	73.14
MS11	38,930,756	38,930,756	77,861,512	33,808,027	67,616,054	86.84	160,408,416	53,520,738	68.74
MS17	24,683,214	24,683,214	49,366,428	22,314,691	44,629,382	90.40	105,489,010	35,407,244	71.72
MS20	13,515,071	13,515,071	27,030,142	12,054,073	24,108,146	89.19	59,264,698	18,737,153	69.32
MS21	22,811,361	22,811,361	45,622,722	20,452,164	40,904,328	89.66	94,070,476	32,892,251	72.10
MS30	21,369,262	21,369,262	42,738,524	19,535,847	39,071,694	91.42	90,791,846	31,308,082	73.25
MS33	30,105,096	30,105,096	60,210,192	26,725,854	53,451,708	88.78	123,531,626	43,273,273	71.87
MS34	42,164,481	42,164,481	84,328,962	37,656,859	75,313,718	89.31	109,040,088	67,031,962	79.49
MS35	25,359,517	25,359,517	50,719,034	21,531,007	43,062,014	84.90	92,910,218	35,164,960	69.33

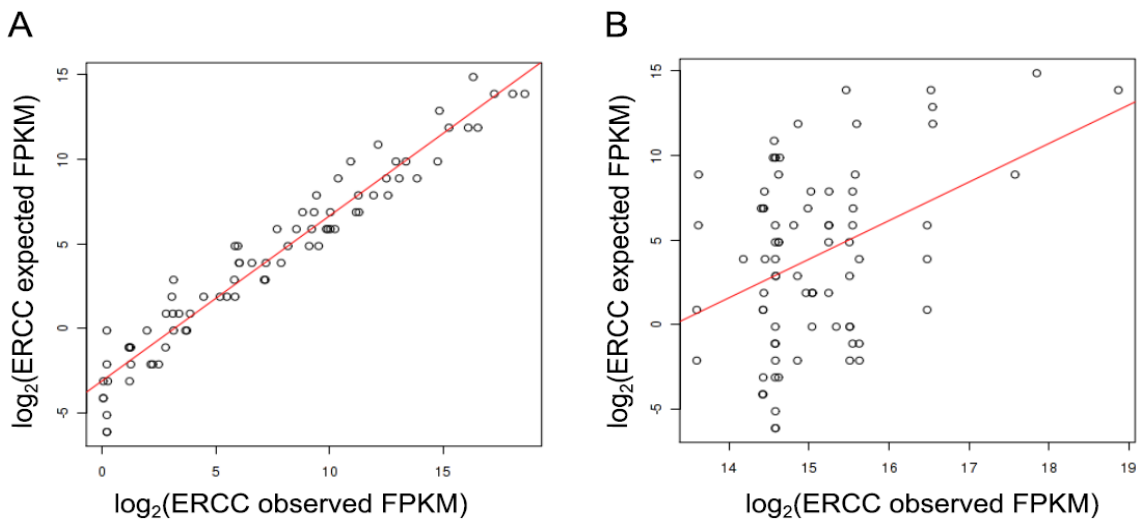


Figure 6.1. Correlation between \log_2 of the observed and expected expression levels of the ERCC spike-in control transcripts. Shown are the examples of sample MS06 from the Douglas-Bell Canada Brain Bank (**A**) and sample 15 from the MRC London Neurodegenerative Diseases Brain Bank (**B**). FPKM, fragments per kilobase of exon per million fragments mapped.

The samples were inspected for contamination by investigating what percentage of reads mapped uniquely to the human genome, to other species genomes or to human ribosomal RNA (rRNA). In order to do this the *FastQ Screen* software was used (Babraham Bioinformatics Group, 2015), which allows to screen a library of sequences against a set of sequence databases. Six samples (18 and 44 from the LNDBB and MS34PFC, MS04PFC, MS09PFC and MS03PFC from the DBCBB) showed some contamination with *Adabidopsis*, yeast and rRNA. **Figure 6.2** presents the example of sample MS02 from the DBCBB, which shows high percentage of unique mapping (light blue) and negligible levels of contamination. **Figure 6.3** shows the example of sample MS34 from the DBCBB, which presents some level of contamination. The contamination of RNA from other species should not be problematic, given that the reads were subsequently mapped to the human genome/transcriptome, however the contamination with human rRNA indicates sub-optimal rRNA removal during prior library preparation (see **Chapter 2 section 2.5.1**) and might be problematic during data analysis. I decided to keep these samples in the dataset and evaluate the consequence of this contamination in downstream analysis (see **section 6.2.8**).

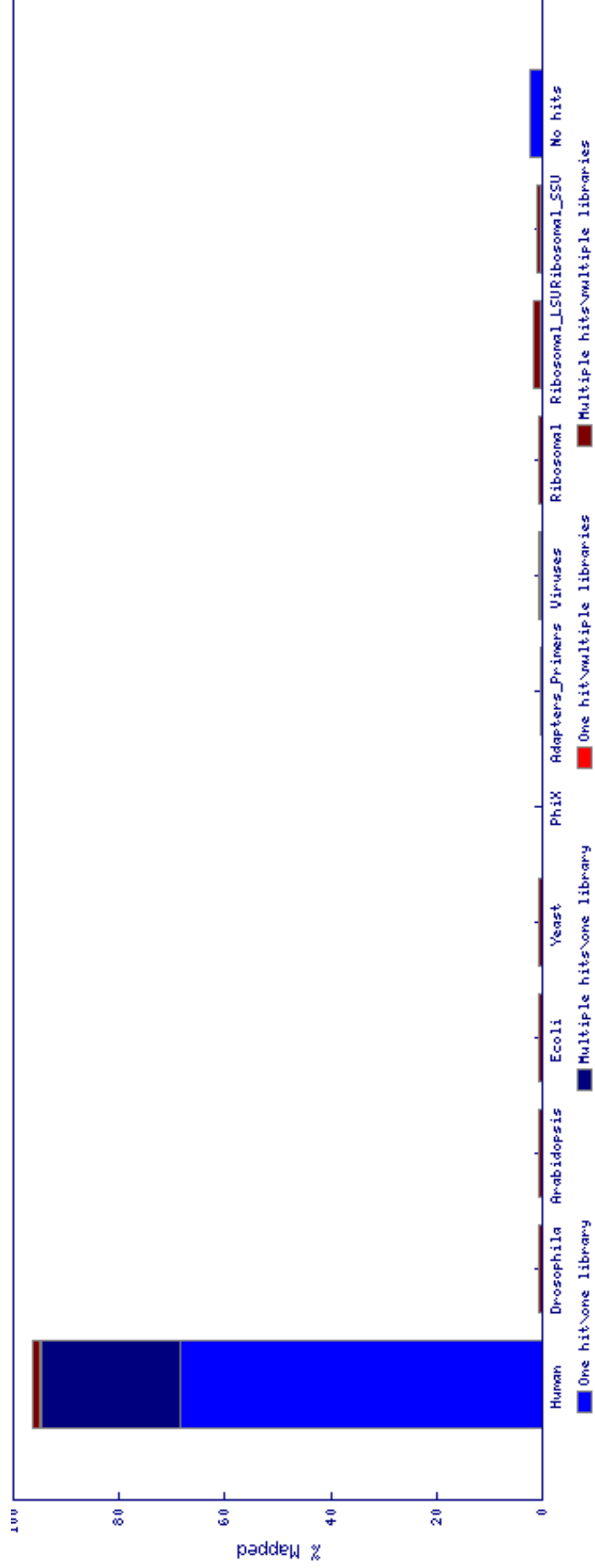


Figure 6.2. Example of plots produced by the *FastQ Screen* tool for sample MS02 from the DBCBB. This example shows high levels of unique mapping (light blue) and negligible levels of contamination by ribosomal RNA and RNA from other species.

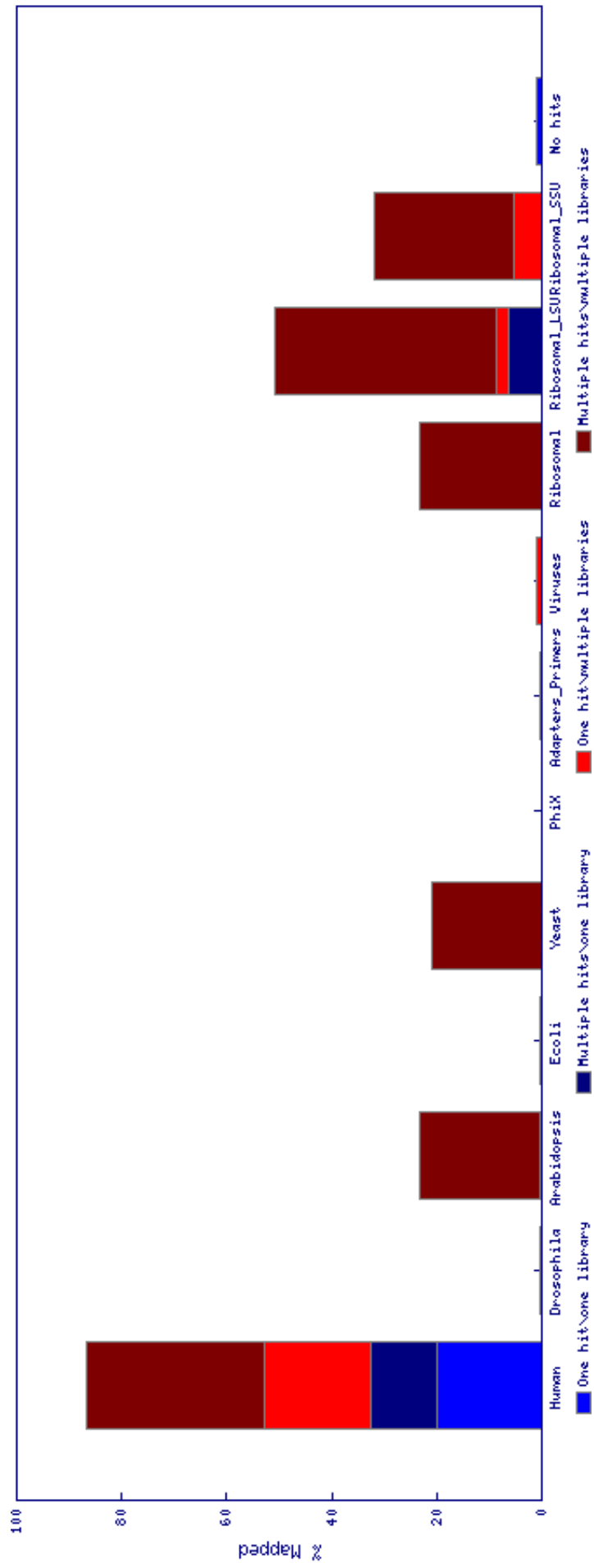


Figure 6.3. Example of plots produced by the FastQ Screen tool for sample MS34 from the DBCBB. This example shows evidence of contamination by ribosomal RNA and RNA from other species.

6.2.4. Inspection of raw data with *FastQC*

I next inspected the raw reads (*.fastq* files of both read 1 and read 2 from each sample) using the *FastQC* software version 0.10.1 (Andrews, 2010). The software provides a modular set of analyses for high throughput sequencing raw data. In this section I present examples of some of the important metrics given by *FastQC* that were used to inspect the RNA-seq data included in this chapter.

6.2.4.1. *Phred* quality scores

One of the important metrics to consider is the 'per base sequence quality'. **Figure 6.4** shows an example of a *FastQC* 'per base sequence quality' plot for read 1 of sample 18 from the LDNBB. The plot shows an overview of the range of quality values across all bases at each position in the *.fastq* file. To provide an estimate of confidence in a given base call, the Illumina sequencing pipeline assigns a quality score (Q, *Phred* scale) to each base called, which estimates the chance that the call is incorrect:

- Q10 = 1 in 10 chance of incorrect base call
- Q20 = 1 in 100 chance of incorrect base call
- Q30 = 1 in 1000 chance of incorrect base call
- Q40 = 1 in 10,000 chance of incorrect base call

A score above 30 is considered good and above 20 is considered acceptable (Andrews, 2010). The quality of calls on the Illumina platform will degrade as the run progresses (towards the end of a read). **Figure 6.5** shows an example of the distribution of *Phred* scores for all read 1 reads of sample 18 from the LDNBB. The plot shows a smooth peak around Q=37, indicating that the majority of reads are of very high quality.

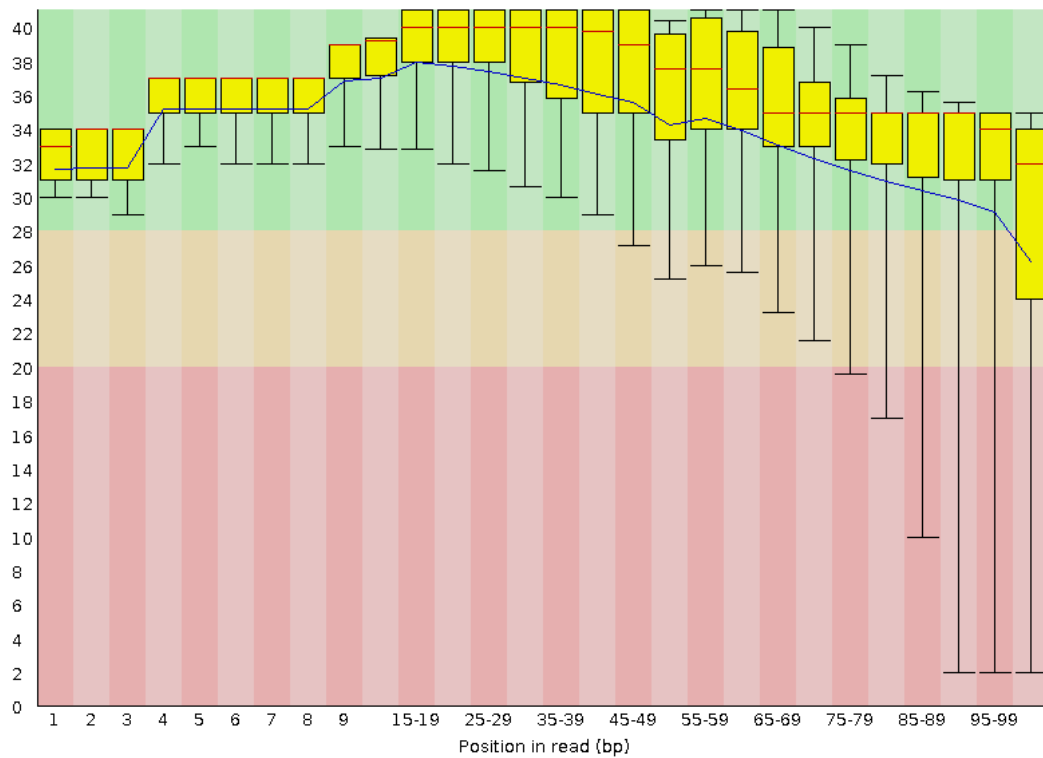


Figure 6.4. Example of a 'per base sequence quality' plot given by the *FastQC* software. Shown is the plot for read 1 of sample 18 from the LNDBB. The y-axis shows the *Phred* score along the read (x-axis). The central red line is the median value; the yellow box represents the inter-quartile range (25-75%), the upper and lower whiskers represent the 10% and 90% points, respectively, and the blue line represents the mean quality.

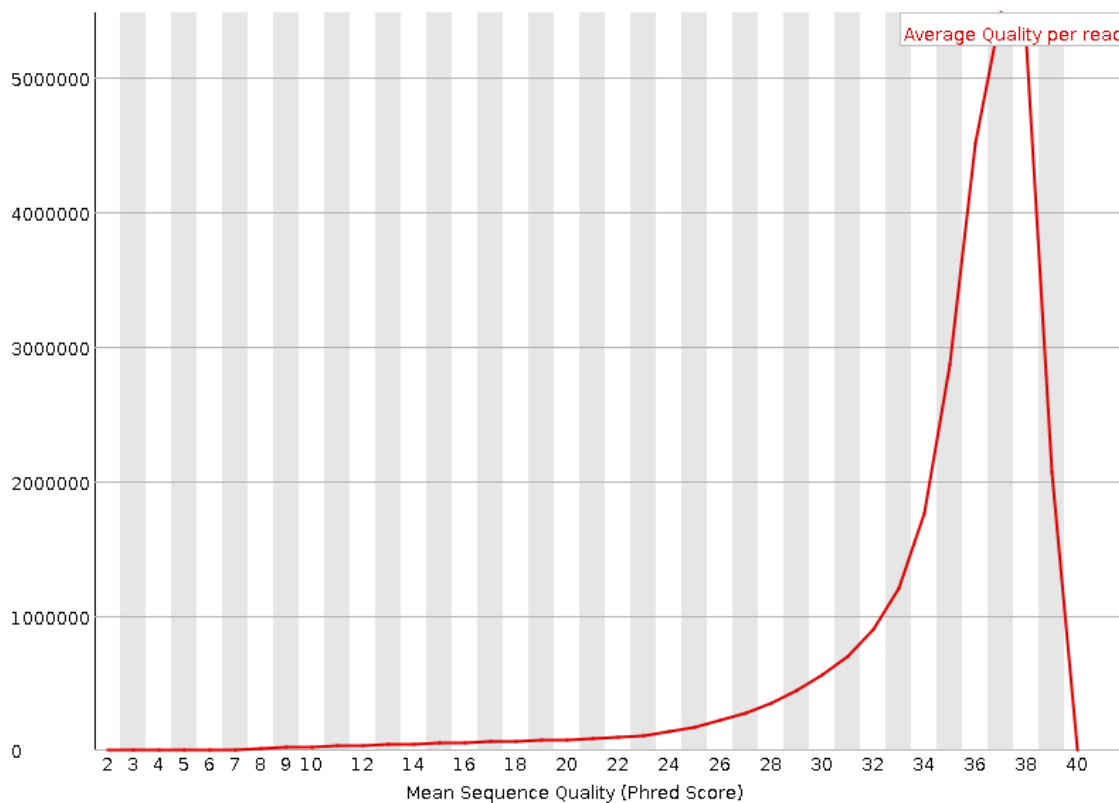


Figure 6.5. Example of a ‘per sequence quality’ plot given by the *FastQC* software. Shown is the plot for read 1 of sample 18 from the LNDBB. The x-axis illustrates the mean *Phred* score per read (y-axis).

6.2.4.2. Per base sequence and GC content

Figures 6.6 and **6.7** show the base (A, C, G and T) and CG content (y-axis) by position in the reads (x-axis), respectively. Ideally, there should be no variation among base calls along the length of the read, and the CG content should be constant along the read. In RNA-seq data generated using Illumina technology there is usually variation of base call and CG content at the beginning of reads. This happens because the random priming that occurs at the beginning of the sequences is not truly random; the first twelve bases (2 hexamer primers) anneal preferentially to sequences that prime more efficiently ((Hansen et al., 2010). This also explains why the *Phred* score is lower in the beginning of the read (**Figure 6.4**). This effect is removed after trimming the sequences (see **Section 6.2.5**) and has no impact on downstream analysis.

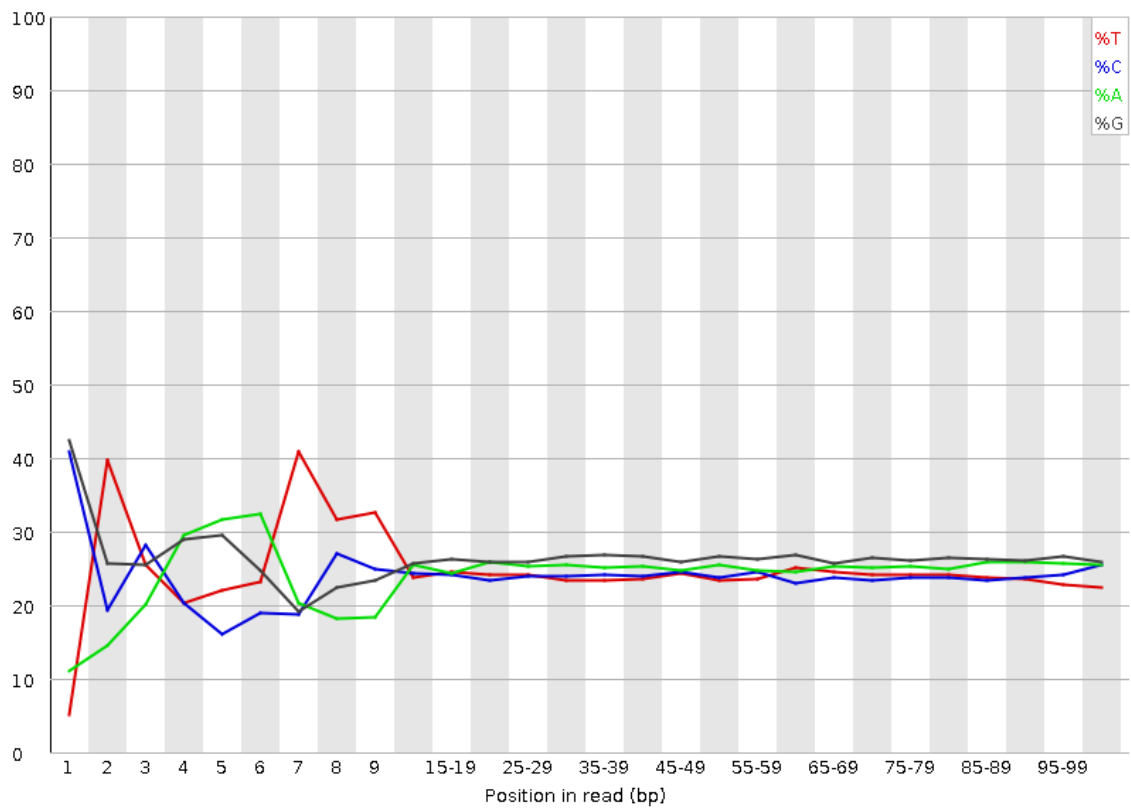


Figure 6.6. Example of a ‘per base sequence content’ plot given by the *FastQC* software. Shown is the plot for read 1 of sample 18 from the LNDBB. The y-axis shows the base call content along the read (x-axis).

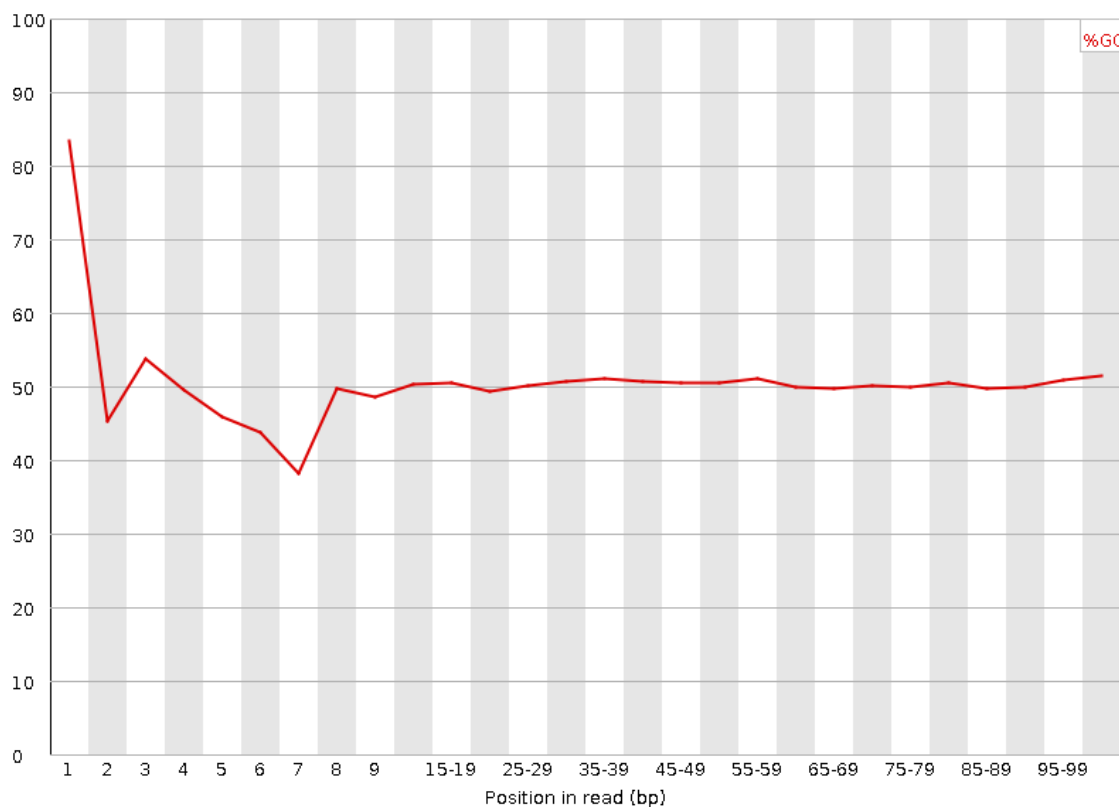


Figure 6.7. Example of a ‘per base CG content’ plot given by the *FastQC* software. Shown is the plot for read 1 of sample 18 from the LNDBB. The y-axis shows the mean CG content along the read (x-axis).

The ‘per sequence GC content’ density plot (**Figure 6.8**) shows the distribution of GC content (x-axis) per reads (y-axis), where the data (red curve) are expected to approximately follow the theoretical distribution (blue curve). If the curve presents a shoulder in a region of high GC content (right of the graphic), it is usually an indication of ribosomal RNA (rRNA) or other species’ RNA contamination. The majority of my samples showed a good approximation to the theoretical distribution. However, contamination by rRNA and other species’ RNA is discussed in more detail in **section 6.2.8**.

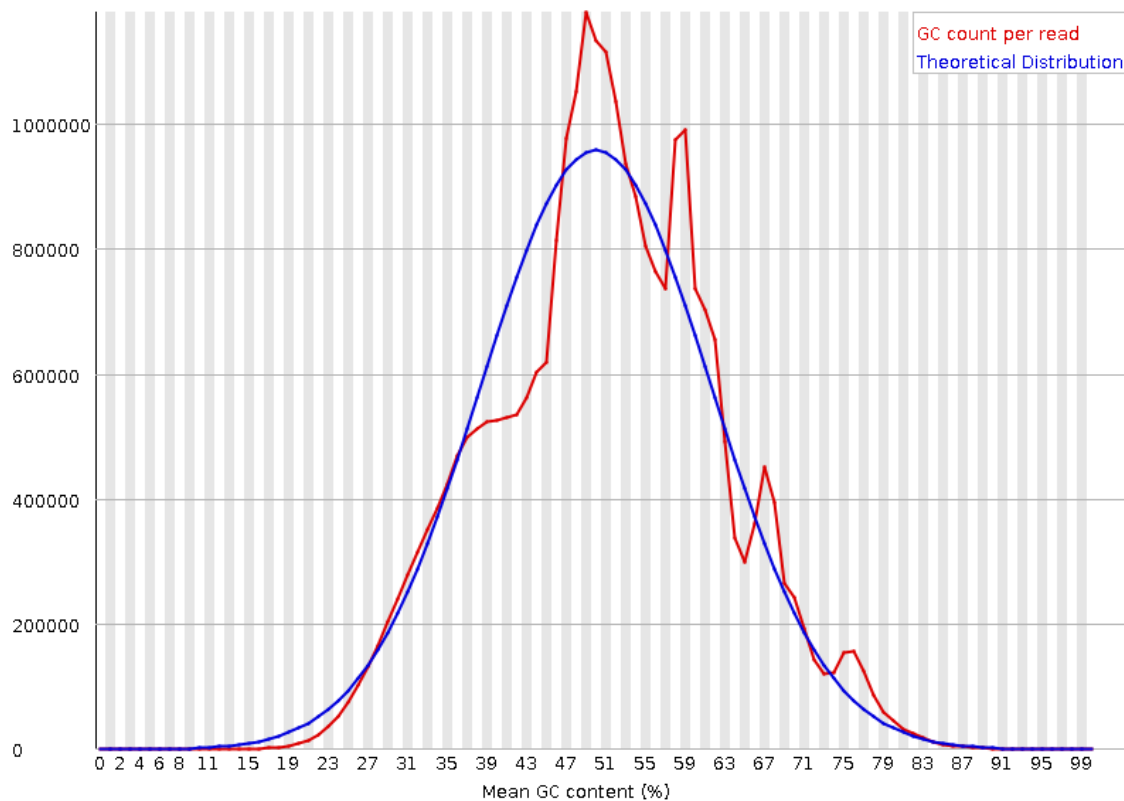


Figure 6.8. Example of a ‘per sequence GC content’ plot given by the *FastQC* software. Shown is the density plot for read 1 of sample 18 from the LNDBB. The x-axis shows the mean CG content (%) per read (y-axis).

6.2.4.3. Sequence duplication levels

Figure 6.9 shows an example of the ‘sequence duplication levels’ plot. This plot presents the level of duplicated sequences in the library. *FastQC* assumes a uniform coverage since it was developed for genomic DNA sequencing. In a library that covers the whole genome uniformly (such as one resulting from genomic DNA sequencing), a high level of duplication is likely to indicate some kind of enrichment bias (e.g. PCR over-amplification). However, in an RNA-seq experiment, genes that are highly expressed will have a very high level of coverage and higher level of duplication is expected.

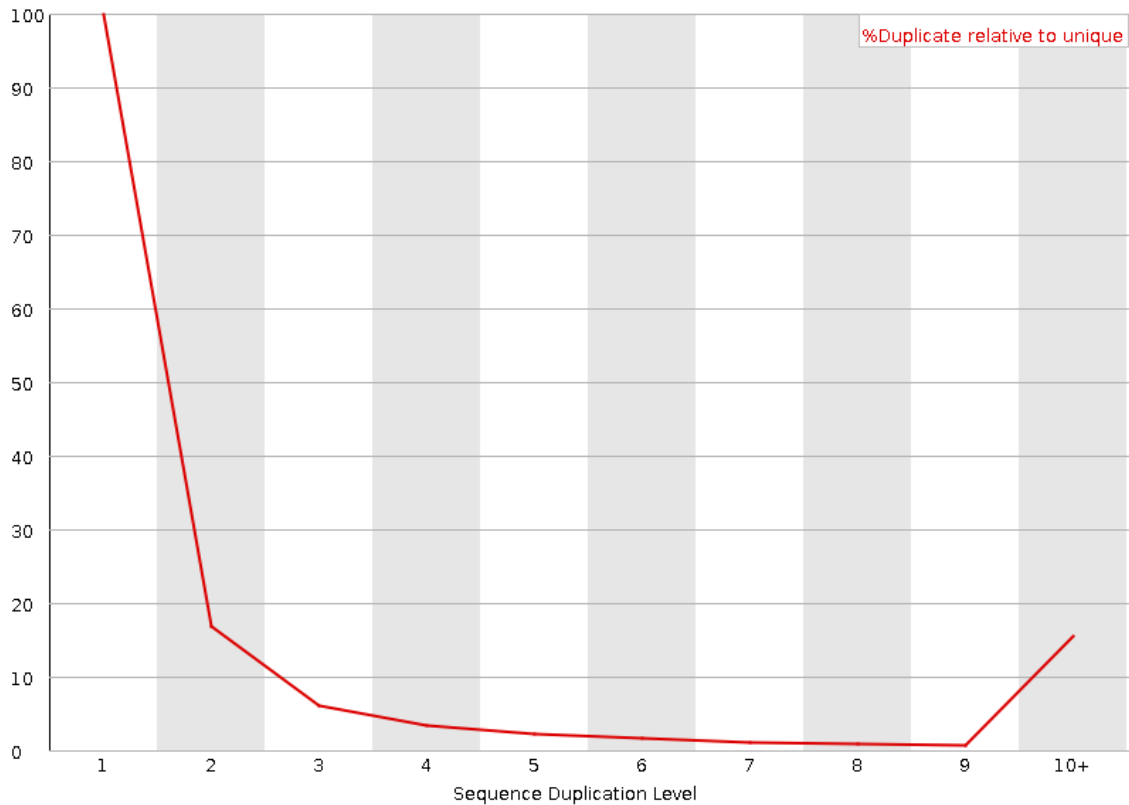


Figure 6.9. Example of a ‘sequence duplication levels’ plot given by the *FastQC* software. Plot for read 1 of sample 18 from the LNDBB. The y-axis shows the percentage of reads considered as duplicates and the x-axis shows the number of reads with that level of duplication.

6.2.5. Trimming of raw reads using *Trimmomatic*

I used *Trimmomatic* version 0.36 (Bolger et al., 2014) to pre-process the raw reads and remove adapter sequences and low quality sequences. *Trimmomatic* is a command line tool that runs within the Linux operating system and uses a set of algorithms to crop and trim the data based on quality measures, as well as remove adapter sequences.

The following list describes the commands used in the raw RNA-seq data used in this Chapter:

ILLUMINACLIP – Exclude adapter and other Illumina-specific sequences from each read.

LEADING - Exclude bases off the start of a read if below a threshold quality number .

TRAILING - Exclude bases off the end of a read if below a threshold quality number.

SLIDINGWINDOW - Performs a sliding window trimming approach. It starts scanning at the 5' end and clips the read once the average quality within the window falls below a threshold.

HEADCROP - Exclude the specified number of bases from the start of the read. These are the 'random' primers that need to be excluded (see **section 6.2.4.2**).

MINLEN - Exclude the entire read if it is below a specified length.

For paired-end data, *Trimmomatic* outputs a 'paired' output file for read 1 and read 2 from each sample, where both reads survived the QC and an 'unpaired' output, where only one or none of the reads survived the processing. The 'paired' output was used for further analysis. **Table 6.4** in **section 6.2.3** shows the number of trimmed reads (read 1, read 2 and paired) for each sample, as well as the percentage of trimmed paired reads in relation to the raw reads for each sample. The paired output for both read 1 and read 2 from each sample was inspected in *FastQC* and compared with the *FastQC* report of the raw reads (see **section 6.2.4.1**). **Figures 6.10** to **6.12** show an example of the comparison between the raw reads and the trimmed reads for the 'per base quality', 'sequence content' and 'CG content' plots. As **Figure 6.10** shows, the low quality end of the reads was successfully trimmed. All three figures indicate that the lower quality at the beginning of the read, due to non-random priming (see **Section 6.2.4.2**), was successfully removed during the trimming process.

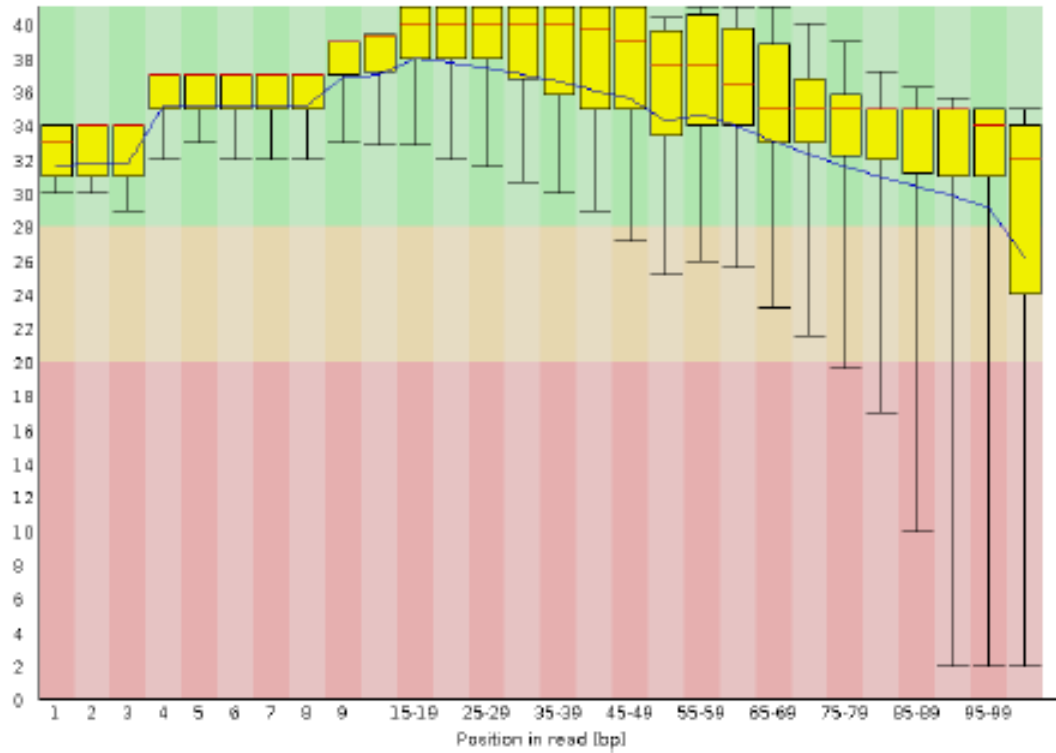
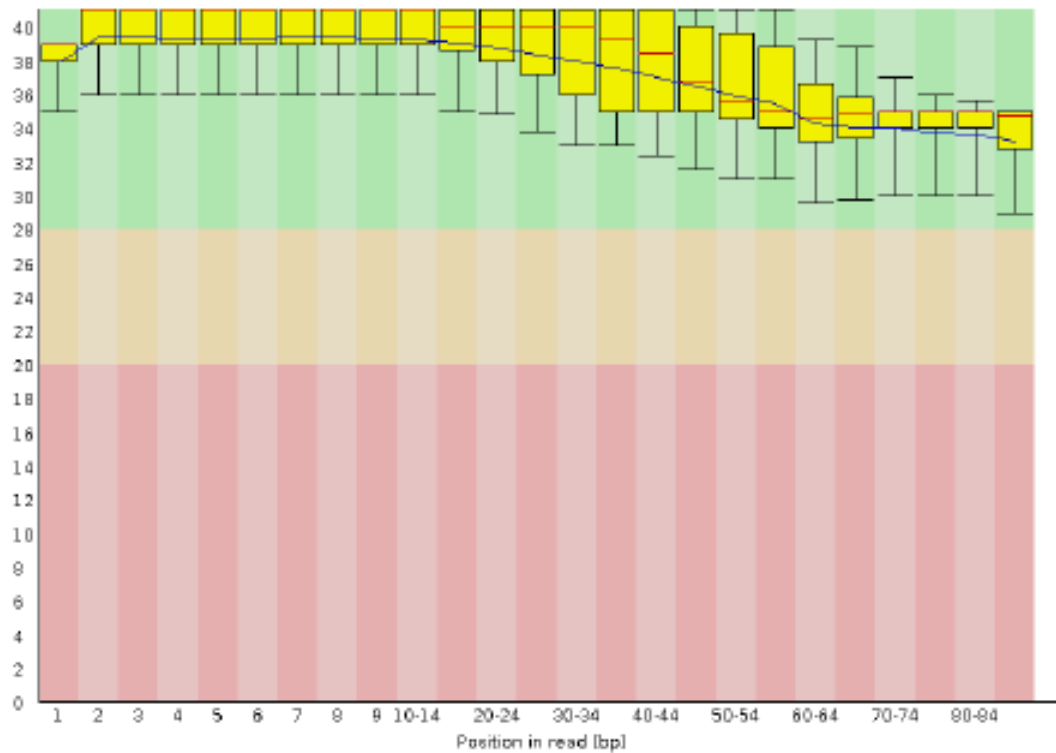
A**B**

Figure 6.10. Example of a ‘per base sequence quality’ plot given by the *FastQC* software before (A) and after (B) using *Trimmomatic*. Shown are the plots for read 1 of sample 18 from the LNDBB. The y-axis shows the *Phred* score along the read (x-axis).

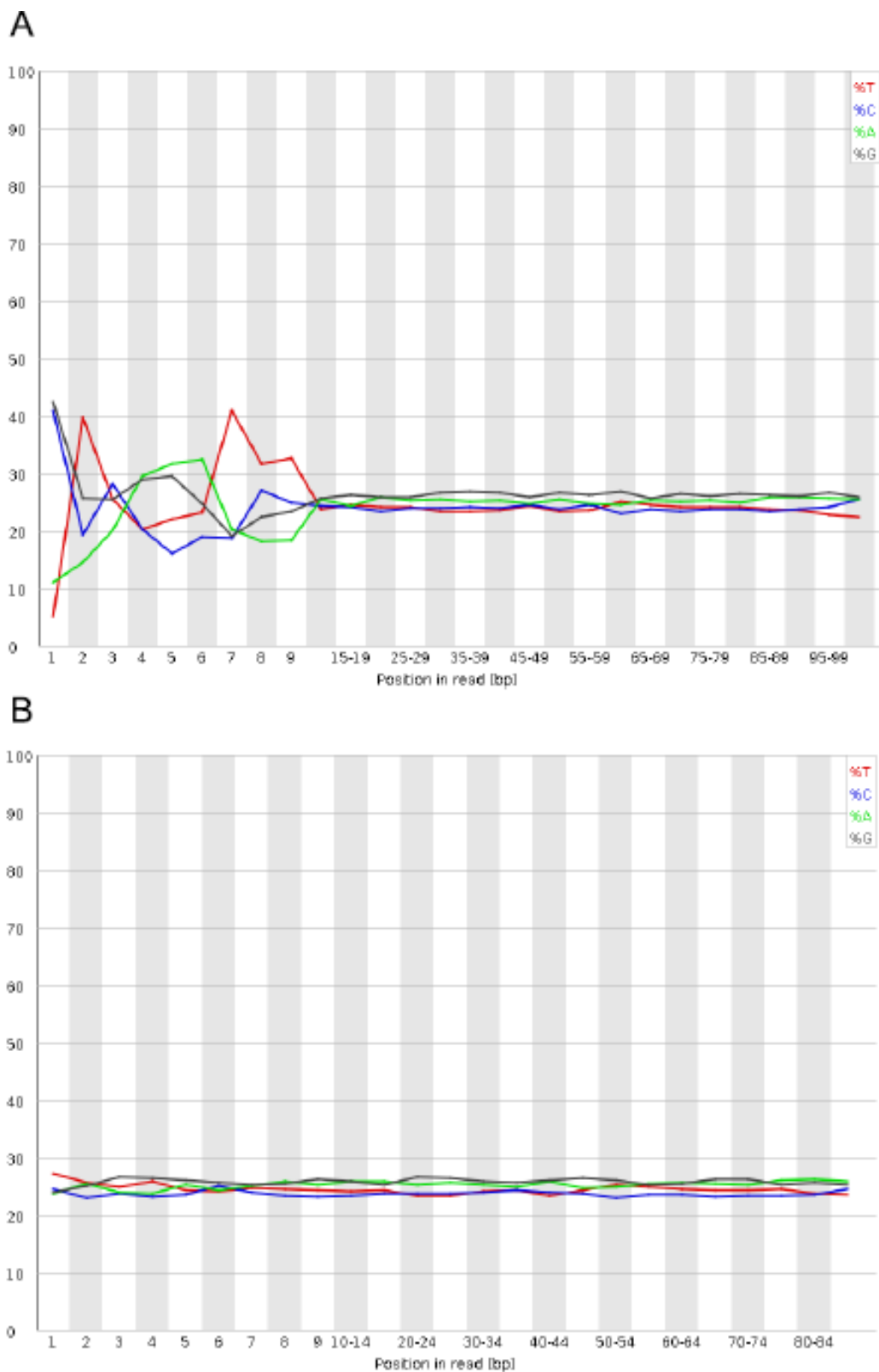


Figure 6.11. Example of a ‘per base sequence content’ plot given by the *FastQC* software before (A) and after (B) using *Trimmomatic*. Plot for read 1 of sample 18 from the MRC London Neurodegenerative Diseases Brain Bank. The y-axis shows the base call content along the read (x-axis).

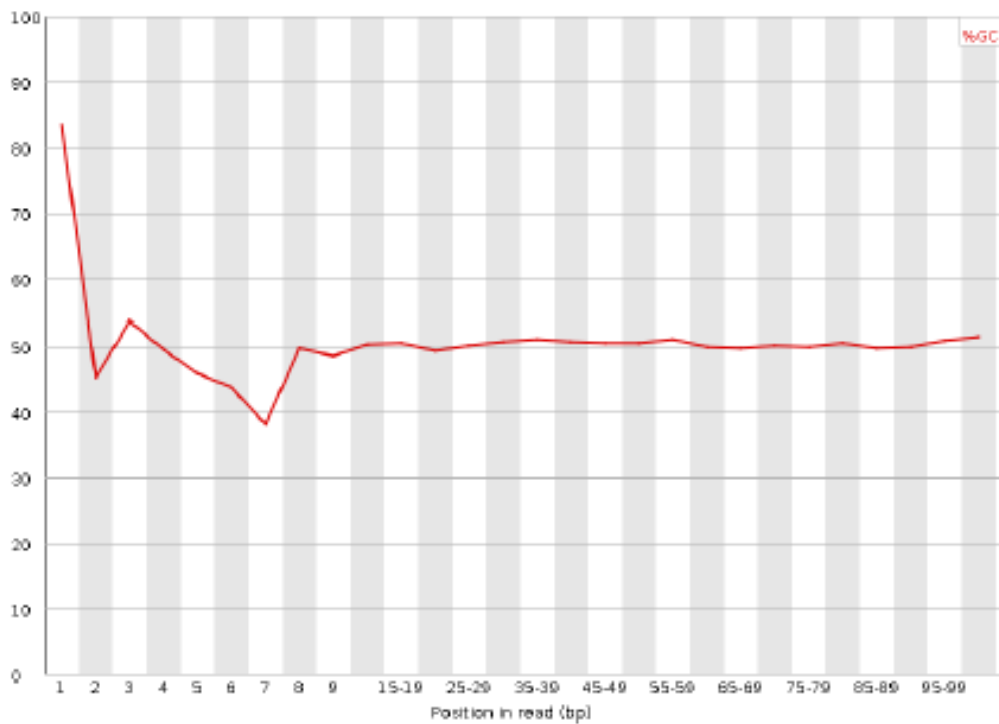
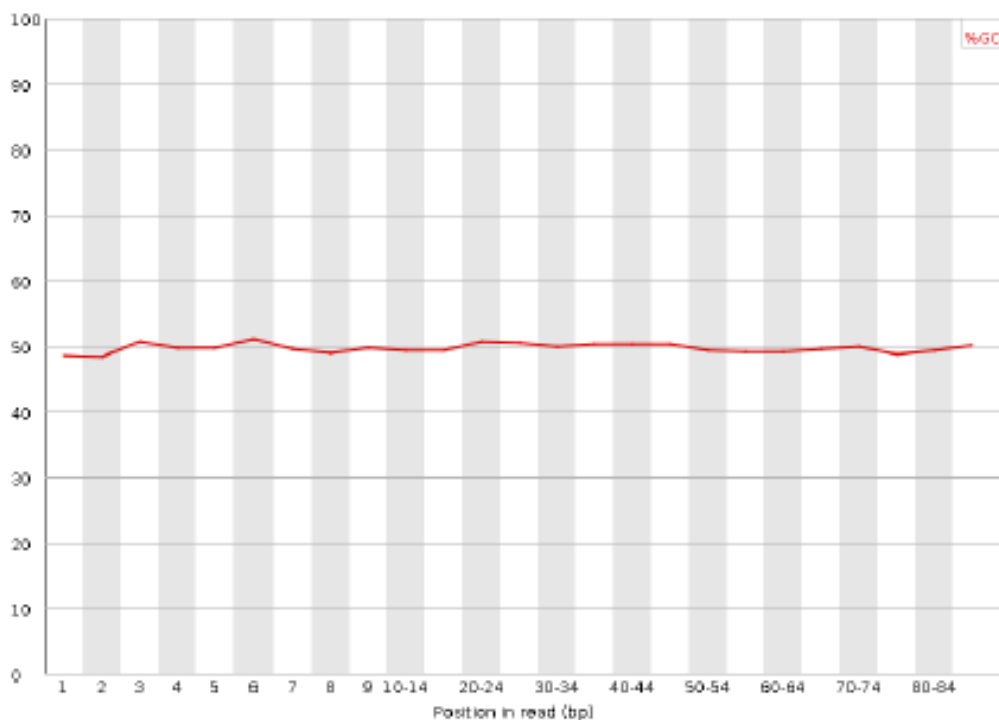
A**B**

Figure 6.12. Example of a ‘per base CG content’ plot given by the *FastQC* software before (A) and after (B) using *Trimmomatic*. Shown are the plots for read 1 of sample 18 from the MRC London Neurodegenerative Diseases Brain Bank. The y-axis shows the mean CG content along the read (x-axis).

6.2.6. Aligning reads to the human reference transcriptome and quantifying gene expression

In order to quantify gene expression levels I next aligned (or mapped) the pre-processed reads to the human reference transcriptome. Mapping to a reference transcriptome rather than the genome is generally faster and more specific but does not enable *de novo* transcript discovery or splicing analysis (Conesa et al., 2016). For the purpose of the analyses presented here I was interested in identifying differently expressed (DE) genes between schizophrenia patients and controls and therefore I mapped the reads to the reference transcriptome.

I first downloaded the reference cDNA sequences from the Genome Reference Consortium Human Build 38 (GRCh38.p5) (genome assembly GCA_000001405.20) from the Ensembl website (for the *ftp* address see Genome Reference Consortium (2013)). I also downloaded the ERRC spike-in sequences from the Thermo Fisher Scientific website (Thermo Fisher Scientific, 2016) and appended these sequences to the human reference transcriptome so I could align the corresponding reads to the control transcripts and remove them from downstream analyses. Next I used *bowtie* (Langmead et al., 2009) within *RSEM* version 1.2.29 (Li and Dewey, 2011) to prepare the reference library. *Bowtie* is a fast and memory-efficient tool designed for the alignment of large sets of short DNA sequences (*i.e.* reads) to large genomes (or transcriptomes). *RSEM* is a software package run under Linux operating system for estimating gene expression levels from RNA-seq data (Li and Dewey, 2011). *RSEM* has built-in support for *bowtie* so the preparation of the reference library, alignment and gene expression calculation can be done within *RSEM*. To achieve this I used the following *RSEM* functions and parameters:

- **Preparing the reference library:**

```
rsem-prepare-reference --transcript-to-gene-map --bowtie -
```

This command uses *bowtie* to prepare the reference library for alignment using the reference human cDNA sequences extracted from Ensembl (Genome Reference Consortium, 2013). The '`--transcript-to-gene-map`' parameter uses the information on the reference transcriptome files to map the transcripts to specific gene IDs.

- **Aligning to the reference transcriptome and calculating gene expression**

`rsem-calculate-expression --paired-end` - This command aligns the input (trimmed) reads against the reference library using *bowtie* and estimates expression values for each gene using the alignment output.

An important note is that after mapping reads to a reference library, these may map uniquely (be assigned to only one position in the reference library) or map to multiple locations (*i.e.* ‘multireads’). When mapping to a reference genome, ‘multireads’ are primarily a result of repetitive sequences or paralogous genes (Conesa et al., 2016). When aligning to a reference transcriptome, ‘multireads’ are more frequent because reads that would have mapped uniquely to a gene DNA sequence can map to all gene isoforms (several transcripts for the same gene) (Conesa et al., 2016).

Table 6.4 (section 6.2.3) presents the number of mapped reads for each sample as well as the number (and percentage relative to the number of original raw reads) of unique mapped reads (unique gene IDs). All samples contained ‘multireads’, which is expected from reads aligned to the transcriptome as explained above. To address this *RSEM* uses an expectation-maximization algorithm to estimate maximum likelihood expression values for each individual gene (Li and Dewey, 2011). The output is a *.bam* file for each sample with the aligned reads and a matrix of “expected counts” per individual gene, which are used for differential expression analysis (see **section 6.2.7**). To merge the “expected counts” files from each sample into a single matrix with expected counts for all samples I used the *abundance_estimates_to_matrix.pl* pipeline within the *Trinity* platform developed by the Broad Institute (Haas et al., 2013). The output for analysis contained counts from all samples for a total of 38,786 genes.

6.2.7. Differential expression analysis

To identify the expressed genes across all samples and differentially expressed genes between schizophrenia patients and controls I used the *edgeR* Bioconductor package (Robinson et al., 2010) in R (R Core Team, 2015). I chose this package from a large range of available software for differential expression analysis since it allows the incorporation of co-variables such as age and sex within the analysis pipeline (McCarthy et al., 2012).

The “expected counts” matrix with gene counts for all samples (see **section 6.2.6**) was imported into R and a *DGEList* object was created using the *DGEList* function in *edgeR*. This object allows the storage of counts and sample information, as all the downstream normalisation and analysis steps in *edgeR*. The object also contains the library size (*i.e.* total gene counts) for each sample. The Bioconductor *biomaRt* package in R (Durinck et al., 2009) was used to annotate the Ensembl gene IDs in the dataset (Flicek et al., 2014) with gene symbols obtained from the HUGO Gene Nomenclature Committee (HGNC) (European Bioinformatics Institute, 2016).

6.2.8. Gene and sample exclusion

First, the ERCC spike-in transcripts and genes on the sex chromosomes were excluded from all libraries. Next, I excluded low expressed genes; genes were kept for further analysis if they had more than 1 counts per million (CPM) in at least 10 samples, as recommended (Robinson et al., 2010). Incorrect assembly sequences and allelic (haplotype) sequences were also excluded (see the Ensembl blog for details (Bronwen (Genebuild) - Ensembl blog, 2011)). In total, 16,920 genes remained after excluding ERCC transcripts (92), genes on the sex chromosomes (1,699 on the X-chromosome and 430 on the Y-chromosome), incorrect and allelic sequences (3,957) and low expressed genes (15,688). **Figure 6.16** in **section 6.2.8.1** presents the distribution of raw counts.

I next calculated principal components (PC) for the data and plotted the first PC against the second PC to look for outliers and batch effects (**Figure 6.13**). The six samples labelled show a greater variance in PC1 than the remaining samples. Of note, these are the samples that showed some degree of contamination with human rRNA and RNA from other species (**section 6.2.3**) and were excluded from further analysis. I next inspected multidimensional

scaling (MDS) plots to check for sex, RNA isolation, library preparation and lane allocation batch effects. **Figures 6.14** and **6.15** show examples of these plots for sex and cohort, respectively. No batch effects were found after exclusion of the six contaminated samples and no further samples were removed from analyses. Criteria for sample exclusion from the analyses are illustrated in **Table 6.5** and **Table 6.6** summarises demographic information of the samples used for analyses in this chapter.

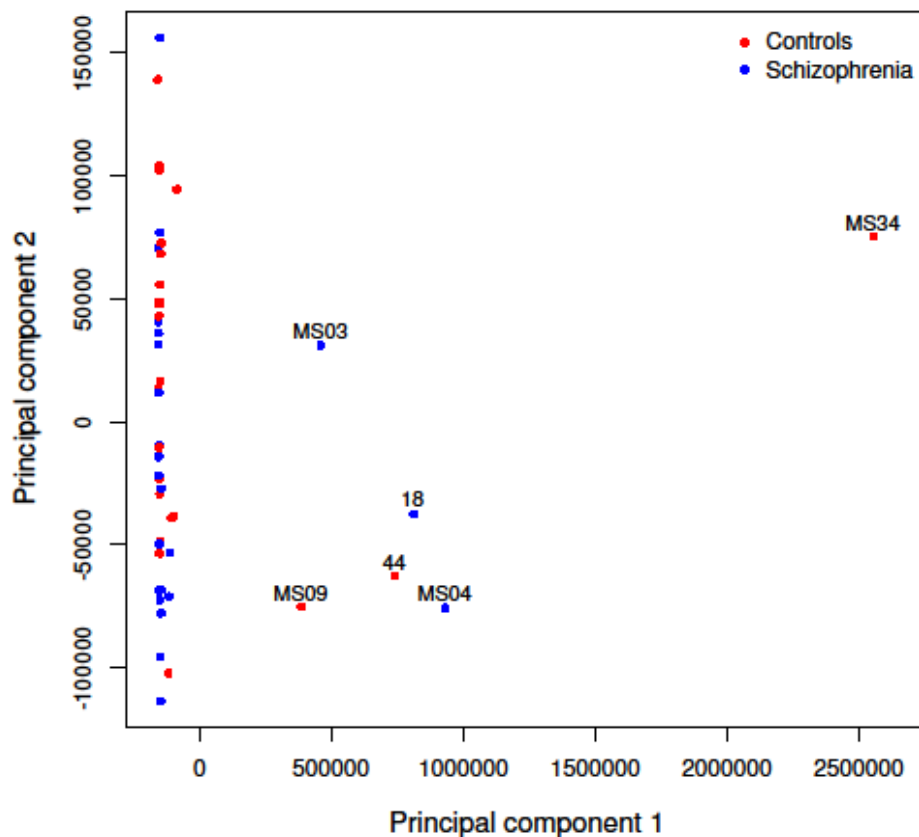


Figure 6.13. Principal component 1 (x-axis) versus principal component 2 (y-axis) of the raw gene counts.

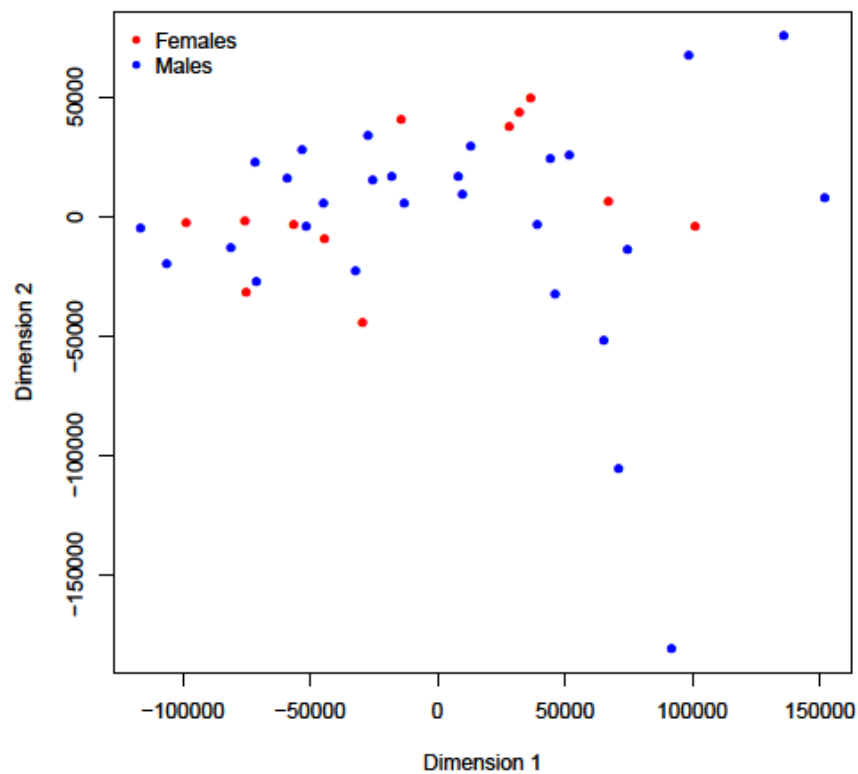


Figure 6.14. Example of multidimensional scaling plots for all samples included in the analyses of this chapter. The samples are coloured by sex.

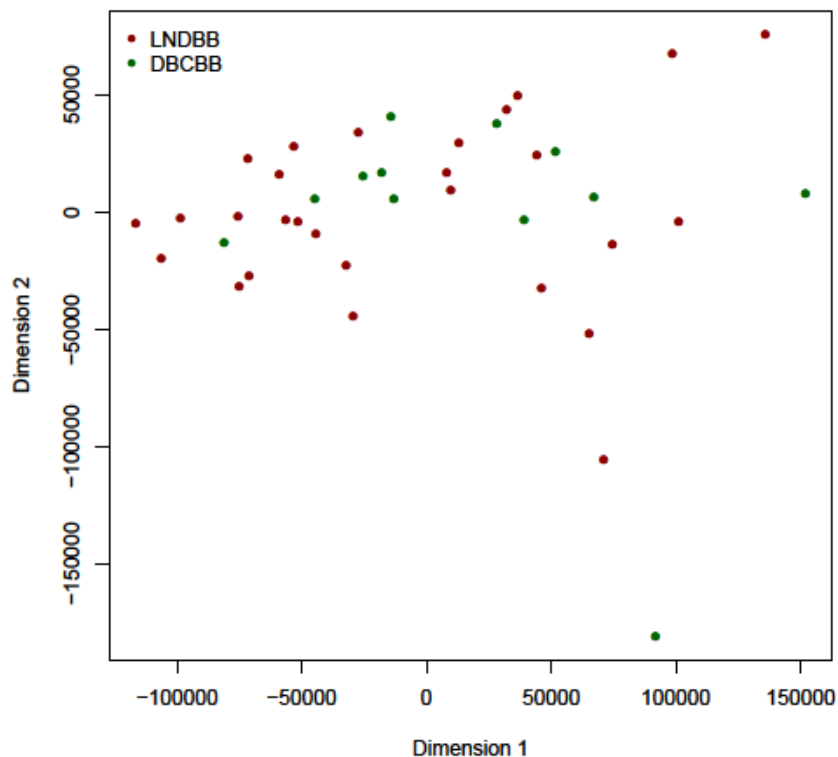


Figure 6.15. Example of multidimensional scaling plots for all samples included in the analyses of this chapter. The samples are coloured by cohort. LNDBB, MRC London Neurodegenerative Diseases Brain Bank; DBCBB, Douglas-Bell Canada Brain Bank.

Table 6.5. Criteria for sample exclusion or inclusion in the analyses performed in this chapter.

Sample	Brain Bank	Group	Sample inclusion/ exclusion
1	LNDBB	schizophrenia	included
2	LNDBB	schizophrenia	included
8	LNDBB	schizophrenia	included
9	LNDBB	schizophrenia	included
11	LNDBB	schizophrenia	included
13	LNDBB	schizophrenia	included
14	LNDBB	schizophrenia	included
15	LNDBB	schizophrenia	failed based on ERCC control QC
16	LNDBB	schizophrenia	included
18	LNDBB	schizophrenia	failed due to rRNA contamination
19	LNDBB	schizophrenia	included
20	LNDBB	schizophrenia	included
22	LNDBB	schizophrenia	included
24	LNDBB	schizophrenia	included
25	LNDBB	control	included
26	LNDBB	control	included
27	LNDBB	control	included
29	LNDBB	control	included
31	LNDBB	control	included
32	LNDBB	control	included
33	LNDBB	control	included
34	LNDBB	control	included
40	LNDBB	control	included
43	LNDBB	control	included
44	LNDBB	control	failed due to rRNA contamination
45	LNDBB	control	included
46	LNDBB	control	included
47	LNDBB	control	included
49	LNDBB	control	included
51	LNDBB	control	included
MS01	DBCBB	schizophrenia	included
MS02	DBCBB	schizophrenia	included
MS03	DBCBB	schizophrenia	failed due to rRNA contamination
MS04	DBCBB	schizophrenia	failed due to rRNA contamination
MS05	DBCBB	control	included
MS06	DBCBB	schizophrenia	included
MS08	DBCBB	control	included
MS09	DBCBB	control	failed due to rRNA contamination
MS11	DBCBB	schizophrenia	included
MS17	DBCBB	control	included
MS20	DBCBB	schizophrenia	included
MS21	DBCBB	schizophrenia	included
MS30	DBCBB	schizophrenia	included
MS33	DBCBB	control	included
MS34	DBCBB	control	failed due to rRNA contamination
MS35	DBCBB	control	included

Table 6.6. Demographic information on the final set of samples included in the analyses performed in this chapter.

	N	Sex (male:female)	Age at death	Brain weight (g)	pH	RIN	% unique mapped reads
LNDBB	Schizophrenia	12	62.92 ± 11.81	1283 ± 129.93	6.69 ± 0.27	6.46 ± 0.87	72.06 ± 4.61
	Controls	15	53.67 ± 15.74	1403.83 ± 189.89	6.62 ± 0.24	6.01 ± 1.25	72.98 ± 1.33
	Total	27	57.78 ± 14.64	1348.91 ± 172.96	6.65 ± 0.25	6.21 ± 1.10	72.57 ± 3.19
	P	-	0.09	0.09	0.51	0.28	0.51
DBCBB	Schizophrenia	7	47.43 ± 17.86	1427.20 ± 200.48	6.19 ± 0.13	7.31 ± 0.71	71.42 ± 1.70
	Controls	5	48.40 ± 16.32	1388.60 ± 130.95	6.05 ± 0.33	6.62 ± 0.73	72.34 ± 2.23
	Total	12	47.83 ± 16.46	1409.65 ± 165.41	6.13 ± 0.23	7.03 ± 0.77	71.80 ± 1.90
	P	-	0.92	0.71	0.41	0.14	0.46
Total	Schizophrenia	19	57.21 ± 15.83	1337.08 ± 169.48	6.5 ± 0.34	6.77 ± 0.9	71.82 ± 3.75
	Controls	20	52.35 ± 15.62	1399.35 ± 170.67	6.45 ± 0.37	6.16 ± 1.16	72.82 ± 1.56
	Total	39	54.72 ± 15.71	1369.16 ± 170.38	6.48 ± 0.35	6.46 ± 1.07	72.33 ± 2.85
	P	-	0.34	0.30	0.66	0.07	0.29

6.2.8.1. Data normalisation

The *calcNormFactors* function was used to normalise the RNA-seq data for differences in library size between samples using the trimmed mean of M-values method (Robinson and Oshlack, 2010). The method finds a set of scaling factors for the library sizes that minimise the log fold-changes between the samples for most genes. These scaling factors are then multiplied by the original library sizes to calculate 'effective library sizes' that will be incorporated in the downstream analyses.

edgeR models the data using a negative binomial distribution. The Poisson distribution is the classical approach to model counts data; however, it does not take into account a gene-wise dispersion parameter, which is a characteristic of RNA-seq data. The negative binomial distribution is an extension to the Poisson distribution, which does take into account this over-dispersion (Hoffman, 2003). Correctly estimating the dispersion and incorporating this information in the differential expression testing model is crucial; underestimating the gene-wise dispersion will give rise to false positives whereas over-estimating it may lead to false negatives (Landau and Liu, 2013).

To estimate the dispersion on multifactorial models, the developers of *edgeR* suggest the use of the Cox-Reid profile-adjusted likelihood method (Cox and Reid, 1987). To implement this I used the *estimateDisp* function to estimate the gene-wise dispersion using sex, age, cohort and neuronal proportion estimates as co-variates. The neuronal proportion estimates were calculated using the *CETS* package (Guintivano et al., 2013) in R from the DNA methylation data from the same samples (details on neuronal proportion estimates calculation can be found in **Chapter 3 section 3.2.5**). For the four samples that did not have neuronal proportion estimates available I used the mean of the other samples estimates. **Figures 6.16, 6.17 and 6.18** show the \log_2 distributions of the raw counts, the counts after exclusion of genes (see **section 6.2.8**) and after data normalisation, respectively.

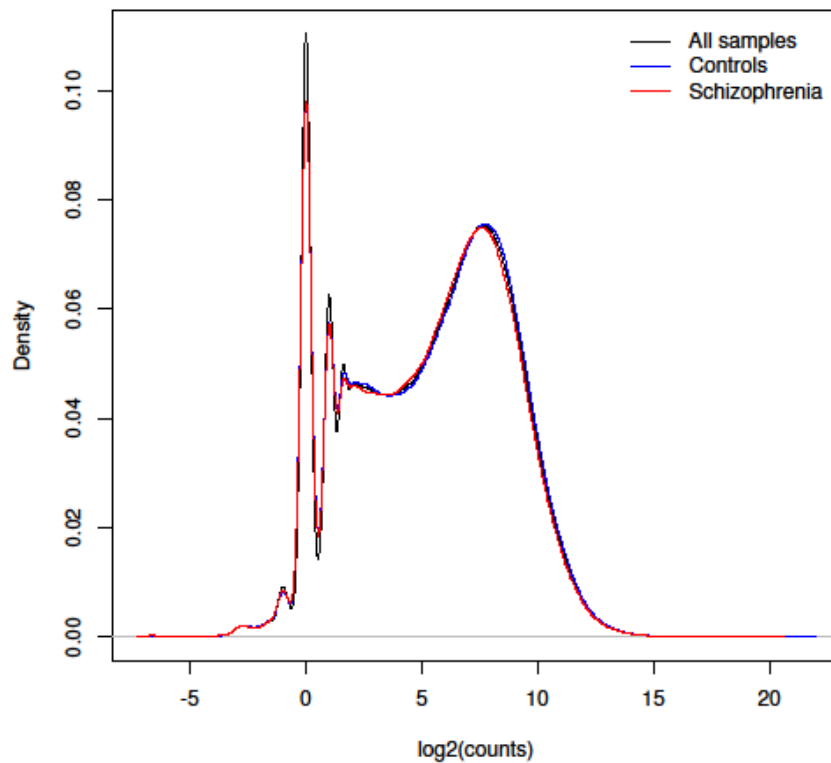


Figure 6.16. \log_2 distribution of the raw gene counts (counts per million) estimated by *RSEM* (Li and Dewey, 2011).

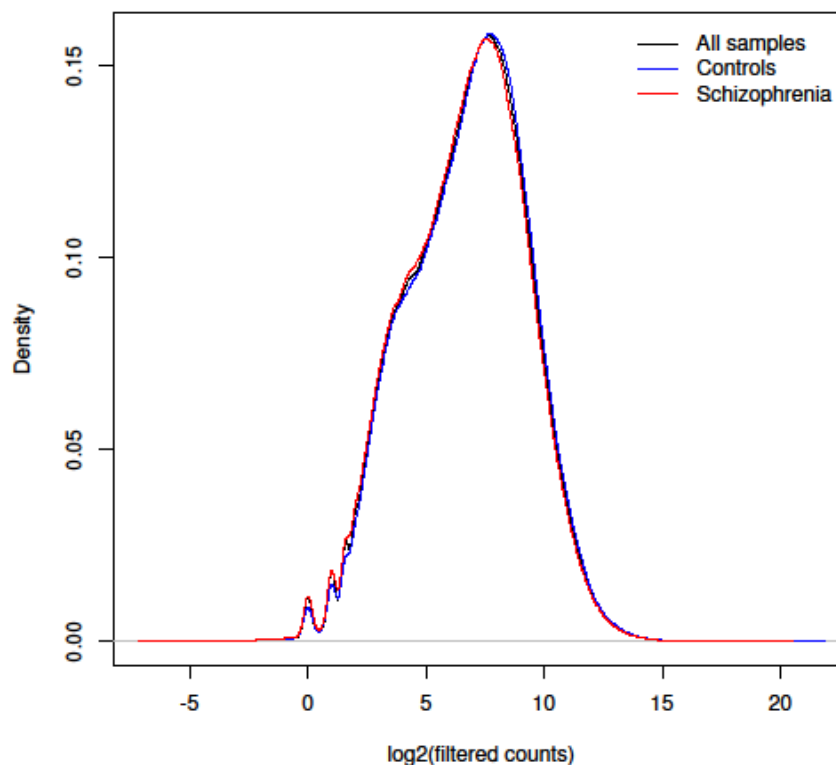


Figure 6.17. \log_2 distribution of the raw gene counts (counts per million) estimated by *RSEM* (Li and Dewey, 2011) after excluding ERCC transcripts, genes on the sex chromosomes, incorrect assembly sequences, allelic variants and low expressed genes.

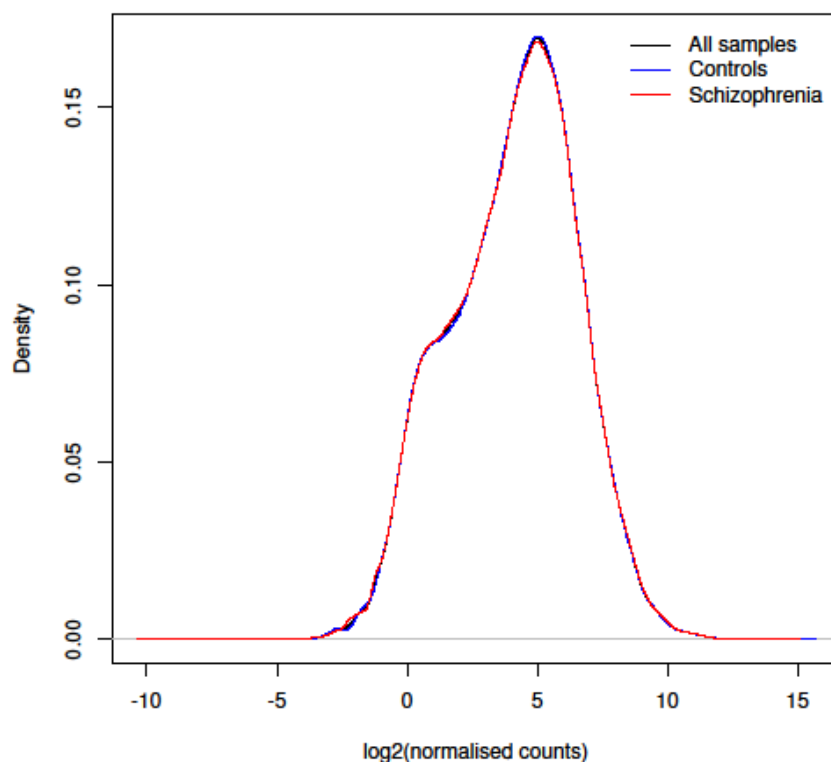


Figure 6.18. \log_2 distribution of the gene counts (counts per million) estimated by *RSEM* (Li and Dewey, 2011) after normalisation with *edgeR* (Robinson et al., 2010).

6.2.8.2. Differential expression analysis

To identify differentially expressed genes on a multifactorial dataset *edgeR* uses a generalised linear model (GLM) quasi-likelihood test (Robinson et al., 2010). To do this I used the *glmQLFit* function to fit a quasi-likelihood negative binomial generalized log-linear model and the *glmQLFTest* function to perform the quasi-likelihood F-test on the 16,920 genes that survived stringent QC steps (see **section 6.2**) including sex, age, cohort and neuronal proportion estimates as co-variates.

6.3. Results

6.3.1. Overview of the experimental strategy

In this Chapter I quantified PFC transcript levels in schizophrenia patients and non-psychiatric controls obtained from two brain banks. Details on the samples cohorts are presented on **Chapter 3 section 3.2.1**. In total, I extracted total RNA from the PFC of 39 schizophrenia patients and 45 controls. I chose 23 schizophrenia cases and 23 controls for RNA-seq analysis based on optimal RNA quality metrics (see **Table 6.2** and **section 6.2.1**). The cDNA libraries for each sample were prepared using the TruSeq Stranded Total RNA with RiboZero Gold Library Preparation LT kit (Illumina, San Diego, CA, USA) and RNA-sequencing was carried out on an Illumina HiSeq 2500 Sequencing System. After stringent QC filtering of the RNA-seq data, one sample was excluded based on spike-in QC measures and 6 other samples were excluded due to rRNA contamination (for sample exclusion criteria see **Table 6.2**). In total, RNA-seq data from 19 schizophrenia cases and 20 non-psychiatric controls were used for analyses. **Table 6.6** summarises the demographic information on the samples used in the analyses. I used a GLM quasi-likelihood F-test to identify DE genes between schizophrenia cases and controls and then I examined the overlap between significantly DE genes and DNA methylation results presented in **Chapter 3**. An overview of the analysis approach in this chapter is given in **Figure 6.19** and a representation on how this analysis integrates with the remaining chapters is given in **Chapter 1 Figure 1.8**.

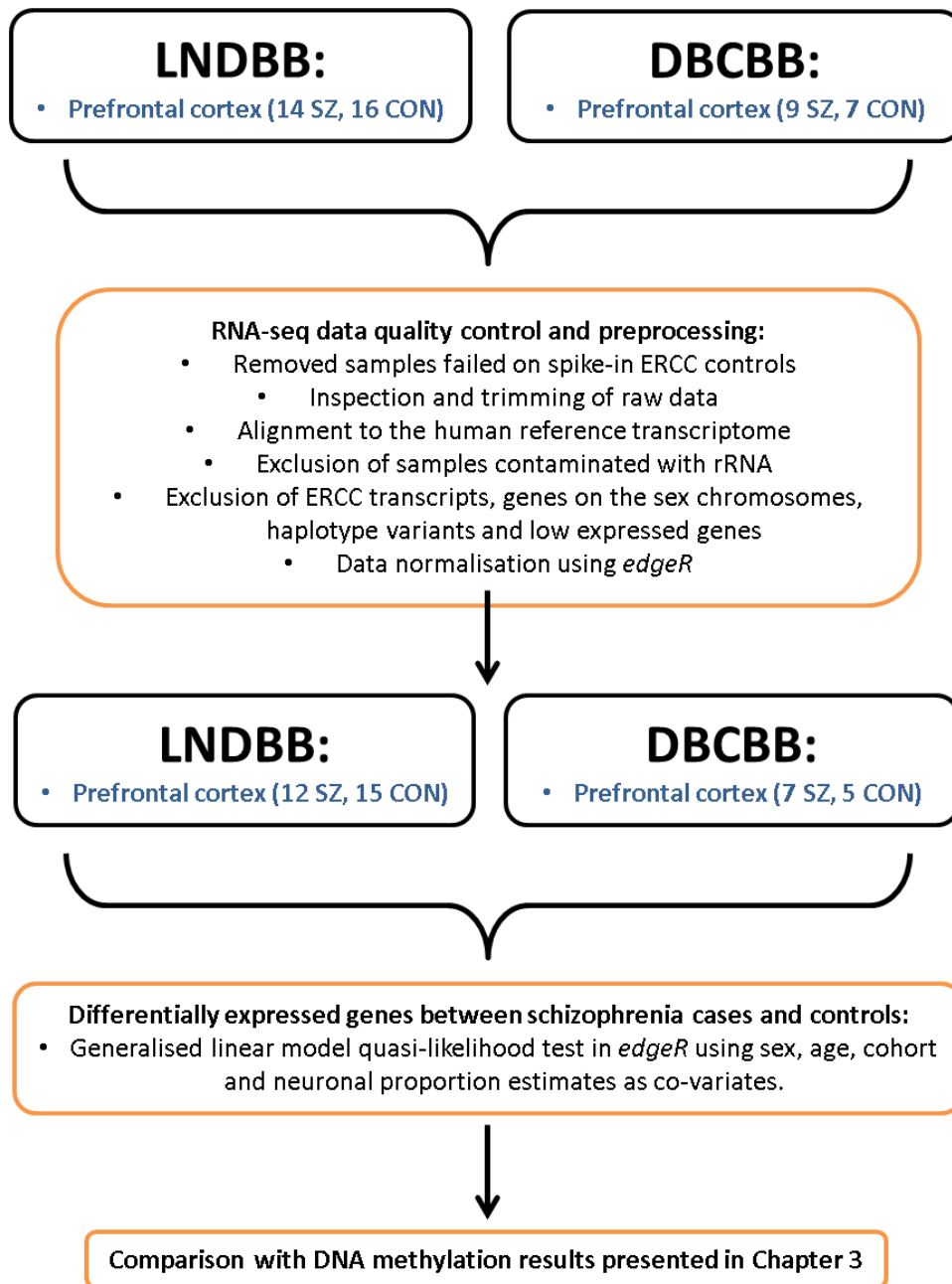


Figure 6.19. Overview of Chapter 6 experimental strategy.

6.3.2. Differentially expressed genes between schizophrenia patients and non-psychiatric controls

The primary aim of this chapter was to identify DE genes in the PFC of schizophrenia patients compared with controls. To do this I used a GLM quasi-likelihood F-test on the 16,920 out of 38,786 genes that survived stringent QC steps and were expressed (see **section 6.2.8**) using sex, age, cohort and neuronal proportion estimates as covariates. **Figure 6.20** shows the quantile-quantile (QQ) plot for the analysis, which shows evidence of under-inflation ($\lambda = 0.69$) and suggests the analysis was moderately under-powered. **Table 6.7** shows the results for the fifty top ranked schizophrenia associated DE genes. **Figure 6.21** presents the \log_2 fold-change in expression (x-axis) versus the $-\log_{10}$ of the P -values for all expressed genes, with the fifty top ranked genes coloured in red.

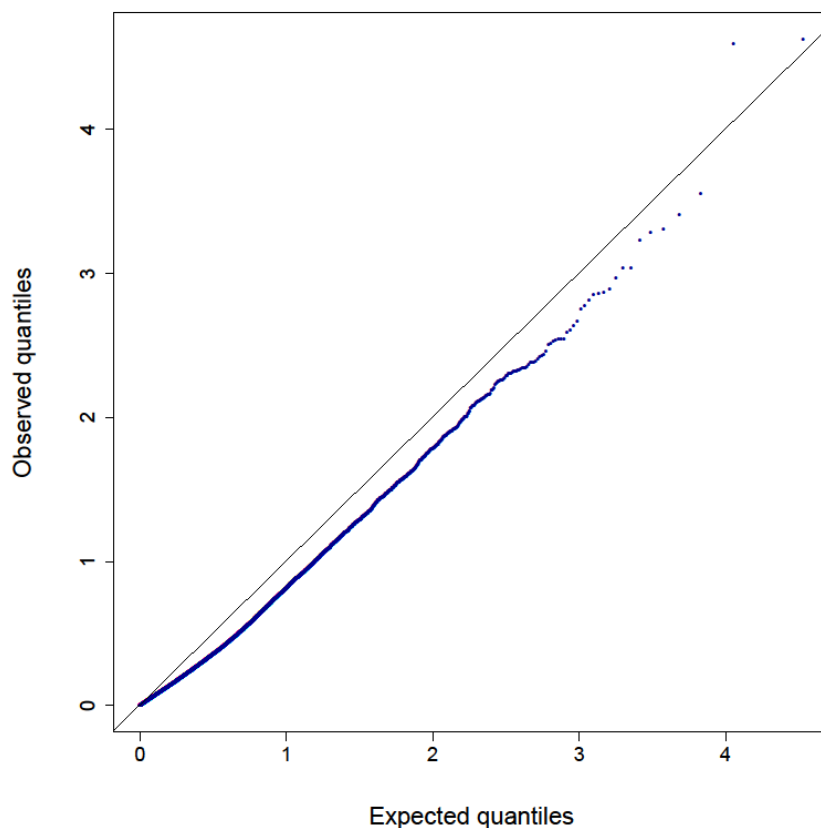


Figure 6.20. Quantile-quantile plot for the differential expression analysis. Shown are the expected (x-axis) and observed (y-axis) quantiles observed in the differential expression analysis of the prefrontal cortex of both the MRC London Neurodegenerative Diseases Brain Bank and Douglas-Bell Canada Brain Bank. $\lambda = 0.69$.

Table 6.7. Top ranked schizophrenia-associated differently expressed genes identified in the prefrontal cortex. Listed are the Ensembl gene IDs (Flicek et al., 2014), the corresponding gene symbols from the HUGO Gene Nomenclature Committee (HGNC) (European Bioinformatics Institute, 2016), the genomic coordinates, the log₂ fold-change (FC), the log₂ counts per million (CPM) across all samples and the *P*-value of the analysis.

Ensembl gene ID	HGNC gene symbol	Genomic position (GRCh38)	log ₂ FC	log ₂ CPM	<i>P</i> -value
ENSG00000064886	<i>CHI3L2</i>	chr1:111200771-111243440	-3.03	1.25	2.38E-05
ENSG00000255769	<i>GOLGA2P10</i>	chr15:82472993-82513950	1.97	0.68	2.57E-05
ENSG00000129951	<i>PLPPR3</i>	chr19:812488-821977	0.44	3.90	2.81E-04
ENSG00000141505	<i>ASGR1</i>	chr17:7173431-7179564	0.52	2.44	3.91E-04
ENSG00000273259		chr14:94592058-94624646	-3.32	4.80	4.93E-04
ENSG00000026508	<i>CD44</i>	chr11:35138870-35232402	-1.77	4.16	5.16E-04
ENSG00000249337	<i>SNX18P25</i>	chr4:49588772-49589529	0.86	0.94	5.84E-04
ENSG00000163638	<i>ADAMTS9</i>	chr3:64515654-64688000	-1.17	4.66	9.17E-04
ENSG00000230528	<i>NOS2P3</i>	chr17:20436337-20447249	1.13	0.56	9.25E-04
ENSG00000165507	<i>C10orf10</i>	chr10:44970981-44978810	-1.01	5.01	1.09E-03
ENSG00000221937	<i>TAS2R40</i>	chr7:143222037-143223079	-1.26	0.45	1.29E-03
ENSG00000141526	<i>SLC16A3</i>	chr17:82228397-82261129	-0.54	3.03	1.35E-03
ENSG00000197993	<i>KEL</i>	chr7:142941114-142962681	-1.15	0.84	1.38E-03
ENSG00000182240	<i>BACE2</i>	chr21:41167801-41282518	-0.49	3.62	1.40E-03
ENSG00000100225	<i>FBXO7</i>	chr22:32474676-32498829	-0.36	6.21	1.55E-03
ENSG00000205129	<i>C4orf47</i>	chr4:185426249-185449826	0.75	0.21	1.68E-03
ENSG00000204655	<i>MOG</i>	chr6:29656981-29672372	-1.89	3.94	1.77E-03
ENSG00000128918	<i>ALDH1A2</i>	chr15:57953424-58497866	-0.51	1.96	2.16E-03
ENSG00000013364	<i>MVP</i>	chr16:29820394-29848039	-0.59	4.59	2.29E-03
ENSG00000179588	<i>ZFPM1</i>	chr16:88453317-88537016	0.46	2.49	2.49E-03
ENSG00000141510	<i>TP53</i>	chr17:7661779-7687550	-0.53	2.60	2.59E-03
ENSG00000167553	<i>TUBA1C</i>	chr12:49188736-49274603	-0.74	2.23	2.84E-03
ENSG00000230549	<i>USP17L1</i>	chr8:7332387-7333979	-0.84	1.17	2.85E-03
ENSG00000196136	<i>SERPINA3</i>	chr14:94612384-94624055	-2.21	3.82	2.86E-03
ENSG00000186326	<i>RGS9BP</i>	chr19:32675407-32678300	0.76	0.70	2.89E-03
ENSG00000136098	<i>NEK3</i>	chr13:52132639-52159861	-0.68	3.50	2.94E-03
ENSG00000170667	<i>RASA4B</i>	chr7:102482445-102517781	0.44	4.40	3.06E-03
ENSG00000139926	<i>FRMD6</i>	chr14:51489100-51730727	0.36	4.53	3.11E-03
ENSG00000106689	<i>LHX2</i>	chr9:124001670-124033301	0.37	4.87	3.49E-03
ENSG00000173110	<i>HSPA6</i>	chr1:161524540-161526910	2.94	3.07	3.66E-03
ENSG00000105808	<i>RASA4</i>	chr7:102573807-102616757	0.33	5.84	3.75E-03
ENSG00000114737	<i>CISH</i>	chr3:50606490-50611831	-0.90	0.17	3.77E-03
ENSG00000013588	<i>GPRC5A</i>	chr12:12890782-12917937	-0.81	0.81	3.92E-03
ENSG00000156253	<i>RWDD2B</i>	chr21:29004384-29019378	-0.38	3.68	4.08E-03
ENSG00000138621	<i>PPCDC</i>	chr15:75023555-75117462	-0.42	1.99	4.13E-03
ENSG00000118785	<i>SPP1</i>	chr4:87975650-87983426	-1.13	6.61	4.13E-03
ENSG00000259271	<i>ANKRD62P1</i>	chr22:16671090-16679493	0.82	0.44	4.18E-03
ENSG00000087510	<i>TFAP2C</i>	chr20:56629302-56639283	1.03	-0.11	4.28E-03
ENSG00000135245	<i>HILPDA</i>	chr7:128455849-128458418	-0.98	3.81	4.49E-03

ENSG00000266714	<i>MYO15B</i>	chr17:75588058-75626501	-0.45	4.99	4.51E-03
ENSG00000198959	<i>TGM2</i>	chr20:38127387-38166578	-0.80	4.84	4.52E-03
ENSG00000164687	<i>FABP5</i>	chr8:81280363-81284777	-0.47	3.74	4.54E-03
ENSG00000130943	<i>PKDREJ</i>	chr22:46255663-46263355	-0.78	1.19	4.62E-03
ENSG00000227057	<i>WDR46</i>	chr6:33279108-33289527	1.85	1.28	4.67E-03
ENSG00000224831		chr3:149982181-149983308	1.07	0.11	4.72E-03
ENSG00000134817	<i>APLNR</i>	chr11:57233577-57237314	-0.99	4.30	4.74E-03
ENSG00000198944	<i>SOWAHA</i>	chr5:132813587-132816797	0.38	6.25	4.76E-03
ENSG00000148926	<i>ADM</i>	chr11:10304680-10307397	-0.99	2.07	4.81E-03
ENSG00000270670		chr10:89837612-89839334	-0.62	1.23	4.88E-03
ENSG00000203710	<i>CR1</i>	chr1:207496147-207640647	-0.85	1.53	4.91E-03

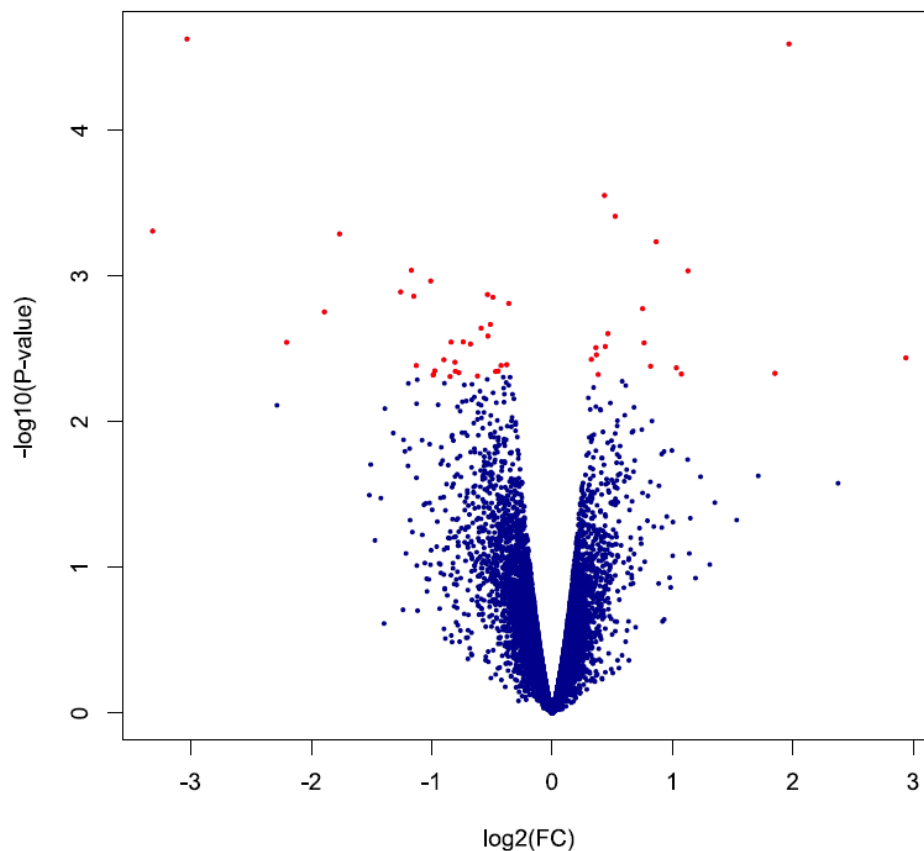


Figure 6.21. Volcano plot for the differential expression analysis. Shown are the \log_2 fold-change (FC; x-axis) versus the $-\log_{10}$ P -values (y-axis) from the differential expression analysis on all expressed genes in the PFC of both the MRC London Neurodegenerative Diseases Brain Bank and Douglas-Bell Canada Brain Bank. The fifty top ranked differentially expressed genes are coloured in red.

Figure 6.22 presents the \log_2 FC for the fifty top ranked DE genes presented in **Table 6.7** and **Figures 6.23** and **6.24** show the CPM for schizophrenia cases and controls for the same genes. Since the level of expression varies considerably across all genes I separated the genes with less than 25 CPM across all samples (**Figure 6.23**) and more than 25 CPM across all samples (**Figure 6.24**).

The top schizophrenia-associated DE gene is *chitinase 3-like-2 (CHI3L2)* which encodes a protein involved in cartilage biogenesis. Although none of the DE genes reached a Bonferroni corrected threshold for the 16,920 genes used in the analysis ($P = 2.96E-06$), two of the top ranked DE genes have been previously found to be differently expressed in schizophrenia patients:

- The myelin oligodendrocyte glycoprotein (*MOG*) gene was down-regulated in the PFC of schizophrenia patients (\log_2 FC = -1.89, $P = 1.77E-03$). This gene encodes a protein expressed on the oligodendrocyte cell membrane and the surface of myelin sheaths. Tkachev and colleagues have also found this gene to be down-regulated in the PFC of schizophrenia patients using gene expression microarrays (FC = -2.91; $P = 7.00E-03$) and quantitative PCR (FC = -2.58; $P = 3.90E-03$) (Tkachev et al., 2003). This gene is located within the major histocompatibility complex (MHC) on chromosome 6. Genetic variants in the MHC *locus* have been strongly linked to schizophrenia GWAS studies (International Schizophrenia et al., 2009, Schizophrenia Working Group of the Psychiatric Genomics, 2014), as discussed in **Chapter 4 section 4.3.3**.

- The serpin family A member 3 (*SERPINA3*) gene was down-regulated in schizophrenia patients (\log_2 FC = -2.21, $P = 2.86E-03$). This gene encodes a plasma protease inhibitor. Its physiological function is unclear although is considered to be an acute-phase inflammatory protein (Horvath and Mirnics, 2014). This gene has been found to be up-regulated in the PFC (Brodmann area (BA) 9) (Arion et al., 2007), dorsolateral PFC (BA 46) (Fillman et al., 2013) and in the middle frontal gyrus (Fillman et al., 2014) of schizophrenia patients. Dysregulation in this protein has also been widely implicated in Alzheimer's disease (Baker et al., 2007).

Additional novel schizophrenia-associated DE genes identified in this study are of potential interest in the context of schizophrenia etiology given their known role in neurobiological function:

- Phospholipid phosphatase related 3 (*PLPPR3*) was up-regulated in the PFC of schizophrenia patients compared to controls (\log_2 FC = 0.44, $P = 2.81E-04$). This gene encodes a membrane protein belonging to the lipid phosphate phosphatase (LPP) family of proteins, which play a role in cell migration and axonal growth in the developing neurons (Brauer et al., 2003).

- *CD44* was down-regulated in schizophrenia patients (\log_2 FC = -1.77, $P = 5.16E-04$). The protein encoded by the *CD44* gene is a cell-surface glycoprotein involved in cell-cell interactions. This gene encodes 38 splice variants (Flicek et al., 2014). Some of the CD44 isoforms have been implicated in the activation of T lymphocytes (Goodison et al., 1999), which play central role in cell-mediated immunity. This is interesting given the potential importance of the immune system in schizophrenia etiology already discussed in **Chapter 1 section 1.1.6**.

- The F-box protein 7 (*FBX07*) also known as Parkinson disease 15 (*PARK15*) was also down-regulated in schizophrenia patients (\log_2 FC = -0.36, $P = 1.55E-03$). Mutations in this gene have been implicated in early-onset Parkinson's disease (Deng et al., 2013), a degenerative disorder of the central nervous system.

- Two genes encoding for members of the GAP1 family of GTPase-activating proteins (*RASA4* and *RASA4B*) were up-regulated in the schizophrenia patients (\log_2 FC = 0.33, $P = 3.75E-03$ and \log_2 FC = 0.44, $P = 3.06E-03$, respectively). This is interesting because a 450K probe (cg24803255) within another gene from this family (*RASA3*) was hypomethylated in the PFC in our DNA methylation analysis (see **Chapter 3 section 3.3.7**). Together these observations suggest that this family of proteins might play a role in schizophrenia.

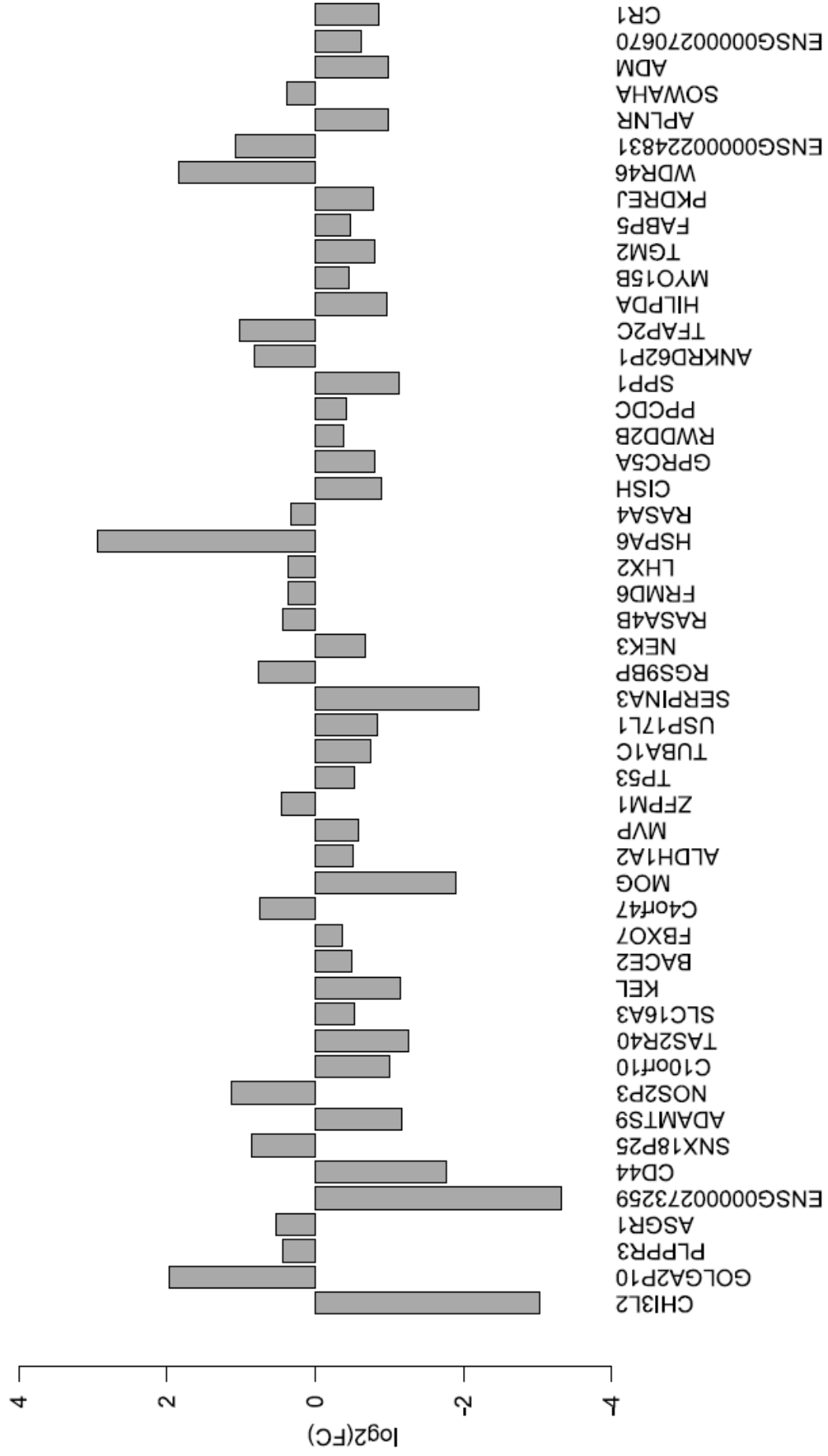


Figure 6.22. Log₂ fold-change (FC) (y-axis) of the fifty top ranked differentially expressed genes in the prefrontal cortex.

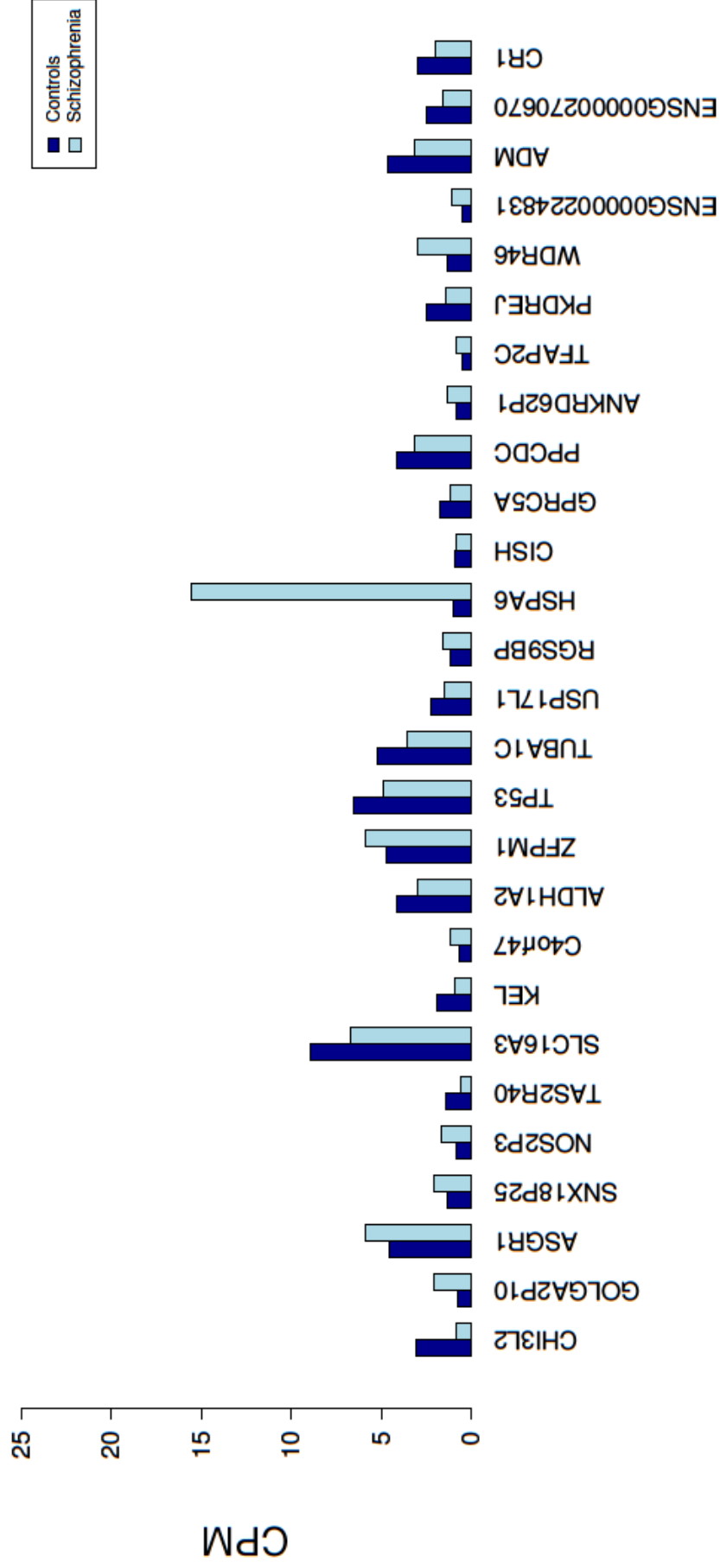


Figure 6.23. Counts per million (CPM) (y-axis) of the top ranked differently expressed genes in the prefrontal cortex with less than 25 CPM. The CPM of the schizophrenia patients (light blue) in comparison with the CPM of the non-psychiatric controls (dark blue) is illustrated.

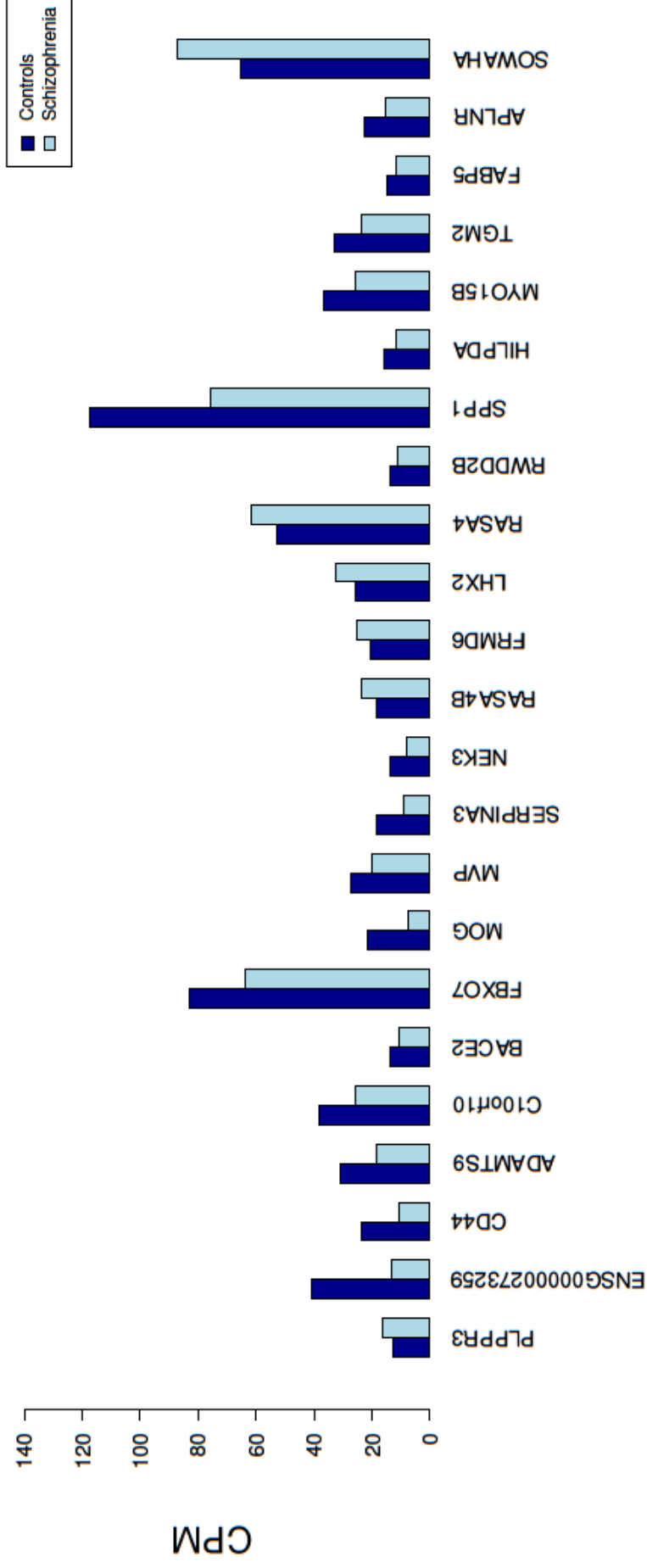


Figure 6.24. Counts per million (CPM) (y-axis) of the top ranked differently expressed genes in the prefrontal cortex with more than 25 CPM. Shown are the CPM of the schizophrenia patients (light blue) in comparison with the CPM of the non-psychiatric controls (dark blue).

6.3.3. Comparison with DNA methylation results

In **Chapter 3** I identified DNA methylation changes associated with schizophrenia using post-mortem tissue from schizophrenia patients and non-psychiatric controls. In this section I explore the overlap between the results from the DNA methylation analyses and the results from the gene expression analyses. Of note, the human genome version used to annotate the 450K array methylation probes was hg19/GRCh37, whereas in the RNA-seq analysis I used the GRCh38 human genome version for annotation. For this reason I compare the RNA-seq and the DNA methylation results based on gene symbols and not genomic location to avoid confusion.

6.3.3.1. DNA methylation probes overlapping DE genes

First I investigated 450K array probes annotated to schizophrenia-associated DE genes identified in **section 6.3.2**. **Figure 6.25** shows a diagram of the approach utilised. I initially investigated 450K probes that were annotated to schizophrenia-associated DE genes using the Illumina annotation (**Figure 6.25 A**). **Table 6.8** presents the selection of these probes that are nominally associated with schizophrenia ($P < 0.05$) in the PFC.

Next, I investigated the probes in the vicinity to the TSS of the schizophrenia-associated DE genes (**Figure 6.25 B**). **Table 6.9** shows probes which are nominally associated with schizophrenia ($P < 0.05$) and whose closest TSS is a DE gene. Fourteen of the DE genes show evidence of nominal schizophrenia-associated DMPs in their vicinity.

Finally, I identified probes nominally associated with schizophrenia that are annotated to a DE gene using the Genomic Regions Enrichment of Annotations Tool (GREAT) (McLean et al., 2010) (**Figure 6.25 C**), instead of the Illumina annotation. GREAT associates genomic regions with genes by defining a *cis*-regulatory region for each gene in the genome. Identifying 450K probes of interest using GREAT annotation can provide additional information on whether these probes lie within putative regulatory regions mapped to DE genes. **Table 6.19** shows schizophrenia nominally-associated DMPs that are annotated to DE genes using the GREAT annotation.

Several of the schizophrenia-associated DE genes have several nominally-associated DMPs annotated to them. For example, the *ZFPM1* gene is annotated to 14 DMPs (12 Illumina annotation and 2 GREAT annotation), the *WDR46* gene is associated with 8 DMPs (Illumina annotation) and the *SLC16A3* gene is annotated to 10 DMPs (7 Illumina annotation and 3 GREAT annotation) and has 2 other DMPs annotated to its TSS. Furthermore, the *CD44* gene is annotated to 9 DMPs (7 Illumina annotation and 2 GREAT annotation) and has 2 other DMPs annotated to its TSS. This gene plays central role in cell-mediated immunity (Goodison et al., 1999) and its potential relevance in the context of schizophrenia has already been discussed in **Section 6.3.2**.

Interestingly, these multiple DMPs per DE gene are not clustered in known regions of regulation (e.g. promoters) but rather are located throughout the gene (e.g. gene body, first exon, etc.). A possible explanation is that the observed methylomic variation in intergenic regions might have a function on regulating the expression of the gene. A potential mechanism is that these events are modulating alternative splicing of these transcripts (see **section 6.4.1** for a more detail discussion).

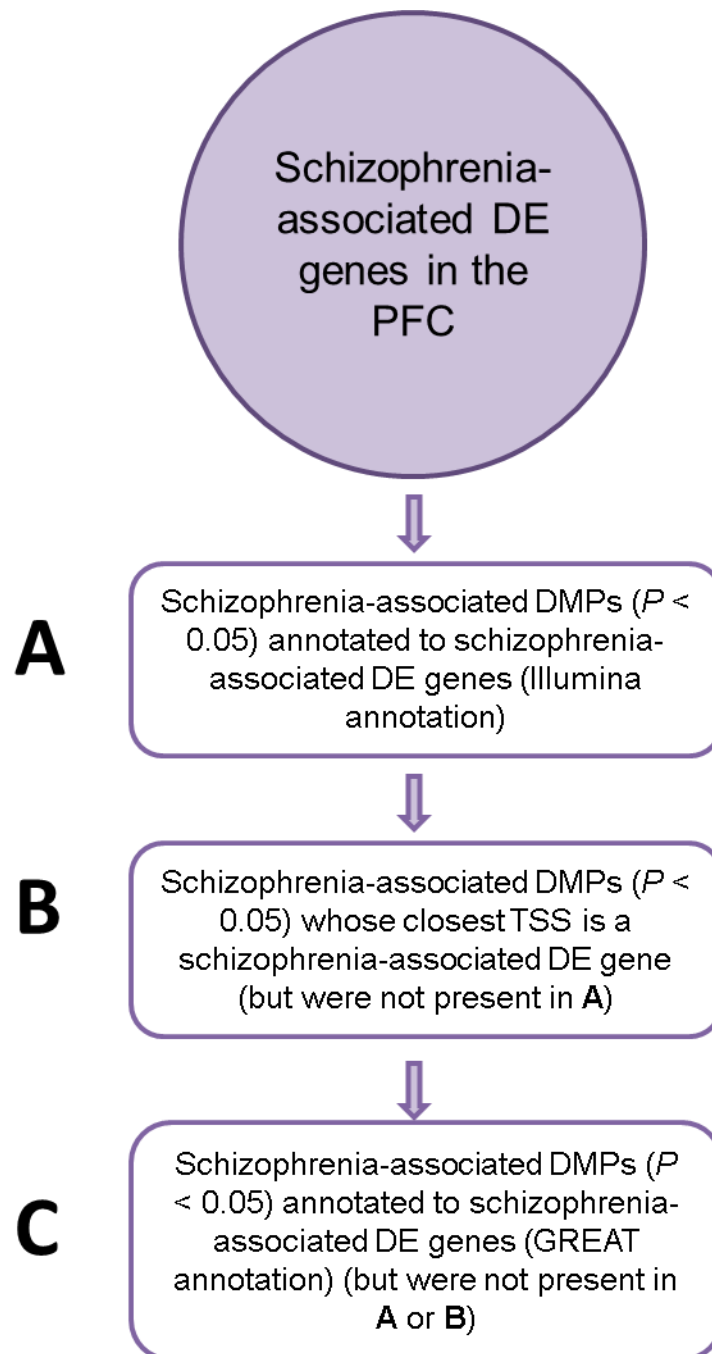


Figure 6.25. Methodological approach to investigate DNA methylation probes overlapping differentially expressed genes in schizophrenia.

Table 6.8. 450K array probes nominally associated with schizophrenia in the prefrontal cortex which are annotated to the differentially expressed genes using the Illumina gene annotation. Shown is the total number of probes annotated to the gene that went into the prefrontal cortex schizophrenia EWAS and how many of those are differentially methylated probes (DMPs) with a *P*-value < 0.05.

Gene expression				DNA methylation			
Ensembl gene ID	Gene symbol	log ₂ FC	<i>P</i> -value	Probes annotated to gene	DMPs <i>P</i> < 0.05	450K Probe ID	Gene region
ENSG00000064886	<i>CH13L2</i>	-3.03	2.38E-05	12	1	cg02590572	Body
ENSG00000141505	<i>ASGR1</i>	0.52	3.91E-04	20	2	cg05331340	Body
						cg20752878	TSS1500
						cg23186333	Body
						cg09077672	5'UTR
						cg04171808	Body
ENSG0000026508	<i>CD44</i>	-1.77	5.16E-04	29	7	cg25096745	TSS1500
						cg01663768	Body
						cg18652941	1stExon
						cg16344511	Body
ENSG00000163638	<i>ADAMTS9</i>	-1.17	9.17E-04	38	2	cg21938436	TSS200
						cg04421973	Body
ENSG00000165507	<i>C10orf10</i>	-1.01	1.09E-03	8	1	cg26002437	Body
						cg15437741	Body; 5'UTR
						cg20531020	5'UTR
						cg18345635	Body
ENSG00000141526	<i>SLC16A3</i>	-0.54	1.35E-03	37	7	cg17932802	TSS1500
						cg08429256	Body
						cg07466788	Body
						cg18083597	1stExon
ENSG00000197993	<i>KEL</i>	-1.15	1.38E-03	9	2	cg26233832	3'UTR; Body
						cg21824300	TSS200
ENSG00000182240	<i>BACE2</i>	-0.49	1.40E-03	22	2	cg08826226	Body
						cg24973205	TSS1500

ENSG00000100225	FBX07	-0.36	1.55E-03	16	3	cg07911523	-0.44	9.19E-03	Body
						cg25267957	-0.32	0.04	Body
						cg07071881	-0.50	0.04	TSS1500
ENSG00000204655	MOG	-1.89	1.77E-03	50	3	cg13682912	-2.65	7.93E-04	Body
						cg05913325	2.31	9.50E-03	Body
						cg02589899	-2.67	0.02	1stExon; 5'UTR; TSS1500
ENSG00000128918	ALDH1A2	-0.51	2.16E-03	18	2	cg07721203	0.38	2.66E-03	Body
						cg14805347	-0.44	0.04	Body
ENSG00000013364	MVP	-0.59	2.29E-03	24	2	cg15777760	2.19	1.90E-03	Body
						cg03849728	1.24	3.63E-03	TSS200; 5'UTR
						cg09535526	1.80	3.31E-04	Body
						cg11846580	-2.44	1.72E-03	TSS1500
						cg08705406	-2.26	6.75E-03	3'UTR
						cg06359968	1.99	8.28E-03	TSS200
						cg06647693	-2.22	0.02	TSS200
ENSG00000179588	ZFPM1	0.46	2.49E-03	112	12	cg05854207	1.09	0.02	1stExon
						cg26568171	1.12	0.03	5'UTR
						cg00986350	1.44	0.03	5'UTR
						cg00473769	1.67	0.03	TSS200
						cg22791932	1.09	0.04	Body
						cg04247152	-2.62	0.04	TSS200
						cg08374494	1.81	0.05	3'UTR; Body
ENSG00000141510	TP53	-0.53	2.59E-03	39	3	cg17461511	-0.57	0.01	3'UTR; Body
						cg06365412	0.85	0.02	TSS200; TSS1500
ENSG00000167553	TUBA1C	-0.74	2.84E-03	15	1	cg15929573	0.76	0.02	TSS200
ENSG00000196136	SERPINA3	-2.21	2.86E-03	5	1	cg08057786	2.03	0.05	Body
ENSG00000186326	RG9BP	0.76	2.89E-03	18	3	cg08297094	-0.72	5.27E-03	3'UTR; Body
						cg24703125	-0.19	9.06E-03	TSS1500
						cg04084088	-1.35	0.01	Body
ENSG00000139926	FRMD6	0.36	3.11E-03	35	4	cg15484023	2.02	5.79E-04	Body
						cg19514905	1.10	9.37E-03	Body
						cg18894781	0.64	0.03	5'UTR
						cg15998247	1.79	0.05	TSS200
ENSG00000173110	HSPA6	2.94	3.66E-03	3	1	cg23691642	-2.43	0.05	Body
ENSG00000114737	CISH	-0.90	3.77E-03	17	1	cg21585138	0.30	0.04	Body

ENSG00000156253	RWDD2B	-0.38	4.08E-03	12	3	cg20220242	3.15	0.02	Body
						cg10822339	0.64	0.04	TSS1500
						cg18001427	2.09	0.04	TSS200; TSS1500
ENSG00000138621	PPCDC	-0.42	4.13E-03	15	2	cg19697512	0.95	0.01	3'UTR; 1stExon
						cg01916610	0.66	0.04	Body
ENSG00000087510	TFAP2C	1.03	4.28E-03	15	1	cg05013064	-0.33	0.01	3'UTR
ENSG00000266714	MYO15B	-0.45	4.51E-03	21	1	cg12184886	-1.70	0.01	TSS1500
ENSG00000198959	TGM2	-0.80	4.52E-03	17	1	cg08545268	-1.25	0.04	Body
ENSG00000130943	PKDREJ	-0.78	4.62E-03	11	2	cg02775765	1.49	0.04	TSS200
						cg08056211	0.87	0.04	Body
						cg21699833	1.09	0.02	TSS1500
						cg01371207	-0.42	0.02	TSS1500
						cg02845534	-1.34	0.03	Body
						cg00578240	-0.31	0.04	TSS200
ENSG00000227057	WDR46	1.85	4.67E-03	108	8	cg04276715	0.58	0.04	TSS1500
						cg11400761	-1.04	0.04	Body
						cg18707500	-0.60	0.04	TSS1500
						cg12745400	-0.59	0.04	3'UTR
ENSG00000203710	CR1	-0.85	4.91E-03	5	1	cg25029035	1.12	0.02	TSS1500; Body

Table 6.9. 450K array probes nominally associated with schizophrenia in the prefrontal cortex whose closest transcription start site is a schizophrenia-associated differentially expressed gene.

Gene expression				DNA methylation						
Ensembl gene ID	Gene symbol	log ₂ FC	P-value	450K Probe ID	DNA methylation difference (%)	P-value	Gene annotation	Gene region	Closest gene TSS	Distance to closest TSS (bp)
ENSG00000064886	CHI3L2	-3.03	2.38E-05	cg15995265	1.16	0.03			CHI3L2	-5423
ENSG00000026508	CD44	-1.77	5.16E-04	cg20740024	-2.09	0.01	SLC1A2	Body	CD44	92231
ENSG00000163638	ADAMTS9	-1.17	9.17E-04	cg25475999	1.65	0.01	SLC1A2	3'UTR	CD44	70665
ENSG00000141526	SLC16A3	-0.54	1.35E-03	cg19846707	1.83	5.83E-03			ADAMTS9	-6289
ENSG00000204655	MOG	-1.89	1.77E-03	cg06682330	-1.47	0.01			SLC16A3	6985
ENSG00000167553	TUBA1C	-0.74	2.84E-03	cg14517001	0.89	0.02			SLC16A3	-6350
ENSG00000139926	FRMD6	0.36	3.11E-03	cg00660167	-1.52	0.05			SLC16A3	7325
ENSG00000106689	LHX2	0.37	3.49E-03	cg12772565	-1.52	0.03			MOG	-6442
ENSG00000156253	RWDD2B	-0.38	4.08E-03	cg06106839	0.87	0.03			TUBA1C	-788
ENSG00000087510	TFAP2C	1.03	4.28E-03	cg05555396	1.65	0.03			TUBA1C	-630
ENSG00000135245	HILPDA	-0.98	4.49E-03	cg14286320	-1.48	0.04			FRMD6	-58222
ENSG00000266714	MYO15B	-0.45	4.51E-03	cg13794404	-1.83	5.29E-03			LHX2	43071
ENSG00000198944	SOWAHA	0.38	4.76E-03	cg14729175	1.09	0.02			RWDD2B	-1624
ENSG00000203710	CR1	-0.85	4.91E-03	cg01209909	-1.19	6.44E-03			TFAP2C	294252
				cg04773827	-1.08	0.04			TFAP2C	-2702
				cg11868041	1.49	0.05			TFAP2C	297426
				cg03955175	0.35	7.24E-03	C7orf68	1stExon; 5'UTR	HILPDA	94
				cg24427302	1.04	0.02			MYO15B	-3196
				cg02699218	-2.08	0.02	ANKRD43	1stExon	SOWAHA	1096
				cg11096629	-0.46	0.03	ANKRD43	TSS200	SOWAHA	-84
				cg07876882	-1.00	0.04	ANKRD43	3'UTR; 1stExon	SOWAHA	2015
				cg10113157	1.43	0.05			CR1	-3125

Table 6.10. 450K array probes nominally associated with schizophrenia in the prefrontal cortex that are annotated to the differentially expressed genes using the GREAT gene annotation (McLean et al., 2010).

Gene expression				DNA methylation			
Ensembl gene ID	Gene symbol	log ₂ FC	P-value	450K Probe ID	DNA methylation difference (%)	P-value	Illumina annotation GREAT annotation GREAT distance
ENSG00000064886	CHI3L2	-3.03	2.38E-05	cg12398575	1.12	4.45E-03	LOC149620 CHI3L2 54817
				cg09138965	1.83	0.01	LOC149620 CHI3L2 52067
				cg19268695	1.32	0.01	DENND2D CHI3L2 -26869
				cg20970369	-1.64	0.03	DENND2D CHI3L2 -26172
ENSG00000141505	ASGR1	0.52	3.91E-04	cg05148465	1.41	5.64E-03	ASGR1 48753
ENSG0000026508	CD44	-1.77	5.16E-04	cg25961618	1.43	0.04	SLC1A2 CD44 200115
				cg21456897	-1.85	1.53E-03	ADAMTS9 419561
				cg11610350	-0.73	0.01	ADAMTS9 419659
				cg11236526	0.38	0.04	ADAMTS9 242424
				cg01165355	-1.62	0.04	ADAMTS9 448256
ENSG00000141526	SLC16A3	-0.54	1.35E-03	cg01048272	2.97	2.93E-03	CCDC57 SLC16A3 -16403
				cg26105045	-1.89	7.90E-03	CCDC57 SLC16A3 -57159
				cg26093898	1.33	0.02	CCDC57 SLC16A3 -48904
ENSG00000197993	KEL	-1.15	1.38E-03	cg214443699	1.78	0.03	C7orf34 KEL 21566
ENSG00000182240	BACE2	-0.49	1.40E-03	cg16246713	-2.81	1.35E-03	C21orf130 BACE2 -19718
ENSG00000100225	FBXO7	-0.36	1.55E-03	cg20476019	1.51	0.01	SYN3 FBXO7 287175
ENSG00000013364	MVP	-0.59	2.29E-03	cg01814495	1.00	0.05	CDIPT MVP 38594
ENSG00000179588	ZFPM1	0.46	2.49E-03	cg00315239	-1.80	0.03	ZFPM1 105088
				cg01783841	-1.17	0.05	ZFPM1 108761
ENSG00000139926	FRMD6	0.36	3.11E-03	cg16685608	2.20	0.02	FRMD6 93004
ENSG00000138621	PPDCDC	-0.42	4.13E-03	cg17125990	1.58	5.75E-03	PPDCDC 154851
ENSG00000087510	TFAP2C	1.03	4.28E-03	cg13236649	-1.79	0.04	BMP7 TFAP2C 630663
				cg27565555	-0.60	0.05	BMP7 TFAP2C 635306
ENSG00000266714	MYO15B	-0.45	4.51E-03	cg10053073	1.45	0.01	RECQL5 MYO15B 14128

6.3.3.2. Expressed genes overlapping differently methylated probes and regions

I was also interested in investigating whether those genes annotated to the top ranked DMPs identified in the PFC and differently methylated regions (DMRs) were also differently expressed. Because the DMRs identified in any of the four brain regions were generally characterised by consistent DNA methylation effects across the other brain regions (see **Chapter 3 Figure 3.41**) I decided to investigate all the DMRs identified in any of the brain regions. **Figure 6.26** presents a diagram of the approach utilised.

First I identified expressed genes annotated to DMRs identified in any of the four brain regions (using both Illumina and GREAT annotation). **Chapter 3 section 3.3.6** presents the DMRs identified. **Table 6.11** shows the \log_2 fold-change and *P*-values of the schizophrenia differential expression analysis for the expressed genes annotated to the DMRs (**Table 3.16**).

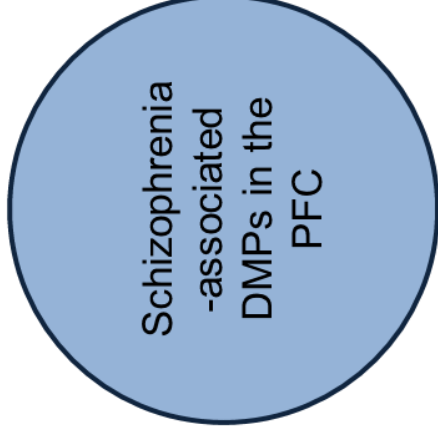
Next I identified expressed genes annotated to the fifty top ranked schizophrenia-associated DMPs identified in the PFC (using both Illumina and GREAT annotation). **Chapter 3 section 3.3.3** presents the DMPs identified. **Table 6.12** shows the \log_2 fold-change and *P*-values of the schizophrenia differential expression analysis for the genes annotated to the DMPs (**Table 3.5**). Surprisingly, none of the genes annotated to DMRs or DMPs were differentially expressed in the PFC of schizophrenia patients, suggesting that the DNA methylation changes observed do not appear to have a direct, *cis*-effect on gene expression.

A



Expressed genes annotated to the DMR (Illumina or GREAT annotation)

B



Expressed genes annotated to the DMP (Illumina annotation)



Expressed genes annotated to the DMP (GREAT annotation)

Figure. 6.26. Methodological approach to investigate expressed genes overlapping schizophrenia-associated differentially methylated regions (DMRs) (A) and top ranked differentially methylated positions (DMPs) in the PFC (B). DMPs and DMRs identified in Chapter 3 sections 3.3.3 and 3.3.6, respectively.

Table 6.11. Results of the schizophrenia differential expression analysis for the expressed genes annotated to the differentially methylated regions (DMRs) identified in Chapter 3. Shown are the genes annotated to all DMRs identified in any of the four brain regions (both Illumina and GREAT (McLean et al., 2010) annotation).

Ensembl gene ID	Gene symbol	log ₂ FC	log ₂ CPM	P-value
ENSG00000162654	<i>GBP4</i>	-0.22	4.05	0.16
ENSG00000171786	<i>NHLH1</i>	0.14	0.02	0.66
ENSG00000235750	<i>KIAA0040</i>	-0.41	2.14	0.15
ENSG00000116147	<i>TNR</i>	0.03	8.78	0.80
ENSG00000162804	<i>SNED1</i>	0.03	5.39	0.80
ENSG00000159674	<i>SPON2</i>	-0.05	2.92	0.78
ENSG00000159692	<i>CTBP1</i>	0.06	7.01	0.58
ENSG00000063978	<i>RNF4</i>	0.02	5.69	0.89
ENSG00000125386	<i>FAM193A</i>	-0.01	5.59	0.94
ENSG00000168884	<i>TNIP2</i>	-0.07	2.48	0.60
ENSG00000204580	<i>DDR1</i>	-0.21	4.60	0.62
ENSG00000182095	<i>TNRC18</i>	0.05	6.81	0.64
ENSG00000155034	<i>FBXL18</i>	0.12	5.42	0.30
ENSG00000155034	<i>FBXL18</i>	0.12	5.42	0.30
ENSG00000167701	<i>GPT</i>	0.20	2.20	0.24
ENSG00000213185	<i>FAM24B</i>	-0.41	0.57	0.06
ENSG00000170430	<i>MGMT</i>	-0.15	3.01	0.24
ENSG00000177947	<i>ODF3</i>	0.21	0.34	0.45
ENSG00000121691	<i>CAT</i>	-0.07	4.64	0.59
ENSG00000196498	<i>NCOR2</i>	-0.04	7.15	0.72
ENSG00000073060	<i>SCARB1</i>	-0.12	5.35	0.31
ENSG00000061936	<i>SFSWAP</i>	0.00	6.05	0.97
ENSG00000150403	<i>TMCO3</i>	-0.04	5.39	0.73
ENSG00000198176	<i>TFDP1</i>	-0.02	4.78	0.85
ENSG00000272636	<i>DOC2B</i>	0.08	5.88	0.61
ENSG00000181031	<i>RPH3AL</i>	-0.25	0.97	0.28
ENSG00000250067	<i>YJEFN3</i>	0.17	4.88	0.13
ENSG00000182871	<i>COL18A1</i>	-0.20	4.54	0.21
ENSG00000173638	<i>SLC19A1</i>	0.11	3.91	0.37

Table 6.12. Results of the schizophrenia differential expression analysis for the expressed genes annotated to the 50 top ranked differentially methylated probes identified in the prefrontal cortex (Chapter 3).

450K Probe ID	DNA methylation			Gene expression					
	Illumina gene annotation	GREAT gene annotation	DNA methylation difference (%)	P-value	Ensembl gene ID	Gene symbol	log ₂ FC	log ₂ CPM	P-value
cg08743050	NCAM1	TTC12	-3.80	1.84E-08	ENSG00000149294	NCAM1	-0.08	9.22	0.44
cg05686445	C7orf54; SND1	LRRC4	-3.65	1.63E-07	ENSG00000197157	SND1	-0.03	6.56	0.80
cg26173173	GSDMD	C8orf73	3.11	8.06E-07	ENSG00000104518	GSDMD	-0.16	1.16	0.35
cg03325693	ABTB2	NAT10	-2.36	8.73E-07	ENSG00000135372	NAT10	-0.05	5.58	0.69
cg16782339	SH3RF3	SEPT10	1.83	9.12E-07	ENSG00000172985	SH3RF3	0.10	4.58	0.40
cg10071493		C10orf8; CACNA1H	3.69	2.13E-06	ENSG00000196557	CACNA1H	-0.09	4.24	0.55
cg18812956	RAB5A		4.68	2.90E-06	ENSG00000144566	RAB5A	0.00	6.26	0.97
cg24281764	MMP17	ULK1	0.71	4.38E-06	ENSG00000198598	MMP17	0.13	5.32	0.23
cg10654165	DPYS		2.24	4.39E-06	ENSG00000147647	DPYS	0.17	1.02	0.38
cg16204289	FAM176A	MRPL19	1.51	4.86E-06	ENSG00000115364	MRPL19	-0.04	5.63	0.74
cg17901382	TSEN54	CASKIN2	2.69	4.98E-06	ENSG00000177303	CASKIN2	-0.19	4.39	0.16
cg10932125	KIF13B		2.37	5.38E-06	ENSG00000197892	KIF13B	-0.31	6.16	0.11
cg20098710	YJEFN3		-2.88	5.61E-06	ENSG00000250067	YJEFN3	0.17	4.88	0.13
cg20383948	COL18A1	SLC19A1	-3.70	5.89E-06	ENSG00000182871	COL18A1	-0.20	4.54	0.21
					ENSG00000173638	SLC19A1	0.11	3.91	0.37

cg16350225	RCSD1	CREG1; MPZL1	4.28	6.08E-06	ENSG00000143162	CREG1	-0.08	4.79	0.52
					ENSG00000198771	RCSD1	-0.07	3.33	0.56
					ENSG00000197965	MPZL1	0.02	5.13	0.84
cg19028706	TRAK1	CCK	-3.49	6.71E-06	ENSG00000182606	TRAK1	0.07	7.11	0.55
					ENSG00000187094	CCK	0.11	6.74	0.36
cg07405426		ZNF629; BCL7C	0.70	7.44E-06	ENSG00000102870	ZNF629	-0.03	5.29	0.82
					ENSG00000099385	BCL7C	0.04	3.67	0.73
cg20044211	NOTCH4	GPSM3	2.69	7.54E-06	ENSG00000204301	NOTCH4	0.06	2.16	0.91
cg10072351	GOSR2		-0.61	8.09E-06	ENSG00000108433	GOSR2	-0.11	5.16	0.35
cg26088561	C6orf136	DHX16	-2.62	8.26E-06	ENSG00000204564	C6orf136	0.21	2.00	0.52
					ENSG00000204560	DHX16	0.02	2.01	0.93
cg04314225	PCNT	DIP2A	2.09	9.18E-06	ENSG00000160299	PCNT	0.04	7.37	0.74
cg06099244	C3orf17		1.90	9.47E-06	ENSG00000163608	C3orf17	0.04	5.47	0.71
cg02272814	TDRD6		2.99	1.06E-05	ENSG00000180113	TDRD6	-0.08	4.12	0.49
cg27059530	MPP5		-1.02	1.08E-05	ENSG00000072415	MPP5	-0.05	6.38	0.64
cg18705408	MA7N3		-1.01	1.26E-05	ENSG00000132031	MA7N3	-0.01	1.23	0.96
cg09741917	VWA3B	CNGA3; TMEM131	1.51	1.40E-05	ENSG00000075568	TMEM131	-0.10	6.31	0.39
					ENSG00000144191	CNGA3	-0.21	1.17	0.27
cg25529303	MTHFD1L		-2.03	1.46E-05	ENSG00000120254	MTHFD1L	-0.07	4.49	0.55
cg16679302		KIAA0182; KIAA0513	-2.86	1.52E-05	ENSG00000135709	KIAA0513	0.06	9.22	0.60
					ENSG00000162643	WDR63	0.03	0.02	0.94
cg02213139	WDR63	MCOLN3; SYDE2	-1.46	1.54E-05	ENSG00000055732	MCOLN3	-0.07	0.37	0.84
					ENSG00000097096	SYDE2	0.08	3.89	0.51
cg27645498		NCOR2; SCARB1	-3.10	1.54E-05	ENSG00000196498	NCOR2	-0.04	7.15	0.72
					ENSG00000073060	SCARB1	-0.12	5.35	0.31

cg02370100	ABCG1	TFF3	-2.04	1.56E-05	ENSG00000160179	ABCG1	-0.11	5.07	0.34
cg24044052	SP140L		2.84	1.75E-05	ENSG00000185404	SP140L	-0.13	2.33	0.37
ch.3.183336F	SETD5	LHFPL4; THUMPD3	-1.78	2.00E-05	ENSG00000134077	THUMPD3	-0.03	4.91	0.79
					ENSG00000168137	SETD5	-0.06	7.11	0.57
					ENSG00000156959	LHFPL4	0.03	5.96	0.81
cg26548293	C10r77; S100A13		3.76	2.11E-05	ENSG00000189171	S100A13	0.05	4.29	0.65
cg15081722	ADARB2	IDI1	4.42	2.12E-05	ENSG00000067064	IDI1	0.03	6.27	0.79
					ENSG00000185736	ADARB2	-0.18	5.78	0.23
cg06477164	EIF2AK2	CCDC75	2.09	2.34E-05	ENSG00000055332	EIF2AK2	0.03	7.24	0.78
cg02565255		PROP1	-1.04	2.54E-05	ENSG00000145911	N4BP3	0.04	4.46	0.70
cg11321921	NFATC1	CTDP1	1.43	2.54E-05	ENSG00000131196	NFATC1	-0.24	1.85	0.20
					ENSG00000060069	CTDP1	-0.11	3.64	0.39
cg09789590	HIF3A		-2.17	2.60E-05	ENSG00000124440	HIF3A	0.02	4.86	0.91
cg03944444	NECAP2	NBPF1	-3.01	2.62E-05	ENSG00000157191	NECAP2	-0.16	4.21	0.17
					ENSG00000219481	NBPF1	0.12	6.06	0.28
cg26819783		HDAC4; NDUFA10	1.35	3.01E-05	ENSG00000068024	HDAC4	0.03	6.44	0.75
					ENSG00000130414	NDUFA10	-0.05	6.18	0.64

6.4. Discussion

6.4.1. Overview of the results

In this Chapter I profiled transcriptomic variation in PFC tissue from schizophrenia patients and non-psychiatric controls obtained from two brain banks. After stringent pre-processing and QC steps, I identified several nominally significant DE genes associated with schizophrenia. Two of the top ranked schizophrenia-associated DE genes have been previously reported to be differentially expressed in schizophrenia brains. First the *MOG* gene, which is down-regulated in the PFC of schizophrenia patients in my data, has been previously reported to be down-regulated in the PFC in schizophrenia patients (Tkachev et al., 2003). Furthermore, this gene is located within the MHC region on chromosome 6. Genetic variants in the MHC *locus* have been strongly linked to schizophrenia in recent large collaborative GWAS studies (International Schizophrenia et al., 2009, Schizophrenia Working Group of the Psychiatric Genomics, 2014). Second, the *SERPINA3* gene, which is down-regulated in schizophrenia patients, has been found to be up-regulated in the PFC (Brodmann area (BA) 9) (Arion et al., 2007), dorsolateral PFC (BA 46) (Fillman et al., 2013) and in the middle frontal gyrus (Fillman et al., 2014) of schizophrenia patients in several other studies. Other schizophrenia-associated DE genes are of potential interest in the context of schizophrenia etiology, such as *PLPPR3* (which may play a role in cell migration and axonal growth in the developing neurons (Brauer et al., 2003)) and *CD44* (isoforms of this gene have been implicated in the activation of T lymphocytes (Goodison et al., 1999), which play central role in cell-mediated immunity).

Furthermore I investigated 450K array probes annotated to schizophrenia-associated DE genes. Several of the schizophrenia-associated DE genes have a number of nominally-associated DMPs annotated to them, such as *ZFPM1*, *WDR46*, *CD44* and *SLC16A3*. Interestingly, these DMPs were not consecutive but were rather located in diverse parts of the genes (e.g. gene body, transcription start site, first exon, etc.). A potential explanation is that these are modulating alternative splicing events. Recent studies provide evidence that DNA methylation within gene bodies correlated positively with gene expression (Ball et al., 2009), and it thought to play a role in alternative splicing (Maunakea et al., 2013). I also identified schizophrenia-associated DMPs in the vicinity to

the transcription start sites of several DE genes. Finally, I investigated whether those genes annotated to the differently methylated probes (DMPs) and regions (DMRs) identified **Chapter 3** were also differently expressed. Surprisingly, none of the genes annotated to DMRs or DMPs are differentially expressed in the PFC of schizophrenia patients, suggesting that the DNA methylation changes observed may not have a direct, *cis*-effect on gene expression.

6.4.2. Limitations, strengths and future directions

This study has a number of limitations and strengths that should be considered. First, although none of the schizophrenia-associated DE genes reaches Bonferroni corrected threshold, I identified several associated DE genes that have been previously found to be aberrantly expressed in schizophrenia brains and are of interest in the context of its etiology. Post-mortem brain samples are difficult to obtain and isolating high quality RNA from these is challenging (see **Chapter 2 section 2.2.4**). Therefore, although underpowered, this is a relatively large RNA-seq study using post-mortem brain tissue from schizophrenia cases and controls. This observation provides encouragement for RNA-seq case-control studies using post-mortem brain tissue in complex disorders such as schizophrenia. Future studies should focus on replication in larger cohorts of samples. Furthermore, these findings should be validated using a gold-standard gene expressing technique, such as qPCR.

Although the role of DNA methylation in genomic regulation is well-established (see **Chapter 1 section 1.2.2.4**), we are far from fully understanding how DNA methylation dynamically regulates the expression of genes. Until recently, the majority of the studies on DNA methylation focused on CpG islands at the TSS of genes, which has influenced general perceptions about the function of DNA methylation on gene expression regulation. Although there is abundant evidence that DNA methylation at the TSS is associated with silencing of some genes, recent studies using epigenome-wide survey techniques have emphasised that the relationship between DNA methylation and gene expression depend on the position of this DNA mark on the gene (Jones, 2012). Furthermore, there is increasing awareness of the importance of 5-hydroxymethyl cytosine (5-hmC) in the human brain (Branco et al., 2012, Kriaucionis and Heintz, 2009), although this modification cannot be

distinguished from DNA methylation using standard bisulfite-based approaches (Lunnon et al., 2016b, Booth et al., 2012). The study of this modification adds another layer of complexity to the intricate role of epigenetic mechanisms in gene expression regulation. It is plausible that many of the differences identified in **Chapter 3** and explored in this chapter are confounded by modifications other than DNA methylation.

In this Chapter I present evidence of schizophrenia-associated DNA methylation variation proximal to schizophrenia-associated DE genes. However, the reverse relationship is not observed; the genes annotated to the top ranked schizophrenia-associated DMPs are not differentially expressed in schizophrenia. Given that the DNA methylation analysis using PFC presented in **Chapter 3** used a larger sample size than the used in the gene expression analysis, it is possible that the transcriptomic analysis is underpowered to detect subtle gene expression changes associated with methylomic variation. Another plausible explanation is that the schizophrenia-associated DNA methylation variation observed is having an indirect, *trans*-impact of gene expression regulation (*i.e.* through insulators and enhancers). Given the limitations discussed above is not possible to draw definite conclusions from these observations. The work from consortiums such as the NIH Roadmap Epigenomics Mapping Consortium as well as studies using a systems-level approach (such as the one described in **Chapter 5**) will be crucial to understand the intricate relationships between epigenetic mechanisms and transcriptional regulation in the near future (Bernstein et al., 2010).

In summary, this Chapter presents the first case-control gene expression study of schizophrenia in samples also profiled for DNA methylation identifying several gene expression changes in the PFC of individuals with the disease. Furthermore, I provide evidence of the overlap between nominally schizophrenia-associated DNA methylation variation and schizophrenia-associated DE genes. Future studies should focus on refining the analytical approach used, replicating the results in a larger sample size and understanding the intricate relationship between DNA methylation variation and gene expression regulation and its implications in complex disease.

Chapter 7 - Epigenomic and transcriptomic signatures of a Klinefelter syndrome (47,XXY) karyotype in the brain

Joana Viana*, Ruth Pidsley*, Claire Troakes, Helen Spiers, Chloe CY Wong, Safa Al-Sarraj, Ian Craig, Leonard Schalkwyk and Jonathan Mill

*These authors contributed equally to this work

This Chapter is presented in the form of a peer-reviewed publication (Viana et al., 2014). The article was published on the scientific journal *Epigenetics* in April of 2014. The supplementary material of this publication is presented in **Appendix B**.

This page has been removed by the author of this thesis for copyright reasons.

<https://dx.doi.org/10.4161/epi.27806>

This page has been removed by the author of this thesis for copyright reasons.

<https://dx.doi.org/10.4161/epi.27806>

This page has been removed by the author of this thesis for copyright reasons.

<https://dx.doi.org/10.4161/epi.27806>

This page has been removed by the author of this thesis for copyright reasons.

<https://dx.doi.org/10.4161/epi.27806>

This page has been removed by the author of this thesis for copyright reasons.

<https://dx.doi.org/10.4161/epi.27806>

This page has been removed by the author of this thesis for copyright reasons.

<https://dx.doi.org/10.4161/epi.27806>

This page has been removed by the author of this thesis for copyright reasons.

<https://dx.doi.org/10.4161/epi.27806>

This page has been removed by the author of this thesis for copyright reasons.

<https://dx.doi.org/10.4161/epi.27806>

This page has been removed by the author of this thesis for copyright reasons.

<https://dx.doi.org/10.4161/epi.27806>

This page has been removed by the author of this thesis for copyright reasons.

<https://dx.doi.org/10.4161/epi.27806>

This page has been removed by the author of this thesis for copyright reasons.

<https://dx.doi.org/10.4161/epi.27806>

This page has been removed by the author of this thesis for copyright reasons.

<https://dx.doi.org/10.4161/epi.27806>

This page has been removed by the author of this thesis for copyright reasons.

<https://dx.doi.org/10.4161/epi.27806>

Chapter 8 - General Discussion

The primary aim of this thesis was to expand the existing knowledge about the extent of methylomic and transcriptomic variation in the brain in schizophrenia; I explored these topics in **Chapters 3 to 6**. Furthermore, in **Chapter 7** I present a methylomic and transcriptomic analysis of two brain regions from an individual with Klinefelter syndrome (KS), identified during my analysis of schizophrenia brain data. In this final chapter I give an overview of the results of my research, placing these in the context of the existing literature on genomic variation in schizophrenia, before concluding with a discussion of the limitations and strengths of my work and a discussion of what I believe to be the future directions for the field.

8.1. Key findings from my research

8.1.1. Methylomic profiling of schizophrenia in the brain

In **Chapter 3** I quantified genome-wide patterns of DNA methylation in post-mortem brain tissue isolated from four different brain region; prefrontal cortex (PFC), striatum (STR), hippocampus (HC) and cerebellum (CER). I identified numerous differentially methylated positions (DMPs) and regions (DMRs) associated with disease in each individual brain region. In addition, I used a multilevel model to identify consistent DNA methylation variation across the PFC, STR and HC - I did not include the CER in this analysis given the distinct DNA methylation profile seen in this brain region (**Chapter 3 section 3.2.2**) (Davies et al., 2012, Hannon et al., 2016, Ladd-Acosta et al., 2007). The multilevel model identified several DMPs and DMRs across all three brain regions. Genes annotated to many of the schizophrenia-associated DMPs and DMRs included *loci* relevant in the context of what we know about the pathophysiology of schizophrenia – for example *NCAM1* (Sunshine et al., 1987, Ronn et al., 1998), *SYNPO* (Focking et al., 2015) and *GBP4* (Sanders et al., 2013).

8.1.2. Methyloomic profiling of schizophrenia polygenic risk burden in the brain

In **Chapter 4** I studied the association between DNA methylation and schizophrenia polygenic risk score (PRS) in post-mortem brain samples isolated from PFC, STR, HC and CER. I identified numerous DMPs and DMRs associated with PRS in individual brain regions as well as across brain regions. Many of the PRS-associated *loci* are relevant to schizophrenia, including several regions in the major histocompatibility complex (MHC) (International Schizophrenia et al., 2009, Schizophrenia Working Group of the Psychiatric Genomics, 2014), *GADD45B* (Gavin et al., 2012), *RGMA* (O'Leary et al., 2013, Matsunaga et al., 2004), the cluster of genes *PCDHA 1 to 4* (Hamada and Yagi, 2001, Kohmura et al., 1998), *AXIN2* (Kikuchi, 1999) (Kalani et al., 2008, Nusse, 2008), *GDNF* (Ibanez, 2008) and *DISC1* (St Clair et al., 1990). Other PRS-associated *loci*, such as *SIGLEC9* and *BPI*, encode proteins that play crucial roles in the immune system (Crocker et al., 2007, Zhang et al., 2000, Angata and Varki, 2000). Many of the DMPs and DMRs associated with increased genetic burden for schizophrenia are independent of the changes observed associated with a diagnosis of schizophrenia itself, identified in the case-control analyses presented in **Chapter 3**. Furthermore, there was no evidence for direct genetic effects on DNA methylation for variants included in the PRS, indicating that the PRS-associated epigenetic variation observed does not directly result from *cis*-genetic influences on DNA methylation.

8.1.3. Systems-level analysis of DNA methylation in the schizophrenia brain

I was interested in studying the co-methylation structure of DNA methylation across the genome in the PFC, STR and CER, and exploring differences in that structure between schizophrenia patients and non-psychiatric controls. In **Chapter 5** I used weighted gene co-methylation analysis (WGCNA) to do this. Five modules of co-methylated *loci* were nominally associated with schizophrenia in the PFC network. Several genes annotated to the 'hub probes' of these modules are particularly interesting in the context of schizophrenia: *KDM3B* (Schizophrenia Working Group of the Psychiatric Genomics, 2014), *ANK3* (Ferreira et al., 2008, Wirgenes et al., 2014) and *RPTOR*. Seven genes

belonging to the schizophrenia-associated modules also showed interactions with genes linked to schizophrenia in a recent study reporting novel interaction networks with schizophrenia-linked genes (Ganapathiraju et al., 2016). Gene ontology enrichment analysis revealed a significant enrichment for neuronal function- and neurodevelopment-relevant pathways in the largest schizophrenia-associated module. Furthermore, five schizophrenia-associated 'fetal network' modules in the PFC were also significantly correlated with brain development in a recent study by Spiers et al. (2015); the largest of these modules was highly enriched for probes annotated to genes in pathways relevant to neurodevelopment (Spiers et al., 2015).

8.1.4. Transcriptomic profiling of schizophrenia prefrontal cortex

In **Chapter 6** I characterised the transcriptome of PFC tissue from schizophrenia patients and non-psychiatric controls. I identified several differentially expressed (DE) genes associated with schizophrenia, several of them relevant in the context of schizophrenia, including *MOG* (Tkachev et al., 2003), *SERPINA3* (Arion et al., 2007, Fillman et al., 2013, Fillman et al., 2014), *PLPPR3* (Brauer et al., 2003) and *CD44* (Goodison et al., 1999). Several of the schizophrenia-associated DE genes have a number of nominally-associated DMPs annotated to them, such as *ZFPM1*, *WDR46*, *CD44* and *SLC16A3*, located in diverse parts of the genes and potentially modulating alternative splicing events (Maunakea et al., 2013). Conversely, none of the genes annotated to DMRs or DMPs are DE genes in the PFC of schizophrenia patients, suggesting that the DNA methylation changes observed may not have a direct, *cis*-effect on gene expression.

8.1.5. Epigenomic and transcriptomic signatures of a Klinefelter syndrome (47,XXY) karyotype in the brain

As part of an integrated '-omics' study of schizophrenia (Pidsley et al., 2014), we identified an individual with KS (a 47,XXY karyotype). Detailed post-mortem records show that although the 47,XXY patient had a similar total brain mass to other patients they had a markedly lower CER mass. The reduced cerebellum mass is consistent with the patient's autopsy report of movement disorders; previous studies demonstrate an association between cerebellar ataxia and

reduced cerebellar size (Richter et al., 2005). Reductions in cerebral volume have been previously reported in KS (Skakkebaek et al., 2016, Skakkebaek et al., 2014, Giedd et al., 2007). Relative to other samples, the 47,XXY patient showed evidence for global DNA hypomethylation in the PFC and hypermethylation in the CER. Furthermore, we identified numerous autosomal regions showing consistent differential DNA methylation in the 47,XXY patient compared with other samples. Of note, several of these *loci* are relevant in the context of this syndrome, including *SPAG1* (Lin et al., 2001), *PIWIL1* (Reuter et al., 2011) and *LHX4* (Machinis et al., 2001). Given the comorbid diagnosis of schizophrenia in this patient, it is interesting that several of the *loci* identified are located in close proximity to other neurobiologically-relevant genes, including *NOTCH4*, *EPHB3* and *KCNN1* (Ho et al., 2009, Liebl et al., 2003, Dolga and Culmsee, 2012). Numerous genes were found to be differentially expressed (DE) in the 47,XXY PFC and CER compared to the remaining samples. There was no evidence for skewed X-chromosome inactivation (XCI) in either of the brain regions from the 47,XXY patient.

KS is often comorbid with psychiatric and neurodevelopmental phenotypes including language-based learning disabilities, decreased verbal intelligence and difficulties with task planning and inhibitory control (Boada et al., 2009). Given that such cognitive symptoms are often present in individuals with KS, future studies should focus on investigating methylomic and gene regulation variation in different brain regions of KS patients. However, post-mortem brain samples from these individuals are difficult to obtain. During the course of my PhD and after the study presented in **Chapter 7** was published (Viana et al., 2014), I identified another individual with a 47,XXY karyotype (see **Chapter 3 section 3.2.2**). Furthermore, I obtained STR and HC tissue from the same individual presented in **Chapter 7**. Currently I am completing a study including DNA methylation, genotyping and transcriptomics (RNA-seq) data from the PFC, STR, HC and CER of these two individuals with KS.

8.2. Limitations

The analyses presented in this thesis have several important limitations that should be considered. Specific limitations to each analysis have already been discussed in each Chapter; here my focus is on the general limitations of using post-mortem brain tissue in molecular epidemiology and what aspects future research should focus on. First, although this represents one of the largest analyses of schizophrenia brain tissues yet undertaken, the number of samples assessed in my work is relatively low. The small number of samples limits the power to detect significant associations, especially given the small effect sizes expected in a complex disease such as schizophrenia (Dempster et al., 2013). Future efforts by the community should focus on extending participation in brain-banking efforts to maximise the number of samples available for molecular epidemiology. In this regard, recent efforts such as the UK Brain Bank Network (Medical Research Council, 2016) and the US CommonMind Consortium (The CommonMind Consortium, 2016) will facilitate advances in understanding the molecular pathology of neuropsychiatric disorders.

Second, because epigenetic processes play an important role in defining cell type-specific patterns of gene expression (Roadmap Epigenomics Consortium et al., 2015, Talens et al., 2010, Varley et al., 2013), the use of 'bulk' tissue from each brain region is a potential confounder in DNA methylation (Guintivano et al., 2013, Heijmans and Mill, 2012) and gene expression studies (Gentles et al., 2015). Despite my efforts to control for the effect of cell type diversity in DNA methylation and gene expression quantification in the analyses using *in silico* approaches to estimate neuronal proportions, this approach is not perfect, not appropriate to estimate the neuronal proportion in the CER, and cannot inform about disease relevant DNA methylation changes specific to individual neuronal cell types. Future efforts should focus on advances in purifying neural cell-types for genomic profiling (Jeffries and Mill, In Press), and developing methods for single cell genomic profiling.

Third, there is increasing awareness of the importance of 5-hydroxymethyl cytosine (5-hmC) in the human brain (Branco et al., 2012, Kriaucionis and Heintz, 2009), although this modification cannot be distinguished from DNA methylation using standard bisulfite-based approaches (Lunnon et al., 2016b,

Booth et al., 2012). It is therefore plausible that many of the differences identified in this study are confounded by modifications other than DNA methylation. To date, no study has evaluated the role of 5-hmC in schizophrenia or any other psychiatric disorder, although novel profiling methods should make this feasible in the near future (Lunnon et al., 2016b).

Fourth, although I controlled for age, sex and derived neuronal composition (where possible) in the analyses presented in this thesis, it is plausible that other factors such as smoking or medication still influenced my results. Post-mortem samples are a precious resource and, when available, are often poorly characterised in terms of medication intake or life style habits such as smoking. Furthermore, even when information on medication is available, it is often impossible to distinguish between medication intake and disease status as all schizophrenia patients are usually prescribed some type of antipsychotic medication during their lifetime. Future efforts should be made to recruit samples for biobanking as early as possible before death so that detailed pre-mortem exposure and phenotypic data can be collected.

8.3. Integration of schizophrenia findings – strengths, implications and future directions

Chapters 3 to 6 represent a comprehensive study of schizophrenia-associated methylomic, transcriptomic and regulatory variation across four brain regions. This section aims to discuss and integrate the findings of the separate Chapters, within the context of the existing literature. In **Table 8.1** I summarise the genes implicated across the different analyses.

Overall, the results presented in this thesis do not support a global change in DNA methylation or gene expression in the brain of schizophrenia patients compared to non-psychiatric controls, which concurs with previous DNA methylation and gene expression studies of schizophrenia (see **Chapter 1 section 1.4**). Instead, I identified changes at specific loci/genes implicated in schizophrenia. To my knowledge, the data presented here represent the most comprehensive combined study of methylomic, genomic and transcriptomic variation across different regions of the brain in schizophrenia to date. The use of PRS derived using data from a large schizophrenia GWAS (Schizophrenia

Working Group of the Psychiatric Genomics, 2014) to investigate methylomic variation associated with schizophrenia polygenic burden that is independent from direct *cis*-genetic effects represents an important step forward in the study of polygenic mediation of the epigenome in disease. Furthermore, the significant difference in PRS between schizophrenia patients and non-psychiatric controls observed in this study (**Chapter 4 Figure 4.4**) highlights the relevance of using PRS as a tool to investigate molecular aetiology of schizophrenia, even in relatively small samples.

In **Chapter 5** I used a systems-level approach to identify modules of co-methylated *loci* that might be dysregulated in schizophrenia. Despite the need to refine the application of WGCNA to DNA methylation data I was able to make several important observations. First, this analysis seems to highlight the importance of the PFC methylome in schizophrenia, with five modules of co-methylated probes associated with disease in this brain region. Second, it allowed identifying evidence of co-methylation at several genes that have been previously shown to interact (Ganapathiraju et al, 2016) with *DISC1* or genes implicated in the latest GWAS (Schizophrenia Working Group of the Psychiatric Genomics, 2014). This provides further support for an interaction between genetic variants associated with schizophrenia and DNA methylation at distinct *loci*, and highlights the importance of undertaking systems-level analyses in complex disorders such as schizophrenia. Finally, the work presented in **Chapter 6** identifies several differentially expressed genes in the PFC in schizophrenia patients, and also provides evidence for an overlap between several of these genes and schizophrenia-associated methylomic variation.

For decades researchers have struggled to understand the biological mechanisms mediating the onset of psychiatric conditions such as schizophrenia, mainly due to their pleiotropic and polymorphic nature. Based on its symptomatology and early epidemiological studies, schizophrenia has been hypothesised to be a disease with neurodevelopmental origin and immunological implications. The work comprised in this thesis represents an important contribution to the field by providing further support for both of these hypotheses.

Several aspects of my data provide further evidence to support a neurodevelopmental origin for schizophrenia: i) several of the genes associated with both schizophrenia diagnosis and schizophrenia polygenic risk burden are genes involved in neurodevelopmental processes, including *ADNP2* (Kushnir et al, 2008), *AXIN2* (Kushnir et al, 2008), *GAT2* (Schmidt and Mirnics, 2015), *PLPPR3* (Brauer et al., 2003), *RPTOR* (Bercury et al, 2014) and *DOC2B* (Groffen et al, 2010); ii) a large schizophrenia-associated module of co-methylated probes in the PFC shows significant enrichment for GO pathways involved in neurodevelopment; and iii) five fetal age-associated modules of co-methylated probes identified in the fetal brain (Spiers et al., 2015) were also associated with schizophrenia in the PFC. Furthermore, several *loci* associated with the schizophrenia PRS have been previously implicated in other neurodevelopmental disorders such as autism-spectrum disorder (ASD) and attention deficit hyperactivity disorder (ADHD), supporting the notion that these different neurodevelopmental disorders might share common biological pathways (Carroll and Owen, 2009).

Additionally, several of the *loci* associated with schizophrenia polygenic risk burden provide further support for the involvement of the immune system in schizophrenia etiology; these *loci* include *BPI* (Marra et al, 1992), *IRF8* (Yanez and Goodridge, 2016), *LSP1* (Pulford et al, 1999) and *SIGLEC9* (Zhang et al, 2000, Angata and Varki, 2000). This evidence is reinforced by the observed association between PRS and DNA methylation at *loci* within the MHC region: e.g. *HLA-DPB2*, *HLA-J* and *RNF39*. Genetic variants in the MHC region have been robustly associated with schizophrenia in recent GWAS studies (International Schizophrenia et al., 2009, Schizophrenia Working Group of the Psychiatric Genomics, 2014). This region spans several megabases on chromosome 6 and contains 18 highly polymorphic human leukocyte antigen (HLA) genes that encode proteins with antigen-presenting roles in the immune system (Benacerraf, 1981). Interestingly, whereas DNA methylation changes at the several neurodevelopmental-relevant *loci* seem to be associated with both schizophrenia diagnosis and schizophrenia polygenic risk burden, changes in DNA methylation at immune-related genes seem to be more often associated with changes in polygenic risk score. A hypothesis arising from this observation would be that the increased burden of schizophrenia genetic risk variants is

associated with DNA methylation variation at immune-related genes. During the course of the disease, DNA methylation status at these loci is potentially changed through the action of antipsychotic medication, explaining why they are not detectable in the diagnosis analysis, where controlling for medication was impossible. My future work is focussed on understanding the genomic changes associated with exposure to antipsychotic medications, enabling me to further explore this hypothesis.

The associations presented in this thesis need to be replicated and validated in larger sample cohorts. Furthermore, it will be important to establish whether the differences reported are causal and have a direct impact on disease etiology or if they are consequences of the disease course and medication intake. Additionally, we need to understand the individual contribution of single variants as well as the impact in molecular mechanism and disease risk of the higher polygenic burden. The development of animal models of schizophrenia should be a focus of future studies. The advance of genome editing technologies, such as the CRISPR/Cas9 system (Capecchi, 2005), will enable to target and modify specific genetic variants and epigenetic modifications. The behavioural and phenotypical analysis of such models should give us large insight on the mechanisms of schizophrenia. These models could be developed in rodents but also in other vertebrate organisms such as zebrafish. Future efforts should also be made to study the effect of antipsychotic medication on epigenetic mechanisms and gene expression using alternative approaches, such as exposure of iPS-derived neurons of schizophrenia patients and animal exposure studies. I am currently assessing the transcriptome and methylome of the brain of zebrafish exposed to antipsychotic medication, which will hopefully provide insight about the molecular implications of antipsychotic exposure on the vertebrate brain.

Another important development in schizophrenia research will be the analysis of the epigenome and transcriptome of individual brain cell types. Ultimately, the integrated profile of DNA methylation, histone modifications, gene expression, open chromatin regions and binding of transcription factors in single cells would be optimal, although at the moment it is not clear how single cell sequencing approaches will be applied to large cohorts of samples. Future work by our group and others is focussing on using novel single-cell approaches to examine

cellular heterogeneity in complex tissues such as the brain and facilitate the identification of pathological changes in specific cells (and cell types).

8.4. Conclusion

In conclusion, the work presented in this thesis represents a comprehensive integrative study of methylomics, genomics and transcriptomics across different regions of the schizophrenia brain and makes an important contribution to the field of psychiatric genomics. I present further evidence to support the neurodevelopmental origin of schizophrenia, as well as a role of the immune system on schizophrenia etiology. My analyses into associations between schizophrenia polygenic burden and DNA methylation suggests that the indirect polygenic mediation of the methylome plays a role in schizophrenia. Future studies will be needed to replicate these results and elucidate the regulatory role of the associations presented in this thesis

Table 8.1. Key genes implicated in the studies presented in my thesis. The table is coloured based on the specific chapter in which the association was made; green: **Chapter 3**, red: **Chapter 4**, orange: **Chapter 5**, blue: **Chapter 6**. CER, cerebellum; DMP, differentially methylated position; DMR, differentially methylated region; FC, fold-change; HC, hippocampus; PFC, prefrontal cortex; PRS, polygenic risk score; STR, striatum.

Gene	Findings	Relevance
ADCY1	PRS-associated DMP in the cross-region multilevel model (PFC, STR and HC) (cg08619378, $P = 1.73E-05$)	Neuronal function
ADNP2	Schizophrenia-associated DMP (cg07500432) in the cross-region multilevel model (PFC, STR and HC) ($P = 3.03E-06$)	Relevant in the context of schizophrenia / Neurodevelopmental origin
ANK3	'Hub probe' (cg22150335) of the schizophrenia-associated PFC 'brown' module	Relevant in the context of schizophrenia / Implicated in other neurodevelopmental or neurological disorders
AXIN2	PRS-associated DMP in the PFC (cg04293307, $P = 6.07E-06$)	Neurodevelopmental origin
BPI	PRS-associated DMP in the PFC (cg01948217, $P = 7.02E-07$)	Implication of the immune system
CACNA1G	HC DMP significantly significant with schizophrenia (cg10383028, $P = 5.30E-06$)	Relevant in the context of schizophrenia
CACNA1H	PFC DMP significantly associated with schizophrenia (cg10071493, $P = 2.13E-06$)	Neuronal function
CD44	Differentially expressed in the PFC of schizophrenia patients ($\log_2 FC = -1.77$, $P = 5.16E-04$). Gene annotated to several PFC DMPs	Implication of the immune system

CHMP1A	PRS-associated DMP in the CER (cg07984684, $P = 3.12E-07$)	Loss-of function mutations in this gene have been linked to reduced cerebellar and cerebral cortical size (Mochida et al, 2012) In the same study, knockout of the CHMP1A orthologue in zebrafish resulted in reduced cerebellum and forebrain volume in these animals	Neuronal function
DCTN1	'Hub probe' (cg06909228) of the schizophrenia-associated PFC 'brown' module	Interacts with <i>DISC1</i> (Ganapathiraju et al, 2016), a gene previously implicated in schizophrenia (see <i>DISC1</i>)	Relevant in the context of schizophrenia
DDR1	Schizophrenia-associated DMR identified in the PFC ($P = 7.87E-03$)	Previously shown to be upregulated during oligodendrocytes differentiation and myelination (Roig et al, 2010, Letzen et al, 2010)	Neuronal function
DISC1	Top ranked PRS-associated DMP in the cross-region multilevel model (PFC, STR and HC) (cg04910228, $P = 6.50E-07$)	A balanced translocation involving this gene that segregates with several major psychiatric disorders including schizophrenia has been intensively studied in a Scottish pedigree (St Clair et al, 1990)	Relevant in the context of schizophrenia
EGR2	'Hub probe' (cg24868421) of the schizophrenia-associated PFC 'black' module	Interacts with <i>NAB2</i> (Ganapathiraju et al, 2016), a gene implicated in the largest schizophrenia GWAS to date (Schizophrenia Working Group of the Psychiatric Genomics, 2014)	Relevant in the context of schizophrenia
FBXO7	Differentially expressed in the PFC of schizophrenia patients ($\log_2 FC = -0.36$, $P = 1.55E-03$). Gene annotated to several PFC DMPs	Mutations in this gene have been implicated in early-onset Parkinson's disease (Deng et al., 2013).	Implicated in other neurodevelopmental or neurological disorders
FOXP1	PRS-associated DMP in the STR (cg01331540, $P = 5.39E-06$)	Deletions, mutations and chromosomal aberrations affecting this gene have been associated with several neurodevelopmental conditions, such as ASD, speech and language deficits and motor development delay (Talkowski et al, 2012, Hamdan et al, 2010, O'Roak et al, 2011) This gene also seems to be important in striatal development in mice (Bacon et al, 2015)	Implicated in other neurodevelopmental or neurological disorders / Neurodevelopmental origin
GAT2	STR DMP significantly associated with schizophrenia (cg15607358, $P = 1.03E-05$)	Encodes a transporter of the key inhibitory neurotransmitter GABA The GABAergic system has been extensively implicated in neurodevelopment and schizophrenia pathology (Schmidt and Mirnics, 2015)	Relevant in the context of schizophrenia / Neurodevelopmental origin
GBP4	STR DMP significantly associated with schizophrenia (cg22221320, $P = 7.88E-08$) Schizophrenia-associated DMR in the cross-region multilevel model (PFC, STR and HC) ($P = 7.88E-08$)	This gene that has been found to be differentially expressed in schizophrenia patients (Sanders et al, 2013)	Relevant in the context of schizophrenia
GDNF	PRS-associated DMR in the cross-region multilevel model (PFC, STR and HC) ($P = 1.73E-06$)	Has been shown to be important for the survival of catecholaminergic neuron survival both <i>in vivo</i> (Pascual et al, 2008) and <i>in vitro</i> (Lin et al, 1993), although this has recently been disputed (Kopra et al, 2015)	Neuronal function

<i>HLA-DPB2</i>	PRS-associated DMR identified in the PFC ($P = 0.04$)	Gene is part of the MHC region	Implication of the immune system
<i>HLA-J</i>	PRS-associated DMR in the cross-region multilevel model (PFC, STR and HC) ($P = 0.02$)	Gene is part of the MHC region	Implication of the immune system
<i>IMMP2L</i>	PRS-associated DMP in the STR (cg19376461, $P = 2.11E-06$)	Encodes a protein involved in processing the signal peptide sequences used to direct mitochondrial proteins to the mitochondria Deletions in this gene have been implicated in several neuropsychiatric disorders ADHD (Elia et al, 2010), ASD (Maestrini et al, 2010) and Tourette syndrome (Patel et al, 2011)	Implicated in other neurodevelopmental or neurological disorders
<i>IRF8</i>	PRS-associated DMR in the cross-region multilevel model (PFC, STR and HC) ($P = 8.76E-03$) PRS-associated DMP in the cross-region multilevel model (PFC, STR and HC) ($P = 4.39E-06$)	Encodes a protein that plays an important role in immune cells differentiation and cell fate (Yanez and Goodridge, 2016)	Implication of the immune system
<i>KDM3B</i>	'Hub probe' (cg03315484) of the schizophrenia-associated PFC 'black' module	Gene implicated in the largest schizophrenia GWAS to date (Schizophrenia Working Group of the Psychiatric Genomics, 2014)	Relevant in the context of schizophrenia
<i>LSP1</i>	PRS-associated DMR in the cross-region multilevel model (PFC, STR and HC) ($P = 8.89E-05$)	Encodes a protein expressed in immune cells such as lymphocytes, neutrophils and macrophages (Pulford et al, 1999)	Implication of the immune system
<i>MAN2A2</i>	'Hub probe' (cg17017272) of the schizophrenia-associated PFC 'brown' module	Interacts with <i>FES</i> (Ganapathiraju et al, 2016), a gene implicated in the largest schizophrenia GWAS to date (Schizophrenia Working Group of the Psychiatric Genomics, 2014)	Relevant in the context of schizophrenia
<i>MAPT</i>	PRS-associated DMP in the cross-region multilevel model (PFC, STR and HC) (cg26019600, $P = 2.99E-05$)	This gene encodes several different isoforms of the tau protein, which have a crucial role in keeping the function of microtubules and axonal transport Several mutations in this gene have been strongly linked to multiple neurodegenerative disorders including Alzheimer's disease, Parkinson's disease, frontotemporal dementia, amongst others (for a review see Zhang et al (2015))	Neuronal function / Implicated in other neurodevelopmental or neurological disorders
<i>MOG</i>	Differentially expressed in the PFC of schizophrenia patients ($\log_2 FC = -1.89$, $P = 1.77E-03$). Gene annotated to several PFC DMPs	Encodes a protein expressed on the oligodendrocyte cell membrane and the surface of myelin sheaths. Down-regulated in the PFC of schizophrenia patients on another study (Tkachev et al, 2003) Located in the MHC region	Relevant in the context of schizophrenia / Implication of the immune system
<i>GAT2</i>	PFC DMP associated with schizophrenia diagnosis (cg08743050, $P = 1.84E-08$)	Encodes a cell adhesion protein with role in neurodevelopment and synaptic plasticity (Ronn et al, 1998, Sunshine et al, 1987)	Neurodevelopmental origin
<i>NDUFA10</i>	'Hub probe' (cg23348161) of the schizophrenia-associated PFC 'black' module	Interacts with <i>CUL3</i> (Ganapathiraju et al, 2016), a gene implicated in the largest schizophrenia GWAS to date (Schizophrenia Working Group of the Psychiatric Genomics, 2014)	Relevant in the context of schizophrenia

NOTCH4	PFC DMP significantly associated with schizophrenia (cg20044211, $P = 7.54E-06$)	Encodes a member of the NOTCH pathway with an important role in neurodevelopment (Lasky and Wu, 2005)	Neuronal function / Neurodevelopmental origin
PCDHA1, PCDHA2, PCDHA3 and PCDHA4	PRS-associated DMP in the PFC (cg19852211, $P = 3.25E-05$)	These genes are organised in a cluster and encode integral plasma membrane, cell adhesion proteins localised at synaptic junctions in neurons (Hamada and Yagi, 2001, Kohmura et al, 1998)	Neuronal function
PLPPR3	Differentially expressed in the PFC of schizophrenia patients ($\log_2 FC = 0.44$, $P = 2.81E-04$).	Encodes a membrane protein belonging to the lipid phosphate phosphatase (LPP) family of proteins, which play a role in cell migration and axonal growth in the developing neurons (Brauer et al, 2003).	Neuronal function / Neurodevelopmental origin
PRDM9	Schizophrenia-associated DMR identified in the CER ($P = 3.65E-05$)	Encodes a protein with histone H3K4 trimethyltransferase activity during meiosis (Berg et al, 2010) and has been previously hypothesised to play a role in schizophrenia (Crow, 2011)	Relevant in the context of schizophrenia
GAP1 family of GTPase-activating proteins (RASAS3, RASAS4 and RASAS4B)	RASAS4 differentially expressed in the PFC of schizophrenia patients ($\log_2 FC = 0.33$, $P = 3.75E-03$) RASAS4B differentially expressed in the PFC of schizophrenia patients ($\log_2 FC = 0.44$, $P = 3.06E-03$) Schizophrenia-associated DMP (cg24803255) in the cross-region multilevel model (PFC, STR and HC) ($P = 1.51E-04$) annotated to RASAS3	RASAS4 and RASAS4B were up-regulated in the schizophrenia patients. A probe annotated to RASAS3 was hypomethylated in the PFC. Together these observations suggest that this family of proteins might play a role in schizophrenia.	Relevant in the context of schizophrenia
RBFOX1	PRS-associated DMP in the PFC (cg0486234, $P = 8.04E-06$)	Encodes a protein thought to regulate a network of genes involved in synaptic function and calcium signalling (Lee et al, 2016) Chromosomal translocations and copy number variations in this gene have been associated with ASD (Martin et al, 2007, Sebat et al, 2007)	Implicated in other neurodevelopmental or neurological disorders
RGMA	PRS-associated DMP in the STR (cg12595281, $P = 6.85E-08$)	Encodes an axon guidance protein thought to be important in interneuron migration and differentiation during neurogenesis (O'Leary et al, 2013, Matsunaga et al, 2004)	Neurodevelopmental origin
RNF39	PRS-associated DMR identified in the PFC ($P = 2.99E-04$) PRS-associated DMR in the cross-region multilevel model (PFC, STR and HC) ($P = 7.36E-04$)	Gene is part of the MHC region	Implication of the immune system

<i>RPH3AL</i> / <i>DOC2B</i>	Schizophrenia associated DMR consistently hypomethylated in schizophrenia patients across all four brain regions DMR validated in the PCF and STR using bisulfite-PCR-pyrosequencing (For the several association <i>P</i> -values see Chapter 3 section 3.3.6)	A consecutive probe also showed significant hypomethylation in PFC, STR and CER, which shows a dramatic Bonferroni-significant increase in DNA methylation associated with brain development in another study (Spiers et al 2015). The DMR is also annotated to the <i>DOC2B</i> gene, which encodes a protein that regulates calcium-dependent neurotransmitter release in synapses (Groffen et al, 2010)	Neuronal function / Neurodevelopmental origin
<i>RPTOR</i>	PRS-associated DMP in the STR (cg15022015, <i>P</i> = 382E-06) 'Hub probe' (cg10281768) of the schizophrenia-associated PFC 'brown' module	Ablation of the protein encoded by this gene in oligodendrocytes has revealed a potential role of this protein in the central nervous system myelination during mouse development (Bercury et al, 2014)	Neuronal function / Neurodevelopmental origin
<i>SEMA7A</i>	'Hub probe' (cg183355991) of the schizophrenia-associated PFC 'brown' module	Interacts with <i>CHRNA5</i> (Ganapathiraju et al, 2016), a gene implicated in the largest schizophrenia GWAS to date (Schizophrenia Working Group of the Psychiatric Genomics, 2014)	Relevant in the context of schizophrenia
<i>SERPINA3</i>	Differentially expressed in the PFC of schizophrenia patients (log2 FC = -2.21, <i>P</i> = 2.86E-03). Gene annotated to several PFC DMPs	Encodes a plasma protease inhibitor. Its physiological function is unclear although is considered to be an acute-phase inflammatory protein (Horvath and Mirnics, 2014). This gene has been found to be up-regulated in the PFC (Arion et al., 2007); dorsolateral PFC (Fillman et al., 2013) and in the middle frontal gyrus (Fillman et al., 2014) of schizophrenia patients. Dysregulation in this protein has also been widely implicated in Alzheimer's disease (Baker et al., 2007)	Relevant in the context of schizophrenia / Implication of the immune system / Implicated in other neurodevelopmental or neurological disorders
<i>SIGLEC9</i>	PRS-associated DMP in the PFC (cg14595786, <i>P</i> = 245E-07)	The SIGLEC9 membrane protein is expressed in monocytes, neutrophils and natural killer cells (Zhang et al, 2000, Angata and Varki, 2000)	Implication of the immune system
<i>SGSH</i>	Hub probes' (cg15774028; cg00141153) of the schizophrenia-associated PFC 'darkgrey' module	Interacts with <i>DRD2</i> (Ganapathiraju et al, 2016), a gene implicated in the largest schizophrenia GWAS to date (Schizophrenia Working Group of the Psychiatric Genomics, 2014)	Relevant in the context of schizophrenia
<i>SYNPO</i>	STR DMP significantly associated with schizophrenia (cg08103144, <i>P</i> = 3.64E-08)	Encodes an actin-associated protein that plays a role in actin-based cell shape and motility that has been shown to be differentially expressed in schizophrenia brains (Focking et al, 2015)	Relevant in the context of schizophrenia
<i>TAOK2</i>	PRS-associated DMP in the CER (cg01682070, <i>P</i> = 4.20E-08)	Encodes a protein that is thought to play an essential role in dendrite morphogenesis (de Anda et al, 2012) Microdeletions and duplications in chromosome 16 affecting this gene have been implicated in ASD (Weiss et al, 2008)	Neuronal function / Implicated in other neurodevelopmental or neurological disorders

TRAK1	PFC DMP significantly associated with schizophrenia (cg19028706, $P = 671E-06$)	Encodes a protein that complexes with the protein encoded by the DISC1 gene (see DISC1)	Relevant in the context of schizophrenia
TULP4	'Hub probe' (cg10296548) of the schizophrenia-associated PFC 'brown' module	Interacts with MAD1L1 (Ganapathiraju et al, 2016), a gene implicated in the largest schizophrenia GWAS to date (Schizophrenia Working Group of the Psychiatric Genomics, 2014)	Relevant in the context of schizophrenia
WNT5A	Schizophrenia-associated DMR in the cross-region multilevel model (PFC, STR and HC) ($P = 8.90E-11$) PRS-associated DMR in the cross-region multilevel model (PFC, STR and HC) ($P = 0.02$)	Encodes for an important neurodevelopmental gene (Horigane et al, 2016)	Neurodevelopmental origin
YJEFN3	Schizophrenia-associated DMR identified in the PFC ($P = 4.49E-02$)	DMR overlaps with the chr19:19374022-19658022 region identified in the latest schizophrenia GWAS	Relevant in the context of schizophrenia
ZAP70	'Hub probe' (cg12332902) of the schizophrenia-associated PFC 'salmon' module	Interacts with CUL3 (Ganapathiraju et al, 2016), a gene implicated in the largest schizophrenia GWAS to date (Schizophrenia Working Group of the Psychiatric Genomics, 2014)	Relevant in the context of schizophrenia
ZNF365	'Hub probe' (cg02712553) of the schizophrenia-associated PFC 'brown' module	Interacts with DISC1 (Ganapathiraju et al, 2016), a gene previously implicated in schizophrenia (see DISC1)	Relevant in the context of schizophrenia

Appendix A – Supplementary Tables

Supplementary Table 1. Demographic data of all samples used in this thesis. Presented are the demographic and phenotypical data (diagnosis group, age, gender) and other relevant information on all samples from the MRC London Neurodegenerative Diseases Brain Bank (LNDBB) and Douglas-Bell Canada Brain Bank (DBCBB) samples.

Individual	Brain Bank	Group	Age	Gender	pH	Brain Weight (g)	Polygenic Risk score	Bisulfite conversion (%)				DNA methylation age				Neuronal proportion estimate			
								PFC	CER	STR	HC	PFC	CER	STR	HC	PFC	CER	STR	HC
1	LNDBB	schizophrenia	67	M	6.36	1313	-17.05	94.12	93.32	94.50	94.79	56.30	53.97	54.65	59.07	0.42	0.51	0.21	0.25
2	LNDBB	schizophrenia	79	M	6.40		-11.05	95.73	94.24	94.44	95.08	54.63	64.77	65.81	66.70	0.45	0.52	0.13	0.16
3	LNDBB	schizophrenia	69	F	6.80		-14.90	94.21	94.52	95.26	95.65	56.81	41.70	60.96	55.90	0.44	0.49	0.05	0.33
4	LNDBB	schizophrenia	76	F	6.25	1143	-17.06	94.29	94.05	94.89	95.43	64.74	49.58	64.78	60.50	0.49	0.50	0.14	0.27
5	LNDBB	schizophrenia	84	F	6.60	1201	-11.70	94.29	94.50	95.18	95.28	62.97	53.24	61.84	61.84	0.44	0.51	0.15	0.18
6	LNDBB	schizophrenia	87	M	6.19	993	-13.55	94.09	93.79	95.68	94.17	71.98	60.67	65.88	75.20	0.45	0.50	0.18	0.29
7	LNDBB	schizophrenia	32	F	6.30	1185	4.10	93.84	93.40	95.04		30.98	33.00	22.63	0.47	0.50	0.24		
8	LNDBB	schizophrenia	70	F	6.17	1193	-12.81	93.47	93.63	94.82		47.11	51.68		0.52	0.52	0.28		
9	LNDBB	schizophrenia	49	F	6.90	1354	11.06	93.70	93.15	94.52	95.16	40.11	47.95	31.33	44.50	0.49	0.48	0.27	0.11
10	LNDBB	schizophrenia	46	M	7.00	1273	-14.74	93.60	95.15	95.23	95.07	38.89	44.02	51.37	47.78	0.38	0.48	0.10	0.28
11	LNDBB	schizophrenia	62	M	7.00	1439	-15.02	93.61	94.20	94.55	94.99	46.43	50.01	54.96	56.08	0.44	0.50	0.05	0.06
12	LNDBB	schizophrenia	31	M	6.30	1273	-3.02	89.16	94.65	96.13	93.77	44.50	27.71	31.79	0.49	0.49	0.15	0.24	
13	LNDBB	schizophrenia	51	M	6.80	1485	-10.95	94.01	93.19	95.07	96.01	35.78	42.43	42.83	50.82	0.51	0.51	0.15	0.15
14	LNDBB	schizophrenia	62	M	7.10		-14.18	93.77	95.57	95.11		50.51	50.31	49.34	0.52	0.50	0.13		
15	LNDBB	schizophrenia	34	F	6.20	1092	-15.44	95.21	90.37	95.64		30.68	34.63	28.63	0.50	0.49	0.28		
16	LNDBB	schizophrenia	75	F	6.60	1314	-20.71	94.97	95.08	94.39	94.82	59.77	49.19	56.99	63.74	0.51	0.49	0.14	0.21
17	LNDBB	schizophrenia	75	F	6.61	1162	-26.59	94.97	94.36	94.80		59.41	52.81	61.31	0.41	0.51	0.10		
18	LNDBB	schizophrenia	64	M	6.70	1239	-13.50	94.01	94.06	94.68	94.12	51.20	48.93	51.84	60.36	0.48	0.49	0.16	0.18
19	LNDBB	schizophrenia	49	M	6.80	1097	-14.18	94.54	95.20	95.45	95.13	44.57	42.08	47.03	48.96	0.49	0.50	0.15	0.14
20	LNDBB	schizophrenia	71	F	6.83	1141	-17.43	94.04	94.38	94.61		60.05	47.92	68.73	0.51	0.49	0.10		
21	LNDBB	schizophrenia	35	M	6.56	1306		93.44	93.82	95.34	93.74								
23	LNDBB	schizophrenia	64	M	6.60	1197	10.22	93.00	92.54	94.78	94.66	47.77	28.06	54.17	60.17	0.45	0.50	0.22	0.24
24	LNDBB	schizophrenia	45	M	6.70	1332	-3.68	94.55	94.58		94.83	40.92			0.46				
25	LNDBB	control	25	M	6.93	1549	-19.28	95.09	94.61	94.96	95.28	23.52	32.20	34.52	22.83	0.46	0.49	0.18	0.29
26	LNDBB	control	49	M	6.70	1231	-7.58	94.71	93.94	95.45	95.59	49.13	42.10	50.06	66.80	0.33	0.50	0.23	0.15
27	LNDBB	control	82	F			-16.20	93.74	94.45	95.73	95.59	65.35	50.14	62.45	0.30	0.50	0.12	0.15	
28	LNDBB	control	82	F	6.33	1216	-15.12	93.74	94.45	94.49				69.31					
29	LNDBB	control	63	F						95.52				56.29					

30	LNDDB	control	68	F	6.02	1196	-23.48	94.78	94.53	95.41	94.83	62.58	40.26	54.06	58.20	0.30	0.49	0.24	0.18
31	LNDDB	control	33	F	6.36	1323	-17.05	92.72	94.28	95.85		28.58	29.26	32.45		0.51	0.50	0.15	
32	LNDDB	control	50	M	6.49	1650	-20.17	93.40	94.74	93.53		36.02	36.74	41.92		0.48	0.50	0.25	
33	LNDDB	control	57	M	6.62	1146	-22.14	93.74	93.85	95.48	95.82	50.59	45.27	49.55	54.08	0.50	0.49	0.12	0.12
34	LNDDB	control	58	M	6.87	1445	-21.11	94.09	94.41	95.81	94.78	60.43	40.24	45.01	56.73	0.33	0.49	0.20	0.21
35	LNDDB	control	68	F	7.10	1137	-15.96	94.06	94.62	94.45		48.18	43.85	48.48		0.48	0.49	0.32	
36	LNDDB	control	86	M			-13.77			95.90				72.75			0.06		
37	LNDDB	control	71	M	6.38	1606	-19.21	94.28	94.86	95.18		75.72	55.74	70.46		0.23	0.52	0.12	
38	LNDDB	control	95	M	6.14	1310	-21.19	93.28	93.74	94.48	94.39	75.13	60.47	60.91	69.96	0.44	0.53	0.28	0.30
39	LNDDB	control	40	M	6.13	1287	6.05	83.47	95.52	95.65		41.96	41.96	39.11			0.49	0.25	
40	LNDDB	control	54	M	6.96	1347	8.69	93.89	94.57	94.60	94.96	47.15	43.11	51.91	49.71	0.40	0.49	0.20	0.11
41	LNDDB	control	76	F	6.41	1175	-11.95	94.77	94.46	94.93		64.12	55.16	60.05		0.34	0.48	0.24	
42	LNDDB	control	67	M	6.06	1336	-19.02	94.19	93.80	94.50	95.85	52.15	56.74	51.86	63.34	0.41	0.49	0.20	0.23
43	LNDDB	control	70	M			-20.88			96.26				56.42			0.14		
44	LNDDB	control	96	F	6.55	1115	-15.11	95.22	94.30	95.61		63.19	58.25	72.19		0.53	0.48	0.14	
45	LNDDB	control	37	M	6.46	1389	-15.18	92.99	94.20	95.28		34.82	36.70	31.28		0.47	0.49	0.23	
46	LNDDB	control	40	M	6.80	1470		94.46	95.28			37.89	38.48			0.46	0.49		
47	LNDDB	control	70	M	6.44	1107	-13.93	93.26	94.08	94.50		54.59	55.31	58.08		0.45	0.49	0.05	0.21
49	LNDDB	control	69	M	6.60	1739	-16.84	94.29	94.95	94.95	94.07	58.76	47.88	57.41	66.68	0.41	0.52	0.24	0.21
50	LNDDB	control	48	M			-22.67			94.76				27.90	39.72		0.37	0.37	0.27
51	LNDDB	control	48	M	6.20	1450	-22.34	93.99	94.94	94.64	95.29	48.47	39.81	46.95	50.81	0.41	0.49	0.15	0.24
52	LNDDB	control	80	M	6.04	1488	-20.36	94.37	94.67	95.58		62.28	51.03	57.23		0.38	0.51	0.22	
53	LNDDB	control	79	M	5.95	1598	-20.94	94.46	93.00	94.82	95.33	61.38	55.69	59.77	70.61	0.36	0.50	0.21	0.22
54	LNDDB	control	55	M	6.90	1452	-21.33	93.19		94.87	95.18	45.57		49.53	48.58	0.34	0.50	0.13	0.18
MS01	DBCBB	schizophrenia	70	M	6.01	1280	-15.93	94.29	94.39	95.89		58.27	45.59	61.15		0.44	0.49	0.13	
MS02	DBCBB	schizophrenia	73	F	6.16		-13.67	91.79		94.99		55.55		55.70		0.44		0.17	
MS03	DBCBB	schizophrenia	30	M	6.42	1321	-18.80	94.15	95.01	95.18		22.15	30.86	25.38		0.43	0.48	0.20	
MS04	DBCBB	schizophrenia	60	F	6.23	1175	-16.95	94.75	94.25	95.23		55.92	49.20	48.01		0.46	0.48	0.18	
MS05	DBCBB	control	57	F	5.73	1250	-18.87	93.84	95.27	94.44		44.35	49.68	48.92		0.47	0.48	0.22	
MS06	DBCBB	schizophrenia	51	F	6.35	1125	-16.83	92.85	94.86	95.09		43.69	43.20	40.30		0.35	0.48	0.23	
MS07	DBCBB	schizophrenia	50	M	6.55	1615	-12.82	94.20	94.19	51.30		46.36	49.56		0.38	0.38	0.49		
MS08	DBCBB	control	57	M	5.72	1400	-15.70	94.06	94.92	94.96		50.60	52.04	43.31		0.31	0.49	0.17	
MS09	DBCBB	control	50	F	6.10	1205	-17.25	95.19	94.34	95.32		49.30	41.77	42.14		0.44	0.49	0.18	
MS10	DBCBB	control	43	M	6.25	1343	-21.00	94.45	95.93	95.41		43.95	46.52	45.04		0.35	0.50	0.19	
MS11	DBCBB	schizophrenia	29	M	6.27	1520		93.30	95.00	95.00		32.45	30.11		0.50	0.47	0.47		
MS12	DBCBB	schizophrenia	24	M	6.01		-20.15	94.53	95.42	95.43		23.49	28.40	23.69		0.43	0.47	0.19	
MS13	DBCBB	control	44	M	5.41	1375.4	-20.58	95.02	94.48	94.98		31.78	34.21	29.69		0.39	0.46	0.23	
MS14	DBCBB	control	28	M	6.59	1565	-8.97	94.83	95.24	95.24		30.85	33.17	26.25		0.46	0.48	0.18	
MS15	DBCBB	control	26	M	6.43	1749	-26.62	94.37	94.15	94.27		33.44	25.84	20.32		0.18	0.48	0.15	
MS16	DBCBB	control	70	M	5.76	1165	-20.73	94.71	95.41	95.00		22.80	51.36	53.75		0.49	0.49	0.16	
MS17	DBCBB	control	30	M	6.22	1517	-17.47	94.71	95.10	94.62			29.80	20.20		0.35	0.46	0.22	

MS18	DBCBB	schizophrenia	69	M	6.23	1295	-15.08	95.62	95.53	95.18	61.80	51.15	52.72	0.38	0.49	0.16
MS19	DBCBB	control	72	F	6.04	1337	-18.92		95.79	95.06		56.53	51.63		0.50	0.27
MS20	DBCBB	schizophrenia	38	M	6.32	1550	-21.03	95.07	95.20	94.90	37.79	39.28	37.07	0.41	0.48	0.18
MS21	DBCBB	schizophrenia	39	M	6.16	1680	-17.73	95.43	95.43	95.44	37.12	37.07	31.16	0.39	0.49	0.19
MS22	DBCBB	control	37	M	6.21	1491	-14.56	95.94	94.61	95.33	34.52	37.60	34.84	0.38	0.52	0.20
MS23	DBCBB	schizophrenia	47	M	5.76	1515.5	-17.56	94.16	95.17	94.79	46.68	41.79	38.03	0.39	0.47	0.26
MS24	DBCBB	control	48	M	6.05	1271.2		94.37	94.52	94.45						
MS25	DBCBB	schizophrenia	65	M	6.27	1320	-11.43	94.91	95.73	94.57	52.87	44.55	57.18	0.47	0.49	0.15
MS26	DBCBB	control	41	M	5.89	1430	-15.78	95.95	94.36	95.66	33.46	36.47	32.10	0.45	0.49	0.18
MS27	DBCBB	schizophrenia	26	M	6.44	1430	-20.06	94.28	94.75	95.45	23.18	33.41	19.46	0.38	0.49	0.19
MS28	DBCBB	schizophrenia	29	M	6.52		-17.82	94.28	95.09	94.72	27.83	29.91	25.19	0.43	0.48	0.22
MS29	DBCBB	schizophrenia	33	M	5.92	1812		93.62	94.93	95.09	25.80		29.82	0.31		0.21
MS30	DBCBB	schizophrenia	32	M	6.05	1408.2	-17.90	94.54	94.63	95.74	29.00	35.51	34.85	0.41	0.50	0.16
MS31	DBCBB	control	33	M	6.34	1670	-16.89	95.09	96.51	95.12	30.15	27.61	28.90	0.41	0.48	0.22
MS32	DBCBB	schizophrenia	54	M	6.47	1430	-12.52	94.96	94.32	95.05	43.47	44.88	49.17	0.40	0.48	0.20
MS33	DBCBB	control	66	M	6.09	1260	-17.88	95.31	95.92	94.85	62.98	53.33	52.40	0.36	0.50	0.24
MS34	DBCBB	control	21	M	6.27	1783	-13.91	94.69	94.31	95.42	20.99	25.65	23.49	0.48	0.47	0.23
MS35	DBCBB	control	32	M	6.49	1516	-20.83	94.57	93.71	96.01	34.54	35.99	31.25	0.29	0.48	0.20
MS36	DBCBB	control	69	M	6.04	1390	-17.51	95.47	94.52	95.87	56.46	54.82	53.88		0.49	0.17
ES01	EBTB	schizophrenia	35	M				95.25	95.61			39.08	36.19		0.47	0.21
ES02	EBTB	control	51	F	6.3			93.19	94.95	93.71	55.62	48.41		0.38	0.48	0.14
ES03	EBTB	control	62	M	6.4			94.21	95.47	94.99	49.51	52.14	51.47	6.61E-05	0.50	0.04
ES04	EBTB	control	55	M	6.63			94.22	94.15	94.08	47.99	49.13	45.87	0.46	0.49	0.27
ES05	EBTB	schizophrenia	25	M	6.4			95.48	95.25	95.04	18.25	31.21	21.55	0.10	0.49	0.24
ES06	EBTB	schizophrenia	42	F	6.69			95.04	94.89	96.28	33.79	42.01	39.24	0.16	0.48	0.15
ES07	EBTB	schizophrenia	42	M	6.51				95.12	94.21		40.47	46.48		0.39	0.16
ES09	EBTB	schizophrenia	18	M	6.38			94.63	95.58	95.53	15.97	24.82	18.62	0.02	0.39	0.18
ES10	EBTB	control	45	M	6.4			94.93	95.01	95.18	38.74	44.70	40.63	0.40	0.49	0.01
ES11	EBTB	schizophrenia	69	M	6.1			93.91	93.60	95.67	55.26	57.78	45.04	0.37	0.49	0.25
ES12	EBTB	schizophrenia	41	M	6.4			95.04	94.14	94.57	36.08	38.27	34.15	0.17	0.15	0.18
ES13	EBTB	control	37	M	6.4			94.28	94.50	95.40	39.14	45.98	45.34	0.32	0.17	0.05
ES14	EBTB	control	25	M	5.9			94.97	95.02	95.52	25.17	23.34	20.31	6.61E-05	0.16	0.22
ES15	EBTB	control	49	M	6.4			93.86	94.69	94.67	46.08	46.90	56.12	0.41	0.14	0.08
ES16	EBTB	control	52	M				94.08	95.33	96.01	21.94	24.42	23.21	0.04	0.11	0.10
ES17	EBTB	control	44	F	6.6			94.89	94.58	95.84	51.75	37.25	46.06	0.38	0.42	0.10
ES18	EBTB	schizophrenia	42	M	6.4			94.26	94.48	94.85	40.15	31.39	39.24	0.34	0.14	0.08

Supplementary Table 2. Sentrix barcode ID information for all samples included in this thesis. Shown are the Illumina Infinium HumanMethylation450 BeadChip (450K) sentrix barcode IDs and the criteria for exclusion from analyses for a few samples. LNDBB, MRC London Neurodegenerative Diseases Brain Bank; DBCBB, Douglas-Bell Canada Brain Bank; PFC, prefrontal cortex; STR, striatum; HC, hippocampus; CER, cerebellum; QC, quality control.

Individual	Brain Bank	Group	PFC 450K Barcode	PFC analysis	CER 450K Barcode	CER analysis	STR 450K Barcode	STR analysis	HC 450K Barcode	HC analysis	Genotyping array barcode	Polygenic risk score analysis
1	LNDBB	schizophrenia	6055432012_R04C02		6042316042_R03C01		9647450064_R04C01		9553932139_R05C01		7942519024_R03C01	
2	LNDBB	schizophrenia	6055432012_R06C01		6042316047_R02C01		9647450027_R06C02		9554599085_R01C01		7942519024_R02C02	
3	LNDBB	schizophrenia	6055432012_R01C02		6042316024_R06C02		9647450035_R06C01		9554599085_R03C01		7942519009_R02C01	
4	LNDBB	schizophrenia	6055432012_R01C01		6042316042_R05C01		9647450081_R05C01		9554599085_R06C01		7942519009_R05C02	
5	LNDBB	schizophrenia	6055432066_R02C01		6042316024_R03C01		9647450100_R02C02	failed	9588557069_R02C01	450K QC	7930649111_R01C01	
6	LNDBB	schizophrenia	6055432029_R02C02		6042316031_R03C02		9647455018_R02C02		9554599066_R03C02		7942519009_R03C01	excluded based on ethnicity
7	LNDBB	schizophrenia	6055432060_R03C01		6042316024_R04C01		9647455027_R01C01				7930649111_R04C02	
8	LNDBB	schizophrenia	6055432012_R04C01	failed 450K QC	6042316024_R04C02		9647455027_R04C02				7942519009_R04C02	excluded based on ethnicity
9	LNDBB	schizophrenia	6055432066_R01C02		6042316031_R05C02		9647450100_R03C01		9553932139_R03C01		7942519009_R01C01	
10	LNDBB	schizophrenia	6055432060_R04C02		6042316024_R02C02		9647450035_R04C02		9554599085_R02C02		7942519009_R04C01	
11	LNDBB	schizophrenia	6055432066_R05C02		6042316024_R02C01		9647450102_R03C02		9554599085_R02C01		7930649095_R06C01	
12	LNDBB	schizophrenia	6055432012_R02C01	failed bisulfite conversion	6042316024_R01C01		9647450035_R05C02		9554599066_R04C01		9933568129_R04C02	excluded based on ethnicity
13	LNDBB	schizophrenia	6055432060_R05C02	failed pyrosequencing	6042316042_R05C02		9647450064_R06C01		9588557069_R03C02		7930649111_R03C02	
14	LNDBB	schizophrenia	6055432066_R03C02		6042316031_R01C01		9647450064_R01C02				7930649111_R03C01	
15	LNDBB	schizophrenia	6055432060_R03C02		6042316047_R03C02		9647455018_R03C02				7930649095_R03C02	

16	LNDBB	schizophrenia	6055432029_R05C01	failed pyrosequencing	6042316031_R06C01	9647450100_R05C01	9554599085_R04C02	7942519009_R06C02	
17	LNDBB	schizophrenia	6055432012_R03C01		6042316024_R05C02	9647450102_R02C02	7942519024_R06C02	7942519024_R06C02	
18	LNDBB	schizophrenia	6055432029_R04C01		6042316042_R04C02	964745081_R06C02	9554599066_R04C02	7942519024_R04C02	
19	LNDBB	schizophrenia	6055432060_R04C01		6042316031_R02C01	964745089_R03C02	9554599085_R06C02	7942519024_R05C01	
20	LNDBB	schizophrenia	6055432029_R03C02		6042316031_R04C02	9647450100_R01C01	7930649095_R05C02	7930649095_R05C02	
21	LNDBB	schizophrenia	6055432066_R06C01	47,XXY	6042316047_R01C02	9588557055_R05C02	47,XXY	7930649095_R01C01	47,XXY
23	LNDBB	schizophrenia	6055432066_R04C02		6042316031_R02C02	964745081_R03C02	9553932139_R02C02	7942519009_R01C02	excluded based on ethnicity
24	LNDBB	schizophrenia	6055432066_R01C01		6042316024_R03C02	failed 450K QC	9588557069_R04C01	7942519024_R01C01	excluded based on ethnicity
25	LNDBB	control	6055432012_R06C02		6042316042_R01C02	964745027_R05C02	9588557069_R05C02	7930649095_R05C01	
26	LNDBB	control	6055432012_R03C02		6042316031_R03C01	964745081_R04C01	7930649095_R03C01	7930649095_R03C01	excluded based on ethnicity
27	LNDBB	control				964745018_R04C02	9553932139_R01C02	9933568081_R07C01	
28	LNDBB	control	6055432012_R05C01		6042316047_R06C01	9647450102_R06C02	7930649095_R04C02	7930649095_R04C02	
29	LNDBB	control				9588557063_R02C01			not run
30	LNDBB	control	6055432060_R05C01		6042316024_R06C01	964745018_R05C01	9588557069_R06C01	7942519009_R02C02	
31	LNDBB	control	6055432029_R02C01		6042316042_R06C02	964745089_R04C01		7942519009_R06C01	
32	LNDBB	control	6055432066_R05C01		6042316047_R05C01	9647450102_R05C01		7930649111_R05C02	
33	LNDBB	control	6055432066_R04C01		6042316042_R02C02	964745018_R05C02	9588557069_R01C01	7930649095_R02C01	
34	LNDBB	control	6055432012_R05C02		6042316031_R06C02	964745081_R01C01	9554599085_R05C01	9933568081_R04C01	
35	LNDBB	control	6055432029_R03C01		6042316047_R05C02	9647450064_R02C01		7942519024_R01C02	
36	LNDBB	control				9588557063_R06C01		9933568129_R06C02	
37	LNDBB	control	6055432012_R02C02		6042316024_R05C01	9647450035_R05C01		7930649111_R02C01	
38	LNDBB	control	6055432066_R02C02		6042316047_R04C02	9647450102_R01C02	9554599085_R03C02	7942519024_R06C01	
39	LNDBB	control	6055432066_R03C01	failed bisulfite conversion	6042316031_R01C02	9647450035_R01C02		9933568129_R11C02	excluded based on ethnicity

40	LNDBB	control	6055432060_R02C02	6042316047_R04C01	9647450100_R02C01	9554599066_R01C02	7930649095_R02C02	excluded based on ethnicity
41	LNDBB	control	6055432060_R06C01	6042316042_R04C01	9588557063_R03C01	9588557069_R02C02	7942519024_R05C02	
42	LNDBB	control	6055432060_R01C01	6042316031_R05C01	9647450102_R05C02	9588557069_R02C02	7930649095_R04C01	
43	LNDBB	control			9588557063_R01C02		9933568081_R08C01	
44	LNDBB	control	6055432060_R06C02	6042316031_R04C01	9647450035_R03C01		7930649111_R06C02	
45	LNDBB	control	6055432029_R01C02	6042316042_R03C02	9647450035_R02C01		7930649111_R01C02	
46	LNDBB	control	6055432029_R04C02	6042316042_R01C01			7930649111_R05C01	
47	LNDBB	control	6055432029_R05C02	6042316042_R02C01	9647455027_R04C01		7942519009_R03C02	excluded based on ethnicity
49	LNDBB	control	6055432060_R01C02	6042316024_R01C02	9647455081_R04C02	9554599066_R02C02	7930649095_R01C02	
50	LNDBB	control			9647450064_R05C01	9554599085_R05C02	9933568081_R11C01	
51	LNDBB	control	6055432029_R06C01	6042316042_R06C01	9647450100_R04C01	9553932139_R04C01	7930649111_R04C01	
52	LNDBB	control	6055432060_R02C01	6042316047_R01C01	9647455089_R02C01		7942519024_R02C01	
53	LNDBB	control	6055432029_R06C02	6042316047_R02C02	9647450102_R02C01	9588557069_R06C02	7942519024_R04C01	
54	LNDBB	control	6055432029_R01C01		9647450102_R04C02	9588557069_R04C02	7930649111_R02C02	
ES01	EBTB	schizophrenia		cohort excluded	cohort excluded			not run
ES02	EBTB	control	9647455034_R03C01	9553932139_R03C02	9588557063_R04C01	9554599066_R06C01		not run
ES03	EBTB	control	9647455034_R03C02	9647455007_R03C01		9554599066_R05C02		not run
ES04	EBTB	control	9647455036_R05C01	9647455007_R05C02	9647455089_R04C02	9554599066_R05C02		not run
ES05	EBTB	schizophrenia	9647455036_R06C01	9647450027_R05C02	9647455027_R03C01	9554599066_R06C02		not run
ES06	EBTB	schizophrenia	9647455036_R01C02	9647450019_R06C02	9647455027_R02C02	9553932139_R01C01		not run
ES07	EBTB	schizophrenia		cohort excluded	cohort excluded			not run
ES09	EBTB	schizophrenia	9647450066_R06C01	9647455007_R05C01	9647455081_R03C01	9553932139_R06C01		not run
ES10	EBTB	control	9647450049_R06C01	9647455007_R06C01	9647455018_R01C01	9554599066_R02C01		not run
ES11	EBTB	schizophrenia	9647450049_R06C02	9647450019_R03C02	9647455089_R02C02	9588557069_R05C01		not run
ES12	EBTB	schizophrenia	9647455036_R02C01	9647455007_R02C01	9647450035_R04C01	9588557069_R01C02		not run
				cohort excluded	cohort excluded	9554599066_R01C01		not run

ES13	EBTB	control	9647455036_R04C01	cohort excluded	9647450027_R01C01	cohort excluded	9647455027_R01C02	cohort excluded	9553932139_R02C01	cohort excluded	9933568081_R02C01	not run
ES14	EBTB	control	9647450066_R03C02	cohort excluded	9647450013_R03C02	cohort excluded	9647455018_R02C01	cohort excluded	9554599085_R01C02	cohort excluded	9933568129_R11C01	not run
ES15	EBTB	control	9647455034_R02C02	cohort excluded	9647450019_R02C02	cohort excluded	9647455089_R05C02	cohort excluded	9554599066_R05C01	cohort excluded	9933568157_R06C02	not run
ES16	EBTB	control	9647450049_R03C02	cohort excluded	9647450019_R02C01	cohort excluded	9647455018_R06C01	cohort excluded	9588557069_R03C01	cohort excluded	9933568129_R03C01	not run
ES17	EBTB	control	9647450066_R05C02	cohort excluded	9647450027_R05C01	cohort excluded	9647455089_R01C02	cohort excluded	9554599066_R03C01	cohort excluded	9933568129_R09C01	not run
ES18	EBTB	schizophrenia	9647450049_R04C01	cohort excluded	9647455007_R01C02	cohort excluded	9647455027_R03C02	cohort excluded	9554599085_R04C01	cohort excluded	9933568129_R08C01	not run
MS01	DBCBB	schizophrenia	9647450049_R03C01		9647450027_R06C01		9647450035_R01C01					
MS02	DBCBB	schizophrenia	9647455034_R06C02				9647455089_R03C01					
MS03	DBCBB	schizophrenia	9647450066_R06C02		9647455007_R02C02		9647450064_R03C01					
MS04	DBCBB	schizophrenia	9647450066_R01C02		9647450013_R02C02		9647455027_R05C01					
MS05	DBCBB	control	9647455034_R01C01		9647450019_R04C02		9647450035_R02C02					
MS06	DBCBB	schizophrenia	9647455034_R05C01		9647450013_R05C02		9647450064_R04C02					
MS07	DBCBB	schizophrenia	9647455036_R03C01		9647450019_R05C02		9647450100_R03C02	failed bisulfite conversion				
MS08	DBCBB	control	9647450049_R01C01		9647450027_R02C01		9647450035_R03C02					
MS09	DBCBB	control	9647455036_R01C01		9647450013_R04C02		9647455027_R02C01					
MS10	DBCBB	control	9647450049_R02C02		9647450019_R06C01		9647450064_R02C02					
MS11	DBCBB	schizophrenia	9647455034_R01C02		9647450013_R01C01		9647450102_R06C01	failed 450K QC				
MS12	DBCBB	schizophrenia	9647450066_R05C01		9647450019_R05C01		9647455089_R05C01					
MS13	DBCBB	control	9647455036_R04C02		9647455007_R01C01		9647450102_R03C01					
MS14	DBCBB	control	9647450066_R02C02		9647450013_R06C02		9647455081_R02C01					excluded based on ethnicity
MS15	DBCBB	control	9647455034_R05C02	failed pyrosequencing	9647450013_R06C01		9647450100_R05C02					
MS16	DBCBB	control			9647450027_R03C01		9647450064_R03C02					
MS17	DBCBB	control	9647450066_R02C01		9647450013_R04C01		9647455027_R06C01					
MS18	DBCBB	schizophrenia	9647455036_R02C02		9647450019_R01C01		9647450100_R06C02					

MS19	DBCBB	control		9553932139_R04C02	964745081_R05C02	9933568081_R06C01
MS20	DBCBB	schizophrenia	9647450066_R04C01	9647455007_R03C02	9647455018_R03C01	9933568129_R01C01
MS21	DBCBB	schizophrenia	9647450049_R04C02	9647450019_R01C02	9647450100_R01C02	9933568081_R10C01
MS22	DBCBB	control	9588557063_R01C01	9553932139_R05C02	9588557063_R05C01	9933568129_R07C02
MS23	DBCBB	schizophrenia	9647450049_R05C01	9647450019_R04C01	964745081_R02C02	9933568129_R10C02
MS24	DBCBB	control	9647455034_R06C01	9647450027_R03C02	9647450100_R04C02	9933568081_R09C01
MS25	DBCBB	schizophrenia	9647455036_R05C02	9647450027_R02C02	9647450102_R01C01	9933568157_R05C02
MS26	DBCBB	control	9647455036_R06C02	9647455007_R04C01	9647455018_R04C01	9933568157_R08C02
MS27	DBCBB	schizophrenia	9647455034_R02C01	9647450027_R01C02	9647455089_R01C01	9933568157_R07C02
MS28	DBCBB	schizophrenia	9647455034_R04C02	9647450013_R02C01	9647450064_R06C02	9933568081_R03C01
MS29	DBCBB	schizophrenia	9647455034_R04C01	9647450019_R03C01	9647450102_R04C01	9933568157_R09C02
MS30	DBCBB	schizophrenia	9647455036_R03C02	9647450013_R01C02	9647450064_R01C01	9933568157_R10C02
MS31	DBCBB	control	9647450066_R01C01	9647455007_R06C02	9647455089_R06C02	9933568129_R01C02
MS32	DBCBB	schizophrenia	9647450066_R04C02	9647450027_R06C02	9647455081_R06C01	9933568129_R05C01
MS33	DBCBB	control	9647450049_R01C02	9553932139_R06C02	9647450064_R05C02	9933568081_R01C01
MS34	DBCBB	control	9647450049_R05C02	9647450027_R04C02	9647455081_R01C02	9933568157_R11C02
MS35	DBCBB	control	9647450049_R02C01	9647450027_R04C01	9647455018_R06C02	9933568129_R12C01
MS36	DBCBB	control	9647450066_R03C01	9647450013_R03C01	9647450035_R06C02	9933568129_R05C02

failed
pyrosequencing

reported
sex

47,XXY

47,XXY

47,XXY

failed QC

Supplementary Table 3. Tissue prediction results for all samples included in Chapter 3 part 1. Shown is the first part of the tissue prediction results using the online DNA methylation age calculator (Horvath, 2016).

Individual	Brain Bank	Group	450K Barcode	Age	Brain region	Sex	Predicted sex	Predicted tissue	Probability from Brain Cerebellum	Probability from Brain frontal cortex	Probability from Brain Occipital Cortex	Probability from Brain PONS	Probability from Brain Prefrontal cortex	Probability from Brain temporal cortex
MS19	DBCBB	control	9553932139_R04C02	72	CER	female	female	Brain CRBLM	0.16	0.55	6.00E-03	0	8.00E-03	0
MS22	DBCBB	control	9553932139_R05C02	37	CER	male	male	Brain CRBLM	0.16	0.54	4.00E-03	4.00E-03	8.00E-03	4.00E-03
MS33	DBCBB	control	9553932139_R06C02	66	CER	male	male	Brain CRBLM	0.15	0.58	6.00E-03	2.00E-03	4.00E-03	8.00E-03
MS11	DBCBB	schizophrenia	9647450013_R01C01	29	CER	male	male	Brain CRBLM	0.15	0.46	2.00E-03	8.00E-03	0.02	0
MS30	DBCBB	schizophrenia	9647450013_R01C02	32	CER	male	male	Brain CRBLM	0.17	0.51	2.00E-03	6.00E-03	6.00E-03	4.00E-03
MS28	DBCBB	schizophrenia	9647450013_R02C01	29	CER	male	male	Brain CRBLM	0.17	0.47	2.00E-03	2.00E-03	0.01	4.00E-03
MS04	DBCBB	schizophrenia	9647450013_R02C02	60	CER	female	female	Brain CRBLM	0.17	0.53	6.00E-03	4.00E-03	6.00E-03	2.00E-03
MS36	DBCBB	control	9647450013_R03C01	69	CER	male	male	Brain CRBLM	0.17	0.48	2.00E-03	8.00E-03	8.00E-03	0
MS17	DBCBB	control	9647450013_R04C01	30	CER	male	male	Brain CRBLM	0.18	0.43	4.00E-03	6.00E-03	0.01	2.00E-03
MS09	DBCBB	control	9647450013_R04C02	50	CER	female	female	Brain CRBLM	0.16	0.49	2.00E-03	2.00E-03	8.00E-03	6.00E-03
MS06	DBCBB	schizophrenia	9647450013_R05C02	51	CER	female	female	Brain CRBLM	0.17	0.48	4.00E-03	6.00E-03	0.01	2.00E-03
MS15	DBCBB	control	9647450013_R06C01	26	CER	male	male	Brain CRBLM	0.19	0.47	6.00E-03	2.00E-03	0.01	6.00E-03
MS14	DBCBB	control	9647450013_R06C02	28	CER	male	male	Brain CRBLM	0.17	0.48	2.00E-03	4.00E-03	0.01	6.00E-03
MS18	DBCBB	schizophrenia	9647450019_R01C01	69	CER	male	male	Brain CRBLM	0.17	0.48	2.00E-03	2.00E-03	0.01	0
MS21	DBCBB	schizophrenia	9647450019_R01C02	39	CER	male	male	Brain CRBLM	0.18	0.51	2.00E-03	0.01	8.00E-03	8.00E-03
MS29	DBCBB	schizophrenia	9647450019_R03C01	33	CER	male	reported sex	failed reported sex	failed reported sex	failed reported sex	failed reported sex	failed reported sex	failed reported sex	failed reported sex
MS23	DBCBB	schizophrenia	9647450019_R04C01	47	CER	male	male	Brain CRBLM	0.18	0.45	4.00E-03	4.00E-03	0.02	4.00E-03
MS05	DBCBB	control	9647450019_R04C02	57	CER	female	female	Brain CRBLM	0.17	0.47	6.00E-03	6.00E-03	0.01	2.00E-03
MS12	DBCBB	schizophrenia	9647450019_R05C01	24	CER	male	male	Brain CRBLM	0.19	0.47	0	6.00E-03	0.01	6.00E-03
MS07	DBCBB	schizophrenia	9647450019_R05C02	50	CER	male	male	Brain CRBLM	0.18	0.48	2.00E-03	2.00E-03	0.01	0
MS10	DBCBB	control	9647450019_R06C01	43	CER	male	male	Brain CRBLM	0.17	0.52	4.00E-03	4.00E-03	0.01	6.00E-03
MS27	DBCBB	schizophrenia	9647450027_R01C02	26	CER	male	male	Brain CRBLM	0.16	0.47	4.00E-03	4.00E-03	0.01	6.00E-03
MS08	DBCBB	control	9647450027_R02C01	57	CER	male	male	Brain CRBLM	0.18	0.48	6.00E-03	8.00E-03	8.00E-03	4.00E-03
MS25	DBCBB	schizophrenia	9647450027_R02C02	65	CER	male	male	Brain CRBLM	0.17	0.45	4.00E-03	8.00E-03	8.00E-03	4.00E-03
MS16	DBCBB	control	9647450027_R03C01	70	CER	male	male	Brain CRBLM	0.16	0.52	2.00E-03	2.00E-03	2.00E-03	4.00E-03
MS24	DBCBB	control	9647450027_R03C02	48	CER	male	47,XXY	47,XXY	47,XXY	47,XXY	47,XXY	47,XXY	47,XXY	47,XXY
MS35	DBCBB	control	9647450027_R04C01	32	CER	male	male	Brain CRBLM	0.17	0.49	4.00E-03	6.00E-03	0.02	4.00E-03
MS34	DBCBB	control	9647450027_R04C02	21	CER	male	male	Brain CRBLM	0.18	0.45	0	0	8.00E-03	2.00E-03
MS01	DBCBB	schizophrenia	9647450027_R06C01	70	CER	male	male	Brain CRBLM	0.18	0.52	6.00E-03	0	8.00E-03	8.00E-03
MS32	DBCBB	schizophrenia	9647450027_R06C02	54	CER	male	male	Brain CRBLM	0.16	0.47	4.00E-03	2.00E-03	8.00E-03	2.00E-03
MS13	DBCBB	control	9647450007_R01C01	44	CER	male	male	Brain CRBLM	0.11	0.47	6.00E-03	8.00E-03	0.03	0.01
MS03	DBCBB	schizophrenia	9647450007_R02C02	30	CER	male	male	Brain CRBLM	0.17	0.44	6.00E-03	4.00E-03	8.00E-03	8.00E-03
MS20	DBCBB	schizophrenia	9647450007_R03C02	38	CER	male	male	Brain CRBLM	0.2	0.48	2.00E-03	6.00E-03	4.00E-03	4.00E-03
MS26	DBCBB	control	9647450007_R04C01	41	CER	male	male	Brain CRBLM	0.16	0.52	4.00E-03	8.00E-03	0.01	6.00E-03
MS31	DBCBB	control	9647450007_R06C02	33	CER	male	male	Brain CRBLM	0.16	0.48	8.00E-03	8.00E-03	0.02	8.00E-03
ES01	EBTB	schizophrenia	9553932139_R03C02	35	CER	male	male	Brain CRBLM	0.18	0.47	4.00E-03	0.01	6.00E-03	4.00E-03

ES14	EBTB	control	schizophrenia	9647450013_R03C02	25	CER	male	failed	failed 450K QC	0.02	0.02	0.04	0.02	0.17	0.07	0.03
ES12	EBTB	schizophrenia	control	9647450013_R05C01	41	CER	male	failed	failed 450K QC	0.01	0.01	0.05	0.05	0.18	0.05	0.03
ES16	EBTB	control	control	9647450019_R02C01	52	CER	male	failed	failed 450K QC	0.01	0.01	0.04	0.05	0.19	0.05	0.02
ES15	EBTB	control	control	9647450019_R02C02	49	CER	male	failed	failed 450K QC	0.02	0.02	0.05	0.03	0.17	0.05	0.02
ES10	EBTB	control	control	9647450019_R03C02	45	CER	male	failed	failed 450K QC	0.17	0.17	0.07	0.01	0.01	6.00E-03	2.00E-03
ES05	EBTB	schizophrenia	control	9647450019_R06C02	25	CER	male	failed	failed 450K QC	0.16	0.16	0.05	4.00E-03	4.00E-03	8.00E-03	8.00E-03
ES13	EBTB	control	control	9647450027_R01C01	37	CER	male	failed	failed 450K QC	0.02	0.02	0.07	0.02	0.21	0.04	0.03
ES17	EBTB	control	control	9647450027_R05C01	44	CER	female	failed	failed 450K QC	0.13	0.13	0.05	6.00E-03	8.00E-03	0.03	0.01
ES04	EBTB	control	control	9647450027_R05C02	55	CER	male	failed	failed 450K QC	0.17	0.17	0.05	6.00E-03	6.00E-03	6.00E-03	2.00E-03
ES18	EBTB	schizophrenia	control	9647455007_R01C02	42	CER	male	failed	failed 450K QC	0.01	0.01	0.04	0.03	0.18	0.06	0.03
ES11	EBTB	schizophrenia	control	9647455007_R02C01	69	CER	male	failed	failed 450K QC	0.16	0.16	0.07	4.00E-03	2.00E-03	0.01	8.00E-03
ES02	EBTB	control	control	9647455007_R03C01	51	CER	female	failed	failed 450K QC	0.19	0.19	0.06	4.00E-03	8.00E-03	2.00E-03	6.00E-03
ES06	EBTB	schizophrenia	control	9647455007_R04C02	42	CER	female	failed	failed 450K QC	0.14	0.14	0.07	4.00E-03	4.00E-03	0.02	4.00E-03
ES07	EBTB	schizophrenia	control	9647455007_R05C01	42	CER	male	failed	failed 450K QC	0.11	0.11	0.04	0.02	0.02	0.04	0.01
ES03	EBTB	control	control	9647455007_R05C02	62	CER	male	failed	failed 450K QC	0.18	0.18	0.05	2.00E-03	6.00E-03	8.00E-03	2.00E-03
ES09	EBTB	schizophrenia	control	9647455007_R06C01	18	CER	male	failed	failed 450K QC	0.11	0.11	0.2	0.02	0.03	0.07	4.00E-03
12	LNDBB	schizophrenia	control	6042316024_R01C01	31	CER	male	failed	failed 450K QC	0.15	0.15	0.06	4.00E-03	4.00E-03	0.02	4.00E-03
49	LNDBB	control	control	6042316024_R01C02	69	CER	male	failed	failed 450K QC	0.18	0.18	0.08	2.00E-03	4.00E-03	0.01	4.00E-03
11	LNDBB	schizophrenia	control	6042316024_R02C01	62	CER	male	failed	failed 450K QC	0.16	0.16	0.08	4.00E-03	6.00E-03	6.00E-03	2.00E-03
10	LNDBB	schizophrenia	control	6042316024_R02C02	46	CER	male	failed	failed 450K QC	0.18	0.18	0.05	6.00E-03	4.00E-03	4.00E-03	0
5	LNDBB	schizophrenia	control	6042316024_R03C01	84	CER	female	failed	failed 450K QC	0.15	0.15	0.08	6.00E-03	6.00E-03	0.02	2.00E-03
24	LNDBB	schizophrenia	control	6042316024_R03C02	45	CER	male	failed	failed 450K QC	0.19	0.19	0.05	2.00E-03	2.00E-03	0.02	failed 450K QC
7	LNDBB	schizophrenia	control	6042316024_R04C01	32	CER	female	failed	failed 450K QC	0.1	0.1	0.09	4.00E-03	4.00E-03	0.01	6.00E-03
8	LNDBB	schizophrenia	control	6042316024_R04C02	70	CER	female	failed	failed 450K QC	0.16	0.16	0.08	4.00E-03	2.00E-03	0.01	8.00E-03
37	LNDBB	control	control	6042316024_R05C01	71	CER	male	failed	failed 450K QC	0.13	0.13	0.07	6.00E-03	8.00E-03	0.01	2.00E-03
17	LNDBB	schizophrenia	control	6042316024_R05C02	75	CER	female	failed	failed 450K QC	0.14	0.14	0.08	4.00E-03	2.00E-03	0.02	4.00E-03
30	LNDBB	control	control	6042316024_R06C01	68	CER	female	failed	failed 450K QC	0.19	0.19	0.06	4.00E-03	4.00E-03	0.01	4.00E-03
3	LNDBB	schizophrenia	control	6042316024_R06C02	69	CER	female	failed	failed 450K QC	0.16	0.16	0.08	4.00E-03	2.00E-03	0.01	4.00E-03
39	LNDBB	schizophrenia	control	6042316031_R01C01	62	CER	male	failed	failed 450K QC	0.16	0.16	0.06	6.00E-03	4.00E-03	0.02	4.00E-03
19	LNDBB	schizophrenia	control	6042316031_R02C01	49	CER	male	failed	failed 450K QC	0.15	0.15	0.06	4.00E-03	4.00E-03	0.01	2.00E-03
23	LNDBB	schizophrenia	control	6042316031_R02C02	64	CER	male	failed	failed 450K QC	0.17	0.17	0.07	2.00E-03	2.00E-03	0.02	2.00E-03
26	LNDBB	control	control	6042316031_R03C01	49	CER	male	failed	failed 450K QC	0.14	0.14	0.06	4.00E-03	4.00E-03	0.02	0
6	LNDBB	schizophrenia	control	6042316031_R03C02	87	CER	male	failed	failed 450K QC	0.17	0.17	0.06	2.00E-03	0.02	0.02	0
44	LNDBB	control	control	6042316031_R04C01	96	CER	female	failed	failed 450K QC	0.18	0.18	0.07	0.01	4.00E-03	0.01	6.00E-03
20	LNDBB	schizophrenia	control	6042316031_R04C02	71	CER	female	failed	failed 450K QC	0.18	0.18	0.07	4.00E-03	6.00E-03	0.01	2.00E-03
42	LNDBB	control	control	6042316031_R05C01	67	CER	male	failed	failed 450K QC	0.15	0.15	0.07	2.00E-03	4.00E-03	0.01	6.00E-03
9	LNDBB	schizophrenia	control	6042316031_R05C02	49	CER	female	failed	failed 450K QC	0.17	0.17	0.07	6.00E-03	4.00E-03	0.02	6.00E-03
16	LNDBB	schizophrenia	control	6042316031_R06C01	75	CER	female	failed	failed 450K QC	0.14	0.14	0.06	2.00E-03	0.01	0.01	2.00E-03
34	LNDBB	control	control	6042316031_R06C02	58	CER	male	failed	failed 450K QC	0.13	0.13	0.07	0	2.00E-03	0.02	2.00E-03
46	LNDBB	control	control	6042316042_R01C01	40	CER	male	failed	failed 450K QC	0.16	0.16	0.08	4.00E-03	8.00E-03	4.00E-03	2.00E-03
25	LNDBB	control	control	6042316042_R01C02	25	CER	male	failed	failed 450K QC	0.18	0.18	0.07	2.00E-03	6.00E-03	0.01	0
47	LNDBB	control	control	6042316042_R02C01	70	CER	male	failed	failed 450K QC	0.16	0.16	0.07	2.00E-03	2.00E-03	0.01	2.00E-03
33	LNDBB	control	control	6042316042_R02C02	57	CER	male	failed	failed 450K QC	0.17	0.17	0.07	0	4.00E-03	0.02	4.00E-03
1	LNDBB	schizophrenia	control	6042316042_R03C01	67	CER	male	failed	failed 450K QC	0.16	0.16	0.08	4.00E-03	4.00E-03	4.00E-03	2.00E-03
45	LNDBB	control	control	6042316042_R03C02	37	CER	male	failed	failed 450K QC	0.14	0.14	0.07	8.00E-03	4.00E-03	0.02	2.00E-03
41	LNDBB	control	control	6042316042_R04C01	76	CER	female	failed	failed 450K QC	0.17	0.17	0.07	6.00E-03	8.00E-03	0.01	8.00E-03
18	LNDBB	schizophrenia	control	6042316042_R04C02	64	CER	male	failed	failed 450K QC	0.18	0.18	0.06	0	4.00E-03	4.00E-03	4.00E-03
4	LNDBB	schizophrenia	control	6042316042_R05C01	76	CER	female	failed	failed 450K QC	0.17	0.17	0.08	2.00E-03	8.00E-03	0.01	2.00E-03

13	LNDBB	schizophrenia	6042316042_R05C02	51	CER	male	Brain CRBLM	0.15	0.48	0.07	6.00E-03	4.00E-03	0.01	2.00E-03
31	LNDBB	control	6042316042_R06C01	48	CER	male	Brain CRBLM	0.16	0.51	0.07	6.00E-03	0	0.02	2.00E-03
31	LNDBB	control	6042316042_R06C02	33	CER	female	Brain CRBLM	0.17	0.49	0.08	4.00E-03	4.00E-03	8.00E-03	2.00E-03
52	LNDBB	control	6042316047_R01C01	80	CER	male	Brain CRBLM	0.14	0.54	0.09	2.00E-03	0	8.00E-03	2.00E-03
21	LNDBB	schizophrenia	6042316047_R01C02	35	CER	male	47_XXY	47_XXY	47_XXY	47_XXY	47_XXY	47_XXY	47_XXY	47_XXY
2	LNDBB	schizophrenia	6042316047_R02C01	79	CER	male	Brain CRBLM	0.15	0.46	0.08	4.00E-03	4.00E-03	0.01	4.00E-03
53	LNDBB	control	6042316047_R02C02	79	CER	male	Brain CRBLM	0.13	0.49	0.06	4.00E-03	2.00E-03	0.01	2.00E-03
15	LNDBB	schizophrenia	6042316047_R03C02	34	CER	female	Brain CRBLM	0.13	0.45	0.07	6.00E-03	0.02	0.02	0.02
40	LNDBB	control	6042316047_R04C01	54	CER	male	Brain CRBLM	0.14	0.48	0.07	8.00E-03	6.00E-03	0.02	2.00E-03
38	LNDBB	control	6042316047_R04C02	95	CER	male	Brain CRBLM	0.17	0.51	0.09	2.00E-03	2.00E-03	8.00E-03	2.00E-03
32	LNDBB	control	6042316047_R05C01	50	CER	male	Brain CRBLM	0.16	0.55	0.07	8.00E-03	2.00E-03	8.00E-03	4.00E-03
35	LNDBB	control	6042316047_R05C02	68	CER	female	Brain CRBLM	0.15	0.52	0.08	2.00E-03	2.00E-03	0.02	4.00E-03
28	LNDBB	control	6042316047_R06C01	82	CER	female	Brain CRBLM	0.14	0.48	0.07	6.00E-03	4.00E-03	0.03	6.00E-03
ES05	EBTB	schizophrenia	9553932139_R01C01	25	HC	male	GliafCell	0.01	0.01	0.05	0.02	0.07	0.08	0.03
ES13	EBTB	control	9553932139_R02C01	37	HC	male	GliafCell	0.01	0.01	0.07	0.04	0.09	0.14	0.06
ES07	EBTB	schizophrenia	9553932139_R06C01	42	HC	male	GliafCell	0.02	0.01	0.07	0.02	0.09	0.11	0.04
ES12	EBTB	schizophrenia	9554599066_R01C01	41	HC	male	GliafCell	0.01	0.02	0.07	0.04	0.09	0.09	0.05
ES09	EBTB	schizophrenia	9554599066_R02C01	18	HC	male	GliafCell	0.02	0.01	0.06	0.03	0.09	0.07	0.04
ES17	EBTB	control	9554599066_R03C01	44	HC	female	GliafCell	2.00E-03	0.01	0.07	0.13	0.03	0.11	0.07
ES15	EBTB	control	9554599066_R05C01	49	HC	male	GliafCell	6.00E-03	0.02	0.03	0.02	0.09	0.06	0.03
ES03	EBTB	control	9554599066_R05C02	62	HC	male	GliafCell	0.01	0.01	0.04	0.02	0.08	0.07	0.02
ES02	EBTB	control	9554599066_R06C01	51	HC	female	GliafCell	0.01	8.00E-03	0.05	0.05	0.08	0.07	0.04
ES04	EBTB	control	9554599066_R06C02	55	HC	male	GliafCell	8.00E-03	0.04	0.04	0.02	0.18	0.13	0.02
ES14	EBTB	control	9554599085_R01C02	25	HC	male	GliafCell	6.00E-03	0.03	0.04	0.04	0.08	0.12	0.04
ES18	EBTB	schizophrenia	9554599085_R04C01	42	HC	male	Neuron	0.01	0.01	0.09	0.11	0.03	0.12	0.07
ES11	EBTB	schizophrenia	9588557069_R01C02	69	HC	male	GliafCell	0.02	0.02	0.06	0.05	0.06	0.09	0.05
ES16	EBTB	control	9588557069_R03C01	52	HC	male	GliafCell	0.01	8.00E-03	0.03	0.02	0.13	0.07	0.03
ES10	EBTB	control	9588557069_R03C02	82	HC	female	GliafCell	0.02	0.02	0.03	0.02	0.07	0.09	0.03
27	LNDBB	control	9553932139_R01C02	64	HC	male	GliafCell	0.01	0.02	0.07	0.04	0.09	0.12	0.05
23	LNDBB	schizophrenia	9553932139_R02C02	64	HC	male	GliafCell	6.00E-03	0.02	0.06	0.05	0.07	0.1	0.06
9	LNDBB	schizophrenia	9553932139_R03C01	49	HC	female	GliafCell	4.00E-03	0.01	0.06	0.02	0.09	0.09	0.03
51	LNDBB	control	9553932139_R04C01	48	HC	male	GliafCell	0.01	0.02	0.05	0.04	0.06	0.09	0.03
1	LNDBB	schizophrenia	9553932139_R05C01	67	HC	male	GliafCell	6.00E-03	0.01	0.08	0.05	0.06	0.14	0.04
49	LNDBB	control	9554599066_R01C02	54	HC	male	GliafCell	8.00E-03	0.02	0.06	0.03	0.09	0.08	0.04
6	LNDBB	schizophrenia	9554599066_R03C02	87	HC	male	GliafCell	8.00E-03	0.01	0.05	0.05	0.08	0.08	0.04
12	LNDBB	schizophrenia	9554599066_R04C02	31	HC	male	GliafCell	0.01	0.03	0.08	0.08	0.07	0.1	0.05
18	LNDBB	schizophrenia	9554599066_R04C01	64	HC	male	GliafCell	4.00E-03	0.01	0.05	0.06	0.07	0.09	0.06
2	LNDBB	schizophrenia	9554599085_R01C01	79	HC	male	GliafCell	8.00E-03	0.01	0.07	0.06	0.08	0.1	0.05
11	LNDBB	schizophrenia	9554599085_R02C01	62	HC	male	GliafCell	0.01	0.02	0.06	0.04	0.08	0.08	0.03
10	LNDBB	schizophrenia	9554599085_R02C02	46	HC	male	GliafCell	0.01	0.01	0.04	0.02	0.17	0.05	0.03
3	LNDBB	schizophrenia	9554599085_R03C01	69	HC	female	GliafCell	0.01	0.02	0.06	0.05	0.04	0.1	0.05
38	LNDBB	control	9554599085_R03C02	95	HC	male	GliafCell	8.00E-03	0.01	0.08	0.06	0.08	0.13	0.05
16	LNDBB	schizophrenia	9554599085_R04C01	75	HC	female	GliafCell	0.01	0.01	0.06	0.03	0.09	0.09	0.03
34	LNDBB	control	9554599085_R05C01	58	HC	male	GliafCell	0.01	0.01	0.05	0.04	0.06	0.08	0.05
50	LNDBB	control	9554599085_R05C02	48	HC	male	GliafCell	8.00E-03	0.01	0.07	0.05	0.07	0.1	0.04
4	LNDBB	schizophrenia	9554599085_R06C01	76	HC	male	GliafCell	6.00E-03	0.01	0.07	0.05	0.06	0.1	0.05
19	LNDBB	schizophrenia	9554599085_R06C02	49	HC	female	GliafCell	8.00E-03	0.02	0.07	0.05	0.07	0.1	0.04
21	LNDBB	schizophrenia	9588557055_R06C02	35	HC	male	47_XXY	47_XXY	47_XXY	47_XXY	47_XXY	47_XXY	47_XXY	47_XXY
33	LNDBB	control	9588557069_R01C01	57	HC	male	GliafCell	0.01	0.02	0.05	0.03	0.09	0.08	0.03

ES09	EBTB	schizophrenia	9647450066_R06C01	18	PFC	male	male	GliaCell	0.01	8.00E-03	0.03	0.02	0.02	0.04	0.03
ES15	EBTB	control	9647455034_R02C02	42	PFC	male	male	GliaCell	6.00E-03	0.01	0.08	0.09	0.09	0.1	0.07
ES02	EBTB	control	9647455034_R03C01	51	PFC	female	female	GliaCell	4.00E-03	0.01	0.08	0.11	0.05	0.14	0.06
ES03	EBTB	control	9647455034_R03C02	62	PFC	male	male	GliaCell	6.00E-03	0.01	0.02	0.01	0.06	0.04	0.03
ES06	EBTB	schizophrenia	9647455036_R01C02	42	PFC	female	female	GliaCell	0.01	0.02	0.06	0.05	0.05	0.08	0.05
ES12	EBTB	schizophrenia	9647455036_R02C01	41	PFC	male	male	GliaCell	0.01	0.02	0.07	0.05	0.05	0.09	0.04
ES13	EBTB	control	9647455036_R04C01	37	PFC	male	male	GliaCell	4.00E-03	0.02	0.11	0.09	0.05	0.13	0.05
ES04	EBTB	control	9647455036_R05C01	55	PFC	male	male	GliaCell	8.00E-03	0.01	0.1	0.11	0.03	0.13	0.06
ES05	EBTB	schizophrenia	9647455036_R06C01	25	PFC	male	male	GliaCell	0.01	0.02	0.06	0.03	0.1	0.12	0.05
4	LNDBB	schizophrenia	6055432012_R01C01	76	PFC	female	female	Neuron	4.00E-03	0.01	0.07	0.1	0.02	0.14	0.07
3	LNDBB	schizophrenia	6055432012_R01C02	69	PFC	female	female	GliaCell	2.00E-03	0.02	0.08	0.09	0.02	0.11	0.05
12	LNDBB	schizophrenia	6055432012_R02C01	31	PFC	male	failed	failed bisulfite conversion	failed bisulfite conversion	failed bisulfite conversion	failed bisulfite conversion	failed bisulfite conversion	failed bisulfite conversion	failed bisulfite conversion	failed bisulfite conversion
37	LNDBB	control	6055432012_R02C02	71	PFC	male	male	GliaCell	4.00E-03	8.00E-03	0.07	0.08	0.02	0.1	0.04
17	LNDBB	schizophrenia	6055432012_R03C01	75	PFC	female	female	GliaCell	2.00E-03	0.01	0.07	0.09	0.03	0.11	0.06
26	LNDBB	control	6055432012_R03C02	49	PFC	male	male	GliaCell	2.00E-03	0.01	0.07	0.09	0.03	0.12	0.05
8	LNDBB	schizophrenia	6055432012_R04C01	70	PFC	female	failed	failed 450K QC	failed 450K QC	failed 450K QC	failed 450K QC	failed 450K QC	failed 450K QC	failed 450K QC	failed 450K QC
1	LNDBB	schizophrenia	6055432012_R04C02	67	PFC	male	male	GliaCell	0	8.00E-03	0.08	0.09	0.02	0.12	0.09
28	LNDBB	control	6055432012_R05C01	82	PFC	female	female	GliaCell	8.00E-03	8.00E-03	0.06	0.07	0.04	0.14	0.06
34	LNDBB	control	6055432012_R05C02	58	PFC	male	male	GliaCell	8.00E-03	0.01	0.05	0.09	0.02	0.12	0.07
2	LNDBB	schizophrenia	6055432012_R06C01	79	PFC	male	male	Neuron	2.00E-03	0.01	0.06	0.09	0.02	0.15	0.05
25	LNDBB	control	6055432012_R06C02	25	PFC	male	male	GliaCell	4.00E-03	0.01	0.07	0.11	0.03	0.13	0.06
54	LNDBB	control	6055432029_R01C01	55	PFC	male	male	GliaCell	4.00E-03	0.01	0.06	0.06	0.04	0.19	0.06
45	LNDBB	control	6055432029_R01C02	37	PFC	male	male	Neuron	6.00E-03	0.01	0.08	0.08	0.03	0.13	0.05
31	LNDBB	control	6055432029_R02C01	33	PFC	female	female	GliaCell	2.00E-03	0.01	0.06	0.09	0.04	0.12	0.05
6	LNDBB	schizophrenia	6055432029_R02C02	87	PFC	male	male	GliaCell	4.00E-03	0.02	0.07	0.07	0.02	0.11	0.04
35	LNDBB	control	6055432029_R03C01	68	PFC	female	female	Neuron	0.01	0.02	0.08	0.1	0.03	0.11	0.04
20	LNDBB	schizophrenia	6055432029_R03C02	71	PFC	female	female	Neuron	2.00E-03	4.00E-03	0.08	0.08	0.03	0.11	0.05
18	LNDBB	schizophrenia	6055432029_R03C02	64	PFC	male	male	Neuron	4.00E-03	8.00E-03	0.06	0.08	0.01	0.13	0.07
46	LNDBB	control	6055432029_R04C02	40	PFC	male	male	GliaCell	6.00E-03	6.00E-03	0.06	0.09	0.02	0.09	0.05
16	LNDBB	schizophrenia	6055432029_R05C01	75	PFC	female	female	Neuron	0	6.00E-03	0.05	0.09	0.01	0.12	0.07
47	LNDBB	control	6055432029_R05C02	70	PFC	male	male	Neuron	0	0.02	0.07	0.08	0.02	0.12	0.05
51	LNDBB	control	6055432029_R06C01	48	PFC	male	male	GliaCell	6.00E-03	0.01	0.06	0.09	0.03	0.16	0.06
53	LNDBB	control	6055432029_R06C02	79	PFC	male	male	GliaCell	4.00E-03	0.02	0.07	0.07	0.04	0.18	0.04
42	LNDBB	control	6055432060_R01C01	67	PFC	male	male	GliaCell	0	4.00E-03	0.07	0.09	0.04	0.1	0.05
49	LNDBB	control	6055432060_R01C02	69	PFC	male	male	GliaCell	4.00E-03	0.01	0.1	0.06	0.04	0.13	0.05
52	LNDBB	control	6055432060_R02C01	80	PFC	male	male	GliaCell	8.00E-03	0.01	0.04	0.08	0.02	0.13	0.05
40	LNDBB	control	6055432060_R02C02	54	PFC	male	male	GliaCell	8.00E-03	0.01	0.05	0.08	0.03	0.13	0.05
7	LNDBB	control	6055432060_R03C01	32	PFC	female	female	GliaCell	2.00E-03	0.01	0.07	0.09	0.03	0.14	0.06
15	LNDBB	schizophrenia	6055432060_R03C02	34	PFC	female	female	Neuron	2.00E-03	0.01	0.06	0.1	0.02	0.1	0.06
19	LNDBB	schizophrenia	6055432060_R04C01	49	PFC	male	male	GliaCell	2.00E-03	0.01	0.07	0.07	0.01	0.1	0.06
10	LNDBB	schizophrenia	6055432060_R04C02	46	PFC	male	male	GliaCell	6.00E-03	0.02	0.05	0.07	0.03	0.13	0.05
30	LNDBB	control	6055432060_R05C01	68	PFC	female	female	GliaCell	0.01	4.00E-03	0.06	0.07	0.03	0.14	0.08
13	LNDBB	schizophrenia	6055432060_R05C02	51	PFC	male	male	GliaCell	6.00E-03	0.02	0.06	0.1	0.02	0.13	0.07
41	LNDBB	control	6055432060_R06C01	76	PFC	female	female	GliaCell	8.00E-03	8.00E-03	0.06	0.08	0.03	0.18	0.07
44	LNDBB	control	6055432060_R06C02	96	PFC	female	female	Neuron	2.00E-03	0.02	0.06	0.08	0.03	0.16	0.06
24	LNDBB	schizophrenia	6055432066_R01C01	45	PFC	male	male	GliaCell	4.00E-03	0.01	0.07	0.11	0.03	0.11	0.06
9	LNDBB	schizophrenia	6055432066_R01C02	49	PFC	female	female	Neuron	2.00E-03	0.02	0.06	0.08	0.03	0.12	0.05

5	LNDDB	schizophrenia	PFC	female	GlialCell	0.01	0.07	0.09	0.02	0.09	0.06
38	LNDDB	control	PFC	male	GlialCell	0.03	0.06	0.12	0.04	0.07	0.07
39	LNDDB	control	PFC	male	failed bisulfite conversion	failed bisulfite conversion	failed bisulfite conversion	failed bisulfite conversion	failed bisulfite conversion	failed bisulfite conversion	failed bisulfite conversion
14	LNDDB	schizophrenia	PFC	male	Neuron	8.00E-03	0.07	0.11	0.02	0.11	0.06
33	LNDDB	control	PFC	male	Neuron	0.01	0.07	0.07	0.02	0.08	0.05
23	LNDDB	schizophrenia	PFC	male	GlialCell	2.00E-03	0.07	0.08	0.03	0.13	0.06
32	LNDDB	control	PFC	male	Neuron	0.01	0.09	0.1	0.02	0.12	0.06
11	LNDDB	schizophrenia	PFC	male	GlialCell	6.00E-03	0.07	0.08	0.03	0.17	0.06
21	LNDDB	schizophrenia	PFC	male	47,XXY	47,XXY	47,XXY	47,XXY	47,XXY	47,XXY	47,XXY
MS22	DBCBB	control	STR	male	GlialCell	4.00E-03	0.06	0.06	0.01	0.1	0.05
MS01	DBCBB	schizophrenia	STR	male	GlialCell	2.00E-03	0.03	0.05	0.08	0.07	0.04
MS05	DBCBB	control	STR	female	GlialCell	8.00E-03	0.06	0.08	0.05	0.1	0.03
MS08	DBCBB	control	STR	male	GlialCell	8.00E-03	0.04	0.06	0.06	0.11	0.06
MS36	DBCBB	control	STR	male	GlialCell	8.00E-03	0.05	0.04	0.09	0.11	0.04
MS30	DBCBB	schizophrenia	STR	male	GlialCell	8.00E-03	0.07	0.04	0.07	0.06	0.06
MS10	DBCBB	control	STR	male	GlialCell	0.01	0.09	0.04	0.05	0.1	0.04
MS03	DBCBB	schizophrenia	STR	male	GlialCell	8.00E-03	0.07	0.05	0.06	0.11	0.05
MS16	DBCBB	control	STR	male	GlialCell	0.01	0.03	0.04	0.06	0.1	0.06
MS06	DBCBB	schizophrenia	STR	female	GlialCell	0.02	0.06	0.06	0.06	0.11	0.04
MS33	DBCBB	control	STR	male	GlialCell	2.00E-03	0.01	0.06	0.07	0.08	0.06
MS28	DBCBB	schizophrenia	STR	male	GlialCell	4.00E-03	0.07	0.07	0.05	0.08	0.05
MS21	DBCBB	schizophrenia	STR	male	GlialCell	0.01	0.06	0.06	0.06	0.14	0.04
MS07	DBCBB	schizophrenia	STR	male	failed bisulfite conversion	failed bisulfite conversion	failed bisulfite conversion	failed bisulfite conversion	failed bisulfite conversion	failed bisulfite conversion	failed bisulfite conversion
MS24	DBCBB	control	STR	male	47,XXY	47,XXY	47,XXY	47,XXY	47,XXY	47,XXY	47,XXY
MS15	DBCBB	control	STR	male	GlialCell	0.01	0.05	0.1	0.05	0.1	0.03
MS18	DBCBB	schizophrenia	STR	male	GlialCell	0.01	0.06	0.07	0.05	0.15	0.04
MS25	DBCBB	schizophrenia	STR	male	GlialCell	0.02	0.06	0.04	0.05	0.08	0.03
MS13	DBCBB	control	STR	male	GlialCell	6.00E-03	0.07	0.04	0.09	0.07	0.03
MS29	DBCBB	schizophrenia	STR	male	GlialCell	0.02	0.07	0.06	0.07	0.09	0.05
MS11	DBCBB	schizophrenia	STR	male	failed 450K QC	failed 450K QC	failed 450K QC	failed 450K QC	failed 450K QC	failed 450K QC	failed 450K QC
MS20	DBCBB	schizophrenia	STR	male	GlialCell	8.00E-03	0.06	0.07	0.05	0.1	0.04
MS26	DBCBB	control	STR	male	GlialCell	0.01	0.05	0.05	0.05	0.08	0.04
MS35	DBCBB	control	STR	male	GlialCell	6.00E-03	0.06	0.06	0.06	0.12	0.05
MS09	DBCBB	control	STR	female	GlialCell	0.01	0.08	0.06	0.07	0.08	0.04
MS04	DBCBB	schizophrenia	STR	female	GlialCell	6.00E-03	0.06	0.07	0.06	0.07	0.06
MS17	DBCBB	control	STR	male	GlialCell	0.01	0.04	0.05	0.05	0.1	0.04
MS34	DBCBB	control	STR	male	GlialCell	6.00E-03	0.01	0.08	0.06	0.07	0.06
MS14	DBCBB	control	STR	male	GlialCell	4.00E-03	0.06	0.04	0.07	0.09	0.04
MS23	DBCBB	schizophrenia	STR	male	GlialCell	0.01	0.05	0.06	0.08	0.11	0.04
MS19	DBCBB	control	STR	female	GlialCell	0.01	0.05	0.05	0.03	0.1	0.03
MS32	DBCBB	schizophrenia	STR	male	GlialCell	0.01	0.05	0.06	0.06	0.06	0.03
MS27	DBCBB	schizophrenia	STR	male	GlialCell	0.01	0.06	0.05	0.04	0.12	0.05
MS02	DBCBB	schizophrenia	STR	female	GlialCell	4.00E-03	0.06	0.06	0.06	0.08	0.04
MS12	DBCBB	schizophrenia	STR	male	GlialCell	8.00E-03	0.01	0.05	0.06	0.09	0.03
MS31	DBCBB	control	STR	male	GlialCell	6.00E-03	0.06	0.06	0.05	0.09	0.04

ES01	EBTB	schizophrenia	9588557063_R04C01	35	STR	male	male	GliaCell	0.02	4.00E-03	0.07	0.07	0.12	0.06
ES11	EBTB	schizophrenia	9647450035_R04C01	69	STR	male	male	GliaCell	4.00E-03	6.00E-03	0.09	0.07	0.1	0.06
ES09	EBTB	schizophrenia	9647455018_R01C01	18	STR	male	male	GliaCell	0.01	0.02	0.05	0.05	0.09	0.04
ES06	EBTB	schizophrenia	9647455018_R01C02	42	STR	female	female	GliaCell	0.01	0.01	0.03	0.03	0.09	0.04
ES14	EBTB	control	9647455018_R02C01	25	STR	male	male	GliaCell	0.01	0.01	0.03	0.03	0.09	0.03
ES16	EBTB	control	9647455018_R06C01	52	STR	male	male	GliaCell	0.01	6.00E-03	0.04	0.1	0.11	0.04
ES13	EBTB	control	9647455027_R01C02	37	STR	male	male	GliaCell	0.02	0.01	0.03	0.06	0.05	0.05
ES05	EBTB	schizophrenia	9647455027_R02C02	25	STR	male	male	GliaCell	8.00E-03	8.00E-03	0.07	0.06	0.08	0.06
ES04	EBTB	control	9647455027_R03C01	55	STR	male	male	GliaCell	0.01	0.02	0.06	0.05	0.09	0.07
ES18	EBTB	schizophrenia	9647455027_R03C02	42	STR	male	male	GliaCell	0.01	0.01	0.05	0.07	0.08	0.05
ES07	EBTB	schizophrenia	9647455081_R03C01	42	STR	male	male	GliaCell	0.01	6.00E-03	0.07	0.06	0.07	0.05
ES17	EBTB	control	9647455089_R01C02	44	STR	female	female	GliaCell	0.02	0.01	0.05	0.07	0.08	0.05
ES10	EBTB	control	9647455089_R02C02	45	STR	male	male	GliaCell	2.00E-03	6.00E-03	0.02	0.01	0.05	0.03
ES03	EBTB	control	9647455089_R04C02	62	STR	male	male	GliaCell	0.01	4.00E-03	0.03	0.02	0.04	0.03
ES15	EBTB	control	9647455089_R05C02	49	STR	male	male	GliaCell	0.01	2.00E-03	0.03	0.03	0.06	0.04
ES12	EBTB	schizophrenia	9647455089_R06C01	41	STR	male	male	GliaCell	6.00E-03	6.00E-03	0.06	0.1	0.1	0.04
21	LNDBB	schizophrenia	9588557055_R05C02	35	STR	male	47,XXY	47,XXY	47,XXY	47,XXY	47,XXY	47,XXY	47,XXY	47,XXY
43	LNDBB	control	9588557063_R01C02	70	STR	male	male	GliaCell	0.01	0.01	0.04	0.05	0.11	0.05
29	LNDBB	control	9588557063_R02C01	63	STR	female	female	GliaCell	0.01	0.02	0.05	0.03	0.07	0.03
41	LNDBB	control	9588557063_R03C01	76	STR	female	female	GliaCell	0.01	0.01	0.07	0.06	0.12	0.05
36	LNDBB	control	9588557063_R06C01	86	STR	male	male	GliaCell	0.01	0.02	0.04	0.01	0.07	0.02
39	LNDBB	control	9647450035_R01C02	40	STR	male	male	GliaCell	8.00E-03	0.01	0.05	0.07	0.1	0.05
45	LNDBB	control	9647450035_R02C01	37	STR	male	male	GliaCell	0.01	0.02	0.06	0.02	0.11	0.04
44	LNDBB	control	9647450035_R03C01	96	STR	female	female	GliaCell	0.01	6.00E-03	0.05	0.04	0.07	0.03
10	LNDBB	schizophrenia	9647450035_R04C02	46	STR	male	male	GliaCell	0.01	0.03	0.03	0.03	0.07	0.04
37	LNDBB	control	9647450035_R05C01	71	STR	male	male	GliaCell	0.01	0.01	0.05	0.04	0.08	0.06
12	LNDBB	schizophrenia	9647450035_R05C02	31	STR	male	male	GliaCell	6.00E-03	0.02	0.06	0.02	0.1	0.07
3	LNDBB	schizophrenia	9647450035_R06C01	69	STR	female	female	GliaCell	4.00E-03	8.00E-03	0.03	0.03	0.06	0.03
14	LNDBB	schizophrenia	9647450064_R01C02	62	STR	male	male	GliaCell	0.02	0.01	0.06	0.04	0.07	0.05
35	LNDBB	control	9647450064_R02C01	68	STR	female	female	GliaCell	6.00E-03	8.00E-03	0.09	0.06	0.07	0.05
1	LNDBB	schizophrenia	9647450064_R04C01	67	STR	male	male	GliaCell	0.02	8.00E-03	0.07	0.06	0.09	0.04
50	LNDBB	control	9647450064_R05C01	48	STR	male	male	Neuron	0.01	0.02	0.11	0.08	0.04	0.06
13	LNDBB	schizophrenia	9647450064_R06C01	51	STR	male	male	GliaCell	4.00E-03	0.01	0.06	0.04	0.08	0.07
20	LNDBB	schizophrenia	9647450100_R01C01	71	STR	female	female	GliaCell	0.01	0.01	0.04	0.04	0.09	0.03
40	LNDBB	control	9647450100_R02C01	54	STR	male	male	GliaCell	8.00E-03	0.02	0.06	0.05	0.11	0.05
5	LNDBB	schizophrenia	9647450100_R02C02	84	STR	female	female	GliaCell	0.01	0.02	0.05	0.05	0.09	0.03
9	LNDBB	schizophrenia	9647450100_R03C01	49	STR	female	female	GliaCell	0.02	0.01	0.07	0.1	0.11	0.05
51	LNDBB	control	9647450100_R04C01	48	STR	male	male	GliaCell	0.01	0.02	0.06	0.04	0.1	0.04
16	LNDBB	schizophrenia	9647450100_R05C01	75	STR	female	female	GliaCell	0.02	0.01	0.05	0.05	0.09	0.03
38	LNDBB	control	9647450102_R01C02	95	STR	male	male	GliaCell	0.02	8.00E-03	0.06	0.06	0.09	0.06
53	LNDBB	control	9647450102_R02C01	79	STR	male	male	GliaCell	0.02	0.01	0.09	0.05	0.07	0.05
17	LNDBB	schizophrenia	9647450102_R02C02	75	STR	female	female	GliaCell	0.01	0.01	0.05	0.03	0.09	0.06
11	LNDBB	schizophrenia	9647450102_R03C02	62	STR	male	male	GliaCell	0.02	0.02	0.03	0.03	0.04	0.03
54	LNDBB	control	9647450102_R04C01	55	STR	male	male	GliaCell	4.00E-03	0.01	0.04	0.04	0.06	0.04
32	LNDBB	control	9647450102_R05C01	50	STR	male	male	GliaCell	4.00E-03	0.01	0.07	0.07	0.07	0.04
42	LNDBB	control	9647450102_R05C02	67	STR	male	male	GliaCell	6.00E-03	0.01	0.06	0.06	0.1	0.05
28	LNDBB	control	9647450102_R06C02	82	STR	female	female	GliaCell	8.00E-03	0.01	0.04	0.05	0.08	0.05
6	LNDBB	schizophrenia	9647455018_R02C02	87	STR	male	male	GliaCell	0.01	0.01	0.07	0.06	0.11	0.04
15	LNDBB	schizophrenia	9647455018_R03C02	34	STR	female	female	GliaCell	0.01	0.01	0.06	0.06	0.1	0.04
27	LNDBB	control	9647455018_R04C02	82	STR	female	female	GliaCell	8.00E-03	0.02	0.07	0.05	0.08	0.04

30	LNDBB	control	9647455018_R05C01	68	STR	female	female	GlialCell	0.01	2.00E-03	0.08	0.07	0.03	0.08	0.06
33	LNDBB	control	9647455018_R05C02	57	STR	male	male	GlialCell	6.00E-03	8.00E-03	0.05	0.04	0.05	0.08	0.04
7	LNDBB	schizophrenia	9647455027_R01C01	32	STR	female	female	GlialCell	0.01	0.02	0.06	0.07	0.07	0.11	0.03
47	LNDBB	control	9647455027_R04C01	70	STR	male	male	GlialCell	0.01	0.01	0.02	0.02	0.08	0.03	0.03
8	LNDBB	schizophrenia	9647455027_R04C02	70	STR	female	female	GlialCell	6.00E-03	0.02	0.08	0.07	0.06	0.12	0.06
25	LNDBB	control	9647455027_R06C02	25	STR	male	male	GlialCell	8.00E-03	8.00E-03	0.05	0.06	0.05	0.08	0.04
2	LNDBB	schizophrenia	9647455027_R06C02	79	STR	male	male	GlialCell	8.00E-03	0.01	0.05	0.05	0.16	0.06	0.03
34	LNDBB	control	9647455081_R01C01	58	STR	male	male	GlialCell	0.02	0.02	0.08	0.04	0.07	0.08	0.05
23	LNDBB	schizophrenia	9647455081_R03C02	64	STR	male	male	GlialCell	8.00E-03	8.00E-03	0.1	0.05	0.06	0.09	0.07
26	LNDBB	control	9647455081_R04C01	49	STR	male	male	GlialCell	2.00E-03	0.02	0.09	0.07	0.07	0.07	0.07
49	LNDBB	control	9647455081_R04C02	69	STR	male	male	GlialCell	0.02	0.01	0.09	0.05	0.05	0.1	0.05
4	LNDBB	schizophrenia	9647455081_R05C01	76	STR	female	female	GlialCell	2.00E-03	0.01	0.05	0.02	0.13	0.04	0.03
18	LNDBB	schizophrenia	9647455081_R06C02	64	STR	male	male	GlialCell	0.01	0.01	0.06	0.04	0.05	0.09	0.06
52	LNDBB	control	9647455089_R02C01	80	STR	male	male	GlialCell	0.01	0.01	0.05	0.09	0.09	0.09	0.04
19	LNDBB	schizophrenia	9647455089_R03C02	49	STR	male	male	GlialCell	6.00E-03	4.00E-03	0.08	0.07	0.04	0.08	0.06
31	LNDBB	control	9647455089_R04C01	33	STR	female	female	GlialCell	4.00E-03	0.01	0.05	0.04	0.06	0.09	0.06

Supplementary Table 4. Tissue prediction results for all samples included in Chapter 3 part 2. Shown is the second part of the tissue prediction results using the online DNA methylation age calculator (Horvath, 2016).

Individual	Probability from Vascular Endothelial Umbilical	Probability from Ape whole blood	Probability from Blood CD4 Tcells	Probability from Blood CD4	Probability from Blood CD14	Probability from Blood Cell Types	Probability from Blood Cord	Probability from Blood peripheral blood mononuclear	Probability from Blood whole blood	Probability from Bone	Probability from Breast	Probability from Breast normal	Probability from Buccal	Probability from Cartilage Knee	Probability from Colon	Probability from Dermal fibroblast	Probability from Epidermis	Probability from Fat Adipocytes	Probability from Gastric	Probability from GliCell	Probability from Head Neck	
MS19	6.00E-03	0.02	0	0	0	4.00E-03	2.00E-03	0	2.00E-03	8.00E-03	2.00E-03	2.00E-03	2.00E-03	8.00E-03	0.01	4.00E-03	0	2.00E-03	0.01	6.00E-03	6.00E-03	
MS22	6.00E-03	0.01	2.00E-03	2.00E-03	2.00E-03	6.00E-03	0	4.00E-03	2.00E-03	0.01	4.00E-03	0	0.01	6.00E-03	2.00E-03	2.00E-03	2.00E-03	0	6.00E-03	0.01	0.01	
MS33	0	6.00E-03	2.00E-03	2.00E-03	2.00E-03	8.00E-03	2.00E-03	2.00E-03	2.00E-03	8.00E-03	2.00E-03	6.00E-03	4.00E-03	4.00E-03	4.00E-03	4.00E-03	2.00E-03	0	6.00E-03	0.01	4.00E-03	
MS11	0	0.02	2.00E-03	2.00E-03	2.00E-03	0.01	2.00E-03	2.00E-03	6.00E-03	8.00E-03	0.01	8.00E-03	8.00E-03	0.01	8.00E-03	4.00E-03	0	0	4.00E-03	0.03	8.00E-03	
MS30	2.00E-03	0.01	2.00E-03	0	6.00E-03	0	2.00E-03	4.00E-03	4.00E-03	0.01	8.00E-03	4.00E-03	2.00E-03	0.01	8.00E-03	6.00E-03	0	0	0	0.03	6.00E-03	
MS28	4.00E-03	0.02	2.00E-03	0	0.01	0	2.00E-03	2.00E-03	2.00E-03	4.00E-03	8.00E-03	2.00E-03	4.00E-03	4.00E-03	6.00E-03	6.00E-03	0	0	6.00E-03	0.03	6.00E-03	
MS04	4.00E-03	0.02	0	2.00E-03	0.01	0	0	2.00E-03	2.00E-03	0.01	4.00E-03	2.00E-03	2.00E-03	4.00E-03	6.00E-03	6.00E-03	2.00E-03	0	2.00E-03	0.02	4.00E-03	
MS36	0	0.03	2.00E-03	0	6.00E-03	0	0	4.00E-03	4.00E-03	0.01	4.00E-03	2.00E-03	2.00E-03	8.00E-03	4.00E-03	4.00E-03	2.00E-03	0	2.00E-03	0.03	2.00E-03	
MS17	8.00E-03	0.02	4.00E-03	0	0.01	0	2.00E-03	4.00E-03	4.00E-03	4.00E-03	0.01	2.00E-03	8.00E-03	0.01	8.00E-03	4.00E-03	0	0	2.00E-03	0.05	0.01	
MS09	2.00E-03	0.02	0	0	0.02	0	0	2.00E-03	2.00E-03	8.00E-03	8.00E-03	0	0.01	8.00E-03	0.01	6.00E-03	2.00E-03	0	2.00E-03	0.02	0.01	
MS06	2.00E-03	0.02	2.00E-03	0	0.01	0	4.00E-03	2.00E-03	2.00E-03	8.00E-03	0.01	4.00E-03	0.01	2.00E-03	4.00E-03	2.00E-03	2.00E-03	0	4.00E-03	0.04	6.00E-03	
MS15	2.00E-03	0.01	4.00E-03	0	0.01	0.01	2.00E-03	0	8.00E-03	8.00E-03	0.01	2.00E-03	8.00E-03	0.01	0	2.00E-03	0	0	2.00E-03	0.02	0.01	
MS14	0	0.03	0	2.00E-03	0.02	0	0	0	6.00E-03	0.01	4.00E-03	0	6.00E-03	6.00E-03	6.00E-03	0	2.00E-03	0	6.00E-03	0.02	4.00E-03	
MS18	2.00E-03	0.02	2.00E-03	2.00E-03	0.02	0	4.00E-03	2.00E-03	2.00E-03	8.00E-03	8.00E-03	4.00E-03	4.00E-03	2.00E-03	6.00E-03	2.00E-03	0	0	2.00E-03	0.03	4.00E-03	
MS21	4.00E-03	0.02	0	2.00E-03	0.01	2.00E-03	0	2.00E-03	2.00E-03	6.00E-03	0.01	4.00E-03	0.01	8.00E-03	8.00E-03	4.00E-03	0	0	2.00E-03	0.01	6.00E-03	
MS29	reported sex	failed sex	failed sex	failed sex	failed sex	failed sex	failed sex	failed sex	failed sex	failed sex	failed sex	failed sex	failed sex	failed sex	failed sex	failed sex	failed sex	failed sex	failed sex	failed sex	failed sex	failed sex
MS23	4.00E-03	0.02	0	2.00E-03	0.01	2.00E-03	0	4.00E-03	4.00E-03	6.00E-03	0.01	0	8.00E-03	4.00E-03	6.00E-03	2.00E-03	0	0	6.00E-03	0.03	8.00E-03	
MS05	4.00E-03	0.02	0	0	0.01	0	0	0	6.00E-03	6.00E-03	6.00E-03	4.00E-03	6.00E-03	6.00E-03	4.00E-03	4.00E-03	0	0	4.00E-03	0.03	6.00E-03	
MS12	0	0.02	0	0	0.01	0	0	0	4.00E-03	8.00E-03	8.00E-03	2.00E-03	4.00E-03	4.00E-03	6.00E-03	2.00E-03	0	0	2.00E-03	0.03	0.02	
MS07	0	0.02	2.00E-03	0	0.01	0	0	4.00E-03	4.00E-03	8.00E-03	0.01	2.00E-03	0	8.00E-03	4.00E-03	4.00E-03	0	0	4.00E-03	0.03	4.00E-03	
MS10	0	0.02	0	2.00E-03	8.00E-03	2.00E-03	8.00E-03	4.00E-03	2.00E-03	6.00E-03	0.01	4.00E-03	0.01	8.00E-03	2.00E-03	6.00E-03	0	0	2.00E-03	0.02	4.00E-03	
MS27	4.00E-03	0.01	2.00E-03	0	0.01	0.01	2.00E-03	2.00E-03	2.00E-03	8.00E-03	0.01	0	6.00E-03	4.00E-03	6.00E-03	2.00E-03	2.00E-03	0	2.00E-03	0.02	0.01	
MS08	2.00E-03	0.02	0	0	4.00E-03	2.00E-03	4.00E-03	8.00E-03	8.00E-03	6.00E-03	0.02	0	4.00E-03	4.00E-03	0	0	0	0	2.00E-03	0.03	4.00E-03	
MS25	2.00E-03	0.03	0	2.00E-03	0.01	0	6.00E-03	2.00E-03	2.00E-03	8.00E-03	8.00E-03	4.00E-03	8.00E-03	8.00E-03	2.00E-03	4.00E-03	0	0	2.00E-03	0.02	4.00E-03	
MS16	2.00E-03	0.02	2.00E-03	2.00E-03	0.01	0	2.00E-03	0	2.00E-03	2.00E-03	0.01	4.00E-03	8.00E-03	8.00E-03	4.00E-03	4.00E-03	2.00E-03	0	2.00E-03	0.02	4.00E-03	

30	0.01	0.02	0	0	8.00E-03	4.00E-03	2.00E-03	4.00E-03	6.00E-03	0.01	2.00E-03	8.00E-03	6.00E-03	6.00E-03	6.00E-03	2.00E-03	0	4.00E-03	0.02	0.01
3	4.00E-03	0.01	0	0	6.00E-03	2.00E-03	2.00E-03	8.00E-03	8.00E-03	0.01	6.00E-03	0	6.00E-03	4.00E-03	8.00E-03	2.00E-03	0	4.00E-03	0.02	0.01
14	2.00E-03	0.02	0	0	6.00E-03	0	0	4.00E-03	6.00E-03	2.00E-03	0	6.00E-03	4.00E-03	6.00E-03	6.00E-03	0	0	2.00E-03	0.02	2.00E-03
39	4.00E-03	8.00E-03	2.00E-03	0	0.01	0	4.00E-03	2.00E-03	2.00E-03	0.01	8.00E-03	4.00E-03	4.00E-03	2.00E-03	0.01	4.00E-03	0	0.01	0.04	0.01
19	4.00E-03	0.01	2.00E-03	0	8.00E-03	0.01	0	4.00E-03	2.00E-03	6.00E-03	2.00E-03	8.00E-03	4.00E-03	4.00E-03	4.00E-03	2.00E-03	0	6.00E-03	0.02	8.00E-03
23	4.00E-03	0.02	2.00E-03	0	8.00E-03	2.00E-03	4.00E-03	2.00E-03	2.00E-03	0.01	6.00E-03	2.00E-03	4.00E-03	4.00E-03	4.00E-03	2.00E-03	2.00E-03	8.00E-03	0.03	0.01
26	4.00E-03	8.00E-03	2.00E-03	0	0.01	0	4.00E-03	0	4.00E-03	0.01	4.00E-03	0	8.00E-03	0.01	4.00E-03	0	0	4.00E-03	0.04	2.00E-03
6	2.00E-03	0.02	2.00E-03	0	4.00E-03	0	0	6.00E-03	8.00E-03	4.00E-03	0	0.01	4.00E-03	2.00E-03	2.00E-03	0	4.00E-03	2.00E-03	0.02	0.01
44	0	0.02	4.00E-03	0	4.00E-03	0	0	8.00E-03	4.00E-03	8.00E-03	2.00E-03	4.00E-03	0.01	4.00E-03	4.00E-03	0	2.00E-03	4.00E-03	0.03	6.00E-03
20	6.00E-03	6.00E-03	2.00E-03	0	8.00E-03	0	0	0.01	6.00E-03	4.00E-03	2.00E-03	6.00E-03	4.00E-03	4.00E-03	4.00E-03	0	0	2.00E-03	0.02	6.00E-03
42	8.00E-03	0.02	4.00E-03	0	8.00E-03	0	2.00E-03	4.00E-03	6.00E-03	8.00E-03	0	0.02	4.00E-03	4.00E-03	2.00E-03	2.00E-03	0	4.00E-03	0.03	0.01
9	2.00E-03	0.02	0	0	0.01	0	2.00E-03	0	6.00E-03	0.01	4.00E-03	0	6.00E-03	6.00E-03	4.00E-03	4.00E-03	0	2.00E-03	0.03	4.00E-03
16	2.00E-03	0.02	0	0	2.00E-03	8.00E-03	4.00E-03	4.00E-03	6.00E-03	0.01	4.00E-03	0	4.00E-03	6.00E-03	2.00E-03	2.00E-03	0	2.00E-03	0.01	4.00E-03
34	6.00E-03	0.01	4.00E-03	0	8.00E-03	2.00E-03	4.00E-03	8.00E-03	8.00E-03	6.00E-03	0	8.00E-03	2.00E-03	0.01	4.00E-03	2.00E-03	0	4.00E-03	0.02	6.00E-03
46	4.00E-03	0.01	0	0	2.00E-03	8.00E-03	0	0	0	0.01	6.00E-03	2.00E-03	4.00E-03	4.00E-03	2.00E-03	0	0	4.00E-03	0.03	4.00E-03
25	2.00E-03	8.00E-03	2.00E-03	0	6.00E-03	0	2.00E-03	0	6.00E-03	0.01	2.00E-03	0.01	2.00E-03	4.00E-03	4.00E-03	0	2.00E-03	4.00E-03	0.04	6.00E-03
47	6.00E-03	0.01	2.00E-03	0	4.00E-03	0	0	2.00E-03	6.00E-03	6.00E-03	2.00E-03	0.02	2.00E-03	6.00E-03	2.00E-03	2.00E-03	0	2.00E-03	0.04	0
33	2.00E-03	0.01	0	0	2.00E-03	6.00E-03	0	0	6.00E-03	0.01	8.00E-03	6.00E-03	8.00E-03	2.00E-03	2.00E-03	2.00E-03	2.00E-03	2.00E-03	0.03	0.01
1	4.00E-03	0.01	2.00E-03	0	2.00E-03	0.01	0	0	2.00E-03	8.00E-03	2.00E-03	8.00E-03	8.00E-03	0	2.00E-03	0	0	2.00E-03	0.02	8.00E-03
45	4.00E-03	8.00E-03	4.00E-03	0	8.00E-03	2.00E-03	6.00E-03	0	6.00E-03	0.01	2.00E-03	0.01	8.00E-03	0.01	2.00E-03	2.00E-03	0	6.00E-03	0.04	0.01
41	4.00E-03	0.01	2.00E-03	0	8.00E-03	2.00E-03	4.00E-03	4.00E-03	6.00E-03	0.01	2.00E-03	2.00E-03	2.00E-03	8.00E-03	4.00E-03	0	0	2.00E-03	0.03	0.01
18	4.00E-03	0.02	0	0	2.00E-03	4.00E-03	2.00E-03	0	4.00E-03	8.00E-03	8.00E-03	8.00E-03	8.00E-03	2.00E-03	4.00E-03	0	0	4.00E-03	0.03	6.00E-03
4	4.00E-03	0.02	0	0	8.00E-03	0	0	6.00E-03	4.00E-03	2.00E-03	2.00E-03	6.00E-03	2.00E-03	2.00E-03	4.00E-03	0	0	4.00E-03	0.03	0
13	4.00E-03	0.02	2.00E-03	0	0.01	2.00E-03	2.00E-03	4.00E-03	4.00E-03	2.00E-03	2.00E-03	2.00E-03	8.00E-03	4.00E-03	4.00E-03	2.00E-03	0	2.00E-03	0.04	6.00E-03
51	8.00E-03	0.02	2.00E-03	0	6.00E-03	0	2.00E-03	8.00E-03	8.00E-03	6.00E-03	0	0.01	4.00E-03	6.00E-03	6.00E-03	0	0	4.00E-03	0.02	6.00E-03
31	4.00E-03	0.01	2.00E-03	0	8.00E-03	2.00E-03	2.00E-03	2.00E-03	2.00E-03	0.01	2.00E-03	4.00E-03	8.00E-03	6.00E-03	2.00E-03	0	0	6.00E-03	0.02	6.00E-03
52	2.00E-03	0.02	2.00E-03	0	0.01	0	0	0	0	6.00E-03	4.00E-03	8.00E-03	4.00E-03	4.00E-03	2.00E-03	0	0	4.00E-03	0.02	4.00E-03
21	47,XXY	47,XXY	47,XXY	47,XXY	47,XXY	47,XXY	47,XXY	47,XXY	47,XXY	47,XXY	47,XXY	47,XXY	47,XXY	47,XXY	47,XXY	47,XXY	47,XXY	47,XXY	47,XXY	47,XXY
2	0	0.02	4.00E-03	2.00E-03	8.00E-03	2.00E-03	4.00E-03	6.00E-03	6.00E-03	0.01	2.00E-03	8.00E-03	0	6.00E-03	0	0	0	4.00E-03	0.04	8.00E-03
53	6.00E-03	0.02	2.00E-03	0	0.01	2.00E-03	2.00E-03	4.00E-03	4.00E-03	0.01	2.00E-03	2.00E-03	4.00E-03	4.00E-03	2.00E-03	2.00E-03	0	8.00E-03	0.04	0.01
15	0.01	8.00E-03	4.00E-03	2.00E-03	8.00E-03	6.00E-03	2.00E-03	0	0.02	6.00E-03	4.00E-03	0.01	0.01	8.00E-03	8.00E-03	6.00E-03	0	4.00E-03	0.02	0.02
40	4.00E-03	0.01	2.00E-03	2.00E-03	8.00E-03	2.00E-03	4.00E-03	4.00E-03	6.00E-03	4.00E-03	2.00E-03	8.00E-03	4.00E-03	4.00E-03	8.00E-03	0	0	6.00E-03	0.01	0.01
38	4.00E-03	0.01	2.00E-03	0	6.00E-03	0	0	2.00E-03	0.01	4.00E-03	0	8.00E-03	4.00E-03	4.00E-03	4.00E-03	0	0	6.00E-03	0.01	0.01
32	4.00E-03	6.00E-03	2.00E-03	0	8.00E-03	2.00E-03	4.00E-03	4.00E-03	8.00E-03	4.00E-03	2.00E-03	0.02	8.00E-03	2.00E-03	2.00E-03	0	0	6.00E-03	8.00E-03	2.00E-03
35	4.00E-03	0.01	2.00E-03	0	6.00E-03	0	4.00E-03	4.00E-03	6.00E-03	2.00E-03	6.00E-03	2.00E-03	4.00E-03	4.00E-03	2.00E-03	0	0	2.00E-03	0.01	2.00E-03
28	4.00E-03	0.01	2.00E-03	0	8.00E-03	0	4.00E-03	4.00E-03	8.00E-03	8.00E-03	4.00E-03	0.01	2.00E-03	2.00E-03	2.00E-03	0	0	6.00E-03	0.02	4.00E-03
ES05	8.00E-03	2.00E-03	2.00E-03	0	2.00E-03	0	2.00E-03	8.00E-03	2.00E-03	0.01	4.00E-03	4.00E-03	2.00E-03	2.00E-03	2.00E-03	0.01	2.00E-03	6.00E-03	0.52	0.02

ES13	6.00E-03	2.00E-03	4.00E-03	2.00E-03	4.00E-03	0	8.00E-03	2.00E-03	2.00E-03	0.02	8.00E-03	8.00E-03	8.00E-03	4.00E-03	8.00E-03	0	2.00E-03	6.00E-03	0.3	0.01	
ES07	0.02	2.00E-03	4.00E-03	0	2.00E-03	4.00E-03	8.00E-03	4.00E-03	0	0.02	8.00E-03	8.00E-03	0.01	8.00E-03	0	0	0	6.00E-03	0.38	0.02	
ES12	0.01	6.00E-03	6.00E-03	0	8.00E-03	0	0	2.00E-03	2.00E-03	0.03	0.01	4.00E-03	6.00E-03	0.01	6.00E-03	0	2.00E-03	8.00E-03	0.34	0.02	
ES09	6.00E-03	0.01	6.00E-03	0	2.00E-03	2.00E-03	2.00E-03	4.00E-03	0	0.02	0.01	4.00E-03	8.00E-03	0.01	4.00E-03	0	2.00E-03	6.00E-03	0.34	0.03	
ES17	2.00E-03	0.01	4.00E-03	2.00E-03	4.00E-03	2.00E-03	6.00E-03	2.00E-03	2.00E-03	0.02	4.00E-03	2.00E-03	2.00E-03	0.01	6.00E-03	0	6.00E-03	6.00E-03	0.19	0.02	
ES15	8.00E-03	4.00E-03	2.00E-03	2.00E-03	4.00E-03	2.00E-03	4.00E-03	2.00E-03	0	0.01	0.01	8.00E-03	0	0.01	6.00E-03	0	0	6.00E-03	0.5	0.04	
ES03	4.00E-03	8.00E-03	4.00E-03	0	4.00E-03	4.00E-03	0	0.01	2.00E-03	0.02	0.01	6.00E-03	4.00E-03	6.00E-03	0.01	0	0	0.01	0.43	0.02	
ES02	0.01	4.00E-03	4.00E-03	0	8.00E-03	0	4.00E-03	4.00E-03	4.00E-03	0.02	6.00E-03	8.00E-03	2.00E-03	0.01	4.00E-03	0	2.00E-03	0.02	0.41	0.02	
ES04	0.01	4.00E-03	0	4.00E-03	2.00E-03	4.00E-03	4.00E-03	4.00E-03	0	0.01	2.00E-03	2.00E-03	6.00E-03	4.00E-03	0.01	0	4.00E-03	4.00E-03	0.33	0.01	
ES14	0.01	8.00E-03	6.00E-03	2.00E-03	2.00E-03	2.00E-03	8.00E-03	4.00E-03	4.00E-03	0.03	0.01	6.00E-03	2.00E-03	0.01	4.00E-03	2.00E-03	2.00E-03	0.01	0.32	0.02	
ES18	8.00E-03	0.01	8.00E-03	0	4.00E-03	6.00E-03	4.00E-03	2.00E-03	4.00E-03	0.03	8.00E-03	2.00E-03	8.00E-03	8.00E-03	2.00E-03	0	0	0	0.13	0.02	
ES11	8.00E-03	0.01	6.00E-03	2.00E-03	8.00E-03	0	8.00E-03	2.00E-03	4.00E-03	0.04	0.02	2.00E-03	4.00E-03	6.00E-03	4.00E-03	2.00E-03	2.00E-03	0.01	0.26	0.02	
ES16	6.00E-03	0	4.00E-03	0	6.00E-03	0	6.00E-03	4.00E-03	4.00E-03	0.01	4.00E-03	2.00E-03	2.00E-03	2.00E-03	6.00E-03	0	0	4.00E-03	0.54	6.00E-03	
ES10	4.00E-03	6.00E-03	6.00E-03	2.00E-03	2.00E-03	2.00E-03	4.00E-03	2.00E-03	4.00E-03	0.02	0.02	6.00E-03	6.00E-03	8.00E-03	0.01	4.00E-03	0	0.01	0.46	0.03	
27	0.01	2.00E-03	2.00E-03	2.00E-03	2.00E-03	0	8.00E-03	4.00E-03	2.00E-03	0.02	0.01	8.00E-03	0	0.01	4.00E-03	0	0	4.00E-03	0.36	0.02	
23	0.01	8.00E-03	4.00E-03	2.00E-03	4.00E-03	0	6.00E-03	6.00E-03	4.00E-03	0.03	6.00E-03	0	2.00E-03	0.01	2.00E-03	2.00E-03	2.00E-03	0.01	0.29	0.02	
9	0.01	4.00E-03	4.00E-03	4.00E-03	4.00E-03	0	4.00E-03	6.00E-03	2.00E-03	0.02	0.01	2.00E-03	2.00E-03	6.00E-03	2.00E-03	0	0	4.00E-03	0.44	0.02	
51	6.00E-03	8.00E-03	4.00E-03	2.00E-03	4.00E-03	0	8.00E-03	0	2.00E-03	0.03	0.01	4.00E-03	2.00E-03	0.01	4.00E-03	2.00E-03	4.00E-03	8.00E-03	0.35	0.02	
1	0.02	6.00E-03	8.00E-03	4.00E-03	2.00E-03	4.00E-03	8.00E-03	8.00E-03	4.00E-03	0.04	0.02	4.00E-03	6.00E-03	6.00E-03	2.00E-03	0	4.00E-03	0.02	0.23	0.02	
40	4.00E-03	2.00E-03	6.00E-03	2.00E-03	6.00E-03	0	6.00E-03	2.00E-03	2.00E-03	0.02	4.00E-03	0	0	6.00E-03	2.00E-03	2.00E-03	2.00E-03	6.00E-03	0.48	0.01	
49	0.01	4.00E-03	4.00E-03	2.00E-03	2.00E-03	0	8.00E-03	4.00E-03	2.00E-03	0.04	4.00E-03	0.01	4.00E-03	0.01	4.00E-03	0	2.00E-03	8.00E-03	0.33	0.02	
6	4.00E-03	0.01	4.00E-03	0	0	0	6.00E-03	2.00E-03	8.00E-03	0.04	0.02	4.00E-03	0	8.00E-03	2.00E-03	0	4.00E-03	0.22	0.02	0.02	
12	4.00E-03	6.00E-03	4.00E-03	0	0	0	0.01	6.00E-03	0	0.02	4.00E-03	0	2.00E-03	0.01	2.00E-03	2.00E-03	2.00E-03	4.00E-03	0.34	0.02	
18	2.00E-03	0.01	2.00E-03	2.00E-03	2.00E-03	0	6.00E-03	4.00E-03	2.00E-03	0.01	2.00E-03	6.00E-03	0	4.00E-03	2.00E-03	0	0	8.00E-03	0.36	0.02	
2	0.01	8.00E-03	4.00E-03	2.00E-03	4.00E-03	2.00E-03	4.00E-03	4.00E-03	4.00E-03	0.02	8.00E-03	2.00E-03	0	8.00E-03	8.00E-03	0	0	8.00E-03	0.4	0.02	
11	4.00E-03	6.00E-03	2.00E-03	2.00E-03	6.00E-03	0	6.00E-03	2.00E-03	2.00E-03	6.00E-03	0	0	0	0	2.00E-03	0	0	6.00E-03	0.51	0.01	
10	6.00E-03	0.01	6.00E-03	2.00E-03	0	0	8.00E-03	4.00E-03	4.00E-03	0.03	8.00E-03	6.00E-03	4.00E-03	0.01	4.00E-03	0	0	4.00E-03	0.26	0.03	
3	4.00E-03	2.00E-03	4.00E-03	0	8.00E-03	0	0.01	2.00E-03	0	0.02	8.00E-03	8.00E-03	2.00E-03	0.01	8.00E-03	2.00E-03	0	0.01	0.25	0.02	
38	0.03	8.00E-03	6.00E-03	2.00E-03	4.00E-03	0	0.01	2.00E-03	8.00E-03	0.05	0.03	0.02	2.00E-03	0.02	8.00E-03	0	6.00E-03	8.00E-03	0.17	0.02	
16	4.00E-03	8.00E-03	4.00E-03	0	2.00E-03	0	8.00E-03	0	2.00E-03	0.03	8.00E-03	0	2.00E-03	0.01	2.00E-03	0	4.00E-03	6.00E-03	0.41	0.02	
34	8.00E-03	6.00E-03	4.00E-03	2.00E-03	6.00E-03	0	8.00E-03	4.00E-03	6.00E-03	0.03	8.00E-03	6.00E-03	4.00E-03	0.01	2.00E-03	2.00E-03	0	0.01	0.33	0.03	
50	0.01	4.00E-03	4.00E-03	2.00E-03	4.00E-03	0	8.00E-03	0.01	4.00E-03	0.04	0.01	4.00E-03	2.00E-03	8.00E-03	4.00E-03	0	0.01	0.27	0.02	0.02	
4	0.01	0.01	6.00E-03	0	6.00E-03	0	8.00E-03	8.00E-03	0.01	0.04	8.00E-03	6.00E-03	2.00E-03	0.01	4.00E-03	2.00E-03	2.00E-03	8.00E-03	0.22	0.02	
19	0.01	4.00E-03	0.01	0	2.00E-03	0	8.00E-03	4.00E-03	2.00E-03	0.02	8.00E-03	6.00E-03	2.00E-03	0.01	6.00E-03	2.00E-03	2.00E-03	4.00E-03	0.42	0.01	
21	47,XXY	47,XXY	47,XXY	47,XXY	47,XXY	47,XXY	47,XXY	47,XXY	47,XXY	47,XXY	47,XXY	47,XXY	47,XXY	47,XXY	47,XXY	47,XXY	47,XXY	47,XXY	47,XXY	47,XXY	
33	0.01	6.00E-03	2.00E-03	2.00E-03	2.00E-03	0	0.01	0	2.00E-03	0.03	0.01	0.01	0	0.02	8.00E-03	0	0	0.02	0.37	0.01	
5	450K QC	450K QC	450K QC	450K QC	450K QC	450K QC	450K QC	450K QC	450K QC	450K QC	450K QC	450K QC	450K QC	450K QC	450K QC	450K QC	450K QC	450K QC	450K QC	450K QC	450K QC

42	4.00E-03	6.00E-03	4.00E-03	0	6.00E-03	0	6.00E-03	0	6.00E-03	0	0.01	0.03	0.02	0.01	4.00E-03	4.00E-03	0.01	4.00E-03	2.00E-03	2.00E-03	6.00E-03	0.27	0.02
13	0.01	2.00E-03	4.00E-03	2.00E-03	6.00E-03	0	6.00E-03	2.00E-03	6.00E-03	0	0.01	0.02	4.00E-03	0.01	6.00E-03	6.00E-03	0.01	2.00E-03	2.00E-03	8.00E-03	0.4	0.02	
24	450K QC	450K QC	450K QC	450K QC	450K QC	450K QC	450K QC	450K QC	450K QC	450K QC	450K QC	450K QC	450K QC	450K QC	450K QC	450K QC	450K QC	450K QC	450K QC	450K QC	450K QC	450K QC	450K QC
54	0.01	8.00E-03	6.00E-03	2.00E-03	2.00E-03	4.00E-03	8.00E-03	4.00E-03	8.00E-03	0.01	0.01	0.03	0.02	0.01	2.00E-03	2.00E-03	0.01	0	0	4.00E-03	0.34	0.02	
25	0.02	6.00E-03	6.00E-03	6.00E-03	4.00E-03	0	8.00E-03	6.00E-03	8.00E-03	0.03	0.03	0.03	0.03	0.01	0	0	0.01	8.00E-03	2.00E-03	4.00E-03	0.01	0.2	0.03
30	4.00E-03	4.00E-03	6.00E-03	2.00E-03	4.00E-03	0	6.00E-03	0	6.00E-03	0.02	0.02	8.00E-03	0	0	2.00E-03	2.00E-03	0	4.00E-03	0	4.00E-03	0.35	0.01	
53	2.00E-03	4.00E-03	2.00E-03	4.00E-03	4.00E-03	0	2.00E-03	2.00E-03	4.00E-03	0.02	0.02	4.00E-03	0	0	6.00E-03	4.00E-03	0	4.00E-03	0	4.00E-03	0.36	0.01	
MS22	2.00E-03	0.01	6.00E-03	4.00E-03	2.00E-03	2.00E-03	6.00E-03	0	4.00E-03	0.02	0.02	2.00E-03	2.00E-03	0	4.00E-03	0	0	4.00E-03	0	4.00E-03	0.2	0.02	
MS08	4.00E-03	6.00E-03	6.00E-03	0	4.00E-03	0	2.00E-03	4.00E-03	2.00E-03	0.02	0.01	4.00E-03	0	6.00E-03	0	2.00E-03	0	0	0	0	0.28	0.02	
MS33	4.00E-03	6.00E-03	6.00E-03	0	0	0	4.00E-03	2.00E-03	4.00E-03	0.03	0.03	8.00E-03	2.00E-03	2.00E-03	0	4.00E-03	0	0	0	0	0.24	0.03	
MS35	4.00E-03	6.00E-03	6.00E-03	4.00E-03	4.00E-03	0	0.01	2.00E-03	2.00E-03	0.01	0.01	4.00E-03	2.00E-03	0	4.00E-03	0	0	4.00E-03	0	2.00E-03	0.3	0.02	
MS10	0	8.00E-03	2.00E-03	4.00E-03	2.00E-03	2.00E-03	4.00E-03	0	4.00E-03	0.03	0.03	2.00E-03	2.00E-03	0	4.00E-03	0	0	8.00E-03	0	2.00E-03	0.23	0.02	
MS01	2.00E-03	6.00E-03	8.00E-03	2.00E-03	4.00E-03	2.00E-03	4.00E-03	4.00E-03	4.00E-03	0.01	0.01	4.00E-03	4.00E-03	0	4.00E-03	0	0	6.00E-03	0	2.00E-03	0.21	0.02	
MS21	2.00E-03	4.00E-03	4.00E-03	4.00E-03	6.00E-03	0	4.00E-03	0	4.00E-03	0.02	0.02	6.00E-03	4.00E-03	4.00E-03	0	2.00E-03	0	2.00E-03	0	2.00E-03	0.19	0.02	
MS23	8.00E-03	0.01	8.00E-03	0	2.00E-03	0	8.00E-03	4.00E-03	2.00E-03	0.02	0.02	6.00E-03	2.00E-03	4.00E-03	0.01	2.00E-03	0	2.00E-03	0	6.00E-03	0.2	0.02	
MS34	2.00E-03	4.00E-03	6.00E-03	4.00E-03	4.00E-03	4.00E-03	0.01	4.00E-03	6.00E-03	0.04	0.04	0.01	6.00E-03	4.00E-03	0.01	2.00E-03	0	2.00E-03	0	2.00E-03	0.13	0.03	
MS31	0.01	8.00E-03	6.00E-03	4.00E-03	4.00E-03	0	4.00E-03	6.00E-03	6.00E-03	0.01	0.01	0.02	2.00E-03	8.00E-03	6.00E-03	2.00E-03	0	2.00E-03	0	2.00E-03	0.13	0.02	
MS04	8.00E-03	0.01	6.00E-03	2.00E-03	0	4.00E-03	4.00E-03	2.00E-03	2.00E-03	0.02	0.02	6.00E-03	2.00E-03	4.00E-03	2.00E-03	0	0	6.00E-03	0	6.00E-03	0.13	8.00E-03	
MS17	6.00E-03	0.01	0.01	2.00E-03	6.00E-03	2.00E-03	4.00E-03	2.00E-03	4.00E-03	0.01	0.01	2.00E-03	0	0.02	4.00E-03	2.00E-03	2.00E-03	0.01	0	0	0.2	0.02	
MS14	0.01	0.01	6.00E-03	2.00E-03	2.00E-03	0	8.00E-03	6.00E-03	6.00E-03	0.02	0.02	0.01	2.00E-03	8.00E-03	0.01	4.00E-03	0	4.00E-03	0	2.00E-03	0.14	0.03	
MS36	2.00E-03	8.00E-03	6.00E-03	2.00E-03	8.00E-03	0	8.00E-03	0	8.00E-03	0.02	0.02	6.00E-03	2.00E-03	2.00E-03	0.01	4.00E-03	0	2.00E-03	0	2.00E-03	0.2	0.02	
MS20	6.00E-03	0.01	2.00E-03	0	2.00E-03	2.00E-03	4.00E-03	0	6.00E-03	0.03	0.03	6.00E-03	0	2.00E-03	0.01	4.00E-03	0	4.00E-03	0	0	0.18	0.03	
MS32	4.00E-03	8.00E-03	6.00E-03	0	2.00E-03	2.00E-03	6.00E-03	2.00E-03	6.00E-03	0.03	0.03	2.00E-03	2.00E-03	4.00E-03	4.00E-03	0	0	4.00E-03	0	4.00E-03	0.21	0.02	
MS12	4.00E-03	6.00E-03	2.00E-03	4.00E-03	6.00E-03	2.00E-03	6.00E-03	2.00E-03	8.00E-03	0.03	0.03	0.01	2.00E-03	8.00E-03	4.00E-03	2.00E-03	0	4.00E-03	0	4.00E-03	0.14	0.02	
MS03	6.00E-03	0.01	6.00E-03	0	2.00E-03	2.00E-03	4.00E-03	4.00E-03	4.00E-03	0.03	0.03	2.00E-03	4.00E-03	2.00E-03	0.01	2.00E-03	0	2.00E-03	0	2.00E-03	0.18	0.02	
MS05	4.00E-03	6.00E-03	4.00E-03	4.00E-03	0	0	6.00E-03	2.00E-03	2.00E-03	0.02	0.02	4.00E-03	4.00E-03	2.00E-03	8.00E-03	0	0	2.00E-03	0	2.00E-03	0.15	0.02	
MS11	0.01	4.00E-03	6.00E-03	0	2.00E-03	2.00E-03	4.00E-03	2.00E-03	4.00E-03	0.04	0.04	4.00E-03	0.01	0.01	0.01	0	0	4.00E-03	0	2.00E-03	0.15	0.04	
MS27	4.00E-03	0.01	4.00E-03	2.00E-03	2.00E-03	2.00E-03	6.00E-03	0	4.00E-03	0.03	0.03	2.00E-03	2.00E-03	4.00E-03	4.00E-03	0	0	2.00E-03	0	2.00E-03	0.15	0.04	
MS29	6.00E-03	8.00E-03	4.00E-03	4.00E-03	4.00E-03	0	6.00E-03	4.00E-03	2.00E-03	0.01	0.01	2.00E-03	2.00E-03	2.00E-03	8.00E-03	2.00E-03	0	2.00E-03	0	2.00E-03	0.2	0.03	
MS28	2.00E-03	8.00E-03	4.00E-03	4.00E-03	4.00E-03	2.00E-03	0.01	2.00E-03	4.00E-03	0.03	0.03	2.00E-03	0	2.00E-03	4.00E-03	0	0	2.00E-03	0	2.00E-03	0.25	0.01	
MS06	0	0.01	4.00E-03	0	4.00E-03	0	4.00E-03	4.00E-03	2.00E-03	0.03	0.03	8.00E-03	4.00E-03	0	6.00E-03	0	0	2.00E-03	0	2.00E-03	0.18	0.03	
MS15	0.01	6.00E-03	6.00E-03	0	4.00E-03	0	0.01	4.00E-03	2.00E-03	0.01	0.01	8.00E-03	2.00E-03	0	4.00E-03	0	0	4.00E-03	0	4.00E-03	0.18	0.02	
MS24	47,XXY	47,XXY	47,XXY	47,XXY	47,XXY	47,XXY	47,XXY	47,XXY	47,XXY	47,XXY	47,XXY	47,XXY	47,XXY	47,XXY	47,XXY	47,XXY	47,XXY	47,XXY	47,XXY	47,XXY	47,XXY	47,XXY	47,XXY
MS02	6.00E-03	0.01	2.00E-03	2.00E-03	0	2.00E-03	8.00E-03	0	2.00E-03	0.02	0.02	0	4.00E-03	2.00E-03	6.00E-03	0	0	2.00E-03	0	2.00E-03	0.19	0.01	
MS09	4.00E-03	0.01	6.00E-03	0	0	2.00E-03	2.00E-03	0	4.00E-03	0.03	0.03	2.00E-03	4.00E-03	0	8.00E-03	2.00E-03	0	8.00E-03	0	0	0.16	0.02	
MS18	6.00E-03	0.01	6.00E-03	2.00E-03	6.00E-03	2.00E-03	4.00E-03	4.00E-03	4.00E-03	0.01	0.01	2.00E-03	0	0	0.01	0	0	2.00E-03	0	2.00E-03	0.18	0.01	
MS07	4.00E-03	2.00E-03	8.00E-03	2.00E-03	4.00E-03	0	6.00E-03	0	4.00E-03	0.01	0.01	0.01	0	4.00E-03	0.01	0	0	2.00E-03	0	2.00E-03	0.23	0.02	

MS30	0.01	0.01	8.00E-03	8.00E-03	0	2.00E-03	2.00E-03	8.00E-03	0.02	0.02	6.00E-03	6.00E-03	0.01	8.00E-03	0	2.00E-03	6.00E-03	0.17	0.02	
MS13	0.01	0.01	0	0	6.00E-03	4.00E-03	0.01	6.00E-03	0.04	6.00E-03	6.00E-03	2.00E-03	8.00E-03	6.00E-03	0	2.00E-03	2.00E-03	0.13	0.02	
MS25	4.00E-03	0.01	2.00E-03	4.00E-03	0	2.00E-03	0.01	0	0.02	0.01	2.00E-03	8.00E-03	0.01	0	0	2.00E-03	2.00E-03	0.14	0.02	
MS26	0.02	6.00E-03	6.00E-03	2.00E-03	2.00E-03	4.00E-03	2.00E-03	6.00E-03	0.01	0.02	6.00E-03	2.00E-03	8.00E-03	4.00E-03	0	4.00E-03	0.01	0.09	8.00E-03	
ES16	6.00E-03	4.00E-03	2.00E-03	2.00E-03	0	2.00E-03	0	0	8.00E-03	4.00E-03	4.00E-03	4.00E-03	4.00E-03	4.00E-03	0	0	2.00E-03	0.6	0.01	
ES18	0.01	0.01	4.00E-03	0	2.00E-03	0	0.02	6.00E-03	0.02	2.00E-03	4.00E-03	2.00E-03	0.01	0	0	0	0	0.2	0.02	
ES10	2.00E-03	0.01	6.00E-03	0	2.00E-03	0	0.01	0	0.02	8.00E-03	2.00E-03	4.00E-03	0.01	0	0	0	6.00E-03	0.14	0.03	
ES11	4.00E-03	6.00E-03	4.00E-03	2.00E-03	0	4.00E-03	0	2.00E-03	0.03	4.00E-03	2.00E-03	4.00E-03	6.00E-03	0	2.00E-03	4.00E-03	0.22	0.02	0.02	
ES14	4.00E-03	0	2.00E-03	0	4.00E-03	0	4.00E-03	0	8.00E-03	4.00E-03	4.00E-03	4.00E-03	2.00E-03	6.00E-03	0	0	2.00E-03	0.67	0.01	
ES17	0.02	8.00E-03	4.00E-03	2.00E-03	2.00E-03	4.00E-03	0.01	4.00E-03	0.03	0.01	6.00E-03	0	0.01	6.00E-03	0	0	0.01	0.18	0.02	
ES09	2.00E-03	0	0	2.00E-03	4.00E-03	0	2.00E-03	4.00E-03	0.01	0	0	0	0	4.00E-03	0	0	6.00E-03	0.72	0.01	
ES15	8.00E-03	6.00E-03	4.00E-03	4.00E-03	2.00E-03	0	0.01	2.00E-03	0.04	6.00E-03	8.00E-03	2.00E-03	0.02	0	0	2.00E-03	4.00E-03	0.15	0.03	
ES02	6.00E-03	0.01	4.00E-03	4.00E-03	4.00E-03	0	8.00E-03	2.00E-03	0.02	8.00E-03	4.00E-03	2.00E-03	8.00E-03	0	0	2.00E-03	8.00E-03	0.17	0.01	
ES03	4.00E-03	0	0	2.00E-03	2.00E-03	0	6.00E-03	0	6.00E-03	4.00E-03	2.00E-03	2.00E-03	4.00E-03	2.00E-03	0	0	0	0.67	0.01	
ES06	2.00E-03	2.00E-03	4.00E-03	2.00E-03	2.00E-03	0	8.00E-03	0	0.02	6.00E-03	2.00E-03	0	4.00E-03	2.00E-03	0	6.00E-03	0.46	0.02	0.02	
ES12	4.00E-03	2.00E-03	6.00E-03	2.00E-03	6.00E-03	0	4.00E-03	2.00E-03	0.01	4.00E-03	2.00E-03	0	8.00E-03	0	0	6.00E-03	0.41	0.01	0.01	
ES13	2.00E-03	8.00E-03	6.00E-03	2.00E-03	2.00E-03	0	4.00E-03	2.00E-03	0.01	2.00E-03	0	0	0.01	4.00E-03	0	0	6.00E-03	0.25	0.03	
ES04	4.00E-03	0.01	0	2.00E-03	0	2.00E-03	0	6.00E-03	0.02	8.00E-03	2.00E-03	0	4.00E-03	0	0	2.00E-03	0.18	0.02	0.02	
ES05	4.00E-03	6.00E-03	0	2.00E-03	0	2.00E-03	0	2.00E-03	0.01	0.01	8.00E-03	0	8.00E-03	4.00E-03	2.00E-03	2.00E-03	0.01	0.38	0.02	
4	4.00E-03	0.01	4.00E-03	2.00E-03	2.00E-03	4.00E-03	8.00E-03	2.00E-03	0.03	4.00E-03	0	2.00E-03	0.01	0	0	2.00E-03	6.00E-03	0.15	0.02	
3	0	0.02	4.00E-03	0	4.00E-03	2.00E-03	6.00E-03	4.00E-03	0.03	6.00E-03	6.00E-03	4.00E-03	0.01	0	0	2.00E-03	2.00E-03	0.16	0.02	
12	failed bisulfite conversio	failed bisulfite conversio	failed bisulfite conversio	failed bisulfite conversio	failed bisulfite conversio	failed bisulfite conversio	failed bisulfite conversio	failed bisulfite conversio	failed bisulfite conversio	failed bisulfite conversio	failed bisulfite conversio	failed bisulfite conversio	failed bisulfite conversio	failed bisulfite conversio	failed bisulfite conversio	failed bisulfite conversio	failed bisulfite conversio	failed bisulfite conversio	failed bisulfite conversio	
37	6.00E-03	8.00E-03	4.00E-03	0	2.00E-03	2.00E-03	4.00E-03	2.00E-03	0.02	8.00E-03	4.00E-03	6.00E-03	4.00E-03	2.00E-03	0	0	0	0.35	0.02	0.02
17	8.00E-03	0.02	0	2.00E-03	2.00E-03	4.00E-03	4.00E-03	8.00E-03	0.02	0.01	2.00E-03	4.00E-03	0.01	2.00E-03	0	0	0	0.21	0.02	0.02
26	8.00E-03	0.01	6.00E-03	2.00E-03	2.00E-03	0	4.00E-03	0	0.02	2.00E-03	0	2.00E-03	4.00E-03	0	0	2.00E-03	0.26	0.02	0.02	
8	450K QC	failed	failed	failed	failed	failed	failed	failed	failed	failed	failed	failed	failed	failed	failed	failed	failed	failed	failed	failed
1	0	0.01	6.00E-03	2.00E-03	0	4.00E-03	6.00E-03	2.00E-03	0.01	2.00E-03	2.00E-03	2.00E-03	4.00E-03	2.00E-03	0	0	2.00E-03	0.23	0.03	0.03
28	0.01	0.01	4.00E-03	0	2.00E-03	0	4.00E-03	0	0.02	4.00E-03	2.00E-03	6.00E-03	6.00E-03	2.00E-03	0	0	2.00E-03	0.31	0.02	0.02
34	2.00E-03	8.00E-03	6.00E-03	0	0	0	2.00E-03	4.00E-03	0.02	4.00E-03	2.00E-03	2.00E-03	8.00E-03	2.00E-03	0	0	0	0.3	0.02	0.02
2	0.02	0.01	2.00E-03	2.00E-03	4.00E-03	2.00E-03	6.00E-03	4.00E-03	0.02	4.00E-03	4.00E-03	0	0.01	2.00E-03	0	0	2.00E-03	0.17	0.02	0.02
25	8.00E-03	8.00E-03	8.00E-03	0	0	6.00E-03	8.00E-03	0	0.02	4.00E-03	4.00E-03	4.00E-03	8.00E-03	0	0	4.00E-03	0.18	0.03	0.03	
54	8.00E-03	8.00E-03	6.00E-03	0	2.00E-03	2.00E-03	0.01	6.00E-03	0.02	6.00E-03	4.00E-03	2.00E-03	6.00E-03	6.00E-03	0	4.00E-03	4.00E-03	0.21	0.02	0.02
45	0.01	0.01	4.00E-03	2.00E-03	0	0	6.00E-03	2.00E-03	0.02	4.00E-03	4.00E-03	4.00E-03	4.00E-03	2.00E-03	0	2.00E-03	6.00E-03	0.17	0.03	0.03
31	4.00E-03	0.01	6.00E-03	0	0	2.00E-03	0.01	6.00E-03	0.02	8.00E-03	4.00E-03	2.00E-03	0.01	0	0	0	4.00E-03	0.17	0.03	0.03
6	2.00E-03	8.00E-03	6.00E-03	2.00E-03	4.00E-03	0	4.00E-03	4.00E-03	0.03	2.00E-03	6.00E-03	2.00E-03	6.00E-03	2.00E-03	0	0	0	0.24	0.02	0.02

35	6.00E-03	0.02	2.00E-03	2.00E-03	0	4.00E-03	8.00E-03	0	4.00E-03	0.02	0	0	0	0	0.18	0.02
20	2.00E-03	0.01	6.00E-03	2.00E-03	0	2.00E-03	0.01	4.00E-03	6.00E-03	0.02	4.00E-03	0	4.00E-03	0	0.16	0.03
18	6.00E-03	0.01	4.00E-03	2.00E-03	2.00E-03	0	4.00E-03	4.00E-03	4.00E-03	0.02	4.00E-03	0	0	0	0.18	0.03
46	2.00E-03	8.00E-03	6.00E-03	2.00E-03	2.00E-03	2.00E-03	6.00E-03	2.00E-03	8.00E-03	0.02	4.00E-03	0	0	2.00E-03	0.18	0.04
16	0	8.00E-03	4.00E-03	2.00E-03	0	2.00E-03	0	2.00E-03	6.00E-03	0.02	8.00E-03	0	2.00E-03	0	0.21	0.02
47	4.00E-03	0.01	4.00E-03	6.00E-03	2.00E-03	0	2.00E-03	4.00E-03	2.00E-03	0.04	8.00E-03	0	0	6.00E-03	0.17	0.03
51	8.00E-03	8.00E-03	6.00E-03	2.00E-03	0	2.00E-03	0.01	0	8.00E-03	0.01	2.00E-03	0	0	4.00E-03	0.22	0.02
53	4.00E-03	0.01	0	4.00E-03	2.00E-03	4.00E-03	6.00E-03	4.00E-03	4.00E-03	0.02	4.00E-03	0	0	4.00E-03	0.2	0.02
42	8.00E-03	4.00E-03	6.00E-03	2.00E-03	2.00E-03	2.00E-03	0.01	2.00E-03	2.00E-03	0.03	2.00E-03	0	0	4.00E-03	0.23	0.03
49	0.01	0.01	2.00E-03	2.00E-03	4.00E-03	0	8.00E-03	0	4.00E-03	0.02	6.00E-03	0	0	0	0.21	0.03
52	0	6.00E-03	8.00E-03	2.00E-03	0	2.00E-03	4.00E-03	0	4.00E-03	0.01	0	0	0	2.00E-03	0.3	0.02
40	4.00E-03	0.01	4.00E-03	2.00E-03	0	4.00E-03	8.00E-03	2.00E-03	8.00E-03	0.02	0	0	0	4.00E-03	0.24	0.01
7	0	6.00E-03	4.00E-03	4.00E-03	0	6.00E-03	6.00E-03	0	8.00E-03	0.03	0	0	2.00E-03	0	0.21	0.02
15	4.00E-03	8.00E-03	4.00E-03	0	0	4.00E-03	4.00E-03	2.00E-03	4.00E-03	0.01	2.00E-03	0	0	2.00E-03	0.17	0.03
19	6.00E-03	0.02	4.00E-03	2.00E-03	0	0	6.00E-03	0	6.00E-03	0.02	2.00E-03	0	0	2.00E-03	0.21	0.04
10	8.00E-03	0.01	8.00E-03	0	0	4.00E-03	2.00E-03	0	4.00E-03	8.00E-03	2.00E-03	0	0	2.00E-03	0.28	0.03
30	4.00E-03	6.00E-03	4.00E-03	2.00E-03	0	4.00E-03	8.00E-03	4.00E-03	2.00E-03	0.02	4.00E-03	0	0	2.00E-03	0.3	0.01
13	4.00E-03	8.00E-03	4.00E-03	0	4.00E-03	2.00E-03	8.00E-03	0	8.00E-03	0.02	4.00E-03	0	0	2.00E-03	0.19	0.03
41	8.00E-03	0	4.00E-03	0	0	2.00E-03	0.01	2.00E-03	4.00E-03	8.00E-03	4.00E-03	0	0	4.00E-03	0.24	0.02
44	8.00E-03	0.01	4.00E-03	2.00E-03	0	4.00E-03	6.00E-03	2.00E-03	2.00E-03	0.02	0.02	2.00E-03	0	2.00E-03	0.1	0.02
24	6.00E-03	6.00E-03	6.00E-03	0	0	2.00E-03	0.01	4.00E-03	8.00E-03	0.01	2.00E-03	0	0	2.00E-03	0.18	0.02
9	8.00E-03	0.01	6.00E-03	2.00E-03	2.00E-03	4.00E-03	8.00E-03	6.00E-03	4.00E-03	0.03	4.00E-03	0	0	4.00E-03	0.15	0.03
5	2.00E-03	2.00E-03	6.00E-03	0	0	0	4.00E-03	0	2.00E-03	0.01	0	0	0	2.00E-03	0.29	0.02
38	4.00E-03	6.00E-03	8.00E-03	0	6.00E-03	0	4.00E-03	2.00E-03	6.00E-03	0.01	4.00E-03	0	0	4.00E-03	0.19	0.02
39	failed bisulfite conversio	failed bisulfite conversio	failed bisulfite conversio	failed bisulfite conversio	failed bisulfite conversio	failed bisulfite conversio	failed bisulfite conversio	failed bisulfite conversio	failed bisulfite conversio	failed bisulfite conversio	failed bisulfite conversio	failed bisulfite conversio	failed bisulfite conversio	failed bisulfite conversio	failed bisulfite conversio	failed bisulfite conversio
14	4.00E-03	0.01	6.00E-03	0	0	0	0.01	2.00E-03	6.00E-03	0.01	4.00E-03	0	0	2.00E-03	0.19	0.03
33	4.00E-03	0.01	4.00E-03	2.00E-03	0	2.00E-03	6.00E-03	2.00E-03	6.00E-03	0.02	4.00E-03	0	0	2.00E-03	0.17	0.03
23	8.00E-03	8.00E-03	4.00E-03	2.00E-03	6.00E-03	2.00E-03	8.00E-03	0	4.00E-03	0.02	2.00E-03	0	0	2.00E-03	0.2	0.03
32	4.00E-03	0.01	4.00E-03	0	2.00E-03	0	8.00E-03	0	6.00E-03	0.03	2.00E-03	0	0	0	0.17	0.02
11	8.00E-03	8.00E-03	6.00E-03	0	2.00E-03	2.00E-03	0.01	0	6.00E-03	0.02	2.00E-03	0	0	2.00E-03	0.21	0.03
21	47,XXY	47,XXY	47,XXY	47,XXY	47,XXY	47,XXY	47,XXY	47,XXY	47,XXY	47,XXY	47,XXY	47,XXY	47,XXY	47,XXY	47,XXY	47,XXY
MS22	4.00E-03	8.00E-03	4.00E-03	0	8.00E-03	0	0.01	0	2.00E-03	0.02	4.00E-03	0	0	4.00E-03	0.35	0.01
MS01	2.00E-03	0	2.00E-03	4.00E-03	6.00E-03	2.00E-03	8.00E-03	6.00E-03	4.00E-03	0.02	8.00E-03	0	0	2.00E-03	0.47	0.01
MS05	0.01	0.02	2.00E-03	0	4.00E-03	2.00E-03	4.00E-03	4.00E-03	4.00E-03	0.02	2.00E-03	0	0	6.00E-03	0.36	0.02
MS08	0.01	0.01	6.00E-03	0	6.00E-03	2.00E-03	6.00E-03	2.00E-03	8.00E-03	0.01	4.00E-03	0	0	0.01	0.36	0.02

MS36	0.01	8.00E-03	6.00E-03	6.00E-03	4.00E-03	4.00E-03	4.00E-03	8.00E-03	2.00E-03	4.00E-03	0.02	0.01	6.00E-03	4.00E-03	0.02	6.00E-03	0	2.00E-03	0.01	2.00E-03	0.32	0.02	
MS30	8.00E-03	6.00E-03	2.00E-03	4.00E-03	2.00E-03	2.00E-03	2.00E-03	0.01	0	6.00E-03	0.03	4.00E-03	2.00E-03	6.00E-03	0.02	4.00E-03	2.00E-03	6.00E-03	2.00E-03	0.01	6.00E-03	0.39	0.02
MS10	8.00E-03	0.01	2.00E-03	4.00E-03	6.00E-03	2.00E-03	2.00E-03	6.00E-03	4.00E-03	2.00E-03	0.02	2.00E-03	4.00E-03	0	0.01	2.00E-03	0	2.00E-03	6.00E-03	0.03	2.00E-03	0.33	0.03
MS03	0.01	6.00E-03	2.00E-03	2.00E-03	6.00E-03	6.00E-03	2.00E-03	0	6.00E-03	2.00E-03	0.01	6.00E-03	6.00E-03	0	0.01	2.00E-03	0	2.00E-03	6.00E-03	0.03	2.00E-03	0.35	0.02
MS16	0.01	2.00E-03	4.00E-03	2.00E-03	0.01	0	6.00E-03	8.00E-03	2.00E-03	2.00E-03	0.02	6.00E-03	4.00E-03	4.00E-03	0.01	6.00E-03	0	4.00E-03	0.01	0.01	4.00E-03	0.34	0.01
MS06	0.01	8.00E-03	4.00E-03	2.00E-03	4.00E-03	0	8.00E-03	2.00E-03	0	2.00E-03	0.02	0	2.00E-03	0	0.01	4.00E-03	2.00E-03	0	8.00E-03	0.01	8.00E-03	0.32	0.01
MS33	8.00E-03	2.00E-03	0	0	0.01	0	6.00E-03	0	0	4.00E-03	0.01	2.00E-03	6.00E-03	0	6.00E-03	0	2.00E-03	6.00E-03	0.01	2.00E-03	0.32	0.01	
MS28	0.01	0.01	2.00E-03	2.00E-03	8.00E-03	4.00E-03	0	6.00E-03	2.00E-03	4.00E-03	0.01	0	4.00E-03	2.00E-03	0.01	6.00E-03	0	2.00E-03	6.00E-03	0.03	2.00E-03	0.33	0.03
MS21	0.01	0	6.00E-03	0	6.00E-03	4.00E-03	0.01	0	0	2.00E-03	0.02	8.00E-03	2.00E-03	0	0.02	2.00E-03	0	0	4.00E-03	0.02	4.00E-03	0.34	0.02
MS07	failed bisulfite conversio n	failed bisulfite conversio n	failed bisulfite conversio n	failed bisulfite conversio n	failed bisulfite conversio n	failed bisulfite conversio n	failed bisulfite conversio n	failed bisulfite conversio n	failed bisulfite conversio n	failed bisulfite conversio n	failed bisulfite conversio n	failed bisulfite conversio n	failed bisulfite conversio n	failed bisulfite conversio n	failed bisulfite conversio n	failed bisulfite conversio n	failed bisulfite conversio n	failed bisulfite conversio n	failed bisulfite conversio n	failed bisulfite conversio n	failed bisulfite conversio n	failed bisulfite conversio n	failed bisulfite conversio n
MS24	47,XXY	47,XXY	47,XXY	47,XXY	47,XXY	47,XXY	47,XXY	47,XXY	47,XXY	47,XXY	47,XXY	47,XXY	47,XXY	47,XXY	47,XXY	47,XXY	47,XXY	47,XXY	47,XXY	47,XXY	47,XXY	47,XXY	47,XXY
MS15	6.00E-03	4.00E-03	6.00E-03	2.00E-03	8.00E-03	0	8.00E-03	0	4.00E-03	2.00E-03	0.01	4.00E-03	4.00E-03	4.00E-03	4.00E-03	4.00E-03	0	0	8.00E-03	0.01	8.00E-03	0.41	0.02
MS18	0.01	8.00E-03	2.00E-03	2.00E-03	2.00E-03	2.00E-03	0.01	4.00E-03	0.01	4.00E-03	0.01	0.01	6.00E-03	0	0.01	8.00E-03	0	0	0.01	0.01	8.00E-03	0.28	8.00E-03
MS25	6.00E-03	6.00E-03	6.00E-03	2.00E-03	8.00E-03	0	2.00E-03	0	2.00E-03	0	0.02	6.00E-03	4.00E-03	0	6.00E-03	0	4.00E-03	2.00E-03	0.02	4.00E-03	0.43	0.02	
MS13	0.02	6.00E-03	6.00E-03	0	4.00E-03	4.00E-03	0.01	4.00E-03	6.00E-03	6.00E-03	0.03	0.01	6.00E-03	6.00E-03	0.01	4.00E-03	2.00E-03	6.00E-03	0.01	2.00E-03	0.2	0.02	
MS29	8.00E-03	4.00E-03	0	4.00E-03	6.00E-03	6.00E-03	0	6.00E-03	2.00E-03	2.00E-03	0.02	4.00E-03	2.00E-03	2.00E-03	4.00E-03	4.00E-03	0	0	0	0	0.33	0.02	0.02
MS11	450K QC	450K QC	450K QC	450K QC	450K QC	450K QC	450K QC	450K QC	450K QC	450K QC	450K QC	450K QC	450K QC	450K QC	450K QC	450K QC	450K QC	450K QC	450K QC	450K QC	450K QC	450K QC	450K QC
MS20	8.00E-03	0.01	6.00E-03	2.00E-03	4.00E-03	4.00E-03	0	8.00E-03	0	6.00E-03	0.02	2.00E-03	2.00E-03	4.00E-03	8.00E-03	0	2.00E-03	0	2.00E-03	0	0.4	0.01	0.01
MS26	6.00E-03	6.00E-03	2.00E-03	2.00E-03	6.00E-03	0	0.01	2.00E-03	2.00E-03	2.00E-03	0.02	2.00E-03	0	2.00E-03	6.00E-03	0	2.00E-03	0	2.00E-03	4.00E-03	0.42	0.02	0.02
MS35	0.01	0.01	2.00E-03	2.00E-03	2.00E-03	2.00E-03	0	8.00E-03	4.00E-03	2.00E-03	0.02	4.00E-03	6.00E-03	0	2.00E-03	0	4.00E-03	0	4.00E-03	0.36	0.01	0.01	0.01
MS09	6.00E-03	0.01	4.00E-03	2.00E-03	4.00E-03	4.00E-03	0	8.00E-03	0	4.00E-03	0.02	6.00E-03	2.00E-03	2.00E-03	0.01	4.00E-03	0	0	6.00E-03	0.34	0.01	0.01	0.01
MS04	4.00E-03	2.00E-03	4.00E-03	0	0.01	0	0	0	0	0	8.00E-03	2.00E-03	2.00E-03	6.00E-03	0.01	2.00E-03	0	0	6.00E-03	0.43	8.00E-03	0.02	0.02
MS17	0.01	4.00E-03	0.01	2.00E-03	4.00E-03	8.00E-03	0.01	4.00E-03	6.00E-03	6.00E-03	0.03	6.00E-03	0.02	2.00E-03	6.00E-03	0.01	2.00E-03	0	2.00E-03	0.01	0.33	0.02	0.02
MS34	4.00E-03	6.00E-03	2.00E-03	0	4.00E-03	0	4.00E-03	0	6.00E-03	2.00E-03	0.03	4.00E-03	8.00E-03	2.00E-03	0.01	0	0	4.00E-03	4.00E-03	0.33	4.00E-03	0.02	0.02
MS14	0.01	2.00E-03	6.00E-03	0	4.00E-03	0	4.00E-03	0	0.01	2.00E-03	0.03	8.00E-03	2.00E-03	0	0.01	4.00E-03	0	0	4.00E-03	0.39	0.01	0.01	0.01
MS23	0.01	2.00E-03	6.00E-03	4.00E-03	2.00E-03	2.00E-03	0.01	0	2.00E-03	0.03	8.00E-03	0.01	4.00E-03	0.01	2.00E-03	2.00E-03	2.00E-03	2.00E-03	0.01	0.25	0.02	0.02	0.02
MS19	0.02	6.00E-03	8.00E-03	2.00E-03	8.00E-03	0.02	6.00E-03	8.00E-03	0.01	0.04	0.02	0.02	4.00E-03	0.01	0.01	0.01	0	0	4.00E-03	0.19	0.03	0.03	0.03
MS32	2.00E-03	4.00E-03	8.00E-03	2.00E-03	8.00E-03	0	4.00E-03	0	2.00E-03	0.02	2.00E-03	2.00E-03	4.00E-03	4.00E-03	4.00E-03	4.00E-03	0	0	6.00E-03	0.44	0.02	0.02	0.02
MS27	0.01	6.00E-03	4.00E-03	0	6.00E-03	0	8.00E-03	0	8.00E-03	0	0.02	6.00E-03	4.00E-03	2.00E-03	6.00E-03	0	4.00E-03	0	4.00E-03	0.39	0.01	0.01	0.01
MS02	4.00E-03	8.00E-03	4.00E-03	2.00E-03	2.00E-03	0	8.00E-03	2.00E-03	0	0.01	4.00E-03	4.00E-03	2.00E-03	2.00E-03	6.00E-03	0	0	0	0.01	0.42	0.02	0.02	0.02
MS12	8.00E-03	4.00E-03	4.00E-03	4.00E-03	6.00E-03	0	6.00E-03	0	6.00E-03	0.02	6.00E-03	8.00E-03	2.00E-03	2.00E-03	4.00E-03	2.00E-03	2.00E-03	2.00E-03	0	0.4	0.02	0.02	0.02
MS31	4.00E-03	8.00E-03	4.00E-03	2.00E-03	2.00E-03	0	4.00E-03	2.00E-03	4.00E-03	0.03	0	2.00E-03	4.00E-03	4.00E-03	0.01	2.00E-03	0	2.00E-03	4.00E-03	0.37	0.01	0.01	0.01
ES01	4.00E-03	6.00E-03	6.00E-03	2.00E-03	6.00E-03	0	8.00E-03	0	8.00E-03	0.02	2.00E-03	2.00E-03	2.00E-03	2.00E-03	0.01	2.00E-03	0	0	6.00E-03	0.32	0.01	0.01	0.01
ES11	6.00E-03	8.00E-03	4.00E-03	0	4.00E-03	2.00E-03	8.00E-03	2.00E-03	2.00E-03	0.01	2.00E-03	0	2.00E-03	2.00E-03	8.00E-03	0.01	2.00E-03	0	8.00E-03	0.27	0.02	0.02	0.02
ES09	0.01	4.00E-03	4.00E-03	2.00E-03	2.00E-03	0	0.01	6.00E-03	8.00E-03	0.02	8.00E-03	4.00E-03	2.00E-03	2.00E-03	0.01	8.00E-03	0	0	6.00E-03	0.32	0.01	0.01	0.01

ES06	2.00E-03	6.00E-03	8.00E-03	2.00E-03	8.00E-03	0	0.01	2.00E-03	4.00E-03	0.01	2.00E-03	0	2.00E-03	6.00E-03	6.00E-03	6.00E-03	6.00E-03	0	2.00E-03	4.00E-03	0.42	0.02
ES14	4.00E-03	0.01	4.00E-03	2.00E-03	2.00E-03	4.00E-03	0.01	2.00E-03	2.00E-03	0.01	2.00E-03	0	2.00E-03	6.00E-03	6.00E-03	0.01	4.00E-03	4.00E-03	0	2.00E-03	0.43	0.01
ES16	8.00E-03	4.00E-03	4.00E-03	0	6.00E-03	0	6.00E-03	2.00E-03	0	0.01	4.00E-03	6.00E-03	6.00E-03	8.00E-03	4.00E-03	4.00E-03	0	0	0	0	0.44	0.01
ES13	4.00E-03	8.00E-03	4.00E-03	2.00E-03	0	2.00E-03	4.00E-03	4.00E-03	2.00E-03	0.02	4.00E-03	2.00E-03	2.00E-03	4.00E-03	0	0	0	0	2.00E-03	2.00E-03	0.55	0.02
ES05	8.00E-03	0.01	8.00E-03	0	8.00E-03	2.00E-03	6.00E-03	0	2.00E-03	0.01	6.00E-03	4.00E-03	2.00E-03	4.00E-03	0	0	0	0	2.00E-03	4.00E-03	0.31	0.01
ES04	4.00E-03	2.00E-03	8.00E-03	4.00E-03	2.00E-03	2.00E-03	8.00E-03	2.00E-03	0	0.02	4.00E-03	6.00E-03	0	0.01	2.00E-03	4.00E-03	6.00E-03	0	4.00E-03	2.00E-03	0.26	0.02
ES18	2.00E-03	2.00E-03	8.00E-03	0	4.00E-03	0	6.00E-03	0	4.00E-03	0.01	2.00E-03	2.00E-03	0	6.00E-03	4.00E-03	2.00E-03	6.00E-03	0	2.00E-03	2.00E-03	0.48	0.02
ES07	0	4.00E-03	4.00E-03	2.00E-03	2.00E-03	2.00E-03	4.00E-03	2.00E-03	2.00E-03	0.02	2.00E-03	0	4.00E-03	0.01	2.00E-03	0	0	0	2.00E-03	4.00E-03	0.42	0.02
ES17	6.00E-03	4.00E-03	4.00E-03	0	8.00E-03	0	8.00E-03	0	2.00E-03	0.01	2.00E-03	4.00E-03	0	2.00E-03	0	0	0	0	2.00E-03	0	0.44	0.01
ES10	0	0	2.00E-03	0	4.00E-03	0	4.00E-03	0	2.00E-03	0.02	4.00E-03	4.00E-03	2.00E-03	2.00E-03	0	0	0	0	2.00E-03	0	0.68	0.01
ES03	4.00E-03	6.00E-03	6.00E-03	2.00E-03	0	0	2.00E-03	2.00E-03	0	0.01	6.00E-03	4.00E-03	0	8.00E-03	4.00E-03	0	0	0	2.00E-03	4.00E-03	0.65	0.02
ES15	8.00E-03	2.00E-03	6.00E-03	0	2.00E-03	0	8.00E-03	0	4.00E-03	0.01	6.00E-03	8.00E-03	0	2.00E-03	2.00E-03	0	0	0	0	0	0.51	0.02
ES12	4.00E-03	8.00E-03	4.00E-03	0	6.00E-03	0	6.00E-03	2.00E-03	2.00E-03	6.00E-03	4.00E-03	0	0	2.00E-03	0	0	0	0	0	0	0.41	0.01
21	47,XXY	47,XXY	47,XXY	47,XXY	47,XXY	47,XXY	47,XXY	47,XXY	47,XXY	47,XXY	47,XXY	47,XXY	47,XXY	47,XXY	47,XXY	47,XXY	47,XXY	47,XXY	47,XXY	47,XXY	47,XXY	47,XXY
43	2.00E-03	4.00E-03	2.00E-03	2.00E-03	2.00E-03	4.00E-03	8.00E-03	2.00E-03	0	0.01	2.00E-03	4.00E-03	0	0.01	0	0	0	0	0	6.00E-03	0.39	6.00E-03
29	0.02	6.00E-03	6.00E-03	0	2.00E-03	0	2.00E-03	4.00E-03	6.00E-03	0.01	6.00E-03	2.00E-03	0	4.00E-03	6.00E-03	2.00E-03	4.00E-03	0	2.00E-03	2.00E-03	0.39	0.01
41	0.01	8.00E-03	6.00E-03	0	4.00E-03	0	2.00E-03	0	0	0.02	4.00E-03	0	0	2.00E-03	2.00E-03	2.00E-03	0	0	6.00E-03	0.3	0.02	
36	0.01	4.00E-03	4.00E-03	2.00E-03	2.00E-03	0	4.00E-03	4.00E-03	2.00E-03	0.01	0.01	2.00E-03	2.00E-03	8.00E-03	6.00E-03	6.00E-03	0	0	2.00E-03	2.00E-03	0.45	0.02
39	4.00E-03	6.00E-03	4.00E-03	0	4.00E-03	0	6.00E-03	2.00E-03	4.00E-03	0.03	6.00E-03	6.00E-03	2.00E-03	4.00E-03	0	2.00E-03	2.00E-03	2.00E-03	4.00E-03	4.00E-03	0.34	0.01
45	4.00E-03	8.00E-03	6.00E-03	0	2.00E-03	0	2.00E-03	0	6.00E-03	0.03	8.00E-03	4.00E-03	0	0.01	2.00E-03	0	0	0	6.00E-03	0	0.3	0.02
44	6.00E-03	4.00E-03	8.00E-03	2.00E-03	6.00E-03	0	8.00E-03	2.00E-03	4.00E-03	0.01	6.00E-03	6.00E-03	2.00E-03	6.00E-03	4.00E-03	0	0	0	0.01	0	0.43	0.03
10	4.00E-03	6.00E-03	8.00E-03	6.00E-03	0	0	4.00E-03	0	4.00E-03	0.02	4.00E-03	2.00E-03	0	4.00E-03	2.00E-03	0	0	0	0	0	0.39	6.00E-03
37	4.00E-03	8.00E-03	2.00E-03	2.00E-03	2.00E-03	0	2.00E-03	0	2.00E-03	0.02	6.00E-03	4.00E-03	0	6.00E-03	2.00E-03	0	0	0	4.00E-03	0	0.43	0.02
12	0.01	6.00E-03	8.00E-03	2.00E-03	4.00E-03	8.00E-03	0.01	2.00E-03	8.00E-03	0.04	6.00E-03	6.00E-03	4.00E-03	4.00E-03	0.02	6.00E-03	0	0	2.00E-03	0.01	0.29	0.02
3	8.00E-03	2.00E-03	2.00E-03	0	2.00E-03	0	2.00E-03	0	0	8.00E-03	2.00E-03	2.00E-03	0	0.01	4.00E-03	0	0	0	6.00E-03	0	0.54	0.02
14	2.00E-03	0	4.00E-03	0	4.00E-03	0	4.00E-03	0	2.00E-03	0.01	4.00E-03	6.00E-03	2.00E-03	6.00E-03	6.00E-03	0	0	0	6.00E-03	0	0.44	0.02
35	0.01	8.00E-03	8.00E-03	4.00E-03	2.00E-03	0	0.01	0	8.00E-03	0.03	6.00E-03	4.00E-03	4.00E-03	0.01	0	4.00E-03	4.00E-03	0	4.00E-03	4.00E-03	0.22	0.02
1	4.00E-03	2.00E-03	6.00E-03	4.00E-03	4.00E-03	0	6.00E-03	0	4.00E-03	0.02	8.00E-03	4.00E-03	0	8.00E-03	0	0	0	0	2.00E-03	4.00E-03	0.35	0.01
50	0.01	0.01	0.01	0	4.00E-03	6.00E-03	4.00E-03	2.00E-03	0	0.02	4.00E-03	6.00E-03	4.00E-03	6.00E-03	6.00E-03	0	0	0	2.00E-03	0	0.17	0.01
13	6.00E-03	8.00E-03	4.00E-03	0	4.00E-03	2.00E-03	4.00E-03	2.00E-03	0	0.01	4.00E-03	6.00E-03	6.00E-03	6.00E-03	2.00E-03	0	0	0	6.00E-03	0	0.44	0.01
20	8.00E-03	4.00E-03	4.00E-03	0	0.01	2.00E-03	2.00E-03	0	2.00E-03	0.01	0	2.00E-03	4.00E-03	4.00E-03	2.00E-03	2.00E-03	0	0	2.00E-03	0	0.46	0.02
40	0.01	2.00E-03	4.00E-03	0	2.00E-03	4.00E-03	4.00E-03	0	0	0.02	2.00E-03	4.00E-03	2.00E-03	6.00E-03	2.00E-03	0	0	0	4.00E-03	0	0.35	0.02
5	6.00E-03	6.00E-03	2.00E-03	0	0.01	2.00E-03	6.00E-03	4.00E-03	6.00E-03	0.02	4.00E-03	2.00E-03	0	0.01	4.00E-03	0	0	0	4.00E-03	6.00E-03	0.36	6.00E-03
9	6.00E-03	0.01	6.00E-03	2.00E-03	2.00E-03	2.00E-03	8.00E-03	0	2.00E-03	0.03	4.00E-03	4.00E-03	0	6.00E-03	2.00E-03	0	0	0	2.00E-03	0.01	0.22	0.02
51	4.00E-03	2.00E-03	2.00E-03	2.00E-03	6.00E-03	6.00E-03	2.00E-03	6.00E-03	0	0.02	2.00E-03	4.00E-03	2.00E-03	2.00E-03	6.00E-03	2.00E-03	0	0	2.00E-03	6.00E-03	0.4	0.01
16	8.00E-03	2.00E-03	4.00E-03	0	0	2.00E-03	6.00E-03	2.00E-03	2.00E-03	0.03	6.00E-03	4.00E-03	0	4.00E-03	2.00E-03	0	0	0	6.00E-03	0	0.39	0.03
38	4.00E-03	6.00E-03	2.00E-03	0	4.00E-03	0	0.01	0	4.00E-03	0.02	0.01	4.00E-03	2.00E-03	6.00E-03	4.00E-03	2.00E-03	2.00E-03	2.00E-03	2.00E-03	2.00E-03	0.24	0.02

53	8.00E-03	8.00E-03	2.00E-03	4.00E-03	0	0	4.00E-03	2.00E-03	0	0.02	6.00E-03	6.00E-03	2.00E-03	6.00E-03	2.00E-03	0	2.00E-03	8.00E-03	0.35	0.01
17	6.00E-03	4.00E-03	6.00E-03	0	0.01	0	2.00E-03	2.00E-03	0	0.02	2.00E-03	0	4.00E-03	2.00E-03	2.00E-03	0	2.00E-03	4.00E-03	0.51	0.01
11	4.00E-03	0	4.00E-03	0	4.00E-03	0	2.00E-03	0	0	2.00E-03	2.00E-03	4.00E-03	6.00E-03	6.00E-03	0	0	4.00E-03	0.57	0.02	
54	6.00E-03	6.00E-03	6.00E-03	0	6.00E-03	0	8.00E-03	2.00E-03	0	0.02	0.01	2.00E-03	2.00E-03	4.00E-03	4.00E-03	0	4.00E-03	0.44	0.02	
32	2.00E-03	0.01	2.00E-03	4.00E-03	2.00E-03	0	0.01	2.00E-03	0	0.03	6.00E-03	6.00E-03	2.00E-03	6.00E-03	2.00E-03	0	4.00E-03	0.28	0.02	
42	4.00E-03	0.01	8.00E-03	4.00E-03	4.00E-03	0	0	0	0	0.01	4.00E-03	4.00E-03	0	4.00E-03	0	0	6.00E-03	0.33	0.01	
28	0.01	6.00E-03	4.00E-03	4.00E-03	6.00E-03	0	4.00E-03	4.00E-03	0	0.02	4.00E-03	4.00E-03	2.00E-03	0.01	2.00E-03	0	6.00E-03	0.45	0.02	
6	8.00E-03	0.02	2.00E-03	0	0	0	6.00E-03	4.00E-03	0	0.02	6.00E-03	4.00E-03	2.00E-03	4.00E-03	2.00E-03	0	8.00E-03	0.33	0.02	
15	2.00E-03	0.01	4.00E-03	0	6.00E-03	0	6.00E-03	0	2.00E-03	0.02	2.00E-03	0	8.00E-03	4.00E-03	4.00E-03	0	4.00E-03	0.27	0.02	
27	4.00E-03	2.00E-03	2.00E-03	0	8.00E-03	2.00E-03	8.00E-03	2.00E-03	0	0.01	0.01	2.00E-03	0	4.00E-03	4.00E-03	0	2.00E-03	0.47	0.01	
30	2.00E-03	6.00E-03	2.00E-03	2.00E-03	0.01	0	8.00E-03	0	2.00E-03	0.01	6.00E-03	2.00E-03	2.00E-03	8.00E-03	2.00E-03	0	4.00E-03	0.33	0.02	
33	8.00E-03	4.00E-03	2.00E-03	4.00E-03	6.00E-03	0	4.00E-03	2.00E-03	0	0.02	4.00E-03	4.00E-03	2.00E-03	8.00E-03	2.00E-03	0	2.00E-03	0.49	0.02	
7	4.00E-03	8.00E-03	4.00E-03	0	0	0	4.00E-03	4.00E-03	8.00E-03	0.02	4.00E-03	4.00E-03	0	0.01	4.00E-03	2.00E-03	2.00E-03	0.3	0.02	
47	2.00E-03	8.00E-03	2.00E-03	0	4.00E-03	0	2.00E-03	4.00E-03	2.00E-03	0.01	2.00E-03	0	4.00E-03	6.00E-03	8.00E-03	4.00E-03	0	0.62	0.01	
8	4.00E-03	2.00E-03	8.00E-03	2.00E-03	8.00E-03	0	6.00E-03	0	2.00E-03	0.01	6.00E-03	0	0	0.01	0	0	2.00E-03	0.26	8.00E-03	
25	6.00E-03	8.00E-03	6.00E-03	2.00E-03	4.00E-03	4.00E-03	2.00E-03	0	4.00E-03	0.01	2.00E-03	0	2.00E-03	0.01	2.00E-03	0	4.00E-03	0.44	0.02	
2	0.01	2.00E-03	0	0	4.00E-03	0	6.00E-03	6.00E-03	4.00E-03	0.02	2.00E-03	2.00E-03	4.00E-03	0.01	0	0	2.00E-03	0.38	0.01	
34	4.00E-03	4.00E-03	2.00E-03	2.00E-03	2.00E-03	0	6.00E-03	2.00E-03	6.00E-03	0.02	6.00E-03	2.00E-03	0.01	8.00E-03	2.00E-03	0	0	0.31	0.03	
23	4.00E-03	2.00E-03	2.00E-03	4.00E-03	8.00E-03	0	4.00E-03	0	4.00E-03	0.02	2.00E-03	4.00E-03	2.00E-03	0.01	0	0	2.00E-03	0.33	8.00E-03	
26	0.01	8.00E-03	4.00E-03	2.00E-03	0.01	2.00E-03	4.00E-03	2.00E-03	0	0.03	6.00E-03	4.00E-03	2.00E-03	6.00E-03	6.00E-03	0	2.00E-03	0.27	0.03	
49	4.00E-03	4.00E-03	4.00E-03	0	6.00E-03	0	0.01	0	2.00E-03	0.03	8.00E-03	6.00E-03	2.00E-03	0.01	0	0	2.00E-03	0.33	8.00E-03	
4	8.00E-03	2.00E-03	8.00E-03	0	8.00E-03	2.00E-03	4.00E-03	2.00E-03	4.00E-03	0.03	2.00E-03	0	8.00E-03	4.00E-03	2.00E-03	0	4.00E-03	0.41	0.02	
18	4.00E-03	0.01	4.00E-03	2.00E-03	0	4.00E-03	4.00E-03	0	4.00E-03	0.02	6.00E-03	2.00E-03	2.00E-03	0.01	2.00E-03	0	8.00E-03	0.4	0.01	
52	4.00E-03	2.00E-03	0	2.00E-03	6.00E-03	0	8.00E-03	2.00E-03	6.00E-03	0.02	4.00E-03	2.00E-03	0	0.01	0	0	8.00E-03	0.3	0.03	
19	4.00E-03	4.00E-03	8.00E-03	0	8.00E-03	0	4.00E-03	0	4.00E-03	0.02	4.00E-03	6.00E-03	2.00E-03	4.00E-03	0	0	4.00E-03	0.39	0.02	
31	4.00E-03	6.00E-03	4.00E-03	0	4.00E-03	2.00E-03	2.00E-03	2.00E-03	2.00E-03	0.02	2.00E-03	2.00E-03	4.00E-03	4.00E-03	0	0	2.00E-03	0.44	0.02	

Supplementary Table 5. Tissue prediction results for all samples included in Chapter 3 part 3. Shown is the third part of the tissue prediction results using the online DNA methylation age calculator (Horvath, 2016).

Individual	Probability from Heart	Probability from Kidney	Probability from Liver	Probability from Liver	Probability from Lung	Probability from Mesenchymal stromal cells	Probability from Muscle	Probability from Neuron	Probability from Placenta	Probability from Prostate normal	Probability from Saliva	Probability from Sperm	Probability from Stomach	Probability from Thyroid	Probability from Uterine Cervix	Probability from Uterine Endomet
MS19	0.01	6.00E-03	4.00E-03	4.00E-03	0	2.00E-03	6.00E-03	0.04	4.00E-03	0.01	4.00E-03	4.00E-03	0	6.00E-03	4.00E-03	4.00E-03
MS22	6.00E-03	0.01	2.00E-03	4.00E-03	0	2.00E-03	4.00E-03	0.04	2.00E-03	6.00E-03	2.00E-03	8.00E-03	0	4.00E-03	0	8.00E-03
MS33	6.00E-03	6.00E-03	4.00E-03	2.00E-03	0	0	0.01	0.03	2.00E-03	6.00E-03	4.00E-03	4.00E-03	0	8.00E-03	2.00E-03	0.01
MS11	0.01	8.00E-03	8.00E-03	4.00E-03	0	4.00E-03	0.01	0.05	8.00E-03	0.01	2.00E-03	6.00E-03	2.00E-03	8.00E-03	6.00E-03	0.02
MS30	0.01	2.00E-03	4.00E-03	4.00E-03	2.00E-03	6.00E-03	4.00E-03	0.05	8.00E-03	2.00E-03	0	4.00E-03	0	6.00E-03	4.00E-03	0.01
MS28	0.01	0.02	6.00E-03	4.00E-03	2.00E-03	4.00E-03	4.00E-03	0.05	2.00E-03	0.01	6.00E-03	8.00E-03	4.00E-03	8.00E-03	2.00E-03	0.02
MS04	8.00E-03	4.00E-03	2.00E-03	4.00E-03	2.00E-03	2.00E-03	8.00E-03	0.05	2.00E-03	0.02	2.00E-03	4.00E-03	2.00E-03	0.01	0	0.01
MS36	0.01	8.00E-03	6.00E-03	8.00E-03	4.00E-03	2.00E-03	8.00E-03	0.06	8.00E-03	0.01	2.00E-03	8.00E-03	0	6.00E-03	0	0.01
MS17	0.01	0.01	8.00E-03	4.00E-03	0	6.00E-03	6.00E-03	0.06	6.00E-03	0.01	6.00E-03	4.00E-03	0	0.01	0	0.03
MS09	8.00E-03	8.00E-03	6.00E-03	4.00E-03	4.00E-03	4.00E-03	6.00E-03	0.05	2.00E-03	0.01	2.00E-03	6.00E-03	0	8.00E-03	2.00E-03	0.02
MS06	6.00E-03	0.01	8.00E-03	2.00E-03	2.00E-03	6.00E-03	6.00E-03	0.04	2.00E-03	0.02	6.00E-03	6.00E-03	2.00E-03	0.01	0	0.01
MS15	8.00E-03	2.00E-03	8.00E-03	2.00E-03	2.00E-03	4.00E-03	4.00E-03	0.06	2.00E-03	0.01	2.00E-03	8.00E-03	0	0.01	6.00E-03	0.02
MS14	4.00E-03	0.01	6.00E-03	2.00E-03	2.00E-03	6.00E-03	4.00E-03	0.05	4.00E-03	0.01	0.01	8.00E-03	2.00E-03	0.01	4.00E-03	0.02
MS18	0.01	6.00E-03	8.00E-03	8.00E-03	2.00E-03	6.00E-03	2.00E-03	0.05	8.00E-03	0.01	2.00E-03	6.00E-03	2.00E-03	0.01	4.00E-03	0.02
MS21	8.00E-03	2.00E-03	4.00E-03	2.00E-03	4.00E-03	6.00E-03	0.01	0.04	2.00E-03	0.01	0	4.00E-03	2.00E-03	4.00E-03	0	0.01
MS29	failed reported sex	failed reported sex	failed reported sex	failed reported sex	failed reported sex	failed reported sex	failed reported sex	failed reported sex	failed reported sex	failed reported sex	failed reported sex	failed reported sex	failed reported sex	failed reported sex	failed reported sex	failed reported sex
MS23	0.01	4.00E-03	6.00E-03	2.00E-03	4.00E-03	6.00E-03	4.00E-03	0.06	8.00E-03	0.01	6.00E-03	2.00E-03	2.00E-03	4.00E-03	2.00E-03	0.02
MS05	0.01	4.00E-03	8.00E-03	2.00E-03	2.00E-03	4.00E-03	0.01	0.06	4.00E-03	0.01	4.00E-03	6.00E-03	2.00E-03	0.02	4.00E-03	0.02
MS12	8.00E-03	8.00E-03	6.00E-03	4.00E-03	2.00E-03	4.00E-03	0.01	0.06	4.00E-03	0.01	4.00E-03	8.00E-03	2.00E-03	8.00E-03	2.00E-03	0.01
MS07	8.00E-03	8.00E-03	6.00E-03	2.00E-03	2.00E-03	8.00E-03	2.00E-03	0.06	6.00E-03	6.00E-03	2.00E-03	6.00E-03	0	6.00E-03	2.00E-03	0.02
MS10	4.00E-03	4.00E-03	6.00E-03	6.00E-03	2.00E-03	8.00E-03	4.00E-03	0.05	0	6.00E-03	4.00E-03	2.00E-03	2.00E-03	4.00E-03	4.00E-03	0.02
MS27	8.00E-03	6.00E-03	6.00E-03	2.00E-03	4.00E-03	0.01	8.00E-03	0.05	6.00E-03	0.01	4.00E-03	0.01	0	0.01	4.00E-03	0.03
MS08	0.01	4.00E-03	6.00E-03	2.00E-03	0	0	6.00E-03	0.06	4.00E-03	8.00E-03	2.00E-03	4.00E-03	0	0.01	2.00E-03	0.02
MS25	4.00E-03	0	8.00E-03	6.00E-03	2.00E-03	4.00E-03	0.01	0.06	6.00E-03	0.02	6.00E-03	8.00E-03	0	0.01	2.00E-03	0.02
MS16	6.00E-03	2.00E-03	4.00E-03	2.00E-03	4.00E-03	4.00E-03	4.00E-03	0.06	4.00E-03	0.01	2.00E-03	8.00E-03	2.00E-03	0.01	4.00E-03	0.02
MS24	47,XXY	47,XXY	47,XXY	47,XXY	47,XXY	47,XXY	47,XXY	47,XXY	47,XXY	47,XXY	47,XXY	47,XXY	47,XXY	47,XXY	47,XXY	47,XXY
MS35	8.00E-03	6.00E-03	6.00E-03	4.00E-03	2.00E-03	4.00E-03	4.00E-03	0.07	4.00E-03	6.00E-03	4.00E-03	0.01	2.00E-03	8.00E-03	0	0.02

MS34	6.00E-03	4.00E-03	0.01	6.00E-03	2.00E-03	6.00E-03	4.00E-03	0.01	8.00E-03	6.00E-03	8.00E-03	4.00E-03	8.00E-03	2.00E-03	0.03
MS01	0.01	4.00E-03	0	4.00E-03	2.00E-03	6.00E-03	4.00E-03	0.02	2.00E-03	4.00E-03	4.00E-03	2.00E-03	4.00E-03	4.00E-03	0.01
MS32	6.00E-03	0.01	8.00E-03	2.00E-03	4.00E-03	4.00E-03	0.01	0.06	6.00E-03	6.00E-03	4.00E-03	0	4.00E-03	4.00E-03	0.02
MS13	0.01	0.01	4.00E-03	4.00E-03	0	0.01	0.01	0.04	2.00E-03	4.00E-03	4.00E-03	0	8.00E-03	0.01	0.02
MS03	0.01	0.01	0.01	2.00E-03	2.00E-03	6.00E-03	0.01	0.05	4.00E-03	2.00E-03	2.00E-03	6.00E-03	0.01	2.00E-03	0.02
MS20	4.00E-03	4.00E-03	4.00E-03	2.00E-03	2.00E-03	4.00E-03	4.00E-03	0.07	4.00E-03	6.00E-03	6.00E-03	0	8.00E-03	6.00E-03	0.01
MS26	0.01	4.00E-03	6.00E-03	2.00E-03	4.00E-03	2.00E-03	8.00E-03	0.06	4.00E-03	6.00E-03	2.00E-03	0	8.00E-03	0	0.02
MS31	4.00E-03	4.00E-03	4.00E-03	2.00E-03	2.00E-03	2.00E-03	0.01	0.03	6.00E-03	6.00E-03	2.00E-03	2.00E-03	6.00E-03	6.00E-03	0.01
ES01	8.00E-03	6.00E-03	4.00E-03	8.00E-03	4.00E-03	4.00E-03	0.01	0.05	4.00E-03	8.00E-03	8.00E-03	4.00E-03	8.00E-03	2.00E-03	0.01
ES14	0.01	0.01	6.00E-03	4.00E-03	0.01	2.00E-03	0.01	0.02	4.00E-03	0	4.00E-03	0.01	0.02	0	0.04
ES12	0.01	8.00E-03	0.01	4.00E-03	0.01	8.00E-03	8.00E-03	0.04	6.00E-03	4.00E-03	2.00E-03	8.00E-03	0.02	2.00E-03	0.04
ES16	0.01	0.01	4.00E-03	8.00E-03	4.00E-03	0	2.00E-03	0.02	2.00E-03	0	4.00E-03	6.00E-03	0.03	2.00E-03	0.04
ES15	0.02	0.02	8.00E-03	6.00E-03	0.01	2.00E-03	8.00E-03	0.03	4.00E-03	2.00E-03	2.00E-03	6.00E-03	0.02	2.00E-03	0.03
ES10	0.01	0.01	0.01	4.00E-03	0	6.00E-03	6.00E-03	0.04	6.00E-03	0	8.00E-03	4.00E-03	4.00E-03	2.00E-03	0.02
ES05	6.00E-03	0.01	8.00E-03	2.00E-03	4.00E-03	0.01	0.01	0.05	2.00E-03	8.00E-03	2.00E-03	0	6.00E-03	4.00E-03	0.02
ES13	6.00E-03	0.02	0.01	0.01	0.02	0	4.00E-03	0.03	6.00E-03	2.00E-03	8.00E-03	6.00E-03	0.01	2.00E-03	0.03
ES17	8.00E-03	0.02	0.01	6.00E-03	4.00E-03	8.00E-03	0.02	0.06	0.01	4.00E-03	4.00E-03	4.00E-03	0.01	0	0.04
ES04	0	6.00E-03	6.00E-03	6.00E-03	2.00E-03	6.00E-03	6.00E-03	0.05	2.00E-03	6.00E-03	2.00E-03	0	8.00E-03	0	0.01
ES18	0.01	8.00E-03	6.00E-03	0.01	0.01	6.00E-03	6.00E-03	0.02	4.00E-03	4.00E-03	8.00E-03	8.00E-03	0.03	2.00E-03	0.04
ES11	4.00E-03	0.01	6.00E-03	4.00E-03	0	2.00E-03	8.00E-03	0.05	0	8.00E-03	8.00E-03	0	8.00E-03	6.00E-03	8.00E-03
ES02	0.01	4.00E-03	6.00E-03	4.00E-03	2.00E-03	6.00E-03	8.00E-03	0.05	6.00E-03	6.00E-03	2.00E-03	2.00E-03	8.00E-03	2.00E-03	0.02
ES06	4.00E-03	0.01	6.00E-03	4.00E-03	0.01	0.01	8.00E-03	0.05	4.00E-03	4.00E-03	4.00E-03	2.00E-03	2.00E-03	0.01	0.02
ES07	6.00E-03	0.02	0.02	6.00E-03	8.00E-03	8.00E-03	0	0.07	8.00E-03	4.00E-03	6.00E-03	4.00E-03	0.03	0	0.05
ES03	0.01	2.00E-03	8.00E-03	0	0	4.00E-03	6.00E-03	0.05	6.00E-03	8.00E-03	2.00E-03	0	8.00E-03	4.00E-03	0.02
ES09	0.02	0.02	0.01	8.00E-03	6.00E-03	0.01	0.02	0.08	4.00E-03	2.00E-03	8.00E-03	8.00E-03	0.02	0	0.03
12	0.01	0.01	6.00E-03	2.00E-03	2.00E-03	0.01	0.01	0.04	6.00E-03	0.01	2.00E-03	0	0.01	4.00E-03	0.03
49	8.00E-03	8.00E-03	6.00E-03	6.00E-03	0	6.00E-03	8.00E-03	0.05	4.00E-03	6.00E-03	2.00E-03	2.00E-03	6.00E-03	0	0.01
11	8.00E-03	8.00E-03	6.00E-03	0	2.00E-03	8.00E-03	4.00E-03	0.03	6.00E-03	4.00E-03	4.00E-03	0	6.00E-03	0	0.02
10	8.00E-03	0.01	0.01	2.00E-03	0	6.00E-03	0	0.06	4.00E-03	6.00E-03	4.00E-03	4.00E-03	0.01	0	0.01
5	8.00E-03	0.01	2.00E-03	2.00E-03	0	2.00E-03	6.00E-03	0.05	6.00E-03	0.01	2.00E-03	0	4.00E-03	2.00E-03	0.01
24	failed 450K QC	failed 450K QC	failed 450K QC	failed 450K QC	failed 450K QC	failed 450K QC	failed 450K QC	failed 450K QC	failed 450K QC	failed 450K QC	failed 450K QC	failed 450K QC	failed 450K QC	failed 450K QC	failed 450K QC
7	8.00E-03	0.01	4.00E-03	2.00E-03	0	8.00E-03	0.01	0.05	6.00E-03	6.00E-03	2.00E-03	0	2.00E-03	0	0.02
8	0.01	6.00E-03	0.01	4.00E-03	0	4.00E-03	0.02	0.05	6.00E-03	8.00E-03	0.01	0	6.00E-03	6.00E-03	0.01
37	0	0.01	0.01	4.00E-03	0	8.00E-03	8.00E-03	0.06	6.00E-03	0.01	4.00E-03	4.00E-03	8.00E-03	6.00E-03	0.02
17	4.00E-03	0.01	0.01	8.00E-03	6.00E-03	6.00E-03	8.00E-03	0.06	4.00E-03	6.00E-03	6.00E-03	0	8.00E-03	8.00E-03	0.02
30	0.01	6.00E-03	8.00E-03	4.00E-03	0	0	4.00E-03	0.05	8.00E-03	4.00E-03	2.00E-03	2.00E-03	4.00E-03	4.00E-03	0.01
3	8.00E-03	0.01	0.01	2.00E-03	0	0	0.01	0.06	4.00E-03	4.00E-03	4.00E-03	0	0.01	0	0.02

14	4.00E-03	4.00E-03	4.00E-03	4.00E-03	6.00E-03	2.00E-03	6.00E-03	4.00E-03	0.05	4.00E-03	0.01	0.01	0.01	2.00E-03	0.01	0.01	2.00E-03	6.00E-03	2.00E-03	2.00E-03	0.02	
39	8.00E-03	0.01	4.00E-03	8.00E-03	8.00E-03	8.00E-03	8.00E-03	4.00E-03	0.06	0.01	4.00E-03	6.00E-03	6.00E-03	0	6.00E-03	8.00E-03	2.00E-03	8.00E-03	8.00E-03	2.00E-03	0.02	
19	0.01	0.01	0.01	2.00E-03	2.00E-03	0	6.00E-03	6.00E-03	0.06	6.00E-03	0.02	4.00E-03	4.00E-03	2.00E-03	0.01	0.01	0	0.01	2.00E-03	2.00E-03	0.02	
23	0.01	2.00E-03	0.01	2.00E-03	2.00E-03	0	6.00E-03	6.00E-03	0.03	0.01	0.02	4.00E-03	4.00E-03	0.02	2.00E-03	8.00E-03	0	4.00E-03	8.00E-03	8.00E-03	0.01	
26	8.00E-03	8.00E-03	0.02	6.00E-03	6.00E-03	0	4.00E-03	4.00E-03	0.06	2.00E-03	0.02	6.00E-03	8.00E-03	4.00E-03	8.00E-03	6.00E-03	2.00E-03	6.00E-03	8.00E-03	8.00E-03	0.01	
6	8.00E-03	6.00E-03	6.00E-03	4.00E-03	4.00E-03	2.00E-03	4.00E-03	4.00E-03	0.06	4.00E-03	0.01	6.00E-03	8.00E-03	2.00E-03	8.00E-03	6.00E-03	2.00E-03	6.00E-03	0	8.00E-03	0.01	
44	2.00E-03	0.01	8.00E-03	8.00E-03	2.00E-03	2.00E-03	6.00E-03	6.00E-03	0.06	0.01	0.01	6.00E-03	4.00E-03	6.00E-03	4.00E-03	6.00E-03	2.00E-03	6.00E-03	0	8.00E-03	0.02	
20	2.00E-03	8.00E-03	8.00E-03	0	4.00E-03	2.00E-03	4.00E-03	4.00E-03	0.05	4.00E-03	0.01	2.00E-03	2.00E-03	0.01	0.01	8.00E-03	0	8.00E-03	0	8.00E-03	0.02	
42	0.01	0.01	4.00E-03	4.00E-03	4.00E-03	4.00E-03	2.00E-03	4.00E-03	0.07	8.00E-03	0.02	8.00E-03	8.00E-03	4.00E-03	8.00E-03	8.00E-03	2.00E-03	0.01	4.00E-03	4.00E-03	0.02	
9	2.00E-03	0.02	4.00E-03	2.00E-03	2.00E-03	2.00E-03	6.00E-03	6.00E-03	0.06	6.00E-03	0.02	4.00E-03	4.00E-03	6.00E-03	4.00E-03	8.00E-03	0	8.00E-03	2.00E-03	2.00E-03	0.01	
16	0.02	2.00E-03	0.01	8.00E-03	6.00E-03	0	4.00E-03	4.00E-03	0.05	8.00E-03	0.01	0	8.00E-03	6.00E-03	8.00E-03	8.00E-03	2.00E-03	8.00E-03	6.00E-03	8.00E-03	0.01	
34	8.00E-03	2.00E-03	8.00E-03	8.00E-03	6.00E-03	2.00E-03	2.00E-03	2.00E-03	0.05	2.00E-03	0.01	8.00E-03	8.00E-03	8.00E-03	8.00E-03	8.00E-03	0	8.00E-03	8.00E-03	8.00E-03	0.01	
46	6.00E-03	2.00E-03	0.01	8.00E-03	4.00E-03	0	4.00E-03	4.00E-03	0.04	4.00E-03	6.00E-03	2.00E-03	8.00E-03	8.00E-03	6.00E-03	6.00E-03	2.00E-03	0.01	2.00E-03	2.00E-03	0.01	
25	6.00E-03	0.01	8.00E-03	4.00E-03	4.00E-03	2.00E-03	6.00E-03	6.00E-03	0.06	6.00E-03	0.01	4.00E-03	8.00E-03	2.00E-03	6.00E-03	8.00E-03	0	0.01	2.00E-03	2.00E-03	0.02	
47	8.00E-03	4.00E-03	6.00E-03	2.00E-03	2.00E-03	0	4.00E-03	4.00E-03	0.06	6.00E-03	4.00E-03	4.00E-03	4.00E-03	8.00E-03	4.00E-03	0.01	2.00E-03	0.01	2.00E-03	2.00E-03	0.01	
33	2.00E-03	0.01	8.00E-03	8.00E-03	0	0	6.00E-03	8.00E-03	0.05	6.00E-03	8.00E-03	6.00E-03	8.00E-03	4.00E-03	8.00E-03	6.00E-03	0	4.00E-03	0	2.00E-03	0.01	
1	4.00E-03	4.00E-03	0.02	0	0	0	6.00E-03	4.00E-03	0.05	6.00E-03	0.01	2.00E-03	2.00E-03	4.00E-03	0.01	0	0	8.00E-03	2.00E-03	2.00E-03	8.00E-03	
45	0.01	6.00E-03	0.01	4.00E-03	4.00E-03	0	4.00E-03	4.00E-03	0.06	0.01	0.01	2.00E-03	2.00E-03	0	0.01	0	0	0.01	0	0	0.01	
41	6.00E-03	0.01	0.01	4.00E-03	4.00E-03	0	6.00E-03	6.00E-03	0.05	2.00E-03	0.01	6.00E-03	4.00E-03	6.00E-03	4.00E-03	2.00E-03	2.00E-03	0.01	2.00E-03	2.00E-03	0.03	
18	4.00E-03	4.00E-03	4.00E-03	4.00E-03	4.00E-03	0	6.00E-03	8.00E-03	0.05	4.00E-03	4.00E-03	8.00E-03	6.00E-03	8.00E-03	6.00E-03	6.00E-03	0	6.00E-03	2.00E-03	2.00E-03	0.02	
4	4.00E-03	0.01	8.00E-03	4.00E-03	4.00E-03	6.00E-03	8.00E-03	4.00E-03	0.06	4.00E-03	0.01	4.00E-03	6.00E-03	4.00E-03	6.00E-03	6.00E-03	0	0.01	0	0	0.01	
13	8.00E-03	8.00E-03	8.00E-03	6.00E-03	6.00E-03	2.00E-03	6.00E-03	6.00E-03	0.05	4.00E-03	0.01	2.00E-03	8.00E-03	6.00E-03	8.00E-03	8.00E-03	2.00E-03	0.01	4.00E-03	4.00E-03	0.01	
51	6.00E-03	4.00E-03	6.00E-03	6.00E-03	0	0	4.00E-03	4.00E-03	0.05	6.00E-03	2.00E-03	2.00E-03	8.00E-03	4.00E-03	8.00E-03	8.00E-03	2.00E-03	8.00E-03	2.00E-03	2.00E-03	8.00E-03	
31	4.00E-03	0.01	4.00E-03	4.00E-03	0	2.00E-03	4.00E-03	4.00E-03	0.05	4.00E-03	0.01	0	4.00E-03	4.00E-03	0	0.01	0	8.00E-03	6.00E-03	6.00E-03	0.02	
52	6.00E-03	0.01	6.00E-03	2.00E-03	2.00E-03	0	4.00E-03	4.00E-03	0.05	4.00E-03	6.00E-03	2.00E-03	6.00E-03	6.00E-03	6.00E-03	0.02	0	0.02	0	0	8.00E-03	0.02
21	4.00E-03	4.00E-03	4.00E-03	4.00E-03	4.00E-03	4.00E-03	4.00E-03	4.00E-03	4.00E-03	4.00E-03	4.00E-03	4.00E-03	4.00E-03	4.00E-03	4.00E-03	4.00E-03	4.00E-03	4.00E-03	4.00E-03	4.00E-03	4.00E-03	
2	6.00E-03	0.01	6.00E-03	4.00E-03	4.00E-03	0	6.00E-03	6.00E-03	0.05	4.00E-03	0.02	2.00E-03	4.00E-03	6.00E-03	6.00E-03	6.00E-03	0	8.00E-03	2.00E-03	2.00E-03	0.01	
53	0.01	6.00E-03	4.00E-03	4.00E-03	2.00E-03	2.00E-03	6.00E-03	6.00E-03	0.05	6.00E-03	6.00E-03	4.00E-03	4.00E-03	0	4.00E-03	4.00E-03	4.00E-03	0.01	2.00E-03	2.00E-03	0.02	
15	8.00E-03	4.00E-03	4.00E-03	6.00E-03	4.00E-03	0	6.00E-03	6.00E-03	0.04	6.00E-03	0.01	2.00E-03	6.00E-03	6.00E-03	6.00E-03	6.00E-03	0	4.00E-03	6.00E-03	6.00E-03	0.01	
40	6.00E-03	8.00E-03	8.00E-03	2.00E-03	2.00E-03	0	4.00E-03	4.00E-03	0.05	8.00E-03	0.01	0	8.00E-03	4.00E-03	8.00E-03	8.00E-03	0	0.01	2.00E-03	2.00E-03	0.03	
38	0.01	4.00E-03	4.00E-03	8.00E-03	8.00E-03	2.00E-03	4.00E-03	4.00E-03	0.05	2.00E-03	4.00E-03	4.00E-03	4.00E-03	6.00E-03	4.00E-03	6.00E-03	0	6.00E-03	6.00E-03	6.00E-03	0.01	
32	6.00E-03	6.00E-03	6.00E-03	6.00E-03	0	0	4.00E-03	6.00E-03	0.04	0	8.00E-03	2.00E-03	6.00E-03	6.00E-03	6.00E-03	0.02	2.00E-03	0	4.00E-03	4.00E-03	0.01	
35	8.00E-03	4.00E-03	4.00E-03	4.00E-03	0	0	4.00E-03	8.00E-03	0.05	0.01	8.00E-03	6.00E-03	6.00E-03	8.00E-03	8.00E-03	0.01	0	6.00E-03	6.00E-03	6.00E-03	0.01	
28	0.01	0.01	8.00E-03	2.00E-03	2.00E-03	2.00E-03	8.00E-03	8.00E-03	0.05	8.00E-03	0.01	2.00E-03	2.00E-03	6.00E-03	2.00E-03	0.01	0	0.01	6.00E-03	6.00E-03	6.00E-03	0.01
ES05	0.01	0.01	4.00E-03	4.00E-03	0	2.00E-03	2.00E-03	4.00E-03	0.01	4.00E-03	8.00E-03	2.00E-03	2.00E-03	6.00E-03	2.00E-03	2.00E-03	8.00E-03	0.01	2.00E-03	2.00E-03	0.03	
ES13	0.02	6.00E-03	4.00E-03	4.00E-03	2.00E-03	8.00E-03	4.00E-03	4.00E-03	0.06	4.00E-03	6.00E-03	6.00E-03	6.00E-03	4.00E-03	6.00E-03	0	4.00E-03	0.02	0	0	0.03	
ES07	0.03	0.01	4.00E-03	4.00E-03	4.00E-03	4.00E-03	4.00E-03	0	8.00E-03	0	4.00E-03	2.00E-03	2.00E-03	4.00E-03	4.00E-03	2.00E-03	6.00E-03	0.02	0	0	0.04	

ES12	0.01	0.02	8.00E-03	6.00E-03	4.00E-03	4.00E-03	2.00E-03	8.00E-03	0.01	0	0.01	4.00E-03	0	4.00E-03	0.01	2.00E-03	0.05
ES09	4.00E-03	0.02	4.00E-03	6.00E-03	4.00E-03	4.00E-03	4.00E-03	4.00E-03	0.01	2.00E-03	0.01	6.00E-03	4.00E-03	2.00E-03	0.03	0	0.06
ES17	8.00E-03	0.01	0.02	8.00E-03	6.00E-03	6.00E-03	4.00E-03	2.00E-03	0.11	2.00E-03	0.01	2.00E-03	2.00E-03	2.00E-03	0.02	2.00E-03	0.05
ES15	0.01	8.00E-03	6.00E-03	4.00E-03	4.00E-03	4.00E-03	4.00E-03	4.00E-03	0.01	0	4.00E-03	0	2.00E-03	2.00E-03	0.02	2.00E-03	0.03
ES03	0.01	0.02	0.01	2.00E-03	0.01	8.00E-03	8.00E-03	0.02	0.01	2.00E-03	4.00E-03	6.00E-03	2.00E-03	4.00E-03	0.02	2.00E-03	0.04
ES02	0.02	0.01	6.00E-03	2.00E-03	6.00E-03	0	0	6.00E-03	0.02	2.00E-03	6.00E-03	4.00E-03	0	4.00E-03	0.02	0	0.04
ES04	0.03	0.01	2.00E-03	0.01	0	0.01	0.01	6.00E-03	0.01	2.00E-03	6.00E-03	2.00E-03	2.00E-03	2.00E-03	0.01	2.00E-03	0.02
ES14	0.01	0.01	6.00E-03	4.00E-03	2.00E-03	2.00E-03	2.00E-03	8.00E-03	0.03	2.00E-03	0.01	4.00E-03	2.00E-03	0.01	0.02	2.00E-03	0.05
ES18	8.00E-03	0.01	4.00E-03	2.00E-03	2.00E-03	2.00E-03	2.00E-03	0	0.19	2.00E-03	8.00E-03	2.00E-03	8.00E-03	2.00E-03	0.02	2.00E-03	0.04
ES11	0.02	0.01	0.01	0.01	0.01	2.00E-03	2.00E-03	0.02	0.04	6.00E-03	0.02	4.00E-03	6.00E-03	2.00E-03	0.01	0	0.06
ES16	4.00E-03	0.01	2.00E-03	2.00E-03	2.00E-03	2.00E-03	2.00E-03	0.01	0.01	0	8.00E-03	2.00E-03	2.00E-03	0	0.01	0	0.02
ES10	0.02	4.00E-03	6.00E-03	2.00E-03	4.00E-03	4.00E-03	2.00E-03	8.00E-03	0.01	4.00E-03	0.01	6.00E-03	0	2.00E-03	0.02	2.00E-03	0.03
27	0.01	8.00E-03	8.00E-03	4.00E-03	6.00E-03	6.00E-03	6.00E-03	4.00E-03	0.03	0	0.01	2.00E-03	4.00E-03	8.00E-03	4.00E-03	2.00E-03	0.03
23	0.01	0.02	8.00E-03	4.00E-03	4.00E-03	4.00E-03	8.00E-03	8.00E-03	0.04	2.00E-03	0.01	2.00E-03	4.00E-03	2.00E-03	0.03	0	0.05
9	0.02	6.00E-03	6.00E-03	2.00E-03	8.00E-03	8.00E-03	4.00E-03	0.02	0.01	8.00E-03	0.01	2.00E-03	0	4.00E-03	0.01	0	0.04
51	0.01	0.02	0.02	6.00E-03	6.00E-03	6.00E-03	8.00E-03	0.01	0.04	2.00E-03	0.01	4.00E-03	4.00E-03	4.00E-03	0.03	0	0.04
1	0.02	0.02	4.00E-03	6.00E-03	0.01	4.00E-03	4.00E-03	6.00E-03	0.04	2.00E-03	0.01	2.00E-03	0	8.00E-03	0.02	0	0.05
40	0.01	0.01	4.00E-03	4.00E-03	0	6.00E-03	6.00E-03	6.00E-03	0.01	0	8.00E-03	2.00E-03	4.00E-03	2.00E-03	0.01	2.00E-03	0.04
49	0.01	0.02	0.01	6.00E-03	8.00E-03	8.00E-03	2.00E-03	8.00E-03	0.02	2.00E-03	0.01	2.00E-03	0	6.00E-03	0.03	2.00E-03	0.05
6	0.02	0.01	0.01	8.00E-03	8.00E-03	8.00E-03	8.00E-03	0.01	0.05	0	0.02	0	2.00E-03	4.00E-03	0.03	0	0.06
12	0.02	0.02	6.00E-03	2.00E-03	0	4.00E-03	4.00E-03	8.00E-03	0.07	0	0.01	2.00E-03	0	0	0.03	2.00E-03	0.05
18	0.02	8.00E-03	6.00E-03	0.01	0	4.00E-03	6.00E-03	6.00E-03	0.04	4.00E-03	8.00E-03	0	6.00E-03	4.00E-03	0.01	2.00E-03	0.04
2	4.00E-03	0.01	6.00E-03	4.00E-03	6.00E-03	4.00E-03	4.00E-03	0.01	0.02	2.00E-03	0.01	6.00E-03	0	6.00E-03	0.03	2.00E-03	0.04
11	0.01	6.00E-03	4.00E-03	6.00E-03	4.00E-03	4.00E-03	2.00E-03	8.00E-03	8.00E-03	0	0.01	2.00E-03	0	4.00E-03	0.01	0	0.03
10	0.02	0.02	0.01	6.00E-03	6.00E-03	6.00E-03	2.00E-03	8.00E-03	0.05	6.00E-03	0.02	4.00E-03	0	2.00E-03	0.02	2.00E-03	0.05
3	0.01	0.02	8.00E-03	0.01	6.00E-03	6.00E-03	2.00E-03	0.01	0.09	4.00E-03	0.01	2.00E-03	2.00E-03	2.00E-03	0.02	6.00E-03	0.04
38	0.02	0.03	0.01	0.01	0.02	0	0	0.02	0.05	0	0.03	6.00E-03	0	4.00E-03	0.03	4.00E-03	0.04
16	0.01	0.02	0.01	2.00E-03	0.01	2.00E-03	6.00E-03	6.00E-03	0.05	4.00E-03	0.01	0	2.00E-03	4.00E-03	0.02	2.00E-03	0.04
34	0.01	0.01	0.01	0	2.00E-03	2.00E-03	6.00E-03	0.02	0.03	2.00E-03	0.01	2.00E-03	0	2.00E-03	0.02	4.00E-03	0.05
50	0.02	8.00E-03	8.00E-03	4.00E-03	6.00E-03	6.00E-03	8.00E-03	4.00E-03	0.05	0	0.02	4.00E-03	4.00E-03	6.00E-03	0.03	2.00E-03	0.05
4	0.02	0.03	0.01	0.01	2.00E-03	2.00E-03	8.00E-03	4.00E-03	0.04	4.00E-03	0.02	4.00E-03	2.00E-03	8.00E-03	0.03	6.00E-03	0.06
19	0.03	0.01	4.00E-03	6.00E-03	0	4.00E-03	4.00E-03	0.01	0.03	2.00E-03	6.00E-03	0	2.00E-03	2.00E-03	0.02	0	0.04
21	47,XXY	47,XXY	47,XXY	47,XXY	47,XXY	47,XXY	47,XXY	47,XXY	47,XXY	47,XXY	47,XXY	47,XXY	47,XXY	47,XXY	47,XXY	47,XXY	47,XXY
33	0.01	0.02	6.00E-03	6.00E-03	4.00E-03	4.00E-03	4.00E-03	0.01	0.01	2.00E-03	0.01	4.00E-03	0	6.00E-03	0.03	4.00E-03	0.05
5	failed 450K QC	failed 450K QC	failed 450K QC	failed 450K QC	failed 450K QC	failed 450K QC	failed 450K QC	failed 450K QC	failed 450K QC	failed 450K QC	failed 450K QC	failed 450K QC	failed 450K QC	failed 450K QC	failed 450K QC	failed 450K QC	failed 450K QC
42	0.01	0.02	8.00E-03	4.00E-03	6.00E-03	6.00E-03	4.00E-03	0.02	0.03	8.00E-03	0.01	4.00E-03	0	6.00E-03	0.03	0	0.05
13	0.01	0.02	4.00E-03	4.00E-03	4.00E-03	4.00E-03	6.00E-03	8.00E-03	0.01	2.00E-03	0.01	0	2.00E-03	0	0.01	2.00E-03	0.04

24	failed 450K QC	failed 450K QC	failed 450K QC	failed 450K QC	failed 450K QC	failed 450K QC	failed 450K QC	failed 450K QC	failed 450K QC	failed 450K QC	failed 450K QC	failed 450K QC	failed 450K QC	failed 450K QC
54	0.02	0.02	0.02	0.02	0.02	0.02	0.02	0.02	0.02	0.02	0.02	0.02	0.02	0.04
25	0.02	0.01	8.00E-03	0.01	8.00E-03	0.01	0.01	8.00E-03	0.01	8.00E-03	0.01	0.01	0.01	0.06
30	6.00E-03	0.01	4.00E-03	4.00E-03	6.00E-03	0.01	0.01	2.00E-03	0.01	2.00E-03	2.00E-03	2.00E-03	0	0.05
53	6.00E-03	8.00E-03	4.00E-03	8.00E-03	8.00E-03	8.00E-03	2.00E-03	4.00E-03	4.00E-03	4.00E-03	0	0	0	0.02
MS22	6.00E-03	0.01	4.00E-03	8.00E-03	8.00E-03	8.00E-03	2.00E-03	2.00E-03	2.00E-03	2.00E-03	2.00E-03	2.00E-03	6.00E-03	0.04
MS08	4.00E-03	0.02	8.00E-03	8.00E-03	8.00E-03	0	0.01	2.00E-03	0.01	2.00E-03	2.00E-03	2.00E-03	2.00E-03	0.06
MS33	0.01	0.01	8.00E-03	8.00E-03	8.00E-03	0.01	0.01	6.00E-03	0.01	6.00E-03	6.00E-03	6.00E-03	6.00E-03	0.05
MS35	0	0.01	0.01	2.00E-03	6.00E-03	2.00E-03	2.00E-03	2.00E-03	8.00E-03	2.00E-03	2.00E-03	2.00E-03	2.00E-03	0.04
MS10	0.01	0.02	0.01	6.00E-03	4.00E-03	6.00E-03	0.01	2.00E-03	0.09	0.01	2.00E-03	2.00E-03	0	0.05
MS01	6.00E-03	0.02	8.00E-03	8.00E-03	8.00E-03	0	0.01	4.00E-03	0.18	0.01	2.00E-03	2.00E-03	0	0.05
MS21	0.01	0.02	2.00E-03	8.00E-03	8.00E-03	2.00E-03	6.00E-03	6.00E-03	0.13	0.02	2.00E-03	2.00E-03	2.00E-03	0.05
MS23	0.01	8.00E-03	8.00E-03	8.00E-03	8.00E-03	0.01	8.00E-03	8.00E-03	0.14	0.02	2.00E-03	2.00E-03	2.00E-03	0.04
MS34	6.00E-03	0.02	8.00E-03	8.00E-03	8.00E-03	2.00E-03	2.00E-03	2.00E-03	0.14	0.02	2.00E-03	2.00E-03	2.00E-03	0.06
MS31	0.01	8.00E-03	0.01	0.01	2.00E-03	0.01	0.01	2.00E-03	0.1	0.01	4.00E-03	4.00E-03	2.00E-03	0.05
MS04	0.01	0.01	6.00E-03	6.00E-03	6.00E-03	2.00E-03	6.00E-03	4.00E-03	0.14	0.02	4.00E-03	4.00E-03	2.00E-03	0.04
MS17	0.01	0.03	6.00E-03	4.00E-03	4.00E-03	2.00E-03	2.00E-03	6.00E-03	0.08	8.00E-03	2.00E-03	2.00E-03	6.00E-03	0.05
MS14	6.00E-03	6.00E-03	6.00E-03	6.00E-03	6.00E-03	2.00E-03	6.00E-03	6.00E-03	0.14	8.00E-03	2.00E-03	2.00E-03	2.00E-03	0.05
MS36	2.00E-03	0.01	6.00E-03	6.00E-03	6.00E-03	0	0	2.00E-03	0.15	0.03	2.00E-03	2.00E-03	2.00E-03	0.04
MS20	4.00E-03	0.01	4.00E-03	4.00E-03	4.00E-03	2.00E-03	2.00E-03	6.00E-03	0.15	0.01	2.00E-03	2.00E-03	2.00E-03	0.04
MS32	2.00E-03	0.02	4.00E-03	4.00E-03	4.00E-03	2.00E-03	2.00E-03	4.00E-03	0.17	0.01	2.00E-03	4.00E-03	6.00E-03	0.04
MS12	6.00E-03	0.02	6.00E-03	6.00E-03	6.00E-03	6.00E-03	6.00E-03	6.00E-03	0.15	0.02	4.00E-03	4.00E-03	2.00E-03	0.04
MS03	4.00E-03	8.00E-03	8.00E-03	8.00E-03	8.00E-03	0.01	0.01	2.00E-03	0.12	6.00E-03	4.00E-03	4.00E-03	4.00E-03	0.04
MS05	8.00E-03	6.00E-03	6.00E-03	6.00E-03	6.00E-03	4.00E-03	4.00E-03	4.00E-03	0.15	0.02	2.00E-03	2.00E-03	2.00E-03	0.06
MS11	4.00E-03	0.01	6.00E-03	6.00E-03	6.00E-03	0	4.00E-03	4.00E-03	0.12	0.02	4.00E-03	4.00E-03	4.00E-03	0.07
MS27	2.00E-03	0.01	0.01	0.01	6.00E-03	0	6.00E-03	6.00E-03	0.15	0.01	4.00E-03	4.00E-03	2.00E-03	0.04
MS29	4.00E-03	8.00E-03	6.00E-03	6.00E-03	6.00E-03	2.00E-03	4.00E-03	4.00E-03	0.11	0.01	2.00E-03	2.00E-03	2.00E-03	0.03
MS28	0.01	0.02	6.00E-03	6.00E-03	6.00E-03	6.00E-03	6.00E-03	6.00E-03	0.14	0.01	4.00E-03	2.00E-03	2.00E-03	0.06
MS06	8.00E-03	8.00E-03	6.00E-03	6.00E-03	6.00E-03	0	4.00E-03	4.00E-03	0.11	0.01	2.00E-03	4.00E-03	4.00E-03	0.04
MS15	8.00E-03	0.02	4.00E-03	4.00E-03	4.00E-03	0	2.00E-03	2.00E-03	0.06	4.00E-03	0	2.00E-03	2.00E-03	0.04
MS24	47,XXY	47,XXY	47,XXY	47,XXY	47,XXY	47,XXY	47,XXY	47,XXY	47,XXY	47,XXY	47,XXY	47,XXY	47,XXY	47,XXY
MS02	0.01	0.02	6.00E-03	6.00E-03	6.00E-03	6.00E-03	4.00E-03	4.00E-03	0.16	0.01	2.00E-03	4.00E-03	4.00E-03	0.04
MS09	8.00E-03	6.00E-03	6.00E-03	6.00E-03	6.00E-03	6.00E-03	4.00E-03	4.00E-03	0.12	0.02	6.00E-03	6.00E-03	6.00E-03	0.04
MS18	6.00E-03	8.00E-03	8.00E-03	8.00E-03	8.00E-03	2.00E-03	2.00E-03	2.00E-03	0.13	0.02	6.00E-03	4.00E-03	8.00E-03	0.03
MS07	0.01	0.02	6.00E-03	6.00E-03	6.00E-03	4.00E-03	4.00E-03	4.00E-03	0.11	0.01	2.00E-03	4.00E-03	2.00E-03	0.04
MS30	0.02	0.01	4.00E-03	4.00E-03	4.00E-03	2.00E-03	2.00E-03	2.00E-03	0.11	0.01	2.00E-03	2.00E-03	4.00E-03	0.03
MS13	0.01	8.00E-03	0.01	8.00E-03	6.00E-03	0.02	6.00E-03	6.00E-03	0.1	0.01	6.00E-03	4.00E-03	4.00E-03	0.04

MS25	0.01	4.00E-03	8.00E-03	6.00E-03	6.00E-03	0	0	0.18	2.00E-03	6.00E-03	0	2.00E-03	2.00E-03	2.00E-03	0.02	0	0.05	
MS26	8.00E-03	0.01	6.00E-03	6.00E-03	6.00E-03	0	8.00E-03	0.13	2.00E-03	2.00E-03	0	4.00E-03	2.00E-03	2.00E-03	0.02	4.00E-03	0.03	
ES16	6.00E-03	6.00E-03	6.00E-03	4.00E-03	2.00E-03	2.00E-03	8.00E-03	0.02	2.00E-03	2.00E-03	2.00E-03	2.00E-03	2.00E-03	2.00E-03	0.02	2.00E-03	0.03	
ES18	8.00E-03	0.01	2.00E-03	2.00E-03	2.00E-03	4.00E-03	6.00E-03	0.1	2.00E-03	0.01	0	8.00E-03	2.00E-03	2.00E-03	0.02	2.00E-03	0.04	
ES10	0.02	0.02	8.00E-03	2.00E-03	6.00E-03	4.00E-03	6.00E-03	0.11	2.00E-03	0.01	2.00E-03	2.00E-03	2.00E-03	2.00E-03	0.01	2.00E-03	0.06	
ES11	2.00E-03	8.00E-03	4.00E-03	2.00E-03	2.00E-03	0	2.00E-03	0.14	4.00E-03	0.01	0	2.00E-03	2.00E-03	2.00E-03	0.01	2.00E-03	0.03	
ES14	6.00E-03	8.00E-03	4.00E-03	0	2.00E-03	0	8.00E-03	8.00E-03	0	0.01	2.00E-03	2.00E-03	2.00E-03	0	0.01	0	0.01	
ES17	0.02	0.01	8.00E-03	0.01	6.00E-03	6.00E-03	8.00E-03	0.08	4.00E-03	0.02	6.00E-03	6.00E-03	4.00E-03	4.00E-03	0.02	2.00E-03	0.05	
ES09	8.00E-03	8.00E-03	4.00E-03	0	2.00E-03	2.00E-03	4.00E-03	0.01	2.00E-03	4.00E-03	2.00E-03	2.00E-03	2.00E-03	2.00E-03	0.01	0	0.02	
ES15	6.00E-03	0.02	8.00E-03	4.00E-03	6.00E-03	0	8.00E-03	0.1	2.00E-03	0.03	2.00E-03	4.00E-03	6.00E-03	6.00E-03	0.02	0	0.08	
ES02	8.00E-03	0.01	6.00E-03	6.00E-03	2.00E-03	2.00E-03	4.00E-03	0.11	2.00E-03	0.02	4.00E-03	2.00E-03	4.00E-03	4.00E-03	0.02	2.00E-03	0.04	
ES03	0	6.00E-03	6.00E-03	6.00E-03	6.00E-03	0.01	2.00E-03	0.01	0	0.01	2.00E-03	2.00E-03	2.00E-03	0	0.01	0	0.03	
ES06	0	0.02	6.00E-03	0	6.00E-03	4.00E-03	6.00E-03	0.04	2.00E-03	8.00E-03	6.00E-03	6.00E-03	2.00E-03	2.00E-03	0.01	0	0.04	
ES12	0.01	0.02	8.00E-03	6.00E-03	2.00E-03	2.00E-03	6.00E-03	0.06	2.00E-03	8.00E-03	2.00E-03	2.00E-03	6.00E-03	4.00E-03	0.02	0	0.03	
ES13	2.00E-03	8.00E-03	4.00E-03	2.00E-03	8.00E-03	0	8.00E-03	0.1	2.00E-03	0.01	0	2.00E-03	4.00E-03	4.00E-03	0.02	2.00E-03	0.04	
ES04	6.00E-03	0.01	4.00E-03	2.00E-03	2.00E-03	2.00E-03	6.00E-03	0.16	4.00E-03	0.01	0	4.00E-03	0	0.01	0	0.04		
ES05	0.01	0.01	4.00E-03	2.00E-03	4.00E-03	4.00E-03	4.00E-03	0.02	2.00E-03	0.01	2.00E-03	2.00E-03	4.00E-03	4.00E-03	0.02	2.00E-03	0.02	
4	0.01	8.00E-03	8.00E-03	6.00E-03	6.00E-03	0	4.00E-03	0.18	0	0.02	2.00E-03	2.00E-03	2.00E-03	2.00E-03	0.02	4.00E-03	0.05	
3	0.01	0.02	8.00E-03	8.00E-03	4.00E-03	2.00E-03	4.00E-03	0.13	2.00E-03	0.02	0	4.00E-03	0	0.03	failed	2.00E-03	0.08	
12	failed	bisulfite	conversion	failed	bisulfite	conversion	failed	bisulfite	conversion	failed	bisulfite	conversion	failed	bisulfite	conversion	failed	bisulfite	conversion
37	6.00E-03	0.01	4.00E-03	4.00E-03	4.00E-03	2.00E-03	2.00E-03	0.1	4.00E-03	0.02	2.00E-03	2.00E-03	2.00E-03	2.00E-03	0.01	2.00E-03	0.05	
17	4.00E-03	0.01	8.00E-03	8.00E-03	4.00E-03	2.00E-03	6.00E-03	0.15	6.00E-03	0.03	4.00E-03	4.00E-03	4.00E-03	0	0.02	0	0.05	
26	2.00E-03	0.02	8.00E-03	6.00E-03	4.00E-03	2.00E-03	2.00E-03	0.15	4.00E-03	0.02	2.00E-03	2.00E-03	2.00E-03	4.00E-03	0.02	0	0.04	
8	failed	450K	QC	failed	450K	QC	failed	450K	QC	failed	450K	QC	failed	450K	QC	failed	450K	QC
1	8.00E-03	0.02	8.00E-03	6.00E-03	4.00E-03	4.00E-03	6.00E-03	0.11	4.00E-03	0.01	2.00E-03	4.00E-03	4.00E-03	0	0.01	2.00E-03	0.04	
28	4.00E-03	8.00E-03	4.00E-03	6.00E-03	2.00E-03	4.00E-03	6.00E-03	0.11	0	0.02	2.00E-03	2.00E-03	6.00E-03	2.00E-03	0.01	0	0.03	
34	6.00E-03	0.01	8.00E-03	4.00E-03	4.00E-03	2.00E-03	4.00E-03	0.12	0	0.02	4.00E-03	4.00E-03	2.00E-03	2.00E-03	0.01	4.00E-03	0.05	
2	0.02	0.02	6.00E-03	6.00E-03	4.00E-03	0	2.00E-03	0.18	0	0.02	2.00E-03	4.00E-03	4.00E-03	0	0.01	4.00E-03	0.04	
25	2.00E-03	0.02	8.00E-03	4.00E-03	2.00E-03	0	4.00E-03	0.17	2.00E-03	0.02	2.00E-03	2.00E-03	2.00E-03	2.00E-03	0.02	2.00E-03	0.04	
54	0.01	8.00E-03	4.00E-03	4.00E-03	0	2.00E-03	6.00E-03	0.12	4.00E-03	0.01	4.00E-03	2.00E-03	2.00E-03	2.00E-03	0.02	2.00E-03	0.03	
45	4.00E-03	0.01	2.00E-03	8.00E-03	8.00E-03	2.00E-03	8.00E-03	0.17	4.00E-03	0.02	2.00E-03	8.00E-03	4.00E-03	4.00E-03	0.03	0	0.05	
31	8.00E-03	0.02	6.00E-03	6.00E-03	4.00E-03	0	2.00E-03	0.17	2.00E-03	0.02	2.00E-03	4.00E-03	4.00E-03	0	0.02	0	0.05	
6	6.00E-03	0.01	8.00E-03	4.00E-03	4.00E-03	0	2.00E-03	0.19	0	0.03	2.00E-03	8.00E-03	2.00E-03	2.00E-03	0.02	0	0.05	
35	4.00E-03	0.01	8.00E-03	6.00E-03	4.00E-03	2.00E-03	6.00E-03	0.19	0	0.01	2.00E-03	6.00E-03	6.00E-03	0	0.01	2.00E-03	0.05	
20	8.00E-03	0.02	8.00E-03	6.00E-03	6.00E-03	0	2.00E-03	0.23	4.00E-03	0.02	2.00E-03	2.00E-03	2.00E-03	0	0.02	2.00E-03	0.04	

18	8.00E-03	0.02	0.01	8.00E-03	4.00E-03	2.00E-03	4.00E-03	0.2	2.00E-03	0.02	8.00E-03	6.00E-03	0	0.01	0	6.00E-03	8.00E-03	0.02	0.05
46	0.01	0.02	0.01	6.00E-03	6.00E-03	2.00E-03	4.00E-03	0.17	6.00E-03	0.02	4.00E-03	2.00E-03	2.00E-03	0.02	2.00E-03	2.00E-03	4.00E-03	0.07	
16	4.00E-03	0.02	8.00E-03	6.00E-03	2.00E-03	2.00E-03	4.00E-03	0.22	0	0.02	2.00E-03	6.00E-03	2.00E-03	0.01	4.00E-03	6.00E-03	0.04		
47	0.01	0.02	0.01	4.00E-03	4.00E-03	0	0	0.2	4.00E-03	0.01	6.00E-03	4.00E-03	0	0.02	2.00E-03	4.00E-03	0.04		
51	0.01	0.01	8.00E-03	4.00E-03	4.00E-03	0	2.00E-03	0.17	0	8.00E-03	0	6.00E-03	0	8.00E-03	0	6.00E-03	0.04		
53	0.01	0.03	0.01	4.00E-03	4.00E-03	0	8.00E-03	0.12	2.00E-03	0.02	8.00E-03	8.00E-03	4.00E-03	0.01	4.00E-03	4.00E-03	0.04		
42	4.00E-03	0.01	6.00E-03	6.00E-03	8.00E-03	0	0	0.15	6.00E-03	0.02	6.00E-03	6.00E-03	4.00E-03	0.02	4.00E-03	6.00E-03	0.07		
49	8.00E-03	0.02	0.01	6.00E-03	2.00E-03	2.00E-03	2.00E-03	0.14	2.00E-03	0.02	2.00E-03	4.00E-03	0	0.02	2.00E-03	2.00E-03	0.05		
52	2.00E-03	8.00E-03	0.01	4.00E-03	4.00E-03	0	2.00E-03	0.15	0	0.02	2.00E-03	4.00E-03	0	0.02	0	4.00E-03	0.04		
40	0.01	0.02	8.00E-03	0.01	4.00E-03	0	0.01	0.16	4.00E-03	0.02	4.00E-03	6.00E-03	2.00E-03	0.01	2.00E-03	2.00E-03	0.03		
7	0	0.03	4.00E-03	4.00E-03	8.00E-03	0	2.00E-03	0.17	4.00E-03	0.02	4.00E-03	4.00E-03	2.00E-03	0.02	2.00E-03	2.00E-03	0.05		
15	0.01	0.02	0.01	6.00E-03	4.00E-03	4.00E-03	4.00E-03	0.22	2.00E-03	0.02	2.00E-03	4.00E-03	2.00E-03	0.02	0	0	0.05		
19	0	0.02	8.00E-03	6.00E-03	4.00E-03	2.00E-03	2.00E-03	0.19	0	0.02	4.00E-03	6.00E-03	0	0.01	0	0	0.05		
10	0.01	0.02	0.01	8.00E-03	8.00E-03	0	4.00E-03	0.13	2.00E-03	0.02	4.00E-03	6.00E-03	6.00E-03	0.01	0	0	0.03		
30	2.00E-03	0.01	2.00E-03	4.00E-03	4.00E-03	2.00E-03	0	0.15	4.00E-03	0.01	2.00E-03	2.00E-03	0	0.01	2.00E-03	2.00E-03	0.03		
13	2.00E-03	0.01	4.00E-03	6.00E-03	2.00E-03	0	2.00E-03	0.19	4.00E-03	0.02	6.00E-03	6.00E-03	0	0.02	4.00E-03	4.00E-03	0.05		
41	0.01	0.01	0.01	6.00E-03	2.00E-03	0	2.00E-03	0.14	2.00E-03	0.02	2.00E-03	2.00E-03	0	8.00E-03	0	0	0.04		
44	0.01	0.01	0.01	2.00E-03	8.00E-03	4.00E-03	6.00E-03	0.23	4.00E-03	0.02	4.00E-03	4.00E-03	4.00E-03	0.02	0	0	0.05		
24	0.02	0.02	6.00E-03	4.00E-03	0	2.00E-03	0	0.17	0	0.01	2.00E-03	2.00E-03	2.00E-03	0.03	0	0	0.05		
9	0.01	0.02	4.00E-03	2.00E-03	0.01	2.00E-03	6.00E-03	0.17	4.00E-03	0.02	2.00E-03	6.00E-03	0.01	0.02	6.00E-03	6.00E-03	0.05		
5	4.00E-03	0.01	2.00E-03	6.00E-03	4.00E-03	2.00E-03	0	0.2	2.00E-03	0.02	4.00E-03	6.00E-03	0	0.01	0	0	0.03		
38	6.00E-03	0.01	6.00E-03	0.01	8.00E-03	0	2.00E-03	0.18	6.00E-03	0.02	0	2.00E-03	4.00E-03	0.02	0	0	0.04		
39	failed bisulfite conversion	failed bisulfite conversion	failed bisulfite conversion	failed bisulfite conversion	failed bisulfite conversion	failed bisulfite conversion	failed bisulfite conversion	failed bisulfite conversion	failed bisulfite conversion	failed bisulfite conversion	failed bisulfite conversion	failed bisulfite conversion	failed bisulfite conversion	failed bisulfite conversion	failed bisulfite conversion	failed bisulfite conversion	failed bisulfite conversion	failed bisulfite conversion	
14	6.00E-03	0.02	8.00E-03	2.00E-03	2.00E-03	2.00E-03	2.00E-03	0.21	2.00E-03	0.02	2.00E-03	6.00E-03	6.00E-03	0.02	2.00E-03	4.00E-03	4.00E-03	0.04	
33	8.00E-03	0.02	6.00E-03	4.00E-03	4.00E-03	0	4.00E-03	0.21	0	0.02	2.00E-03	6.00E-03	2.00E-03	0.02	0	0	0	0.06	
23	4.00E-03	0.02	0.01	8.00E-03	2.00E-03	4.00E-03	0	0.16	2.00E-03	0.02	4.00E-03	2.00E-03	0	0.02	0	0	0	0.04	
32	8.00E-03	0.01	0.01	8.00E-03	4.00E-03	0	0	0.2	0	0.01	2.00E-03	2.00E-03	2.00E-03	0.02	0	0	0	0.03	
11	2.00E-03	0.01	4.00E-03	6.00E-03	8.00E-03	0	6.00E-03	0.13	0	0.01	6.00E-03	6.00E-03	6.00E-03	0.02	2.00E-03	2.00E-03	0.04		
21	47,XXY	47,XXY	47,XXY	47,XXY	47,XXY	47,XXY	47,XXY	47,XXY	47,XXY	47,XXY	47,XXY	47,XXY	47,XXY	47,XXY	47,XXY	47,XXY	47,XXY	47,XXY	
MS22	8.00E-03	0.02	8.00E-03	2.00E-03	6.00E-03	2.00E-03	6.00E-03	0.06	4.00E-03	0.02	2.00E-03	4.00E-03	4.00E-03	0.02	2.00E-03	2.00E-03	0	0.04	
MS01	6.00E-03	0.02	0.01	2.00E-03	0.01	2.00E-03	6.00E-03	0.05	2.00E-03	0.01	0	2.00E-03	4.00E-03	0.01	0	0	0	0.02	
MS05	8.00E-03	0.02	4.00E-03	6.00E-03	0.01	0	2.00E-03	0.08	4.00E-03	0.02	0	4.00E-03	2.00E-03	0.02	0	0	0	0.03	
MS08	0.02	0.01	0.01	6.00E-03	8.00E-03	0	8.00E-03	0.05	2.00E-03	0.01	8.00E-03	4.00E-03	4.00E-03	0.02	0	0	0	0.03	
MS36	0.02	8.00E-03	0.01	4.00E-03	6.00E-03	6.00E-03	4.00E-03	0.03	6.00E-03	0.01	4.00E-03	6.00E-03	6.00E-03	0.03	6.00E-03	6.00E-03	0	0.02	
MS30	0.01	8.00E-03	2.00E-03	6.00E-03	6.00E-03	6.00E-03	6.00E-03	0.03	4.00E-03	0.01	4.00E-03	4.00E-03	0	0.02	2.00E-03	2.00E-03	0	0.03	
MS10	0.01	8.00E-03	0.01	4.00E-03	8.00E-03	4.00E-03	8.00E-03	0.07	6.00E-03	0.01	6.00E-03	0	2.00E-03	0.02	2.00E-03	2.00E-03	0	0.04	

MS03	6.00E-03	0.01	8.00E-03	2.00E-03	6.00E-03	0.07	4.00E-03	0.02	0	4.00E-03	4.00E-03	0.02	0	4.00E-03	4.00E-03	0.02	0	0.04
MS16	0.01	0.02	6.00E-03	0.01	6.00E-03	0.05	4.00E-03	0.01	0	0.02	2.00E-03	0.02	2.00E-03	2.00E-03	0.02	0.03		
MS06	6.00E-03	0.01	2.00E-03	2.00E-03	4.00E-03	0.08	2.00E-03	0.02	4.00E-03	4.00E-03	2.00E-03	0.02	0	2.00E-03	2.00E-03	0.02	0	0.03
MS33	8.00E-03	0.02	0.01	8.00E-03	6.00E-03	0.09	8.00E-03	0.02	8.00E-03	2.00E-03	2.00E-03	0.02	0	2.00E-03	2.00E-03	0.02	0	0.03
MS28	0.01	0.02	0.01	2.00E-03	6.00E-03	0.07	6.00E-03	0.02	2.00E-03	2.00E-03	0	0.03	0	0	0.03	0.03		
MS21	0.01	2.00E-03	4.00E-03	4.00E-03	0	0.07	4.00E-03	0.01	0	2.00E-03	2.00E-03	0.02	0	2.00E-03	2.00E-03	0.02	0	0.05
MS07	failed bisulfite conversion	failed bisulfite conversion	failed bisulfite conversion	failed bisulfite conversion	failed bisulfite conversion	failed bisulfite conversion	failed bisulfite conversion	failed bisulfite conversion	failed bisulfite conversion	failed bisulfite conversion	failed bisulfite conversion	failed bisulfite conversion	failed bisulfite conversion	failed bisulfite conversion	failed bisulfite conversion	failed bisulfite conversion	failed bisulfite conversion	failed bisulfite conversion
MS24	47,XXY	47,XXY	47,XXY	47,XXY	47,XXY	47,XXY	47,XXY	47,XXY	47,XXY	47,XXY	47,XXY	47,XXY	47,XXY	47,XXY	47,XXY	47,XXY	47,XXY	47,XXY
MS15	4.00E-03	8.00E-03	0.01	6.00E-03	6.00E-03	0.06	4.00E-03	0.01	4.00E-03	8.00E-03	2.00E-03	0.01	2.00E-03	2.00E-03	0.01	2.00E-03	2.00E-03	0.04
MS18	0.02	0.01	6.00E-03	6.00E-03	2.00E-03	0.04	6.00E-03	0.01	0	8.00E-03	4.00E-03	0.02	0	4.00E-03	4.00E-03	0.02	0	0.04
MS25	4.00E-03	0.03	0.01	2.00E-03	4.00E-03	0.04	6.00E-03	0.01	0	6.00E-03	2.00E-03	0.02	0	2.00E-03	2.00E-03	0.02	0	0.03
MS13	0.03	0.02	0.01	8.00E-03	0.01	0.05	0	0.02	0	2.00E-03	6.00E-03	0.03	4.00E-03	6.00E-03	0.03	0.08		
MS29	0.02	0.01	8.00E-03	6.00E-03	0.01	0.06	4.00E-03	0.01	2.00E-03	2.00E-03	0	0.03	2.00E-03	2.00E-03	0.03	0.04		
MS11	failed 450K QC	failed 450K QC	failed 450K QC	failed 450K QC	failed 450K QC	failed 450K QC	failed 450K QC	failed 450K QC	failed 450K QC	failed 450K QC	failed 450K QC	failed 450K QC	failed 450K QC	failed 450K QC	failed 450K QC	failed 450K QC	failed 450K QC	failed 450K QC
MS20	8.00E-03	0.02	2.00E-03	0	8.00E-03	0.06	4.00E-03	0.01	2.00E-03	6.00E-03	2.00E-03	0.01	2.00E-03	2.00E-03	0.01	0	0.03	
MS26	8.00E-03	0.01	6.00E-03	6.00E-03	6.00E-03	0.07	6.00E-03	8.00E-03	2.00E-03	2.00E-03	0	0.02	0	0	0.03	0.03		
MS35	0.01	0.01	6.00E-03	4.00E-03	4.00E-03	0.04	2.00E-03	0.02	0	6.00E-03	6.00E-03	0.03	0	6.00E-03	6.00E-03	0.03	0	0.03
MS09	0.01	0.02	0.01	4.00E-03	2.00E-03	0.06	6.00E-03	0.02	2.00E-03	4.00E-03	4.00E-03	0.02	0	4.00E-03	4.00E-03	0.02	0	0.03
MS04	8.00E-03	0.01	4.00E-03	2.00E-03	4.00E-03	0.06	4.00E-03	6.00E-03	0	0	0	0.03	0	0	0.02	0.02		
MS17	0.01	0.02	6.00E-03	2.00E-03	6.00E-03	0.05	4.00E-03	0.02	8.00E-03	8.00E-03	8.00E-03	0.02	4.00E-03	8.00E-03	0.02	0.05		
MS34	8.00E-03	0.01	6.00E-03	4.00E-03	4.00E-03	0.06	6.00E-03	0.02	2.00E-03	8.00E-03	6.00E-03	0.01	0	6.00E-03	6.00E-03	0.01	0	0.05
MS14	8.00E-03	0.02	8.00E-03	2.00E-03	2.00E-03	0.06	2.00E-03	0.01	2.00E-03	4.00E-03	4.00E-03	0.01	2.00E-03	4.00E-03	8.00E-03	0.04		
MS23	0.01	0.02	8.00E-03	6.00E-03	6.00E-03	0.08	2.00E-03	0.02	4.00E-03	6.00E-03	6.00E-03	0.02	0	2.00E-03	2.00E-03	0.02	0	0.07
MS19	0.02	0.02	0.02	6.00E-03	0.01	0.08	2.00E-03	0.01	0	0.01	4.00E-03	0.02	2.00E-03	4.00E-03	0.02	0.04		
MS32	6.00E-03	0.01	0.01	4.00E-03	4.00E-03	0.06	4.00E-03	0.01	0	4.00E-03	6.00E-03	0.02	0	6.00E-03	6.00E-03	0.02	0	0.03
MS27	4.00E-03	0.02	4.00E-03	2.00E-03	2.00E-03	0.05	6.00E-03	0.01	0	2.00E-03	6.00E-03	0.03	0	6.00E-03	6.00E-03	0.03	0	0.03
MS02	2.00E-03	0.01	0	4.00E-03	2.00E-03	0.08	0	0.02	0	4.00E-03	0	0.02	0	0	0.03	0.03		
MS12	4.00E-03	0.01	0.01	2.00E-03	4.00E-03	0.07	6.00E-03	0.01	2.00E-03	4.00E-03	2.00E-03	0.02	0	2.00E-03	2.00E-03	0.02	0	0.04
MS31	6.00E-03	0.01	8.00E-03	4.00E-03	4.00E-03	0.07	6.00E-03	0.02	0	8.00E-03	4.00E-03	0.01	0	4.00E-03	4.00E-03	0.01	0	0.05
ES01	6.00E-03	4.00E-03	0.01	2.00E-03	4.00E-03	0.07	2.00E-03	0.02	2.00E-03	4.00E-03	4.00E-03	8.00E-03	0	4.00E-03	4.00E-03	0.01	0	0.04
ES11	6.00E-03	0.01	0.01	2.00E-03	6.00E-03	0.12	4.00E-03	8.00E-03	2.00E-03	6.00E-03	2.00E-03	0.01	0	2.00E-03	2.00E-03	0.01	0	0.03
ES09	0.01	0.02	8.00E-03	2.00E-03	8.00E-03	0.02	0	0.02	4.00E-03	4.00E-03	2.00E-03	0.02	0	2.00E-03	2.00E-03	0.02	0	0.05
ES06	0.01	8.00E-03	0.01	4.00E-03	8.00E-03	0.05	4.00E-03	0.01	2.00E-03	0	0	0.02	0	0	0.03	0.03		
ES14	0.02	0.02	0.01	4.00E-03	6.00E-03	0.03	4.00E-03	0.01	2.00E-03	2.00E-03	8.00E-03	0.01	0	8.00E-03	8.00E-03	0.01	0	0.03
ES16	0.02	0.01	6.00E-03	4.00E-03	4.00E-03	0.03	0	0.01	2.00E-03	4.00E-03	2.00E-03	0.01	0	2.00E-03	2.00E-03	0.01	0	0.03

ES13	8.00E-03	0.01	6.00E-03	4.00E-03	4.00E-03	0	8.00E-03	0.02	4.00E-03	6.00E-03	0	2.00E-03	4.00E-03	6.00E-03	0	0.03
ES05	8.00E-03	0.01	2.00E-03	6.00E-03	6.00E-03	0	6.00E-03	0.1	6.00E-03	0.02	0	4.00E-03	2.00E-03	0.01	0	0.05
ES04	2.00E-03	0.02	6.00E-03	6.00E-03	6.00E-03	0	6.00E-03	0.11	6.00E-03	0.01	2.00E-03	4.00E-03	2.00E-03	0.02	0	0.06
ES18	6.00E-03	6.00E-03	6.00E-03	2.00E-03	2.00E-03	0	2.00E-03	0.05	0	4.00E-03	2.00E-03	0	0	0.01	0	0.03
ES07	8.00E-03	8.00E-03	8.00E-03	8.00E-03	8.00E-03	0	6.00E-03	0.06	4.00E-03	0.01	2.00E-03	0	4.00E-03	8.00E-03	0	0.04
ES17	0.01	0.01	4.00E-03	8.00E-03	4.00E-03	2.00E-03	0.01	0.06	2.00E-03	0.01	2.00E-03	0	4.00E-03	0.01	0	0.03
ES10	8.00E-03	4.00E-03	2.00E-03	0	8.00E-03	0	2.00E-03	0.01	0	0.01	2.00E-03	0	4.00E-03	0.02	0	0.02
ES03	0.01	8.00E-03	2.00E-03	2.00E-03	2.00E-03	0	4.00E-03	0.01	0	6.00E-03	2.00E-03	2.00E-03	0	0.01	0	0.02
ES15	0.02	0.02	0	2.00E-03	2.00E-03	0	4.00E-03	0.04	4.00E-03	4.00E-03	2.00E-03	2.00E-03	2.00E-03	0.01	0	0.04
ES12	0.01	0.01	4.00E-03	4.00E-03	8.00E-03	0	4.00E-03	0.08	2.00E-03	0.01	0	6.00E-03	0	0.02	0	0.02
21	47,XXY	47,XXY	47,XXY	47,XXY	47,XXY	47,XXY	47,XXY	47,XXY	47,XXY	47,XXY	47,XXY	47,XXY	47,XXY	47,XXY	47,XXY	47,XXY
43	0.01	0.01	4.00E-03	2.00E-03	4.00E-03	6.00E-03	0	0.05	4.00E-03	8.00E-03	2.00E-03	2.00E-03	2.00E-03	0.02	2.00E-03	0.03
29	0.01	8.00E-03	0	6.00E-03	8.00E-03	2.00E-03	2.00E-03	0.03	2.00E-03	8.00E-03	4.00E-03	2.00E-03	4.00E-03	0.02	0	0.05
41	6.00E-03	4.00E-03	8.00E-03	2.00E-03	8.00E-03	0	4.00E-03	0.1	4.00E-03	0.02	0	6.00E-03	2.00E-03	0.01	0	0.05
36	0.02	0.01	8.00E-03	2.00E-03	2.00E-03	6.00E-03	8.00E-03	0.01	0	4.00E-03	2.00E-03	4.00E-03	4.00E-03	0.02	6.00E-03	0.03
39	8.00E-03	0.01	0.01	4.00E-03	4.00E-03	2.00E-03	4.00E-03	0.08	4.00E-03	0.01	0	2.00E-03	0	0.02	0	0.06
45	8.00E-03	0.01	0.01	6.00E-03	8.00E-03	4.00E-03	8.00E-03	0.09	8.00E-03	0.02	0	0.01	0	0.02	0	0.05
44	6.00E-03	8.00E-03	2.00E-03	2.00E-03	2.00E-03	4.00E-03	0.01	0.04	2.00E-03	0.01	4.00E-03	0	0.01	0.02	4.00E-03	0.04
10	8.00E-03	0.02	0.01	4.00E-03	6.00E-03	0	4.00E-03	0.04	0	0.02	4.00E-03	0	8.00E-03	0.01	0	0.03
37	8.00E-03	2.00E-03	8.00E-03	8.00E-03	8.00E-03	2.00E-03	6.00E-03	0.06	4.00E-03	8.00E-03	2.00E-03	2.00E-03	4.00E-03	0.01	0	0.03
12	0.03	0.02	0.01	4.00E-03	4.00E-03	6.00E-03	0.02	0.02	2.00E-03	0.01	4.00E-03	6.00E-03	8.00E-03	0.03	0	0.04
3	0.01	0.01	4.00E-03	4.00E-03	2.00E-03	4.00E-03	6.00E-03	0.02	2.00E-03	0.01	4.00E-03	4.00E-03	8.00E-03	0.01	0	0.04
14	8.00E-03	0.02	6.00E-03	4.00E-03	4.00E-03	2.00E-03	4.00E-03	0.02	0	8.00E-03	6.00E-03	0	2.00E-03	0.01	0	0.04
35	0.01	0.02	0.01	0.01	6.00E-03	4.00E-03	8.00E-03	0.07	4.00E-03	0.01	0	2.00E-03	0	0.02	0	0.02
1	4.00E-03	0.01	0.01	2.00E-03	4.00E-03	4.00E-03	4.00E-03	0.13	4.00E-03	0.01	0	2.00E-03	4.00E-03	0.02	0	0.07
50	8.00E-03	0.01	0.01	2.00E-03	6.00E-03	2.00E-03	8.00E-03	0.19	2.00E-03	0.01	2.00E-03	2.00E-03	6.00E-03	0.02	0	0.04
13	0.01	8.00E-03	6.00E-03	2.00E-03	2.00E-03	0	4.00E-03	0.06	2.00E-03	0.01	0	8.00E-03	4.00E-03	0.02	0	0.03
20	0.01	0.01	8.00E-03	0	6.00E-03	8.00E-03	6.00E-03	0.04	4.00E-03	0	2.00E-03	2.00E-03	2.00E-03	0.01	0	0.02
40	0.01	0.01	6.00E-03	2.00E-03	2.00E-03	2.00E-03	6.00E-03	0.1	2.00E-03	0.01	4.00E-03	6.00E-03	2.00E-03	0.01	2.00E-03	0.04
5	2.00E-03	0.01	8.00E-03	8.00E-03	8.00E-03	0	6.00E-03	0.03	0	8.00E-03	2.00E-03	0	6.00E-03	0.02	0	0.03
9	6.00E-03	0.02	0.01	2.00E-03	2.00E-03	0	8.00E-03	0.13	2.00E-03	0.01	2.00E-03	4.00E-03	0	0.02	0	0.04
51	0.01	0.01	6.00E-03	4.00E-03	4.00E-03	4.00E-03	4.00E-03	0.05	4.00E-03	0.01	2.00E-03	2.00E-03	2.00E-03	0.01	0	0.04
16	6.00E-03	8.00E-03	0.01	4.00E-03	4.00E-03	0	6.00E-03	0.04	2.00E-03	8.00E-03	2.00E-03	0	8.00E-03	0.02	0	0.03
38	0.02	0.02	0.01	0.01	0.03	0	4.00E-03	0.11	6.00E-03	0.02	2.00E-03	2.00E-03	4.00E-03	0.02	0	0.08
53	4.00E-03	0.01	8.00E-03	2.00E-03	6.00E-03	4.00E-03	2.00E-03	0.07	4.00E-03	0.02	0	0	4.00E-03	0.02	2.00E-03	0.04
17	6.00E-03	8.00E-03	8.00E-03	4.00E-03	4.00E-03	4.00E-03	4.00E-03	0.03	4.00E-03	6.00E-03	0	0	2.00E-03	0.01	0	0.03
11	0.01	0.01	2.00E-03	6.00E-03	6.00E-03	0	8.00E-03	0.03	2.00E-03	6.00E-03	0	0	4.00E-03	8.00E-03	2.00E-03	0.02

54	8.00E-03	0.01	2.00E-03	4.00E-03	6.00E-03	4.00E-03	6.00E-03	0.02	0	0	2.00E-03	2.00E-03	8.00E-03	0.01	0	0.04
32	8.00E-03	0.03	8.00E-03	0.01	2.00E-03	2.00E-03	0.01	0.1	4.00E-03	0.02	2.00E-03	2.00E-03	6.00E-03	0.02	0	0.07
42	2.00E-03	0.01	0.01	2.00E-03	0.01	2.00E-03	6.00E-03	0.1	2.00E-03	0.02	0	4.00E-03	2.00E-03	0.01	0	0.04
28	8.00E-03	6.00E-03	8.00E-03	6.00E-03	2.00E-03	4.00E-03	2.00E-03	0.03	0	8.00E-03	0	2.00E-03	2.00E-03	0.01	0	0.03
6	2.00E-03	0.01	0.01	8.00E-03	8.00E-03	4.00E-03	2.00E-03	0.07	2.00E-03	2.00E-03	2.00E-03	2.00E-03	0.01	0.03	0	0.03
15	0.01	0.01	0.01	6.00E-03	6.00E-03	4.00E-03	2.00E-03	0.12	4.00E-03	0.02	0	4.00E-03	2.00E-03	0.02	0	0.04
27	0.01	0.02	6.00E-03	2.00E-03	6.00E-03	4.00E-03	6.00E-03	0.05	0	8.00E-03	0	4.00E-03	0	0.02	0	0.02
30	8.00E-03	4.00E-03	0.01	4.00E-03	0.02	6.00E-03	2.00E-03	0.11	4.00E-03	0.01	0	4.00E-03	2.00E-03	0.01	0	0.04
33	6.00E-03	0.01	4.00E-03	0	4.00E-03	4.00E-03	6.00E-03	0.06	2.00E-03	0.01	0	2.00E-03	0	8.00E-03	0	0.03
7	0.01	0.01	0.01	6.00E-03	0.02	2.00E-03	6.00E-03	0.06	4.00E-03	0.02	0	4.00E-03	6.00E-03	0.02	0	0.03
47	2.00E-03	4.00E-03	4.00E-03	2.00E-03	6.00E-03	0	8.00E-03	0.03	2.00E-03	8.00E-03	0	2.00E-03	6.00E-03	0.01	0	0.03
8	6.00E-03	0.01	8.00E-03	4.00E-03	6.00E-03	2.00E-03	8.00E-03	0.12	4.00E-03	0.01	0	0.01	2.00E-03	0.01	0	0.04
25	0.02	0.01	4.00E-03	4.00E-03	8.00E-03	2.00E-03	6.00E-03	0.06	2.00E-03	6.00E-03	6.00E-03	0	0	0.02	0	0.03
2	6.00E-03	0.02	8.00E-03	4.00E-03	0.01	0	8.00E-03	0.03	6.00E-03	0.02	2.00E-03	2.00E-03	6.00E-03	0.02	0	0.04
34	8.00E-03	0.02	6.00E-03	6.00E-03	0.02	2.00E-03	0.02	0.07	0	0.01	8.00E-03	6.00E-03	6.00E-03	0.02	0	0.04
23	8.00E-03	6.00E-03	8.00E-03	2.00E-03	2.00E-03	2.00E-03	6.00E-03	0.1	2.00E-03	0.01	4.00E-03	2.00E-03	6.00E-03	0.02	0	0.04
26	4.00E-03	0.01	0.01	2.00E-03	6.00E-03	4.00E-03	6.00E-03	0.1	4.00E-03	0.02	0	2.00E-03	0	0.01	0	0.03
49	6.00E-03	0.01	6.00E-03	2.00E-03	8.00E-03	4.00E-03	0	0.1	2.00E-03	0.01	2.00E-03	2.00E-03	2.00E-03	0.01	0	0.04
4	6.00E-03	0.02	6.00E-03	0.01	0.01	0	4.00E-03	0.03	4.00E-03	0.02	4.00E-03	0	2.00E-03	0.02	0	0.04
18	8.00E-03	0.01	2.00E-03	2.00E-03	4.00E-03	6.00E-03	4.00E-03	0.08	4.00E-03	8.00E-03	4.00E-03	0	2.00E-03	0.02	0	0.03
52	0.01	0.02	0.01	4.00E-03	2.00E-03	2.00E-03	4.00E-03	0.07	4.00E-03	0.02	0	0	2.00E-03	0.03	0	0.04
19	0.01	0.01	0.01	2.00E-03	4.00E-03	6.00E-03	0	0.07	4.00E-03	0.01	2.00E-03	6.00E-03	0	0.02	0	0.03
31	0.01	0.01	8.00E-03	0	8.00E-03	0	2.00E-03	0.06	0.01	8.00E-03	0	6.00E-03	0	0.01	0	0.03

Supplementary Table 6. Methylation QTLs (mQTL) identified in the prefrontal cortex for SNPs included in the schizophrenia polygenic risk score (PRS). Shown are associations between DNA methylation at specific Illumina 450K probes and genetic variants used to derive PRS in Chapter 4, in addition to the corresponding *P*-values for PRS-associated DNA methylation variation at the same probe.

SNP	SNP genomic location (hg19)	mQTL <i>P</i>	CpG	CpG genomic location (hg19)	EWAS <i>P</i>
rs9726753	chr1:153591652	5.88E-49	cg08477332	chr1:153590243	0.36
rs117194038	chr17:43927290	1.65E-47	cg17117718	chr17:43663208	0.97
rs12635522	chr3:125708174	4.79E-46	cg15145296	chr3:125709740	0.09
rs35059736	chr7:158224692	1.83E-44	cg01191920	chr7:158217561	0.54
rs76344840	chr9:33120204	2.97E-43	cg20290983	chr6:43655470	0.34
rs12635522	chr3:125708174	9.23E-38	cg04553112	chr3:125709451	0.06
rs12635522	chr3:125708174	1.68E-37	cg02807482	chr3:125708958	0.07
rs4792919	chr17:41873309	1.98E-37	cg26893861	chr17:41843967	0.71
rs12635522	chr3:125708174	2.29E-34	cg06494592	chr3:125709126	0.1
rs10857676	chr10:134970598	1.74E-33	cg00753039	chr10:134969141	0.29
rs6680259	chr1:7122308	2.50E-33	cg20409752	chr1:7122726	0.01
rs10920265	chr1:201822955	9.59E-33	cg11586189	chr1:201857591	0.25
rs117194038	chr17:43927290	5.30E-32	cg22968622	chr17:43663579	0.43
rs907033	chr16:83987856	1.14E-30	cg27171569	chr16:83987465	0.14
rs11734838	chr4:7980737	1.43E-30	cg22688802	chr4:7980661	0.51
rs9933817	chr16:83972660	3.25E-30	cg16457916	chr16:83968360	0.56
rs4880509	chr10:1511150	7.38E-29	cg13684379	chr10:1511173	0.66
rs4880509	chr10:1511150	1.71E-28	cg09316607	chr10:1511024	0.93
rs2800973	chr22:19168616	2.02E-27	cg02655711	chr22:19163373	0.41
rs60668498	chr19:44642672	9.76E-26	cg23489630	chr19:44645078	0.92
rs4880509	chr10:1511150	1.48E-25	cg04012681	chr10:1511277	0.52
rs13282161	chr8:1705041	7.43E-25	cg17694851	chr8:1707553	0.07
rs13065	chr14:100996312	1.04E-23	cg18516195	chr14:101012996	0.86
rs10271372	chr7:157793023	1.56E-23	cg12440927	chr7:157791721	0.04
rs4807546	chr19:4182060	2.24E-23	cg23999422	chr19:4173466	0.64
rs9348260	chr6:170516123	3.49E-23	cg22739554	chr6:170500876	0.1
rs7833924	chr8:144996029	5.06E-23	cg10276948	chr8:144986694	0.06
rs7833924	chr8:144996029	7.35E-23	cg09374673	chr8:144986488	0.06
rs9933817	chr16:83972660	1.30E-22	cg16528738	chr16:83968260	0.94
rs907033	chr16:83987856	2.05E-22	cg07978099	chr16:83986941	0.24
rs2412322	chr17:48578726	3.11E-22	cg00901687	chr17:48585270	0.06
rs4689604	chr4:7129556	1.06E-21	cg16307866	chr4:7129517	0.19
rs7496866	chr15:27102200	1.31E-21	cg10318222	chr15:27111940	0.2
rs6435711	chr2:213410065	1.54E-21	cg16329650	chr2:213403929	0.78
rs13147452	chr4:1078124	3.25E-21	cg27284194	chr4:1044797	0.6
rs1156782	chr6:115995564	6.21E-21	cg04193905	chr6:115989126	0.76
rs2568198	chr2:85403546	8.25E-21	cg22128724	chr2:85402928	0.78
rs4928043	chr3:54085900	9.48E-21	cg15798837	chr3:54122146	0.48
rs10058772	chr5:180033292	1.31E-20	cg06967124	chr5:180045597	0.52
rs5412	chr17:7184046	1.37E-20	cg01757206	chr17:7183913	0.18
rs30927	chr16:55317598	1.54E-20	cg01064265	chr16:55363058	0.11
rs13065	chr14:100996312	1.67E-20	cg19590140	chr14:101012492	0.81
rs7833924	chr8:144996029	2.76E-20	cg06045337	chr8:145013910	0.01
rs2412322	chr17:48578726	3.49E-20	cg11440486	chr17:48585216	0.08
rs212781	chr6:133771248	4.13E-20	cg25075347	chr6:133731801	0.53
rs1735173	chr8:146071261	4.84E-20	cg20672363	chr8:146075022	0.9
rs10079713	chr5:28692468	6.95E-20	cg07881623	chr6:80731107	0.39
rs13147452	chr4:1078124	9.41E-20	cg04106633	chr4:1044584	0.52

rs16961809	chr19:29226299	9.75E-20	cg12756686	chr19:29218302	0.26
rs7516453	chr1:15972558	1.52E-19	cg17385448	chr1:15911702	0.9
rs1350543	chr4:56014389	2.10E-19	cg01777861	chr4:56023843	0.79
rs454759	chr12:125799159	2.43E-19	cg03923277	chr12:104359732	0.18
rs11650633	chr17:80083807	2.92E-19	cg16920238	chr17:80076378	0.56
rs57550038	chr17:14078445	3.24E-19	cg00902417	chr17:15492168	0.25
rs4807546	chr19:4182060	3.25E-19	cg01287132	chr19:4173254	0.97
rs2978902	chr8:6690173	6.20E-19	cg11878365	chr8:6692387	0.24
rs7201047	chr16:86335556	6.38E-19	cg04352168	chr16:86334058	0.47
rs1341741	chr10:888073	6.63E-19	cg26597838	chr10:835615	0.45
rs1341741	chr10:888073	8.95E-19	cg20503657	chr10:835505	0.76
rs16961809	chr19:29226299	9.06E-19	cg14983838	chr19:29218262	0.11
rs11636395	chr15:45535684	1.04E-18	cg25801113	chr15:45476975	0.58
rs9876131	chr3:136726790	1.34E-18	cg21827317	chr3:136751795	0.27
rs16961809	chr19:29226299	1.90E-18	cg03161606	chr19:29218774	0.19
rs11984421	chr7:100266633	2.09E-18	cg02938413	chr7:100330587	0.24
rs1350543	chr4:56014389	2.39E-18	cg09978860	chr4:56023921	0.76
rs12924275	chr16:9191790	2.77E-18	cg08831531	chr16:9218945	0.08
rs9936140	chr16:10193417	2.88E-18	cg08242859	chr7:128032651	0.63
rs56340588	chr7:127799341	3.00E-18	cg02301128	chr7:127792165	0.74
rs2062480	chr1:197905400	3.12E-18	cg00114966	chr1:197893920	0.49
rs74002504	chr2:241828338	3.34E-18	cg04034577	chr2:241836375	0.1
rs9643305	chr8:134610055	4.90E-18	cg22582999	chr8:134594669	0.54
rs8082590	chr17:17958402	5.31E-18	cg04398451	chr17:18023971	0.86
rs12097673	chr1:2843180	5.61E-18	cg21402748	chr1:2838849	0.03
rs72732566	chr5:36744234	7.70E-18	cg03995615	chr5:36744219	0.54
rs7803698	chr7:64427895	8.13E-18	cg12143784	chr7:64541923	0.29
rs9769809	chr7:64956889	1.06E-17	cg12143784	chr7:64541923	0.29
rs3128778	chr4:2402474	1.07E-17	cg01601518	chr4:2404284	0.86
rs7512217	chr1:15586878	1.13E-17	cg08815479	chr1:15573596	0.93
rs79175383	chr12:96336533	1.49E-17	cg25229172	chr12:96336121	0.31
rs7206985	chr17:9159202	1.57E-17	cg12361772	chr17:9160821	0.88
rs2800973	chr22:19168616	1.61E-17	cg24911827	chr22:19170109	0.96
rs2342082	chr12:123090380	1.85E-17	cg23029597	chr12:123009494	0.39
rs6565516	chr17:78965146	1.89E-17	cg10070101	chr17:78963290	0.6
rs6685767	chr1:46823929	2.25E-17	cg15580309	chr1:46814106	0.45
rs7257916	chr19:45482884	2.38E-17	cg13119609	chr19:45449297	0.72
rs2505949	chr6:80804414	2.48E-17	cg08355045	chr6:80787529	0.87
rs11675057	chr2:26399481	2.89E-17	cg22920501	chr2:26401640	0.78
rs11688491	chr2:98167020	3.06E-17	cg26665480	chr2:98280029	0.58
rs4555948	chr6:160094492	3.17E-17	cg13221458	chr6:160112632	0.64
rs7257916	chr19:45482884	3.24E-17	cg09555818	chr19:45449301	0.81
rs7470675	chr9:132588337	3.47E-17	cg13529314	chr9:132598258	0.88
rs74002504	chr2:241828338	3.63E-17	cg07537917	chr2:241836409	0.49
rs6676743	chr1:110296338	4.07E-17	cg10807101	chr1:110282274	0.16
rs56378923	chr10:72316604	4.21E-17	cg22643110	chr10:72319345	0.74
rs908951	chr16:89697625	4.97E-17	cg08949735	chr16:89699720	0.74
rs2246207	chr17:61987576	5.00E-17	cg06873352	chr17:61820015	0.61
rs72635991	chr10:788658	5.00E-17	cg24280607	chr15:41709584	0.4
rs62014776	chr16:1339750	5.51E-17	cg03705235	chr16:1371463	0.63
rs7496866	chr15:27102200	5.62E-17	cg03325535	chr15:27111949	0.37
rs13147452	chr4:1078124	7.37E-17	cg21130718	chr4:1044621	0.34
rs930526	chr17:6473353	7.39E-17	cg23551722	chr17:6546898	0.66
rs60061503	chr1:185364328	7.89E-17	cg11066601	chr1:185373486	0.58
rs113935737	chr15:65123276	8.14E-17	cg25489524	chr15:65127973	0.84
rs9812936	chr3:50043654	9.76E-17	cg12257692	chr3:49977190	0.96
rs59462516	chr12:1165012	1.32E-16	cg07813377	chr12:1192425	0.68
rs12467950	chr2:220275736	1.38E-16	cg15015639	chr2:220282977	0.8
rs9348260	chr6:170516123	1.85E-16	cg21597487	chr6:170500638	0.19
rs1350543	chr4:56014389	1.93E-16	cg16572876	chr4:56024045	0.93
rs4929922	chr11:8975776	2.09E-16	cg21881798	chr11:8931708	0
rs12595938	chr16:8958081	2.14E-16	cg08308162	chr16:8889244	0.8

rs28839814	chr4:13555899	2.63E-16	cg20477448	chr4:13656704	0.38
rs1730794	chr4:3451960	3.04E-16	cg25120210	chr4:3464653	0.54
rs9726753	chr1:153591652	3.13E-16	cg05659314	chr1:153590020	0.1
rs3021270	chr22:40396409	3.35E-16	cg21771250	chr22:40406049	0.93
rs6968990	chr7:32552159	3.51E-16	cg06627557	chr7:32535165	0.31
rs62185165	chr2:241251453	3.62E-16	cg21947394	chr2:241260110	0.35
rs1375813	chr3:142809577	4.50E-16	cg01520402	chr3:142790398	0.31
rs9812936	chr3:50043654	4.87E-16	cg05623727	chr3:50126028	0.56
rs12653391	chr5:439796	4.91E-16	cg00049323	chr5:472564	0.34
rs58635565	chr8:41561181	5.08E-16	cg07533533	chr8:41559593	0.92
rs12691433	chr7:154989404	5.13E-16	cg07944445	chr7:155006275	0.85
rs13283037	chr9:97018520	5.44E-16	cg13980266	chr9:97022269	0.78
rs117194038	chr17:43927290	5.52E-16	cg01934064	chr17:44064242	0.73
rs10793287	chr11:77846706	6.02E-16	cg09721595	chr11:77773924	0.88
rs1812214	chr8:105344070	7.22E-16	cg04554929	chr8:105342491	0.73
rs9769809	chr7:64956889	7.61E-16	cg01136167	chr7:65037704	0.55
rs2370234	chr1:25304464	7.89E-16	cg23273869	chr1:25296894	0.47
rs7662812	chr4:24983413	8.17E-16	cg19676182	chr4:24981695	0.14
rs7402982	chr15:99193269	8.24E-16	cg03437748	chr15:99193247	0.03
rs12022839	chr1:58089133	8.59E-16	cg00026909	chr1:58089001	0.63
rs11149799	chr16:75174049	8.71E-16	cg00897404	chr16:75182368	0.77
rs7514450	chr1:220991171	8.91E-16	cg08655206	chr1:221058198	0.34
rs4782336	chr16:89151518	1.01E-15	cg00697672	chr16:89151343	0.63
rs45537633	chr6:41117824	1.18E-15	cg03644281	chr6:41068752	0.23
rs11060115	chr12:129554644	1.19E-15	cg01290755	chr12:129554587	0.17
rs4789846	chr17:80225545	1.29E-15	cg22805688	chr17:80197841	0.84
rs7574691	chr2:240044687	1.30E-15	cg15934368	chr2:240044021	0.07
rs11712066	chr3:151830309	1.48E-15	cg27098685	chr3:151867537	0.85
rs30927	chr16:55317598	1.65E-15	cg07592723	chr16:55365146	0.32
rs6597862	chr10:126649723	1.69E-15	cg06432487	chr10:126623651	0.54
rs9817966	chr3:46650540	1.78E-15	cg24524379	chr3:46600244	0.16
rs12674529	chr8:127885599	1.82E-15	cg21238284	chr8:127889295	0.78
rs455104	chr17:10618227	1.89E-15	cg00549475	chr17:10632715	0.44
rs30927	chr16:55317598	2.12E-15	cg06722193	chr16:55359355	0.17
rs2276968	chr4:7070118	2.26E-15	cg06697600	chr4:7070879	0.55
rs4571937	chr1:20897033	2.30E-15	cg00750606	chr1:20899121	0.85
rs4770476	chr13:24269820	2.35E-15	cg07031408	chr13:24269867	0.51
rs57094537	chr4:40261798	2.39E-15	cg25243082	chr4:40267141	0.83
rs7016869	chr8:2474928	2.58E-15	cg02472801	chr8:2480483	0.18
rs2637657	chr10:133993806	2.60E-15	cg18037376	chr10:134004552	0.52
rs11675057	chr2:26399481	2.70E-15	cg25036284	chr2:26402008	0.81
rs1919784	chr7:33105268	2.89E-15	cg22798885	chr7:33102694	0.74
rs7663448	chr4:10054787	2.91E-15	cg26043149	chr18:55253948	0.29
rs10987908	chr9:130936530	3.07E-15	cg10071929	chr9:130955135	0.72
rs392124	chr17:9669921	3.17E-15	cg13468767	chr17:9672024	0.26
rs13147452	chr4:1078124	3.59E-15	cg04016957	chr4:1044486	0.42
rs3793202	chr7:6207142	4.84E-15	cg22849526	chr7:6199437	0.82
rs6711715	chr2:130330516	5.25E-15	cg05903289	chr2:130345205	0.06
rs11179581	chr12:37892432	5.32E-15	cg10856724	chr12:34555212	0.18
rs117194038	chr17:43927290	5.58E-15	cg01341218	chr17:43662625	0.46
rs7104785	chr11:804212	5.81E-15	cg01741372	chr11:783889	0.93
rs9284725	chr2:102744854	5.95E-15	cg22835712	chr2:102737379	0.71
rs7833924	chr8:144996029	5.96E-15	cg27082292	chr8:145001361	0.26
rs11675057	chr2:26399481	6.22E-15	cg27170947	chr2:26402098	0.5
rs4314559	chr7:2365892	6.93E-15	cg16553052	chr7:2349605	0.67
rs12028536	chr1:228743706	7.56E-15	cg06261630	chr1:228741351	0.74
rs4910458	chr11:9379402	8.41E-15	cg19695805	chr11:9385645	0.96
rs7496866	chr15:27102200	8.56E-15	cg01378667	chr15:27111911	0.44
rs257701	chr5:123737922	8.80E-15	cg01806427	chr5:123737813	0.76
rs13044479	chr20:62245686	8.94E-15	cg09650180	chr20:62225654	0.74
rs7833924	chr8:144996029	9.08E-15	cg05696706	chr8:145013932	0.01
rs10987908	chr9:130936530	9.61E-15	cg09976142	chr9:130955436	0.58

rs4770476	chr13:24269820	9.62E-15	cg10885151	chr13:24270087	0.57
rs12129745	chr1:28572317	1.07E-14	cg04993605	chr1:28573052	0.23
rs34228916	chr12:115942842	1.14E-14	cg18639984	chr12:115943877	0.11
rs8016689	chr14:103319981	1.21E-14	cg23020514	chr14:103360112	0.09
rs8008761	chr14:90739754	1.29E-14	cg10090757	chr14:90744615	0.91
rs4782336	chr16:89151518	1.30E-14	cg07845093	chr16:89151447	0.88
rs2269906	chr17:42294337	1.34E-14	cg13607699	chr17:42295918	0.43
rs10175462	chr2:113988492	1.41E-14	cg21550016	chr2:113992930	0.51
rs72781258	chr2:20274213	1.73E-14	cg24657347	chr2:20261756	0.94
rs8057544	chr16:537650	1.96E-14	cg27494100	chr16:537705	0.82
rs72755098	chr15:64427587	2.09E-14	cg02848875	chr15:64387786	0.28
rs9998888	chr4:824575	2.10E-14	cg24793722	chr4:824416	0.7
rs193930	chr2:8107520	2.21E-14	cg03155496	chr2:8117019	0.46
rs8053397	chr16:87573468	2.32E-14	cg08031982	chr16:87577539	0.18
rs4984688	chr16:785717	2.32E-14	cg18653534	chr16:772142	0.37
rs117194038	chr17:43927290	2.36E-14	cg22433210	chr17:43662623	0.82
rs7143780	chr14:96154609	2.44E-14	cg03043804	chr14:96152706	0.49
rs9782	chr12:103351826	2.56E-14	cg27569040	chr12:103351855	0.86
rs9915323	chr17:37770481	2.59E-14	cg00129232	chr17:37814104	0.92
rs17333520	chr11:31058834	2.60E-14	cg26647111	chr11:31128758	0.09
rs111543213	chr19:37642385	2.61E-14	cg08835041	chr19:37461278	0.16
rs9912302	chr17:44916982	2.75E-14	cg25836567	chr17:44929689	0.16
rs10920265	chr1:201822955	2.87E-14	cg06775570	chr1:201857621	0.25
rs2376584	chr17:76402116	3.21E-14	cg05887092	chr17:76393375	0.46
rs16961809	chr19:29226299	3.22E-14	cg25267487	chr19:29217858	0.12
rs3128778	chr4:2402474	3.27E-14	cg13053151	chr4:2403559	0.59
rs3808524	chr8:23161983	3.42E-14	cg24531534	chr8:23162162	0.53
rs10773762	chr12:130765366	3.60E-14	cg14604444	chr12:130766091	0.48
rs12977777	chr19:35323365	3.64E-14	cg15695738	chr19:35329860	0.13
rs11230570	chr11:60782634	3.68E-14	cg27098804	chr11:60776124	0.45
rs4866663	chr5:2727471	4.15E-14	cg27345924	chr5:2727758	0.91
rs6560691	chr10:134140245	4.24E-14	cg23771949	chr10:134165390	0.05
rs7015233	chr8:144381511	5.46E-14	cg12888521	chr8:144346762	0.42
rs10151225	chr14:52589352	5.59E-14	cg12071775	chr14:52591786	0.25
rs28520336	chr6:17555977	5.81E-14	cg09879382	chr6:17581248	0.93
rs10492997	chr1:19769371	6.19E-14	cg17081867	chr1:19768096	0.25
rs7016869	chr8:2474928	6.30E-14	cg01414268	chr8:2480911	0.2
rs10987908	chr9:130936530	6.90E-14	cg13642260	chr9:130955380	0.63
rs10773762	chr12:130765366	7.12E-14	cg27633287	chr12:130766243	0.44
rs2205661	chr22:45731759	7.17E-14	cg00733150	chr22:45705707	0.12
rs12698058	chr7:157225536	7.24E-14	cg03453431	chr7:157225567	0.44
rs10175462	chr2:113988492	7.76E-14	cg11763394	chr2:113992921	0.47
rs4143866	chr16:85716366	7.96E-14	cg26571870	chr16:85723150	0.54
rs7455225	chr7:73241386	9.64E-14	cg02874145	chr7:73246406	0.32
rs10888514	chr1:152707929	9.78E-14	cg07796016	chr1:152779584	0.98
rs4475020	chr3:14599121	1.10E-13	cg21529591	chr3:14596904	0.32
rs6421977	chr11:407708	1.12E-13	cg18351999	chr11:406901	0.52
rs4965672	chr15:101089241	1.20E-13	cg02597199	chr15:101098829	0.77
rs6711715	chr2:130330516	1.21E-13	cg05962382	chr2:130345044	0.71
rs2021560	chr19:22373470	1.23E-13	cg22620746	chr19:22234992	0.44
rs4789885	chr17:77310495	1.30E-13	cg08223357	chr17:77302162	0.79
rs16965349	chr17:36614524	1.32E-13	cg12050358	chr17:36612909	0.78
rs12208321	chr6:56132243	1.35E-13	cg07143470	chr6:56111812	0.1
rs12097673	chr1:2843180	1.35E-13	cg00996827	chr1:2838805	0.14
rs3793969	chr11:1318884	1.36E-13	cg14329644	chr11:1253904	0.73
rs4900242	chr14:95151985	1.45E-13	cg16462006	chr14:95155784	0.42
rs58069944	chr8:2294105	1.46E-13	cg11900328	chr8:2263331	0.99
rs2297475	chr10:90984623	1.55E-13	cg17741809	chr10:90985055	0.44
rs29655	chr5:180267436	1.61E-13	cg19091830	chr5:180286094	0.21
rs6946060	chr7:157644761	1.67E-13	cg22216157	chr7:157643037	0.82
rs6946060	chr7:157644761	1.74E-13	cg25449441	chr7:157644471	0.94
rs4928043	chr3:54085900	1.84E-13	cg01296889	chr3:54122032	0.22

rs45537633	chr6:41117824	1.87E-13	cg04346459	chr6:41068666	0.74
rs28400431	chr8:143698404	1.87E-13	cg10104451	chr8:143696006	0.68
rs72704639	chr1:150798335	1.91E-13	cg04414720	chr1:150670196	0.07
rs2453606	chr17:19387091	1.92E-13	cg19949948	chr17:19361230	0.68
rs28452050	chr16:29317318	1.94E-13	cg05645661	chr16:29329490	0.77
rs668338	chr11:60713358	1.97E-13	cg06257669	chr11:60702218	0.43
rs2870479	chr19:57449293	2.03E-13	cg12414181	chr15:75287860	0.86
rs7794450	chr7:6625847	2.05E-13	cg19149522	chr7:6616423	0.13
rs143349430	chr10:32183019	2.18E-13	cg04359828	chr10:32216031	0.24
rs12653230	chr5:159735611	2.21E-13	cg17267804	chr5:159735392	0.07
rs1055150	chr19:18499784	2.34E-13	cg21088460	chr19:18499786	0.87
rs9525735	chr13:43661306	2.36E-13	cg14729962	chr13:43597565	0
rs2145848	chr6:3035894	2.56E-13	cg05728019	chr6:3024023	0.86
rs890393	chr18:74102435	2.60E-13	cg24786174	chr18:74118243	0.18
rs11650633	chr17:80083807	2.65E-13	cg00755572	chr17:80077754	0.36
rs7018316	chr8:144630169	2.85E-13	cg20458811	chr8:144631810	0.11
rs11675057	chr2:26399481	3.21E-13	cg04944784	chr2:26401820	0.76
rs10058772	chr5:180033292	3.26E-13	cg00744924	chr5:180042471	0.72
rs75934331	chr1:183182029	3.30E-13	cg01417625	chr1:183187433	0.48
rs5023799	chr13:47095293	3.55E-13	cg11342437	chr13:47126328	0.03
rs12761857	chr10:7105868	3.56E-13	cg00998146	chr19:18284560	0.79

Supplementary Table 7. Methylation QTLs (mQTL) identified in the striatum for SNPs included in the schizophrenia polygenic risk score (PRS). Shown are associations between DNA methylation at specific Illumina 450K probes and genetic variants used to derive PRS in Chapter 4, in addition to the corresponding *P*-values for PRS-associated DNA methylation variation at the same probe.

SNP	SNP genomic location (hg19)	mQTL <i>P</i>	CpG	CpG genomic location (hg19)	EWAS <i>P</i>
rs6680259	chr1:7122308	1.55E-52	cg20409752	chr1:7122726	0.07
rs9726753	chr1:153591652	3.54E-50	cg08477332	chr1:153590243	0.29
rs12635522	chr3:125708174	5.95E-46	cg15145296	chr3:125709740	0.61
rs117194038	chr17:43927290	2.87E-45	cg17117718	chr17:43663208	0.5
rs76344840	chr9:33120204	4.29E-43	cg20290983	chr6:43655470	0.38
rs4792919	chr17:41873309	1.00E-39	cg26893861	chr17:41843967	0.99
rs35059736	chr7:158224692	2.93E-34	cg01191920	chr7:158217561	0.58
rs12635522	chr3:125708174	3.18E-34	cg02807482	chr3:125708958	0.59
rs12635522	chr3:125708174	5.04E-34	cg06494592	chr3:125709126	0.95
rs9348260	chr6:170516123	1.16E-31	cg22739554	chr6:170500876	0.03
rs12635522	chr3:125708174	1.92E-31	cg04553112	chr3:125709451	0.43
rs117194038	chr17:43927290	3.19E-31	cg22968622	chr17:43663579	0.31
rs7833924	chr8:144996029	5.67E-31	cg10276948	chr8:144986694	0.02
rs907033	chr16:83987856	9.19E-31	cg27171569	chr16:83987465	0.29
rs4880509	chr10:1511150	1.74E-30	cg09316607	chr10:1511024	0.71
rs72732566	chr5:36744234	1.80E-30	cg03995615	chr5:36744219	0.95
rs4880509	chr10:1511150	4.08E-30	cg13684379	chr10:1511173	0.49
rs4807546	chr19:4182060	2.74E-28	cg23999422	chr19:4173466	0.76
rs12653230	chr5:159735611	1.13E-27	cg17267804	chr5:159735392	0.02
rs10857676	chr10:134970598	1.43E-27	cg00753039	chr10:134969141	0.54
rs9933817	chr16:83972660	1.46E-27	cg16528738	chr16:83968260	0.36
rs11650633	chr17:80083807	2.21E-26	cg16920238	chr17:80076378	0.63
rs6597862	chr10:126649723	3.79E-26	cg06432487	chr10:126623651	0.92
rs4880509	chr10:1511150	3.79E-26	cg04012681	chr10:1511277	0.71
rs7833924	chr8:144996029	6.96E-26	cg09374673	chr8:144986488	0.05
rs199503	chr17:44862162	2.97E-25	cg22968622	chr17:43663579	0.31
rs11636395	chr15:45535684	4.47E-25	cg25801113	chr15:45476975	0.04
rs117194038	chr17:43927290	5.23E-25	cg01934064	chr17:44064242	0.84
rs4807546	chr19:4182060	7.48E-25	cg01287132	chr19:4173254	0.62
rs9348260	chr6:170516123	1.05E-24	cg21597487	chr6:170500638	0.05
rs9348260	chr6:170516123	1.14E-24	cg21235075	chr6:170500610	0.2
rs11060115	chr12:129554644	6.89E-24	cg01290755	chr12:129554587	0.3
rs199503	chr17:44862162	8.32E-24	cg17117718	chr17:43663208	0.5
rs2412322	chr17:48578726	8.83E-24	cg00901687	chr17:48585270	0.09
rs2505949	chr6:80804414	1.55E-23	cg08355045	chr6:80787529	0.47
rs13065	chr14:100996312	1.68E-23	cg18516195	chr14:101012996	0.12
rs2800973	chr22:19168616	4.34E-23	cg02655711	chr22:19163373	0.56
rs4555948	chr6:160094492	5.15E-23	cg13221458	chr6:160112632	0.26
rs5412	chr17:7184046	5.65E-23	cg01757206	chr17:7183913	0.53
rs6455887	chr6:163674175	6.75E-23	cg07343445	chr6:163673130	0.11
rs73752005	chr6:88092421	9.34E-23	cg06087457	chr6:88040249	0.41
rs56340588	chr7:127799341	2.61E-22	cg02301128	chr7:127792165	0.54
rs9933817	chr16:83972660	2.70E-22	cg16457916	chr16:83968360	0.8
rs13147452	chr4:1078124	7.13E-22	cg27284194	chr4:1044797	0.59
rs72755098	chr15:64427587	1.99E-21	cg02848875	chr15:64387786	0.32
rs74002504	chr2:241828338	2.82E-21	cg04034577	chr2:241836375	0.33
rs1350543	chr4:56014389	4.64E-21	cg09978860	chr4:56023921	0.97
rs60061503	chr1:185364328	7.87E-21	cg11066601	chr1:185373486	0.85
rs454759	chr12:125799159	9.47E-21	cg03923277	chr12:104359732	0.4

rs1350543	chr4:56014389	1.43E-20	cg01777861	chr4:56023843	0.81
rs257701	chr5:123737922	1.59E-20	cg01806427	chr5:123737813	0.26
rs7131362	chr11:1689325	3.18E-20	cg04938738	chr11:1689429	0.62
rs60668498	chr19:44642672	3.93E-20	cg23489630	chr19:44645078	0.87
rs12595938	chr16:8958081	6.21E-20	cg08308162	chr16:8889244	0.39
rs28839814	chr4:13555899	8.95E-20	cg20477448	chr4:13656704	0.82
rs28452050	chr16:29317318	1.09E-19	cg05645661	chr16:29329490	0.32
rs35037013	chr10:54656418	1.12E-19	cg05984115	chr10:54631212	0.92
rs2291393	chr17:80585094	1.13E-19	cg27136344	chr17:80606911	0.54
rs16961809	chr19:29226299	1.20E-19	cg14983838	chr19:29218262	0.18
rs11230233	chr11:55349858	1.27E-19	cg20623702	chr11:55431584	0.73
rs650241	chr11:75277757	1.71E-19	cg26104986	chr11:75275303	0.08
rs4143866	chr16:85716366	1.92E-19	cg26571870	chr16:85723150	0.68
rs6685767	chr1:46823929	2.97E-19	cg15580309	chr1:46814106	0.12
rs8082590	chr17:17958402	3.07E-19	cg04398451	chr17:18023971	0.56
rs1341741	chr10:888073	4.50E-19	cg26597838	chr10:835615	0.94
rs2412322	chr17:48578726	4.74E-19	cg11440486	chr17:48585216	0.11
rs13147452	chr4:1078124	5.33E-19	cg21130718	chr4:1044621	0.74
rs12097673	chr1:2843180	5.33E-19	cg21402748	chr1:2838849	0.84
rs10793287	chr11:77846706	5.40E-19	cg09721595	chr11:77773924	0.73
rs1294417	chr6:6741932	5.59E-19	cg06612196	chr6:6737390	0.81
rs7803698	chr7:64427895	7.87E-19	cg12143784	chr7:64541923	0.13
rs212781	chr6:133771248	1.12E-18	cg25075347	chr6:133731801	0.69
rs62014776	chr16:1339750	1.21E-18	cg03705235	chr16:1371463	0.6
rs9726753	chr1:153591652	1.23E-18	cg05659314	chr1:153590020	0.69
rs6565516	chr17:78965146	1.41E-18	cg10070101	chr17:78963290	0.63
rs2066700	chr13:50887725	1.58E-18	cg17976839	chr13:50923823	0.06
rs11675057	chr2:26399481	1.61E-18	cg22920501	chr2:26401640	0.74
rs4689604	chr4:7129556	1.69E-18	cg16307866	chr4:7129517	0.88
rs16961809	chr19:29226299	1.88E-18	cg03161606	chr19:29218774	0.14
rs2342082	chr12:123090380	2.10E-18	cg23029597	chr12:123009494	0.09
rs13282161	chr8:1705041	2.29E-18	cg17694851	chr8:1707553	0.05
rs684337	chr17:727349	2.30E-18	cg05176970	chr17:724273	0.72
rs199503	chr17:44862162	2.40E-18	cg01934064	chr17:44064242	0.84
rs62185165	chr2:241251453	2.58E-18	cg21947394	chr2:241260110	0.64
rs3793202	chr7:6207142	3.00E-18	cg22849526	chr7:6199437	0.24
rs3891052	chr14:105672895	3.86E-18	cg27037305	chr14:105689766	0.54
rs16961809	chr19:29226299	4.54E-18	cg12756686	chr19:29218302	0.21
rs45537633	chr6:41117824	4.90E-18	cg03644281	chr6:41068752	0.68
rs4475020	chr3:14599121	5.36E-18	cg21529591	chr3:14596904	0.61
rs10058772	chr5:180033292	5.48E-18	cg06967124	chr5:180045597	0.47
rs13065	chr14:100996312	5.57E-18	cg19590140	chr14:101012492	0.47
rs9390343	chr6:146010527	6.69E-18	cg01476807	chr6:146125657	0.94
rs57550038	chr17:14078445	7.18E-18	cg00902417	chr17:15492168	0.33
rs7257916	chr19:45482884	7.23E-18	cg09555818	chr19:45449301	0.65
rs6801145	chr3:167312146	8.54E-18	cg18801567	chr3:167450363	0.02
rs7662812	chr4:24983413	8.97E-18	cg19676182	chr4:24981695	1
rs57094537	chr4:40261798	9.01E-18	cg25243082	chr4:40267141	0.58
rs392124	chr17:9669921	1.16E-17	cg13468767	chr17:9672024	0.36
rs4928043	chr3:54085900	1.34E-17	cg15798837	chr3:54122146	0.37
rs6435711	chr2:213410065	2.36E-17	cg16329650	chr2:213403929	0.38
rs2978902	chr8:6690173	2.70E-17	cg11878365	chr8:6692387	0.77
rs10897269	chr11:62162088	2.70E-17	cg23876832	chr11:62092739	0.13
rs9876131	chr3:136726790	3.09E-17	cg21827317	chr3:136751795	0.82
rs7015233	chr8:144381511	3.83E-17	cg20232550	chr8:144344793	0.95
rs890393	chr18:74102435	4.51E-17	cg24786174	chr18:74118243	0.14
rs66712530	chr12:132664285	4.93E-17	cg26320244	chr12:132663455	0.44
rs2568198	chr2:85403546	5.14E-17	cg22128724	chr2:85402928	0.72
rs144716806	chr4:38854783	5.17E-17	cg26681822	chr4:38858561	0.38
rs72704639	chr1:150798335	5.97E-17	cg09365446	chr1:150670422	0.15
rs2014453	chr7:44142792	6.41E-17	cg12399411	chr7:44134432	0.59
rs12214357	chr6:77577369	7.43E-17	cg17141972	chr6:77547510	0.53

rs13147452	chr4:1078124	8.06E-17	cg04106633	chr4:1044584	0.58
rs12698058	chr7:157225536	9.93E-17	cg03453431	chr7:157225567	0.49
rs9769809	chr7:64956889	1.03E-16	cg12143784	chr7:64541923	0.13
rs13283037	chr9:97018520	1.09E-16	cg13980266	chr9:97022269	0.81
rs10175462	chr2:113988492	1.12E-16	cg21550016	chr2:113992930	0.99
rs4910458	chr11:9379402	1.16E-16	cg19695805	chr11:9385645	0.63
rs9917823	chr3:183673780	1.39E-16	cg01324343	chr3:183735012	0.06
rs12129745	chr1:28572317	1.48E-16	cg04993605	chr1:28573052	0.85
rs4802745	chr19:51320111	1.71E-16	cg02725269	chr19:51327177	0.35
rs3128778	chr4:2402474	1.78E-16	cg13053151	chr4:2403559	0.77
rs2475509	chr6:39890217	1.79E-16	cg10871120	chr6:39891273	0.07
rs2062480	chr1:197905400	1.85E-16	cg00114966	chr1:197893920	0.34
rs12450494	chr17:7207887	2.22E-16	cg04514024	chr17:7222668	0.31
rs7833924	chr8:144996029	2.22E-16	cg06045337	chr8:145013910	0.16
rs10175462	chr2:113988492	2.53E-16	cg11763394	chr2:113992921	0.88
rs28400431	chr8:143698404	2.54E-16	cg10104451	chr8:143696006	0.25
rs4984688	chr16:785717	2.65E-16	cg18653534	chr16:772142	0.46
rs4571937	chr1:20897033	2.83E-16	cg00750606	chr1:20899121	0.91
rs9936140	chr16:10193417	2.84E-16	cg08242859	chr7:128032651	0.41
rs13147452	chr4:1078124	3.33E-16	cg04016957	chr4:1044486	0.5
rs4789846	chr17:80225545	3.71E-16	cg22805688	chr17:80197841	0.96
rs1058167	chr22:42538029	3.83E-16	cg09322432	chr22:42527611	0
rs2553022	chr7:100401862	3.90E-16	cg12616177	chr7:100434510	0.09
rs12028536	chr1:228743706	4.04E-16	cg06261630	chr1:228741351	0.51
rs4965672	chr15:101089241	4.41E-16	cg02597199	chr15:101098829	0.54
rs72704639	chr1:150798335	5.04E-16	cg04414720	chr1:150670196	0.44
rs11650633	chr17:80083807	5.82E-16	cg00755572	chr17:80077754	0.78
rs10987908	chr9:130936530	6.99E-16	cg10071929	chr9:130955135	0.67
rs62120467	chr2:3382624	7.07E-16	cg12447832	chr2:3383257	0.19
rs9549822	chr13:112691814	7.07E-16	cg16875032	chr8:121823916	0.01
rs7104785	chr11:804212	7.10E-16	cg01741372	chr11:783889	0.76
rs274692	chr5:6734625	7.52E-16	cg10857441	chr5:6722123	0.43
rs9817966	chr3:46650540	7.80E-16	cg24524379	chr3:46600244	0.38
rs1341741	chr10:888073	1.02E-15	cg20503657	chr10:835505	0.59
rs111543213	chr19:37642385	1.05E-15	cg08835041	chr19:37461278	0.45
rs34228916	chr12:115942842	1.16E-15	cg18639984	chr12:115943877	0.93
rs4782336	chr16:89151518	1.28E-15	cg07845093	chr16:89151447	0.6
rs72781258	chr2:20274213	1.33E-15	cg24657347	chr2:20261756	0.86
rs7018316	chr8:144630169	1.35E-15	cg20458811	chr8:144631810	0.95
rs883138	chr7:150042793	1.54E-15	cg12556325	chr7:150026731	0.54
rs193572	chr7:116835734	1.67E-15	cg16444922	chr7:116842338	0.42
rs7514450	chr1:220991171	1.68E-15	cg15450098	chr1:221057561	0.05
rs10753541	chr1:23061992	1.92E-15	cg05266663	chr1:23061564	0.54
rs28701975	chr1:38272307	2.06E-15	cg00095214	chr1:38272200	0.44
rs907033	chr16:83987856	2.70E-15	cg07978099	chr16:83986941	0.39
rs7854075	chr9:96571211	2.70E-15	cg14396892	chr9:96623032	0.11
rs10175462	chr2:113988492	3.31E-15	cg07772999	chr2:113993052	0.96
rs2370234	chr1:25304464	3.33E-15	cg23273869	chr1:25296894	0.05
rs6517397	chr21:38352125	3.52E-15	cg21871091	chr21:38349937	0.66
rs2205661	chr22:45731759	3.64E-15	cg00733150	chr22:45705707	0.07
rs12022839	chr1:58089133	4.85E-15	cg00026909	chr1:58089001	0.5
rs11675057	chr2:26399481	4.93E-15	cg04944784	chr2:26401820	0.54
rs10079713	chr5:28692468	5.93E-15	cg07881623	chr6:80731107	0.58
rs1350543	chr4:56014389	6.00E-15	cg16572876	chr4:56024045	0.94
rs1571624	chr13:112164791	6.50E-15	cg25943066	chr13:112164965	0.93
rs1183079	chr7:2904672	6.75E-15	cg14668632	chr7:2872130	0.97
rs930526	chr17:6473353	6.79E-15	cg23551722	chr17:6546898	0.87
rs4648729	chr1:1808769	6.96E-15	cg03396347	chr1:1875803	0.8
rs8044982	chr16:58521090	7.09E-15	cg02036364	chr16:58521443	0.75
rs10987908	chr9:130936530	7.42E-15	cg13642260	chr9:130955380	0.47
rs4793213	chr17:41307101	8.37E-15	cg23758822	chr17:41437982	0.16
rs7663448	chr4:10054787	8.99E-15	cg15882809	chr6:26285828	0.91

rs11251278	chr10:2544043	9.11E-15	cg18171855	chr10:2543474	0.47
rs12097673	chr1:2843180	9.33E-15	cg00996827	chr1:2838805	0.55
rs62120467	chr2:3382624	9.82E-15	cg01472464	chr2:3383078	0.05
rs7663448	chr4:10054787	9.89E-15	cg26043149	chr18:55253948	0.28
rs8140485	chr22:50529146	1.05E-14	cg24864161	chr22:50528282	0.43
rs9812936	chr3:50043654	1.11E-14	cg12257692	chr3:49977190	0.97
rs1055150	chr19:18499784	1.15E-14	cg21088460	chr19:18499786	0.17
rs1316524	chr1:31972540	1.25E-14	cg07096763	chr1:31971752	0.48
rs4708675	chr6:168555071	1.34E-14	cg04463397	chr6:168556793	0.01
rs4808736	chr19:18117488	1.39E-14	cg21649277	chr19:18117794	0.75
rs7606595	chr2:15900274	1.43E-14	cg26669897	chr2:15909070	0.02
rs7574691	chr2:240044687	1.48E-14	cg15635302	chr2:240043224	0.72
rs16961809	chr19:29226299	1.51E-14	cg25267487	chr19:29217858	0.15
rs28647894	chr17:80340483	1.55E-14	cg07797397	chr2:177052527	0.13
rs2665971	chr17:74010038	1.58E-14	cg10138630	chr17:74024966	0.15
rs6711715	chr2:130330516	1.62E-14	cg05962382	chr2:130345044	0.72
rs2003181	chr14:105642016	1.63E-14	cg15868425	chr14:105643522	0.32
rs12445614	chr16:89166832	1.70E-14	cg09427016	chr16:89167018	0.91
rs4145082	chr6:86352016	1.75E-14	cg03285617	chr6:86179345	1
rs12924275	chr16:9191790	2.20E-14	cg08831531	chr16:9218945	0.12
rs2872542	chr20:61664872	2.81E-14	cg08045932	chr20:61659980	0.71
rs7734278	chr5:178761358	2.82E-14	cg26694831	chr5:178763419	0.11
rs12517252	chr5:149910986	2.83E-14	cg02633363	chr5:149906179	0.3
rs7206985	chr17:9159202	2.94E-14	cg12361772	chr17:9160821	0.21
rs7545884	chr1:67665785	3.00E-14	cg23726106	chr1:67600229	0.53
rs1557026	chr1:228383367	3.10E-14	cg01200585	chr1:228362443	0.45
rs30927	chr16:55317598	3.32E-14	cg02198701	chr16:55364614	0.06
rs6711715	chr2:130330516	3.50E-14	cg05903289	chr2:130345205	0.35
rs7305397	chr12:42850058	3.95E-14	cg19980929	chr12:42632907	0.7
rs7710436	chr5:54056541	3.99E-14	cg06536806	chr5:54081633	0.5
rs58069944	chr8:2294105	4.37E-14	cg11900328	chr8:2263331	0.91
rs13224850	chr7:40168950	4.41E-14	cg13264672	chr7:39993440	0.74
rs7016869	chr8:2474928	4.45E-14	cg02472801	chr8:2480483	0.49
rs732215	chr7:50544063	4.58E-14	cg00647317	chr7:50633725	0.04
rs6500602	chr16:4497451	4.86E-14	cg01793945	chr16:4420291	0.06
rs12904722	chr15:42304003	4.90E-14	cg03080639	chr15:42302379	0.8
rs17333520	chr11:31058834	4.92E-14	cg06552810	chr11:31128660	0.52
rs2246207	chr17:61987576	5.22E-14	cg06873352	chr17:61820015	0.33
rs7470605	chr9:136890107	5.38E-14	cg13789015	chr9:136890014	0.93
rs9630726	chr17:43068628	5.49E-14	cg20215112	chr17:43065055	0.45
rs2295232	chr6:153365384	6.81E-14	cg17707550	chr6:153380415	0.37
rs10987908	chr9:130936530	8.00E-14	cg09976142	chr9:130955436	0.85
rs45537633	chr6:41117824	8.16E-14	cg09580153	chr6:41068724	0.93
rs6421977	chr11:407708	8.33E-14	cg18351999	chr11:406901	0.69
rs9782	chr12:103351826	8.83E-14	cg27569040	chr12:103351855	0.44
rs13269498	chr8:54578332	9.49E-14	cg10225865	chr8:54605566	0.96
rs6946060	chr7:157644761	9.51E-14	cg24524099	chr7:157643007	0.74
rs6702840	chr1:246626857	9.63E-14	cg04798314	chr1:246668601	0.61
rs7560311	chr2:1803605	9.89E-14	cg21862353	chr2:1801628	0.35
rs113935737	chr15:65123276	1.09E-13	cg07915896	chr15:65129816	0.43
rs9525735	chr13:43661306	1.11E-13	cg05035143	chr13:43597297	0.03
rs6946060	chr7:157644761	1.14E-13	cg22216157	chr7:157643037	0.96
rs6968990	chr7:32552159	1.19E-13	cg06627557	chr7:32535165	0.21
rs2872542	chr20:61664872	1.25E-13	cg23505145	chr19:12996616	0.15
rs74002504	chr2:241828338	1.27E-13	cg07537917	chr2:241836409	0.41
rs909832	chr1:25754025	1.33E-13	cg24991732	chr1:25594486	0.27
rs2637647	chr10:133954267	1.35E-13	cg02162534	chr10:133956875	0.71
rs10271372	chr7:157793023	1.35E-13	cg12440927	chr7:157791721	0.27
rs7765960	chr6:13958385	1.43E-13	cg24233211	chr6:14002749	0.23
rs143349430	chr10:32183019	1.58E-13	cg04359828	chr10:32216031	0.1
rs6946377	chr7:64324352	1.62E-13	cg16681239	chr7:64349915	0.16
rs13084718	chr3:13610039	1.81E-13	cg02146340	chr3:13610059	0.18

rs2376584	chr17:76402116	2.10E-13	cg02836325	chr17:76403955	0.12
rs4557742	chr8:145508113	2.15E-13	cg15151778	chr8:145502134	0.21
rs571780	chr9:136001763	2.60E-13	cg13753488	chr9:136001623	0.83
rs699664	chr2:85780536	2.61E-13	cg02493740	chr2:85810744	0.36
rs9998888	chr4:824575	2.70E-13	cg24793722	chr4:824416	0.86
rs4807546	chr19:4182060	2.74E-13	cg18542377	chr19:4172961	0.27
rs4334037	chr11:69256482	2.91E-13	cg23478547	chr11:69259265	0.09
rs2800973	chr22:19168616	3.10E-13	cg24911827	chr22:19170109	0.51
rs9861843	chr3:54159358	3.11E-13	cg12173409	chr3:54154746	0.55
rs6027929	chr20:59535741	3.48E-13	cg19181528	chr20:59542589	0.16
rs11251278	chr10:2544043	3.58E-13	cg05625103	chr10:2543513	0.28
rs2993317	chr13:113687143	3.64E-13	cg07204236	chr13:113705910	0.66

Supplementary Table 8. Methylation QTLs (mQTL) identified in the cerebellum for SNPs included in the schizophrenia polygenic risk score (PRS). Shown are associations between DNA methylation at specific Illumina 450K probes and genetic variants used to derive PRS in Chapter 4, in addition to the corresponding *P*-values for PRS-associated DNA methylation variation at the same probe.

SNP	SNP genomic location (hg19)	mQTL <i>P</i>	CpG	CpG genomic location (hg19)	EWAS <i>P</i>
rs12635522	chr3:125708174	2.67E-45	cg02807482	chr3:125708958	0.53
rs12635522	chr3:125708174	1.67E-42	cg15145296	chr3:125709740	0.61
rs2141182	chr12:131401591	1.06E-41	cg07816006	chr12:131401305	0.99
rs9726753	chr1:153591652	2.20E-41	cg08477332	chr1:153590243	0.08
rs12635522	chr3:125708174	9.50E-41	cg06494592	chr3:125709126	0.59
rs10205909	chr2:3526603	2.28E-36	cg21240684	chr2:3526841	0.48
rs557873	chr9:135336912	2.36E-36	cg21190742	chr9:135336993	0.34
rs2141182	chr12:131401591	4.21E-35	cg10021924	chr12:131401275	0.92
rs7803698	chr7:64427895	4.72E-35	cg24247132	chr7:64458642	0.23
rs12635522	chr3:125708174	1.80E-34	cg04553112	chr3:125709451	0.28
rs4789846	chr17:80225545	8.17E-34	cg02744699	chr17:80197898	0.37
rs117194038	chr17:43927290	1.67E-33	cg22968622	chr17:43663579	0.52
rs6680259	chr1:7122308	3.31E-33	cg20409752	chr1:7122726	0.03
rs4807546	chr19:4182060	2.72E-31	cg01287132	chr19:4173254	0.74
rs35059736	chr7:158224692	6.83E-31	cg01191920	chr7:158217561	0.76
rs1726866	chr7:141672705	3.11E-30	cg19476643	chr7:141672455	0.8
rs11712066	chr3:151830309	8.01E-30	cg27098685	chr3:151867537	0.31
rs10857676	chr10:134970598	1.21E-29	cg00753039	chr10:134969141	0.55
rs4792919	chr17:41873309	4.15E-29	cg26893861	chr17:41843967	0.99
rs3214023	chr12:53682986	5.41E-29	cg04065151	chr12:53682969	0.88
rs2800973	chr22:19168616	8.83E-29	cg02655711	chr22:19163373	0.51
rs2412322	chr17:48578726	9.29E-29	cg00901687	chr17:48585270	0.01
rs117194038	chr17:43927290	5.51E-28	cg10094238	chr17:43483251	0.78
rs4807546	chr19:4182060	9.43E-28	cg23999422	chr19:4173466	0.48
rs76344840	chr9:33120204	1.29E-27	cg20290983	chr6:43655470	0.08
rs10793287	chr11:77846706	9.62E-27	cg09721595	chr11:77773924	0.67
rs13065	chr14:100996312	1.23E-26	cg18516195	chr14:101012996	0.15
rs6968990	chr7:32552159	3.17E-26	cg06133097	chr7:32552212	0.12
rs4807546	chr19:4182060	5.63E-26	cg07492962	chr19:4173315	0.96
rs117194038	chr17:43927290	5.91E-26	cg27244773	chr17:43483116	0.68
rs4789846	chr17:80225545	4.83E-25	cg22805688	chr17:80197841	0.19
rs12507178	chr4:86920281	5.94E-25	cg13324779	chr4:86923558	0.89
rs650241	chr11:75277757	1.13E-24	cg26104986	chr11:75275303	0.16
rs62185165	chr2:241251453	1.81E-24	cg21947394	chr2:241260110	0.19

rs13226756	chr7:149015681	2.87E-24	cg07762347	chr7:149016554	0.42
rs2553022	chr7:100401862	3.03E-24	cg12616177	chr7:100434510	0.91
rs1341741	chr10:888073	3.40E-24	cg26597838	chr10:835615	0.4
rs16961809	chr19:29226299	3.48E-24	cg14983838	chr19:29218262	0.04
rs2468300	chr12:84901620	3.71E-24	cg09278098	chr12:84902512	0.46
rs4984688	chr16:785717	5.25E-24	cg18653534	chr16:772142	0.28
rs2800973	chr22:19168616	5.97E-24	cg24911827	chr22:19170109	0.23
rs12099513	chr12:5267322	1.98E-23	cg01414572	chr12:5248588	0.67
rs16961809	chr19:29226299	6.17E-23	cg12756686	chr19:29218302	0.11
rs2568198	chr2:85403546	8.69E-23	cg22128724	chr2:85402928	0.2
rs2342082	chr12:123090380	1.11E-22	cg23029597	chr12:123009494	0.66
rs164080	chr5:141391532	1.24E-22	cg25940447	chr5:141391533	0.04
rs28452050	chr16:29317318	1.31E-22	cg05645661	chr16:29329490	0.38
rs400132	chr1:2141866	2.46E-22	cg24578937	chr1:2090814	0.95
rs9812936	chr3:50043654	2.71E-22	cg05623727	chr3:50126028	0.54
rs2412322	chr17:48578726	3.26E-22	cg11440486	chr17:48585216	0.03
rs930526	chr17:6473353	3.49E-22	cg23551722	chr17:6546898	0.7
rs60668498	chr19:44642672	3.60E-22	cg23489630	chr19:44645078	0.38
rs62154034	chr2:101953138	4.28E-22	cg23685994	chr2:101959022	0.75
rs9921300	chr16:5641315	7.95E-22	cg03979510	chr16:5641033	0.59
rs8053397	chr16:87573468	9.76E-22	cg08031982	chr16:87577539	0.79
rs1345145	chr8:102144280	2.66E-21	cg13263591	chr8:102142199	0.02
rs16965349	chr17:36614524	2.88E-21	cg12050358	chr17:36612909	0.8
rs7496866	chr15:27102200	3.36E-21	cg10318222	chr15:27111940	0.04
rs1285820	chr14:91840017	4.02E-21	cg10511902	chr14:91842949	0.19
rs3760312	chr17:13970282	1.02E-20	cg27005118	chr17:13972210	0.82
rs2620032	chr17:71745091	1.25E-20	cg24457076	chr17:71744550	0.52
rs4807546	chr19:4182060	1.89E-20	cg09617135	chr19:4173482	0.53
rs8053397	chr16:87573468	2.18E-20	cg03020503	chr16:87577655	0.38
rs12672284	chr7:32825576	2.92E-20	cg11105292	chr7:32802564	0.26
rs2269481	chr4:2386139	2.94E-20	cg11208915	chr4:2401758	0.47
rs4729915	chr7:103081125	3.42E-20	cg21537297	chr8:144298583	0.03
rs7833924	chr8:144996029	3.44E-20	cg06045337	chr8:145013910	0.47
rs11738251	chr5:177819313	3.72E-20	cg00986130	chr5:177821799	0.79
rs4789846	chr17:80225545	4.40E-20	cg21034531	chr17:80197757	0.89
rs1780033	chr1:118339119	5.46E-20	cg01778345	chr1:118427435	0.99
rs4264326	chr14:105411700	6.84E-20	cg21017887	chr14:105400489	0
rs11146990	chr12:133027749	7.52E-20	cg15402627	chr12:133021489	0.58
rs75934331	chr1:183182029	9.41E-20	cg01417625	chr1:183187433	0.75
rs9769809	chr7:64956889	1.20E-19	cg24247132	chr7:64458642	0.23
rs4737	chr16:75238103	1.23E-19	cg06389950	chr16:75240536	0.37
rs1888502	chr21:41545747	1.41E-19	cg10828127	chr21:41550814	0.67
rs74002504	chr2:241828338	1.85E-19	cg07537917	chr2:241836409	0.35
rs1881191	chr2:236607924	2.76E-19	cg24888581	chr2:236616026	0.47
rs117194038	chr17:43927290	3.41E-19	cg17117718	chr17:43663208	0.76
rs6676743	chr1:110296338	3.47E-19	cg10807101	chr1:110282274	0.33
rs16961809	chr19:29226299	4.01E-19	cg03161606	chr19:29218774	0.02
rs6982268	chr8:12994642	4.62E-19	cg03231596	chr8:12987546	0.45
rs2447027	chr10:14003363	4.69E-19	cg27572370	chr10:14002394	0.45
rs2645673	chr4:77816229	4.95E-19	cg21917090	chr4:77816250	0.22
rs9933817	chr16:83972660	5.08E-19	cg16528738	chr16:83968260	0.85
rs17385407	chr1:160473286	5.46E-19	cg22696814	chr1:160398070	0.05
rs117194038	chr17:43927290	5.58E-19	cg14260695	chr17:43506184	0.54
rs7496866	chr15:27102200	9.61E-19	cg01378667	chr15:27111911	0.07
rs77841981	chr7:5231658	9.82E-19	cg07508942	chr7:5267994	0.96
rs3861297	chr18:75380032	1.05E-18	cg11874321	chr18:75380364	0.45
rs11248093	chr4:2276047	1.20E-18	cg19771469	chr4:2275994	0.07
rs144716806	chr4:38854783	1.31E-18	cg26681822	chr4:38858561	0.98
rs4314559	chr7:2365892	1.32E-18	cg16553052	chr7:2349605	0.19
rs7470605	chr9:136890107	1.51E-18	cg13789015	chr9:136890014	0.09
rs11146990	chr12:133027749	1.92E-18	cg11090202	chr12:133021713	0.96
rs4689604	chr4:7129556	2.21E-18	cg16307866	chr4:7129517	0.94

rs881347	chr10:134000130	2.66E-18	cg10144198	chr10:134001728	0.43
rs12595938	chr16:8958081	3.12E-18	cg08308162	chr16:8889244	0.45
rs1341741	chr10:888073	3.31E-18	cg20503657	chr10:835505	0.49
rs274692	chr5:6734625	3.32E-18	cg10857441	chr5:6722123	0.16
rs75231006	chr14:102987539	3.89E-18	cg23712530	chr14:102964522	0.07
rs7807840	chr7:35834025	4.20E-18	cg11531232	chr7:35808197	0.16
rs77841981	chr7:5231658	4.76E-18	cg12631105	chr7:5267896	0.96
rs77617940	chr20:61814968	5.27E-18	cg17237881	chr20:61867533	0.59
rs2276947	chr4:8233943	5.40E-18	cg25777912	chr4:8233394	0.45
rs11248093	chr4:2276047	5.63E-18	cg22029856	chr4:2276003	0.24
rs13147452	chr4:1078124	6.30E-18	cg13468214	chr4:1046988	0.93
rs11688491	chr2:98167020	8.16E-18	cg26665480	chr2:98280029	0.92
rs7710436	chr5:54056541	1.12E-17	cg06536806	chr5:54081633	0.2
rs73494059	chr7:154468109	1.21E-17	cg15618646	chr7:154473202	0.64
rs9390343	chr6:146010527	1.21E-17	cg25629118	chr6:146113270	0.5
rs117194038	chr17:43927290	2.21E-17	cg12609785	chr17:43660871	0.51
rs35037013	chr10:54656418	2.36E-17	cg05984115	chr10:54631212	0.47
rs11633474	chr15:22939192	2.46E-17	cg26344513	chr15:22930613	0.58
rs8082590	chr17:17958402	2.56E-17	cg04398451	chr17:18023971	0.27
rs11995562	chr8:1427444	2.72E-17	cg16582891	chr8:1430303	0.09
rs964757	chr2:183114225	3.16E-17	cg17054006	chr2:183107046	0.38
rs56340588	chr7:127799341	4.36E-17	cg02301128	chr7:127792165	0.25
rs62285061	chr4:1688981	4.82E-17	cg05026014	chr4:1749153	0.19
rs6946060	chr7:157644761	5.48E-17	cg24524099	chr7:157643007	0.87
rs74002504	chr2:241828338	5.49E-17	cg01588581	chr2:241832900	0.34
rs887687	chr7:44185805	6.62E-17	cg18628255	chr7:44152333	0.32
rs2666873	chr8:55090128	6.67E-17	cg20636351	chr8:55087400	0.31
rs6503422	chr17:43163851	7.09E-17	cg25538415	chr17:43129957	0.5
rs77841981	chr7:5231658	9.84E-17	cg16035714	chr7:5267749	0.91
rs73494059	chr7:154468109	1.68E-16	cg23463533	chr7:154473289	0.9
rs55674909	chr15:31525516	1.97E-16	cg03330558	chr15:31516127	0.3
rs11123564	chr2:3683615	2.10E-16	cg14926093	chr2:3680421	0.55
rs113661747	chr14:75894945	2.26E-16	cg22143352	chr14:75897841	0.26
rs3861297	chr18:75380032	2.34E-16	cg27582240	chr18:75380514	0.76
rs10271372	chr7:157793023	2.57E-16	cg12440927	chr7:157791721	0.64
rs2978902	chr8:6690173	2.71E-16	cg11878365	chr8:6692387	1
rs7455225	chr7:73241386	2.93E-16	cg02874145	chr7:73246406	0.36
rs6968990	chr7:32552159	3.63E-16	cg06627557	chr7:32535165	0.01
rs6514834	chr20:18010631	3.71E-16	cg02912291	chr20:17944845	0.8
rs4959982	chr6:4464320	3.75E-16	cg12916580	chr6:4403020	0.35
rs454759	chr12:125799159	4.45E-16	cg03923277	chr12:104359732	0.43
rs55674909	chr15:31525516	4.89E-16	cg12689679	chr15:31516316	0.9
rs890393	chr18:74102435	5.18E-16	cg24786174	chr18:74118243	0.35
rs34228916	chr12:115942842	5.22E-16	cg18639984	chr12:115943877	0.46
rs1476835	chr4:17665456	5.29E-16	cg04450456	chr4:17643702	0.36
rs2244746	chr15:43695083	5.85E-16	cg05490132	chr15:43661835	0.12
rs4689604	chr4:7129556	6.23E-16	cg13998369	chr4:7129440	0.89
rs12342201	chr9:95894964	6.61E-16	cg13713821	chr9:95899302	0.05
rs13147452	chr4:1078124	6.95E-16	cg09755784	chr4:1047097	0.49
rs6946060	chr7:157644761	7.11E-16	cg22216157	chr7:157643037	0.81
rs11675057	chr2:26399481	7.13E-16	cg22920501	chr2:26401640	0.85
rs1058167	chr22:42538029	7.55E-16	cg11915388	chr22:42470451	0
rs77841981	chr7:5231658	8.64E-16	cg01000248	chr7:5267360	0.77
rs13008444	chr2:36909816	9.00E-16	cg21931986	chr2:36922916	0.16
rs7018316	chr8:144630169	9.41E-16	cg16976870	chr8:144631524	0.73
rs13147452	chr4:1078124	1.02E-15	cg01815783	chr4:1047043	0.84
rs6711715	chr2:130330516	1.03E-15	cg05903289	chr2:130345205	0.67
rs7018316	chr8:144630169	1.14E-15	cg18649319	chr8:144631768	0.68
rs12129745	chr1:28572317	1.26E-15	cg04993605	chr1:28573052	0.73
rs7514450	chr1:220991171	1.38E-15	cg15450098	chr1:221057561	0.04
rs34474195	chr1:3178582	1.41E-15	cg26520908	chr1:3191876	0.64
rs2968475	chr16:88976663	1.45E-15	cg08484992	chr16:88977278	0.88

rs74002504	chr2:241828338	1.53E-15	cg04034577	chr2:241836375	0.84
rs74002504	chr2:241828338	1.53E-15	cg21187597	chr2:241846305	0.71
rs9912302	chr17:44916982	1.62E-15	cg25836567	chr17:44929689	0.54
rs13147452	chr4:1078124	1.71E-15	cg10407489	chr4:1043616	0.83
rs8116218	chr20:44496330	1.80E-15	cg04807470	chr20:44452801	0
rs1919784	chr7:33105268	2.04E-15	cg22798885	chr7:33102694	0.62
rs7730045	chr5:56077993	2.17E-15	cg20203395	chr5:56204925	0.44
rs7376288	chr4:741742	2.18E-15	cg14024328	chr4:719362	0.21
rs3793202	chr7:6207142	2.40E-15	cg22849526	chr7:6199437	0.62
rs7833924	chr8:144996029	2.52E-15	cg27082292	chr8:145001361	0.31
rs72713299	chr15:34034124	2.85E-15	cg16888559	chr15:34031029	0.09
rs56303414	chr16:67466435	3.04E-15	cg25341653	chr16:67233277	0.54
rs3021270	chr22:40396409	3.14E-15	cg21771250	chr22:40406049	0.83
rs2270115	chr17:9804724	3.29E-15	cg26853458	chr17:9805074	0.17
rs3093182	chr19:15994924	3.49E-15	cg26851661	chr19:16045708	0.73
rs7730045	chr5:56077993	3.53E-15	cg18230493	chr5:56204884	0.48
rs2857851	chr4:3043512	4.44E-15	cg14003022	chr4:3043019	1
rs62285061	chr4:1688981	5.82E-15	cg08488569	chr4:1749241	0.44
rs137934836	chr17:16312563	6.28E-15	cg08466034	chr17:16318930	0.92
rs72755098	chr15:64427587	6.84E-15	cg02848875	chr15:64387786	0.32
rs7549293	chr1:205312280	7.42E-15	cg00407231	chr1:205312199	0.67
rs732215	chr7:50544063	8.49E-15	cg00647317	chr7:50633725	0.12
rs9902733	chr17:7271219	8.50E-15	cg25737411	chr17:7286288	0.36
rs1350543	chr4:56014389	8.63E-15	cg09978860	chr4:56023921	0.86
rs72634702	chr1:3661182	8.84E-15	cg19903298	chr1:3659644	0.84
rs557888	chr11:94258480	9.91E-15	cg20289045	chr11:94270260	0.93
rs557934	chr1:182548607	1.01E-14	cg27563952	chr1:182557982	0.22
rs10079713	chr5:28692468	1.09E-14	cg07881623	chr6:80731107	0.38
rs8116218	chr20:44496330	1.14E-14	cg12112556	chr20:44455373	0
rs2221903	chr4:123538912	1.17E-14	cg10583651	chr4:123538969	0.71
rs117194038	chr17:43927290	1.18E-14	cg05485769	chr17:44820573	0.93
rs256881	chr5:16572798	1.20E-14	cg24531590	chr5:16559541	0.57
rs117194038	chr17:43927290	1.28E-14	cg10780632	chr17:43973522	0.67
rs55674909	chr15:31525516	1.32E-14	cg19666541	chr15:31516111	0.5
rs6518257	chr21:47210107	1.37E-14	cg18931629	chr21:47287357	0.45
rs4915215	chr1:201077212	1.44E-14	cg22815214	chr1:201083145	0.29
rs9615062	chr22:45602573	1.46E-14	cg20078807	chr22:45608713	0.3
rs9881242	chr3:134032225	1.46E-14	cg26387619	chr3:134032421	0.21
rs13147452	chr4:1078124	1.52E-14	cg27284194	chr4:1044797	0.75
rs16961809	chr19:29226299	1.61E-14	cg25267487	chr19:29217858	0.03
rs7455225	chr7:73241386	1.62E-14	cg17787108	chr7:73246044	0.46
rs6504120	chr17:60830725	1.67E-14	cg23831897	chr17:60827363	0.15
rs62444320	chr7:5111830	1.70E-14	cg02215787	chr7:5107766	0.45
rs4557742	chr8:145508113	1.71E-14	cg15151778	chr8:145502134	0.13
rs571780	chr9:136001763	1.91E-14	cg13753488	chr9:136001623	0.85
rs9826313	chr3:57943818	1.93E-14	cg07735586	chr3:57945651	0.18
rs2062480	chr1:197905400	1.96E-14	cg00114966	chr1:197893920	0.09
rs2872542	chr20:61664872	2.22E-14	cg16240275	chr20:61666158	0.86
rs7539178	chr1:65383002	2.27E-14	cg09765463	chr1:65393430	0.43
rs28676999	chr15:40569884	2.33E-14	cg19335742	chr15:40566880	0.43
rs2637657	chr10:133993806	2.35E-14	cg18037376	chr10:134004552	0.82
rs111543213	chr19:37642385	2.43E-14	cg08835041	chr19:37461278	0.55
rs11230570	chr11:60782634	2.49E-14	cg27098804	chr11:60776124	0.28
rs117194038	chr17:43927290	2.52E-14	cg01341218	chr17:43662625	0.08
rs13724	chr8:142221032	2.64E-14	cg17525220	chr8:142204116	0.81
rs1554948	chr17:7286326	2.72E-14	cg18632631	chr17:7284049	0.18
rs903759	chr2:241078945	2.81E-14	cg03314473	chr2:241083794	0.39
rs3907645	chr4:7338501	2.97E-14	cg19931925	chr4:7338730	0.72
rs62014776	chr16:1339750	3.05E-14	cg03705235	chr16:1371463	0.94
rs8053397	chr16:87573468	3.13E-14	cg16596957	chr16:87575150	0.91
rs1554948	chr17:7286326	3.19E-14	cg25737411	chr17:7286288	0.36
rs9627788	chr22:50300438	3.58E-14	cg15880211	chr22:50250494	0.55

rs12761857	chr10:7105868	3.74E-14	cg00998146	chr19:18284560	0.43
rs2159397	chr17:14486205	3.93E-14	cg17334453	chr17:14479244	0.02
rs1055150	chr19:18499784	4.00E-14	cg21088460	chr19:18499786	0.25
rs67327962	chr16:89366932	4.06E-14	cg27251473	chr16:89359053	0.4
rs11136381	chr8:1273538	4.41E-14	cg24513387	chr8:1273604	0.16
rs7252903	chr19:16075619	4.61E-14	cg26851661	chr19:16045708	0.73
rs9817966	chr3:46650540	4.72E-14	cg24524379	chr3:46600244	0.09
rs1996370	chr11:35546199	4.84E-14	cg14642338	chr11:35547903	0.81
rs2297776	chr9:34372931	5.03E-14	cg14096074	chr9:34255149	0.82
rs7702622	chr5:122548721	5.23E-14	cg04547002	chr5:122551801	0.63
rs2367209	chr3:160398885	6.09E-14	cg03789276	chr3:160170225	0.03
rs73494059	chr7:154468109	6.11E-14	cg11537355	chr7:154473324	0.38
rs7920264	chr10:134046083	6.53E-14	cg05225883	chr10:134043755	0.55
rs12608939	chr19:3652680	6.99E-14	cg10996109	chr19:3637309	0.24
rs340111	chr5:178773203	7.06E-14	cg27054655	chr5:178772969	0.35
rs10773762	chr12:130765366	7.10E-14	cg14604444	chr12:130766091	0.29
rs117194038	chr17:43927290	7.28E-14	cg08318660	chr17:44122580	0.64
rs2665971	chr17:74010038	7.35E-14	cg00498401	chr17:74024829	0.23
rs9615062	chr22:45602573	7.41E-14	cg02541592	chr22:45608686	0.09
rs6959895	chr7:142434960	7.66E-14	cg02329916	chr7:142457299	0.71
rs2290769	chr17:73826406	9.20E-14	cg06407111	chr17:73872650	0.63
rs71559409	chr7:101006835	9.39E-14	cg15127702	chr7:101079617	0.41
rs2475509	chr6:39890217	9.54E-14	cg10871120	chr6:39891273	0.03
rs11738251	chr5:177819313	1.02E-13	cg06730250	chr5:177821870	0.57
rs1557026	chr1:228383367	1.12E-13	cg24846680	chr1:228362309	0.43
rs56303414	chr16:67466435	1.15E-13	cg19514469	chr16:67233432	0.36
rs1072231	chr2:118634348	1.17E-13	cg24461052	chr2:118607738	0.89
rs12473344	chr2:106959895	1.18E-13	cg24419520	chr2:106959257	0.55
rs7730045	chr5:56077993	1.19E-13	cg24531977	chr5:56204891	0.84
rs7305397	chr12:42850058	1.20E-13	cg19980929	chr12:42632907	0.89
rs9365604	chr6:164171914	1.20E-13	cg18405330	chr6:164171960	0.53
rs2317947	chr1:55431003	1.25E-13	cg15129052	chr1:55416755	0.62
rs342778	chr13:53185730	1.25E-13	cg05335186	chr13:53173507	0.31
rs13268456	chr8:28473911	1.29E-13	cg23665710	chr8:28476677	0.97
rs66964681	chr2:242915902	1.42E-13	cg23069297	chr2:242833648	0.81
rs7803698	chr7:64427895	1.43E-13	cg12143784	chr7:64541923	0.63
rs36062268	chr9:27585697	1.45E-13	cg14297867	chr9:27526172	0.39
rs11149799	chr16:75174049	1.48E-13	cg00897404	chr16:75182368	0.53
rs1957841	chr14:89588834	1.61E-13	cg09271279	chr14:89588740	0.38
rs135572	chr22:46527242	1.64E-13	cg00004775	chr22:46516503	0.32
rs7514450	chr1:220991171	1.67E-13	cg26440142	chr1:221057573	0.21
rs12976309	chr19:3864966	1.75E-13	cg22553301	chr19:3839231	0.66
rs7018316	chr8:144630169	1.76E-13	cg10438391	chr8:144631915	0.79
rs61821477	chr1:159383337	1.77E-13	cg25076881	chr1:159409836	0.41
rs73210894	chr8:20019512	1.84E-13	cg09628359	chr8:20039283	0.75
rs12433009	chr14:104196405	1.86E-13	cg01849466	chr14:104193079	0.02
rs6754331	chr2:236441590	1.98E-13	cg00059854	chr2:236443857	0.76
rs2816607	chr14:105718385	2.25E-13	cg10792982	chr14:105748885	0.32
rs2246207	chr17:61987576	2.30E-13	cg06873352	chr17:61820015	0.76
rs12291981	chr11:681502	2.34E-13	cg00115288	chr11:705892	0.51
rs6711715	chr2:130330516	2.38E-13	cg05962382	chr2:130345044	0.91
rs1474256	chr15:79463847	2.39E-13	cg17916960	chr15:79447300	0.52
rs11230570	chr11:60782634	2.43E-13	cg04046629	chr11:60775831	0.7
rs4793213	chr17:41307101	2.48E-13	cg23758822	chr17:41437982	0.19
rs1939686	chr11:115785356	2.57E-13	cg26145504	chr11:115801162	0.09
rs73036509	chr12:6165814	2.58E-13	cg04053108	chr12:6166028	0.02
rs939421	chr3:46576081	2.91E-13	cg24524379	chr3:46600244	0.09
rs1267813	chr11:133981075	2.94E-13	cg20138604	chr11:134023651	0.9
rs11871657	chr17:49714763	3.15E-13	cg05229989	chr17:49724713	0.95
rs11610602	chr12:8070815	3.31E-13	cg01627669	chr12:8068706	0.42
rs8044407	chr16:29154849	3.33E-13	cg07505478	chr16:29193318	0.87
rs58474699	chr17:79257728	3.53E-13	cg03823431	chr17:79229385	0.82

Supplementary Table 9. Overlap of probes assigned to each pair of schizophrenia cases and non-psychiatric controls modules.
 Shown is the number of overlapping probes between each pair of cases and controls modules presented in **Chapter 5 section 5.5.1.1**.

Schizophrenia network ->

	1	2	3	4	5	6	7	8	9	10	11	12	13	14	15	16	17	18	19	20	21	22	23	24	25	26	27	28	29	30	31	32	33	34	35	36	37	38	39	40	41	42	43	44	45	46	47	48	49	50	51	52	53	54
1	29178	1641	3347	1985	1391	708	366	392	982	959	499	359	391	222	145	679	428	335	469	176	346	431	122	105	161	267	94	123	84	114	202	42	49	61	104	74	179	82	108	77	22	86	54	53	25	36	75	20	16	20	7	11	15	
2	3193	514	623	689	339	145	80	98	178	122	135	61	95	60	45	199	75	58	88	59	40	64	19	23	32	52	24	26	42	29	36	12	14	36	31	41	28	18	20	15	12	17	11	19	8	6	10	4	5	11	2	4	9	7
3	1072	3538	577	108	117	188	86	160	71	51	40	24	46	460	23	20	38	36	13	23	11	17	133	36	18	10	124	13	21	15	10	28	68	66	12	14	11	9	5	8	55	6	8	9	4	3	2	3	1	1	3	2	1	
4	1407	1663	721	152	176	202	92	206	99	107	56	43	77	262	50	36	60	37	32	29	24	34	132	65	36	19	139	34	12	33	35	26	53	17	20	21	19	14	9	13	20	8	16	7	7	11	5	3	4	2	12	6	3	2
5	1527	258	411	111	161	138	148	118	96	65	119	130	159	25	290	76	43	64	63	98	33	20	21	35	34	21	11	28	95	31	28	8	11	8	21	11	7	22	11	15	12	6	16	13	9	52	3	9	7	5	6	9	8	4
6	2282	366	666	131	188	148	88	144	172	127	56	78	93	52	51	50	64	83	70	44	80	35	34	30	32	39	17	22	11	38	27	10	12	17	20	14	27	23	24	11	5	19	10	17	10	6	4	4	7	4	0	0	1	
7	2562	379	553	329	275	133	75	68	168	116	85	51	91	42	33	57	62	62	95	58	31	45	32	14	36	41	21	19	16	33	21	9	14	16	17	11	25	17	29	8	6	19	12	18	12	4	8	2	4	6	1	2	11	
8	1468	804	455	107	117	196	155	124	105	62	57	39	52	90	64	35	63	54	54	47	26	28	24	32	19	14	19	19	14	26	19	19	29	171	12	18	8	14	12	11	15	14	11	4	6	4	5	6	3	2	5	1	4	
9	1799	162	445	60	112	122	941	109	56	55	48	554	50	21	310	28	41	36	19	29	83	12	11	47	14	16	7	18	15	13	12	15	14	3	9	10	6	15	8	6	0	3	9	7	8	5	4	1	7	3	1	6	2	3
10	1501	258	465	156	172	156	116	96	114	91	64	81	84	40	74	48	47	69	51	47	46	25	18	38	41	16	13	42	17	31	18	16	12	10	26	18	11	32	20	15	9	10	12	10	14	16	4	3	9	2	5	1	2	
11	2202	293	327	293	245	102	67	55	94	100	77	28	54	39	29	70	41	36	58	46	25	46	14	14	35	38	19	17	30	23	17	7	14	5	11	15	11	11	12	13	11	16	17	10	8	4	5	11	1	8	3	1	2	0
12	2137	325	501	171	216	125	65	74	109	94	63	66	59	41	31	67	54	46	49	32	33	42	35	16	27	41	22	20	15	20	21	10	8	14	9	17	15	17	13	16	13	10	11	13	5	2	3	1	8	2	1	3	2	
13	2344	297	476	149	158	128	55	66	125	103	52	38	63	26	26	64	79	63	52	26	41	40	19	13	11	32	17	21	13	15	17	8	17	12	11	7	12	15	8	15	5	8	11	9	16	6	6	8	3	1	1	2	5	1
14	1429	254	480	96	142	153	147	85	141	77	55	70	93	42	56	32	55	66	41	49	42	21	18	42	29	17	13	26	17	25	22	15	9	21	16	13	14	18	12	13	5	12	4	11	8	12	2	3	2	6	4	2	0	4
15	2277	215	332	1088	292	66	39	40	73	60	103	46	53	20	16	78	29	28	58	30	19	32	19	13	18	23	11	10	9	14	18	2	7	10	5	11	14	6	9	6	7	5	8	4	1	4	3	3	5	2	2	6	0	
16	1467	335	482	112	131	152	129	145	112	95	42	98	71	68	87	34	40	51	35	32	27	27	28	16	29	18	21	20	26	11	13	6	17	11	23	14	17	10	5	17	6	8	8	2	5	1	1	2	6	4	1			
17	1683	234	381	229	184	106	73	69	109	80	65	57	77	34	50	49	40	35	64	54	25	30	25	17	23	29	18	21	27	21	28	3	14	12	13	17	11	14	11	14	0	8	5	11	5	13	4	3	2	4	1	3	1	4
18	1914	600	335	139	150	129	88	69	62	109	52	66	37	93	22	31	64	33	32	17	32	28	14	20	14	25	21	13	10	7	11	17	9	9	15	7	16	5	6	6	12	5	3	2	3	2	0	1	2	5	2	0	2	
19	1168	162	386	76	96	115	467	68	81	50	47	201	55	16	190	18	48	34	15	29	55	11	11	43	23	14	11	32	16	8	17	13	6	4	17	8	1	24	12	9	7	12	8	8	16	7	8	3	2	3	9	1	1	

20 1636 161 340 220 183 91 38 83 69 65 75 49 50 24 16 41 40 42 41 19 18 32 18 13 17 29 14 13 17 18 20 6 14 6 9 13 14 10 11 12 5 8 8 8 4 2 4 1 3 2 0 0 1 2
21 719 829 259 48 68 131 60 90 56 34 37 25 36 96 26 14 48 31 14 14 15 9 18 34 7 9 32 13 5 12 6 25 25 12 8 6 1 1 7 2 12 7 7 4 2 6 1 0 0 0 7 2 1
22 1426 167 255 183 172 79 34 25 52 55 67 26 28 24 16 42 25 22 48 17 15 19 14 12 16 15 7 11 13 9 13 3 7 6 9 7 15 10 8 8 2 7 1 7 0 2 2 1 0 3 1 0 5 1
23 1266 154 283 127 139 71 46 38 71 44 37 35 47 14 21 30 26 25 34 23 16 25 13 12 9 23 15 16 10 18 5 10 3 2 8 11 7 10 6 13 4 10 9 10 5 4 7 1 3 3 0 3 2
24 1356 146 317 99 110 76 87 43 60 59 37 77 52 20 32 21 35 21 13 10 20 21 12 11 10 15 13 10 5 15 8 7 4 2 11 6 9 14 3 4 3 7 2 2 5 1 3 3 1 1 0 1 0 2
25 882 143 178 197 185 73 36 136 28 36 90 28 30 24 17 74 24 19 30 36 7 8 8 4 23 15 5 15 21 3 5 12 3 4 10 41 2 2 8 11 3 6 7 7 1 1 18 4 2 3 2 0 8 1
26 1204 113 174 115 113 61 21 63 57 66 38 15 40 21 12 27 23 29 33 30 25 22 6 9 12 16 5 7 19 12 14 2 1 6 11 7 8 5 5 8 1 9 8 5 1 2 1 6 1 3 2 2 1 0
27 760 146 230 52 88 75 84 50 66 29 36 43 48 22 46 18 22 36 17 30 19 6 9 20 16 10 9 10 10 15 3 6 5 4 9 4 5 4 11 6 8 9 5 12 6 1 3 2 4 0 2 2 1
28 880 442 204 58 65 76 32 43 35 32 30 32 30 17 29 26 15 17 17 22 12 11 10 12 10 11 18 13 5 11 7 3 7 11 9 5 5 10 8 7 6 3 5 3 3 1 0 1 0 0 5 2
29 709 153 220 61 89 73 50 73 62 30 31 20 48 17 24 20 24 28 31 21 12 23 6 24 19 8 9 17 10 12 10 8 9 1 8 7 2 4 13 15 1 9 8 8 3 3 5 2 1 1 3 1 1 0
30 1081 129 277 63 64 50 47 35 34 40 26 45 24 17 8 9 19 21 12 10 32 14 12 8 5 17 7 9 2 10 17 5 7 7 2 14 4 4 1 1 8 2 4 2 3 0 0 3 0 0 2 0
31 722 128 237 44 68 64 95 37 38 34 30 66 28 17 36 16 34 30 18 15 45 15 7 22 4 8 7 13 4 8 4 1 3 7 5 7 4 8 4 5 0 7 9 6 1 7 0 4 4 5 1 2 0 1
32 444 952 202 41 37 41 17 32 31 10 17 10 23 90 8 14 10 12 17 6 8 10 35 6 5 3 29 4 4 5 6 2 10 25 3 2 10 1 0 5 31 2 2 10 0 0 1 4 0 0 1 0 1 0
33 833 117 178 47 73 46 35 36 50 45 25 33 13 16 23 18 22 25 20 26 14 7 15 10 16 7 13 6 7 7 2 6 6 5 3 6 13 5 6 0 11 0 3 2 7 3 2 7 1 3 0 1 1
34 622 328 218 41 50 51 40 45 34 33 20 24 29 58 12 16 21 23 14 11 16 10 23 7 7 11 24 8 5 9 9 10 9 13 5 3 4 4 4 4 5 3 6 5 0 2 1 1 0 2 2 2 1 0
35 842 98 181 54 68 56 19 34 38 30 23 8 27 11 12 22 17 19 14 21 15 7 5 4 10 2 14 2 6 9 5 4 5 5 5 10 6 8 4 0 6 1 3 0 2 2 1 3 5 0 0 0 1
36 790 118 161 57 64 51 21 61 47 35 19 15 32 16 11 16 25 25 17 6 15 14 4 11 9 8 9 4 9 9 3 3 3 5 4 5 3 6 6 4 1 6 4 1 1 2 4 7 2 1 0 4 1 2
37 574 212 169 26 50 59 26 32 15 19 25 16 13 18 7 8 46 16 5 7 23 11 2 6 4 5 7 11 3 5 3 40 5 3 4 3 7 5 1 2 2 0 2 3 1 2 1 3 0 1 1 1 0 0
38 454 117 134 43 47 49 45 30 48 21 14 19 31 17 19 10 11 21 16 19 9 6 7 9 4 10 1 14 3 14 8 3 4 6 4 0 4 10 4 1 8 2 5 3 3 0 0 1 2 1 4 1 2
39 482 80 155 21 40 40 52 28 24 23 11 41 21 12 44 11 15 31 13 8 22 7 8 8 9 7 2 11 5 8 4 3 5 1 3 4 9 6 5 5 1 3 3 7 3 5 0 0 0 1 1 0 1 0
40 555 50 138 30 52 32 36 23 16 27 17 35 11 8 10 8 13 19 11 3 22 9 4 8 5 6 3 7 6 7 9 3 0 1 8 3 1 1 1 0 1 3 1 1 1 0 5 1 1 2 0 0 2 2
41 280 62 66 13 26 25 72 16 35 11 24 58 31 9 90 7 6 11 14 17 6 3 3 21 1 5 1 7 9 3 3 1 5 0 2 3 5 1 1 0 4 3 4 2 1 8 1 1 4 1 3 4 1 0
42 398 52 92 28 37 36 36 24 29 19 13 26 17 5 9 14 15 12 10 10 7 4 7 9 6 3 8 4 8 6 0 2 2 4 1 6 2 4 4 1 3 2 3 2 3 3 0 2 0 0 0 1 1
43 195 478 119 24 25 20 11 24 8 8 4 4 8 38 3 7 12 3 8 2 2 0 48 9 0 3 15 3 0 2 3 3 25 21 2 4 5 0 2 0 5 1 1 2 1 0 0 0 0 1 0 0 1
44 177 144 80 16 18 44 17 47 11 7 12 10 7 11 6 5 14 7 5 2 6 3 3 4 6 1 2 2 2 0 0 111 3 3 1 3 1 3 1 2 3 3 2 4 1 2 1 1 0 1 0 1 0 1
45 288 54 66 22 32 19 10 12 21 15 9 7 12 4 5 4 10 11 5 2 7 1 2 4 7 2 0 3 2 3 4 5 3 2 1 3 4 3 1 2 1 2 3 2 0 2 0 2 1 0 0 0 0 0
46 210 39 52 17 26 18 16 13 20 9 8 6 20 8 5 7 1 9 4 4 0 3 2 6 6 8 1 5 2 11 2 4 3 1 0 4 1 2 5 1 1 5 7 2 1 0 1 1 0 1 1 0 0 0

47 164 29 54 12 18 15 15 35 17 7 12 7 14 2 13 4 5 3 2 6 5 4 2 3 3 2 0 4 1 7 1 0 5 1 4 2 1 1 2 2 1 1 5 0 1 0 0 1 0 0 3 2 0 1
48 173 20 45 13 20 15 11 20 11 12 10 6 7 2 5 12 5 5 10 8 3 2 2 2 11 2 0 1 5 1 2 1 2 0 13 1 2 4 1 2 1 1 0 2 1 2 1 1 0 0 0 1 0
49 168 25 25 11 23 9 5 9 11 6 5 5 6 5 10 6 3 3 5 5 2 3 2 1 6 3 0 4 3 3 2 0 0 0 1 1 2 1 1 4 1 0 0 0 2 0 0 0 0 0 0
50 118 34 24 16 18 11 7 5 6 9 12 3 3 2 7 24 1 1 4 12 1 0 0 1 5 7 1 2 6 1 1 3 0 0 1 1 0 2 1 2 1 1 0 2 2 1 0 1 1 0 0 1 0 0
51 89 23 32 6 17 9 0 12 10 7 6 6 12 2 9 4 7 2 4 9 1 2 1 2 3 1 0 2 6 2 1 1 1 0 0 3 0 2 0 0 1 1 1 1 1 4 0 0 1 2 0 0 0
52 70 2 10 1 14 5 124 3 2 0 1 60 2 0 102 1 0 0 0 0 0 1 0 1 0 0 1 1 0
53 50 185 29 4 8 3 1 9 3 0 0 1 5 17 0 4 1 1 2 1 0 1 9 1 2 0 9 0 5 1 1 0 2 2 2 1 0 1 0 0 39 0 0 0 0 0 0 0 0 0 0 0 1 0
54 41 29 16 3 6 12 6 155 6 7 2 1 3 3 9 2 3 3 3 1 1 1 0 2 1 0 2 3 0 1 0 0 1 2 0 0 1 0 0 0 1 1 0 0 0 0 0 0 0 0 0 0 2 0 0
55 53 51 15 9 15 14 3 17 7 4 13 3 3 8 2 0 8 2 0 3 0 2 1 1 3 0 2 0 0 2 0 11 1 0 0 0 2 1 0 0 0 1 0 1 0 0 1 1 0 0 2 1 1 0
56 129 20 31 8 12 5 5 4 9 5 2 3 2 1 1 3 2 4 1 1 4 4 0 1 1 2 1 0 0 2 1 0 0 2 2 1 0 1 1 0 1 0 0 2 0 0 0 1 1 0 0 0 0
57 48 133 6 5 5 5 6 2 1 0 2 1 15 1 0 2 1 0 1 0 0 5 3 0 0 1 1 0 1 0 2 1 1 0 1 0 0 1 0 1 0 0 0 0 1 0 1 0 0 0 0 1 0
58 85 37 25 18 2 3 2 4 3 5 5 3 4 6 2 2 1 1 6 1 1 3 4 1 1 2 1 0 1 0 2 0 2 2 2 0 1 0 2 0 0 0 0 0 0 0 0 1 0 0 0 0 2
59 23 102 21 10 8 6 6 5 2 0 5 1 1 4 1 1 1 2 1 0 1 0 1 1 2 1 0 0 1 0 1 4 5 1 0 1 1 0 0 0 0 0 0 0 0 0 0 0 0 0 1 1 0 0
60 26 9 7 8 10 3 0 2 3 2 4 0 0 1 1 3 1 1 0 6 1 2 1 0 1 1 0 1 1 0 1 0 1 0
61 36 3 10 1 5 7 7 1 0 3 1 1 1 0 2 0 1 1 4 2 2 0 0 4 1 1 0 0 1 2 0 1
62 41 8 13 2 5 7 3 0 2 1 1 1 3 1 0 1 0 0 1 2 0 0 0 2 0 1 0
63 18 19 3 1 2 4 3 39 2 1 2 2 0 1 1 1 0 0 1 1 1 0 0 0 1 0
64 28 3 13 3 7 6 0 2 3 2 5 3 3 0 0 1 1 1 3 1 0 3 1 0 3 1 0 2 0 0 1 0 2 0 0 0 0 1 1 0 1 2 0 0 0 0 1 0 0 1 0 0 0 0 0
65 33 3 2 0 5 1 4 5 1 1 1 3 1 2 1 1 0 3 1 1 0 1 1 1 1 1 0 2 0
66 25 8 12 1 6 2 0 5 0 1 2 1 1 0 0 1 2 0 1 3 1 2 1 0 0 0 1 0 0 1 1 1 0 0 1 1 0 0 1 1 0 0 1 0 0 0 0 0 0 0 0 0 0 0 0
67 41 4 6 14 8 0 2 1 1 2 3 1 1 0 0 3 1 0 1 1 0 1 0 1 0 1 0 0 0 0 1 2 0 1 0 0 0 0 1 0 0 0 0 0 0 0 0 0 0 0 0 0 0 0
68 23 6 1 0 0 4 7 0 2 1 1 1 0 0 3 3 0 0 1 0 0 0 0 4 0
69 11 32 6 1 2 5 1 5 1 0 0 1 0 4 2 0 1 0 0 0 0 0 3 1 0

Supplementary Table 10. Percentage of probes in each of the non-psychiatric controls modules overlapping with each of the schizophrenia cases modules (1 to 27). Shown is the percentage of overlap between the controls and schizophrenia modules presented in Chapter 5 section 5.5.1.1.

	Schizophrenia network ->																										
	1	2	3	4	5	6	7	8	9	10	11	12	13	14	15	16	17	18	19	20	21	22	23	24	25	26	27
1	50.46	2.84	5.79	3.43	2.41	1.22	0.63	0.68	1.70	1.66	0.86	0.62	0.68	0.38	0.25	1.17	0.74	0.58	0.81	0.30	0.60	0.75	0.21	0.18	0.28	0.46	0.16
2	31.89	5.13	6.22	6.88	3.39	1.45	0.80	0.98	1.78	1.22	1.35	0.61	0.95	0.60	0.45	1.99	0.75	0.58	0.88	0.59	0.40	0.64	0.19	0.23	0.32	0.52	0.24
3	10.94	36.10	5.89	1.10	1.19	1.92	0.88	1.63	0.72	0.52	0.41	0.24	0.47	4.69	0.23	0.20	0.39	0.37	0.13	0.23	0.11	0.17	1.36	0.37	0.18	0.10	1.27
4	15.51	18.33	7.95	1.68	1.94	2.23	1.01	2.27	1.09	1.18	0.62	0.47	0.85	2.89	0.55	0.40	0.66	0.41	0.35	0.32	0.26	0.37	1.46	0.72	0.40	0.21	1.53
5	17.88	3.02	4.81	1.30	1.88	1.62	1.73	1.38	1.12	0.76	1.39	1.52	1.86	0.29	3.39	0.89	0.50	0.75	0.74	1.15	0.39	0.23	0.25	0.41	0.40	0.25	0.13
6	28.08	4.50	8.20	1.61	2.31	1.82	1.08	1.77	2.12	1.56	0.69	0.96	1.14	0.64	0.63	0.62	0.79	1.02	0.86	0.54	0.98	0.43	0.42	0.37	0.39	0.48	0.21
7	31.77	4.70	6.86	4.08	3.41	1.65	0.93	0.84	2.08	1.44	1.05	0.63	1.13	0.52	0.41	0.71	0.77	0.77	1.18	0.72	0.38	0.56	0.40	0.17	0.45	0.51	0.26
8	19.92	10.91	6.17	1.45	1.59	2.66	2.10	1.68	1.42	0.84	0.77	0.53	0.71	1.22	0.87	0.47	0.85	0.73	0.73	0.64	0.35	0.38	0.33	0.43	0.26	0.19	0.26
9	25.57	2.30	6.32	0.85	1.59	1.73	13.37	1.55	0.80	0.78	0.68	7.87	0.71	0.30	4.41	0.40	0.58	0.51	0.27	0.41	1.18	0.17	0.16	0.67	0.20	0.23	0.10
10	21.96	3.77	6.80	2.28	2.52	2.28	1.70	1.40	1.67	1.33	0.94	1.18	1.23	0.59	1.08	0.70	0.69	1.01	0.75	0.69	0.67	0.37	0.26	0.56	0.60	0.23	0.19
11	33.15	4.41	4.92	4.41	3.69	1.54	1.01	0.83	1.42	1.51	1.16	0.42	0.81	0.59	0.44	1.05	0.62	0.54	0.87	0.69	0.38	0.69	0.21	0.21	0.53	0.57	0.29
12	32.71	4.97	7.67	2.62	3.31	1.91	0.99	1.13	1.67	1.44	0.96	1.01	0.90	0.63	0.47	1.03	0.83	0.70	0.75	0.49	0.51	0.64	0.54	0.24	0.41	0.63	0.34
13	35.98	4.56	7.31	2.29	2.43	1.96	0.84	1.01	1.92	1.58	0.80	0.58	0.97	0.40	0.40	0.98	1.21	0.97	0.80	0.40	0.63	0.61	0.29	0.20	0.17	0.49	0.26
14	22.38	3.98	7.52	1.50	2.22	2.40	2.30	1.33	2.21	1.21	0.86	1.10	1.46	0.66	0.88	0.50	0.86	1.03	0.64	0.77	0.66	0.33	0.28	0.66	0.45	0.27	0.20
15	36.24	3.42	5.28	17.32	4.65	1.05	0.62	0.64	1.16	0.95	1.64	0.73	0.84	0.32	0.25	1.24	0.46	0.45	0.92	0.48	0.30	0.51	0.30	0.21	0.29	0.37	0.18
16	24.46	5.59	8.04	1.87	2.18	2.53	2.15	2.42	1.87	1.58	0.70	1.63	1.18	1.13	1.45	0.57	0.67	0.85	0.58	0.53	0.45	0.45	0.45	0.45	0.47	0.27	0.48
17	28.31	3.94	6.41	3.85	3.10	1.78	1.23	1.16	1.83	1.35	1.09	0.96	1.30	0.57	0.84	0.82	0.67	0.59	1.08	0.91	0.42	0.50	0.42	0.29	0.39	0.49	0.30
18	33.32	10.45	5.83	2.42	2.61	2.25	1.53	1.20	1.08	1.90	0.91	1.15	0.64	1.62	0.38	0.54	1.11	0.57	0.56	0.30	0.56	0.49	0.24	0.35	0.24	0.44	0.37

19	5386	21.69	3.01	7.17	1.41	1.78	2.14	8.67	1.26	1.50	0.93	0.87	3.73	1.02	0.30	3.53	0.33	0.89	0.63	0.28	0.54	1.02	0.20	0.20	0.80	0.43	0.26	0.20
20	4969	32.92	3.24	6.84	4.43	3.68	1.83	0.76	1.67	1.39	1.31	1.51	0.99	1.01	0.48	0.32	0.83	0.80	0.85	0.83	0.38	0.36	0.64	0.36	0.26	0.34	0.58	0.28
21	4461	16.12	18.58	5.81	1.08	1.52	2.94	1.34	2.02	1.26	0.76	0.83	0.56	0.81	2.15	0.58	0.31	1.08	0.69	0.31	0.31	0.34	0.20	0.40	0.76	0.16	0.20	0.72
22	3968	35.94	4.21	6.43	4.61	4.33	1.99	0.86	0.63	1.31	1.39	1.69	0.66	0.71	0.60	0.40	1.06	0.63	0.55	1.21	0.43	0.38	0.48	0.35	0.30	0.40	0.38	0.18
23	3960	31.97	3.89	7.15	3.21	3.51	1.79	1.16	0.96	1.79	1.11	0.93	0.88	1.19	0.35	0.53	0.76	0.66	0.63	0.86	0.58	0.40	0.63	0.33	0.30	0.23	0.58	0.38
24	3902	34.75	3.74	8.12	2.54	2.82	1.95	2.23	1.10	1.54	1.51	0.95	1.97	1.33	0.51	0.82	0.54	0.90	0.54	0.33	0.26	0.51	0.54	0.31	0.28	0.26	0.38	0.33
25	3585	24.60	3.99	4.97	5.50	5.16	2.04	1.00	3.79	0.78	1.00	2.51	0.78	0.84	0.67	0.47	2.06	0.67	0.53	0.84	1.00	0.20	0.22	0.22	0.11	0.64	0.42	0.14
26	3451	34.89	3.27	5.04	3.33	3.27	1.77	0.61	1.83	1.65	1.91	1.10	0.43	1.16	0.61	0.35	0.78	0.67	0.84	0.96	0.87	0.72	0.64	0.17	0.26	0.35	0.46	0.14
27	3431	22.15	4.26	6.70	1.52	2.56	2.19	2.45	1.46	1.92	0.85	1.05	1.25	1.40	0.64	1.34	0.52	0.64	1.05	0.50	0.87	0.55	0.17	0.26	0.58	0.47	0.29	0.26
28	3361	26.18	13.15	6.07	1.73	1.93	2.26	0.95	1.28	1.28	1.04	0.95	0.89	0.95	0.89	0.51	0.86	0.77	0.45	0.51	0.51	0.65	0.36	0.33	0.30	0.36	0.30	0.30
29	3230	21.95	4.74	6.81	1.89	2.76	2.26	1.55	2.26	1.92	0.93	0.96	0.62	1.49	0.53	0.74	0.62	0.74	0.87	0.96	0.65	0.37	0.71	0.19	0.74	0.59	0.25	0.28
30	2950	36.64	4.37	9.39	2.14	2.17	1.69	1.59	1.19	1.15	1.36	0.88	1.53	0.81	0.58	0.27	0.31	0.64	0.71	0.41	0.34	1.08	0.47	0.41	0.27	0.17	0.58	0.24
31	2926	24.68	4.37	8.10	1.50	2.32	2.19	3.25	1.26	1.30	1.16	1.03	2.26	0.96	0.58	1.23	0.55	1.16	1.03	0.62	0.51	1.54	0.51	0.24	0.75	0.14	0.27	0.24
32	2839	15.64	33.53	7.12	1.44	1.30	1.44	0.60	1.13	1.09	0.35	0.60	0.35	0.81	3.17	0.28	0.49	0.35	0.42	0.60	0.21	0.28	0.35	1.23	0.21	0.18	0.11	1.02
33	2779	29.97	4.21	6.41	1.69	2.63	1.66	1.26	1.30	1.80	1.62	0.90	1.19	1.19	0.47	0.58	0.83	0.65	0.79	0.90	0.72	0.94	0.50	0.25	0.54	0.36	0.58	0.25
34	2708	22.97	12.11	8.05	1.51	1.85	1.88	1.48	1.66	1.26	1.22	0.74	0.89	1.07	2.14	0.44	0.59	0.78	0.85	0.52	0.41	0.59	0.37	0.85	0.26	0.26	0.41	0.89
35	2428	34.68	4.04	7.45	2.22	2.80	2.31	0.78	1.40	1.57	1.24	0.95	0.33	1.11	0.45	0.49	0.91	0.70	0.70	0.78	0.58	0.86	0.62	0.29	0.21	0.16	0.41	0.08
36	2388	33.08	4.94	6.74	2.39	2.68	2.14	0.88	2.55	1.97	1.47	0.80	0.63	1.34	0.67	0.46	0.67	1.05	1.05	0.71	0.25	0.63	0.59	0.17	0.46	0.38	0.34	0.38
37	2192	26.19	9.67	7.71	1.19	2.28	2.69	1.19	1.46	0.68	0.87	1.14	0.73	0.59	0.82	0.32	0.36	2.10	0.73	0.23	0.32	1.05	0.50	0.09	0.27	0.18	0.23	0.32
38	2099	21.63	5.57	6.38	2.05	2.24	2.33	2.14	1.43	2.29	1.00	0.67	0.91	1.48	0.81	0.91	0.48	0.52	1.00	0.76	0.91	0.43	0.29	0.33	0.43	0.19	0.48	0.05
39	1966	24.52	4.07	7.88	1.07	2.03	2.03	2.64	1.42	1.22	1.17	0.56	2.09	1.07	0.61	2.24	0.56	0.76	1.58	0.66	0.41	1.12	0.36	0.41	0.41	0.46	0.36	0.10
40	1732	32.04	2.89	7.97	1.73	3.00	1.85	2.08	1.33	0.92	1.56	0.98	2.02	0.64	0.46	0.58	0.46	0.75	1.10	0.64	0.17	1.27	0.52	0.23	0.46	0.29	0.35	0.17
41	1646	17.01	3.77	4.01	0.79	1.58	1.52	4.37	0.97	2.13	0.67	1.46	3.52	1.88	0.55	5.47	0.43	0.36	0.67	0.85	1.03	0.36	0.18	0.18	1.28	0.06	0.30	0.06
42	1503	26.48	3.46	6.12	1.86	2.46	2.40	2.40	1.60	1.93	1.26	0.86	1.73	1.13	0.33	0.60	0.93	1.00	0.80	0.67	0.67	0.47	0.27	0.47	0.60	0.40	0.20	
43	1411	13.82	33.88	8.43	1.70	1.77	1.42	0.78	1.70	0.57	0.57	0.28	0.28	0.57	2.69	0.21	0.50	0.85	0.21	0.57	0.14	0.14	0	3.40	0.64	0	0.21	1.06
44	1341	13.20	10.74	5.97	1.19	1.34	3.28	1.27	3.50	0.82	0.52	0.89	0.75	0.52	0.82	0.45	0.37	1.04	0.52	0.37	0.15	0.45	0.22	0.22	0.30	0.45	0.07	0.15
45	1021	28.21	5.29	6.46	2.15	3.13	1.86	0.98	1.18	2.06	1.47	0.88	0.69	1.18	0.39	0.49	0.39	0.98	1.08	0.49	0.20	0.69	0.10	0.20	0.39	0.69	0.20	0
46	906	23.18	4.30	5.74	1.88	2.87	1.99	1.77	1.43	2.21	0.99	0.88	0.66	2.21	0.88	0.55	0.77	0.11	0.99	0.44	0.44	0	0.33	0.22	0.66	0.66	0.88	0.11

47	787	20.84	3.68	6.86	1.52	2.29	1.91	1.91	4.45	2.16	0.89	1.52	0.89	1.78	0.25	1.65	0.51	0.64	0.38	0.25	0.76	0.64	0.51	0.25	0.38	0.38	0.25	0	
48	724	23.90	2.76	6.22	1.80	2.76	2.07	1.52	2.76	1.52	1.66	1.38	0.83	0.83	0.97	0.28	0.69	1.66	0.69	0.69	1.38	1.10	0.41	0.28	0.28	0.28	1.52	0.28	0
49	592	28.38	4.22	4.22	1.86	3.89	1.52	0.84	1.52	1.86	1.01	0.84	0.84	1.01	0.84	1.69	1.01	0.51	0.51	0.84	0.84	0.34	0.51	0.34	0.17	1.01	0.51	0	
50	544	21.69	6.25	4.41	2.94	3.31	2.02	1.29	0.92	1.10	1.65	2.21	0.55	0.55	0.37	1.29	4.41	0.18	0.18	0.74	2.21	0.18	0	0	0.18	0.92	1.29	0.18	
51	524	16.98	4.39	6.11	1.15	3.24	1.72	0	2.29	1.91	1.34	1.15	1.15	2.29	0.38	1.72	0.76	1.34	0.38	0.76	1.72	0.19	0.38	0.19	0.38	0.57	0.19	0	
52	483	14.49	0.41	2.07	0.21	2.90	1.04	25.7	0.62	0.41	0	0.21	12.42	0.41	0	21.12	0.21	0	0	0	0	0	0	0	0.21	0	0.21	0	
53	472	10.59	39.19	6.14	0.85	1.69	0.64	0.21	1.91	0.64	0	0	0.21	1.06	3.60	0	0.85	0.21	0.21	0.42	0.21	0	0.21	1.91	0.21	0.42	0	1.91	
54	469	8.74	6.18	3.41	0.64	1.28	2.56	1.28	33.05	1.28	1.49	0.43	0.21	0.64	0.64	1.92	0.43	0.64	0.64	0.64	0.21	0.21	0	0.43	0.21	0	0.43	0.43	
55	440	12.05	11.59	3.41	2.05	3.41	3.18	0.68	3.86	1.59	0.91	2.95	0.68	0.68	1.82	0.45	0	1.82	0.45	0	0.68	0	0.45	0.23	0.23	0.68	0	0.45	
56	379	34.04	5.28	8.18	2.11	3.17	1.32	1.32	1.06	2.37	1.32	0.53	0.79	0.53	0.26	0.26	0.79	0.53	1.06	0.26	0.26	1.06	1.06	0	0.26	0.26	0.53	0.26	
57	336	14.29	39.58	1.79	1.49	1.49	1.49	1.49	1.79	0.60	0.30	0	0.60	0.30	4.46	0.30	0	0.60	0.30	0	0.30	0	0	1.49	0.89	0	0	0.30	
58	334	25.45	11.08	7.49	5.39	0.60	0.90	0.60	1.20	0.90	1.50	1.50	0.90	1.20	1.80	0.60	0.60	0.30	0.30	1.80	0.30	0.30	0.90	1.20	0.30	0.30	0.60	0.30	
59	291	7.90	35.05	7.22	3.44	2.75	2.06	2.06	1.72	0.69	0	1.72	0.34	0.34	1.37	0.34	0.34	0.34	0.69	0.34	0	0.34	0	0.34	0.34	0.69	0.34	0	
60	170	15.29	5.29	4.12	4.71	5.88	1.76	0	1.18	1.76	1.18	2.35	0	0	0.59	0.59	1.76	0.59	0.59	0	3.53	0.59	1.18	0.59	0	0.59	0.59	0	
61	160	22.50	1.88	6.25	0.63	3.13	4.38	4.38	0.63	0	1.88	0.63	0.63	0.63	0	1.25	0	0.63	0.63	2.50	1.25	1.25	0	0	2.50	0.63	0.63	0	
62	160	25.63	5.00	8.13	1.25	3.13	4.38	1.88	0	1.25	0.63	0.63	0.63	1.88	0.63	0	0.63	0	0	0.63	1.25	0	0	0	1.25	0	0	0	
63	159	11.32	11.95	1.89	0.63	1.26	2.52	1.89	24.53	1.26	0.63	1.26	1.26	0	0.63	0.63	0	0.63	0	0	0.63	0	0	0.63	0	0.63	0	0	
64	144	19.44	2.08	9.03	2.08	4.86	4.17	0	1.39	2.08	1.39	3.47	2.08	2.08	0	0	0.69	0.69	0.69	2.08	0.69	0	2.08	0.69	0	1.39	0	0	
65	125	26.40	2.40	1.60	0	4.00	0.80	3.20	4.00	0.80	0.80	0.80	2.40	0.80	1.60	0.80	0.80	0	2.40	0.80	0.80	0.80	0.80	0.80	0.80	0.80	0.80	0.80	
66	124	20.16	6.45	9.68	0.81	4.84	1.61	0	4.03	0	0.81	1.61	0.81	0.81	0	0	0.81	1.61	0	0.81	2.42	0.81	1.61	0.81	0	0	0	0.81	
67	117	35.04	3.42	5.13	11.97	6.84	0	1.71	0.85	0.85	1.71	2.56	0.85	0.85	0	0	2.56	0.85	0	0.85	0.85	0	0.85	0	0.85	0	0	0	
68	108	21.30	5.56	0.93	0	3.70	6.48	0	0	3.70	6.48	0	1.85	0.93	0.93	0	2.78	2.78	2.78	0	0	0.93	0	0	0	3.70	0	0	
69	108	10.19	29.63	5.56	0.93	1.85	4.63	0.93	4.63	0.93	0	0	0.93	0	3.70	1.85	0	0.93	0	0	0	0	0	0	2.78	0.93	0	0	

Supplementary Table 11. Percentage of probes in each of the non-psychiatric controls modules overlapping with each of the schizophrenia cases modules (28 to 54). Shown is the percentage of overlap between the controls and schizophrenia modules presented in Chapter 5 section 5.5.1.1.

	Total no. probes in control network	Schizophrenia network ->																										
		28	29	30	31	32	33	34	35	36	37	38	39	40	41	42	43	44	45	46	47	48	49	50	51	52	53	54
1	57824	0.21	0.15	0.20	0.35	0.07	0.08	0.11	0.18	0.13	0.31	0.14	0.19	0.13	0.04	0.15	0.09	0.09	0.09	0.04	0.06	0.13	0.03	0.03	0.03	0.01	0.02	0.03
2	10014	0.26	0.42	0.29	0.36	0.12	0.14	0.36	0.31	0.41	0.28	0.18	0.20	0.15	0.12	0.17	0.11	0.19	0.08	0.06	0.10	0.04	0.05	0.11	0.02	0.04	0.09	0.07
3	9801	0.13	0.21	0.15	0.10	0.29	0.69	0.67	0.12	0.14	0.11	0.09	0.05	0.08	0.56	0.06	0.08	0.09	0.08	0.04	0.03	0.02	0.03	0.01	0.01	0.03	0.02	0.01
4	9072	0.37	0.13	0.36	0.39	0.29	0.58	0.19	0.22	0.23	0.21	0.15	0.10	0.14	0.22	0.09	0.18	0.08	0.08	0.12	0.06	0.03	0.04	0.02	0.13	0.07	0.03	0.02
5	8542	0.33	1.11	0.36	0.33	0.09	0.13	0.09	0.25	0.13	0.08	0.26	0.13	0.18	0.14	0.07	0.19	0.15	0.11	0.61	0.04	0.11	0.08	0.06	0.07	0.11	0.09	0.05
6	8126	0.27	0.14	0.47	0.33	0.12	0.15	0.21	0.25	0.17	0.33	0.28	0.30	0.14	0.06	0.23	0.12	0.21	0.12	0.07	0.07	0.05	0.05	0.09	0.05	0	0	0.01
7	8064	0.24	0.20	0.41	0.26	0.11	0.17	0.20	0.21	0.14	0.31	0.21	0.36	0.10	0.07	0.24	0.15	0.22	0.15	0.05	0.10	0.02	0.02	0.05	0.07	0.01	0.02	0.14
8	7369	0.26	0.19	0.35	0.26	0.26	0.39	2.32	0.16	0.24	0.11	0.19	0.16	0.15	0.20	0.19	0.15	0.15	0.05	0.08	0.05	0.07	0.08	0.04	0.03	0.07	0.01	0.05
9	7036	0.26	0.21	0.18	0.17	0.21	0.20	0.04	0.13	0.14	0.09	0.21	0.11	0.09	0	0.04	0.13	0.10	0.11	0.07	0.06	0.01	0.10	0.04	0.01	0.09	0.03	0.04
10	6836	0.61	0.25	0.45	0.26	0.23	0.18	0.15	0.38	0.26	0.16	0.47	0.29	0.22	0.13	0.15	0.18	0.15	0.20	0.23	0.06	0.04	0.04	0.13	0.03	0.07	0.01	0.03
11	6642	0.26	0.45	0.35	0.26	0.11	0.21	0.08	0.17	0.23	0.17	0.17	0.18	0.20	0.17	0.24	0.26	0.15	0.12	0.06	0.08	0.17	0.02	0.12	0.05	0.02	0.03	0
12	6533	0.31	0.23	0.31	0.32	0.15	0.12	0.12	0.21	0.14	0.26	0.23	0.26	0.20	0.24	0.20	0.15	0.17	0.20	0.08	0.03	0.05	0.02	0.12	0.03	0.02	0.05	0.03
13	6514	0.32	0.20	0.23	0.26	0.12	0.26	0.18	0.17	0.11	0.18	0.23	0.12	0.23	0.08	0.12	0.17	0.14	0.25	0.09	0.09	0.12	0.05	0.02	0.02	0.03	0.08	0.02
14	6386	0.41	0.27	0.39	0.34	0.23	0.14	0.33	0.25	0.20	0.22	0.28	0.19	0.20	0.08	0.19	0.06	0.17	0.13	0.19	0.03	0.05	0.03	0.09	0.06	0.03	0	0.06
15	6283	0.16	0.14	0.22	0.29	0.03	0.11	0.16	0.08	0.18	0.22	0.10	0.14	0.10	0.11	0.08	0.13	0.06	0.02	0.02	0.06	0.05	0.05	0.08	0.03	0.03	0.10	0
16	5997	0.30	0.35	0.33	0.43	0.18	0.22	0.10	0.28	0.18	0.38	0.23	0.28	0.17	0.08	0.28	0.10	0.13	0.13	0.13	0.03	0.08	0.02	0.02	0.03	0.10	0.07	0.02
17	5945	0.35	0.45	0.35	0.47	0.05	0.24	0.20	0.22	0.29	0.19	0.24	0.19	0.24	0	0.13	0.08	0.19	0.08	0.22	0.07	0.05	0.03	0.07	0.02	0.05	0.02	0.07
18	5744	0.23	0.17	0.12	0.19	0.30	0.16	0.16	0.26	0.12	0.28	0.09	0.10	0.10	0.21	0.09	0.09	0.05	0.03	0.05	0.03	0	0.02	0.03	0.09	0.03	0	0.03
19	5386	0.59	0.30	0.15	0.32	0.24	0.11	0.07	0.32	0.15	0.02	0.45	0.22	0.17	0.13	0.22	0.15	0.15	0.30	0.13	0.13	0.15	0.06	0.04	0.06	0.17	0.02	0.02
20	4969	0.26	0.34	0.36	0.40	0.12	0.28	0.12	0.18	0.26	0.28	0.20	0.22	0.24	0.10	0.16	0.16	0.16	0.08	0.04	0.08	0.02	0.06	0.04	0	0	0.02	0.04

21	4461	0.29	0.11	0.27	0.13	0.56	0.27	0.18	0.13	0.02	0.02	0.16	0.04	0.27	0.16	0.09	0.04	0.13	0.02	0	0	0	0	0.16	0.04	0.02			
22	3968	0.28	0.33	0.23	0.33	0.08	0.18	0.15	0.23	0.18	0.38	0.25	0.20	0.20	0.05	0.18	0.03	0.18	0	0.05	0.05	0.03	0	0.08	0.03	0	0.13	0.03	
23	3960	0.40	0.25	0.45	0.13	0.25	0.08	0.05	0.20	0.28	0.18	0.25	0.15	0.33	0.10	0.25	0.23	0.25	0.13	0.10	0.10	0.18	0.03	0.08	0.08	0	0.08	0.05	
24	3902	0.26	0.13	0.38	0.21	0.18	0.10	0.05	0.28	0.15	0.23	0.36	0.08	0.10	0.08	0.18	0.05	0.05	0.13	0.03	0.08	0.08	0.03	0.03	0	0.03	0	0.05	
25	3585	0.42	0.59	0.08	0.14	0.33	0.08	0.11	0.28	1.14	0.06	0.06	0.22	0.31	0.08	0.17	0.20	0.20	0.03	0.03	0.50	0.11	0.06	0.08	0.06	0	0.22	0.03	
26	3451	0.20	0.55	0.35	0.41	0.06	0.03	0.17	0.32	0.20	0.23	0.14	0.14	0.23	0.03	0.26	0.23	0.14	0.03	0.06	0.03	0.17	0.03	0.09	0.06	0.06	0.03	0	
27	3431	0.29	0.29	0.44	0.09	0.17	0.15	0.12	0.26	0.12	0.15	0.12	0.12	0.32	0.17	0.23	0.26	0.15	0.35	0.17	0.03	0.09	0.06	0.12	0	0.06	0.06	0.03	
28	3361	0.33	0.54	0.39	0.15	0.33	0.21	0.09	0.21	0.33	0.27	0.15	0.15	0.30	0.24	0.21	0.18	0.09	0.15	0.09	0.09	0.03	0	0.03	0	0	0.15	0.06	
29	3230	0.53	0.31	0.37	0.31	0.25	0.28	0.03	0.25	0.22	0.06	0.12	0.40	0.46	0.03	0.28	0.25	0.25	0.09	0.09	0.15	0.06	0.03	0.03	0.09	0.03	0.03	0	
30	2950	0.31	0.07	0.34	0.58	0.17	0.24	0.24	0.24	0.07	0.47	0.14	0.14	0.03	0.03	0.27	0.07	0.14	0.07	0.10	0	0	0.10	0	0	0	0	0.07	0
31	2926	0.44	0.14	0.27	0.14	0.03	0.10	0.24	0.17	0.24	0.14	0.27	0.14	0.17	0	0.24	0.31	0.21	0.03	0.24	0	0.14	0.14	0.17	0.03	0.07	0	0.03	
32	2839	0.14	0.14	0.18	0.21	0.07	0.35	0.88	0.11	0.07	0.35	0.04	0	0.18	1.09	0.07	0.07	0.35	0	0	0.04	0.14	0	0	0.04	0	0	0.04	0
33	2779	0.47	0.22	0.25	0.25	0.07	0.22	0.22	0.18	0.11	0.22	0.47	0.18	0.22	0	0.40	0	0.11	0.07	0.25	0.11	0.07	0.25	0.04	0	0.07	0.07	0.04	0.04
34	2708	0.30	0.18	0.33	0.33	0.37	0.33	0.48	0.18	0.11	0.15	0.15	0.15	0.15	0.18	0.11	0.22	0.18	0	0.07	0.04	0.04	0	0.07	0.07	0.07	0.04	0	
35	2428	0.58	0.08	0.25	0.37	0.21	0.16	0.21	0.21	0.21	0.41	0.25	0.33	0.16	0	0.25	0.04	0.12	0	0.08	0.08	0.04	0.12	0.21	0	0	0	0.04	
36	2388	0.17	0.38	0.38	0.13	0.13	0.13	0.21	0.17	0.21	0.13	0.25	0.25	0.17	0.04	0.25	0.17	0.04	0.04	0.08	0.17	0.29	0.08	0.04	0	0.17	0.04	0.08	
37	2192	0.50	0.14	0.23	0.14	1.82	0.23	0.14	0.18	0.14	0.32	0.23	0.05	0.09	0.09	0	0.09	0.14	0.05	0.09	0.05	0.14	0	0.05	0.05	0	0	0	
38	2099	0.67	0.14	0.67	0.38	0.14	0.19	0.29	0.29	0.19	0	0.19	0.48	0.19	0.05	0.38	0.10	0.24	0.14	0.14	0	0	0.05	0.10	0.05	0.19	0.05	0.10	
39	1966	0.56	0.25	0.41	0.20	0.15	0.25	0.05	0.15	0.20	0.46	0.31	0.25	0.25	0.05	0.15	0.15	0.36	0.15	0.25	0	0	0	0.05	0.05	0	0.05	0	
40	1732	0.40	0.35	0.40	0.52	0.17	0	0.06	0.46	0.17	0.06	0.06	0.06	0	0.06	0.17	0.06	0.06	0.06	0	0.29	0.06	0.06	0.12	0	0	0.12	0.12	
41	1646	0.43	0.55	0.18	0.18	0.06	0.30	0	0.12	0.18	0.30	0.06	0.06	0	0.24	0.18	0.24	0.12	0.06	0.49	0.06	0.24	0.06	0.18	0.24	0.06	0	0	
42	1503	0.53	0.27	0.53	0.40	0	0.13	0.13	0.27	0.07	0.40	0.13	0.27	0.27	0.07	0.20	0.13	0.20	0.13	0.20	0.20	0	0.13	0	0	0	0.07	0.07	
43	1411	0.21	0	0.14	0.21	0.21	1.77	1.49	0.14	0.28	0.35	0	0.14	0	0.35	0.07	0.07	0.14	0.07	0	0	0	0	0	0.07	0	0	0.07	
44	1341	0.15	0.15	0	0	8.28	0.22	0.22	0.07	0.22	0.07	0.22	0.07	0.15	0.22	0.22	0.15	0.30	0.07	0.15	0.07	0.07	0	0.07	0	0.07	0	0.07	
45	1021	0.29	0.20	0.29	0.39	0.49	0.29	0.20	0.10	0.29	0.39	0.29	0.10	0.20	0.10	0.20	0.29	0.20	0	0.20	0	0.20	0.10	0	0	0	0	0	
46	906	0.55	0.22	1.21	0.22	0.44	0.33	0.11	0	0.44	0.11	0.22	0.55	0.11	0.11	0.55	0.77	0.22	0.11	0	0.11	0.11	0	0.11	0.11	0	0	0	
47	787	0.51	0.13	0.89	0.13	0	0.64	0.13	0.51	0.25	0.13	0.13	0.25	0.25	0.13	0.13	0.64	0	0.13	0	0	0.13	0	0	0.38	0.25	0	0.13	
48	724	0.14	0.69	0.14	0.28	0.14	0.28	0	1.80	0.14	0.28	0.55	0.14	0.28	0.14	0.14	0	0.28	0.14	0.28	0.14	0.14	0	0	0	0	0	0.14	0

49	592	0.68	0.51	0.51	0.34	0	0	0	0.17	0.17	0.17	0.34	0.17	0.17	0.68	0.17	0	0	0	0.34	0	0	0	0	0	0			
50	544	0.37	1.10	0.18	0.18	0.55	0	0	0.18	0.18	0	0.37	0.18	0.37	0.18	0	0.37	0.37	0.18	0	0.18	0.18	0	0	0.18	0	0		
51	524	0.38	1.15	0.38	0.19	0.19	0.19	0	0	0.57	0	0.38	0	0	0.19	0.19	0.19	0.19	0.76	0	0	0.19	0.38	0	0	0	0		
52	483	0	0.21	0.21	0	0	0	0	0	0	0	0	0	0	0	0	0.41	0	0	0	0	6.21	0	0	0.21	0	0		
53	472	0	1.06	0.21	0.21	0	0.42	0.42	0.42	0.21	0	0.21	0	0	8.26	0	0	0	0	0	0	0	0	0	0	0	0.21	0	
54	469	0.64	0	0.21	0	0	0.21	0.43	0	0	0.21	0	0	0	0.21	0.21	0.21	0	0.21	0	0	0	0	0	0	0.43	0	0	
55	440	0	0	0.45	0	2.50	0.23	0	0	0	0.45	0.23	0	0	0.23	0	0.23	0	0.23	0.23	0	0	0.45	0.23	0.23	0	0	0	
56	379	0	0	0.53	0.26	0	0	0.53	0.53	0.26	0	0.26	0.26	0.26	0.26	0	0.53	0	0	0.53	0	0	0.26	0.26	0	0	0	0	
57	336	0.30	0	0.30	0	0.60	0.30	0.30	0	0.30	0	0.30	0	0.30	0	0.30	0	0	0.30	0	0	0	0	0	0.30	0	0	0	
58	334	0	0.30	0	0.60	0	0.60	0.60	0.60	0	0.30	0	0.60	0	0	0	0	0	0	0	0.30	0	0	0	0	0	0	0	0.60
59	291	0	0.34	0	0.34	1.37	1.72	0.34	0	0.34	0.34	0	0	0	0	0	0	0	0	0	0	0	0	0	0.34	0.34	0	0	
60	170	0.59	0.59	0	0.59	0	0	0	0	0	0	0	0	0	0.59	0	0	0	0	0	0	0	0	0	0	0	0	0	
61	160	0	0.63	1.25	0	0	0	0	0	0.63	0	0	0	0	0.63	0.63	0.63	0	0.63	0	0	0	0	0	0	0	0	0	0.63
62	160	0	0	0.63	0	0	0	0	0	0	0.63	0	0	0.63	0.63	0	0.63	0	0.63	0	0	0	0	0	0.63	0.63	0	0	0
63	159	0.63	0.63	0	0	0	0.63	0	0	0	0	1.26	1.26	0	0.63	0	0	0	0	0	0	0	0	0	0	0	0	0	
64	144	0.69	0	1.39	0	0	0	0	0.69	0.69	0	0.69	1.39	0	0	0	0.69	0	0.69	0.69	0	0	0	0	0	0	0	0	0
65	125	0	1.60	0	0	0	0	0	0	0	0.80	0	1.60	0	0	0	0	0	0	0	0	0	0	0	0	0	0	0	0
66	124	0	0	0.81	0.81	0.81	0	0	0.81	0.81	0	0.81	0	0	0.81	0	0	0	0	0.81	0	0	0.81	0	0	0	0	0	0
67	117	0.85	1.71	0	0.85	0	0	0	0	0	0.85	0	0	0	0	0	0	0	0	0	0	0	0	0	0	0	0	0	0
68	108	0	0	0.93	0	0	0	0	0	0	0	0	0	0	0.93	0	0.93	0	0.93	0	0	0	0	0	0	0	0	0	0
69	108	0	0	0	0	0.93	0.93	0	0	0	0.93	0	0	0	0	0	0	0	0	0	0	0	0	0	0	0	0	0	0

Supplementary Table 12. P-values of the hypergeometric test between pairs of non-psychiatric controls and schizophrenia (1 to 27) modules. Shown are P-values of the hypergeometric test between the controls and schizophrenia modules presented in Chapter 5 section 5.5.1.1.

	1	2	3	4	5	6	7	8	9	10	11	12	13	14	15	16	17	18	19	20	21	22	23	24	25	26	27	
Controls network																												
1	0	1.00	1.00	4.22E-38	1.00	1.00	1.00	1.00	1.51E-03	1.66E-29	1.00	1.00	1.00	1.00	1.00	3.37E-30	0.58	1.00	6.91E-08	1.00	1.51E-06	2.15E-27	1.00	1.00	1.00	1.00	8.01E-06	1.00
2	2.69E-23	1.00	0.56	5.45E-115	3.56E-07	1.00	1.00	1.00	1.00	0.03	4.61E-04	1.00	0.61	1.00	1.00	5.32E-33	0.47	0.89	1.90E-03	0.36	0.84	2.34E-03	1.00	1.00	1.00	0.82	4.17E-03	0.97
3	1.00	0	0.94	1.00	1.00	0.93	1.00	0.38	1.00	1.00	1.00	1.00	1.00	1.08E-182	1.00	1.00	1.00	1.00	1.00	1.00	1.00	2.22E-35	0.56	1.00	1.00	1.00	2.19E-34	
4	1.00	2.30E-278	4.68E-11	1.00	1.00	0.26	1.00	4.94E-07	1.00	0.44	1.00	1.00	0.89	1.63E-59	1.00	1.00	0.82	1.00	1.00	1.00	1.00	0.83	3.71E-38	1.01E-06	0.36	0.99	1.72E-47	
5	1.00	1.00	1.00	1.00	1.00	1.00	0.28	0.95	1.00	1.00	2.87E-04	1.21E-06	3.25E-14	1.00	8.08E-89	0.09	1.00	0.20	0.12	7.57E-11	0.86	1.00	0.98	0.30	0.36	0.96	1.00	
6	0.11	1.00	1.39E-12	1.00	0.93	0.98	1.00	0.10	3.59E-05	6.24E-04	1.00	0.58	0.06	1.00	0.98	0.94	0.31	1.78E-04	7.38E-03	0.59	7.45E-10	0.55	0.28	0.53	0.38	0.03	0.99	
7	3.48E-18	1.00	0.01	3.80E-15	2.36E-06	1.00	1.00	1.00	1.00	0.01	0.32	1.00	0.08	1.00	1.00	0.71	0.38	0.15	1.77E-08	0.03	0.86	0.06	0.39	1.00	0.15	0.01	0.90	
8	1.00	1.32E-32	0.61	1.00	1.00	1.04E-03	1.56E-03	0.27	0.81	1.00	0.98	1.00	0.99	2.25E-03	0.35	1.00	0.13	0.27	0.15	0.19	0.93	0.78	0.77	0.20	0.96	0.99	0.90	
9	1.00	1.00	0.40	1.00	1.00	0.99	0	0.61	1.00	1.00	1.00	1.32E-312	0.99	1.00	7.51E-124	1.00	0.94	0.96	1.00	0.96	4.69E-14	1.00	1.00	1.30E-04	1.00	0.97	1.00	
10	1.00	1.00	0.03	0.96	0.61	0.19	0.38	0.90	0.21	0.10	0.71	0.05	0.02	1.00	0.01	0.71	0.69	7.46E-04	0.13	0.08	8.03E-03	0.82	0.95	0.01	2.23E-03	0.96	0.99	
11	4.82E-25	1.00	1.00	8.88E-18	2.45E-08	1.00	1.00	1.00	0.81	5.79E-03	0.10	1.00	0.91	1.00	1.00	4.28E-03	0.88	0.91	1.00E-02	0.08	0.85	1.84E-03	0.99	0.99	0.03	0.03	2.49E-03	0.78
12	2.59E-21	1.00	2.01E-06	0.47	1.42E-04	0.89	1.00	1.00	0.21	0.02	0.62	0.40	0.72	0.99	1.00	8.89E-03	0.21	0.38	0.13	0.78	0.31	9.31E-03	0.02	0.96	0.29	0.04	3.13E-04	0.51
13	7.08E-52	1.00	2.75E-04	0.95	0.77	0.82	1.00	1.00	8.99E-03	1.25E-03	0.96	1.00	0.51	1.00	1.00	0.02	1.96E-05	3.12E-03	0.05	0.97	0.03	0.02	0.88	0.99	1.00	0.03	0.87	
14	1.00	1.00	2.24E-05	1.00	0.96	0.07	4.88E-05	0.96	2.49E-05	0.37	0.87	0.18	1.08E-04	0.98	0.33	0.99	0.13	5.19E-04	0.47	0.02	0.01	0.91	0.90	3.70E-04	0.15	0.88	0.98	
15	5.98E-53	1.00	1.00	0	1.82E-21	1.00	1.00	1.00	1.00	0.94	1.42E-06	0.98	0.85	1.00	1.00	2.45E-05	1.00	0.99	3.35E-03	0.81	0.98	0.20	0.84	0.99	0.87	0.41	0.99	
16	1.00	1.00	1.66E-08	1.00	0.97	0.02	1.63E-03	8.37E-07	0.02	1.73E-03	0.99	1.20E-06	0.05	0.03	6.04E-07	0.96	0.74	0.05	0.69	0.60	0.21	0.44	0.18	0.17	0.12	0.87	0.04	
17	0.07	1.00	0.31	6.05E-09	6.22E-03	0.97	1.00	1.00	1.00	0.04	0.09	0.24	7.38E-03	1.00	0.45	0.28	0.72	0.79	4.33E-05	0.68	0.22	0.29	0.87	0.42	0.04	0.68		
18	4.60E-23	1.00	1.62E-20	0.91	0.81	0.42	0.26	0.76	1.00	7.43E-07	0.77	0.10	1.00	6.44E-08	1.00	0.98	9.17E-04	0.82	0.77	1.00	0.15	0.28	0.96	0.61	0.95	0.14	0.36	
19	1.00	1.00	3.13E-03	1.00	1.00	0.48	2.70E-185	0.98	0.59	0.95	0.83	1.72E-56	0.35	1.00	7.39E-61	1.00	0.10	0.64	1.00	0.57	7.96E-08	1.00	0.99	4.00E-06	0.25	0.87	0.96	

20	8.12E-18	1.00	0.04	6.15E-14	1.32E-06	0.93	1.00	0.32	0.82	0.16	3.63E-04	0.48	0.39	1.00	1.00	0.29	0.28	0.07	0.05	0.96	0.85	0.02	0.55	0.90	0.62	5.04E-03	0.75
21	1.78E-141	1.00	0.89	1.00	1.00	1.67E-04	0.95	0.01	0.95	1.00	0.88	1.00	0.87	1.28E-14	0.97	1.00	6.16E-03	0.41	1.00	0.99	0.89	1.00	0.37	8.11E-05	0.99	0.96	7.10E-05
22	6.51E-32	1.00	0.32	2.28E-13	5.33E-11	0.71	1.00	1.00	0.89	0.09	3.10E-05	0.98	0.96	0.98	1.00	0.02	0.78	0.81	2.05E-05	0.86	0.77	0.33	0.57	0.75	0.35	0.36	0.97
23	1.59E-10	1.00	0.01	9.64E-03	1.70E-04	0.93	0.99	1.00	0.10	0.60	0.65	0.72	0.08	1.00	0.98	0.48	0.71	0.61	0.04	0.41	0.68	0.04	0.67	0.75	0.93	0.01	0.31
24	6.88E-24	1.00	1.55E-06	0.59	0.16	0.77	3.03E-03	0.99	0.50	0.02	0.61	1.19E-08	0.01	1.00	0.50	0.95	0.12	0.84	0.99	1.00	0.30	0.16	0.74	0.81	0.88	0.33	0.50
25	1.00	1.00	1.00	5.71E-22	1.60E-18	0.63	1.00	9.26E-20	1.00	0.80	7.81E-15	0.89	0.78	0.92	0.99	3.55E-14	0.67	0.85	0.07	5.44E-04	0.99	0.98	0.93	1.00	6.80E-03	0.23	0.99
26	4.67E-22	1.00	1.00	4.37E-03	5.40E-03	0.93	1.00	0.13	0.29	6.57E-05	0.26	1.00	0.13	0.97	1.00	0.41	0.67	0.11	0.01	0.01	0.02	0.04	0.98	0.85	0.56	0.12	0.98
27	1.00	1.00	0.13	1.00	0.49	0.39	2.51E-04	0.72	0.04	0.96	0.37	0.05	7.22E-03	0.94	9.46E-04	0.94	0.73	5.42E-03	0.84	9.46E-03	0.20	0.99	0.85	0.03	0.17	0.69	0.76
28	0.95	5.52E-35	0.66	1.00	0.99	0.28	1.00	0.93	0.89	0.73	0.59	0.68	0.52	0.48	0.98	0.23	0.38	0.95	0.81	0.63	0.05	0.74	0.65	0.74	0.52	0.66	0.63
29	1.00	1.00	0.09	1.00	0.24	0.29	0.66	1.82E-03	0.04	0.89	0.57	0.98	2.40E-03	0.99	0.68	0.81	0.46	0.09	0.01	0.23	0.75	0.01	0.97	9.47E-04	0.03	0.82	0.69
30	5.91E-28	1.00	1.71E-11	0.95	0.91	0.95	0.57	0.96	0.96	0.15	0.72	2.28E-03	0.80	0.97	1.00	1.00	0.70	0.37	0.94	0.95	0.34	0.35	0.79	0.97	0.02	0.81	
31	1.00	1.00	3.23E-05	1.00	0.79	0.39	6.87E-10	0.92	0.85	0.47	0.42	7.40E-10	0.50	0.97	0.01	0.90	5.58E-03	0.01	0.52	0.60	4.60E-12	0.24	0.88	1.22E-03	0.99	0.72	0.80
32	1.00	0	0.03	1.00	1.00	1.00	1.00	0.98	0.98	1.00	0.99	1.00	0.80	3.26E-24	1.00	0.95	0.99	0.95	0.56	1.00	0.92	0.72	1.33E-09	0.92	0.96	0.99	1.73E-07
33	1.54E-03	1.00	0.36	1.00	0.41	0.96	0.95	0.89	0.13	0.01	0.68	0.13	0.12	0.99	0.93	0.31	0.68	0.20	0.04	0.12	4.71E-04	0.27	0.84	0.07	0.49	0.03	0.75
34	1.00	1.06E-20	8.93E-05	1.00	0.99	0.80	0.74	0.36	0.89	0.36	0.91	0.67	0.28	1.64E-09	0.99	0.83	0.38	0.12	0.75	0.84	0.15	0.67	2.09E-04	0.81	0.81	0.27	0.05
35	2.77E-15	1.00	7.83E-03	0.87	0.22	0.25	1.00	0.76	0.44	0.34	0.57	1.00	0.22	0.99	0.97	0.18	0.55	0.40	0.16	0.41	3.42E-03	0.08	0.72	0.90	0.95	0.26	0.99
36	6.55E-10	1.00	0.16	0.73	0.35	0.46	1.00	2.13E-04	0.05	0.08	0.83	0.96	0.03	0.87	0.98	0.66	0.04	0.02	0.28	0.98	0.11	0.12	0.95	0.21	0.43	0.49	0.33
37	0.91	4.88E-06	2.84E-03	1.00	0.79	0.03	0.96	0.66	1.00	0.89	0.23	0.87	0.97	0.60	1.00	0.99	3.83E-10	0.33	1.00	0.93	1.79E-04	0.28	0.99	0.73	0.92	0.80	0.50
38	1.00	1.00	0.39	0.94	0.82	0.24	0.04	0.70	4.13E-03	0.73	0.94	0.60	0.01	0.62	0.31	0.93	0.86	0.03	0.20	0.02	0.53	0.83	0.56	0.29	0.90	0.14	0.99
39	1.00	1.00	1.73E-03	1.00	0.93	0.58	5.48E-04	0.70	0.87	0.45	0.98	5.32E-06	0.30	0.90	3.51E-09	0.82	0.40	1.00E-05	0.39	0.79	9.39E-05	0.65	0.35	0.34	0.22	0.41	0.97
40	1.16E-05	1.00	1.97E-03	0.99	0.12	0.77	1.00	0.79	0.98	0.06	0.49	4.15E-05	0.92	0.97	0.86	0.91	0.42	0.02	0.44	0.99	1.40E-05	0.25	0.80	0.22	0.65	0.43	0.85
41	1.00	1.00	1.00	1.00	1.00	0.96	1.53E-13	0.98	0.03	0.97	0.03	1.27E-16	2.92E-04	0.93	2.57E-44	0.94	0.96	0.45	0.12	7.51E-03	0.66	0.94	0.88	7.36E-07	0.99	0.54	0.98
42	0.80	1.00	0.56	0.96	0.57	0.21	0.01	0.45	0.10	0.31	0.66	2.81E-03	0.23	0.99	0.81	0.19	0.11	0.23	0.38	0.24	0.10	0.36	0.69	0.22	0.07	0.30	0.77
43	1.00	1.34E-189	5.22E-04	0.98	0.97	0.97	1.00	0.33	1.00	0.98	1.00	1.00	0.93	1.92E-09	1.00	0.85	0.26	0.99	0.56	0.99	0.96	1.00	2.70E-30	0.05	1.00	0.75	5.42E-05
44	1.00	6.53E-07	0.65	1.00	1.00	1.00	0.85	4.13E-07	0.99	0.99	0.60	0.77	0.95	0.55	0.93	0.94	0.08	0.70	0.86	0.98	0.45	0.85	0.76	0.58	0.25	0.95	0.85
45	0.29	0.99	0.36	0.79	0.11	0.68	0.95	0.83	0.08	0.15	0.58	0.79	0.21	0.95	0.85	0.89	0.15	0.05	0.64	0.93	0.11	0.94	0.75	0.35	0.04	0.71	0.97

46	1.00	1.00	1.00	0.72	0.91	0.25	0.56	0.34	0.59	0.05	0.62	0.57	0.79	3.42E-04	0.43	0.77	0.40	0.99	0.10	0.69	0.59	0.99	0.58	0.68	0.06	0.06	6.22E-03	0.83	
47	1.00	1.00	1.00	0.22	0.97	0.65	0.61	0.24	3.79E-08	0.07	0.70	0.06	0.52	0.01	0.97	7.53E-03	0.72	0.54	0.78	0.88	0.17	0.17	0.28	0.59	0.36	0.35	0.54	0.94	
48	0.98	1.00	1.00	0.48	0.90	0.32	0.48	0.54	7.61E-03	0.45	0.09	0.12	0.58	0.42	0.96	0.56	4.67E-03	0.46	0.37	8.28E-03	0.02	0.45	0.63	0.53	0.52	3.02E-05	0.48	0.92	
49	0.29	1.00	1.00	0.98	0.85	0.02	0.81	0.93	0.48	0.22	0.54	0.55	0.53	0.36	0.45	0.01	0.17	0.65	0.58	0.19	0.12	0.53	0.27	0.40	0.66	8.33E-03	0.17	0.87	
50	1.00	0.77	0.96	0.96	0.26	0.12	0.49	0.68	0.87	0.74	0.11	4.21E-03	0.79	0.78	0.87	0.09	2.52E-12	0.91	0.89	0.27	2.00E-05	0.73	0.91	0.88	0.62	0.02	0.14	0.56	0.84
51	1.00	0.99	0.51	0.98	0.14	0.68	1.00	1.00	0.08	0.20	0.27	0.28	0.27	2.41E-03	0.85	0.01	0.38	0.05	0.69	0.25	9.99E-04	0.71	0.42	0.60	0.32	0.14	0.56	0.84	
52	1.00	1.00	1.00	1.00	1.00	0.27	0.95	1.01E-107	0.95	0.98	1.00	0.96	1.22E-46	0.85	0.99	2.26E-109	0.89	0.97	0.96	0.96	0.94	0.90	0.89	0.85	0.55	0.84	0.52	0.82	
53	1.00	4.01E-87	0.49	0.99	0.86	0.99	1.00	1.00	0.23	0.94	1.00	0.99	0.95	0.32	4.93E-07	0.98	0.30	0.87	0.83	0.59	0.75	0.89	0.62	1.98E-05	0.54	0.27	0.82	8.46E-06	
54	1.00	0.76	1.00	1.00	0.96	0.21	0.66	0.66	1.28E-155	0.60	0.19	0.85	0.95	0.68	0.61	6.86E-03	0.70	0.47	0.40	0.36	0.75	0.65	0.62	0.84	0.27	0.53	0.82	0.23	
55	1.00	2.88E-04	0.99	0.71	0.11	0.05	0.93	0.93	3.38E-04	0.38	0.59	2.01E-04	0.63	0.63	0.02	0.71	0.97	6.55E-03	0.58	0.94	0.24	0.88	0.31	0.51	0.50	0.09	0.80	0.20	
56	2.09E-03	0.91	0.05	0.66	0.19	0.82	0.60	0.60	0.73	0.08	0.29	0.74	0.52	0.72	0.86	0.83	0.33	0.54	0.12	0.70	0.64	0.04	0.03	0.77	0.43	0.42	0.16	0.38	
57	1.00	5.32E-64	1.00	0.87	0.87	0.72	0.48	0.48	0.29	0.90	0.90	0.97	0.65	0.84	1.12E-07	0.77	0.93	0.46	0.67	0.89	0.57	0.80	0.78	2.14E-03	0.04	0.72	0.70	0.33	
58	0.78	3.33E-03	0.15	1.47E-03	0.99	0.93	0.92	0.92	0.62	0.76	0.20	0.13	0.42	0.23	0.03	0.53	0.47	0.71	0.67	6.43E-03	0.57	0.47	0.06	0.01	0.37	0.36	0.12	0.33	
59	1.00	5.99E-44	0.21	0.14	0.34	0.43	0.21	0.32	0.83	0.97	0.08	0.78	0.78	0.78	0.13	0.70	0.66	0.64	0.32	0.56	0.81	0.40	0.73	0.31	0.31	0.10	0.28	0.64	
60	1.00	0.78	0.84	0.04	4.91E-03	0.49	0.94	0.94	0.51	0.27	0.32	0.03	0.82	0.81	0.45	0.42	0.04	0.36	0.32	0.67	6.14E-05	0.19	0.04	0.14	0.48	0.14	0.13	0.45	
61	0.91	1.00	1.00	0.42	0.92	0.23	0.02	5.53E-03	0.73	0.92	0.12	0.48	0.47	0.47	0.77	0.15	0.71	0.34	0.30	3.98E-03	0.06	0.04	0.51	0.46	4.09E-04	0.12	0.11	0.43	
62	0.66	0.81	0.13	0.79	0.23	0.02	0.28	0.28	0.92	0.45	0.56	0.48	0.47	0.07	0.42	0.74	0.35	0.70	0.67	0.28	0.06	0.53	0.51	0.46	0.02	0.46	0.44	0.43	
63	1.00	9.98E-03	0.99	0.92	0.78	0.25	0.27	0.27	1.34E-35	0.41	0.19	0.24	0.06	0.05	0.73	0.38	0.35	0.70	0.66	0.27	0.60	0.53	0.51	0.13	0.46	0.12	0.44	0.43	
64	0.98	0.99	0.07	0.52	0.52	0.03	0.04	0.91	0.41	0.19	0.24	3.63E-03	0.06	0.05	0.73	0.70	0.30	0.29	0.26	0.01	0.19	0.16	4.18E-03	0.11	0.42	0.02	0.40	0.40	
65	0.56	0.98	0.99	0.96	0.11	0.75	0.06	0.06	0.02	0.58	0.43	0.36	0.04	0.35	0.10	0.28	0.25	0.61	0.01	0.19	0.16	0.45	0.11	0.08	0.08	0.08	0.07	0.07	
66	0.96	0.53	0.05	0.84	0.04	0.50	0.87	0.87	0.02	0.86	0.43	0.13	0.35	0.34	0.68	0.65	0.25	0.07	0.57	0.19	5.71E-03	0.12	0.02	0.08	0.38	0.38	0.36	0.07	
67	0.03	0.93	0.60	4.57E-07	0.92	0.92	0.31	0.31	0.56	0.55	0.16	0.03	0.32	0.32	0.65	0.63	0.01	0.22	0.55	0.17	0.14	0.42	0.10	0.36	0.07	0.36	0.34	0.34	
68	0.91	0.66	0.99	0.94	0.94	0.08	4.62E-04	0.83	0.24	0.36	0.30	0.30	0.29	0.66	0.62	0.01	9.92E-03	9.06E-03	0.52	0.50	0.13	0.40	0.38	0.34	0.34	6.45E-05	0.32	0.31	
69	1.00	4.40E-13	0.52	0.78	0.53	0.03	0.54	0.54	8.04E-03	0.50	0.72	0.67	0.29	0.66	3.10E-03	0.06	0.57	0.19	0.52	0.50	0.46	0.40	0.38	8.63E-04	0.06	0.34	0.32	0.31	

Supplementary Table 13. P-values of the hypergeometric test between pairs of non-psychiatric controls and schizophrenia (28 to 54) modules. Shown are P-values of the hypergeometric test between the controls and schizophrenia modules presented in Chapter 5 section 5.5.1.1.

	Schizophrenia network ->																													
	28	29	30	31	32	33	34	35	36	37	38	39	40	41	42	43	44	45	46	47	48	49	50	51	52	53	54			
1	1.00	1.00	1.00	1.11E-05	1.00	1.00	1.00	0.98	1.00	9.40E-11	1.00	0.37	1.00	1.00	0.84	1.00	1.00	0.95	1.00	0.93	2.03E-06	1.00	1.00	1.00	0.90	1.00	1.00	1.00	0.85	
2	0.87	0.04	0.54	0.03	1.00	0.99	8.12E-03	0.02	3.52E-05	0.02	0.57	0.29	0.72	0.84	0.39	0.81	0.09	0.80	0.89	0.17	0.89	0.54	0.01	0.84	0.38	5.65E-03	0.02	0.02	0.02	
3	1.00	0.97	1.00	1.00	0.23	2.48E-14	8.25E-14	0.98	0.93	0.97	0.99	1.00	0.99	2.81E-15	1.00	0.95	0.90	0.78	0.97	0.95	0.98	0.83	0.97	0.94	0.57	0.73	0.85	0.85	0.85	
4	0.19	1.00	0.12	0.01	0.23	5.94E-09	0.83	0.40	0.29	0.32	0.76	0.97	0.76	0.08	0.96	0.20	0.95	0.80	0.23	0.72	0.92	0.62	0.89	3.12E-04	0.08	0.46	0.60	0.60	0.60	
5	0.45	4.00E-25	0.13	0.10	1.00	0.99	1.00	0.23	0.95	0.99	0.07	0.85	0.48	0.66	0.99	0.14	0.35	0.50	3.93E-25	0.90	0.13	0.13	0.35	0.10	2.77E-03	0.03	0.17	0.17	0.17	
6	0.79	1.00	3.76E-03	0.09	0.99	0.96	0.67	0.23	0.74	3.18E-03	0.03	9.13E-03	0.80	0.99	0.05	0.66	0.05	0.31	0.73	0.46	0.75	0.52	0.09	0.31	0.96	0.96	0.77	0.77	0.77	
7	0.92	0.98	0.03	0.46	1.00	0.89	0.74	0.47	0.92	9.80E-03	0.30	2.61E-04	0.95	0.98	0.05	0.42	0.03	0.13	0.92	0.19	0.95	0.85	0.47	0.08	0.84	0.60	2.34E-05	0.60	0.60	
8	0.83	0.98	0.18	0.47	0.42	6.14E-03	4.66E-11	0.80	0.23	0.95	0.46	0.59	0.68	0.17	0.24	0.41	0.37	0.92	0.64	0.69	0.51	0.15	0.59	0.66	0.08	0.78	0.11	0.11	0.11	0.11
9	0.83	0.94	0.96	0.93	0.71	0.75	1.00	0.94	0.88	0.98	0.29	0.90	0.97	1.00	1.00	0.60	0.79	0.40	0.73	0.65	0.97	0.06	0.56	0.83	0.03	0.51	0.22	0.22	0.22	0.22
10	6.14E-05	0.84	0.01	0.44	0.57	0.86	0.94	2.33E-03	0.15	6.68E-06	2.59E-06	0.02	0.18	0.69	0.57	0.22	0.39	0.01	9.04E-04	0.62	0.78	0.57	5.70E-03	0.61	0.06	0.74	0.41	0.41	0.41	0.41
11	0.82	0.03	0.21	0.48	0.99	0.67	1.00	0.77	0.34	0.64	0.63	0.44	0.32	0.42	0.05	0.01	0.36	0.34	0.81	0.42	6.23E-03	0.90	0.01	0.36	0.75	0.47	0.90	0.90	0.90	0.90
12	0.57	0.90	0.41	0.15	0.94	0.98	0.98	0.44	0.89	0.09	0.20	0.06	0.30	0.05	0.20	0.38	0.23	0.02	0.67	0.89	0.74	0.90	0.01	0.58	0.75	0.24	0.39	0.39	0.39	0.39
13	0.48	0.96	0.83	0.45	0.98	0.34	0.79	0.74	0.97	0.50	0.20	0.84	0.14	0.96	0.75	0.27	0.46	1.45E-03	0.51	0.25	0.07	0.53	0.88	0.80	0.49	0.04	0.65	0.65	0.65	0.65
14	0.11	0.75	0.08	0.08	0.56	0.95	0.06	0.22	0.49	0.27	0.05	0.38	0.27	0.95	0.26	0.96	0.21	0.30	0.02	0.88	0.73	0.73	0.07	0.17	0.48	0.92	0.07	0.07	0.07	0.07
15	0.99	1.00	0.85	0.30	1.00	0.99	0.89	0.99	0.68	0.25	0.96	0.71	0.94	0.82	0.95	0.59	0.95	0.99	0.99	0.99	0.55	0.72	0.51	0.14	0.55	0.47	0.01	0.88	0.88	0.88
16	0.59	0.30	0.27	5.86E-03	0.83	0.62	0.99	0.10	0.62	9.25E-04	0.19	0.03	0.52	0.93	0.01	0.79	0.49	0.24	0.17	0.85	0.32	0.87	0.85	0.52	0.01	0.08	0.61	0.61	0.61	0.61

17	0.32	0.03	0.19	1.44E-03	1.00	0.50	0.68	0.40	0.09	0.49	0.18	0.40	0.13	1.00	0.65	0.88	0.15	0.66	4.01E-03	0.50	0.68	0.68	0.24	0.76	0.22	0.67	0.05
18	0.90	0.98	1.00	0.82	0.22	0.90	0.89	0.18	0.92	0.06	0.97	0.90	0.89	0.16	0.91	0.85	0.97	0.96	0.84	0.83	0.99	0.85	0.63	0.05	0.41	0.89	0.31
19	6.47E-04	0.57	0.98	0.18	0.51	0.98	1.00	0.05	0.81	1.00	7.59E-05	0.19	0.51	0.67	0.11	0.41	0.37	1.79E-04	0.20	0.06	0.03	0.39	0.58	0.23	8.12E-05	0.61	0.55
20	0.75	0.35	0.18	0.03	0.97	0.25	0.95	0.63	0.18	0.07	0.37	0.20	0.12	0.83	0.43	0.32	0.29	0.66	0.89	0.35	0.90	0.33	0.53	0.90	0.87	0.57	0.24
21	0.60	1.00	0.59	0.95	1.19E-04	7.09E-05	0.28	0.62	0.83	1.00	1.00	0.57	0.99	0.04	0.45	0.34	0.77	0.88	0.18	0.87	0.97	0.93	0.92	0.87	5.28E-04	0.25	0.45
22	0.65	0.41	0.76	0.17	0.99	0.76	0.84	0.35	0.61	5.73E-03	0.15	0.30	0.29	0.96	0.33	0.98	0.21	0.99	0.78	0.60	0.81	0.90	0.18	0.54	0.80	4.57E-03	0.39
23	0.16	0.73	0.03	0.95	0.43	0.99	1.00	0.48	0.14	0.51	0.15	0.58	0.01	0.78	0.07	0.07	0.03	0.29	0.39	0.20	0.01	0.68	0.18	0.11	0.80	0.07	0.15
24	0.73	0.99	0.14	0.70	0.78	0.96	1.00	0.14	0.72	0.23	0.01	0.93	0.83	0.89	0.32	0.93	0.92	0.28	0.91	0.37	0.36	0.67	0.64	0.83	0.47	0.78	0.15
25	0.14	3.90E-03	0.99	0.91	0.13	0.98	0.93	0.16	1.94E-18	0.97	0.97	0.21	0.03	0.84	0.38	0.17	0.15	0.91	0.88	1.31E-10	0.15	0.35	0.14	0.23	0.77	1.21E-05	0.35
26	0.88	0.01	0.25	0.04	0.99	1.00	0.73	0.07	0.45	0.23	0.66	0.60	0.18	0.98	0.06	0.08	0.38	0.90	0.69	0.75	0.02	0.60	0.13	0.21	0.17	0.38	0.69
27	0.57	0.55	0.06	0.98	0.77	0.85	0.92	0.21	0.85	0.66	0.79	0.75	0.02	0.34	0.12	0.03	0.37	1.84E-04	0.07	0.75	0.28	0.33	0.05	0.79	0.16	0.15	0.33
28	0.43	0.02	0.14	0.88	0.16	0.59	0.96	0.44	0.06	0.13	0.63	0.58	0.04	0.11	0.19	0.24	0.71	0.18	0.46	0.27	0.73	0.86	0.56	0.79	0.75	2.04E-03	0.11
29	0.02	0.47	0.18	0.24	0.44	0.28	1.00	0.26	0.38	0.95	0.75	2.97E-03	3.49E-04	0.97	0.04	0.05	0.05	0.50	0.43	0.04	0.46	0.57	0.54	0.06	0.38	0.35	0.67
30	0.50	1.00	0.28	1.08E-03	0.76	0.44	0.42	0.30	0.95	8.59E-04	0.67	0.63	0.97	0.96	0.06	0.81	0.42	0.65	0.36	0.90	0.90	0.10	0.81	0.74	0.70	0.11	0.64
31	0.11	0.96	0.52	0.88	1.00	0.93	0.41	0.60	0.29	0.67	0.12	0.62	0.43	0.99	0.11	0.01	0.13	0.84	0.01	0.90	0.08	0.03	6.56E-03	0.39	0.12	0.68	0.26
32	0.96	0.95	0.86	0.62	0.98	0.10	1.45E-08	0.86	0.94	0.03	0.97	0.99	0.41	6.47E-17	0.85	0.79	3.13E-03	0.96	0.95	0.65	0.07	0.81	0.80	0.37	0.69	0.30	0.62
33	0.08	0.79	0.60	0.45	0.97	0.53	0.51	0.55	0.84	0.30	1.29E-03	0.40	0.24	0.99	2.65E-03	0.98	0.57	0.61	8.91E-03	0.18	0.36	2.75E-04	0.46	0.04	0.68	0.29	0.24
34	0.53	0.87	0.30	0.18	0.09	0.14	7.09E-03	0.53	0.83	0.61	0.60	0.55	0.54	0.29	0.65	0.11	0.20	0.95	0.53	0.63	0.62	0.80	0.20	0.13	0.10	0.28	0.60
35	0.02	0.98	0.60	0.11	0.58	0.71	0.53	0.42	0.41	9.09E-03	0.19	0.04	0.45	0.98	0.11	0.88	0.46	0.94	0.46	0.30	0.56	0.06	2.69E-03	0.67	0.63	0.61	0.20
36	0.89	0.25	0.19	0.87	0.86	0.84	0.52	0.58	0.40	0.68	0.18	0.15	0.43	0.91	0.10	0.28	0.86	0.75	0.45	0.04	6.26E-04	0.17	0.39	0.67	3.09E-03	0.23	0.05
37	0.06	0.92	0.65	0.83	2.24E-22	0.45	0.77	0.51	0.68	0.07	0.25	0.91	0.76	0.70	0.97	0.63	0.39	0.71	0.39	0.51	0.09	0.73	0.35	0.26	0.22	0.57	0.53
38	4.81E-03	0.91	2.21E-03	0.11	0.78	0.59	0.25	0.17	0.46	0.98	0.38	1.97E-03	0.33	0.86	9.00E-03	0.60	0.08	0.21	0.17	0.81	0.80	0.35	0.12	0.25	1.78E-03	0.19	0.04

39	0.03	0.61	0.14	0.59	0.74	0.36	0.95	0.61	0.41	5.90E-03	0.09	0.15	0.15	0.84	0.41	0.33	8.31E-03	0.18	0.02	0.79	0.78	0.69	0.30	0.23	0.55	0.18	0.49
40	0.21	0.33	0.16	0.02	0.64	0.99	0.92	0.01	0.50	0.85	0.85	0.82	0.96	0.78	0.32	0.73	0.71	0.58	0.83	2.70E-03	0.39	0.27	0.07	0.55	0.51	0.03	0.02
41	0.18	0.04	0.73	0.63	0.92	0.22	0.98	0.69	0.46	0.11	0.83	0.80	0.95	0.14	0.29	0.10	0.42	0.56	6.55E-05	0.37	0.36	3.09E-03	0.24	7.20E-03	6.10E-04	0.13	0.43
42	0.06	0.53	0.04	0.11	0.98	0.72	0.70	0.23	0.83	0.03	0.56	0.14	0.14	0.71	0.24	0.39	0.17	0.24	0.07	0.03	0.69	0.06	0.57	0.50	0.46	0.11	0.09
43	0.68	0.99	0.80	0.51	0.48	6.81E-15	1.30E-11	0.59	0.18	0.06	0.94	0.48	0.92	0.03	0.68	0.62	0.33	0.47	0.77	0.67	0.67	0.56	0.55	0.14	0.44	0.42	0.08
44	0.82	0.81	0.98	0.97	3.20E-129	0.42	0.40	0.78	0.32	0.74	0.26	0.70	0.44	0.18	0.18	0.32	0.05	0.45	0.16	0.28	0.28	0.55	0.17	0.46	0.10	0.40	0.08
45	0.43	0.64	0.37	0.13	0.05	0.25	0.45	0.65	0.17	0.05	0.14	0.56	0.28	0.50	0.24	0.07	0.18	0.68	0.09	0.55	0.05	0.12	0.44	0.37	0.34	0.33	0.29
46	0.08	0.56	2.74E-05	0.43	0.08	0.19	0.64	0.86	0.05	0.53	0.26	6.92E-03	0.49	0.44	4.28E-03	7.70E-05	0.14	0.27	0.61	0.16	0.16	0.41	0.09	0.07	0.31	0.29	0.27
47	0.12	0.72	3.03E-03	0.61	0.87	0.01	0.57	0.03	0.23	0.45	0.45	0.18	0.17	0.37	0.37	1.28E-03	0.68	0.22	0.56	0.46	0.12	0.37	0.36	5.07E-04	4.22E-03	0.26	0.03
48	0.69	0.03	0.64	0.30	0.55	0.26	0.83	1.12E-09	0.45	0.17	0.01	0.38	0.14	0.34	0.34	0.66	0.09	0.20	0.04	0.11	0.11	0.35	0.33	0.28	0.26	0.03	0.22
49	0.05	0.13	0.11	0.21	0.78	0.77	0.76	0.72	0.36	0.32	0.32	0.10	0.29	0.26	3.24E-03	0.22	0.57	0.49	0.46	0.37	0.01	0.29	0.28	0.24	0.21	0.20	0.18
50	0.27	2.19E-03	0.49	0.42	0.05	0.74	0.73	0.33	0.32	0.65	0.09	0.26	0.08	0.23	0.23	0.55	0.04	0.02	0.11	0.35	0.07	0.04	0.26	0.22	0.02	0.19	0.17
51	0.25	1.78E-03	0.21	0.40	0.39	0.37	0.72	0.68	0.03	0.64	0.08	0.62	0.61	0.22	0.21	0.18	0.17	0.12	2.36E-04	0.34	0.33	0.04	3.35E-03	0.21	0.19	0.18	0.16
52	0.80	0.46	0.43	0.72	0.71	0.70	0.69	0.65	0.64	0.61	0.61	0.59	0.58	0.55	0.55	0.51	0.03	0.42	0.39	0.32	0.31	5.44E-53	0.24	0.20	0.02	0.17	0.15
53	0.79	4.72E-03	0.42	0.35	0.70	0.11	0.11	0.08	0.27	0.60	0.23	0.58	0.57	1.81E-54	0.54	0.50	0.49	0.41	0.39	0.31	0.31	0.24	0.23	0.19	0.17	0.01	0.15
54	0.07	0.78	0.41	0.71	0.70	0.32	0.11	0.64	0.63	0.23	0.60	0.58	0.57	0.18	0.18	0.15	0.49	0.10	0.38	0.31	0.30	0.24	0.23	0.19	9.79E-04	0.17	0.15
55	0.76	0.76	0.15	0.69	2.44E-09	0.30	0.65	0.61	0.61	0.06	0.21	0.55	0.55	0.52	0.16	0.48	0.13	0.39	0.36	0.05	0.05	0.23	0.22	1.14E-03	0.01	0.01	0.14
56	0.71	0.71	0.11	0.26	0.62	0.61	0.06	0.05	0.19	0.52	0.17	0.15	0.15	0.47	0.13	0.43	0.42	9.42E-03	0.32	0.26	0.25	0.02	0.02	0.16	0.14	0.14	0.12
57	0.30	0.66	0.27	0.59	0.06	0.20	0.19	0.52	0.16	0.48	0.48	0.13	0.46	0.11	0.43	0.39	0.38	0.32	0.29	0.03	0.23	0.18	0.17	0.14	0.13	7.60E-03	0.11
58	0.67	0.29	0.64	0.06	0.57	0.05	0.05	0.04	0.51	0.14	0.48	0.02	0.45	0.42	0.42	0.39	0.38	0.31	0.29	0.23	0.03	0.18	0.17	0.14	0.13	0.12	2.20E-04

59	0.62	0.24	0.58	0.18	9.78E-04	9.74E-05	0.16	0.47	0.13	0.11	0.43	0.41	0.41	0.38	0.38	0.35	0.34	0.28	0.26	0.20	0.20	0.16	0.15	8.04E-03	6.41E-03	0.11	0.09		
60	0.11	0.11	0.40	0.07	0.35	0.34	0.34	0.31	0.30	0.28	0.28	0.27	0.26	0.03	0.24	0.22	0.22	0.17	0.16	0.13	0.12	0.10	0.09	0.07	0.07	0.06	0.06	0.06	
61	0.41	0.10	0.01	0.34	0.34	0.33	0.32	0.29	0.05	0.27	0.27	0.25	0.25	0.03	0.03	0.02	0.21	0.17	0.15	0.12	0.12	0.09	0.09	0.07	0.06	0.06	1.42E-03	0.06	
62	0.41	0.40	0.08	0.34	0.34	0.33	0.32	0.29	0.29	0.04	0.27	0.25	0.03	0.03	0.23	0.02	0.21	0.17	0.15	7.22E-03	0.12	0.09	0.09	0.07	2.00E-03	1.80E-03	0.05	0.05	
63	0.10	0.09	0.38	0.34	0.33	0.06	0.32	0.29	0.29	0.27	3.79E-03	3.22E-03	0.25	0.03	0.23	0.21	0.20	0.16	0.15	0.12	0.12	0.09	0.09	0.07	0.06	0.06	0.06	0.05	0.05
64	0.08	0.37	9.73E-03	0.32	0.31	0.30	0.29	0.04	0.04	0.24	0.03	2.44E-03	0.23	0.21	0.21	0.19	0.02	0.15	0.14	5.89E-03	5.72E-03	0.08	0.08	0.06	0.06	0.05	0.05	0.05	0.05
65	0.34	7.99E-03	0.31	0.28	0.27	0.27	0.26	0.24	0.23	0.03	0.22	1.63E-03	0.20	0.19	0.19	0.17	0.16	0.13	0.12	0.12	0.09	0.09	0.07	0.06	0.05	0.05	0.05	0.04	0.04
66	0.33	0.33	0.05	0.04	0.04	0.26	0.26	0.03	0.03	0.21	0.21	0.02	0.20	0.19	0.02	0.17	0.16	0.13	0.12	4.41E-03	0.09	0.07	2.28E-03	0.06	0.05	0.05	0.05	0.04	0.04
67	0.06	6.67E-03	0.30	0.04	0.26	0.25	0.25	0.22	0.22	0.02	0.20	0.19	0.19	0.18	0.18	0.16	0.15	0.12	0.11	0.11	0.09	0.09	0.07	0.06	0.05	0.05	0.04	0.04	0.04
68	0.30	0.30	0.04	0.25	0.24	0.23	0.23	0.21	0.21	0.19	0.19	0.18	0.18	0.01	0.16	0.01	0.14	0.11	0.11	0.08	0.08	0.06	0.06	0.06	0.05	0.04	0.04	0.04	0.04
69	0.30	0.30	0.28	0.25	0.03	0.03	0.23	0.21	0.21	0.02	0.19	0.18	0.18	0.16	0.16	0.15	0.14	0.11	0.11	0.08	0.08	0.06	0.06	0.06	0.05	0.04	0.04	0.04	0.04

Supplementary Table 14. P-values of the Fisher's exact test between pairs of non-psychiatric controls and schizophrenia (1 to 27) modules. Shown are P-values of the hypergeometric test between the controls and schizophrenia modules presented in Chapter 5 section 5.5.1.1.

		Schizophrenia network ->																											
		1	2	3	4	5	6	7	8	9	10	11	12	13	14	15	16	17	18	19	20	21	22	23	24	25	26	27	
Controls network	1	0	1.00	1.00	5.92E-38	1.00	1.00	1.00	1.00	1.69E-03	2.54E-29	1.00	1.00	1.00	1.00	1.00	5.68E-30	0.60	1.00	9.18E-08	1.00	2.04E-06	4.05E-27	1.00	1.00	1.00	1.00	1.10E-05	
	2	3.35E-23	1.00	0.57	1.57E-114	4.80E-07	1.00	1.00	1.00	1.00	0.04	0.34	6.38E-04	1.00	0.65	1.00	1.46E-32	0.51	0.91	2.72E-03	0.41	0.88	3.53E-03	1.00	1.00	1.00	0.87	6.43E-03	
	3	1.00	0	0.94	1.00	1.00	0.94	1.00	0.41	1.00	1.00	1.00	1.00	1.00	6.54E-182	1.00	1.00	1.00	1.00	1.00	1.00	1.00	1.00	8.48E-35	0.62	1.00	1.00	8.66E-34	
	4	1.00	6.96E-278	1.00	1.00	1.00	0.28	1.00	7.23E-07	1.00	0.48	1.00	1.00	0.91	5.63E-59	1.00	1.00	0.85	1.00	1.00	1.00	1.00	1.00	1.52E-37	2.00E-06	0.43	1.00	8.32E-47	
	5	1.00	1.00	1.00	1.00	1.00	1.00	0.31	0.96	1.00	1.00	4.11E-04	1.92E-06	6.41E-14	1.00	3.62E-88	0.11	1.00	0.24	0.15	1.60E-10	0.90	1.00	0.99	0.36	0.42	0.97	1.00	
	6	0.11	1.00	1.88E-12	1.00	0.94	0.98	1.00	0.12	5.05E-05	8.66E-04	1.00	0.63	0.08	1.00	0.99	0.96	0.36	2.79E-04	0.01	0.65	1.63E-09	0.61	0.34	0.60	0.45	0.05	0.99	
	7	4.31E-18	1.00	0.01	6.14E-15	3.21E-06	1.00	1.00	1.00	1.31E-04	0.02	0.36	1.00	0.10	1.00	1.00	0.76	0.43	0.19	3.38E-08	0.05	0.90	0.08	0.46	1.00	0.19	0.02	0.93	
	8	1.00	2.13E-32	0.63	1.00	1.00	1.34E-03	0.99	0	0.83	1.00	0.99	1.00	1.00	3.19E-03	0.40	1.00	0.16	0.32	0.19	0.23	0.95	0.83	0.83	0.26	0.97	1.00	0.93	
	9	1.00	1.00	0.42	1.00	1.00	1.00	0.99	0	0.65	1.00	1.00	1.29	0.99	1.00	4.45E-123	1.00	0.96	0.97	1.00	0.97	1.24E-13	1.00	1.00	2.42E-04	1.00	0.98	1.00	
	10	1.00	1.00	0.03	0.96	0.64	0.21	0.41	0.91	0.24	0.12	0.75	0.06	0.02	1.00	0.02	0.76	0.74	1.16E-03	0.16	0.11	0.01	0.87	0.97	0.02	0.03	3.76E-03	0.97	0.99
	11	6.35E-25	1.00	1.00	1.56E-17	3.61E-08	1.00	1.00	1.00	0.84	7.78E-03	0.12	1.00	0.93	1.00	1.00	6.18E-03	0.91	0.93	0.01	0.10	0.89	3.03E-03	1.00	1.00	0.04	4.26E-03	0.84	
	12	3.35E-21	1.00	2.53E-06	1.88E-04	0.50	0.90	1.00	1.00	0.24	0.03	0.66	0.45	0.76	0.99	1.00	0.01	0.25	0.44	0.16	0.83	0.37	0.01	0.04	0.98	0.36	5.83E-04	0.60	
	13	1.06E-51	1.00	3.29E-04	0.96	0.80	0.84	1.00	1.00	0.01	1.76E-03	0.97	1.00	0.56	1.00	1.00	0.03	3.32E-05	4.66E-03	0.07	0.98	0.04	0.03	0.91	1.00	1.00	0.05	0.91	
	14	1.00	1.00	2.76E-05	1.00	0.97	0.08	7.01E-05	0.97	3.65E-05	0.41	0.90	0.21	1.68E-04	0.99	0.38	1.00	0.16	8.26E-04	0.53	0.02	0.94	0.93	6.77E-04	0.20	0.92	0.99		

15	9.05E-53	1.00	1.00	0	3.41E-21	1.00	1.00	1.00	1.00	0.95	2.39E-06	0.99	0.88	1.00	1.00	4.14E-05	1.00	0.99	5.07E-03	0.86	0.99	0.25	0.88	1.00	0.91	0.49	1.00
16	1.00	2.20E-08	1.00	0.98	0.02	2.20E-03	1.31E-06	2.45E-03	2.06E-06	1.00	2.06E-06	0.07	0.04	1.09E-06	0.97	0.79	0.07	0.74	0.67	0.74	0.26	0.51	0.24	0.22	0.16	0.91	0.05
17	0.08	1.00	0.33	9.21E-09	7.72E-03	0.98	1.00	1.00	0.12	0.28	0.62	0.01	1.00	1.00	0.50	0.33	0.77	0.83	7.60E-05	7.40E-04	0.75	0.28	0.36	0.91	0.50	0.07	0.76
18	6.12E-23	2.48E-20	0.92	0.83	0.45	0.29	0.79	1.00	1.25E-06	0.81	0.13	1.00	1.20E-07	1.00	0.99	1.44E-03	0.86	0.82	1.00	0.19	0.35	0.98	0.69	0.97	0.19	0.45	
19	1.00	1.00	0.05	3.69E-03	1.00	0.51	1.62E-184	0.98	0.64	0.96	0.86	0.40	1.00	3.37E-60	1.00	0.13	0.70	1.00	0.64	1.82E-07	1.00	0.99	0.64	0.94	0.71	0.82	
20	1.06E-17	1.00	0.05	1.08E-13	1.94E-06	0.94	1.00	0.36	0.85	0.20	5.68E-04	0.53	0.45	1.00	0.34	0.34	0.10	0.07	0.97	0.90	0.03	0.64	0.94	0.71	8.89E-03	0.82	
21	1.00	5.40E-141	0.90	1.00	1.00	2.38E-04	0.96	0.02	0.96	1.00	0.91	1.00	0.90	3.20E-14	1.00	9.44E-03	0.49	1.00	0.99	0.93	1.00	0.46	1.73E-04	1.00	0.98	1.56E-04	
22	9.71E-32	1.00	0.34	4.19E-13	9.31E-11	0.75	1.00	1.00	0.91	0.12	5.43E-05	0.99	0.97	1.00	0.03	0.83	0.86	4.08E-05	0.91	0.84	0.41	0.67	0.83	0.45	0.46	0.99	
23	1.99E-10	1.00	0.01	0.01	2.41E-04	0.94	1.00	1.00	0.13	0.66	0.71	0.77	0.11	1.00	0.99	0.56	0.77	0.68	0.06	0.49	0.77	0.06	0.76	0.83	0.97	0.02	0.41
24	9.74E-24	1.00	0.06	2.08E-06	0.63	0.18	0.81	1.00	0.55	0.03	0.68	2.49E-08	0.02	1.00	0.57	0.97	0.16	0.89	1.00	1.00	0.39	0.23	0.82	0.88	0.93	0.43	0.61
25	1.00	1.00	1.00	1.26E-21	3.35E-18	0.68	1.00	2.30E-19	1.00	0.84	2.03E-14	0.92	0.83	1.00	1.00E-13	0.73	0.89	0.09	1.03E-03	1.00	0.99	0.97	1.00	0.01	0.31	0.99	
26	6.65E-22	1.00	1.00	5.82E-03	7.16E-03	0.94	1.00	0.16	0.34	1.13E-04	0.32	1.00	0.16	1.00	0.98	0.49	0.74	0.15	0.02	0.02	0.03	0.07	0.99	0.91	0.66	0.19	0.99
27	1.00	1.00	0.15	1.00	0.54	0.43	3.88E-04	0.77	0.05	0.97	0.43	0.07	0.01	0.96	1.61E-03	0.97	0.79	8.95E-03	0.89	0.02	0.27	1.00	0.91	0.05	0.24	0.79	0.85
28	0.96	1.10E-34	0.69	1.00	0.99	0.32	1.00	0.94	0.92	0.78	0.66	0.74	0.59	0.55	0.99	0.29	0.46	0.97	0.87	0.72	0.08	0.82	0.75	0.83	0.63	0.77	0.74
29	1.00	1.00	0.11	1.00	0.28	0.33	0.71	2.70E-03	0.06	0.92	0.64	0.99	3.85E-03	0.99	0.75	0.86	0.54	0.12	0.02	0.30	0.83	0.02	0.99	2.00E-03	0.05	0.89	0.79
30	9.09E-28	1.00	1.00	2.69E-11	0.96	0.93	0.96	0.97	0.97	0.19	0.78	3.73E-03	0.85	0.98	1.00	1.00	0.77	0.45	0.97	2.00E-05	0.45	0.47	0.88	0.99	0.04	0.89	
31	1.00	1.00	1.00	4.34E-05	1.00	0.82	1.40E-09	0.94	0.89	0.54	0.49	1.77E-09	0.58	0.98	0.02	0.94	9.34E-03	0.02	0.61	1.59E-11	0.33	0.93	0.93	2.61E-03	1.00	0.82	0.88
32	1.00	0	0.03	1.00	1.00	1.00	1.00	0.99	0.99	1.00	0.99	1.00	0.85	1.21E-23	1.00	0.97	1.00	0.97	0.65	1.00	0.96	0.81	4.53E-09	0.96	0.98	1.00	5.42E-07
33	1.76E-03	1.00	0.39	1.00	0.45	0.97	0.96	0.92	0.17	0.02	0.75	0.17	0.16	1.00	0.95	0.39	0.76	0.27	0.06	1.01E-03	0.36	0.91	0.12	0.62	0.05	0.85	

34	1.00	1.91E-20	1.00	1.00	0.84	0.79	0.42	0.91	0.43	0.94	0.74	0.34	4.08E-09	0.99	0.88	0.46	0.17	0.83	0.90	0.22	0.77	5.00E-04	0.89	0.89	0.38	4.73E-05	
35	3.92E-15	1.00	9.72E-03	0.90	0.26	0.30	1.00	0.81	0.41	0.65	1.00	0.28	1.00	0.98	0.25	0.64	0.49	0.23	0.52	6.90E-03	0.13	0.83	0.95	0.98	0.38	1.00	
36	8.62E-10	1.00	0.18	0.77	0.40	0.52	1.00	3.57E-04	0.06	0.11	0.88	0.05	0.91	0.99	0.74	0.06	0.03	0.37	0.99	0.16	0.19	0.98	0.31	0.56	0.63	0.46	
37	0.92	6.91E-06	3.65E-03	1.00	0.83	0.05	0.97	0.72	1.00	0.93	0.30	0.92	0.98	1.00	0.99	1.14E-09	0.43	1.00	0.97	4.31E-04	0.39	1.00	0.84	0.97	0.89	0.64	
38	1.00	1.00	0.42	0.96	0.86	0.28	0.05	0.76	6.47E-03	0.79	0.96	0.68	0.02	0.71	0.40	0.96	0.91	0.06	0.28	0.04	0.66	0.91	0.70	0.41	0.96	0.23	1.00
39	1.00	1.00	2.28E-03	1.00	0.95	0.64	9.26E-04	0.76	0.91	0.53	0.99	1.19E-05	0.38	0.94	9.95E-09	0.89	0.50	2.47E-05	0.50	0.87	0.78	0.49	0.48	0.34	0.56	0.99	
40	1.46E-05	1.00	2.63E-03	0.99	0.15	0.82	0.10	0.84	0.99	0.09	0.58	9.04E-05	0.95	0.99	0.91	0.95	0.53	0.03	0.56	1.00	4.09E-05	0.37	0.90	0.35	0.79	0.59	0.94
41	1.00	1.00	1.00	1.00	1.00	0.97	4.26E-13	0.99	0.04	0.98	0.05	4.79E-16	6.01E-04	0.96	1.82E-43	0.97	0.98	0.57	0.18	0.02	0.79	0.98	2.66E-06	1.00	0.70	1.00	
42	0.81	1.00	0.60	0.98	0.64	0.27	0.02	0.53	0.14	0.40	0.75	5.34E-03	0.31	1.00	0.88	0.27	0.16	0.33	0.50	0.35	0.18	0.51	0.83	0.35	0.13	0.45	0.90
43	1.00	9.03E-189	7.42E-04	0.99	0.98	0.98	1.00	0.41	1.00	0.99	1.00	1.00	0.97	6.11E-09	1.00	0.92	0.37	1.00	0.69	1.00	0.99	1.00	2.58E-29	0.10	1.00	0.88	1.83E-04
44	1.00	1.04E-06	0.69	1.00	1.00	4.11E-03	0.89	9.60E-07	0.99	1.00	0.70	0.85	0.98	0.67	0.97	0.98	0.14	0.81	0.93	1.00	0.61	0.94	0.89	0.75	0.40	0.99	0.95
45	0.31	0.99	0.41	0.85	0.15	0.76	0.97	0.89	0.12	0.22	0.70	0.88	0.30	0.98	0.93	0.95	0.24	0.10	0.79	0.98	0.21	0.99	0.90	0.55	0.10	0.88	1.00
46	1.00	1.00	0.76	0.94	0.32	0.65	0.43	0.69	0.08	0.73	0.70	0.88	8.45E-04	0.57	0.87	0.55	1.00	0.17	0.83	0.76	1.00	0.77	0.86	0.14	0.14	0.02	0.96
47	1.00	1.00	0.26	0.98	0.73	0.71	0.33	1.14E-07	0.11	0.81	0.11	0.66	0.03	0.99	0.02	0.85	0.70	0.90	0.96	0.29	0.32	0.47	0.81	0.58	0.58	0.77	1.00
48	0.99	1.00	0.54	0.94	0.41	0.58	0.66	0.01	0.57	0.15	0.20	0.72	0.57	0.99	0.72	0.01	0.63	0.55	0.02	0.06	0.66	0.83	0.77	0.76	1.36E-04	0.73	1.00
49	0.33	1.00	0.99	0.91	0.04	0.89	0.97	0.61	0.32	0.69	0.71	0.70	0.52	0.62	0.03	0.31	0.82	0.77	0.33	0.25	0.77	0.49	0.67	0.90	0.03	0.36	1.00
50	1.00	0.81	0.97	0.35	0.17	0.61	0.80	0.94	0.85	0.19	0.01	0.91	0.90	0.96	0.17	1.59E-11	0.98	0.98	0.46	8.77E-05	0.92	1.00	1.00	0.88	0.06	3.92E-03	0.85
51	1.00	1.00	0.58	0.99	0.20	0.79	1.00	0.14	0.30	0.42	0.44	0.42	6.42E-03	0.95	0.03	0.57	0.10	0.87	0.44	3.52E-03	0.92	0.68	0.87	0.60	0.32	0.85	1.00
52	1.00	1.00	1.00	1.00	0.37	0.98	2.13E-106	0.98	1.00	1.00	0.99	1.79E-45	0.95	1.00	7.48E-108	0.98	1.00	1.00	1.00	1.00	1.00	1.00	1.00	0.84	1.00	0.82	1.00
53	1.00	3.40E-86	0.57	1.00	0.92	1.00	1.00	0.35	0.98	1.00	1.00	0.99	0.49	2.18E-06	1.00	0.49	0.97	0.96	0.81	0.93	1.00	0.88	1.13E-04	0.84	0.54	1.00	5.33E-05

54	1.00	0.82	1.00	1.00	0.98	0.30	0.79	4.00E-154	0.74	0.31	0.95	0.99	0.84	0.80	0.02	0.88	0.68	0.62	0.58	0.93	0.89	0.88	1.00	0.54	0.83	1.00	0.49
55	1.00	5.13E-04	1.00	0.81	0.17	0.09	0.98	9.11E-04	0.53	0.76	6.66E-04	0.81	0.81	0.05	0.88	1.00	0.02	0.80	1.00	0.46	1.00	0.59	0.82	0.81	0.24	1.00	0.46
56	2.95E-03	0.94	0.08	0.77	0.28	0.91	0.75	0.86	0.14	0.46	0.90	0.73	0.89	0.97	0.96	0.56	0.78	0.26	0.91	0.89	0.11	0.09	1.00	0.77	0.77	0.40	0.73
57	1.00	4.58E-63	1.00	0.94	0.94	0.85	0.66	0.45	0.97	0.98	1.00	0.85	0.96	6.20E-07	0.94	1.00	0.72	0.90	1.00	0.85	1.00	1.00	0.01	0.14	1.00	1.00	0.69
58	0.81	5.74E-03	0.21	3.43E-03	1.00	0.97	0.98	0.78	0.89	0.35	0.25	0.64	0.42	0.08	0.77	0.73	0.92	0.90	0.02	0.85	0.79	0.19	0.04	0.72	0.72	0.34	0.69
59	1.00	4.26E-43	0.28	0.23	0.48	0.59	0.35	0.50	0.94	1.00	0.17	0.94	0.94	0.27	0.91	0.89	0.89	0.59	0.85	1.00	0.75	1.00	0.68	0.67	0.30	0.65	1.00
60	1.00	0.86	0.91	0.08	0.01	0.71	1.00	0.76	0.49	0.59	0.09	1.00	1.00	0.79	0.76	0.14	0.72	0.69	1.00	4.68E-04	0.55	0.18	0.48	1.00	0.48	0.46	1.00
61	0.94	1.00	0.55	0.99	0.40	0.06	0.02	0.92	1.00	0.29	0.80	0.80	0.79	1.00	0.39	1.00	0.70	0.67	0.02	0.23	0.17	1.00	1.00	3.50E-03	0.46	0.44	1.00
62	0.73	0.89	0.20	0.92	0.40	0.06	0.50	1.00	0.71	0.85	0.80	0.80	0.21	0.77	1.00	0.71	1.00	1.00	0.64	0.23	1.00	1.00	1.00	0.13	1.00	1.00	1.00
63	1.00	0.02	1.00	0.99	0.92	0.44	0.49	2.77E-34	0.71	0.85	0.48	0.47	1.00	0.76	0.74	0.71	1.00	1.00	0.64	1.00	1.00	1.00	0.46	1.00	0.46	1.00	1.00
64	0.99	1.00	0.12	0.73	0.08	0.09	1.00	0.67	0.39	0.50	0.02	0.17	0.17	1.00	1.00	0.67	0.66	0.63	0.07	0.56	1.00	0.03	0.43	1.00	0.11	1.00	1.00
65	0.64	0.99	1.00	1.00	0.22	0.93	0.15	0.05	0.86	0.77	0.72	0.13	0.71	0.31	0.65	0.62	1.00	0.05	0.55	0.51	1.00	0.43	0.38	0.38	0.38	0.36	0.35
66	0.98	0.67	0.09	0.96	0.10	0.75	1.00	0.05	1.00	0.77	0.36	0.71	0.71	1.00	1.00	0.62	0.24	1.00	0.55	0.03	0.44	0.11	0.38	1.00	1.00	1.00	0.35
67	0.04	0.97	0.75	2.52E-06	0.01	1.00	0.58	0.85	0.84	0.40	0.12	0.69	0.68	1.00	1.00	0.06	0.58	1.00	0.53	0.49	1.00	0.41	1.00	0.36	1.00	1.00	1.00
68	0.94	0.79	1.00	1.00	1.00	0.20	2.24E-03	1.00	0.50	0.72	0.67	0.66	1.00	1.00	0.06	0.05	0.05	1.00	1.00	0.46	1.00	1.00	1.00	8.24E-04	1.00	1.00	1.00
69	1.00	2.50E-12	0.68	0.94	0.77	0.08	0.84	0.03	0.82	1.00	1.00	0.66	1.00	0.02	0.23	1.00	0.56	1.00	1.00	1.00	1.00	8.69E-03	0.34	1.00	1.00	1.00	1.00

Supplementary Table 15. P-values of the Fisher's exact test between pairs of non-psychiatric controls and schizophrenia (28 to 54) modules. Shown are P-values of the hypergeometric test between the controls and schizophrenia modules presented in Chapter 5 section 5.5.1.1.

	Schizophrenia network ->																											
	28	29	30	31	32	33	34	35	36	37	38	39	40	41	42	43	44	45	46	47	48	49	50	51	52	53	54	
1	1.00	1.00	1.00	1.59E-05	1.00	1.00	1.00	0.98	1.00	1.68E-10	1.00	0.41	1.00	1.00	0.86	1.00	1.00	0.96	1.00	0.95	3.94E-06	1.00	1.00	0.93	1.00	1.00	1.00	0.90
2	0.91	0.06	0.61	0.04	1.00	0.99	0.01	0.03	7.28E-05	0.04	0.66	0.37	0.80	0.90	0.49	0.88	0.14	0.88	0.95	0.27	0.95	0.70	0.03	0.94	0.58	0.02	0.06	0.06
3	1.00	0.98	1.00	1.00	0.29	7.52E-14	2.48E-13	0.99	0.95	0.98	1.00	1.00	1.00	1.04E-14	1.00	0.98	0.94	0.86	0.99	0.98	1.00	0.93	1.00	0.99	0.76	0.89	0.97	0.97
4	0.24	1.00	0.16	0.02	0.30	1.50E-08	0.88	0.49	0.37	0.41	0.84	0.98	0.83	0.12	0.98	0.28	0.98	0.89	0.33	0.84	0.97	0.78	0.96	1.05E-03	0.17	0.68	0.82	0.82
5	0.53	1.49E-24	0.17	0.14	1.00	0.99	1.00	0.30	0.97	1.00	0.11	0.91	0.58	0.75	1.00	0.21	0.46	0.63	2.67E-24	0.96	0.22	0.24	0.52	0.20	8.61E-03	0.02	0.33	0.33
6	0.85	1.00	6.27E-03	0.13	1.00	0.98	0.75	0.30	0.82	5.94E-03	0.05	0.02	0.87	1.00	0.08	0.77	0.08	0.44	0.84	0.62	0.88	0.70	0.17	0.51	1.00	1.00	0.94	0.94
7	0.95	0.99	0.05	0.55	1.00	0.93	0.82	0.57	0.96	0.02	0.39	5.59E-04	0.98	0.99	0.08	0.54	0.05	0.21	0.97	0.30	0.99	0.95	0.66	0.17	0.96	0.82	1.11E-04	0.82
8	0.88	0.99	0.24	0.57	0.51	0.01	5.47E-110	0.87	0.31	0.97	0.56	0.69	0.78	0.24	0.33	0.53	0.49	0.97	0.77	0.83	0.68	0.27	0.78	0.85	0.18	0.94	0.24	0.24
9	0.88	0.97	0.98	0.96	0.79	0.82	1.00	0.97	0.93	0.99	0.39	0.94	0.99	1.00	1.00	0.72	0.88	0.54	0.85	0.80	1.00	0.12	0.76	0.96	0.07	0.75	0.43	0.43
10	1.22E-04	0.89	0.02	0.53	0.67	0.91	0.97	4.49E-03	0.21	0.78	6.76E-06	0.03	0.26	0.80	0.69	0.32	0.52	0.03	2.31E-03	0.79	0.90	0.77	0.02	0.82	0.15	0.93	0.68	0.68
11	0.88	0.05	0.28	0.58	1.00	0.76	1.00	0.85	0.44	0.74	0.74	0.55	0.42	0.54	0.09	0.02	0.48	0.48	0.91	0.60	0.02	0.98	0.04	0.59	0.93	0.73	1.00	1.00
12	0.65	0.93	0.50	0.21	0.97	0.99	0.99	0.54	0.94	0.14	0.29	0.10	0.40	0.08	0.29	0.50	0.34	0.04	0.80	0.96	0.88	0.98	0.03	0.80	0.93	0.46	0.65	0.65
13	0.56	0.98	0.88	0.55	0.99	0.44	0.86	0.83	0.98	0.62	0.28	0.91	0.21	0.98	0.84	0.38	0.59	3.54E-03	0.66	0.41	0.14	0.74	0.97	0.95	0.74	0.11	0.89	0.89

14	0.16	0.82	0.12	0.13	0.66	0.98	0.10	0.30	0.60	0.36	0.08	0.50	0.37	0.98	0.36	0.99	0.31	0.43	0.04	0.96	0.87	0.89	0.15	0.33	0.73	1.00	0.17
15	1.00	1.00	0.90	0.39	1.00	0.99	0.94	1.00	0.78	0.34	0.98	0.81	0.97	0.89	0.98	0.72	0.98	1.00	1.00	0.73	0.87	0.72	0.28	0.78	0.73	0.04	1.00
16	0.68	0.39	0.36	0.01	0.90	0.72	1.00	0.16	0.73	2.00E-03	0.28	0.05	0.64	0.97	0.02	0.88	0.63	0.37	0.28	0.95	0.50	0.97	0.76	0.04	0.20	0.87	
17	0.40	0.05	0.26	2.79E-03	1.00	0.60	0.77	0.51	0.14	0.61	0.27	0.52	0.19	1.00	0.76	0.94	0.24	0.80	9.74E-03	0.69	0.84	0.87	0.43	0.94	0.44	0.90	0.15
18	0.94	0.99	1.00	0.89	0.30	0.94	0.93	0.26	0.96	0.10	0.99	0.95	0.95	0.25	0.96	0.93	0.99	0.99	0.94	1.00	0.97	0.83	0.12	0.68	1.00	0.58	
19	1.26E-03	0.67	0.99	0.26	0.61	0.99	1.00	0.08	0.88	1.00	1.90E-04	0.28	0.64	0.79	0.18	0.55	0.51	5.25E-04	0.32	0.13	0.06	0.61	0.81	0.45	3.97E-04	0.84	
20	0.83	0.44	0.25	0.04	0.99	0.34	0.98	0.74	0.26	0.11	0.49	0.30	0.19	0.91	0.57	0.46	0.42	0.81	0.96	0.55	0.98	0.56	0.77	1.00	1.00	0.85	0.51
21	0.70	1.00	0.69	0.98	2.84E-04	1.75E-04	0.39	0.74	0.91	1.00	1.00	0.71	1.00	0.07	0.60	0.49	0.88	0.96	0.31	0.97	1.00	1.00	1.00	1.00	2.48E-03	0.51	0.78
22	0.75	0.52	0.84	0.25	1.00	0.86	0.92	0.48	0.74	0.01	0.24	0.44	0.43	0.99	0.48	1.00	0.35	1.00	0.92	0.82	0.95	1.00	0.38	0.84	1.00	0.02	0.74
23	0.24	0.82	0.06	0.98	0.55	1.00	1.00	0.62	0.23	0.65	0.24	0.73	0.03	0.89	0.12	0.14	0.06	0.46	0.58	0.38	0.04	0.90	0.38	0.27	1.00	0.20	0.39
24	0.82	1.00	0.21	0.80	0.87	0.99	1.00	0.22	0.83	0.35	0.02	0.97	0.92	0.96	0.46	0.98	0.98	0.45	0.98	0.59	0.58	0.90	0.89	1.00	0.80	1.00	0.38
25	0.21	7.78E-03	1.00	0.96	0.21	0.99	0.97	0.25	1.13E-17	0.99	0.99	0.33	0.06	0.94	0.54	0.29	0.26	0.98	0.98	9.41E-10	0.30	0.62	0.33	0.49	1.00	8.43E-05	0.71
26	0.94	0.02	0.35	0.08	1.00	1.00	0.84	0.13	0.60	0.36	0.80	0.75	0.29	1.00	0.12	0.15	0.55	0.98	0.87	0.93	0.05	0.87	0.31	0.47	0.41	0.74	1.00
27	0.69	0.67	0.10	0.99	0.87	0.92	0.97	0.32	0.93	0.80	0.90	0.87	0.05	0.50	0.21	0.07	0.55	6.48E-04	0.15	0.93	0.50	0.60	0.13	1.00	0.41	0.38	0.69
28	0.55	0.03	0.22	0.94	0.24	0.72	0.99	0.59	0.11	0.21	0.78	0.73	0.09	0.20	0.32	0.38	0.86	0.33	0.67	0.49	0.93	1.00	0.85	1.00	1.00	0.01	0.32
29	0.04	0.60	0.27	0.35	0.58	0.40	1.00	0.39	0.53	0.99	0.87	7.43E-03	1.00E-03	1.00	0.09	0.11	0.10	0.71	0.65	0.11	0.71	0.85	0.84	0.18	0.73	0.71	1.00
30	0.63	1.00	0.40	2.62E-03	0.87	0.59	0.57	0.45	0.99	2.35E-03	0.82	0.79	1.00	0.99	0.12	0.93	0.61	0.85	0.59	1.00	1.00	0.25	1.00	1.00	1.00	0.31	1.00
31	0.17	0.99	0.66	0.95	1.00	0.98	0.56	0.75	0.43	0.82	0.21	0.78	0.61	1.00	0.21	0.03	0.25	0.96	0.03	1.00	0.19	0.10	0.03	0.74	0.33	1.00	0.63
32	0.98	0.98	0.93	0.76	0.99	0.17	5.70E-08	0.94	0.98	0.05	1.00	1.00	0.58	4.65E-16	0.95	0.92	8.92E-03	1.00	1.00	0.89	0.18	1.00	1.00	0.73	1.00	0.67	1.00
33	0.13	0.88	0.73	0.60	0.99	0.68	0.66	0.71	0.93	0.46	3.54E-03	0.57	0.39	1.00	7.32E-03	1.00	0.76	0.82	0.03	0.37	0.63	1.42E-03	0.79	0.14	1.00	0.66	0.61

34	0.66	0.94	0.43	0.29	0.16	0.23	0.02	0.69	0.93	0.77	0.77	0.73	0.72	0.46	0.82	0.22	0.35	1.00	0.77	0.88	0.88	1.00	0.45	0.35	0.30	0.65	1.00	
35	0.03	1.00	0.74	0.19	0.74	0.85	0.70	0.60	0.59	0.02	0.33	0.08	0.64	1.00	0.21	0.97	0.68	1.00	0.71	0.57	0.85	0.17	0.01	1.00	1.00	1.00	0.56	
36	0.95	0.37	0.30	0.95	0.94	0.93	0.68	0.76	0.57	0.84	0.32	0.27	0.63	0.98	0.20	0.47	0.97	0.93	0.71	0.12	2.85E-03	0.41	0.74	1.00	0.02	0.60	0.20	
37	0.92	6.91E-06	3.65E-03	1.00	0.83	0.05	0.97	0.72	1.00	0.93	0.30	0.92	0.98	0.69	1.00	0.99	1.14E-09	0.43	1.00	0.97	4.31E-04	0.39	1.00	0.84	0.97	0.89	0.64	
38	1.00	1.00	0.42	0.96	0.86	0.28	0.05	0.76	6.47E-03	0.79	0.96	0.68	0.02	0.71	0.40	0.96	0.91	0.06	0.28	0.04	0.66	0.91	0.70	0.41	0.96	0.23	1.00	
39	1.00	1.00	2.28E-03	1.00	0.95	0.64	9.26E-04	0.76	0.91	0.53	0.99	1.19E-05	0.38	0.94	9.95E-09	0.89	0.50	2.47E-05	0.50	0.87	2.42E-04	0.78	0.49	0.48	0.34	0.56	0.99	
40	1.46E-05	1.00	2.63E-03	0.99	0.15	0.82	0.10	0.84	0.99	0.09	0.58	9.04E-05	0.95	0.99	0.91	0.95	0.53	0.03	0.56	1.00	4.09E-05	0.37	0.90	0.35	0.79	0.59	0.94	
41	1.00	1.00	1.00	1.00	1.00	0.97	4.26E-13	0.99	0.04	0.98	0.05	4.79E-16	6.01E-04	0.96	1.82E-43	0.97	0.98	0.57	0.18	0.02	0.79	0.98	0.95	2.66E-06	1.00	0.70	1.00	
42	0.81	1.00	0.60	0.98	0.64	0.27	0.02	0.53	0.14	0.40	0.75	5.34E-03	0.31	1.00	0.88	0.27	0.16	0.33	0.50	0.35	0.18	0.51	0.83	0.35	0.13	0.45	0.90	
43	1.00	9.03E-189	7.42E-04	0.99	0.98	0.98	1.00	0.41	1.00	0.99	1.00	1.00	0.97	6.11E-09	1.00	0.92	0.37	1.00	0.69	1.00	0.99	1.00	2.58E-29	0.10	1.00	0.88	1.83E-04	
44	1.00	1.04E-06	0.69	1.00	1.00	4.11E-03	0.89	9.60E-07	0.99	1.00	0.70	0.85	0.98	0.67	0.97	0.98	0.14	0.81	0.93	1.00	0.61	0.94	0.89	0.75	0.40	0.99	0.95	
45	0.31	0.99	0.41	0.85	0.15	0.76	0.97	0.89	0.12	0.22	0.70	0.88	0.30	0.98	0.93	0.95	0.24	0.10	0.79	0.98	0.21	0.99	0.90	0.55	0.10	0.88	1.00	
46	1.00	1.00	0.76	0.94	0.32	0.65	0.43	0.69	0.08	0.73	0.70	0.88	8.45E-04	0.57	0.87	0.55	1.00	0.17	0.83	0.76	1.00	0.77	0.86	0.14	0.14	0.02	0.96	
47	1.00	1.00	0.26	0.98	0.73	0.71	0.33	1.14E-07	0.11	0.81	0.11	0.66	0.03	0.99	0.02	0.85	0.70	0.90	0.96	0.29	0.32	0.47	0.81	0.58	0.58	0.77	1.00	
48	0.99	1.00	0.54	0.94	0.41	0.58	0.66	0.01	0.57	0.15	0.20	0.72	0.57	0.99	0.72	0.01	0.63	0.55	0.02	0.06	0.66	0.83	0.77	0.76	1.36E-04	0.73	1.00	
49	0.33	1.00	0.99	0.91	0.04	0.89	0.97	0.61	0.32	0.69	0.71	0.70	0.52	0.62	0.03	0.31	0.82	0.77	0.33	0.25	0.77	0.49	0.67	0.90	0.03	0.36	1.00	
50	1.00	0.81	0.97	0.35	0.17	0.61	0.80	0.94	0.85	0.19	0.01	0.91	0.90	0.96	0.17	1.59E-11	0.98	0.98	0.46	8.77E-05	0.92	1.00	1.00	0.88	0.06	3.92E-03	0.85	
51	1.00	1.00	0.58	0.99	0.20	0.79	1.00	0.14	0.30	0.42	0.44	0.42	6.42E-03	0.95	0.03	0.57	0.10	0.87	0.44	3.52E-03	0.92	0.68	0.87	0.60	0.32	0.85	1.00	
52	1.00	1.00	1.00	1.00	0.37	0.98	2.13E-106	0.98	1.00	1.00	0.99	1.79E-45	0.95	1.00	7.48E-108	0.98	1.00	1.00	1.00	1.00	1.00	1.00	1.00	1.00	0.84	1.00	0.82	1.00
53	1.00	3.40E-86	0.57	1.00	0.92	1.00	1.00	0.35	0.98	1.00	1.00	0.99	0.49	2.18E-06	1.00	0.49	0.97	0.96	0.81	0.93	1.00	0.88	1.13E-04	0.84	0.54	1.00	5.33E-05	

54	1.00	0.82	1.00	1.00	0.98	0.30	0.79	4.00E-154	0.74	0.31	0.95	0.99	0.84	0.80	0.02	0.88	0.68	0.62	0.58	0.93	0.89	0.88	1.00	0.54	0.83	1.00	0.49
55	1.00	5.13E-04	1.00	0.81	0.17	0.09	0.98	9.11E-04	0.53	0.76	6.66E-04	0.81	0.81	0.05	0.88	1.00	0.02	0.80	1.00	0.46	1.00	0.59	0.82	0.81	0.24	1.00	0.46
56	2.95E-03	0.94	0.08	0.77	0.28	0.91	0.75	0.86	0.14	0.46	0.90	0.73	0.89	0.97	0.96	0.56	0.78	0.26	0.91	0.89	0.11	0.09	1.00	0.77	0.77	0.40	0.73
57	1.00	4.58E-63	1.00	0.94	0.94	0.85	0.66	0.45	0.97	0.98	1.00	0.85	0.96	6.20E-07	0.94	1.00	0.72	0.90	1.00	0.85	1.00	1.00	0.01	0.14	1.00	1.00	0.69
58	0.81	5.74E-03	0.21	3.43E-03	1.00	0.97	0.98	0.78	0.89	0.35	0.25	0.64	0.42	0.08	0.77	0.73	0.92	0.90	0.02	0.85	0.79	0.19	0.04	0.72	0.72	0.34	0.69
59	1.00	4.26E-43	0.28	0.23	0.48	0.59	0.35	0.50	0.94	1.00	0.17	0.94	0.94	0.27	0.91	0.89	0.89	0.59	0.85	1.00	0.75	1.00	0.68	0.67	0.30	0.65	1.00
60	1.00	0.86	0.91	0.08	0.01	0.71	1.00	0.76	0.49	0.59	0.09	1.00	1.00	0.79	0.76	0.14	0.72	0.69	1.00	4.68E-04	0.55	0.18	0.48	1.00	0.48	0.46	1.00
61	0.94	1.00	0.55	0.99	0.40	0.06	0.02	0.92	1.00	0.29	0.80	0.80	0.79	1.00	0.39	1.00	0.70	0.67	0.02	0.23	0.17	1.00	1.00	3.50E-03	0.46	0.44	1.00
62	0.73	0.89	0.20	0.92	0.40	0.06	0.50	1.00	0.71	0.85	0.80	0.80	0.21	0.77	1.00	0.71	1.00	1.00	0.64	0.23	1.00	1.00	1.00	0.13	1.00	1.00	1.00
63	1.00	0.02	1.00	0.99	0.92	0.44	0.49	2.77E-34	0.71	0.85	0.48	0.47	1.00	0.76	0.74	0.71	1.00	1.00	0.64	1.00	1.00	1.00	0.46	1.00	0.46	1.00	1.00
64	0.99	1.00	0.12	0.73	0.08	0.09	1.00	0.67	0.39	0.50	0.02	0.17	0.17	1.00	1.00	0.67	0.66	0.63	0.07	0.56	1.00	0.03	0.43	1.00	0.11	1.00	1.00
65	0.64	0.99	1.00	1.00	0.22	0.93	0.15	0.05	0.86	0.77	0.72	0.13	0.71	0.31	0.65	0.62	1.00	0.05	0.55	0.51	1.00	0.43	0.38	0.38	0.38	0.36	0.35
66	0.98	0.67	0.09	0.96	0.10	0.75	1.00	0.05	1.00	0.77	0.36	0.71	0.71	1.00	1.00	0.62	0.24	1.00	0.55	0.03	0.44	0.11	0.38	1.00	1.00	1.00	0.35
67	0.04	0.97	0.75	2.52E-06	0.01	1.00	0.58	0.85	0.84	0.40	0.12	0.69	0.68	1.00	1.00	0.06	0.58	1.00	0.53	0.49	1.00	0.41	1.00	0.36	1.00	1.00	1.00
68	0.94	0.79	1.00	1.00	1.00	0.20	2.24E-03	1.00	0.50	0.72	0.67	0.66	1.00	1.00	0.06	0.05	0.05	1.00	1.00	0.46	1.00	1.00	1.00	1.00	8.24E-04	1.00	1.00
69	1.00	2.50E-12	0.68	0.94	0.77	0.08	0.84	0.03	0.82	1.00	1.00	0.66	1.00	0.02	0.23	1.00	0.56	1.00	1.00	1.00	1.00	1.00	8.69E-03	0.34	1.00	1.00	1.00

Appendix B – Supplementary material of Chapter 7

This page has been removed by the author of this thesis for copyright reasons.

<https://dx.doi.org/10.4161/epi.27806>

This page has been removed by the author of this thesis for copyright reasons.

<https://dx.doi.org/10.4161/epi.27806>

This page has been removed by the author of this thesis for copyright reasons.

<https://dx.doi.org/10.4161/epi.27806>

This page has been removed by the author of this thesis for copyright reasons.

<https://dx.doi.org/10.4161/epi.27806>

This page has been removed by the author of this thesis for copyright reasons.

<https://dx.doi.org/10.4161/epi.27806>

This page has been removed by the author of this thesis for copyright reasons.

<https://dx.doi.org/10.4161/epi.27806>

This page has been removed by the author of this thesis for copyright reasons.

<https://dx.doi.org/10.4161/epi.27806>

This page has been removed by the author of this thesis for copyright reasons.

<https://dx.doi.org/10.4161/epi.27806>

This page has been removed by the author of this thesis for copyright reasons.

<https://dx.doi.org/10.4161/epi.27806>

This page has been removed by the author of this thesis for copyright reasons.

<https://dx.doi.org/10.4161/epi.27806>

This page has been removed by the author of this thesis for copyright reasons.

<https://dx.doi.org/10.4161/epi.27806>

This page has been removed by the author of this thesis for copyright reasons.

<https://dx.doi.org/10.4161/epi.27806>

This page has been removed by the author of this thesis for copyright reasons.

<https://dx.doi.org/10.4161/epi.27806>

This page has been removed by the author of this thesis for copyright reasons.

<https://dx.doi.org/10.4161/epi.27806>

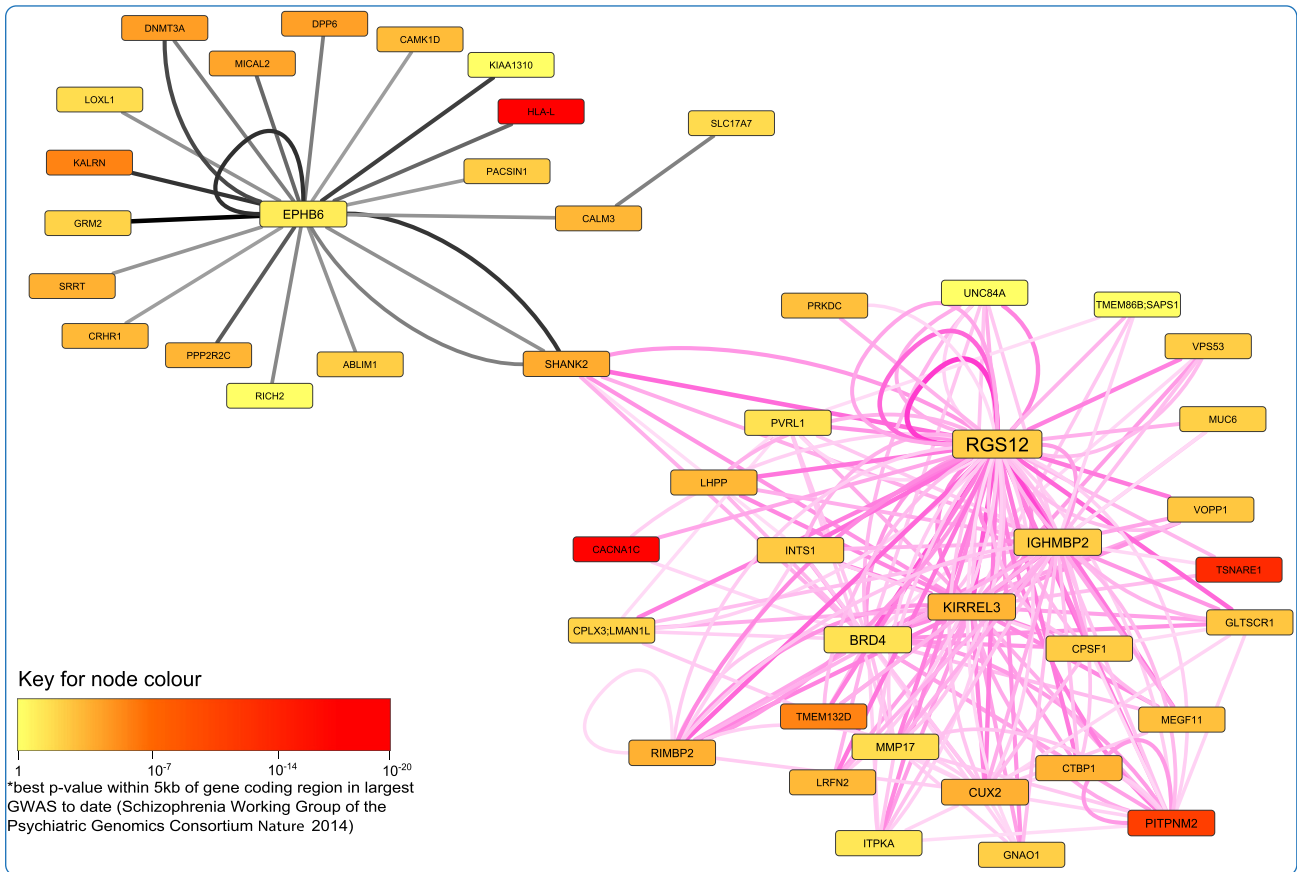
This page has been removed by the author of this thesis for copyright reasons.

<https://dx.doi.org/10.4161/epi.27806>

This page has been removed by the author of this thesis for copyright reasons.

<https://dx.doi.org/10.4161/epi.27806>

Appendix C – Additional publications



Methylomic profiling of human brain tissue supports a neurodevelopmental origin for schizophrenia

Pidsley *et al.*

RESEARCH

Open Access

Methylomic profiling of human brain tissue supports a neurodevelopmental origin for schizophrenia

Ruth Pidsley^{1,2}, Joana Viana³, Eilis Hannon³, Helen Spiers¹, Claire Troakes¹, Safa Al-Saraj¹, Naguib Mechawar⁴, Gustavo Turecki⁴, Leonard C Schalkwyk^{1,5}, Nicholas J Bray¹ and Jonathan Mill^{1,3*}

Abstract

Background: Schizophrenia is a severe neuropsychiatric disorder that is hypothesized to result from disturbances in early brain development. There is mounting evidence to support a role for developmentally regulated epigenetic variation in the molecular etiology of the disorder. Here, we describe a systematic study of schizophrenia-associated methylomic variation in the adult brain and its relationship to changes in DNA methylation across human fetal brain development.

Results: We profile methylomic variation in matched prefrontal cortex and cerebellum brain tissue from schizophrenia patients and controls, identifying disease-associated differential DNA methylation at multiple loci, particularly in the prefrontal cortex, and confirming these differences in an independent set of adult brain samples. Our data reveal discrete modules of co-methylated loci associated with schizophrenia that are enriched for genes involved in neurodevelopmental processes and include loci implicated by genetic studies of the disorder. Methylomic data from human fetal cortex samples, spanning 23 to 184 days post-conception, indicates that schizophrenia-associated differentially methylated positions are significantly enriched for loci at which DNA methylation is dynamically altered during human fetal brain development.

Conclusions: Our data support the hypothesis that schizophrenia has an important early neurodevelopmental component, and suggest that epigenetic mechanisms may mediate these effects.

Background

Schizophrenia is a severe neuropsychiatric disorder characterized by episodic psychosis and altered cognitive function. With a lifetime prevalence of approximately 1%, schizophrenia contributes significantly to the global burden of disease [1]. Although schizophrenia does not typically manifest until late adolescence or early adulthood, evidence from neuroimaging, neuropathology and epidemiological studies has led to its conceptualization as a neurodevelopmental disorder, with etiological origins before birth [2]. To date, however, the neurobiological mechanisms underlying the disorder remain largely

undefined, and molecular evidence for *in utero* disturbances in schizophrenia is currently lacking.

Schizophrenia is known to have a substantial genetic component, involving a large number of common variants with individually small effects on risk for the disorder [3], as well as rarer mutations [4] and copy number variants [5] of greater effect size. Of note, several of the most robustly supported schizophrenia susceptibility genes have known roles in early brain development and appear to impact on schizophrenia risk during this period [6,7]. Epidemiological research suggests that prenatal environmental insults are also important, with established associations between hypoxia [8], maternal infection [9], maternal stress [10], and maternal malnutrition or famine [11] and risk for developing schizophrenia. These observations have led to a growing interest in the role of developmentally regulated epigenetic variation in the molecular etiology of schizophrenia [12]. The notion that epigenetic processes

* Correspondence: j.mill@exeter.ac.uk

¹Institute of Psychiatry, King's College London, London, SE5 8AF, UK

³University of Exeter Medical School, University of Exeter, Exeter, UK, RILD Building, Royal Devon & Exeter Hospital, Barrack Road, Exeter EX2 5DW, UK
Full list of author information is available at the end of the article

are involved in the onset of schizophrenia is supported by recent methylomic studies of disease-discordant monozygotic twins [13], clinical sample cohorts [14], and post-mortem brain tissue [15].

Here, we describe a systematic study of schizophrenia-associated methylomic variation in the adult brain and its relationship to changes in DNA methylation during human fetal brain development. We profiled DNA methylation in matched prefrontal cortex (PFC) and cerebellum brain tissue from schizophrenia patients and controls, subsequently assessing disease-associated regions in human fetal cortex samples spanning 23 to 184 days post-conception. Our data support the hypothesis that schizophrenia has an important early neurodevelopmental component, and suggest that epigenetic mechanisms likely contribute to these disturbances.

Results and discussion

Identification of schizophrenia-associated differentially methylated positions in the prefrontal cortex

Our 'discovery' cohort comprised PFC and cerebellum samples from schizophrenia patients and matched (for sex, age and sample quality markers (for example, pH)) control donors archived in the MRC London Brain Bank

for Neurodegenerative Diseases (LBBND; see Materials and methods; Tables S1 and S2 in Additional file 1). Genome-wide patterns of DNA methylation were quantified using the Illumina Infinium HumanMethylation450 BeadChip (450K array) (Illumina Inc., San Diego, CA, USA), performing pre-processing, normalization and stringent quality control as previously described [16] (see Materials and methods; Table S3 in Additional file 1). In total, data from 43 PFC (20 schizophrenia and 23 controls) and 44 cerebellum (21 schizophrenia and 23 controls) samples passed quality control metrics and were used for analysis. The top-ranked differentially methylated positions (DMPs) in each brain region are shown in Tables S4 and S5 in Additional file 1. Most notably, highly significant DMPs were identified in the PFC (Table 1), with probes in four genes being significantly associated with schizophrenia at a false discovery rate (FDR) ≤ 0.05 : *GSDMD* (cg26173173: control = 78.9 ± 3.0 , schizophrenia = 83.3 ± 1.3 , FDR = 0.03); *RASA3* (cg24803255: control = 65.1 ± 4.7 , schizophrenia = 56.4 ± 4.1 , FDR = 0.03); *HTR5A* (cg00903099: control = 11.5 ± 1.7 , schizophrenia = 9.2 ± 1.2 , FDR = 0.03); and *PPFIA1* (cg08171022: control = 53.1 ± 3.2 , schizophrenia = 47.6 ± 3.2 , FDR = 0.03) (Figure 1A). As epigenetic epidemiological research can be confounded

Table 1 Schizophrenia-associated differentially methylated positions in the prefrontal cortex

Probe ID	Genomic position (hg19)	Gene	Gene region	P-value	FDR	Mean SZ	Mean control	Beta difference
cg26173173	chr8:144642813	<i>GSDMD</i>	Body	1.16E-07	0.03	0.83	0.79	0.04
cg24803255	chr13:114807060	<i>RASA3</i>	Body	1.25E-07	0.03	0.56	0.65	-0.09
cg00903099	chr7:154862441	<i>HTR5A</i>	TSS200	2.40E-07	0.03	0.09	0.12	-0.02
cg08171022	chr11:70185278	<i>PPFIA1</i>	Body	2.85E-07	0.03	0.48	0.53	-0.05
cg02857643	chr17:48696108	<i>CACNA1G</i>	Body	1.63E-06	0.1	0.87	0.92	-0.05
cg00236305	chr2:1796076	<i>MYT1L</i>	Body	1.75E-06	0.1	0.67	0.73	-0.06
cg14966346	chr14:104152124	<i>KLC1</i>	Body	2.51E-06	0.1	0.72	0.77	-0.05
cg13079528	chr7:4027346	<i>SDK1</i>	Body	2.75E-06	0.1	0.71	0.79	-0.08
cg14429765	chr8:6492531	<i>MCPH1</i>	Body	2.79E-06	0.1	0.79	0.76	0.03
cg08602214	chr8:22864392	<i>RHOBTB2</i>	Body	2.87E-06	0.1	0.69	0.75	-0.07
cg19735533	chr2:241196887	-	-	2.94E-06	0.1	0.76	0.81	-0.06
cg09507608	chr22:29873338	-	-	2.95E-06	0.1	0.56	0.62	-0.06
cg23844013	chr1:57383752	<i>C8A</i>	3' UTR	3.20E-06	0.1	0.82	0.79	0.03
cg26578910	chr19:47204096	<i>PRKD2</i>	Body	3.47E-06	0.1	0.67	0.71	-0.04
cg21847368	chr13:113744010	<i>MCF2L</i>	Body	3.70E-06	0.1	0.80	0.84	-0.03
cg03607729	chr16:25138698	<i>LCMT1</i>	Body	4.19E-06	0.1	0.70	0.75	-0.04
cg10248981	chr10:126157948	<i>LHPP</i>	Body	4.32E-06	0.1	0.55	0.63	-0.07
cg03445663	chr2:242170236	<i>HDLBP</i>	Body	4.59E-06	0.1	0.51	0.59	-0.08
cg15079231	chr3:42572745	<i>VIPR1</i>	Body	4.93E-06	0.1	0.76	0.80	-0.04
cg21341878	chr4:2278462	<i>ZFYVE28</i>	Body	5.14E-06	0.1	0.75	0.81	-0.05
cg04922803	chr12:104444418	<i>GLT8D2</i>	TSS1500	5.19E-06	0.1	0.68	0.62	0.06
cg18857062	chr6:43276478	<i>CRIP3</i>	Body	5.29E-06	0.1	0.21	0.26	-0.04

Listed are all probes associated with schizophrenia (SZ) with FDR ≤ 0.1 . The 100 top-ranked DMPs are listed in Table S4 in Additional file 1.

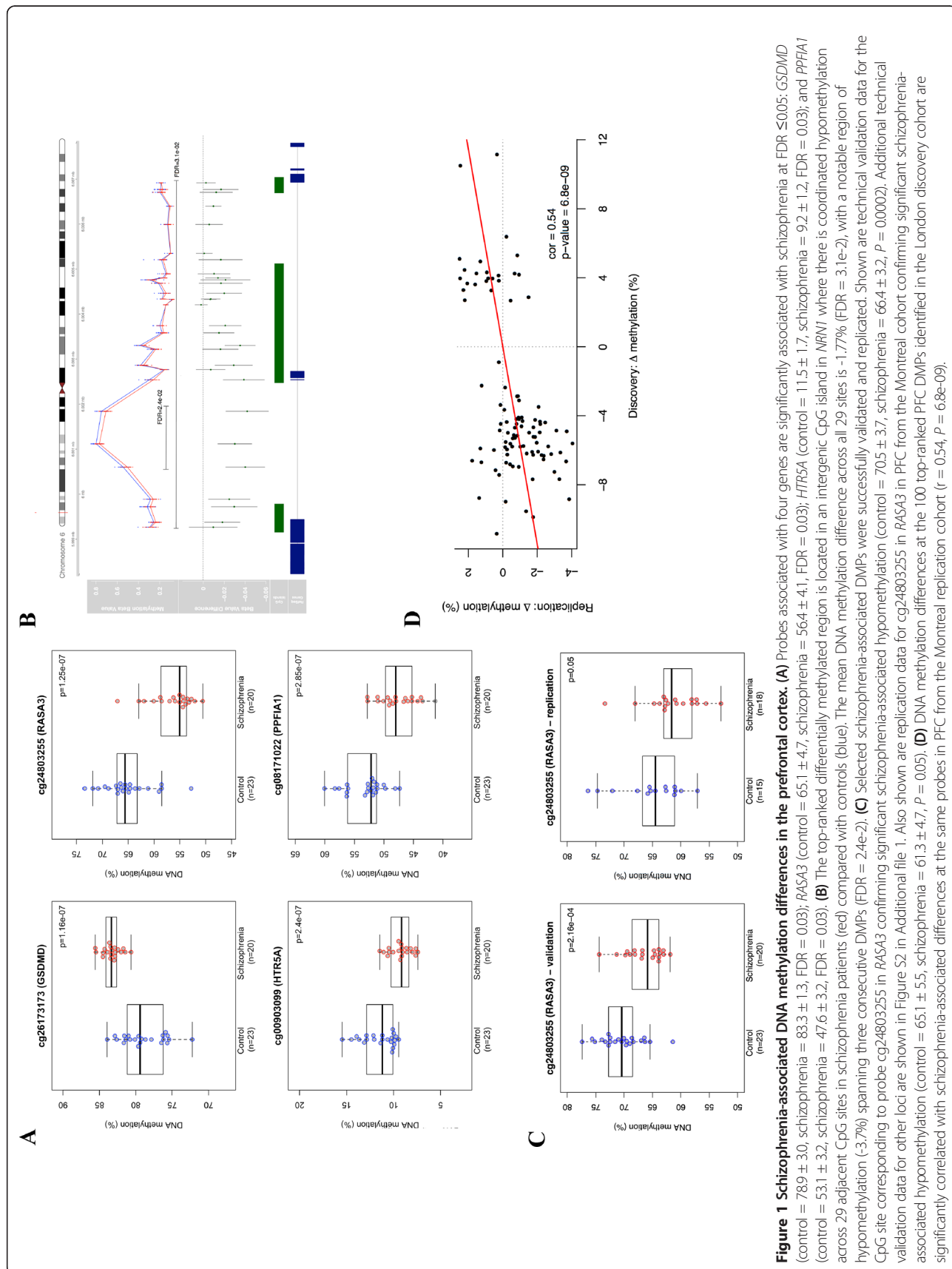


Figure 1 Schizophrenia-associated DNA methylation differences in the prefrontal cortex. (A) Probes associated with four genes are significantly associated with schizophrenia at $FDR \leq 0.05$: GSDMD (control = 78.9 ± 3.0 , schizophrenia = 83.3 ± 1.3 , $FDR = 0.03$); RAS43 (control = 65.1 ± 4.7 , schizophrenia = 56.4 ± 4.1 , $FDR = 0.03$); HTR5A (control = 11.5 ± 1.7 , schizophrenia = 9.2 ± 1.2 , $FDR = 0.03$); and PPF1A1 (control = 53.1 ± 3.2 , schizophrenia = 47.6 ± 3.2 , $FDR = 0.03$). (B) The top-ranked differentially methylated region is located in an intergenic CpG island in *NR1* where there is coordinated hypomethylation across 29 adjacent CpG sites in schizophrenia patients (red) compared with controls (blue). The mean DNA methylation difference across all 29 sites is -1.77% ($FDR = 3.1e-2$), with a notable region of hypomethylation (-3.7%) spanning three consecutive DMPs ($FDR = 2.4e-2$). (C) Selected schizophrenia-associated DMPs were successfully validated and replicated. Shown are technical validation data for the CpG site corresponding to probe cg24803255 in RAS43 confirming significant schizophrenia-associated hypomethylation (control = 70.5 ± 3.7 , schizophrenia = 66.4 ± 3.2 , $P = 0.0002$). Additional technical validation data for other loci are shown in Figure S2 in Additional file 1. Also shown are replication data for cg24803255 in RAS43 in PFC from the Montreal cohort confirming significant schizophrenia-associated hypomethylation (control = 65.1 ± 5.5 , schizophrenia = 61.3 ± 4.7 , $P = 0.05$). (D) DNA methylation differences at the 100 top-ranked PFC DMPs identified in the London discovery cohort are significantly correlated with schizophrenia-associated differences at the same probes in PFC from the Montreal replication cohort ($r = 0.54$, $P = 6.8e-09$).

by cellular heterogeneity [17,18], we used an *in silico* algorithm to assess the extent to which DMPs are influenced by differences in neuronal proportions between individuals [19]. Notably, all top-ranked PFC DMPs remained significantly associated with schizophrenia after correction for the estimated neuronal proportion in each sample (Table S4 in Additional file 1). In contrast to the PFC, few schizophrenia-associated DMPs (none at $FDR \leq 0.05$) were identified in the cerebellum (Table S5 in Additional file 1), suggesting that disease-associated epigenetic differences are likely to be brain region-specific.

Region-based analysis of altered DNA methylation in schizophrenia

As DNA methylation is often correlated across adjacent CpG sites [20,21], we used the Illumina Methylation Analyser (IMA) [22] package to aggregate and assess DNA methylation across adjacent probes within annotated regions of the genome. Again, we observe widespread evidence for schizophrenia-associated DNA methylation differences, occurring specifically in the PFC (Figure S1 and Table S6 in Additional file 1). Most notably we observe a large (approximately 8 kb) region spanning the gene body of the *Neuritin 1* (*NRN1*) gene across which 29 adjacent CpG sites are consistently hypomethylated in schizophrenia patients compared with controls (Figure 1B). The mean DNA methylation difference across all 29 sites is -1.77% ($FDR = 3.1e-2$), with a notable region of hypomethylation (-3.7%) spanning three consecutive DMPs ($FDR = 2.4e-2$). This is of particular interest because *NRN1* plays a well-established role in neurodevelopment and synaptic plasticity [23], and genetic variation in the gene has been linked to cognitive phenotypes in schizophrenia [24].

Validation and replication of schizophrenia-associated DNA methylation differences in the prefrontal cortex

To confirm the array data, bisulfite-pyrosequencing was used to validate schizophrenia-associated DMPs in the vicinity of three genes (*NRN1* (cg00565348), *C8A* (cg23844013), and *RASA3* (cg24803255)) in the same samples. Bisulfite-PCR amplification was performed in duplicate using the primers and assay conditions in Table S7 in Additional file 1. Fully methylated and fully unmethylated control samples were included in all experiments. For each amplicon we confirmed significant DNA methylation differences in the same direction as reported by the 450K array (Figure 1C; Figure S2 and Table S8 in Additional file 1). We subsequently generated a replication PFC (BA9) 450K dataset using schizophrenia and control brains archived at the Douglas Bell-Canada Brain Bank, Montreal, Canada ($n = 33$, 18 schizophrenia and 15 controls; Tables S9 and S10 in Additional file 1) using the Illumina 450K array as described above.

Strikingly, DNA methylation differences at the top-ranked PFC DMPs identified in the 'LBBND' cohort (listed in Table S11 in Additional file 1) were strongly correlated with schizophrenia-associated differences at the same probes in PFC tissue from the Montreal replication samples ($r = 0.54$, $P = 6.8e-09$) with a consistent direction of effect observed across both cohorts and significant differences observed for top-ranked DMPs (Figure 1C,D).

Evidence for schizophrenia-associated gene co-methylated modules in the prefrontal cortex

We next employed weighted gene co-methylation network analysis (WGCNA) to undertake a systems-level view of the DNA methylation differences associated with schizophrenia in the PFC [25,26]. Using probe-wise DNA methylation data we identified 110 modules (representing discrete networks of co-methylated sites), and the first principal component of each individual module (termed the 'eigengene') was used to assess the relationship with disease status. Twelve PFC modules were significantly associated with schizophrenia, most notably the 'black' ($n = 6,647$ probes, $r = -0.52$, $P = 0.0004$) and 'pink' modules ($n = 4,399$ probes, $r = -0.45$, $P = 0.002$) (Figure 2A). Module membership in both modules is strongly correlated with probe-level disease significance (black module: $r = 0.39$, $P < 1e-200$; pink module: $r = 0.22$, $P = 2.4e-49$) (Figure 2B). Repeating WGCNA on the cerebellum data yielded no schizophrenia-associated modules, providing further evidence of brain region-specific DNA methylation differences in schizophrenia. Furthermore, a comparison of modules across the two brain regions showed that while a subset of 43 PFC modules correlated strongly ($r > 0.8$) with 51 cerebellum modules, none of the PFC schizophrenia-associated modules were correlated with modules in the cerebellum. Finally, despite the low number of samples and lack of power for replicating WGCNA associations in the Montreal replication dataset, the modular structure of DNA methylation in the PFC was found to be strongly preserved across both brain cohorts (Figure S3 in Additional file 1), with both the black and pink modules being highly conserved and negatively correlated with schizophrenia (black module: $r = -0.26$; pink module: $r = -0.10$).

Schizophrenia-associated co-methylated modules are enriched for neurodevelopmental pathways and loci previously implicated in the disorder

To test whether the identified schizophrenia-associated modules were biologically meaningful, pathway and gene ontology analyses were performed using Ingenuity Pathway Analysis (IPA) and EASE (DAVID) software [28]. Enrichment for specific pathways and biological functions was determined relative to the relevant microarray

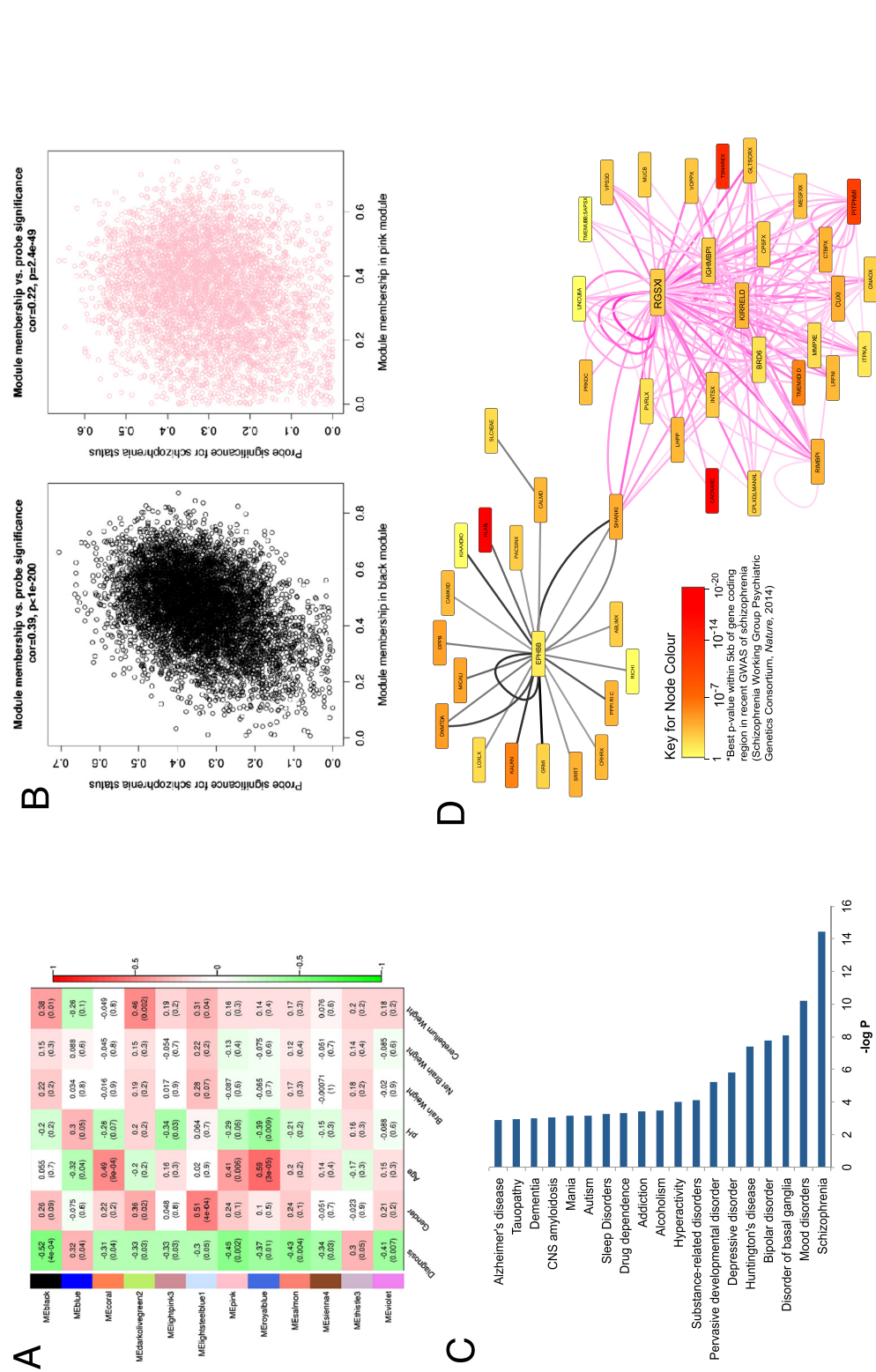
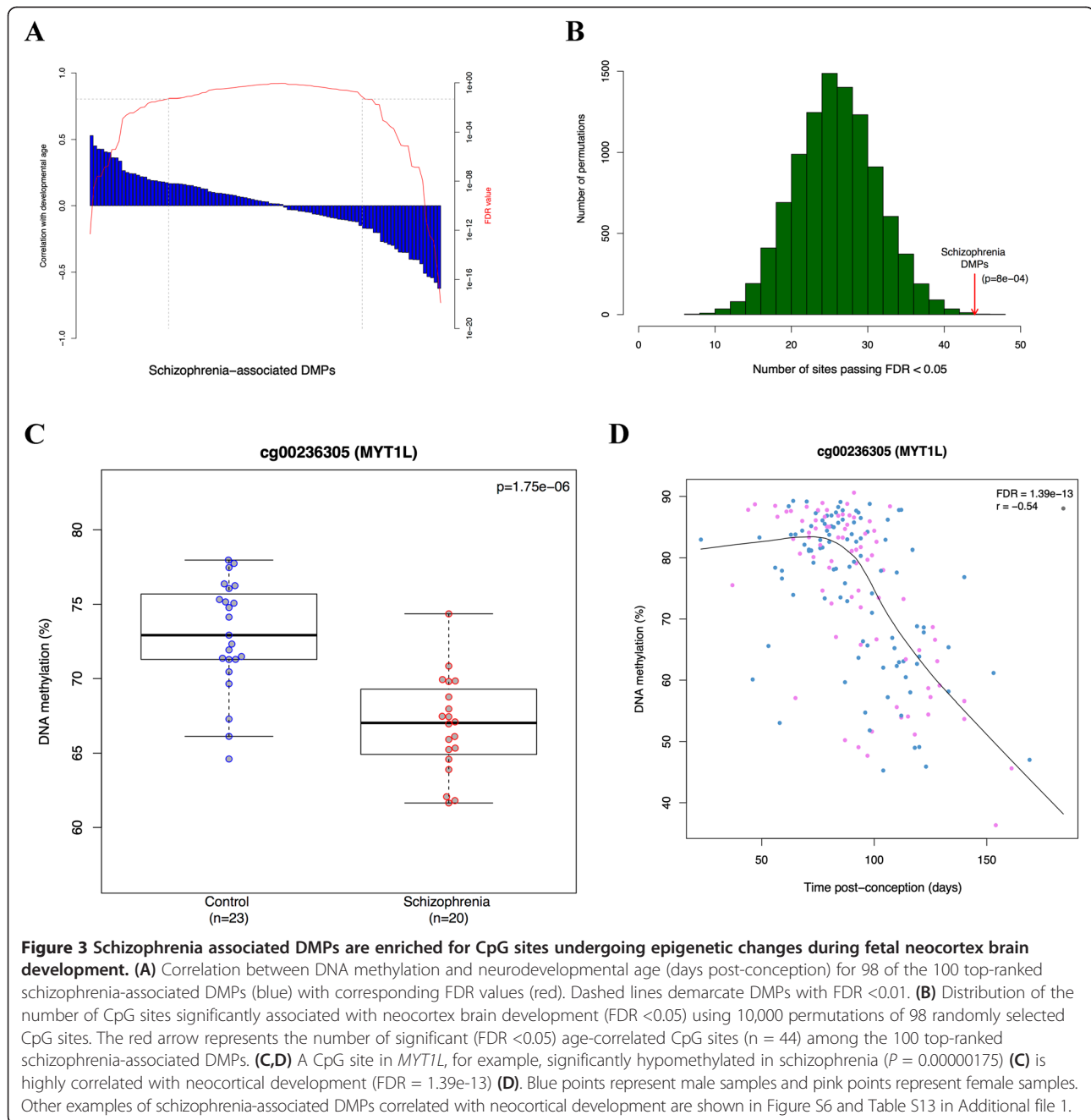


Figure 2 Schizophrenia-associated gene co-methylation modules in the prefrontal cortex. Each row represents a specific module, indicated by an arbitrary module color labeled on the y-axis. Dark red indicates strong positive correlation, dark green indicates strong negative correlation, and white indicates no correlation, as indicated in color scale bar. *P*-values are given in parentheses. The black ($P = 0.0004$) and pink ($P = 0.002$) WGCNA modules are most significantly associated with schizophrenia in the PFC. **(B)** Module membership in both modules is strongly correlated with probe significance with disease (black module: $r = 0.22$, $P = 2.4e-49$). **(C)** Ingenuity Pathway Analysis of genes associated with CpG sites in the black module reveals a highly significant enrichment of disease pathways related to schizophrenia and other neuropsychiatric disease. **(D)** Co-methylation networks between the top 1% of loci in the black and pink modules ranked by their module membership, where thicker lines indicate more connected genes. Black edges represent co-methylation between probes in the black module and pink edges represent co-methylation in the pink module; thicker and deeper colored edges indicate stronger correlations between probes. Interestingly, the two modules are connected by *SHANK2*, which encodes a molecular scaffold protein that plays a role in synaptogenesis. Furthermore, several of the genes are associated with schizophrenia in recent collaborative genome-wide association studies (GWAS) [27]. GWAS significance for SNPs in the vicinity of each locus is depicted by color.



gene list using a right-tailed Fisher's test. IPA of genes associated with CpG sites in the top-ranked PFC modules reveals a highly significant enrichment of disease pathways related to 'schizophrenia and other neuropsychiatric disorders' in the black module ($P = 3.67 \times 10^{-15}$ to 1.27×10^{-3} ; Figure 2C), and 'nervous system development and function' in both the black ($P = 3.80 \times 10^{-18}$ to 1.37×10^{-3} ; Figure S4 in Additional file 1) and pink ($P = 4.04 \times 10^{-15}$ to 3.16×10^{-3} ; Figure S5 in Additional file 1) modules. Consistent with the IPA results, gene ontology analysis using EASE (DAVID) [28] shows that both modules are significantly

enriched for functions related to nervous system and neuron development, synaptic transmission and calcium ion binding (Table S12 in Additional file 1). An analysis of co-methylation networks between the top-ranked 'hub' probes in the black and pink modules shows that they are connected by DNA methylation in the vicinity of *SHANK2*, a molecular scaffold protein that plays a critical role in neurodevelopment and synaptogenesis, and has been widely implicated in several neurodevelopmental disorders, including schizophrenia [29] (Figure 2D). Furthermore, several of the probes are located in genes that have been strongly

implicated in schizophrenia by a recent large collaborative genome-wide association study (GWAS; for example, *CACNA1C*, *TSNARE1*, *PITPNM2*, and *HLA-L*) [27].

Schizophrenia-associated DMPs are enriched for CpG sites undergoing epigenetic changes during fetal neocortex brain development

Given previous evidence for a neurodevelopmental basis to schizophrenia [2], and our analyses demonstrating an enrichment of neurodevelopmental pathways involved in disease, we next investigated whether schizophrenia-associated DMPs are enriched for CpG sites undergoing dynamic DNA methylation changes during human fetal brain development. For each of the top-ranked PFC DMPs we assessed the correlation between DNA methylation and days post-conception in a 450K DNA methylation dataset generated by our lab using human fetal brain tissue ($n = 179$, range = 23 to 184 days post-conception, number of matching 450K probes in fetal dataset after quality control and filtering = 98/100; HH Spiers *et al.*, in preparation). Strikingly, DNA methylation at 44% of the schizophrenia-associated DMPs is significantly associated (at FDR <0.05) with post-conception age in the developing fetal brain (Figure 3A), reflecting a highly significant enrichment for neurodevelopmental DMPs (10,000 permutations, $P = 8e-04$) amongst schizophrenia-associated loci (Figure 3B) and reinforcing the notion that neurodevelopmental dysfunction is involved in schizophrenia. For example, one of the top-ranked schizophrenia-associated DMPs (cg00236305), located in the gene body of *MYTIL*, is significantly hypomethylated ($P = 1.75e-6$) in patients compared with controls (Figure 3C). *MYTIL* encodes a potent transcription factor integral to neurodevelopment [30], and the same probe is highly correlated with neocortical development (FDR = $1.39e-13$; Figure 3D). Other examples of schizophrenia-associated DMPs strongly correlated with neocortical development are shown in Figure S6 and Table S13 in Additional file 1.

Conclusions

In this study we have found schizophrenia-associated variation in DNA methylation in the PFC, and identified discrete modules of co-methylated loci associated with the disorder that are significantly enriched for genes involved in neurodevelopmental processes. Methyloomic profiling in human fetal cortex samples confirmed that disease-associated DMPs are significantly enriched for loci at which DNA methylation is dynamically altered during human fetal brain development. These data strongly support the hypothesis that schizophrenia has an important early neurodevelopmental component, and suggest that epigenetic mechanisms may mediate the relationship between neurodevelopmental disturbances and risk of disease.

Materials and methods

Samples and sample processing

London Brain Bank for Neurodegenerative Disorders

PFC and cerebellum samples were obtained from 47 brains archived in the LBBND. Subjects were approached in life for written consent for brain banking, and all tissue donations were collected and stored following legal and ethical guidelines (NHS reference number 08/MRE09/38; the HTA license number for the LBBND brain bank is 12293). The study is also approved by the University of Exeter Medical School Research Ethics Committee (reference number 13/02/009). Samples were dissected by a trained neuropathologist, snap-frozen and stored at -80°C . Schizophrenia patients were diagnosed by trained psychiatrists according to Diagnostic and Statistical Manual of Mental Disorders (DSM) criteria. Demographic information for the samples is summarized in Tables S1 and S2 in Additional file 1. Samples were randomized with respect to gender and disease status to avoid batch effects throughout all experimental procedures. Genomic DNA was isolated using a standard phenol-chloroform extraction protocol. DNA was tested for degradation and purity using spectrophotometry and gel electrophoresis.

Douglas Bell-Canada Brain Bank, Montreal

PFC samples from 18 schizophrenia cases and 15 controls were obtained from the Douglas Bell-Canada Brain Bank (DBCBB) [31]. Brain specimens used in this study were collected postmortem following consent obtained with next of kin, according to tissue banking practices regulated by the Quebec Health Research Fund [32], and based on the OECD Guidelines on Human Biobanks and Genetic Research Databases [33]. Samples were dissected by neuropathology technicians, snap-frozen and stored at -80°C . Psychiatric diagnoses were based on best-estimate diagnostic procedures, following SCID I diagnostic interviews conducted with informants, as described elsewhere [34]. Demographic information for the DBCBB samples is summarized in Tables S8 and S9 in Additional file 1. Genomic DNA was isolated using a standard phenol-chloroform extraction protocol. DNA was tested for degradation and purity using spectrophotometry and gel electrophoresis.

Genome-wide quantification of DNA methylation

Microarray processing

DNA (500 ng) from each sample was treated with sodium bisulfite in duplicate, using the EZ-96 DNA methylation kit (Zymo Research, Irvine, CA, USA). DNA methylation was quantified using the Illumina Infinium HumanMethylation450 BeadChip (Illumina Inc.) run on an Illumina HiScan System (Illumina) using the manufacturers' standard protocol.

Data processing and quality control of discovery data

Signal intensities for each probe were extracted using Illumina GenomeStudio software and imported into R [35] using the *methylnumi* and *minfi* packages [36,37]. Multi-dimensional scaling plots of variable probes on the sex chromosomes were used to check that the predicted gender corresponded with the reported gender for each individual. One sample showed a discrepancy between measured and reported sex and was subsequently identified as having an XXY karyotype and removed from the current study for independent investigation [38]. Comparison of non-CpG SNP probes on the array confirmed that matched PFC and cerebellum tissues were sourced from the same individual. Raw beta values of probes within brain region-specific DMRs (extracted from [39]) were used to confirm the tissue identity of each sample. Probes containing a SNP with minor allele frequency >5% within 10 bp of the single base extension site based on Illumina's database and probes identified by Chen and colleagues [40] ($n = 34,548$) were removed from all analyses. Further data quality control and processing steps were conducted using the *watermelon* package [16] in R. The *pfilter* function was used to filter data by beadcount and detection P -value. Samples with >1% probes with a detection P -value >0.05 were removed (PFC: $n = 3$ samples; cerebellum: $n = 1$ sample). Probes with a detection P -value >0.05 in at least 1% of samples and/or a beadcount <3 in 5% of samples were removed across all samples to stringently control for poor quality probes. Quality control sample exclusions are summarized in Table S3 in Additional file 1. The *dasen* function was used to normalize the data as previously described [16], with probes on the sex chromosomes removed from all subsequent analysis.

Statistical analysis

First, analyses were performed to test for DNA methylation differences between schizophrenia cases and controls at the individual probe level. To model the effect of sample-specific variables we performed linear regression for each probe using age, gender and disease status as independent variables. Regression tests were performed using the *Limma* [41] package in R, and prior to analyses β -values were log-transformed to M -values to improve sensitivity. P -values were adjusted for multiple testing according to the FDR procedure of Benjamini-Hochberg. The CETS package in R [19] was used to check that our top-ranked DMPs were not mediated by the effect of differential neuronal cell proportions across samples. To identify DMRs we used the Illumina Methylation Analyzer (IMA) [22] package to compute region-level summaries of DNA methylation in the PFC and cerebellum, which were then tested for association with disease using *Limma*. P -values were adjusted for multiple testing

according to the FDR procedure of Benjamini-Hochberg. Significant DMRs were selected at a 5% FDR and visualized using *RCircos* [42] and *Gviz* [43] packages. To investigate whether schizophrenia-associated DMPs are enriched for sites undergoing epigenetic changes during neurodevelopment, we used an unpublished 450K DNA methylation dataset of fetal cortex brain samples ($n = 179$, range 23 to 184 days post-conception) collected as part of ongoing work in our group (HH Spiers *et al.*, in preparation). For the top 100 schizophrenia-associated DMPs in our dataset, we extracted β -values of 98 matched probes in the neurodevelopmental dataset ($n = 2$ probes removed during quality control of fetal dataset). We then used Pearson's correlation tests to assess the number of probes showing a significant relationship (FDR <0.05) between DNA methylation and days post-conception. To evaluate the genome-wide significance of this result we compared the above correlation with an estimated null distribution from 10,000 randomizations of the data. On each randomization we randomly selected 98 probes and computed the number of probes with FDR <0.05, as described above. One-tail significance was assessed by comparing the original number of significant probes (FDR <0.05) to the estimated null distribution.

Bisulfite-pyrosequencing

Independent verification analysis was performed on three PFC schizophrenia-associated DMPs (in the vicinity of *NRN1*, *C8A*, and *RASA3*), based on results from both the probe-wise and region-level analysis. Pyrosequencing assays were designed using the PyroMark Assay design software (Qiagen, Hilden, Germany). Bisulfite-PCR amplification was performed in duplicate using the primers and assay conditions in Table S7 in Additional file 1. Fully methylated and fully unmethylated control samples were included in all experiments.

Replication analysis

DNA samples from the Montreal cohort were analyzed using the Illumina Infinium HumanMethylation450 BeadChip using the same processing and quality control steps as described above. For the top 100 schizophrenia-associated DMPs in the LBBND cohort (Table S4 in Additional file 1), we extracted β -values for matched probes in the Montreal dataset. Pearson's correlation was used to assess the relationship between disease-associated DNA methylation differences in the two datasets at these probes.

Weighted gene co-methylation network analysis

Network analysis was performed on normalized probe-wise DNA methylation data (PFC: $n = 445,617$ probes; cerebellum: $n = 440,836$ probes) using WGCNA [26]. For each brain region pair-wise correlations were used to identify modules of highly co-methylated probes,

independent of disease status. Specifically, an unsigned network was created with a soft threshold parameter of 6 using the *blockwiseModules* function based on a block size of 20,000. Each module was then labeled with a unique color name. The first principle component of the methylation matrix of each module was calculated to give a 'module eigengene' (ME) for each module (a weighted average methylation profile). To identify modules associated with schizophrenia, each of the ME values was regressed on disease status, in addition to other sample-specific variables: pH, age, gender, brain weight and cerebellum weight. To test whether the identified schizophrenia-associated modules were biologically meaningful, pathway and gene ontology analyses were performed using IPA [44] and EASE (DAVID) [28,45]. Correlations were performed between the ME and DNA methylation values to calculate the module membership of each probe (the extent to which a given probe contributes to the ME). This module membership value was used to identify the 'hub' genes in each module. The function *modulePreservation* in the WGCNA package was used to calculate module preservation statistics for the Montreal PFC data based on the PFC modules built from the discovery dataset.

Accession numbers

The Gene Expression Omnibus accession numbers for the 450K array data reported in this paper are GSE61431 (LBBND dataset) and GSE61380 (DBCBB dataset).

Additional file

Additional file 1: Supplementary Figures S1 to S6 and Supplementary Tables S1 to S13.

Abbreviations

DBCBB: Douglas Bell-Canada Brain Bank; DMP: differentially methylated position; DMR: differentially methylated region; FDR: false discovery rate; GWAS: genome-wide association study; IPA: Ingenuity Pathway Analysis; LBBND: London Brain Bank for Neurodegenerative Diseases; ME: module eigengene; PFC: prefrontal cortex; SNP: single-nucleotide polymorphism; UTR: untranslated region; WGCNA: weighted gene co-methylation network analysis.

Competing interests

The authors declare that they have no competing interests.

Authors' contributions

RP ran 450K arrays, performed data analysis, and helped draft the manuscript. JV undertook validation and replication work and helped draft the manuscript. EH undertook data analysis and helped draft the manuscript. HS and NB undertook the fetal brain analyses. CT, SAS, NM, and GT provided brain tissue. LS assisted in data analysis. JM oversaw the study, was involved in data analysis, helped draft the manuscript, and obtained funding. All authors read and approved the final version of the manuscript.

Acknowledgements

This work was supported by grants from the UK Medical Research Council (MRC) (grant number MR/K013807/1) and US National Institutes of Health (grant number AG036039) to JM. RP and HS were funded by MRC PhD studentships. The human embryonic and fetal material was provided by the

Joint MRC (grant number G0700089)/Wellcome Trust (grant number GR082557) Human Developmental Biology Resource.

Author details

¹Institute of Psychiatry, King's College London, London, SE5 8AF, UK. ²Garvan Institute of Medical Research, Sydney, NSW 2010, Australia. ³University of Exeter Medical School, University of Exeter, Exeter, UK, RILD Building, Royal Devon & Exeter Hospital, Barrack Road, Exeter EX2 5DW, UK. ⁴Douglas Mental Health Institute, McGill University, Montreal, QC, H4H 1R3, Canada. ⁵School of Biological Sciences, University of Essex, Colchester CO4 3SQ, UK.

Received: 8 June 2014 Accepted: 24 September 2014

Published online: 28 October 2014

References

1. Bebbington P: **The World Health Report 2001.** *Soc Psychiatry Psychiatr Epidemiol* 2001, **36**:473–474.
2. Fatemi SH, Folsom TD: **The neurodevelopmental hypothesis of schizophrenia, revisited.** *Schizophr Bull* 2009, **35**:528–548.
3. Purcell SM, Wray NR, Stone JL, Visscher PM, O'Donovan MC, Sullivan PF, Sklar P: **Common polygenic variation contributes to risk of schizophrenia and bipolar disorder.** *Nature* 2009, **460**:748–752.
4. Purcell SM, Moran JL, Fromer M, Ruderfer D, Solovieff N, Roussos P, O'Dushlaine C, Chambert K, Bergen SE, Kahler A, Duncan L, Stahl E, Genovese G, Fernández E, Collins MO, Komiyama NH, Choudhary JS, Magnusson PKE, Banks E, Shakir K, Garimella K, Fennell T, DePristo M, Grant SG, Haggarty SJ, Gabriel S, Scolnick EM, Lander ES, Hultman CM, Sullivan PF, et al: **A polygenic burden of rare disruptive mutations in schizophrenia.** *Nature* 2014, **506**:185–190.
5. The International Schizophrenia Consortium: **Rare chromosomal deletions and duplications increase risk of schizophrenia.** *Nature* 2008, **455**:237–241.
6. Kirov G, Rujescu D, Ingason A, Collier DA, O'Donovan MC, Owen MJ: **Neurexin 1 (NRXN1) deletions in schizophrenia.** *Schizophr Bull* 2009, **35**:851–854.
7. Hill MJ, Bray NJ: **Evidence that schizophrenia risk variation in the ZNF804A gene exerts its effects during fetal brain development.** *Am J Psychiatry* 2012, **169**:1301–1308.
8. Cannon M, Jones PB, Murray RM: **Obstetric complications and schizophrenia: historical and meta-analytic review.** *Am J Psychiatry* 2002, **159**:1080–1092.
9. Brown AS, Derkits EJ: **Prenatal infection and schizophrenia: a review of epidemiologic and translational studies.** *Am J Psychiatry* 2010, **167**:261–280.
10. Khashan AS, Abel KM, McNamee R, Pedersen MG, Webb RT, Baker PN, Kenny LC, Mortensen PB: **Higher risk of offspring schizophrenia following antenatal maternal exposure to severe adverse life events.** *Arch Gen Psychiatry* 2008, **65**:146–152.
11. Susser E, Neugebauer R, Hoek HW, Brown AS, Lin S, Labovitz D, Gorman JM: **Schizophrenia after prenatal famine. Further evidence.** *Arch Gen Psychiatry* 1996, **53**:25–31.
12. Dempster E, Viana J, Pidsley R, Mill J: **Epigenetic studies of schizophrenia: progress, predicaments, and promises for the future.** *Schizophr Bull* 2013, **39**:11–16.
13. Dempster EL, Pidsley R, Schalkwyk LC, Owens S, Georgiades A, Kane F, Kalidindi S, Picchioni M, Kravariti E, Touloupoulou T, Murray RM, Mill J: **Disease-associated epigenetic changes in monozygotic twins discordant for schizophrenia and bipolar disorder.** *Hum Mol Genet* 2011, **20**:4786–4796.
14. Aberg KA, McClay JL, Nerella S, Clark S, Kumar G, Chen W, Khachane AN, Xie L, Hudson A, Gao G, Harada A, Hultman CM, Sullivan PF, Magnusson PK, van den Oord EJ: **Methylome-wide association study of schizophrenia: identifying blood biomarker signatures of environmental insults.** *JAMA Psychiatry* 2014, **71**:255–264.
15. Mill J, Tang T, Kaminsky Z, Khare T, Yazdanpanah S, Bouchard L, Jia P, Assadzadeh A, Flanagan J, Schumacher A, Wang SC, Petronis A: **Epigenomic profiling reveals DNA-methylation changes associated with major psychosis.** *Am J Hum Genet* 2008, **82**:696–711.
16. Pidsley R, CC YW, Volta M, Lunnon K, Mill J, Schalkwyk LC: **A data-driven approach to preprocessing Illumina 450K methylation array data.** *BMC Genomics* 2013, **14**:293.

17. Mill J, Heijmans BT: **From promises to practical strategies in epigenetic epidemiology.** *Nat Rev Genet* 2013, **14**:585–594.
18. Jaffe AE, Irizarry RA: **Accounting for cellular heterogeneity is critical in epigenome-wide association studies.** *Genome Biol* 2014, **15**:R31.
19. Guintivano J, Aryee M, Kaminsky Z: **A cell epigenotype specific model for the correction of brain cellular heterogeneity bias and its application to age, brain region and major depression.** *Epigenetics* 2013, **8**:290–302.
20. Eckhardt F, Lewin J, Cortese R, Rakyan VK, Attwood J, Burger M, Burton J, Cox TV, Davies R, Down TA, Haefliger C, Horton R, Howe K, Jackson DK, Kunde J, Koenig C, Liddle J, Niblett D, Otto T, Pettett R, Seemann S, Thompson C, West T, Rogers J, Olek A, Berlin K, Beck S: **DNA methylation profiling of human chromosomes 6, 20 and 22.** *Nat Genet* 2006, **38**:1378–1385.
21. Ball MP, Li JB, Gao Y, Lee JH, LeProust EM, Park IH, Xie B, Daley GQ, Church GM: **Targeted and genome-scale strategies reveal gene-body methylation signatures in human cells.** *Nat Biotechnol* 2009, **27**:361–368.
22. Wang D, Yan L, Hu Q, Stucheston LE, Higgins MJ, Ambrosone CB, Johnson CS, Smiraglia DJ, Liu S: **IMA: an R package for high-throughput analysis of Illumina's 450K Infinium methylation data.** *Bioinformatics* 2012, **28**:729–730.
23. Fujino T, Leslie JH, Eavri R, Chen JL, Lin WC, Flanders GH, Borok E, Horvath TL, Nedivi E: **CPG15 regulates synapse stability in the developing and adult brain.** *Genes Dev* 2011, **25**:2674–2685.
24. Chandler D, Dragovic M, Cooper M, Badcock JC, Mullin BH, Faulkner D, Wilson SG, Hallmayer J, Howell S, Rock D, Palmer LJ, Kalaydjieva L, Jablensky A: **Impact of Neuritin 1 (NRN1) polymorphisms on fluid intelligence in schizophrenia.** *Am J Med Genet B Neuropsychiatr Genet* 2010, **153B**:428–437.
25. Zhang B, Horvath S: **A general framework for weighted gene co-expression network analysis.** *Stat Appl Genet Mol Biol* 2005, **4**:Article17.
26. Langfelder P, Horvath S: **WGCNA: an R package for weighted correlation network analysis.** *BMC Bioinformatics* 2008, **9**:559.
27. Schizophrenia Working Group of the Psychiatric Genomics Consortium: **Biological insights from 108 schizophrenia-associated genetic loci.** *Nature* 2014, **511**:421–427.
28. Hosack DA, Dennis G Jr, Sherman BT, Lane HC, Lempicki RA: **Identifying biological themes within lists of genes with EASE.** *Genome Biol* 2003, **4**:R70.
29. Guilmatre A, Huguet G, Delorme R, Bourgeron T: **The emerging role of SHANK genes in neuropsychiatric disorders.** *Dev Neurobiol* 2014, **74**:113–122.
30. Ambasadhan R, Talantova M, Coleman R, Yuan X, Zhu S, Lipton SA, Ding S: **Direct reprogramming of adult human fibroblasts to functional neurons under defined conditions.** *Cell Stem Cell* 2011, **9**:113–118.
31. **The Douglas-Bell Canada Brain Bank.** [http://douglasbrainbank.ca/]
32. Thibaut F: **Why schizophrenia genetics needs epigenetics: a review.** *Psychiatr Danub* 2012, **24**:25–27.
33. Spadaro PA, Bredy TW: **Emerging role of non-coding RNA in neural plasticity, cognitive function, and neuropsychiatric disorders.** *Front Genet* 2012, **3**:132.
34. McGirr A, Tousignant M, Routhier D, Pouliot L, Chawky N, Margolese HC, Turecki G: **Risk factors for completed suicide in schizophrenia and other chronic psychotic disorders: a case-control study.** *Schizophr Res* 2006, **84**:132–143.
35. Team RDC: *In R: A Language and Environment for Statistical Computing.* Edited by Computing RFFS. 2005.
36. Hansen KD, Aryee M: **minfi: Analyze Illumina's 450k methylation arrays. R package version 1.2.0.** 2012, [http://bioconductor.org/packages/release/bioc/html/minfi.html]
37. Davis S, Du P, Bilke S, Triche T, Bootwalla M: **Methylumi: handle illumina methylation data, R package.** 2012, [http://www.bioconductor.org/packages/release/bioc/html/methylumi.html]
38. Viana J, Pidsley R, Troakes C, Spiers H, Wong CC, Al-Sarraj S, Craig I, Schalkwyk L, Mill J: **Epigenomic and transcriptomic signatures of a Klinefelter syndrome (47, XXY) karyotype in the brain.** *Epigenetics* 2014, **9**:587–599.
39. Davies MN, Volta M, Pidsley R, Lunnon K, Dixit A, Lovestone S, Coarfa C, Harris RA, Milosavljevic A, Troakes C, Al-Sarraj S, Dobson R, Schalkwyk LC, Mill J: **Functional annotation of the human brain methylome identifies tissue-specific epigenetic variation across brain and blood.** *Genome Biol* 2012, **13**:R43.
40. Chen YA, Lemire M, Choufani S, Butcher DT, Grafodatskaya D, Zanke BW, Gallinger S, Hudson TJ, Weksberg R: **Discovery of cross-reactive probes and polymorphic CpGs in the Illumina Infinium HumanMethylation450 microarray.** *Epigenetics* 2013, **8**:203–209.
41. Smyth GK: **Linear models and empirical bayes methods for assessing differential expression in microarray experiments.** *Stat Appl Genet Mol Biol* 2004, **3**:Article3.
42. Zhang H, Meltzer P, Davis S: **RCircos: an R package for Circos 2D track plots.** *BMC Bioinformatics* 2013, **14**:244.
43. Florian Hahne SD, Robert I, Arne M, Steve L, Ge T: **Gviz: Plotting data and annotation information along genomic coordinates, R package version 1.6.0.** 2014, [http://www.bioconductor.org/packages/release/bioc/html/Gviz.html]
44. **Ingenuity Pathway Analysis.** 2014, [http://www.ingenuity.com/]
45. **DAVID Bioinformatics Resources.** 2014, [http://david.abcc.ncifcrf.gov]

doi:10.1186/s13059-014-0483-2

Cite this article as: Pidsley et al.: Methyloomic profiling of human brain tissue supports a neurodevelopmental origin for schizophrenia. *Genome Biology* 2014 **15**:483.

Submit your next manuscript to BioMed Central and take full advantage of:

- **Convenient online submission**
- **Thorough peer review**
- **No space constraints or color figure charges**
- **Immediate publication on acceptance**
- **Inclusion in PubMed, CAS, Scopus and Google Scholar**
- **Research which is freely available for redistribution**

Submit your manuscript at
www.biomedcentral.com/submit



This page has been removed by the author of this thesis for copyright reasons.

<http://dx.doi.org/10.1080/15592294.2015.1099797>

This page has been removed by the author of this thesis for copyright reasons.

<http://dx.doi.org/10.1080/15592294.2015.1099797>

This page has been removed by the author of this thesis for copyright reasons.

<http://dx.doi.org/10.1080/15592294.2015.1099797>

This page has been removed by the author of this thesis for copyright reasons.

<http://dx.doi.org/10.1080/15592294.2015.1099797>

This page has been removed by the author of this thesis for copyright reasons.

<http://dx.doi.org/10.1080/15592294.2015.1099797>

This page has been removed by the author of this thesis for copyright reasons.

<http://dx.doi.org/10.1080/15592294.2015.1099797>

This page has been removed by the author of this thesis for copyright reasons.

<http://dx.doi.org/10.1080/15592294.2015.1099797>

This page has been removed by the author of this thesis for copyright reasons.

<http://dx.doi.org/10.1080/15592294.2015.1099797>

This page has been removed by the author of this thesis for copyright reasons.

<http://dx.doi.org/10.1080/15592294.2015.1099797>

This page has been removed by the author of this thesis for copyright reasons.

<http://dx.doi.org/10.1080/15592294.2015.1099797>

This page has been removed by the author of this thesis for copyright reasons.

<https://dx.doi.org/10.1038/nn.4182>

This page has been removed by the author of this thesis for copyright reasons.

<https://dx.doi.org/10.1038/nn.4182>

This page has been removed by the author of this thesis for copyright reasons.

<https://dx.doi.org/10.1038/nn.4182>

This page has been removed by the author of this thesis for copyright reasons.

<https://dx.doi.org/10.1038/nn.4182>

This page has been removed by the author of this thesis for copyright reasons.

<https://dx.doi.org/10.1038/nn.4182>

This page has been removed by the author of this thesis for copyright reasons.

<https://dx.doi.org/10.1038/nn.4182>

This page has been removed by the author of this thesis for copyright reasons.

<https://dx.doi.org/10.1038/nn.4182>

This page has been removed by the author of this thesis for copyright reasons.

<https://dx.doi.org/10.1038/nn.4182>

This page has been removed by the author of this thesis for copyright reasons.

<https://dx.doi.org/10.1038/nn.4182>

This page has been removed by the author of this thesis for copyright reasons.

<https://dx.doi.org/10.1093/hmg/ddw373>

This page has been removed by the author of this thesis for copyright reasons.

<https://dx.doi.org/10.1093/hmg/ddw373>

This page has been removed by the author of this thesis for copyright reasons.

<https://dx.doi.org/10.1093/hmg/ddw373>

This page has been removed by the author of this thesis for copyright reasons.

<https://dx.doi.org/10.1093/hmg/ddw373>

This page has been removed by the author of this thesis for copyright reasons.

<https://dx.doi.org/10.1093/hmg/ddw373>

This page has been removed by the author of this thesis for copyright reasons.

<https://dx.doi.org/10.1093/hmg/ddw373>

This page has been removed by the author of this thesis for copyright reasons.

<https://dx.doi.org/10.1093/hmg/ddw373>

This page has been removed by the author of this thesis for copyright reasons.

<https://dx.doi.org/10.1093/hmg/ddw373>

This page has been removed by the author of this thesis for copyright reasons.

<https://dx.doi.org/10.1093/hmg/ddw373>

This page has been removed by the author of this thesis for copyright reasons.

<https://dx.doi.org/10.1093/hmg/ddw373>

This page has been removed by the author of this thesis for copyright reasons.

<https://dx.doi.org/10.1093/hmg/ddw373>

This page has been removed by the author of this thesis for copyright reasons.

<https://dx.doi.org/10.1093/hmg/ddw373>

This page has been removed by the author of this thesis for copyright reasons.

<https://dx.doi.org/10.1093/hmg/ddw373>

This page has been removed by the author of this thesis for copyright reasons.

<https://dx.doi.org/10.1093/hmg/ddw373>

This page has been removed by the author of this thesis for copyright reasons.

<https://dx.doi.org/10.1093/hmg/ddw373>

This page has been removed by the author of this thesis for copyright reasons.

<https://dx.doi.org/10.1093/hmg/ddw373>

Bibliography

- ABDOLMALEKY, H. M., CHENG, K. H., FARAONE, S. V., WILCOX, M., GLATT, S. J., GAO, F., SMITH, C. L., SHAFI, R., AEALI, B., CARNEVALE, J., PAN, H., PAPAGEORGIS, P., PONTE, J. F., SIVARAMAN, V., TSUANG, M. T. & THIAGALINGAM, S. 2006. Hypomethylation of MB-COMT promoter is a major risk factor for schizophrenia and bipolar disorder. *Hum Mol Genet*, 15, 3132-45.
- ABDOLMALEKY, H. M., CHENG, K. H., RUSSO, A., SMITH, C. L., FARAONE, S. V., WILCOX, M., SHAFI, R., GLATT, S. J., NGUYEN, G., PONTE, J. F., THIAGALINGAM, S. & TSUANG, M. T. 2005. Hypermethylation of the reelin (RELN) promoter in the brain of schizophrenic patients: a preliminary report. *Am J Med Genet B Neuropsychiatr Genet*, 134B, 60-6.
- ABDOLMALEKY, H. M., YAQUBI, S., PAPAGEORGIS, P., LAMBERT, A. W., OZTURK, S., SIVARAMAN, V. & THIAGALINGAM, S. 2011. Epigenetic dysregulation of HTR2A in the brain of patients with schizophrenia and bipolar disorder. *Schizophr Res*, 129, 183-90.
- ABERG, K. A., MCCLAY, J. L., NERELLA, S., CLARK, S., KUMAR, G., CHEN, W., KHACHANE, A. N., XIE, L., HUDSON, A., GAO, G., HARADA, A., HULTMAN, C. M., SULLIVAN, P. F., MAGNUSSON, P. K. & VAN DEN OORD, E. J. 2014. Methylome-wide association study of schizophrenia: identifying blood biomarker signatures of environmental insults. *JAMA Psychiatry*, 71, 255-64.
- AHMED, T., HARALDSEN, J. T., REHR, J. J., DI VENTRA, M., SCHULLER, I. & BALATSKY, A. V. 2014. Correlation dynamics and enhanced signals for the identification of serial biomolecules and DNA bases. *Nanotechnology*, 25, 125705.
- ALEMAN, A., KAHN, R. S. & SELTEN, J. P. 2003. Sex differences in the risk of schizophrenia: evidence from meta-analysis. *Arch Gen Psychiatry*, 60, 565-71.
- ALLIS, C. D., CAPARROS, M. L., JENUWEIN, T. & REINBERG, D. 2015. *Epigenetics*, Cold Spring Harbor Laboratory Press.
- AMERICAN PSYCHIATRIC ASSOCIATION 1994. *Diagnostic and statistical manual of mental disorders: DSM-IV*, Washington, DC, USA, American Psychiatric Association.
- AMERICAN PSYCHIATRIC ASSOCIATION 2013. *Diagnostic and statistical manual of mental disorders (5th Edition)*, Washington, DC, USA, American Psychiatric Association.
- ANDREASEN, N. C. & PIERSON, R. 2008. The role of the cerebellum in schizophrenia. *Biol Psychiatry*, 64, 81-8.
- ANDREWS, S. 2010. FastQC: A quality control tool for high throughput sequence data. Available online at: <http://www.bioinformatics.babraham.ac.uk/projects/fastqc>.
- ANGATA, T. & VARKI, A. 2000. Cloning, characterization, and phylogenetic analysis of siglec-9, a new member of the CD33-related group of siglecs. Evidence for co-evolution with sialic acid synthesis pathways. *J Biol Chem*, 275, 22127-35.
- ARION, D., UNGER, T., LEWIS, D. A., LEVITT, P. & MIRNICS, K. 2007. Molecular evidence for increased expression of genes related to immune

- and chaperone function in the prefrontal cortex in schizophrenia. *Biol Psychiatry*, 62, 711-21.
- ARYEE, M. J., JAFFE, A. E., CORRADA-BRAVO, H., LADD-ACOSTA, C., FEINBERG, A. P., HANSEN, K. D. & IRIZARRY, R. A. 2014. Minfi: a flexible and comprehensive Bioconductor package for the analysis of Infinium DNA methylation microarrays. *Bioinformatics*, 30, 1363-9.
- ASHBURNER, M., BALL, C. A., BLAKE, J. A., BOTSTEIN, D., BUTLER, H., CHERRY, J. M., DAVIS, A. P., DOLINSKI, K., DWIGHT, S. S., EPPIG, J. T., HARRIS, M. A., HILL, D. P., ISSEL-TARVER, L., KASARSKIS, A., LEWIS, S., MATESE, J. C., RICHARDSON, J. E., RINGWALD, M., RUBIN, G. M. & SHERLOCK, G. 2000. Gene ontology: tool for the unification of biology. The Gene Ontology Consortium. *Nat Genet*, 25, 25-9.
- AVNER, P. & HEARD, E. 2001. X-chromosome inactivation: counting, choice and initiation. *Nat Rev Genet*, 2, 59-67.
- BABRAHAM BIOINFORMATICS GROUP. 2015. *FastQ Screen tool website* [Online]. http://www.bioinformatics.babraham.ac.uk/projects/fastq_screen/: Babraham Institute. [Accessed 2015].
- BACHMAN, K. E., ROUNTREE, M. R. & BAYLIN, S. B. 2001. Dnmt3a and Dnmt3b are transcriptional repressors that exhibit unique localization properties to heterochromatin. *J Biol Chem*, 276, 32282-7.
- BACHMAN, M., URIBE-LEWIS, S., YANG, X., BURGESS, H. E., IURLARO, M., REIK, W., MURRELL, A. & BALASUBRAMANIAN, S. 2015. 5-Formylcytosine can be a stable DNA modification in mammals. *Nat Chem Biol*, 11, 555-557.
- BACHMAN, M., URIBE-LEWIS, S., YANG, X., WILLIAMS, M., MURRELL, A. & BALASUBRAMANIAN, S. 2014. 5-Hydroxymethylcytosine is a predominantly stable DNA modification. *Nat Chem*, 6, 1049-1055.
- BACON, C., SCHNEIDER, M., LE MAGUERESSE, C., FROELICH, H., STICHT, C., GLUCH, C., MONYER, H. & RAPPOLD, G. A. 2015. Brain-specific Foxp1 deletion impairs neuronal development and causes autistic-like behaviour. *Mol Psychiatry*, 20, 632-9.
- BAKER, C., BELBIN, O., KALSHEKER, N. & MORGAN, K. 2007. SERPINA3 (aka alpha-1-antichymotrypsin). *Front Biosci*, 12, 2821-35.
- BALL, M. P., LI, J. B., GAO, Y., LEE, J. H., LEPROUST, E. M., PARK, I. H., XIE, B., DALEY, G. Q. & CHURCH, G. M. 2009. Targeted and genome-scale strategies reveal gene-body methylation signatures in human cells. *Nat Biotechnol*, 27, 361-8.
- BALLEINE, B. W., DELGADO, M. R. & HIKOSAKA, O. 2007. The role of the dorsal striatum in reward and decision-making. *J Neurosci*, 27, 8161-5.
- BARABASI, A. L. & OLTVAI, Z. N. 2004. Network biology: understanding the cell's functional organization. *Nat Rev Genet*, 5, 101-13.
- BARRY, G. 2014. Integrating the roles of long and small non-coding RNA in brain function and disease. *Mol Psychiatry*, 19, 410-6.
- BENACERRAF, B. 1981. Role of MHC gene products in immune regulation. *Science*, 212, 1229-38.
- BENES, F. M. & BERRETTA, S. 2001. GABAergic interneurons: implications for understanding schizophrenia and bipolar disorder. *Neuropsychopharmacology*, 25, 1-27.

- BENROS, M. E., NIELSEN, P. R., NORDENTOFT, M., EATON, W. W., DALTON, S. O. & MORTENSEN, P. B. 2011. Autoimmune diseases and severe infections as risk factors for schizophrenia: a 30-year population-based register study. *Am J Psychiatry*, 168, 1303-10.
- BERCURY, K. K., DAI, J., SACHS, H. H., AHRENDSEN, J. T., WOOD, T. L. & MACKLIN, W. B. 2014. Conditional ablation of raptor or rictor has differential impact on oligodendrocyte differentiation and CNS myelination. *J Neurosci*, 34, 4466-80.
- BERG, I. L., NEUMANN, R., LAM, K. W., SARBAJNA, S., ODENTHAL-HESSE, L., MAY, C. A. & JEFFREYS, A. J. 2010. PRDM9 variation strongly influences recombination hot-spot activity and meiotic instability in humans. *Nat Genet*, 42, 859-63.
- BERGER, S. L. 2007. The complex language of chromatin regulation during transcription. *Nature*, 447, 407-12.
- BERNSTEIN, B. E., STAMATOYANNOPOULOS, J. A., COSTELLO, J. F., REN, B., MILOSAVLJEVIC, A., MEISSNER, A., KELLIS, M., MARRA, M. A., BEAUDET, A. L., ECKER, J. R., FARNHAM, P. J., HIRST, M., LANDER, E. S., MIKKELSEN, T. S. & THOMSON, J. A. 2010. The NIH Roadmap Epigenomics Mapping Consortium. *Nat Biotechnol*, 28, 1045-8.
- BIBIKOVA, M., BARNES, B., TSAN, C., HO, V., KLOTZLE, B., LE, J. M., DELANO, D., ZHANG, L., SCHROTH, G. P., GUNDERSON, K. L., FAN, J. B. & SHEN, R. 2011. High density DNA methylation array with single CpG site resolution. *Genomics*, 98, 288-95.
- BIRD, A. 2007. Perceptions of epigenetics. *Nature*, 447, 396-8.
- BIRD, A. P. 1986. CpG-rich islands and the function of DNA methylation. *Nature*, 321, 209-13.
- BOADA, R., JANUSZ, J., HUTAFF-LEE, C. & TARTAGLIA, N. 2009. The cognitive phenotype in Klinefelter syndrome: a review of the literature including genetic and hormonal factors. *Dev Disabil Res Rev*, 15, 284-94.
- BOCK, C. 2009. Epigenetic biomarker development. *Epigenomics*, 1, 99-110.
- BOKS, M. P., DE JONG, N. M., KAS, M. J., VINKERS, C. H., FERNANDES, C., KAHN, R. S., MILL, J. & OPHOFF, R. A. 2012. Current status and future prospects for epigenetic psychopharmacology. *Epigenetics*, 7, 20-8.
- BOLGER, A. M., LOHSE, M. & USADEL, B. 2014. Trimmomatic: a flexible trimmer for Illumina sequence data. *Bioinformatics*, 30, 2114-20.
- BOOTH, M. J., BRANCO, M. R., FICZ, G., OXLEY, D., KRUEGER, F., REIK, W. & BALASUBRAMANIAN, S. 2012. Quantitative sequencing of 5-methylcytosine and 5-hydroxymethylcytosine at single-base resolution. *Science*, 336, 934-7.
- BOOTH, M. J., MARSICO, G., BACHMAN, M., BERALDI, D. & BALASUBRAMANIAN, S. 2014. Quantitative sequencing of 5-formylcytosine in DNA at single-base resolution. *Nat Chem*, 6, 435-40.
- BOOTH, M. J., OST, T. W., BERALDI, D., BELL, N. M., BRANCO, M. R., REIK, W. & BALASUBRAMANIAN, S. 2013. Oxidative bisulfite sequencing of 5-methylcytosine and 5-hydroxymethylcytosine. *Nat Protoc*, 8, 1841-51.
- BOSIA, M., PIGONI, A. & CAVALLARO, R. 2015. Genomics and epigenomics in novel schizophrenia drug discovery: translating animal models to clinical research and back. *Expert Opin Drug Discov*, 10, 125-39.

- BOWDEN, N. A., SCOTT, R. J. & TOONEY, P. A. 2008. Altered gene expression in the superior temporal gyrus in schizophrenia. *BMC Genomics*, 9, 199.
- BRANCO, M. R., FICZ, G. & REIK, W. 2012. Uncovering the role of 5-hydroxymethylcytosine in the epigenome. *Nat Rev Genet*, 13, 7-13.
- BRAUER, A. U., SAVASKAN, N. E., KUHN, H., PREHN, S., NINNEMANN, O. & NITSCH, R. 2003. A new phospholipid phosphatase, PRG-1, is involved in axon growth and regenerative sprouting. *Nat Neurosci*, 6, 572-8.
- BRONWEN (GENEBUILD) - ENSEMBL BLOG. 2011. *Accessing alternate sequences in human* [Online]. <http://www.ensembl.info/blog/2011/05/20/accessing-non-reference-sequences-in-human/>. [Accessed 2016].
- BROWN, A. S. & DERKITS, E. J. 2010. Prenatal infection and schizophrenia: a review of epidemiologic and translational studies. *Am J Psychiatry*, 167, 261-80.
- BROWN, A. S., HOOTON, J., SCHAEFER, C. A., ZHANG, H., PETKOVA, E., BABULAS, V., PERRIN, M., GORMAN, J. M. & SUSSER, E. S. 2004. Elevated maternal interleukin-8 levels and risk of schizophrenia in adult offspring. *Am J Psychiatry*, 161, 889-95.
- BUNDO, M., TOYOSHIMA, M., OKADA, Y., AKAMATSU, W., UEDA, J., NEMOTO-MIYAUCHI, T., SUNAGA, F., TORITSUKA, M., IKAWA, D., KAKITA, A., KATO, M., KASAI, K., KISHIMOTO, T., NAWA, H., OKANO, H., YOSHIKAWA, T., KATO, T. & IWAMOTO, K. 2014. Increased I1 retrotransposition in the neuronal genome in schizophrenia. *Neuron*, 81, 306-13.
- BURMEISTER, M., MCINNIS, M. G. & ZOLLNER, S. 2008. Psychiatric genetics: progress amid controversy. *Nat Rev Genet*, 9, 527-40.
- CANNON, M., JONES, P. B. & MURRAY, R. M. 2002. Obstetric complications and schizophrenia: historical and meta-analytic review. *Am J Psychiatry*, 159, 1080-92.
- CAPECCHI, M. R. 2005. Gene targeting in mice: functional analysis of the mammalian genome for the twenty-first century. *Nat Rev Genet*, 6, 507-12.
- CARLSON, M. R., ZHANG, B., FANG, Z., MISCHEL, P. S., HORVATH, S. & NELSON, S. F. 2006. Gene connectivity, function, and sequence conservation: predictions from modular yeast co-expression networks. *BMC Genomics*, 7, 40.
- CARRARD, A., SALZMANN, A., MALAFOSSE, A. & KAREGE, F. 2011. Increased DNA methylation status of the serotonin receptor 5HTR1A gene promoter in schizophrenia and bipolar disorder. *J Affect Disord*, 132, 450-3.
- CARROLL, L. S. & OWEN, M. J. 2009. Genetic overlap between autism, schizophrenia and bipolar disorder. *Genome Medicine*, 1, 1-7.
- CHANG, C. C., CHOW, C. C., TELLIER, L. C., VATTIKUTI, S., PURCELL, S. M. & LEE, J. J. 2015. Second-generation PLINK: rising to the challenge of larger and richer datasets. *Gigascience*, 4, 7.
- CHEN, C., ZHANG, C., CHENG, L., REILLY, J. L., BISHOP, J. R., SWEENEY, J. A., CHEN, H. Y., GERSHON, E. S. & LIU, C. 2014. Correlation between DNA methylation and gene expression in the brains of patients with bipolar disorder and schizophrenia. *Bipolar Disord*, 16, 790-9.

- CHEN, T., UEDA, Y., DODGE, J. E., WANG, Z. & LI, E. 2003. Establishment and maintenance of genomic methylation patterns in mouse embryonic stem cells by Dnmt3a and Dnmt3b. *Mol Cell Biol*, 23, 5594-605.
- CHEN, Y., ZHANG, J., ZHANG, L., SHEN, Y. & XU, Q. 2012. Effects of MAOA promoter methylation on susceptibility to paranoid schizophrenia. *Hum Genet*, 131, 1081-7.
- CHEN, Y. A., LEMIRE, M., CHOUFANI, S., BUTCHER, D. T., GRAFODATSKAYA, D., ZANKE, B. W., GALLINGER, S., HUDSON, T. J. & WEKSBERG, R. 2013. Discovery of cross-reactive probes and polymorphic CpGs in the Illumina Infinium HumanMethylation450 microarray. *Epigenetics*, 8, 203-9.
- CHENG, Y., BERNSTEIN, A., CHEN, D. & JIN, P. 2015. 5-Hydroxymethylcytosine: A new player in brain disorders? *Exp Neurol*, 268, 3-9.
- CLOUDGENE. 2016. *Michigan Imputation Server* [Online]. <https://imputationserver.sph.umich.edu/start.html#!pages/home>. [Accessed 16th March 2016].
- COLD SPRING HARBOR LABORATORY. 2009. *Genes to Cognition Online* [Online]. <http://www.g2conline.org/>. [Accessed 14th March 2016].
- CONESA, A., MADRIGAL, P., TARAZONA, S., GOMEZ-CABRERO, D., CERVERA, A., MCPHERSON, A., SZCZESNIAK, M. W., GAFFNEY, D. J., ELO, L. L., ZHANG, X. & MORTAZAVI, A. 2016. A survey of best practices for RNA-seq data analysis. *Genome Biol*, 17, 13.
- COX, D. R. & REID, N. 1987. Parameter orthogonality and approximate conditional inference. *Journal of the Royal Statistical Society. Series B (Methodological)*, 1-39.
- CRADDOCK, N., O'DONOVAN, M. C. & OWEN, M. J. 2005. The genetics of schizophrenia and bipolar disorder: dissecting psychosis. *J Med Genet*, 42, 193-204.
- CROCKER, P. R., PAULSON, J. C. & VARKI, A. 2007. Siglecs and their roles in the immune system. *Nat Rev Immunol*, 7, 255-66.
- CROW, T. J. 2011. 'The missing genes: what happened to the heritability of psychiatric disorders?'. *Mol Psychiatry*, 16, 362-4.
- DALACK, G. W., HEALY, D. J. & MEADOR-WOODRUFF, J. H. 1998. Nicotine dependence in schizophrenia: clinical phenomena and laboratory findings. *Am J Psychiatry*, 155, 1490-501.
- DANECEK, P., AUTON, A., ABECASIS, G., ALBERS, C. A., BANKS, E., DEPRISTO, M. A., HANDSAKER, R. E., LUNTER, G., MARTH, G. T., SHERRY, S. T., MCVEAN, G., DURBIN, R. & GENOMES PROJECT ANALYSIS, G. 2011. The variant call format and VCFtools. *Bioinformatics*, 27, 2156-8.
- DAVIES, M. N., VOLTA, M., PIDSLEY, R., LUNNON, K., DIXIT, A., LOVESTONE, S., COARFA, C., HARRIS, R. A., MILOSAVLJEVIC, A., TROAKES, C., AL-SARRAJ, S., DOBSON, R., SCHALKWYK, L. C. & MILL, J. 2012. Functional annotation of the human brain methylome identifies tissue-specific epigenetic variation across brain and blood. *Genome Biol*, 13, R43.
- DAVIES, W., ISLES, A. R. & WILKINSON, L. S. 2005. Imprinted gene expression in the brain. *Neurosci Biobehav Rev*, 29, 421-30.
- DAVIS S, D. P., BILKE S, TRICHE T, JR. AND BOOTWALLA M 2015. methylumi: Handle Illumina methylation data. R package version 2.17.0, .

- DAWLATY, M. M., BREILING, A., LE, T., RADDATZ, G., BARRASA, M. I., CHENG, A. W., GAO, Q., POWELL, B. E., LI, Z., XU, M., FAULL, K. F., LYKO, F. & JAENISCH, R. 2013. Combined deficiency of Tet1 and Tet2 causes epigenetic abnormalities but is compatible with postnatal development. *Dev Cell*, 24, 310-23.
- DE ANDA, F. C., ROSARIO, A. L., DURAK, O., TRAN, T., GRAFF, J., MELETIS, K., REI, D., SODA, T., MADABHUSHI, R., GINTY, D. D., KOLODKIN, A. L. & TSAI, L. H. 2012. Autism spectrum disorder susceptibility gene TAOK2 affects basal dendrite formation in the neocortex. *Nat Neurosci*, 15, 1022-31.
- DE LEON, J. & DIAZ, F. J. 2005. A meta-analysis of worldwide studies demonstrates an association between schizophrenia and tobacco smoking behaviors. *Schizophr Res*, 76, 135-57.
- DEDEURWAERDER, S., DEFRANCE, M., CALONNE, E., DENIS, H., SOTIRIOU, C. & FUKS, F. 2011. Evaluation of the Infinium Methylation 450K technology. *Epigenomics*, 3, 771-84.
- DELANEAU, O., MARCHINI, J. & ZAGURY, J. F. 2012. A linear complexity phasing method for thousands of genomes. *Nat Methods*, 9, 179-81.
- DEMPSTER, E., VIANA, J., PIDSLEY, R. & MILL, J. 2013. Epigenetic studies of schizophrenia: progress, predicaments, and promises for the future. *Schizophr Bull*, 39, 11-6.
- DEMPSTER, E. L., MILL, J., CRAIG, I. W. & COLLIER, D. A. 2006. The quantification of COMT mRNA in post mortem cerebellum tissue: diagnosis, genotype, methylation and expression. *BMC Med Genet*, 7, 10.
- DEMPSTER, E. L., PIDSLEY, R., SCHALKWYK, L. C., OWENS, S., GEORGIADES, A., KANE, F., KALIDINDI, S., PICCHIONI, M., KRAVARITI, E., TOULOPOULOU, T., MURRAY, R. M. & MILL, J. 2011. Disease-associated epigenetic changes in monozygotic twins discordant for schizophrenia and bipolar disorder. *Hum Mol Genet*, 20, 4786-96.
- DENG, H., LIANG, H. & JANKOVIC, J. 2013. F-box only protein 7 gene in parkinsonian-pyramidal disease. *JAMA Neurol*, 70, 20-4.
- DINGER, M. E., AMARAL, P. P., MERCER, T. R., PANG, K. C., BRUCE, S. J., GARDINER, B. B., ASKARIAN-AMIRI, M. E., RU, K., SOLDA, G., SIMONS, C., SUNKIN, S. M., CROWE, M. L., GRIMMOND, S. M., PERKINS, A. C. & MATTICK, J. S. 2008. Long noncoding RNAs in mouse embryonic stem cell pluripotency and differentiation. *Genome Res*, 18, 1433-45.
- DOI, A., PARK, I. H., WEN, B., MURAKAMI, P., ARYEE, M. J., IRIZARRY, R., HERB, B., LADD-ACOSTA, C., RHO, J., LOEWER, S., MILLER, J., SCHLAEGER, T., DALEY, G. Q. & FEINBERG, A. P. 2009. Differential methylation of tissue- and cancer-specific CpG island shores distinguishes human induced pluripotent stem cells, embryonic stem cells and fibroblasts. *Nat Genet*, 41, 1350-3.
- DOLGA, A. M. & CULMSEE, C. 2012. Protective Roles for Potassium SK/K(Ca)₂ Channels in Microglia and Neurons. *Front Pharmacol*, 3, 196.
- DOUGLAS-BELL CANADA BRAIN BANK WEBSITE. 2016. <http://douglasbrainbank.ca/>. [Accessed 27th February 2016].
- DUDBRIDGE, F. 2013. Power and predictive accuracy of polygenic risk scores. *PLoS Genet*, 9, e1003348.

- DURINCK, S., SPELLMAN, P. T., BIRNEY, E. & HUBER, W. 2009. Mapping identifiers for the integration of genomic datasets with the R/Bioconductor package biomaRt. *Nat Protoc*, 4, 1184-91.
- ECKHARDT, F., LEWIN, J., CORTESE, R., RAKYAN, V. K., ATTWOOD, J., BURGER, M., BURTON, J., COX, T. V., DAVIES, R., DOWN, T. A., HAEFLIGER, C., HORTON, R., HOWE, K., JACKSON, D. K., KUNDE, J., KOENIG, C., LIDDLE, J., NIBLETT, D., OTTO, T., PETTETT, R., SEEMANN, S., THOMPSON, C., WEST, T., ROGERS, J., OLEK, A., BERLIN, K. & BECK, S. 2006. DNA methylation profiling of human chromosomes 6, 20 and 22. *Nat Genet*, 38, 1378-85.
- ECKLE, V. S., SHCHEGLOVITOV, A., VITKO, I., DEY, D., YAP, C. C., WINCKLER, B. & PEREZ-REYES, E. 2014. Mechanisms by which a CACNA1H mutation in epilepsy patients increases seizure susceptibility. *J Physiol*, 592, 795-809.
- EDINBURGH BRAIN AND TISSUE BANKS WEBSITE. 2016. <http://www.wiki.ed.ac.uk/display/edinburghbrainbanks/EDINBURGH+BR+AIN+AND+TISSUE+BANKS>. [Accessed 27th February 2016].
- EGGER, G., LIANG, G., APARICIO, A. & JONES, P. A. 2004. Epigenetics in human disease and prospects for epigenetic therapy. *Nature*, 429, 457-63.
- ELIA, J., GAI, X., XIE, H. M., PERIN, J. C., GEIGER, E., GLESSNER, J. T., D'ARCY, M., DEBERARDINIS, R., FRACKELTON, E., KIM, C., LANTIERI, F., MUGANGA, B. M., WANG, L., TAKEDA, T., RAPPAPORT, E. F., GRANT, S. F., BERRETTINI, W., DEVOTO, M., SHAIKH, T. H., HAKONARSON, H. & WHITE, P. S. 2010. Rare structural variants found in attention-deficit hyperactivity disorder are preferentially associated with neurodevelopmental genes. *Mol Psychiatry*, 15, 637-46.
- ELLIOTT, H. R., TILLIN, T., MCARDLE, W. L., HO, K., DUGGIRALA, A., FRAYLING, T. M., DAVEY SMITH, G., HUGHES, A. D., CHATURVEDI, N. & RELTON, C. L. 2014. Differences in smoking associated DNA methylation patterns in South Asians and Europeans. *Clin Epigenetics*, 6, 4.
- EMBL-EBI. 2016. *1000 Genomes Project* [Online]. <http://www.1000genomes.org/>. [Accessed 16th March 2016].
- ENCODE PROJECT CONSORTIUM 2012. An integrated encyclopedia of DNA elements in the human genome. *Nature*, 489, 57-74.
- ENCODE PROJECT CONSORTIUM, BIRNEY, E., STAMATOYANNOPOULOS, J. A., DUTTA, A., GUIGO, R., GINGERAS, T. R., MARGULIES, E. H., WENG, Z., SNYDER, M., DERMITZAKIS, E. T., THURMAN, R. E., KUEHN, M. S., TAYLOR, C. M., NEPH, S., KOCH, C. M., ASTHANA, S., MALHOTRA, A., ADZHUBEI, I., GREENBAUM, J. A., ANDREWS, R. M., FLICEK, P., BOYLE, P. J., CAO, H., CARTER, N. P., CLELLAND, G. K., DAVIS, S., DAY, N., DHAMI, P., DILLON, S. C., DORSCHNER, M. O., FIEGLER, H., GIRESI, P. G., GOLDY, J., HAWRYLYCZ, M., HAYDOCK, A., HUMBERT, R., JAMES, K. D., JOHNSON, B. E., JOHNSON, E. M., FRUM, T. T., ROSENZWEIG, E. R., KARNANI, N., LEE, K., LEFEBVRE, G. C., NAVAS, P. A., NERI, F., PARKER, S. C., SABO, P. J., SANDSTROM, R., SHAFER, A., VETRIE, D., WEAVER, M., WILCOX, S., YU, M., COLLINS, F. S., DEKKER, J., LIEB, J. D., TULLIUS, T. D., CRAWFORD, G. E., SUNYAEV, S.,

- NOBLE, W. S., DUNHAM, I., DENOEUDE, F., REYMOND, A., KAPRANOV, P., ROZOWSKY, J., ZHENG, D., CASTELO, R., FRANKISH, A., HARROW, J., GHOSH, S., SANDELIN, A., HOFACKER, I. L., BAERTSCH, R., KEEFE, D., DIKE, S., CHENG, J., HIRSCH, H. A., SEKINGER, E. A., LAGARDE, J., ABRIL, J. F., SHAHAB, A., FLAMM, C., FRIED, C., HACKERMULLER, J., HERTEL, J., LINDEMEYER, M., MISSAL, K., TANZER, A., WASHIETL, S., KORBEL, J., EMANUELSSON, O., PEDERSEN, J. S., HOLROYD, N., TAYLOR, R., SWARBRECK, D., MATTHEWS, N., DICKSON, M. C., THOMAS, D. J., WEIRAUCH, M. T., et al. 2007. Identification and analysis of functional elements in 1% of the human genome by the ENCODE pilot project. *Nature*, 447, 799-816.
- EUROPEAN BIOINFORMATICS INSTITUTE. 2016. *HUGO Gene Nomenclature Committee at the European Bioinformatics Institute* [Online]. <http://www.genenames.org/>. [Accessed May 2016].
- EXETER SEQUENCING SERVICE. 2015. *Exeter Sequencing Service website* [Online]. <http://sequencing.exeter.ac.uk/>. [Accessed 11th May 2016].
- EZKURDIA, I., JUAN, D., RODRIGUEZ, J. M., FRANKISH, A., DIEKHANS, M., HARROW, J., VAZQUEZ, J., VALENCIA, A. & TRESS, M. L. 2014. Multiple evidence strands suggest that there may be as few as 19,000 human protein-coding genes. *Hum Mol Genet*, 23, 5866-78.
- FATEMI, S. H. & FOLSOM, T. D. 2009. The neurodevelopmental hypothesis of schizophrenia, revisited. *Schizophr Bull*, 35, 528-48.
- FAUL, F., ERDFELDER, E., LANG, A. G. & BUCHNER, A. 2007. G*Power 3: a flexible statistical power analysis program for the social, behavioral, and biomedical sciences. *Behav Res Methods*, 39, 175-91.
- FELSENFELD, G. & GROUDINE, M. 2003. Controlling the double helix. *Nature*, 421, 448-53.
- FERREIRA, M. A., O'DONOVAN, M. C., MENG, Y. A., JONES, I. R., RUDERFER, D. M., JONES, L., FAN, J., KIROV, G., PERLIS, R. H., GREEN, E. K., SMOLLER, J. W., GROZEVA, D., STONE, J., NIKOLOV, I., CHAMBERT, K., HAMSHERE, M. L., NINGAONKAR, V. L., MOSKVINA, V., THASE, M. E., CAESAR, S., SACHS, G. S., FRANKLIN, J., GORDON-SMITH, K., ARDLIE, K. G., GABRIEL, S. B., FRASER, C., BLUMENSTIEL, B., DEFELICE, M., BREEN, G., GILL, M., MORRIS, D. W., ELKIN, A., MUIR, W. J., MCGHEE, K. A., WILLIAMSON, R., MACINTYRE, D. J., MACLEAN, A. W., ST, C. D., ROBINSON, M., VAN BECK, M., PEREIRA, A. C., KANDASWAMY, R., MCQUILLIN, A., COLLIER, D. A., BASS, N. J., YOUNG, A. H., LAWRENCE, J., FERRIER, I. N., ANJORIN, A., FARMER, A., CURTIS, D., SCOLNICK, E. M., MCGUFFIN, P., DALY, M. J., CORVIN, A. P., HOLMANS, P. A., BLACKWOOD, D. H., GURLING, H. M., OWEN, M. J., PURCELL, S. M., SKLAR, P., CRADDOCK, N. & WELLCOME TRUST CASE CONTROL, C. 2008. Collaborative genome-wide association analysis supports a role for ANK3 and CACNA1C in bipolar disorder. *Nat Genet*, 40, 1056-8.
- FICZ, G., BRANCO, M. R., SEISENBERGER, S., SANTOS, F., KRUEGER, F., HORE, T. A., MARQUES, C. J., ANDREWS, S. & REIK, W. 2011. Dynamic regulation of 5-hydroxymethylcytosine in mouse ES cells and during differentiation. *Nature*, 473, 398-402.
- FILLMAN, S. G., CLOONAN, N., CATTS, V. S., MILLER, L. C., WONG, J., MCCROSSIN, T., CAIRNS, M. & WEICKERT, C. S. 2013. Increased

- inflammatory markers identified in the dorsolateral prefrontal cortex of individuals with schizophrenia. *Mol Psychiatry*, 18, 206-14.
- FILLMAN, S. G., SINCLAIR, D., FUNG, S. J., WEBSTER, M. J. & SHANNON WEICKERT, C. 2014. Markers of inflammation and stress distinguish subsets of individuals with schizophrenia and bipolar disorder. *Transl Psychiatry*, 4, e365.
- FINNEGAN, E. J. & MATZKE, M. A. 2003. The small RNA world. *J Cell Sci*, 116, 4689-93.
- FISHER, R. A. 1922. On the interpretation of χ^2 from contingency tables, and the calculation of P. *Journal of the Royal Statistical Society*, 85, 87-94.
- FLICEK, P., AMODE, M. R., BARRELL, D., BEAL, K., BILLIS, K., BRENT, S., CARVALHO-SILVA, D., CLAPHAM, P., COATES, G., FITZGERALD, S., GIL, L., GIRON, C. G., GORDON, L., HOURLIER, T., HUNT, S., JOHNSON, N., JUETTEMANN, T., KAHARI, A. K., KEENAN, S., KULESHA, E., MARTIN, F. J., MAUREL, T., MCLAREN, W. M., MURPHY, D. N., NAG, R., OVERDUIN, B., PIGNATELLI, M., PRITCHARD, B., PRITCHARD, E., RIAT, H. S., RUFFIER, M., SHEPPARD, D., TAYLOR, K., THORMANN, A., TREVANION, S. J., VULLO, A., WILDER, S. P., WILSON, M., ZADISSA, A., AKEN, B. L., BIRNEY, E., CUNNINGHAM, F., HARROW, J., HERRERO, J., HUBBARD, T. J., KINSELLA, R., MUFFATO, M., PARKER, A., SPUDICH, G., YATES, A., ZERBINO, D. R. & SEARLE, S. M. 2014. Ensembl 2014. *Nucleic Acids Res*, 42, D749-55.
- FLUSBERG, B. A., WEBSTER, D. R., LEE, J. H., TRAVERS, K. J., OLIVARES, E. C., CLARK, T. A., KORLACH, J. & TURNER, S. W. 2010. Direct detection of DNA methylation during single-molecule, real-time sequencing. *Nat Methods*, 7, 461-5.
- FOCKING, M., LOPEZ, L. M., ENGLISH, J. A., DICKER, P., WOLFF, A., BRINDLEY, E., WYNNE, K., CAGNEY, G. & COTTER, D. R. 2015. Proteomic and genomic evidence implicates the postsynaptic density in schizophrenia. *Mol Psychiatry*, 20, 424-32.
- FRANK, J., LANG, M., WITT, S. H., STROHMAIER, J., RUJESCU, D., CICHON, S., DEGENHARDT, F., NOTHEN, M. M., COLLIER, D. A., RIPKE, S., NABER, D. & RIETSCHER, M. 2015. Identification of increased genetic risk scores for schizophrenia in treatment-resistant patients. *Mol Psychiatry*, 20, 150-1.
- FROMMER, M., MCDONALD, L. E., MILLAR, D. S., COLLIS, C. M., WATT, F., GRIGG, G. W., MOLLOY, P. L. & PAUL, C. L. 1992. A genomic sequencing protocol that yields a positive display of 5-methylcytosine residues in individual DNA strands. *Proc Natl Acad Sci U S A*, 89, 1827-31.
- FUKS, F., BURGERS, W. A., BREHM, A., HUGHES-DAVIES, L. & KOUZARIDES, T. 2000. DNA methyltransferase Dnmt1 associates with histone deacetylase activity. *Nat Genet*, 24, 88-91.
- FUKS, F., BURGERS, W. A., GODIN, N., KASAI, M. & KOUZARIDES, T. 2001. Dnmt3a binds deacetylases and is recruited by a sequence-specific repressor to silence transcription. *EMBO J*, 20, 2536-44.
- FULLARD, J. F., HALENE, T. B., GIAMBARTOLOMEI, C., HAROUTUNIAN, V., AKBARIAN, S. & ROUSSOS, P. 2016. Understanding the genetic liability to schizophrenia through the neuroepigenome. *Schizophr Res*.

- FURY, W., BATLIWALLA, F., GREGERSEN, P. K. & LI, W. T. 2006. Overlapping probabilities of top ranking gene lists, hypergeometric distribution, and stringency of gene selection criterion. *2006 28th Annual International Conference of the IEEE Engineering in Medicine and Biology Society, Vols 1-15*, 4877-4880.
- GAMAZON, E. R., BADNER, J. A., CHENG, L., ZHANG, C., ZHANG, D., COX, N. J., GERSHON, E. S., KELSOE, J. R., GREENWOOD, T. A., NIEVERGELT, C. M., CHEN, C., MCKINNEY, R., SHILLING, P. D., SCHORK, N. J., SMITH, E. N., BLOSS, C. S., NURNBERGER, J. I., EDENBERG, H. J., FOROUD, T., KOLLER, D. L., SCHEFTNER, W. A., CORYELL, W., RICE, J., LAWSON, W. B., NWULIA, E. A., HIPOLITO, M., BYERLEY, W., MCMAHON, F. J., SCHULZE, T. G., BERRETTINI, W. H., POTASH, J. B., ZANDI, P. P., MAHON, P. B., MCINNIS, M. G., ZOLLNER, S., ZHANG, P., CRAIG, D. W., SZELINGER, S., BARRETT, T. B. & LIU, C. 2013. Enrichment of cis-regulatory gene expression SNPs and methylation quantitative trait loci among bipolar disorder susceptibility variants. *Mol Psychiatry*, 18, 340-346.
- GANAPATHIRAJU, M. K. 2012-2016. *Schizo-Pi* [Online]. <http://severus.dbmi.pitt.edu/schizo-pi/>. [Accessed 2016].
- GANAPATHIRAJU, M. K., THAHIR, M., HANDEN, A., SARKAR, S. N., SWEET, R. A., NIMGAONKAR, V. L., LOSCHER, C. E., BAUER, E. M. & CHAPARALA, S. 2016. Schizophrenia interactome with 504 novel protein–protein interactions. *Npj Schizophrenia*, 2, 16012.
- GARDINER-GARDEN, M. & FROMMER, M. 1987. CpG islands in vertebrate genomes. *J Mol Biol*, 196, 261-82.
- GARDINER, E. J., CAIRNS, M. J., LIU, B., BEVERIDGE, N. J., CARR, V., KELLY, B., SCOTT, R. J. & TOONEY, P. A. 2013. Gene expression analysis reveals schizophrenia-associated dysregulation of immune pathways in peripheral blood mononuclear cells. *J Psychiatr Res*, 47, 425-37.
- GAVIN, D. P., SHARMA, R. P., CHASE, K. A., MATRISCIANO, F., DONG, E. & GUIDOTTI, A. 2012. Growth arrest and DNA-damage-inducible, beta (GADD45b)-mediated DNA demethylation in major psychosis. *Neuropsychopharmacology*, 37, 531-42.
- GENE ONTOLOGY CONSORTIUM. 2015. *Gene ontology website* [Online]. <http://geneontology.org/>. [Accessed 7th April 2016].
- GENOME REFERENCE CONSORTIUM. 2013. *cDNA sequences from the Genome Reference Consortium Human Build 38 (GRCh38.p5 -assembly GCA_000001405.20)* [Online]. ftp://ftp.ensembl.org/pub/release-84/fastq/homo_sapiens/cdna/; Ensembl. [Accessed February 2016].
- GENTLES, A. J., NEWMAN, A. M., LIU, C. L., BRATMAN, S. V., FENG, W., KIM, D., NAIR, V. S., XU, Y., KHUONG, A., HOANG, C. D., DIEHN, M., WEST, R. B., PLEVITIS, S. K. & ALIZADEH, A. A. 2015. The prognostic landscape of genes and infiltrating immune cells across human cancers. *Nat Med*, 21, 938-45.
- GHADIRIVASFI, M., NOHESARA, S., AHMADKHANIHA, H. R., ESKANDARI, M. R., MOSTAFAVI, S., THIAGALINGAM, S. & ABDOLMALEKY, H. M. 2011. Hypomethylation of the serotonin receptor type-2A Gene (HTR2A) at T102C polymorphic site in DNA derived from the saliva of patients with schizophrenia and bipolar disorder. *Am J Med Genet B Neuropsychiatr Genet*, 156B, 536-45.

- GIBBS, J. R., VAN DER BRUG, M. P., HERNANDEZ, D. G., TRAYNOR, B. J., NALLS, M. A., LAI, S. L., AREPALLI, S., DILLMAN, A., RAFFERTY, I. P., TRONCOSO, J., JOHNSON, R., ZIELKE, H. R., FERRUCCI, L., LONGO, D. L., COOKSON, M. R. & SINGLETON, A. B. 2010. Abundant quantitative trait loci exist for DNA methylation and gene expression in human brain. *PLoS Genet*, 6, e1000952.
- GIEDD, J. N., CLASEN, L. S., WALLACE, G. L., LENROOT, R. K., LERCH, J. P., WELLS, E. M., BLUMENTHAL, J. D., NELSON, J. E., TOSSELL, J. W., STAYER, C., EVANS, A. C. & SAMANGO-SPROUSE, C. A. 2007. XXY (Klinefelter syndrome): a pediatric quantitative brain magnetic resonance imaging case-control study. *Pediatrics*, 119, e232-40.
- GOODISON, S., URQUIDI, V. & TARIN, D. 1999. CD44 cell adhesion molecules. *Mol Pathol*, 52, 189-96.
- GRAYSON, D. R., JIA, X., CHEN, Y., SHARMA, R. P., MITCHELL, C. P., GUIDOTTI, A. & COSTA, E. 2005. Reelin promoter hypermethylation in schizophrenia. *Proc Natl Acad Sci U S A*, 102, 9341-6.
- GREWAL, S. I. & JIA, S. 2007. Heterochromatin revisited. *Nat Rev Genet*, 8, 35-46.
- GROFFEN, A. J., MARTENS, S., DIEZ ARAZOLA, R., CORNELISSE, L. N., LOZOVAYA, N., DE JONG, A. P., GORIOUNOVA, N. A., HABETS, R. L., TAKAI, Y., BORST, J. G., BROSE, N., MCMAHON, H. T. & VERHAGE, M. 2010. Doc2b is a high-affinity Ca²⁺ sensor for spontaneous neurotransmitter release. *Science*, 327, 1614-8.
- GU, T. P., GUO, F., YANG, H., WU, H. P., XU, G. F., LIU, W., XIE, Z. G., SHI, L., HE, X., JIN, S. G., IQBAL, K., SHI, Y. G., DENG, Z., SZABO, P. E., PFEIFER, G. P., LI, J. & XU, G. L. 2011. The role of Tet3 DNA dioxygenase in epigenetic reprogramming by oocytes. *Nature*, 477, 606-10.
- GUIDOTTI, A., AUTA, J., DAVIS, J. M., DI-GIORGI-GEREVINI, V., DWIVEDI, Y., GRAYSON, D. R., IMPAGNATIELLO, F., PANDEY, G., PESOLD, C., SHARMA, R., UZUNOV, D. & COSTA, E. 2000. Decrease in reelin and glutamic acid decarboxylase67 (GAD67) expression in schizophrenia and bipolar disorder: a postmortem brain study. *Arch Gen Psychiatry*, 57, 1061-9.
- QUINTIVANO, J., ARYEE, M. J. & KAMINSKY, Z. A. 2013. A cell epigenotype specific model for the correction of brain cellular heterogeneity bias and its application to age, brain region and major depression. *Epigenetics*, 8, 290-302.
- GUTIERREZ-ARCELUS, M., LAPPALAINEN, T., MONTGOMERY, S. B., BUIL, A., ONGEN, H., YUROVSKY, A., BRYOIS, J., GIGER, T., ROMANO, L., PLANCHON, A., FALCONNET, E., BIELSER, D., GAGNEBIN, M., PADIOLEAU, I., BOREL, C., LETOURNEAU, A., MAKRYTHANASIS, P., GUIPPONI, M., GEHRIG, C., ANTONARAKIS, S. E. & DERMITZAKIS, E. T. 2013. Passive and active DNA methylation and the interplay with genetic variation in gene regulation. *Elife*, 2, e00523.
- HAAS, B. J., PAPANICOLAOU, A., YASSOUR, M., GRABHERR, M., BLOOD, P. D., BOWDEN, J., COUGER, M. B., ECCLES, D., LI, B., LIEBER, M., MACMANES, M. D., OTT, M., ORVIS, J., POCHET, N., STROZZI, F., WEEKS, N., WESTERMAN, R., WILLIAM, T., DEWEY, C. N., HENSCHER, R., LEDUC, R. D., FRIEDMAN, N. & REGEV, A. 2013. De

- novo transcript sequence reconstruction from RNA-seq using the Trinity platform for reference generation and analysis. *Nat Protoc*, 8, 1494-512.
- HAAS, B. J. & ZODY, M. C. 2010. Advancing RNA-Seq analysis. *Nat Biotechnol*, 28, 421-3.
- HAFNER, H., MAURER, K., LOFFLER, W., FATKENHEUER, B., AN DER HEIDEN, W., RIECHER-ROSSLER, A., BEHRENS, S. & GATTAZ, W. F. 1994. The epidemiology of early schizophrenia. Influence of age and gender on onset and early course. *Br J Psychiatry Suppl*, 29-38.
- HAMADA, S. & YAGI, T. 2001. The cadherin-related neuronal receptor family: a novel diversified cadherin family at the synapse. *Neurosci Res*, 41, 207-15.
- HAMDAN, F. F., DAOUD, H., ROCHEFORT, D., PITON, A., GAUTHIER, J., LANGLOIS, M., FOOMANI, G., DOBRZENIECKA, S., KREBS, M. O., JOOBER, R., LAFRENIERE, R. G., LACAILE, J. C., MOTTRON, L., DRAPEAU, P., BEAUCHAMP, M. H., PHILLIPS, M. S., FOMBONNE, E., ROULEAU, G. A. & MICHAUD, J. L. 2010. De novo mutations in FOXP1 in cases with intellectual disability, autism, and language impairment. *Am J Hum Genet*, 87, 671-8.
- HANNON, E., SPIERS, H., VIANA, J., PIDSLEY, R., BURRAGE, J., MURPHY, T. M., TROAKES, C., TURECKI, G., O'DONOVAN, M. C., SCHALKWYK, L. C., BRAY, N. J. & MILL, J. 2016. Methylation QTLs in the developing brain and their enrichment in schizophrenia risk loci. *Nat Neurosci*, 19, 48-54.
- HANSEN, K. D., BRENNER, S. E. & DUDOIT, S. 2010. Biases in Illumina transcriptome sequencing caused by random hexamer priming. *Nucleic Acids Res*, 38, e131.
- HARTWELL, L. H., HOPFIELD, J. J., LEIBLER, S. & MURRAY, A. W. 1999. From molecular to modular cell biology. *Nature*, 402, C47-52.
- HE, Y. F., LI, B. Z., LI, Z., LIU, P., WANG, Y., TANG, Q., DING, J., JIA, Y., CHEN, Z., LI, L., SUN, Y., LI, X., DAI, Q., SONG, C. X., ZHANG, K., HE, C. & XU, G. L. 2011. Tet-mediated formation of 5-carboxylcytosine and its excision by TDG in mammalian DNA. *Science*, 333, 1303-7.
- HECKERS, S. 2001. Neuroimaging studies of the hippocampus in schizophrenia. *Hippocampus*, 11, 520-8.
- HEIJMANS, B. T. & MILL, J. 2012. Commentary: The seven plagues of epigenetic epidemiology. *Int J Epidemiol*, 41, 74-8.
- HERT, M., SCHREURS, V., VANCAMPFORT, D. & WINKEL, R. 2009. Metabolic syndrome in people with schizophrenia: a review. *World Psychiatry*, 8, 15-22.
- HILL, M. J. & BRAY, N. J. 2012. Evidence that schizophrenia risk variation in the ZNF804A gene exerts its effects during fetal brain development. *Am J Psychiatry*, 169, 1301-8.
- HO, S. K., KOVACEVIC, N., HENKELMAN, R. M., BOYD, A., PAWSON, T. & HENDERSON, J. T. 2009. EphB2 and EphA4 receptors regulate formation of the principal inter-hemispheric tracts of the mammalian forebrain. *Neuroscience*, 160, 784-95.
- HOFFMAN, D. 2003. Negative binomial control limits for count data with extra-Poisson variation. *Pharmaceutical Statistics*, 2, 127-132.
- HORIGANE, S., AGETA-ISHIHARA, N., KAMIJO, S., FUJII, H., OKAMURA, M., KINOSHITA, M., TAKEMOTO-KIMURA, S. & BITO, H. 2016. Facilitation

- of axon outgrowth via a Wnt5a-CaMKK-CaMKIalpha pathway during neuronal polarization. *Mol Brain*, 9, 8.
- HORVATH, S. 2013a. DNA methylation age of human tissues and cell types. *Genome Biol*, 14, R115.
- HORVATH, S. 2013b. *Tutorial for the Online Age Calculator: Estimate DNA methylation age* [Online].
<https://labs.genetics.ucla.edu/horvath/dnamage/TUTORIALOnlineCalculator.pdf>. [Accessed 1st March 2016].
- HORVATH, S. 2015. Erratum to: DNA methylation age of human tissues and cell types. *Genome Biol*, 16, 96.
- HORVATH, S. 2016. *DNA Methylation Age Calculator* [Online].
<https://dnamage.genetics.ucla.edu/home>. [Accessed 01st March 2016].
- HORVATH, S. & MIRNICS, K. 2014. Immune system disturbances in schizophrenia. *Biol Psychiatry*, 75, 316-23.
- HOUSEMAN, E. A., KELSEY, K. T., WIENCKE, J. K. & MARSIT, C. J. 2015. Cell-composition effects in the analysis of DNA methylation array data: a mathematical perspective. *BMC Bioinformatics*, 16, 95.
- HOWIE, B., FUCHSBERGER, C., STEPHENS, M., MARCHINI, J. & ABECASIS, G. R. 2012. Fast and accurate genotype imputation in genome-wide association studies through pre-phasing. *Nat Genet*, 44, 955-9.
- HWANG, Y., KIM, J., SHIN, J. Y., KIM, J. I., SEO, J. S., WEBSTER, M. J., LEE, D. & KIM, S. 2013. Gene expression profiling by mRNA sequencing reveals increased expression of immune/inflammation-related genes in the hippocampus of individuals with schizophrenia. *Transl Psychiatry*, 3, e321.
- IBANEZ, C. F. 2008. Catecholaminergic neuron survival: getting hooked on GDNF. *Nat Neurosci*, 11, 735-6.
- IKEGAME, T., BUNDO, M., SUNAGA, F., ASAI, T., NISHIMURA, F., YOSHIKAWA, A., KAWAMURA, Y., HIBINO, H., TOCHIGI, M., KAKIUCHI, C., SASAKI, T., KATO, T., KASAI, K. & IWAMOTO, K. 2013. DNA methylation analysis of BDNF gene promoters in peripheral blood cells of schizophrenia patients. *Neurosci Res*, 77, 208-14.
- ILLUMINA. 2013. *Innium HTS Assay Protocol Guide* [Online].
http://support.illumina.com/downloads/infinium_hts_assay_protocol_user_guide_15045738_a.html. [Accessed 22nd April 2016].
- ILLUMINA. 2015. *Innium HD Assay Methylation Protocol Guide* [Online].
[http://support.illumina.com/downloads/infinium_hd_methylation_assay_protocol_guide_\(15019519_b\).html](http://support.illumina.com/downloads/infinium_hd_methylation_assay_protocol_guide_(15019519_b).html). [Accessed 22nd April 2016].
- IMPAGNATIELLO, F., GUIDOTTI, A. R., PESOLD, C., DWIVEDI, Y., CARUNCHO, H., PISU, M. G., UZUNOV, D. P., SMALHEISER, N. R., DAVIS, J. M., PANDEY, G. N., PAPPAS, G. D., TUETING, P., SHARMA, R. P. & COSTA, E. 1998. A decrease of reelin expression as a putative vulnerability factor in schizophrenia. *Proc Natl Acad Sci U S A*, 95, 15718-23.
- INTERNATIONAL HAPMAP, C. 2005. A haplotype map of the human genome. *Nature*, 437, 1299-320.
- INTERNATIONAL SCHIZOPHRENIA, C. 2009. Common polygenic variation contributes to risk of schizophrenia that overlaps with bipolar disorder. *Nature*, 460, 748-752.

- INTERNATIONAL SCHIZOPHRENIA, C., PURCELL, S. M., WRAY, N. R., STONE, J. L., VISSCHER, P. M., O'DONOVAN, M. C., SULLIVAN, P. F. & SKLAR, P. 2009. Common polygenic variation contributes to risk of schizophrenia and bipolar disorder. *Nature*, 460, 748-52.
- ITO, S., SHEN, L., DAI, Q., WU, S. C., COLLINS, L. B., SWENBERG, J. A., HE, C. & ZHANG, Y. 2011. Tet proteins can convert 5-methylcytosine to 5-formylcytosine and 5-carboxylcytosine. *Science*, 333, 1300-3.
- IWAMOTO, K., BUNDO, M., YAMADA, K., TAKAO, H., IWAYAMA-SHIGENO, Y., YOSHIKAWA, T. & KATO, T. 2005. DNA methylation status of SOX10 correlates with its downregulation and oligodendrocyte dysfunction in schizophrenia. *J Neurosci*, 25, 5376-81.
- JABLENSKY, A. 2010. The diagnostic concept of schizophrenia: its history, evolution, and future prospects. *Dialogues Clin Neurosci*, 12, 271-87.
- JACKSON, M. O. 2010. An overview of social networks and economic applications. *The handbook of social economics*, 1, 511-85.
- JAENISCH, R. & BIRD, A. 2003. Epigenetic regulation of gene expression: how the genome integrates intrinsic and environmental signals. *Nat Genet*, 33 Suppl, 245-54.
- JAFFE, A. E., GAO, Y., DEEP-SOBOSLAY, A., TAO, R., HYDE, T. M., WEINBERGER, D. R. & KLEINMAN, J. E. 2016. Mapping DNA methylation across development, genotype and schizophrenia in the human frontal cortex. *Nat Neurosci*, 19, 40-7.
- JAFFE, A. E. & IRIZARRY, R. A. 2014. Accounting for cellular heterogeneity is critical in epigenome-wide association studies. *Genome Biol*, 15, R31.
- JEFFRIES, A. R. & MILL, J. In Press. Profiling Regulatory Variation in the Brain: Methods for Exploring the Neuronal Epigenome. *Biological Psychiatry*.
- JIANG, L., SCHLESINGER, F., DAVIS, C. A., ZHANG, Y., LI, R., SALIT, M., GINGERAS, T. R. & OLIVER, B. 2011. Synthetic spike-in standards for RNA-seq experiments. *Genome Res*, 21, 1543-51.
- JIRTLE, R. L. & SKINNER, M. K. 2007. Environmental epigenomics and disease susceptibility. *Nat Rev Genet*, 8, 253-62.
- JONES, H. J., STERGIAKOULI, E., TANSEY, K. E., HUBBARD, L., HERON, J., CANNON, M., HOLMANS, P., LEWIS, G., LINDEN, D. E., JONES, P. B., DAVEY SMITH, G., O'DONOVAN, M. C., OWEN, M. J., WALTERS, J. T. & ZAMMIT, S. 2016. Phenotypic Manifestation of Genetic Risk for Schizophrenia During Adolescence in the General Population. *JAMA Psychiatry*, 73, 221-8.
- JONES, P. A. 2012. Functions of DNA methylation: islands, start sites, gene bodies and beyond. *Nat Rev Genet*, 13, 484-92.
- JONES, P. A. & BAYLIN, S. B. 2002. The fundamental role of epigenetic events in cancer. *Nat Rev Genet*, 3, 415-28.
- KALANI, M. Y., CHESHER, S. H., CORD, B. J., BABABEYGY, S. R., VOGEL, H., WEISSMAN, I. L., PALMER, T. D. & NUSSE, R. 2008. Wnt-mediated self-renewal of neural stem/progenitor cells. *Proc Natl Acad Sci U S A*, 105, 16970-5.
- KAPRANOV, P., CHENG, J., DIKE, S., NIX, D. A., DUTTAGUPTA, R., WILLINGHAM, A. T., STADLER, P. F., HERTEL, J., HACKERMULLER, J., HOFACKER, I. L., BELL, I., CHEUNG, E., DRENKOW, J., DUMAIS, E., PATEL, S., HELT, G., GANESH, M., GHOSH, S., PICCOLBONI, A., SEMENTCHENKO, V., TAMMANA, H. & GINGERAS, T. R. 2007. RNA

- maps reveal new RNA classes and a possible function for pervasive transcription. *Science*, 316, 1484-8.
- KASOWSKI, M., KYRIAZOPOULOU-PANAGIOTOPOULOU, S., GRUBERT, F., ZAUGG, J. B., KUNDAJE, A., LIU, Y., BOYLE, A. P., ZHANG, Q. C., ZAKHARIA, F., SPACEK, D. V., LI, J., XIE, D., OLARERIN-GEORGE, A., STEINMETZ, L. M., HOGENESCH, J. B., KELLIS, M., BATZOGLOU, S. & SNYDER, M. 2013. Extensive variation in chromatin states across humans. *Science*, 342, 750-2.
- KENDELL, R. E. 1987. Diagnosis and classification of functional psychoses. *Br Med Bull*, 43, 499-513.
- KHASHAN, A. S., ABEL, K. M., MCNAMEE, R., PEDERSEN, M. G., WEBB, R. T., BAKER, P. N., KENNY, L. C. & MORTENSEN, P. B. 2008. Higher risk of offspring schizophrenia following antenatal maternal exposure to severe adverse life events. *Arch Gen Psychiatry*, 65, 146-52.
- KIKUCHI, A. 1999. Roles of Axin in the Wnt signalling pathway. *Cell Signal*, 11, 777-88.
- KILPINEN, H., WASZAK, S. M., GSCHWIND, A. R., RAGHAV, S. K., WITWICKI, R. M., ORIOLI, A., MIGLIAVACCA, E., WIEDERKEHR, M., GUTIERREZ-ARCELUS, M., PANOUSIS, N. I., YUROVSKY, A., LAPPALAINEN, T., ROMANO-PALUMBO, L., PLANCHON, A., BIELSER, D., BRYOIS, J., PADIOLEAU, I., UDIN, G., THURNHEER, S., HACKER, D., CORE, L. J., LIS, J. T., HERNANDEZ, N., REYMOND, A., DEPLANCKE, B. & DERMITZAKIS, E. T. 2013. Coordinated effects of sequence variation on DNA binding, chromatin structure, and transcription. *Science*, 342, 744-7.
- KINOSHITA, M., NUMATA, S., TAJIMA, A., SHIMODERA, S., ONO, S., IMAMURA, A., IGA, J., WATANABE, S., KIKUCHI, K., KUBO, H., NAKATAKI, M., SUMITANI, S., IMOTO, I., OKAZAKI, Y. & OHMORI, T. 2013. DNA methylation signatures of peripheral leukocytes in schizophrenia. *Neuromolecular Med*, 15, 95-101.
- KIROV, G., RUJESCU, D., INGASON, A., COLLIER, D. A., O'DONOVAN, M. C. & OWEN, M. J. 2009. Neurexin 1 (NRXN1) deletions in schizophrenia. *Schizophr Bull*, 35, 851-4.
- KITANO, H. 2002. Systems biology: a brief overview. *Science*, 295, 1662-4.
- KLOSE, R. J. & BIRD, A. P. 2006. Genomic DNA methylation: the mark and its mediators. *Trends Biochem Sci*, 31, 89-97.
- KOHMURA, N., SENZAKI, K., HAMADA, S., KAI, N., YASUDA, R., WATANABE, M., ISHII, H., YASUDA, M., MISHINA, M. & YAGI, T. 1998. Diversity revealed by a novel family of cadherins expressed in neurons at a synaptic complex. *Neuron*, 20, 1137-51.
- KOPRA, J., VILENIUS, C., GREALISH, S., HARMA, M. A., VARENDI, K., LINDHOLM, J., CASTREN, E., VOIKAR, V., BJORKLUND, A., PIEPPONEN, T. P., SAARMA, M. & ANDRESSOO, J. O. 2015. GDNF is not required for catecholaminergic neuron survival in vivo. *Nat Neurosci*, 18, 319-22.
- KOUZARIDES, T. 2007. Chromatin modifications and their function. *Cell*, 128, 693-705.
- KRIAUCIONIS, S. & HEINTZ, N. 2009. The nuclear DNA base 5-hydroxymethylcytosine is present in Purkinje neurons and the brain. *Science*, 324, 929-30.

- KU, C. S., NAIDOO, N., WU, M. & SOONG, R. 2011. Studying the epigenome using next generation sequencing. *J Med Genet*, 48, 721-30.
- KUMARASINGHE, N., TOONEY, P. A. & SCHALL, U. 2012. Finding the needle in the haystack: a review of microarray gene expression research into schizophrenia. *Aust N Z J Psychiatry*, 46, 598-610.
- KUSHNIR, M., DRESNER, E., MANDEL, S. & GOZES, I. 2008. Silencing of the ADNP-family member, ADNP2, results in changes in cellular viability under oxidative stress. *J Neurochem*, 105, 537-45.
- LABRIE, V., PAI, S. & PETRONIS, A. 2012. Epigenetics of major psychosis: progress, problems and perspectives. *Trends Genet*, 28, 427-35.
- LADD-ACOSTA, C., PEVSNER, J., SABUNCIYAN, S., YOLKEN, R. H., WEBSTER, M. J., DINKINS, T., CALLINAN, P. A., FAN, J. B., POTASH, J. B. & FEINBERG, A. P. 2007. DNA methylation signatures within the human brain. *Am J Hum Genet*, 81, 1304-15.
- LANDAU, W. M. & LIU, P. 2013. Dispersion estimation and its effect on test performance in RNA-seq data analysis: a simulation-based comparison of methods. *PLoS One*, 8, e81415.
- LANGFELDER, P. & HORVATH, S. 2008. WGCNA: an R package for weighted correlation network analysis. *BMC Bioinformatics*, 9, 559.
- LANGMEAD, B., TRAPNELL, C., POP, M. & SALZBERG, S. L. 2009. Ultrafast and memory-efficient alignment of short DNA sequences to the human genome. *Genome Biol*, 10, R25.
- LASKY, J. L. & WU, H. 2005. Notch signaling, brain development, and human disease. *Pediatr Res*, 57, 104R-109R.
- LASZLO, A. H., DERRINGTON, I. M., BRINKERHOFF, H., LANGFORD, K. W., NOVA, I. C., SAMSON, J. M., BARTLETT, J. J., PAVLENOK, M. & GUNDLACH, J. H. 2013. Detection and mapping of 5-methylcytosine and 5-hydroxymethylcytosine with nanopore MspA. *Proc Natl Acad Sci U S A*, 110, 18904-9.
- LEE, J. A., DAMIANOV, A., LIN, C. H., FONTES, M., PARIKSHAK, N. N., ANDERSON, E. S., GESCHWIND, D. H., BLACK, D. L. & MARTIN, K. C. 2016. Cytoplasmic Rbfox1 Regulates the Expression of Synaptic and Autism-Related Genes. *Neuron*, 89, 113-28.
- LETZEN, B. S., LIU, C., THAKOR, N. V., GEARHART, J. D., ALL, A. H. & KERR, C. L. 2010. MicroRNA expression profiling of oligodendrocyte differentiation from human embryonic stem cells. *PLoS One*, 5, e10480.
- LI, B. & DEWEY, C. N. 2011. RSEM: accurate transcript quantification from RNA-Seq data with or without a reference genome. *BMC Bioinformatics*, 12, 323.
- LI, W.-W., GONG, L. & BAYLEY, H. 2013. Single-Molecule Detection of 5-Hydroxymethylcytosine in DNA through Chemical Modification and Nanopore Analysis. *Angewandte Chemie International Edition*, 52, 4350-4355.
- LIEBERS, D. T., PIROOZANIA, M., SEIFFUDIN, F., MUSLINER, K. L., ZANDI, P. P. & GOES, F. S. 2016. Polygenic Risk of Schizophrenia and Cognition in a Population-Based Survey of Older Adults. *Schizophr Bull*.
- LIEBL, D. J., MORRIS, C. J., HENKEMEYER, M. & PARADA, L. F. 2003. mRNA expression of ephrins and Eph receptor tyrosine kinases in the neonatal and adult mouse central nervous system. *J Neurosci Res*, 71, 7-22.

- LIN, L. F., DOHERTY, D. H., LILE, J. D., BEKTESH, S. & COLLINS, F. 1993. GDNF: a glial cell line-derived neurotrophic factor for midbrain dopaminergic neurons. *Science*, 260, 1130-2.
- LIN, W., ZHOU, X., ZHANG, M., LI, Y., MIAO, S., WANG, L., ZONG, S. & KOIDE, S. S. 2001. Expression and function of the HSD-3.8 gene encoding a testis-specific protein. *Mol Hum Reprod*, 7, 811-8.
- LIU, J., CHEN, J., EHRlich, S., WALTON, E., WHITE, T., PERRONE-BIZZOZERO, N., BUSTILLO, J., TURNER, J. A. & CALHOUN, V. D. 2014. Methylation patterns in whole blood correlate with symptoms in schizophrenia patients. *Schizophr Bull*, 40, 769-76.
- LODGE, D. J. & GRACE, A. A. 2008. Hippocampal dysfunction and disruption of dopamine system regulation in an animal model of schizophrenia. *Neurotox Res*, 14, 97-104.
- LOPES, C. T., FRANZ, M., KAZI, F., DONALDSON, S. L., MORRIS, Q. & BADER, G. D. 2010. Cytoscape Web: an interactive web-based network browser. *Bioinformatics*, 26, 2347-8.
- LOTT, S. A., BURGHARDT, P. R., BURGHARDT, K. J., BLY, M. J., GROVE, T. B. & ELLINGROD, V. L. 2013. The influence of metabolic syndrome, physical activity and genotype on catechol-O-methyl transferase promoter-region methylation in schizophrenia. *Pharmacogenomics J*, 13, 264-71.
- LUGER, K., MADER, A. W., RICHMOND, R. K., SARGENT, D. F. & RICHMOND, T. J. 1997. Crystal structure of the nucleosome core particle at 2.8[thinsp]Å resolution. *Nature*, 389, 251-260.
- LUNNON, K., HANNON, E., SMITH, R. G., DEMPSTER, E., WONG, C., BURRAGE, J., TROAKES, C., AL-SARRAJ, S., KEPA, A., SCHALKWYK, L. & MILL, J. 2016a. Variation in 5-hydroxymethylcytosine across human cortex and cerebellum. *Genome Biol*, 17, 27.
- LUNNON, K., HANNON, E., SMITH, R. G., DEMPSTER, E., WONG, C., BURRAGE, J., TROAKES, C., AL-SARRAJ, S., KEPA, A., SCHALKWYK, L. & MILL, J. 2016b. Variation in 5-hydroxymethylcytosine across human cortex and cerebellum. *Genome Biol*, 17, 27.
- LV, J., LIU, H., YU, S., LIU, H., CUI, W., GAO, Y., ZHENG, T., QIN, G., GUO, J., ZENG, T., HAN, Z., ZHANG, Y. & WU, Q. 2015. Identification of 4438 novel lincRNAs involved in mouse pre-implantation embryonic development. *Mol Genet Genomics*, 290, 685-97.
- LYKO, F., RAMSAHOYE, B. H., KASHEVSKY, H., TUDOR, M., MASTRANGELO, M. A., ORR-WEAVER, T. L. & JAENISCH, R. 1999. Mammalian (cytosine-5) methyltransferases cause genomic DNA methylation and lethality in *Drosophila*. *Nat Genet*, 23, 363-6.
- MACHINIS, K., PANTEL, J., NETCHINE, I., LEGER, J., CAMAND, O. J., SOBRIER, M. L., DASTOT-LE MOAL, F., DUQUESNOY, P., ABITBOL, M., CZERNICHOW, P. & AMSELEM, S. 2001. Syndromic short stature in patients with a germline mutation in the LIM homeobox LHX4. *Am J Hum Genet*, 69, 961-8.
- MAESTRINI, E., PAGNAMENTA, A. T., LAMB, J. A., BACCHELLI, E., SYKES, N. H., SOUSA, I., TOMA, C., BARNBY, G., BUTLER, H., WINCHESTER, L., SCERRI, T. S., MINOPOLI, F., REICHERT, J., CAI, G., BUXBAUM, J. D., KORVATSKA, O., SCHELLENBERG, G. D., DAWSON, G., DE BILD, A., MINDERAA, R. B., MULDER, E. J., MORRIS, A. P., BAILEY, A. J., MONACO, A. P. & IMGSAAC 2010. High-density SNP association

- study and copy number variation analysis of the AUTS1 and AUTS5 loci implicate the IMMP2L-DOCK4 gene region in autism susceptibility. *Mol Psychiatry*, 15, 954-68.
- MARRA, M. N., WILDE, C. G., COLLINS, M. S., SNABLE, J. L., THORNTON, M. B. & SCOTT, R. W. 1992. The role of bactericidal/permeability-increasing protein as a natural inhibitor of bacterial endotoxin. *J Immunol*, 148, 532-7.
- MARTIN, C. L., DUVALL, J. A., ILKIN, Y., SIMON, J. S., ARREAZA, M. G., WILKES, K., ALVAREZ-RETUERTO, A., WHICHELLO, A., POWELL, C. M., RAO, K., COOK, E. & GESCHWIND, D. H. 2007. Cytogenetic and molecular characterization of A2BP1/FOX1 as a candidate gene for autism. *Am J Med Genet B Neuropsychiatr Genet*, 144B, 869-76.
- MARTIN, J. A. & WANG, Z. 2011. Next-generation transcriptome assembly. *Nat Rev Genet*, 12, 671-82.
- MATSUNAGA, E., TAUSZIG-DELAMASURE, S., MONNIER, P. P., MUELLER, B. K., STRITTMATTER, S. M., MEHLEN, P. & CHEDOTAL, A. 2004. RGM and its receptor neogenin regulate neuronal survival. *Nat Cell Biol*, 6, 749-55.
- MATTICK, J. S. & MAKUNIN, I. V. 2006. Non-coding RNA. *Hum Mol Genet*, 15 Spec No 1, R17-29.
- MAUNAKEA, A. K., CHEPELEV, I., CUI, K. & ZHAO, K. 2013. Intragenic DNA methylation modulates alternative splicing by recruiting MeCP2 to promote exon recognition. *Cell Res*, 23, 1256-69.
- MAURANO, M. T., HUMBERT, R., RYNES, E., THURMAN, R. E., HAUGEN, E., WANG, H., REYNOLDS, A. P., SANDSTROM, R., QU, H., BRODY, J., SHAFER, A., NERI, F., LEE, K., KUTYAVIN, T., STEHLING-SUN, S., JOHNSON, A. K., CANFIELD, T. K., GISTE, E., DIEGEL, M., BATES, D., HANSEN, R. S., NEPH, S., SABO, P. J., HEIMFELD, S., RAUBITSCHKE, A., ZIEGLER, S., COTSAPAS, C., SOTOODEHNIA, N., GLASS, I., SUNYAEV, S. R., KAUL, R. & STAMATOYANNOPOULOS, J. A. 2012. Systematic localization of common disease-associated variation in regulatory DNA. *Science*, 337, 1190-5.
- MAYCOX, P. R., KELLY, F., TAYLOR, A., BATES, S., REID, J., LOGENDRA, R., BARNES, M. R., LARMINIE, C., JONES, N., LENNON, M., DAVIES, C., HAGAN, J. J., SCORER, C. A., ANGELINETTA, C., AKBAR, M. T., HIRSCH, S., MORTIMER, A. M., BARNES, T. R. & DE BELLEROCHE, J. 2009. Analysis of gene expression in two large schizophrenia cohorts identifies multiple changes associated with nerve terminal function. *Mol Psychiatry*, 14, 1083-94.
- MCCARTHY, D. J., CHEN, Y. & SMYTH, G. K. 2012. Differential expression analysis of multifactor RNA-Seq experiments with respect to biological variation. *Nucleic Acids Res*, 40, 4288-97.
- MCDONALD, P. P., O'REILLY, R. & SINGH, S. M. 2011. Methylation analysis of the NOTCH4 -25 C/T polymorphism in schizophrenia. *Psychiatr Genet*, 21, 5-13.
- MCGRATH, J., SAHA, S., CHANT, D. & WELHAM, J. 2008. Schizophrenia: a concise overview of incidence, prevalence, and mortality. *Epidemiol Rev*, 30, 67-76.
- MCLEAN, C. Y., BRISTOR, D., HILLER, M., CLARKE, S. L., SCHAAR, B. T., LOWE, C. B., WENGER, A. M. & BEJERANO, G. 2010. GREAT

- improves functional interpretation of cis-regulatory regions. *Nat Biotechnol*, 28, 495-501.
- MCVICKER, G., VAN DE GEIJN, B., DEGNER, J. F., CAIN, C. E., BANOVICH, N. E., RAJ, A., LEWELLEN, N., MYRTHIL, M., GILAD, Y. & PRITCHARD, J. K. 2013. Identification of Genetic Variants That Affect Histone Modifications in Human Cells. *Science*, 342, 747-749.
- MEDICAL RESEARCH COUNCIL. 2016. *UK Brain Bank Network* [Online]. <http://www.mrc.ac.uk/research/facilities-and-resources-for-researchers/brain-banks/>. [Accessed 2nd December 2016].
- MELAS, P. A., ROGDAKI, M., OSBY, U., SCHALLING, M., LAVEBRATT, C. & EKSTROM, T. J. 2012. Epigenetic aberrations in leukocytes of patients with schizophrenia: association of global DNA methylation with antipsychotic drug treatment and disease onset. *FASEB J*, 26, 2712-8.
- MERENLENDER-WAGNER, A., MALISHKEVICH, A., SHEMER, Z., UDAWELA, M., GIBBONS, A., SCARR, E., DEAN, B., LEVINE, J., AGAM, G. & GOZES, I. 2015. Autophagy has a key role in the pathophysiology of schizophrenia. *Mol Psychiatry*, 20, 126-32.
- MILL, J. & HEIJMANS, B. T. 2013. From promises to practical strategies in epigenetic epidemiology. *Nat Rev Genet*, 14, 585-94.
- MILL, J., TANG, T., KAMINSKY, Z., KHARE, T., YAZDANPANA, S., BOUCHARD, L., JIA, P., ASSADZADEH, A., FLANAGAN, J., SCHUMACHER, A., WANG, S. C. & PETRONIS, A. 2008. Epigenomic profiling reveals DNA-methylation changes associated with major psychosis. *Am J Hum Genet*, 82, 696-711.
- MISTRY, M., GILLIS, J. & PAVLIDIS, P. 2013. Genome-wide expression profiling of schizophrenia using a large combined cohort. *Mol Psychiatry*, 18, 215-25.
- MIYAMOTO, S., DUNCAN, G. E., MARX, C. E. & LIEBERMAN, J. A. 2005. Treatments for schizophrenia: a critical review of pharmacology and mechanisms of action of antipsychotic drugs. *Mol Psychiatry*, 10, 79-104.
- MOCHIDA, G. H., GANESH, V. S., DE MICHELENA, M. I., DIAS, H., ATABAY, K. D., KATHREIN, K. L., HUANG, H. T., HILL, R. S., FELIE, J. M., RAKIEC, D., GLEASON, D., HILL, A. D., MALIK, A. N., BARRY, B. J., PARTLOW, J. N., TAN, W. H., GLADER, L. J., BARKOVICH, A. J., DOBYNS, W. B., ZON, L. I. & WALSH, C. A. 2012. CHMP1A encodes an essential regulator of BMI1-INK4A in cerebellar development. *Nature Genetics*, 44, 1260-1264.
- MONTANO, C., TAUB, M. A., JAFFE, A., BRIEM, E., FEINBERG, J. I., TRYGVADOTTIR, R., IDRIZI, A., RUNARSSON, A., BERNDSEN, B., GUR, R. C., MOORE, T. M., PERRY, R. T., FUGMAN, D., SABUNCIYAN, S., YOLKEN, R. H., HYDE, T. M., KLEINMAN, J. E., SOBELL, J. L., PATO, C. N., PATO, M. T., GO, R. C., NIMGAONKAR, V., WEINBERGER, D. R., BRAFF, D., GUR, R. E., FALLIN, M. D. & FEINBERG, A. P. 2016. Association of DNA Methylation Differences With Schizophrenia in an Epigenome-Wide Association Study. *JAMA Psychiatry*, 73, 506-14.
- MORISON, I. M., RAMSAY, J. P. & SPENCER, H. G. 2005. A census of mammalian imprinting. *Trends Genet*, 21, 457-65.
- MRC LONDON NEURODEGENERATIVE DISEASE BRAIN BANK WEBSITE. 2016. <http://www.kcl.ac.uk/ioppn/depts/bcn/Our>

- [research/Neurodegeneration/brain-bank.aspx](#). [Accessed 27th February 2016].
- MUELLE, O., LIGHTFOOT, S. & SCHROEDER, A. 2004. *RNA Integrity Number (RIN) – Standardization of RNA Quality Control* [Online]. <https://www.agilent.com/>: Agilent Technologies. [Accessed 21st April 2016].
- NAGALAKSHMI, U., WANG, Z., WAERN, K., SHOU, C., RAHA, D., GERSTEIN, M. & SNYDER, M. 2008. The transcriptional landscape of the yeast genome defined by RNA sequencing. *Science*, 320, 1344-9.
- NAN, X., NG, H. H., JOHNSON, C. A., LAHERTY, C. D., TURNER, B. M., EISENMAN, R. N. & BIRD, A. 1998. Transcriptional repression by the methyl-CpG-binding protein MeCP2 involves a histone deacetylase complex. *Nature*, 393, 386-9.
- NARAYAN, S., TANG, B., HEAD, S. R., GILMARTIN, T. J., SUTCLIFFE, J. G., DEAN, B. & THOMAS, E. A. 2008. Molecular profiles of schizophrenia in the CNS at different stages of illness. *Brain Res*, 1239, 235-48.
- NATURE EDUCATION. 2014. *Gene Expression* [Online]. <http://www.nature.com/scitable/topicpage/gene-expression-14121669>. [Accessed 2016].
- NEUMANN, P. 2007. *Progress in DNA Methylation Research*, Humana Press Inc.
- NEW ENGLAND BIOLABS. 2016. *New England Biolabs webpage* [Online]. <https://www.neb.com/>. [Accessed 21st April 2016].
- NG, S. Y. & STANTON, L. W. 2013. Long non-coding RNAs in stem cell pluripotency. *Wiley Interdiscip Rev RNA*, 4, 121-8.
- NIELSEN, P. R., LAURSEN, T. M. & MORTENSEN, P. B. 2013. Association between parental hospital-treated infection and the risk of schizophrenia in adolescence and early adulthood. *Schizophr Bull*, 39, 230-7.
- NISHIOKA, M., BUNDO, M., KOIKE, S., TAKIZAWA, R., KAKIUCHI, C., ARAKI, T., KASAI, K. & IWAMOTO, K. 2013. Comprehensive DNA methylation analysis of peripheral blood cells derived from patients with first-episode schizophrenia. *J Hum Genet*, 58, 91-7.
- NOHESARA, S., GHADIRIVASFI, M., MOSTAFAVI, S., ESKANDARI, M. R., AHMADKHANIHA, H., THIAGALINGAM, S. & ABDOLMALEKY, H. M. 2011. DNA hypomethylation of MB-COMT promoter in the DNA derived from saliva in schizophrenia and bipolar disorder. *J Psychiatr Res*, 45, 1432-8.
- NORKETT, R., MODI, S., BIRSA, N., ATKIN, T. A., IVANKOVIC, D., PATHANIA, M., TROSSBACH, S. V., KORTH, C., HIRST, W. D. & KITTLER, J. T. 2016. DISC1-dependent Regulation of Mitochondrial Dynamics Controls the Morphogenesis of Complex Neuronal Dendrites. *J Biol Chem*, 291, 613-29.
- NUMATA, S., YE, T., HERMAN, M. & LIPSKA, B. K. 2014. DNA methylation changes in the postmortem dorsolateral prefrontal cortex of patients with schizophrenia. *Front Genet*, 5, 280.
- NUSSE, R. 2008. Wnt signaling and stem cell control. *Cell Res*, 18, 523-7.
- O'DONOVAN, M. C. 2015. What have we learned from the Psychiatric Genomics Consortium. *World Psychiatry*, 14, 291-3.
- O'LEARY, C., COLE, S. J., LANGFORD, M., HEWAGE, J., WHITE, A. & COOPER, H. M. 2013. RGMa regulates cortical interneuron migration and differentiation. *PLoS One*, 8, e81711.

- O'ROAK, B. J., DERIZIOTIS, P., LEE, C., VIVES, L., SCHWARTZ, J. J., GIRIRAJAN, S., KARAKOC, E., MACKENZIE, A. P., NG, S. B., BAKER, C., RIEDER, M. J., NICKERSON, D. A., BERNIER, R., FISHER, S. E., SHENDURE, J. & EICHLER, E. E. 2011. Exome sequencing in sporadic autism spectrum disorders identifies severe de novo mutations. *Nat Genet*, 43, 585-9.
- OGAWA, F., MALAVASI, E. L., CRUMMIE, D. K., EYKELENBOOM, J. E., SOARES, D. C., MACKIE, S., PORTEOUS, D. J. & MILLAR, J. K. 2014. DISC1 complexes with TRAK1 and Miro1 to modulate anterograde axonal mitochondrial trafficking. *Hum Mol Genet*, 23, 906-19.
- OTA, V. K., NOTO, C., GADELHA, A., SANTORO, M. L., SPINDOLA, L. M., GOUVEA, E. S., STILHANO, R. S., ORTIZ, B. B., SILVA, P. N., SATO, J. R., HAN, S. W., CORDEIRO, Q., BRESSAN, R. A. & BELANGERO, S. I. 2014. Changes in gene expression and methylation in the blood of patients with first-episode psychosis. *Schizophr Res*, 159, 358-64.
- OWEN, M. J., O'DONOVAN, M. C., THAPAR, A. & CRADDOCK, N. 2011. Neurodevelopmental hypothesis of schizophrenia. *Br J Psychiatry*, 198, 173-5.
- OZSOLAK, F. & MILOS, P. M. 2011. RNA sequencing: advances, challenges and opportunities. *Nat Rev Genet*, 12, 87-98.
- PARIKSHAK, N. N., LUO, R., ZHANG, A., WON, H., LOWE, J. K., CHANDRAN, V., HORVATH, S. & GESCHWIND, D. H. 2013. Integrative functional genomic analyses implicate specific molecular pathways and circuits in autism. *Cell*, 155, 1008-21.
- PASCUAL, A., HIDALGO-FIGUEROA, M., PIRUAT, J. I., PINTADO, C. O., GOMEZ-DIAZ, R. & LOPEZ-BARNEO, J. 2008. Absolute requirement of GDNF for adult catecholaminergic neuron survival. *Nat Neurosci*, 11, 755-61.
- PATEL, C., COOPER-CHARLES, L., MCMULLAN, D. J., WALKER, J. M., DAVISON, V. & MORTON, J. 2011. Translocation breakpoint at 7q31 associated with tics: further evidence for IMMP2L as a candidate gene for Tourette syndrome. *Eur J Hum Genet*, 19, 634-9.
- PAUL, C. L. & CLARK, S. J. 1996. Cytosine methylation: quantitation by automated genomic sequencing and GENESCAN analysis. *Biotechniques*, 21, 126-33.
- PEDERSEN, B. S., SCHWARTZ, D. A., YANG, I. V. & KECHRIS, K. J. 2012. Comb-p: software for combining, analyzing, grouping and correcting spatially correlated P-values. *Bioinformatics*, 28, 2986-8.
- PETRONIS, A., GOTTESMAN, II, KAN, P., KENNEDY, J. L., BASILE, V. S., PATERSON, A. D. & POPENDIKYTE, V. 2003. Monozygotic twins exhibit numerous epigenetic differences: clues to twin discordance? *Schizophr Bull*, 29, 169-78.
- PICKARD, B. S. 2015. Schizophrenia biomarkers: translating the descriptive into the diagnostic. *J Psychopharmacol*, 29, 138-43.
- PIDSLEY, R., CC, Y. W., VOLTA, M., LUNNON, K., MILL, J. & SCHALKWYK, L. C. 2013. A data-driven approach to preprocessing Illumina 450K methylation array data. *BMC Genomics*, 14, 293.
- PIDSLEY, R. & MILL, J. 2011. Epigenetic studies of psychosis: current findings, methodological approaches, and implications for postmortem research. *Biol Psychiatry*, 69, 146-56.

- PIDSLEY, R., VIANA, J., HANNON, E., SPIERS, H., TROAKES, C., AL-SARAJ, S., MECHAWAR, N., TURECKI, G., SCHALKWYK, L. C., BRAY, N. J. & MILL, J. 2014. Methylomic profiling of human brain tissue supports a neurodevelopmental origin for schizophrenia. *Genome Biol*, 15, 483.
- POCKLINGTON, A. J., O'DONOVAN, M. & OWEN, M. J. 2014. The synapse in schizophrenia. *Eur J Neurosci*, 39, 1059-67.
- PORTEOUS, D. J., THOMSON, P. A., MILLAR, J. K., EVANS, K. L., HENNAH, W., SOARES, D. C., MCCARTHY, S., MCCOMBIE, W. R., CLAPCOTE, S. J., KORTH, C., BRANDON, N. J., SAWA, A., KAMIYA, A., RODER, J. C., LAWRIE, S. M., MCINTOSH, A. M., ST CLAIR, D. & BLACKWOOD, D. H. 2014. DISC1 as a genetic risk factor for schizophrenia and related major mental illness: response to Sullivan. *Mol Psychiatry*, 19, 141-3.
- POWER, R. A., STEINBERG, S., BJORNSDOTTIR, G., RIETVELD, C. A., ABDELLAOUI, A., NIVARD, M. M., JOHANNESSEN, M., GALESLOOT, T. E., HOTTENGA, J. J., WILLEMSSEN, G., CESARINI, D., BENJAMIN, D. J., MAGNUSSON, P. K., ULLEN, F., TIEMEIER, H., HOFMAN, A., VAN ROOIJ, F. J., WALTERS, G. B., SIGURDSSON, E., THORGEIRSSON, T. E., INGASON, A., HELGASON, A., KONG, A., KIEMENEY, L. A., KOELLINGER, P., BOOMSMA, D. I., GUDBJARTSSON, D., STEFANSSON, H. & STEFANSSON, K. 2015. Polygenic risk scores for schizophrenia and bipolar disorder predict creativity. *Nat Neurosci*, 18, 953-5.
- PRESTON, A. R., SHOHAMY, D., TAMMINGA, C. A. & WAGNER, A. D. 2005. Hippocampal function, declarative memory, and schizophrenia: anatomic and functional neuroimaging considerations. *Curr Neurol Neurosci Rep*, 5, 249-56.
- PRICE, M. E., COTTON, A. M., LAM, L. L., FARRE, P., EMBERLY, E., BROWN, C. J., ROBINSON, W. P. & KOBOR, M. S. 2013. Additional annotation enhances potential for biologically-relevant analysis of the Illumina Infinium HumanMethylation450 BeadChip array. *Epigenetics Chromatin*, 6, 4.
- PSYCH, E. C., AKBARIAN, S., LIU, C., KNOWLES, J. A., VACCARINO, F. M., FARNHAM, P. J., CRAWFORD, G. E., JAFFE, A. E., PINTO, D., DRACHEVA, S., GESCHWIND, D. H., MILL, J., NAIRN, A. C., ABYZOV, A., POCHAREDDY, S., PRABHAKAR, S., WEISSMAN, S., SULLIVAN, P. F., STATE, M. W., WENG, Z., PETERS, M. A., WHITE, K. P., GERSTEIN, M. B., AMIRI, A., ARMOSKUS, C., ASHLEY-KOCH, A. E., BAE, T., BECKEL-MITCHENER, A., BERMAN, B. P., COETZEE, G. A., COPPOLA, G., FRANCOEUR, N., FROMER, M., GAO, R., GRENNAN, K., HERSTEIN, J., KAVANAGH, D. H., IVANOV, N. A., JIANG, Y., KITCHEN, R. R., KOZLENKOV, A., KUNDAKOVIC, M., LI, M., LI, Z., LIU, S., MANGRAVITE, L. M., MATTEI, E., MARKENSCOFF-PAPADIMITRIOU, E., NAVARRO, F. C., NORTH, N., OMBERG, L., PANCHISION, D., PARIKSHAK, N., POSCHMANN, J., PRICE, A. J., PURCARO, M., REDDY, T. E., ROUSSOS, P., SCHREINER, S., SCUDERI, S., SEBRA, R., SHIBATA, M., SHIEH, A. W., SKARICA, M., SUN, W., SWARUP, V., THOMAS, A., TSUJI, J., VAN BAKEL, H., WANG, D., WANG, Y., WANG, K., WERLING, D. M., WILLSEY, A. J., WITT, H., WON, H., WONG, C. C., WRAY, G. A., WU, E. Y., XU, X., YAO, L., SENTHIL, G., LEHNER, T., SKLAR, P. & SESTAN, N. 2015. The PsychENCODE project. *Nat Neurosci*, 18, 1707-12.

- PSYCHIATRIC GENOMICS CONSORTIUM. 2015. *Psychiatric Genomics Consortium* [Online]. <https://www.med.unc.edu/pgc/downloads>. [Accessed 16th March 2016].
- PSYCHIATRIC GENOMICS CONSORTIUM. 2016. *Psychiatric Genomics Consortium website* [Online]. <http://www.med.unc.edu/pgc/>. [Accessed 2016].
- PULFORD, K., JONES, M., BANHAM, A. H., HARALAMBIEVA, E. & MASON, D. Y. 1999. Lymphocyte-specific protein 1: a specific marker of human leucocytes. *Immunology*, 96, 262-71.
- PURCELL, S., NEALE, B., TODD-BROWN, K., THOMAS, L., FERREIRA, M. A., BENDER, D., MALLER, J., SKLAR, P., DE BAKKER, P. I., DALY, M. J. & SHAM, P. C. 2007. PLINK: a tool set for whole-genome association and population-based linkage analyses. *Am J Hum Genet*, 81, 559-75.
- PURCELL, S. M., MORAN, J. L., FROMER, M., RUDERFER, D., SOLOVIEFF, N., ROUSSOS, P., O'DUSHLAINE, C., CHAMBERT, K., BERGEN, S. E., KAHLER, A., DUNCAN, L., STAHL, E., GENOVESE, G., FERNANDEZ, E., COLLINS, M. O., KOMIYAMA, N. H., CHOUDHARY, J. S., MAGNUSSON, P. K., BANKS, E., SHAKIR, K., GARIMELLA, K., FENNELL, T., DEPRISTO, M., GRANT, S. G., HAGGARTY, S. J., GABRIEL, S., SCOLNICK, E. M., LANDER, E. S., HULTMAN, C. M., SULLIVAN, P. F., MCCARROLL, S. A. & SKLAR, P. 2014. A polygenic burden of rare disruptive mutations in schizophrenia. *Nature*, 506, 185-90.
- QIAGEN. 2010. *RNeasy MinElute Cleanup Kit Handbook* [Online]. <https://www.qiagen.com/>. [Accessed 21st April 2016].
- QIAGEN. 2014. *miRNeasy Mini Kit Handbook* [Online]. <https://www.qiagen.com/>. [Accessed 21st April 2016].
- QIAGEN. 2016. *Qiagen website* [Online]. <https://www.qiagen.com/gb/resources/technologies/pyrosequencing-resource-center/technology-overview/>. [Accessed 22nd April 2016].
- QUINODOZ, M., GOBET, C., NAEF, F. & GUSTAFSON, K. B. 2014. Characteristic bimodal profiles of RNA polymerase II at thousands of active mammalian promoters. *Genome Biol*, 15, R85.
- QURESHI, I. A. & MEHLER, M. F. 2012. Emerging roles of non-coding RNAs in brain evolution, development, plasticity and disease. *Nat Rev Neurosci*, 13, 528-41.
- R CORE TEAM 2015. R: A language and environment for statistical computing. Vienna, Austria: R Foundation for Statistical Computing.
- RAKYAN, V. K., DOWN, T. A., THORNE, N. P., FLICEK, P., KULESHA, E., GRAF, S., TOMAZOU, E. M., BACKDAHL, L., JOHNSON, N., HERBERTH, M., HOWE, K. L., JACKSON, D. K., MIRETTI, M. M., FIEGLER, H., MARIONI, J. C., BIRNEY, E., HUBBARD, T. J., CARTER, N. P., TAVARE, S. & BECK, S. 2008. An integrated resource for genome-wide identification and analysis of human tissue-specific differentially methylated regions (tDMRs). *Genome Res*, 18, 1518-29.
- RANGANATH, C., MINZENBERG, M. J. & RAGLAND, J. D. 2008. The cognitive neuroscience of memory function and dysfunction in schizophrenia. *Biol Psychiatry*, 64, 18-25.
- RAPOPORT, J. L., GIEDD, J. N. & GOGTAY, N. 2012. Neurodevelopmental model of schizophrenia: update 2012. *Mol Psychiatry*, 17, 1228-38.

- RAPOPORT, M., VAN REEKUM, R. & MAYBERG, H. 2000. The role of the cerebellum in cognition and behavior: a selective review. *J Neuropsychiatry Clin Neurosci*, 12, 193-8.
- REUTER, M., BERNINGER, P., CHUMA, S., SHAH, H., HOSOKAWA, M., FUNAYA, C., ANTONY, C., SACHIDANANDAM, R. & PILLAI, R. S. 2011. Miwi catalysis is required for piRNA amplification-independent LINE1 transposon silencing. *Nature*, 480, 264-7.
- RICHARDS, A. L., JONES, L., MOSKVINA, V., KIROV, G., GEJMAN, P. V., LEVINSON, D. F., SANDERS, A. R., MOLECULAR GENETICS OF SCHIZOPHRENIA, C., INTERNATIONAL SCHIZOPHRENIA, C., PURCELL, S., VISSCHER, P. M., CRADDOCK, N., OWEN, M. J., HOLMANS, P. & O'DONOVAN, M. C. 2012. Schizophrenia susceptibility alleles are enriched for alleles that affect gene expression in adult human brain. *Mol Psychiatry*, 17, 193-201.
- RICHARDS, E. J. 2006. Inherited epigenetic variation--revisiting soft inheritance. *Nat Rev Genet*, 7, 395-401.
- RICHTER, S., DIMITROVA, A., MASCHKE, M., GIZEWSKI, E., BECK, A., AURICH, V. & TIMMANN, D. 2005. Degree of cerebellar ataxia correlates with three-dimensional mri-based cerebellar volume in pure cerebellar degeneration. *Eur Neurol*, 54, 23-7.
- RILEY, B. & KENDLER, K. S. 2006. Molecular genetic studies of schizophrenia. *Eur J Hum Genet*, 14, 669-80.
- RIVERA, C. M. & REN, B. 2013. Mapping human epigenomes. *Cell*, 155, 39-55.
- ROADMAP EPIGENOMICS CONSORTIUM, KUNDAJE, A., MEULEMAN, W., ERNST, J., BILENKY, M., YEN, A., HERAVI-MOUSSAVI, A., KHERADPOUR, P., ZHANG, Z., WANG, J., ZILLER, M. J., AMIN, V., WHITAKER, J. W., SCHULTZ, M. D., WARD, L. D., SARKAR, A., QUON, G., SANDSTROM, R. S., EATON, M. L., WU, Y. C., PFENNING, A. R., WANG, X., CLAUSSNITZER, M., LIU, Y., COARFA, C., HARRIS, R. A., SHORESH, N., EPSTEIN, C. B., GJONESKA, E., LEUNG, D., XIE, W., HAWKINS, R. D., LISTER, R., HONG, C., GASCARD, P., MUNGALL, A. J., MOORE, R., CHUAH, E., TAM, A., CANFIELD, T. K., HANSEN, R. S., KAUL, R., SABO, P. J., BANSAL, M. S., CARLES, A., DIXON, J. R., FARH, K. H., FEIZI, S., KARLIC, R., KIM, A. R., KULKARNI, A., LI, D., LOWDON, R., ELLIOTT, G., MERCER, T. R., NEPH, S. J., ONUCHIC, V., POLAK, P., RAJAGOPAL, N., RAY, P., SALLARI, R. C., SIEBENTHALL, K. T., SINNOTT-ARMSTRONG, N. A., STEVENS, M., THURMAN, R. E., WU, J., ZHANG, B., ZHOU, X., BEAUDET, A. E., BOYER, L. A., DE JAGER, P. L., FARNHAM, P. J., FISHER, S. J., HAUSSLER, D., JONES, S. J., LI, W., MARRA, M. A., MCMANUS, M. T., SUNYAEV, S., THOMSON, J. A., TLSTY, T. D., TSAI, L. H., WANG, W., WATERLAND, R. A., ZHANG, M. Q., CHADWICK, L. H., BERNSTEIN, B. E., COSTELLO, J. F., ECKER, J. R., HIRST, M., MEISSNER, A., MILOSAVLJEVIC, A., REN, B., STAMATOYANNOPOULOS, J. A., WANG, T. & KELLIS, M. 2015. Integrative analysis of 111 reference human epigenomes. *Nature*, 518, 317-30.
- ROBINSON, M. D., MCCARTHY, D. J. & SMYTH, G. K. 2010. edgeR: a Bioconductor package for differential expression analysis of digital gene expression data. *Bioinformatics*, 26, 139-40.

- ROBINSON, M. D. & OSHLACK, A. 2010. A scaling normalization method for differential expression analysis of RNA-seq data. *Genome Biol*, 11, R25.
- ROIG, B., FRANCO-PONS, N., MARTORELL, L., TOMAS, J., VOGEL, W. F. & VILELLA, E. 2010. Expression of the tyrosine kinase discoidin domain receptor 1 (DDR1) in human central nervous system myelin. *Brain Res*, 1336, 22-9.
- ROMANOSKI, C. E., GLASS, C. K., STUNNENBERG, H. G., WILSON, L. & ALMOUZNI, G. 2015. Epigenomics: Roadmap for regulation. *Nature*, 518, 314-6.
- RONN, L. C., HARTZ, B. P. & BOCK, E. 1998. The neural cell adhesion molecule (NCAM) in development and plasticity of the nervous system. *Exp Gerontol*, 33, 853-64.
- ROUSSOS, P., KATSEL, P., DAVIS, K. L., SIEVER, L. J. & HAROUTUNIAN, V. 2012. A system-level transcriptomic analysis of schizophrenia using postmortem brain tissue samples. *Arch Gen Psychiatry*, 69, 1205-13.
- RUZICKA, W. B., SUBBURAJU, S. & BENES, F. M. 2015. Circuit- and Diagnosis-Specific DNA Methylation Changes at gamma-Aminobutyric Acid-Related Genes in Postmortem Human Hippocampus in Schizophrenia and Bipolar Disorder. *JAMA Psychiatry*, 72, 541-51.
- SAHA, R. N. & PAHAN, K. 2006. HATs and HDACs in neurodegeneration: a tale of disconcerted acetylation homeostasis. *Cell Death Differ*, 13, 539-50.
- SAINZ, J., MATA, I., BARRERA, J., PEREZ-IGLESIAS, R., VARELA, I., ARRANZ, M. J., RODRIGUEZ, M. C. & CRESPO-FACORRO, B. 2013. Inflammatory and immune response genes have significantly altered expression in schizophrenia. *Mol Psychiatry*, 18, 1056-7.
- SANDERS, A. R., GORING, H. H., DUAN, J., DRIGALENKO, E. I., MOY, W., FREDA, J., HE, D., SHI, J., MGS & GEJMAN, P. V. 2013. Transcriptome study of differential expression in schizophrenia. *Hum Mol Genet*, 22, 5001-14.
- SANGER, F., NICKLEN, S. & COULSON, A. R. 1977. DNA sequencing with chain-terminating inhibitors. *Proc Natl Acad Sci U S A*, 74, 5463-7.
- SCHIZOPHRENIA WORKING GROUP OF THE PSYCHIATRIC GENOMICS, C. 2014. Biological insights from 108 schizophrenia-associated genetic loci. *Nature*, 511, 421-7.
- SCHMIDT, M. J. & MIRNICS, K. 2015. Neurodevelopment, GABA system dysfunction, and schizophrenia. *Neuropsychopharmacology*, 40, 190-206.
- SCHMITT, A., LEONARDI-ESSMANN, F., DURRENBERGER, P. F., PARLAPANI, E., SCHNEIDER-AXMANN, T., SPANAGEL, R., ARZBERGER, T., KRETZSCHMAR, H., HERRERA-MARSCHITZ, M., GRUBER, O., REYNOLDS, R., FALKAI, P. & GEBICKE-HAERTER, P. J. 2011. Regulation of immune-modulatory genes in left superior temporal cortex of schizophrenia patients: a genome-wide microarray study. *World J Biol Psychiatry*, 12, 201-15.
- SCHWARZER, G. 2015. meta: General Package for Meta-Analysis.
- SCHWIKOWSKI, B., UETZ, P. & FIELDS, S. 2000. A network of protein-protein interactions in yeast. *Nat Biotechnol*, 18, 1257-61.
- SEBAT, J., LAKSHMI, B., MALHOTRA, D., TROGE, J., LESE-MARTIN, C., WALSH, T., YAMROM, B., YOON, S., KRASNITZ, A., KENDALL, J., LEOTTA, A., PAI, D., ZHANG, R., LEE, Y. H., HICKS, J., SPENCE, S. J.,

- LEE, A. T., PUURA, K., LEHTIMAKI, T., LEDBETTER, D., GREGERSEN, P. K., BREGMAN, J., SUTCLIFFE, J. S., JOBANPUTRA, V., CHUNG, W., WARBURTON, D., KING, M. C., SKUSE, D., GESCHWIND, D. H., GILLIAM, T. C., YE, K. & WIGLER, M. 2007. Strong association of de novo copy number mutations with autism. *Science*, 316, 445-9.
- SHENTON, M. E., DICKEY, C. C., FRUMIN, M. & MCCARLEY, R. W. 2001. A review of MRI findings in schizophrenia. *Schizophr Res*, 49, 1-52.
- ŠIDÁK, Z. 1967. Rectangular confidence region for the means of multivariate normal distributions. *Journal of the American Statistical Association*, 62, 626-633.
- SIMPSON, E. H., KELLENDONK, C. & KANDEL, E. 2010. A possible role for the striatum in the pathogenesis of the cognitive symptoms of schizophrenia. *Neuron*, 65, 585-96.
- SKAKKEBAEK, A., GRAVHOLT, C. H., RASMUSSEN, P. M., BOJESEN, A., JENSEN, J. S., FEDDER, J., LAURBERG, P., HERTZ, J. M., OSTERGAARD, J. R., PEDERSEN, A. D. & WALLENTIN, M. 2014. Neuroanatomical correlates of Klinefelter syndrome studied in relation to the neuropsychological profile. *Neuroimage Clin*, 4, 1-9.
- SKAKKEBAEK, A., GRAVHOLT, C. H., RASMUSSEN, P. M., BOJESEN, A., JENSEN, J. S., FEDDER, J., LAURBERG, P., HERTZ, J. M., OSTERGAARD, J. R., PEDERSEN, A. D. & WALLENTIN, M. 2016. Corrigendum to "Neuroanatomical correlates of Klinefelter syndrome studied in relation to the neuropsychological profile" [*NeuroImage: Clin* 4 (2014) 1-9]. *Neuroimage Clin*, 11, 52.
- SLIEKER, R. C., BOS, S. D., GOEMAN, J. J., BOVÉE, J. V., TALENS, R. P., VAN DER BREGGEN, R., SUCHIMAN, H. E., LAMEIJER, E. W., PUTTER, H., VAN DEN AKKER, E. B., ZHANG, Y., JUKEMA, J. W., SLAGBOOM, P. E., MEULENBELT, I. & HEIJMANS, B. T. 2013. Identification and systematic annotation of tissue-specific differentially methylated regions using the Illumina 450k array. *Epigenetics Chromatin*, 6, 26.
- SORENSEN, H. J., MORTENSEN, E. L., REINISCH, J. M. & MEDNICK, S. A. 2009. Association between prenatal exposure to bacterial infection and risk of schizophrenia. *Schizophr Bull*, 35, 631-7.
- SPENCER, V. A. & DAVIE, J. R. 1999. Role of covalent modifications of histones in regulating gene expression. *Gene*, 240, 1-12.
- SPIERS, H., HANNON, E., SCHALKWYK, L. C., SMITH, R., WONG, C. C., O'DONOVAN, M. C., BRAY, N. J. & MILL, J. 2015. Methyloomic trajectories across human fetal brain development. *Genome Res*, 25, 338-52.
- ST CLAIR, D., BLACKWOOD, D., MUIR, W., CAROTHERS, A., WALKER, M., SPOWART, G., GOSDEN, C. & EVANS, H. J. 1990. Association within a family of a balanced autosomal translocation with major mental illness. *Lancet*, 336, 13-6.
- STEFANSSON, H., MEYER-LINDENBERG, A., STEINBERG, S., MAGNUSDOTTIR, B., MORGEN, K., ARNARSDOTTIR, S., BJORNSDOTTIR, G., WALTERS, G. B., JONSDOTTIR, G. A., DOYLE, O. M., TOST, H., GRIMM, O., KRISTJANSDOTTIR, S., SNORRASON, H., DAVIDSDOTTIR, S. R., GUDMUNDSSON, L. J., JONSSON, G. F., STEFANSDOTTIR, B., HELGADOTTIR, I., HARALDSSON, M.,

- JONSDOTTIR, B., THYGESEN, J. H., SCHWARZ, A. J., DIDRIKSEN, M., STENSBOL, T. B., BRAMMER, M., KAPUR, S., HALLDORSSON, J. G., HREIDARSSON, S., SAEMUNDSEN, E., SIGURDSSON, E. & STEFANSSON, K. 2014. CNVs conferring risk of autism or schizophrenia affect cognition in controls. *Nature*, 505, 361-6.
- STURROCK, R. R. 1989a. Age related changes in Purkinje cell number in the cerebellar nodulus of the mouse. *J Hirnforsch*, 30, 757-60.
- STURROCK, R. R. 1989b. Changes in neuron number in the cerebellar cortex of the ageing mouse. *J Hirnforsch*, 30, 499-503.
- STURROCK, R. R. 1990. A comparison of quantitative histological changes in different regions of the ageing mouse cerebellum. *J Hirnforsch*, 31, 481-6.
- SULLIVAN, P. F. 2013. Questions about DISC1 as a genetic risk factor for schizophrenia. *Mol Psychiatry*, 18, 1050-2.
- SUNSHINE, J., BALAK, K., RUTISHAUSER, U. & JACOBSON, M. 1987. Changes in neural cell adhesion molecule (NCAM) structure during vertebrate neural development. *Proc Natl Acad Sci U S A*, 84, 5986-90.
- SUSSER, E., NEUGEBAUER, R., HOEK, H. W., BROWN, A. S., LIN, S., LABOVITZ, D. & GORMAN, J. M. 1996. Schizophrenia after prenatal famine. Further evidence. *Arch Gen Psychiatry*, 53, 25-31.
- TAHILIANI, M., KOH, K. P., SHEN, Y., PASTOR, W. A., BANDUKWALA, H., BRUDNO, Y., AGARWAL, S., IYER, L. M., LIU, D. R., ARAVIND, L. & RAO, A. 2009. Conversion of 5-methylcytosine to 5-hydroxymethylcytosine in mammalian DNA by MLL partner TET1. *Science*, 324, 930-5.
- TALENS, R. P., BOOMSMA, D. I., TOBI, E. W., KREMER, D., JUKEMA, J. W., WILLEMSSEN, G., PUTTER, H., SLAGBOOM, P. E. & HEIJMANS, B. T. 2010. Variation, patterns, and temporal stability of DNA methylation: considerations for epigenetic epidemiology. *FASEB J*, 24, 3135-44.
- TALKOWSKI, M. E., ROSENFELD, J. A., BLUMENTHAL, I., PILLALAMARRI, V., CHIANG, C., HEILBUT, A., ERNST, C., HANSCOM, C., ROSSIN, E., LINDGREN, A. M., PEREIRA, S., RUDERFER, D., KIRBY, A., RIPKE, S., HARRIS, D. J., LEE, J. H., HA, K., KIM, H. G., SOLOMON, B. D., GROPMAN, A. L., LUCENTE, D., SIMS, K., OHSUMI, T. K., BOROWSKY, M. L., LORANGER, S., QUADE, B., LAGE, K., MILES, J., WU, B. L., SHEN, Y., NEALE, B., SHAFFER, L. G., DALY, M. J., MORTON, C. C. & GUSELLA, J. F. 2012. Sequencing chromosomal abnormalities reveals neurodevelopmental loci that confer risk across diagnostic boundaries. *Cell*, 149, 525-37.
- TAMMINGA, C. A. & BUCHSBAUM, M. S. 2004. Frontal cortex function. *Am J Psychiatry*, 161, 2178.
- TAMMINGA, C. A., STAN, A. D. & WAGNER, A. D. 2010. The hippocampal formation in schizophrenia. *Am J Psychiatry*, 167, 1178-93.
- TAN, L. & SHI, Y. G. 2012. Tet family proteins and 5-hydroxymethylcytosine in development and disease. *Development*, 139, 1895-902.
- TANDON, R., GAEBEL, W., BARCH, D. M., BUSTILLO, J., GUR, R. E., HECKERS, S., MALASPINA, D., OWEN, M. J., SCHULTZ, S., TSUANG, M., VAN OS, J. & CARPENTER, W. 2013. Definition and description of schizophrenia in the DSM-5. *Schizophr Res*, 150, 3-10.
- THE COMMONMIND CONSORTIUM. 2016. *The CommonMind Consortium* [Online]. <http://commonmind.org>. [Accessed 2nd December 2016].

- THERMO FISHER SCIENTIFIC. 2012. *ERCC RNA Spike-In Control Mixes user guide* [Online].
https://tools.thermofisher.com/content/sfs/manuals/cms_086340.pdf.
 [Accessed 11th May 2016].
- THERMO FISHER SCIENTIFIC. 2016. *ERCC RNA Spike-In Mix Catalog page* [Online].
<https://www.thermofisher.com/order/catalog/product/4456740>.
 [Accessed February 2016].
- TKACHEV, D., MIMMACK, M. L., RYAN, M. M., WAYLAND, M., FREEMAN, T., JONES, P. B., STARKEY, M., WEBSTER, M. J., YOLKEN, R. H. & BAHN, S. 2003. Oligodendrocyte dysfunction in schizophrenia and bipolar disorder. *Lancet*, 362, 798-805.
- TOCHIGI, M., IWAMOTO, K., BUNDO, M., KOMORI, A., SASAKI, T., KATO, N. & KATO, T. 2008. Methylation status of the reelin promoter region in the brain of schizophrenic patients. *Biol Psychiatry*, 63, 530-3.
- TOLOSA, A., SANJUAN, J., DAGNALL, A. M., MOLTO, M. D., HERRERO, N. & DE FRUTOS, R. 2010. FOXP2 gene and language impairment in schizophrenia: association and epigenetic studies. *BMC Med Genet*, 11, 114.
- TORKAMANI, A., DEAN, B., SCHORK, N. J. & THOMAS, E. A. 2010. Coexpression network analysis of neural tissue reveals perturbations in developmental processes in schizophrenia. *Genome Res*, 20, 403-12.
- TOST, J. & GUT, I. G. 2007. DNA methylation analysis by pyrosequencing. *Nat Protoc*, 2, 2265-75.
- TSAI, M. C., MANOR, O., WAN, Y., MOSAMMAPARAST, N., WANG, J. K., LAN, F., SHI, Y., SEGAL, E. & CHANG, H. Y. 2010. Long noncoding RNA as modular scaffold of histone modification complexes. *Science*, 329, 689-93.
- VAN RIJN, S., ALEMAN, A., SWAAB, H. & KAHN, R. 2006. Klinefelter's syndrome (karyotype 47,XXY) and schizophrenia-spectrum pathology. *Br J Psychiatry*, 189, 459-60.
- VARLEY, K. E., GERTZ, J., BOWLING, K. M., PARKER, S. L., REDDY, T. E., PAULI-BEHN, F., CROSS, M. K., WILLIAMS, B. A., STAMATOYANNOPOULOS, J. A., CRAWFORD, G. E., ABSHER, D. M., WOLD, B. J. & MYERS, R. M. 2013. Dynamic DNA methylation across diverse human cell lines and tissues. *Genome Res*, 23, 555-67.
- VIANA, J., PIDSLEY, R., TROAKES, C., SPIERS, H., WONG, C. C., AL-SARRAJ, S., CRAIG, I., SCHALKWYK, L. & MILL, J. 2014. Epigenomic and transcriptomic signatures of a Klinefelter syndrome (47,XXY) karyotype in the brain. *Epigenetics*, 9, 587-99.
- VOINEAGU, I., WANG, X., JOHNSTON, P., LOWE, J. K., TIAN, Y., HORVATH, S., MILL, J., CANTOR, R. M., BLENCOWE, B. J. & GESCHWIND, D. H. 2011. Transcriptomic analysis of autistic brain reveals convergent molecular pathology. *Nature*, 474, 380-4.
- WADDINGTON, C. H. 1942. The epigenotype. *Endeavour*, 18-20.
- WADDINGTON, C. H. 1957. *The strategy of the genes; a discussion of some aspects of theoretical biology*, London, Allen & Unwin.
- WAGNER, J. R., BUSCHE, S., GE, B., KWAN, T., PASTINEN, T. & BLANCHETTE, M. 2014. The relationship between DNA methylation, genetic and expression inter-individual variation in untransformed human fibroblasts. *Genome Biology*, 15, R37-R37.

- WANG, H., FERGUSON, G. D., PINEDA, V. V., CUNDIFF, P. E. & STORM, D. R. 2004. Overexpression of type-1 adenylyl cyclase in mouse forebrain enhances recognition memory and LTP. *Nat Neurosci*, 7, 635-42.
- WANG, H. & ZHANG, M. 2012. The role of Ca²(+)-stimulated adenylyl cyclases in bidirectional synaptic plasticity and brain function. *Rev Neurosci*, 23, 67-78.
- WANG, P. 2012. *Cellphone data helps pinpoint source of traffic tie-ups* [Online]. MIT News. [Accessed 2016].
- WANG, R. Y., GEHRKE, C. W. & EHRLICH, M. 1980. Comparison of bisulfite modification of 5-methyldeoxycytidine and deoxycytidine residues. *Nucleic Acids Res*, 8, 4777-90.
- WANG, T., GUAN, W., LIN, J., BOUTAOUI, N., CANINO, G., LUO, J., CELEDON, J. C. & CHEN, W. 2015. A systematic study of normalization methods for Infinium 450K methylation data using whole-genome bisulfite sequencing data. *Epigenetics*, 10, 662-9.
- WANG, Z., GERSTEIN, M. & SNYDER, M. 2009. RNA-Seq: a revolutionary tool for transcriptomics. *Nat Rev Genet*, 10, 57-63.
- WEBER, M., DAVIES, J. J., WITTIG, D., OAKELEY, E. J., HAASE, M., LAM, W. L. & SCHUBELER, D. 2005. Chromosome-wide and promoter-specific analyses identify sites of differential DNA methylation in normal and transformed human cells. *Nat Genet*, 37, 853-62.
- WEINBERGER, D. R. 1995. From neuropathology to neurodevelopment. *Lancet*, 346, 552-7.
- WEISS, L. A., SHEN, Y., KORN, J. M., ARKING, D. E., MILLER, D. T., FOSSDAL, R., SAEMUNDSEN, E., STEFANSSON, H., FERREIRA, M. A., GREEN, T., PLATT, O. S., RUDERFER, D. M., WALSH, C. A., ALTSHULER, D., CHAKRAVARTI, A., TANZI, R. E., STEFANSSON, K., SANTANGELO, S. L., GUSELLA, J. F., SKLAR, P., WU, B. L., DALY, M. J. & AUTISM, C. 2008. Association between microdeletion and microduplication at 16p11.2 and autism. *N Engl J Med*, 358, 667-75.
- WELLCOME TRUST SANGER INSTITUTE. 2016. *HapMap Phase 3* [Online]. <http://www.sanger.ac.uk/resources/downloads/human/hapmap3.html>. [Accessed 16th March 2016].
- WILHELM-BENARTZI, C. S., KOESTLER, D. C., KARAGAS, M. R., FLANAGAN, J. M., CHRISTENSEN, B. C., KELSEY, K. T., MARSIT, C. J., HOUSEMAN, E. A. & BROWN, R. 2013. Review of processing and analysis methods for DNA methylation array data. *Br J Cancer*, 109, 1394-402.
- WILHELM, B. T. & LANDRY, J. R. 2009. RNA-Seq-quantitative measurement of expression through massively parallel RNA-sequencing. *Methods*, 48, 249-57.
- WIRGENES, K. V., TESLI, M., INDERHAUG, E., ATHANASIU, L., AGARTZ, I., MELLE, I., HUGHES, T., ANDREASSEN, O. A. & DJUROVIC, S. 2014. ANK3 gene expression in bipolar disorder and schizophrenia. *Br J Psychiatry*, 205, 244-5.
- WOCKNER, L. F., MORRIS, C. P., NOBLE, E. P., LAWFORD, B. R., WHITEHALL, V. L., YOUNG, R. M. & VOISEY, J. 2015. Brain-specific epigenetic markers of schizophrenia. *Transl Psychiatry*, 5, e680.
- WOCKNER, L. F., NOBLE, E. P., LAWFORD, B. R., YOUNG, R. M., MORRIS, C. P., WHITEHALL, V. L. & VOISEY, J. 2014. Genome-wide DNA

- methylation analysis of human brain tissue from schizophrenia patients. *Transl Psychiatry*, 4, e339.
- WORLD HEALTH ORGANIZATION 2013. *The World Health Report 2013: Research for Universal Health Coverage*, World Health Organization.
- WORLD HEALTH ORGANIZATION. 2015. *Schizophrenia Fact sheet N°397* [Online]. <http://www.who.int/mediacentre/factsheets/fs397/en/>. [Accessed 26th February 2016].
- WU, J. Q., WANG, X., BEVERIDGE, N. J., TOONEY, P. A., SCOTT, R. J., CARR, V. J. & CAIRNS, M. J. 2012. Transcriptome sequencing revealed significant alteration of cortical promoter usage and splicing in schizophrenia. *PLoS One*, 7, e36351.
- XIAO, Y., CAMARILLO, C., PING, Y., ARANA, T. B., ZHAO, H., THOMPSON, P. M., XU, C., SU, B. B., FAN, H., ORDONEZ, J., WANG, L., MAO, C., ZHANG, Y., CRUZ, D., ESCAMILLA, M. A., LI, X. & XU, C. 2014. The DNA methylome and transcriptome of different brain regions in schizophrenia and bipolar disorder. *PLoS One*, 9, e95875.
- XU, B., ROOS, J. L., DEXHEIMER, P., BOONE, B., PLUMMER, B., LEVY, S., GOGOS, J. A. & KARAYIORGOU, M. 2011. Exome sequencing supports a de novo mutational paradigm for schizophrenia. *Nat Genet*, 43, 864-8.
- XU, J., SUN, J., CHEN, J., WANG, L., LI, A., HELM, M., DUBOVSKY, S. L., BACANU, S. A., ZHAO, Z. & CHEN, X. 2012. RNA-Seq analysis implicates dysregulation of the immune system in schizophrenia. *BMC Genomics*, 13 Suppl 8, S2.
- YAMAGUCHI, S., HONG, K., LIU, R., SHEN, L., INOUE, A., DIEP, D., ZHANG, K. & ZHANG, Y. 2012. Tet1 controls meiosis by regulating meiotic gene expression. *Nature*, 492, 443-7.
- YANEZ, A. & GOODRIDGE, H. S. 2016. Interferon regulatory factor 8 and the regulation of neutrophil, monocyte, and dendritic cell production. *Curr Opin Hematol*, 23, 11-7.
- YANG, J., LEE, S. H., GODDARD, M. E. & VISSCHER, P. M. 2011. GCTA: a tool for genome-wide complex trait analysis. *Am J Hum Genet*, 88, 76-82.
- YU, M., HON, G. C., SZULWACH, K. E., SONG, C. X., ZHANG, L., KIM, A., LI, X., DAI, Q., SHEN, Y., PARK, B., MIN, J. H., JIN, P., REN, B. & HE, C. 2012. Base-resolution analysis of 5-hydroxymethylcytosine in the mammalian genome. *Cell*, 149, 1368-80.
- ZHANG, A. P., YU, J., LIU, J. X., ZHANG, H. Y., DU, Y. Y., ZHU, J. D., HE, G., LI, X. W., GU, N. F., FENG, G. Y. & HE, L. 2007. The DNA methylation profile within the 5'-regulatory region of DRD2 in discordant sib pairs with schizophrenia. *Schizophr Res*, 90, 97-103.
- ZHANG, B. & HORVATH, S. 2005. A general framework for weighted gene co-expression network analysis. *Stat Appl Genet Mol Biol*, 4, Article17.
- ZHANG, C. C., XING, A., TAN, M. S., TAN, L. & YU, J. T. 2015. The Role of MAPT in Neurodegenerative Diseases: Genetics, Mechanisms and Therapy. *Mol Neurobiol*.
- ZHANG, J. Q., NICOLL, G., JONES, C. & CROCKER, P. R. 2000. Siglec-9, a novel sialic acid binding member of the immunoglobulin superfamily expressed broadly on human blood leukocytes. *J Biol Chem*, 275, 22121-6.

- ZHANG, L., LU, X., LU, J., LIANG, H., DAI, Q., XU, G. L., LUO, C., JIANG, H. & HE, C. 2012. Thymine DNA glycosylase specifically recognizes 5-carboxylcytosine-modified DNA. *Nat Chem Biol*, 8, 328-30.
- ZHAO, Z., XU, J., CHEN, J., KIM, S., REIMERS, M., BACANU, S. A., YU, H., LIU, C., SUN, J., WANG, Q., JIA, P., XU, F., ZHANG, Y., KENDLER, K. S., PENG, Z. & CHEN, X. 2015. Transcriptome sequencing and genome-wide association analyses reveal lysosomal function and actin cytoskeleton remodeling in schizophrenia and bipolar disorder. *Mol Psychiatry*, 20, 563-72.
- ZILLER, M. J., HANSEN, K. D., MEISSNER, A. & ARYEE, M. J. 2015. Coverage recommendations for methylation analysis by whole-genome bisulfite sequencing. *Nat Meth*, 12, 230-232.
- ZYMO RESEARCH WEBPAGE. 2016. *EZ DNA Methylation-Gold kit specifications webpage* [Online].
<https://www.zymoresearch.com/epigenetics/dna-methylation/bisulfite-conversion/ez-dna-methylation-gold-kit>: Zymo Research. [Accessed 21st April 2016].